International Indian Ocean Expedition

Collected reprints V

Published upon the recommendation
of the Scientific Committee on Oceanic Research (SCOR)
and the
Intergovernmental Oceanographic Commission (IOC)

Unesco

UNESCO ARCHIVES

International Indian Ocean Expedition. Collected reprints V

Copyright in each paper reprinted in this
collected edition remains in the possession
of each author and publisher, from whom
permission to reproduce has been obtained.

Collected edition published in 1968 by the United Nations
Educational, Scientific and Cultural Organization,
Place de Fontenoy, 75 Paris-7e
Printed by Les Presses Saint-Augustin, Bruges

SC.68/D.37/5A
Printed in Belgium

Preface

The fifth volume of collected reprints of the International Indian Ocean Expedition consists of papers received by Unesco between January and September 1967.

For convenience of presentation the papers have been grouped, in a very approximate classification, under the following six main headings:

I. Marine biology;
II. Marine chemistry;
III. Physical oceanography and marine meteorology;
IV. Marine geology and geophysics;
V. Cruise and general reports;
VI. Papers presented by title only.

It is envisaged that both author and subject indexes will eventually be prepared for the whole series of Collected Reprints volumes.

Collected reprints of the IIOE

List of reprints

Part I. Marine biology

289. Frontier, S. Zooplankton récolté en Mer d'Arabie, Golfe Persique et Golfe d'Aden (3e campagne océanographique du *Commandant Robert Giraud*). I: Données générales—Répartition quantitative. *Océanographie (Nosy Bé)*, no. 3, 1963, p. 17-30 (Cahiers ORSTOM) 3

290. Frontier, S. Notes sur quelques larves atypiques de décapodes brachyoures récoltées dans le plankton de Nosy Bé. *Océanographie (Nosy Bé)*, no. 3, 1963, p. 31-59 (Cahiers ORSTOM) 19

291. Frontier, S. Zooplankton récolté en Mer d'Arabie, Golfe Persique et Golfe d'Aden. II: Ptéropodes—systématique et répartition. *Océanographie (Nosy Bé II)*, no. 6, 1963, p. 233-254 (Cahiers ORSTOM) 49

292. Frontier, S. Hétéropodes et ptéropodes récoltés dans le plankton de Nosy Bé. *Océanographie (Nosy Bé II)*, no. 6, 1963, p. 213-227 (Cahiers ORSTOM). 71

293. Frontier, S. Présence de Creseis chierchiae (BOAS) dans l'Océan Indien. *Océanographie (Nosy Bé II)*, no. 6, 1963, p. 229-232 (Cahiers ORSTOM) 87

294. Sakamoto, Ichitaro. Falling model on the planktonic diatoms. *Report of Faculty of Fisheries, Prefectural University of Mie*, vol. 5, no. 1, 1964, p. 33-49 91

295. Dyson, N.; Jitts, H. R.; Scott, B. D. Techniques for measuring oceanic primary production using radioactive carbon. Australia, CSIRO, Division of Fisheries and Oceanography, 1965, 12 p. (Technical paper no. 18) 109

296. Barnes, H.; Tranter, D. J. A statistical examination of the catches, numbers and biomass taken by three commonly used plankton nets. *Aust. J. Mar. Freshw. Res.*, vol. 16, 1965, p. 293-306 121

297. Doty, Maxwell S.; Jitts, H. R.; Koblentz-Mishke, O. J.; Saijo, Y. Intercalibration of marine plankton primary productivity techniques. *Limnol. and Oceanogr.*, vol. 10, no. 2, 1965, p. 282-286 135

298. Fox, Denis L.; Crozier, George F. Absence or singular specificity of carotenoids in some lower fishes. *Science*, vol. 150, no. 3,697, 1965, p. 771-773 141

299. Frontier, S. Le problème des Creseis. *Océanographie*, vol. III, no. 2, 1965, p. 11-17 (Cahiers ORSTOM) . . 143

300. Frontier, S. Notes morphologiques sur les *Atlanta* récoltées dans le plancton de Nosy Bé (Madagascar). *Océanographie*, vol. IV, no. 2, 1966, p. 131-139 (Cahiers ORSTOM) . . 151

301. Frontier, S. Liste complémentaire des ptéropodes du plancton de Nosy Bé (Madagascar). *Océanographie*, vol. IV, no. 2, 1966, p. 141-146 (Cahiers ORSTOM). 161

302. Frontier, S. Zooplankton de la région de Nosy Bé. I: Programme des recoltés et techniques d'études. II: Plancton de surface aux stations 5 et 10. *Océanographie*, vol. IV, no. 3, 1966, p. 3-36 (Cahiers ORSTOM) 167

303. Sakamoto, I.; Matsuike, K. A preliminary report on the primary productivity in the Eastern Indian Ocean in winter. IIOE report on productivity, 1963-1964. *Umitaka-Maru*. Methods of experiments, data and outlines. *J. Tokyo Univ. Fish.*, vol. 8, no. 2, 1966, p. 173-226. 205

304. Russell, Anthony P. The invertebrate acid deoxyribonucleases and molecular taxonomy. *Comp. Biochem. Physiol.*, vol. 18, 1966, p. 961-969 259

305. Gross, W. J.; Lasiewski, R. C.; Dennis, M.; Rudy, Jr., P. Salt and water balance in selected crabs of Madagascar. *Comp. Biochem. Physiol.*, vol. 17, 1966, p. 641-660. . . 269

306. Hida, T. S.; Pereyra, W. T. Results of bottom trawling in Indian seas by R.V. *Anton Bruun* in 1963. *Proc. Indo-Pacific Fish. Coun.*, vol. 11, no. II, 1966, p. 156-171. . . . 290

307. Humphrey, G. F. The concentration of chlorophyllis *a* and *c* in the south-east Indian Ocean. *Aust. J. Mar. Freshw. Res.*, vol. 17, 1966, p. 135-145 307

308. Cressey, R. A new species of *Dentigryps* Wilson (Copepoda, Caligoida) from Madagascar. *Proc. Biol. Soc. Wash.*, vol. 79, 1966, p. 91-94 319

309. Cressey, R. F. *Bariaka alopiae* n. gen. n. sp. (Copepoda, Caligoida) a parasite on the gills of a thresher shark. *Bull. mar. Sci.*, vol. 16, no. 2, 1966, p. 324-329 324

310. Nevenzel, J. C.; Rodecker, W.; Mead, J. F.; Gordon, M. S. Lipids of the living coelacanth, *Latimeria chalumnae*. *Science*, vol. 152, no. 3,730, 1966, p. 1753-1755 331

311. Ryther, J. J.; Hall, J. R.; Pease, A. K.; Bakun, A.; Jones, M. M. Primary organic production in relation to the chemistry and hydrography of the Western Indian Ocean. *Limnol. and Oceanogr.*, vol. 11, no. 3, 1966, p. 371-380 . . 333

312. Della Croce, N.; Frontier, S. Thecosomatous pteropods from the Mozambique Channel. *Boll. Mus. Ist. biol. Univ. Genova*, vol. XXXIV, no. 207, 1966, p. 107-113 . . . 343

313. Della Croce, N.; Castle, P. H. J. Leptocephali from the Mozambique Channel. *Boll. Mus. Ist. biol. Univ. Genova*, 1966, vol. XXXIV, no. 211, p. 149-164 351

314. Hansen, V. Kr. The Indian Ocean Biological Centre: the centre for sorting plankton samples of the International Indian Ocean Expedition. *Deep-sea Res.*, vol. 13, 1966, p. 229-234 367

315. Panikkar, N. K. Fishery resources of the Indian Ocean. *Curr. Sci.*, vol. 35, no. 18, 1966, p. 451-455 374

316. Panikkar, N. K.; Jayaraman, R. Biological and oceanographic differences between the Arabian Sea and the Bay of Bengal as observed from the Indian region. *Proc. Ind. Acad. Sci.*, vol. LXIV, no. 5, sect. B, 1966, p. 231-240 . . . 379

317. Thiel, H. Quantitative Untersuchungen über die Meiofauna des Tiefseebodens. *Veröff. Inst. Meeresforsch. Bremerh.*, Sonderband II, 1966, p. 131-147 389

318. Gunkel, W. Bakteriologische Untersuchungen im Indischen Ozean. *Veröff. Inst. Meeresforsch. Bremerh.*, Sonderband II, 1966, p. 255-263 406

319. Gordon, M. S.; Boëtius, J.; Boëtius, I.; Evans, D. H.; McCarthy, R.; Oglesby, L. C. Salinity adaptation in the mudskipper fish *Periophthalmus sobrinus*. *Hvalråd. Skr.*, no. 48, p. 85-93 417

320. Gordon, M. S. Adapting to dry land. *Discovery*, vol. XXVII, no. 4, 1966, p. 26-30 426

321. Humes, Arthur G. New species of *Macrochiron* (Copepoda, Cyclopoida) associated with hydroids in Madagascar. *Beaufortia* (Zoological Museum, Amsterdam), vol. 14, no. 165, 1966, 24 p. 431

322. Fenaux, R. Une variété de *Fritillaria pellucida* (Busch), 1851, récoltée dans la Mer d'Oman. *Océanographie*, vol. IV, no. 2, 1966, p. 147-151 (Cahiers ORSTOM) 455

323. Fenaux, R. Les appendiculaires de la Mer Rouge (Note faunistique). *Bull. Mus. Nat. d'Hist. Natur.* (Paris), 2nd series, vol. 38, no. 6, 1966 (1967), p. 784-785 461

324. Sournia, A. Sur la variabilité infraspécifique du genre *Ceratium* (Péridinien planctonique) en milieu marin. *C. R. Acad. Sc. Paris*, series D, vol. 263, 1966, p. 1980-1983 . . . 463

325. Humes, A. G.; Ho, Ju-shey. New cyclopoid copepods associated with the alcyonarian coral *Tubipora musica* (Linnaeus) in Madagascar. *Proc. U.S. Nat. Mus.*, vol. 121, no. 3,573, 1967, p. 1-24 467

326. Grice, G. D.; Hulsemann, K. Bathypelagic calanoid copepods of the Western Indian Ocean. *Proc. U.S. Nat. Mus.*, vol. 122, no. 3,583, 1967, p. 1-67 491

327. Humes, A. G.; Ho, Ju-shey. New cyclopoid copepods associated with the coral *Psammocora contigua* (Esper) in Madagascar. *Proc. U.S. Nat. Mus.*, vol. 122, no. 3,586, 1967, p. 1-32 559

328. Humes, A. G.; Ho, Ju-shey. New cyclopoid copepods associated with polychaete annelids in Madagascar. *Bull. Mus. Comp. Zool.* (Harvard), vol. 135, no. 7, 1967, p. 377-413 . 591

329. Robertson, R. *Heliacus* (Gastropoda: Architectonicidae) symbiotic with *Zoanthiniaria* (coelenterata). *Science*, vol. 156, no. 3,772, 1967, p. 246-248 628

330. ЗЕРНОВА, В. В. О биолюминесценции планктона в Индийском океане по материалам 35-го рейса экспедиционного судна «Витязь». *Биоэнергетика и биологическая спектрофотометрия*. Академия Наук СССР, Научный совет по биофизике, Сибирское отделение. Москва, Наука, 1967 г., стр. 46-52 . . 630
Zernova. V. V. On the bioluminescent plankton of the Indian Ocean from the data collected during the 35th cruise of the *Vitijaz. Bioenergetica i Biologicheskaya Spectrophotometria*. U.S.S.R. Academy of Sciences, Scientific Council on Biophysics, Siberian Branch. Moscow, Nauka, 1967, p. 46-52

Part II. Marine chemistry

331. Mullin, M. M. Size fractionation of particulate organic carbon in the surface waters of the Western Indian Ocean. *Limnol. and Oceanogr.*, vol. 10, no. 3, 1965, p. 459-462 . . 639

332. Mullin, Michael M. Size fractionation of particulate organic carbon in the surface waters of the Western Indian Ocean: Addendum. *Limnol. and Oceanogr.*, vol. 10, no. 4, 1965, p. 610-611 643

Part III. Physical oceanography and marine meteorology

333. Bien, G. S.; Rakestraw, N. W.; Suess, H. E. Radiocarbon in the Pacific and Indian Oceans and its relation to deep water movements. *Limnol. and Oceanogr.* vol. 10, supplement, November 1965, p. R25-R37 647

334. Ramage, C. S. The summer atmospheric circulation over the Arabian Sea. *J. atmos. Sci.*, vol. 23, no. 2, 1966, p. 144-150 660

335. Gangadhara Rao, L. V.; Jayaraman, R. Upwelling in the Minicoy region of the Arabian Sea. *Curr. Sci.*, vol. 35, no. 15, 1966, p. 378-380 667

336. Swallow, J. C.; Bruce, J. G. Current measurements off the Somali coast during the southwest monsoon of 1964. *Deep-sea Res.*, vol. 13, 1966, p. 861-888 669

337. Gordon, A. H. The mean wind structure over Bahrein and Aden in 1962. *J. atmos. Sci.*, vol. 23, no. 6, 1966, p. 712-719 697

Part IV. Marine geology and geophysics

338. ANANTHA PADMANABHA SHETTY, M. G. Submarine canyons off Madras coast. *Curr. Sci.*, vol. 33, no. 22, 1964, p. 685 . 707

339. УДИНЦЕВ, Г. Б. Новые данные о строении дна Индийского океана. *Океанология*, том. V, вып. 6, 1965 г., стр. 993-998 709
UDINTSEV, G. B. New data on the bottom structure of the Indian Ocean. *Okeanologia*, vol. V, no. 6, 1965, p. 993-998

340. УДИНЦЕВ, Г. Б. 36-й рейс научно-исследовательского судна «Витязь». *Океанология*, том. V, вып. 6, 1965 г., стр. 1113-1119 715
UDINTSEV, G. B. 36th cruise of R.V. *Vityaz*. *Okeanologia*, vol. V, no. 6, 1965, p. 1113-1119 . . . . . .

341. УДИНЦЕВ, Г. Б.; ЧЕРНЫШЕВА, В. И. Образцы пород верхней мантии земли из рифтовой зоны Индийского океана. *Докл. Акад. Наук СССР*, том. 165, № 5, 1965 г., стр. 1147-1150 723
UDINTSEV, G. B.; CHERNYSHEVA, V. I. Samples of the upper mantle material from the rift zone of the Indian Ocean. *Dokl. Akad. Nauk SSSR*, vol. 165, no. 5, 1965, p. 1147-1150

342. KNOTT, S. T.; BUNCE, E. T.; CHASE, R. L. Red Sea seismic reflection studies. *International upper mantle project—The world rift system. Report of symposium, Ottawa, Canada, 4-5 September 1965*, p. 33-61 (GSC paper 66-14) . . . 727

343. ANDEL, T. H. van. Morphology and sediments of the Sahul Shelf, Northwestern Australia. *Trans. N.Y. Acad. Sci.*, series II, vol. 28, no. 1, 1965, p. 81-89 757

344. NESTEROFF, W. D.; HEEZEN, B. C.; CONOLLY, J. R. Découverte de turbidités hétérogènes dans le bassin australien. *C.R. Acad. Sc. Paris*, series D, vol. 263, 1966, p. 1052-1054 767

345. KELLER, George H.; RICHARDS, Adrian F. Sediments of the Malacca Strait, Southeast Asia. *J. sedimentary Petrology*, March 1967, p. 102-127 770

346. BUNCE, T. Elizabeth; LANGSETH, M. G.; CHASE, R. L.; EWING, M. Structure of the Western Somali Basin. *J. geophys. Res.*, vol. 72, no. 10, 1967, p. 2547-2555 . . 797

347. ИСАЕВА, А. Б. Химический состав железно-марганцовых конкреций Индийского океана. *Литология и полезные ископаемые*, № 3, 1967 г., стр. 43-56 . . 807
ISAEVA, A. B. Chemical composition of ferro-manganese nodules of the Indian Ocean. *Litologia i Poleznye Iskopaemye*, no. 3, 1967, p. 43-56

Part V. Cruise and general reports

348. TRANTER, D. J. The International Indian Ocean expedition. *Aust. natur. Hist.*, vol. XIV, no. 10, 1964, p. 323-325 . . 823

349. PRUTER, A. T.; SHOMURA, R. International co-operation in the Indian Ocean. *Nautilus*, no. 1, 1966, p. 7-8. Basle (Switzerland), J. R. Geigy S.A. [*Anton Bruun* cruises] . . 827

Part VI. Papers presented by title

350-399. SMITH, J. L. B. Bibliography of papers on ichthyology of the Indian Ocean 833

400-406. *Annales de la Faculté des Sciences et des Techniques de Madagascar (Travaux de la station marine de Tuléar)*, no. 1, 1962 834

407-409. *Annales de la Faculté des Sciences et des Techniques de Madagascar (Travaux de la station marine de Tuléar)*, no. 2, 1964 834

410. *Annales de la Faculté des Sciences et des Techniques de Madagascar (Travaux de la station marine de Tuléar)*, no. 3, 1965 834

411-413. *Annales de la Faculté des Sciences et des Techniques de Madagascar (Travaux de la station marine de Tuléar)*, no. 4, 1966 834

414-417. Admiralty marine science publications. Hydrographic Department, 1963 834

418-419. National Oceanographic Data Center (Washington)/ World Data Center A (Oceanography) publications .

Part I

Marine biology

Reprinted from *Océanographie (Nosy Bé)*, no. 3, 1963, p. 17-30

ZOOPLANKTON RÉCOLTÉ EN MER D'ARABIE, GOLFE PERSIQUE ET GOLFE D'ADEN

(3e Campagne Océanographique du "Commandant Robert Giraud")

I - DONNÉES GÉNÉRALES - RÉPARTITION QUANTITATIVE *

par **S. FRONTIER**,

D'avril à juin 1961 l'aviso "Commandant Robert Giraud" a procédé, sous la direction de M. MENACHE, à une campagne océanographique qui s'est étendue aux secteurs nord et nord-ouest de la Mer d'Arabie, au Golfe Persique et au Golfe d'Aden. 98 stations hydrologiques profondes ont été occupées. Des récoltes de Zooplankton ont été effectuées lors de 80 de ces stations, l'état de la mer n'ayant pas toujours permis la mise à l'eau des filets.

Trois techniques de récolte ont été utilisées :

1 - Des traits verticaux (numérotés RGV 1 à 189) effectués à l'aide de filets fermants de 2,20 m de longueur (dont 1,50 m pour la partie pêchante), 0,70 m de diamètre d'ouverture, et constitués de deux secteurs de soie à bluter, successivement de :

625	et	1 115	mailles/cm^2	(modèle	A)
625	et	625	"	("	B)
81	et	625	"	("	C)

Les filets étaient remontés à la vitesse de 50 cm/sec. environ. La plus grande partie de ces traits verticaux avaient lieu entre 100 m et la surface. Des profondeurs plus grandes ont été atteintes aux stations RG 185 (420 m), RG 196 (1 500 m), RG 209 (2 000 m), RG 215 (903 m).

2 - Des traits horizontaux de surface (numérotés RGH 1 à 8) de filets non fermants, de 4,50 m de longueur, 1 m de diamètre d'ouverture, et constitués de 4 secteurs successifs de soie à bluter de 81, 625, 1 115 et 1 890 mailles/cm^2. Le filet était remorqué à la vitesse de 50 cm/sec. et maintenu à une immersion soit de 1 m, soit de 10 m.

3 - Des pêches au lamparo (numérotées RGL 1 à 5). Le plankton attiré par la lumière était recueilli à l'aide d'épuisettes (soie de 625 mailles/cm^2).

Les tables qui suivent indiquent les conditions de chaque récolte, ainsi que le volume de plankton recueilli. Il s'agit du volume par déplacement mesuré suivant la technique d'EALEY (1954) les individus d'un cm^3 ou plus ayant été retirés de la récolte avant la mesure.

Les résultats hydrologiques ne sont pas encore connus.

Dans le but d'obtenir des chiffres plus comparables concernant les volumes de plankton recueillis, les résultats ont été repris pour les seules récoltes effectuées dans la couche supérieure

* La deuxième partie de cet article paraîtra dans le n° 6 des Cahiers ORSTOM - Océanographie.

(généralement de 50 m à la surface) avec les filets de modèle A, et divisés par la distance parcourue dans l'eau par le filet, c'est-à-dire par la longueur de câble mouillée. Les résultats sont alors les suivants :

Station	Volume (mm3) par mètre d'avancement	Station	Volume (mm3) par mètre d'avancement	Station	Volume (mm3) par mètre d'avancement
RG 185	40	RG 213	36	RG 256	12
186	48	214	42	257	34
188	28	215	34	258	14
189	37	216	56	259	10
190	109	217	40	260	18
191	40	218	91	262	16
192	34	220	36	263	62
193	22	222	34	264	76
194	24	223	43	265	40
195	45	225	54	266	22
196	52	229	189	267	58
197	54	231	205	268	18
198	66	233	20	269	10
200	24	235	40	270	10
201	0	237	21	271	12
203	470	239	37	272	0
204	982	241	48	273	0
205	63	243	128	274	6
206	295	244	68	275	6
207	228	245	164	276	6
208	52,5	246	30	277	50
209	32	247	36	278	4
210	24	248	130	279	10
211	20	249	42	280	4
212	32	250	74	281	34

On remarque que malgré la transformation faite, les chiffres restent irréguliers, ce qui était prévisible vu l'hétérogénéité bien connue de la répartition de Zooplankton, ses migrations verticales et les variations du rendement d'un même filet de plankton suivant l'état de la mer et celui du plankton lui-même. Il ne saurait donc être question de considérer ces chiffres de façon absolue, encore moins d'ébaucher des lignes d'égale densité planktonique à travers la zône prospectée.

La séparation des chiffres en deux ensembles suivant qu'ils correspondent à des stations de jour ou de nuit n'apporte aucune régularisation des résultats : l'hétérogénéité de la répartition dans l'espace masque totalement le cycle de migrations nycthémérales, et de forts volumes peuvent être trouvés en plein midi alors que douze heures plus tard, dans le même secteur océanique, nous ne trouvons qu'un volume très réduit.

Nous sommes donc amenés à considérer les chiffres obtenus de façon globale et sans distinction d'heure. Dans ces conditions il est possible, en dépit de la grande variabilité dont nous venons de parler, de reconnaître quelques caractères généraux de la répartition des volumes (carte 2)

Dans la Mer d'Arabie, Golfe d'Oman inclus et jusqu'à l'entrée du Golfe Persique, mais exception faite du secteur nord-est, les valeurs obtenues sont moyennes = en général de 25 à 65 mm^3 de plankton par mètre d'avancement du filet. Une récolte plus abondante se remarque localement (RG 248).

La partie nord-est de la Mer d'Arabie se remarque par une richesse extrême en plankton jusqu'à 982 mm^3 (RG 204, par 2 020 m de fond) et 470 mm^3 (RG 203, fond 1 120 m). Les stations RG 205 et 244 font exception. Cette abondance est très probablement en rapport avec les importants apports terrigènes de ce secteur.

Le Golfe d'Aden semble très riche dans son premier tiers (189 et 205 mm^3), le reste étant à densité du même ordre que celle de la Mer d'Arabie.

On constate un appauvrissement très net, par contre, le long de la section J qui suit approximativement la côte sud-est de l'Arabie. Cet appauvrissement se prolonge peut-être le long de la rive sud-ouest du Golfe Persique. Le Golfe d'Aden est extrêmement pauvre, à l'exception des deux stations côtières RG 277 et 281.

Entre ces deux dernières zones appauvries on retrouve un secteur de richesse planktonique moyenne qui semble s'étendre dans un rayon d'une centaine de milles autour du Cap Gardafui. Cet enrichissement pourrait être en rapport avec l'upwelling découvert par M. MENACHE le long de la côte des Somalies lors des deuxième et quatrième campagne océanographique du "Robert Giraud".

BIBLIOGRAPHIE

EALEY (E.H.M.) 1954 - Net plankton determinations.
Cons. Int. Expl. Mer - J. du Conseil, *19*, p.368.

FRONTIER (S.) 1961 - En mission océanographique avec l'aviso "Cdt Robert Giraud".
La Revue Maritime, *182* (nov.1961)

MENACHE (M.) 1962 - Quatrième campagne océanographique du "Commandant Robert Giraud".
C.R. séance du 23 nov.1962 du Comité National Malgache de Recherche Océanique, fig. VI et VII.

TRAITS VERTICAUX

Station n°	Date (1961)	Coordonnées nord	Coordonnées est	Fond (mètres)	Plankton n°	Heure locale	Profondeur début A	Profondeur début B	Profondeur fin A	Filet	Volume (cm^3)
Mer d'Arabie											
Section A (1ère partie)											
RG 185	22/4	18°55'	66°06'	3040	RGV 1	11.30	400	20°	220	A	# 0
					RGV 2	12.00	420	40°	225	C	# 0
					RGV 3	12.30	200	40°	0	A	8,0
					RGV 4	12.45	200	40°	0	C	9,5
RG 186	22/4	19°03'	67°32'	3300	RGV 5	18.15	50	50°	0	A	2,4
					RGV 6	18.30	50	50°	0	C	1,2
RG 188	23/4	18°55'	69°43'	1585	RGV 7	12.45	100	60°	52	A	5,0
					RGV 8	13.15	100	35°	49	C	1,0
					RGV 9	13.30	50	40°	0	A	1,4
					RGV 10	13.45	50	60°	0	C	1,9
					RGV 11	14.30	400	35°	200 ?	A	# 0
					RGV 12	14.45	200	40°	100	A	0,8
RG 189	23/4	19°01'	69°54'	196 à 170	RGV 13	16.30	60	50°	0	A	2,2
					RGV 14	16.45	60	50°	0	C	1,4
Section B											
RG 190	29/4	22°36'	67°46'	70	RGV 15	11.45	70	50°	0	A	7,6
					RGV 16	12.00	60	45°	0	C	2,1
RG 191	29/4	22°34'	67°16'	220 à 206	RGV 17	14.00	100	30°	0	A	1,6
					RGV 18	14.15	100	30°	40	C	1,2
					RGV 19	14.30	50	30°	0	A	2,0

(A) longueur du câble mouillé (en mètres)
(B) angle du câble avec la verticale

Station n°	Date (1961)	Coordonnées nord	Coordonnées est	Fond (mètres)	Plankton n°	Heure locale	Profondeur début A	Profondeur début B	Profondeur fin	Filet	Volume (cm^3)
RG 192	29/4	22°33'	67°13'	700 à 530	RGV 20	15.00	100	30°	53	A	1,8
					RGV 21	15.15	53	25°	0	A	1,8
RG 193	29/4	22°30'	67°06'	1 500 à 1 370	RGV 22	17.00	100	25°	54	A	1,1
					RGV 23	17.15	54	30°	0	A	1,2
RG 194	29/4	22°33'	66°28'	1 500	RGV 24	22.30	100	18°	52	A	0,5
					RGV 25	22.45	50	23°	0	A	1,2
RG 195	30/4	22°34'	65°23'	2 230	RGV 26	04.45	100	45°	0	A	4,5
RG 196	30/4	22°32'	64°17'	2 225	RGV 27	11.45	100	45°	0	A	8,8
					RGV 28	12.00	50	45°	0	A	2,6
					RGV 29	14.30	1 500	30°	0	A	2,6 (1)
					RGV 30	15.15	800	30°	500	A	≠ 0
					RGV 31	16.00	500	35°	96	A	≠ 0
RG 197	30/4	22°33'	63°07'	?	RGV 32	22.15	100	50°	54	A	6,2
					RGV 33	22.30	50	39°	0	A	2,7
RG 198	1/5	22°33'	62°05'	3 010	RGV 34	04.15	100	50°	0	A	6,6
RG 200	1/5	22°37'	60°20'	2 680 à 2 850	RGV 35	18.15	50	57°	0	A	1,2
					RGV 36	18.45	100	60°	0	A	9,8
RG 201	1/5	22°37'	60°01'	1 110	RGV 37	22.45	100	5°	60 ?	A	0,6
					RGV 38	23.00	60	20°	0	A	≠ 0
Section C											
RG 203	6/5	24°44'	66°01'	1 120	RGV 39	20.15	100	10°	45	A	38,0
					RGV 40	20.45	60	38°	0	A	28,2
RG 204	6/5	24°38'	65°35'	2 020	RGV 41	23.30	100	40°	50 ?	A	0;9
					RGV 42	23.45	50	33°	0	A	49,1

(A) Longueur de câble mouillé (en mètres)
(B) Angle du câble avec la verticale
(1) RGV 29 : Fermeture non déclenchée mais vitesse rapide de remontée à partir de 500 m.

Station n°	Date (1961)	Coordonnées nord	Coordonnées est	Fond (mètres)	Plankton n°	Heure locale	Profondeur début A	Profondeur début B	Profondeur fin	Filet	Volume (cm^3)
RG 205	7/5	24°26'	64°21'	2 350	RGV 43	06.15	100	25°	40	A	1,4
					RGV 44	06.45	40	25°	0	A	2,5
RG 206	7/5	24°10'	63°23'	3 140	RGV 45	12.30	100	20°	49	A	2,4
					RGV 46	13.30	65	57°	25	A	19,2
					RGV 46bis	13.30	25		0	A	0
RG 207	7/5	23°46'	62°20'	3 310	RGV 47	21.00	100	27°	0	A	4,2
					RGV 48	21.30	50	57°	0	A	11,4
RG 208	8/5	23°43'	61°15'	3 320	RGV 49	04.15	100	43°	48	A	3,8
					RGV 50	05.00	80	40°	0	A	4,2
RG 209	8/5	23°25'	60°12'	3 330	RGV 51	11.00	100	5°	43	A	1,4
					RGV 52	11.15	50	10°	0	A	1,6
					RGV 53	13.45	2 000	22°	920 ?	C	0 (1)
					RGV 54	14.45	1 000	19°	530	C	# 0 (1)
					RGV 55	15.15	500	12°	0	C	1,4 (1)
					RGV 56	15.45	100	4°	0	C	2,5
RG 210	8/5	23°15'	59°07'	1 560	RGV 57	20.45	50	12°	0	A	1,2
					RGV 58	21.15	100	20°	50	A	0,6
Golfe d'Oman											
Section D											
RG 211	9/5	23°44'	58°39'	1 060	RGV 59	02.00	100	12°	45	A	# 0
					RGV 60	02.15	50	12°	0	A	1,0
RG 212	9/5	23°51'	58°44'	2 300	RGV 61	03.30	100	15°	0	A	# 0
					RGV 62	03.30	50	5°	0	A	1,6

(A) longueur de câble mouillé (en mètres)
(B) angle du câble avec la verticale
(1) RGV 53, 54, 55 : remonté à 1,50 m/sec.

Station n°	Date (1961)	Coordonnées nord	Coordonnées est	Fond (mètres)	Plankton n°	Heure locale	Profondeur début A	Profondeur fin B	Profondeur fin	Filet	Volume (cm^3)
RG 213	9/5	24°17'	58°57'	3 220	RGV 63	07.30	100	5°	50	A	0,3
					RGV 64	07.45	50	17°	0	A	1,8
RG 214	9/5	24°42'	59°16'	1 770	RGV 65	12.00	100	28°	40	A	0,8
					RGV 66	12.15	50	45°	0	A	2,1
RG 215	9/5	24°58'	59°30'	1 000	RGV 67	15.15	100	30°	51	A	# 0
					RGV 68	15.30	50	31°	35	A	0,8
					RGV 69	16.00	35	38°	17	A	0,7
					RGV 70	16.15	17	25°	0	A	0,2
					RGV 71	17.15	903	28°	530	A	# 0
					RGV 72	17.45	530	21°	210	A	1,6
					RGV 73	18.15	210	16°	95	A	perdu
RG 216	9/5	25°11'	59°41'	400	RGV 74	19.45	100	45°	51	A	3,4
					RGV 75	20.00	50	40°	0	A	2,8
Section E											
RG 217	10/5	24°21'	57°01'	292	RGV 76	09.00	100	0°	50	A	2,0
					RGV 77	09.45	50	20°	0	A	2,0
RG 218	10/5	24°30'	57°05'	394	RGV 78	11.30	100	42°	0	A	9,1
RG 220	10/5	25°02'	57°29'	1 300	RGV 79	19.30	100	12°	50	A	12,1
					RGV 80	20.15	50	20°	0	A	1,8
RG 222	11/5	25°28'	57°38'	196	RGV 81	00.45	100	20°	50	A	7,2
					RGV 82	01.15	50	8°	0	A	1,7

(A) longueur du câble mouillé (en mètres)
(B) angle du câble avec la verticale

Station n°	Date (1961)	Coordonnées nord	Coordonnées est	Fond (mètres)	Plankton n°	Heure locale	Profondeur début A	Profondeur fin B	Profondeur fin	Filet	Volume (cm^3)
Golfe persique											
Section F											
RG 223	11/5	26°59'	56°37'	26	RGV 83	10.15	30	20°	0	A	1,3
RG 225	11/5	26°43'	56°34'	56	RGV 84	12.00	69	30°	0	A	3,7
RG 226	11/5	26°35'	56°33'	76	RGV 85	13.15	100	40°	0	A	? (1)
Section G											
RG 227	11/5	26°22'	55°56'	64	RGV 86	16.30	75	10°	0	A	? (1)
RG 229	11/5	26°00'	54°35'	74	RGV 87	23.15	70	38°	0	A	13,2
RG 231	12/5	26°22'	52°56'	76	RGV 88	07.15	95	35°	0	A	19,5
RG 233	12/5	26°54'	51°47'	66	RGV 89	14.15	66	18°	0	A	1,3
RG 235	12/5	27°35'	50°40'	50	RGV 90	20.00	60	22°	0	A	2,4
Section H											
RG 237	13/5	29°10'	50°27'	25	RGV 91	05.15	33	42°	0	A	0,7
RG 239	13/5	28°47'	49°31'	40	RGV 92	10.30	60	38°	0	A	2,2
RG 241	13/5	28°06'	50°10'	53	RGV 93	18.15	60	38°	0	A	2,9
Mer d'Arabie											
Section I											
RG 243	18/5	24°57'	63°39'	380	RGV 94	17.30	100	50°	48	A	3,8
					RGV 95	17.45	50	50°	0	A	6,4

(A) longueur du câble mouillé (en mètres)
(B) angle du câble avec la verticale
(1) mesure du volume rendu impossible par l'abondance des Salpes

Station n°	Date (1961)	Coordonnées nord	Coordonnées est	Fond (mètres)	Plankton n°	Heure locale	Profondeur début A	Profondeur fin B	Profondeur fin	Filet	Volume (cm^3)
RG 244	18/5	24°47'	63°40'	1 060	RGV 96	19.00	100	52°	49	A	5,0
					RGV 97	19.15	50	14°	0	A	3,4
RG 245	19/5	23°42'	63°43'	2 420	RGV 98	01.45	100	40°	80	A	0,5
					RGV 99	02.00	80	40°	46	A	4,9
					RGV 100	02.15	50	53°	0	A	8,2
RG 246	19/5	22°31'	63°38'	2 400	RGV 101	09.00	100	37°	49	A	1,3
					RGV 102	09.15	50	32°	0	A	1,5
RG 247	19/5	21°19'	63°48'	3 170	RGV 103	16.30	100	45°	45	A	3,2
					RGV 104	16.45	50	45°	0	A	2,3
RG 248	20/5	20°10'	63°44'	3 360	RGV 105	01.15	100	50°	50	A	3,2
					RGV 106	01.45	50	60°	0	A	6,5
Section A (2ème partie)											
RG 249	20/5	18°57'	63°42'	3 560	RGV 107	09.15	100	52°	52	A	2,3
					RGV 108	09.45	50	48°	0	A	2,1
					RGV 109	10.00	50	45°	0	B	0,8
RG 250	20/5	18°52'	62°34'	3 620	RGV 110	18.45	100	46°	50	A	1,7
					RGV 111	19.00	50	59°	0	A	3,7
					RGV 112	19.30	100	48°	0	B	5,6
Section J											
RG 256	22/5	18°22'	57°40'	430	RGV 113	16.45	100	5 à 10°	48	A	0,5
					RGV 114	17.00	50	25°	0	A	0,6
					RGV 115	17.15	100	30° à 35°	0	B	0,6

(A) longueur de câble mouillé (en mètres)
(B) angle du câble avec la verticale

Station n°	Date (1961)	Coordonnées nord	Coordonnées est	Fond (mètres)	Plankton n°	Heure locale	Profondeur début A	Profondeur fin B	Profondeur fin	Filet	Volume (cm^3)
RG 257	23/5	17°29'	56°42'	1 330	RGV 116	00.15	50	45°	0	A	1,7
					RGV 117	00.30	100	30°	0	A	1,8
					RGV 118	00.45	100	20°	50	B	0,3
RG 258	23/5	16°43'	55°53'	3 270	RGV 119	08.00	100	35°	50	A	0,9
					RGV 120	08.15	50	0°	0	A	0,7
					RGV 121	08.30	100	20°	51	B	1,4
					RGV 122	08.45	50	25°	0	B	0,4
RG 259	23/5	15°51'	55°09'	2 570	RGV 123	18.30	100	45°	54	A	0,6
					RGV 124	18.45	50	45°	0	A	0,5
					RGV 125	19.00	100	40°	50	B	# 0
					RGV 126	19.15	50	45°	0	B	0,3
RG 260	24/5	14°56'	54°16'	1 360	RGV 127	03.45	100	10°	52	A	0,7
					RGV 128	04.00	50	10°	0	A	0,9
					RGV 129	04.15	100	15°	52	B	0,3
					RGV 130	04.30	50	15°	0	B	1,3
RG 262	24/5	13°20'	52°37'	2 200	RGV 131	18.00	100	45°	44	A	0,25
					RGV 132	18.15	50	45°	0	A	0,8
					RGV 133	18.30	100	30°	0	B	0,6
RG 263	25/5	12°45'	51°50'	500	RGV 134	01.00	50	20°	0	A	3,1 (1)
RG 264	25/5	12°03'	51°21'	410	RGV 135	06.30	50	45°	0	B	3,8
					RGV 136	06.45	100	35°	50	B	1,0
Golfe d'Aden											
Section K											
RG 265	25/5	12°12'	51°05'	180	RGV 137	08.45	100	25°	0	A	4,0

(A) longueur de câble mouillé (en mètres)
(B) angle du câble avec la verticale
(1) angle du câble très variable

Station n°	Date (1961)	Coordonnées nord	Coordonnées est	Fond (mètres)	Plankton n°	Heure locale	Profondeur début A	Profondeur fin B	Profondeur fin	Filet	Volume (cm³)
RG 266	25/5	12°49'	50°54'	2 130	RGV 138	13.00	100	20°	50	A	1,8
					RGV 139	13.15	50	20°	0	A	1,1
					RGV 140	13.45	100	20°	52	B	0,5
					RGV 141	14.00	50	18°	0	B	1,0
RG 267	25/5	13°29'	50°38'	2 500	RGV 142	18.45	100	30°	50	A	0,5
					RGV 143	19.00	50	30°	0	A	2,9
					RGV 144	19.15	100	30°	48	B	0,4
					RGV 145	19.30	50	15°	0	B	1,4
RG 268	25/5	14°03'	50°21'	2 210	RGV 146	23.45	100	0°	50	A	# 0
	26/5				RGV 147	00.15	50	5°	0	A	0,9
					RGV 148	00.30	100	5°	52	B	# 0
					RGV 149	00.30	50	0°	0	B	1,0
RG 269	26/5	14°38'	50°04'	462	RGV 150	05.30	100	15°	51	A	# 0
					RGV 151	05.45	50	10°	0	A	0,5
					RGV 152	06.00	100	5°	0	B	0,5
Section L											
RG 270	26/5	12°05'	48°04'	2 200	RGV 153	19.30	100	35°	52	A	0,7
					RGV 154	20.00	50	22°	0	A	0,5
					RGV 155	20.15	100	15°	0	B	0,6
RG 271	27/5	12°02'	47°22'	1 670	RGV 156	01.00	100	10°	51	A	0,5
					RGV 157	01.15	50	0°	0	A	0,6
					RGV 158	02.00	100	5°	50	B	1,1
RG 272	27/5	12°00'	46°41'	1 940	RGV 159	06.00	100	10°	45	A	0
					RGV 160	06.15	50	0°	0	A	# 0
					RGV 161	06.30	100	5°	0	B	0,7
RG 273	27/5	12°01'	46°01'	1 420	RGV 162	10.30	100	8°	49	A	0,15
					RGV 163	10.45	50	12°	0	A	0
					RGV 164	11.00	100	30°	51	B	0,6

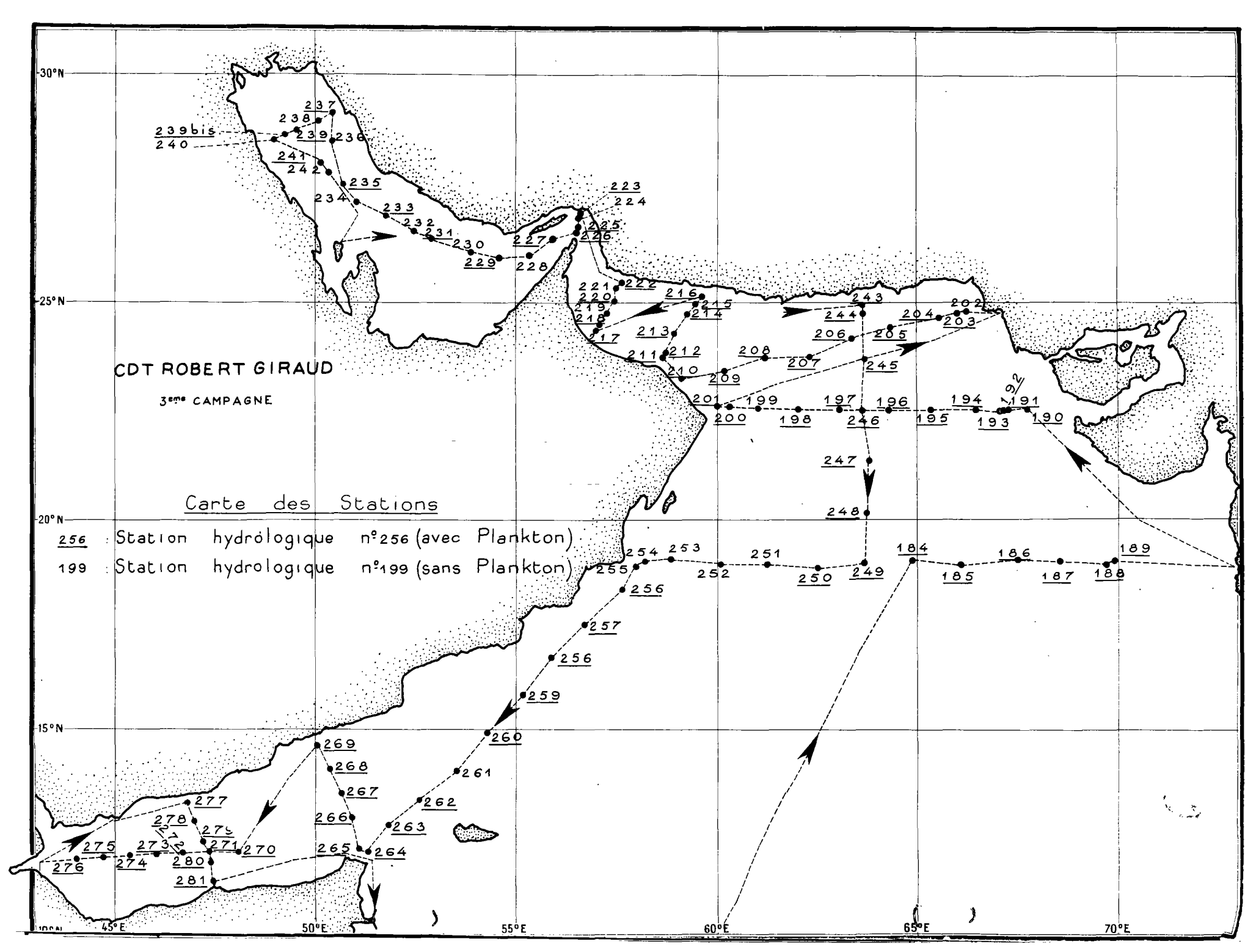
(A) Longueur de câble mouillé (en metres).
(B) Angle du câble avec la verticale.

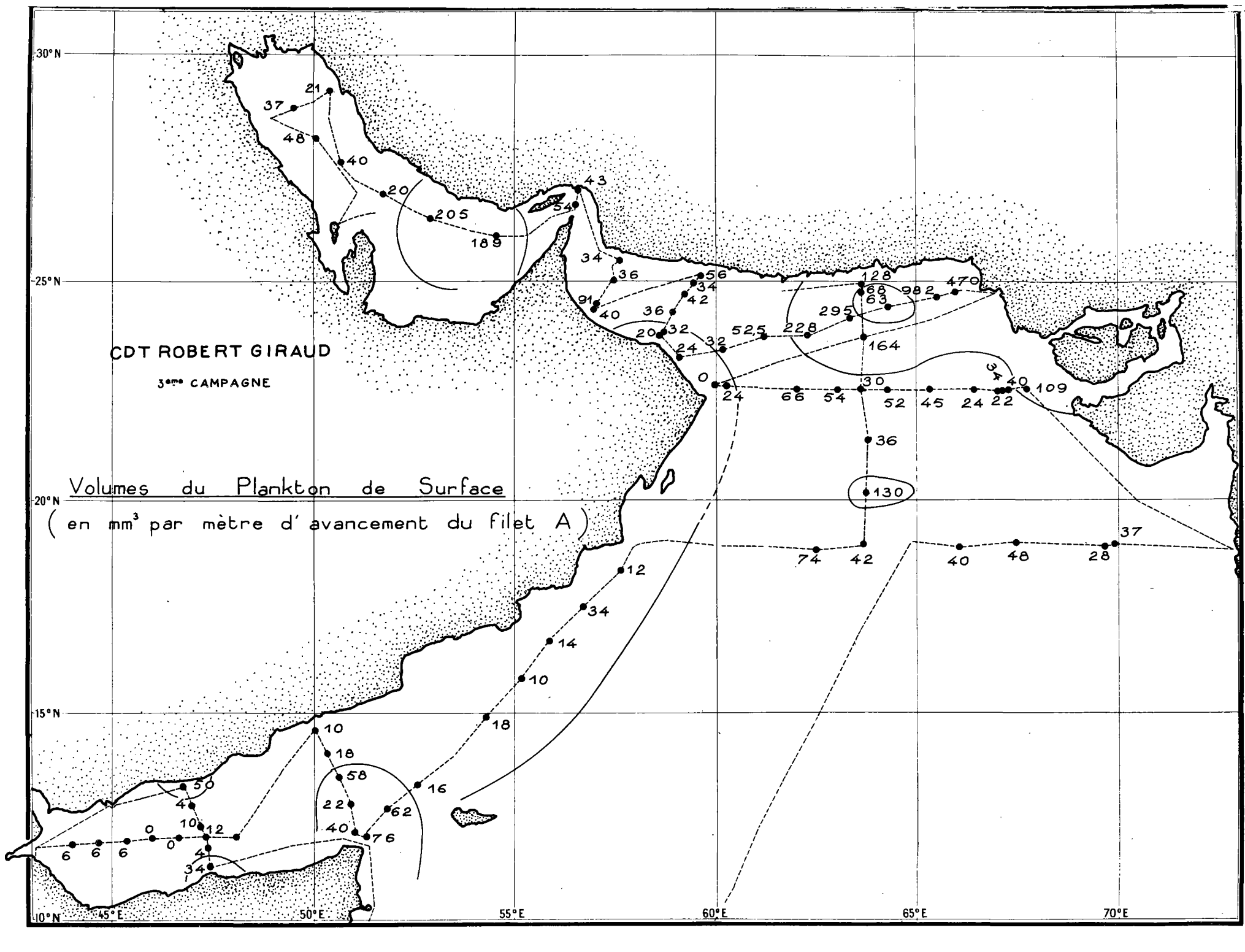
Station n°	Date (1961)	Coordonnées nord	Coordonnées est	Fond (mètres)	Plankton n°	Heure locale	Profondeur début A	Profondeur début B	Profondeur fin A	Filet	Volume (cm^3)
RG 274	27/5	11°57'	45°23'	1 050	RGV 165	14.45	100	30°	52	A	# 0
					RGV 166	15.00	50	5°	0	A	0,3
					RGV 167	15.15	100	15°	0	B	0,1
RG 275	27/5	11°54'	44°40'	830	RGV 168	19.30	100	10°	55	A	0,2
					RGV 169	19.45	50	15°	0	A	0,3
					RGV 170	20.15	100	28°	0	B	0,7
RG 276	28/5	11°52'	44°02'	570	RGV 171	00.00	100	10°	50	A	0,2
					RGV 172	00.15	50	8°	0	A	0,3
					RGV 173	00.30	100	10°	0	B	1,2
Section M											
RG 277	1/6	13°17'	46°49'	560	RGV 174	07.15	100	5°	52	A	0,2
					RGV 175	07.30	50	3°	0	A	2,5
					RGV 176	08.15	60	20°	0	B	2,5
RG 278	1/6	12°50'	47°00'	1 580	RGV 177	10.45	100	40°	51	A	0,5
					RGV 178	11.00	50	10°	0	A	0,2
					RGV 179	11.15	100	10°	0	B	0,1
RG 279	1/6	12°19'	47°11'	1 150	RGV 180	15.00	100	9°	51	A	0,3
					RGV 181	15.15	50	15°	0	A	0,5
					RGV 182	15.30	100	14°	0	B	0,5
RG 280	1/6	11°51'	47°23'	2 030	RGV 183	19.45	100	35°	52	A	0,8
					RGV 184	20.00	50	25°	0	A	0,2
					RGV 185	20.15	100	20°	0	B	1,0
RG 281	2/6	11°20'	47°24'	700	RGV 186	00.45	100	21°	52	A	0,6
					RGV 187	01.00	50	15°	0	A	1,7
					RGV 188	01.15	100	25°	51	B	# 0
					RGV 189	01.30	50	15°	0	B	0,2

(A) longueur de câble mouillé (en mètres)
(B) angle du câble avec la verticale

TRAITS HORIZONTAUX ET PÊCHES A LA LUMIÈRE

Station n°	Date (1961)	Coordonnées nord	Coordonnées est	Fond (mètres)	Plankton n°	Heure locale début	Heure locale fin	Immersion du filet
RG 184	22/4	19°02'	64°54'	3 150 à 3 300	RGL 1	00.00	01.30	
RG 187	23/4	18°59'	68°34'	3 265	RGH 1	03.55	04.25	1 m
					RGH 2	04.35	05.05	10 m
RG 194	29/4	22°33'	66°28'	1 500	RGH 3	21.35	21.50	1 m
					RGH 4	22.10	22.25	10 m
RG 210	8/5	23°15'	59°07'	1 560	RGL 2	20.45	?	
RG 268	26/5	14°03'	50°21'	2 210	RGL 3	00.00	01.00	
					RGL 4	01.00	02.00	
RG 271	27/5	12°02'	47°22'	1 670	RGH 5	01.10	01.30	1 m
					RGH 6	01.50	02.10	10 m
RG 276	27/5	11°52'	44°02'	570	RGL 5	23.50	00.40	
RG 280	1/6	11°51'	47°23'	2 030	RGH 7	20.00	20.20	1 m
					RGH 8	20.40	21.00	10 m


CDT ROBERT GIRAUD
3ème CAMPAGNE
Carte des Stations
256 : Station hydrologique n°256 (avec Plankton)
199 : Station hydrologique n°199 (sans Plankton)
30°N
25°N
20°N
15°N
45°E
50°E
55°E
60°E
65°E
70°E


CDT ROBERT GIRAUD
3ème CAMPAGNE
Volumes du Plankton de Surface
(en mm³ par mètre d' avancement du filet A)
30°N
25°N
20°N
15°N
10°N
45°E
50°E
55°E
60°E
65°E
70°E

Reprinted from *Océanographie (Nosy Bé)*, no. 3, 1963, p. 31-59

NOTES SUR QUELQUES LARVES ATYPIQUES DE DÉCAPODES BRACHYOURES RÉCOLTÉES DANS LE PLANKTON DE NOSY BÉ

par

S. FRONTIER

Une cinquantaine de récoltes effectuées en surface dans le secteur de Nosy Bé, entre octobre et décembre 1960, ont montré une proportion étonnante de larves de Crustacés Décapodes et Stomatopodes, qui surpassaient parfois numériquement les Entomostracés et leurs larves. (1)

Un premier examen de ce riche matériel, portant plus spécialement sur les larves de Brachyoures, a permis de constater parmi ces dernières toute une catégorie de formes dont la morphologie s'éloignait fortement de la morphologie habituelle du groupe. Quelques unes de ces formes ont été choisies à titre d'exemple pour être decrites ici. L'intérêt de telles descriptions est simplement d'ordre taxonomique, l'examen d'un matériel exceptionnellement abondant et varié permettant de démontrer que l'éventail morphologique d'un groupe larvaire jusqu'ici considéré comme particulierement homogène, est en fait bien plus étendu.

Aucun nom d'espèce ne peut encore, évidemment, être avancé pour aucune de ces larves. Toutefois deux d'entre elles sont attribuables au genre *Tetralia* (*Xanthidae*), et une aux *Hymenosomidae*.

***ZOE BRACHYOURE* 10 NB** stade 3 (fig. 1a à 1g)

A - Description

Longueur de la carapace : 0,96 mm. Epine rostrale : 0,58 mm. Epine dorsale : 0,58 mm. Distance entre les extrémités des épines rostrale et dorsale : 1,76 mm. Longueur du telson : 0,80 mm.

Cette zoé de grande taille se singularise par une multiplication considérable des épines de la carapace et de l'abdomen. Epines dorsale et rostrale assez courtes, plumeuses dans leur partie distale : la rostrale est droite, la dorsale légèrement incurvée vers l'arrière et porte sur la face antérieure, au tiers de sa longueur, une soie plumeuse.

En plus de ces deux épines typiques, la carapace possède 42 paires d'épines courtes disposées de la façon suivante : une paire à la base du rostre ; une très petite sur la face antérieure de

(1) La maille du filet utilisé étant suffisomment faible pour pouvoir en principe retenir la totalité des Entomostracés, on peut considérer cette importance des larves de Crustacés supérieurs comme un caractère fondamental des eaux prospectées, et non comme un simple effet de sélection dû au filet.

chaque pédoncule oculaire ; 12 paires sur les bords d'une expansion frontale en forme de fer à cheval à concavité tournée vers le bas ; 28 paires sur les flancs de la carapace. Toutes ces épines sont entièrement plumeuses, à l'exception de la petite épine du pédoncule oculaire, glabre.

La carapace porte, de plus, deux tubercules sagittaux cylindriques et tronqués au sommet, l'un, court, en arrière de l'épine dorsale, l'autre environ trois fois plus long que large et situé entre les deux yeux.

Les lobes latéraux de la carapace sont bombés et peu développés vers le bas, laissant à découvert les ébauches d'appendices thoraciques.

Abdomen formé de 6 segments plus le telson. Premier segment pourvu de 5 grandes soies dorsales ; 2ème au 6ème à bord postérieur frangé d'une douzaine de soies très courtes ; 2ème au 5ème munis, à mi-longueur, d'une courte carène transversale portant une paire de soies proches du plan de symétrie, et à chacune de ses extrémités un petit tubercule cônique lui-même terminé par une courte soie. Ces derniers sont très réduits sur le 5ème segment. Deuxième segment abdominal pourvu d'une paire de forts crochets latéraux-dorsaux dirigés vers le bas et terminés par une courte soie. 3ème au 5ème segment portant, insérée au même point que les crochets latéraux du 2ème segment, une paire de fortes épines incurvées atteignant le tiers du segment suivant. Ces épines sont plumeuses sur leur moitié distale. Les angles postéro-ventraux de ces mêmes segments sont prolongés par une paire d'épines très longues et fines (chacune dépassant l'extrémité postérieure du segment suivant) et plumeuses sur leur moitié distale. L'épine postérieure du 5ème segment est plus longue que les autres.

Telson long, à épines furcales longues, minces et divergentes, pourvues d'une courte pilosite. Bord postérieur profondément échancré. Trois paires d'épines internes atteignant les trois-quarts de la longueur des épines furcales, ciliées (quelques cils plus longs à mi-longueur de la face interne de la paire la plus interne). Une paire d'épines externes très longues et minces (2/5 de la longueur de l'épine furcale), ciliées.

Yeux allongés verticalement, pédonculés.

Antennule assez volumineuse, avec quatre aesthètes apicaux, deux (plus petits) subapicaux, et une ébauche de rame interne.

Antenne très longue. Processus épineux atteignant une fois et demie la longueur du rostre, spinuleux sur ses deux tiers distaux. Exopodite atteignant les 2/5 du processus épineux, terminé par trois épines : une très épaisse et très longue, atteignant l'extrémité du processus épineux et de même structure que ce dernier, et deux courtes, inermes. Endopodite insegmenté, atteignant les deux tiers du processus épineux et portant deux soies courtes à son extrémité tronquée.

Mandibules pourvues d'un palpe inarticulé sans soie. (A fins d'allègement, les autres pièces buccales ne seront pas décrites dans cette étude préliminaire).

Pléopodes présents sur les segments abdominaux 2 à 6, atteignant la longueur du segment abdominal suivant chez les trois premiers, plus courts chez les deux suivants. Ebauche d'endopodite presente, sauf sur la dernière paire.

B - Affinités

Un rapprochement s'impose entre cette Zoé et celle décrite par WILLIAMSON (1960) : on retrouve la multiplication des épines, encore plus accentuée ici, une paire d'épines sur le 2ème segment abdominal, deux paires sur les segments 3 à 6, toutes ces épines étant plumeuses (WILLIAMSON ne mentionne pas d'autre armature de l'abdomen). Le telson est presque identique. L'antenne est de même structure (l'exopodite se terminant, chez la larve de WILLIAMSON, par trois branches épaisses et spinuleuses, au lieu d'une branche de ce type et de deux soies ordinaires chez la larve décrite ici). On retrouve le tubercule sagittal situé en arrière de la dorsale ; quant au tubercule frontal allongé, il semble correspondre exactement à ce que WILLIAMSON interprète

comme la base du rostre cassé, qui serait dirigé perpendiculairement à la face frontale ; la Zoé de Nosy Bé possède par contre un rostre typique. Notons enfin que chez la Zoé de WILLIAMSON les faces latérales de la carapace sont bien plus développées vers le bas.

Malgré quelques nettes différences, il se trouve donc un grand nombre de points communs entre ces deux larves et il semble naturel de les rapprocher. Dès lors, il convient de remarquer que la présence d'un stade 3 chez la "Zoé Brachyrhynque 10 NB" (8 soies natatoires aux exopodites des maxillipèdes 1 et 2) éloigne cette forme des *Majidae*, auxquels WILLIAMSON est tenté de rattacher sa larve. L'antenne et le telson n'en sont pas moins d'un type que l'on rencontre dans cette famille (antenne type *Maia*, telson type *Inachus*), et l'état de développement des pattes thoraciques et abdominales au stade 3 est remarquable.

Terminons par une remarque qui pourrait avoir ultérieurement un intérêt phylogénétique : il s'agit des deux tubercules cylindriques à sommet tronqué que l'on observe chez l'une et l'autre larve, dans le plan sagittal de la carapace. Ils sont à rapprocher d'une part des tubercules sagittaux plus ou moins développés que l'on remarque sur la carapace de nombreuses Zoés de Brachyoures de types divers ; d'autre part aux organes sagittaux frontal et post-dorsal, cylindriques et à sommet tronqué, qui ont été remarqué chez un certain nombre de larves de Crustacés Décapodes : Stades *Protozoé* et *Mysis I* des *Sergestidae* ainsi que du *Penaeidae Solenocera*, larves d'*Eryoneicus*, et celles attribuées à *Homola*. Ces larves se caractérisent par rapport aux formes voisines par une multiplication hypertélique des épines de la carapace et de l'abdomen. La Zoé Brachyoure 10 NB et celle décrite par WILLIAMSON s'inscrivent dans la même ligne.

Rappelons que ces organes sagittaux avaient été homologués par HANSEN (1921) à l'organe frontal des Entomostracés. Par ailleurs la multiplication des épines a également été considérée comme un caractère primitif : on observerait ainsi la coincidence assez régulière de deux caractères ancestraux.

***ZOE BRACHYOURE* 11 NB** stade 3 (fig. 2a à 2e)

Longueur de la carapace : 1,21 mm. Epine rostrale : 0,81 mm. Epine dorsale : 1,57 mm. Distance entre les extrémités des épines rostrale et dorsale : 3,38 mm. Distance entre les extrémités des épines latérales : 2,60 mm. Longueur de telson : 0,72 mm.

Carapace de forme allongée, légèrement bosselée ; une carène part de la base des pédoncules oculaires, inclinée à 45° vers le haut. Rostre long, incliné à 45° vers l'avant. Epine dorsale très longue, inclinée à 45° vers l'arrière, et garnie de quelques soies molles. Epines latérales assez longues, fortement incurvées vers le bas. Le bord de la carapace montre une échancrure caractéristique au niveau des mandibules. Lobes latéraux de la carapace peu étendus vers le bas. Un tubercule frontal tronqué, et un semblable au bord postérieur de la carapace, flanqué de deux bosses demi-sphériques portant une petite soie raide à leur sommet. La moitié supérieure de la carapace (au-dessus des épines latérales) porte de nombreux poils épais et fortement crochus.

Abdomen de six articles plus le telson. Premier article abdominal avec 4 soies dorsales. Segments 2 à 5 avec une paire de soies dorsales située à mi-longueur sur une légère carène transversale ; les segments 4 et 5 ont, de plus, deux soies rapprochées sur le bord postérieur. Segments 2 à 5 à crochets latéraux : grands et recourbés vers le bas sur le deuxième segment, vers le bas et l'arrière sur le troisième ; réduits et recourbés vers l'arrière sur les quatrième et cinquième. Segments 3 à 5 munis, de plus, d'une paire d'épines latéro-ventrales épaisses et très longues (une fois et demie la longueur du segment), à l'extrémité arrondie.

Telson large, court sans les épines furcales, celles-ci fortes, longues et très écartées. Bord postérieur à échancrure large et peu profonde. Trois paires d'épines internes typiques ciliées, deux paires de soies internes supplémentaires, les plus internes glabres, les plus externes plumeuses. Trois paires d'épines externes : une latérale grande et deux dorsales petites.

Yeux longuement pédonculés.

Antennule assez longue, portant 4 aesthètes apicales et une subapicale.

Antenne : processus épineux atteignant le tiers du rostre, et de longueur double de l'exopodite ; celui-ci terminé par trois soies dont une très longue, atteignant la moitié du rostre. Endopodite insegmenté, de même longueur que l'exopodite.

Maxillipèdes 1 et 2 : exopodites avec 8 soies apicales plus une neuvième petite, subapicale, sur mxp2.

Pléopodes 2 à 6 présents, petits et uniramés (pl2 atteint le tiers de la longueur du segment abdominal ; pl6 est représenté par un simple bourgeon).

***ZOE BRACHYRHYNQUE* 12 NB** stade 1 (fig. 3a à 3e)

Longueur de la carapace : 0,51 mm. Epine rostrale : 0,35 mm. Epine dorsale (distance rectiligne de la base au sommet) 0,50 mm. Distance entre extrémités des épines rostrale et dorsale 1,10 mm. Distance entre les extrémités des épines latérales inférieures : 0,87 mm. Longueur du telson : 0,50 mm.

Carapace de forme allongée et peu haute. Rostre peu incliné à l'origine, puis s'infléchissant vers le bas. Epine dorsale à base très épaisse et presque verticale, amincie vers l'arrière au niveau d'un coude brusque, portant deux denticules latéraux. Un tubercule frontal arrondi et un en arrière de la dorsale. Deux paires d'épines latérales côniques, l'une inférieure, l'autre supérieure, à bases coalescentes ; leur extrémité est brusquement effilée ; quelques petits denticules, et une soie sur la face ventrale de l'épine supérieure.

Abdomen de cinq segments plus le telson. Deuxième segment avec un fort crochet latéral dirigé vers l'arrière et le bas, à l'extrémité arrondie. Segments 3 à 5 avec une paire d'épines dorsales dirigées vers l'arrière et l'extérieur. Cinquième segment avec de plus une paire d'épines ventrales dirigées vers l'arrière.

Telson profondément échancré. Deux paires de soies internes supplémentaires courtes et glabres. Deux paires d'épines externes, latérales, dont une très petite. Epines furcales pourvues de deux rangées de cils.

Yeux pédonculés.

Antennule avec trois aesthètes.

Antenne : processus épineux atteignant l'extrémité du rostre, portant deux rangs de spinules; exopodite court, terminé par trois soies dont une très grande (atteignant presque l'extrémité du processus épineux), et muni d'un rang de spinules. Endopodite absent.

Pléopodes absents.

***ZOE TETRALIA* 2 NB** stade 2 à 4 (fig. 4a à 4j)

Longueur de la carapace :	stade 2 : 0,64 mm	stade 3 : 1,00	stade 4 : 1,25
Epine rostrale	1,80	3,30	3,75
Epine dorsale (distance base-sommet)	0,71		1,60
Epine latérale (inférieure	1,00	1,25	1,88
(supérieure			1,10
Longueur du telson	0,73	1,00	1,25

Forme très voisine de la larve de *Tetralia glaberrima* (Herbst) décrite par GURNEY (1938).

Rostre extrêmement long, droit, portant quelques spinules sur ses faces dorsale et ventrale dans le tiers proximal. Dorsale longue, d'abord droite et verticale, puis brusquement coudée vers

l'arrière et le bas ; quelques courtes soies sur la face antérieure. Un tubercule frontal arrondi et un semblable près du bord postérieur de la carapace. Deux paires d'épines latérales longues : une inférieure et une supérieure, la première dirigée vers le bas, la seconde vers le haut. Ces deux épines sont élargies à l'extrémité en palettes, terminées par une pointe aigue ; les palettes, non indiquées par GURNEY au stade 1 sont ébauchées seulement au stade 2, déjà nettes au stade 3 et très larges au stade 4 ; elles portent quelques spinules sur leurs bords. Bords latéraux de la carapace très développés vers le bas.

Abdomen de 5 segments plus le telson chez le stade 2, de 6 segments à partir du stade 3. Segments 2 à 5 (ou 6) pourvus d'une paire de soies dorsales. Segment 2 avec une paire de crochets latéraux recourbés vers l'avant. Segments 3 à 5 pourvus d'une paire d'épines postéro-ventrales courtes au stade 2, plus longues au stade 3 (celles des segments 4 et 5 atteignant la moitié de la longueur du segment), et atteignant au stade 4 les trois-quarts de la longueur du segment abdominal.

Telson identique au stade 2 à celui de la larve de GURNEY (1938) ; une paire de soies internes supplémentaires glabres, très courtes au stade 3, plus longues au stade 4. Deux paires d'épines externes.

Yeux pédonculés.

Antennule avec trois aesthètes plus une soie aux stades 2 et 3 ; cinq aesthètes apicaux (dont un petit) et 7 en une rangée subapicale au stade 4.

Antenne de structure identique, au stade 2, à celle de la larve de GURNEY. Au stade 3, endopodite atteignant les 2/5 de la longueur du processus épineux, et les 3/4 de cette longueur au stade 4.

Pléopodes absents au stade 2, présents au stade 3 à l'état de bourgeons sur les segments abdominaux 2 à 6, et atteignant presque au stade 4 la longueur des segments.

***ZOE TETRALIA* (?) 1 NB** stade 1 (fig. 5a à 5e)

Longueur de la carapace : 0,56 mm. Epine rostrale : 0,85 mm. Epine dorsale : 0,65 mm. Distance entre extrémités des épines rostrale et dorsale : 1,72 mm. Distance entre extrémités des épines latérales supérieures : 1,52 mm. Longueur du telson : 0,48 mm.

Larve nettement apparentée à la précédente. Rostre moins long, légèrement courbé vers le bas, et pourvu sur toute sa longueur d'une double rangée de spinules antérieurs. Dorsale fortement recourbée sur toute sa longueur, avec une double rangée de spinules sur chacune de ses faces antérieure et postérieure. Latérale supérieure bien développée, courbée vers le bas, avec une double rangée de spinules sur sa face dorsale. Latérale inférieure réduite à un court processus cônique et effilé à l'extrémité, glabre. Pas de tubercule en arrière de l'épine dorsale, mais un frontal. Une paire de soies en arrière de la dorsale.

Abdomen de 5 segments plus le telson. Deuxième et troisième segments pourvus d'une paire de processus latéraux, ceux du 2ème en crochets dirigés vers l'avant, ceux du 3ème très réduits. Segments 3 à 5 avec une paire de très petites épines postéro-ventrales.

Telson portant des épines furcales très longues proportionnellement au reste de l'abdomen, divergentes et recourbées vers la face dorsale. Echancrure médiane large et peu profonde. Trois paires de longues épines internes plumeuses ; pas de soies internes supplémentaires. Deux paires d'épines externes, une latérale et une dorsale, plus une courte soie à la base de cette dernière.

Yeux pédonculés.

Antennule avec trois aesthètes apicaux.

Antenne identique à celle de la larve précédente.

Pléopodes absents.

***ZOE* groupe A 9 NB** stade 4 (fig. 6a à 6e)

Longueur de la carapace : 2,64 mm. Epine rostrale : 1,36 mm. Epine dorsale : 1,12 mm. Distance entre extrémités des épines rostrale et dorsale : 3,69 mm. Distance entre extrémités des épines latérales : 3,04 mm. Longueur du telson : 1,20 mm.

Carapace bosselée : partie frontale déprimée en selle, faces latérales très saillantes, mais déprimées en arrière des yeux. Bord inférieur de la carapace profondément échancré au niveau de la mandibule. Epines rostrale et dorsale fines et droites, munies de quelques paires de soie sur leurs faces antérieures. Une paire de forts denticules à la base du rostre. Un tubercule sagittal arrondi en arrière de la dorsale ; au-dessus des yeux, un processus cylindrique et tronqué au sommet, perpendiculaire à l'axe du rostre, très analogue à celui décrit ci-dessus chez la larve "*Brachyoure* 10 NB", mais plus allongé encore. Epine latérale courte et droite, insérée au sommet de la zone saillante du flanc de la carapace, et portant contre sa base, face ventrale, un bouton évoquant l'ébauche d'une seconde épine latérale. Bords postéro-inférieurs de la carapace frangés de longues soies. Quelques paires de soies entre l'épine dorsale et le processus sagittal frontal.

Abdomen de six articles et telson. Chaque segment avec une paire de soies dorsales postérieures. Segments 2 et 3 porteurs d'une paire de protubérances latérales en forme de boutons coniques à sommets arrondis. Segments 4 et 5 munis de très longues expansions latéro-postérieures étroites, à extrémités arrondies, qui encadrent le sixième segment abdominal et la base du telson.

Telson de forme générale quadrangulaire, à bords latéraux arrondis. Epines furcales très courtes, à base large et brusquement amincies à mi-longueur. Echancrure médiane très peu profonde, anguleuse. Trois paires d'épines internes à ciliature très courte. Deux paires de très petites épines externes.

Antennule portant dix aesthètes au sommet de la rame externe et un au sommet de la rame interne.

Antenne : processus épineux court et mince, portant une rangée de denticules. Endopodite atteignant la moitié du rostre, avec une ébauche de segmentation. Endopodite extrèmement réduit, mais portant trois soies apicales dont une dépasse l'endopodite.

Exopodites des maxillipèdes 1 et 2 avec dix soies apicales plus deux subapicales plus petites.

Pléopodes présents sur les segments abdominaux 1 à 6, avec une ébauche d'endopodite sur les segments 2 à 5 seulement.

On remarquera que l'antenne est voisine de celles décrites chez *Ocypode gaudichaudi* (CRANE 1950) ou *O. Platytarsis* (RAJA BAI NAIDU 1951). Le telson est d'un type rencontré également chez *Ocypode*, mais aussi chez certains *Grapsidae* (Planes ...) et chez certaines "*Grapsizoeae*" de AIKAWA ; mais en regard des nombreux caractères particuliers de cette forme larvaire, les quelques ressemblances mentionnées ci-dessus ne peuvent donner que des présomptions quant à ses affinités.

***ZOE HYMENOSOMIDAE* 1 NB** stade 1 à 4 (fig. 7a à 7d)

	stade 1	stade 2	stade 3	stade 4
Longueur de la carapace :	0,90 mm	1,00	1,28	1,40
Distance entre extrémités des épines latérales supérieures :	0,78	1,16	1,48	1,40
Distance entre extrémités des épines latérales inférieures :	0,92	1,10	1,16	1,00
Longueur du telson :	0,25	0,28		0,40

Cette forme semble identique à une Zoé non nommée, figurée par CLAUS (1876).

Carapace globuleuse, à bords latéro-inférieurs très développés vers le bas et prolongés en

angles ; échancrure abdominale profonde et étroite : ces caractères sont ceux des Zoés d'*Hymenosomidae*.

Rostre réduit à une dent triangulaire. Deux paires de courtes épines latérales : une paire supérieure plantée de part et d'autre du sommet de la carapace ; une paire inférieure insérée par une base large près de l'angle latéro-inférieur de la carapace. La taille relative des épines latérales inférieures décroit du stade 1 au stade 4. Deux tubercules sagittaux arrondis : l'un frontal, l'autre en avant des épines latérales supérieures.

Abdomen court, le plus souvent replié sous la carapace, comme cela se rencontre chez les Zoés de *Pinnotheridae*, *Leucosidae* et *Hymenosomidae*. Cinq segments aux stades 1 à 3, six au stade 4, telson exclus. Les segments 1 à 3 sont cylindriques ; le quatrième présente deux expansions latérales aux angles postérieurs ; le cinquième est très élargi et présente deux lobes latéraux arrondis et foliacés, très développés, encadrant la base du telson et le sixième segment en entier quand il existe : c'est donc un abdomen typique de Zoé d'*Hymenosomidae*. Segments 2 et 3 pourvus d'une paire d'expansions dorso-latérales foliacées, celles du deuxième segment triangulaires et mucronées à l'extrémité, celles du troisième segment arrondies. Telson presque rectangulaire, plus large que long surtout aux stades âgés. Epines furcales courtes, fortes, parallèles. Bord postérieur droit. Trois paires d'épines internes ciliées, légèrement plus courtes que la furca au stade 1, plus longues aux stades suivants ; ces épines présentent un léger étranglement au tiers environ de leur longueur. Une paire de très petites épines externes, presque invisibles aux stades âgés.

Antenne vestigiale.

Mandibule volumineuse, sans palpe.

Exopodite des maxillipèdes 1 et 2 avec quatre soies au stade 1, sept au stade 2, dix aux stades 3 et 4.

Pléopodes ébauchés au stade 2. Ceux du sixième segment apparaissent au stade 3 alors que le segment n'est pas encore distinct du telson.

***PTEROCARIS* 1 NB** stade 5 (fig. 8a à 8e)

Longueur de la carapace : 2,90 mm. Plus grande largeur de la carapace : 6,75 mm. Epine rostrale : 2,10 mm ? (cassée à l'extrémité ?). Epine dorsale cassée. Longueur du telson : 1,94 mm.

Cette forme parait identique à la larve figurée par CLAUS (1876) (à qui l'on doit le terme de *Pterocaris*) et qui provenait de Zanzibar.

Cette forme se singularise au premier abord par une paire d'expansions latérales considérables de la carapace, formant deux poches en forme de cylindres plats, ovales en vue dorsale. Elles enveloppent complètement les péréiopodes et le troisième maxillipède. L'arête ventrale de cette expansion porte, au bord postérieur latéral, une forte épine. Bord postéro-inférieur de la carapace en bourrelet, et portant de chaque côté une dizaine de longues soies. Echancrure abdominale profonde et étroite.

Rostre long et mince ; épine dorsale probablement cassée sur le specimen étudié (CLAUS figure une épine dorsale longue et mince).

Abdomen de six segments plus le telson. Premier segment abdominal avec trois soies dorsales. Segments 3 à 4 munis de processus latéraux : celui du deuxième segment cônique et légèrement courbé vers l'avant, ceux des segments 3 et 4 minuscules, le dernier recourbé vers l'arrière. Segments 3 à 5 avec épines latérales, celles du troisième segment courtes, celles des segments 4 et 5 très longues.

Telson allongé, à bords parallèles. Epines furcales fines et parallèles, échancrure médiane profonde, en ogive. Trois paires d'épines internes courtement ciliées ; la plus interne porte sur sa face proximale une dizaine de soies plus longues. Deux paires de soies internes supplémentaires

UNESCO ARCHIVES

longues et glabres. Deux paires d'épines externes, dont une réduite à une soie.

Yeux pédonculés.

Antennule de trois segments et munie de nombreuses aesthètes disposées en trois séries ; une ébauche de rame interne.

Antenne : processus épineux portant deux séries de spinules, plus des spinules disséminés. Endopodite insegmenté plus court que le processus épineux. Exopodite plus court que l'endopodite, avec trois soies apicales dont une très courte et une dépassant l'extrémité du processus épineux.

Mandibule à petit palpe. Exopodites des maxillipèdes 1 et 2 pourvus de douze soies natatoires apicales auxquelles s'ajoutent trois soies subapicales plus courtes.

Péréiopodes bien développés, la première paire chéliforme.

Pléopodes présents sur les segments abdominaux 2 à 6, munis, sauf la dernière paire, d'ébauches d'endopodite.

***PTEROCARIS* 2 NB** stade 1 (fig. 9a à 9d)

Longueur de la carapace : 0,70 mm. Plus grande largeur de la carapace : 1,36 mm. Epine rostrale : 0,72 mm. Epine dorsale 0,44 mm. Distance entre extrémités des épines rostrale et dorsale : 1,68 mm. Longueur du telson : 0,65 mm.

Voisine de la forme précédente ; mais les poches latérales de la carapace sont proportionnellement moins développées. Bord postéro-inférieur de la carapace dépourvu de soies. Arête dorsale de la poche latérale de la carapace peu nette ; arête ventrale mieux prononcée et garnie d'une douzaine de denticules arrondis ; l'angle postéro-latéral de chacune de ces arêtes est muni d'une forte épine.

Rostre long et mince, dirigé à 45° vers l'avant. Dorsale courte, épaisse, arrondie au sommet, très inclinée en arrière.

Abdomen de cinq segments plus le telson. Segments 2 à 5 munis de processus latéro-dorsaux ; ceux des deux premiers très réduits (le premier arrondi, le second cônique), ceux des deux derniers en forts crochets dirigés vers l'arrière. Segments abdominaux 4 et 5 munis d'épines postérieures.

Antennule avec trois aesthètes plus deux soies apicales.

Antenne : processus épineux long et fin, muni de deux rangées de spinules. Endopodite absent. Exopodite court, terminé par trois soies dont une atteignant presque l'extrémité du processus épineux, les deux autres très courtes.

BIBLIOGRAPHIE

AIKAWA (H.) 1933 - On larval forms of some Brachyura. II) A note on indeterminates zoëas. Rec. Ocean. Wks. Jap. *5*, pp.124-254.

CLAUS (C.) 1876 - Untersuchungen zur Erforschung der genealogischen Grundlage des Crustaceen-System. Ein Beitrag zur Descendenzlehre. Wien, 1876.

CRANE (J.) 1940 - On the postembryonic development of Brachyuran Crabs of the genus *Ocypoda*. Zoologica, *25*, pp. 65-82.

GURNEY (R.) 1938 - Notes on some Decapod Crustacea from the Red Sea. VI. Some Brachyuran *larvae*.
Proc. Zool. Soc. London, série B, *108*, pp.73-84, 6 pl.

" 1942 - Larvae of Decapod Crustacea.
Ray Society, n° *129*.

HANSEN (H.J.) 1921 - - Studies on Arthropodu. 1.-On the postembryonic occurence of the median "dorsal organ" in Crustacea Malacostraca.
Copenhagen, pp.66-80.

HYMAN (O.W.) 1925 - Studies on larvae of Crabs of the family *Grapsidae*.
Proc. U.S.Nat. Mus., 65-10-pp. 1-8.

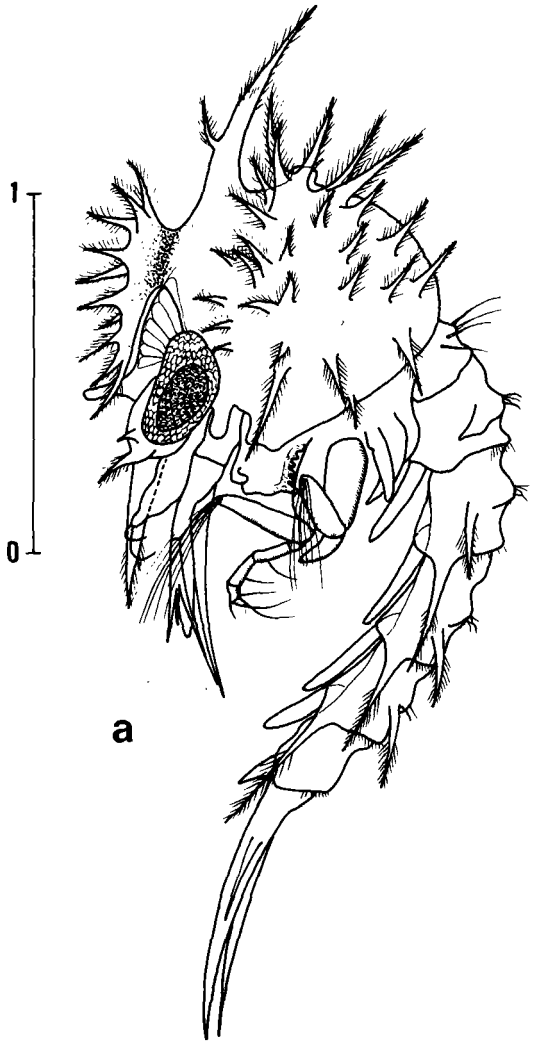
LEBOUR (M.V.) 1944 - Larval Crabs from Bermuda.
Zoologica, *29* -pp. 113-128.

RAJA-BAI (N.K.G.) 1951 - Some stages in the developpement and the bionomics of *Ocypoda platytarsis*.
Proc. Ind. Acad. Sc., B *33* pp.32-40, 2 pl.

WILLIAMSON (D.I.) 1960 - A remarkable *Zoea*, attribuable to *Majidae*.
Ann. Mag. Nat. Hist., 3-27 pp.141-144.

Zoe Brachyoure 10 NB

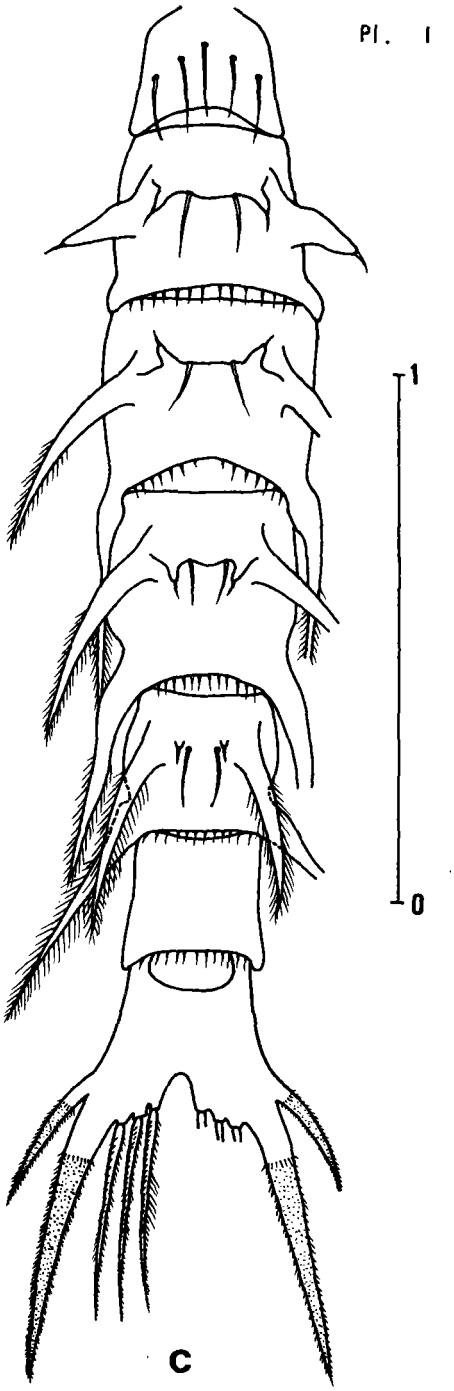
- 1a Vue latérale
- 1b Carapace : vue frontale
- 1c Abdomen, face dorsale
- 1d Abd 4 à 6, face ventrale



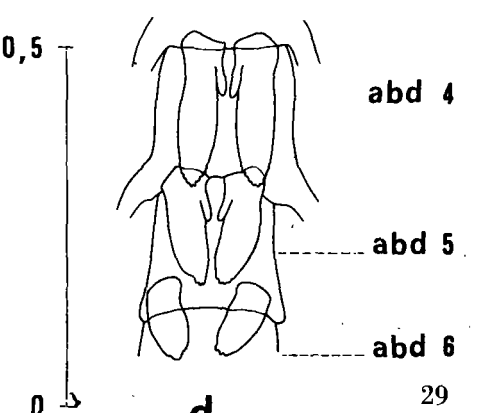
a



b



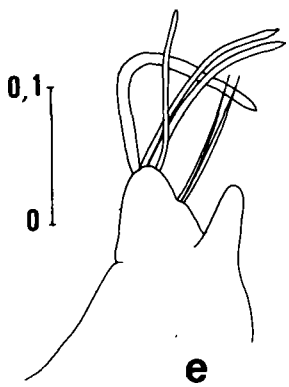
c



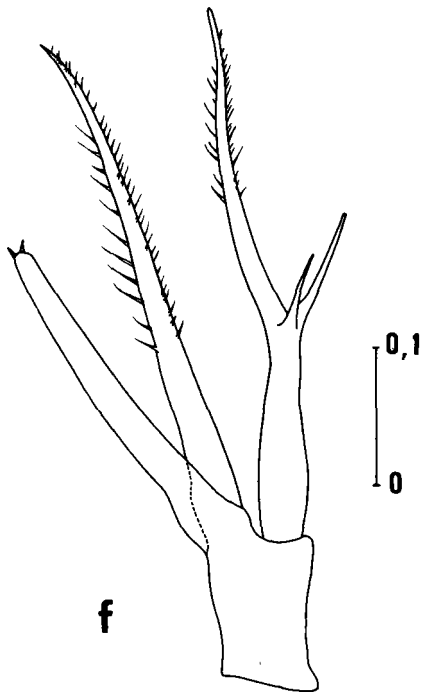
d

Zoe Brachyoure 10 NB

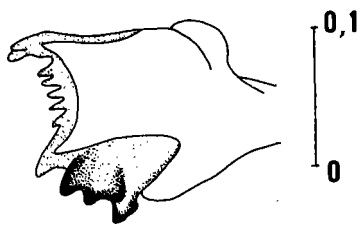
- 1e Antennule
- 1f Antenne
- 1g Mandibule



e



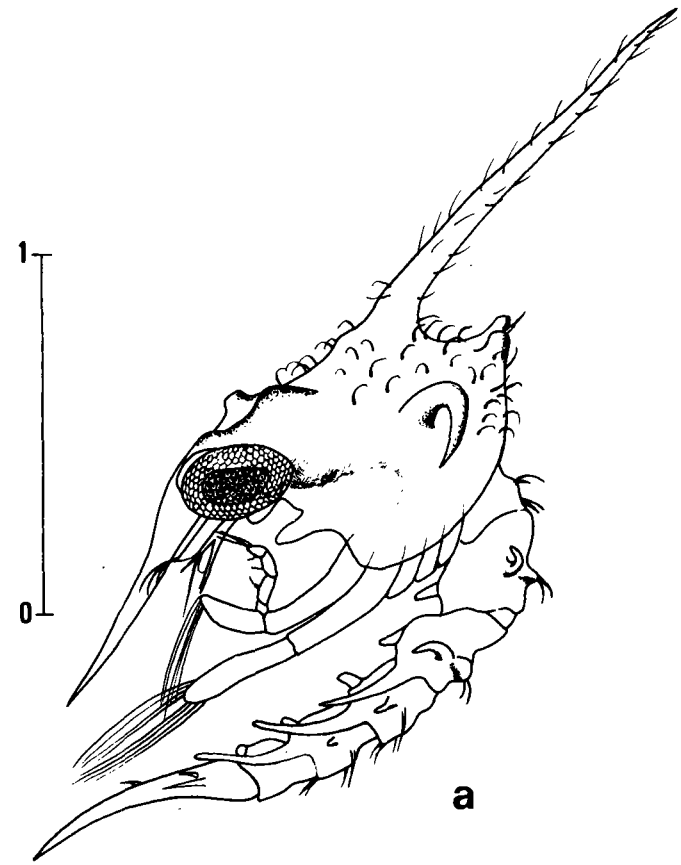
f

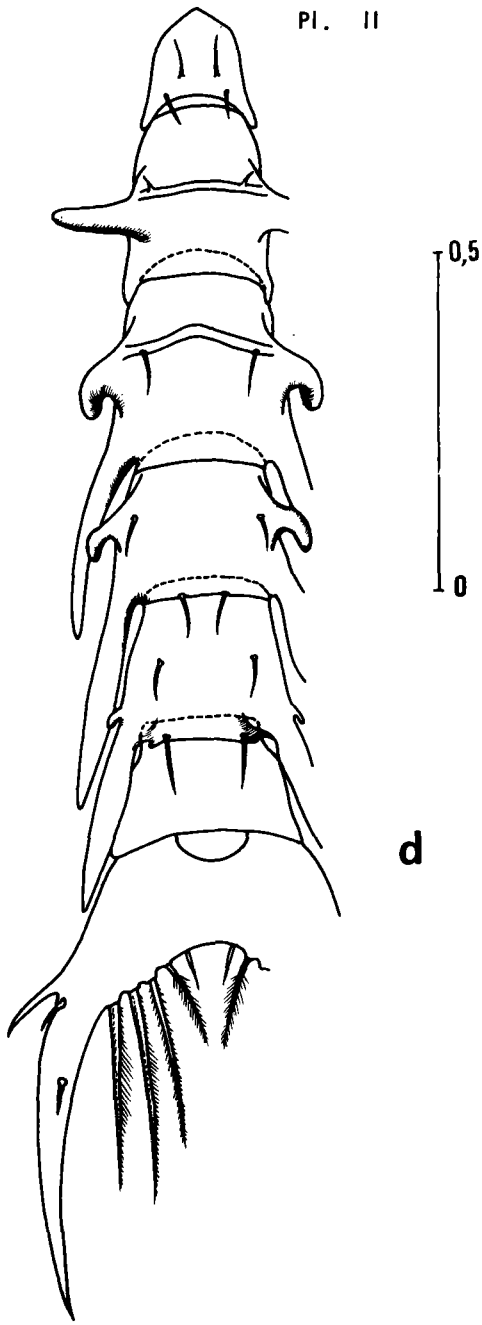


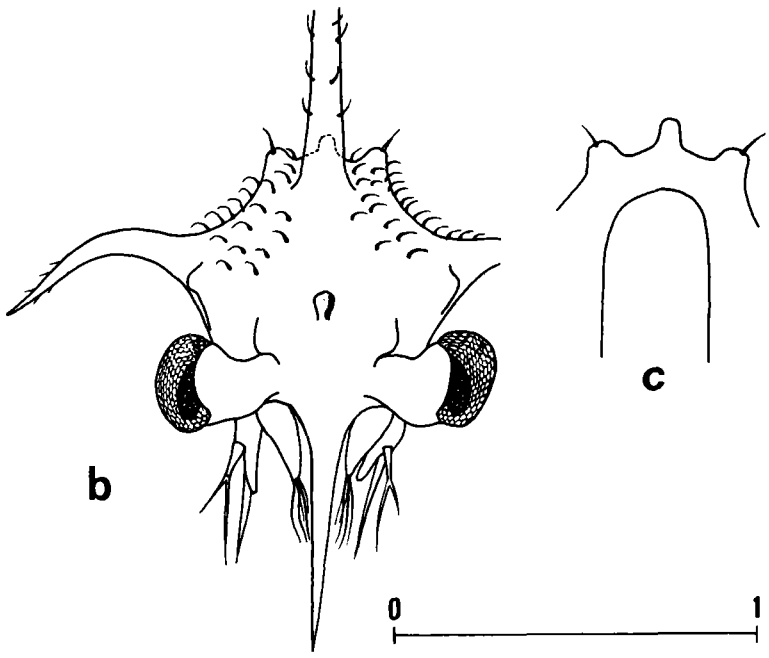
g

Zoe Brachyoure 11 NB

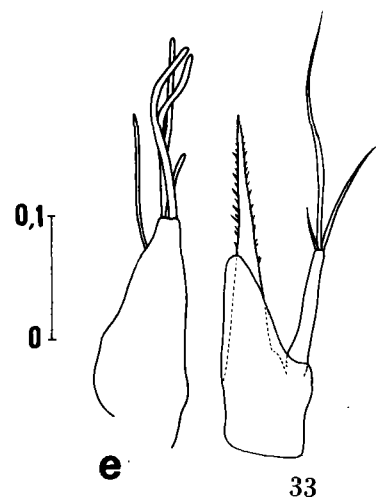
- 2a Vue latérale
- 2b Carapace : vue frontale
- 2c Bord postérieur de la carapace
- 2d Abdomen face dorsale
- 2e Antennule et Antenne


1
0
a


0,5
0
d

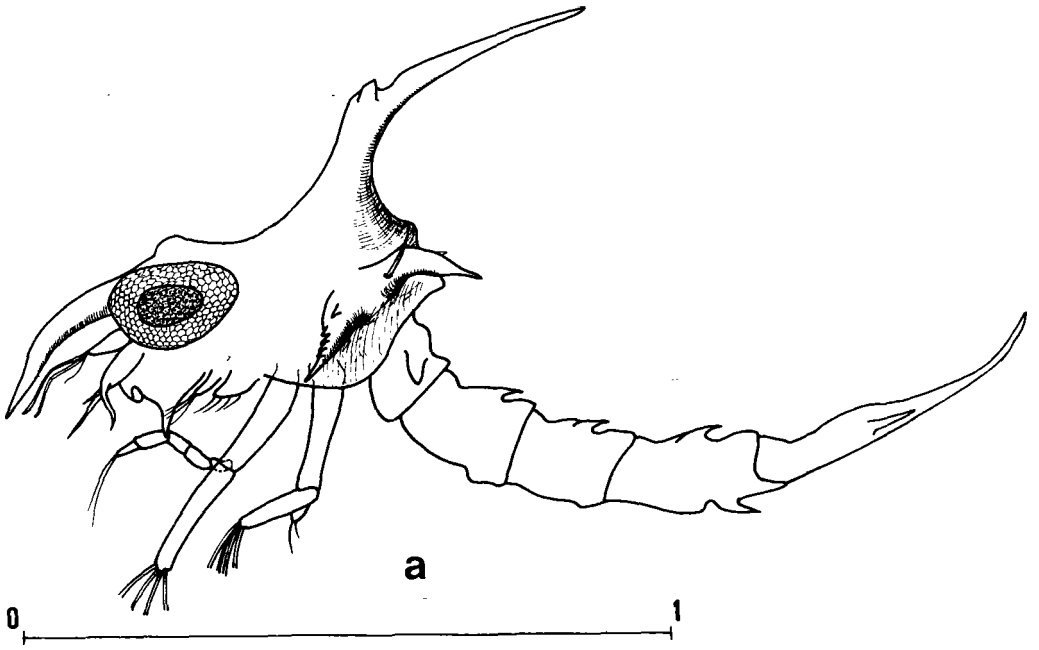

b
0
1

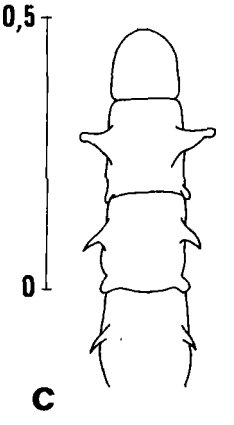
c

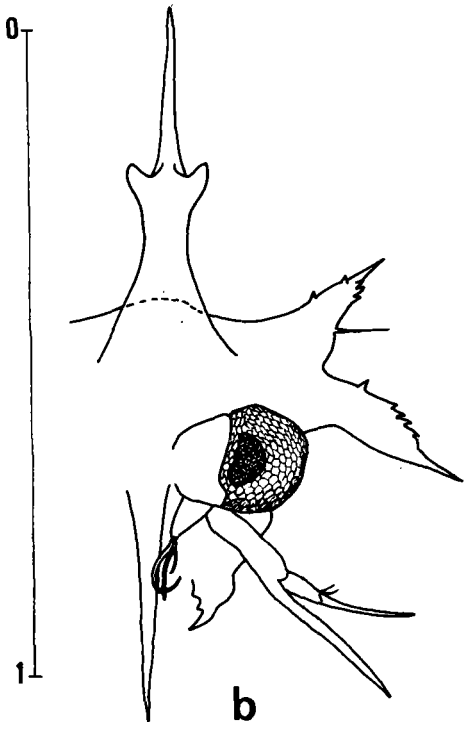

0,1
0
e

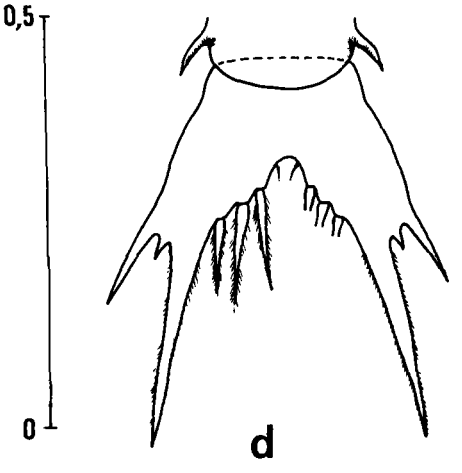
Zoe Brachyoure 12 NB

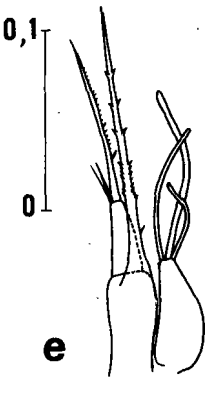
- 3a Vue latérale
- 3b Carapace : vue frontale
- 3c Abd 1 à 4, face dorsale
- 3d Telson
- 3e Antennule et Antenne


a
0
1


0,5
0
c

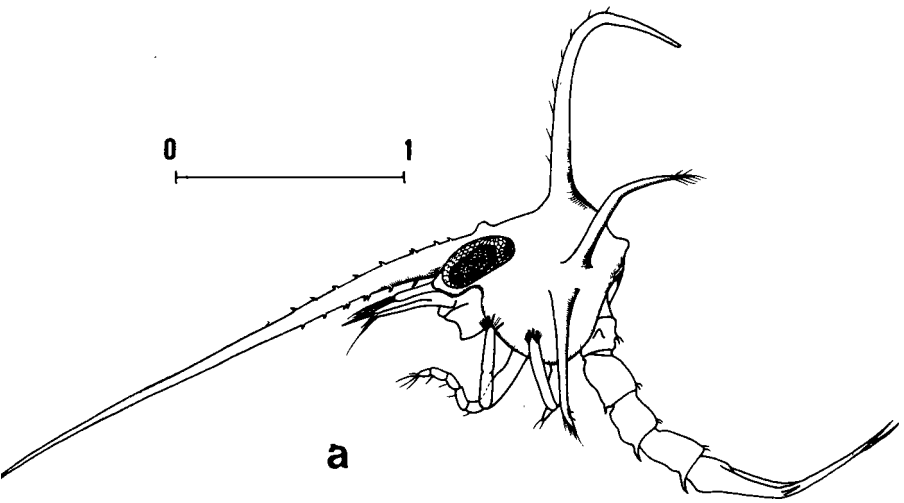

0
1
b


0,5
0
d

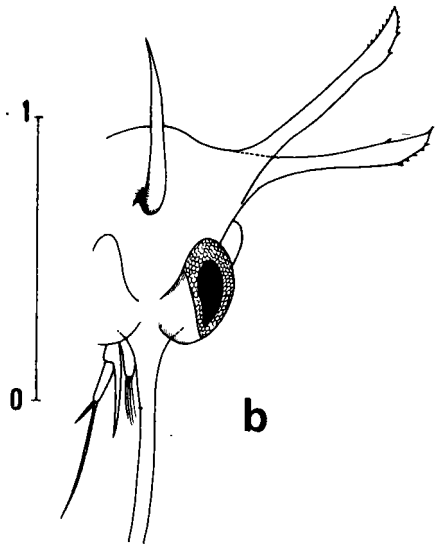

0,1
0
e

Zoe Tetralia 2 NB

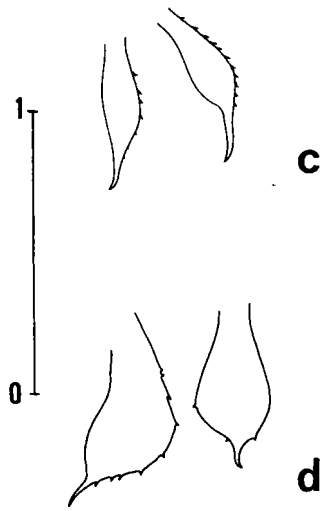
- 4a Vue latérale, stade 2
- 4b Carapace, vue dorsale, stade 2
- 4c Extrémité des épines latérales, stade 3
- 4d Idem, stade 4
- 4e Abd 2 et 3, stade 2
- 4f Telson, face dorsale, stade 2
- 4g Telson : base de l'épine furcale, face latérale, stade 2
- 4h Antennule, stade 2
- 4i Antenne, stade 2
- 4j Idem, stade 4



a

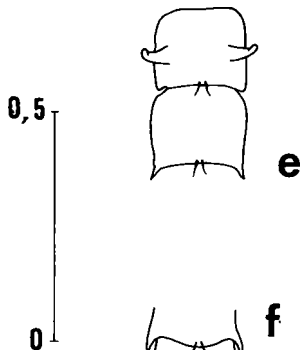


b



c

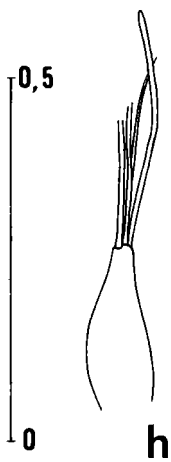
d



e

f

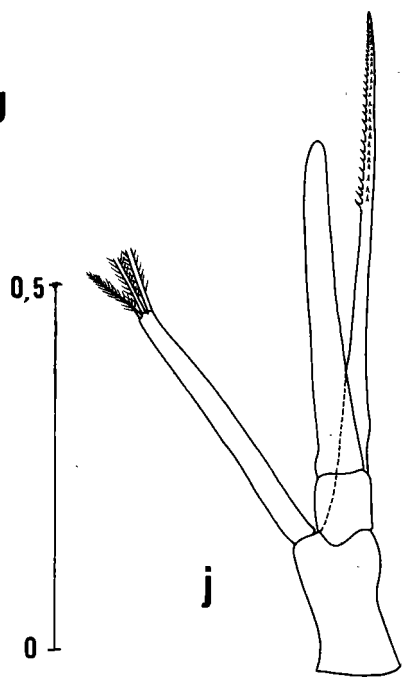
g



h



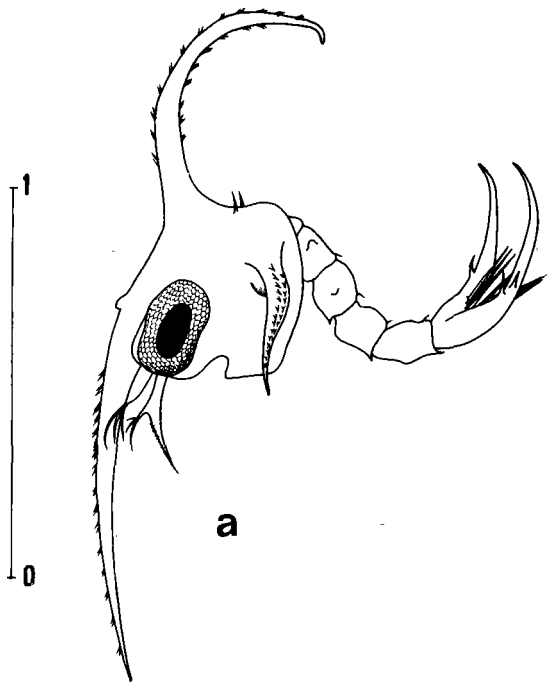
i



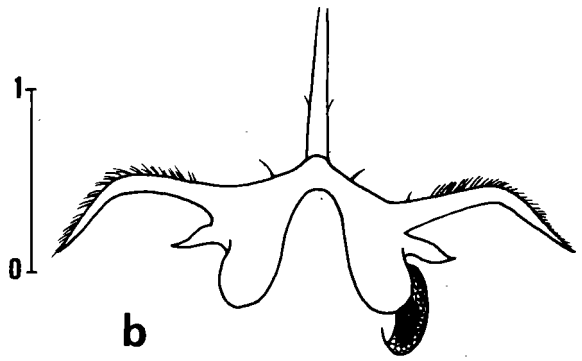
j

Zoe Tetralia (?) 1 NB

- 5a Vue latérale
- 5b Carapace, vue postérieure
- 5c Abd. 2 et 3
- 5d Antennule
- 5e Telson



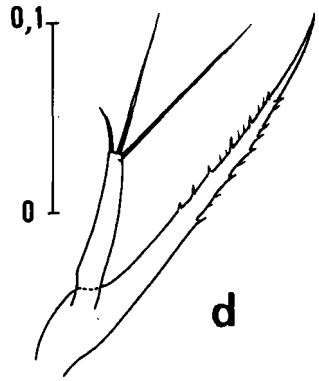
a



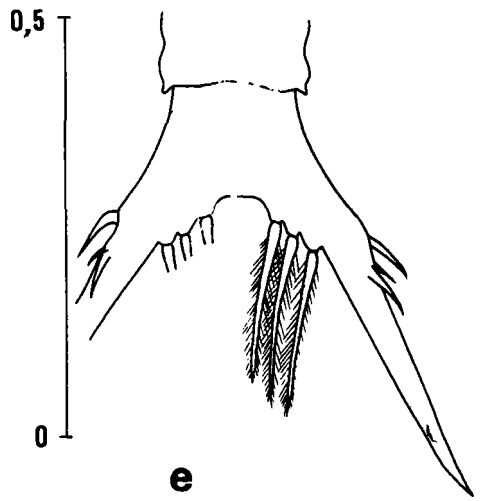
b



c



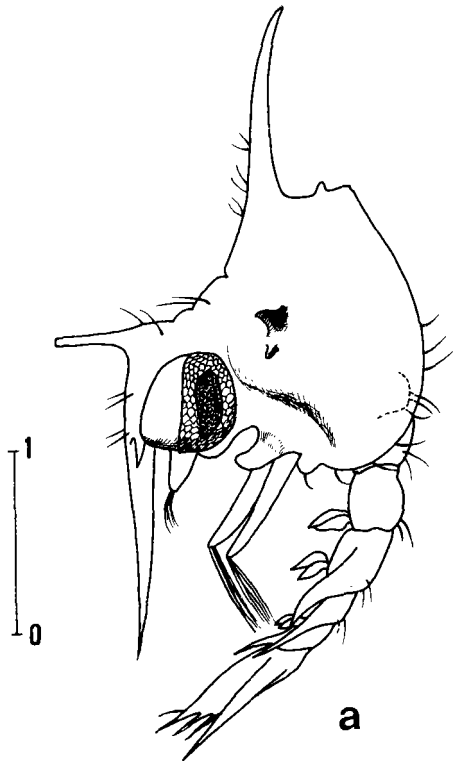
d



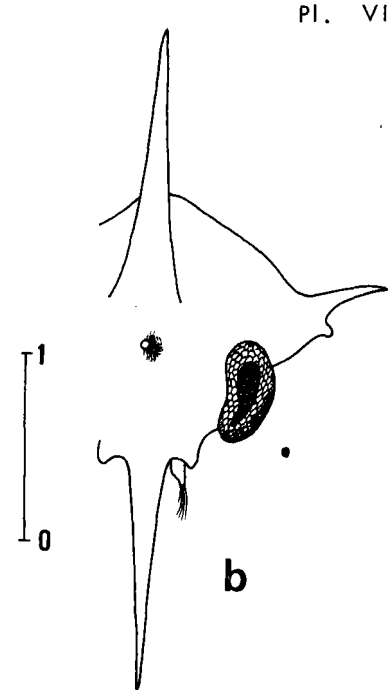
e

Zoe groupe A 9 NB

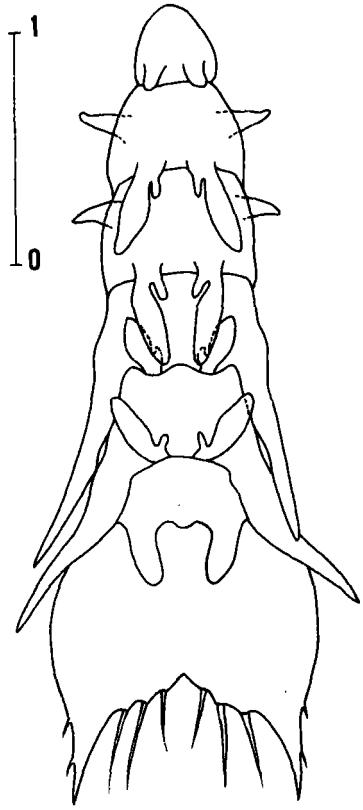
- 6a Vue latérale
- 6b Carapace, vue frontale
- 6c Abdomen, face ventrale
- 6d Antennule
- 6e Antenne



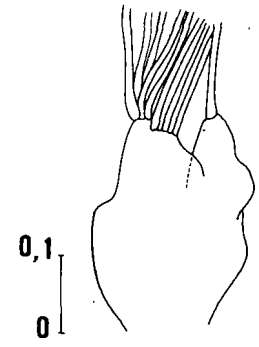
a



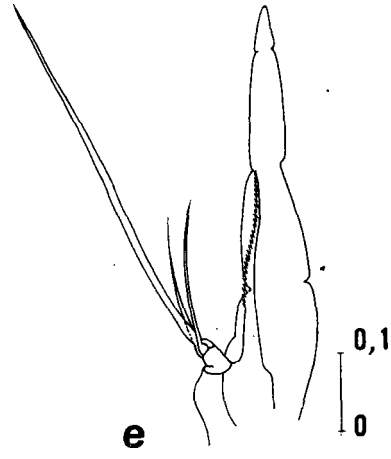
b



c



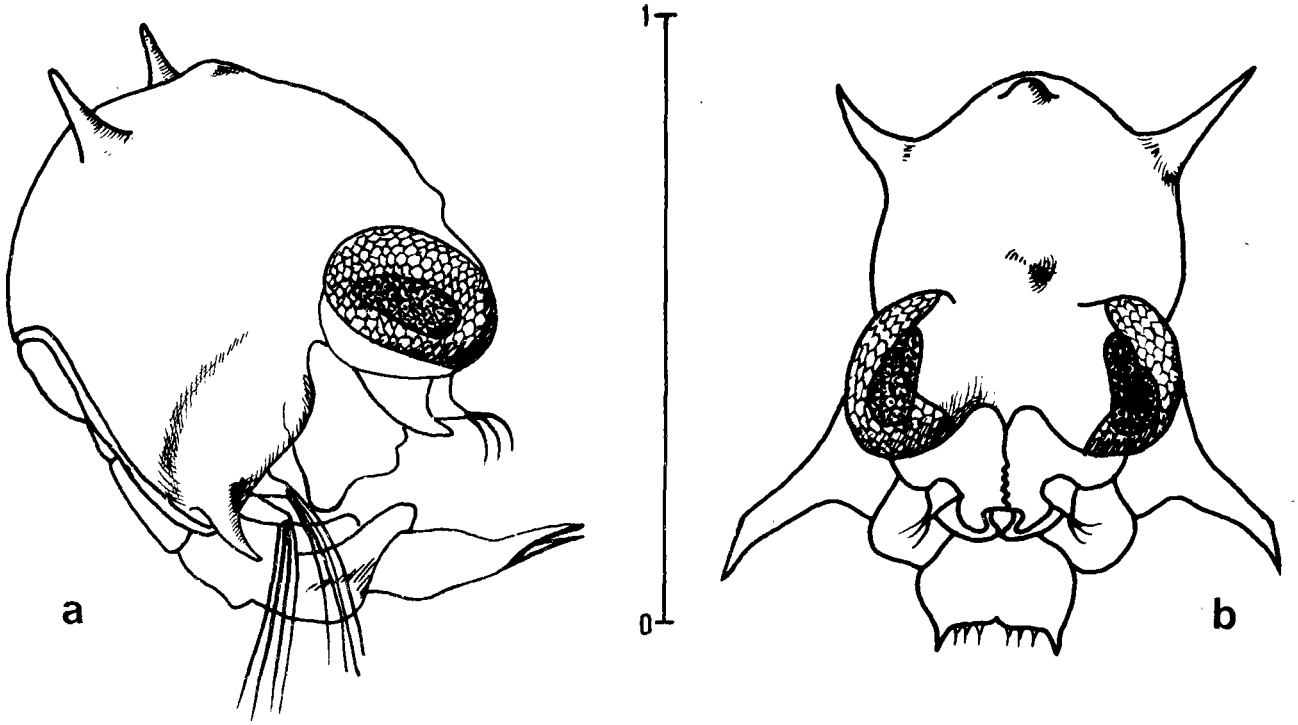
d

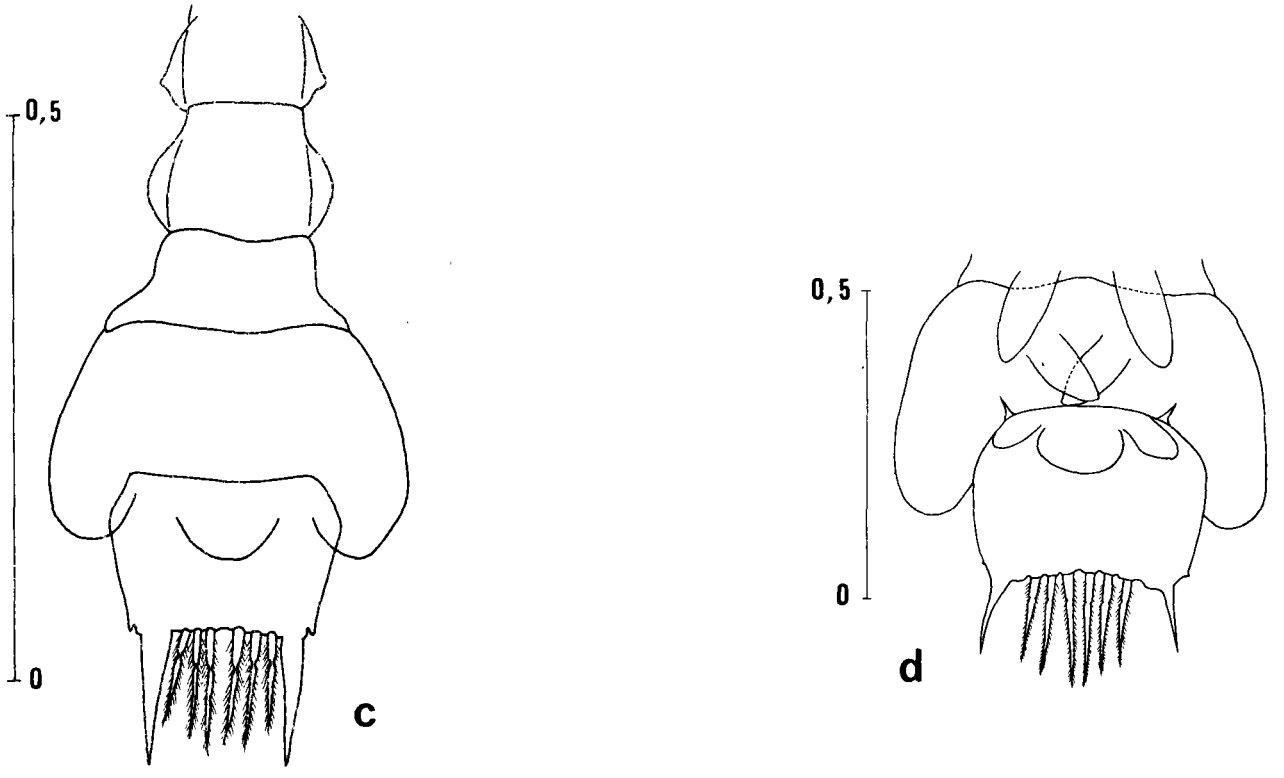


e

Zoe Hymenosomide 1 NB

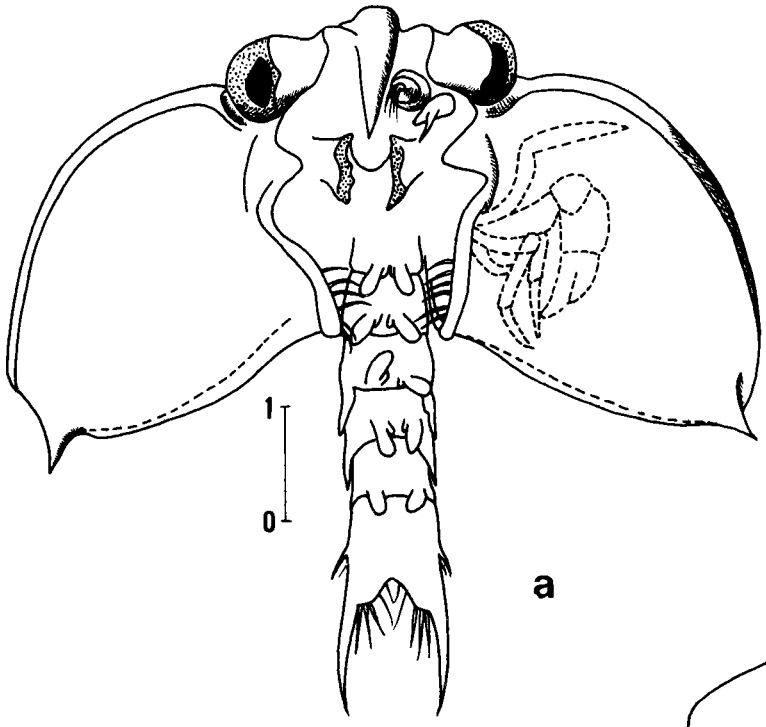
- 7a Vue latérale, stade 1
- 7b Carapace, vue frontale, stade 1
- 7c Abdomen, stade 1
- 7d Idem, stade 4


a
1
0
b

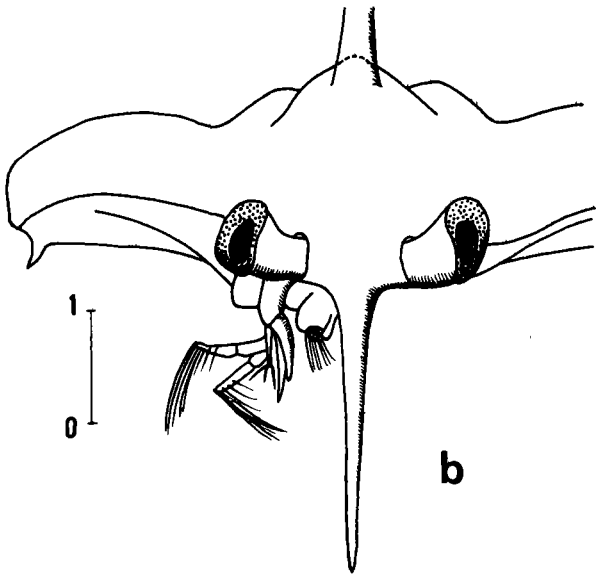

0,5
0
c
0,5
0
d

Pterocaris 1 NB

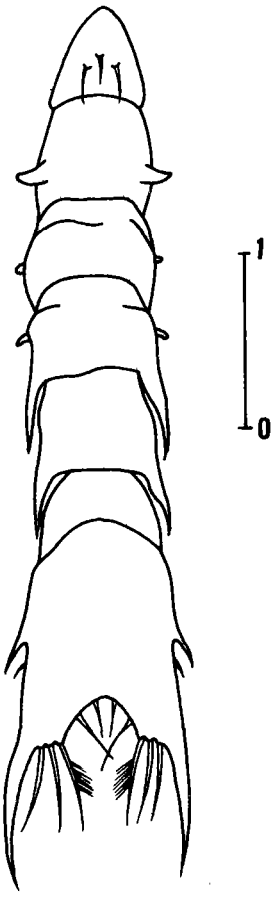
- 8a Face ventrale
- 8b Vue frontale
- 8c Abdomen, face dorsale
- 8d Abd 2 à 5, face latérale
- 8e Antenne



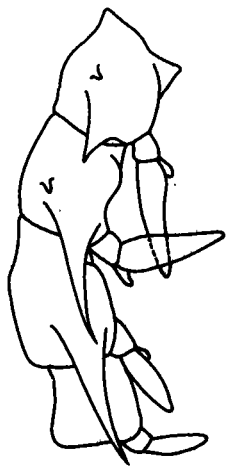
a



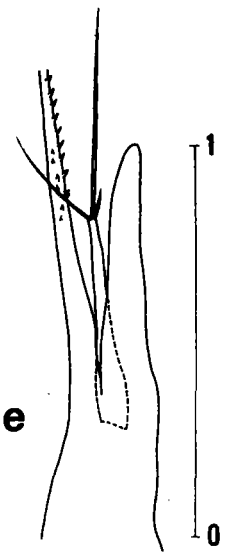
b



c



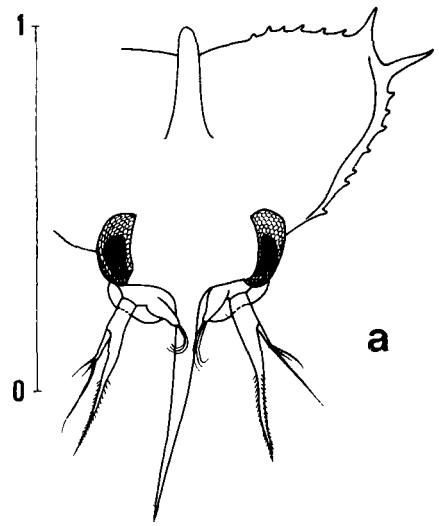
d

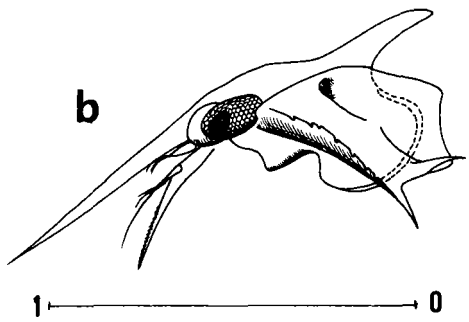


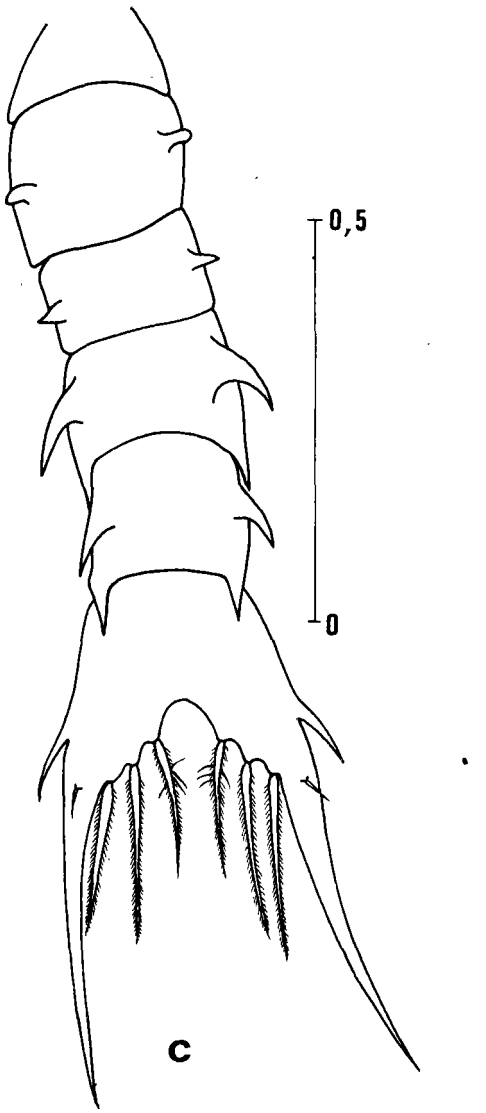
e

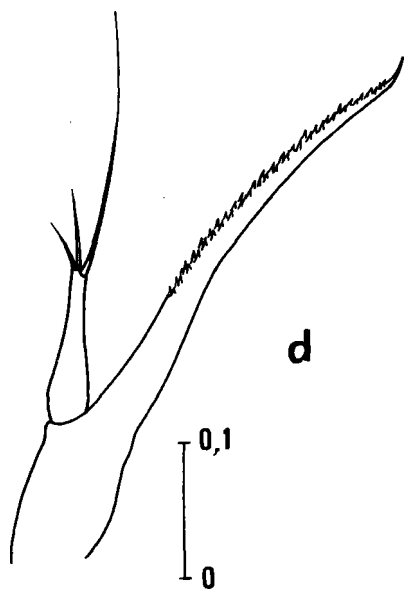
Pterocaris 2 NB

- 9a Carapace, vue dorsale
- 9b Carapace, vue latérale
- 9c Abdomen face dorsale
- 9d Antenne


1
0
a


b
1
0


0,5
0
c


d
0,1
0

Reprinted from *Océanographie (Nosy Bé II)*, no. 6, 1963, p. 233-254

ZOOPLANKTON RÉCOLTÉ EN MER D'ARABIE, GOLFE PERSIQUE ET GOLFE D'ADEN

(3e Campagne Océanographique du
"Commandant Robert Giraud"
Avril à Juin 1961)

II - PTEROPODES : SYSTEMATIQUE ET REPARTITION

par

S. FRONTIER[1]

Les Ptéropodes constituent un élément remarquablement constant du plankton recueilli lors de la 3ème campagne océanographique du "Robert Giraud" (2) : ils n'ont manqué complètement qu'à la station 188 à laquelle n'a été effectuée qu'une pêche au lamparo.

7054 individus ont été dénombrés, se répartissant comme suit :

	Nombre d'individus	Nombre de stations auxquelles l'espèce était présente sur un total de 80 stations
Limacinidae		
Limacina inflata (d'Orbigny)	754	46
Limacina Lesueuri (d'Orbigny)	2	2
Limacina bulimoides (d'Orbigny)	85	15
Limacina trochiformis (d'Orbigny)	58	20
Cavolinidae		
Creseis acicula Rang	1131	66
Creseis virgula Rang	2315	75
Creseis chierchiae (Boas)	10	3
Cuvierina columnella (Rang)	4	4
Hyalocylix striata (Rang)	47	13
Euclio pyramidata (Linné)	125	21
Cavolinia spp.	328	54
Diacria quadridentata (Lesueur)	324	39
Peraclidae		
Peraclis spp.	284	27

(1) Océanographe biologiste de l'O.R.S.T.O.M. au Centre d'Océanographie et des Pêches de Nosy-Bé (Madagascar)

(2) Liste et carte des stations données dans : Zooplankton récolté en Mer d'Arabie, Golfe Persique et Golfe d'Aden - I) Données Générales - Répartition quantitative par S. FRONTIER - Cahiers du C.O.P.N., N° 1.

	Nombre d'individus	Nombre de stations auxquelles l'espèce était présente sur un total de 80 stations
Cymbuliidae		
Cymbulia spp.	134	39
Corolla spp.	16	11
Desmopteridae		
Desmopterus papilio Chun	1244	65
Desmopterus Gardineri Tesch	21	9
Pneumodermatidae		
Pneumodermopsis paucidens (Boas)	46	2
Cliopsidae		
Cliopsis Krohni Troschel	1	1
Clionidae		
Clionina longicaudata (Souleyet)	55	15
Larves de Gymnosomes indéterminés	70	30

Du fait de l'acidité du formol utilisé pour la fixation la plupart des coquilles se sont trouvées dissoutes lors de l'examen des échantillons. Il s'ensuit que les genres chez lesquels les distinctions spécifiques ne peuvent, dans l'état actuel de nos connaissances, être établies d'après les seules parties molles n'ont pu être déterminés : c'est le cas de *Cavolinia* et de *Peraclis* , qui seront donc envisagés globalement.

Par ailleurs, comme cela se produit très généralement, les pseudoconques des *Cymbulia* et *Corolla* étaient détachées du corps des animaux, et même la plupart du temps perdues, de sorte que la détermination spécifique de ces 2 genres n'a pas non plus été possible.

Les espèces ou groupes d'espèces envisagés se rangent en ce qui concerne la fréquence (nombre de stations) et l'abondance (nombre d'individus), de la façon suivante :

Ordre de fréquence	Ordre d'abondance
Creseis virgula	*Creseis virgula*
Creseis acicula	*Desmopterus papilio*
Desmopterus papilio	*Creseis acicula*
Cavolinia	*Limacina inflata*
Limacina inflata	*Cavolinia*
Diacria quadridentata	*Peraclis*
Cymbulia	*Diacria quadridentata*
Larves de Gymnosomes indéterminés	*Cymbulia*
Peraclis	*Euclio pyramidata*
Euclio pyramidata	*Limacina bulimoides*
Limacina trochiformis	Larves de Gymnosomes indéterminés
Limacina bulimoides	*Limacina trochiformis*
Clionina longicaudata	*Clionina longicaudata*
Hyalocylix striata	*Hyalocylix striata*
Corolla	*Pneumodermopsis paucidens*
Desmopterus Gardineri	*Desmopterus Gardineri*
Cuvierina columnella	*Corolla*
Creseis chierchiae	*Creseis chierchiae*
Limacina Lesueuri	*Cuvierina columnella*
Pneumodermopsis paucidens	*Limacina Lesueuri*
Cliopsis Krohni	*Cliopsis Krohni*

On voit que les deux classements coincident à quelques inversions près.

Le nombre moyen d'individus recueillis par un trait de filet de 100 m. à la surface varie pour l'ensemble des stations de 1 à 278, mais ne se répartit pas géographiquement de façon suggestive. Par contre le nombre d'espèces récoltées dans une station est sujet à d'importantes variations en fonction de la localisation géographique.

Une première constatation est la pauvreté en espèces du Golfe Persique : deux ou trois espèces par station, soit au total 8 espèces dont une seule abondante et pratiquement constante :

Creseis virgula (10 stations sur 11, 164 individus), et trois relativement abondantes :

Limacina inflata (20 individus en 3 stations proches de l'entrée)

Cavolinia sp. (6 stations, 18 individus)

Desmopterus papilio (5 stations, 16 individus)

On remarque que ces quatre espèces sont parmi les plus abondantes et parmi les plus fréquentes pour l'ensemble de la campagne : il s'agit sans doute d'espèces tolérantes vis à vis d'une eau de caractéristiques très particulières.

Les autres espèces rencontrées sont très rares :

Creseis acicula (2 individus à l'entrée du Golfe)

Hyalocylix striata (2 individus à l'entrée du Golfe)

Corolla sp. (1 individu à l'entrée du Golfe)

Clionina longicaudata (1 individu)

Cette pauvreté en espèces doit être rapprochée de la relative abondance quantitative du plankton de cette zone, ainsi qu'il ressort de l'étude des volumes recueillis (FRONTIER 1963 - a). Ces deux propriétés caractérisent une eau essentiellement néritique, les fonds du Golfe Persique n'excédant guère 75 m.

A l'opposé on doit noter une richesse particulière en espèces dans Golfe d'Aden, pour lequel l'étude des volumes de plankton recueillis avait conclu à une extrême pauvreté quantitative. A un moindre degré ce caractère a son répondant dans le Golfe d'Oman, ce qui semblerait indiquer une certaine parenté, du point de vue écologique, entre ces deux secteurs. En effet un certain nombre d'espèces ne sont présentes ou abondantes que dans ces deux golfes - la zone du Golfe d'Oman s'étendant parfois à tout l'extrême Nord de la Mer d'Arabie et celle du Golfe d'Aden à la côte Sud-Est de l'Arabie. C'est le cas de *Limacina inflata*, *Limacina trochiformis*, *Corolla spp.*, *Clionina longicaudata*. Le Golfe d'Aden reste néanmoins plus riche en espèces que le Golfe d'Oman : *Limacina bulimoides*, *Limacina Lesueuri* et *Pneumodermopsis paucidens* n'ont été récoltés qu'en Golfe d'Aden. *Peraclis* sp. est pratiquement constant dans le Golfe d'Aden et le long de la côte Sud-Ouest d'Arabie, sporadique dans le Nord de la Mer d'Arabie et absent dans le Golfe d'Oman comme du Gofe Persique ; il en est de même de *Euclio pyramidata*. *Diacria quadridentata* et *Cymbulia spp.*, sont assez constants dans le Golfe d'Aden et la Mer d'Arabie, et absents ou presque du Golfe d'Oman.

EUTHECOSOMATA

LIMACINIDAE —

Limacina inflata (d'Orbigny) - (Carte 1) : Espèce venant au 4e rang pour l'abondance et au 5e rang pour la fréquence; abondante surtout dans le Nord de la Mer d'Arabie et dans le Golfe d'Aden. Quelques individus dans trois stations du Golfe Persique.

Cette espèce disparait presque complètement pendant le jour de la couche 100 m. - surface. Sur 80 stations auxquelles du plankton a été récolté 44 eurent lieu pendant le jour et 36 pendant la nuit; les récoltes diurnes n'ont ramené que 60 individus au total dans la couche des 100 premiers mètres, contre 686 pour les récoltes nocturnes. Le phénomène est particulièrement net pour les deux régions où l'espèce est le moins sporadique : l'extrême Nord de la Mer d'Arabie et le Golfe d'Aden. Pour le premier secteur on ne trouve que 8 individus récoltés entre 100 m. et la surface pendant le jour : 4 à 18h. 15 et 4 à 06h. 15, c'est-à-dire au coucher du soleil et à l'aurore. Par ailleurs des récoltes plus profondes effectuées pendant la journée ont ramené quelques individus : 2 de 1500 m. à la surface (station 196, 14h. 30), 4 de 500 à 100 m. (station 196, 16h. 00), 2 de 500 m. à la surface (station 209, 15h. 15); en fait le très petit nombre de récoltes profondes effectuées au cours de cette campagne ne permet pas de déterminer les profondeurs à laquelle se tient *Limacina inflata* pendant le jour. Dans le Golfe d'Aden 9 individus ont été récoltés de jour contre 290 de nuit.

Limacina lesueuri (d'Orbigny) - Espèce présente de façon rare et sporadique dans tout l'Océan Indien. La collection du "Robert Giraud" n'en contient que 2 spécimens, récoltés en deux stations du Golfe d'Aden :

	Latitude	Longitude	Immersion	Heure
263	12°45' S	51°50' E	50 m - surface	01h. 00
272	12°00' S	46°41' E	50 m - surface	06h. 15

Limacina bulimoides (d'Orbigny) - (Carte 2) : 85 individus récoltés en 13 stations du Golfe d'Aden et en deux stations (un individu à chacune d'elles) au large de la côte Sud-Est d'Arabie. La plupart ont été récoltés la nuit; 6 individus seulement proviennent de 4 stations occupées pendant le jour.

Limacina trochiformis (d'Orbigny) - (Carte 3) : 58 individus répartis de la façon suivante : 10 stations dans le Golfe Persique, trois au large de la côte Sud d'Arabie et 7 dans le Nord et l'Est de la Mer d'Arabie, à peu de distance des côtes de l'Inde et du Pakistan. Généralement un à trois individus par récolte; quatre à neuf aux 4 stations 263, 264, 265 et 266, voisines du Cap Gardafui.

Contrairement aux trois espèces précédentes qui effectuent des migrations verticales importantes, celle-ci semble appartenir à l'épiplankton. En effet sur les 20 stations auxquelles elle a été trouvée, 10 ont eu lieu de jour et 10 de nuit. Elle était également présente, à l'exclusion d'autres *Limacina*, dans les récoltes à l'épuisette en surface aux stations 260 et 271.

CAVOLINIDAE —

Creseis acicula Rang. Troisième espèce dans l'ordre d'abondance, seconde dans l'ordre de fréquence. Absente du Golfe Persique, sauf deux individus non loin de l'entrée du Golfe. Présente à toutes les autres stations sauf deux, en nombre très variable mais nettement inférieur aux stations de jour qu'aux stations de nuit (278 individus dans 32 stations de jour, sur 66 où les 1131 individus ont été trouvés).

Creseis virgula Rang. Cette espèce est à la fois la plus abondante et la plus fréquente, constituant en nombre le tiers de l'effectif total des Ptéropodes, et ayant été récoltée à toutes les stations sauf 3. C'est en particulier la seule espèce présente en quantité notable dans le Golfe Persique, où elle ne manque qu'en une station. Le tiers environ des individus a été récolté de jour.

Creseis chierchiae (Boas). 10 individus récoltés en 3 stations (deux en Mer d'Arabie, une dans le Golfe d'Aden), ainsi qu'il a été mentionné dans une note antérieure (FRONTIER 1963 - c).

Cuvierina columnella (Rang) - (Carte 4) - 4 individus juvéniles récoltés en 4 stations de la Mer d'Arabie et du Golfe d'Aden.

Hyalocylix striata. (Rang) - (Carte 4) - 47 individus répartis sporadiquement en Mer d'Arabie et Golfe d'Aden, ainsi qu'en une station du Golfe d'Oman (un individu) et une à l'entrée du Golfe Persique (2 individus). 8 individus seulement proviennent de stations de jour.

Euclio pyramidata (Linné) - (Carte 5) - 125 individus. L'espèce est assez constante dans le Golfe d'Aden, et sporadique dans la moitié Ouest de la Mer d'Arabie. Un individu dans le Golfe d'Oman.

Cavolinia spp. - 328 individus, répartis assez sporadiquement dans toute la zone prospectée; absentes cependant de la moitié Sud-Est du Golfe Persique, et d'une zone située au voisinage du Ras el Had. Autant d'individus capturés de jour que de nuit.

Vu le mauvais état ou la disparition complète des coquilles, la détermination spécifique n'a été possible que dans 15 récoltes, soit en 12 stations réparties dans toute la zone prospectée : 82 individus, appartenant tous à l'espèce *C. longirostris* (Lesueur), et adultes.

Diacria quadridentata (Lesueur) - (Carte 6) - 233 individus. La répartition de cette espèce est singulière : à peu près constante dans la Mer d'Arabie proprement dite et le Golfe d'Aden, elle manque totalement dans le Golfe Persique et le Golfe d'Oman ainsi qu'en quelques stations proches du Ras el Had. Un tiers environ des individus a été capturé de jour.

PSEUDOTHECOSOMATA

PERACLIDAE —

Peraclis spp. (Carte 7) - Les déterminations spécifiques ont été impossibles pour ce genre en raison de la dissolution complète des coquilles.

284 individus, localisés principalement dans le Golfe d'Aden et aux stations longeant la côte Sud-Est de l'Arabie (ils ne manquent qu'en deux stations de ce secteur océanique). De plus 8 individus ont été capturés en 4 stations du centre de la Mer d'Arabie.

Même nombre d'individus récoltés de jour et de nuit.

CYMBULIIDAE —

Cymbulia spp. (Carte 8) - 134 individus, tous détachés de leur pseudoconque, plus une cinquantaine de pseudoconques isolées appartenant à l'espèce *Cymbulia sibogae* Tesch.

Répartition assez régulière dans le Golfe d'Aden et la Mer d'Arabie; deux individus dans le Golfe d'Oman; aucun dans le Golfe Persique. Captures de jour et de nuit d'importances presque égales.

Corolla spp. (Carte 9) - 16 individus (tous détachés de leur pseudoconque), récoltés en 11 stations situées d'une part dans le Golfe d'Oman ou près de son entrée, d'autre part dans le Golfe d'Aden. 4 individus seulement ont été récoltés de nuit.

DESMOPTERIDAE —

Desmopterus papilio Chun (Carte 10; Fig. 1 et 3) - Cette espèce, jusqu'ici trouvée en un petit nombre de stations dans l'Océan Indien (MEISENHEIMER 1903 : 10 stations de la *Tiefsee Expédition*), et complètement absente du matériel du DANA (TESCH 1948), se trouve curieusement être ici la troisième en fréquence (65 stations sur 80) et la seconde en abondance (1244 individus, soit presque le cinquième de l'effectif total des Ptéropodes récoltés). C'est une des rares espèces représentées dans le Golfe Persique. Sa répartition d'ensemble est assez irrégulière, le nombre d'individus par récolte variant de 1 à 79. Autant d'individus capturés de jour et de nuit.

Desmopterus Gardineri Tesch (Carte 11; Fig. 2 et 4) - Cette espèce n'était connue jusqu'à présent que par un seul spécimen récolté près des Chagos (TESCH 1910). La collection du "Robert Giraud" en contient 21, récoltés en 9 stations de la Mer d'Arabie, du Golfe d'Aden et du Golfe d'Oman. Tous sont juvéniles : tentacules postérieurs des parapodies à l'état de moignon; envergure comprise entre 0,9 et 1,5 mm.

Cette espèce se distingue essentiellement de *Desmopterus papilio* par la musculature des parapodies, dont les fibres se groupent en un double système de bandelettes entrecroisées qui restent distinctes d'une extrémité à l'autre, contrairement à l'espèce précédente chez laquelle ces fibres se mêlent de façon confuse - au moins dans la partie médiane -, et sans jamais former de bandelettes. Ces deux dispositions sont visibles sur les photographies des figures 1 et 2, représentant les parapodies des deux espèces, la figure 1 représentant un *D. papilio* approximativement au même stade que les *D. Gardineri* récoltés (tentacules parapodiaux réduits à une paire de moignons).

Contrairement à l'exemplaire décrit par TESCH, le bord extérieur de la parapodie est très convexe et non légèrement concave. Par ailleurs un second caractère distinguant les deux espèces, que n'avait pas signalé l'auteur précédent, est la plus grande taille du corps de l'animal en comparaison des parapodies chez *D. Gardineri* (fig. 2 et 3 représentant les deux espèces à des stades à peu près équivalents). Toutefois ces deux derniers caractères sont peut-être des caractères juvéniles de *D. Gardineri* et ne sont peut-être pas à retenir en tant que caractères spécifiques.

GYMNOSOMES

PNEUMODERMATIDAE —

Pneumodermopsis paucidens (Boas) - 46 spécimens, récoltés dans des traits horizontaux près de la surface, en deux stations voisines du Golfe d'Aden :

271	12°02' N	47°22'5 E	immersion : 10 m.	(7 individus)
280	11°51' N	47°23' E	immersion : 1 m.	(32 individus)
			immersion : 10 m.	(7 individus)

Longueur à l'extension : 1,2 à 3 mm. Cette espèce n'avait pas encore été signalée en Océan Indien.

CLIONIDAE —

Clionina longicaudata (Souleyet) - (Carte 12) - 55 individus, récoltés presque tous de nuit dans le Golfe d'Oman et le Golfe d'Aden, plus un individu dans le Golfe Persique et un dans le centre de la Mer d'Arabie.

Cette espèce n'avait été signalée précédemment qu'en deux stations de l'Océan Indien : une au Sud du Canal de Mozambique et une autre au large de Sumatra (TESCH 1950), ainsi qu'au voisinage de Nosy Bé. (FRONTIER 1963 b).

CLIOPSIDAE —

Cliopsis krohni Troschel (= *grandis* Boas d'après PRUVOT-FOL 1924). 1 individu de 32 mm. à la station 209 (entrée du Golfe d'Oman), entre 500 m. et la surface.

Cette espèce est déjà connue de l'Océan Indien (PRUVOT-FOL 1942; TESCH 1950).

BIBLIOGRAPHIE

BOAS (J.E.V.) 1886 - Spolia atlantica : Bidtrag til Pteropodernes-Morfologi og Systematic samt til Kundskaben om deres geografiske Udbredelse.
Dansk. Vidensk. Selk. Skrifter - 6. Raekke, Afd 4, Bd 1, pp. 1-231, pl.8

FRONTIER (S.) 1963 a - Zooplankton récolté en Mer d'Arabie, Golfe Persique et Golfe d'Aden (3ème campagne océanographique du "Commandant Robert Giraud" - Avril à Juin 1961. I) Données générales, répartition quantitative. *Cahiers du Centre d'Océanographie et des Pêches de Nosy Bé, 1, pp. 17-30*

1963 b - Hétéropodes et Ptéropodes récoltés dans le plankton de Nosy Bé.
Ibid., 2, pp. 213-227

1963 c - Présence de *Creseis chierchiae* (Boas) dans l'Océan Indien.
Ibid. pp. 229-232

KWIETNIEWSKI (C.) 1903 - Contribuzioni alla conoscenza anatomo-zoologica del Pteropoda Gimnosomi del Mare Mediterranea.
Rich. Lab. Anat. Norm. Univ. Roma, 9., pp. 245-343, 3 pl.

MEISENHEIMER (J.) 1905 - Pteropoda
Tiefsee Expedition "Valdivia" 9 (1). pp. 1-314, Cartes 1-9, pl. 1-27

PRUVOT-FOL (A.) 1924 - Etude de quelques Gymnosomes méditarranéens des pêches de l'"Orvet" en 1921-1922.
Arch. Z. Exp., 62

1926 - Mollusques Ptéropodes Gymnosomes provenant des campagnes du Prince Albert Premier de Monaco.
Rés. Camp. Sc. Monaco, 70, pp. 1-60, pl. 1-3.

1942 - Les Gymnosomes
Dana rep., 20, pp. 1-54

TAKI (L.) et OKUTANI (T.) 1962 - Report on the biological results of the "Umitoka Maru" Expedition. II) Planktonic Gastropods collected from the Pacific and Indian Oceans.
J. Fac. Fish. and Animal Husbandry, Hiroshima Univ. 4, pp. 81-96

TESCH (J.J.) 1904 - The Thecosomata and Gymnosomata of the Siboga Expedition.
Siboga Exp., Livr.16, Monogr.52, pp.1-89, pl.1-6.

TESCH (J.J.) 1910 - The Percy Sladen Trust Expedition in Indian Ocean. X) Pteropoda and Heteropoda.
Trans. Lin. Soc. London, 2e série, 14 (1), pp. 165-189 pl. 12-14

1913 - Pteropoda
Bronn's Tierreich, Lief.36, pp. 1-154

1946 - The Thecosomatous Pteropods. I) The Atlantic.
Dana Rep. 28, pp. 1-82, pl. 1-8

1948 - The Thecosomatous Pteropods. II) The Indopacific.
Ibid., 30, pp. 1-45, pl. 1-3

1950 - Gymnosomata II
Ibid., 36, pp. 1-55

VINOGRADOV (M. E.) et VORONINA (N. M.) 1962 - "Données sur la distribution du Zooplankton dan
le Nord de l'Océan Indien". (en russe)
Trudy Inst. Okean. 58, pp.80-113

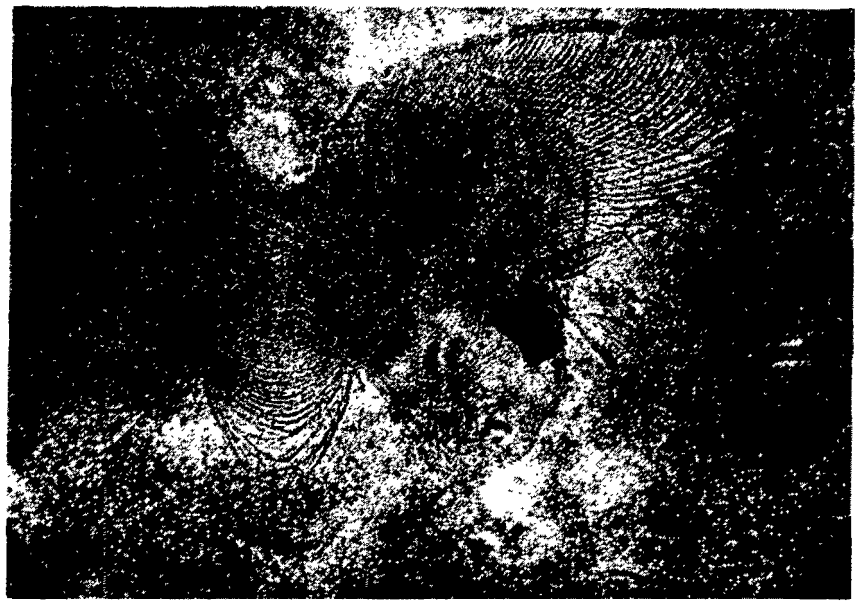
FIGURES

1 - Parapodies d'un *Desmopterus papilio* jeune.

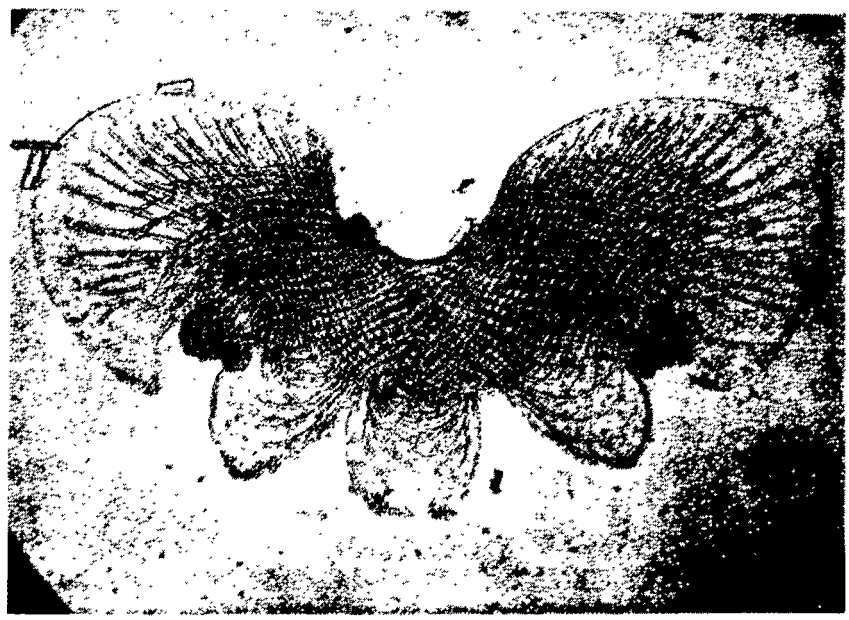
2 - Parapodies d'un *Desmopterus Gardineri* jeune.

3 - *Desmopterus papilio* jeune, vue latérale, parapodies rabattues vers la face ventrale.

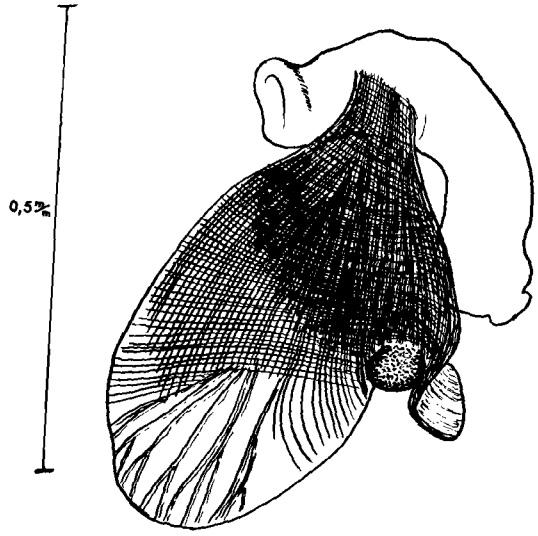
4 - *Desmopterus Gardineri* jeune, même disposition.



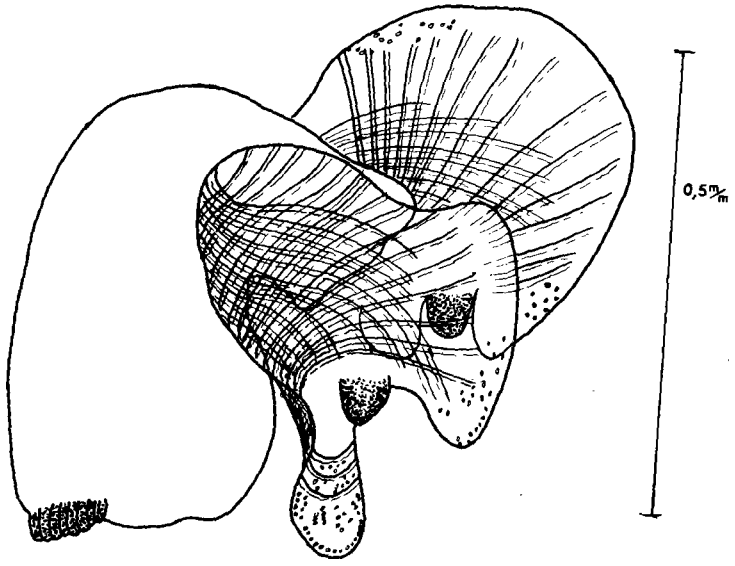
1



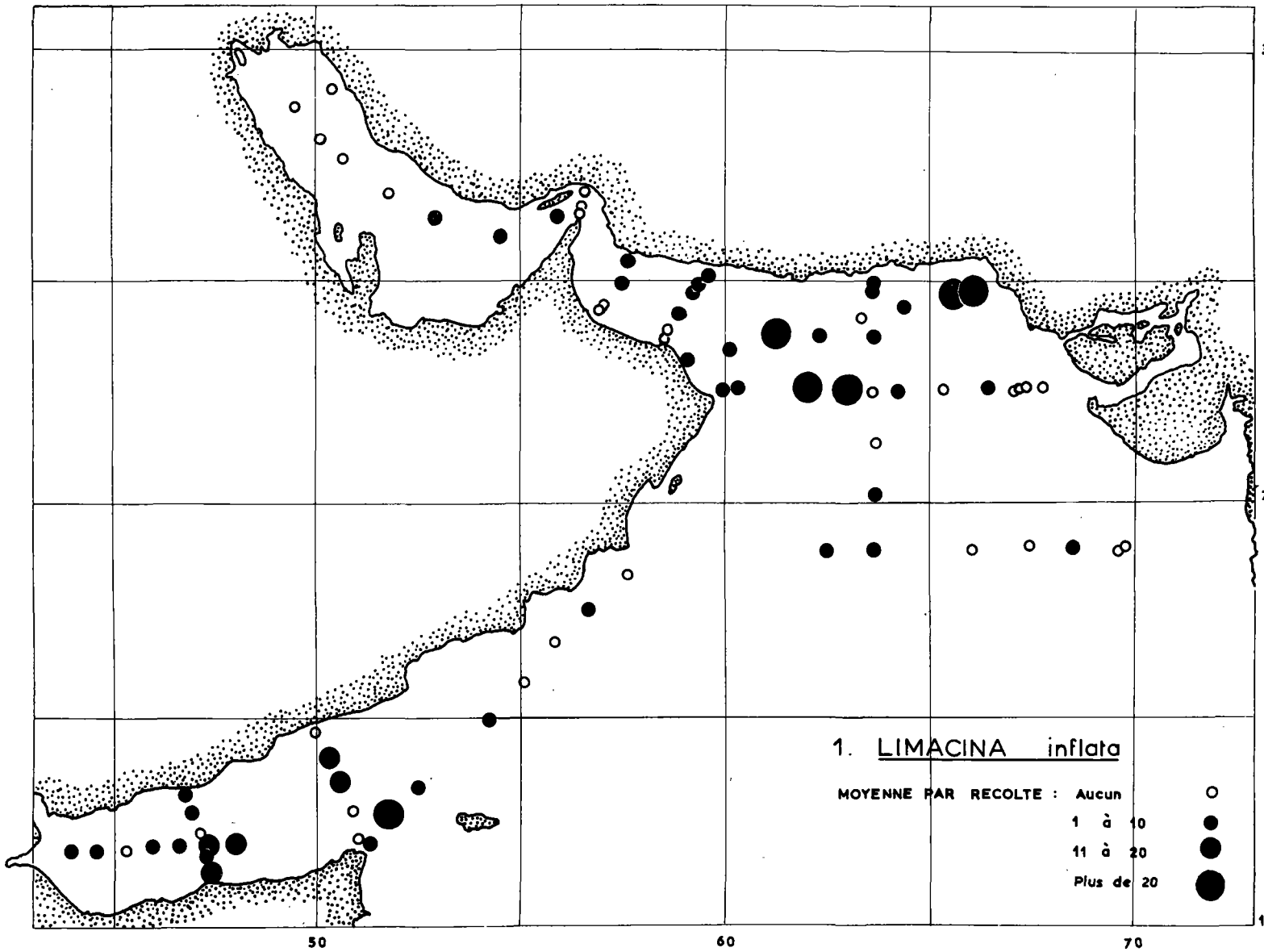
2

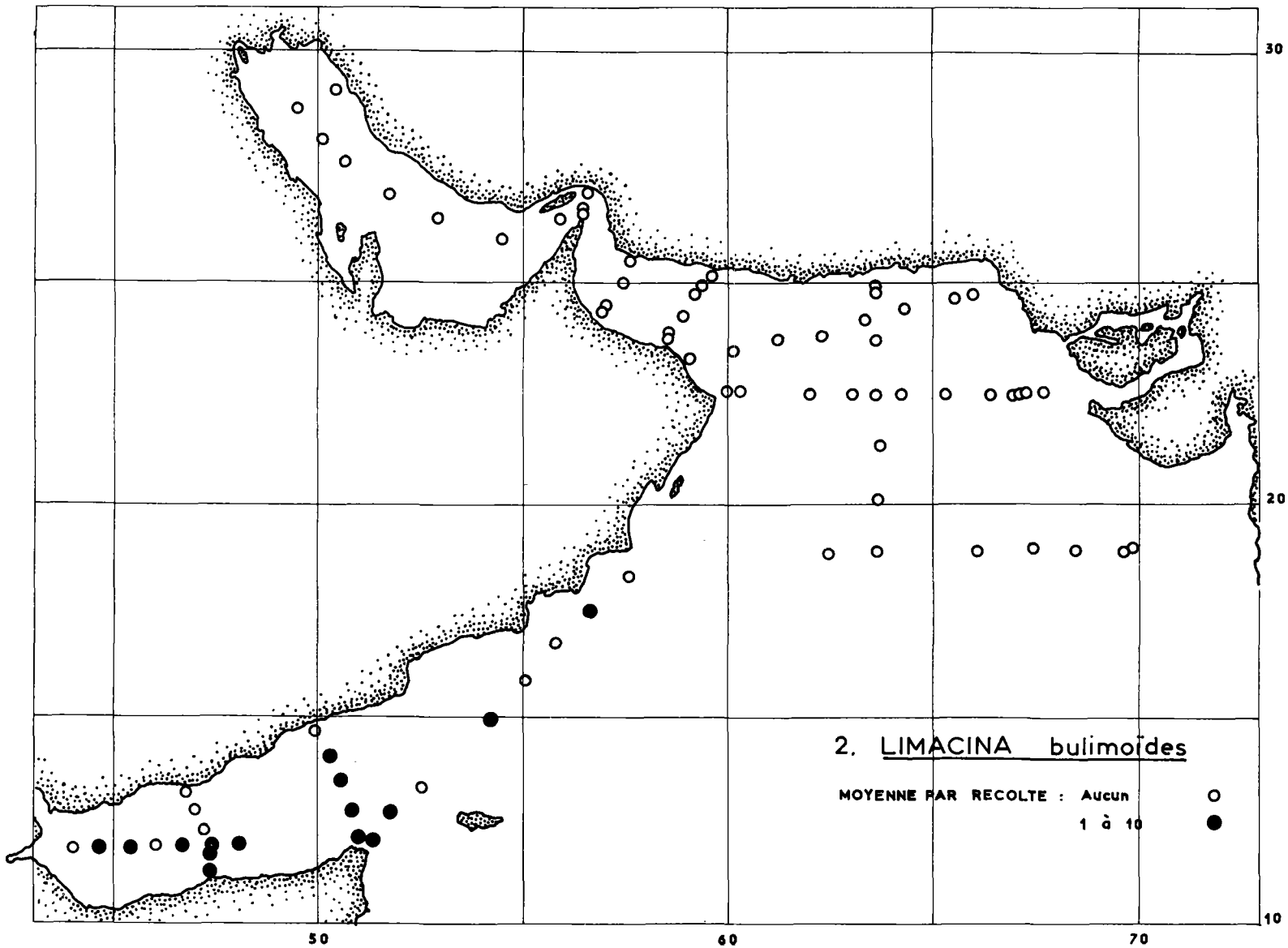


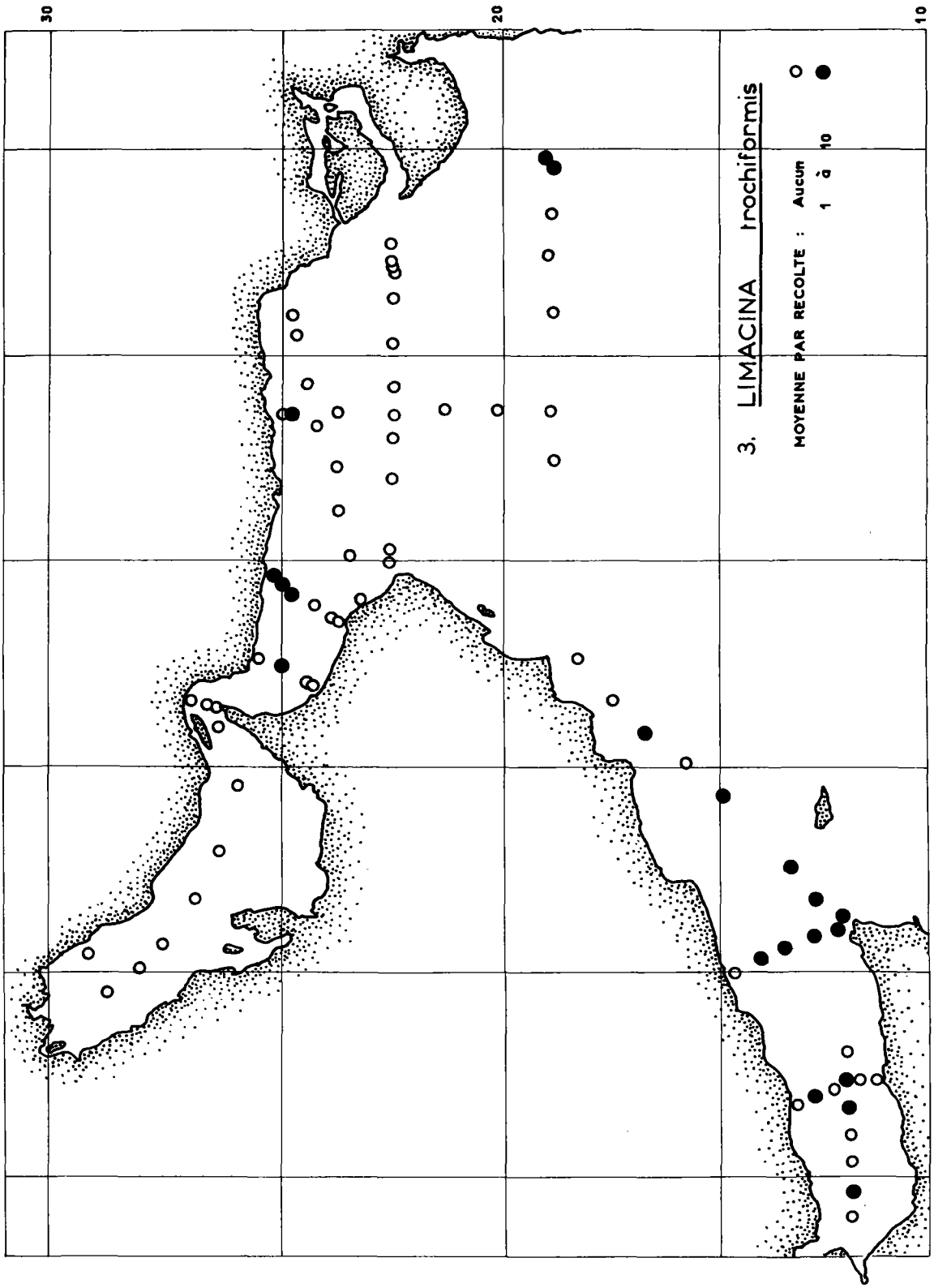
3

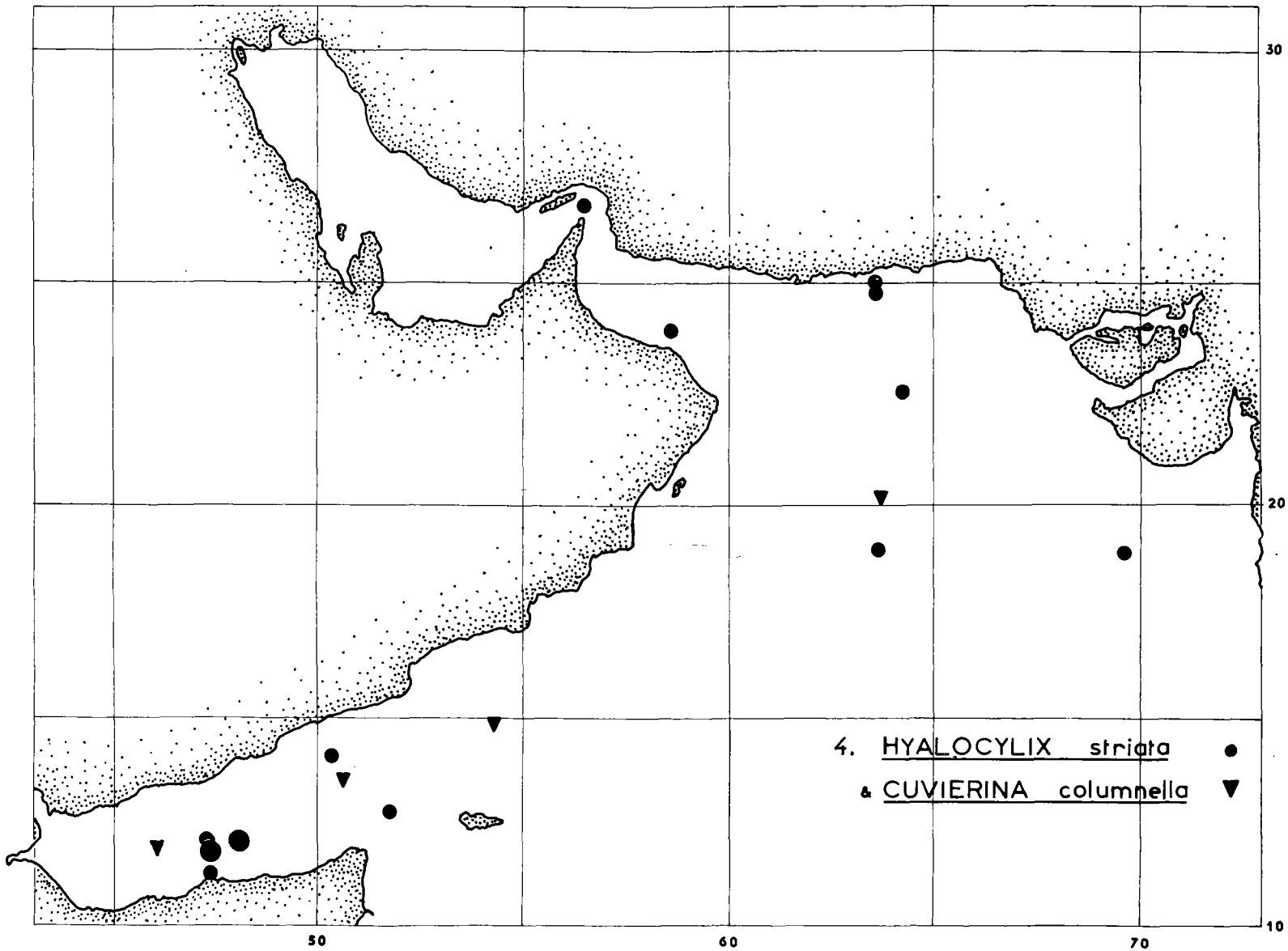


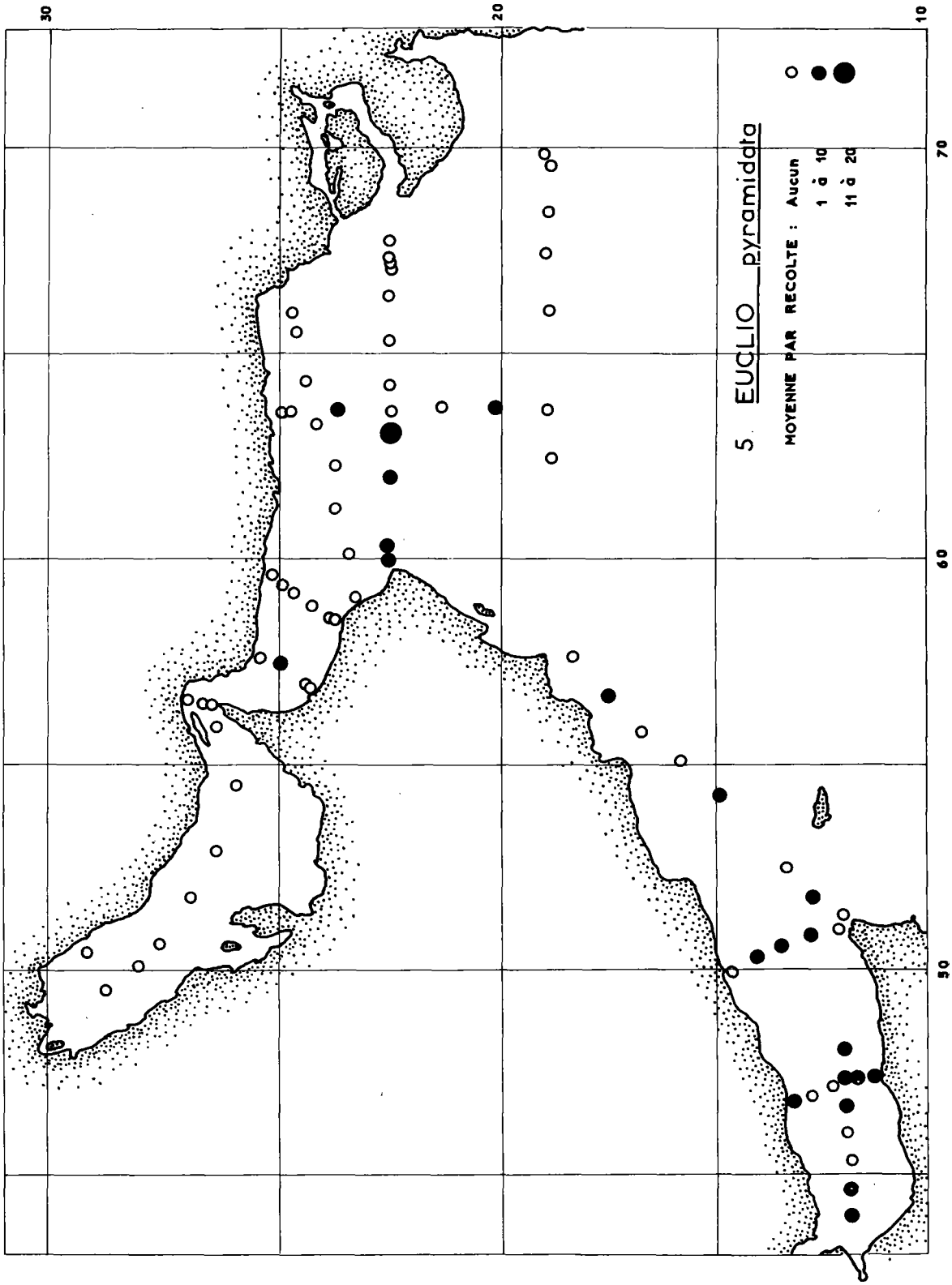
4

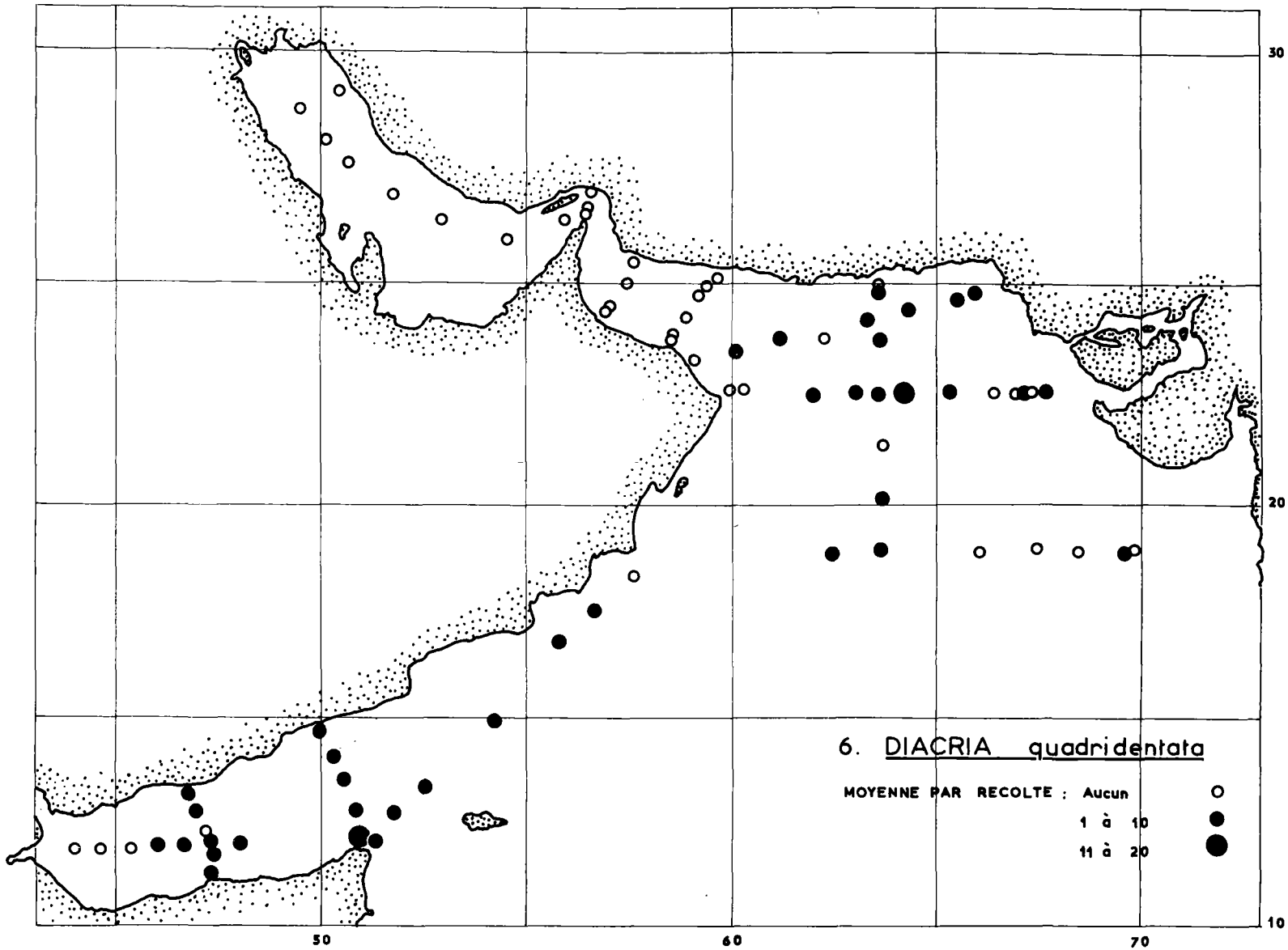

30
20
10
50
60
70
1. LIMACINA inflata
MOYENNE PAR RECOLTE : Aucun
1 à 10
11 à 20
Plus de 20

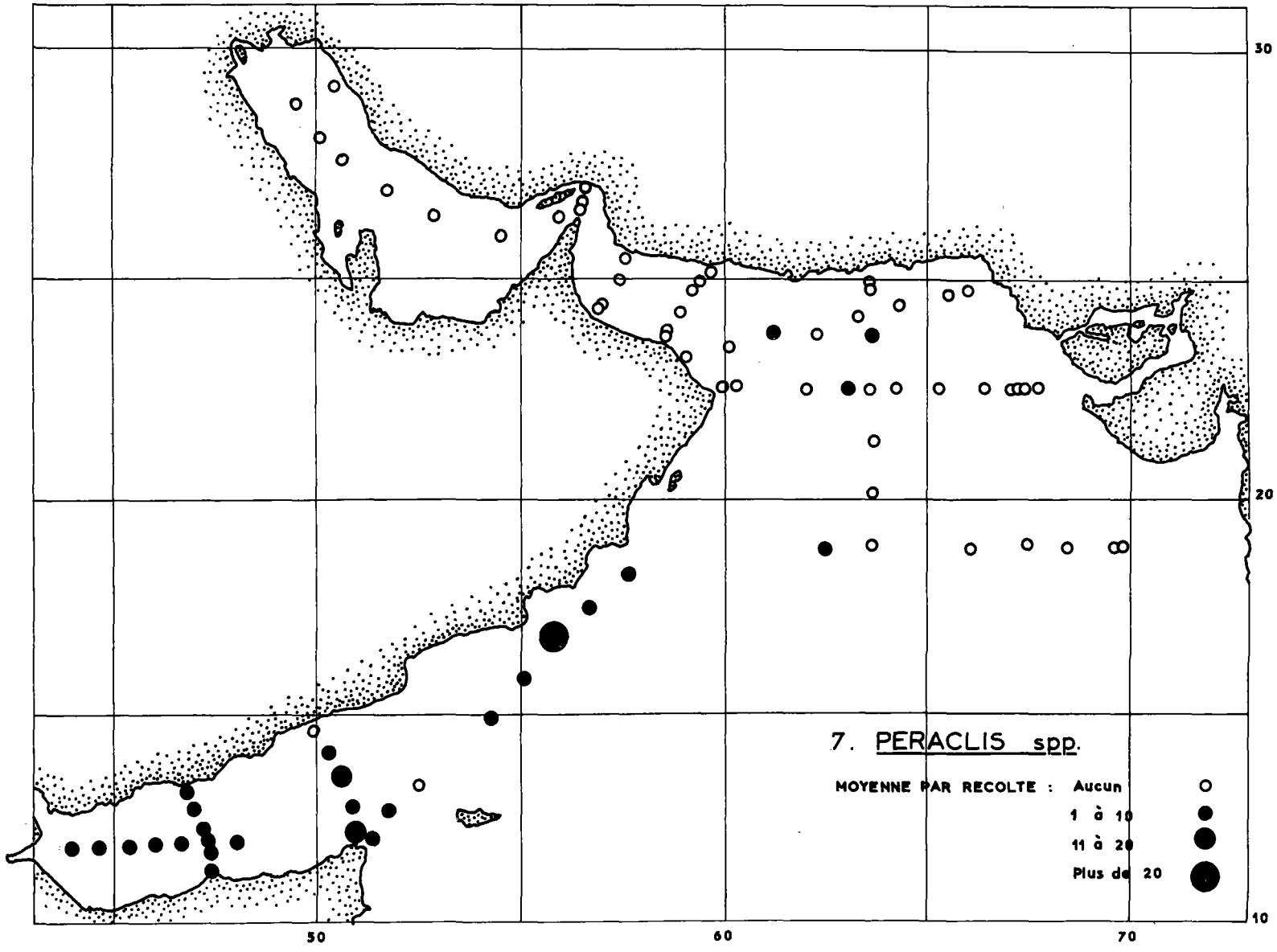

30
20
10
50
60
70
2. LIMACINA bulimoïdes
MOYENNE PAR RECOLTE : Aucun
1 à 10

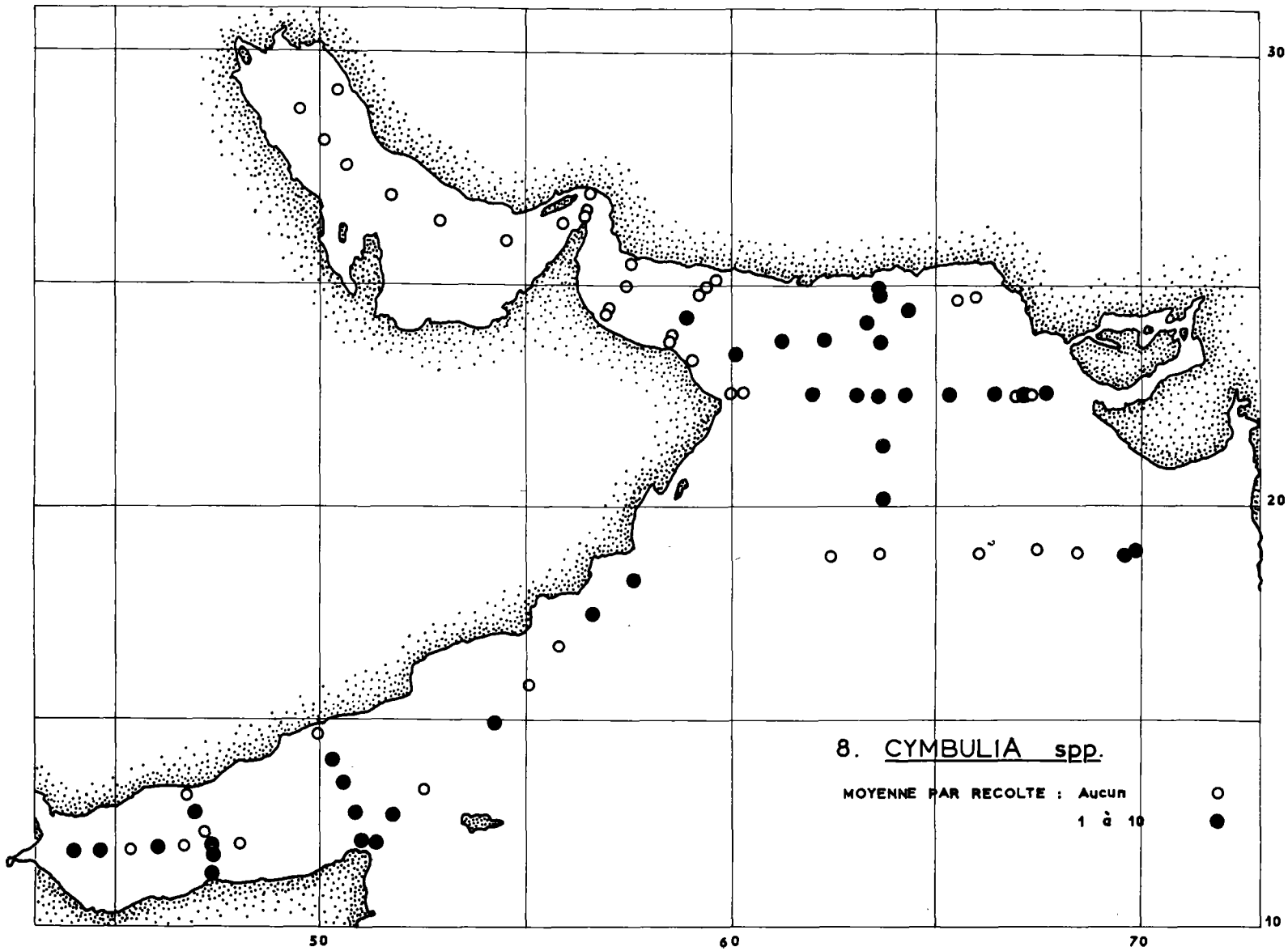

3. LIMACINA trochiformis
MOYENNE PAR RECOLTE : Aucun
1 à 10
30
20
10
70
60
50

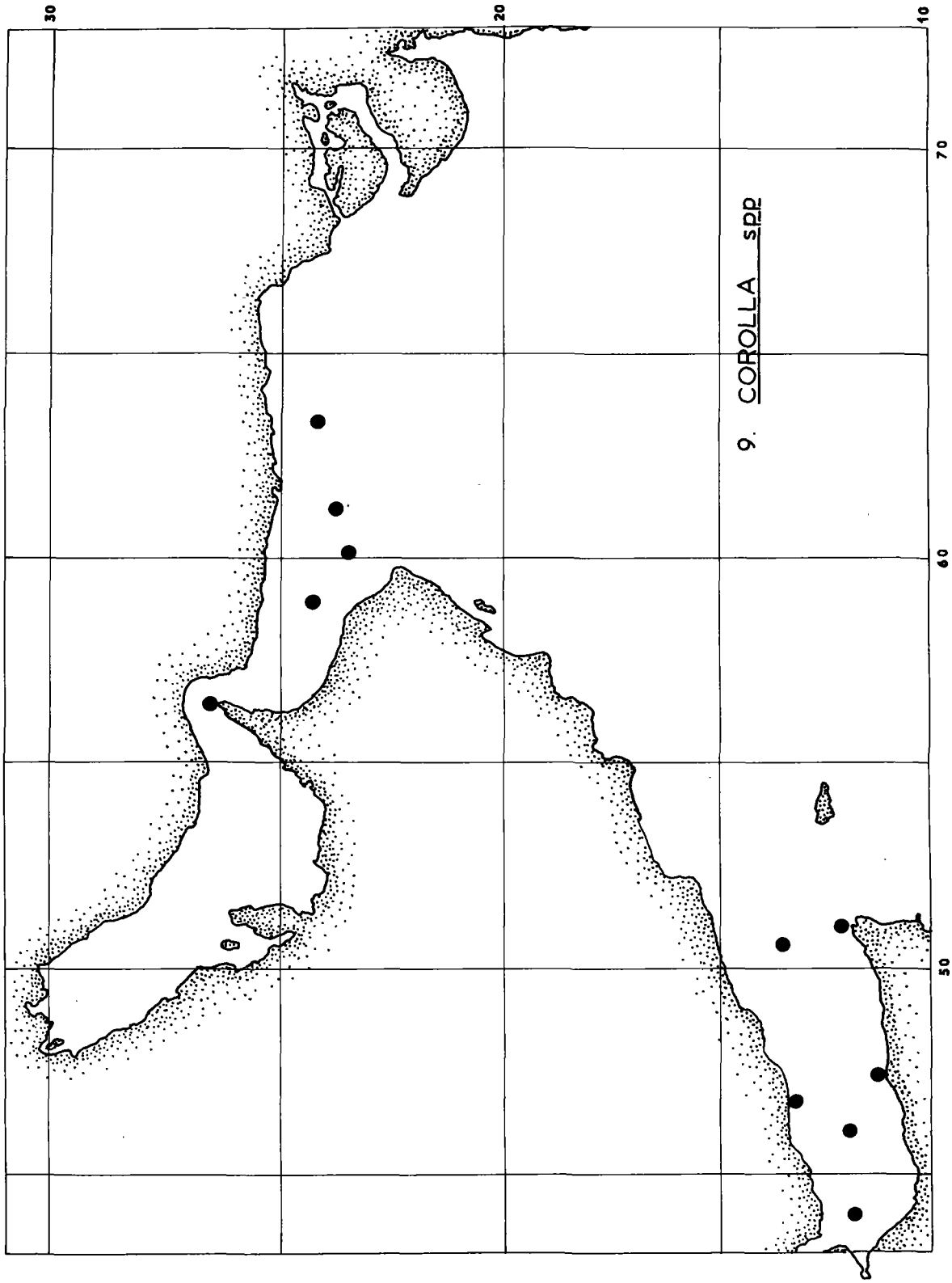

30
20
10
50
60
70
4. HYALOCYLIX striata
& CUVIERINA columnella

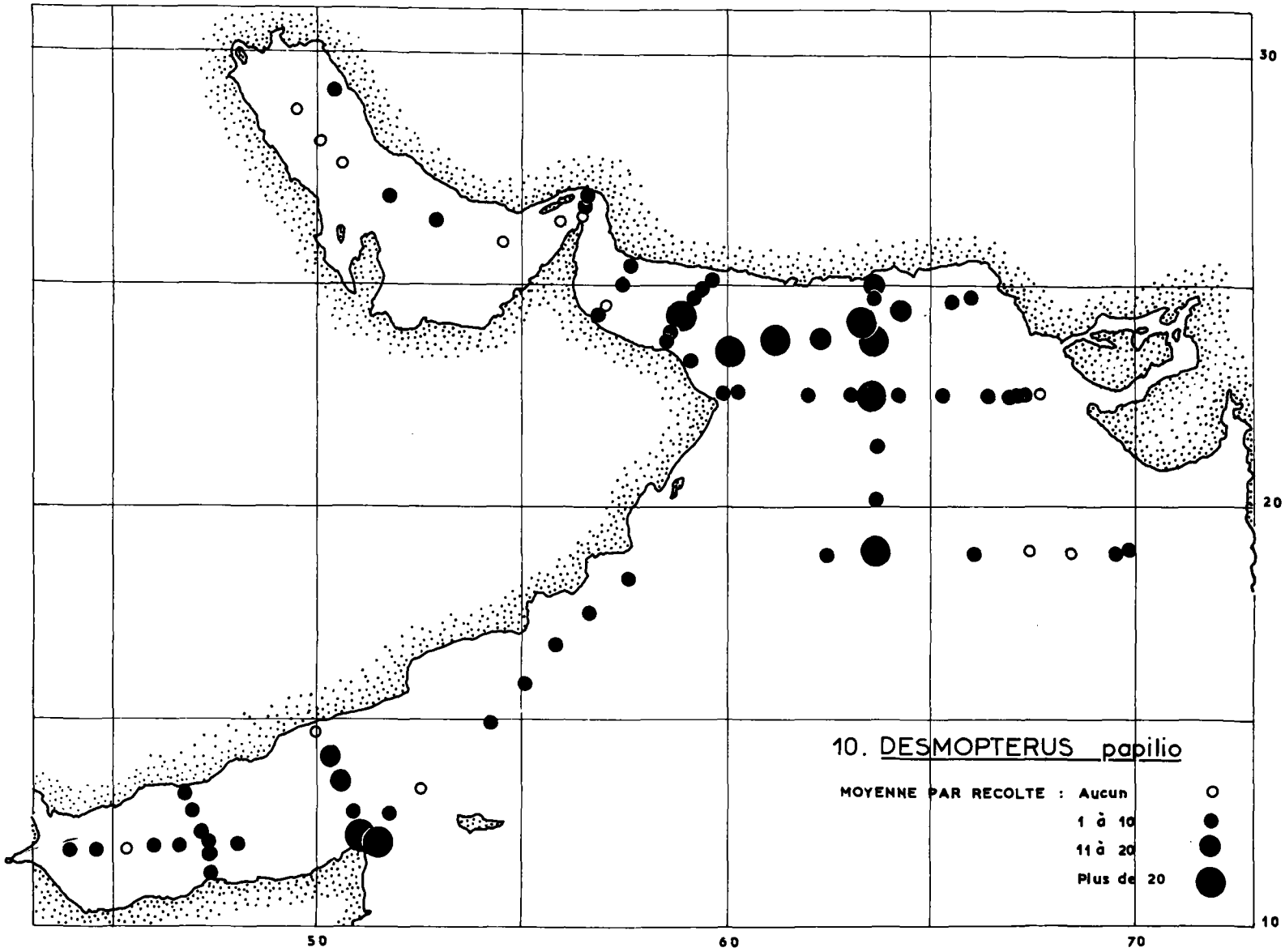

30
20
10
70
60
50
5 EUCLIO pyramidata
MOYENNE PAR RECOLTE : Aucun
1 à 10
11 à 20

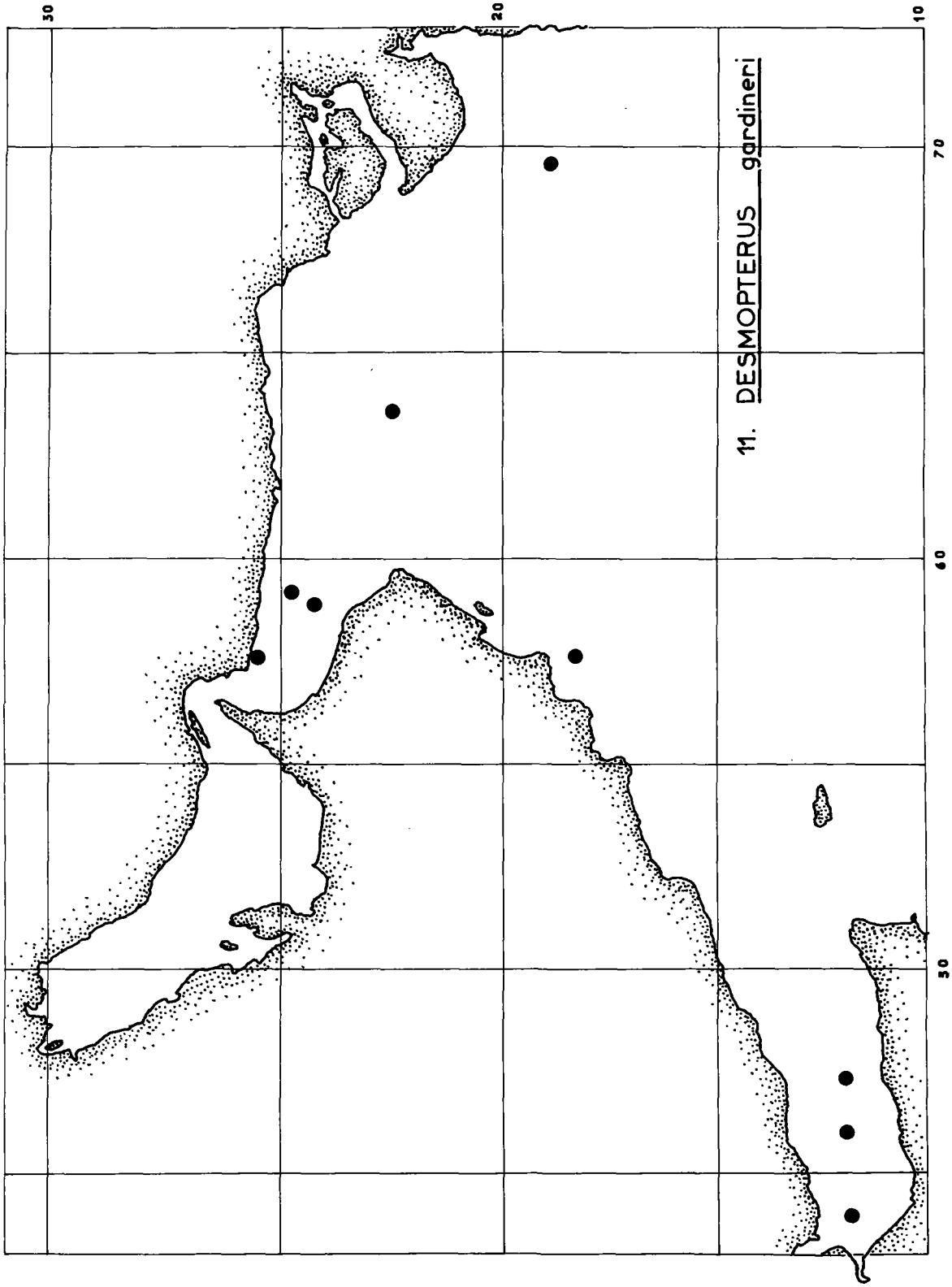

30
20
10
50
60
70
6. DIACRIA quadridentata
MOYENNE PAR RECOLTE : Aucun
1 à 10
11 à 20

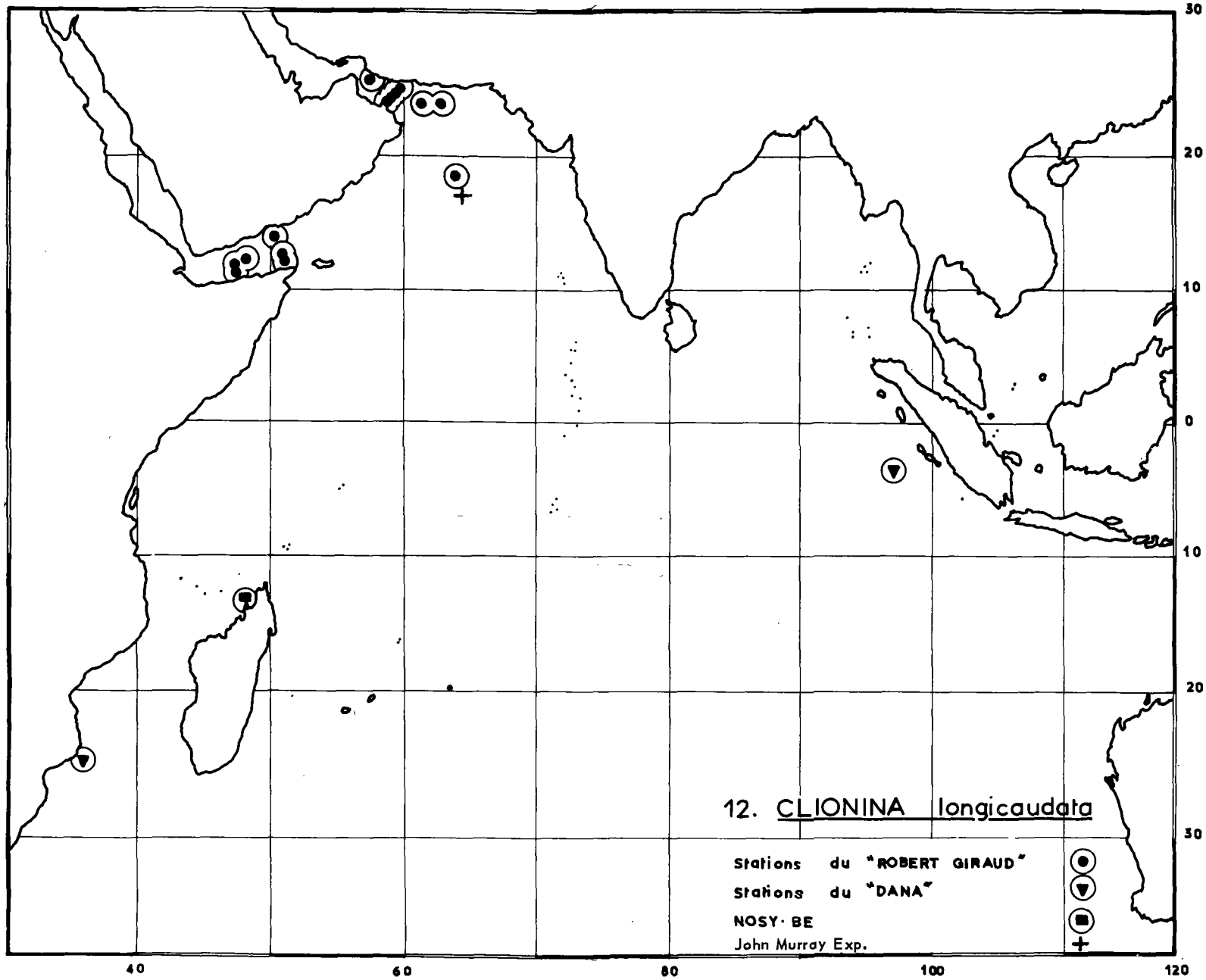

30
20
10
50
60
70
7. PERACLIS spp.
MOYENNE PAR RECOLTE : Aucun
1 à 10
11 à 20
Plus de 20


30
20
10
50
60
70
8. CYMBULIA spp.
MOYENNE PAR RECOLTE : Aucun
1 à 10


30
20
10
70
60
50
9. COROLLA spp


30
20
10
50
60
70
10. DESMOPTERUS papilio
MOYENNE PAR RECOLTE : Aucun
1 à 10
11 à 20
Plus de 20


30
20
10
70
60
50
11. DESMOPTERUS gardineri


30
20
10
0
10
20
30
40
60
80
100
120
12. CLIONINA longicaudata
Stations du "ROBERT GIRAUD"
Stations du "DANA"
NOSY-BE
John Murray Exp.

Reprinted from *Océanographie (Nosy Bé II)*, no. 6, 1963, p. 213-227

HETEROPODES ET PTEROPODES RÉCOLTES DANS LE PLANKTON DE NOSY-BE

par

S. FRONTIER[1]

I - ESPECES RENCONTREES - REPARTITION GENERALE

La présente étude est le résultat de l'examen de 54 récoltes de plankton effectuées dans le voisinage de Nosy-Bé entre Octobre et Décembre 1960.

L'ile de Nosy-Bé est située sur un vaste plateau corallien semé d'herbiers de Zostéracées, attenant au continent malgache; les fonds sont généralement compris entre 15 et 50 mètres. Le fond de nombreuses baies, tant sur la côté de Nosy-Bé que sur celle de Madagascar même, est vaseux et garni de mangrove, recevant fréquemment des apports d'eau douce. Au large le plateau continental tombe très brutalement vers des fonds de l'ordre de 1000 à 1500 mètres. L'on devait s'attendre à trouver une influence pélagique en explorant les abords du talus continental, influence manquant au contraire totalement à l'intérieur des rades vaseuses.

Le premier échantillonnage de zooplankton que constituent les 54 récoltes étudiées ici a permis d'ébaucher une comparaison entre ces deux types de localisation. 35 récoltes en effet ont eu lieu vers l'ouverture de la Rade d'Hellville (côte Sud de Nosy-Bé : point A de la carte), qui appartient à la catégorie mentionnée ci-dessus. 19 récoltes ont au contraire été effectuées plus au large, non loin de la bordure du plateau continental, ainsi que suivant trois radiales chevauchant cette dernière à trois latitudes différentes : radiale BB' au large de Nosy Mitsio; radiale CC' au large de Nosy Sakatia; radiale DD' au large de Nosy Iranja. De cette façon six récoltes ont été effectuées au-dessus des grands fonds, et deux à l'aplomb du talus continental.

L'examen du zooplankton récolté a confirmé la différence de nature présumée entre les eaux des deux secteurs. En ce qui concerne les Mollusques, 12 espèces d'Hétéropodes et 17 de Ptéropodes ont été dénombrées au total. La plupart n'ont été rencontrées régulièrement qu'au large ou à proximité immédiate du bord du plateau. La faune habituelle de la Rade semble se limiter aux espèces suivantes : *Atlanta gaudichaudi* (SOULEYET), *Atlanta lesueuri* (SOULEYET), *Limacina inflata* (d'ORBIGNY), *Limacina trochiformis* (d'ORBIGNY), *Creseis acicula* (RANG), *Creseis virgula* (RANG) et *Cavolinia longirostris* (LESUEUR).

Les récoltes des 18, 19 et 20 Octobre dans la Rade d'Hellville font exception : s'y trouvaient, outre les espèces mentionnées ci-dessus, douze autres rencontrées habituellement plus au large : il semble qu'il y ait eu jusqu'au point A, pendant ces trois jours, apport d'eau provenant de la partie extérieure du plateau continental.

6 espèces ont été rencontrées exclusivement ou presque exclusivement le long des radiales et surtout dans les stations situées le plus au large.

Au total, l'ensemble des espèces rencontrées dans ces 54 récoltes peut être divisé en trois groupes :

- Un groupe d'espèces présentes régulièrement dans la Rade, quoique toujours plus abondamment représentées le long des radiales :

Atlanta gaudichaudi SOULEYET
Atlanta lesueuri SOULEYET
Limacina inflata (d'ORBIGNY)
Limacina trochiformis (d'ORBIGNY)
Creseis acicula RANG
Creseis virgula RANG
Cavolinia longirostris (LESUEUR)

(1) Océanographe biologiste de l'O.R.S.T.O.M au Centre d'Océanographie et des Pêches de Nosy-Bé (Madagascar)

- Un groupe d'espèces du large

Atlanta fusca SOULEYET
Limacina bulimoides (d'ORBIGNY)
Cuvierina columnella RANG
Styliola subula (QUOY & GAYMARD)
Euclio pyramidata (L.)
Cavolinia inflexa (LESUEUR)

- Un troisième groupe pouvant être constitué soit d'éléments propres à une zone intermédiaire, soit d'espèces pélagiques plus tolérantes que celles du groupe précédent et pouvant occasionnellement être entraînées jusqu'en zone côtière :

Oxygyrus keraudreni LESUEUR
Atlanta helicinoides SOULEYET
Atlanta inclinata SOULEYET
Atlanta inflata SOULEYET
Atlanta peroni LESUEUR
Atlanta turriculata d'ORBIGNY
Firoloida demaresti LESUEUR
Hyalocylix striata (RANG)
Diacria quadridentata (LESUEUR)
Desmopterus papilio CHUN
Clionina longicaudata (SOULEYET)

Le cas de *Cavolinia tridentata* (FORSKAL) reste douteux, cette espèce n'ayant été récoltée que les 18, 19 et 20 Octobre au point A. On ne peut rien conclure non plus concernant *Protatlanta souleyeti* (EDG. A. SMITH), *Cardiopoda placenta* LESSON, *Cavolinia globulosa* (RANG), *Cymbulia* sp., trouvés en un ou deux exemplaires chacun.

Poussant plus loin l'analyse, il a été possible de remarquer d'une part que les espèces du premier groupe, bien que rencontrées fréquemment en Rade d'Hellville, y dominent dans presque toutes dans les récoltes effectuées les 18, 19 et 20 Octobre - dates de l'apport présumé d'eau du large - ainsi que dans les récoltes effectuées le long des radiales. Trois espèces : *Atlanta lesueuri*, *Limacina inflata* et *Limacina trochiformis* sont nettement plus abondantes au-dessus des grands fonds ; *Atlanta gaudichaudi* prédomine au contraire au-dessus du plateau continental, et *Cavolinia longirostris* dans la rade même ; *Creseis acicula* et *virgula* ont une répartition indifférente.

D'autre part plus de la moitié des espèces du troisième groupe marque une prédominance plus ou moins nette des stations situées le plus au large, c'est-à-dire au-dessus des grands fonds ou au-dessus de l'accore. Seule *Atlanta inclinata* et (si l'on veut tenir compte de la répartition des 4 spécimens récoltés de cette espèce) *Desmopterus papilio* caractérisent surtout la périphérie du plateau continental. *Firoloida demaresti* semble se répartir indifféremment entre le large et le bord du plateau.

Il semble finalement qu'à part *Atlanta gaudichaudi*, *Atlanta inclinata*, *Cavolinia longirostris* et peut être *Desmopterus papilio* les Ptéropodes et Hétéropodes récoltés fassent partie d'une seule et même faune d'origine pélagique, et que les trois groupes délimités plus haut, plutôt que des peuplements différents, représentent des degrés de tolérance vis-à-vis des caractères de l'eau néritique.

Il n'a malheureusement pas été possible, au cours de ces récoltes, de procéder à des observations hydrologiques qui auraient permis de préciser cette différence de nature entre les eaux explorées, et ces degrés de tolérance. Un aperçu sur les conditions régnant dans la zone étudiée est toutefois donné dans une récente récapitulation des données hydrologiques recueillies jusqu'à ce jour dans la région de Nosy Bé (1).

Ajoutons enfin que les récoltes qui font l'objet de cet article ont été effectuées de nuit, entre 18h.30 et 04h.45 heures locales. L'immersion du filet était de 1 à 4 m.

---

(1) ANGOT (M.) & MENACHE (M.) 1963 - Premières données hydrologiques sur la région voisine de Nosy Bé (Nord-Ouest de Madagascar). Cahiers du Centre d'Océanographie et des Pêches de Nosy Bé N° 1.

II - PARTIE SYSTEMATIQUE

HETEROPODA

ATLANTIDAE - Toutes les espèces reconnues actuellement ont été rencontrées; la plupart, bien que surtout abondantes le long des trois radiales effectuées, ont été trouvées au moins une fois en rade même.

Dans ce qui suit deux mensurations seront indiquées pour chaque espèce :

1°) - Le diamètre maximum de la coquille : AA'.

2°) - Cette même dimension au stade, s'il existe, où la dernière spire commence à chevaucher la carène; pour effectuer cette mesure l'on suit jusqu'à son extrémité externe la strie d'accroissement (fig. 1, ligne aa') commençant au point exact où apparaît la carène sur l'avant-dernière spire; le segment a'a" est le diamètre cherché.

Oxygyrus keraudreni (Lesueur). A été trouvé dans 4 récoltes : une en rade d'Helville (2 spécimens) et trois le long de radiales (20 spécimens au total, dont 19 au-dessus des grands fonds). Il s'agissait toujours d'individus jeunes, à coquille calcifiée sur la moitié de sa surface. Diamètre 0,88 à 1,56 mm.

Protatlanta souleyeti (Edg. A. Smith). Un seul specimen, récolté au début d'une radiale (fond : 23 m).

Atlanta peroni Lesueur. Espèce peu abondante : rencontrée dans 5 des 54 récoltes (deux en rade d'Hellville et trois au-dessus des grands fonds), à l'état dispersé : un à cinq individus par récolte, avec une légère prédominance au large.

Diamètre 1,81 à 3,38 mm. La dernière spire chevauche la carène à partir du stade 2,0 à 2,3 mm.

Atlanta gaudichaudi Souleyet. Une des espèces les plus abondantes, mais rencontrée surtout sur la partie externe du plateau continental. Présente dans 18 récoltes, dont 9 en rade d'Hellville (essentiellement les 18, 19, 20 Octobre) à l'état dispersé, et 9 le long des radiales où elle forme parfois au contraire des concentrations notables.

Diamètre 1,18 à 3,94 mm. La dernière spire chevauche la carène à partir du stade 2,6 à 2,8 mm.

Atlanta inclinata Souleyet. Présente dans 8 récoltes : 3 en rade d'Hellville (les 19 et 20 Octobre) et 5 le long des radiales. Un à trois individus par récolte.

Diamètre 1,36 à 2,63 mm. La dernière spire chevauche la carène à partir du stade 1,5 à 2,3 mm.

Atlanta lesueuri Souleyet. C'est l'espèce la plus commune : rencontrée dans 17 récoltes à raison de 1 à 10 individus par récolte, sauf une récolte du large qui en contenait 25; 9 de ces récoltes en rade d'Hellville (essentiellement du 18 au 21 Octobre), 8 le long des radiales.

Diamètre 1,38 à 2,90 mm. La dernière spire chevauche la carène à partir du stade 1,8 à 2,6 mm.

Atlanta helicinoides Souleyet. Présente dans 10 récoltes : une en rade d'Hellville (le 20 Octobre), les autres le long des radiales. 1 à 8 individus par récolte, avec prédominance au large et au voisinage de l'accore.

Diamètre 0,80 à 1,91 mm. La dernière spire ne chevauche jamais la carène.

Atlanta inflata Souleyet. Présente dans 13 récoltes : 3 en rade d'Hellville (18 au 20 Octobre), 10 sur les radiales. Des concentrations notables ont été rencontrées au-dessus des grands fonds.

Diamètre 0,75 à 1,65 mm. La dernière spire ne chevauche jamais la carène.

Atlanta fusca Souleyet. Peu fréquente : 1 ou 2 spécimens par récolte dans 5 stations du large.

Diamètre 0,90 à 2,10 mm. La dernière spire chevauche la carène à partir du stade 1,85 mm (mesuré sur un seul individu). Fig. 1.

Atlanta turriculata d'Orbigny. Présente dans 12 récoltes dont une seule en rade d'Hellville (le 20 Octobre : quelques spécimens jeunes), les autres le long des radiales avec une légère prédominance au large.

Diamètre 1,00 à 1,50 mm. La dernière spire ne chevauche jamais la carène.

CARINARIIDAE —

Cardiopoda placenta (Lesson). Un mâle de 17 mm. capturé au large.

PTEROTRACHAEIDAE —

Firoloida demaresti Lesueur. Rencontrée dans 9 récoltes : 3 en rade d'Hellville (les 18 et 19 Octobre), 6 le long des radiales. Un ou deux spécimens par récolte.

PTEROPODA

EUTHECOSOMES

LIMACINIDAE —

Limacina bulimoides (d'Orbigny). Présente dans 7 stations, toutes situées le long des radiales, avec prédominance au large.

Hauteur de la coquille, 1,12 à 1,32 mm.

Limacina inflata (d'Orbigny). Présente dans 15 récoltes dont une seule en rade d'Hellville (environ 30 formes jeunes le 11 Octobre) les autres effectuées le long des radiales ; prédominance au large.

Diamètre maximum de la coquille : 0,5 à 1,55 mm.

Limacina trochiformis (d'Orbigny). Rare et sporadique : rencontrée dans 7 récoltes (4 en rade d'Hellville et 3 sur une radiale). Une certaine concentration notée dans la station la plus au large.

Hauteur de la coquille 0,7 à 0,8 mm.

CAVOLINIDAE —

Creseis acicula Rang. Présente dans 31 récoltes, dont 17 en rade d'Hellville, principalement du 18 au 21 Octobre, et sur 13 des 19 récoltes effectuées le long de radiales. Généralement de 1 à 10 individus par récolte en rade ; des concentrations appréciables, par contre, le long des radiales.

Longueur maxima : 17 mm.

Coquille embryonnaire subcylindrique, 4 à 5,5 fois plus longue que large, arrondie à l'extrémité, et séparée de la coquille adulte par une constriction légère mais nette au niveau de laquelle la paroi se trouve légèrement épaissie. Longueur 0,35 à 0,45 mm ; plus grande largeur 0,09 mm. Fig. 2.

Creseis virgula Rang. Moins commune que la précédente : récoltée dans 19 stations, 8 en rade d'Hellville (presque uniquement du 18 au 20 Octobre), 11 le long des radiales.

Longueur maximum : 2,9 mm.

Coquille embryonnaire sans délimitation nette d'avec le reste de la coquille. L'extrémité de la coquille, de forme générale évasée contrairement aux coquilles de *Creseis acicula*, est de modèle variable mais possède très généralement un étranglement plus ou moins profond mais toujours bien plus étendu en longueur que chez l'espèce précédente, et le plus souvent précédé d'un élargissement sensible de la coquille. Il ne peut donc y avoir confusion entre les deux espèces citées. Fig. 3.

Il ne nous a pas été donné d'observer la coquille embryonnaire de type *Creseis acicula* décrite par TOKIOKA (1955) comme caractéristique de *Creseis acicula clava* (= *C. virgula clava* TESCH 1948) toutes les coquilles récoltées, droites comme courbes, étant du type *virgula* par leur extrémité.

Styliola subula (Quoy & Gaymard). Présente dans 11 stations, toutes le long des radiales. Généralement 1 à 10 individus par récolte, 40 dans la station située le plus au large d'une des radiales.

Longueur de la coquille 3 à 7,5 mm.
Coquille embryonnaire : longueur 0,15 à 0,18 mm
largeur max. 0,1 mm

Hyalocylix striata (Rang). Présente dans 8 récoltes : 3 en rade d'Hellville (les 19 et 20 Octobre), 5 sur les radiales avec prédominance au large. De 1 à 5 individus par récolte.

Longueur de la coquille 1,1 à 6,0 mm.
Coquille embryonnaire toujours détachée.

Cuvierina columnella (Rang). forme *urceolaris* (Mörch). Présente dans 7 récoltes, toutes le long des radiales : 5 situées au-dessus des grands fonds, une au-dessus de l'accore et une non loin de celui-ci. De 2 à 6 individus par récolte, 12 dans la récolte effectuée le plus au large.

Longueur de la coquille complète (trouvée telle chez un seul individu) : 9,9 mm.

Longueur de la coquille définitive, la partie postérieure s'étant rompue : 5,5 à 6,6 mm; sa plus grande largeur : 2,15 mm.

Coquille embryonnaire allongée et ovoïde, présentant sa plus grande largeur aux deux tiers environ à partir de l'apex, et séparée du reste de la coquille par un col au niveau duquel la paroi est épaissie. Longueur 0,4 mm; plus grande largeur 0,14 mm Fig. 4.

Euclio pyramidata (L). Rencontré dans 3 récoltes du large : 5 individus au total.

Longueur de la coquille 4,8 à 7,5 mm.

Coquille embryonnaire voisine de celle de *Styliola subula*, à la taille près : longueur 0,35 mm, plus grande largeur 0,23 mm. Apex mucroné.

Diacria quadridentata (Lesueur). Espèce fréquemment rencontrée, surtout à l'état juvénile. Présente dans 23 récoltes, 14 en rade d'Hellville (uniquement du 18 au 20 Octobre), 9 le long des radiales avec prédominance du large; des formes adultes n'ont été rencontrées que dans 4 récoltes faites en rade et 7 sur les radiales.

Longueur de la coquille définitive 1,9 à 2,4 mm; plus grande largeur (c'est-à-dire distance entre les angles postéro-latéraux) 1,75 à 1,9 mm ; distance entre les angles postérieurs 0,95 à 1,05 mm.

A côté de ces dimensions typiques, ont été rencontrés quelques individus de plus petite taille bien qu'ayant atteint la forme définitive : longueur 1,45 à 1,6 mm; distance entre les épines latérales : 1,1 à 1,2 mm; distance entre les épines postérieures 0,65 à 0,7 mm.

Coquille embryonnaire globuleuse, de 0,22 mm de longueur sur 0,16 mm de plus grande largeur. La coquille jeune croît en s'évasant, jusqu'à une longueur d'environ 3,8 mm (à ce moment la distance entre les angles latéraux est de 2,1 mm en moyenne, soit la distance signalée ci-dessus entre les épines latérales). A ce stade l'animal se détache du fond de sa coquille et se rétracte dans la partie antérieure de cette dernière pendant que la partie postérieure se détache à une distance de l'apex d'environ 2,3 mm; à ce niveau de rupture la largeur de la coquille est de 1,1 à 1,2 mm, soit la distance signalée ci-dessus entre les épines postérieures de la coquille définitive. La partie antérieure secrète alors un mince diaphragme immédiatement au-dessus de la rupture; enfin les deux lèvres, dorsale et ventrale, se mettent à croître de façon différente pour adopter leur forme définitive. Les stades successifs, d'aspect très différent,de cette espèce sont ainsi aisément reconnaissables. Fig. 5 a à d.

Cavolinia longirostris longirostris (Lesueur). Présente dans 17 récoltes dont 4 seulement (4 individus au total) hors de la rade. Des formes juvéniles ont été rencontrées dans 12 de ces récoltes; à l'état dispersé; formes adultes dans 6 récoltes en rade d'Hellville à raison de 1 à 6 individus par récolte.

Coquille adulte : longueur 4 à 5,5 mm; coquilles juvéniles rencontrées : de 0,95 à 1,85 mm de longueur sur 0,5 à 1,4 mm de plus grande largeur.

La coquille embryonnaire était détachée sauf sur le spécimen le plus petit (longueur 0,95 mm) Fig. 6.

Cavolinia longirostris angulata (Souleyet). Un individu, capturé dans la rade d'Hellville le 20 Octobre. Longueur de la coquille 3,1 mm.

Cavolinia globulosa (Rang). 2 individus capturés au large. Longueur de la coquille 5,0 à 5,2 mm. Coquille embryonnaire détachée.

Cavolinia inflexa (Lesueur). forme *lata* Boas - 5 individus, dont 3 juvéniles, tous capturés au large.

Les deux spécimens adultes récoltés se caractérisent par la présence de processus latéraux extrêmement allongés et grêles : longueur de la coquille 4,5 et 4,8 mm, distance entre les extrémités des appendices latéraux 4,35 et 4,5 mm, soit un rapport longueur/plus grande largeur égal à 0,96 et 0,97 alors que TESCH (1948) indique pour valeur de ce rapport 0,6 pour les spécimens provenant de l'Atlantique et 0,8 pour ceux de l'Océan Indien. Fig. 7 a.

Coquilles juvéniles : longueur 1,4 à 3,0 mm : plus grande largeur 0,8 à 2,3 mm. Coquilles embryonnaires détachées. Fig. 7 b.

Cavolinia tridentata (Forskal). 5 individus juvéniles et subadultes recueillis dans 3 récoltes en rade d'Hellville les 19 et 20 Octobre.

Longueur de la coquille 1,7 mm à 7,1 mm; plus grande largeur 0,7 à 5,05 mm. Coquille embryonnaire persistante, arrondie et sans délimitation nette. Fig. 8.

PSEUDOTHECOSOMES

CYMBULIIDAE—

Cymbulia sp.- Deux individus de petite taille, sans pseudoconque. Rade d'Hellville les 18 et 20 Octobre.

DESMOPTERIDAE—

Desmopterus papilio Chun. 4 individus, récoltés deux fois en rade d'Hellville (18 et 20 Octobre) et une fois à l'aplomb du talus continental. Envergure 2,1 à 3,3 mm.

GYMNOSOMES

CLIONIDAE—

Clionina longicaudata (Souleyet). 14 individus, rencontrés dans une station en rade d'Hellville le 18 Octobre et 7 le long de radiales.

Longueur à l'extension (trompe exclue) 1,65 à 2,7 mm.

Enfin quelques *larves de Clionidae* indéterminables ont été récoltées aux trois stations les plus éloignées d'une des radiales.

Longueur à l'extension : 1,15 à 2,15 mm Fig. 9.

BIBLIOGRAPHIE

FOL (H.) 1875 - Sur le développement des Ptéropodes
Arch. Zool. Exp. Série 1 - 4 - pp. 1-214 ; pl. I-X.

MENZIES (R. J.) 1958 - Shell bearing Pteropod Gastropods from mediterranean plankton (Cavoliniade).
Pub. Sta. Zool. Napoli 30 - pp. 381-401

TESCH (J. J.) 1904 - The Thecosomata and Gymnosomata of the Siboga-Expedition
Siboga Expeditie 29, Livr. 16 pp. 1-92 ; pl. 1-6

1906 - Die Heteropoden der Siboga-Expedition
Ibid. Livr. 29, pp. 1-112 ; pl. 1-14

1913 - Pteropoda
Das Tierreich, Lief, 36, pp. 1-154

1946 - The Thecosomatous Pteropods. I) The Atlantic. *Dana Rep. 28, pp. 1-82 ; pl. 1-8.*

1948 - The Thecosomatous Pteropods. II) The Indopacific.
Ibid. 30, pp. 1-45, pl. 1-3

1949 - Heteropoda
Ibid. 34, pp. 1-55, pl. 1-5

1950 - Gymnosomata
Ibid. 36, pp. 1-55

TOKIOKA (T.) 1955 - On some planktonic animals collected by the Suynkotu-Maru in May-June 1954. II) Shells of Atlantidae. *Pub. Seto Mar. Biol. Lab. 4, pp. 227-236, pl. 15-16*

1955 - Shells of Atlantidae (Heteropoda) collected by the Soyo-Maru in the Southern waters of Japan.
Ibid. pp. 237-250, pl. 17-18

1955 - On some planktonic animals collected by the Suynkotu-Maru in May 6 June 1954. IV) Thecosomatous Pteropods.
Ibid. 5, pp. 59-74, pl. 7-13

1961 - The structure of the operculum of the species of Atlantidae as taxonomic criterion, with records of some pelagic Molluscs in the North Pacific.
Ibid. 9, pp. 226-332

FIGURES

1 - *Atlanta fusca* Souleyet. Mensurations effectuées sur les coquilles d'Atlantidae :

AA' = diamètre
aa' = strie d'accroissement
a'a" = diamètre au stade où la dernière spire commence à chevaucher la carène.

2 - *Creseis acicula* Rang. Extrémités de coquilles

3 - *Creseis virgula* Rang. Extrémités de coquilles

4 - *Cuvierina columnella* (Rang) a = coquille complète
b = coquille embryonnaire

5 - *Diacria quadridentata* (Lesueur)

a = coquille juvénile
b = coquille juvénile proche de se rompre
c = coquille juvénile peu de temps après la rupture
d = coquille adulte

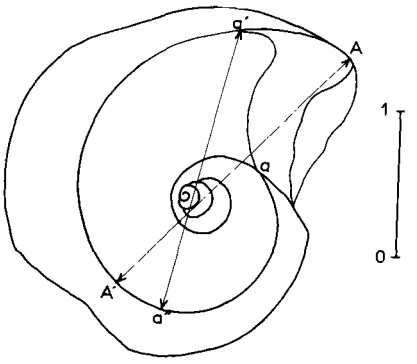
6 - *Cavolinia longirostris* (Lesueur). Coquilles juvéniles

7 - *Cavolinia inflexa* (Lesueur)

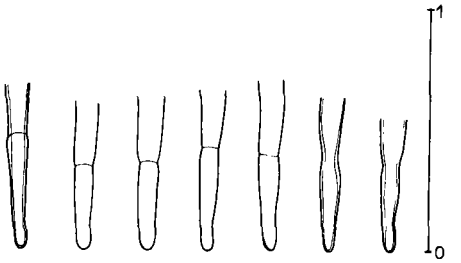
a = adulte, faces ventrale et latérale
b = coquilles juvéniles

8 - *Cavolinia tridentata* (Forskal). Coquilles juvéniles

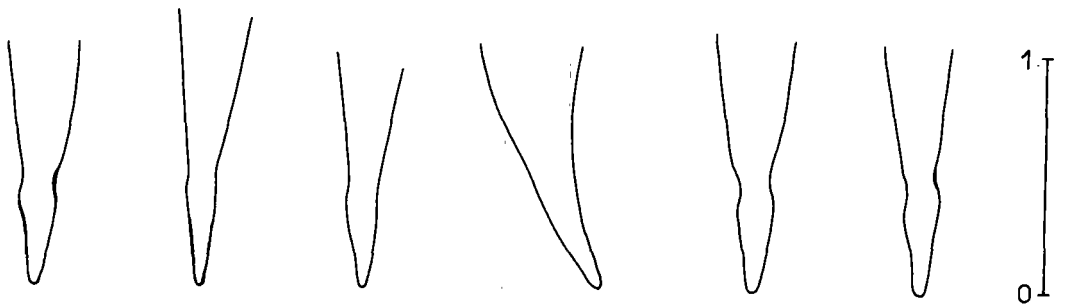
9 - Larve de *Clionidae*

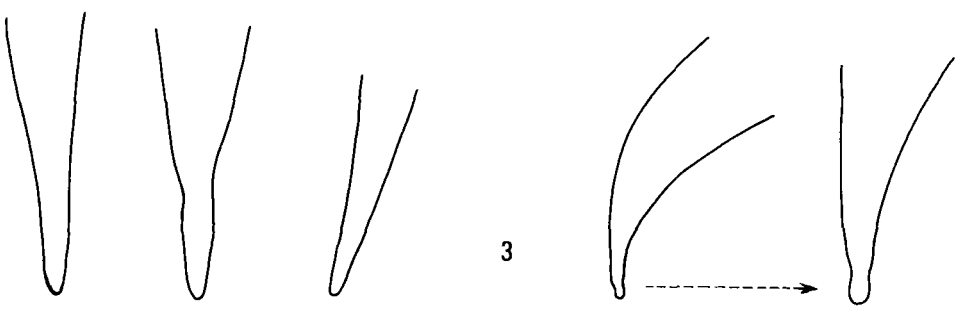


1

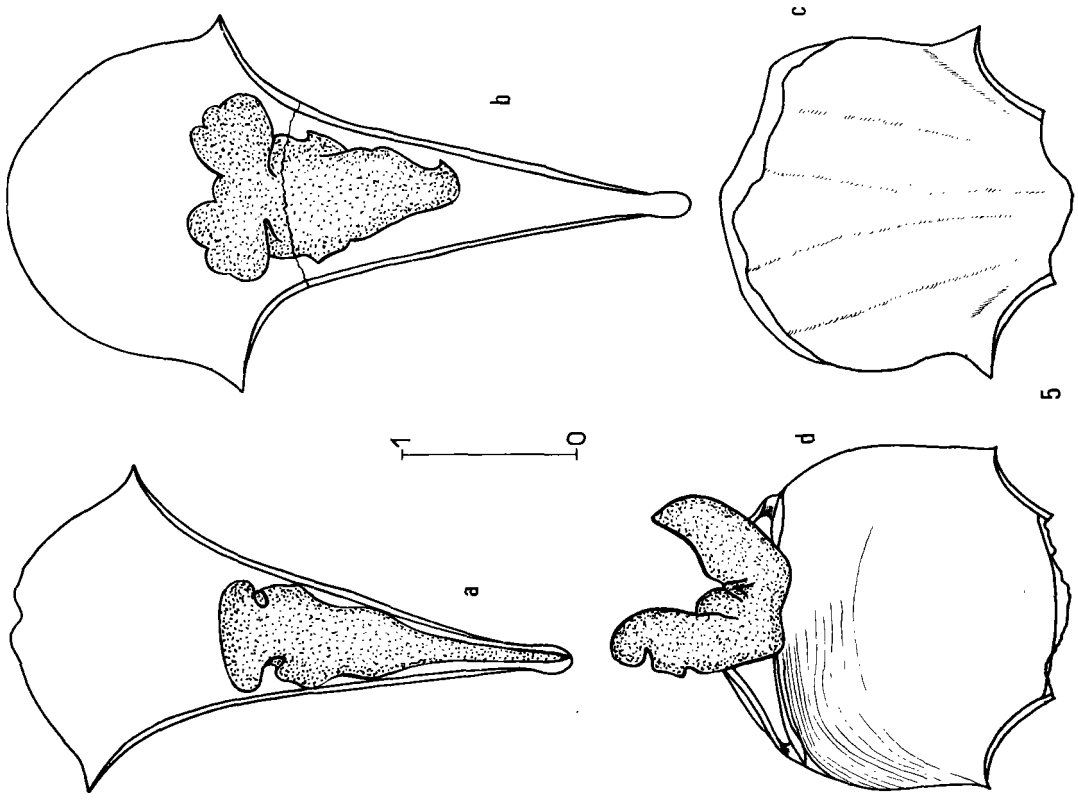


2

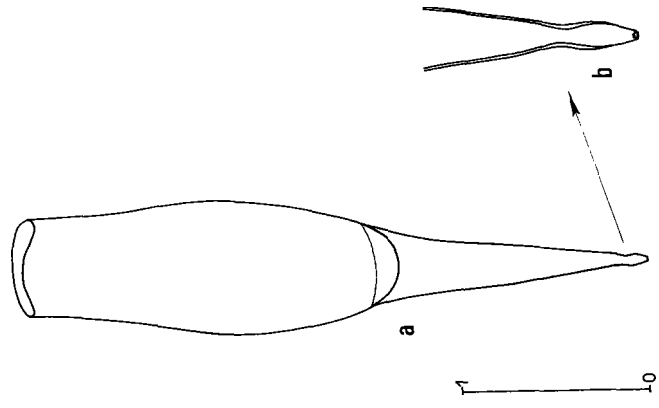




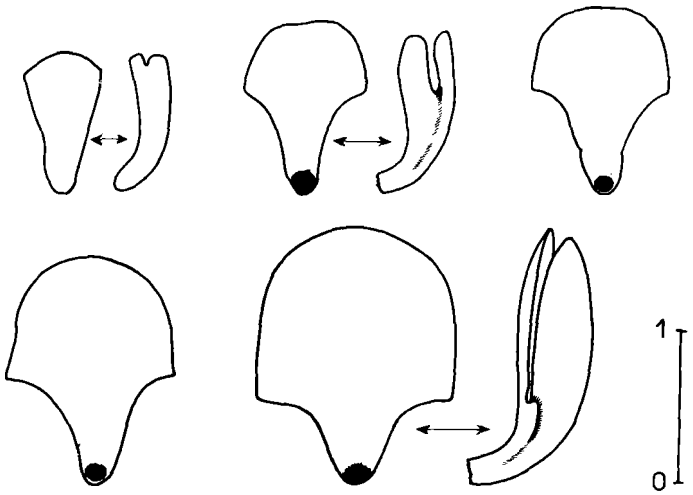
3



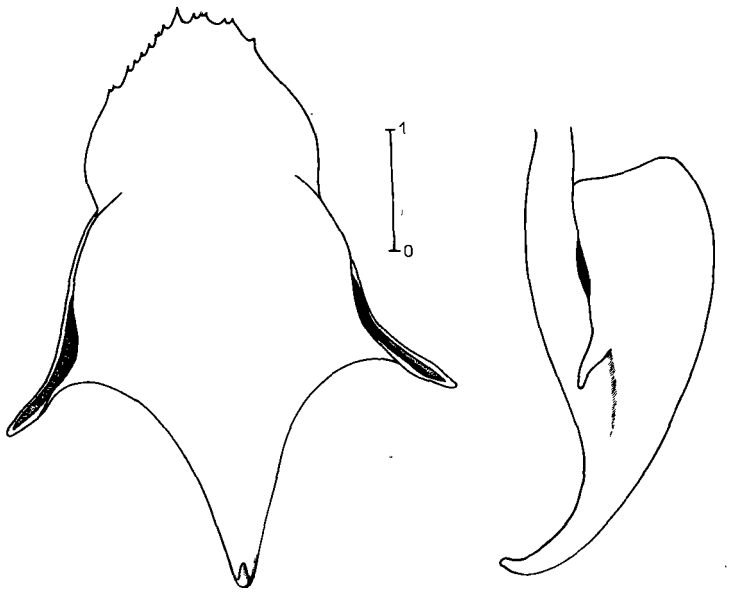
5



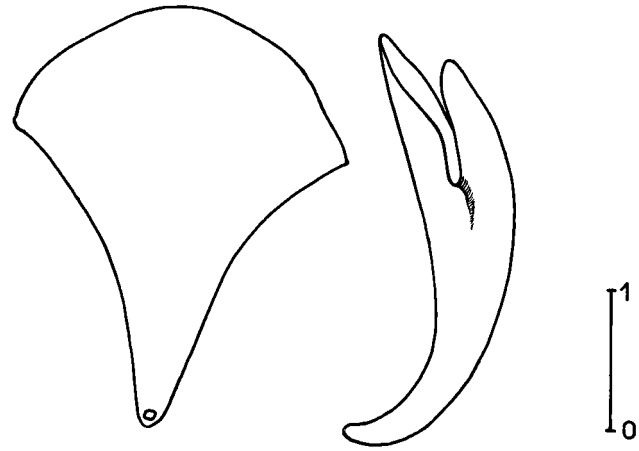
4

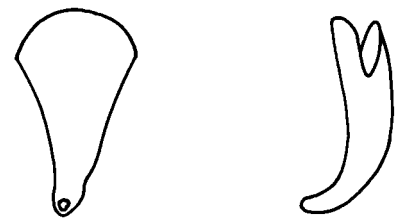


6

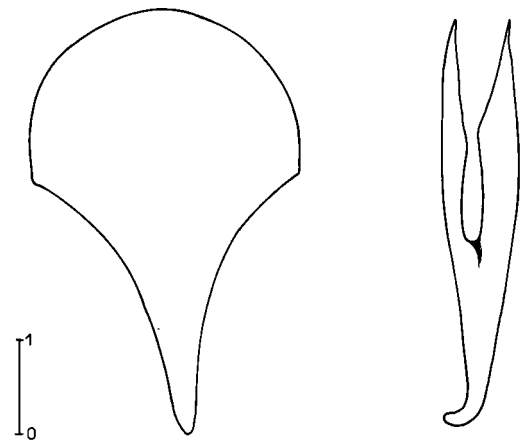


7 a

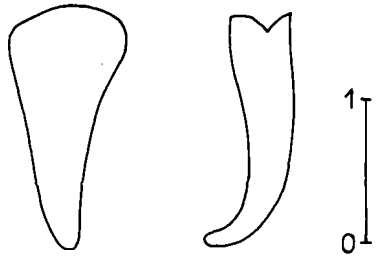




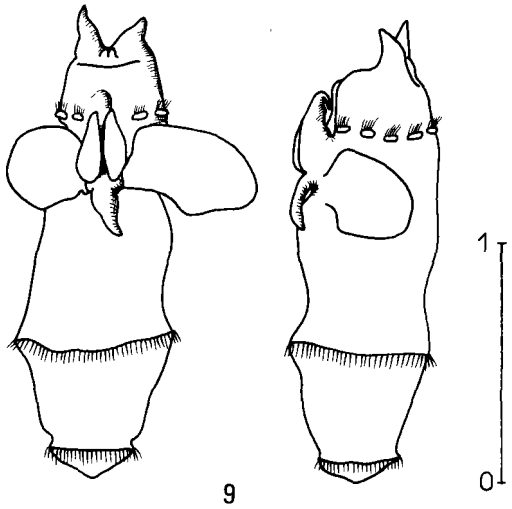
7b



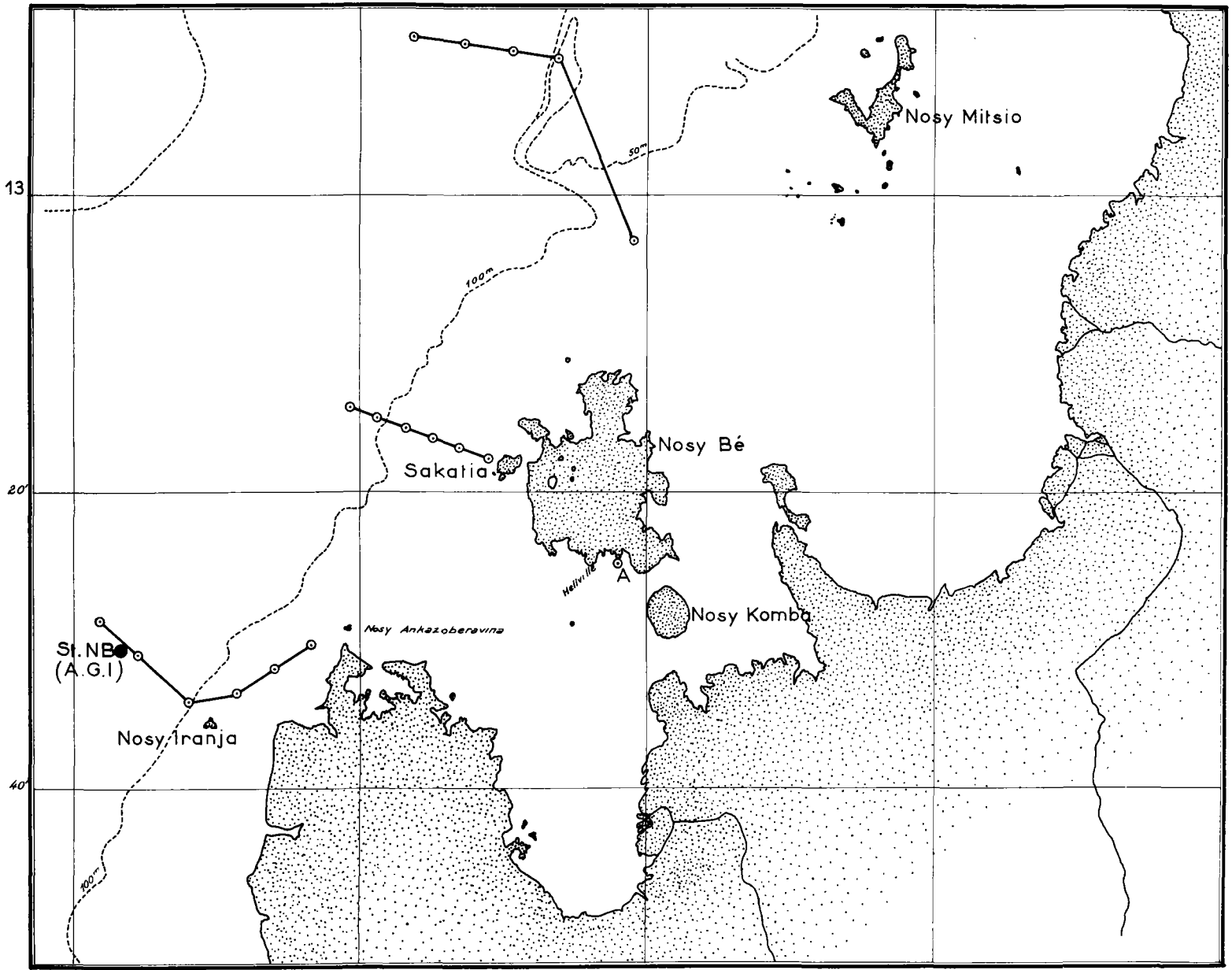
8a



8b



9



Carte des récoltes de Plankton (Oct_Déc. 60)

Reprinted from *Océanographie (Nosy Bé II)*, no. 6, 1963, p. 229-232

PRÉSENCE DE CRESEIS CHIERCHIAE (BOAS) DANS L'OCÉAN INDIEN

par

S. FRONTIER[1]

Cette espèce a été établie par BOAS (1886) d'après quelques exemplaires récoltés par 10°N et 137°W (entre les Carolines et les Philippines). Elle a été retrouvée ensuite au large de la Floride (DALL 1872) et en plusieurs localités proches de Panama (PELSENEER 1887). Récemment MENZIES (1958) la signale en une station de la Méditerranée Orientale.

10 exemplaires de cette espèce ont été récoltés lors de la troisième campagne océanographique du "COMMANDANT ROBERT GIRAUD" (Avril à Juin 1961) aux stations suivantes :

	Latitude	Longitude	Heure	Immersion
194	22°33' N	66°28' E	21h. 35	1 m.
			22h. 10	10 m.
198	22°33' N	62°05' E	04h. 15	trait vertical 100 m - surface
271	12°02' N	47°22' 5E	01h. 10	1 m.

Par ailleurs l'examen du plankton récolté autour de Nosy Bé (Madagascar) entre Mars et Mai 1963 a permis de découvrir près d'un millier d'exemplaires de la même espèce, essentiellement localisés dans une zone typiquement néritique, située hors de l'influence des eaux pélagiques mais en dehors d'une zone d'influence directe des rivières, alors envahie par un phytoplankton abondant. 8 individus seulement ont été récoltés en dehors de cette zone dont la salinité était comprise pendant cette période entre 29,81 et 34,54 ‰, et la température entre 28,05 et 30,47°C.

Cette espèce semble être - comme l'avait remarqué MENZIES - une espèce de surface. Les récoltes étaient effectuées à l'aide d'un filet d'un mètre de diamètre d'ouverture trainé, à chaque station, à 2 mètres puis à 10 mètres d'immersion; les traits effectués à 10 m. ont ramené environ 250 individus, les traits à 2 m.,700, toutes récoltes étant effectuées de jour.

Description

Coquille droite et cônique (longueur = environ 4 fois le plus grand diamètre), extrêmement mince et fragile, transparente, et possédant sur une partie de sa longueur une annulation très caractéristique (environ 35 replis par millimètre). Très petite taille : 2,5 mm. de longueur au maximum. La coquille embryonnaire paraît tout à fait identique à celle de *Creseis virgula* . L'annulation de la coquille ne débutant qu'à environ 0,75 mm. de l'extrémité, il n'est pas possible de distinguer les individus très jeunes de *Creseis chierchiae* de ceux de *Creseis virgula*; les effectifs indiqués pour *Creseis chierchiae* sont donc probablement sous-estimés, vu que *Creseis virgula* est très abondante dans toute la zone prospectée, et que la proportion de juvéniles est forte.

(1) Océanographe Biologiste de l'O.R.S.T.O.M. au Centre d'Océanographie et des Pêches de Nosy Bé. (Madagascar).

Cette description est conforme à celle de BOAS et à sa figuration. La description de MENZIES par contre semble s'éloigner notablement du type : coquille droite et parallèle, environ 5 fois plus longue que le plus grand diamètre, et possédant une dizaine de replis annulaires. De plus la figure qu'il donne indique une extrémité de coquille très différente des figures de BOAS, et se rapprochant au contraire du type *"Creseis acicula"* (cf TOKIOKA 1955). Il semble donc que les spécimens récoltés par MENZIES appartiennent non pas à *Creseis chierchiae* , mais à une espèce non encore décrite. Dans cette hypothèse *Creseis chierchiae* resterait une espèce tropicale.

BIBLIOGRAPHIE

BOAS (J.E.V.) 1886 - Bidtrag til Pteropodernes. *Dansk. Vidensk. Selsk. Skr. 4, p. 62, pl. 3 et 4.*

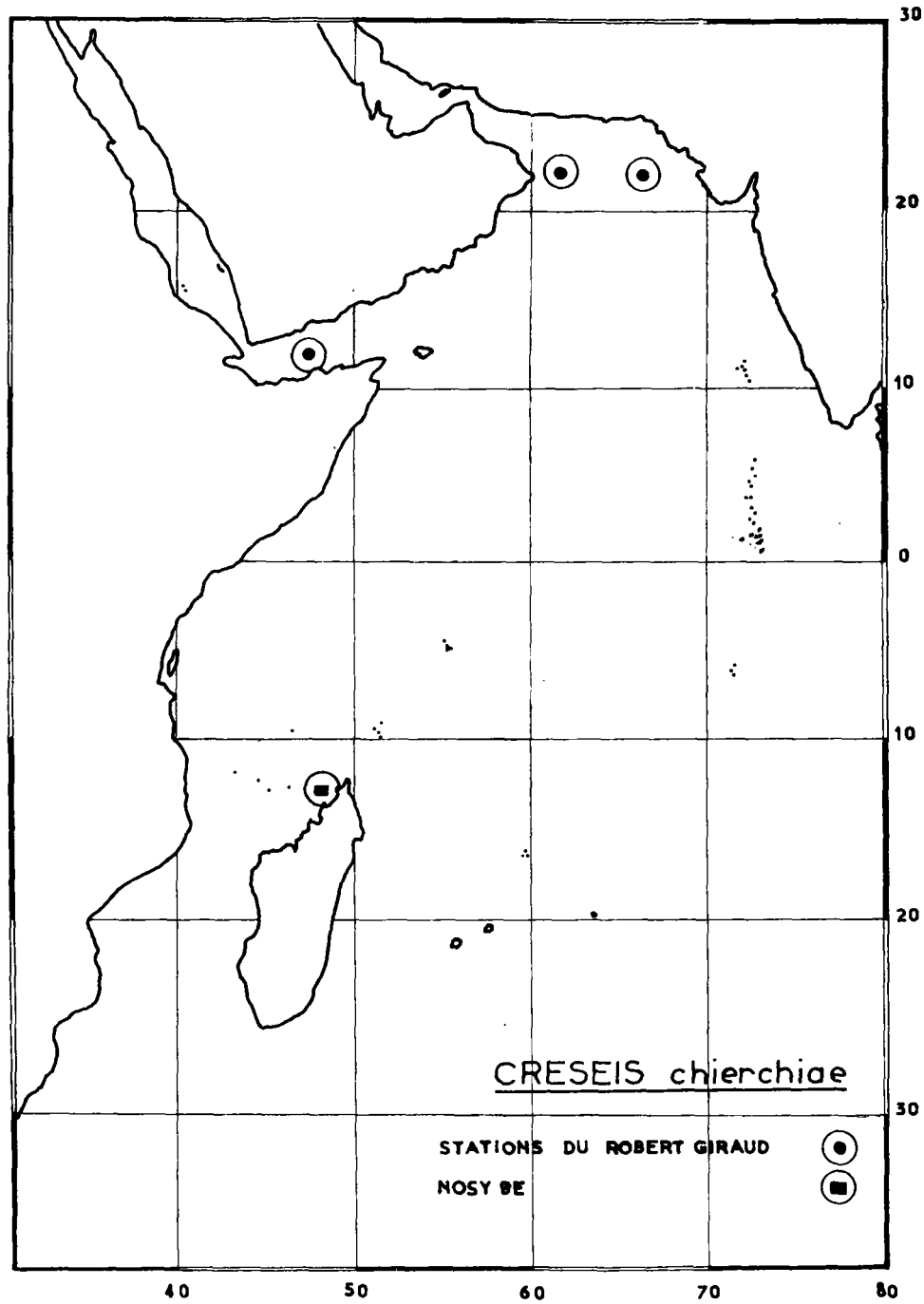
DALL (WH) 1872 - Description of 60 new forms of Mollusks from the West coast of North America. *Amer J. Conchyl. 7*

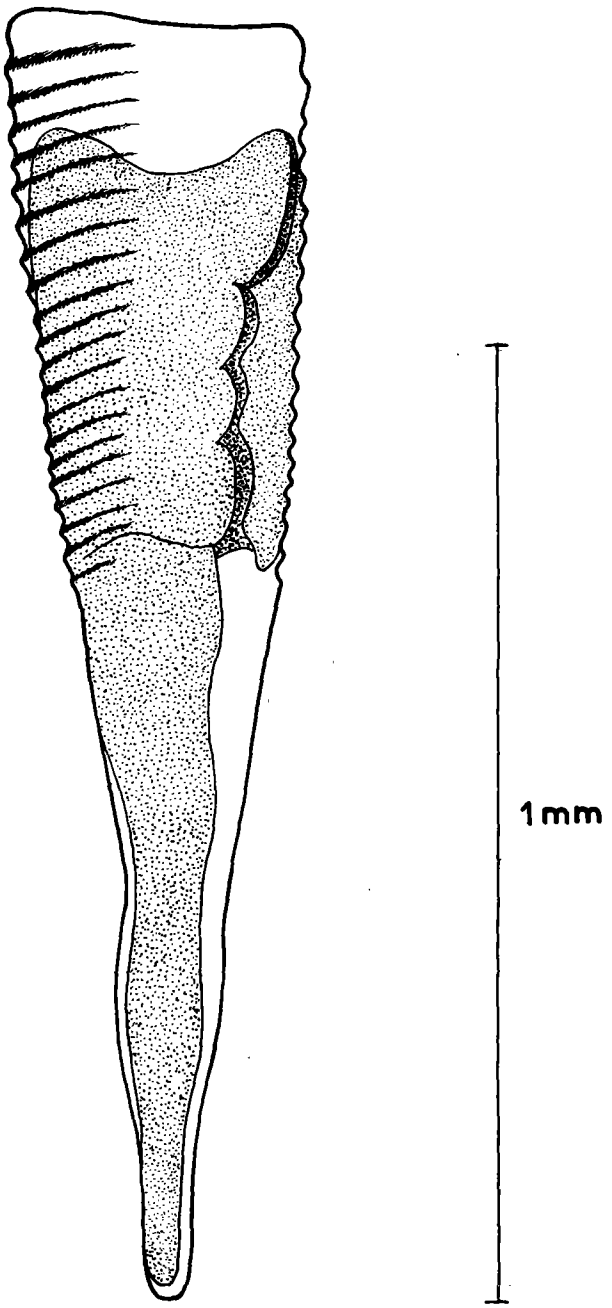
FRONTIER (S.) 1963 - Zooplankton récolté en Mer d'Arabie, Golfe Persique et Golfe d'Aden (3ème campagne océanographique du Robert Giraud. Mars à Juin 1961) - 1. Données générales ; répartition quantitative. *Cahiers du C.O.P.N. 1, pp. 17-30.*

MENZIES (R.J.) 1958 - Shell bearing Pteropod Gastropods from mediterranean plankton. *Pub. Staz. Zool. Napoli, 3, pp. 384 et 386 - 387*

PELSENEER (P.) 1887 - Pteropoda Thecosomata. *Challenger Rep., 23 (65)p. 53*

TOKIOKA (T.) 1955 - On some plankton animals collected by the Suynkotu-Maru in May-June 1854. IV) Thecosomatous Pteropods. *Pub. Seto Mar. Biol. Lab., 5, pp. 63-64, pl. 9.*


30
20
10
0
10
20
30
40
50
60
70
80
CRESEIS chierchiae
STATIONS DU ROBERT GIRAUD
NOSY BE


1mm

Reprinted from *Report of Faculty of Fisheries, Prefectural University of Mie, vol.* 5, no. 1, 1964, p. 33-49

Falling Model on the Planktonic Diatoms

Ichitaro SAKAMOTO

(With 9 Figures and 3 Tables)

Introduction

The research of planktonic organisms originally started from an ecological interest has now developed to such a stage that a quantitative analysis of production physiology can be assayed.

In order to analyze the balancing mechanism of Standing crops in controlling the spatial or lapse-time distribution, the in-situ physiological condition of organisms and also mechanisms of the physical and chemical effects of in-situ environment upon the organisms must ought to be clarified first.

Moreover, it is necessary to grasp a definite the concept of the physical characters of planktonic organisms when these are considered as non biological (i.e. physical) bodies.

In this report, a model of planktonic diatoms will be discussed in reference to their falling velocity.

I. In-situ Density of the Planktonic Diatom

The vertical distribution of phyto-planktons in the sea shows that the layers maximum in population density is different according to the species. This implies that there exists a particular layer in which the organisms are hydrostatic balance.

It seems that the most important of the factors which control the vertical distribution of phyto-planktons is the balance between the actual density of plankton cell and that of environmental water, even when in-situ oceanic conditions may have eddy turbulences and currents.

One of the ecological characteristics of planktonic diatoms consists in that can propagate only when they maintain their own density same as that of environmental water.

Their *Bathyscaphe* like three states, up-floating, neutral-floating, and falling, occur according to the changes in the specific gravity which have resulted from their physiological conditions.

Amnog the components of diatom cells, those which have a density considerably differing from that of environmental water are 1) the shell composed of silicate, and 2) the oil particles dispersed within the protoplasm as reserve substances produced by photosynthesis.

On the other hand, the cell-sap is isotonic to the environmental water. Though the density of the cell-sap does not seem to have ever been measured, it may probably be approximately equal to (most probably a little greater than) the density of environmental water.

For the sake of simplification, it is assumed that a diatom cell comprises a shell and a protoplasm, each separable from the other by plasmolysis, and the protoplasm is composed of cell-sap and oil particles.

Denotations and Assumptions:

d : In-situ density of environmental water, which is generally within the range of 0.99 to 1.03.

dp: In-situ density of diatom particle.

ds : Density of diatom shell, assumed to be constantly equal to that of quartz (2.7).

dl': In-situ density of protoplasm, that is average density of inner-shell's volume.

dl : In-situ density of cell sap (on the assumption that the cell-sap is the portion of protoplasm minus oil particles), assumed tentatively equal to d.

do: Density of oil particles, (the effects of hydrostatic pressure and water temperature upon their volumes are ignored) assumed to be constant, displaced for 0.925 from the mode of the typical vegetable oil.

S : Volume ratio of shell to cell.

X : Volume ratio of oil particles to cell

Now, the condition for the neutral state, or $dp=d$, is to be obtained

$$dp = 2.7 \cdot S + dl' \cdot (1 - S) = d \qquad \cdots\cdots\cdots(1)$$

So that

$$dl' = (d - 2.7 \cdot S) \cdot (1 - S)^{-1} \qquad \cdots\cdots\cdots(2)$$

dl' has the connotation as indicated in the following formula.

$$dl' = \{0.925 \cdot X + d \cdot (1 - S - X)\} \cdot (1 - S)^{-1} \qquad \cdots\cdots\cdots(3)$$

The correlation between S and X for achieving $dp=d$ can be obtained from formula (2) and (3).

$$S \cdot X^{-1} = (d - 0.925) \cdot (2.7 - d)^{-1} \qquad \cdots\cdots\cdots(4)$$

The maximum of the volume ratio of shell (S max) in a neutral state should be less than a value estimated on the assumption that the interior of shell was exclusively occupied by oil.

$$S \text{ max} \leqq (d - 0.925) \cdot 1.775^{-1} \qquad \cdots\cdots\cdots(5)$$

Therefore, the diatom whose S is greater than S max cannot maintain its planktonic state in the mid-layer, unless any moving mechanism is present.

S obtained from the silicate quantity, which was determined through chemical analysis of *Coscinodiscus Janischii* by J. NAKAI (1942), is 1.13% and about 20% of

S max when it is assumed that $ds = 2.7$.

According to the "Table of Plankton Equivalents" reviewed by R. H. FLEMING (1940), his weight ratio of Dry-Wet plankton samples exactly corresponds to that obtained by NAKAI. For these diatoms, in keeping neutral state in the environmental water with in-situ density (***d***) of 1.02, ***X*** ought to be 20% calculated from the formula (4).

When the oil content increases with photosynthesis, the diatoms get up-floating force, but when they dissipated oil content, they begin to fall. For example, when ***X*** decrease to 18.9%, the diatoms fall down to the layer with ***d*** of 1.025, in which they become re-balanced and stay.

From these it may be considered that the compensation depth give the optimum condition to the photosynthetic planktons in maintaining neutral state.

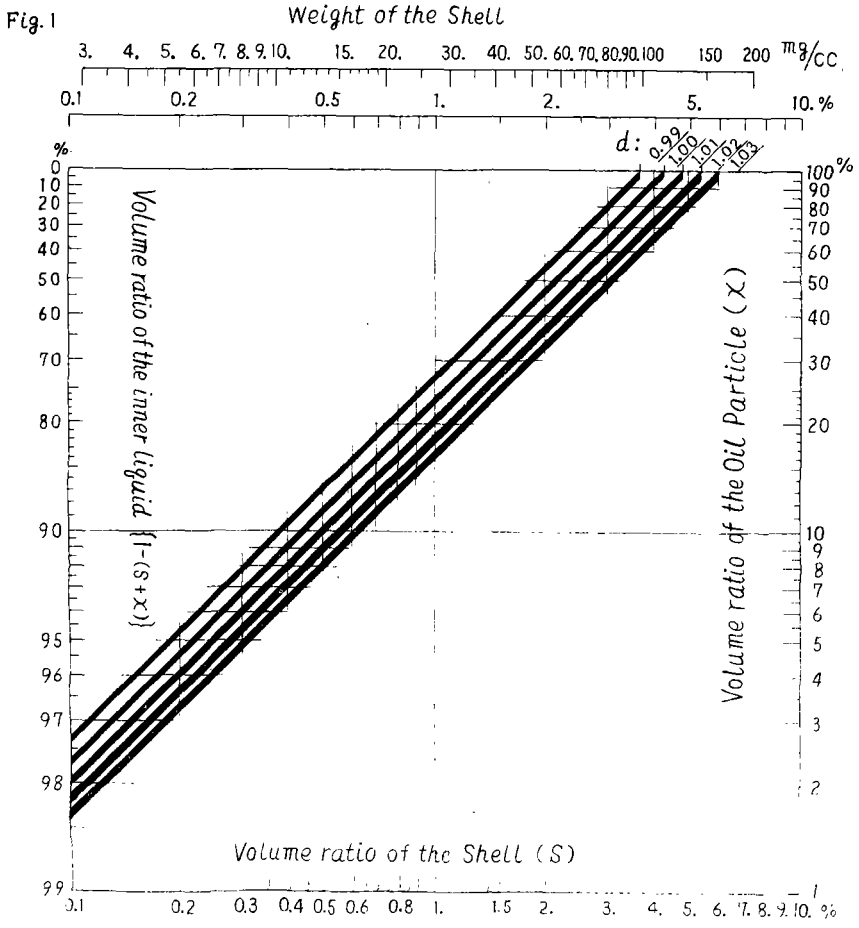


Fig. 1. Correlation between the volume ratio of diatom shell (**S**) and that of the oil particles (**X**), for in neutral state ($dp = d$). Formula (4).

Not only an increase (decrease) in oil quantity but also a decrease (increase) in shell substances accelerate the up-floating (falling) movement of diatoms. Formation of resting-spore would accelerate the falling motion, and an increase in hydrostatic water pressure under a low temperature would cause the silicate components to dissolve, resulting in the decrease of falling velocity.

Since the dissolution velocity of silicate is much smaller than that of the decomposition of organic constituents, and in so far as the dissolved quantity of silicate is presumed to be a function of time, the volume ratio of dissolution during the descent of a given distance is greater for the smaller diatoms. It is presumed that this may give one of the clues in solving the problem why smaller types are relatively few among the dead diatom shells constituting the diatom-ooze.

The maximum of ***dp*** (***dp*** max) occurs when oil particles become extinct.

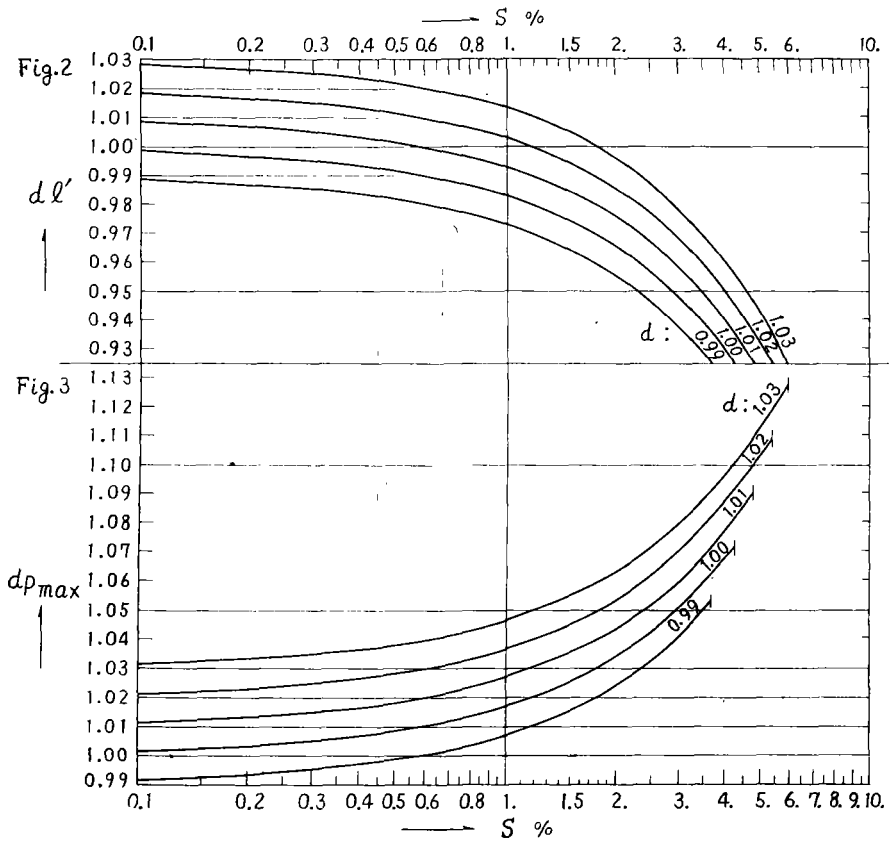


Fig. 2. Correlation between ***S*** and *in-situ* density of protoplasm (***dl'***), for in neutral state. Formula (2).

Fig. 3. Correlation between ***S*** and in-situ maximum density of the diatom particles (***dp*** max). Formula (6).

According to the present assumptions extinction of oil particles corresponds to the state that $dl' = d$, or to the one in which protoplasm is completely replaced by the environmental water.

That is, $$dp \max = 2.7S + (1 - S)\cdot d \qquad \cdots\cdots(6)$$

This value shows the condition in which the dead shells get the maximum falling velocity.

Within the range of S less than S max represented in the formula (6), results of formulae (4), (2) and (6) are shown in *Fig. 1*, *Fig. 2*, and *Fig. 3* correspondingly.

II. Structural Adaptation of Planktonic Diatoms

Floating adaptation of diatoms is represented in expansion of their surface as well as in regulation of their density. Expanding of their surface produces two effects upon them, one being increasing in the efficiency of nutrients uptake, and the other decrease in their falling velocity due to increase of resistance against water.

For a comparative analysis of these efficiency depending upon the shape of cell, all kinds of diatom cells and colonies, the shape of which vary from a hair type through needle type-cylinder type-disc type, to a membrane type, are assumed for convenience to have a disc shape.

Correlations between the dimensions of disc body and those of the equivolume sphere are shown in the following equations.

Denotations:

V : Volume. Discs and sphere are equi-volume.
D : Diameter of sphere.
D' : Diameter of disc.
h : Height of disc.
s : Symbol of sphere.
d : symbol of disc.
S_H: } Section of the disc. { Horizontal position.
S_V: } { Vertical position.
S_s : Section of the sphere.

That is,

volume, $$V_s = \pi\cdot D^3/6 = \pi\cdot h\cdot D'^2/4 = V_d \qquad \cdots\cdots(7)$$

surface, $$\left.\begin{aligned} A_s &= \pi\cdot D^2 = 6\cdot V/D \\ A_d &= \pi\cdot D'\cdot(2\cdot h + D')/2 = 2\cdot V\cdot(2/D' + 1/h) \end{aligned}\right\} \qquad \cdots\cdots(8)$$

diameter, height of disc body $$\left.\begin{aligned} D &= \sqrt[3]{6\cdot V/\pi} = 1.24\cdot \sqrt[3]{V} \\ D' &= \sqrt{4\cdot V/\pi\cdot h} = 1.128\cdot \sqrt{V/h} \\ h &= 4\cdot V/\pi\cdot D'^2 = 1.273\cdot V/D'^2 \end{aligned}\right\} \qquad \cdots\cdots(9)$$

surface-ratio $Ad/As=(2/D'+1/h)\cdot D/3=(D'/D)^2/2+(D/D')\cdot 2/3$ ···(10)

disc-ratio $h/D'=4\cdot V/\pi\cdot D'^3=(D/D')^3\cdot 2/3$ ·····(11)

section
$$\left.\begin{aligned} Ss &= \pi\cdot D^2/4 \\ S_V &= \pi\cdot D'^2/4=(D'/D)^2\cdot\pi\cdot D^2/4 \\ S_H &= h\cdot D'=4\cdot V/\pi\cdot D'=(D/D')\cdot 2\cdot D^2/4 \end{aligned}\right\} \quad \cdots\cdots(12)$$

section-ratio
$$\left.\begin{aligned} S_V/Ss &= (D'/D)^2 \\ S_H/Ss &= (D/D')\cdot 8/3\cdot\pi \end{aligned}\right\} \quad \cdots\cdots(13)$$

section ratio of disc $S_H/S_V=(D/D')^3\cdot 8/3\cdot\pi$ ·····(14)

Generally speaking the surface-ratio in any individual diatom is smaller than 10. This may, however, become far greater in the diatoms with spines.

Thickness of a shell (τ) is in inverse proportion to the surface ratio for equi-volume body. Therefore the equi-volume sphere has the maximum value of τ/D.

Thickness of a sphere shell (τs) and the same of shell of the equi-volume disc (τ) are;

$$\tau s/D=(1-\sqrt[3]{1-S})/2, \quad \tau=\tau s\cdot Ad/As \qquad \cdots\cdots(15)$$

Fig.4

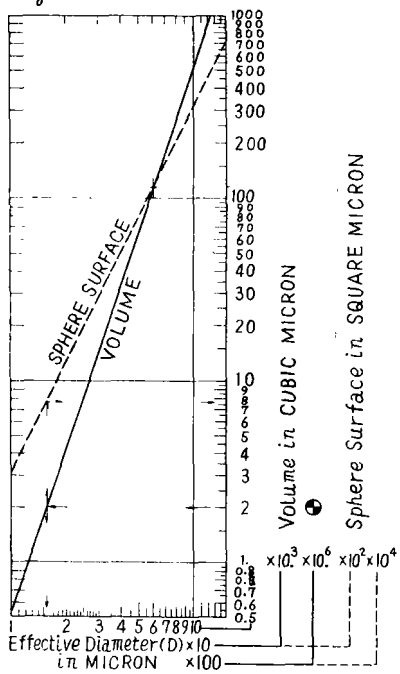


Fig. 4. Diagram of finding the effective diameter (D) from the particle volume. Formula (7).

Fig. 5

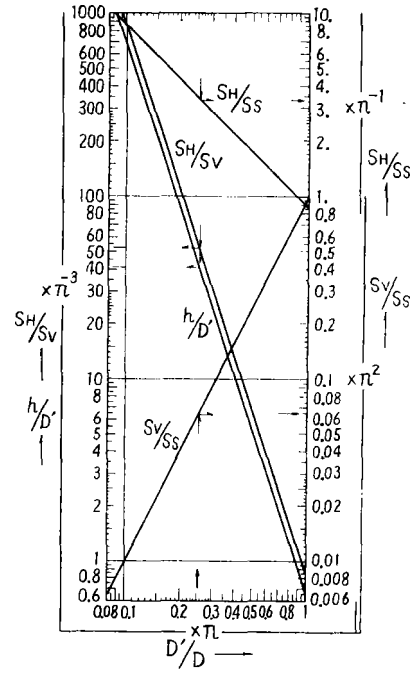


Fig. 5. Correlations between the diameter ratio (D'/D) and the shape character of disc-body (h/D' and S_H/S_V) and also between former and section-ratio (S_H/Ss and S_V/Ss). Formula (11, 13 and 14).

It must be remembered that density of shell has been assumed 2.7. Since shell contains a considerable amount of bonding water and has a basket-frame structure, as demonstrated by IZUKA and IRIE (1963) with Electron Micrography, the thick-

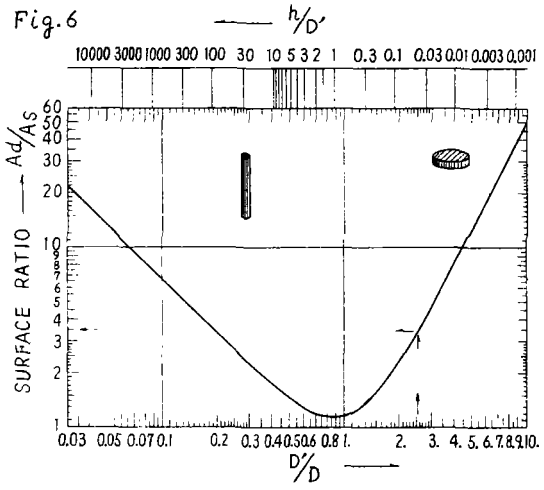


Fig. 6. Diagram of finding the surface-ratio from the diameter-ratio. Formula (10).

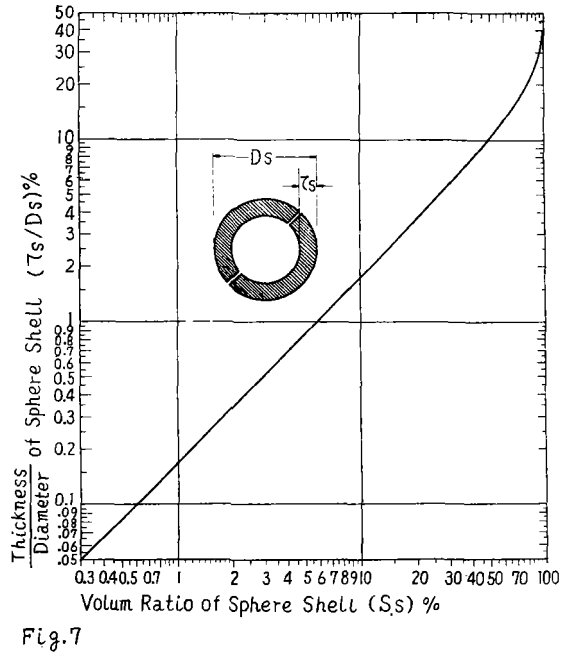


Fig. 7. Correlation between the volume-ratio (S) and the thickness (τs) of the spherical shell. Formula (15).

ness measured with ordinary microscope may be greater than the value calculated.

The formula (8) showing the relation between the effective diameter and the surface of an equi-volume sphere and the formula (9) showing the relation between the former and the volume of an equi-volume sphere are diagrammatically represented in *Fig.* (*4*).

A diagram of the formula (11) for finding the diameter of equi-volume sphere from the direct sight of diatom cell, and the same of formulae (13) and (14) for finding the section ratio from the diameter-ratio are shown together in *Fig.* 5.

A diagram of the formula (10) for finding the surface-ratio from the diameter-ratio of equi-volume disc is shown in *Fig.* 6. The correlation between the volume-ratio and the thickness of sphere shells defined by the formula (15) are shown in *Fig.* 7. Thus, the structural character of objective diatoms easily state in figures by means of those diagrams.

For example, in *Coscinodiscus janischii* studied by J. NAKAI (1942) mentioned above, its individual weight is 2 micrograms, so that the individual volume is about $2 \cdot 10^6$ cubic micron. The volume ratio of shell (S) is 1.13% when their dp is neutral to the water of $d = 1.02$.

In this case X is 19.5% from *Fig.* 1, dl' is 1.0005 from *Fig.* 2, and $dp\ max$ is 1.039, from *Fig.* 3 when $dl' = d$. The diameter of this diatom (D') is estimated at 396 microns after NAKAI's microscopical measurement.

Dimension of a sphere, which is equi-volume to this diatom, is estimated from the *Fig.* 4, and *Fig.* 7 as follows:

$$D = 156.3 \text{ micron}$$
$$As = 7.69 \cdot 10^4 \text{ square micron}$$
$$\tau s = 0.295 \text{ micron}$$

So that, the diameter-ratio is:

$$\frac{D'}{D} = \frac{396}{156.3} = 2.53$$

Now, dimension of this diatom is estimated as follows:

From *Fig.* 5. $\frac{h}{D'} = 0.0412$

therefore, $h = 396 \cdot 0.0412 = 16.3$ micron

section-ratio $\frac{Sv}{Ss} = 6.4, \quad \frac{SH}{Ss} = 0.336, \quad \frac{SH}{Sv} = 0.0525$

From *Fig.* 6. surface ratio = 3.46

therefore $Ad(\text{surface}) = 7.69 \cdot 10^4 \cdot 3.46 = 26.6 \cdot 10^4$ square micron

$\tau(\text{thickness of the shell}) = \frac{0.295}{3.46} = 0.086$ micron

H. H. GRAN (1912) classified the shape of diatoms into four types: 1) the bladder type, 2) the needle or hair type, 3) the ribbon type, and 4) the branched type. He remarked at the same time that the bladder type falls in a zigzag course and that the needle type falls fast when it is in vertical position and slow when it is in horizontal position, which compels it to fall describing a great wide circles. In other words, the falling velocity of diatoms vary according to their pose against the gravitational direction.

Give α to the inclination of disc's axle to the gravitational direction, then the ratio between the projection of this disc and the same of the equi-volume sphere can be represented by the following formula.

$$Projection\ Ratio = (D'/D)^2 \cdot \cos\alpha + (D/D') \cdot \sin\alpha \cdot 8/3 \cdot \pi \quad \cdots\cdots(16)$$

However, so far as resistance of water against falling particles of extreme minuteness acts upon the totol surface, it is difficult to say whether the shape coefficient in the formula of falling velocity is mainly determined by the surface ratio, or by the gravitational projection-ratio, even in the diatoms of prototype.

It seems necessary, therefore, to examine the correlation between the surface, ratio, or the projection, and the shape coefficient to be used in the equation of falling velocity in various prototypes.

A method appropriate for the model experimentation of minute particles must be first proposed and discussed.

III. The Maximum Falling Velocity of Dead Diatom Shells

According to Stokes' law, known as the falling velocity equation for minute spherical particles, the falling velocity (v) is in inverse proportion to the viscosity of medium solution, and in direct proportion to the difference between dp and d, and the square diameter of particles.

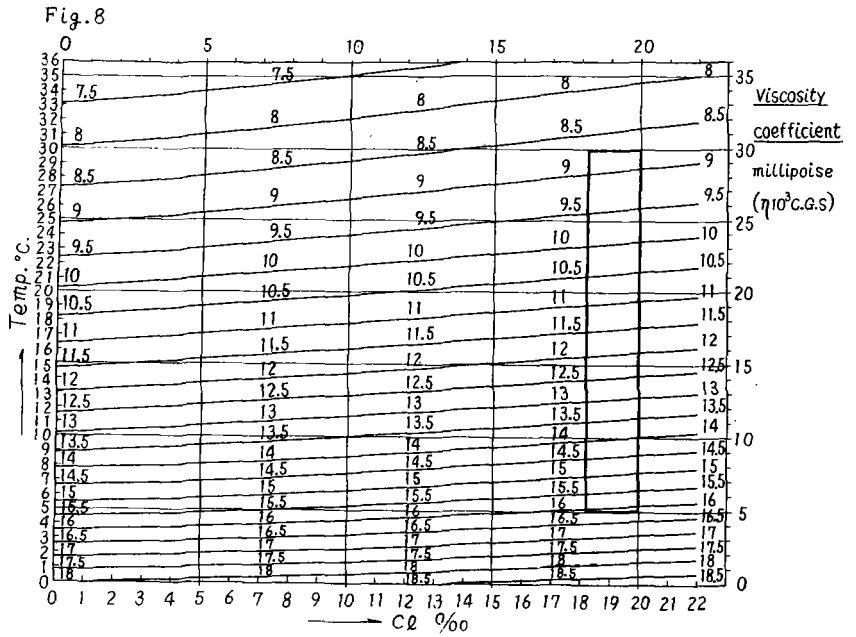
$$v = \frac{2}{9} \cdot \frac{(dp-d)}{\eta} \cdot g \cdot r^2 \text{ cm/sec.} \quad \cdots\cdots(17)$$

Denotations:

g: Acceleration due to gravity.
r: Radius of the particle in cm.
η: Absolute viscosity in poise.

η estimated from temperature and chlorinity (salinity) of sea water becomes larger as salinity rises and temperature falls. Under natural conditions the effect of salinity variation is considerably smaller than that of the temperature.

If the pressure effect is ignored, the maximum viscosity in the poise in sea water is 0.019 and the minimum viscosity in the poise in fresh water is 0.007.
T-Cl diagram of viscosity is shown in *Fig. 8*.



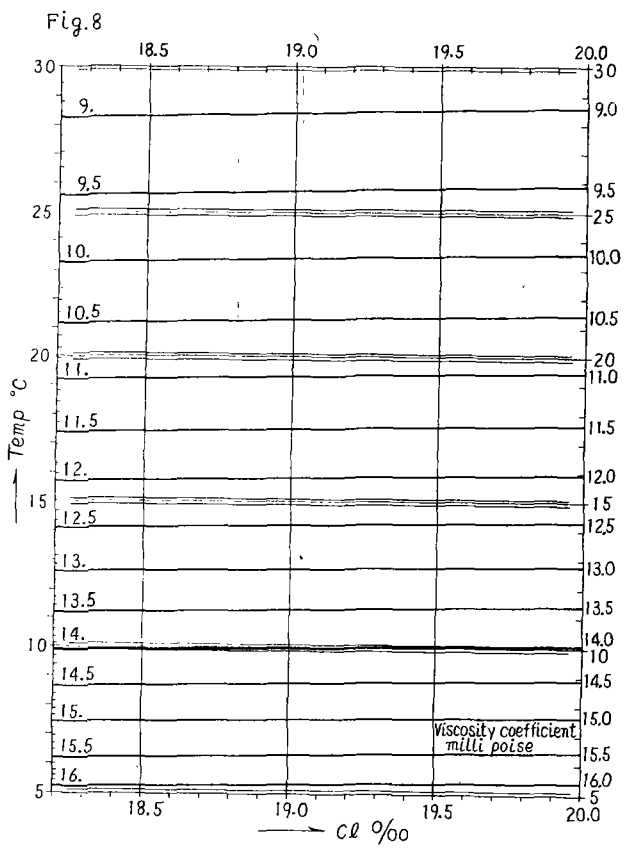


Fig. 8. ***T-Cl*** diagram of the viscosity.

Now, by transforming the formula (17), the falling velocity equation of diatom cells under the condition $dp > d$ is sought as in the following.

Denotations:

Vel: Falling velocity in cm/day.
D: Effective diameter (diameter of equi-volume sphere) $=1.24\cdot\sqrt[3]{V}$ in micron.
μ: Absolute viscosity of sea water in millipoise.
d: In-situ density of sea water. $=1+\sigma_{tD}/10^3$
K: Coefficient of shape resistance. (sphere$=1$).

$$Vel=\frac{47.088}{\mu}\cdot\frac{\{(1700-\sigma_{tD})\cdot S-X\cdot(75+\sigma_{tD})\}}{10^3}\cdot\frac{D^2}{K} \quad \cdots\cdots(18)$$

The maximum falling velocity of dead diatom shells (***Vel*** max) is obtained at $X=0$, namely at the time when oil particles become extinct and dl' equals to d in the formula (18).

$$Vel_{max.}=\frac{47.088}{\mu}\cdot\frac{(1700-\sigma_{tD})}{10^3}\cdot\frac{S\cdot D^2}{K}=\upsilon\cdot\frac{S\cdot D^2}{K}=\frac{1.502\cdot\upsilon\cdot S\cdot V^{2/3}}{K} \quad \cdots(19)$$

υ is estimated from the environmental **T-Cl.**

υ stands for the falling velocity coefficient of environment for dead diatom shells, and is shown in *Table 1*.

Table 1.: Coefficient of the maximum falling velocity for the dead diatom shells by means of the environmental character (σ_{tD} and viscosity). (υ in cm/day.)

σ_{tD} \ μ viscosity in millipoise	7	8	9	10	11	12	13	14	15	16	17	18	19
0	11.44	10.01	8.90	8.00	7.28	6.68	6.154	5.75	5.34	5.015	4.71	4.45	4.22
10	11.37	9.95	8.86	7.96	7.23	6.64	6.12	5.695	5.31	4.99	4.68	4.43	4.19
20	11.31	9.90	8.80	7.91	7.19	6.60	6.08	5.66	5.275	4.96	4.65	4.40	4.17
30	11.24	9.84	8.75	7.86	7.15	6.56	6.045	5.63	5.24	4.93	4.63	4.375	4.14

Table 1 agrees well with the table for the falling velocity of quartz spheres of one micron diameter, or with the condition in which s, k and D all equal to 1.

As may be clear from the table, the main factor of environmental effect on υ is the viscosity of water, the effect of in-situ water density being much smaller.

The viscosity of sea water is mainly influenced by temperature under normal conditions. We have no information on the characteristics of viscosity under the deep sea conditions with high pressure and low temperature, though the property of deep sea waters are now going to be studied by SASAKI, T. and T. NAGATA (1964) in Japan.

Both the effective diameter and the volume ratio of shell substances are defined by volume. Although they can be obtained by measurement, the value of K, which

may represent the shape resistance characteristics, is still unknown as mentioned before.

The correlation between effective diameter and maximum falling velocity under the conditions that $S=1$ and $K=1$ in the formula (19) is shown in *Fig. 9.*

Fig. 9.

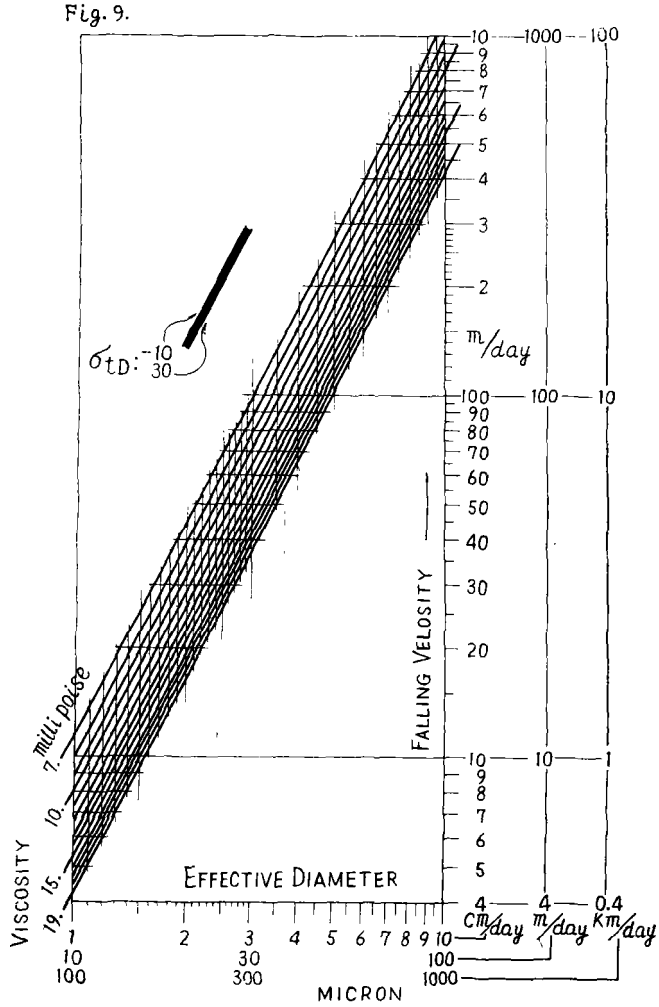


Fig. 9. Diagram of finding the falling velocity for quartz sphere ($K=1$, $\sigma_{tD}=1$ or 3) from the effective diameter and also viscosity. Formula (18).

In the case of *Coscinodiscus janischii* measured by NAKAI, when μ is assumed to be 10 millipoise, the maximum falling velocity corresponding to equi-volume sphere ($K=1$, $S=1$, $D=156.3$ micron) is 1900 m/day as seen from *Fig. 9.*

Therefore, when $S=0.0113$ is put into this value, we get 21.5 m/day for the

Vel max of a sphere shell.

If application of surface ratio to K were possible, the maximum falling velocity of this diatom would be $21.5/3.46=6.21$ m/day. When projection ratio is applied, the maximum falling velocity is $21.5/6.4=3.36$ m/day in vertical position, and $21.5/0.336=64$ m/day in horizontal position.

Data concerning the falling velocity of diatom shells exist very little even in the field of marine geology.

The table that Ph. H. KUENEN (1950) compiled gives the velocity of 0.15 cm/sec ($=129.6$ m/day) in a diatom (species undetermined) of a diameter of 40 micron. This equals to the velocity of quartz sphere of $S=1$, under the condition of $\mu=10$ millipoise. Even if this diatom is assumed to have a spherical shape (or $K=1$), such may not be possible with an individual cell. It seems some potential errors exist in his datum.

In many cases, diatoms form a chained colony by their propagation, and then their dead cells form by flocculation a large mass (so-called Marine Snow), sometimes which may get a larger falling velocity. The self-coagulate-precipitation, though, cannot be expected in the case of a sparse population.

In his study of size distribution of primary production in the ocean, using ^{14}C and millipore filters of various pore sizes, SAIJŌ, Y. (1963) reported that the main portion of the production is originates in the microorganisms which can passing away through the plankton net (XX13).

At the International Indian Ocean Expedition (I.I.O.E.) in which the author participated on board Umitaka-maru, HA type millipore-filter of pore size 0.4 micron was prescribed for use in experimentation of primary productivity and determination of chlorophyll. He got from some samples taken from surface water on a return voyage the same results as SAIJŌ's as shown in *Table 2* below.

Table 2.: The size distribution of primary production on some of the surface samples at the Far East waters. (percentage)

Sample / Filter				SS	RA		AA	DA		HA	PH	GS
Lat.	Long.	Date	Pore Dia:	3	1.2		0.8	0.65		0.45	0.3	0.22 micron
09-41.1 S	103-35.0 E	1964 Jan. 16	55.9	6.5	18.1			18.2			1.3	
05-04.0 N	113-48.5 E	Feb. 4	93.9	zero				zero			6.1	
11-13.2 N	118-22.5 E	Feb. 6	69.1	10.9				5.6			14.5	
16-16.6 N	119-32.0 E	Feb. 7	55.4	4.3				38.6			1.7	
20-41.0 N	121-02.0 E	Feb. 8	59.8	7.4				24.6			8.2	
26-50.5 N	123-23.5 E	Feb. 9	78.4	20.6				1.0			zero	
28-51.7 N	125-39.8 E	Feb. 10	91.0	4.6				4.4			zero	
33-09.0 N	135-34.0 E	Feb. 15	46.7	38.3	6.4			4.0	2.9		1.6	0.1

This means that about a half of the production frequently makes its appearance in the size section smaller than three micron, and that sometimes the size fraction smaller than 0.8 micron reaches about 40% of whole.

During on board Umitaka-maru in the I.I.O.E. (1963–1964), the author carried out the experiment of primary productivity on the basis of 311 water-samples. On that occasion, in order to make clear the constitution of the standing crops, he attempted to concentrate the micro-organisms contained in 2 liters of each sample exclusively.

For the concentration of sample, 22-hours settling-precipitating method with a settling cylinder of one-meter length was employed to save expenditures in many large bottles. Such a concentration method has been widely used for the research of microplanktons.

The minimum particle, which is possible to fall down through one meter of the cylinder within 22 hours, is a quartz sphere of 3.7 micron-diameter as may be seen from Fig. 9 for 10 millipoise-viscosity.

Even if the shapes of dead diatoms (turned into $dl'=d$) are assumed to be spherical ($K=1$) and they are smaller than those, the dimensions of which are indicated below, they can not fall down under the above mentioned condition.

volume ratio of the diatom shell (S)	1.0	0.06	0.05	0.04	0.03	0.02	0.01	0.005
Effective diameter in micron (D)	3.7	15.0	16.5	18.5	21.3	27.5	37.0	52.5

In short, it is obvious that, unless the population density of organisms in the sample water is in such a condition as unexpectedly favorable for creating a flocculation, any successful concentration of organisms smaller than 30 micron-diameter cannot be expected.

Since this settling method has a fatal weakness for oceanic samples of sparse population as pointed out before, the author hopes that the persons concerned bear the limit of the method in mind so as not to repeat his failure.

The co-precipitation method is excellent for the pre-treatment in determining the trace elements and radio-active substances in sea water owing to its simplicity of operation and of apparatus necessary for it.

To make use this method as perfectly as possible in concentrating the micro-organisms, he wishes to suggest to reconsider the way of its use.

Another countermeasure with mechanical method is prepared for increasing of g in formula (17) by the use of centrifugal force instead of the acceleration of gravity.

The centrifugal force is illustrated in the following equations:

$$\text{centrifugal force} = \frac{(\text{linear velocity})^2}{\text{radius of rotation}} = \frac{(R\cdot\omega)^2}{R}$$

$$= R\cdot\omega^2 = R\cdot(2\cdot\pi\cdot N)^2$$

where ω: Angular velocity.
N: Number of revolutions per second.

BAVER, L. D. (1948) represents the time required for driving a particle in a centrifuge from R_1 (the distance from the axis of rotation) to a given depth R_2, as in the following formula.

$$t \text{ in second} = \frac{9}{2} \cdot \frac{\eta}{(dp-d)\cdot r^2} \cdot \frac{ln \frac{R_2}{R_1}}{(2\cdot\pi\cdot N)^2} \quad \cdots\cdots\cdots(20)$$

In applying the formula (20) to diatoms, the denotations and assumptions are given as follows:

$R_2/R_1 = 2$

T: The time required for centrifugal separation in minutes.

$n = \frac{60\cdot N}{1000}$: Number of revolutions in thousand per minutes.

Vel: Falling velocity in cm per day in the formula (18) and (19).

Then, the actual equation to be obtained by transforming the formula (20) is as in the following,

$$T = \frac{24\cdot 60\cdot 2.303\cdot \log 2}{Vel} \cdot \frac{3600\cdot 980}{(10^3\cdot n)^2} = 89.3/(Vel\cdot n^2) \text{ minutes} \cdots\cdots\cdots(21)$$

The correlations between n and T for the diatoms which are smaller than 5 micron-diameter and assumed to be of spherical shape ($K=1$), and in which $dl' = d$ and $S=0.01$, under the conditions of $\mu=10$ millipoise, are shown in the table inserted below.

Table 3.: The requisite time **in minutes** for centrifugal separation. From the Fig. 9 and formula (21).

Revolutions / Diameter	1	2	3	4	6	8	10	12	15	20	$25\cdot10^3$ /min.
micron											
0.5	4570.	1145.	509.	286.	127.3	71.6	45.7	31.8	20.4	11.45	7.35
1	1115.	279.	124.	69.8	31.0	17.45	11.15	7.75	4.96	2.79	1.79
2	284.	71.	31.6	17.8	7.9	4.45	2.84	1.97	1.26	0.71	0.46
3	127.5	31.9	14.2	8.0	3.6	2.00	1.28	0.89	0.57	0.32	0.21
4	71.4	17.9	7.9	4.5	2.0	1.12	0.72	0.50	0.32	0.18	0.12
5	46.0	11.5	5.1	2.9	1.3	0.72	0.46	0.32	0.21	0.12	0.074

In the case of a quartz particle ($S=1.0$, $dp=2.7$), requisite time is only one percent of the table value as mentioned above.

Table 3 shows that, when sampling is aimed at the same organisms as the objective microorganisms used as material for the experiments of primary productivity in the ocean, the ultra-centrifuge of over 15000 revolutions per minute should

be necessary.

Moreover, for the reason that the density of actual living diatoms (***dp***) is close to that of environmental water (***d***) and their shape coefficients (***K***) are much larger than ***I***, the author would like it may be well to suggest that, for such a centrifuging, it will be necessary to plan the one combined with the use of chemical coagulants, or precipitants.

References:

BAVER, L. D., (1948). Soil Physics. New York, John Wiley & Sons, Inc., 398 pp.

FLEMING, R. H., (1940). Composition of plankton and units for reporting populations and production. Sixth Pacific Sci. Congr. Calif., 1939, Proc., V. 3. 535-540.

GRAN, H. H., (1912). Pelagic plant life. In Murray and Hjort, Depth of the Ocean. London. Macmillan, 821 pp., 307-386.

IIZUKA, S. & H. IRIE, (1963). Electron Micrographic Study on the Marine Diatoms, especially *Skeletonema costatum* (GREV.) CLEVE. Bulletin of the Faculty of Fisheries, Nagasaki Univ., 15. 92-99.

KUENEN, Ph. H., (1950). Marine Geology. New York, John Wiley & Sons, Inc., 568 pp.

NAKAI, J., (1942). The chemical composition, volume, weight and size of the important marine plankton. Journ. Oceanog. Soc. Jap., 1. 45-55. in Japanese.

SAIJŌ, Y., (1963). Problem in the Study of Primary Production in the Sea. Information Bulletin on Planktology in Japan. 10. 9-17. in Japanese.

SASAKI, T. & T. NAGATA, (1964). Preliminary Reports on the Properties of Deep Sea Waters. Lectured on Oceanog. Soc. Jap., 1964. in Japanese.

Résumé

In this report physical models of diatoms were schematically constructed as an attempt to study the falling velocity of diatoms and the density *in-situ*, and the dimensions related to their shape were also discussed in some detail.

The model of diatom cells is composed of three elements, namely, the shell, oil particles and cell sap.

The constitutional condition of diatom cell necessary for its staying in neutral state was discussed on the assumption that density of the three constituents are respectively $\boldsymbol{ds}=2.7$, $\boldsymbol{do}=0.925$, $\boldsymbol{dl}=\boldsymbol{d}$ (*in-situ* density of environmental water).

The formula obtained is:

$$\boldsymbol{S}\cdot\boldsymbol{X}^{-1}=(\boldsymbol{d}-0.925)\,(2.7-\boldsymbol{d})^{-1}$$

where, $\boldsymbol{S}=\dfrac{\text{volume of shell}}{\text{volume of cell}}$

$$\boldsymbol{X}=\frac{\text{volume of oil particles}}{\text{volume of cell}}$$

$$\boldsymbol{S}+\boldsymbol{X}<1$$

The density of dead diatom cell reaches its maximum point when protoplasm

of the cell is replaced by the environmental water, or when $X=0$.

Namely,

$$dp \text{ max} = 2.7 \cdot S - (1 - S) \cdot d$$

Stokes' law (formula for the velocity of the falling particle) is transformed into the following equation.

$$Vel = \frac{47.088}{\mu} \cdot \frac{\{S \cdot (1700 - \sigma_{tD}) - X \cdot (75 + \sigma_{tD})\}}{10^3} \cdot \frac{D^2}{K} \text{ cm/day}$$

where, μ = Viscosity in millipoise.
$d = 1 + \sigma_{tD}/10^3$
$D = 1.24 \sqrt[3]{V}$ = effective diameter in micron.
K = Resistance coefficient due to the shape.

The maximum falling velocity which occurs at dp_{max} is obtained from the following formula.

$$Vel \text{ max.} = \frac{47.088}{\mu} \cdot \frac{(1700 - \sigma_{tD})}{10^3} \cdot \frac{S \cdot D^2}{K} = \upsilon \cdot \frac{S \cdot D^2}{K} = \frac{1.502 \cdot \upsilon \cdot S \cdot V^{2/3}}{K} \text{ cm/day}$$

A practical formula of the requisite time necessary for centrifugal separation is obtained as shown below.

$$T = \frac{89.3}{n^2 \cdot Vel} \text{ minutes}$$

where n: Rotation number in 10^3 revolutions/minnute.

The shape of planktonic diatoms, which actually varies from a needle-form to a membranous-form, was tentatively represented by a disc, and a study was made with respect to the relationship between the changes in shape and the surface ratio, or the section ratios.

The relationship between the surface ratio, or the section ratio, and the coefficient of resistance due to shape (K) needs further confirmation with some new experimental methods.

In the quantitative study of micro plankton based upon the water-sampling method, it is absolutely necessary to find out a unfailing, sure method of concentration in accordance with the size of objective organisms.

Both the settling method and the centrifuge one are inappropriate themselves for such a study as the experiment on the primary productivity of the ocean.

Techniques for Measuring Oceanic Primary Production Using Radioactive Carbon

By N. Dyson, H. R. Jitts, and B. D. Scott

Division of Fisheries and Oceanography
Technical Paper No. 18

Commonwealth Scientific and Industrial
Research Organization, Australia
Melbourne 1965

Collected reprints of the International Indian Ocean Expedition, vol. V, contribution no. 295

TECHNIQUES FOR MEASURING OCEANIC PRIMARY PRODUCTION USING RADIOACTIVE CARBON

By N. DYSON,* H. R. JITTS,* and B. D. SCOTT*

[*Manuscript received February* 5, 1965]

Summary

Changes made since 1957 in the ^{14}C technique are described. Descriptions are given of a modified sampler which automatically introduces ^{14}C, plastic filtration units for use with membrane filters, two constant light incubators, and a windowless gas-flow counter. Tests of sampling errors gave coefficients of variation between 10 and 30%; it is concluded that measurements which differ by more than 80% are significantly different.

I. INTRODUCTION

The ^{14}C method of measuring primary production of organic matter has been used by this Laboratory for extensive surveys in both the Indian and Pacific Oceans. Since the techniques used were described by Jitts (1957), modifications have been made both in the equipment and in the treatment of samples and data. These changes, and studies of the sampling errors involved in the ^{14}C method, are described in this report.

II. METHODS

(*a*) *Preparation of Ampoules*

$Na_2{}^{14}CO_3$ solution of high specific activity is obtained from the Radiochemical Centre, Amersham. It is diluted with CO_2-free distilled water, and NaCl and Na_2CO_3 added so that the solution contains 10 μc of ^{14}C, 30 mg NaCl, and 0·09 mg CO_2 in each millilitre. This solution is filtered through an HA Millipore filter.

One ml ($\pm$0·01 ml) aliquots of the solution are sealed in 2 ml glass ampoules and the ampoules are autoclaved at 15 lb/in^2 for 15 min. They are then immersed in a dye bath under a pressure of 75 lb/in^2, and inspected visually for leaks, volume, and particulate matter.

(*b*) *Collection and Treatment of Samples, 1957–61*

Until 1962, samples were taken with the twin 400 ml Perspex samplers (Fig. 1) described by Jitts (1957). These were incubated either *in situ* or in the upright position in an artificial light bath (Fig. 2) between two banks of three horizontal 20 W fluorescent tubes (Philips TLS 20 W/33), giving a light intensity of about 1100 f.c. For some experimental *in situ* measurements the twin 400 ml sampler was modified (Fig. 3) to allow the automatic introduction of ^{14}C without bringing the samples to the surface. As the sampler closed, a glass ampoule of the ^{14}C solution was broken in the sampler and a spring-loaded Perspex propeller stirred the contents.

* Division of Fisheries and Oceanography, CSIRO, Cronulla, N.S.W.

After incubation, the samples were filtered through 24 mm Millipore HA filters in the Perspex filtration units shown in Figure 4. In all other respects the treatment of samples was as described in the next section.

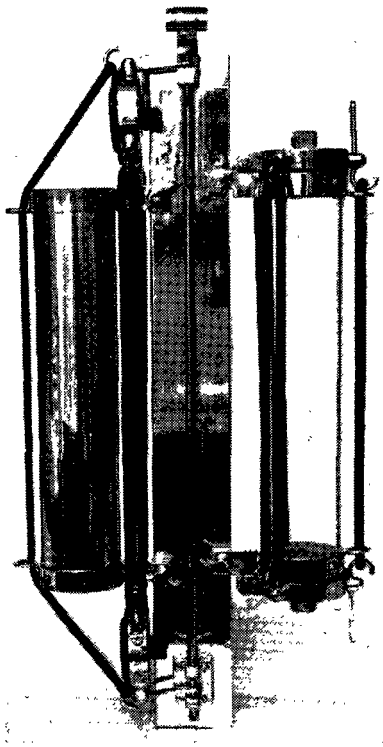


Fig. 1

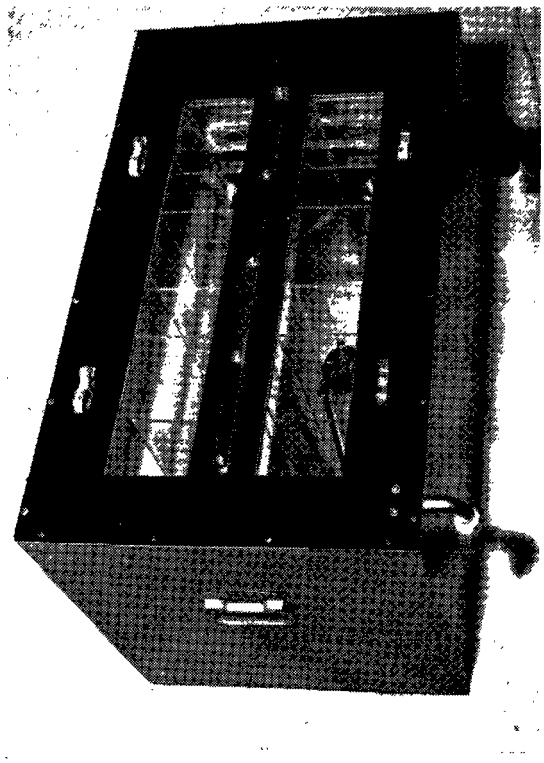


Fig. 2

Fig. 1.—A twin 400 ml light and dark plastic sampler for measuring primary production in sea-water without the need for further transfers of the samples. The light bottle is shown closed and the dark hooked open. The bottles can be detached from the frame for incubation in a light bath.

Fig. 2.—A constant artificial light incubator for use with the 400 ml samplers shown in Figure 1. The three banks of three horizontal fluorescent tubes (Philips TLS 20 W/33) give a light intensity of about 1100 f.c.

(*c*) *Collection and Treatment of Samples, 1962 onwards*

In 1962 the twin 400 ml Perspex samplers were superseded by a twin 6 l. sampler described by Jitts (1964). This sampler is used to enable samples for other work (phytoplankton, pigments, and particulate carbon) to be collected simultaneously.

The samples are collected from various predetermined depths, usually 0, 25, 50, 75, 100, and 150 m, or from depths determined by the "balance by depth" method of photometry described by Jitts (1963). Subsamples are drawn from these samplers into two 300 ml Pyrex glass bottles, one of which is clear and the other light-proofed

with black-painted adhesive bandage. Before incubation, the stoppers of the dark bottles are light-proofed by covering them with a sheet of aluminium foil.

The contents of a ^{14}C ampoule are added to the sample with a hypodermic syringe, the ampoule washed with 1 ml of the sample, and the washings added to the sample.

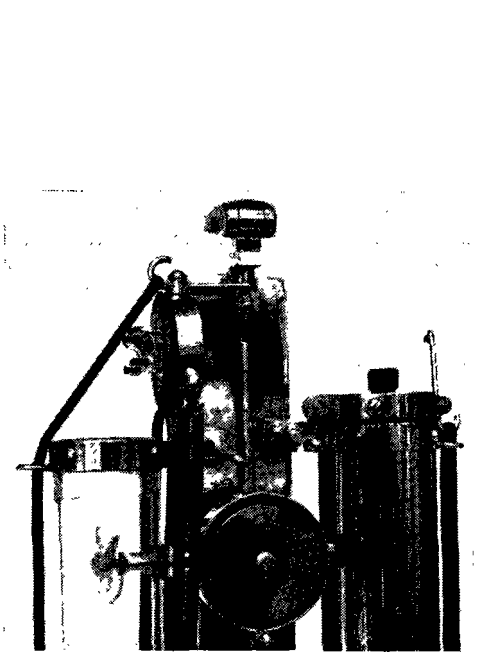


Fig. 3

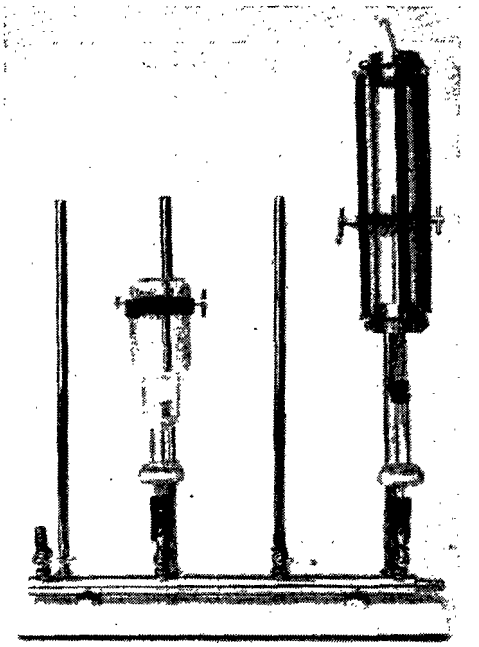


Fig. 4

Fig. 3.—A modification of the twin 400 ml plastic sampler shown in Figure 1; this allows the automatic introduction of ^{14}C into the sample when the sampler is closed. A glass ampoule containing the ^{14}C is inserted in the holder under the lid. When this closes, the ampoule is broken against the plastic rod across the top of the tube. At the same time the spring-loaded propeller is released and stirs the contents of the sampler.

Fig. 4.—Two types of plastic filtration units for use with 24 mm membrane filters. The one on the left is shown with a 300 ml bottle inverted into the unit. The unit on the right is shown connected to a 400 ml plastic sampler.

For measuring productivity under constant artificial light the bottles are placed in an incubator as shown in Figure 5. The samples are kept cool by surface sea-water passed through the Perspex tanks containing the bottles. This incubator is very similar to one described by Doty and Oguri (1959).

For measuring *in situ* production the bottles are placed either on wire clamps for *in situ* incubation or in the simulated *in situ* incubator described by Jitts (1963). The samples are incubated by either of these two methods for a half-day period, i.e. from sunrise to noon or, more frequently, from noon to sunset.

After incubation the bottles are inverted into the Perspex filter units (Fig. 4) and the sample is filtered through a 24 mm Millipore HA filter, using a vacuum of not more than 15 inHg. The vacuum is provided by a diaphragm or rotary oil pump via two 6 gal tanks connected in series. These act as a vacuum reservoir and container for the filtrate. After filtration the filters are washed with 10 ml 0·001N HCl in 3% NaCl, followed by 10 ml 3% NaCl to remove any inorganic ^{14}C remaining on the

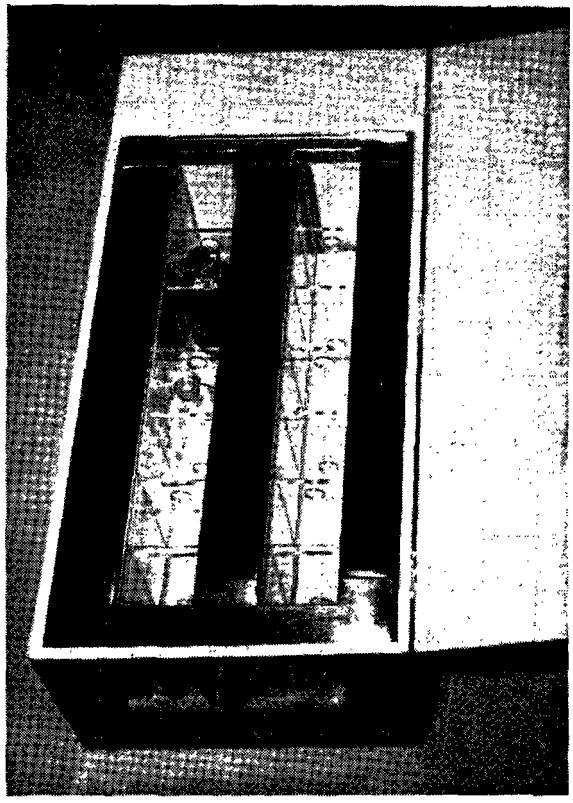


Fig. 5.—A constant artificial light incubator for use with 300 ml glass bottles. The three banks of two horizontal fluorescent tubes (Philips TLS 20 W/33) give a light intensity of about 1100 f.c.

filter. The filters are sucked dry and placed in numbered plastic holders, held by a smear of petroleum jelly. These are placed in a metal desiccator with silica gel and the filters dried for about two days before counting. Immediately before counting, the filters are numbered in the margin for identification.

After use, the glass bottles are washed with conc. HCl, then rinsed twice with fresh water and left to drain. The plastic samplers are rinsed with fresh water and drained dry after each use, but are also washed with conc. HCl and detergents before initial use and at about monthly intervals during cruises.

(*d*) *Counting*

A windowless gas-flow Geiger counter is used with an Ekco N530 scaler. The counter was made in this Laboratory. It has three planchet positions, a chromium-plated brass counting chamber, and a tungsten electrode; it is shielded by aluminium and lead (Fig. 6). This counter has a starting voltage of 1300 V and the Geiger plateau has a slope of 2% with no signs of continuous discharge below 1800 V. Using an operating voltage of 1450 V the counting efficiency is approximately 50% and the background is between 10 and 15 counts/min. The counter is used in an air-conditioned room to give greater stability.

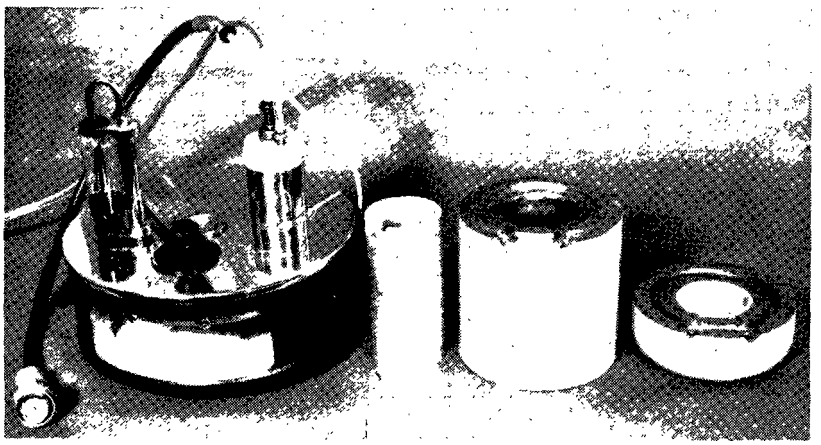


Fig. 6.—A windowless gas flow Geiger counter. Shown with the aluminium and lead shields removed from the chrome-plated brass counting chamber.

The filters, mounted on brass planchet holders, are preflushed with Tracerlab Q gas (helium with isobutanol) in the counter for 5 min at the rate of one bubble per second; the planchet carrier plate is then rotated and the sample counted for 5 min or 30,000 counts, whichever occurs first. After every second count, a ^{14}C standard is counted to correct for instability in the counter. This standard is a piece of poly (methyl-^{14}C) methacrylate (Amersham CFP 2) having the same geometry as the filtering area of the filters and a known activity of approximately 6000 counts/min. The counter background is determined by counting a blank filter for 1 hr on each day that counting is done.

The method of Jitts and Scott (1961) is used to determine the efficiency of the Geiger counter and the absolute and zero-thickness activities of the ampoules. These are standardized with a Hexadecane Reference Standard (Amersham, CFR 2) by liquid scintillation counting.

III. Calculation of Results

Raw data for samples collected at each station are recorded on the sheets shown in Table 1. Calculations are done by an electronic computer. The raw data are punched on cards and the results obtained printed out in the form shown in Table 2.

TABLE 1

LOG SHEET FOR RECORDING RAW DATA

CSIRO DIVISION OF FISHERIES AND OCEANOGRAPHY PRODUCTIVITY LOG SHEET NO. 2

Sheet No. 29 of 55

Vessel	Cruise	Station No.	Year	Month	Day	Time	TZ*	Latitude	NS	Longitude	EW	Observer
Diamantina	1	34	63	4	6	0930	−8	11° 06′	S	109° 57′	E	B. Scott

Sonic Depth	Dist. Coast	Incub. Meth.		Stock No.		Stock Activity	TE*	Bkgd†	CT*	OI*	Time In	Out	Period
4938		Bath	0	15		$9{\cdot}59\times10^{6}$		10	08		1000	1330	3·50

Depth	Temp.	Lt. Bottle		Dk. Bottle		Raw Count		St. Correction		DD*	CT*	OI*	Corrected Counts			Production	
		No.	Filter	No.	Filter	Light	Dark	Light	Dark				Light	Dark	Net	A	B
0		1	1641	7	1647	2106	422	0·96	1·00		80		395	74	321	0·26	
25		2	1642	8	1648	2258	279	0·99	0·98				437	45	392	0·29	
50		3	1643	9	1649	3244	265	0·99	0·98				633	42	591	0·43	
75		4	1644	10	1650	930	201	0·99	0·97				174	29	145	0·11	
100		5	1645	11	1651	392	201	0·99	0·97				67	29	38	0·03	
150		6	1646	12	1652	201	240	1·00	1·00				30	38	0	0·00	0·26

Remarks:

* Qualitative symbols used in the computer program.

† Bkgd is the background in counts/min.

TABLE 2

COMPUTER PRINT-OUT

SHIP	CRUISE	ST. NO.	YEAR	MONTH	DAY	TIME	LATITUDE	LONGITUDE
11	1	34	63	4	6	0930 H	11 06 S	109 57 E

SONIC DEPTH	DISTANCE FROM COAST	INCUBATION METHOD	STOCK NUMBER	STOCK ACTIVITY	BACKGROUND
4938	190	0	15	9·590	10

DEPTH	LIGHT COUNT	LIGHT COUNT	MEAN LIGHT	DARK COUNT	DARK USED	NET COUNT	INCUBATION PERIOD	PRODUCTION A	PRODUCTION B	LIGHT STANDARD	LIGHT STANDARD	DARK STANDARD
0	394	—	—	74	36	358	3·500	·26	·00	·96		1·00
25	437	—	—	45	45	392	3·500	·29	·07	·99		·98
50	633	—	—	42	42	591	3·500	·43	·16	·99		·98
75	174	—	—	29	29	145	3·500	·11	·23	·99		·97
100	67	—	—	29	29	38	3·500	·03	·25	·99		·97
150	30	—	—	38	38	−8	3·500	·00	·26	1·00		1·00

In the computer program, the raw count is reduced to counts/min, then corrected by the factor obtained from the ^{14}C standard count. From this the background is subtracted. The net activity is obtained by subtracting the dark bottle result from that of the light bottle. The rate of production in mg C/hr/m^3 (Production A) is calculated using the formula:

$$\text{Rate of Production} = \frac{\text{Net Activity}}{\text{Added Activity}} \times \frac{\text{Total } CO_2}{\text{Hours of Incubation}},$$

where the "Added Activity" is the zero-thickness Geiger activity in counts/min of the ^{14}C ampoules used and "Total CO_2" is assumed for oceanic waters to be constant at 24,500 mg C/m^3 (90 mg CO_2/l.).

In the case of *in situ* or simulated *in situ* incubations the rate of production in mg C/day/m^3 is calculated using the formula:

$$\text{Rate of Production} = \frac{\text{Net Activity}}{\text{Added Activity}} \times \frac{\text{Total } CO_2}{\text{Days of Incubation}},$$

where a "day" is assumed to be the period from sunrise to sunset.

The rate of production under 1 m^2 of the water column sampled in g C/day^2/m^2 (Production B) is obtained by integrating the results of all the samples in the column by the formula:

$$\text{Column Production} = \frac{f}{1000}\left[(d_1-d_0)\left(\frac{a+b}{2}\right)+(d_2-d_1)\left(\frac{b+c}{2}\right)+\ldots\right],$$

where d_0, d_1, d_2 are the depths sampled;

a, b, c are the respective production rates;

f is a factor for converting the units to production per day.

When incubation is *in situ* or simulated *in situ*, f is 1. When incubation is under a constant artificial light it is 10, because the daily rate is assumed to be 10 times the hourly rate.

The results of both Production A and Production B are rounded off to two decimal places. If duplicate light bottles are counted, the mean of the corrected counts is taken. If the dark count is missing or rejected as aberrant, i.e. it is greater than 50 counts/min and also greater than 10% of the mean light count, the mean dark count of all the non-aberrant values at the station is used. If all the dark counts are aberrant, an arbitrary figure of 20 counts/min is used.

IV. Errors in Estimation

The errors in estimation of production by the ^{14}C method described in the preceding sections were determined at: (i) two all-day stations carried out by F.R.V. *Derwent Hunter* on July 25 and 30, 1959, during which the ship was drifting about 50 miles off the coast near Sydney, (ii) seven stations by H.M.A.S. *Kimbla* from September 14 to 16, 1959, all at least 20 miles off the continental shelf between Coff's Harbour and Sydney, and (iii) a station in the Indian Ocean (19° 25′ S., 94° 27′ E.) by H.M.A.S. *Diamantina* on July 21, 1960 (Dm2/143/60).

In the first series, the errors due to the method were estimated by measuring the productivity of replicate subsamples from a large sample of well-mixed surface sea-water. Surface sea-water was collected with a plastic bucket and poured through Discovery N70 net into a 44 gal drum which had been lined with an epoxy resin. The water was stirred vigorously for 10 min with a wooden paddle, and subsamples dipped from it and poured through a plastic funnel into the clear plastic 400 ml samplers (Fig. 1). The productivity of each of these subsamples was then estimated as described earlier. The coefficients of variation of these measurements varied from 13 to 20% (Table 3).

TABLE 3

SAMPLING ERRORS IN THREE TESTS OF ^{14}C UPTAKE BY REPLICATE SAMPLES TAKEN FROM BARRELS OF SURFACE SEA-WATER

Ship Date Time	Mean Activity (counts/min)	No. of Samples	Standard Deviation	Coefficient of Variation
Derwent Hunter 25.vii.59 0530	329	8	43	13
Derwent Hunter 25.vii.59 1530	221	10	45	20
Kimbla 14.ix.59 1640	332	10	54	16
				Mean: 17

In the second series, several samples were taken at depths of 0, 25, and 50 m from a drifting ship. At each depth the samples were taken in succession within 20 min of each other with the 400 ml clear plastic samplers. The errors in this series (Table 4) include those due to the method and also to the variations of plankton distribution. The mean coefficients of variation at the three depths were 29, 12, and 22% respectively.

In the third series, 14 surface samples were taken at 5 min intervals with a plastic bucket from a ship (*Diamantina*, July 21, 1960) steaming at 2 knots along two lines bisecting each other at right angles. These were poured through plastic funnels into 300 ml glass bottles, and their productivity was measured. The mean productivity was 0·11 mg C/hr/m^3 with a coefficient of variation of 18%.

In the fourth series, the productivity of the column of sea-water under 1 m^2 was examined. The errors in this type of estimation were determined from casts taken with 400 ml plastic samplers at depths of 0, 25, and 50 m. Successive casts taken within 20 min of each other gave a mean coefficient of variation of 11% (Table 5).

The estimate of technique error in the first series of tests gave a mean coefficient of variation of 17%. This is somewhat higher than the 10% quoted by Doty and

TABLE 4

VARIATIONS BETWEEN SAMPLES TAKEN IN QUICK SUCCESSION

Ship Date Time	Depth (m)	Mean Activity (counts/min)	No. of Samples	Standard Deviation	Coefficient of Variation	Mean Coefficient at Each Depth
Derwent Hunter 30.vii.59 0500	0	655	12	218	33	29
Kimbla 15.ix.59 0630	0	656	12	168	26	
Derwent Hunter 30.vii.59 1200	25	1071	10	111	10	12
Kimbla 15.ix.59 1200	25	481	10	61	13	
Kimbla 15.ix.59 1800	50	510	10	112	22	22
						Mean: 21

TABLE 5

VARIATIONS IN SAMPLING A COLUMN OF WATER IN SUCCESSIVE CASTS FROM DEPTHS OF 0, 25, AND 50 M

Ship Date Name	Mean Activity/m^2	No. of Casts	Standard Deviation	Coefficient of Variation
Kimbla 16.ix.59 0630	2101	4	252	12
Kimbla 16.ix.59 1200	5336	4	546	10
Kimbla 16.ix.59 1700	2828	4	287	10
				Mean: 11

Oguri (1959) for a similar technique. On a culture of *Skeletonema*, Cassie (1962) found a range of from 9 to 15%, and pointed out that it is probable that sampling errors contribute a large part of this estimate of technique errors even in aliquots from a large well-mixed sample.

The results from the second, third, and fourth series show that the sampling plus method errors gave coefficients of variation varying from 10 to 33%. Doty and Oguri (1959) quote up to 25% for an experiment similar to the third series, whilst Cassie (1962) found 14 to 37% for sets of 25 samples taken simultaneously in close proximity to each other.

None of the tests reported here or those referred to showed a coefficient of variation of more than 40%, whereas most of them gave from 10 to 30%. This allows the conclusion that two measurements in which one is 80% greater than the other are significantly different. However, when considering measurements of productivity of samples incubated under constant light it should be remembered that the effects of diurnal variations (Doty and Oguri 1957) can cause considerably greater variations than 80% unless the samples were taken at the same time of day.

V. References

Cassie, R. M. (1962).—Microdistribution and other error components of ^{14}C primary production estimates. *Limnol. Oceanogr.* **7**: 121–30.

Doty, M. S., and Oguri, M. (1957).—Evidence for a photosynthetic daily periodicity. *Limnol. Oceanogr.* **2**: 37–40.

Doty, M. S., and Oguri, M. (1959).—The carbon-fourteen technique for determining primary plankton productivity. *Pubbl. Staz. Zool. Napoli* **31**: 70–94.

Jitts, H. R. (1957).—The ^{14}C method for measuring CO_2 uptake in marine productivity studies. CSIRO Aust. Div. Fish. Oceanogr. Rep. No. 8.

Jitts, H. R. (1963).—The simulated *in situ* measurement of oceanic primary production. *Aust. J. Mar. Freshw. Res.* **14**: 139–47.

Jitts, H. R. (1964).—A twin six-litre plastic sampler. *Limnol. Oceanogr.* **9**: 452.

Jitts, H. R., and Scott, B. D. (1961).—The determination of zero-thickness activity in Geiger counting of ^{14}C solutions used in marine productivity studies. *Limnol. Oceanogr.* **6**: 116–23.

Reprinted from *Aust. J. mar. freshw. Res.*, vol 16, 1965, p. 293-306

A STATISTICAL EXAMINATION OF THE CATCHES, NUMBERS, AND BIOMASS TAKEN BY THREE COMMONLY USED PLANKTON NETS

By H. BARNES* and D. J. TRANTER†

[*Manuscript received October* 28, 1964]

Summary

A comparison has been made between the Indian Ocean standard net (IOSN), the tropical Juday net (TJN), and the Clarke–Bumpus sampler (CBS). Various components of the zooplankton have been counted and the results submitted to analyses of variance.

The variability of the catches is greatest with the TJN, the percentage standard deviation of a single observation ranging from 73 to 135 %; the values for the IOSN and the CBS are similar to each other: 42–51 %. The greater variability of the TJN is ascribed to its smaller mesh with consequent clogging, and arises from variability in the volume filtered and from the difficulty of washing down such a large and fine net efficiently.

There is no evidence that the larger zooplankton avoid the smaller CBS any more successfully than they avoid the two large nets; as expected, the smaller zooplankton organisms escape more readily through the IOSN with its coarser meshes than through the other two nets.

The catches for the IOSN and the CBS agree very well when expressed per volume of water filtered.

The main advantage of the larger nets—as regards the organisms considered here—is in the greater volume of water filtered; this would be of importance if a large bulk of material were required for, say, chemical analysis or if a search were being made for rare organisms.

I. INTRODUCTION

The purpose of this investigation was to compare quantitatively the performance of three commonly used plankton nets, namely, the Indian Ocean standard net (IOSN), the tropical Juday net (TJN), and the Clarke–Bumpus sampler (CBS); a preliminary account of this work has already been given by Tranter (1963). The IOSN is described by Currie (1963), the TJN by Bogorov (1957), and the [Australian] CBS by Tranter (1965). Figure 1 shows the relative sizes and shapes of the nets, the specifications of which are collected together in Table 1.

The hauls were made during August 1962 from the Soviet expedition ship *Vityaz* at SCOR–UNESCO Reference Station No. 1 in the south-east Indian Ocean (32°S., 111°50′E.).

II. METHODS

(*a*) *Collection of Samples*

Sampling extended from 2100 hr on August 6 to 0700 hr on August 7. The sampling duration consisted of three periods in each of which three replicates were

* Marine Station, Millport, Scotland.
† Division of Fisheries and Oceanography, CSIRO, Cronulla, N.S.W.

made with each of the three nets. Thus, 27 hauls were made in all, consisting of nine replicates with each net. The water column from 200 m to surface was sampled with each net in turn as rapidly as possible. All but the last three hauls were made in darkness. The IOSN and TJN hauls were "vertical"; in practice ship's drift gave rise to considerable wire angles—sometimes as much as 50° from the vertical. The amount of wire out to place the net at 200 m was determined from the wire angle—this being standard practice on board *Vityaz*, where the related values are engraved on the winch. The IOSN was hauled at 1 m per sec, and the TJN at 0·6–0·8 m per sec, these being the recommended speeds. Hauls with the CBS were oblique at 0·4 m per sec with the ship under way at 2–3 kt, and with the wire angle maintained at 45–50° throughout; thus the speed of the CBS through the water was 50% faster than the IOSN and twice as fast as the TJN.

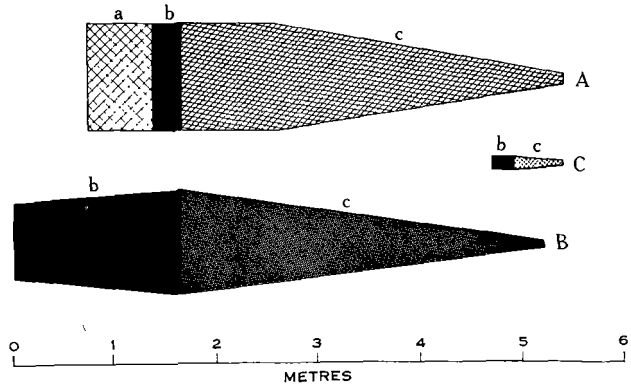


Fig. 1.—The zooplankton samplers drawn to scale. *A*, Indian Ocean standard net (IOSN); *B*, Soviet tropical Juday net (TJN); *C*, Australian model of the Clarke–Bumpus sampler (CBS). (See Table 1 for *a*, *b*, and *c*.)

The standard procedure on board *Vityaz* for washing both the IOSN and the TJN is as follows: the catch is first withdrawn from the cod-end and transferred to the storage vessel; the net is then re-immersed up to the mouth and brought inboard; the washings are added to the original contents, and preservatives added. The contents of the bucket of the CBS were transferred to the storage vessel, and the net washed down on deck by hand until all visible traces of plankton were collected.

(*b*) *Subsequent Treatment of Samples*

When necessary, subsamples were taken using the whirling device of Kott (1953); the general practice was to take $\frac{1}{10}$ of the whole from the IOSN, and $\frac{1}{5}$ from the TJN samples, the fraction being determined by the sample size. The CBS material was not subsampled. For the estimation of biomass, the whole samples were separated from preservative by draining through a plastic weighing dish with a base of monel metal gauze (80 meshes per in.); this retained all the organisms. The retained material was washed with 50% alcohol, air dried, and weighed. This weight is termed wet weight biomass.

(c) *Estimation of Volume of Water Filtered*

For both the IOSN and the TJN the volume of water filtered was estimated by multiplying the cross-sectional area of the opening of the net by the length of wire out. For the CBS, it was estimated from the readings of a flowmeter (previously calibrated in tank tests) placed in the mouth of the net. The method of estimation

TABLE 1

CHARACTERISTICS OF THE THREE PLANKTON NETS BEING COMPARED

As shown in Tranter (1963)

Net	Specifications						
	Section	Material	Diameter (cm)	Length (cm)	Mesh Type	Meshes per 1 cm	Mesh Aperture (mm)
IOSN (large, non-truncate)	*a*	French netting	113	70	Coarse	—	Approx. 20
	b	Terylene cloth	113	30	—	—	—
	c	Nylon	113–10	400	Medium coarse	21·5	0·33
TJN (large, truncate)	*b*	Canvas	80–113	175	—	—	—
	c	Silk	113–7	374	Fine	38	0·17
CBS (small, truncate)	*b*	Stainless steel	12·3	23	—	—	—
	c	Nylon	12·3	56	Medium	24·4	0·27

used for the two large nets is subject to a number of well-known errors unrelated to the plankton. First, the water filtered may be less than that calculated because of the incapacity of the nets to "accept" all the water at the hauling speeds used; that is, the filtration coefficient (Hensen 1895) is less than unity. The filtration coefficient is a function of the hydrodynamic properties of the net, of the net area, and of the mesh, all in relation to the speed of hauling. The large nets were designed to have a filtration coefficient of unity under the conditions used; the TJN has a truncated opening and was hauled relatively more slowly; the IOSN has a relative coarse-meshed filtering section and a cylindrical forward part (Currie 1963). A second, and quite distinct, source of error has been stressed by Motoda (1963); in a "vertical" haul from a drifting ship where there is considerable wire angle, the length of wire paid out to place the net at a selected depth is, because of the ship's drift, an underestimate of the column of water through which the net passes.

(*d*) *Groups Counted*

The numbers present in a haul were expressed per 20 m^3 of water filtered. Various organisms were counted and the counts collected into sets according to their character as shown in Table 2. Species counts included immature stages where these could be recognized.

TABLE 2

TAXONOMIC GROUPS COUNTED

Series I (selected groups)	Series II (euphausiid stages)	Series III (selected copepods)
Copepods	*Calyptopis*	*Euchaeta* sp.
Decapod larvae	*Furcilia*+*Cyrtopia*	*Pleuromamma abdominalis*
Ostracods	Adults	*Oncaea* sp.
Chaetognaths		*Lucicutia flavicornis*
Salps		*Pleuromamma piseki*
Euphausiid larvae		*Corycaeus* sp.
Euphausiid adults		*Candacia* sp.
Appendicularians		*Eucalanus* sp.
Polychaete larvae		*Haloptilus longicornis*

(*e*) *Analysis of the Data*

An appropriate statistical procedure for the analysis of data of this kind is the analysis of variance. Before analysis, the catches were converted to their log $(n+1)$ values, such a transformation being usually required in zooplankton sampling (Barnes 1952). For the analyses the hauls were assumed to have some "statistical" identity, that is, haul 1 in one period is assumed to have some relation to haul 1 in any other period; similarly with hauls 2 and 3. First-order interactions with hauls may then be separated. There is some justification for this assumption; the net may be drier and its filtration coefficient and selectivity slightly different at the beginning of a set of hauls; more care may be given to the first haul of a set. The alternative would be to consider the hauls as random samples; the results on this assumption are readily obtained from the analysis described above.

The following abbreviations are used: nets (N), taxonomic groups (G), sampling periods (P), hauls within sampling periods (H).

III. RESULTS

We may first examine the components of variance for each net, taken separately, over the whole sampling period (during which changes in the population sampled may have taken place). In series I there are nine groups of animals, taken in three successive hauls, and repeated at three different periods during the investigation. The results for series I are given in Table 3. The source of variation and the number of degrees of freedom are the same for all the nets.

A comparison of the first-order interactions with the residual shows that, for the IOSN and the CBS, none is significant so that their sums of squares can be

pooled to give a better estimate of the error variance; the values are 0·0295 (IOSN) and 0·0218 (CBS). For the TJN, neither $G \times H$ nor $G \times P$ is significant and these may be pooled with $G \times H \times P$ (residual) to give 0·0249; the value of $H \times P$ is very high and indicates a much greater variability with this net. The P values indicate significant population changes. For the IOSN and CBS the variance for a single observation

TABLE 3

COMPARISON OF NETS, FOR ORGANISMS IN SERIES I

Analysis of variance, showing the components of variance for each net, taken separately, over the whole sampling period

Source of Variation	D.F.	Mean Square for Nets:		
		IOSN	TJN	CBS
Groups (G)	8	3·7683	7·3394	4·8268
Hauls (H)	2	0·0427	0·0063	0·0877
Periods (P)	2	0·1373	0·3470	0·1474
$G \times H$	16	0·0275	0·0202	0·0249
$G \times P$	16	0·0184	0·0196	0·0226
$H \times P$	4	0·0607	0·4318	0·0125
Residual	32	0·0320	0·0298	0·0211

(one group counted from one haul) over a sampling period for which the present results can be considered representative is $\sigma_H^2 + \sigma_0^2$; calculation from the components of variance gives 0·0300 (IOSN) and 0·0242 (CBS). For the TJN $\sigma_0^2 + \sigma_{HP}^2$ is required,

TABLE 4

COMPARISON OF SAMPLING PERIODS, FOR ORGANISMS IN SERIES I

Analysis of variance, showing the components of variance for each sampling period, with groups, nets, and hauls as the variables

Source of Variation	D.F.	Mean Square for Periods:		
		1	2	3
Groups (G)	8	5·0707	4·9787	4·7397
Nets (N)	2	0·9123	1·0698	1·6407
Hauls (H)	2	0·1841	0·0125	0·2347
$G \times N$	16	0·1451	0·1453	0·1428
$G \times H$	16	0·0396	0·0271	0·0317
$N \times H$	4	0·1721	0·0802	0·1052
Residual	32	0·0190	0·0196	0·0315

$= 0·0701$. These are logarithmic values; they correspond to percentage standard deviations of 49% (IOSN), 84% (TJN), and 43% (CBS). The values for the IOSN and CBS are similar to those obtained in other plankton sampling; for example, Winsor and Clarke (1940) found that vertical hauls when made with a good technique

UNESCO ARCHIVES

had standard deviations between 45 and 50% of the mean. The value for the TJN clearly shows the great variability of this net.

As an alternative to the preceding analysis the results may be considered period by period, with Groups, Nets, and Hauls as the variables (Table 4). Attention is particularly drawn to the high values for Nets and $G \times N$; these arise from differences in the total catches and in the proportion of the various groups taken by the three nets. It is now necessary to look at the catches themselves; the group totals (raw data) summed over all the hauls of the three periods are given in Table 5.

TABLE 5

COMPARISON OF NETS, FOR ORGANISMS IN SERIES I

Using the raw data (counts/20 m³); the values are the totals for the whole sampling period

Group	Net		
	IOSN	TJN	CBS
Copepods	6825	79,048	22,211
Euphausiid larvae	931	1148	1439
Euphausiid adults	162	145	223
Decapod larvae	37	64	70
Ostracods	450	987	1220
Salps	190	235	263
Appendicularians	354	3734	2606
Chaetognaths	939	1672	1230
Polychaetes	109	428	283

It is quite evident that the group totals are in many cases much lower with the IOSN, and that the groups are taken in different proportions by the three nets. The difference is most marked with the copepods and appendicularians and this difference

TABLE 6

COMPARISON OF NETS, FOR ORGANISMS IN SERIES II

Analysis of variance, showing the components for each net, taken separately, over the whole sampling period

Source of Variation	D.F.	Mean Square for Nets:		
		IOSN	TJN	CBS
Groups (G)	2	1·0619	1·1151	1·1887
Hauls (H)	2	0·0046	0·0055	0·0574
Periods (P)	2	0·1253	0·2067	0·0456
$G \times H$	4	0·0267	0·0429	0·0109
$G \times P$	4	0·0149	0·0703	0·0177
$H \times P$	4	0·0689	0·3340	0·0279
Residual	8	0·0130	0·0230	0·0168

dominates the contrast between the IOSN and the other nets. Before discussing these results further, the analysis of the data from the remaining two series will be considered, presenting them as for series I.

TABLE 7

COMPARISON OF SAMPLING PERIODS, FOR ORGANISMS IN SERIES II

Analysis of variance, showing the components of variance for each sampling period, with groups, nets, and hauls as the variables

Source of Variation	D.F.	Mean Square for Periods:		
		1	2	3
Groups (G)	2	1·3102	1·4689	0·7128
Nets (N)	2	0·1419	0·0301	0·0421
Hauls (H)	2	0·1297	0·0330	0·1268
$G \times N$	4	0·0063	0·0086	0·0249
$G \times H$	4	0·0227	0·0091	0·0095
$N \times H$	4	0·2401	0·0130	0·0667
Residual	8	0·0235	0·0080	0·0409

Series II consists of various euphausiid stages; the results of the analysis of variance are given in Table 6.

As in series I the value of $H \times P$ for the TJN is very high. After pooling the values which are not significant, the variance and the percentage standard deviation of a

TABLE 8

COMPARISON OF NETS, FOR ORGANISMS IN SERIES II

Using the raw data (counts/20 m³); the values are the totals for the whole sampling period

Group	Net		
	IOSN	TJN	CBS
Calyptopis	733	857	1063
Furcilia + *Cyrtopia*	197	281	252
Adults	162	145	223

single haul may be calculated from the components of the variance, with the following results: IOSN, 43%; TJN, 135%; CBS, 42%. The values for the IOSN and the CBS are similar to those found for series I; that for the TJN is even higher; confirming the great variability of the catches with this net. The results were again analysed for the three separate periods, with Nets, Groups, and Hauls as the variables (Table 7).

The value for Nets is relatively smaller than in series I, and the net totals cannot be considered to show significant differences; the value for $G \times N$ is small and similarly

not significant. The facts are reflected in the group totals (Table 8) from which it is clear that with these organisms the catches were much more consistent for the three nets (contrast Table 5).

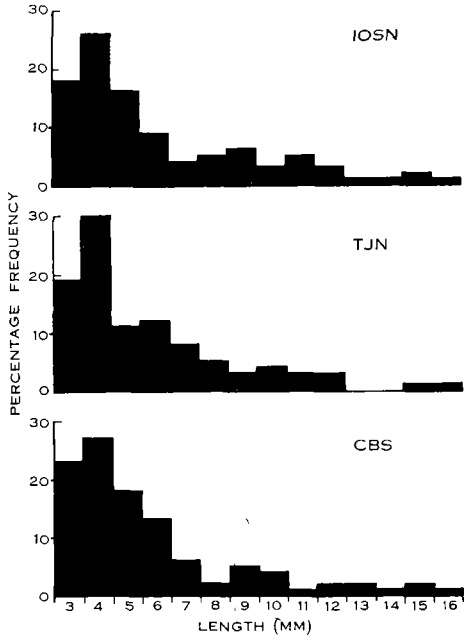


Fig. 2.—Length-frequency distributions of adult euphausiids.

One important point is emphasized by Table 8, namely, that the catching power of the small CBS (per unit area of mouth) is in no way inferior to that of the two much

TABLE 9

COMPARISON OF NETS, FOR ORGANISMS IN SERIES III

Analysis of variance, showing the components of variance for each net, taken separately, over the whole sampling period

Source of Variation	D.F.	Mean Square for Nets: IOSN	TJN	CBS
Groups (G)	8	0·7611	4·2415	1·1606
Hauls (H)	2	0·0032	0·0405	0·0662
Periods (P)	2	0·0079	0·2832	0·0582
$G \times H$	16	0·0108	0·0163	0·0108
$G \times P$	16	0·0197	0·0150	0·0282
$H \times P$	4	0·0639	0·3776	0·0660
Residual	32	0·0092	0·0166	0·0166

larger nets as regards these euphausiid stages. This is further emphasized by the plot of the size frequency of adult euphuasiids (Fig. 2), the histograms for the three nets being very similar.

Series III consisted of selected copepod genera and species, and the analysis of the data is given in Table 9. Again the value for $H \times P$ is extremely high for the TJN and here the values for both P and G are high for the same net. As before, after pooling

TABLE 10

COMPARISON OF SAMPLING PERIODS, FOR ORGANISMS IN SERIES III

Analysis of variance, showing the components of variance for each sampling period, with groups, nets, and hauls as the variables

Source of Variation	D.F.	Mean Square for Periods: 1	2	3
Groups (G)	8	1·6245	1·6258	1·4912
Nets (N)	2	0·3055	0·7365	0·9729
Hauls (H)	2	0·2404	0·0272	0·1839
$G \times N$	16	0·2474	0·2579	0·2555
$G \times H$	16	0·0276	0·0103	0·0317
$N \times H$	4	0·1746	0·1192	0·0442
Residual	32	0·0180	0·0115	0·0116

the values which are not significant the following percentage standard deviations are obtained: IOSN, 38%; TJN, 73%; CBS, 51%. Once more the TJN stands out on account of its much greater variability. The analysis by periods for this series is given in Table 10.

TABLE 11

COMPARISON OF NETS, FOR ORGANISMS IN SERIES III

Using the raw data (counts/20 m³); the values are the totals for the whole sampling period

Group	Net: IOSN	TJN	CBS
Euchaeta sp.	178	178	253
Haloptilus longicornis	141	113	263
Pleuromamma abdominalis	233	263	262
P. piseki	774	889	902
Oncaea sp.	357	14,212	1899
Corycaeus sp.	330	2249	694
Lucicutia flavicornis	610	1137	1005
Candacia sp.	89	121	150
Eucalanus sp.	336	406	430

As in series I, the values for Nets and $G \times N$ are high and indicate differences in the net totals and the proportion caught in the three nets. The group totals are shown in Table 11.

It is clear from Table 11 that the high values in Table 10 for Nets and $G \times N$ occur largely because of the failure of the IOSN to take some of the animals; the catches

of *Oncaea* sp., *Corycaeus* sp., and to a lesser extent *Candacia* sp. are low with this net, and to a lesser extent with the CBS, but markedly high with the TJN.

To summarize, the results of the three series are consistent amongst themselves and indicate: firstly, the variability of the catches with the IOSN and CBS is similar and of the same order as previously found for plankton sampling, while that of the TJN is much higher; secondly, the IOSN fails to catch some of the organisms taken by the other nets; thirdly, the small, and in many ways much more convenient CBS, is in no way less efficient in its catching power, as regards the organisms dealt with here, than the two larger nets.

IV. Discussion

(a) Sampling Properties of the Three Nets

An explanation may now be sought for the greater variability of catches with the TJN, and for the reduced catches of the IOSN. The mesh aperture of the filtering

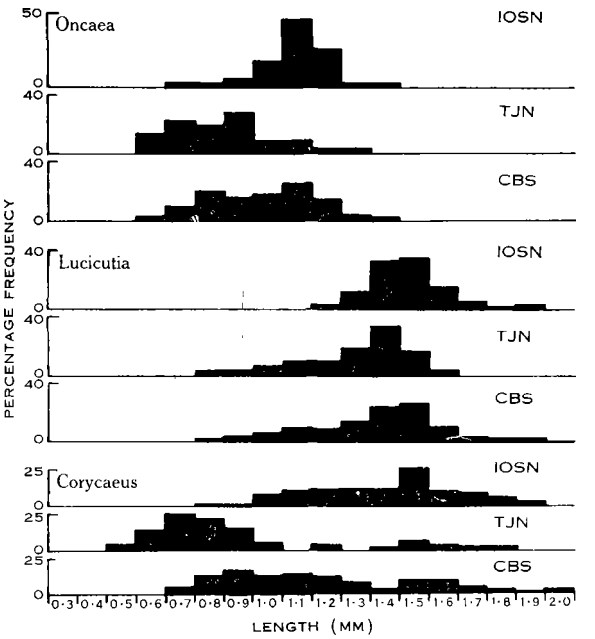


Fig. 3.—Length-frequency distributions of three small copepods.

portion of the TJN is much smaller than that of the other nets (Table 1) and it will, therefore, retain more phytoplankton and the smaller zooplankton organisms. Both will tend to clog the net and to increase variability, the effect probably being exaggerated by the patchiness of these organisms. Further, the presence of clogging organisms in the net may make the efficient washing down difficult, particularly in view of its large size. The smaller number of some of the species taken by the IOSN is almost certainly due to the larger mesh size of the filtering portion; the deficient species are the smaller ones.

This is amply confirmed by Figure 3 which gives the size-frequency distribution of some of the smaller copepod genera taken by the three nets. The results for *Oncaea* most clearly demonstrate that copepods less than 1·0 mm are rarely taken by the IOSN, whereas the CBS retains those as small as 0·8 mm, and the TJN down to 0·6 mm. The *Corycaeus* group covers a wide range, and here the excess of the smaller size groups taken by the TJN is clearly emphasized. Both these genera were taken in far greater numbers (see Table 11) by the TJN than by the two other nets, the catches for the IOSN being by comparison particularly low.

If the net is required to collect only those organisms which have a lower size limit near to 1·0 mm then either the IOSN or the CBS may be used and the results with these nets are directly comparable. Further, there is no evidence that the larger zooplankton organisms—adult euphausiids in the present instance—avoid the small CBS any more than the larger nets; this may be due to its faster speed through the water. It should perhaps be pointed out that most of the hauls of the present series were taken in darkness; avoidance may be a more severe problem during daylight hours (Regan 1963). Therefore, a Clarke–Bumpus sampler used as in the present investigations and for the same purpose has much to recommend it. There are occasions when a large net would be advantageous: when a bulk of material is required for some purpose such as chemical analysis, or when rare organisms are sought, since their chance of capture is increased by increasing the volume of water filtered.

TABLE 12

RELATIONSHIP OF TOTAL BIOMASS TO NUMBERS OF COPEPODS, APPENDICULARIANS, AND OTHER ORGANISMS

Analysis of regression, using data for all three nets for whole sampling period

Source of Variation	D.F.	Mean Square
Regression on X_1, X_2, X_3 (overall)	3	1467·1
Regression on other plankton (X_3)	1	1218·5
Regression on copepods (X_1)	1	20·795
Regression on appendicularians (X_2)	1	46·919
Error	14	177·8

(b) Estimations of Numbers and Biomass

Reference has already been made to the fact that wet weight biomass was determined before the samples were counted. From an analysis of the biomass data, Tranter (1963) found that the values for the three nets were comparable but that the variability of the estimate from the TJN was far higher than for the IOSN and the CBS: this second conclusion has been amply confirmed.

The biomass estimates were as follows:

IOSN 40 mg/m^3; S.D. single haul 6·1 mg/m^3
TJN 56 mg/m^3; S.D. single haul 22·9 mg/m^3
CBS 53 mg/m^3; S.D. single haul 11·8 mg/m^3.

The differences between the biomass estimates are quite clearly much less than the differences between the numbers taken in the nets (see Table 11) and some explanation of this discrepancy is called for. It has been shown above that the excess catches in the TJN (and to a less extent in the CBS) are largely on account of the bias produced by the smaller mesh size with the result that more smaller animals are retained. The explanation would seem to lie in the fact that the weight of the smaller animals makes relatively little contribution to the total biomass.

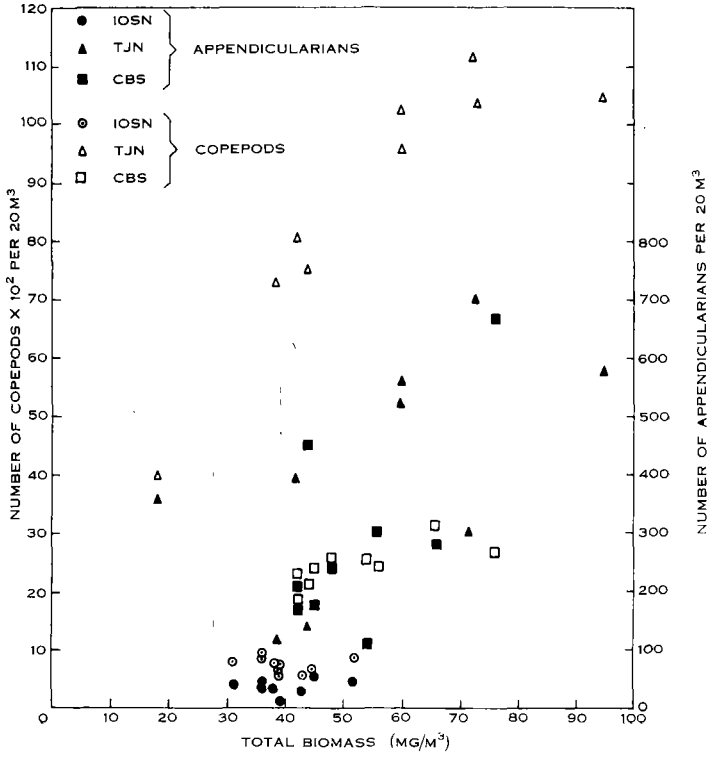


Fig. 4.—Relation between biomass and numbers of some organisms.

The appropriate method for an examination of the correlation between the biomass and the components of which it is made up is that of multiple regression. For simplicity (and in the absence of a computer) the data have been analysed, using *all* the values irrespective of nets, with respect to three components which have been shown to be concerned in the discrepancy, namely, copepods (X_1), appendicularians (X_2), and other plankton (X_3). The partial regression coefficients of biomass (Y) on these components using data for all three nets for the whole sampling period are:

$b_{y(1:2,3)} = 0{\cdot}000335$; $b_{y(2:1,3)} = 0{\cdot}010273$; $b_{y(3:1,2)} = 0{\cdot}065806$

It is evident that the effect of "other plankton" (X_3) is by far the most important while that of the copepods and appendicularians may not be significant. The analysis of variance is given in Table 12.

Neither the value for copepods nor for appendicularians is significant and their contribution to the relation may be neglected. It is suggested that the copepods are

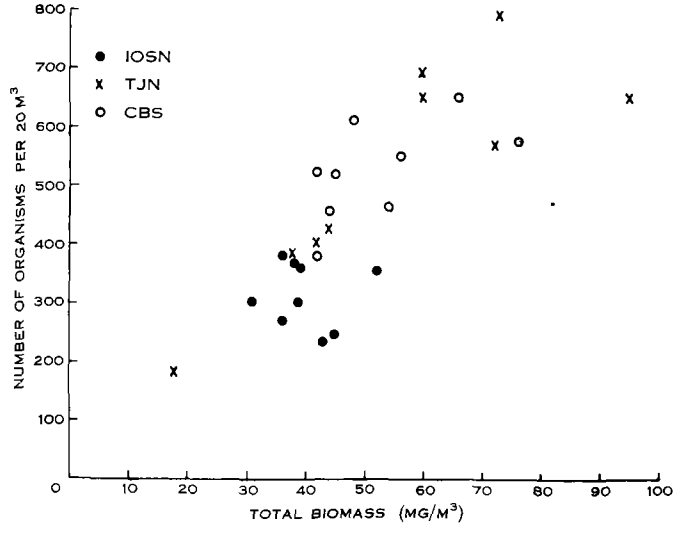


Fig. 5.—Relation between biomass and numbers of organisms other than copepods and appendicularians.

made up of large numbers of small animals which contribute little weight relative to the other parts of the catch. This is of course only true in the present instance when the relation is considered over *all* nets together; with other nets and even

TABLE 13

COMPARISON OF CRITERIA FOR ABUNDANCE

Numbers of total copepods, *Oncaea*, and appendicularians present in a particular TJN sample, and the biomass of these three components. Total biomass of sample: 5740 mg

Taxonomic Group	Number of Individuals	Biomass (mg)
Total copepoda	60,050	2200
Oncaea	12,600	211
Appendicularia	3305	105

with these nets fishing a population of a different composition, this need not, and in many instances would not, be true. The point is further illustrated in Figures 4 and 5, in which the number of copepods, appendicularians, and other organisms are plotted against the total biomass for the three nets for all the hauls. There is no

correlation *overall* between copepod and appendicularian numbers and biomass, although there is for the TJN and the CBS considered *separately*. By contrast, the number of other organisms and the total biomass show a very distinct correlation which is independent of the net. The same components were weighed (wet) and counted in one of the TJN hauls. The results are shown in Table 13. *Oncaea* are a dominant component of the copepod counts, making up $\frac{1}{5}$ of the total, and yet they constitute only $\frac{1}{10}$ of the copepod biomass and $\frac{1}{20}$ of the total biomass. Since out of the whole size spectrum of the genus *Oncaea*, it is the smaller ones which pass through the IOSN, it is clear that their loss will have a small effect on the total wet weight biomass taken by the latter net.

The results show that a net which takes only a fraction of certain (small) components of the plankton (the IOSN in this instance) may give a biomass similar to a net (TJN and CBS) which takes a greater fraction of these same components.

V. Acknowledgments

We wish to make the following acknowledgments: to Dr. M. E. Vinogradov, Institute of Oceanology, U.S.S.R., for the original incentive to carry out this investigation; to Dr. I. Sukhanova (U.S.S.R.), Dr. Daniel (India), and Dr. Kanagaratnam (Ceylon) for their generous assistance with the field work; and to Dr. D. I. Williamson (Port Erin) who counted the euphausiid stages.

VI. References

Barnes, H. (1952).—The use of transformations in marine biological statistics. *J. Cons. Perm. Int. Explor. Mer*, **18**: 61–71.

Bogorov, B. G. (1957).—Unification of plankton research. *Annls. Biol. Copenh.* **33**: 299–315.

Currie, R. I. (1963).—The Indian Ocean standard net. *Deep Sea Res.* **10**: 27–32.

Hensen, V. (1895).—Methodik der Untersuchungen. Ergebn.Plankton-Exped. Humboldt-Stiftung Kiel. Vol. I*B*, pp. 1–200.

Kott, P. (1953).—Modified whirling apparatus for the sub-sampling of plankton. *Aust. J. Mar. Freshw. Res.* **4**: 387–93.

Motoda, S. (1963).—Proposed method of estimation of quantity of water filtered by vertical net haul, and its application on illustrating distribution of zooplankton biomass in the eastern Indian Ocean. *Inf. Bull. Planktol. Japan* **10**: 22–8.

Regan, L. (1963).—Field trials with the Clarke–Bumpus sampler. Effects of coarse and fine-meshed nets over a range of speeds on euphausiid collections. Inst. Oceanog. Univ. British Columbia, Manuscript Rep. No. 16.

Tranter, D. J. (1963).—A comparison of zooplankton biomass determinations by Indian Ocean standard net, Juday net, and Clarke–Bumpus sampler. *Nature, Lond.* **198**: 1179–80.

Tranter, D. J. (1965).—The Australian Clarke–Bumpus sampler and calibration tank. CSIRO Div. Fish. Oceanogr. Tech. Pap. No. 20.

Winsor, C. P., and Clarke, G. L. (1940).—A statistical study of variation in the catch of plankton nets. *J. Mar. Res.* **3**: 1–34.

Reprinted from *Limnol. and Oceanogr.*, vol. 10, no. 2, 1965, p. 282-286

INTERCALIBRATION OF MARINE PLANKTON PRIMARY PRODUCTIVITY TECHNIQUES

BY MAXWELL S. DOTY, HARRY R. JITTS, OLGA J. KOBLENTZ-MISHKE AND YATSUKE SAIJO

Intercalibration of Marine Plankton Primary Productivity Techniques[1]

Biological oceanographers of several countries now use carbon-14 methods for estimating primary phytoplankton production. In connection with the International Indian Ocean Expeditions (IIOE), intercalibration meetings were initiated. The authors have represented their National Committees in a series of such meetings sponsored by the Scientific Committee on Oceanic Research (SCOR) and the United Nations Educational, Scientific and Cultural Organization (UNESCO) at the invitation of Dr. George Humphrey, President of SCOR. During the meetings, the various techniques were discussed and in some cases applied to the same waters. Only one report of these meetings (Doty 1962) has been published.

The most recent meeting was held aboard the research ship *Vityaz* of the Institute of Oceanology of the USSR working in the Indian Ocean off Fremantle, Western Australia. The authors, none working exactly according to his accustomed procedures, each measured the productivity of

[1] Work instigated and funded by the Scientific Committee on Oceanic Research (SCOR) of the International Council of Scientific Unions and the United Nations Educational, Scientific and Cultural Organization, U.S. Atomic Energy Commission Contract No. AT-(04-3)-15, and Office of Naval Research Contract Nonr-4108(00).

the sea on four different days (3, 5, 6, and 7 August 1962) near the positions given. Each used his own equipment and methods (Table 1) separately as much as possible. In addition, two other types of measurements were made which at one time or another have been suggested as reference methods for the IIOE phytoplankton primary productivity work.

The data were incomplete in some instances, but an idea of the variability due to the different technical modifications can be presented. Thus far, it has been impossible for the group to obtain comparative values having any satisfactory confidence level. From the four replicate sets of data (Table 2), it is difficult to predict the number of replications required to obtain any given confidence level, but the data do permit a first approximation of the differences to be expected among measurements made using the different techniques.

Note the uniformity of the *in situ* measurements (Table 2), repeated on what seems to have been the same water mass except for the 3 August station that was closer inshore. The *in situ* method was selected as the IIOE reference method because it is thought to reflect production rates better than other techniques. The application of the method was unsatisfactory (e.g., no samples were incubated in the upper levels), and thus, the close agreement of the last three measurements may be fortuitous.

The coefficient of variation (Table 2) between the relative productivity measurements made (in per cent) by the different national groups on each of the four days is given. The mean is 26%. Each participant felt serious concern for the lack of adherence to the details of his technique, and there were many irregularities in all routines.

It is thought that the Russian results (Table 2) are generally higher than the *in situ* results because of differences in estimating ^{14}C stock activity, but the results for 5 and 6 August are nearly identical to the general mean per cent of the *in situ* value for the four national methods on all four days—95% (Table 2, columns 5–8). Perhaps the IIOE prototype and the American results were low because the sampling did not extend as deeply into the sea as did that for the *in situ* and Russian measurements.

Measurements of primary productivity in marine waters may vary from 0.001 to as

TABLE 1. *The major differences between the different techniques used**

Technique	Outstanding features
In situ	Essentially as described by Steemann Nielsen (1952). Eleven to 12 depths sampled, samples inoculated and resuspended in the sea at the sample depths for the incubation period. Water samples used were subsamples of light-level samples for the other methods.
Prototype IIOE	Nylon net layers used around bottles submerged in a tray in sunlight to simulate light intensities at five sample depths, otherwise as described by Doty and Oguri (1958, 1959).
American	Nylon net layers used around bottles in ca. 140 lux intensity fluorescent light to simulate five light depths from which the samples were taken. (Doty and Oguri 1958, 1959).
Australian	Similar to prototype IIOE method but sunlit incubator light intensity adjusted with flat, blue glass sheets. Six depths used. (Jitts 1963).
Japanese	Similar to protoype IIOE method but perforated metal screen used to adjust sunlight intensity to that of six sample depths. (Saijo and Ichimura 1960, 1963).
Russian	Samples from 10 to 14 depths incubated in sunlight subdued about 50% by nylon netting. Values thus obtained adjusted for the characteristic *in situ* behavior of plankton in the area. (Koblentz-Mishke 1960; Ges 1960).

* The sampling depths were usually selected by the participants either so that the light intensity was equivalent to that passed by the filters they used or to achieve the desired sampling of the water. The selection was from curves, prepared by the hydrophotometric group, of light penetration as a function of depth with the light intensity at deck level accepted as 100%. The Australian group sampled at depths where the light balanced the electric output from two photocells, one under the respective incubator filter and the other suspended in the sea. The techniques are described by Sorokin (1958), Vinberg (1960 and 1963), Jitts (1963), Doty and Oguri (1958 and 1959), and Saijo and Ichimura (1963).

TABLE 2. *A summary of comparative values and of statistics from the application of six techniques for measuring primary marine productivity off Perth, Western Australia, August 1962. The values were converted to carbon fixed in mg^{-3} (12-hr day)$^{-1}$ by integrating the values obtained by the methods in Table 1 for the different depths. The productivity values in columns 4–8 are in per cent of the related value in column 3*

Date	S lat and E long	*In situ** productivity	Per cent of *in situ* value					Coefficient of variation† %
			IIOE prototype	National group results				
				American	Australian	Japanese	Russian	
(1)	(2)	(3)	(4)	(5)	(6)	(7)	(8)	(9)
3	32°26′ 115°00′	123	75	112	90	146	143‡	26
5	31°53′ 111°43′	196	61	65	59	47	95	30
6	31°01′ 112°57′	197	68	55	76	105	91	24
7	31°01′ 112°46′	206	86	96	132	76	139	24
Mean		181	73	82	89	94	117	
C, %		21.4	14.7	32.3	34.9	45.2	23.8	

* Surface fixation estimated as an average of that from the other five techniques, since surface samples were not processed *in situ*.

† For results from all six techniques.

‡ The mean ratio between the results from full sunlight and 50% uniform light incubations on other days was used to obtain a surface fixation rate for this day in full sunlight.

much as 100 mg C m^{-3} hr^{-1} and 1 mg to 20 mg m^{-2} day^{-1} at different times in different geographic areas. In the light of such a wide range of variation (five orders of magnitude), the mean of the coefficients of variation (29%) between each of the five techniques and the *in situ* results is almost negligible. However, if each of the authors had been able to adhere to his technique and to work simultaneously with each other, the variation might have been less. In a subsequent independent study by one of us (HRJ), a similar analysis of the results from the use of one technique gave a coefficient of variation of about 20%.

That none of the national techniques was used without modification is reflected by the larger coefficients of variation (bottom line, Table 2) for the national results (columns 5–8) than for the reference results (columns 3 and 4). The probable causes for this larger variation were lack of the facilities normally used and time restrictions.

With only four replications, little confidence can be placed in the observed differences. Although the group techniques averaged 91% of the *in situ* values, six of the 16 group results (columns 5–8) were higher than the correlated *in situ* values.

The internal consistency ($C = 14.7\%$) of the results from the IIOE prototype incubation method, simplest of all the methods, indicates that it merits further attention. This consistency may indicate that the complexities of the other techniques introduce random or chance variations. It does appear that the IIOE prototype method yields results (Table 2, column 4) significantly lower than the others.

A series of experiments was suggested during the conferences held aboard the *Vityaz* and in Cronulla, Australia in connection with this last intercalibration session. Several were related to the effects of the relatively high light intensity on the plankton when the samples were brought aboard ship—"light shock." Because several of us had observed apparently significant reductions in productivity as a result of light shock, one of us carried out a series of experiments to investigate this phenomenon.

In one experiment, all bottles were filled at the same time from opaque samplers in the dim light of a below-decks laboratory.

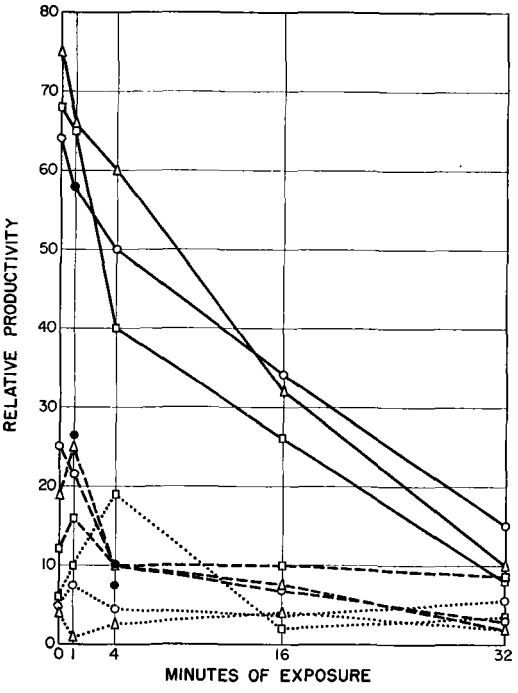


FIG. 1. The effect of sunlight on the ability of phytoplankton to photosynthesize as determined in separate experiments on three successive days. The exposure to direct sunlight was made on the ship's deck. The temperature in the bottles was not allowed to rise more than 1C. Each point represents the mean of two light-bottle values except in the two cases (solid circles) when the higher of the two values was used. —— surface meter of water; ------ depth at which 32% of surface light remains; .... depth at which 1% of surface light remains; ○ = 2 Oct 1963, 1218 lux; △ = 3 Oct 1963, 1046 lux; and □ = 4 Oct 1963, 697 lux.

The experimental bottles were then brought into the sunlight at times that terminated sunlight exposure simultaneously for all of them. All bottles, including the controls that had been kept in the laboratory, were then inoculated and incubated, using the carbon-14 incubator described by Doty and Oguri (1958). The surface samples were uniformly exposed to about 140 lux while incubating, those from the 32% light depth to about 45 lux and the 1% light depth samples to about 14 lux. These intensities were obtained by using calibrated black nylon netting sleeves around the 32 and 1% light-level bottles. The incubations were

TABLE 3. *The comparison of primary productivity measurements by four different techniques when subsamples from arbitrary depths and* in situ *incubation were used*

Date, August 1962	Depth (m)	Mg C/m³			
		American	Australian	Japanese	Russian
6	0	0.36	0.40	0.39	0.50
	5	0.27	0.21	0.33	0.39
	10	0.30	0.35	0.30	0.55
	25	0.18	0.19	0.21	0.36
	50	0.15	0.12	0.17	0.24
	75	0.05	0.04	0.04	0.10
7	0	0.33	0.31	0.35	0.44
	5	0.25	0.27	0.28	0.34
	10	0.21	0.29	0.37	0.56
	25	0.31	0.27	0.30	0.55
	50	0.15	0.15	0.17	0.25
	75	0.04	0.04	0.04	0.09

simultaneous and of nearly uniform duration. This experiment (Fig. 1) and other somewhat different experiments gave similar results, indicating a strong depressing effect even from a few minutes of exposure to bright sunlight. The inference is that samples must be kept out of bright sunlight, and the use of opaque samplers and the handling of samples inside a laboratory are recommended. Special precautions should be taken in initiating *in situ* experiments to avoid light shock when the bottles are assembled and put in the sea.

Twice during the trials, experiments were conducted to test each of the four techniques for differences due to factors other than the methods of incubation and the determination of depths of sampling. This was done by taking large samples from specified depths, dividing them into aliquots for each of the national groups, who thereafter dealt with them by their own methods, for example, bottles, carbon-14 solutions, filtration, counting, and so on, except that the subsamples were incubated uniformly by resuspending them to the same depths from which they were taken and for the same period, that is, from about 0700 hours to 1100 hours.

The coefficients of variation of the per cent ratios of each group with respect to each of the other three for 12 paired results (Table 3) were calculated. The coeffi-

cients of variation between the four groups were similar with an index value or average of about 20% among the results. This, as opposed to the 34% variation found in comparing the four techniques to *in situ* measurements, can be interpreted as an indication that incubation conditions and sampling depths are major causes of variation.

These trials have also demonstrated the need for more careful measurements of light intensities both in the ocean and in incubators.

CONCLUSIONS

Any method used for the measurement of primary production should be carefully calibrated against *in situ* measurements. If the calibration of a technique against *in situ* measurements is independent, it is necessary to ensure that comparable *in situ* measurements are obtained. Such methods could be explored during future intercalibration trials or by international adoption of the same or comparable methods for *in situ* measurements, for standardization of carbon-14 stock solutions, and for the determination of Geiger counting efficiencies. To achieve this goal by intercalibration trials, each participant would have to use his own technique without modification, and concurrently with other participants, as well as with sufficient replication over a wide range of water types to obtain satisfactory confidence levels.

MAXWELL S. DOTY
University of Hawaii,
Honolulu, Hawaii.

HARRY R. JITTS
C.S.I.R.O.,
Division of Fisheries and Oceanography,
Cronulla, N.S.W., Australia.

OLGA J. KOBLENTZ-MISHKE
Institute of Oceanology,
Academy of Science, USSR,
Sadovaya St. 1,
Lublino, Moscow J387, USSR.

YATSUKE SAIJO
Water Research Laboratory,
Faculty of Science,
University of Nagoya,
Nagoya, Japan.

REFERENCES

DOTY, M. S. 1962. An analysis of data on primary production obtained at the time of simultaneous methodological work by scientists of various countries in the region of the Hawaiian Islands. Okeanologiya, **2**: 543–553. (Translated and abbreviated by Olga Koblentz-Mishke.)

———, AND M. OGURI. 1958. Selected features of the isotopic carbon primary productivity technique. Rappt. Proces-Verbaux Reunions, Conseil Perm. Intern. Exploration Mer, **144**: 47–55.

———, AND ———. 1959. The carbon-14 technique for determining primary plankton productivity. Pubbl. Staz. Zool. Napoli, **31**: 70–94.

GES, N. D. [ed.] 1960. Technique guide for determining the primary production of organic material in bodies of water by means of the radiocarbon method. Prepared by a committee of the Institute of Oceanology of the Academy of Sciences of the USSR and including G. G. Vinberg, Y. G. Kabanova, O. I. Koblentz-Mishke, and N. N. Ksmeleva. Belorussian State University of Lenin, Minsk. 26 p.

JITTS, H. R. 1963. The simulated in situ measurement of oceanic primary production. Aust. J. Marine Freshwater Res., **14**: 139–147.

KOBLENTZ-MISHKE, O. 1960. On the study of primary production in the sea by Soviet scientists. Intern. Rev. ges. Hydrobiol., **45**: 319–326.

SAIJO, Y., AND S. ICHIMURA. 1960. Primary production in the Northwestern Pacific Ocean. J. Oceanog. Soc. Japan, **16**: 139–145.

———, AND ———. 1963. A review of the recent development of techniques measuring primary production. Proc. Conf. Primary Productivity Measurement, Marine Freshwater held at Honolulu, 1961. U.S. At. Energy Comm., Division of Technical Information TID-7633, Biology and Medicine, p. 91–94.

SOROKIN, YU. I. 1958. Results and prospects of using isotopic carbon for the investigation of carbon cycle in water basins. Intern. Conf. Radioisotopes, UNESCO, Paris, **4**: 633–648.

STEEMANN NIELSEN, E. 1952. The use of radioactive carbon (C^{14}) for measuring organic production in the sea. J. Conseil, Conseil Perm. Intern. Exploration Mer, **18**: 117–140.

VINBERG, G. G. 1960. The primary production of bodies of water. The Institute of Biology of the Belorussian Academy of Sciences, Minsk. [In Russian.] 329 p.

———. 1963. The primary production of bodies of water. [Transl. from Russian.] U.S. At. Energy Comm., Division of Technical Information, AEC-tr-5692. Book 1, p. 1–235, and Book 2, p. 236–601.

Reprinted from *Science*, vol. 150, no. 3,697, p. 771-773

Absence or Singular Specificity of Carotenoids in Some Lower Fishes

Abstract. *No colored carotenoids were recovered from the scales or liver of the coelacanth,* Latimeria chalumnae, *or from skin, immature eggs, or liver of the Pacific hagfish,* Eptatretus stoutii. *Zeaxanthin, present as esters in the skin and largely unesterified in the liver, was the only carotenoid identified in the thornback ray,* Platyrhinoidis triseriata, *and in the horned shark,* Heterodontus francisci, *whereas the skin of the Pacific mako shark,* Isurus glaucus, *yielded no carotenoids.*

An earlier review (*1*), surveying the wide occurrence of carotenoids in fishes, indicated the preponderance of the oxygenated or xanthophyllic class, while the hydrocarbon or carotene type was represented uncommonly and in minor proportions. Two xanthophylls resembling taraxanthin and lutein, which are common in plants, were encountered most frequently; astaxanthin was placed third in order; and zeaxanthin was listed as being of rare or questionable incidence.

Among the lower fishes, the larvae and the adult skin of two cyclostome lampreys, *Lampetra fluviatilis* and *L. planeri*, yielded lutein, which was reported also to be present in the skin of two elasmobranch species, the rays *Raja batis* and *R. clavata*.

More recently, Fisher (*2*) reported concentrations of total lipids, vitamin A, and collective carotenoids in livers from 17 species of sharks and dogfishes, 13 species of skates and rays, and from the chimaerid species, *Chimaera monstrosa*. He found wide variations, average values equivalent to the extremes of 0.06 to 2.3 mg/100 g wet weight for the sharks and dogfishes, and from 0.08 to 1.3 mg/100 g for the livers of the skates, rays, and chimaerid. The greater average figure for the latter group was considered as due, perhaps, to the composition of the natural food consumed. Fisher did not identify the carotenoids present, but measured the light-absorption of the collective yield at 450 mμ in normal hexane, a maximum close to that of β-carotene and to that of its mono- and dihydroxy derivatives, cryptoxanthin and zeaxanthin.

We report here on two species, widely separated in the evolutionary procession, that apparently are without colored carotenoids and two elasmobranchs whose liver and skin yielded only zeaxanthin.

Specimens of the hagfish, *Eptatretus stoutii*, were captured in baited screen-traps at depths of about 200 m a few kilometers seaward from San Diego (*3*). We received scales and liver tissue from a specimen of the coelacanth, *Latimeria chalumnae*, which was nearly 2 m in length, taken on 11 December 1964 from waters off Mutsamudu, Anjouan, Isles Comores (*4*). The tissues had been preserved in 10 percent formaldehyde promptly after capture of the animal. A piece of the preserved liver, sectioned on 8 February 1965, was analyzed 2 days later. The thornback ray, *Platyrhinoidis triseriata*, the horned shark, *Heterodontus francisci*, and the Pacific mako shark, *Isurus glaucus*, were caught in neighboring waters.

Each tissue to be analyzed (except the scales) was minced with scissors and finely comminuted in several volumes of ethanol in a Waring Blendor. The solid and fluid materials were transferred to glass-stoppered flasks and were covered with an atmosphere of nitrogen; they were then stored overnight or longer in a dark refrigerator before being clarified through celite and washed until the filtrate showed no more pigment. All lipids and lipid-soluble pigments were transferred to *n*-hexane. Carotenoids were resolved into chromatographically separable fractions on columns of MgO and celite (1 : 1); they were eluted individually with hexane that contained graded concentrations of methanol from 0.1 to 5.0 percent.

For identification with authentic carotenoids we used thin-layer chromatography with silica gel as adsorbent and with 20 percent acetone in hexane, or equal volumes of ethyl acetate and benzene, as eluants in a modified Davies concentration chamber (*5*). Profiles of the absorption spectra and concentrations of carotenoid were determined with a Bausch & Lomb 505 recording photoelectric spectrophotometer; the factor for β-carotene, the ratio of the molecular weight to the extinction coefficient 0.0041, was used throughout (Table 1).

No traces of pigment soluble in ethanol were found in the skin and liver of one hagfish specimen and the liver of a second one, more recently captured. Also, the pale-yellow or dirty cream-colored maturing eggs from a recently captured specimen yielded no carotenoid after these eggs were ground in ethanol and allowed to stand in it for several days; the solvent was then filtered. *Eptatretus stoutii* thus differs from the two lutein-storing *Lampetra* species.

The coelacanth, *Latimeria chalumnae* (of the crossopterygian order Actinistia

Table 1. Assays for carotenoids in five species of lower fishes.

Tissue and wet weight	Color of ethanol extract	Total carotenoids (mg/100 g)	Identity and proportions of carotenoids (%)
	Cyclostome: *Eptatretus stoutii* (hagfish)		
Captive 3 mo at 7°C			
Liver (1.99 g)	Colorless	None	
Skin (4.60 g)	Colorless	None	
Captive 1 wk at 7°C			
Liver (1.51 g)	Colorless	None	
Eggs	Colorless	None	
	Crossopterygian: *Latimeria chalumnae* (coelacanth)		
Preserved 2 mo with formaldehyde			
Scales	Colorless	None	
Liver piece (33.56 g)	Pale cloudy yellow	None; much lipid; typical reactions for sterols by Salkowski's and Liebermann-Burchard tests	
	Elasmobranch: *Platyrhinoidis triseriata* (thornback ray)		
Skin (10.85 g)	Yellow	0.17	Zeaxanthin esters, 100
Liver (3.47 g)	Yellow	7.86	Free zeaxanthin, 93; zeaxanthin esters, 7
	Elasmobranch: *Heterodontus francisci* (horned shark)		
Skin (6.91 g)	Yellow	1.92	Zeaxanthin esters, 100
Liver (14.12 g)	Yellow	4.57	Free zeaxanthin, 65.3; zeaxanthin esters, 34.7
	Elasmobranch: *Isurus glaucus* (Pacific mako shark)		
Skin (10.44 g)	Colorless	None	

which may be dated back to the lower Carboniferous), yielded no carotenoid from its heavy, partially melanized scales overlying the white flesh when these scales were soaked in hot ethanol. A section of the formaldehyde-preserved liver (wet weight, 33.56 g; dry weight, 40 percent of wet weight) contained much waxy lipid material and yielded pale-yellow ethanolic and hexane extracts. Hydrolysis of the whole extract left very little pale-yellow, hexane-soluble material, which showed a green fluorescence under ultraviolet illumination and showed no spectral absorption maxima in the visible portion, but only a steady rise into the blue-violet region. Upon treatment with concentrated H_2SO_4 alone or in the presence of acetic anhydride (Salkowski's and Liebermann-Burchard reactions), chloroform solutions of the hexane extract exhibited series of blue, green, and red colors typical of unsaturated sterols. The liver and other tissues had been preserved with 10 percent formaldehyde solution for the 2-month period since the animal's capture; this should have denatured proteins, including any lipoxidases that might otherwise have tended to degrade carotenoids. Thus it was surprising to encounter such a firm, lipid-rich section of liver lacking in these pigments.

The skin of both the thornback ray and the horned shark yielded only xanthophyllic esters, while the uncombined xanthophyll (93 percent of total carotenoids) predominated over its esters in the ray's liver and comprised two-thirds of the carotenoids in the horned shark's liver.

The liver of *Platyrhinoidis* and that of *Heterodontus* each yielded two chromatographically separable esters and the skin of the latter, three ester fractions; but all xanthophyllic material, whether free or esterified, showed the same absorption profile within minor limits of error. The typical values were: 475, 447.3, and an inflection or sloping shoulder at about 424 mμ, but varying between 420 and 425 mμ. All 13 values for the first maximum were located from 474 to 476 mμ except for one fraction which gave a maximum centering at 471, and another, a value of 478 mμ. All loci for the chief maximum not actually at 447 mμ were within 2 or 3 mμ above or below it. Minor departures of this kind, if not indeed within instrumental error, may arise either from a degree of isomerization or from the presence of fatty acid conjugants or incidental lipids.

The spectral absorption maxima of the xanthophyll present in these fishes agreed very closely with those of authentic zeaxanthin: 475, 447, and 422 to 424 mμ in the same solvent (*n*-hexane) and measured with the same instrument. The experimental xanthophyll likewise exhibited the same partition ratio (11 : 89) between hexane and 95 percent methanol as pure zeaxanthin does [as measured by Petracek and Zechmeister (*6*) and by us].

Co-chromatography of a purified sample (from *Platyrhinoidis* liver) with isozeaxanthin, prepared by us from canthaxanthin, showed wide separation between the two xanthophylls. Moreover, Goodwin's test (*7*) for allylic hydroxyl groups resulted in noticeable darkening of isozeaxanthin and reversed the hypophasic behavior, but the shark-liver xanthophyll remained unchanged, as zeaxanthin also does.

Finally, an isolated sample of the xanthophyll, obtained from the hydrolytic treatment of collective carotenoids from *Heterodontus* liver, was co-chromatographed on thin-layered silica gel with some of the authentic, crystalline zeaxanthin (*8*). The two gave identical R_F values on individual chromatograms and a single zone when combined in the same solution, which shows the identity between our xanthophyll and zeaxanthin.

It should be emphasized that contaminating lipids may distort chromatographic zonation as well as behavior on partition and position of absorption maxima. Accordingly, it was necessary sometimes to first adsorb a xanthophyll ester upon powdered MgO or Al_2O_3, discard the supernatant colorless, cloudy solvent, and then rinse the colored powder several times before eluting the carotenoid in preparation for diagnostic examination (*5*).

Our values for the collective liver carotenoid fractions (7.86 and 4.57 mg/100 g, respectively, for the ray and the shark analyzed), although somewhat higher than Fisher's, lie well within the order of magnitude of his analyses, while the skin of the shark yielded more than ten times as much zeaxanthin esters as the skin of the ray. It was surprising that no carotenoid was recovered from the skin of a pelagic shark, *Isurus glaucus*, after a 3-day extraction with ethanol, since Fisher's findings would suggest that carotenoids are present, although in relatively low concentrations, in the livers of all or most sharks, and hence might be expected also, at least in minor quantities, in the integument of this species, as in other fishes (*1*).

Note added in proof: Since this report went to press, Professor C. L. Hubbs kindly made available to us for analysis 70.95 g (wet weight) of liver tissue from a black-skinned chimaerid (*Hydrolagus* sp., being described by him), measuring about 1 m in length, freshly captured off Baja California at a depth of 1200 m. The dark, melanistic, very fatty liver involved less than 0.04 mg of suspected carotenoids, whose recovery was rendered impracticable by the presence of the high concentrations of lipids.

DENIS L. FOX
GEORGE F. CROZIER
Department of Marine Biology, Scripps Institution of Oceanography, La Jolla, California

References and Notes

1. D. L. Fox, in *The Physiology of Fishes*, M. E. Brown, Ed. (Academic Press, New York, 1957), chap. 7.
2. R. L. Fisher, *Vitamin A, carotenoids and total lipids in the livers of some elasmobranchs*, Marine Research No. 2, Dept. of Agr. and Fisheries for Scotland, Edinburgh (Her Majesty's Stationery Office, London, 1964).
3. Kindly supplied by Dr. David Jensen.
4. Through the generosity of Dr. Malcolm Gordon and the U.S. Program in Biology, International Indian Ocean Expedition, sponsored by the National Science Foundation.
5. D. L. Fox and T. S. Hopkins, *Nature* **206**, 307 (1965).
6. F. J. Petracek and L. Zechmeister, *Anal. Chem.* **28**, 1484 (1956).
7. T. W. Goodwin, *Biochem. J.* **63**, 481 (1952).
8. Kindly furnished by Professor L. Zechmeister.
9. We acknowledge the support given this research through grant GB-2312 (to D.L.F.) from the National Science Foundation. Contribution of the Scripps Institution of Oceanography, University of California, San Diego, La Jolla, California.

2 July 1965

Reprinted from *Océanographie*, vol. III, no. 2, 1965, p. 11-17

LE PROBLEME DES CRESEIS

par

S. **FRONTIER** *

L'orientation des travaux récents concernant les *Cavolinidae* (**Tokioka** 1955, **Menzies** 1958, **Frontier** 1963, **Chin Chen** et **Be** 1964) semble faire apparaître l'importance des coquilles embryonnaires dans la systématique de cette famille. Chez la plupart des espèces, en effet, la coquille embryonnaire persiste à l'extrémité de la coquille adulte - au moins pendant une partie de la vie - et est moins sujette que cette dernière aux fluctuations morphologiques d'origine phéno ou génotypique. Ce caractère de constance s'étend à la partie de la coquille qui suit immédiatement la coquille embryonnaire, et qui peut être utilisée dans le même but taxonomique lorsque celle-ci n'est pas nettement distincte, ou manque de caractéristiques nettes (*Cavolinia*).

Il semble en particulier, que le problème des différentes formes de *Creseis* doive être résolu par l'examen attentif des extrémités de coquilles : les caractères de cette région pourraient servir à délimiter les espèces, alors que les variations de forme de la coquille adulte ne donneraient lieu qu'à des distinctions de sous-espèces voire de formes sans valeur systématique.

Sans prétendre donner un avis définitif, j'exposerai ici quelques conclusions qu'il me semble légitime de tirer après examen d'un abondant matériel tropical provenant, d'une part, de la région de Nosy Be (environ 600 récoltes, non encore entièrement examinées), d'autre part d'une bande d'Atlantique tropical de 120 à 4000 milles de large située le long des côtes d'Afrique entre l'Equateur et la latitude de 18° S (1) : soit 182 récoltes, auxquelles j'ai pu adjoindre une petite collection provenant de la Rade de Dakar (33 récoltes) que m'a communiquée M. **G. Seguin**.

L'unité du genre *Creseis* semble bien établie par des caractéristiques constantes tant de la coquille (allongée et conique, à section circulaire, sans ornementations latérales; coquille embryonnaire arrondie à l'extrémité et très légèrement renflée, fréquemment teintée de brun ou de pourpre), que des parties molles par lesquelles il se distingue sans confusion possible des autres *Cavolinidae* lors même que la coquille a disparu (parapodies munies chacune d'un court tentacule antérieur et d'une tache glandulaire à la base de ce dernier; lobe postérieur du pied très court. **Meisenheimer** 1905, **Tesch** 1946).

Les anciens auteurs avaient noté le polymorphisme de *Creseis*, la variabilité observée portant sur l'allongement et la courbure de la coquille. En 1828 **Rang** crée les trois espèces *virgula*, *clava* et *acicula*. **Eschscholtz** (1829) distingue *acus*, *conica*, *unguis*, *cornucopiae*, *caligula*. D'autres dénominations sont encore proposées pour rendre compte de formes intermédiaires : une synonymie en est donnée par **Tesch** (1904) qui ne reconnait que les espèces

* Océanographe Biologiste au Centre O.R.S.T.O.M. de Nosy-Bé (Madagascar)

(1) Campagnes 12, 13 et 14 de l'Ombango effectuées par le Centre O.R.S.T.O.M. de Pointe Noire.

virgula et *acicula* après que **Boas** (1886) ait établi et figuré la continuité des variations morphologiques des coquilles de *Creseis* et conclu à l'impossibilité de délimiter des espèces - la distinction entre *acicula* et *clava* étant toutefois reconnue plus nette qu'entre les autres formes.

En 1913 dans le «Tierreich», **Tesch** reconnait les deux espèces *acicula*, à coquille droite et *virgula*, à coquille courbée, avec les quatre sous-espèces *acicula* (coquille longue) et *clava* (coquille courte) pour la première, *virgula* (coquille à forte courbure vers l'extrémité) et *conica* (coquille faiblement courbée) pour la seconde. C'est cette classification qui a prévalu jusqu'à ce jour, à ceci près que la sous-espèce *clava* a été placée par **Tesch** en 1946 et 1948 dans l'espèce *virgula*, puis replacée dans *acicula* par **Tokioka** (1955) et à nouveau dans *virgula* par **Chin Chen** et **Be** (1964).

Il est reconnu enfin deux autres espèces de *Creseis* : *C. chierchiae* (*Cleodora chierchiae* **Boas** 1886), et *C. caliciformis* **Meisenheimer** 1905, cette dernière n'ayant été récoltée qu'en deux exemplaires.

Il revient à **Tokioka** (1955) d'avoir eu pour la première fois recours à la coquille embryonnaire pour la distinction des deux espèces litigieuses *acicula* et *virgula*. L'auteur décrit d'abord la coquille embryonnaire de *C. acicula acicula* :
«Embryonal shell is elongate, with rounded tip and shows a slight swelling. The constriction at the base is very slight, but distinct; the shell is slighty thickened at this constricted part.»
Puis il écrit à propos de *clava* :
«The specimens treated here resemble superficialy *Cr. virgula conica*, especially closely in the younger shells, although they have embryonal shells of the «*acicula*-type» differing distinctly from those of *Cr. virgula* and its varieties and forms.»
A ce titre il considère *clava* comme une sous-espèce d'*acicula*.

L'exemplaire de *clava* figuré par **Chin Chen** et **Be** (1964) montre une coquille embryonnaire très voisine de celles figurées par **Tokioka** mais ne présentant pas de légère constriction la séparant de la coquille adulte - le texte mentionne cependant cette constriction; les dimensions sont pratiquement les mêmes : 0,38 × 0,14 et 0,17 mm respectivement pour les deux exemplaires dessinés par **Tokioka**, et 0,33 × 0,20 mm d'après le dessin de **Chin Chen** et **Be**. Les coquilles adultes sont toujours parfaitement droites.

Toutes les autres coquilles sont attribuées à *Creseis virgula*, qui comprend donc des formes recourbées et des formes droites : **Tokioka** nomme *C. virgula virgula* un individu dont la coquille fait un angle de 40°, et *C. virgula conica* ceux dont l'angle est compris entre 0 et 30°. Il devient dès lors impossible d'attribuer à *conica* ou à *clava*, dans leurs acceptions actuelles, les formes droites décrites et figurées dans la littérature et en particulier, malheureusement, les coquilles proches de la forme *acicula* figurées par **Boas** dans sa série morphologique (**Boas** 1886 pl. 6 fig. 94 s et t).

Chin Chen et **Be** déterminent comme *virgula virgula* une coquille présentant un angle d'environ 28°. D'autre part, ces auteurs établissent une nouvelle sous-espèce; *Creseis virgula constricta*, de petite taille (holotype : 3,5 mm). à coquille à peine courbée, et possédant une région juvénile séparée du reste par une constriction très nette précédée d'un renflement. Cette conformation n'est pas nouvelle puisqu'elle avait été signalée, plus ou moins prononcée et sans qu'il lui soit donné de valeur systématique, chez certains individus déterminés comme *C. virgula, conica* ou *clava* (**Boas** 1886, **Tesch** 1913, **Menzies** 1958) et chez les espèces *C. chierchiae* (**Boas** 1886, **Tesch** 1913, **Frontier** 1963) et *C. caliciformis* (**Meisenheimer** 1905). Cependant la création d'une unité systématique nouvelle me semble tout à fait opportune pour autant que le renflement de la coquille juvénile, et l'étranglement qui sépare cette dernière de la coquille adulte soient nettement plus prononcés que chez les spécimens de v. *virgula* et v. *conica* où cette disposition est ébauchée. Or cela semble être le cas d'une part dans le matériel examiné par **Chin Chen** et **Bé**, d'autre part dans les collections provenant de Madagascar et de la côte atlantique d'Afrique que j'ai pu étudier jusqu'ici.

Je n'ai observé aucune *constricta* dans les récoltes d'Afrique; celles-ci ne contenaient que les formes *virgula virgula* et *virgula conica*, ces dernières comprenant une forte proportion

d'individus à coquille droite ou presque droite. L'extrémité de la coquille chez v. *virgula* comme chez v. *conica* peut être régulièrement conique, mais le plus souvent présente un léger renflement suivi d'une zone rétrécie, le diamètre le plus étroit se trouvant à une distance de 0,6 à 0,8 mm de l'apex, et le diamètre au niveau du renflement variant entre 0,15 et 0,20 mm. Aucune différence dans les coquilles juvéniles ne semble distinguer les sous-espèces *virgula* et *conica* qui restent donc caractérisées par la forme de la coquille adulte (fig. 4 à 8 pl. II et III).

Dans le matériel de Nosy Be, *Creseis virgula conica* se montre très rare, *C. virgula virgula* nettement plus abondante ; toutes deux coïncident exactement avec les exemplaires d'Afrique. Mais la grande majorité des *Creseis* est constituée - *acicula* mise à part - par deux formes :

1°. *Une forme qui semble coïncider avec C. virgula constricta* : coquille de petite taille (inférieure à 3 mm), droite ou le plus souvent très légèrement courbée, pourvue à son extrémité d'une partie juvénile à renflement net suivi d'un étranglement net et bien moins étendu en longueur que chez les deux premières formes ; distance entre le milieu de l'étranglement et l'apex de la coquille : 0,4 à 0,5 mm ; diamètre au niveau du renflement : 0,13 à 0,15 mm : au total un aspect moins effilé que pour v. *virgula* et v. *conica*. (fig. 11 pl. IV). La figure 11 (a) représente l'extrémité de la coquille d'un individu chez lequel ces caractères sont le moins accusés : ils restent encore bien reconnaissables. Il s'ajoute à cela un caractère de proportion : la coquille mesure en longueur de 4 à 5 fois son diamètre d'ouverture, contre 6 fois environ pour les coquilles de *conica* droites ou presque droites.

2°. L'espèce *Creseis chierchiae* (BOAS) dont la coquille possède la même forme, les mêmes proportions, les mêmes dimensions et la même coquille juvénile que la forme précédente (**Frontier** 1963) et n'en diffère que par la présence d'une annulation (environ 35 replis par mm) de la coquille, et par la minceur caractéristique de celle-ci. De plus une proportion notable d'individus, en certaines stations où les «*constricta*» typiques se remarquent par une minceur inhabituelle de la coquille, réalisent plusieurs types de formes intermédiaires : individus présentant une annulation plus effacée et moins serrée, allant jusqu'à se distinguer difficilement des irrégularités de croissance, ou bien individus ne possédant l'annulation caractéristique que sur un ou deux courts segments de la coquille, les deux modalités pouvant être associées (fig. 10 pl. IV). A titre d'exemple les effectifs d'une récolte à 2 mètres étaient les suivants :

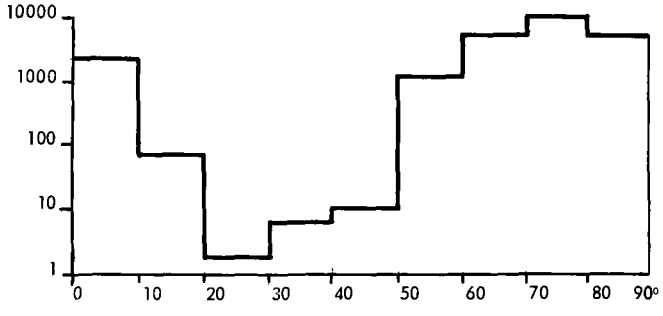
chierchiae typiques : 163
«*constricta*» typiques : 110
intermédiaires : 105

C'est donc sans hésitation que j'identifie les deux formes sous le nom de *Creseis chierchiae* (BOAS) : la priorité joue en effet en faveur de cette dernière dénomination ; d'autre part j'ai quelques scrupules à identifier dès maintenant les formes lisses de *Creseis chierchiae* que j'ai trouvées à Nosy Be avec la *Creseis virgula constricta* de **Chin Chen** et **Be**, n'ayant pas eu ce dernier matériel sous les yeux, et l'holotype montrant quelques différences avec mes specimens : la coquille juvénile (jusqu'à l'étranglement) mesure 0,54 sur 0,12 mm, donc est plus effilée que celle de *C. chierchiae*, et la longueur de la coquille adulte (3,5 mm) est égale à 9 fois le diamètre d'ouverture (6 fois seulement d'après le dessin).

Remarquons enfin que la *Creseis caliciformis* de **Meisenheimer** (1905) possède une coquille juvénile de forme très voisine de celle de *C. chierchiae*, mais dont les dimensions ne sont pas indiquées. Dans l'hypothèse où ces dimensions coïncideraient elles aussi avec celles de *C. chierchiae*, il ne serait pas absurde de penser que l'on a à faire là aussi à des *Creseis chierchiae* à coquille lisse : en effet les deux individus récoltés par **Meisenheimer** mesurent 8 et 10 mm de longueur, et la dilatation ne s'amorce qu'à mi-longueur de la coquille environ ; en deçà celle-ci est régulièrement conique et environ 5 fois plus longue que le diamètre maximum d'après le dessin. Il pourrait alors s'agir soit d'une anomalie de croissance, soit de la forme normale que prend *Creseis chierchiae* lorsqu'exceptionnellement elle atteint une telle taille.

Un dernier point litigieux est la limite à adopter entre C. *virgula virgula* et C. *virgula conica*. Il ne peut s'agir, nous l'avons vu, que d'une limite concernant la courbure de la coquille adulte, les coquilles juvéniles étant identiques. J'ai tenté de préciser cette limite en mesurant l'angle fait par l'axe longitudinal de la coquille âgée avec l'axe de la coquille juvénile sur les spécimens qui m'avaient été envoyés d'Afrique (plus exactement, sur tous ceux dont l'état de la coquille permettait une telle mesure). Les résultats sont les suivants :

Angles	**Effectifs**
0-10°	2600
10-20°	67
20-30°	2
30-40°	6
40-50°	8
50-60°	1100
60-70°	4500
70-80°	8800
80-90°	3600 (1)



Il en résulte un histogramme nettement bimodal dont les deux maxima correspondent évidemment à v. *virgula* et v. *conica*. La limite entre les deux sous-espèces pourrait être prise commodément à 30°, les individus dont l'angle est voisin de cette valeur restant douteux.

Notons enfin un caractère de proportion de la coquille adulte : pour une même longueur le diamètre d'ouverture est plus grand chez v. *virgula* que chez v. *conica*.

En ce qui concerne *clava* je ne puis me permettre un avis définitif, n'en ayant pas encore eu d'exemplaire sous les yeux. Il me semblerait cependant judicieux, puisque les coquilles embryonnaires comme les coquilles adultes diffèrent notablement et ne semblent pas être réunies par une série d'intermédiaires avec *acicula*, d'élever la forme *clava* au rang d'espèce - conformément à l'idée première de **Rang** bien que le critère d'espèce ne soit plus celui auquel se référait cet auteur.

En conclusion la classification du genre *Creseis* proposée ici se résume de la façon suivante :

Creseis acicula RANG

Creseis clava TOKIOKA nec RANG

Creseis virgula RANG, comprenant les deux sous-espèces *virgula* RANG et *conica* ESCHSCHOLTZ.

Creseis chierchiae (BOAS) (= C. *virgula constricta* CHIN CHEN et BE ?, = *C.calciformis* MEISENHEIMER ?), comprenant une forme à coquille épaisse et lisse, une forme à coquille mince et annelée, et des formes intermédiaires.

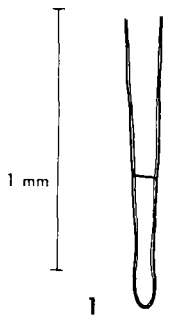
J'insiste sur le caractère de suggestion que je tiens à donner à cette classification. Le matériel examiné jusqu'ici, bien qu'assez abondant provient de localités encore trop peu nombreuses. Le problème reste ouvert et ne pourra être résolu définitivement que par la comparaison de collections en provenance de toutes les mers. (2)

(1) Les effectifs élevés des quatre dernières classes sont dus essentiellement à une seule récolte contenant près de 18000 *Creseis virgula virgula* de 10mm de longueur environ (et jusqu'à 11mm) - taille encore jamais signalée (fig. 8 pl. III). Les caractéristiques de cette récolte sont les suivantes : Coordonnées : 8° 35'E, 15° 35'S ; fond 4800m ; date : 3 mars 1961 ; heure : 13h,20 à 13h,35; longueur de câble mouillé : 150m ; filet à mailles de 1 mm de côté traîné à 2,5 nœuds.

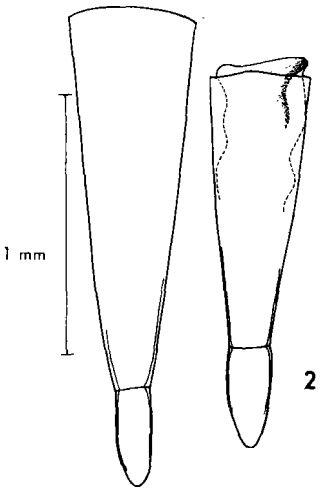
Exception faite de cette récolte les effectifs sont respectivement : 15 - 17 - 12 - 5.

(2) Il resterait pour être complet à mentionner la « *Creseis chierchiae* » dont Menzies (1958) signale la présence en Méditerranée. En fait ni la description de l'animal ni le dessin qui l'accompagne ne correspondent à l'espèce nommée. L'extrémité de la coquille semble se rapprocher de celle de *Creseis acicula*, mais avec une coquille embryonnaire deux fois moins longue, et des annulations transversales dès le début de la coquille adulte (fig. 3 pl. I). Les dimensions ne sont pas indiquées.

PLANCHE I



1. Creseis acicula acicula : extrémité de coquille.

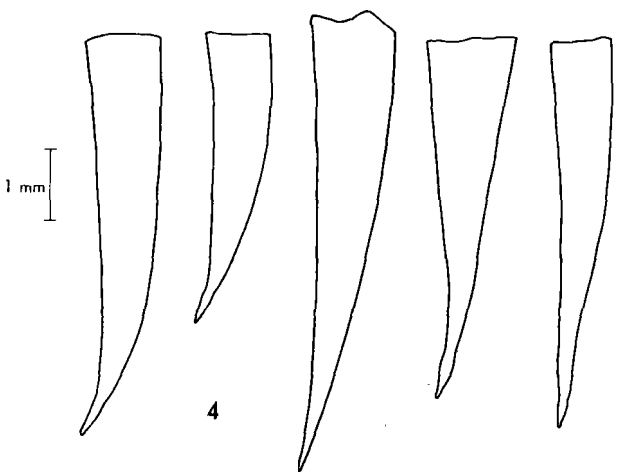


2. Creseis acicula clava : d'après Tokioka (1955)

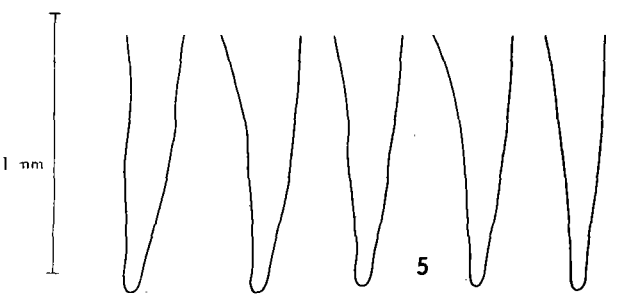


3. Creseis chierchiae : d'après Menziès (1958)

PLANCHE II

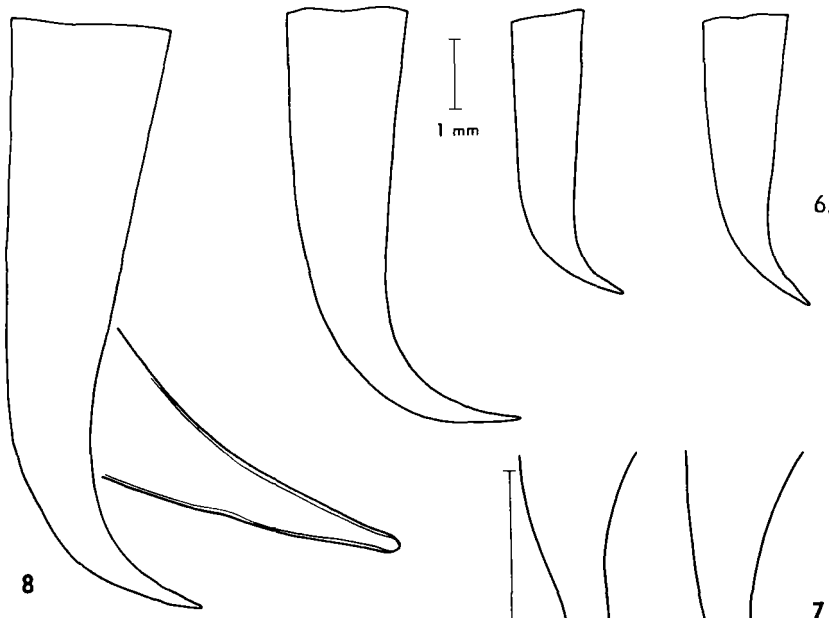


4. *Creseis virgula conica* : coquilles entières



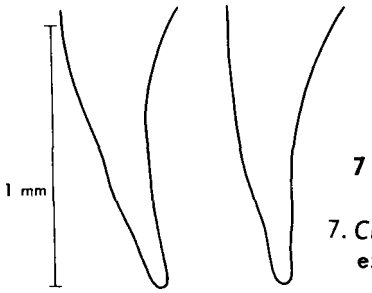
5. *Creseis virgula conica* : extrémités de coquilles.

PLANCHE III



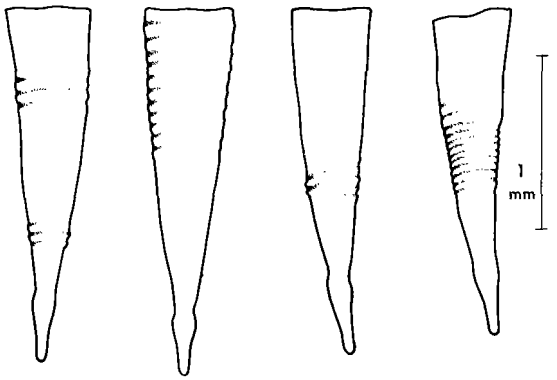
6. *Creseis virgula virgula* : coquilles entières

8. *Creseis virgula virgula* : exemplaire de très grande taille récolté au large des côtes d'Angola.

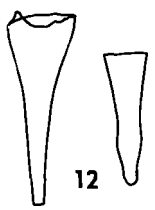


7. *Creseis virgula virgula* : extrémités de coquilles

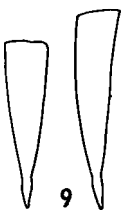
PLANCHE IV



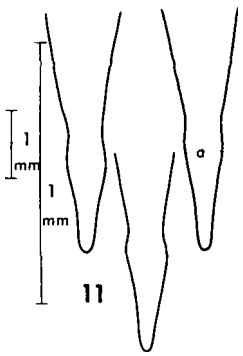
10. *Creseis chierchiae* : formes intermédiaires, coquilles entières.



12. *Creseis caliciformis* : d'après Meisenheimer (1905.)



9. *Creseis chierchiae* : formes lisses, coquilles entières.



11. *Creseis chierchiae* : extrémités de coquilles

BIBLIOGRAPHIE

BOAS, J.E.V.- 1886, Spolia Atlantica. Bidtrag til Pteropodernes Morphologi og systematic sant til Kundskaben om deres geografiske Udbredelse. *Dansk. Vidensk. Selsk. Skrifter, 6. Raekke, Naturvid. og Math.*, Afd 4, Bd 1, pp. 1-231, 8 pl.

CHIN CHEN & BE, A.W.H.- 1964, Seasonal distribution of Euthecosomatous Pteropods in the surface waters of five stations in the western North Atlantic *Bul. Mar. Sc. Gulf and Carrib.* 14 (2), pp. 185-220.

FRONTIER, S.- 1963, a - Hétéropodes et Ptéropodes récoltés dans le plancton de Nosy Be. *Cah. O.R.S.T.O.M. Océanographie* N° 6, pp. 213-227.

1963, b - Présence de *Creseis chierchiae* (BOAS) dans l'Océan Indien. *Ibid.*, pp. 229-232.

MEISENHEIMER, J.- 1905, Pteropoda. *Wiss. Erg. der deutschen Tiefsee Exp. (Valdivia)* 9 (1), pp. 1-314, cartes 1-9, pl. 1-27.

MENZIES, R.J.- 1958, Shell bearing Pteropods Gastropods from mediterranean plancton *(Cavolinidae). Pub. St. Zool, Napoli* 30 (3), pp. 381-401.

TESCH, J.J.- 1904, The Thecosomata and Gymnosomata of the Siboga Expedition. *Siboga Exp.*, Monogr. 52, pp. 1-89, 6 pl.

1946, The Thecosomatous Pteropods. I) The Atlantic. *Dana Report* 28, pp. 1-82, 8 pl.

1948, The Thecosomatous Pteropods. II) The Indopacific *Ibid.* 30, pp. 1-45, 3 pl.

TOKIOKA, T.- 1955, On some plancton animals collected by the Syunkotu-Maru in May-June 1954. IV Thecosomatous Pteropods. *Pub. Seto Mar. Biol. Lab.* 5 (1), pp. 59-74, 7 pl.

Reprinted from *Océanographie*, vol. IV, no. 2, 1966, p. 131-139

NOTES MORPHOLOGIQUES SUR LES *ATLANTA* RÉCOLTÉES DANS LE PLANCTON DE NOSY BÉ (MADAGASCAR)

par Serge FRONTIER*

RÉSUMÉ

La détermination des Atlanta est facilitée par l'examen minutieux des premiers tours de spire de la coquille. La détermination des individus juvéniles est, de ce fait, rendue possible. Les espèces Atlanta inclinata SOULEYET *et* Atlanta helicinoides SOULEYET *se présentent chacune sous deux formes dans le matériel examiné. Une espèce nouvelle,* Atlanta peresi, *est décrite.*

* * *

Les récoltes de plancton effectuées depuis trente mois autour de Nosy Bé ont permis de rassembler une grande quantité d'*Atlantidae* à tous les stades de développement. J'ai ainsi été amené à établir des séries morphologiques quasi continues permettant de relier de façon indiscutable les adultes de toutes les espèces rencontrées aux formes les plus jeunes trouvées dans les récoltes.

Les données concernant la partie juvénile des coquilles d'*Atlantidae* sont rares. TOKIOKA (1955 a) figure un *Atlanta turriculata* de 0,58 mm de diamètre, un *Atlanta lesueuri* de 0,6 mm, et un individu de 0,6 mm de diamètre attribué à *Atlanta inflata*. Pour le reste on ne dispose que de dessins, généralement approximatifs, des premiers tours de spire et de leur ornementation, de sorte que les formes extrêmement jeunes d'*Atlanta* restent le plus souvent indéterminées (1).

Le matériel récolté autour de Nosy Bé a permis de constater que, non seulement les coquilles juvéniles des différentes espèces se distinguent les unes des autres de façon extrêmement nette, mais que l'examen attentif des premiers tours de spire est d'une aide précieuse pour la détermi-

* Océanographe biologiste de l'O.R.S.T.O.M., Centre O.R.S.T.O.M. de Nosy Bé.

(1) TOKIOKA (1961) signale toutefois des individus très jeunes de toutes les espèces qu'il cite, mais sans figurer ni décrire les coquilles.

nation parfois délicate des adultes, et des jeunes. Au moins en ce qui concerne le matériel de Nosy Bé, les caractères à retenir pour la détermination des espèces d'*Atlanta* se sont révélés être les suivants :

1°) Diamètre et nombre de tours de la partie centrale de la coquille, c'est-à-dire de la partie située avant l'apparition de la carène. La largeur moyenne des spires dans cette partie centrale résulte des deux caractéristiques, et peut être reconnue sur les spécimens très jeunes.

2°) Angle apical du cône que constituent les premiers tours de spire à la face supérieure de la coquille. Cet angle peut, lui aussi, être reconnu chez les spécimens très jeunes.

3°) Profil de la spire au-dessous du cône. Ce profil, donné pour les différentes espèces aux figures 1, 6, 9, 11, 13, 17, 19, 24, 26, 31 à 33, dépend à la fois de l'épaisseur de la spire comparativement à son diamètre et de l'inclinaison de la tranche de la coquille vers l'ombilic. Il ne peut être observé que chez les spécimens juvéniles, le profil du dernier tour de spire étant toujours très différent des précédents et n'aidant que peu à la détermination.

4°) L'ornementation (stries, côtes) de la partie centrale de la coquille.

Les 8 espèces classiques d'*Atlanta* (1) se caractérisent alors de la façon suivante :

Atlanta peroni Lesueur (fig. 1 à 5). — Partie centrale de la coquille : 0,9 à 1,0 mm., 4 tours ; angle apical d'environ 80°.

L'ornementation de la coquille est limitée à une strie longitudinale fine qui longe de très près la suture ; cette strie se trouve partiellement recouverte d'un tour de spire au suivant de sorte qu'elle apparaît par segments, d'une façon variant selon les individus, à la surface du cône. Le profil de la spire est donné à la figure 1.

Atlanta gaudichaudi Souleyet (fig. 6 à 8). — Partie centrale d'un diamètre assez variable : 0,7 à 0,9 mm., l'évasement du deuxième tour de spire pouvant varier (fig. 7 et 8), mais comprenant toujours, sur les individus récoltés à Nosy Bé, exactement trois tours ; angle apical d'environ 90°.

Le profil de la spire est donné à la figure 7. La tranche de la coquille est pourvue d'un grand nombre de stries longitudinales extrêmement fines, souvent difficiles à apercevoir et parfois complètement effacées par le séjour de l'échantillon dans le formol. Le cône supérieur, ainsi que la zone entourant l'ombilic à la face inférieure, sont lisses.

Atlanta lesueuri Souleyet (fig. 9 et 10). — Partie centrale de la coquille : 0,35 à 0,4 mm de de diamètre, 1 3/4 tour. L'évasement caractéristique apparaît dès le deuxième tour. Angle apical d'environ 140°.

Le profil de la spire est donné à la figure 9. La coquille est entièrement lisse.

Atlanta inclinata Souleyet (fig. 11 à 16). — Partie centrale de la coquille : 0,75 à 0,9 mm., 4 à 5 tours ; angle apical d'environ 80°.

Le profil de la spire est donné aux figures 11 et 13. L'ornementation du centre de la coquille a été décrite par Tesch (1908) sur des exemplaires nommés *Atlanta inclinata* et *Atlanta gibbosa* — la seconde dénomination étant par la suite tombée en synonymie avec la première —, et par Tokioka (1955 a). Elle consiste en un système de stries transversales et longitudinales extrêmement ténues, reproduit aux figures 11, 15, et 16. L'altération des coquilles par le fixateur fait souvent disparaître plus ou moins complètement ces stries, et c'est sans doute la raison pour laquelle Tesch ne décrit les stries transversales que chez *Atlanta inclinata* et la strie longitudinale longeant la suture que chez *Atlanta gibbosa*.

(1) Seule *Atlanta megalope* Richter 1961 n'a pas été rencontrée avec certitude dans le plancton de Nosy Bé.

Le matériel récolté autour de Nosy Bé comprend un grand nombre d'individus différant sensiblement de la description classique par l'aspect du cône central, qui est droit (fig. 13) et non légèrement convexe comme dans la forme typique (fig. 11).

Atlanta inflata Souleyet (fig. 17-18). — Partie centrale de la coquille : 0,5 à 0,6 mm de diamètre, 3 1/4 tours. Angle apical d'environ 100°.

Le profil de la spire est donné à la figure 17. La tranche de la coquille et sa face inférieure montrent un système de stries longitudinales très fines rappelant celles d'*Atlanta gaudichaudi* — plus marquées, cependant, que chez cette espèce, et s'étendant jusqu'à l'ombilic. Le cône possède trois à quatre côtes très nettes par tour de spire.

Tokioka (1961) a découvert un caractère permettant de déterminer à coup sûr cette espèce : le premier tour de spire de l'opercule est garni sur les trois quarts de sa longueur, de denticules très visibles. Le caractère est aisément observable chez les juvéniles, car les denticules se trouvent alors sur le bord libre de l'opercule et sont visibles sans dissection ni coloration (1).

Atlanta helicinoïdes Souleyet (fig. 19 à 25). — Partie centrale de la coquille : 0,4 à 0,7 mm. de diamètre, 3 3/4 à 4 tours ; angle apical d'environ 130 à 140°.

Le profil de la spire est donné à la figure 19. On observe 16 côtes longitudinales très marquées, plus quelques côtes moins fortes au voisinage de l'ombilic ; 9 des 16 côtes principales sont situées sur le versant inférieur de la spire et 7 sur le versant supérieur ; de ces dernières, 4 sont recouvertes d'un tour de spire à l'autre de sorte qu'il n'apparaît que 3 côtes par tour de spire à la surface du cône.

Les *Atlanta helicinoïdes* examinés se groupent — du moins en ce qui concerne les individus assez âgées — chez lesquels le dernier tour de spire a fait son apparition — en deux ensembles. Un premier ensemble (forme A : fig. 20 et 21) se caractérise par une spire épaisse, une partie centrale de fort diamètre et une ornementation externe très accusée. Le second type possède une coquille surbaissée à partie centrale plus étroite et une striation bien plus effacée (forme B : fig. 22 et 23). De façon plus précise les deux formes se caractérisent par les mensurations suivantes :

	Épaisseur de la coquille (Distance de l'apex au plan moyen de la face inférieure)	Diamètre de la partie centrale
Forme A	0,4 à 0,5 mm	0,5 à 0,7 mm
Forme B.....	0,3 à 0,4 mm	0,4 à 0,5 mm

La distinction n'est en fait aisée que chez les individus relativement âgés (à partir de l'apparition de la carène), et les juvéniles sont difficiles à attribuer à une forme ou à l'autre.

Les deux formes se trouvent souvent réunies dans la même récolte.

Atlanta fusca Souleyet (fig. 24 et 25). — Partie centrale de la coquille : 0,6 mm. de diamètre, 3 tours ; angle apical d'environ 90°.

Le profil de la spire est donné à la figure 24. Il montre environ 12 côtes longitudinales fines mais très nettes sur la tranche et sur la face inférieure : le trajet des ces côtes est finement sinueux

(1) L'observation des opercules d'*Atlantidae* est grandement facilitée par la coloration au Rose Bengale ; l'objet est immergé une dizaine d'heures dans une solution aqueuse à 1 %.

et rappelle l'ornementation de la coquille d'*Oxygyrus keraudreni* (TOKIOKA 1961, fig. 2a). On remarque deux côtes longitudinales sinueuses par tour de spire au début du cône, trois à partir de deux tours et demi.

Atlanta turriculata d'ORBIGNY (fig. 26). — Partie centrale de la coquille : 0,45 mm de diamètre, 2 ½ tours ; angle apical d'environ 40°.

Le profil de la spire est donné à la figure 26. On observe 10 côtes longitudinales fines sur la tranche de la spire, la côte la plus rapprochée de l'apex du cône n'étant pas recouverte d'un tour de spire à l'autre et apparaissant donc à la surface du cône. La limite entre la face externe et la tranche de la spire est suivie par une très courte membrane dressée perpendiculairement à la surface de la coquille, dépendant sans doute du periostracum. Cette membrane est figurée par TOKIOKA (1955 a : fig. 5 U) mais sans mention dans le texte.

Description d'Atlanta peresi n. sp. (fig. 27 à 26). — Une cinquantaine d'individus, surtout juvéniles, récoltés au large de Nosy Bé, ne répondent à la description d'aucune des huit espèces mentionnées ci-dessus ni à celle d'*Atlanta megalope* récemment décrite (RICHTER 1961). Quatre adultes ont été rencontrés jusqu'ici, pour lesquels la clé des *Atlanta* publiée par TESCH (1949) aboutirait à la détermination *Atlanta lesueuri*. Ces individus diffèrent cependant à de nombreux égards de cette dernière espèce. Il convient d'en faire une espèce nouvelle.

Le type est un adulte possédant une coquille de 2,69 mm de diamètre maximum, pour 3 tours 1/2 de spire. La carène (0,72 mm dans sa partie la plus haute) apparaît au stade 0,52 mm (3 tours 1/4 de spire), et se trouve chevauchée par la dernière spire à partir du stade 1,40 mm. (3 tours de spire). La spire s'élargit, à partir du centre de la coquille, de façon très régulière et sans montrer l'évasement caractéristique d'*Atlanta lesueuri*. Reprenant les notations de TOKIOKA (1955), on trouve comme *whorl formula* (1 : 0,29 : 0,11), contre 1 : 0,17 : 0,07) pour les exemplaires de même taille d'*Atlanta lesueuri* étudiés par cet auteur.

Deux tours de spire sont visibles à la face inférieure de la coquille. L'ouverture de celle-ci est relativement basse et large : rapport hauteur / largeur maximum égal à 1,3. Le profil de la spire chez les spécimens juvéniles est donné aux figures 31 à 33. L'angle apical varie entre 110 et 130°, donc est presque aussi plat que chez *Atlanta lesueuri*. On n'observe aucune ornementation de la coquille, qui est d'un blanc laiteux légèrement teinté de fauve sur le dernier tour de spire.

L'opercule (fig. 30) ressemble à celui d'*Atlanta lesueuri*, mais est plus large ; reprenant les notations de TOKIOKA (1961), on trouve les mensurations suivantes :

L (longueur)	0,98	mm.
W (largeur maxima)	0,78	mm.
W / L	0,79	mm.
A / L	0,315	mm.
B / A	0,42	mm.
D / C	0,83	mm.

BIBLIOGRAPHIE

FRANC (A.) 1948. — Véligères et Mollusques Gastéropodes des Baies d'Alger et de Banyuls. *J. Conchyl.* 88, *pp. 13-35.*

— 1949. — Hétéropodes et autres Gastéropodes planctoniques de Méditerranée occidentale. *J. Conchyl.* 89, *pp.* 209-230.

FRONTIER (S.) 1963. — Hétéropodes et Ptéropodes récoltés dans le plancton de Nosy Bé. *Cahiers O.R.S.T.O.M. Océanographie 1 (6) (Travaux du Centre d'Océanographie et des Pêches de Nosy Bé n° 2) pp. 213-227.*

RICHTER (G.) 1961. — Die Radula der Atlantiden und ihre Bedeutung fur die Systematik und Evolution der Familie. *Z. Morph. Oekol. Tiere* 50, *pp. 163-238.*

TESCH (J.J.) 1906. — Heteropoden der Siboga Expedition. *Siboga Exp., 112 p., 12 pl.*

— 1908. — Systematic monography of the Atlantidae. *Notes Leyden Mus.* 30, *pp.* 1-30, 5 *pl.*

TESCH (J.J.) 1949. — Heteropoda. *Dana Report 34, pp. 1-55, 5 pl.*

TOKIOKA (T.) 1955 a. — On some planctonic animals collected by the Syunkotu-Maru in May-June 1954. II) Shells of Atlantidae. *Pub. Seto Mar. Biol. Lab. 4 (2), pp. 227-236, pl. 15-16.*

— 1955 b. — Shells of Atlantidae (Heteropoda) collected by the Sôyô-Maru in the Southern waters of Japan. *Ibid. 4 (2), pp. 237-250, pl. 17-18.*

— 1961. — The structure of the operculum of the species of Atlantidae as taxonomic criterion, with records of some pelagic Molluscs in the North Pacific. *Ibid. 9 (2) pp. 266-332.*

Les échelles représentent 1 mm.

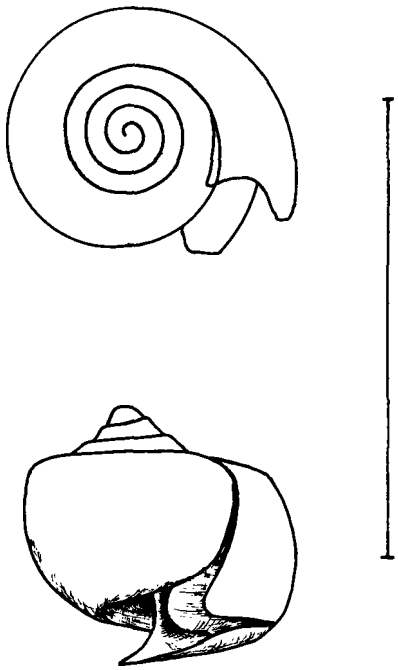


Fig. 1 et 2. — *Atlanta peroni*, coquille de 0,66 mm de diamètre maximum.

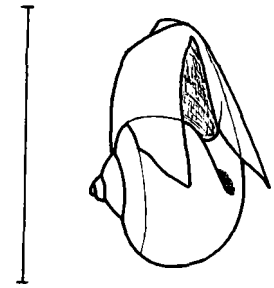


Fig. 3. — *Atlanta peroni*, coquille de 1,00 mm de diamètre.

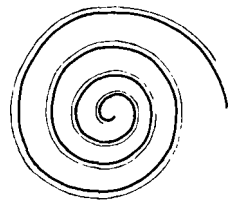


Fig. 5. — *Atlanta peroni*, autre individu : centre de la spire.

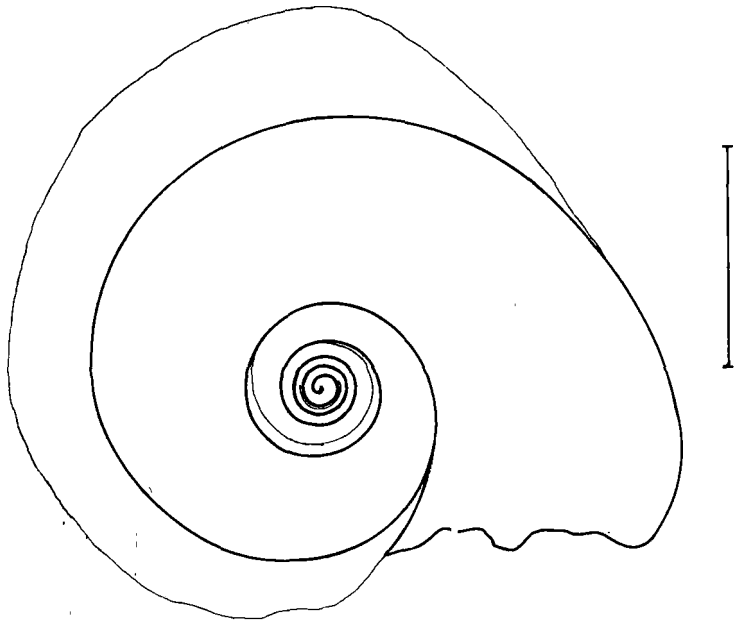


Fig. 4. — *Atlanta peroni*, coquille adulte.

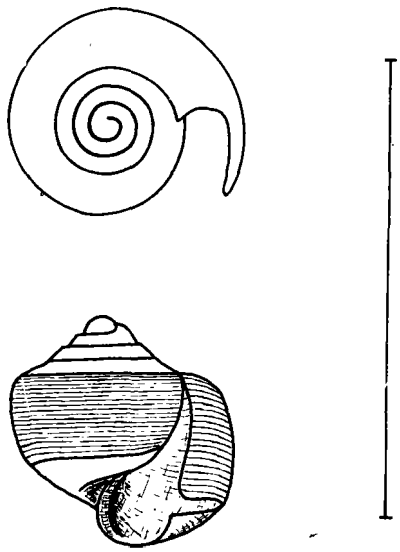


Fig. 6 et 7 — *Atlanta gaudichaudi*, coquille de 0,52 mm de diamètre maximum.

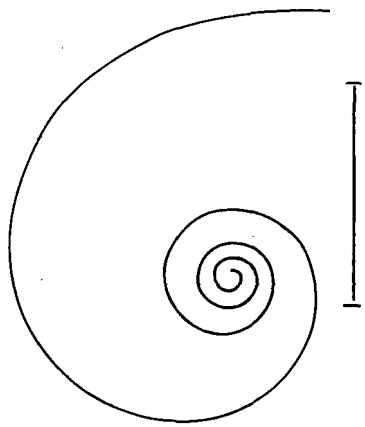


Fig. 8. — *Atlanta gaudichaudi*, coquille adulte : centre de la spire.

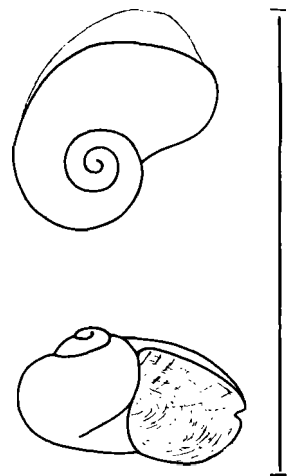
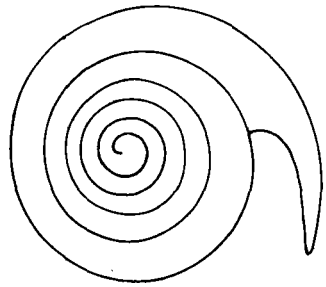
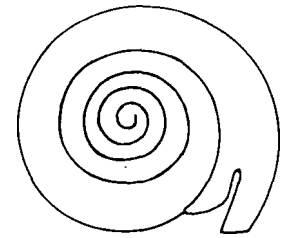


Fig. 9 et 10. — *Atlanta lesueuri*, coquille de 0,49 mm de diamètre maximum.

Les échelles représentent 1 mm.





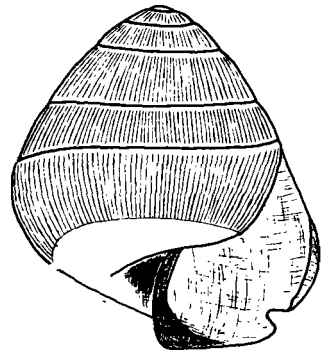


Fig. 11 et 12. — *Allanta inclinata*, forme typique, coquille de 0,72 mm de diamètre maximum.

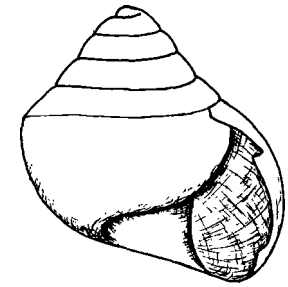


Fig. 13 et 14. — Idem, forme atypique, coquille de 0,58 mm de diamètre maximum.

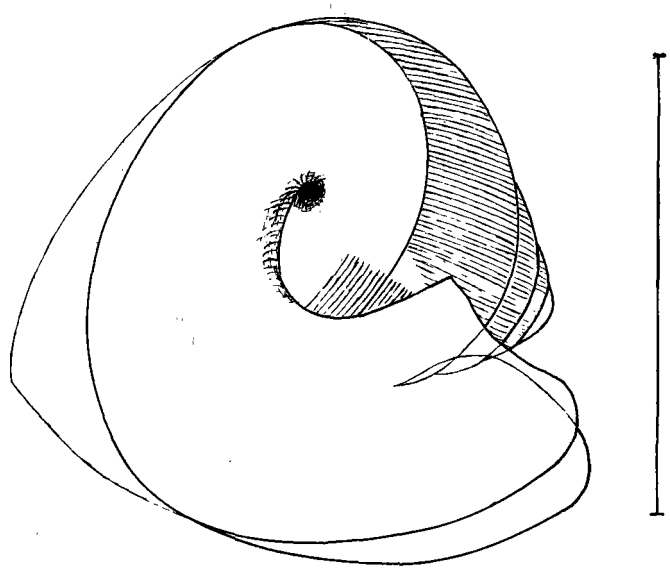


Fig. 15 — *Allanta inclinata*, coquille jeune.

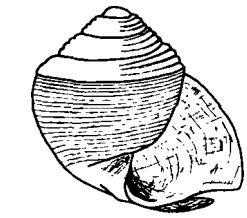


Fig. 17. — *Allanta inflata*, coquille de 0,50 mm de diamètre maximum.

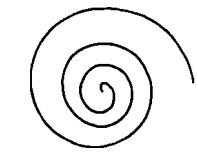


Fig. 18. — Idem coquille adulte, centre de la spire.

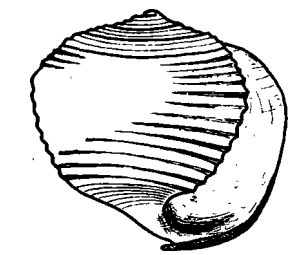


Fig. 19. — *Allanta helicinoides*, coquille de 0,56 mm de diamètre maximum.

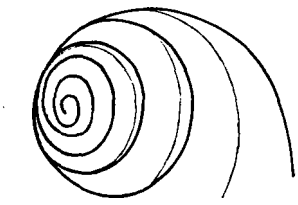


Fig. 16. — Idem coquille jeune.

Les échelles représentent 1 mm.

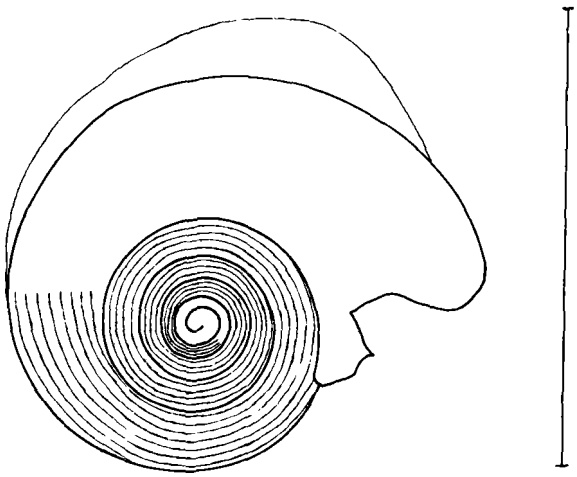


Fig. 20 *Atlanta helicinoides*, forme A, coquille de 1,03 mm de diamètre maximum.

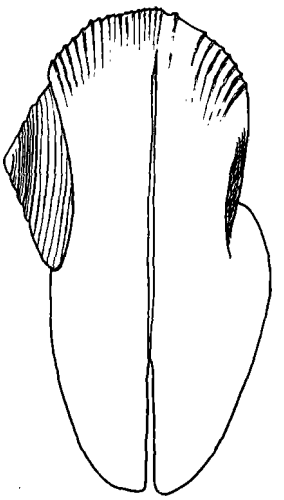


Fig. 21. — *Atlanta helicinoides*, forme A, coquille de 1,03 mm de diamètre maximum.

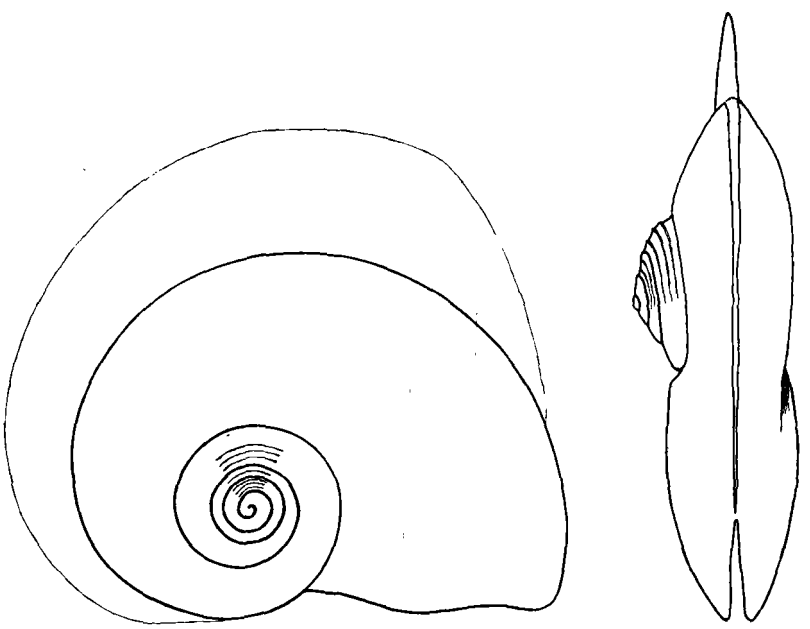


Fig. 22 et 23. — *Atlanta helicinoides*, forme B, coquille de 1,14 mm de diamètre maximum.

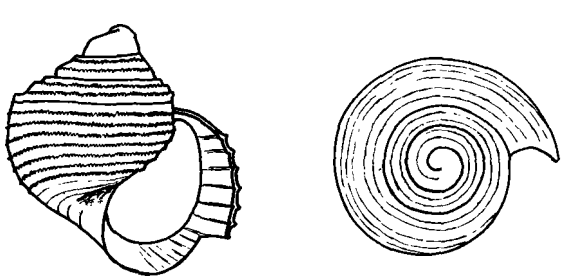


Fig. 24 et 25. — *Atlanta fusca*, coquille de 0,49 mm de diamètre maximum.

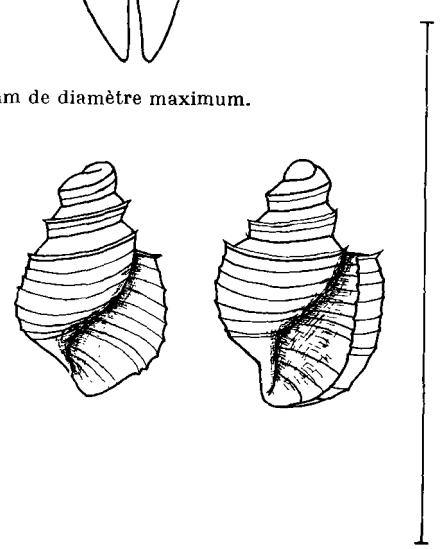
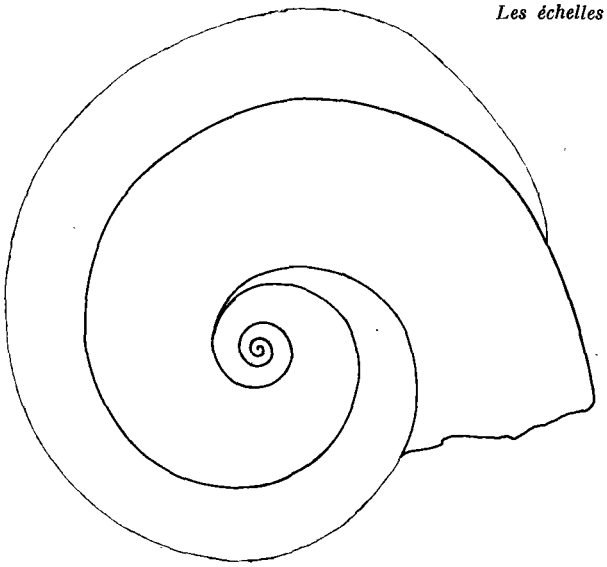


Fig. 26. — *Atlanta turriculata*, coquilles de 0,28 et 0,35 mm de diamètre maximum.

Les échelles représentent 1 mm.



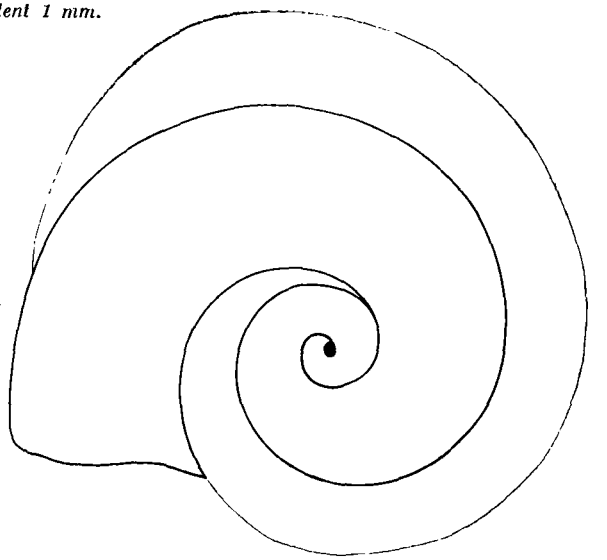


Fig. 29. — *Atlanta peresi*, face inférieure.



Fig. 27. — *Atlanta peresi* n. sp. (type), face supérieure. Diamètre maximum 2,69 mm.
Fig. 28. — Idem, centre de la spire.

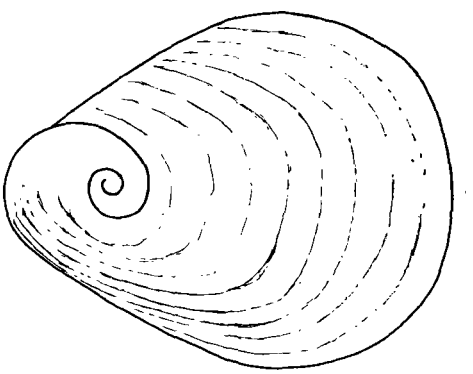


Fig. 30. — *Atlanta peresi*, opercule.

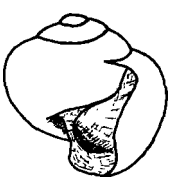


Fig. 31. — *Atlanta peresi*, coquille de 0,36 mm de diamètre maximum.

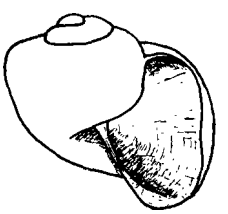


Fig. 32. — *Atlanta peresi*, coquille de 0,48 mm de diamètre maximum.

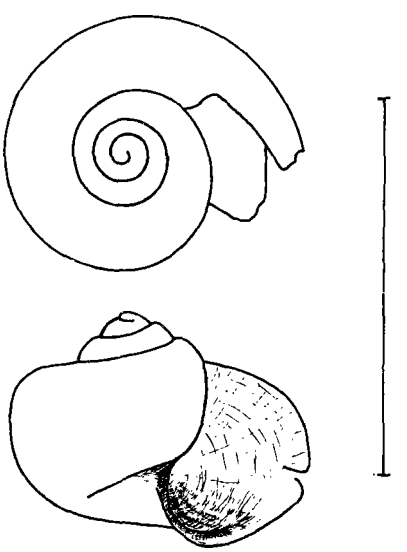


Fig. 33 et 34. — *Atlanta peresi*, coquille de 0,66 mm de diamètre maximum (individu à cône relativement prononcé).

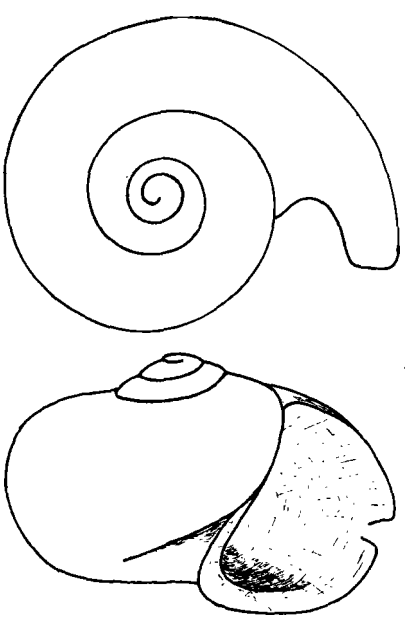


Fig. 35 et 36. — *Atlanta peresi*, coquille de 0,80 mm de diamètre maximum (individu à cône relativement peu prononcé).

Reprinted from *Océanographie*, vol. IV, no. 2, 1966, p. 141-146

LISTE COMPLÉMENTAIRE DES PTÉROPODES DU PLANCTON DE NOSY BÉ (MADAGASCAR)

par S. FRONTIER*

RÉSUMÉ

L'auteur signale 12 espèces et une sous-espèce supplémentaires de Ptéropodes dans le secteur de Nosy Bé. Trois espèces sont nouvelles pour l'Océan Indien. Des remarques morphologiques sont faites concernant Diacria quadridentata (LESUEUR), Cuvierina columnella (RANG) *et* Cavolinia longirostris (LESUEUR).

* * *

Une première liste de Ptéropodes récoltés dans un rayon d'une cinquantaine de milles autour de Nosy Bé a été publiée en 1963 (FRONTIER 1963 a) ; elle comprenait 17 espèces. *Creseis chierchiae* (BOAS), très abondante au-dessus du plateau continental, a été signalée ultérieurement (FRONTIER 1963 b et 1965). Outre cette espèce, 12 autres, toutes très rares et localisées aux eaux du large ont été rencontrées depuis l'établissement de la première liste, ainsi qu'une sous-espèce.

EUTHECOSOMES.

Limacina lesueuri (d'ORBIGNY). — Déjà signalée dans l'Océan Indien (MEISENHEIMER 1905), cette espèce y est indiquée comme très rare. L'expédition du « Dana » n'en a récolté, aucun exemplaire (TESCH 1948). Quelques individus ont été récoltés au voisinage de Nosy Bé, toujours dans les eaux du large : en un cycle annuel (24 récoltes par station en un an), une station située presque à l'aplomb du talus continental en a fourni 17 individus, et une station située au-dessus des fonds de 1400 m, 8.

Euclio cuspidata (Bosc). — Un individu jeune capturé à l'aplomb du talus continental.

Cuvierina columnella columnella (RANG). — Un individu adulte capturé au large (tous les autres *Cuvierina columnella* capturés appartiennent à la sous-espèce *urceolaris* (MÖRCH)).

Diacria trispinosa (LESUEUR). — Deux individus juvéniles capturés au large.

---

* Océanographe biologiste de l'O.R.S.T.O.M., Centre O.R.S.T.O.M. de Nosy Bé.

PSEUDOTHECOSOMES.

Peraclis reticulata (d'ORBIGNY). — Deux individus capturés au large.

Corolla sp. — 7 individus jeunes capturés au large. Pseudoconques perdues.

Gleba cordata FORSKAL. — Espèce non encore signalée en Océan Indien. Trois individus ont été capturés en une station située au large.

GYMNOSOMES.

Pneumodermopsis sp. — Deux individus en une station du large.

Pneumoderma atlanticum (OKEN). — Un individu capturé au large.

Spongiobranchaea australis (d'ORBIGNY). — Trois individus jeunes capturés au large. L'espèce était considérée jusqu'ici comme circumantarctique, n'ayant jamais été capturée au nord de la latitude 30°15'S (TESCH 1950) près de la côte sud africaine — où elle apparaissait sans doute à la faveur du courant de Benguela. Sa présence au large de Nosy Bé à la latitude de 13°34'S s'explique peut-être par des remontées d'eau profonde (1).

Nolobranchaea macdonaldi (PELSENEER). — Un individu jeune capturé au large.

Thalassopterus zancleus (KWIETNIEWSKI). — Un individu capturé au large. Cette espèce néoténique n'était connue jusqu'ici que de la Méditerranée (KWIETNIEWSKI 1910 et 1912).

Hydromyles globulosa (RANG). — Deux individus capturés en une station du large. L'espèce est signalée comme très abondante dans l'Indopacifique tropical (TESCH 1950).

Toutes les espèces mentionnées ont été capturées à l'aide du filet « TREGOUBOFF » (TREGOUBOFF G. et ROSE M. 1957) entre 10 m. de profondeur et la surface.

NOTES MORPHOLOGIQUES

Diacra quadridentata (LESUEUR). — Les individus adultes appartiennent à deux formes nettement distinctes, souvent mêlées dans la même récolte : une forme de grande taille (longueur de la coquille 2,0 à 2,4 mm. ; largeur maximum 1,9 à 2,15 mm. ; rapport longueur / largeur 1,05 à 1,18) et une forme de petite taille à coquille généralement plus allongée (longueur de la coquille 1,45 à 1,6 mm ; largeur maximum 1,2 à 1,3 mm ; rappport longueur / largeur 1,13 à 1,28). Il n'a pas été trouvé d'intermédiaires entre ces deux formes. Les coquilles juvéniles des deux formes ne peuvent être distinguées, sauf évidemment celles qui ont atteint une très grande taille et ne peuvent appartenir qu'à la première forme.

Cuvierina columnella (RANG) (fig. 1). — J'ai représenté en 1963 une coquille juvénile à extrémité cassée ; je figure cette fois une coquille intacte. L'apex est arrondi. Un sillon externe très fin situé au niveau du rétrécissement sépare la partie embryonnaire du reste de la coquille. Dimensions de la coquille embryonnaire : $0{,}40 \times 0{,}17$ mm.

Cavolinia longirostris longirostris (LESUEUR) (fig. 2a à 2 h). — L'obtention d'un abondant matériel provenant des récoltes effectuées au-dessus du plateau continental a permis d'établir une série morphologique quasi-continue réunissant la forme adulte à des formes extrêmement jeunes. Ces dernières, ainsi qu'il apparaît aux figures 2 et 3, diffèrent nettement de la forme juvénile « *Hyalaea laevigata* » que l'on considère depuis PELSENEER (1887) comme la forme juvénile de *Cavolinia longirostris*.

(1) Les mêmes récoltes contenaient les espèces *Lanceola aestiva* (STEBBING) et *Lanceola pacifica* SAY, Amphipodes Hypériens considérés comme bathypélagiques.

« *Hyalaea laevigata* » a par ailleurs été trouvée en assez grand nombre dans le secteur de Nosy Bé, mais presque uniquement aux stations du large.

Les coquilles juvéniles de *Cavolinia longirostris longirostris* observées dans le matériel de Nosy Bé ne sont pas calcifiées mais parfaitement transparentes et souples — contrairement à toutes les formes juvéniles décrites sous le nom générique d'*Hyalaea* qui sont calcifiées d'emblée. Les stries d'accroissement sont visibles en éclairage latéral. La partie postérieure se détruit au fur à mesure que croît la partie antérieure, de sorte que l'on arrive à la forme adulte progressivement et non par perte de la partie jeune de la coquille à un stade déterminé du développement, comme PELSENEER en avait fait l'hypothèse.

La lèvre dorsale tend à croître au-delà de la lèvre ventrale depuis les stades les plus jeunes (fig. 2a) ; le bombement caractéristique de la lèvre ventrale n'apparaît par contre qu'à un stade relativement tardif (fig. 2 g'), au moment où la coquille se calcifie. La courbure sagittale caractérisant les formes juvéniles de *Cavolinia* n'est visible, en raison de la destruction progressive de l'extrémité de la coquille, que sur les plus petites coquilles examinées ; elle est d'ailleurs presque imperceptible (fig. 2 a' et b') ; sur ces mêmes coquilles on peut également observer la coquille embryonnaire, hémisphérique comme chez les autres *Cavolinia*, insérée sur l'extrémité tronquée de la coquille secondaire (fig. 2a et a').

Il semble bien que les coquilles se déforment en grandissant au cours des premiers stades de la croissance : la partie basale s'élargit graduellement, de sorte qu'il est impossible de superposer les dessins de deux stades successifs de coquilles juvéniles dans leurs parties homologues. Cette déformation graduelle est probablement rendue possible par la nature purement organique de la coquille à ces stades du développement. Il est difficile d'établir s'il s'agit d'un remaniement ou simplement d'un aplatissement et d'un étirement de la coquille dans le sens dorso-ventral ; j'opterais cependant plutôt pour la seconde hypothèse vu l'aspect normal des stries d'accroissement à tous les stades.

L'identité de la forme « *Hyalaea laevigata* » (fig. 3) se trouve alors mise en doute. PELSENEER l'avait rattachée à *Cavolinia longirostris* pour des raisons anatomiques, mais sans avoir observé les stades intermédiaires. Or ces raisons anatomiques sont justifiées, et d'autre part *Hyalaea laevigata* ne peut correspondre à aucune espèce connue de *Cavolinia* hormis *Cavolinia longirostris* ; en effet toutes les autres espèces conservant la partie juvénile de leur coquille à l'état adulte, et chez aucune d'entre elles cette partie juvénile ne peut se superposer à *Hyalaea laevigata*.

Les coquilles juvéniles de toutes les espèces de *Cavolinia* identifiées dans le plancton de Nosy Bé ont été observées dans ce même plancton à l'exception de *Cavolinia globulosa* dont il n'a été récolté qu'une petit nombre de coquilles adultes au large (la forme juvénile de cette espèce, dite « *Hyalaea rotundata* », est aisément reconnaissable) et de *Cavolinia longirostris angulata*. Or, il est à remarquer que cette dernière sous-espèce, tout comme *Hyalaea laevigata*, ne se rencontre pratiquement qu'au large.

Il vient à l'esprit qu'*Hyalaea laevigata* pourrait être la forme juvénile de *Cavolinia longirostris angulata*, qui est à Nosy Bé la forme du large de *Cavolinia longirostris*. En fait, la morphologie aberrante des coquilles juvéniles de *Cavolinia longirostris longirostris* décrites ici, très différentes de la forme « *Hyalaea* », pourrait s'expliquer par leur absence de calcification, qui permettrait l'élargissement de la partie basale sous l'action mécanique des pressions internes. Nous avons remarqué en effet que les tout premiers stades (fig. 2a) présentent beaucoup plus l'aspect « *Hyalaea* » que les suivants, qui s'élargissent graduellement.

Une décalcification des coquilles à mesure que l'eau devient plus côtière a déjà été notée pour *Creseis chierchiae* (FRONTIER 1965) qui se présente autour de Nosy Bé sous deux formes : l'une peu ou pas calcifiée, transparente et à annulation très visible, localisée au plateau continental et abondante surtout à l'intérieur des baies ; l'autre à coquille lisse et calcifiée, de plus en plus abondante à mesure qu'on s'éloigne des côtes, et seule présente dans les eaux du large. Ce dimorphisme semble devoir être rapproché de celui constaté ci-dessus dans l'hypothèse où *Hyalaea laevigata* représente la forme du large de la coquille juvénile de *Cavolinia longirostris*, et celle décrite plus haut, la forme néritique. Plutôt qu'une dissemblance singulière entre les formes juvéniles de deux sous-espèces très voisines à l'état adulte, nous serions en présence d'un dimorphisme lié en partie aux conditions écologiques.

BIBLIOGRAPHIE

FRONTIER (S.) 1963 a. — Hétéropodes et Ptéropodes récoltés dans le plancton de Nosy Bé. *Cahiers O.R.S.T.O.M. Océanographie (Travaux du Centre d'Océanographie et des Pêches de Nosy Bé) 1 (6) pp. 255-283.*

— 1963 b. — Présence de *Creseis chierchiae* dans l'Océan Indien. *Ibid. pp. 229-232.*

— 1965. — Le problème des *Creseis. Ibid. 3 (2) pp.* 11-17.

KWIETNIEWSKI (C.) 1910. — Ueber die Larven eines unbekannten Gymnosomen Pteropoden. *Zool. Anz. 36 pp. 257-271.*

— 1912. — Ueber der Larve mit Segellappen eines Gymnosomen Pteropoden *(Thalassopterus zancleus). Ibid. 39 pp. 589-062.*

MEISENHEIMER (J.) 1905. — Pteropoda. *Tiefsee Exp. Valdivia 9 (1) pp. 1-314, carles 1-9, pl. 1-27.*

PELSENEER (P.) 1887. — Report on Pteropoda. II) Thecosomata. *Challenger Rep. 23, pp. 1-132, 2 pl.*

PRUVOT-FOL (A.) 1942. — Les Gymnosomes (I). *Dana Rep. 20 pp. 1-54.*

TESCH (J.J.) 1913. — Pteropoda. *Bronn's Tierreich, Lief. 36, pp. 1-154.*

— 1946. — The Thecosomatous Pteropods. I) The Atlantic. *Dana Rep. 28 pp. 1-82, 8 pl.*

— 1948. — The Thecosomatous Pteropods. II) The Indo-Pacific. *Ibid. 30 pp. 1-45, 3 pl.*

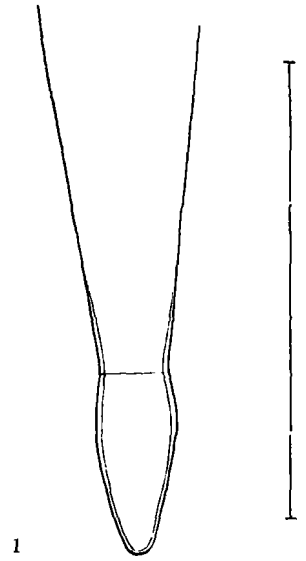
— 1950. — Gymnosomata (II). *Ibid. 36 pp. 1-55.*

PLANCHES

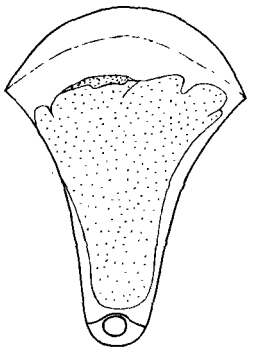
(légendes des figures)

1. — *Cuvierina columnella.* Extrémité de coquille jeune.
2. — *Cavolinia longirostris longirostris.* Coquilles juvéniles (2 a à 2 h).
3. — " *Hyalaea laevigata* ".

Les échelles représentent 1 mm.



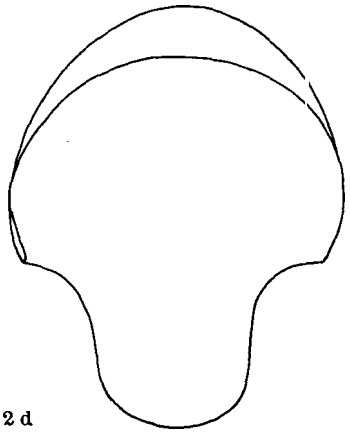
1



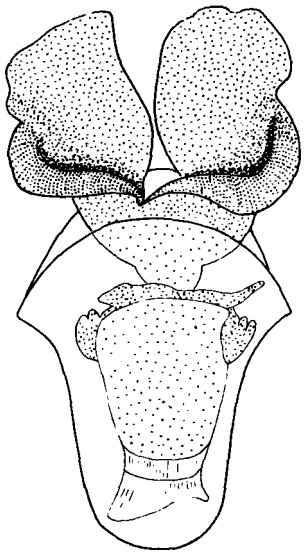
2 a



2 a'



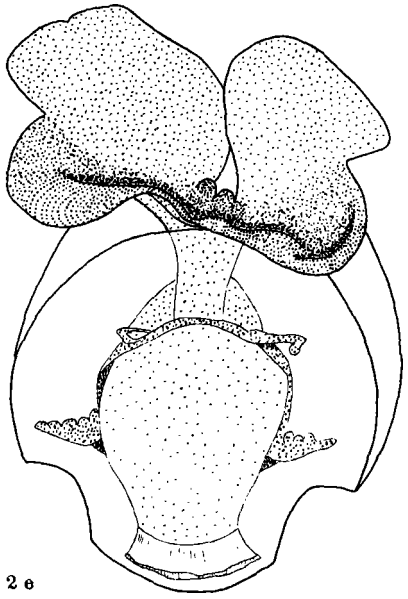
2 d



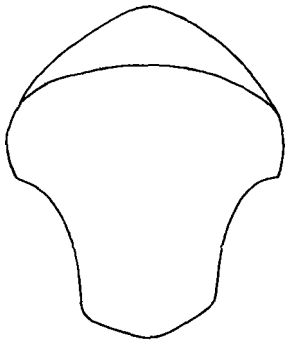
2 b



2 b'



2 e

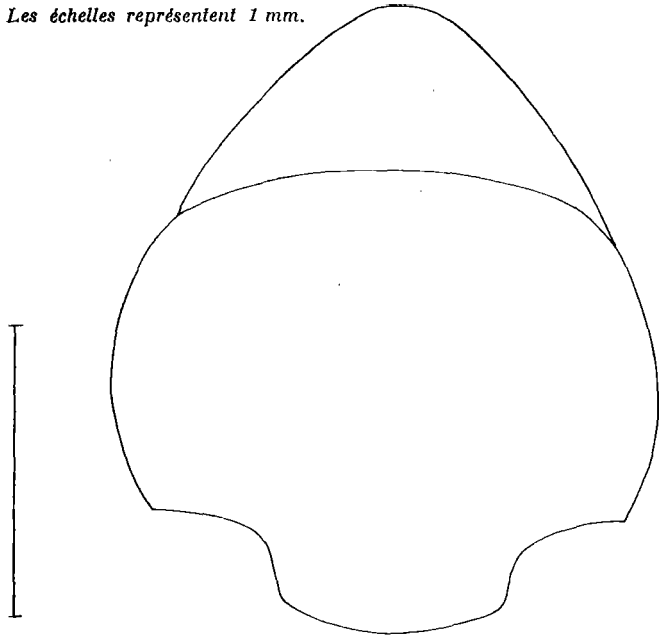


2 c

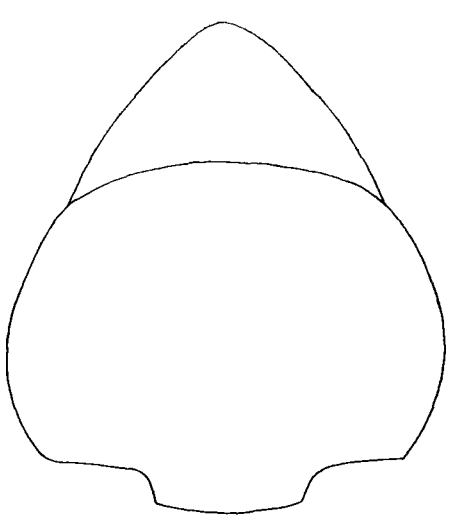


2 c'

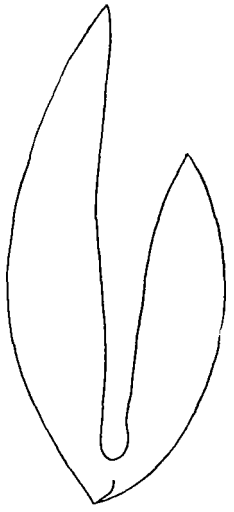
Les échelles représentent 1 mm.



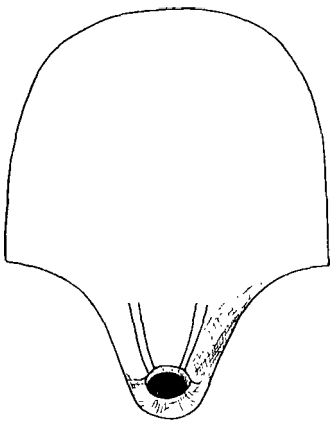
2 f



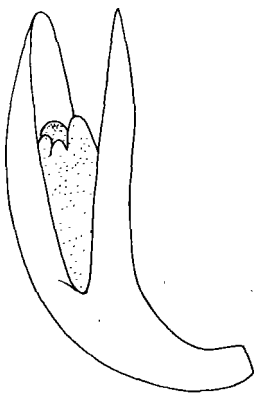
2 g



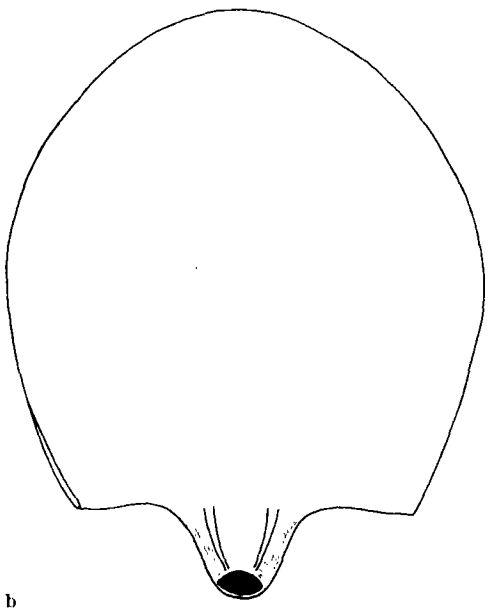
2 g'



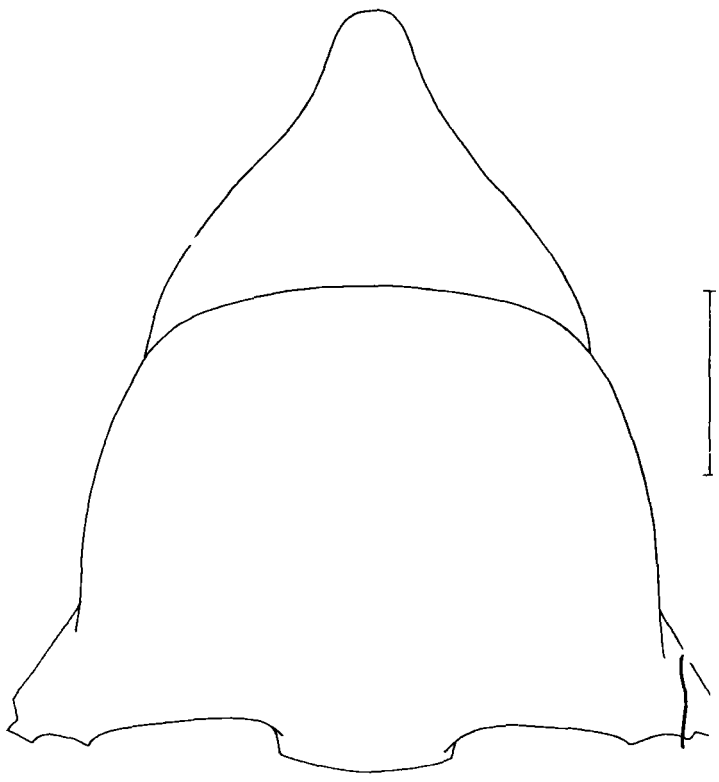
3 a



3 a'



3 b



2 h

Reprinted from *Océanographie*, vol. IV, no. 3, 1966, p. 3-36

ZOOPLANCTON DE LA RÉGION DE NOSY BÉ.
I. PROGRAMME DES RÉCOLTES ET TECHNIQUES D'ÉTUDES.
II. PLANCTON DE SURFACE AUX STATIONS 5 ET 10

par S. FRONTIER*

RÉSUMÉ

L'auteur expose les méthodes de récoltes utilisées (filets), une méthode d'estimation d'abondance des groupes zoologiques (cotation d'abondance de 0 à 7 correspondant à une progression exponentielle) et de représentation graphique des résultats (comptages et cotes d'abondance portés en échelle (log)²).

L'analyse des résultats hydrologiques de surface en deux stations — l'une située au-dessus du plateau continental, l'autre au-dessus des fonds de 800 m — aboutit à une division de l'année en quatre saisons.

Les variations d'abondance des Dolioles, Appendiculaires, larves de Décapodes Brachyoures, Anomoures, Natantia, larves de Stomatopodes, Cladocères, Annélides, Chaetognathes, Ptéropodes, Hétéropodes, Cténaires, Siphonophores au cours d'un cycle annuel effectué aux deux stations citées, sont exposées et commentées. Ces groupes montrent, dans leur ensemble, au cours de l'année étudiée, des fluctuations soit dans leur abondance absolue, soit dans la stabilité (ou l'homogénéité) des populations qu'ils constituent. Ces fluctuations se situent facilement par rapport à la division de l'année en quatre saisons; elles se montrent bien plus considérables à la station située au-dessus du plateau continental qu'à celle du large.

L'étude systématique des Hétéropodes (14 espèces) et des Ptéropodes (24 espèces) fait ressortir le très petit nombre d'espèces présentes régulièrement dans les eaux du plateau continental. Les autres semblent appartenir à une faune du large qui n'apparaît dans la zone néritique qu'à la faveur d'apports d'eau pélagique; en particulier un parallélisme très net est constaté entre les variations du nombre d'espèces d'Hétéropodes rencontrées au-dessus du plateau continental, et les variations d'abondance de ce même groupe au large.

---

* Océanographe biologiste de l'O.R.S.T.O.M., Centre O.R.S.T.O.M. de Nosy Bé (Madagascar).

* * *

Cette note inaugure une série d'exposés sur le zooplancton rencontré dans un rayon d'une cinquantaine de milles autour de Nosy Bé, et sur les fluctuations saisonnières dont ce plancton semble être l'objet.

Un tel exposé ne peut encore être que très global, le dépouillement précis des récoltes n'ayant pu, faute de temps, être effectué que pour un très petit nombre de groupes zoologiques. Il tire son intérêt de l'ignorance quasi-totale dans laquelle nous nous trouvons encore actuellement concernant le peuplement planctonique de la partie ouest de l'Océan Indien, en particulier du Canal de Mozambique. L'implantation d'un Centre O.R.S.T.O.M. d'Océanographie sur le rivage de ce dernier est de nature à permettre enfin une étude exhaustive du plancton en un point précis de cette zone océanique. Certes le travail entamé ici n'a pas la prétention d'aboutir à cette étude exhaustive, cependant nous espérons que les distinctions de peuplements et les périodicités saisonnières entrevues puissent servir de cadre à des examens ultérieurs plus complets.

Une première série de récoltes autour de Nosy Bé avait été effectuée de novembre 1959 à décembre 1960 par A. Crosnier et moi-même. De leur examen, dont quelques résultats ont été publiés (1), il semblait ressortir que trois types de peuplement devaient être distingués : le premier limité à l'intérieur des baies vaseuses bordées de mangroves, recevant en saison humide d'abondants apports d'eau douce ; ce peuplement, que je nommerai *peuplement néritique interne*, se remarque par une pullulation fréquente de Cyanophycées et de Diatomées en chaînes qui encombrent les récoltes faites au filet à mailles fines ; le zooplancton y est pauvre en espèces, et souvent en individus. Le second peuplement, appelé *néritique externe*, caractérise les eaux recouvrant la moitié externe du plateau continental, à l'ouest d'une ligne approximative Nosy Be-Nosy Mitsio ; c'est un peuplement riche qualitativement et quantitativement. Enfin un troisième peuplement définit les *eaux du large*, pauvres en individus mais riches en espèces.

Les limites spatiales de ces peuplements varient au cours de l'année et, en outre, ne peuvent être définies avec netteté car les trois types d'eau s'interpénètrent plus ou moins profondément. Les récoltes de 1959-60 avaient révélé la présence sporadique, en des points situés parfois très en-deçà de la ligne des 100 m, d'espèces du large (Chaetognathes : Furnestin & Radiguet 1964 ; Hérétopodes et Ptéropodes : Frontier 1963), semblant indiquer des allées et venues de l'eau de surface et des apports d'eau du large au-dessus du plateau continental. En ce qui concerne les Hétéropodes et les Ptéropodes la plus grande partie du stock d'espèces semblait appartenir en propre à l'eau du large, les espèces se distinguant les unes des autres par un degré de tolérance variable vis-à-vis du mélange de leur eau d'origine avec l'eau néritique. Il semblait qu'il serait possible d'établir une échelle d'espèces telle que l'inventaire d'une récolte permît une estimation du degré de mélange de l'eau dont elle proviendrait.

Dans le but de confirmer ou d'infirmer ces hypothèses, dans l'intention également de déceler des variations saisonnières tant dans l'extension géographique de ces peuplements qu'au sein des peuplements eux-mêmes, un nouveau programme de récoltes a été mis en train en mars 1963. Il se poursuit actuellement, et l'examen des échantillons obtenus a déjà permis de dégager un certain nombre de faits.

Dans ce premier article le programme de récoltes et les techniques de travail seront décrites, puis quelques résultats significatifs provenant de deux stations occupées pendant un an seront exposés et commentés. Une de ces stations se trouve à la limite des eaux néritiques externe et interne, l'autre à la limite entre la zone néritique externe et l'eau du large.

---

(1) Frontier (S.), 1963 a et b ; Furnestin (M. L.) et Radiguet (J.), 1964 ; Nouvel (H.), 1964.

I) PROGRAMME DES RÉCOLTES ET TECHNIQUES DE TRAVAIL

A. Stations occupées (Carte des stations p. 6). — Un premier cycle annuel de récoltes a été exécuté entre mars 1963 et mars 1964 : un itinéraire situé dans un rayon d'environ 50 milles autour de Nosy Be a été suivi chaque mois pendant un an. Au cours de cet itinéraire, huit stations principales (numérotées 3 à 10) et deux stations « intermédiaires » (4A et 5A) étaient tout d'abord occupées. A partir de juillet la station 3 a été complétée par une station 3A située très près de la côte, la station 7 a été déplacée vers le large et la station 9 remplacée par les deux stations 9A et 9B. Quelques stations au voisinage des îles Mitsio (4α, 4β, 4γ) ont été occupées sporadiquement. Par contre la station 10, proche du Centre, l'a été en moyenne tous les quinze jours. Les stations 4α à 5A (radiale est-ouest au large des Mitsio) avaient lieu de nuit, la station 6 (à l'extrémité de cette radiale) au lever du jour, toutes les autres au cours de la journée.

A partir d'avril 1964, la distinction des trois zones de peuplement s'étant trouvée confirmée, trois stations seulement ont été retenues soit une dans chaque zone : les stations 3, 4 et 5A jusqu'en août, puis à partir de septembre les stations 3, 11 et 12, ces deux dernières étant situées cette fois dans le sud de la région étudiée. Les stations 4, 5A, 11 et 12 étaient occupées de nuit ; la 3 continuait à l'être vers le milieu de la journée.

Les positions des stations sont données dans le tableau ci-dessous :

Station n°		Coordonnées Sud	Est	Fond (mètres)
3		13°15'	48°39'	22
3A		13°15'	48°47'	4
4α		12°51,5'	48°34'	34
4β		12°59'	48°27'	30
4γ		12°54'	48°28'	44
4		12°56'	48°23'	50
4A		12°56'	48°16'	80
5		12°56'	48°10'	800
5A		12°56'	48°00'	830
6		12°56'	47°50'	1940
7	ancienne position	13°10'	47°57'	1570
7	nouvelle position	13°04'	47°55,5'	1920
8		13°24'	48°08,5'	40
9		13°39'	48°14.5'	30
9A		13°42'	48°18'	4
9B		13°39,5'	48°10,5'	45
10		13°26,5'	48°17,5'	16
11		13°27,5'	48°07'	48
12		13°34'	47°44'	1400

B. Méthodes de récolte. — Trois types de filets ont été utilisés :

1° **Filets verticaux fermants, type « Discovery ».** Diamètre d'ouverture 0,70 m, longueur 2,20 m dont 1,50 m, pour la partie pêchante : cette dernière constituée de deux secteurs successifs de gaze à bluter, respectivement de 626 et 1115 mailles par cm².

Le filet était remonté à l'aide d'un treuil à main à la vitesse approximative de 50 cm/sec., de 100 m à 50 m d'immersion puis de 50 m à la surface aux stations situées au-dessus des grands fonds, ou du fond à la surface aux stations situées au-dessus du plateau continental. La fermeture du filet avait lieu sans interruption de la course de ce dernier : pour celà le messager était lâché à un instant calculé de telle sorte qu'il rencontre le filet à la profondeur désirée.

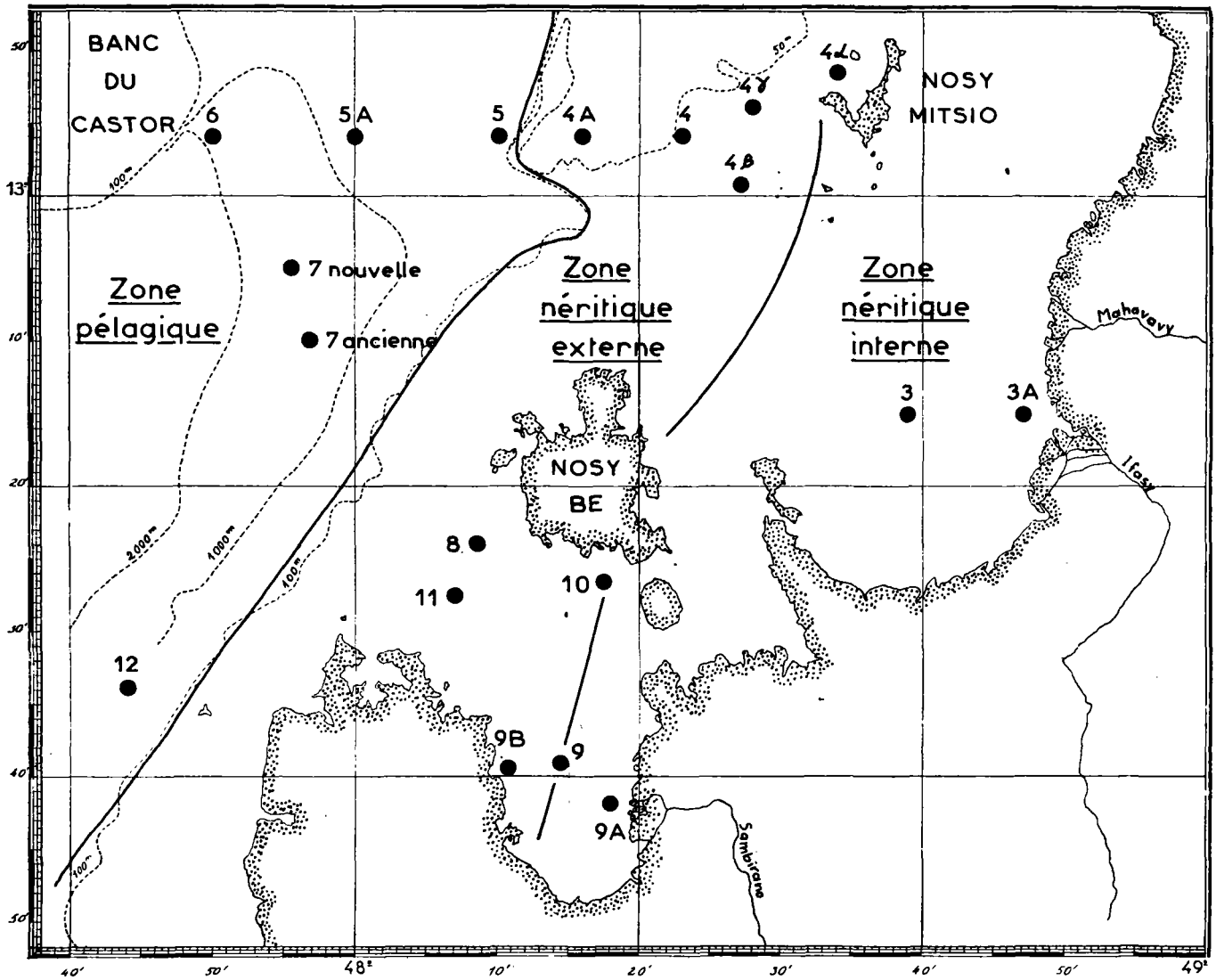


Fig. 1. — Carte des stations.

Ces filets verticaux n'ont été utilisés qu'au cours du premier cycle annuel (mars 1963-mars 1964) et pour les stations 3, 4, 5, 6, 7, 8, 9 et 9B.

2° **Filets horizontaux non fermants, type « Tregouboff »,** conformes à la description donnée dans TREGOUBOFF et ROSE 1957 : diamètre d'ouverture 1 m, longueur 4,50 m dont 4 m pour la partie pèchante ; cette dernière constituée de quatre secteurs successifs de gaze à bluter, respectivement de 81, 625, 1115 et 3500 mailles par cm².

Le filet était traîné horizontalement derrière le bateau, à la vitesse très régulière de 50 cm/sec., pendant 5 minutes comptées au compte-minutes de laboratoire, et maintenu à une immersion de 2 m ou de 10 m grâce à un orin de cette longueur le reliant à une bouée profilée.

La plus grande partie des récoltes effectuée autour de Nosy Bé l'a été au moyen de ce filet. Ce choix peut surprendre : étant constitué de quatre secteurs successifs de mailles différentes filtrant des volumes d'eau différents, ce modèle de filet est, pour autant que cela soit possible,

encore plus inadapté que les autres modèles à l'estimation même grossière du volume d'eau concerné par la récolte. Il a par contre la grande qualité de recueillir un très large éventail de *tailles* d'organismes (pratiquement : depuis les plus petites formes larvaires grâce à son dernier secteur, jusqu'à des formes de grande taille et rapides grâce au faible refoulement d'ouverture que permet son premier secteur à grandes mailles). On ne peut évidemment rapporter les différents, comptages à un volume d'eau déterminé puisque ce volume varie (et d'une façon que nous ignorons) pour les différentes tailles d'organisme. Cependant si l'on admet que le filet « travaille » de la même façon d'une fois à l'autre — et ceci est sans doute ni plus ni moins vrai que pour les autres types de filets —, mis à part les cas de colmatation par des organismes gélatineux, les comptages d'organismes pris dans des limites de taille convenables doivent se trouver comparables d'une récolte à l'autre ; les variations d'effectifs obtenus dans ces conditions doivent alors refléter les fluctuations naturelles.

L'on peut ainsi compter séparément, au sein d'une même espèce, divers stades de développement. L'on obtient pour chacun d'eux des maxima et des minima d'effectif dont on peut observer la succession dans le temps, ce qui fournit des indications sur le cycle biologique de cette espèce. Nous donnons ci-dessous à titre d'illustration de cette méthode les résultats des comptages d'une espèce abondante à la station 5 : *Limacina inflata* (d'ORBIGNY) (Ptéropodes Thécosomes), pour laquelle trois stades ont été arbitrairement distingués :

— stade très jeune (moins d'un tour et demi de spire) ;

— stade jeune ;

— stade adulte ou subadulte (dent sagittale de la coquille bien constituée).

Il ne peut être question de comparer entre eux, à aucun instant, les effectifs des divers stades. On peut toutefois constater qu'en avril et mai l'effectif des « jeunes » présente un maximum puis diminue au profit des « adultes ». En août-septembre a sans doute lieu une ponte, d'où une brusque augmentation des « très jeunes » et la disparition d'une partie des « adultes », qui meurent peut-être. Un nouveau maximum de « jeunes » apparaît en janvier, provenant vraisemblablement de la croissance des « très jeunes » apparus en août.

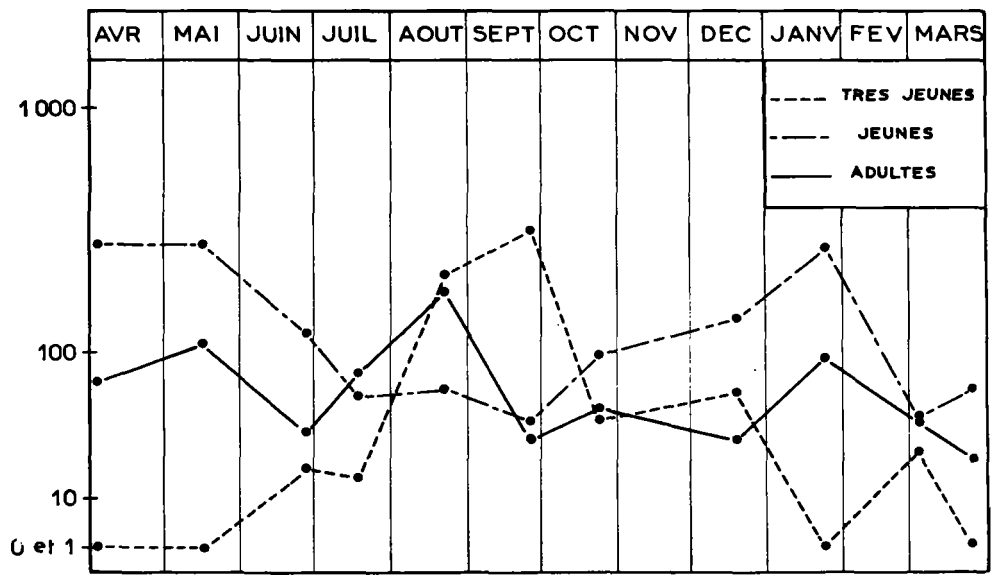


Fig. 2. — *Limacina inflata*, station 5, moyenne entre les effectifs à 2 m et à 10 m. (Pour l'échelle des ordonnées, voir § I-D).

3° **Filets horizontaux non fermants dits « à larves de Poissons ».** Mêmes dimensions que le filet « TREGOUBOFF », mais en nylon de 49 mailles par cm². Le filet était traîné horizontalement pendant 10 minutes à la vitesse régulière de 1,50 m/sec., et maintenu à 2 m ou à 10 m d'immersion.

Signalons enfin que chaque récolte de plancton était accompagnée d'observations hydrologiques (températures et salinités). Toutes les corrections thermométriques et mesures de salinité ont été effectuées par le Laboratoire d'Océanographie Physique du Centre de Nosy Bé, sous la responsabilité de R. GÉRARD.

C. ESTIMATIONS D'ABONDANCE DES GROUPES ZOOLOGIQUES. — Certains groupes ou certaines espèces ont été comptés intégralement, soit dans la récolte complète, soit dans une de ses parties aliquotes. Les autres groupes ont été l'objet de comptages approximatifs, les résultats étant exprimés suivant la cotation ci-après :

Cotes d'abondance		effectifs
0	(absents)	0
1	(très rares)	1 à 3
2	(rares)	4 à 18
3	(assez rares)	19 à 80
4	(assez nombreux)	80 à 350
5	(nombreux)	350 à 1500
6	(très nombreux)	1500 à 6500
7	(constituant fondamental de la récolte)	plus de 6500

La suite (1, 4, 19, 350, 1500, 6500) est très voisine d'une progression exponentielle de raison 4.3 — choisie empiriquement.

D. REPRÉSENTATION GRAPHIQUE DES RÉSULTATS. — Les résultats de comptages sont habituellement portés sur les graphiques en échelle logarithmique, qui atténue l'amplitude des fluctuations. Mais il arrive que cette échelle atténue les fluctuations au point de masquer les phénomènes : les maxima peuvent être exagérément réduits, par ailleurs une importance trop grande est accordée aux variations dans le domaine des petits nombres. Or ces derniers sont sujets à des fluctuations aléatoires que l'on doit éviter de confondre avec des variations significatives (la transformation logarithmique aboutit par exemple à donner autant d'importance à une variation du nombre d'individus de 1 à 10 et à une variation de 100 à 1000, ce qui semble difficilement admissible).

Afin d'atténuer ces inconvénients, tout en conservant les avantages de la transformation logarithmique, nous avons adopté l'échelle $(\log)^2$. Les effectifs faibles sont alors rapprochés entre eux, les maxima sont plus distincts, et la partie médiane de la courbe reste inchangée dans son allure (1). Les figures 3 et 4 illustrent la comparaison entre les échelles log et $(\log)^2$.

Les cotes d'abondance (I-C) ont été portées sur les graphiques en échelle $(\text{cote})^2$, très voisine de l'échelle $(\log)^2$ sans coïncider exactement avec celle-ci. Les figures 5 et 6, obtenues l'une à partir des comptages intégraux des Ptéropodes, l'autre des comptages des Chaetognathes d'une partie aliquote de chaque récolte, montrent une coïncidence assez satisfaisante entre les courbes obtenues par comptages et au moyen de la cotation d'abondance. L'on peut ainsi espérer que, pour les groupes n'ayant pas fait l'objet de comptages exacts, la méthode permette d'obtenir l'allure approximative des variations saisonnières.

(1) La transformation $(\log)^2$ n'a pas de justification mathématique, et ne saurait donc entrer dans un modèle mathématique de population. Il s'agit seulement d'une technique de dessin.

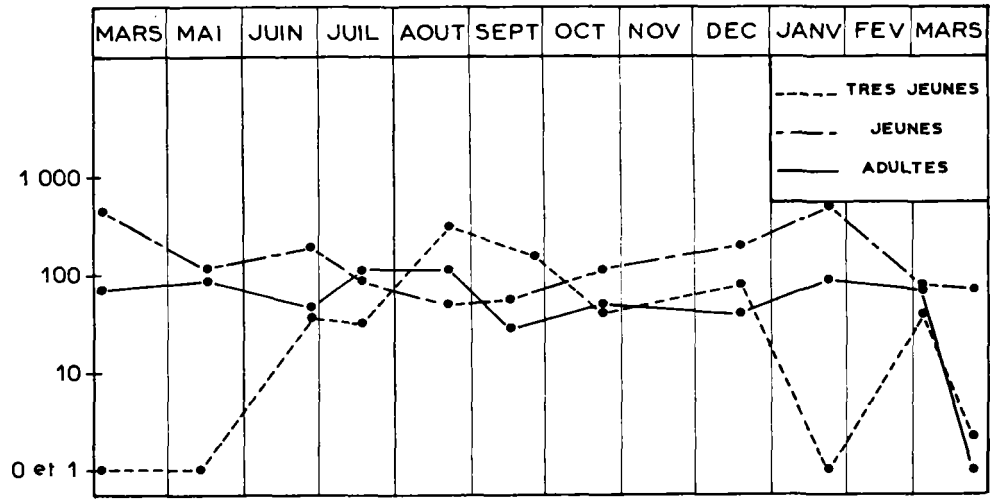


Fig. 3. — *Limacina inflata*, station 5, 2 m, échelle logarithmique.

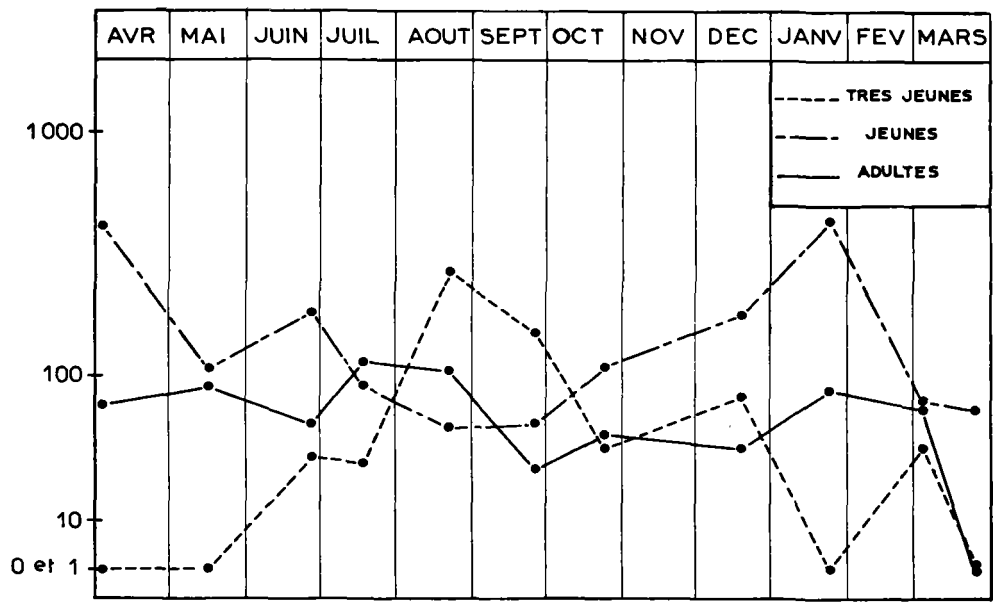


Fig. 4. — *Limacina inflata*, station 5, 2 m, échelle (log).[2]

II. ZOOPLANCTON DE SURFACE DES STATIONS 5 ET 10

A. Le milieu hydrologique. — Les résultats hydrologiques mensuels aux différentes stations pour la période mars 1963-mars 1964 ont été publiés précédemment (Angot M. & Gérard R. 1963, 1965 a et b) et ont fait l'objet d'un texte de synthèse (Angot M. 1965). Je reprendrai ici les résultats obtenus aux stations 5 et 10 à 2 et 10 m d'immersion ; ces résultats sont portés sur les diagrammes T-S des figures 7 à 10, qui permettent une vision synthétique des conditions saisonnières. Le diagramme de la station 10, occupée 27 fois entre mars 1963 et mars 1964, présente ainsi quatre régions distinctes :

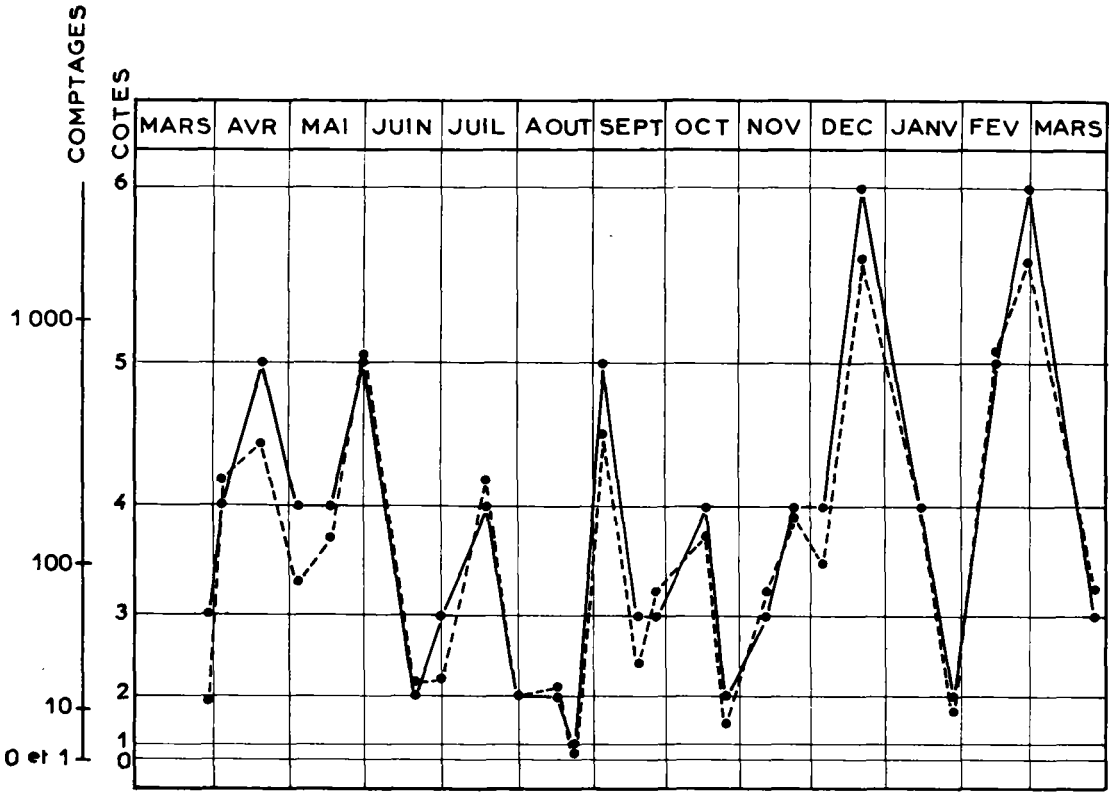


Fig. 5. — Ptéropodes, station 10, 2 m.

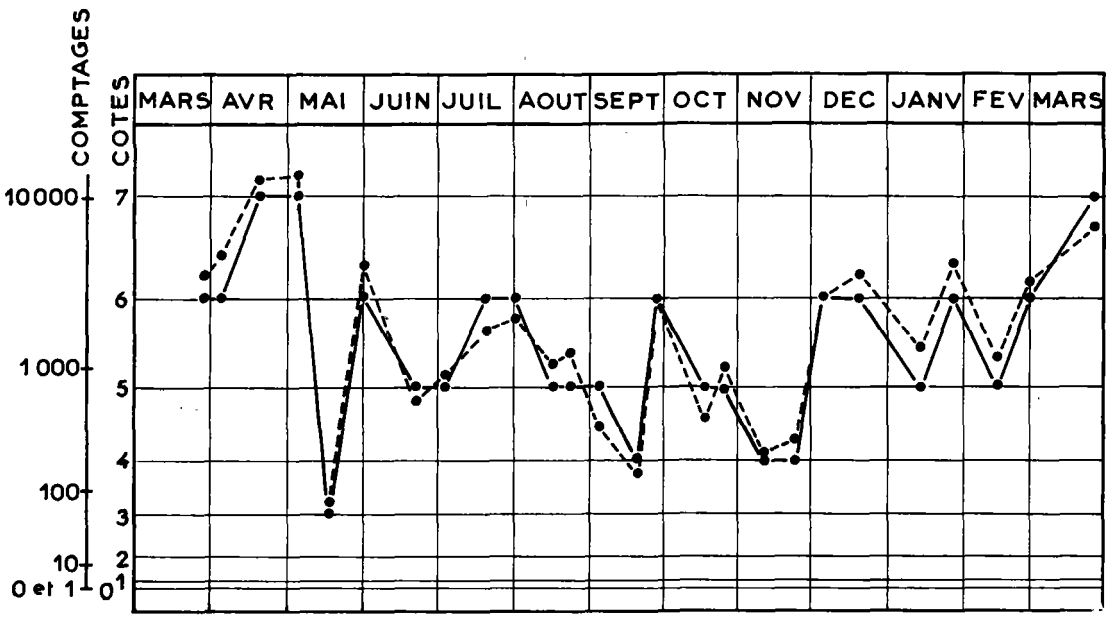


Fig. 6. — Chaetognathes, station 10, 2 m.

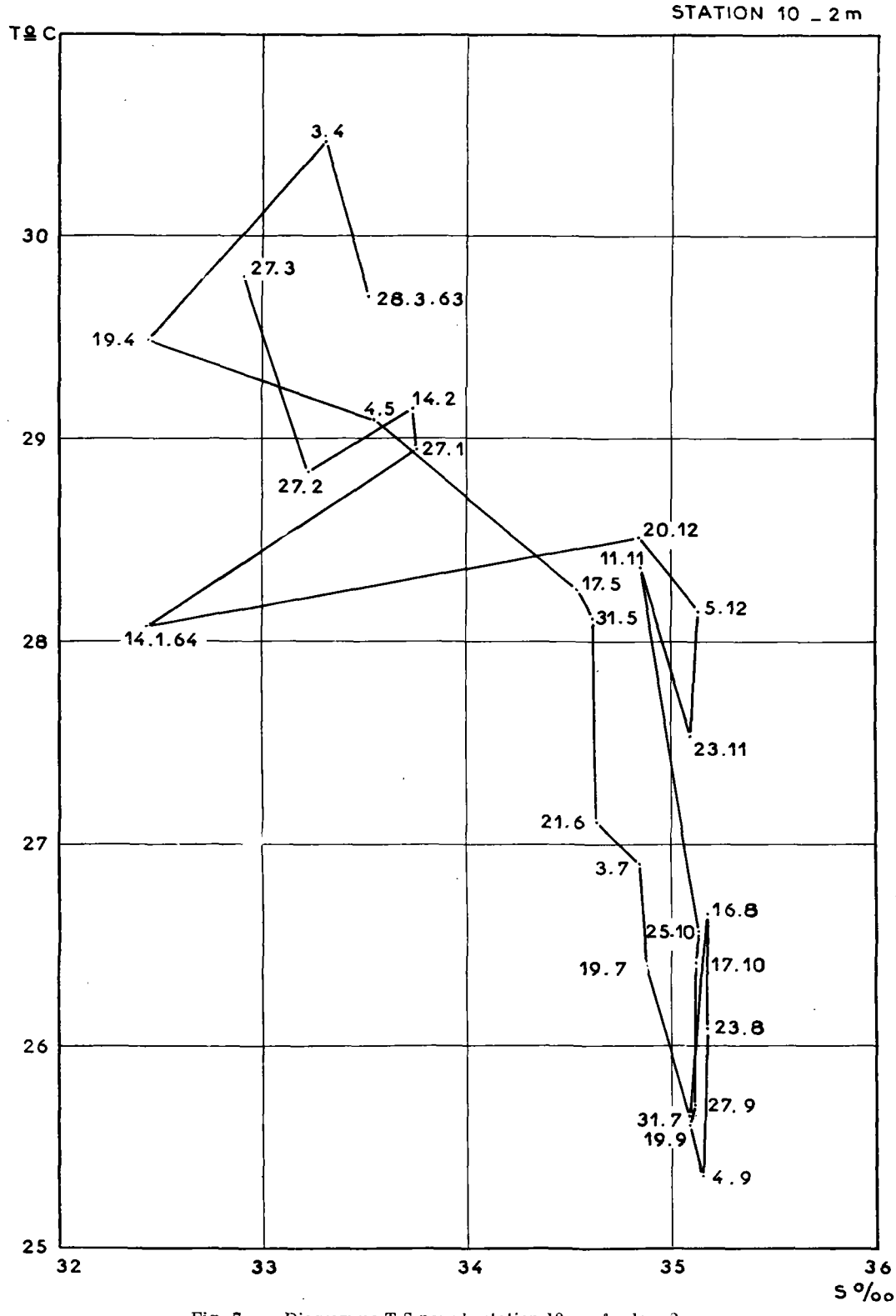


Fig. 7. — Diagramme T-S pour la station 10, profondeur 2 m.

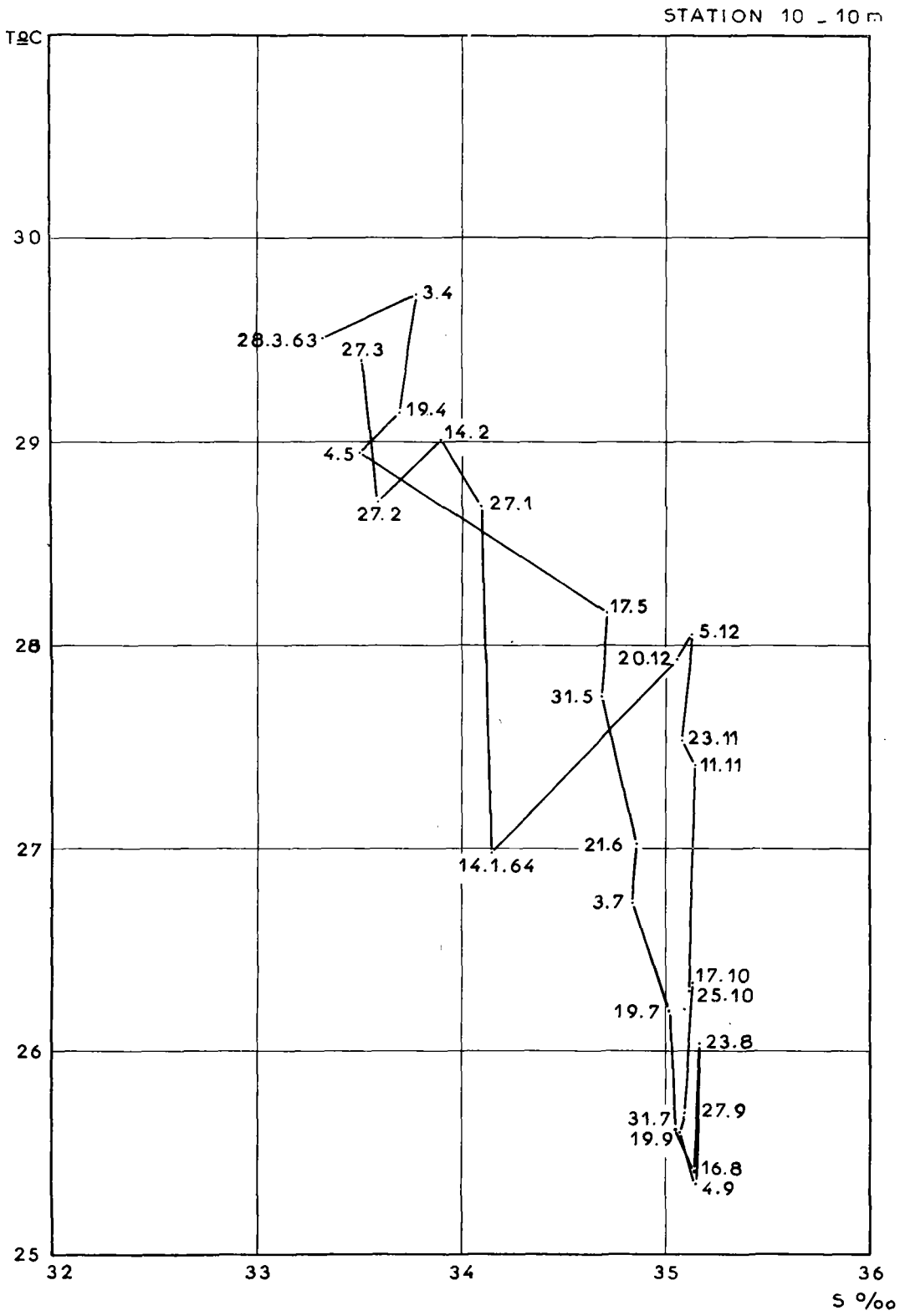


Fig. 8. — Diagramme T-S pour la station 10, profondeur 10 m.

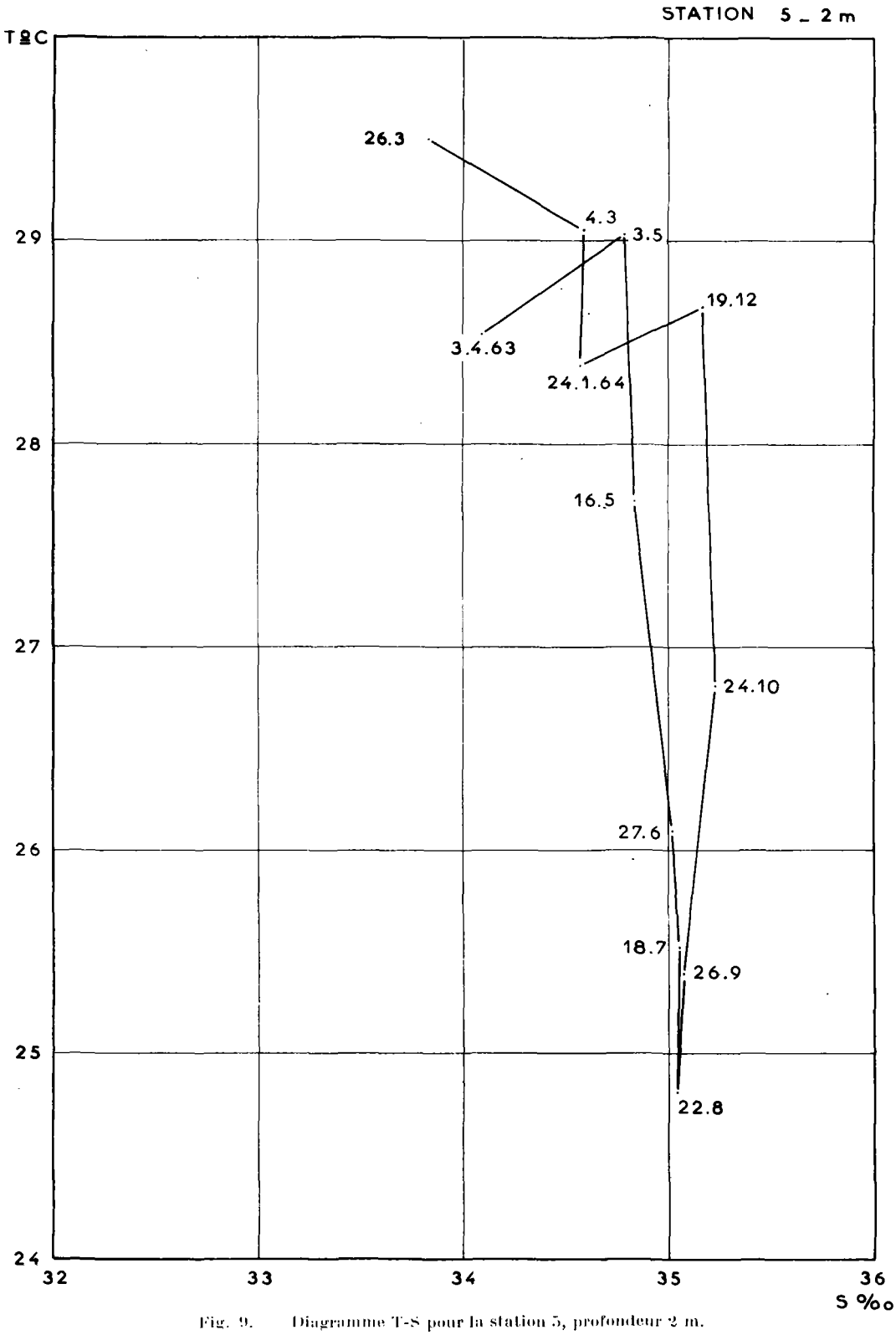


Fig. 9. Diagramme T-S pour la station 5, profondeur 2 m.

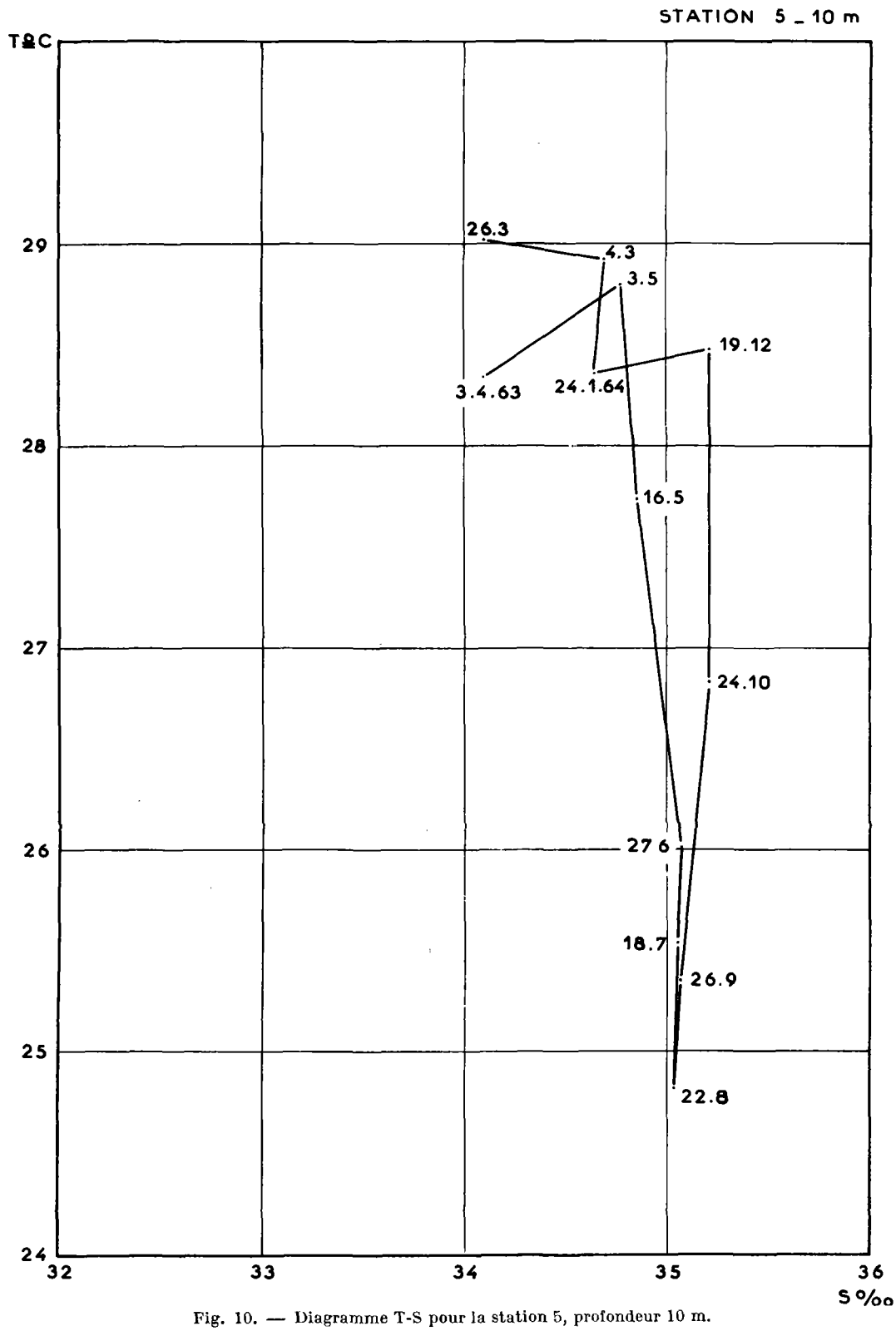


Fig. 10. — Diagramme T-S pour la station 5, profondeur 10 m.

1 — **De fin décembre à début mai :** températures élevées (28 à 30,5°C) salinités faibles (32,4 à 34,5 °/₀₀), et fondamentalement forte *instabilité* des conditions hydrologiques. C'est l'**été austral.**

2 — **De mai à juillet :** le diagramme rejoint par une courbe régulière la région de basses températures et de fortes salinités qui caractérise la saison suivante. On peut nommer cette période **automne austral.**

3 — **Août et septembre :** période de *stabilité hydrologique*, la température restant localisée entre 25.3 et 26,6° C et la salinité entre 35,1 et 35,2 °₀₀/. C'est le plein **hiver austral.**

4 — **D'octobre à décembre :** période que l'on peut appeler **printemps austral**, au cours de laquelle la température remonte jusque vers 28 ou 28,5°C sans diminution de la salinité. A l'issue de cette période on se retrouve dans la saison chaude et hydrologiquement instable.

L'instabilité caractéristique de la saison d'été est moins marquée à 10 m de profondeur qu'à 2 m à la station 10 — les apports d'eau douce propres à cette époque de l'année affectant principalement les couches superficielles — , et moins encore aux profondeurs 2 et 10 m de la station 5, éloignée du rivage.

Mise à part cette période estivale, les diagrammes T-S des deux stations sont presque superposables, le diagramme de la station 10 étant cependant situé, dans l'ensemble, plus à gauche (salinités légèrement plus faibles) que celui de la station 5. Au plus fort de l'hiver austral les températures sont légèrement plus basses à la station 5 qu'à la 10 (24,8 au lieu de 25,3°C) et les salinités très légèrement plus faibles (35,05 au lieu de 35,15 °/₀₀).

B. Variations d'abondance de quelques groupes zoologiques. — Un certain nombre de groupes zoologiques présentent dans leur ensemble, soit à la station 5 soit à la station 10, des fluctuations significatives d'abondance au cours de l'année étudiée. Nous nous bornerons ici à l'examen de ces quelques groupes, la totalité des résultats étant par ailleurs fournie en annexe.

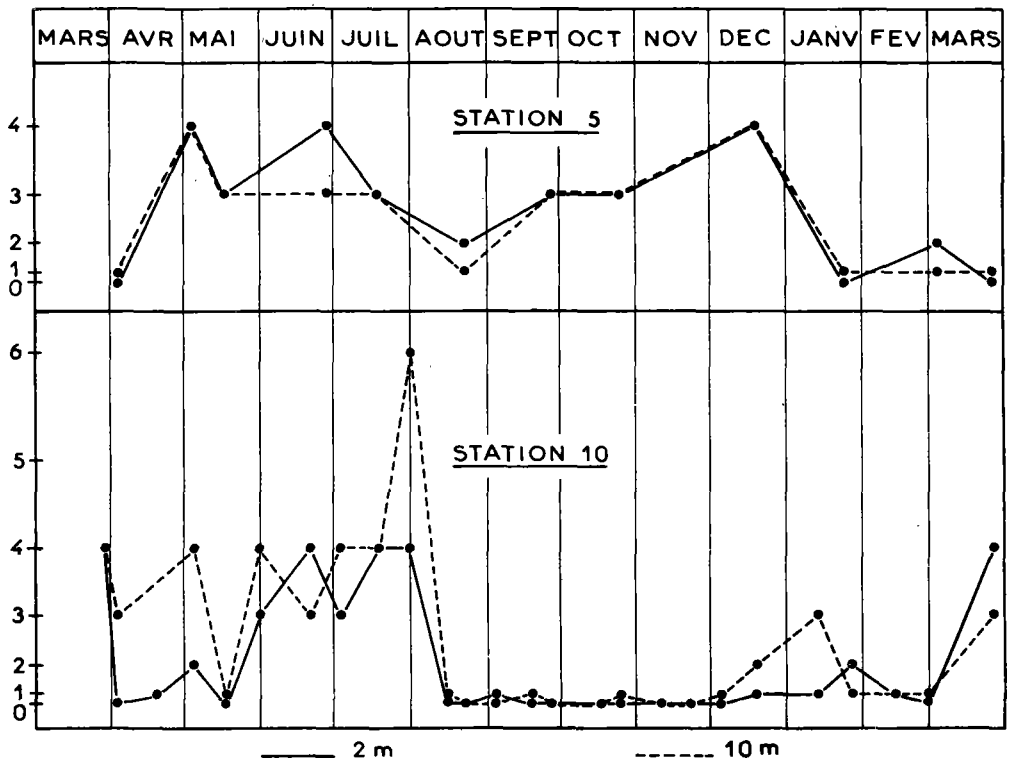


Fig. 11. Abondance des Dolioles aux stations 5 et 10.

DOLIOLES (Fig. 11). — On contate deux périodes tranchées : l'une s'étendant de janvier à mars pour la station 5, d'août à février pour la station 10, pendant laquelle les Dolioles sont absents ou rares. L'autre au cours de laquelle ce groupe est « assez rare » (cote 3) à « assez nombreux » (cote 4), et s'étendant d'avril à janvier pour la station 5, de mars à juillet pour la station 10. Les époques d'abondance relative ne coïncident donc pas entre les deux stations, et la période de quasi-disparition du groupe est deux fois plus étendue à la station 10 qu'à la station 5.

APPENDICULAIRES (Fig. 12). — Deux périodes se remarquent pour la station 10 : de janvier à juin les populations semblent être assez stables, cotées « nombreuses » (5) ou « très nombreuses » (6). De juillet à décembre a lieu une période d'instabilité (ou d'hétérogénéité) du peuplement en Appendiculaires, la cote d'abondance de ce groupe variant entre 2 et 7 d'une récolte à l'autre.

Cette distinction ne s'observe pas à la station 5.

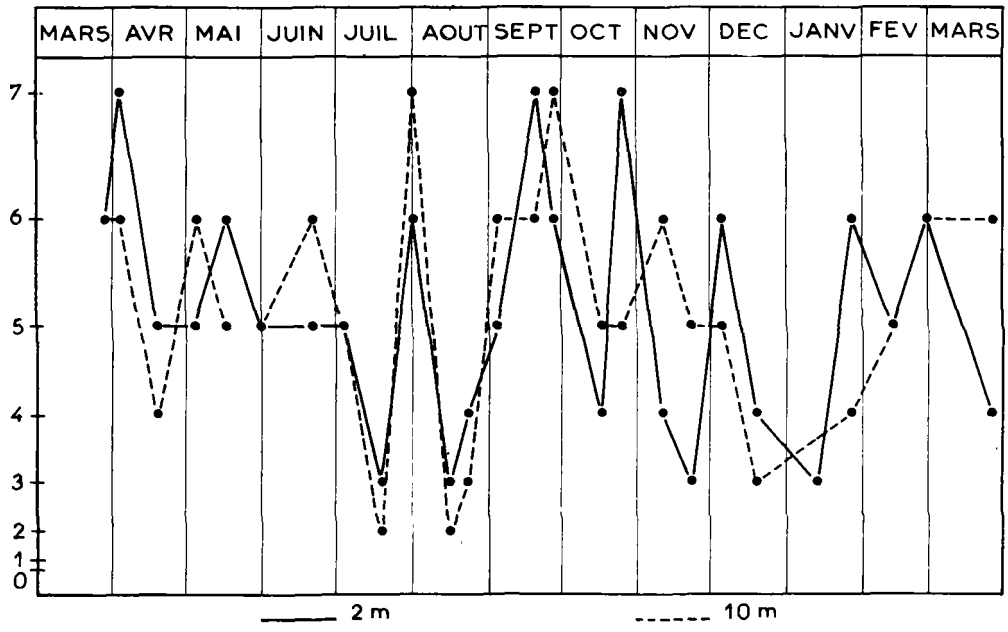


Fig. 12. Abondance des Appendiculaires à la station 10.

LARVES DE DÉCAPODES BRACHYOURES (Fig. 13). — On remarque une augmentation d'abondance dans la seconde partie du cycle annuel, nette surtout à la station 5, et localisée de décembre à février pour cette dernière (l'état de la mer n'a pas permis de récolter du plancton en novembre), d'octobre à février pour la station 10.

LARVES DE DÉCAPODES ANOMOURES (Fig. 14), *DÉCAPODES NATANTIA* (Fig. 15) *ET STOMATOPODES* (Fig. 16). — Mêmes constatations que pour les larves de Brachyoures aux deux stations pour les Anomoures, à la station 5 seulement pour les Natantia et Stomatopodes.

CLADOCÈRES (Fig. 17). — Absents ou rares toute l'année à la station 5, ainsi que de mai à octobre (saison sèche) à la station 10. Les populations s'installent à partir de novembre et se maintiennent, probablement groupées en essaims denses (cote d'abondance variant de 1 à 7 d'une récolte à l'autre) jusqu'en mars inclusivement. Elles diminuent brusquement en avril, mais ne sont complètement absentes qu'en aout et septembre.

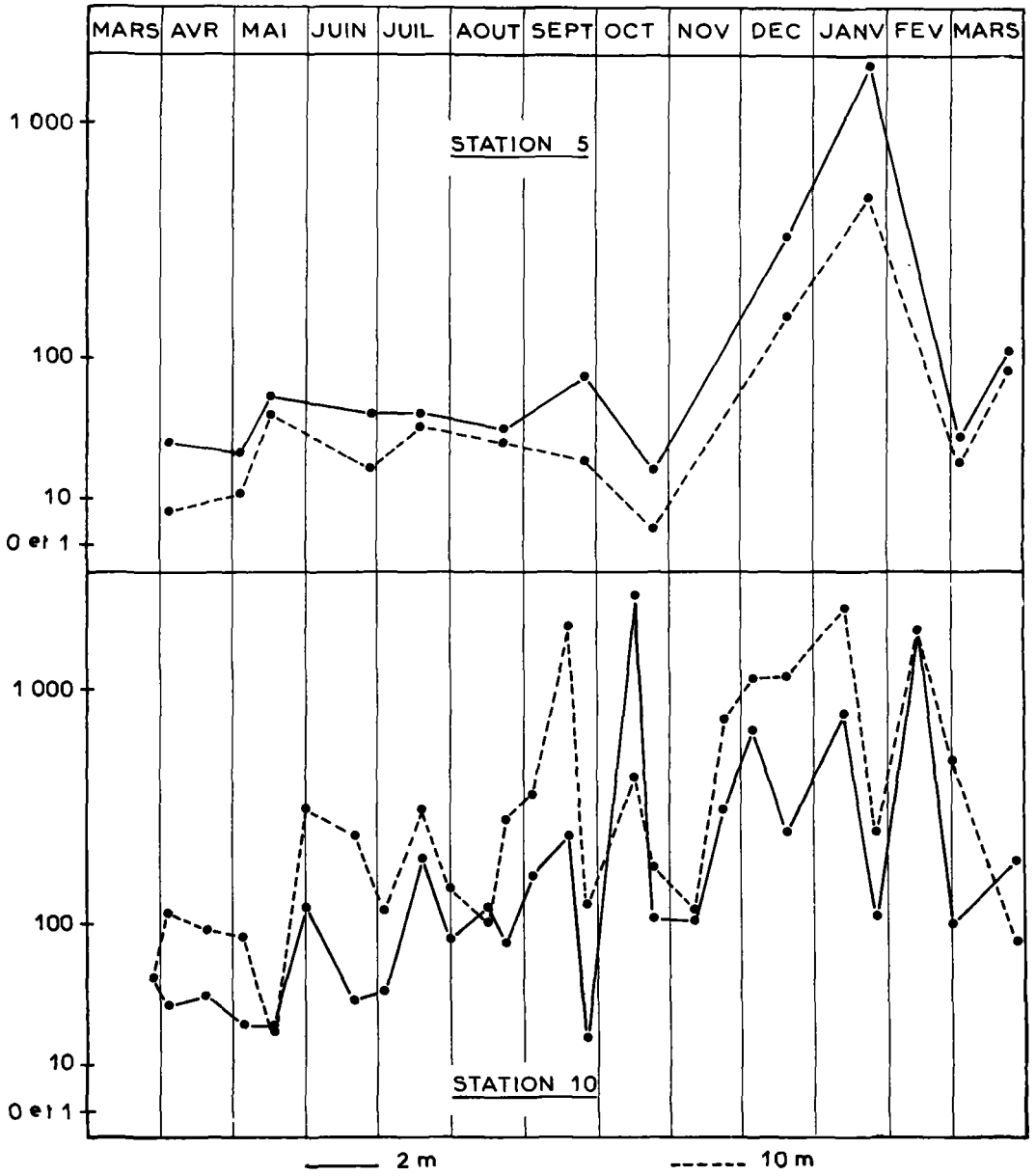


Fig. 13. — Comptages approximatifs des larves de Décapodes Brachyoures aux stations 5 et 10.

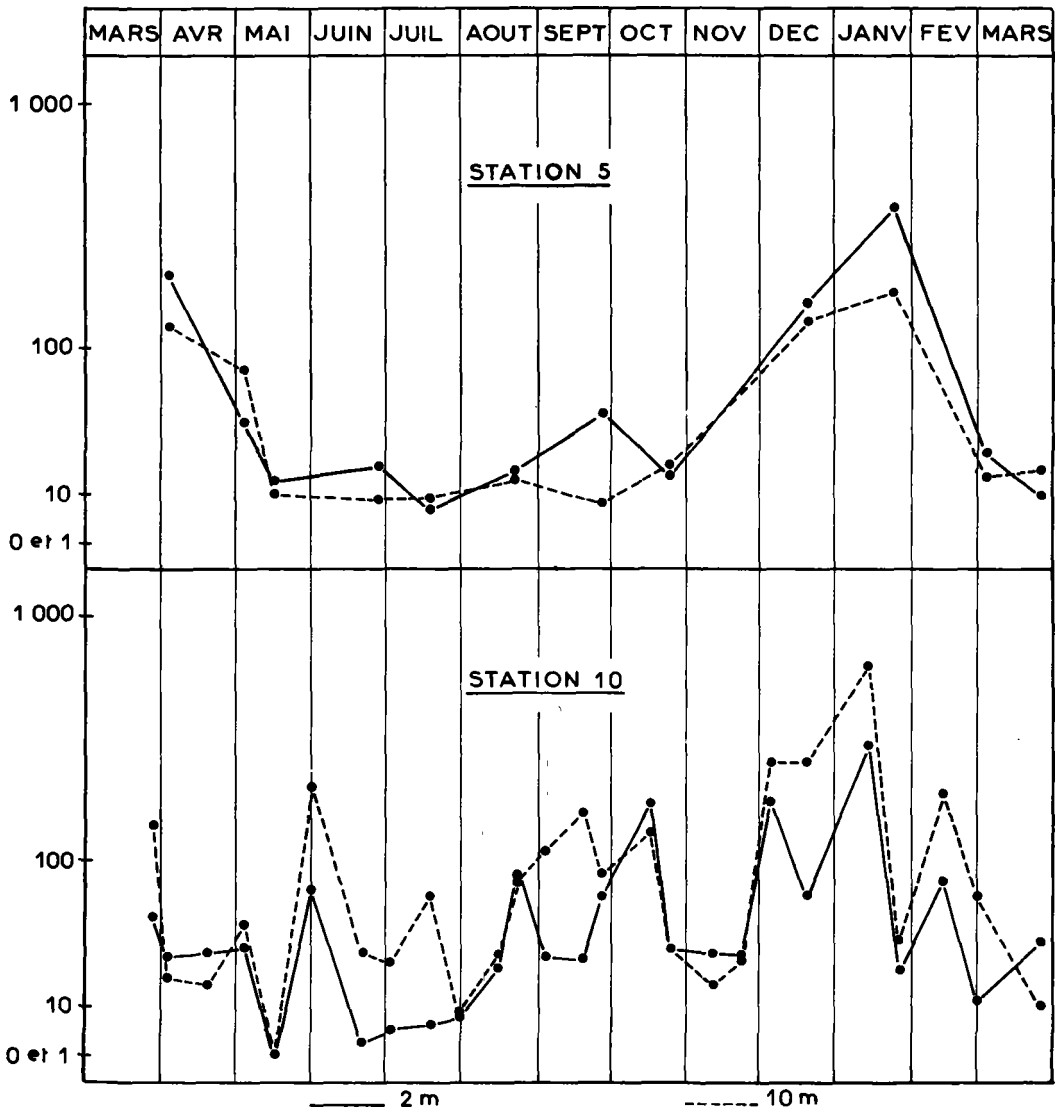


Fig. 14. — Comptages approximatifs des larves de Décapodes Anomoures aux stations 5 et 10.

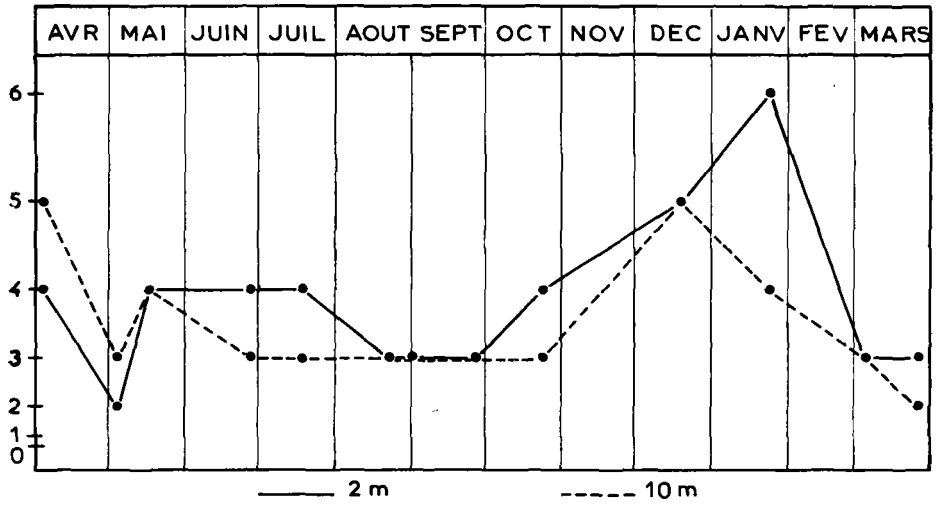


Fig. 15. — Abondance des larves de Décapodes Natantia à la station 5.

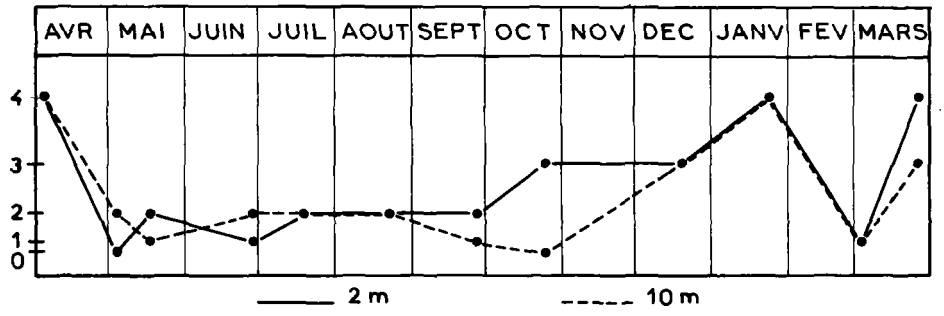


Fig. 16. — Abondance des larves de Stomatopodes à la station 5.

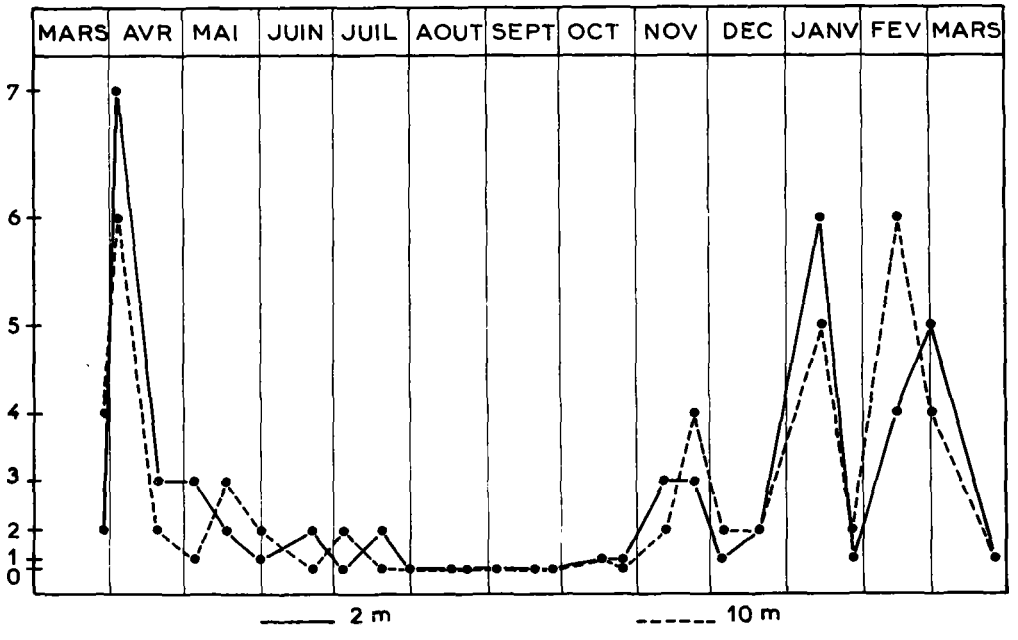


Fig. 17. — Abondance des Cladocères à la station 10.

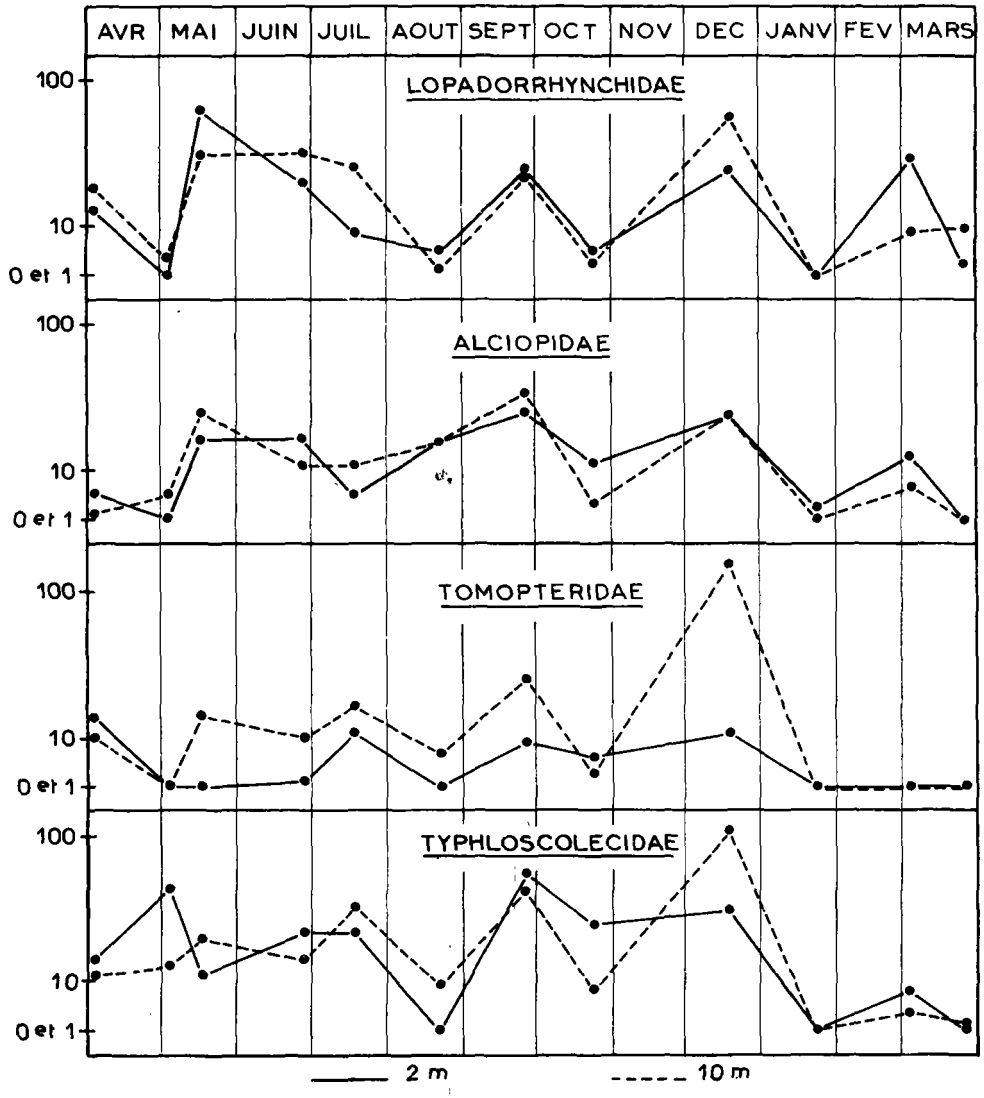


Fig. 18. — Comptages des quatre principales familles d'Annélides holoplanctoniques à la station 5.

POLYCHÈTES (Fig. 18). — Les comptages ont été effectués séparément pour les quatre familles principales de Polychètes pélagiques : *Lopadorrhynchidae*, *Alciopidae*, *Tomopteridae*, *Typhloscolecidae*. Les moyennes par récolte pour ces quatre familles aux stations 5 et 10 sont portées dans le tableau suivant.

		Lopadorrh.		*Alcoipidae*		*Tomopteridae*		*Typhloscolec.*	
Station 5	2 m...	22,3		12,8		4,7		17,5	
	10 m...		20,3		13,3		19,4		20,3
Station 10	2 m...	0,1		6,5		7,8		5,5	
	10 m...		0,3		7,4		8,9		7,2

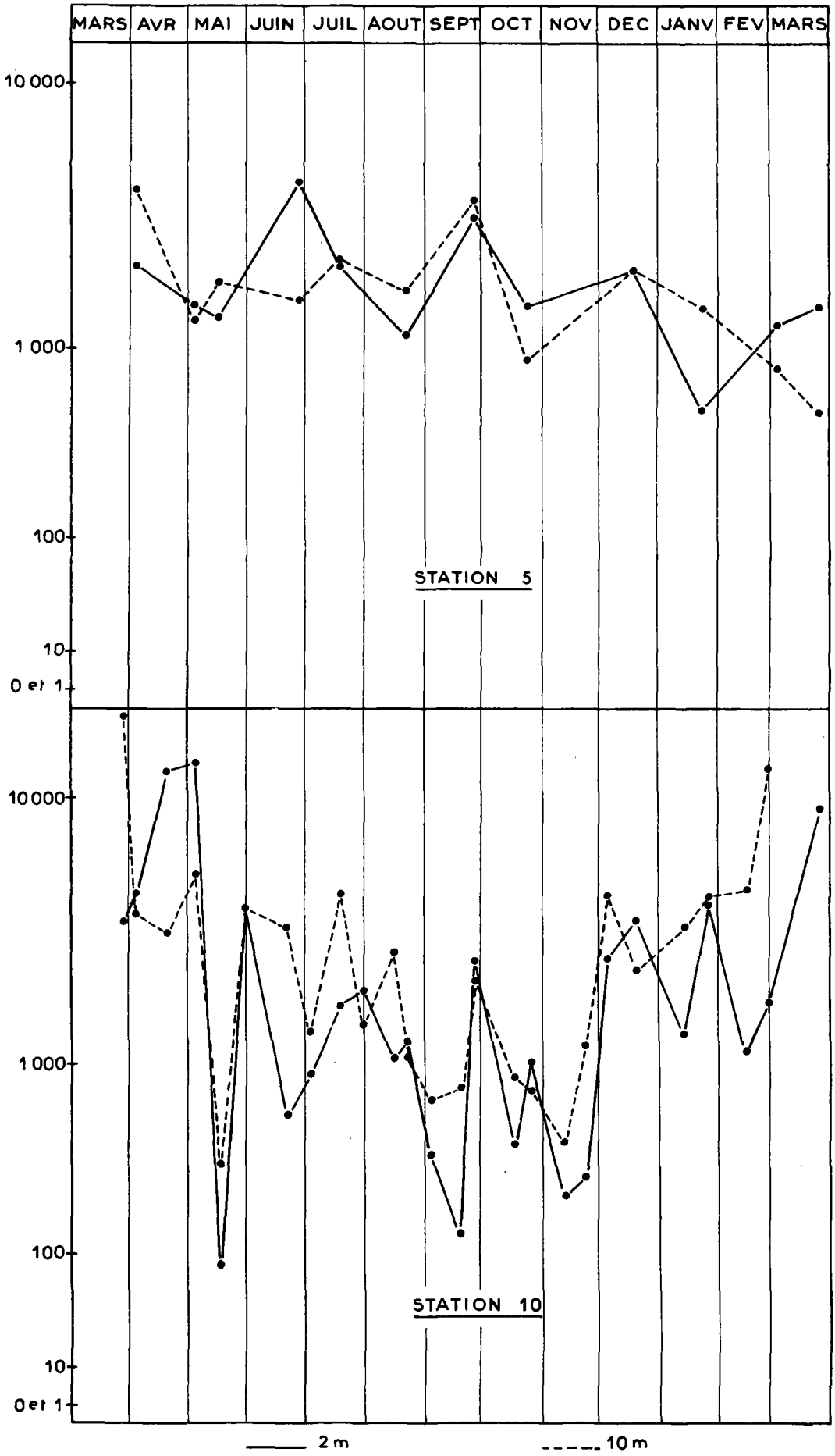


Fig. 19. Comptages des Chaetognathes aux stations 5 et 10.

On constate que les quatre familles sont plus abondantes à la station du large qu'à la station 10 voisine de la côte, et régulièrement plus abondantes à 10 m qu'à 2 m à l'exception des Lopadorrhynchidae de la station 5 (cette dernière famille est toujours très rare ou absente à la station 10). Rappelons cependant que la station 5 a été occupée de nuit (sauf le 3 mai) alors que la 10 ne l'a été que pendant la journée, ce qui limite la valeur de la comparaison entre les deux stations.

Pris dans leur ensemble les Polychètes planctoniques de la station 10 montrent une augmentation régulière d'abondance entre octobre 1963 et mars 1964, date à laquelle les effectifs à 2 m et à 10 m atteignent des valeurs bien supérieures à celles atteintes en mars 1963. A la station 5 on observe des fluctuations d'assez grande amplitude mais sans qu'il soit possible de déceler des périodes bien tranchées. Un fait intéressant se détache cependant des graphiques ci-dessous qui figurent les variations d'effectif par récolte des quatre familles prises séparément. Les quatre familles évoluent parallèlement, ce qui tendrait à faire penser que les facteurs écologiques et internes responsables des fluctuations d'abondance des populations agissent de la même façon sur les différentes familles d'Annélides. Ce problème sera repris ultérieurement à la lumière des résultats fournis par les autres stations.

CHAETOGNATHES (Fig. 19). — Les variations d'abondance à la station 10 présentent une allure très nette avec — les récoltes du 16 mai mises à part — évolution graduelle entre un *maximum en février-avril* et un *minimum en septembre-novembre*. Cette évolution ne se retrouve pas à la station 5, où la population de Chaetognathes semble plus stable. En moyenne pour l'année on trouve 1950 individus par récolte à la station 5 et 2600 à la station 10.

Trois espèces ont été comptées séparément :

Pterosagitta draco KROHN. L'abondance de cette espèce dans le secteur de Nosy Bé avait été remarquée par Mmes FURNESTIN et RADIGUET (1964). Sa présence dans les eaux néritiques est généralement considérée comme dépendant des eaux de pente, qui sont probablement importantes au voisinage de la station 5 ; la migration nocturne doit aussi expliquer en partie l'abondance régulière de cette espèce à la station 5 pendant une partie de l'année (mai à décembre) — pendant laquelle les effectifs varient entre 30 et 1120 par récolte (soit en moyenne 183 individus par

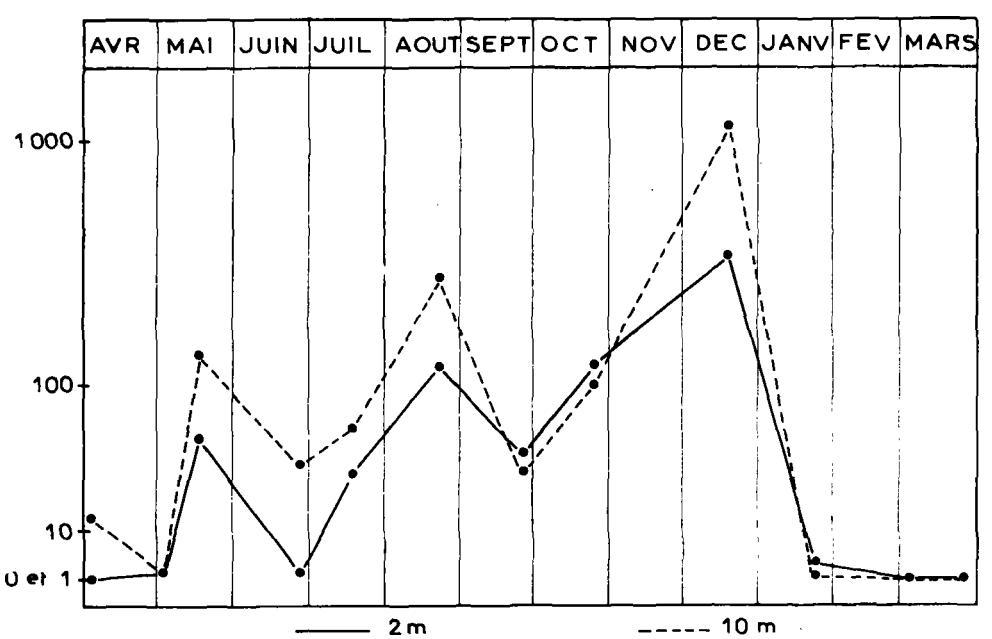


Fig. 20. — Comptages de *Pterosagitta draco* à la station 5.

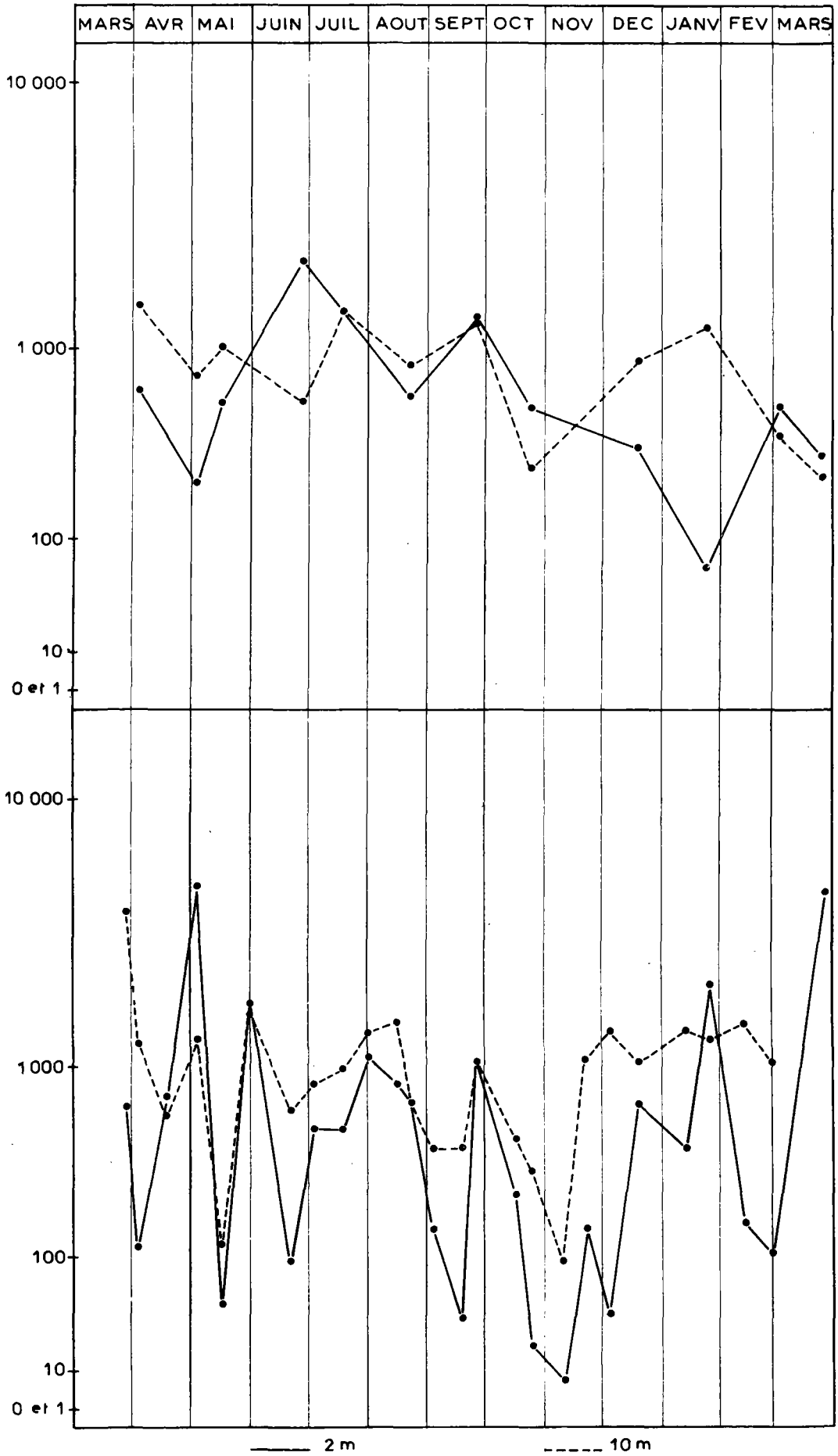


Fig. 21. — Comptages de *Sagitta enflata* aux stations 5 et 10.

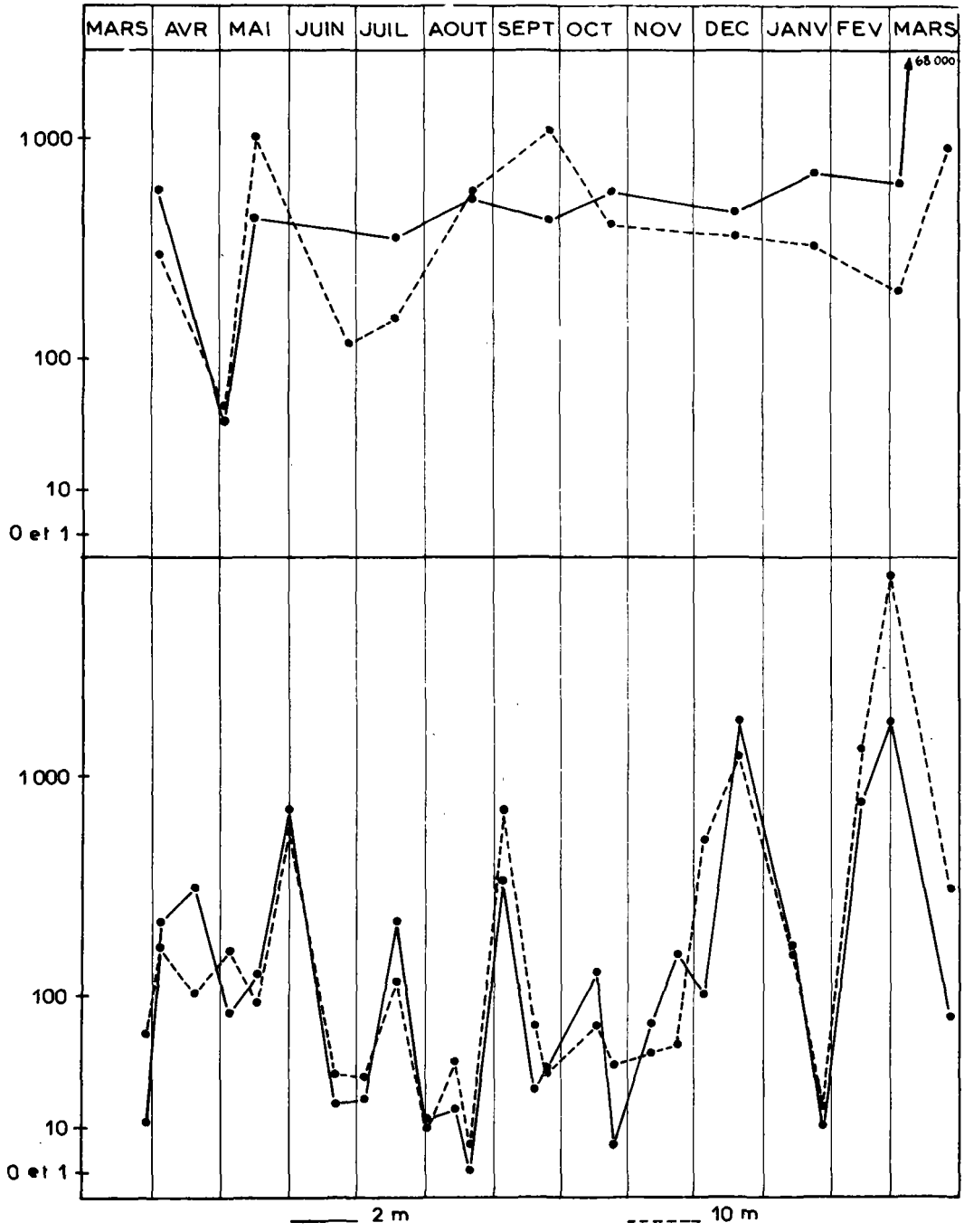


Fig. 22. — Comptages des Ptéropodes aux stations 5 et 10.

récolte). Par contre l'espèce manque presque complètement entre janvier et début mai, c'est-à-dire exactement pendant l'été hydrologique tel qu'il a été défini plus haut (II-A). Sa présence est alors limitée à un intervalle de salinité relativement étroit (34,84 à 35,21 ‰), l'intervalle de température toléré étant au contraire assez large (24,82 à 28,69°C). L'effectif le plus élevé (1120 individus pour la récolte du 19 décembre à 10 m) a été obtenu pour une température de 28,48°C et une salinité de 35,21 ‰.

A la station 10 *Pterosagitta draco* est sporadique, sa présence ne résultant sans doute que d'un transport d'eau pélagique au-dessus du plateau continental. 168 individus y ont été récoltés au total, dans 21 récoltes sur 52 effectuées ; 165 de ces individus ont été capturés pendant l'époque où l'espèce est abondante au large, et parmi ces derniers 131 au cours du mois de septembre (6 récoltes).

Sagitta hexaptera d'Orbigny. C'est une espèce d'eau profonde. Deux exemplaires seulement ont été récoltés à la station 10. L'espèce est par contre assez régulière à la station 5, où elle apparaît sans doute en surface à la faveur de la migration nocturne : elle y est présente dans 20 récoltes sur 24 effectuées, à raison de 3,4 individus en moyenne par récolte.

Sagitta enflata Grassi. Espèce semi-néritique très abondante dans tout le secteur prospecté : 830 individus en moyenne par récolte à la station 5 (où elle représente 43 % de la totalité des Chaetognathes), et 960 par récolte à la station 10 (37 %). A cette dernière station l'abondance de cette espèce varie au cours de l'année comme pour l'ensemble des Chaetognathes, bien qu'un peu moins régulièrement. A la station 5 on observe seulement une diminution régulière d'effectif entre mars 1963 et mars 1964 (Fig. 21).

PTÉROPODES (Fig. 22). — Ce groupe se trouve abondant dans la plupart des récoltes. L'effectif par récolte est, à la station 10, extrêmement variable ; l'on peut toutefois déceler une période de faible abondance moyenne entre juin et novembre, et de décembre à mars la présence d'essaims très denses mais sporadiques. La station 5 se caractérise par une constance remarquable du nombre de Ptéropodes à 2 m : généralement de 400 à 650 individus par récolte (il convient de mettre à part les récoltes du 3 mai 1963, effectuées de jour, et du 26 mars 1964, qui contenait environ 68 000 *Creseis acicua* juvéniles) ; à 10 m de profondeur l'effectif en Ptéropodes est nettement plus variable, sans qu'il soit possible de distinguer des périodes dans l'année.

HÉTÉROPODES (Fig. 23). — Le nombre d'Hétéropodes varie, à la station 10, de 0 à 90 par récolte sans tendance saisonnière nette. A la station 5 on note un minimum entre mai et juillet (moins de 75 par récolte) et un maximum en septembre et octobre (150 à 600 par récolte avec majorité de juvéniles) — rappelons qu'il n'a pas été récolté de plancton à la station 5 en novembre.

CTÉNAIRES (Fig. 24). — Absents ou rares à la station 5, ils sont plus abondants quoique sporadiques à la 10, montrant un maximum en mars-avril et un minimum en septembre-octobre. Il s'agit essentiellement de Cydippoides, les autres formes étant toujours très rares.

SIPHONOPHORES (Fig. 25). — Il s'agit presque exclusivement de Calycophores. La station 10 présente deux périodes tranchées : de novembre à avril les populations de Siphonophores sont abondantes et stables (cote d'abondance variant entre 0 et 7) ; de mai à novembre on constate une abondance moyenne plus faible et surtout une instabilité (ou une hétérogénéité) des populations faisant varier la cote d'abondance entre 0 et 6 d'une récolte à la suivante.

Résumons ces données en les situant par rapport au schéma saisonnier déduit plus haut de l'hydrologie des deux stations.

L'**été austral** (fin décembre-début mai) se caractérise par l'abondance des larves de Crustacés Décapodes et Stomatopodes (au moins pendant la première partie de cette période) pour les deux stations ; par l'absence de Dolioles jusqu'au mois d'avril à la station 5, jusqu'au mois de

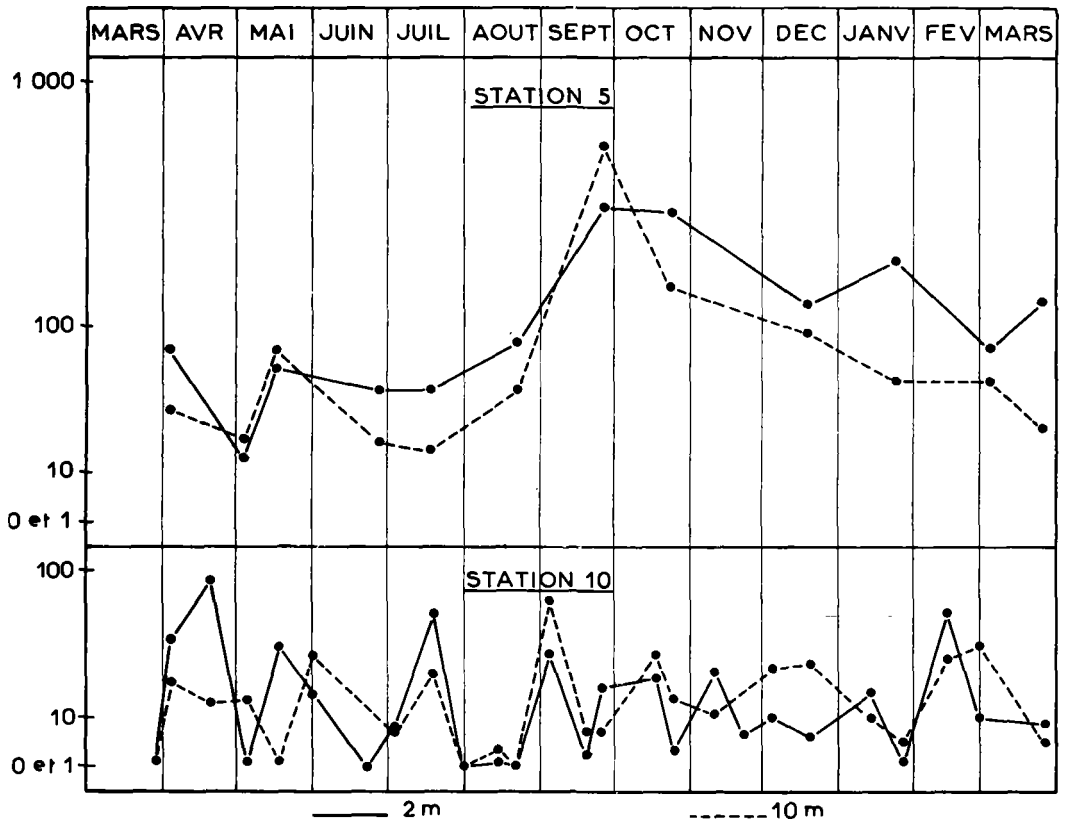


Fig. 23. — Comptages des Hétéropodes aux stations 5 et 10.

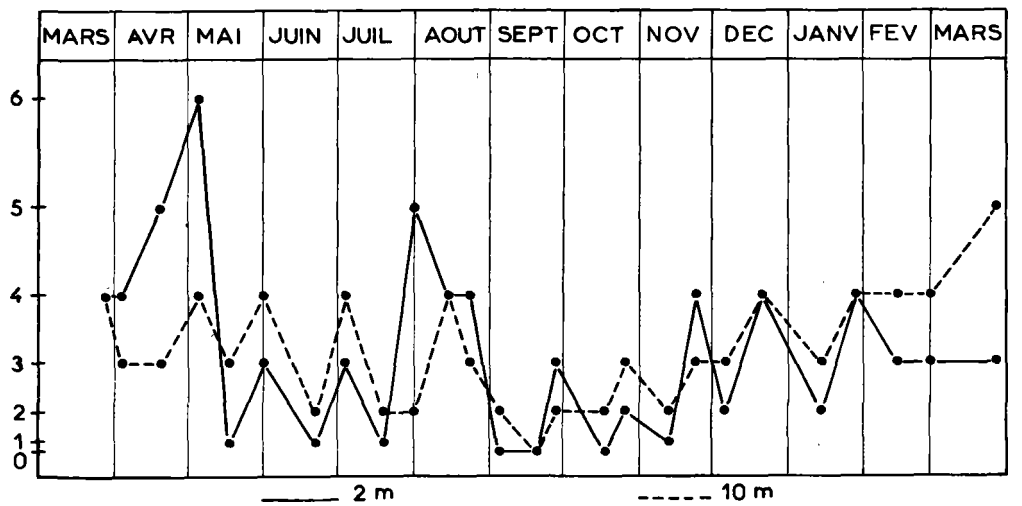


Fig. 24. — Abondance des Cténaires à la station 10.

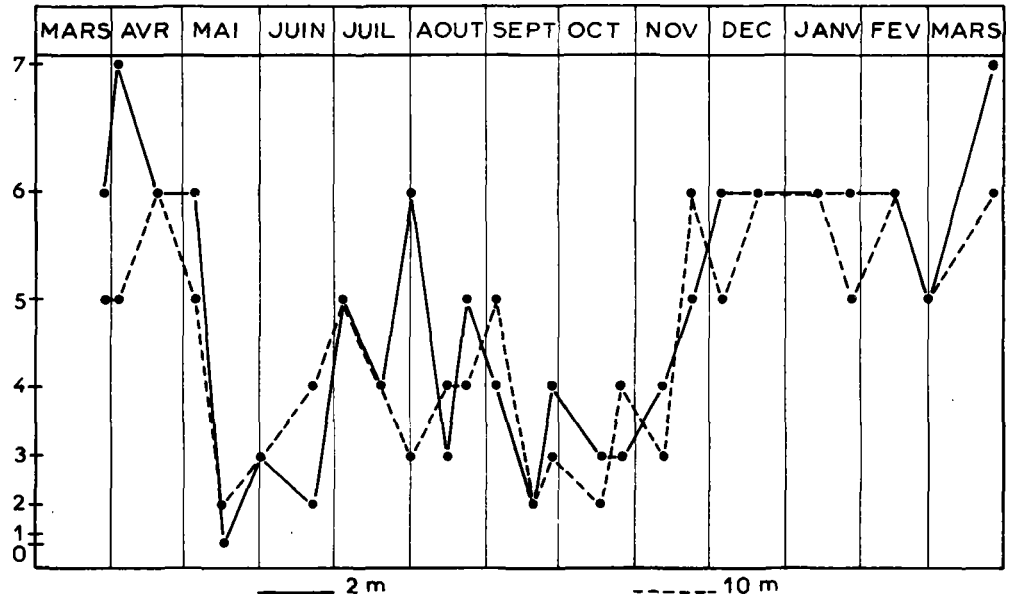


Fig. 25. — Abondance des Siphonophores à la station 10.

mars à la station 10 ; par l'abondance de Chaetognathes, Cladocères, Cténaires et Siphonophores à la station 10 ; enfin, par l'absence quasi-totale de *Pterosagitta draco* à la station 5.

L'**automne austral** (mai-juillet) se remarque par une richesse générale des eaux en Dolioles, la quasi-disparition des Cladocères à la station 10 et, à cette même station. la diminution progressive des Chaetognathes et Cténaires, et brutale des Siphonophores.

L'**hiver austral** (août-septembre) marque la disparition des Dolioles à la station 10 (les populations se maintenant à la station 5) ; à la même station l'effectif des Chaetognathes et Cténaires reste bas, tandis que celui des Hétéropodes subit un accroissement brusque entre août et septembre.

Au **printemps austral** (octobre à décembre) apparaissent à la station 10 une instabilité caractéristique des populations d'Appendiculaires, une augmentation du nombre de Chaetognathes, de Cténaires et de Cladocères ; l'absence de Dolioles à cette station se maintient, ainsi que l'instabilité des populations de Siphonophores, qui restent à un niveau très bas avant de réaugmenter brusquement en décembre.

Au total *les variations quantitatives constatées au cours de ce premier cycle annuel se montrent bien plus considérables à la station 10, proche de terre, qu'à la station 5 située à l'aplomb du talus continental et à 40 milles des côtes.* L'on ne saurait perdre de vue toutefois que ces données ne peuvent encore constituer que des indications préliminaires, qui ne tireront la plus grande partie de leur signification que de la comparaison avec les données fournies par les autres stations prospectées. Par ailleurs le caractère saisonnier des fluctuations observées au cours de ce premier cycle annuel devra être confirmé — ou infirmé — par une comparaison avec les années suivantes.

C. Hétéropodes et Ptéropodes. — 14 espèces d'Hétéropodes et 24 espèces de Ptéropodes ont été dénombrées à la station 5, 10 espèces d'Hétéropodes et 10 de Ptéropodes à la station 10, réparties en nombre comme suit :

	Station 5 (24 récoltes)	Station 10 (52 récoltes)
HÉTÉROPODES		
Oxygyrus keraudreni (LESUEUR)	24	1
Protatlanta souleyeti (E. A. SMITH)	4	1
Atlanta peroni LESUEUR	48	2
Atlanta gaudichaudi SOULEYET	638	710
Atlanta peresi FRONTIER	9	
Atlanta lesueuri SOULEYET	514	28
Atlanta inclinata SOULEYET	105	
Atlanta inflata SOULEYET	45	36
Atlanta helicinoides SOULEYET	1029	105
Atlanta turriculata d'ORBIGNY	203	13
Atlanta fusca SOULEYET	18	1
Pterotrachaea hippocampus PHILIPPI	1	
Firoloida demaresti LESUEUR	75	1
Cardiapoda placenta (LESSON)	6	
PTÉROPODES EUTHÉCOSOMES		
Limacina inflata (d'ORBIGNY)	7166	1533
Limacina trochiformis (d'ORBIGNY)	756	157
Limacina bulimoides (d'ORBIGNY)	36	
Limacina lesueuri (d'ORBIGNY)	17	
Creseis acicula RANG	71000 (1)	8811
Creseis virgula virgula RANG	109	16
Creseis virgula conica ESCHOSCHOLTZ	184	6
Creseis chierchiae (BOAS)	670	7593
Styliola subula (QUOY & GAYMARD)	130	
Hyalocylix striata (RANG)	63	
Cuvierina columnella (RANG)	4	
Euclio pyramidata (L.)	4	
Euclio cuspidata (BOSC)	1	
Diacria quadridentata (LESUEUR)	282	1
Diacria trispinosa (LESUEUR)	1	
Cavolina globulosa (RANG)	2	
Cavolina inflexa (LESUEUR)	35	
Cavolina tridentata (FORSKAL)	1	
Cavolina longirostris longirostris (LESUEUR)	12	87
Cavolinia longirostris angulata (SOULEYET)	7	1
« *Hyalaea laevigata* » (2)	58	
PTÉROPODES PSEUDOTHÉCOSOMES		
Peraclis reticulata (d'ORBIGNY)	1	
Cymbulia sp	8	
Corolla sp	4	1
Desmopterus papilio CHUN	33	2
PTÉROPODES GYMNOSOMES		
Pneumodermopsis sp	2	
Clionina longicaudata (SOULEYET)	13	27
larves de Clionidae	17	17

(1) Dont 68.000 dans une seule récolte.

(2) Pour la mise en doute de l'identification de *Hyalaea laevigata* comme forme juvénile de *Cavolinia longirostris*, voir FRONTIER 1965.

La station 5 est donc bien plus riche que la station 10 en Mollusques pélagiques, tant du point de vue du nombre d'individus que du nombre d'espèces. On remarque que toutes les espèces présentes à la station 10 sont présentes aussi à la station 5 et y sont plus abondantes en moyenne par récolte, à l'exception de *Creseis chierchiae*. de *Creseis acicula* si l'on ne tient pas compte de la récolte du 26 mars 1964 à la station 5 ayant ramené 68000 individus juvéniles, et de *Cavolinia longirostis longirostris*.

La seule espèce importante d'Hétéropodes de la station 10 est *Atlanta gaudichaudi* qui, bien qu'elle soit moins abondante qu'à la station 5 (13,8 individus en moyenne par récolte contre 26,6 à la station 5) se rencontre très régulièrement, étant présente dans toutes les récoltes sauf 6 — qui ne contenaient d'ailleurs aucun Hétéropode.

Atlanta helicinoides, lesueuri, inflata, turriculata sont sporadiques et bien moins abondantes (respectivement 2,0-0,5-0,7-0,25 individus en moyenne par récolte). Les autres espèces d'Hétéropodes n'ont pas été récoltés à la station 10 ou l'ont été en un ou deux exemplaires pour tout le cycle annuel.

En représentant graphiquement le nombre d'espèces d'Hétéropodes rencontrées à la station 10 on se rend compte que les espèces autres qu'*Atlanta gaudichaudi* n'apparaissent qu'à deux époques : de début avril à début mai (3 ou 4 espèces par récolte : *Atlanta lesueuri, inflata* et *turriculata*, toujours en très petit nombre) et surtout de septembre à décembre. Or cette période correspond à un maximum très accusé de l'abondance des Hétéropodes au large (fig. 23). La figure 26 montre le parallélisme frappant qui existe entre les variations d'abondance des Hétéropodes dans leur ensemble à la station du large, et celles du nombre d'espèces à la station 10. Cela semble confirmer l'hypothèse selon laquelle les espèces d'Hétéropodes autres qu'*Atlanta gaudichaudi* ne se rencontrent au-dessus du plateau continental qu'à la faveur d'apports pélagiques

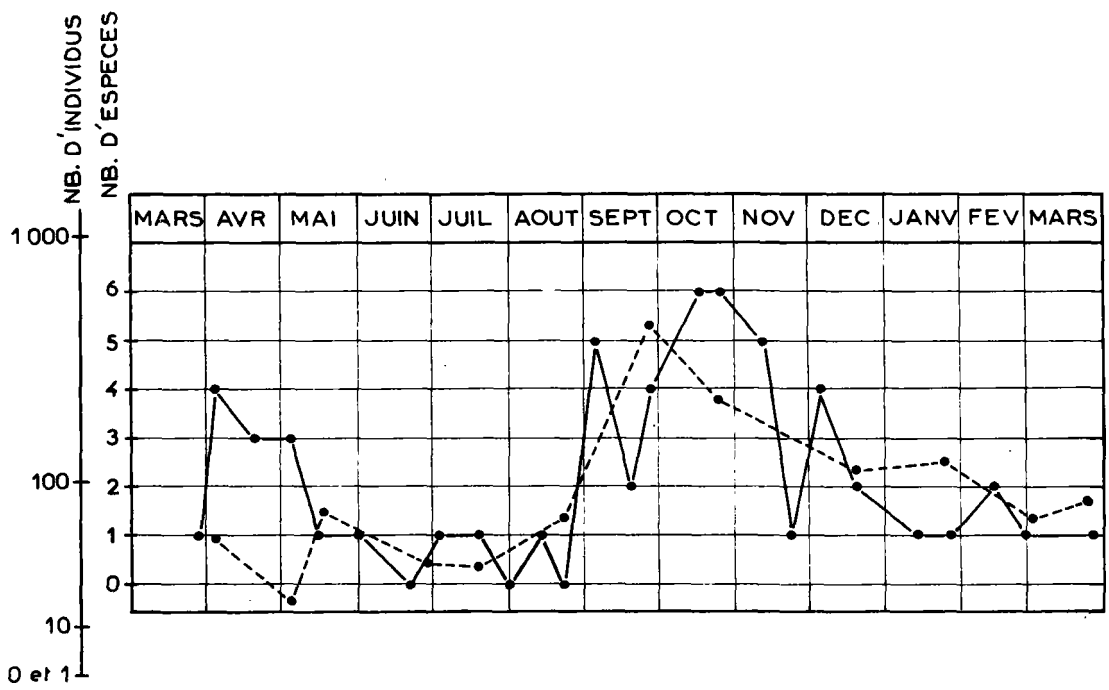


Fig. 26. — Nombre d'espèces d'Hétéropodes à la station 10 (trait plein) et nombre d'individus par récolte moyenne entre 2 et 10 m) à la station 5 (trait interrompu).

On retrouve à la station 5 le maximum du nombre d'espèces par récolte (10 à 12 espèces) de septembre-décembre, mais non celui d'avril. Trois espèces sont abondantes : *Atlanta helicinodes* (43 individus en moyenne par récolte), *gaudichaudi* (27) et *lesueuri* (21). Ces trois espèces sont, de plus, régulièrement présentes : elles ne manquent que dans une à trois récoltes sur les 24 effectuées. Suivent, dans l'ordre d'abondance, *Atlanta turriculata* (présente dans 18 récoltes à raison de 8,4 individus en moyenne), *Atlanta inclinata*, *Firoloida demaresti* et *Atlanta peroni* (présentes chacune dans 11 des 24 récoltes, à raison respectivement de 4,4-3,1-2,0 individus en moyenne par récolte). Toutes les autres espèces sont sporadiques ou très rares.

Le nombre total d'Hétéropodes à la station 5 a été représenté à la figure 23. On remarque une rapide augmentation d'effectif en août et septembre ; cette augmentation est due en majorité à une apparition massive d'*Atlanta* juvéniles appartenant à toutes les espèces mentionnées ci-dessus (mais fondamentalement à *A. helicinoides* et *lesueuri*). Ce phénomène apparaît nettement sur le graphique suivant, où sont portés les effectifs totaux d'*Atlanta* à 2 et 10 m d'immersion ; les comptages ont été effectués séparément pour les individus « très jeunes » (carène non encore apparue), « jeunes » (carène présente sur moins de trois quarts de tour de spire) et « adultes ou subadultes » (plus de trois quarts de tour).

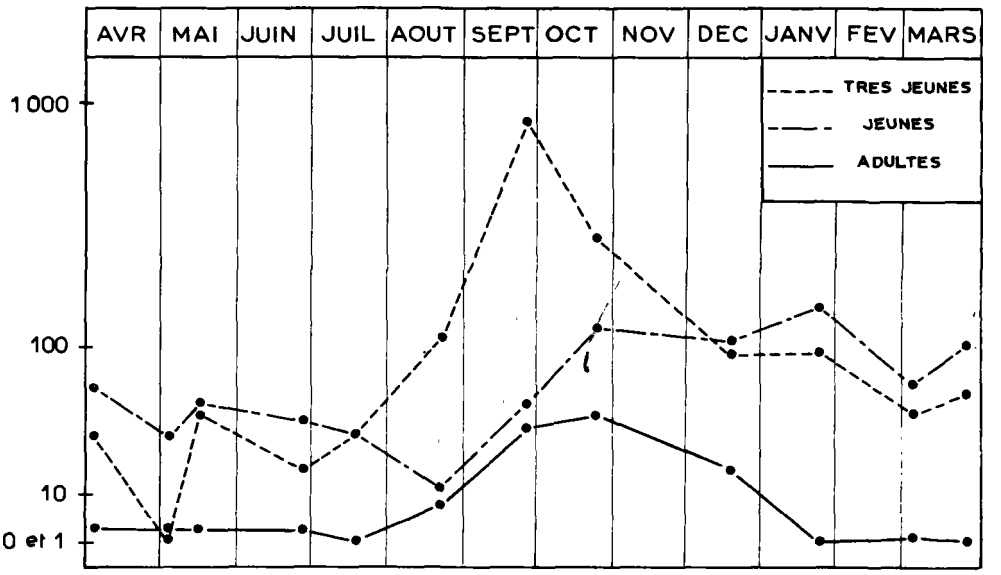


Fig. 27. — Comptages des *Atlanta spp.* à 2 et 10 m, station 5.

Les « jeunes » présentent un maximum d'abondance entre octobre et janvier ; les « adultes » sont très rares sauf entre août et décembre.

Trois espèces de Ptéropodes sont abondantes à la station 10 : *Creseis acicula* (169 individus en moyenne par récolte ; présente à toutes les récoltes sauf une), *Creseis chierchiae* (1) (146 individus par récolte ; présente dans toutes les récoltes sauf deux) et *Limacina inflata* (30 individus par récolte ; présente dans 32 récoltes sur 52). Les deux premières espèces sont — si l'on excepte la récolte contenant 68000 *Creseis acicula* juvéniles — nettement plus abondantes qu'à la station 5. *Limacina inflata* au contraire est moins abondante à la station 10 et s'y présente essentiellement sous forme juvénile, les adultes étant très rares tout au long de l'année ; par ailleurs 87 % des *Limacina inflata* capturés à la station 10 l'ont été entre septembre et décembre.

(1) Pour l'identification de cette espèce, voir FRONTIER 1965.

Cavolinia longirostris longirostris est peu abondante au total mais semble caractéristique du plateau continental, la station 5 n'ayant ramené que 12 individus, tous jeunes ou très jeunes. *Limacina trochiformis* est présente à la station 10 dans 25 des 52 récoltes, à raison de 3 individus en moyenne par récolte, presque tous jeunes ou très jeunes ; 81 % des individus de cette espèce récoltés à la station 10 l'ont été entre septembre et décembre.

Les autres espèces recensées à la station 10 sont très rares et sporadiques.

Ces différences faunistiques entre les stations 5 et 10 s'interprètent de la façon la plus simple en admettant l'existence de deux peuplements fondamentaux : l'un, très riche, caractéristique des eaux du large, l'autre de celles du plateau continental et limité aux espèces suivantes :

Atlanta gaudichaudi
Creseis acicula
Creseis chierchiae
Cavolinia longirostris longirostris (1)

Des éléments de la faune du large arrivent occasionnellement jusqu'à la station 10, particulièrement pendant la période que j'ai appelée « printemps austral », c'est-à-dire de septembre à décembre. Il se pourrait que les brassages d'eau entre le plateau continental et le large soient particulièrement intense pendant cette période.

Les espèces de la station 10 sont également présentes avec une abondance variable, à la station 5, et sans qu'il soit possible de déceler une époque préférentielle. J'anticiperai enfin sur les comptes-rendus ultérieurs qui seront consacrés aux stations situées plus au large que la 5, en faisant savoir que plusieurs espèces rares ou très rares à la station 5 *(Styliola subula, Hyalocylix striata, Cuvierina columnella, Euclio pyramidata)* sont nettement plus abondantes au-dessus des fonds de 1000 à 2000 m. Le peuplement à la station 5 semble donc être un peuplement du large appauvri par l'influence néritique.

(1) *Cavolinia longirostris angulata* — ainsi que « *Hyalaea laevigata* » — sont caractéristiques des eaux du large.

ANGOT (M.) 1965. — Cycle annuel de l'hydrologie dans la région proche de Nosy Bé. *Cahiers O.R.S.T.O.M. Océanographie 3 (1), pp.* 55-66.

ANGOT (M.) et GÉRARD (R.) 1963. — Hydrologie de la région de Nosy Bé : mars à juin 1963. *Ibid. 1 (6), pp. 255-288.*

— 1965 a — Hydrologie de la région de Nosy Bé : juillet à novembre 1963. *Ibid. 3 (1) pp. 3-30.*

— 1965 b — Hydrologie de la région de Nosy Bé : décembre 1963 à mars 1964. *Ibid. 3 (1), pp. 31-54.*

FRONTIER (S.) 1963 a. — Notes sur quelques larves atypiques de Décapodes Brachyoures récoltées dans le plancton de Nosy Bé. *Cahiers O.R.S.T.O.M. Océanographie (Travaux du Centre d'Océanographie et des Pêches de Nosy Bé) 1 (3) pp. 31-59.*

— 1963 b — Hétéropodes et Ptéropodes récoltés dans le plancton de Nosy Bé. *Ibid. 1 (6), pp. 213-227.*

— 1963 c — Présence de Creseis chierchiae (BOAS) dans l'Océan Indien. *Ibid. 1 (6), pp. 229-232.*

— 1965 — Le problème des Creseis. Cah. ORSTOM. sér. Océanogr. III, 2, pp. 11-17.

— 1966 a — Notes morphologiques sur les Atlanta récoltées dans le plancton de Nosy Bé (Madagascar). Cah. ORSTOM. sér. Océanogr. IV, 2, pp. 131-139.

— 1966 b — Liste complémentaire de Ptéropodes du plancton de Nosy Bé (Madagascar). *Ibid.* pp. 141-144.

FURNESTIN (M. L.) et RADIGUET (J.) 1964. — Chaetognathes de Madagascar (Secteur de Nosy Bé). *Cahiers O.R.S.T.O.M. sér., Océanogr. II, 4, pp. 55-98.*

NOUVEL (H.) 1964. — Mysidacés récoltés par S. FRONTIER à Nosy Bé. I — Description de deux Leptomysini. *Bull. Soc. Hist. Nat. Toulouse 99 (1-2), pp. 107-123.*

— 1965 — *Id.* II. Description de deux Mysini appartenant aux genres *Diamysis et Acanthomysis. Ibid.* 100 (3-4), pp. 107-123).

TESCH (J. J.) 1913. — Pteropoda. *Bronn's Tierreich, Lief 36, pp. 1-154.*

— 1946. — The Thecosomatous Pteropods. I) The Atlantic. *Dana rep. 28, pp. 1-,82 pl. 1-8.*

— 1948. — The Thecosomatous Pteropods. II) The Indo-pacific. *Ibid. 30, pp. 1-45, pl. 1-3.*

— 1949. — Heteropoda. *Ibid. 34, pp. 1-55, pl. 1-6.*

— 1950. — Gymnosomata II. *Ibid. 36, pp. 1-55.*

TOKIOKA (T.) 1955 a. — On some planctonic animals collected by the Syunkotu-Maru in May-June 1954. II) Shells of Atlantidae. *Pub. Seto. Mar. Biol. Lab.* 4 *(2), pp. 227-236, pl. 15-16.*

— 1955 b. — Shells of Atlantidae (Heteropoda collected by the Sôyô-Maru in the Southern waters of Japan. *Ibid. 4 (2), pp. 237-250, pl. 17-18.*

— 1955 c. — On some plankton animals collected by the Syunkotu-Maru in May-June 1954. IV) Thecosomatous Pteropods. *Ibid. 5 (1), pp. 59-72, pl. 7-13.*

— 1961. — The structure of the operculum of the species of Atlantidae as taxonomic criterion with records of some pelagic Molluscs in the North Pacific. *Ibid. 9 (2), pp. 266-332.*

TREGOUBOFF (G.) et ROSE (M.) 1957. — Manuel de planctonologie méditerranéenne. *C.N.R.S. 2 tomes.*

Annexe I

Cotations d'abondance par groupes zoologiques aux stations 5 et 10 entre mars 1963 et mars 1964.

(Pour chaque date de récolte les résultats concernant la récolte à 2 m de profondeur sont portés sur la première ligne ; ceux concernant la récolte à 10 m, sur la deuxième ligne et en retrait.)

Cotation adoptée		
	0.....	0 individu
	1.....	1 à 3 individus
	2.....	4 à 18 individus
	3.....	19 à 80 individus
	4.....	80 à 350 individus
	5.....	350 à 1500 individus
	6.....	1500 à 6500 individus
	7.....	plus de 6500 individus dans la récolte.

Annexe II

Comptages des Hétéropodes et Ptéropodes aux stations 5 et 10 entre mars 1963 et mars 1964.

(Pour chaque date de récolte et pour chaque espèce les résultats concernant la récolte à 2m sont portés sur la première ligne ; ceux concernant la récolte à 10 m sur la deuxième ligne et en retrait).

ANNEXE I

STATION 5				*Salpes*	*Dolioles*	*Appendiculaires*	*Lucifer*	Larves de *Brachyoures*	Larves d'*Anomoures*	Larves de *Palinoures*	Larves de *Natantia*	Larves de *Stomatopodes*	*Euphausiaces*	*Hyperiens*	*Isopodes*	*Mysidaces*	*Cumaces*	*Gammariens*	*Copépodes*	*Ostracodes*	*Cladocères*	*Ptéropodes*	*Hétéropodes*	*Annélides*	*Chaëtognathes*	*Cténaires*	*Méduses*	*Siphonophores*
Date	heure	Temp. (°C)	Salinité (‰)																									
3 IV	01.00	28,55	34,09	4	0	5	3	3	4	0	4	4	6	2	0	0	0	1	7	1	1	5	3	3	6	1	3	5
	01.15	28,34	34,09	4	1	5	4	3	4	1	5	4	6	2	1	0	1	1	7	3	0	4	3	3	6	2	3	5
3 V	14.40	29,04	34,79	1	4	5	0	3		0	2	0	1	3	0	0	0	0	7	0	0	3	2	2	6	1	3	4
	15.00	28,80	34,77	3	4	6	3	3		0	3	2	3	3	0	0	0	0	7	0	0	3	3	3	5	1	4	5
16 V	23.40	27,73	34,84	3	3	6	4	4	3	0	4	2	5	3	2	2	0	0	7	3	0	5	3	4	5	1	3	5
	23.55	27,73	34,85	3	3	4	4	3		0	4	1	5	3	0	0	0	0	7	3	0	5	3	4	6	1	3	5
27 VI	23.00	26,11	35,02	4	4	2	3	3	2	1	4	1	5	3	1	0	0	1	7	5	0	5	3	4	6	1	3	5
	23.15	26,01	35,07	3	3	2	2	3	2	1	3	2	5	3	1	1	0	0	7	5	0	4	3	4	6	1	3	5
18 VII	03.30	25.53	35,05	4	3	4	4	3	2	0	4	2	5	3	2	0	0	1	7	5	1	5	3	4	6	2	4	5
	03.45	25,53	35,05	4	3	3	4	3	2	0	3	2	5	3	1	1	0	1	7	5	0	4	2	4	6	2	4	5
22 VIII	02.25	24,82	35,04	1	2	4	4	3	2	1	3	2	5	2	1	2	0	1	7	6	0	5	4	3	5	0	3	4
	02.35	24,82	35,04	0	1	4	3	3	2	0	3	2	5	2	2	0	0	0	7	6	0	5	3	3	6	0	3	3
26 IX	02.10	25,40	35,07	3	3	4	6	4	3	1	3	2	5	4	2	2	1	0	7	4	0	5	4	4	6	2	4	4
	02.25	25,36	35,06	4	3	5	6	3	3	1	3	1	5	4	1	1	1	0	7	5	0	5	5	4	6	1	4	5
24 X	01.55	26,82	35,23	3	3	4	5	3	2	0	4	3	6	4	2	3	1	1	7	4	0	5	4	3	6	1	3	3
	02.10	26,83	35,21	3	3	4	5	2	2	0	3	0	5	4	0	1	0	0	7	4	0	5	4	2	5	1	3	3
19 XII	01.30	28,69	35,17	0	4	4	5	5	6	0	5	3	6	3	1	2	0	0	7	5	1	5	4	4	6	0	4	4
	01.40	28,48	35,21	3	4	5	5	4	4	0	5	3	6	3	1	1	0	0	7	4	0	5	4	4	6	1	4	4
24 I	02.20	28,39	34,57	5	0	3	3	6	5	2	6	4	5	2	2	3	2	0	7	3	1	5	4	2	5	0	3	2
	02.35	28,36	34,64	4	1	3	2	5	4	2	4	4	5	2	2	1	0	0	7	3	2	5	3	2	6	0	3	1
4 III	03.00	29,07	34,59	5	2	4	4	3	3	0	3	1	4	4	1	1	0	0	7	3	0	5	3	4	5	1	4	5
	03.10	28,93	34,69	5	1	3	4	3	2	0	3	1	5	3	1	0	0	0	7	3	0	4	3	3	5	1	1	5
26 III	01.45	29,51	33,83	1	0	3	4	4	2	0	3	4	3	1	2	1	1	0	7	1	3	7	1	2	5	0	2	3
	02.00	29,02	34,09	2	1	5	4	4	2	1	2	3	4	1	1	0	0	0	7	3	2	5	3	3	5	1	3	4

STATION 10				*Salpes*	*Doliolés*	*Appendiculaires*	*Lucifer*	Larves de *Brachyoures*	Larves d'*Anomoures*	Larves de *Palinoures*	Larves de *Natantia*	Larves de *Stomatopodes*	*Euphausiacés*	*Hyperiens* + *Synopidae*	*Isopodes*	*Mysidacés*	*Cumacés*	*Gammariens* sauf *Synopidae*	*Copépodes*	*Ostracodes*	*Cladocères*	*Ptéropodes*	*Hétéropodes*	*Annélides*	*Chaetognathes*	*Cténaires*	*Méduses*	*Siphonophores*
Date	heure	Temp. (°C)	Salinité (‰)																									
28 III	10.15	29,70	33,52	3	4	6	1	3	3	0	5	3	0	2	0	0	0	0	7	0	2	2	1	2	6	4	5	6
	10.50	29,51	33,32	3	4	6	3	3	4	1	5	3	1	3	0	0	0	0	7	0	1	3	2	3	7	4	5	5
3 IV	15.25	30,47	33,31	5	0	7	2	3	3	0	4	4	0	2	0	0	0	0	7	0	7	4	3	2	6	4	5	7
	15.40	29,73	33,78	6	3	6	4	4	2	0	5	4	0	3	0	0	0	0	7	0	6	4	3	2	6	3	5	5
19 IV	13.10	29,49	32,44	3	1	5	4	5	3	0	6	4	4	3	1	0	0	0	7	0	3	5	4	2	7	5	4	6
	13.20	29,15	33,70	3		4	5	4	2	1	5	4	2	2	0	0	0	0	7	2	2	4	2	2	6	3	3	6
4 V	10.55	29,10	33,54	1	2	5	0	3	3	0	4	3	3	4	0	0	0	0	7	4	3	4	1	3	7	6	5	6
	11.05	28,95	33,50	1	4	6	2	4	3	1	5	4	4	4	1	0	0	0	7	5	1	4	2	3	6	4	4	5
17 V	19.40	28,26	34,54	3	0	6	5	3	0	0	3	2	1	1	0	2	1	0	6	2	2	4	3	1	3	1	2	0
	19.50	28,16	34,71	2	1	5	5	3	1	0	4	0	0	0	0	2	1	0	6		3	4	1	1	4	3	4	2
31 V	10.15	28,12	34,62	2	3	5	3	4	3	0	4	3	3	2	0	0	0	0	7	0	1	5	2	3	6	3	4	3
	10.25	27,75	34,69	3	4	5	5	5	4	1	5	4	4	3	0	0	0	0	7	6	2	5	3	3	6	4	4	3
21 VI	17.00	27,11	34,63	7	4	5	2	3	2	1	3	3	1	3	1	0	0	0	6	2	2	2	0	2	5	0	3	2
	17.10	27,02	34,86	7	3	6	3	4	3	1	5	3	5	3	1	0	0	0	6	3	0	3	0	3	6	2	4	4
3 VII	10.30	26,91	34,84	2	3	5	5	3	2	0	4	2	0	3	0	0	0	0	6	0	0	3	2	3	5	3	4	5
	10.40	26,73	34,84	2	4	5	6	4	3	1	4	3	1	1	0	0	0	0	6	2	2	3	2	3	5	4	4	5
19 VII	17.25	26,40	34,88	4	4	3	3	4	2	1	5	4	0	2	0	0	0	0	7	4	2	4	3	4	6	0	4	4
	17.35	26,20	35,02	2	4	2	6	5	3	1	6	3	4	4	0	0	0	0	7	3	0	4	3	4	6	2	4	4
31 VII	09.25	25,65	35,09	3	4	6	0	4	2	0	6	4	2	1	0	0	0	0	7	0	0	2	0	2	6	5	5	6
	09.35	25,61	35,05	3	6	7	0	4	2	1	5	3	4	2	1	0	0	0	7	1	0	2	0	3	5	2	4	3
16 VIII	16.00	26,66	35,17	4	0	3	3	4	3	0	5	3	0	3	0	0	0	0	7	0	0	2	1	0	5	4	4	3
	16.10	25,40 ?	35,15	4	1	2	4	4	3	2	5	4	0	3	0	0	0	0	7	1	0	3	2	2	6	4	3	4
23 VIII	09.15	25,09	35,17	1	0	4	6	4	3	0	5	3	1	1	0	0	0	0	7	1	0	1	0	0	5	4	3	5
	09.25	26,04	35,17	4	0	3	6	4	3	2	5	4	1	1	1	0	0	0	6	1	0	2	0	2	5	3	3	4
4 IX	16.35	25,36	35,15	4	1	5	3	4	3	0	4	3	3	1	1	0	0	0	7	0	0	5	3	1	5	0	3	4
	16.40	25,34	35,15	4	0	6	0	5	4	1	4	4	4	2	1	0	0	0	7	0	0	5	3	2	5	2	3	5
19 IX	16.55	25,61	35,09	1	0	7	0	4	3	0	3	1	6	0	0	0	0	0	7	1	0	3	1	2	4	0	2	2
	17.10	25,59	35,07	1	1	6	1	6	4	1	4	2	6	2	1	0	0	0	7	2	0	3	2	2	5	0	3	2
27 IX	09.20	25,71	35.11	6	0	6	0	3	3	1	5	4	6	3	2	0	0	0	7	1	0	3	2	2	6	3	4	4
	09.30	27,70	35,10	4	0	7	0	4	4	2	5	4	7	2	3	0	0	0	7	2	0	3	2	3	6	2	4	3
17 X	18.50	26,41	35,12	7	0	4	4	6	4	0	5	4	6	2	3	4	4	4	7	5	1	4	3	3	5	0	4	3
	19.00	26,34	35,13	5	0	5	3	5	4	1	5	3	6	3	2	4	4	0	7	4	1	3	3	2	5	2	3	2
25 X	09.10	26,57	35,13	2	0	7	2	4	3	0	2	3	1	2	0	0	0	0	7	0	1	2	2		5	2	2	3
	09.20	26,29	35,12	2	1	5	1	4	3	0	4	3	3	3	2	0	0	0	7	0	0	3	2	2	5	3	3	4
11 XI	11.00	28,37	34,85	3	0	4	0	4	3	0	3	3	2	2	1	0	1	1	6	0	3	3	3	3	4	1	2	4
	11.10	27,41	35,14	5	0	6	1	4	2	0	4	0	4	3	1	0	0	0	6	0	2	3	2	2	5	2	4	3
23 XI	07.15	27,53	35,09	0	0	3	3	5	3	2	4	4	2	2	1	0	0	0	6	1	3	4	2	0	4	4	3	5
	07.25	27,53	35,08	1	0	5	3	5	3	3	4	4	0	2	0	1	0	0	7	0	4	3	2	1	5	3	3	6
5 XII	10.50	28,16	35,13	0	0	6	0	5	4	0	4	4	1	2	0	0	0	0	7	0	1	4	2	3	6	2	4	6
	11.00	28,05	35,13	0	1	5	4	5	4	1	6	3	6	3	0	0	0	0	7	1	2	5	3	3	6	3	3	5
20 XII	07.40	28,52	34,81	5	1	4	6	5	3	0	5	3	0	1	1	0	0	0	7	0	2	6	2	3	6	4	4	6
	07.55	27,93	35,05	5	2	3	6	5	4	2	5	4	1	1	1	0	0	0	7	2	2	5	3	3	6	4	4	6
14 I	10.45	28,08	32,13	4	1	3	6	5	4	2	5	3	0	3	0	0	0	0	7	3	6	4	2	3	5	2	4	6
	10.55	26,99	34,15	2	3	3	6	6	5	1	5	4	0	3	0	0	0	0	7	4	5	4	2	3	6	3	4	6
27 I	09.05	28,95	33,75	0	2	6	2	4	3	0	4	2	2	3	0	0	0	0	7	3	1	2	1	2	6	4	5	6
	09.10	28,69	34,10	0	1	4	3	4	3	0	5	4	1	2	1	0	0	0	7	3	2	2	2	2	6	4	5	5
14 II	09.40	29,15	33,73	1	1	5	4	6	3	0	4	3	1	2	0	0	0	0	7	1	4	5	3	4	5	3	4	6
	09.45	29,02	33,90	1	1	5	5	6	4	0	5	4	2	3	0	0	0	0	7	2	6	5	3	4	6	4	4	6
27 II	08.20	28,81	33,22	0	0	6	4	4	2	0	4	3	2	1	1	0	0	0	7	0	5	6	2	4	6	3	4	5
	08.30	28,71	33,59	2	1	6	5	5	3	0	6	5	3	2	0	1	0	0	7	2	4	6	3	4	7	4	5	5
27 III	08.50	29,80	32,91	1	4	4	2	4	3	1	5	5	5	3	1	0	0	0	7	4	1	3	2	5	7	3	7	7
	09.00	29,40	33,51	2	3	6	3	4	2	0	4	5	3	2	0	0	0	0	7	3	1	1	2	4		5	6	6

ANNEXE II

STATION 5

	3 avril	4 mai	16 mai	27 juin	18 juil.	22 août	26 sept.	24 oct.	19 déc.	24 janv.	1 mars	26 mars
Oxygyrus keraudreni				1	1		1	8				
							1	3	6	3		
Protatlanta souleyeti				1				1			1	
								1				
Atlanta peroni	3				5		3	6	3			
	2		1				9	11	3		2	
Atlanta gaudichaudi	43	6	7	10	3	8	31		32	126	39	135
	27		23	1	2	14	50	27	17	11	26	25
Atlanta peresi						3		1				
						4		1				
Atlanta lesueuri		7	18	24	17	31	79	83	12	2	2	
	1	14	12	6	5	10	145	36	3	4	3	
Atlanta inclinata			3			1	1	44	10		4	
			1			2	15	15	9			
Atlanta inflata					6			25	1	2		
		1		1				7	2			
Atlanta helicinoïdes	15	1	4	8	18	34	213	115	46	59	15	
	1	4	10	4	5	13	332	51	42	30	9	
Atlanta turriculata	2		4		1	3	12	40	24	13	3	
			5	2	2	5	41	30	12	3	1	
Atlanta fusca				1			4	6	1			
				1			4	1				
Pterotrachaea hippocampus			1									
Firoloida demaresti	2		22	2							13	
	1	1	22	2			1		2		7	
Cardiapoda placenta			1				1					
			1		2		1					
Limacina inflata	526		200	287	240	459	247	200	311	614	223	70
	216	3	698	74	62	524	591	179	266	324	42	110
Limacina trochiformis	41	34	20	54	35	28	46	76	19	6	29	8
	45	23	37	24	11	14	155	25	20	4	8	3
Limacina bulimoides			1	1	3		1	4	5	2		
			1			1	3	2	4	8		
Limacina lesueuri				2			3	5				
						1	4	2				
Creseis acicula	42		92	50	40	62	90	249	118	55	322	68000
	29	2	113	11	38	49	147	155	149	16	123	796
Creseis virgula virgula		5	24	1	2	7	3				8	
	3	18	26	1		5	1			1	4	
Creseis virgula conica			1			6	41	10			6	
					1	3	106	3	7			
Creseis chierchiae	22		90	8	23	13	4		33	47	64	141
	21	3	87	2	15	15	2		12	11	38	19
Styliola subula			25	1	11	1	3	9		7		
			28	2	6	8	1	12	3	1		

ANNEXE II (suite)

STATION 5 (fin)

	3 avril	4 mai	16 mai	27 juin	18 juil.	22 août	26 sept.	24 oct.	19 déc.	24 janv.	4 mars	26 mars
Hyalocylix striata	11		9 16		1 3		1 2	2 3	3		8 4	
Cuvierina columnella				1				1 2				
Euclio pyramidata						1	1	2				
Euclio cuspidata					1							
Diacria quadridentata	5 1		7 16	5 3	23 14	2 6	31 36	56 44	12 16	1	2 1	1
Diacria trispinosa								1				
Cavolinia globulosa				1							1	
Cavolinia inflexa	1		4	2 2	9 6	1		2	2 5	3		
Cavolinia tridentata							1					
Cavolinia longirostris longirostris			4		4 4							
Cavolinia longirostris angulata									1		6	
« *Hyalaea laevigata* »	1		2 1	1 2	8 7	1	4 8	6 10	1 3		2	1 1
Peraclis reticulata							1					
Cymbulia sp.	1	1	1					1	4			
Corolla sp.					1 1							2
Desmopterus papilio			1					3 3	11 15			
Pneumodermopsis sp.					1				1			
Clionina longicaudata		1 1		1 1					3		6	
larves de Clionidae	1 2	1	1 3	2		3 1			1 1	1		

	28 mars	3 avril	19 avril	4 mai	17 mai	31 mai	21 juin	3 juil.	19 juil.	31 juil.	16 août
Oxygyrus keraudreni			/								
Protatlanta souleyeti				1							
Atlanta peroni											
Atlanta gaudichaudi	2 6	29 19	86 13	2 13	36 2	17 32		8 7	67 24		2 4
Atlanta lesueuri		2 1	3 1	1							
Atlanta inflata		8	1								
Atlanta helicinoides											
Atlanta fusca											
Atlanta turriculata		2									
Firoloida demaresti											
Limacina inflata		1 2	4 3		1		1		1 2		
Limacina trochiformis		3	4 2				4	1	1 2	1	
Creseis acicula	3 21	10 10	115 36	11 55	85 29	29 40	7 4	6 13	223 110	1 3	7 12
Creseis v. virgula		6 1	2								
Creseis v. conica											
Creseis chierchiae	8 6	235 145	226 62	63 115	40 63	718 552	8 20	14 14	16 12	10 7	10 28
Diacria quadridentata				1							
Cavolinia l. longirostris	1 4	1 26	1	6 4	10 1	4 12		2	1		
Cavolinia l. angulata				1							
Corolla sp.										1	
Desmopterus papilio				1							
Clionina longicaudata			2 2			2 1	2 4	1	1		
larves de Clionidae						3 5					

suite)

19 sept.	27 sept.	17 oct.	25 oct.	11 nov.	23 nov.	5 déc.	20 déc.	14 janv.	27 janv.	14 févr.	27 févr.	27 mars
			1									
		1										
2	4	7	2	8	6	4	6	12	2	53	10	9
7	6		3	2	7	21	27	10	5	30	38	5
	6	3		1								
		3	4									
				10		1				7		
		7		1		1						
1	8	7		6		5	1					
		21	6	7		3						
			1									
		4	1									
		1	1	1		1						
	1											
20	24	115	6	63	1	26	8	5		104	2	
44	6	53	28	35		41	1	1	1	50	8	
2	6	6		4		3	1	1		9		1
8	9		2			2	2			1		
	4	5	1	5	109	44	786	42	7	55	1250	44
9	14	10	3	3	32	35	672	95	7	147	4200	280
		2		2						7		
2	2	14		1	61	30	821	140	4	522	319	30
9	2	6	3	5	21	499	517	76	7	100	729	64
1							2	1				
	1						5	1	1	2		
				1								
					2					1		1
							6			2		
							2	1				1
										1	4	

Reprinted from *J. Tokio Univ. Fish.*, vol. 8, no. 2, 1966, p. 173-226

A PRELIMINARY REPORT ON THE PRIMARY PRODUCTIVITY IN THE EASTERN INDIAN OCEAN IN WINTER

— IIOE Report on Productivity, 1963-1964, Umitaka-maru — — Methods of Experiments, Data, and Outlines —

Ichitaro SAKAMOTO* and Kanau MATSUIKE**

(Jan. 11, 1965)

I. Introduction

During the International Indian Ocean Expedition (IIOE) on the Umitaka-maru, experiments on primary productivity were carried out mainly in the Eastern Indian waters, and data were obtained at 30 all-round observation stations. Experiments were carried on throughout the voyage from Nov. 2, 1963 to Feb. 14, 1964. At the same time 37 sampling stations, including some in the Far East and the Northeast Pacific waters, were added for the study of the surface water.

Examined sample waters amounted to 311 in total.

Our experimentation plan was carried out as follows. Solar insolation was measured by the Robitzsch recording actinograph for three and a half months contiunously. At each of the all-round observation stations sample water of over 20 liters each was taken from the following 9 layers, 0 m, 10 m, 25 m, 50 m, 75 m, 100 m, 125 m, 150 m, 200 m, during 8 a. m.–10 a. m. local mean time.

Transparency and submarine relative irradiance were measured immediately before the apparent noon.

Each sample water was prepared for the measurement of chlorophyll, seston, microplankton, and sample waters of the 7 layers above 125 m were prepared for photosynthetic experimentations with the radio-active ^{14}C.

Experiments of photosynthesis were carried out with 4-hour exposure under the fluolescent light for the tank experiment, and with day-light exposure from the apparent noon to the sunset for in-situ experiment and on-deck experiment.

Measurement of these test materials were done after the expedition returned to Japan. Measurement of absorbancy of chlorophyll materials, and counting of ^{14}C activity of photosynthetic materials were undertaken by Mr. K. TAKESUE of Fisheries College. Examination on the spectral sensitivity of the submarine irradiance-meter was undertaken by Prof. T. SASAKI of Tokyo University of Fisheries, and Dr. G. ŌSHIBA of the Institute of Physical and Chemical Research. The authors would like to express their deep gratitude to their wholesome cooperation.

* Miye Prefectural University.
** Tokyo University of Fisheries.

Among the environmental factors which contribute to primary productivity, water temperature, salinity, current, nutrients, bio-mass of macro-planktons and D.S.L. animals were measured by colleagues in physical oeeanography, chemical oceanography and marine biology. Their data will soon be made public.

Since primary productivity is understood as a synthetic reflection of such oceanic conditions as biochemical activity, chemical and optical potential productivity, thermal, chemical and dynamic effects, and population density of bio-mass, discussions and remarks on the conclusion will have to wait until all the related data are put in order. This report presents only a brief description on the methods used by the authors, and the full data, and deals with only the obvious facts in outline.

The authors would like to acknowledge Prof. S. MOTODA of Hokkaido Univ., Prof. Y. MATSUDAIRA of Hiroshima Univ., Dr. Y. SAIJO of Nagoya Univ., and Prof. M. UDA of Tokyo Univ. of Fisheries who had given them useful suggestions prior to the expedition; Prof. J. SENO of Tokyo Univ. of Fisheries, the head of the expedition, and the staff members who constantly encouraged and cooperated with the authors in operation; the staff of the Umitaka-maru under Captain K. OZAWA and students of Tokyo Univ. of Fisheries who were on board for their training, without whose willing cooperation the authors would have encounted great many hardships.

II. Methods of observation and the data

1. Solar insolation

For the measurement of solar insolation two Robitzsch actinographs were insituted, one on each side of the upper deck of the bridge, thereby correcting errors arising from the structural shades. Measurement was carried on smoothly. However, two kinds of structural defects were noted in this type of actinographs. One is that the time lag is rather great, other is that it gives more or less greater indication when the sun's altitude lowers, the cause of which seems to be inside reflection of the glass dome.

Relationship between the sun's altitude and the correction on the measured data will be reported in a separate paper together with a report on relationship between insolation and cloudiness.

Table 1 shows the time and position of sunrise, apparent noon and sunset, and the azimuth and altitude of the sun.

Table 2 shows the raw data on solar insolation per each one hour with the apparent noon as the standard time.

2. Submarine irradiance

Submarine irradiation, with solar insolation as its light source, is itself one of the potential resources on primary production, and it decreases exponentially as the depth increases.

It has been generally held that measurement of submarine irradiation in the oceanic conditions is quite difficult unless favored by best conditions. This is mostly

due to the difficulty in operation of a large ship to readjust the cable inclination to zero.

Accuracy in determination of the depth of the observed layer is particularly important for measurement of submarine irradiance which shows exponential decrease against the depth.

At the same time, since directionality of insolation flux under the clear sky reaches a considerable depth in a clear ocean, corrections on the inclination angle against incoming light flux on the receiving surface of submarine irradiance-meter cannot be neglected.

A depth-finder "Net Zonde" of a telemeter type, developed by the Furuno Denki Co. Ltd. to determine the depth of a trawlnet in operation, was fixed on the cable of the submarine irradiance-meter to determine the relationship between the depth of photo cells on the one hand, and the length of the let out cable and the cable's inclination angle on the deck side on the other hand. The inclination angle of photo

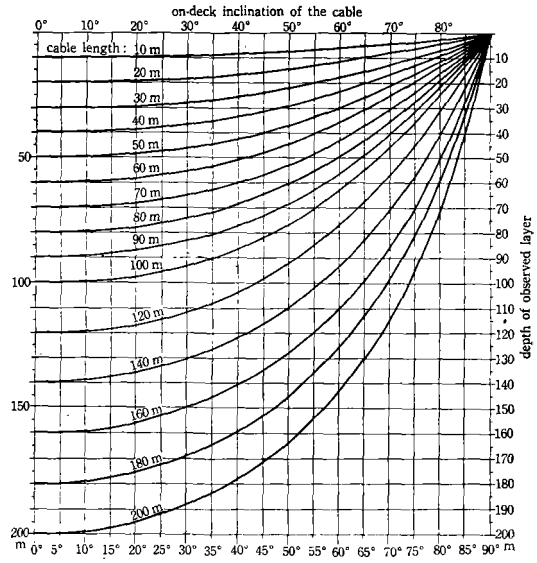


Fig. 1. Diagram for finding the depth of observed layers from the on-deck inclination of the cable and the cable length.

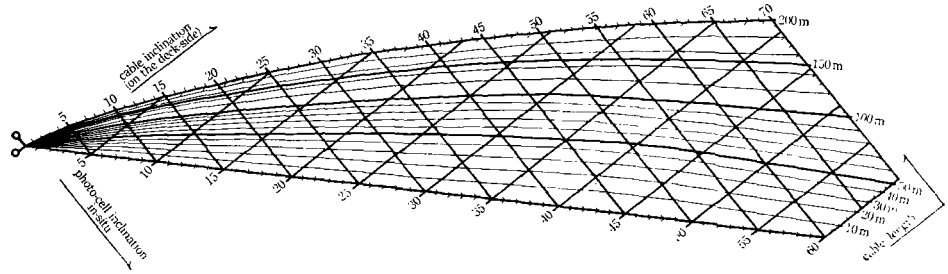


Fig. 2. Diagram for finding the photo-cell inclination from the cable inclination on the deck side and the cable length.

cells obtained from drawings. Resulting diagrams are shown in Fig. 1 and 2.

Since submarine irradiance is measured under the condition in which the relative position and direction of photo cells against light flux change in response to continuous changes in the sun's altitude and azimuth, uncorrected raw data will have no meaning except as the data of the instrument's responsiveness.

The authors have corrected the raw data of measured irradiance (i) with variation of insolation (s) and photo cell's light-collecting surface (c).

Thus, the relative irradiance at z meter depth (I_z) is shown as in the following equation.

$$I_z\,\% = \frac{i_z/s_z \cdot c_z}{i_0/s_0 \cdot c_0} \cdot 10\,, \tag{1}$$

i_0/c_0 stands for irradiance measured at right angle to the sun in the air using the submarine irradiance-meter, and s_0 is the on deck insolation at the same time. i_z/c_z stands for underwater (z meter depth) irradiance measured at right angle to the insolation flux and s_z is the on deck insolation at the time when i_z was measured.

s_0 and s_z were normally recorded by the actinograph, but in case of rapid fluctuations due to clouds "Tōshiba-No. 5-Luxmeter" was substituted for the measurement of the maximum solar irradiance in the air while measuring submarine irradiance.

For calculation of C the following formula was devised

$$\begin{aligned} C &= \cos\alpha \cdot \cos\beta + \sin\alpha \cdot \sin\beta \cdot \cos\varphi \\ &= \cos\chi\,, \end{aligned} \tag{2}$$

Fig. 3 shows an illustration of denotation in the formula (2).

α: Refraction angle of solar insolation, is determined by the sun's altitude (a) when the refractive index (n) is made constant in

$$n = \frac{\sin(90^\circ - a)}{\sin\alpha} \fallingdotseq 1.3388_{43} \quad [\lambda_D \cdot 25^\circ\mathrm{C} \cdot 19\,{}^0/_{00}\,\mathrm{Cl}]$$

β: Inclination angle of the photocell at the time of measurement, that is, the inclination angle of the normal line of the photo cell against the vertical line.

φ: Angle enclosed by the sun's azimuth and the bearing of the normal line of the photo cell $=180^\circ - \varphi'$

φ': Difference between the cable's bearing ($B'g$) and the sun's azimuth.

χ: Angle enclosed by the incoming insolation flux and the normal line of the photo cell.

For calculation of the attenuation coefficient (K), the light path $\left(\frac{z_2 - z_1}{\cos\alpha}\right)$ and not the difference in depth of the observed layer ($z_2 - z_1$) was used as in shown below.

$$I_{z2} = I_{z1} \cdot e^{-K \cdot (z_2 - z_1/\cos\alpha)} \tag{3}$$

Moreover, upward irradiance (Eu) was measured at five stations by turning the

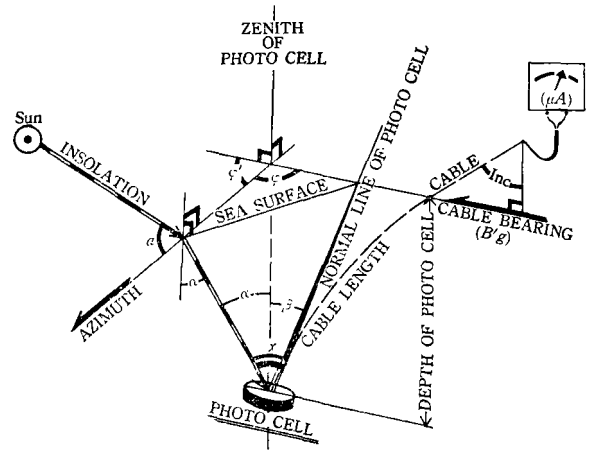


Fig. 3. Illustration of the method for finding the submarine irradiance.

photo cell downward. Eu was corrected only with s_z. Irradiance ratio (reflectance $R=Eu/Ed$) was shown by the ratio of the above mentioned Eu with $Ed=i_z/s_z \cdot c_z$.

Measurement of irradiance was carried out wholly with the "Type-A submarine irradiance-meter" manufactured by Murayama Denki Seisakusho Co.

The light-receiving surface of this instrument has four photo cells, each covered by a different kind of filter (opal, blue, green, amber).

Relative spectral sensitivity of each photo cell is shown in Fig. 4.

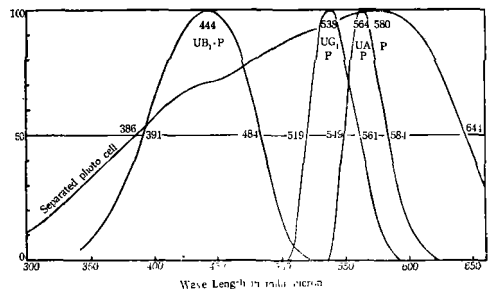


Fig. 4. Spectral sensitivity of the Umitaka-maru's submarine irradiance-meter.

Table 3 shows relative irradiance (I_z %) and attenuation coefficient (K), and Table 4 shows reflectance (R).

In the "Cooperative Studies on Primary Productivity in the Coastal Waters of Japan, 1962–63", depths of sampling layers were determined with transparency as a basis. This decision was based on the assumption that the relative irradiance at transparency depth is 15 %. Our data are shown in Table 5 in order to have application of this assumption into the Indian Ocean examined.

3. Experimentation of Primary Production

Method of experimentation are similar to the ones reported by Y. MATSUDAIRA, et al. (1964). Only the different points will be described here.

"Van Dorn water sampler" with double 6-liter vessels were used twice to get 24 liters of sample water from each layer. In order to carry on the operation speedily we abstained from letting out the corrective wire. Instead we determined depths of layers from the data obtained by the "Net Zonde depth finder". Wires were stretched down to 200 meter for sampling of the 9 layers at each station.

i. Experiment of Photosynthesis

Photosynthesis of each sample was measured by both the tank method and the SOROKIN's method. In addition, measurement by in-situ method was successfully carried out at 15 stations. In all these experiments two light bottle and one dark bottle (about 280 ml in capacity) were used, and 1 ml water solution of the radioactive $Na_2{}^{14}CO_3$ (10 micro curie/ml) was added into each bottle.

After exposure samples were filtered through Millipore-filter·HA of diameter 24 mm (0.45 micron dia. pores).

Incubation in tank experiment was done precisely for four hours with 10 k lux. irradiation of fluorescent lamps while keeping water temperature of the tank constantly within 1°C. of the temperature of surface water by pouring sea water from the sanitary tank.

From measurement by the submarine irradiance-meter, insolation whose irradiance is equal to one hour irradiation of the tank was calculated as below.

(Types of filters) Wave length of maximum response	(Blue) 444 mμ	(Green) 538 mμ	(Amber) 580 mμ
Insolation in g cal/cm²	12.6	12.6	13.8

Photosynthetic experiment by SOROKIN's method was carried out on the upper deck using a revolving tank (devised by I. SAKAMOTO) covered with 2 (or 3 on rare occasions) white polyethylene plate of 2 mm thickness. Light bottles were set on the turbine-affixed floating ring inside the tank, and were revolved on the surface of water by the rushing sea water from the pump.

Unavoidable partial irradiance inside the tank due to the structural shades of the ship was nullified by revolving the samples. Water temperature was constantly kept equal to that of sea water immediatly below its surface, and polyethylene covers were effective enough to scatter and decrease insolation.

Light transmittancy in % of polyethylene covers, measured by the submarine irradiance-meter, has as the following table indicates, a flat characteristic.

No. of cover / Wave length	1 plate	2 plates	3 plates
(Blue) 444 mμ	50.4	25.4	12.8
(Green) 538 mμ	55.7	31.0	17.3
(Amber) 580 mμ	57.5	33.1	19.0
	%	%	%

Samples were given exposure from the apparent noon to the sunset.

A new attempt to nullify inclination of the wire was done in case of in-situ experiment by fixing a "deplessor" to the end of the wire. Samples were fixed to a wire at the same length as of sampling in all caces except when water sample for the surface was fixed at 2 m of the wire. A buoy-system from which wires were suspended with samples, was connected with the ship by a guide wire, and left drifting and exposed to daylight from the apparent noon to the sunset.

Irradiance distribution of the fluorescent-lighted tank, an illustration of the SAKAMOTO-revolving tank to be used under daylight irradiance, and an illustration of the drifting method used for in-situ experiment on the Umitaka-maru are shown in Fig. 5.

In these three kinds of photosynthetic experiments a photochemical method was applied to check the received amount of total irradiation. Mixtures of potassium iodide solution and dilute sulphuric acid cause liberation of iodine when irradiated. Since the speed of

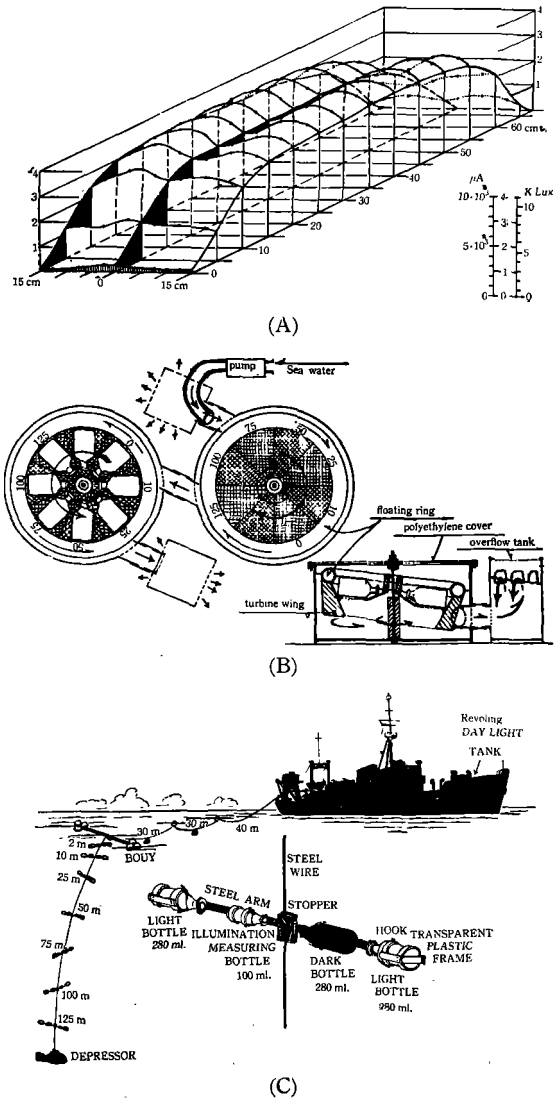


Fig. 5. Photosynthetic experiments.
(A): Distribution of irradiation inside the flusrescent lamp-lighted tank.
(B): Illustration of the SAKAMOTO-revolving tank for daylight conditions.
(C): Illustration of the in-situ method on the Umitaka-maru.

iodine liberation varies according to the concentration of sulphuric acid, the following mixtures were used according to the experimental light conditions.

A: Equi-volume mixture of n/10 KI and n/50 H_2SO_4···for strong irradiation

B: Equi-volume mixture of n/10 KI and n/10 H_2SO_4···for medium irradiation

C: Equi-volume mixture of n/10 KI and n/2 H_2SO_4 ···for weak irradiation

These fluid were filled in 100 ml oxygen bottles and titrated after exposure with n/100 $Na_2S_2O_3$ solution.

Irradiation and titration are in direct proportion until titration reaches about 5 ml. Though action spectrum of photosynthesis does not coincide with that of this photochemical reaction, a standard can be obtained from this method. If sensitive papers for blue print devised by FRIEND; D. T. C. (1961), and various materials of different wave lengths of reaction were applied, very effective results would surely be obtained.

Test filters were given prescribed treatment and kept dry under the low temperature of −10∼−20°C. During April—June 1964 these filters were put to counting with 2π gasflow-counter by Mr. K. TAKESUE of the college of Fisheries. Carbon assimilation was calculated as follows:

$$\frac{\{\text{Total carbon dioxide in water (mg C/}l\text{)}\}\cdot 10^3\cdot \{\text{Count of light bottle (c. p. m.)}-\text{Count of dark bottle (c. p. m.)}\}}{^{14}\text{C added to sample (c. p. m.)}} = \text{Assimilation (mg C/m}^3\text{)} \quad (4)$$

It must be noted here that all experiments were carried out on the assumption that the total carbon dioxide in water is constantly 24.6 mg C/l. ^{14}C, which was added to the samples, has been found to have the accepted activity of 9,633,500 c. p. m. Error of the gas-flow-counter has been ascertained to be within 7 %.

The larger value of double samples was taken for the value of assimilation. In the tank method production, was expressed in **mg C/m³·10 KLux·hour**. Production per unit chlorophyll-a, expressed in **mg C/mg chl-a·10 KLux·hour**, indicates of biological activity on photosynthesis.

Production, experimented under the daylight condition, was expressed in **mg C/m³·half day**.

The integrated vertical data on production measured by in-situ method gives the unit area production in **mg C/m²·half day**.

ii. Chlorophyll measurement

About 10 liters of each sample water was filtered through Millipore-filter-HA of 47 mm diameter. Filters were then treated with hot steam and preserved day in low temperature for later filtration. These filters were examined by Mr. K. TAKESUE during June—August 1964 for the purpose of chlorophyll measurement; their optical density of the following wave lengths, 750 mμ, 665 mμ, 645 mμ, 630 mμ, in the aceton extraction fluid.

Optical density of 510 mμ, 480 mμ, 430 mμ, also was measured on 70 samples after

station UM-6323 for carotenoids measurement.

Calculations of chlorophyll-a, b, c, and carotenoids were done using the RICHARDS and THOMPSON's formula (1952).*

iii. Seston

Each sample was filtered as chlorophyll measurement, through Millipore-filterHA of 47 mm diameter which had been dried and weighed, and then the filter was washed through with 100 ml of pure water. Filters thus depickled were preserved like chlorophyll samples, and have been weighed again to measure seston quantity since the expedition returned to Japan.

We would like to acknowledge Mr. R. ADACHI (Technical-employee of Miye Prefectural Univ.) for his faithful cooperation.

iii. Micro plankton

2 liters of sample water were fixed with 20 ml of 40 % formalin, and left to settle for 22 hours in a 1 m-long settling cylinner, and thus concentrated to 250 ml. These are still being counted.

It has been found during examinations on their falling velocity that this concentration method failed in concentrating organisms whose effective diameters are smaller than about 40 micron. Since the photosynthetic experiments are dealing with micro-organisms of 0.45 micron, it seems now apparent that adoption of centrifugal method must be seriously considered as well as application of coagulants and precipitants.

Table 6 shows data on conditions in the photosynthetic experiment, and Table 7 shows data on photosynthetic production by tank method, SOROKIN's method and in-situ method. Table 9 shows data on chlorophyll-a. b. c, and carotenoids. Table 10 shows data on seston and attenuation coefficients.

On the return cruise surface water was sampled at 16 places. Seven of these samples were filtered through Millipore-filters of various pore sizes as a preliminary step toward the study of the size distribution of production. The findings are shown in Table 8.

---

* Chl-a mg/L $=15.6\cdot D_{665}-2.0\cdot D_{645}-0.8\cdot D_{630}$
Chl-b mg/L $=-4.4\cdot D_{665}+25.4\cdot D_{645}-10.3\cdot D_{630}$
Chl-c MSPU/L $=-12.5\cdot D_{665}-28.7\cdot D_{645}+109.0\cdot D_{630}$
Car-ac MSPU/L $=2.0\cdot(4.45\cdot D_{res.\,510}-D_{res.\,480})$
Car-nac MSPU/L $=7.6\cdot(-1.49\cdot D_{res.\,510}+D_{res.\,480})$
$\left[\begin{array}{l} D_{res.\,510}=D_{510}-0.0026\cdot\text{Chl-a}-0.0035\cdot\text{Chl-b}-0.0021\cdot\text{Chl-C} \\ D_{res.\,480}=D_{480}-0.0019\cdot\text{Chl-a}-0.0136\cdot\text{Chl-b}-0.0054\cdot\text{Chl-C} \end{array}\right]$

III. Outline Remarks

Spectral and attenuative characteristics of submarine irradiation defined in terms of relative irradiance in the researched waters can be summarized in the following table.

IG 538 mμ	100	30	10	3	1	0.3	0.1	%
IB 444 mμ	100	69	48	22.8	9			
IA 564 mμ	100	16.5	3.8	0.78	0.21	0.048	0.012	%
Depth of occurrence in the Eastern Indian Ocean in winter	Surface	6	18	29	45	61	73 m	minimum
		21	41	61	73	89	109	median
		36	56	78	87	110	127	maximum

If one use filters of the same spectral transmittancy as in the table above, one will find no difficulty of radiant source in the simulated in-situ method.

Relative irradiance of transparency-depth, considered as a standard of irradiation is found to be no standard, as the following table clearly illustrates.

Wave length in mμ	444 (Blue)	538 (Green)	564 (Amber)
$I_{Tr.}$ in %	33-83	6.3-27	2.6-15.2

Experiment under varying meteorological conditions for continuous days is production measurement by in-situ method. To discuss geographical distribution of production, it is necessary to find latitudinal distribution of the lapse time variation of the sun's altitude (**a**) with a particular sun's declination as the basis, to find the transmission coefficient of the air (**q**) under a typical weather during the season, and then to correct each datum. This q is defined by the following equation

$$I_H = J_0 \cdot \sin a \cdot q^{(\sin a)^{-1}} \qquad \log q = \sin a \cdot \log \frac{I_H}{J_0 \cdot \sin a}$$

a : sun's altitude.

I_H: in-come insolation on the sea surface.

J_0: incoming solar insolation measured at right angle outside of the atmosphere.

In our experiment the winter solstics was taken as the basis and 0.7 was considered an appropriate figure for q of the season.

Both attenuation coefficient and reflectance of irradiance indicate turbidity in the sea, but no inevitable relation with the amount of seston has been found. This is probably due to the great variety of coagulating forms of seston particles in the sea.

A conspicuous maximum layer of chlorophyll-a exists between 75-100 m, and shows a peculiar surface distribution parallel to iso-σ_{tD} or iso-viscosity surface. This maximum surface has discontinuous lines stretched to east-west direction at 6.5°S (100°E), 10.5°S

(120°E)~14.5°S (106°E) and 15.5°S (120°E)~180°S (106°E). The first two are not so clear as the last one.

The maximum zone of seston exists in a vertical belt from along the discontinuous lines of the chlorophyll-a maximum surface, and its stratification is not so clear. Therefore, no regularity in relation between the amount of seston and chlorophyll-a quantity can be found.

The maximum photosynthetic production measured by the tank method under near a light-saturated condition, appear in the upper part of the chlorophyll-a maximum surface show much smaller photosynthetic production.

Assimilation number (**mg C/mg chl-a·10 KLux·hr.**) which indicates biological activity has its maximum in 10–25 m layer. Though chemical productivity is quite small in this layer, assimilation number shows such a great value as over 10. The fact that assimilation number is a little smaller for samples taken from the surface layer is considered to be a result of obstruction by strong irradiation. In the chlorophyll-a maximum layer assimilation number is shows the normal value of 2~3.

Condition of irradiation in in-situ method is quite different from that in tank method. That many samples taken from lower layers have blue-lighting ratio greater than production ratio is found from compearing quantity of production and received irradiation in in-situ experiment with those in tank experiment. Therefore it seems that the blue element of 10 KLux irradiation in the tank causes obstractive effects of strong lighting on samples taken from layers below 75 m, where they are adapted to weak blue irradiation.

Samples from layers above 75 m show the light saturation response on blue lighting during in-situ experiment. Above 10–25 m layer light saturation occur on amber lighting too.

One-day production per unit area reaches over 150 mg C/m², and even 450 mg C/m² at the upwelling area southeast of Java.

Between the depth of the chlorophyll maximum surfrce (**D m**) and the amount of in-situ production (**C mg/m²·day**) there exists a relation apparoximately expressed in the following equation.

$$C=545-3.16\cdot D \qquad (30<D<130)$$

The chlorophyll-a maximum surface is considered as an accumulation layer of dead chlorophyll and also as a slack production layer of photosynthetic organisms adapted to weak irradiation.

High preservancy of standing crops in this layer seems to be due to the fact that the layer approximately corresponds to the compensation depth. That nutrient salts, especially nitrate, abruptly increases in quantity below this layer is a very significant feature.

Color-turning phenomenon, considered as an indication of a physiological weakness

of plants, is conspicuous in the upper and lower parts of the maximum layer of chlorophyll.

This indicates an abnormality, but production itself has both positive and negative relations and is never constant.

The following remarks can safely be made from the data obtained through a preliminary research on the size distribution of production at several places. Photosynthesis of organisms smaller than 3 micron in diameter sometimes accounted for 60 % of the total quantity. Cases where 40 % of the total photosynthesis was shared by organisms of 0.5–0.8 micron diameter were also observed. But, since Millipore-filter-HA failed to catch only 15 % of the total photosynthesis at the most, it seems proper to use Millipore-filter-HA in experiments of production.

As far as the Far Eastern waters is concerned, it was recognized organisms of 0.8–3 micron diameter increase their share in the total photosynthetic production while those of diameter less than 0.45 micron decrease their share as the location move to a higher latitude.

An abnormally high rate of biological activity for photosynthesis was noticed in the euphotic zone of the Eastern Indian Ocean during winter. Since optical potential productivity is provided sufficiently during this season, a high rate of production could be expected in this area if only chemical potential productivity were supplied sufficiently.

The fact that standing crops in upper layers remain in poor level seems to be due to an unfavorable preservance condition formed by obstructive effects of strong lighting and low viscosity caused by high water temperature.

Accordingly, it seems that the compensation depth reaches down to 75–100 m where vertical gradient of viscosity increases abruptly, and that the maximum layer of standing crops, represented by the amount of chlorophyll-a, is formed in this depth.

This makes a nice contrast with the fact that, in the upper layer of water at high latitude where both irradiation and temperature are low, standing crops are preserved in large quantity despite low biological activity and therefore comparatively larger amount of production can be observed in the uppermost layer.

Literature

FRIEND, D.T.C. (1961): A Simple Method of Measuring Integrated Light Values in the Field. Ecology, 42, (3), 577–580.

MATUSDAIRA, Y., et al., (1964): Cooperative Studies on Primary Productivity in the Coastal Waters of Japan 1962-63. Information Bulletin on Planktology in Japan, 11, 24-73.

RICHARDS, F.A. and T.G. THOMPSON, (1962): The Estimation and Characterization of Plankton Populations by Pigment Analyses II. A Spectrophotometric Method for the Estimation of Plankton Pigments. Journal of Marine Research, X, (2), 156–172.

SAKAMOTO, I. (1964): Falling Model on the Planktonic Diatoms. Report of Faculty of Fisheries, Prefectural University of Miye, 5, (1), 33-49.

List of Tables

Table 1. The time and position of sunrise, apparent noon, sunset; the azimuth and the altitude of the sun. p. 186
Table 2. Raw data of solar insolation on the horizontal surface (for each one hour with the meridian passage as the standard time). p. 190
Table 3. Relative irradiance (I_Z %) and attenuation coefficients (K). p. 194
Table 4. Reflectance (irradiance ratio)=Eu/Ed. p. 206
Table 5. Transparency, relative irradiance at the transparency depth (I_{T_r}) and the mean attenuation coefficient ($\overline{K_{T_r}}$). p. 207
Table 6. Conditions at the time of productivity experiment. p. 208
Table 7. Data on production measured by ^{14}C method. p. 217
Table 8. The size distribution of production on the surface of the Far Eastern waters. p. 219
Table 9. Data on the quantity of chlorophyll-a, b, c, and carotenoids. p. 220
Table 10. Quantity of seston and attenuation coefficients (K) at the layer of water sampling. p. 224

Table 1. The time and position of sunries, apparent noon,

Date	Time				Position			
					Sun Rise		Apparent Noon	
	Zone	Sun Rise	Mer. Pass	Sun Set	Lat.	Long	Lat.	Long
	h							
1963 Nov. 3	+9-00	06-02	11-31-16	17-03	32-31.5 N	138-37.0 E	31-30.7 N	138-05.0 E
4	+9-00	06-04	11-38-08	17-15	27-46.5 N	136-46.0 E	26-41.0 N	136-23.7 E
5	+9-00	06-06	11-44-36	17-26	23-16.3 N	135-10.0 E	22-13.8 N	134-46.5 E
6	+9-00	06-08	11-50-37	17-37	18-48.7 N	133-39.5 E	17-47.5 N	133-16.3 E
7	+9-00	06-09	11-57-00	17-49	14-17.3 N	132-02.5 E	13-10.0 N	131-40.5 E
8	+9-00	06-10	12-03-27	18-00	09-40.0 N	130-24.3 E	08-32.0 N	129-58.5 E
9	+9-00	06-12	12-09-00	18-11	05-04.0 N	128-17.5 E	04-08.0 N	128-47.5 E
10	+9-00	06-13	12-16-52	18-22	01-16.7 N	126-56.3 E	00-00.8 S	126-45.0 E
11	+9-00	06-14	12-20-05	18-33	03-10.2 S	125-46.0 E	04-13.0 S	125-54.0 E
12	+9-00	06-07	12-16-03	18-29	06-28.6 S	126-25.0 E	07-26.6 S	126-58.1 E
13	+9-00	05-58	12-13-30	18-30	09-20.3 S	127-36.2 E	09-44.3 S	127-36.5 E
14	+9-00	05-52	12-06-21	18-21	10-57.2 S	128-36.0 E	11-37.0 S	129-22.5 E
15	From 00-00 +9-30				Darwin			
16	From 00-00 +9-30							
17	From 00-00 +9-30							
18	From 00-00 +9-30							
19	From 08-00 +9-00	06-20	12-16-09	18-43	12-22.0 S	128-37.0 E	12-25.0 S	127-19.0 E
20	From 08-00 +8-30	06-09	12-05-51	18-32	12-45.0 S	123-36.0 E	12-25.0 S	122-24.0 E
21	From 08-00 +8-00	05-56	11-45-48	18-07	11-07.0 S	119-50.0 E	11-13.6 S	119-48.8 E
22	+8-00	05-24	11-45-35	18-09	12-38.0 S	119-59.0 E	12-38.0 S	119-55.8 E
23	+8-00	05-21	11-45-51	18-11	14-01.0 S	119-55.8 E	14-01.7 S	119-55.7 E
24	+8-00	05-18	11-46-30	18-15	15-31.0 S	119-58.5 E	15-34.7 S	119-59.0 E
25	+8-00	05-16	11-46-45	18-18	17-01.0 S	120-01.5 E	17-01.5 S	119-57.0 E
26	+8-00	05-16	11-48-19	18-18	17-15.0 S	120-07.5 E	17-03.0 S	119-39.0 E
27	+8-00	05-14	11-47-37	18-18	18-13.5 S	119-54.0 E	18-32.5 S	120-04.0 E
28					Broome			
29								
30	+8-00		11-40-21	18-18	Broome		17-55.0 S	122-00.0 E
Dec. 1	+8-00	05-18	11-49-43	18-22	18-28.0 S	119-25.0 E	18-15.8 S	119-45.5 E
2	+8-00	05-15	11-51-51	18-26	18-44.3 S	118-54.5 E	18-41.4 S	119-15.5 E
3	+8-00	05-24	12-01-44	18-34	17-22.0 S	118-05.0 E	16-33.0 S	116-56.5 E
4	+8-00	05-43	12-12-23	18-36	13-24.0 S	115-02.0 E	12-16.5 S	114-22.0 E
5	From 08-00 +7-30	05-59	11-48-15	18-11	09-04.0 S	113-02.9 E	09-03.0 S	113-02.5 E
6	+7-30	05-31	11-48-28	18-11	10-28.3 S	113-08.5 E	11-01.9 S	113-03.0 E
7	+7-30	05-25	11-49-53	18-16	12-33.0 S	112-48.0 E	13-04.0 S	112-48.9 E
8	+7-30	05-21	11-49-19	18-19	14-28.0 S	113-00.0 E	14-57.5 S	113-04.7 E
9	+7-30	05-19	11-49-57	18-23	16-15.5 S	113-03.2 E	16-56.0 S	113-00.8 E
10	+7-30	05-17	11-50-24	18-27	18-20.5 S	113-03.0 E	18-58.5 S	113-03.0 E
11	+7-30	05-12	11-51-31	18-32	20-25.0 S	112-55.5 E	21-03.3 S	112-50.2 E
12	From 20-00 +8-00	05-06	11-51-19	18-37	22-32.0 S	113-02.5 E	23-54.0 S	113-01.0 E
13		05-26	12-16-45		27-11.0 S	113-27.0 E	28-30.0 S	114-10.0 E
14								
15	+8-00	05-20		19-15				
16								
17								
18	+8-00	05-34	12-25-11	19-16	25-30.0 S	112-44.0 E	25-11.0 S	112-40.5 E
19	+8-00	05-34	12-26-13	19-17	25-04.0 S	112-48.0 E	25-02.0 S	112-41.0 E
20	+8-00	05-35	12-26-50	19-18	25-24.5 S	112-38.9 E	25-03.0 S	112-41.0 E
21	+8-00	05-36	12-27-40	19-15	24-42.0 S	112-40.0 E	24-59.0 S	112-29.7 E
22	+8-00	05-41	12-27-10	19-14	23-20.5 S	112-29.2 E	22-59.0 S	112-44.0 E
23	+8-00	05-45	12-31-00	19-19	23-52.6 S	111-56.0 E	24-41.3 S	111-55.4 E
24	+8-00	05-40	12-33-38	19-29	26-04.2 S	111-16.0 E	26-48.7 S	111-22.0 E
25	+8-00	05-30	12-26-40	19-24	27-53.0 S	112-55.8 E	28-43.0 S	113-19.2 E
26		05-19	12-19-42	19-24	30-32.5 S	114-26.0 E	31-36.1 S	115-07.8 E

sunsent ; the azimuth and the altitude of the sun.

Sun Set		Azimuth of the Sun			Altitude of the Sun at Apparent Noon	Drift	
Lat.	Long	Sun Rise	Mer. Pass	Sun Set		Dir.	Vel. Knot
30-25.4 N	137-42.0 E	S 73.2 E	S	S 72.8 W	43°-41	90°	0.8
25-35.5 N	136-02.4 E	S 73.5 E	S	S 73.1 W	48-12	180	0.5
21-07.3 N	134-24.1 E	S 73.6 E	S	S 73.3 W	52-21	320	0.6
16-40.0 N	132-52.5 E	S 73.7 E	S	S 73.5 W	56-29	320	0.6
12-03.0 N	131-18.3 E	S 73.8 E	S	S 73.6 W	60-48	270	0.7
07-19.6 N	129-43.2 E	S 73.6 E	S	S 73.4 W	65-08	270	0.6
03-16.3 N	128-11.5 E	S 73.4 E	S	S 73.2 W	69-15	70	1.5
01-14.2 S	126-44.0 E	S 73.2 E	S	S 73.0 W	73-06	45	1.5
04-35.3 S	125-47.5 E	S 72.8 E	S	S 72.7 W	77-01	Coasting	
08-27.5 S	127-32.2 E	S 72.4 E	S	S 72.3 W	79-58	Coasting	
09-49.0 S	127-30.5 E	S 72.0 E	S	S 71.9 W	82-00	2000-Noon 190	0.6
12-12.0 S	130-36.0 E	S 71.6 E	S	S 71.5 W	83-36	2000-Noon 190	0.4
Carwin							
12-30.0 S	126-03.0 E	S 70.4 E	S	S 70.3 W	83-09	Almost Nil	
11-51.0 S	121-19.0 E	S 70.1 E	S	S 70.0 W	82-54	80	0.8
11-04.0 S	119-46.0 E	S 70.0 E	S	S 69.9 W	81-29	210	0.6
12-38.0 S	120-04.0 E	S 69.6 E	S	S 69.5 W	82-40	270	0.4
14-06.5 S	120-04.7 E	S 69.3 E	S	S 69.1 W	83-49		
15-45.0 S	120-01.5 E	S 68.9 E	S	S 68.7 W	85-11	110	0.3
17-11.5 S	119-59.0 E	S 68.5 E	S	S 68.3 W	86-26	Almost Nil	
17-01.0 S	119-54.0 E	S 68.3 E	S	S 68.2 W	86-05		
18-29.0 S	120-09.0 E	S 68.1 E	S	S 68.0 W	87-33		
18-02.0 S	120-34.0 E	S 67.1 E	S	S 67.3 W	86-24		
18-07.0 S	119-55.0 E	S 66.9 E	S	S 67.0 W	86-35		
18-29.0 S	119-30.0 E	S 66.9 E	S	S 66.8 W	86-51		
15-27.0 S	116-15.0 E	S 67.2 E	S	S 67.1 W	84-40	30	0.3
11-04.0 S	113-53.0 E	S 67.4 E	S	S 67.4 W	80-08	330	0.3
08-58.0 S	113-01.5 E	S 67.2 E	S	S 67.3 W	76-47	230	0.5
11-04.0 S	112-58.0 E	S 66.9 E	S	S 67.1 W	78-38	280	0.5
13-00.5 S	112-49.0 E	S 66.6 E	S	S 66.8 W	80-28	270	0.6
14-51.5 S	113-03.3 E	S 66.4 E	S	S 66.5 W	82-20	unknoun	
16-55.8 S	113-08.2 E	S 66.0 E	S	S 66.3 W	84-11	80	0.4
18-54.3 S	113-04.0 E	S 65.4 E	S	S 65.9 W	86-07	80	0.7
20-58.5 S	112-54.5 E	S 65.0 E	S	S 65.2 W	88-07	310	0.4
25-14.0 S	113-46.0 E	S 64.0 E	N	S 64.4 W	89-07	40	0.3
Geraldton (15h20m)		S E	N	S W	84-40	Coasting	
Geraloton							
25-04.0 S	112-44.5 E	S 64.0 E	N	S 64.0 W	88-13		
24-47.0 S	112-45.5 E	S 64.0 E	N	S 64.0 W	88-22		
24-53.5 S	112-34.0 E	S 64.0 E	N	S 64.0 W	88-22		
24-40.5 S	112-53.0 E	S 63.9 E	N	S 63.9 W	88-27	Var.	
22-54.5 S	112-48.0 E	S 64.4 E	S	S 64.4 W	89-32		
24-56.8 S	112-16.5 E	S 64.4 E	N	S 64.2 W	88-45		
26-57.0 S	111-45.5 E	S 63.7 E	N	S 63.5 W	86-38	06-00 350	0.7
29-02.5 S	113-27.4 E	S 63.3 E	N	S 63.1 W	84-42	06-00 110	0.8
Fremantle			N		81-47	160	0.2

Table 1. continued

Date	Time				Position			
					Sun Rise		Apparent Noon	
	Zone	Sun Rise	Mer. Pass	Sun Set	Lat.	Long	Lat.	Long
	h							
27								
28								
29								
30								
31								
1964 Jun. 1								
2	+8-80			19-28			Fremantle	
3	From 08-00 +7-30	05-32	12-06-49	19-08	29-58.2 S	113-01.5 E	29-03.0 S	111-43.9 E
4	From 08-00 +7-00	05-24	11-54-18	18-50	26-41.3 S	108-43.5 E	25-55.2 S	107-32.5 E
5	+7-00	05-12	12-00-57	18-50	24-58.5 S	105-58.7 E	25-01.2 S	106-02.6 E
6	+7-00	05-18	12-01-09	18-46	23-33.5 S	106-00.5 E	23-12.0 S	106-04.5 E
7	+7-00	05-26	12-07-20	18-50	22-06.5 S	105-05.0 E	22-02.5 S	104-39.5 E
8	+7-00	05-25	12-02-17	18-47	21-18.0 S	105-18.0 E	20-57.2 S	105-52.0 E
9	+7-00	05-26	12-02-43	18-39	19-17.5 S	106-01.9 E	18-57.5 S	105-59.6 E
10	+7-00	05-29	12-03-08	18-36	17-28.8 S	106-03.9 E	16-58.5 S	106-06.0 E
11	+7-00	05-34	12-03-33	18-33	15-31.5 S	106-05.0 E	15-05.8 S	106-02.5 E
12	+7-00	05-36	12-03-33	18-29	13-39.0 S	106-06.0 E	12-59.0 S	106-06.0 E
13	+7-00	05-41	12-04-20	18-26	11-17.0 S	106-05.0 E	11-01.0 S	106-02.5 E
14	+7-00	05-49	12-06-43	18-27	09-53.5 S	105-07.0 E	11-03.4 S	105-31.5 E
15	+7-00	05-48	12-05-25	18-23	09-22.7 S	106-00.2 E	08-59.0 S	105-55.1 E
16	From 20-00 +6-30	05-54	12-18-27	18-43	09-32.4 S	103-59.2 E	09-58.8 S	102-47.0 E
17	+6-30	05-38	12-00-48	18-22	11-03.0 S	99-52.0 E	11-01.8 S	99-45.1 E
18	+6-30	05-40	12-00-08	18-28	09-23.3 S	100-03.0 E	09-24.0 S	99-59.0 E
19	+6-30	05-44	12-00-28	18-15	07-58.5 S	100-02.0 E	08-03.5 S	100-03.5 E
20	+6-30	05-48	12-01-27	18-15	06-44.6 S	99-51.0 E	06-47.0 S	99-59.0 E
21	+6-30	05-50	12-01-05	18-12	05-29.0 S	99-58.0 E	05-29.0 S	99-57.4 E
22	+6-30	05-53	12-03-06	18-14	03-55.1 S	99-34.2 E	03-55.0 S	99-35.9 E
23	+6-30	06-02	12-16-46	18-25	03-52.0 S	97-29.4 E	03-48.5 S	96-12.7 E
24	+6-30	06-13	12-16-42	18-19	00-11.2 S	96-16.9 E	01-05.0 N	96-18.0 E
25	+6-30	06-24	12-23-17	18-18	03-28.0 N	94-44.0 E	04-45.0 N	94-44.5 E
26	From 20-00 +7-30	06-24	12-13-55	18-05	07-14.1 N	96-00.0 E	07-13.7 N	97-11.6 E
27					Penang			
28								
29								
30								
31	+7-30	07-06	13-02-59	19-02	Penang		04-48.2 N	100-05.3 E
Feb. 1	+7-30	06-56	12-50-58	18-50	02-10.0 N	102-03.0 E	01-23.0 N	103-08.0 E
2	+7-30	06-37	12-34-01	18-32	01-57.2 N	106-24.5 E	02-15.8 N	107-24.0 E
3	+7-30	06-24	12-20-09	18-16	03-29.9 N	109-59.0 E	03-46.0 N	110-55.7 E
4	+7-30	06-11	12-06-32	18-00	04-54.0 N	113-36.0 E	05-27.0 N	114-17.5 E
5	+7-30	06-05	11-58-30	17-49	07-33.0 N	115-52.3 E	08-17.0 N	116-22.0 E
6	+7-30	06-00	11-49-15	17-37	10-54.4 N	118-12.3 E	11-49.5 N	118-44.0 E
7	From 20-00 +8-00	06-00	11-45-56	17-28	15-06.7 N	119-17.8 E	16-16.6 N	119-32.0 E
8	+8-00	06-19	12-09-51	17-47	19-55.0 N	120-52.0 E	21-07.0 N	121-06.5 E
9	+8-00	06-26	12-00-40	17-31	24-47.8 N	122-53.5 E	25-50.5 N	123-23.5 E
10	From 20-00 +9-00	06-22	11-51-32	17-22	28-11.0 N	125-04.8 E	28-51.7 N	125-39.8 E
11	+9-00	07-28	12-49-09	18-20	29-21.5 N	126-17.2 E	29-19.8 N	126-13.5 E
12	+9-00	07-17	12-47-02	18-15	29-43.0 N	126-30.0 E	30-19.2 N	126-53.5 E
13	+9-00	07-06	12-32-30	18-00	30-55.8 N	129-19.0 E	30-55.4 N	130-30.4 E
14	+9-00	06-59	12-30-29	17-55	Ariake-wan		31-23.4 N	131-04.4 E
15	+9-00	06-47	12-12-35	17-05	32-53.5 N	134-19.5 E	33-09.0 N	135-34.0 E
16	+9-00	06-30	11-54-46	17-23	34-39.0 N	139-11.5 E	35-00.0 N	139-50.5 E
17	+9-00	06-27	11-55-05	17-24	Tōkyō		35-39.0 N	139-46.0 E

Table 1. continued

Sun Set		Azimuth of the Sun			Altitude of the Sun at Apparent Noon	Drift	
Lat.	Long	Sun Rise	Mer. Pass	Sun Set		Dir.	Vel. Knot
31-21.2 S	114-48.0 E		N	S 62.9 W	83-53	19-00	
28-05.0 S	110-30.2 E	S 63.2 E	N	S 63.8 W	83-53	16.00-05.00 40 / 05.00-12.00 230	0.2 / 0.4
25-15.0 S	106-20.0 E	S 64.2 E	N	S 64.5 W	86-54	Nil	
24-55.4 S	106-06.0 E	S 64.8 E	N	S 64.8 W	87-42	20	0.3
23-11.5 S	106-08.5 E	S 65.3 E	N	S 65.4 W	89-25	180	0.4
22-05.0 S	104-40.0 E	S 65.6 E	S	S 65.7 W	89-55	Almost nil	
20-47.0 S	105-52.0 E	S 65.9 E	S	S 66.0 W	88-35		
18-50.0 S	105-58.7 E	S 66.2 E	S	S 66.5 W	86-43	360	0.7
16-52.0 S	106-07.0 E	S 66.7 E	S	S 66.9 W	84-53		
15-01.5 S	106-04.8 E	S 67.2 E	S	S 67.4 W	83-09	90	0.4
12-52.0 S	106-05.5 E	S 67.5 E	S	S 67.7 W	81-12	350	0.4
10-59.0 S	106-02.0 E	S 67.9 E	S	S 68.0 W	79-22	340	0.4
10-11.3 S	105-35.1 E	S 68.1 E	S	S 68.2 W	78-35		
08-55.0 S	105-50.7 E	S 68.3 E	S	S 68.3 W	77-41	330	0.4
10-25.0 S	101-38.0 E	S 68.5 E	S	S 68.5 W	78-52	300	0.4
10-57.5 S	99-53.3 E	S 68.8 E	S	S 68.7 W	80-06	near Station 300	0.8
09-17.5 S	100-11.4 E	S 68.9 E	S	S 69.0 W	78-41	near Station 300	0.2
07-58.1 S	100-19.2 E	S 69.4 E	S	S 69.3 W	77-31	150	0.5
06-50.0 S	99-50.7 E	S 69.5 E	S	S 69.4 W	76-28	120	0.7
05-15.0 S	99-51.3 E	S 69.7 E	S	S 69.8 W	75-22	05.00-12.00 290	0.4
03-53.4 S	99-12.8 E	S 70.0 E	S	S 70.1 W	74-02	330	0.2
02-39.0 S	96-14.0 E	S 70.2 E	S	S 70.3 W	74-09	270	0.3
02-00.9 N	95-56.5 E	S 70.5 E	S	S 70.6 W	69-29	Var. Weak	
06-55.5 S	94-41.2 E	S 70.7 E	S	S 70.8 W	67-04	10	0.5
06-44.0 N	97-52.6 E	S 70.8 E	S	S 71.0 W	63-50	330	0.5
03-37.2 N	100-16.3 E	S E	S	S 72.4 W	67-33	Coasting	
01-21.0 N	104-23.0 E	S 72.6 E	S	S 72.8 W	71-15	Coasting	
02-50.9 N	108-15.0 E	S 72.9 E	S	S 73.0 W	70-39	180	1.0
04-02.0 N	111-52.0 E	S 73.1 E	S	S 73.3 W	69-26	240	0.8
06-14.2 N	114-54.8 E	S 73.4 E	S	S 73.5 W	68-01	240	0.8
09-07.9 N	117-02.5 E	S 73.5 E	S	S 73.6 W	65-29	250	0.8
12-51.5 N	118-58.7 E	S 73.6 E	S	S 73.6 W	62-15	Coasting	
17-26.6 N	119-59.3 E	S 73.7 E	S	S 73.6 W	58-05	Coasting	
22-16.3 N	121-30.0 E	S 73.6 E	S	S 73.7 W	53-35	310	1.1
26-35.5 N	123-46.7 E	S 73.3 E	S	S 73.2 W	49-10	—	
29-13.7 N	125-56.4 E	S 73.3 E	S	S 73.3 W	46-48	—	
29-23.0 N	125-59.0 E	S 73.5 E	S	S 73.6 W	46-22	—	
31-02.5 N	127-20.2 E	S 73.7 E	S	S 73.6 W	45-39	—	
Ariake-wan		S 73.9 E	S	S	45-22	—	
31-42.4 N	131-53.4 E	S E	S	S 74.3 W	45-15	—	
33-33.6 N	136-34.9 E	S 73.4 E	S	S 73.4 W	43-48	—	
Tōkyō			S	S W	42-18		
Tōkyō			S	S W	42-00		

Table 2. Rawdata of solar insolation on the horizontal surface

Station No.	Data 1963	Δt_R* min.	Half day total g·cal/cm²	Each 1 hour g·cal/cm². Before Mer. Pass						Mer. Pass	
				6h	5h	4h	3h	2h	1h	Alt -⊙-	g·cal/cm²·min
	Nov. 4	—	—	—	—	—	—	19.5	20.7	19.5	48-12	0.383
	5	+5	225.9	0	3.0	18.4	35.6	51.7	54.0	63.2	52-21	1.072
	6	+10	238.1	0	4.6	23.0	39.1	56.4	64.4	50.6	56-29	1.149
	7	−40	149.2	0	0	8.7	21.2	34.0	42.3	43.0	60-48	0.735
	8	0	—	0	5.8	18.4	41.4	—	—	—	65-08	—
	9	0	280.4	0	7.8	25.3	44.9	59.8	69.0	73.6	69-15	1.225
	10	0	268.7	0	8.1	26.4	40.2	54.3	65.5	74.2	73-06	1.265
	11	0	262.7	0	6.2	21.4	39.3	55.9	67.4	72.5	77-01	1.245
	12	−5	286.2	0	6.9	27.1	46.4	61.9	69.9	74.0	79-58	1.320
	13	0	253.0	0.1	6.2	20.7	38.6	54.5	63.2	69.7	82-00	1.190
	14	+3	268.6	0.2	5.8	18.4	40.7	62.1	64.4	77.0	83-36	1.320
	15	—	290.0	0.1	5.8	29.2	50.6	58.2	71.3	74.8		1.245
	16	—	245.0	0	1.0	18.4	36.1	52.9	65.6	71.0		1.225
	17	—	284.5	0.5	9.2	27.6	45.3	59.8	68.5	73.6		1.265
	18	—	289.1	0.9	12.0	34.5	43.7	57.5	67.4	73.1		1.265
	19	+5	275.5	0.5	9.0	29.9	51.0	63.2	46.5	75.4	83-09	1.300
	20	+5	321.6	0.9	10.8	32.2	53.4	66.7	75.9	81.7	82-54	1.300
UM-6301	21	+10	298.6	0.7	11.5	27.6	47.6	64.4	70.4	76.4	81-29	1.340
UM-6302	22	+10	297.3	0.9	11.5	30.6	45.5	61.1	72.0	75.7	82-40	1.380
UM-6303	23	0	262.3	0.7	11.2	27.1	34.5	57.0	62.1	69.7	83-49	1.380
UM-6304	24	+5	300.7	0.8	13.1	33.6	46.7	59.4	71.2	75.9	85-11	1.300
UM-6305	25	−5	300.6	0.9	9.2	29.4	48.7	57.9	74.0	80.5	86-26	1.360
	26	0	299.2	0.9	7.4	31.0	50.4	59.6	72.4	77.5	86-05	1.340
UM-6306′	27	0	290.0	1.8	11.5	30.1	45.1	54.3	69.0	78.2	87-33	1.340
	28	—	300.4	0.9	11.5	28.0	49.9	62.1	71.0	77.0		1.320
	29	—	215.4	5.5	20.4	34.7	44.2	42.1	35.9	32.6		0.500
	30	—	285.2	1.6	13.8	28.3	38.9	52.9	70.1	79.6	86-24	1.350
	Dec. 1	+15	299.8	1.8	12.9	31.5	49.2	61.2	69.0	74.2	86-35	1.265
	2	+5	298.9	2.3	10.8	29.2	50.6	61.4	67.8	76.8	86-51	1.320
	3	0	304.0	1.6	12.4	31.3	50.1	62.8	70.8	75.0	84-40	1.280
	4	0	302.4	1.4	11.5	32.0	51.0	62.1	71.0	73.4	80-08	1.285
UM-6306	5	0	235.0	0.1	7.1	20.2	33.8	55.6	56.8	61.4	76-47	1.110
UM-6307	6	0	270.4	0.1	6.9	20.7	44.9	59.8	69.0	69.0	78-38	1.270
UM-6308	7	−10	274.5	0.7	6.9	23.4	43.2	56.3	69.0	75.0	80-28	1.300
UM-6309	8	0	301.3	1.6	12.0	30.4	46.7	59.8	71.9	78.9	82-20	1.340
UM-6310	9	0	302.6	0.7	9.2	29.9	48.3	62.1	73.5	78.9	84-11	1.360
UM-6311	10	0	305.1	1.6	11.5	32.2	48.5	62.5	70.6	78.2	86-07	1.400
UM-6312	11	0	289.0	1.6	12.2	25.3	44.1	62.1	63.2	80.5	88-07	1.450
	12	0	292.7	0.7	8.5	19.8	40.0	60.7	79.1	83.9	89-07	1.450
	13	0	302.1	3.0	9.7	25.0	45.5	60.9	73.6	84.4	84-40	1.510
	14	—	279.4	0.2	3.9	21.1	46.0	61.0	69.0	78.2		1.380
	15	—	352.2	8.8	24.2	36.1	56.8	73.4	71.3	81.6		1.380
	16	—	331.8	3.5	17.7	34.9	53.8	66.7	75.9	79.3		1.360
	17	—	343.6	5.8	21.8	36.8	53.8	66.7	75.9	82.8		1.400
	18	−20	190.7	1.2	4.4	13.8	25.3	44.8	43.7	57.5	88-13	1.000
	19	+5	345.0	4.6	18.4	34.5	55.2	71.3	78.2	82.8	88-22	1.430
	20	−5	323.7	1.8	15.4	31.0	51.5	66.3	77.0	80.7	88-22	1.420
UM-6313′	21	−5	301.5	3.5	12.2	32.6	41.4	50.1	78.9	82.8	88-27	1.435
UM-6313	22	−5	301.8	2.3	12.0	29.9	50.6	64.4	73.6	69.0	89-32	1.460
	23	0	252.5	2.3	8.3	20.7	35.6	46.0	62.1	77.5	88-45	1.420
	24	−15	193.8	2.3	7.8	23.0	23.9	29.9	39.8	67.1	86-38	1.460
	25	0	269.0	4.4	16.5	32.6	33.4	42.8	65.1	74.2	84-42	1.540
	26	0	215.0	2.1	6.9	15.6	26.0	36.6	65.3	62.5	81-47	1.360
	27	—	307.8	?	11.5	32.2	52.2	58.9	69.5	83.5		1.435
	28	—	343.1	9.2	25.3	29.9	59.8	66.7	83.2	69.0		1.520
	29	—	304.2	2.3	16.1	29.9	53.6	61.6	69.4	71.3		1.555
	30	—	373.9	9.2	27.6	45.1	61.1	71.5	75.9	83.5		1.460
	31	—	370.3	10.1	27.1	46.7	61.4	71.0	74.0	80.0		1.380

(for each one hour with the meridian passage as the standard time).

Each 1 hour g·cal/cm². After Mer. Pass							Half day total g·cal/cm²	Δt_S** min.	q***	Cloudiness	
1h	2h	3h	4h	5h	6h				at apparent noon		
39.5	42.5	36.8	19.5	10.6	0.9	0	149.8	+5	0.366	Sc, Cu	6
62.1	57.5	48.3	34.5	17.2	2.3	0	221.9	+5	0.743	Cu	2
66.7	62.0	52.9	36.8	17.2	4.6	0	240.2	+5	0.741	Cu	3
36.8	21.2	26.9	18.4	13.1	3.9	0	120.3	0	0.475	Ac	10
—	—	—	—	—	—	—		0		As, Cu	6
71.3	65.3	56.6	40.9	23.7	5.1	0	262.9	0	0.732	Cu	2
75.0	64.8	64.4	43.7	23.7	6.9	0	278.5	+15	0.680	Ac	3
71.5	63.2	56.1	39.8	20.2	6.4	0	257.2	0	0.653	As, Ac	7
78.2	73.6	64.4	32.2	32.2	12.4	0.2	293.2	+5	0.681	Ac, Cu	2
69.0	64.0	54.5	37.9	21.8	7.6	0.5	255.3	0	0.611	Sc	10
78.2	73.1	63.2	47.6	27.6	7.8	0.1	297.6	0	0.683	Cu	1
72.5	66.7	55.1	41.8	22.7	9.2	0.5	268.5	—			
72.5	64.0	58.6	43.7	23.0	10.3	1.4	273.5	—			
73.6	68.5	59.3	40.7	21.6	9.0	1.4	274.1	—			
71.3	68.5	60.2	43.9	20.7	6.2	0.3	271.1	—			
72.9	51.7	52.2	64.9	25.3	8.5	1.2	276.7	+30	0.657	Sc	1
83.5	82.2	73.6	57.0	36.8	14.2	1.2	348.5	+20	0.661	Cc	1
75.7	69.9	55.2	44.6	24.2	6.9	0.6	277.1	0	0.685	Cu	2
77.5	69.9	60.2	43.9	19.8	6.5	0.5	278.3	0	0.701	Cc, Cu	3
66.9	71.7	58.2	43.9	28.3	11.5	1.2	281.7	+5	0.699	St, Cu	6
77.7	73.0	63.2	48.1	29.0	10.1	0.8	301.9	0	0.657	Ac, Cu	2
79.6	75.4	66.0	52.7	31.3	12.9	1.4	319.3	+5	0.685	Cs	2
78.2	74.0	58.4	49.4	32.0	14.7	1.2	307.9	0	0.675	Sc, Cc	2
78.2	73.6	63.5	50.6	32.9	9.9	1.6	310.3	+10	0.673	As, Cs	1
78.2	73.6	57.7	46.4	26.5	12.0	1.8	296.2	—			
63.0	61.9	28.0	15.9	19.3	12.6	1.6	202.3	—			
79.1	68.8	60.9	46.9	28.0	10.6	0.9	295.2	0	0.679	As	3
74.0	66.7	56.8	46.4	29.9	11.3	0.9	286.0	0	0.631	Cu	10
75.7	70.6	60.5	44.6	23.2	6.9	0.9	282.4	0	0.664	St	4
74.0	68.5	58.2	44.4	28.5	12.2	1.2	287.0	+5	0.645	Cu	3
75.2	67.4	58.2	44.1	29.0	7.8	0.3	282.0	−5	0.657	Cu	1
59.1	62.1	58.0	39.8	30.4	11.0	1.0	261.4	0	0.580	As, Sc	6
75.9	71.3	51.0	39.1	25.3	7.6	0.2	270.4	−5	0.654	Cu	5
74.0	70.2	59.8	37.5	23.9	9.2	1.4	276.0	0	0.663	St	6
77.7	72.6	64.4	49.0	29.4	10.6	0.2	303.9	+5	0.688	Cs	1
80.2	75.9	67.8	55.2	36.8	17.2	2.3	335.4	+10	0.695		0
79.3	76.6	68.9	55.8	39.5	18.4	2.3	340.8	+5	0.704	Ac	4
85.1	75.9	72.9	57.5	39.8	23.0	5.1	359.3	+20	0.725	Sc, Cu	4
83.9	80.5	73.1	59.1	42.3	20.7	4.6	364.2	+10	0.725	Cu	1
75.0	54.0	58.8	51.8	30.8	16.1	2.3	283.8	—	0.758	Ci, Cu	4
80.5	78.2	68.3	56.4	40.0	20.0	6.9	350.3	—			
66.7	69.0	52.7	37.2	22.3	6.9	0.3	255.1	0			
79.3	73.6	64.4	50.6	35.6	20.7	4.8	329.0	—			
81.7	77.0	67.8	54.7	40.7	23.0	6.7	351.6	—			
80.5	71.3	50.6	50.6	25.3	11.5	2.3	292.1	0	0.501	Ac, St	9
82.8	73.6	69.0	52.9	34.5	16.1	2.3	331.2	−10	0.715	Ac, Cu	4
79.3	73.4	69.0	56.1	39.3	21.1	4.6	342.8	+10	0.710	Cs	3
84.4	76.6	65.6	56.1	42.1	17.5	4.1	346.4	+15	0.718	Ac, Cu	6
80.5	74.5	67.4	60.3	40.5	20.9	4.8	348.9	+5	0.728	St, Cc	6
81.5	73.3	53.8	44.8	27.6	16.1	4.1	301.2	+10	0.710	Ac	6
83.5	80.7	55.9	35.4	20.0	12.6	4.4	292.5	+5	0.732	Cu	5
82.8	69.9	71.3	60.7	40.7	22.1	4.4	351.9	0	0.774	Ac, Cu	7
71.7	75.9	64.0	43.7	32.2	17.9	7.4	312.8	+10	0.697	St	9
83.2	80.5	70.1	57.0	39.1	23.0	6.0	358.9	—			
85.1	73.1	37.9	17.0	14.9	11.5	6.0	245.5	—			
68.0	69.7	62.8	34.7	27.6	13.8	6.9	283.5	—			
84.0	81.4	71.3	56.6	39.8	19.8	4.4	357.3	—			
81.2	76.3	65.3	49.0	33.3	12.6	3.0	320.7	—			

Table 2. continued

Station No.	Data 1963	Δt_R* min.	Half day total g·cal/cm²	Each 1 hour g·cal/cm². Before Mer. Pass							Mer. Pass	
				6h	5h	4h	3h	2k	1h		Alt -⊙-	g·cal/cm²·min
	1964											
	Jan. 1	—	351.1	6.9	23.0	42.5	58.2	69.0	70.0	81.5		1.420
	2	—	381.7	6.9	26.4	47.4	61.9	73.6	80.2	85.3		1.470
	3	+15	391.9	10.0	28.7	47.6	63.2	74.3	81.9	86.2	83-53	1.455
	4	−15	213.8	3.0	6.4	14.7	23.9	44.4	42.5	78.9	86-54	1.470
UM-6314	5	0	156.2	3.5	11.5	12.2	16.1	27.6	30.6	54.7	87-42	1.420
UM-6315	6	+5	343.4	3.9	21.4	42.5	51.0	65.5	75.9	83.2	89-25	1.430
	7	+10	340.2	4.1	19.8	42.7	55.2	70.1	74.8	73.5	89-55	1.500
UM-6316	8	−10	272.0	1.6	10.3	25.5	20.7	56.8	80.5	76.6	88-35	1.435
UM-6317	9	+5	311.0	2.3	9.2	33.8	46.0	62.1	73.6	84.0	86-43	1.450
UM-6318	10	−20	248.9	0.2	4.6	18.4	45.1	47.2	62.1	71.3	84-53	1.570
UM-6319	11	0	260.9	1.4	8.7	17.2	33.4	67.2	53.0	80.0	83-09	1.435
UM-6320	12	0	329.1	1.4	13.8	34.5	57.5	66.7	73.6	81.6	81-12	1.390
UM-6321	13	+5	306.3	1.4	12.9	31·0	44.8	64.4	73.6	78.2	79-22	1.430
	14	−5	241.3	0	5.3	20.7	37.5	60.5	69.0	48.3	78-35	1.430
UM-6322	15	−10	159.9	0	8.7	23.2	39.7	37.7	27.6	23.0	77-41	0.520
	16	+5	316.0	0.7	9.9	28.8	54.0	66.7	76.8	79.1	78-52	1.420
UM-6323	17	0	250.7	1.6	11.5	26.4	36.8	51.8	42.1	80.5	80-06	1.210
UM-6324	18	+5	305.8	0.7	10.8	28.7	50.6	65.5	72.5	77.0	78-41	1.320
UM-6325	19	+20	161.6	0.5	5.8	15.0	29.9	36.8	36.8	36.8	77-31	0.650
UM-6326	20	+10	296.0	0.5	9.2	28.8	50.5	57.5	75.9	73.6	76-28	1.380
UM-6327	21	0	260.6	0.2	10.8	24.4	43.7	62.1	60.7	58.7	75-22	1.340
UM-6338	22	0	270.7	0	5.1	27.1	46.5	51.7	66.7	73.6	74-02	1.300
	23	−5	271.4	0	4.6	23.0	45.5	57.5	67.0	73.8	74-09	1.420
	24	−105	37.5	0	0	0	3.5	6.4	11.5	16.1	69-29	0.326
	25	+5	173.7	0	5.8	16.1	31.0	24.2	48.3	48.3	67-04	0.460
	26	0	251.9	0	4.1	20.7	40.2	50.6	63.2	73.1	63-50	1.260
	27	—	287.9	0	5.8	28.7	48.3	62.1	71.3	71.7		1.200
	28	—	284.7	0	8.7	26.4	49.5	61.0	67.8	71.3		1.220
	29	—	279.5	0	6.4	24.8	45.1	60.5	69.7	73.0		1.220
	30	—	271.3	0	4.6	23.0	42.5	58.6	69.0	73.6		1.250
	31	0	262.1	0	3.5	23.0	41.3	59.8	70.1	64.4	67-33	0.800 ~1.360
	Feb. 1	0	254.4	0	3.0	20.7	36.8	55.2	65.1	73.6	71-15	1.420
	2	+5	102.2	0	3.5	10.3	17.2	18.4	17.2	35.6	70-39	0.880
	3	0	242.3	0	4.6	18.4	37.9	45.1	60.2	76.1	69-26	1.250
	4	0	250.2	0	5.3	16.1	38.0	58.6	63.2	69.0	68-01	1.150
	5	+10	280,8	0	5.3	21.4	45.5	59.8	72.5	76.3	65-29	1.310
	6	+5	246.1	0	4.6	17.3	39.1	54.0	59.8	71.3	62-15	1.210 ~1.150
	7	0	281.8	0	5.8	27.6	46.0	61.0	69.0	72.4	58-05	1.230
	8	−5	243.6	0	1.2	19.5	35.6	52.9	64.4	70.0	53-35	1.190
	9	+10	254.8	0	2.5	22.3	42.1	56.8	64.4	66.7	49-10	1.220
	10	−25	48.7	0	0	2.3	6.9	11.5	14.2	13.8	46-48	0.190
	11	−32	20.4	0	0	1.2	3.0	4.6	5.8	5.8	46-22	0.115
	12	−20	48.2	0	0	2.3	4.6	12.6	14.9	13.8	45-39	0.290 ~0.640
	13	0	63.9	0	0.7	4.6	6.9	18.4	17.2	16.1	45-22	0.375
	14	−5	215.0	0	0	13.8	32.2	46.0	57.5	65.5	45-15	1.090
	15	+5	39.1	0	0	2.3	6.9	6.9	10.8	12.2	43-48	0.203
	16	+5	198.6	0	1.2	11.0	26.9	42.5	56.3	60.7	42-18	0.995
	17	0	146.9	0	0	8.8	13.8	28.8	40.3	55.2	42-00	0.980

* Δt_R { +: Sensitive from betore the sunrise. −: Sensitive from after the sunrise. } expressed in minutes.

** Δt_S { +: Insensitive from after the sunset. −: Insensitive from befor the sunset. }

*** q: Transmission coefficient of the Air. $I_H = J_0 \cdot \sin a \cdot q^{1/\sin a}$.
J_0: Solar constant

Table 2. continued

Each 1 hour g·cal/cm². After Mer. Pass							Half day total g·cal cm²	Δt_S** min.	q***	Cloudiness	
1h	2h	3h	4h	5h	6h				at apparent noon		
79.3	77.7	68.3	54.7	38.4	20.5	5.3	344.2	—			
85.3	80.5	67.1	50.6	33.1	18.4	3.7	338.7	—			
83.7	76.8	67.6	54.5	34.3	20.2	5.3	342.4	0	0.741	Ac	2
83.5	72.7	52.9	32.9	20.0	10.1	0.7	272.8	−20	0.735	Ac, Cu	3
37.5	47.9	49.7	43.5	24.8	15.4	3.5	222.3	+5	0.709	Sc, Cu	8
84.6	79.8	69.2	45.3	25.8	14.0	4.1	322.8	+15	0.713	Cu	2
84.0	75.0	66.7	55.0	35.9	13.8	2.8	333.2	+15	0.748	St, Cu	5
82.8	77.0	65.1	43.7	19.5	10.3	1.8	300.2	−5	0.715	Sc, Cu	6
83.2	57.0	38.8	33.1	25.8	12.6	2.1	252.6	+10	0.727	Cu	3
80.5	64.9	57.7	36.8	24.6	14.0	1.5	280.0	0	0.787	Sc, Cu	6
81.6	75.4	67.8	53.8	35.2	14.2	0.9	328.9	0	0.724	Sc, Cu	5
81.6	74.3	66.7	55.2	32.2	11.5	1.2	322.7	0	0.706	As, Cu	2
69.0	62.1	66.7	52.9	34.5	13.1	0.9	299.2	- +5	0.731	As, St	4
81.6	74.8	60.2	51.0	34.7	16.3	2.3	320.9	+20	0.733	Ci, Cu	7
35.6	29.9	56.3	49.5	32.5	15.8	4.4	224.0	+40	0.274	Sc, Cu	9
70.0	54.0	50.1	36.6	23.7	9.2	0.4	244.0	+10	0.727	Sc, Cu	6
60.5	68.3	52.2	28.1	12.0	5.1	0	226.2	−10	0.619	St, Cu	10
78.6	72.5	63.0	46.7	25.3	6.9	0.2	292.6	0	0.677	Ci, Cu	4
55.1	44.8	36.8	41.4	29.9	6.9	0.7	215.6	+15	0.341	Sc, Cu	9
75.9	65.0	57.0	42.1	21.8	6.9	0.2	268.9	0	0.716	Ci, Cu	8
74.0	67.2	57.5	43.7	26.4	8.1	0.2	277.1	+10	0.700	Ac, Cu	6
59.8	23.0	32.0	42.1	23.7	8.1	0.5	189.2	0	0.685	St, Cu	4
66.7	66.7	52.9	41.2	24.2	8.1	0	259.8	+5	0.668	Cb, Cu	6
20.7	6.9	4.6	10.3	9.2	4.1	0	55.8	−10	0.194	St	10
64.4	64.4	55.2	36.3	16.3	2.3	0	238.9	+5	0.280	Sc, Cu	7
73.6	63.2	56.8	43.7	18.4	2.3	0	258.0	0	0.729	Ac, Ci	2
69.0	59.8	48.3	36.3	17.9	3.0	0	234.3	—			
70.0	63.2	46.0	31.8	15.6	2.3	0	228.9	—			
72.6	66.7	57.0	36.4	16.1	4.4	0	253.2	—			
72.5	66.7	55.9	39.1	20.7	5.3	0	260.2	—			
69.0	51.7	52.9	33.8	26.4	5.3	0	239.1	0			
74.8	47.1	19.5	18.4	12.6	4.6	0	177.0	0	0.764	Cs, Cu	7
43.9	58.2	35.6	18.4	6.9	2.3	0	165.3	0	0.489	Cb, Cu	9
69.2	59.8	58.2	35.6	19.5	3.5	0	245.8	0	0.687	Ci, Cu	6
69.0	65.5	43.7	28.8	12.6	3.5	0	223.1	+5	0.645	As, Cs	5
76.0	66.7	58.6	36.8	11.5	2.3	0	251.9	−15	0.744	As, Cu	6
65.5	62.1	55.2	34.5	16.1	1.6	0	235.0	0	0.717 0.686	As, St	6
71.3	63.2	33.3	34.5	20.7	3.5	0	226.5	+5	0.764	As, Cu	3
69.0	63.2	49.4	34.5	16.1	0.2	0	232.4	0	0.788	Cu	1
29.4	26.0	32.9	20.0	6.4	1.1	0	115.8	+45	0.853	Sc, Cu	8
11.5	8.1	6.9	4.6	4.6	2.3	0	38.0	−25	0.227	As, Sc	10
12.9	10.6	6.0	4.6	2.3	0	0	36.4	−10	0.162	Sc, Ns	10
21.2	20.7	18.4	11.5	4.6	0.2	0	76.6	−15	0.321 0.565	Sc	10
41.4	50.6	42.5	17.7	8.1	1.2	0	161.5	+30	0.389	Sc	10
62.1	58.6	46.0	27.6	10.3	0	0	204.6	+15	0.833	Sc	1
13.3	12.6	7.6	5.1	1.2	0	0	39.8	+25	0.266	As, Sc	10
57.5	52.5	41.4	25.3	9.4	0.5	0	186.6	0	0.820		0
57.5	50.6	25.3	6.5	0.5	0	0	140.4	−25	0.822	Sc	4

UNESCO ARCHIVES

Table 3. Relative irradiance (Iz %) and attenuation coefficients ($K \cdot 10^3$).

3-0

i	Station UM-	vii	Z: Layer of Observation (m)
ii	(L. M. T. h m	viii	C: Collecting Surface (%)
iii	(Sun's Alt. -⊙-	ix x xi	Iz: Relative Irradiation (%) { Blue 444 / Green 538 / Amber 564
iv	Insolation $g \cdot cal/cm^2 \cdot min.$	xii	Δl: Light Path (m)
v	Date	xiii xiv xv	$K \cdot 10^3$ Attenuation Coefficient { Blue 444 / Green 538 / Amber 564
vi	Position		

3-1

i 6301	ii ↑10-00 h m / 9-42	iii ↑59.8° / 55.8	iv ↑1.155 / 1.103	v 1963 Nov.-21	vi 11-08.3 S / 119-49.2 E	
On deck	viii C. 86.6	x Iz. G.	xi Iz. A. —— 100 ——	xii Δl	xiv $K_G \cdot 10^3$	xv $K_A \cdot 10^3$
vii Z m	%	%	%	m		
0	92.7	93.4	93.4			
2	92.1			5.5	14.6	87.4
5	90.0	86.5	57.8	5.4	61	98
10	89.2	62.5	34.0	10.9	49.5	85.5
20	89.4	36.5	13.5	10.9	60.6	76
30	87.2	18.9	5.93	10.9	48	85.5
40	87.5	11.2	2.29	10.4	63.5	105
49.5	87.0	5.82	0.773	10.9	85.5	78
59.5	87.1	2.32	0.331	10.9	84.5	95
69.5	87.3	0.93	0.117	10.4	91.4	
79	87.1	0.36		10.9	44	
89	87.2	0.223		11.0	32.7	
99	85.4	0.156		11.0	41.8	
109	84.5	0.0985				

3-2

6302	↑9-40 / 9-05	↑55.8 / 47.3	↑1.017 / 0.886	Nov.-22	12-38.4 S / 120-02.3 E	
On deck	C. 82.9	Iz. G.	Iz. A. —— 100 ——	Δl	$K_G \cdot 10^3$	$K_A \cdot 10^3$
Z m				m		
0	90.6	91.5	91.5			
2	90.6	67.4	83.0	2.2	138.5	45.4
5	90.6	42.6	45.7	3.3	140	182
10	89.9	32.0	29.6	5.6	50	78.5
20	89.9	16.15	10.5	11.1	61.3	93
30	89.9	9.94	4.69	11.1	44.2	73
40	89.1	4.70	1.99	11.2	67	76.8
50	89.1	2.97	0.714	11.2	41	91
60	89.1	1.54	0.294	11.2	59	79.5
70	88.3	0.823	0.208	11.3	55	31
80	88.3	0.486	0.091	11.3	46.9	73.5
90	88.3	0.241	0.0413	11.3	62	70
100	87.5	0.133	0.0207	11.5	51.3	60
120	87.5	0.049	0.00576	22.9	44.1	56.5
140	87.5	0.0186	0.00225	22.9	42.8	41
160	86.6	0.00686	0.00076	23.1	43.3	47.3
180	86.6	0.00256		23.1	42.5	

Table 3. continued

3-3

6303	↑9-15 ↓9-26	↑58.7 ↓52.8	⇅0.957 ⇵0.990	Nov.-23	14-01.8 S 120-03.5 E	
On deck	C. 85.7	Iz. G.	Iz. A.	Δl	$K_G \cdot 10^3$	$K_A \cdot 10^3$
		—— 100 ——				
Z m				m		
0	92.1	93.0	93.0	2.2	105.6	70.8
2	92.1	73.9	79.0	3.4	107	95.3
5	92.1	51.5	57.3	5.5	91	160.3
10	89.0	31.1	23.9	10.95	72.2	90.5
20	85.8	14.1	8.92	9.3	64.6	58.1
28.5	79.8	7.77	5.19	8.75	40.6	72
36.5	77.0	5.25	2.77	9.4	26.6	82
45	72.7	4.25	1.29	8.8	41	62
53	73.3	2.96	0.75	9.95	88	72.9
62	70.7	1.24	0.363	7.2	117	
68.5	69.2	0.533		9.45	41.3	
77	69.7	0.360		11.1	43.7	
87	70.1	0.222		18.0	57.5	
103	71.7	0.079		21.3		
122	72.7					

3-4

6304	↑9-35 ↓9-06	↑54.8 ↓48.4	↑0.934 ↓0.829	Nov.-24	15-41.5 S 119-58.5 E	
On deck	C. 81.9	Iz. G.	Iz. A.	Δl	$K_G \cdot 10^3$	$K_A \cdot 10^3$
		—— 100 ——				
Z m				m		
0	89.9	91.2	91.2	2.2	327	77.4
2	89.9	44.3	77.1	3.3	100	78.8
5	89.9	31.8	59.3	5.5	108.3	115.5
10	88.1	17.5	31.3	11.2	34.8	64.3
20	86.4	11.8	15.2	9.6	51.3	71.2
28.5	82.9	7.2	7.70	9.0	44.5	82.2
36.5	83.0	4.84	3.68	9.0	57.8	116
44.5	81.2	2.87	1.29	5.1	51.0	94
49	77.1	2.22	0.798	7.9	48.1	36.7
56	74.4	1.51	0.594	9.1	61.6	50.6
64	75.6	0.865	0.375	5.7	73.6	118
69	73.5	0.566	0.191	4.6	54.3	82.6
73	71.4	0.440	0.130	10.3	73.8	
82	71.4	0.205		19.4	38.6	
99	72.6	0.097		27.4	34.3	
123	76.7	0.0381				

Table 3. continued

3-5

6305	↑9-29 ↑8-58	↑54.1 ↑46.7	↑0.938 ↑0.827	Nov.-25	17-06.0 S 119-58.4 E	
On deck	C. 80.9	Iz. G. —— 100 ——	Iz. A.	Δl	$K_G \cdot 10^3$	$K_A \cdot 10^3$
Z m				m		
0	89.9	90.0	90.0	2.2	49.2	94
2	89.9	81.0	81.0	3.4	94.1	79.4
5	89.9	58.9	61.9	5.6	80.5	78.6
10	90.3	37.6	40.0	10.7	38.8	93
19.5	90.3	24.8	14.8	10.1	30.7	50
28.5	88.9	18.2	8.91	8.5	29.4	86
36	88.4	14.2	4.31	9.6	70	88.5
44.5	88.0	7.27	1.85	6.2	51.6	110
50	86.9	5.25	0.935	7.9	84.2	79.8
57	88.5	2.70	0.500	3.4	69.1	67.7
60	83.9	2.14	0.398	10.3	45.6	66
69	86.9	1.33	0.201	2.3	126	108.7
71	88.8	1.00	0.166	16.2	45.7	
85	88.6	0.480		20.2	29.7	
102.5	88.4	0.263		20.4	29	
120	87.4	0.145		18.7	51.3	
136	88.2	0.056				

3-6

6305′	↑9-16.5 ↑8-50	↑51.3 ↑45.1	↑1.000 ↑0.876	Nov.-27	18-35.0 S 119-51.8 E	
On deck	C. 77.7	Iz. G. —— 100 ——	Iz. A.	Δl	$K_G \cdot 10^3$	$K_A \cdot 10^3$
Z m				m		
0	88.3	88.0	88.0	2.3	88.4	145.5
2	88.3	72.4	63.2	3.4	82.4	127
5	87.5	55.0	41.2	5.7	128	112.5
10	90.2	32.1	21.7	11.45	60.3	102.2
20	91.2	16.0	6.77	11.6	57.3	75
30	89.9	9.20	2.84	11.6	47.3	62
40	90.0	5.30	1.38	11.0	48.1	55.5
49.5	90.2	3.10	0.751	11.7	65.9	59
59.5	89.7	1.45	0.376	11.7	65	79.5
69.5	89.8	0.678	0.149	9.3	87.2	95.8
77.5	92.9	0.302	0.0612	11.2	46.4	47.2
87	92.4	0.181	0.0362	8.25	51	54.6
94	94.7	0.119	0.0231			

Table 3. continued

3-7

6306	↑13-52 13-17	↑59.9 67.2	⇕1.222 0.883	Dec.-5	09-02.8 S 113-02.3 E	
On deck	C. 86.6	Iz. G. —— 100 ——	Iz. A.	Δl	$K_G \cdot 10^3$	$K_A \cdot 10^3$
Z m				m		
0	92.7	93.5	93.5			
2	92.7	71.8	62.7	2.2	120.5	185
5	92.7	58.4	46.8	3.24	64.9	92.6
				5.35	67.3	82.5
10	93.4	40.8	30.2			
20	93.4	19.8	14.0	10.7	68.3	72.0
30	93.4	10.4	5.30	10.7	59.8	90.7
				10.65	59.1	66.6
40	93.9	5.53	2.61			
50	93.7	2.55	0.99	10.65	73.2	91
60	93.3	1.35	0.397	10.65	59.1	86.4
				10.1	71.3	83.2
69.5	92.8	0.659	0.172			
79	93.5	0.389	0.0895	10.06	52.7	64.6
89	93.7	0.203	0.0425	10.6	61.3	70.7
				10.6	56.6	76.4
99	93.9	0.111	0.0189			
119	95.2	0.0316	0.00896	21.0	60.0	36.7
137.5	95.7	0.0104	0.00484	19.5	57.5	31.8
				21.6	37.9	
158	95.7	0.00459				
178.5	96.1	0.00289		21.4	21.5	
197.5	95.7	0.00236		19.9	10.5	

3-8

6307	↑11-44 10-55	↑78.0 70.7	↑1.271 1.225	Dec.-6	11-02.2 S 113-03.3 E	
On deck	C. 97.8	Iz. G. —— 100 ——	Iz. A.	Δl	$K_G \cdot 10^3$	$K_A \cdot 10^3$
Z m				m		
0	98.8	99.0	99.0			
2	98.8	72.8	63.2	2	153	229
5	98.5	41.05	35.6	3.1	187	187
				5.1	110	179
10	98.5	23.4	14.3			
20	98.5	12.15	5.66	10.2	64.8	91.4
30	98.5	4.41	1.65	10.2	99.2	121
				10.2	88.3	98.2
40	98.0	1.71	0.606			
50	97.6	0.701	0.203	10.2	87.3	108
60	97.3	0.360	0.0894	10.2	64.7	80.5
				10.2	39.2	56
70	96.1	0.242	0.0506			
80	96.3	0.147	0.0260	10.2	49	65.7
89	95.5	0.0836	0.0131	9.2	62	74
				10.2	82.8	53.5
99	95.0	0.0359	0.00752			
116	92.8	0.0188	0.00534	17.4	37.4	19.5
131	90.2	0.0133		15.4	22.4	
				16.9	52	
147.5	89.7	0.0055				
155	89.6			7.7		
176	90.0			21.6		

Table 3. continued

3-9

6308	↑11-42.5 ↓11-06.5	↑79.6 ↓74.1	↑1.267 ↓1.230	Dec.-7	13-0.41 S 112-48.4 E	
On deck	C. 98.5	Iz. G.	Iz. A.	Δl	$K_G \cdot 10^3$	$K_A \cdot 10^3$
		— 100 —				
Z m				m		
0	99.0	99.6	99.6			
2	99.0	84.0	74.6	2.0	84.2	143.5
5	98.8	63.5	62.4	3.0	92	59.2
				5.1	43.4	114.5
10	98.8	51.0	35.0			
20	97.7	39.2	13.0	10.1	26.1	97.8
30	95.9	18.3	6.32	10.1	75.0	72
				19.6	50.9	57
39.5	95.9	11.25	3.65			
49.5	95.5	6.25	1.755	10.3	57.3	71
59.5	95.6	3.84	0.684	10.3	47.6	91.3
				9.8	68.6	98.3
69	95.3	1.96	0.261			
78.5	95.7	0.865	0.0989	9.8	84.0	99.3
87.5	95.3	0.376	0.0405	9.3	91.8	96.1
				9.8	37.9	52.2
97	94.2	0.255	0.0244			
115	92.9	0.0779	0.00625	18.5	64.4	73.6
134	93.7	0.0247	0.00344	19.5	60	30.8
				19.5	47.1	16.4
153	94.5	0.00985	0.00249			
171	93.8	0.00423		18.4	45.6	
192	94.6	0.00225		21.5	29.3	

3-10

6309	↑11-39 ↓10-54	↑80.8 ↓72.7	↑1.301 ↓1.259		Dec.-8	14-57.9 S 113-04.1 E		
On deck	C. 98.8	Iz. B.	Iz. G.	Iz. A.	Δl	$K_B \cdot 10^3$	$K_G \cdot 10^3$	$K_A \cdot 10^3$
			— 100 —					
Z m					m			
0	99.3	99.6	99.6	99.6				
2	99.3	85.5	86.4	78.9	2.0	74.3	69.4	114.0
5	99.0	80.2	66.0	60.0	3.0	19.7	88.8	92.1
					5.1	19.8	81.2	103.0
10	99.0	72.3	44.0	35.6				
20	96.2	65.1	29.8	17.4	10.15	10.8	54.2	71.0
29.5	96.0	54.9	19.6	7.71	9.6	17.7	60.5	85.5
					9.6	21.9	44.7	72.8
39	94.2	44.5	12.7	3.80				
48.5	94.0	34.2	7.16	1.99	9.6	28.1	60.4	66.6
56.5	90.5	24.0	3.98	0.913	8.1	43.2	72.8	96.3
					8.65	53.2	70.5	92.5
65	89.9	15.2	2.17	0.411				
72.5	88.7	8.75	1.25	0.189	7.6	72.5	72.5	103.0
77	85.9	3.74	0.74	0.115	4.6	185	113	108.8
					5.1	188	82.5	120.0
82	82.3	1.45	0.485	0.0629				
95	82.8	0.281	0.230	0.0304	13.3	123	56.5	54.1
110	82.1	0.0831	0.0842	0.0104	15.3	80	65.5	70.0
					18.4	71.3	49.0	37.0
128	84.4	0.0203	0.0343	0.00530				
145	84.3	0.00189	0.0130	0.00372	17.4	136	56.3	20.1
173	88.4	0.000605	0.00311		28.8	39.6	49.7	

Table 3. continued

3-11

6310	↑15-37 ↑14-56	↑38.8 ↑48.3	↑0.919 ↑1.071		Dec.-9	16-55.2 S 113-04.1 E		
On deck	C. 62.9	Iz. B.	Iz. G.	Iz. A.				
			100					
Z m					m			
0	81.9	77.0	77.0	77.0	2.5	36.9	111	230
2	81.9	70.4	58.8	44.2	3.7	68.3	87.5	87.4
5	81.9	54.8	42.8	32.1	6.05	18.2	77.7	97.5
10	82.9	48.9	26.8	17.9	12.1	15.7	32.3	63
20	78.2	40.6	18.2	8.38	11.5	11.3	53	76.5
29.5	72.8	35.5	9.94	3.50	10.15	17.7	61.1	68
38	70.5	29.6	5.36	1.75	10.75	14.9	26.1	49.4
47	66.7	25.4	4.03	1.03	8.34	21.5	46.7	71.9
54	62.2	21.2	2.81	0.561	8.45	34.3	55.6	85.2
62	60.9	15.7	1.75	0.274	7.1	43.7	46.5	46.5
68	56.8	11.5	1.26	0.197	5.9	33.9	33.9	45.7
73	52.6	9.45	1.03	0.150	5.9	56	37.3	50.8
78	51.0	6.8	0.83	0.111	10.5		63.8	78
87	49.3		0.43	0.0487	14.0		52.2	43.7
99	46.0		0.206	0.0264	19.9		31.1	30.1
116	50.1		0.111	0.0145	15.6		62.2	26.3
129.5	56.7		0.0425	0.00956	23.7		34.6	
150	57.8		0.0188					

3-12

6311	↑12-05.5 ↑11-33.5	↑86.1 ↑82.6	⇑1.362 ⇓1.371		Dec.-10	18-58.9 S 113-02.1 E		
On deck	C. 97.0	Iz. B.	Iz. G.	Iz. A.				
			100					
Z m					m			
0		97.0	97.0	97.0	2.0	25	45	22.5
2		92.2	88.5	62.2	3.0	30	76.7	133.5
5	99.9	84.0	70.5	41.6	5.0	28	26	74
10	99.1	73.3	61.7	28.6	9.5	40	54.8	69.5
19.5	96.2	49.9	36.7	14.8	9.5	21	42.2	64.3
29	92.3	41.0	24.63	8.03	7.5	17.3	70.1	84
36.5	89.6	36.2	14.55	4.28	8.0	13.8	53.9	61.3
44.5	87.4	32.3	9.50	2.63	3.0	10	70	90
47.5	80.7	31.2	7.71	2.00	4.5	24.4	57.6	117
52	75.5	27.9	5.92	1.21	4.0	35	100	152
56	74·2	24.2	3.98	0.662	8.0	21.2	42.4	44.9
64	75.7	20.4	2.82	0.463	5.0	34	66	32
69	76.3	17.3	2.03	0.349	13.1	14.6	41.4	48.3
82	77.5	14.3	1.18	0.210	11.1		31.5	77.5
93	74.4		0.833	0.0881	10.1		49.7	54.7
103	79.1		0.506	0.0510	10.1		59.7	71.7
119	75.1		0.278	0.0248	17.1		74.4	67
130	75.7		0.0785	0.0079				

Table 3. continued

3-13

6312	↑10-52.5 10-06.5	↑74.2 63.6	↑1.231 ∓1.056		Dce.-11	21-04.8 S 112-49.7 E		
On deck	C. 96.1	Iz. B.	Iz. G.	Iz. A.	Δl	$K_B \cdot 10^3$	$K_G \cdot 10^3$	$K_A \cdot 10^3$
			100					
Z m					m			
0	97.8	98.5	98.5	98.5	2.0	14.7	63.8	34.3
2	97.8	95.4	84.6	91.6	3.1	13	48.8	35.7
5	97.4	91.8	74.1	82.0	5.2	12.6	44.7	55.4
10	98.0	85.9	58.7	61.6	10.3	14.6	33	108.0
20	97.9	74.1	41.6	20.4	9.3	20.6	71.1	83.0
29	95.8	61.0	21.6	9.44	9.3	14.6	59.2	92.7
38	95.9	53.3	12.4	3.99	6.7	7.5	64.2	88.1
44.5	92.7	50.7	8.06	2.22	9.85	21.4	68	73.2
54	93.7	41.1	4.11	1.09	5.7	40.2	64.7	98.0
59.5	90.9	32.8	2.84	0.625	8.35	25.2	35.4	70.7
67.5	91.5	26.6	2.11	0.348	1.6	31.8	66.8	(236)
69	86.4	25.3	1.90	0.240	8.4	38.6	86.6	90.8
77	87.1	18.3	0.917	0.113	15.7	44.6	54.8	68.9
92	89.7	9.06	0.387	0.038	19.0	23.1	60.0	58.0
110	90.9	5.84	0.128	0.0127	19.1	22.0	89.0	51.8
128	91.8	3.84	0.0398	0.00462	14.8	17.6	62.1	41.9
142	91.4	2.96	0.0158	0.0025	19.1		62.4	
160	91.6		0.00484					

3-14

6313′	↑9-07 8-43	↑50.5 46.9	↑110 ∓32 112 K Lux	
On deck	C. 76.6	Iz. G. 100	Δl	$K_G \cdot 10^3$
Z m			m	
0	84.8	90.4	2.35	162.5
2	85.7	62.0	3.5	60
5	84.3	50.3	5.25	36.2
9.5	76.6	41.6	11.1	32.4
19	77.3	29.0	11.7	55.5
29	76.6	15.2	8.8	34.2
36.5	73.6	11.3	9.35	31.0
44.5	71.0	8.39	4.1	66.0
48	65.6	6.40	5.85	83.8
53	62.5	3.94		
Dec.-21	25-01.4 S 112-28.6 E		Photo-cells were damaged by the Sea-Water Leak*	

* Observations from the Dec. 22nd on were carried out with the spare cells.

Table 3. continued

3-15

6313	↑10-13 ↑9-43	↑64.0 ↑58.5	↑1.171 ↑1.148		Dec.-22*	23-01.7 S 112-43.5 E		
On deck	C. 90.6	Iz. B.	Iz. G. 100	Iz. A.	Δl	$K_B \cdot 10^3$	$K_G \cdot 10^3$	$K_A \cdot 10^3$
Z m								
0	94.6	95.6	95.6	95.6				
2	94.6	91.0	85.8	74.2	2.1	22.6	52.0	120.0
5	94.6	85.2	60.0	50.4	3.2	20.5	113.5	121.5
10	90.5	83.9	47.5	40.3	5.3	3.2	44.2	43.3
19	85.8	76.0	34.4	23.5	9.6	10.5	33.4	56.5
29	85.2	67.9	24.7	11.9	10.7	10.7	30.8	63.5
36.5	79.9	61.7	14.1	7.62	8.05	12.4	69.6	54.7
46	80.1	54.3	9.35	4.10	10.3	37.0	39.0	60.5
55.5	80.5	40.5	6.11	2.62	9.2	32.6	45.7	49.0
65	80.7	34.7	4.07	1.58	10.3	16.0	38.8	48.5
69	81.4	26.0	2.75	0.941	4.3	65.5	89.7	119.8

3-16

6314	↑11-08 ↑10-42.5	↑80.7 ↑73.9	↑1.360 ↑1.410	123.K Lux ↘	1964 Jan.-6	23-12.7 S 106-03.9 E		
On deck	C. 97.8	Iz. B.	Iz. G. 100	Iz. A.	Δl	$K_B \cdot 10^3$	$K_G \cdot 10^3$	$K_A \cdot 10^3$
Z m					m			
0	98.8	98.9	98.9	98.9				
1.9	98.5	85.2	69.4	64.2	1.9	83.0	192.0	223.5
4.8	98.5	83.6	63.3	53.5	2.84	5.6	31.7	65.0
9.6	98.5	78.9	49.4	36.8	4.9	11.6	51.0	75.5
19	98.2	74.5	39.3	20.7	9.6	67.9	24.0	59.5
29	98.2	67.3	19.5	10.4	10.2	9.3	68.6	66.6
38.5	97.8	55.9	13.4	5.90	9.7	18.5	38.1	58.6
48	97.3	48.1	8.43	2.81	9.7	15.4	47.4	76.6
58	97.2	39.6	5.22	1.45	10.2	19.1	47.1	64.7
67	96.6	31.8	3.08	0.767	9.25	23.8	57.4	69.2
76	96.6	22.0	1.79	0.382	9.25	40.0	58.4	75.7
80	95.9	17.3	1.22	0.304	4.1	58.5	92.6	58.5

3-17

6315	↑11-01 ↑10-50	↑80.7 ↑73.9	↑1.36 ↑1.36	123.K Lux ↘	Jan.-6	23-12.7 S 106-03.9 E		
On deck	C. 98.8	Iz. B.	Iz. G. 100	Iz. A.	Δl	$K_B \cdot 10^3$	$K_G \cdot 10^3$	$K_A \cdot 10^3$
Z m					m			
0	99.3	99.5	99.5	99.5				
2	99.0	96.5	92.5	80.5	2.0	14.9	32.2	107.0
5	99.0	94.5	81.2	75.8	3.0	5.9	43.0	18.8
8	98.5	92.8	71.8	58.6	3.0	5.9	41.3	85.9
13	98.2	91.2	65.3	38.6	5.1	3.6	18.8	81.0
22	98.2	82.1	39.8	23.5	9.1	1.5	56.4	53.9
32	98.1	73.7	27.4	13.8	10.2	10.8	36.4	52.1
42	98.0	62.8	19.3	7.33	10.2	15.7	34.4	62.0
51	98.2	50.4	9.08	3.52	9.2	24.0	82.0	81.0
61	98.2	39.5	6.30	1.76	10.2	23.5	35.3	67.6
70	98.4	24.4	3.10	0.780	9.2	52.4	77.5	88.5
80	98.0	16.5	1.54	0.379	10.25	38.1	68.4	70.4

Table 3. continued

3-18

6316	↑13-31 ↑12-59	↑69.3 76.6	↑1.265 1.420	110.K Lux ↘	Jan.-8	20-55.6 S 105-52.1 E		
On deck	C. 98.4	Iz. B.	Iz. G.	Iz. A.	Δl	$K_B \cdot 10^3$	$K_G \cdot 10^3$	$K_A \cdot 10^3$
			100					
Z m					m			
0	96.6	96.7	96.7	96.7	2.1		72.6	89.5
2	96.6		83.4	80.4	3.1		16.2	74.2
5	97.0		79.2	64.0	5.15	2.2	25.3	60.2
10	93.0		69.5	47.0	8.25		29.7	34.5
18	84.9	92.4	54.5	35.3	9.25	4.3	20.6	19.5
27	83.1	89	45.1	29.6	8.2	4.9	46.2	80.4
35	83.5	85.7	30.9	15.3	9.2	13.1	56.5	77.2
44	84.2	76	18.5	7.53	7.2	18.85	81.0	81.0
51	82.3	66.4	10.3	4.21	6.1	19.65	44.2	72.1
57	80.2	59.1	7.88	2.71	6.1	45.9	57.4	80.3
63	80.4	44.7	5.56	1.67	4.1	50.4	51.7	93.5
67	81.0	36.4	4.51	1.14				

3-19

6317	↑11-33 ↑10-04	↑83.0 76.6	↑1.400 1.365	122.K Lux ↘	Jan.-9	18-59.0 S 106-00.0 E		
On deck	C. 99.3	Iz. B.	Iz. G.	Iz. A.	Δl	$K_B \cdot 10^3$	$K_G \cdot 10^3$	$K_A \cdot 10^3$
			100					
Z m					m			
0	99.5	99.8	99.8	99.8	2.01	7.5	16.5	84.8
2	99.5	98.1	96.2	84.4	3.02	8.3	39.7	81.2
5	99.5	95.7	85.4	66.0	5.04	3.0	45.6	62.5
10	99.3	94.1	68.0	48.2	9.06	5.5	35.4	45.2
19	98.2	89.6	49.5	32.1	10.1	5.0	22.7	35.4
29	95.4	85.0	39.6	22.6	8.1	6.2	46.9	93.8
37	93.9	80.6	27.0	10.6	7.1	4.9	43.7	60.6
44	88.0	77.8	19.8	6.88	9.1	8.8	53.9	45.6
53	89.6	71.8	12.2	4.45	7.1	16.2	59.3	77.6
60	86.5	63.9	7.98	2.61	8.1	20.9	51.7	90.0
68	92.9	53.9	5.27	1.26	6.1	18.1	54.2	46.0
74	93.0	48.4	3.79	0.953				

3-20

6318	↑11-26 ↑10-57	↑80.5 74.3	↕0.593 ↕1.015	34.~42. ↘ K Lux	Jan.-10	16-59.4 S 106-05.9 E		
On deck	C. 98.5	Iz. B.	Iz. G.	Iz. A.	Δl	$K_B \cdot 10^3$	$K_G \cdot 10^3$	$K_A \cdot 10^3$
			100					
Z m					m			
0	99.0	99.5	99.5	99.5	2.0	49.5	173.0	258.0
2	99.0	90.0	70.0	59.0	3.0	46.2	73.3	82.6
5	99.0	78.2	56.2	46.1	5.1	36.6	43.5	55.4
10	98.8	65.0	45.0	35.0	9.1	28.6	44.0	61.5
19	97.0	50.3	30.1	20.05	10.1	15.8	45.9	87.0
29	96.5	42.9	18.6	8.36	8.1	20.9	46.8	86.1
37	92.6	36.4	12.9	4.12	8.1	25.8	66.5	61.5
45	91.4	29.5	7.50	2.50	10.2	23.1	56.9	59.9
55	92.4	23.4	4.19	1.37	10.2	32.4	43.2	55.0
65	93.4	17.4	2.70	0.780	10.2	21.6	44.1	61.9
75	94.0	14.0	1.72	0.412	3.1	39.1	68.4	133.5
78	91.0	12.5	1.39	0.274				

Table 3. continued

3-21

6319	↑11-22 ↑10-54.5	↑78.7 ↑73.0	·↑1.460 ∓0.264	104.K Lux ↘	Jan.-11	15-06.6 S 106-02.1 E		
On deck	C. 98.2	Iz. B.	Iz. G.	Iz. A.	Δl	$K_B \cdot 10^3$	$K_G \cdot 10^3$	$K_A \cdot 10^3$
			100					
Z m					m			
0	98.8	99.4	99.4	99.4	2.03	27.1	64.1	86.4
2	98.8	94.1	87.5	83.5	3.04	18.1	74.0	65.9
5	98.8	88.8	70.0	68.1	5.1	18.7	73.6	80.5
10	98.5	80.8	48.0	45.1	9.15	15.9	36.1	62.4
19	98.5	70.0	34.5	25.7	10.15	14.8	27.6	43.4
29	97.1	60.3	26.1	16.5	9.15	13.5	39.4	13.7
38	95.2	52.7	18.2	14.52	9.15	18.6	59.6	71.0
47	94.6	44.6	8.80	7.59	9.2	22.9	58.8	126.0
57	94.6	36.1	4.25	2.38	9.2	17.4	45.7	53.3
66	94.0	30.8	2.79	1.46	9.2	44.6	67.5	79.5
75	93.6	20.5	1.50	0.698	5.13	70.2	97.5	66.2
80	93.3	14.3	0.910	0.498				

3-22

6320	↑11-39.5 ↑11-16.5	↑79.9 ↑76.4	↑1.360 ↑1.340	110.K Lux ↘	Jan.-12	12-59.4 S 106-06.6 E		
On deck	C. 98.5	Iz. B.	Iz. G.	Iz. A.	Δl	$K_B \cdot 10^3$	$K_G \cdot 10^3$	$K_A \cdot 10^3$
			100					
Z m					m			
0	99.0	99.6	99.6	99.6	2.02	7.4	44.9	99.0
2	99.0	98.0	91.0	78.2	3.03	3.3	26.6	46.2
5	99.0	97.1	84.2	68.0	5.05	4.0	12.9	46.0
10	99.0	94.5	78.6	54.0	9.2	8.7	37.0	49.0
19	98.8	87.5	56.1	34.4	10.2	9.3	58.7	75.4
29	97.4	79.6	30.8	16.0	9.2	13.0	39.1	59.8
38	96.5	70.8	21.5	9.22	10.2	9.3	35.2	51.8
48	96.6	64.3	14.9	5.42	10.25	18.5	57.6	50.7
58	96.9	53.3	8.27	3.22	9.24	41.7	69.4	101.0
67	96.6	36.3	4.37	1.27	9.24	41.7	65.0	76.9
76	96.1	24.7	2.40	0.625	5.1	54.6	72.1	66.3
81	96.1	18.6	1.66	0.445				

3-23

6321	↑11-00 ↑10-32	↑72.1 ↑66.5	↑1.340 ↑1.300	111.K Lux ↘	Jan.-13	11-01.7 S 106-02.9 E		
On deck	C. 95.1	Iz. B.	Iz. G.	Iz. A.	Δl	$K_B \cdot 10^3$	$K_G \cdot 10^3$	$K_A \cdot 10^3$
			100					
Z m					m			
0	97.0	98.0	98.0	98.0	2.06	7.3	17.0	51.4
2	97.0	96.5	94.5	88.2	3.1	9.7	22.7	49.9
5	97.0	93.6	88.1	75.5	5.15	7.2	67.0	66.0
10	97.0	90.0	62.3	54.0	9.33	3.2	42.3	83.0
19	96.6	83.0	42.0	24.9	10.35	16.4	22.2	46.9
29	96.6	70.2	33.2	15.3	9.4	14.4	36.2	69.3
38	94.6	61.4	23.6	8.00	10.4	20.2	69.7	66.4
48	94.4	49.9	11.4	4.01	10.4	31.7	50.5	58.6
58	94.0	35.8	6.75	2.18	9.4	41.5	71.3	97.9
67	93.9	23.8	3.46	0.870	9.4	66.0	73.4	81.9
76	93.9	12.9	1.73	0.405	7.3	67.6	62.9	71.0
83	93.9	7.81	1.09	0.241				

Table 3. continued

3-24

6322	↑10-51 ↑10-29	↑69.4 ↑64.8	↑0.441 ↑0.468	18.5K Lux ↘	Jan.-15	08-59.5 S 105-55,5 E		
On deck	C. 93.4	Iz. B.	Iz. G.	Iz. A.	Δl	$K_B \cdot 10^3$	$K_G \cdot 10^3$	$K_A \cdot 10^3$
			100					
Z m					m			
0	96.1	97.2	97.2	97.2	2.08	115.5	163.5	202.0
2	96.1	76.7	69.0	63.5	3.1	57.8	54.5	89.9
5	96.1	64.2	58.4	47.8	5.2	28.8	44.2	104.0
10	96.1	55.5	46.5	27.8	9.4	5.3	52.5	52.1
19	95.6	52.7	28.3	16.5	10.5	7.7	40.1	56.5
29	92.1	48.7	18.6	9.09	9.4	24.9	48.2	66.8
38	92.1	38.6	11.8	4.85	10.5	26.3	53.5	66.9
48	92.1	29.3	6.76	2.42	10.5	22.4	60.0	58.0
58	91.6	23.2	4.28	1.31	9.45	62.5	61.4	61.4
67	91.1	12.8	2.40	0.738	8.4	77.3	66.6	72.0
75	89.6	6.68	1.37	0.403	7.4	33.8	24.3	58.1
82	88.8	5.22	1.144	0.262				

3-25

6323	↑10-01 ↑9-39	↑59.7 ↑54.9	↑1.000 ∓0.900	87.K Lux ↘	Jan.-17	11-02.6 S 99-50.1 E		
On deck	C. 86.6	Iz. B.	Iz. G.	Iz. A.	Δl	$K_B \cdot 10^3$	$K_G \cdot 10^3$	$K_A \cdot 10^3$
			100					
Z m					m			
0	92.1	94.0	94.0	94.0	2.2	25.2	55.2	80.5
2	92.1	89.0	83.0	79.0	3.04	13.2	62.5	62.5
4.8	92.1	85.4	68.8	65.5	5.2	11.5	54.6	75.6
9.6	87.5	80.4	51.8	44.0	10.3	97.2	58.3	94.2
19	84.9	72.7	28.2	16.7	10.9	8.3	35.7	59.5
29	82.9	66.5	19.1	8.80	9.85	38.1	68.0	76.1
38	82.9	45.6	9.76	4.19	9.94	33.2	51.3	76.4
47	80.9	32.7	5.85	1.97	11.0	13.6	49.0	67.1
57	80.9	28.2	3.41	0.940	8.8	41.3	64.6	60.6
65	80.9	19.5	1.93	0.550	11.0	45.3	72.5	65.3
75	79.8	11.8	0.868	0.268	5.5	83.5	56.2	91.6
80	79.8	7.41	0.639	0.162				

3-26

6324	↑9-39 ↑9-16	↑54.2 ↑49.0	↑1.111 ↑1.019	110.K Lux ↘	Jan.-18	09-20.2 S 100-06.5 E		
On deck	C. 80.9	Iz. B.	Iz. G.	Iz. A.	Δl	$K_B \cdot 10^3$	$K_G \cdot 10^3$	$K_A \cdot 10^3$
			100					
Z m					m			
0	89.9	90.0	90.0	90.0	2.2	6.8	27.0	67.6
2	89.9	88.5	84.7	77.3	3.1	11.3	32.1	57.9
4.8	89.9	85.5	76.9	64.5	5.4	16.7	126.0	126.0
9.6	89.1	78.0	38.8	32.6	10.6	13.3	24.6	58.6
19	80.9	67.9	29.9	17.6	10.1	12.9	42.5	63.2
28	73.0	59.5	19.4	9.27	10.2	17.6	54.0	61.3
37	72.0	49.6	11.2	4.97	10.2	45.1	63.7	84.3
46	72.0	31.3	5.88	2.10	10.3	35.5	53.0	45.7
55	69.6	21.7	3.41	1.10	9.7	59.7	53.5	56.5
63.5	69.6	12.2	2.02	0.640	9.7	77.2	64.3	82.3
72	68.4	5.77	1.08	0.287	4.0	21.3	101.3	104.0
75.5	67.2	5.30	0.720	0.189				

Table 3. continued

3-27

6325	↑9-38 ↑8-54	↑54.2 ↑49.0	↕0.804 ↕0.569		Jan.-19	07-57.2 S 100-07.5 E		
On deck	C. 79.9	Iz. B.	Iz. G. — 100 —	Iz. A.	Δl	$K_B \cdot 10^3$	$K_G \cdot 10^3$	$K_A \cdot 10^3$
Z m					m			
0	89.1	89.7	89.7	89.7	2.25	11.3	91.2	178.0
2	89.1	87.0	73.0	60.0	3.1	10.5	46.2	111.5
4.8	89.1	84.0	63.1	47.0	5.45	8.8	23.8	43.1
9.6	88.3	80.0	55.4	37.2	10.1	6.9	21.8	49.5
18.5	75.2	74.7	44.5	22.6	11.35	7.9	53.7	58.1
28.5	74.0	68.0	24.3	11.7	8.5	25.9	57.0	72.4
36	70.7	54.7	14.9	6.30	10.3	25.2	45.0	59.0
45	71.9	42.1	9.35	3.42	10.9	36.7	50.5	61.6
54.5	72.9	28.2	5.37	1.75	11.45	42.9	47.2	56.0
64.5	73.9	17.2	3.13	0.920	9.8	83.5	82.5	71.4
73	73.8	7.60	1.40	0.455	4.04	69.4	64.5	37.2
76.5	72.8	5.77	1.08	0.400				

3-28

6326	↑9-38.5 ↑9-14.5	↑53.2 ↑47.7	↑1.003 ↑0.931	116.K Lux ↘	Jan.-20	06-46.4 S 99-51.3 E		
On deck	C. 79.9	Iz. B.	Iz. G. — 100 —	Iz. A.	Δl	$K_B \cdot 10^3$	$K_G \cdot 10^3$	$K_A \cdot 10^3$
Z m					m			
0	89.1	89.7	89.7	89.7	2.24	42.4	89.3	105.0
2	89.1	81.6	73.6	71.0	3.14	11.2	17.5	38.2
4.8	89.1	78.5	69.7	63.0	5.44	4.6	31.3	49.7
9.6	88.3	76.7	58.8	48.1	10.7	5.2	42.0	68.2
19	88.3	72.3	37.6	23.1	11.35	11.0	44.1	58.1
29	88.3	63.6	22.7	11.9	10.9	15.2	60.8	79.2
38.5	87.5	54.0	11.6	5.03	10.9	38.6	49.2	66.2
48	87.5	35.7	6.81	2.45	11.45	46.3	57.7	57.7
58	87.5	21.0	3.50	1.25	11.0	54.6	57.3	52.0
67.5	86.6	11.5	1.87	0.509	5.2	67.3	50.0	166.0
72	89.0	8.06	1.45	0.216				

3-29

6327	↓9.57 ↓10.27	↓56.7 ↓63.0	↕1.182 ↕1.231	113.K Lux ↘	Jan.-21	05-25.0 S 99-56.3 E		
On deck	C. 89.1	Iz. B.	Iz. G. — 100 —	Iz. A.	Δl	$K_B \cdot 10^3$	$K_G \cdot 10^3$	$K_A \cdot 10^3$
Z m					m			
0	91.4	97.5	97.5	97.5	2.2	68.5	45.6	96.0
2	91.4	84.0	88.1	79.0	3.06	8.2	21.3	32.6
4.8	91.4	81.9	82.7	71.5	5.2	4.8	51.9	61.5
9.6	92.1	80.0	63.2	51.9	10.25	2.9	31.2	64.5
19	92.1	77.5	45.6	25.75	10.9	6.9	45.9	51.4
29	92.1	71.9	30.0	15.3	10.3	11.7	40.5	57.6
38.5	92.7	63.8	19.8	8.45	9.7	16.5	45.3	80.2
47.5	93.8	54.7	12.8	3.88	9.2	14.2	42.0	53.4
56	92.7	47.8	8.71	2.38	9.2	30.5	43.6	67.6
64.5	92.6	36.2	5.82	1.28	9.1	56.0	74.7	75.9
73	94.4	22.8	2.95	0.64				

Table 3. continued

3-30

6328	↑8-58 ↓8-34	↑42.9 ↓37.4	↑0.881 ↓0.766	116.K Lux ↘	Jan.-22	03-55.0 S 99-35.0 E		
On deck	C. 68.2	Iz. B.	Iz. G. ——100——	Iz. A.	Δl	$K_B \cdot 10^3$	$K_G \cdot 10^3$	$K_A \cdot 10^3$
Z m					m			
0	83.9	81.3	81.3	81.3				
1.5	82.9	78.0	76.0	69.6	1.8	22.1	35.9	88.5
4.3	82.9	73.8	70.4	58.0	3.4	16.3	22.2	53.3
9.1	82.9	70.3	49.9	38.4	5.8	8.3	58.8	70.9
18.5	82.9	57.1	26.8	16.3	11.35	18.5	55.1	75.9
28.5	81.9	45.6	14.9	6.84	12.2	18.5	48.4	71.5
38.	81.9	33.4	7.42	3.20	11.6	26.7	60.3	65.5
47.5	81.9	27.5	4.83	1.60	11.6	16.8	37.0	59.5
57.5	81.9	18.4	2.86	0.912	12.2	32.8	42.6	46.3
67.	80.9	11.1	1.42	0.467	11.8	42.4	59.3	56.8
72.	80.9	6.59	0.725	0.199	6.2	84.0	108.3	141.0

Table 4. Reflectance (irradiance ratio) = Eu/Ed.

4-1

Station UM-6322	L.M.T. ↑11-30.5 ↓11-05.5	Suns Alt. ↑75.8 ↓72.0	Insolation ↑0.407 ↓0.264
Layer	R_B	R_G	R_A
broadside	9.9 %	7.7 %	6.5 %
0 m	9.25	6.00	0.44
2	6.18	1.02	0.60
5	5.87	1.09	0.65
10	5.93	1.09	0.84
19	4.26	1.10	0.83
29	3.59	1.12	1.08
38	2.95	1.22	1.46
47	2.20	1.06	2.24
57	1.15	0.56	3.24
66	0.95		3.98
75	0.95		6.74
82	0.66		9.74

4-2

6324	↑10-21 ↓9-54	↑63.6 ↓57.6	↑1.222 ↓1.145
Layer	R_B	R_G	R_A
broadside	12.95%	3.91%	3.76 %
0 m	10.82		3.28
2	5.98	0.97	0.62
4.8	5.66	0.87	0.56
9.6	5.48	1.45	0.81
19	4.92	1.14	0.84
29	4.08	1.13	0.96
37	2.92	1.23	1.36
46.5	2.37	1.32	1.65
56	1.49	1.10	1.82
65.5	1.09	0.69	2.31
74	1.05		3.84
79	0.94		7.31

4-3

6326	↑10-12.5 ↓9-51.5	↑60.7 ↓56.1	↑1.157 ↓0.881
Layer	R_B	R_G	R_A
broadside	16.1 %	6.0%	6.18%
0 m	10.4	3.9	4.48
2	6.07	0.85	0.99
4.8	5.80	0.85	0.46
9.6	4.90	0.80	0.46
19	4.01	0.84	0.50
29	3.20	0.80	0.58
38.5	2.17	0.93	0.71
48	1.86	0.94	1.08
58	1.34	0.84	1.41
67.5	1.42	0.60	1.77
72	1.41		3.36
			6.55

4-4

6327	↓9-28 ↓9-52	↓50.2 ↓55.6	↓1.015 ↓1.141
Layer	R_B	R_G	R_A
broadside	%	%	%
0 m	14.13	4.27	4.16
2	6.90	0.97	0.54
4.8	6.50	0.91	0.51
9.6	5.74	0.98	0.51
19	4.25	0.86	0.57
29	2.74	0.75	0.59
38.5	2.02	0.69	0.70
47.5	1.68	0.63	1.07
56	1.34	0.65	1.24
64.5	1.02	0.49	1.75
72	1.00	0.49	2.52

4-5

6328	↑9-32 ↓9-08	↑50.5 ↓45.2	↑0.734 ∓0.477
Layer	R_B	R_G	R_A
broadside	%	8.65%	6.68 %
0 m	16.2	9.06	8.03
1	5.75	1.17	0.74
3.8	5.22	1.03	0.61
8.6	4.61	1.14	0.63
18	4.05	0.96	0.83
28	3.50	1.00	1.14
37.5	3.16	1.15	1.64
47	2.99		2.98
57	1.56		4.09
66.5	1.42		6.09
71.5	1.66		11.80

Eu: Upward irradiance.
Ed: Downward irradiance.

Table 5. Transparency, relative irradiance at the transparency depth (I_{T_r}) and the mean attenuation coefficient ($\overline{K_{T_r}}$).

Station	Transparency m. (Wire Inclination)	Relafive Irradiane ot the T_r depth			Mean Attenuation Coefficient		
		$I_{T_r}B$	$I_{T_r}G$	$I_{T_r}A$	$\overline{K_{T_r}B}\cdot10^3$	$\overline{K_{T_r}G}\cdot10^3$	$\overline{K_{T_r}A}\cdot10^3$
UM-6301	30 (13°)	×	19.0	5.8	×	55.7	95.0
6302	31.5 (6°)	×	8.9	4.2	×	77.2	100.7
6303	31 (35°)	×	7.1	4.5	×	85.8	100.3
6304	31 (45°)	×	6.3	6.2	×	89.4	89.7
6305	38.5 (40°)	×	12.7	3.9	×	54.0	85.0
6305′	30 (29°)	×	9.2	2.8	×	80.0	119.4
6306	29 (20°)	×	11.2	5.8	×	75.9	98.3
6307	26 (10°)	×	6.5	2.6	×	105.4	140.3
6308	35 (30°)	×	14.7	4.7	×	55.1	87.5
6309	38 (36°)	46.0	13.2	4.0	20.5	53.6	84.7
6310	32 (25°)	33.5	7.6	2.8	34.4	80.7	112.0
6311	43 (56°)	33.0	10.0	2.8	25.8	53.5	82.3
6312	37 (50°)	53.5	13.0	4.2	17.0	55.4	85.1
6313	37 (50°)	62.0	14.0	7.4	13.0	53.2	70.3
6313′	28 (53°)	×	16.5	×		64.6	
6314	30 (15°)	66.0	18.6	10.0	14.0	56.0	76.7
6315	36.5 (15°)	70.0	24.0	10.7	9.9	39.2	62.0
6316	38 (43°)	83.0	27.0	11.8	5.0	34.5	56.1
6317	37 (35°)	81.0	27.0	10.8	5.95	36.0	60.0
6318	34.5 (39°)	39.0	14.5	5.1	27.3	56.3	85.8
6319	35 (30°)	56.0	20.7	15.2	16.6	49.9	54.3
6320	35 (23°)	74.5	24.3	10.9	8.6	40.3	64.6
6321	37 (19°)	62.0	25.0	8.4	13.0	37.6	66.8
6322	32.5 (10°)	45.0	15.6	7.0	24.6	57.2	81.9
6323	34 (30°)	56.0	13.0	5.9	17.1	60.0	83.2
6324	29 (38°)	59.0	18.3	8.9	18.3	58.2	83.8
6325	31 (35°)	63.0	20.2	9.3	14.9	51.3	77.1
6326	35 (8°)	58.0	15.0	6.7	15.4	54.4	76.9
6327	33 (23°)	69.0	26.3	12.6	11.2	40.9	63.0
6328	28 (10°)	46.0	15.1	7.1	27.8	67.8	94.6

Table 6. Conditions at the

Station	UM-6300	6301	6302	6303	6304	6305	6305′
Position S	09-04.1	11-04.1	12-38.0	14-05.4	15-45.9	17-12.0	18-35.0
Position E	127-40.1	119-46.2	120-04.5	150-08.3	120-00.0	119-59.2	119-51.8
Date	1963 Nov. 13	Nov. 21	Nov. 22	Nov. 23	Nov. 24	Nov. 25	Nov. 27
Time (L.M.T.)	10-45 11-11	8-50 10-04	8-48 9-56	8-35 9-38	8-58 10-01	8-54 10-00	8-43 9-13
Layer	Water Temperature** in °C.						
0 m	29.0	29.7	30.0	29.5	28.6	27.9	27.3
10	28.5	29.07	29.57	29.61	28.51	25.01	27.22
20	—	28.99	29.11	28.58	28.23	24.63	27.05
25	27.7						
30	—	27.18	29.05	28.09	27.40	24.43	26.30
50	27.2	24.61	26.80	25.50	26.21	24.10	24.42
75	25.0	22.41	25.33	23.35	24.80	22.44	23.85
100	21.2	20.89	23.53	21.34	23.71	20.29	
125	18.5	18.08	20.79	19.69	22.29	19.48	
150	16.8	16.73	17.66	18.84	19.98	17.03	
200	14.7	13.24	13.93	14.58	17.22	15.95	
Wire Length	Depth of the Sampling in m.						
0 m	0	0	0	0	0	0	0
10	10	10	10	10	10	10	10
25	25	25	25	25	24	25	25
50	50	50	50	49	48	49	50
75	74	75	75	74	73	72	75
100	99	100	100	99	97	97	99
125	124	125	125	123	121	118	
150	148	150	150	148	145	143	
200	198	200	200	198	192	191	
Sampling Wire Length	Depth of the in situ experiment in m.						
0 m							
10							
25							
50							
75							
100							
125							
Half Day's Insolation g·cal/cm²	255.3	277.1	278.3	281.7	301.9	319.3	310.3

time of productivity experiment.

6306	6307	6308	6309	6310	6311	6312	6313
09-02.0 113-02.3	11-02.2 113-00.9	13-02.7 112-49.1	14-56.0 113-05.0	16-55.3 113-07.0	18-57.5 113-30.0	21-01.0 112-51.6	22-58.4 112-45.0
Dec. 5	Dec. 6	Dec. 7	Dec. 8	Dec. 9	Dec. 10	Dec. 11	Dec. 22
8-58 9-58	9-05 9-54	8-52 9-46	8-41 9-39	9-56 10-52	9-46 10-37	9-36 10-44	8-58 9-30
28.6	28.8	29.5	29.0	27.7	26.8	25.7	24.8
28.38	27.79	29.18	28.80	27.18	26.76	25.61	24.49
26.38	24.74	28.96	28.70	26.65	26.64	25.61	23.38
25.86	23.52	28.67	28.49	26.65	26.41	25.62	24.38
24.56	20.48	26.36	27.26	25.46	24.95	25.28	24.16
20.95	19.00	24.99	25.57	23.84	23.64	23.18	21.18
17.69	16.95	23.71	24.34	21.97	22.27	22.03	20.45
16.33	15.56	22.35	23.52	20.88	21.09	21.16	19.86
15.43	14.47	20.94	21.99	20.47	20.06	19.98	19.05
13.42	12.63	17.68	17.62	18.06	18.21	18.81	17.74
0	0	0	0	0	0	0	0
10	10	10	10	10	9	9	9
25	25	25	25	24	24	24	23.5
50	50	50	49	49	48	48	48
75	75	75	74	74	71	72	71
99	100	100	98	99	95	97	95
124	124	124	121	123	117	122	114
150	149	149	144	146	140	145	138
200	198	198	192	195	188	197	176
2	2	2	2		2	2	2
10	10	10	9.5		9	9.5	9
25	24.5	25	24		23	24	23.5
50	49	49.5	48.5		46.5	48.5	47.5
74.5	74	74.5	73		70	73	71.5
99.5	99	99.5	98		93.5	98	95.5
124.5	124	124	122		117	122	119
261.4	270.4	276.0	303.9	335.4	340.8	359.3	348.9

Table 6. continued

Station	UM-6313′	6314	6315	6316	6317	6318	6819
Position S E	25-01.0 112-28.8	24-59.5 106-02.8	23-11.8 106-05.3	20-52.6 105-52.1	18-55.1 105-59.4	16-56.1 106-04.3	15-04.6 106-03.0
Date	1963 Dec. 21	1964 Jan. 5	Jan. 6	Jan. 8	Jan. 9	Jan. 10	Jan. 11
Time (L.M.T.)	8-34 9-35	8-41 9-40	8-49 9-41	9-46 10-54	8-57 9-52	8-53 9-47	8-40 9-42
Layer	Water Temperature** in °C.						
0 m	23.5	23.7	24.5	24.0	24.4	26.0	27.6
10	23.47	23.20	24.27	23.99	24.44	25.93	27.50
20	23.30	23.03	23.80	23.97	24.41	25.91	27.43
25							
30	23.25	22.92	23.44	23.76	24.40	25.90	27.42
50	22.64	22.65	22.59	22.70	24.34	25.74	27.15
75	21.08	20.68	20.98	21.46	23.50	24.61	25.22
100		19.88	20.00	20.37	22.39	22.74	23.45
125		18.87	19.41	19.68	22.01	21.53	21.75
150		18.36	18.92	19.09	21.12	20.82	20.24
200		17.25	17.80	18.05	18.65	19.83	17.84
Wire Length	Depth of the Sampling in m.						
0 m	0	0	0	0	0	0	0
10	8.5	10	10	9.5	9	10	10
25	22	25	25	23.5	25	24	24
50	41	50	49	47	49	48	49
75	66	75	74	70	72	73	73
100	90	99	100	93	96	98	99
125	125	124	125	115	121	122	123
150	(Bottom)	148	150	140	144	145	147
200		198	200	184	192	192	196
Sampling Wire Length	Depth of the in situ experiment in m.						
0 m		2	2		2	2	2
10		10	9		9	9	9.5
25		25	23.5		23.5	23.5	24
50		49.5	47		47.5	47.5	48.5
75		74.5	70.5		71.5	71.5	73
100		99.5	94.5		96	96	98
125		124	118		120	120	122
Half Day's Insolation g·cal/cm²	346.4	222.3	322.8	300.2	252.6	280.0	328.9

Table 6. continued

6320	6321	6322	6323	6324	6325	6326	6327	6328
12-56.9 106-05.9	10-59.8 106-02.1	08-58.1 105-53.8	10-57.9 99-53.7	09-17.3 100-12.0	07-58.0 100-19.1	06-49.5 99-50.0	05-16.0 99-51.0	03-55.4 99-34.2
Jan. 12	Jan. 13	Jan. 15	Jan. 17	Jan. 18	Jan. 19	Jan. 20	Jan. 21	Jan. 22
9-34 10-18	8-51 9-39	8-39 9-26	8-39 9-25	8-42 9-32	8-32 9-14	8-39 9-23	8-58 9-49	8-05 8-52
28.2	29.3	29.1	28.7	28.9	28.6	29.5	29.5	29.0
27.69	28.48	28.88	28.59	28.71	28.51	28.84	28.87	28.89
27.63	28.33	28.88	28.60	28.56	28.59	28.82	28.77	28.83
27.61	27.34	28.78	28.57	27.55	28.58	28.84	28.70	28.86
27.49	25.75	26.50	27.84	25.38	27.16	28.28	28.08	28.75
25.40	23.47	22.93	23.77	21.30	24.34	26.59	26.58	27.66
23.69	20.84	18.23	20.50	18.39	21.04	23.84	22.50	22.94
21.65	18.64	15.58	18.28	16.46	17.89	21.42	19.32	16.33
19.60	16.62	14.20	16.48	14.83	15.48	17.60	16.05	14.15
15.44	13.60	12.36	13.72	12.16	13.34	12.91	13.06	12.87
0	0	0	0	0	0	0	0	0
10	10	10	10	10	10	10	10	10
25	25	25	25	25	25	25	25	25
50	50	49	50	49	49	50	49	50
75	75	73	74	73	73	75	74	75
99	100	97	99	97	98	100	99	100
124	125	122	123	121	120	125	123	125
148	149	146	146	144	143	150	147	150
198	199	192	192	192	192	199	194	200
2	2	2						
9.5	10	9						
24.5	25	23.5						
49	49.5	47.5						
74	74.5	71.5						
99	99.5	96						
123.5	124	120						
322 7	299.2	224.0	226.2	292.6	215.6	268.9	277.1	189.2

Table 6. continued

Station	UM-6300	6301	6302	6303	6304	6305	6305′
Position S	09-40.9	11-04.1	12-38.0	14-05.4	15-45.9	17-12.0	18-35.0
Position E	127-40.1	119-46.2	120-04.5	150-08.3	120-00.0	119-59.2	119-51.8
Date	1963 Nov. 13	Nov. 21	Nov. 22	Nov. 23	Nov. 24	Nov. 25	Nov. 27
Time (L.M.T.)	10-45 11-11	8-50 10-04	8-48 9-56	8-35 9-38	8-58 10-01	8-54 10-00	8-43 9-13
Transparency m		30	31.5	31	31	38.5	30
Wire Length	Relative Blue-light Intensity (λ: 391·444·484 mμ) in %.						
2 m							
10							
25							
50							
75							
100							
125							
Wire Length	Relative Green-light Intensity (λ: 519·538·561 mμ) in %.						
2 m							
10		63	32	32	18	37	33
25		24.5	13	10	9.4	20	12
50		5.3	3.0	3.8	2.4	5.5	2.9
75		0.53	0.65	0.64	0.44	0.93	0.37
100		0.15	0.135	0.29	0.105	0.31	0.085
125		0.05	0.039	0.076	0.041	0.12	
Wire Length	Relative Amber-light Intensity (λ: 549·564·584 mμ) in %.						
2 m							
10		34	30	25	31	41	31
25		8.7	7.1	6.8	11	13	4.3
50		0.70	0.75	1.0	0.86	1.05	0.74
75		0.06	0.14	0.14	0.13	0.15	0.075
100			0.021		0.033		0.016
125			0.0045				
Filter***		2	2	2	2	2	2
Wire Length	Phosphate-P Microgram-atoms/L.***						
0 m		0.12	0.31	0.16	0.10	0.07	0.15
10		0.12	0.12	0.07	0.12	0.12	0.12
25		0.18	0.14	0.13	0.10	0.18	0.12
50		0.56	0.24	0.16	0.14	0.34	0.21
75		0.93	0.20	0.64	0.36	0.64	0.35
100		1.11	0.52	0.99	0.66	1.04	0.43
125		1.31	1.06	1.14	0.81	1.14	
150		1.51	1.35	1.08	0.98	1.34	
200		1.77	1.97	1.62	1.34	1.53	

Table 6. continued

6306	6307	6308	6309	6310	6311	6312	6313
09-02.0 113-02.3	11-02.2 113-00.9	13-02.7 112-49.1	14-56.0 113-05.0	16-55.3 113-07.0	18-57.5 113-30.0	21-01.0 112-51.6	22-58.4 112-45.0
Dec. 5	Dec. 6	Dec. 7	Dec. 8	Dec. 9	Dec. 10	Dec. 11	Dec. 22
8-58 9-58	9-05 9-54	8-52 9-46	8-41 9-39	9-56 10-52	9-46 10-37	9-36 10-44	8-58 9-30
29	26	35	38	32	43	37	37
			85	49	94	95	91
			73	38	76	86	84
			60	24	46	66	73
			33	8.5	31.5	48	52
			6	1.6	17.0	22	19
			0.18		12.0	7.7	
			0.037			4.4	
72	75	73	87		88	88	84
41	24	51	45	27	63	60	51
14.5	7.3	25	25	15	32	29	30.5
2.6	0.72	6.2	6.4	3.7	8.1	6.0	8.6
0.5	0.195	1.02	0.93	0.96	2.0	1.4	1.8
0.105	0.034	0.22	0.17	0.2	0.82	0.28	
0.022	0.016	0.039	0.04	0.053	0.21	0.06	
66	63	84	67		61	91	75
31	12	36	36	18	30	64	43
8.0	3.0	8.9	11.5	5.6	12	14	17.5
1.0	0.21	1.7	1.8	0.84	2.2	1.7	3.6
0.12	0.038	0.16	0.15	0.14	0.34	0.16	0.6
0.018	0.0073	0.021	0.023	0.026	0.087	0.026	
0.0074	0.0024	0.0044	0.0058	0.011	0.019	0.0055	
2	2	2	2	2	2	2	2
0.08	0.14	0.04	0.18	0.08	0.12	0.18	0.10
0.07	0.09	0.03	0.09	0.04	0.06	0.05	0.10
0.11	0.25	0.02	0.10	0.08	0.02	0.11	0.10
0.30	1.11	0.07	0.15	0.03	0.12	0.14	0.25
0.88	1.20	0.10	0.32	0.14	0.23	0.26	0.14
1.30	1.37	0.38	0.54	0.53	0.42	0.50	0.14
1.46	1.44	0.58	0.68	0.74	0.54	0.52	0.14
14.8	1.62	0.93	0.66	0.63	0.60	0.51	0.17
17.9	1.94	1.08	1.31	0.60	0.45	0.46	0.24

Table 6. continued

Station	UM-6313′	6314	6315	6316	6317	6318	6319
Position S	25-01.0	24-59.5	23-11.8	20-52.6	18-55.1	16-56.1	15-04.6
Position E	112-28.8	106-02.8	106-05.3	105-52.1	105-59.4	106-04.3	106-03.0
Date	1963 Dec. 21	1964 Jan. 5	Jan. 6	Jan. 8	Jan. 9	Jan. 10	Jan. 11
Time (L.M.T.)	8-34	8-41	8-49	9-46	8-57	8-53	8-40
	9-35	9-40	9-41	10-54	9-52	9-47	9-42
Transparency m	28	30	36.5	38	37	34.5	35
Wire Length	Relative Blue-light Intensity (λ: 391·444·484 mμ) in %.						
2 m		86	96		98	91	95
10		79	92	94	94	68	81
25		71	79	90	88	47	65
50		47	53	68	75	28	43
75		24	20	32	50.5	15.3	21
100		5.0	5.6	6.6		6.0	2.7
125							
Wire Length	Relative Green-light Intensity (λ: 519·538·561 mμ) in %.						
2 m		70	92		95	70	84
10	41	49	70	70	70	47	49
25	21	27	36	48	45	24	29
50	5.4	7.7	10	11	17	6.3	7.1
75	0.44	1.9	2.3	2.8	4.4	2.0	1.6
100		0.25	0.12	0.64		0.38	0.14
125							
Wire Length	Relative Amber-light Intensity (λ: 549·564·584 mμ) in %.						
2 m		66	81		85	60	87
10		36	50	48	51	37	46
25		14	20	32	28	14	19
50		2.5	4	4.7	5.8	2.2	4.8
75		0.42	0.55	0.6	1.05	0.55	0.7
100		0.11	0.048	0.066			0.13
125							
Filter*	2	2	2	2	2	2	2
Wire Length	Phosphate-P Microgram-atoms/L.***						
0 m	0.10	0.12	0.05	0.14	0.14	0.10	0.08
10	0.04	0.06	0.05	0.05	0.06	0.10	0.16
25	0.03	0.10	0.08	0.05	0.06	0.08	0.13
50	0.11	0.10	0.10	0.14	0.09	0.06	0.12
75	0.08	0.16	0.11	0.10	0.13	0.10	0.16
100	0.13	0.14	0.11	0.15	0.12	0.41	0.42
125	0.21	0.25	0.24	0.18	0.30	0.52	0.66
150		0.28	0.20	0.26	0.32	0.51	0.89
200		0.33	0.29	0.18	0.66	0.36	0.98

Table 6. continued

6320	6321	6322	6323	6324	6325	6326	6327	6328
12-56.9 106-05.9	10-59.8 106-02.1	08-58.1 105-53.8	10-57.9 99-53.7	09-17.3 100-12.0	07-58.0 100-19.1	06-49.5 99-50.0	05-16.0 99-51.0	03-55.4 99-34.2
Jan. 12	Jan. 13	Jan. 15	Jan. 17	Jan. 18	Jan. 19	Jan. 20	Jan. 21	Jan. 22
9-34 10-18	8-51 9-39	8-39 9-26	8-39 9-25	8-42 9-32	8-32 9-14	8-39 9-23	8-58 9-49	8-05 8-52
35	37	32.5	34	29	31	35	33	28
98	96	78						
95	91	55	79	79	80	76	80	70
83	75	51	69	62	72	68	74	50
64	48	30	32	27	37	32	54	25
27	14.5	8.5	12.5	5.4	7.6	6.5	21	5.2
7.0	2.5	3.7	1.9	1.8	1.1	1.1	3.6	0.48
91	95	70						
80	64	49	49	39	54	57	63	42
40	37	24	23	24	31	28	35	18.5
14	10.5	7.0	5.0	4.6	7.5	6.0	11.8	4.3
2.7	1.9	1.65	0.87	0.98	1.4	1.18	2.8	0.52
0.45	0.38	0.80	0.19	0.10	0.2	0.22	0.39	
79	89	66						
58	54	30	40	32	36	47	51	35
22	19	12.5	12	12	15	15.5	19	9.1
5.2	3.8	2.5	1.6	1.6	2.55	2.1	3.4	1.4
0.73	0.42	0.52	0.27	0.26	0.45	0.15	0.58	0.125
0.11	0.074	0.12			0.12		0.074	
2	2	2	2	2	2	2	2	2
0.13	0.05	0.07	0.10	0.06	0.09	0.06	0.06	0.03
0.15	0.10	0.10	0.07	0.15	0.12	0.10	0.06	0.06
0.08	0.06	0.08	0.10	0.09	0.12	0.09	0.11	0.09
0.11	0.11	0.14	0.06	0.14	0.18	0.16	0.05	0.10
0.16	0.46	0.56	0.38	0.67	0.52	0.46	0.48	0.28
0.39	0.94	1.27	0.88	1.18	0.96	0.98	1.18	1.20
0.96	1.37	1.58	1.23	1.40	1.32	1.42	1.50	1.78
1.07	1.38	1.76	1.45	1.57	1.58	1.66	1.80	1.94
1.67	2.00	2.13	1.46	1.83	1.96	2.02	2.06	1.96

Table 6. continued

Surface Station	Position		Date	Time of Sampling (L.M.T.)	Water Temp. °C	Half Day's Insolation g·cal/cm²	Filter*
	Lat.	Long·E					
UM	Tateyama		1963 Nov.				
A-01	35-00 N	139-50	2	11-50	22.0	—	
A-02	N		2	20-20	25.9	—	
A-03	32-09 N	138-26.1	3	09-32	26.3	—	
A-04	27-23.5 N	136-37.7	4	09-10	26.5	149.8	
A-05	22-55.2 N	135-02.1	5	08-18	27.4	221.9	
A-06	18-29.2 N	133-32.1	6	08-13	28.1	240.2	3
A-07	13-55.1 N	131-54.9	7	08-06	27.8	120.3	3
A-08	09-18.7 N	130-16.7	8	07-58	28.0	—	2
A-09	04-44.8 N	129-14.5	9	07-55	28.2	262.9	2
A-10	00-56.9 N	126-45.2	10	07-43	29.7	278.5	2
A-11	03-28.6 S	125-46.8	11	07-40	31.0	257.2	2
A-12	06-45.6 S	126-32.4	12	07-40	30.5	293.2	2
Darwin							
A-13	12-48.6 S	123-08.0	Nov. 20	08-02	30.0	348.5	2
Broome							
A-14	17-02.7 S	117-37.5	Dec. 3	08-35	—	287.0	2
A-15	13-00.3 S	114-48.1	4	08-22	30.0	282.0	2
A-16	23-06.7 S	113-01.5	12	08-36	(23.6)	(364.2)	2
A-17	25-14.0 S	113-46.0	12	20-13	(22.5)	(283.8)	2
A-18	27-38.3 S	113-44.6	13	07-11	24.5	156 / 283.8	2
Geraldton Fremantle							
			1964 Jan.				
A-19	26-17.5 S	108-13.2	4	08-44	21.5	272.8	2
A-20	09-41.1 S	103-35.0	16	08-20	29.0	244.0	2
A-21	03-52.0 S	97-03.8	23	19-18	29.5	(259.8)	2
A-22	00-10.5 N	96-17.2	24	08-14	26.3	(55.8)	2
A-23	03-48.0 N	94-44.2	25	08-07	28.4	238.9	2
A-24	07-14.3 N	96-19.0	26	08-10	28.3	258.0	2
Penang							
A-25	02-01.9 N	102-14.4	Feb. 1	08-30	27.0	177.0	2
A-26	02-01.5 N	106-38.0	2	08-19	27.2	165.3	2
A-27	05-04.0 N	113-48.5	4	08-18	26.0	223.1	2
A-28	11-13.2 N	118-22.5	6	10-09	26.0	235.0	2
A-29	16-16.6 N	119-32.0	7	11-12	26.8	226.5	2
A-30	20-41.0 N	121-02.0	8	09-48	24.3	232.4	2
A-31	25-50.5 N	123-23.5	9	10-57	24.0	115.8	2
A-32	28-51.7 N	125-39.8	10	11-06	15.8	38.0	2
A-33	30-19.2 N	126-53.5	12	11-11	(14.6)	76.6	
A-34	30-55.4 N	130-30.4	13	12-17	(17.2)	161.5	
A-35	31-14.5 N	131-11.2	13	15-29	(17.2)	161.5	
A-36	33-09.0 N	135-34.0	15	11-47	18.0	39.8	

*: Number of covers (Filier-plate) using in SOROKIN's method.
**: Data of Temperature are taken from the Physical report.
***: Figures in the Table of Phosphate-P are interpolated on Chemical data.

Table 7. Data on production measured by ^{14}C method.

Station	UM-6300	6301	6302	6303	6304	6305	6305′	6306	6307	6308	6309	6310	6311	6312	6313
Wire Length	Assimilation by the Tank-Experimen (microgram C/m³·10KLux·hr.)											150m 39 200m 88			
0 m	296	423	204	265	271	244	359	522	835	177	248	39	144	308	181
10	388	435	411	400	281	372	573	778	847	324	201	128	194	328	241
25	96	646	437	421	247	407	514	1442	855	316	219	188	219	419	279
50	293	990	467	930	299	241	632	245	770	832	509	173	251	417	283
75	270	260	273	103	302	312	468	142	62	233	245	431	312	364	356
100	27	68	176	35	20	251	506	210	116	49	47	102	578	101	93
125	6	65	4	25	53	19		56	135	100	9	4	59	49	40
Wire Length	Assimilation by the SAKAMOTO-revolving-tank Experiment under the daylight condition (microgram C/m³·halfday)														
0 m		1950	1082	1975	1210	1332	1665	1070	4250	775	830	506	740	887	848
10		1490	1452	5045	1845	2185	1600	2645	3665	921	636	707	1125	810	982
25		1740	1005	1947	1306	2100	1185	7150	3695	778	935	830	1167	1417	865
50		2155	803	3875	1115	1400	146	1325	944	1925	1072	828	1122	1080	1090
75		513	682	529	1321	1610	179	427	337	1107	472	1058	1419	1202	1670
100		56	74	117	306	500	151	795	204	74	570	324	1200	337	557
125		15	117	32	260	33		646	383	651	590	128	417	950	217
Wire Length	Assimilation by the in-situ-Experiment (microgram C/m³·halfday)														
0 m								1520	4840	1188	685		993	936	974
10								2396	4500	1355	809		1203	959	706
25								3940	4200	1358	988		1490	1500	1520
50								1462	1015	2750	1920		1528	1360	1285
75								1790	179	1595	1325		1172	890	1062
100								815	26	89	166		1190	113	217
125								64	146	932	23		322	49	327
	Unit area production (mg C/m²·halfday)							226	198	190	117		150	100	113

Table 7. continued

Station	6313′	6314	6315	6316	6317	6318	6319	6320	6321	6322	6323	6324	6325	6326	6327	6328
Wire Length	Assimilation by the Tank-Experiment (microgram C/m³·10 KLux·hr.)															
0 m	109	180	264	126	168	226	113	180	446	381	118	193	314	210	137	596
10	177	221	195	132	174	204	287	203	410	254	218	291	270	281	156	834
25	157	227	264	229	194	269	236	224	461	340	278	355	287	298	265	440
50	194	153	175	209	215	267	306	284	260	636	330	420	272	396	260	424
75	336	194	276	267	232	183	173	231	610	228	223	360	244	154	379	501
100	264	150	248	199	244	222	160	49	124	65	115	20	98	29	68	61
125	81	24	73	22	123	97	17	7	28	20	18	16	52	49	10	69
Wire Length	Assimilation by the SAKAMOTO-revolving-tank Experiment under the daylight condition (microgram C/m³·halfday)															
0 m	146	597	2165	733	682	640	1660	777	1350	1560	690	837	1535	710	1175	2090
10	390	930	833	687	700	922	1087	979	1350	937	606	1028	940	1111	1193	2000
25	595	646	805	906	687	1180	912	1222	1540	1010	748	1160	1469	1274	1304	1474
50	769	590	646	1020	509	1033	1100	1050	1042	2540	1133	794	158	1710	1228	1613
75	1118	197	784	1112	667	1065	617	853	2080	1370	541	1092	495	345	1470	2485
100	1069	302	753	493	745	603	497	399	577	202	207	309	516	122	553	105
125	232	166	64	140	82	207	163	253	330	256	151	56	189	219	169	125
Wire Length	Assimilation by the in-situ-Experiment (microgram C/m³·halfday)															
0 m		427	757		317	429	817	440	1165	1400						
10		826	915		383	880	840	745	1700	902						
25		627	1060		722	1040	898	1100	1720	1080						
50		504	442		610	686	940	1185	855	1480						
75		683	568		823	640	503	1635	640	733						
100		640	317		866	222	623	284	189	107						
125		470	199		204	220	179	230	33	0						
(mg C/m²·halfday)		85	75		83	75	88	119	97	93						

Table 7. continued

Surface Station	Tank-Exp. μg C/m^3·hr.	SAKAMOTO's Revolving Tank-Exp.
UM-		
A- 1	6550	μg C/m^3·halfday
A- 2	916	
A- 3	429	
A- 4	361	
A- 5	59	
A- 6	252	639
A- 7	342	848
A- 8	171	590
A- 9	938	3050
A-10	1040	4200
A-11	1550	8700
A-12	484	995
Darwin		
A-13	289	1270
Broome		
A-14	×	511
A-15	285	1850
A-16	182	396 (2.5 hr.)
A-17	366	707 (2.5 hr.)
A-18	1140	2575 (2.5 hr.)
Geraldton·Fremantle		
UM-		
A-19	300	828
A-20	450	1260
A-21	180	1115
A-22	407	1485
A-23	165	514
A-24	630	1042
Penang		
A-25	4580	16020
A-26	1270	6410
A-27	3550	13300
A-28	1120	5990
A-29	264	2090
A-30	234	930
A-31	1120	2500
A-32	1575	1800
A-33	1610	μg C/m^3·halfday
A-34	647	
A-35	994	
A-36	1097	

Table 8. The size distribution of production on the Far Eastern waters.

Surface Station	Position		Date	Type of Filter pore Dia. μ.		SS.	RA.	AA.	DA.	HA.	PH.	GS.
	Lat.	Long. E	1964			3	1.2	0.8	0.65	0.45	0.3	0.22
A-20	09-41.1 S	103-35.0	Jan. 16	%	55.9	6.5	18.1	18.2			1.3	
A-27	05-04.0 N	113-48.5	Feb. 4		93.9	zero		zero			6.1	
A-28	11-13.2 N	118-22.5	Feb. 6		69.1	10.9		5.6			14.5	
A-29	16-16.6 N	119-32.0	Feb. 7		55.4	4.3		38.6			1.7	
A-30	20-41.0 N	121-02.0	Feb. 8		59.8	7.4		24.6			8.2	
A-31	26-50.5 N	123-23.5	Feb. 9		78.4	20.6		1.0			zero	
A-32	28-51.7 N	125-39.8	Feb. 10		91.0	4.6		4.4			zero	
A-36	33-09.0 N	135-34.0	Feb. 15		46.7	38.3	6.4	4.0	2.9		1.6	0.1

Table 9. Data on the quantity of chlorophyll a, b, c, and carotenoids.

Station	UM-6300	6301	6302	6303	6304	6305	6305′	6306	6307	6308	6309	6310	6311	6312	6313
Wire Length	Chlorophyll-a microgram/m³														
0 m	18	11	37	41	18	21	36	27	41	16	11.4	30.2	27.8	22.7	59.6
10	27	24	24	34	20	15	18	33	51	24.4	14.8	23.9	28.1	26.9	61.3
25	26	35	30	24	19	15	32	160	93	21.3	14.3	23.2	33.0	24.1	60.5
50	39	62	51	406	29	30	116	122	177	55.8	29.0	20.4	38.8	29.9	62.2
75	84	83	120	138	80	35	165	36	111	88.3	115.0	76.1	49.3	49.0	85.5
100	27	49	84	46	88	127	171	17	57	88.9	100.0	93.3	126.5	172.7	142.0
125	8	31	40	27	89	55		20	26	69.3	57.9	87.5	115.9	77.6	190.8
150	2	26	56	21	35	44		19	17	46.6	49.3	55.6	98.6	68.9	91.9
200	8	18	15	23	13	22		27	26	27.1	25.7	55.8	22.8	37.7	80.9
Wire Length	Chlorophyll-b microgram/m³														
0 m	5.3	5.7	24.1	19.8	16.9	20.2	33.7	11.1	7.8	11.4		32.4	21.5	27.7	78.0
10	12.2	9.5	8.7	18.8	7.9	4.7	11.6	12.9	18.3	14.6	0.13	24.7	34.0	26.7	80.2
25	17.3	3.0	16.8	16.0	8.3	11.2	28.6	56.0	30.5	11.6	3.4	21.8	29.0	21.8	82.0
50	14.4	30.1	20.3	124	16.1	27.4	63.6	42.6	36.5	20.9	4.3	19.2	32.4	38.8	86.4
75	38.2	37.8	42.5	46	20	22.8	61.4	24.4	44.3	36.4	44.8	51.3	41.0	32.3	81.2
100	7.3	28.3	22.0	20	38.2	66.2	56.2	10.3	28.0	31.4	42.2	44.0	67.6	80.5	109.0
125	5.0	20.9	21.0	14.5	37.4	21.0		14.5	12.2	25.9	52.0	51.2	54.1	42.8	125.5
150	3.5	18.7	60.0	23.3	24.8	17.4		14.9	9.4	23.8	30.0	35.0	62.1	52.5	83.3
200	2.4	5.3	11.3	16.2	10.8	10.6		24.3	15.4	18.8	27.6	53.5	28.1	50.5	82.4
Wire Length	Chlorophyll-c m s p u/m³														
0 m	0.116	0.097	0.532	0.219	0.165	0.193	0.375	0.130	0.095	0.107		0.273	0.169	0.266	0.603
10	0.094	0.116	0.088	0.186	0.127	0.100	0.118	0.095	0.160	0.150	0.0116	0.203	0.241	0.254	0.532
25	0.141	0.059	0.117	0.143	0.096	0.108	0.247	0.332	0.315	0.130	0.011	0.150	0.214	0.184	0.520
50	0.338	0.220	0.193	0.841	0.109	0.271	0.569	0.302	0.340	0.194	0.0645	0.140	0.266	0.234	0.529
75	0.239	0.294	0.277	0.334	0.157	0.161	0.393	0.203	0.269	0.253	0.187	0.309	0.324	0.231	0.586
100	0.175	0.243	0.195	0.227	0.246	0.347	0.398	0.119	0.190	0.164	0.220	0.296	0.465	0.495	0.640
125	0.076	0.163	0.177	0.117	0.203	0.186		0.106	0.111	0.177	0.205	0.280	0.312	0.319	0.908
150	0.081	0.144	0.487	0.273	0.189	0.164		0.151	0.062	0.198	0.163	0.222	0.411	0.363	0.554
200	0.117	0.111	0.101	0.146	0.067	0.134		0.210	0.139	0.122	0.159	0.437	0.245	0.397	0.552

Table 9. continued

Station	6313′	6314	6315	6316	6317	6318	6319	6320	6321	6322	6323	6324	6325	6326	6327	6328
Wire Length	Chlorophyll-a microgram/m³															
0 m	124.1	68.6	80.0	24.7	29.0	24.3	35.5	36.7	20.9	37.1	34.9	21.9	35.0	27.7	21.6	68.0
10	98.0	38.0	49.1	11.3	26.3	21.0	20.3	17.1	24.0	21.4	18.4	24.1	15.0	22.0	22.5	48.7
25	85.5	47.0	15.0	20.8	24.2	14.2	13.6	11.9	20.9	28.9	18.4	25.5	23.3	19.4	24.2	40.9
50	95.6	46.3	18.7	20.7	14.1	24.2	23.0	19.7	27.8	56.2	27.7	40.7	42.7	45.4	30.5	45.2
75	98.3	49.0	21.9	34.9	21.1	14.5	36.0	49.0	94.8	126.2	58.0	198.3	122.1	96.1	57.5	109.0
100	138.4	89.0	65.0	98.5	25.8	58.0	56.2	87.9	110.4	101.0	114.2	103.5	129.8	68.2	112.1	96.8
125	232.7	108.3	88.2	63.6	92.0	68.4	57.5	58.7	47.0	45.8	67.7	43.4	66.5	43.5	60.5	38.5
150		72.4	67.1	52.5	86.5	39.2	41.0	22.6	23.3	28.9	28.3	22.5	35.9	45.3	41.8	22.1
200		41.2	23.1	31.5	28.7	21.9	27.0	19.3	17.1	43.0	23.0	24.2	21.2	29.5	17.7	26.4
Wire Length	Chlorophyll-b microgram/m³															
0 m	184.0	76.4	81.0	22.2	29.9	23.2	32.8	32.2	30.0	34.5	40.2	43.5	25.9	36.2	20.4	35.3
10	131.0	55.7	43.7	2.9	30.6	15.6	14.6	12.3	13.3	32.5	16.7	14.0	18.8	19.6	23.9	19.2
25	118.0	68.5	5.01	13.9	27.6	11.9	12.6	11.2	17.9	38.6	27.4	15.2	23.2	20.6	16.8	23.5
50	106.2	53.3	8.74	18.7	17.8	17.7	18.1	15.6	21.5	32.4	22.7	25.4	26.1	33.3	22.6	25.0
75	113.0	63.4	13.2	23.6	16.1	20.0	22.5	23.9	54.5	62.3	33.1	69.6	47.2	52.1	43.7	42.3
100	125.3	91.5	32.3	55.4	20.6	30.0	37.4	45.0	48.5	43.7	54.5	47.1	63.1	42.4	60.7	47.1
125	165.3	60.5	46.3	41.5	50.0	41.3	33.8	39.8	40.3	28.3	40.0	25.0	29.6	39.3	38.2	29.1
150		53.4	32.7	37.6	64.3	42.9	25.8	20.8	15.1	19.7	25.3	18.1	24.5	34.1	12.5	17.6
200		35.6	15.8	11.3	22.5	20.6	22.9	21.4	10.2	24.8	24.9	17.8	20.4	24.7	17.7	26.9
Wire Length	Chlorophyll-c m s p U/m³															
0 m	1.181	0.518	0.552	0.252	0.301	0.146	0.149	0.340	0.209	0.238	0.353	0.186	0.271	0.2735	0.164	0.245
10	0.922	0.448	0.208	0.169	0.219	0.0567	0.095	0.139	0.0632	0.225	0.136	0.194	0.120	0.152	0.1915	0.243
25	0.730	0.430	0.051	0.151	0.203	0.075	0.0573	0.1023	0.193	0.214	0.1335	0.1016	0.177	0.187	0.168	0.172
50	0.838	0.462	0.087	0.116	0.158	0.130	0.146	0.073	0.1685	0.252	0.104	0.1685	0.214	0.244	0.217	0.196
75	0.871	0.509	0.103	0.137	0.146	0.0895	0.128	0.140	0.314	0.376	0.1654	0.463	0.318	0.341	0.2795	0.305
100	0.815	0.565	0.223	0.321	0.150	0.191	0.136	0.300	0.371	0.316	0.3495	0.3055	0.429	0.283	0.386	0.328
125	1.152	0.452	0.320	0.274	0.293	0.204	0.168	0.2595	0.212	0.278	0.239	0.1823	0.211	0.3225	0.254	0.187
150		0.371	0.228	0.275	0.430	0.225	0.171	0.1718	0.1265	0.231	0.216	0.1268	0.203	0.260	0.135	0.127
200		0.255	0.141	0.151	0.257	0.1145	0.215	0.2045	0.0834	0.3035	0.222	0.195	0.185	0.184	0.1295	0.224

Table 9. continued

Station	6323	6324	6325	6326	6327	6328
Wire Length	Nonastacin type Carotenoids M S P U/m³					
0 m	0.086	0.047	0.119	0.076	0.044	0.044
10	0.036	0.038	0.047	0.044	0.045	0.039
25	0.035	0.052	0.042	0.039	0.040	0.035
50	0.037	0.041	0.058	0.060	0.040	0.046
75	0.047	0.067	0.063	0.064	0.054	0.045
100	0.065	0.053	0.082	0.061	0.063	0.048
125	0.052	0.074	0.055	0.090	0.046	0.043
150	0.055	0.041	0.064	0.071	0.040	0.046
200	0.059	0.059	0.075	0.060	0.034	0.039
Wire Length	Astacin type Carotenoids M S P U/m³					
0 m	(−0.007)	0.003	(−0.022)	0.008	0.003	0.017
10	0.004	0.006	(−0.002)	0.002	0.001	0.019
25	0.006	(−0.005)	0.007	0.007	0.0035	0.015
50	0.007	0.015	0.012	0.021	0.002	0.026
75	0.034	0.114	0.076	0.043	0.020	0.074
100	0.064	0.065	0.069	0.026	0.064	0.067
125	0.034	(−0.010)	0.038	(−0.012)	0.028	0.019
150	0.002	0.001	0.012	0.009	0.021	0.003
200	(−0.001)	(−0.011)	(−0.018)	0.003	0.008	0.008
Wire Length	Ratio of Absorbencies D430/D665					
0 m	14.0	15.7	17.29	21.9	14.8	6.7
10	14.5	13.12	19.5	15.0	13.5	8.13
25	15.44	12.62	14.47	16.9	12.8	8.21
50	11.5	9.3	11.94	12.7	11.2	8.96
75	8.97	5.89	7.67	8.03	9.45	7.35
100	7.52	7.34	8.14	9.38	7.39	7.30
125	8.55	11.05	10.1	12.5	8.69	9.7
150	15.0	14.52	15.55	12.6	10.43	15.3
200	17.4	15.08	18.15	15.5	17.55	11.9

Table 9. continued

Surface Station	Chlorophyll microgram/m³			Calotenoid MSPU/m³		D430/D665
	a	b	c	Non Astacin	Astacin	
UM-						
A- 1	321	125	0.911			
A- 2	77	32	0.375			
A- 3	47	32.6	0.212			
A- 4	51	35	0.319			
A- 5	20	11.5	0.204			
A- 6	16	9.2	0.139			
A- 7	19	4.1	0.036			
A- 8	33	9.4	0.077			
A- 9	59	10.2	0.196			
A-10	77	8.8	0.203			
A-11	63	8.8	0.128			
A-12						
Darwin						
A-13	30	7.8	0.100			
Broome						
A-14	44	33.2	0.246			
A-15	35	26.9	0.134			
A-16	56.2	62.4	0.538			
A-17	64.3	46.4	0.275			
A-18	249.0	223.0	1.623			
Geraldton · Fremantle						
A-19	107.0	128.3	0.885			
A-20	28.1	16.6	0.135	0.030	0.018	10.23
A-21	77.0	165.0	1.138	0.016	0.009	14.7
A-22	273.0	92.7	0.970	0.092	0.076	5.3
A-23	44.1	34.5	0.253	0.041	0.026	9.26
A-24	41.5	10.8	0.140	(−0.001)	0.048	9.5
Penang						
A-25	530.8	119.2	1.151	0.171	0.178	5.4
A-26	133.8	48.2	0.3134	0.058	0.065	6.4
A-27	466.2	102.8	1.099	0.157	0.206	6.06
A-28	77.4	28.1	0.228	0.056	0.032	7.53
A-29	22.9	29.6	0.2345	0.045	0.028	17.5
A-30	49.5	21.4	0.180	0.040	0.026	8.62
A-31	219.0	49.6	0.640	0.081	0.124	6.48
A-32	307.9	82.5	0.555	0.096	0.134	5.65
A-33	323.7	80.1	0.705	0.149	0.151	6.5
A-34	203.2	77.7	0.575	0.167	0.068	7.75
A-35	320.5	66.5	0.549	0.056	0.157	5.05
A-36	365.0	59.0	0.536	0.054	0.189	4.94

Table 10. Quantity of seston and attenuation coefficients ($K \cdot 10^3$) at the layer of water sampling.

Station	UM-6300	6301	6302	6303	6304	6305	6305′	6306	6307	6308	6309	6310	6311	6312	6313
Wire Length	Seston mg/m³														
0 m	1200	1170	1410	510	650	650	660	460	1000	650	280	330	1020	430	290
10	×	870	500	100	430	410	290	280	800	510	190	370	490	170	270
25	×	530	630	320	480	510	280	380	540	530	240	300	370	260	230
50	560	1240	×	200	200	290	580	300	620	620	340	300	330	320	330
75	720	560	×	120	100	400	500	540	160	530	190	420	410	390	310
100	×	1000	710	90	210	320	550	380	390	620	250	470	360	410	650
125	×	400	1060	180	870	480		360	410	450	270	550	370	330	410
150	×	360	×	230	710	550		360	550	440	360	340	360	270	210
200	×	820	910	350	1250	490		980	630	460	270	1300	290	110	330
Wire Length	Attenuation Coefficient of Blue Irradiation $K_B \cdot 10^3$ (λ: 391·444·484 mμ)														
0 m											129	12	24	16	23
10											15	16	28	14	3
25											18	11	20	21	11
50											38	19	15	16	34
75											187	49	21	39	82
100											87			22	
125											69			24	
150											120			14	
200											34				
Wire Length	Attenuation Coefficient of Green Irradiation $K_G \cdot 10^3$ (λ: 519·538·561 mμ)														
0 m		13	134	99	320	38	91	170	144	80	68	132	12	72	38
10		57	53	84	65	68	104	70	80	28	63	50	23	43	37
25		63	39	66	56	30	58	59	106	81	64	54	38	76	31
50		79	53	44	48	49	61	64	87	49	73	43	59	69	45
75		95	43	37	59	50	97	31	48	86	122	34	58	92	110
100		37	48	61	35	28	63	57	67	64	66	43	46	55	
125			43	62	36	31		60	19	63	49	68	71	95	
150			43		39	62		35	40	48	59	36	72	61	
200								7	32	30	46				
Wire Length	Attenuation Coefficient of Amber Irradiation $K_A \cdot 10^3$ (λ: 549·564·584 mμ)														
0 m		88	41	61	78	102	159	253	251	215	143	280	13	34	105
10		96	85	137	87	85	107	79	151	110	87	85	73	68	42
25		75	70	55	73	37	73	99	133	71	88	79	62	79	65
50		86	87	58	88	108	52	89	97	85	90	63	105	71	56
75		100	75	72	71	69	106	63	66	100	101	49	37	94	140
100			60				64	57	38	76	67	36	56	59	
125			40					33		29	36	29	67	50	
150			49							10	12	10	64	40	
200										12	10				

Table 10. continued

Station	UM-6313′	6314	6315	6316	6317	6318	6319	6320	6321	6322	6323	6324	6325	6326	6327	6328
Wire Length	Seston	mg/m³														
0 m	×	130	560	470	420	180	460	320	400	300	460	650	1150	350	600	300
10	×	270	60	290	270	210	230	550	150	180	210	230	380	440	210	200
25	×	350	290	260	300	90	330	760	90	230	550	240	470	360	130	170
50	×	460	210	270	120	190	290	490	80	200	300	310	190	320	210	270
75	×	290	340	410	130	10	180	490	80	210	480	310	390	300	230	180
100	×	560	80	510	360	100	360	210	100	180	350	290	200	540	110	400
125	×	140	240	400	420	170	340	310	70	260	240	310	250	390	190	230
150		290	160	380	330	160	260	430	10	120	400	300	140	200	90	210
200		280	180	260	190	160	580	410	170	160	410	760	180	300	220	180
Wire Length	Attenuation Coefficient of Blue Irradiation $K_B \cdot 10^3$ (λ: 391·444·484 mμ)															
0 m		130	20	2	6	50	38	9	6	147	39	5	16	65	107	23
10		32	3	2	3	32	19	5	5	10	10	16	9	4	3	9
25		6	11	6	4	13	15	10	23	7	8	13	7	13	7	17
50		18	23	19	9	25	24	13	28	23	14	34	41	43	15	31
75		50	37	50	18	22	56	42	74	68	45	28	82	72	64	91
100																
125																
150																
200																
Wire Length	Attenuation Coefficient of Green Irradiation $K_G \cdot 10^3$ (λ: 519·538·561 mμ)															
0 m	245	260	30	130	14	238	60	53	17	250	48	26	119	130	60	52
10	32	37	18	30	43	43	64	17	65	50	57	100	21	37	42	59
25	57	72	39	18	20	46	26	62	20	37	30	46	60	42	49	48
50	31	51	83	89	55	61	65	53	55	58	39	55	52	53	43	40
75		57	65	40	56	47	79	66	69	67	71	95	82	46	84	116
100																
125																
150																
200																
Wire Length	Attenuation Coefficient of Amber Irradiation $K_A \cdot 10^3$ (λ: 549·564·584 mμ)															
0 m		300	190	100	86	300	93	144	55	260	98	83	186	175	132	122
10		66	83	53	49	59	77	48	78	80	85	94	46	56	66	74
25		66	50	16	31	92	45	78	41	58	55	64	60	56	50	72
50		63	83	82	42	60	137	49	56	57	69	42	64	59	51	45
75		73	63	96	38	66	81	66	76	72	77	100	60	190	80	162
100																
125																
150																
200																

Table 10. continued

Surface Station	Seston mg/m³
UM-A- 1	1700
A- 2	420
A- 3	450
A- 4	190
A- 5	250
A- 6	90
A- 7	180
A- 8	160
A- 9	210
A-10	180
A-11	290
A-12	230
Darwin	
A-13	540
Broome	
UM-A-14	900
A-15	930
A-16	330
A-17	240
A-18	600
Geraldton-Fremantle	
A-19	740
A-20	220
A-21	690
A-22	560
A-23	250
A-24	390
Penang	
UM-A-25	550
A-26	630
A-27	880
A-28	380
A-29	290
A-30	300
A-31	790
A-32	1180
A-33	1720
A-34	460
A-35	840
A-36	×

Reprinted from *Comp. Biochem. Physiol.*, vol. 18, 1966, p. 961-969

THE INVERTEBRATE ACID DEOXYRIBONUCLEASES AND MOLECULAR TAXONOMY*

ANTHONY P. RUSSELL†

Department of Biology, Boston University, Boston, Massachusetts

(*Received* 21 *February* 1966)

Abstract—1. The effects of three salts at one concentration on the kinetics of crude preparations of acid DNase from 38 invertebrates were measured.

2. Taxonomically related animals have enzymes with a similar response to the salts but the taxonomic rank of animals with similar enzymes vary.

3. These findings were interpreted as representing the divergent evolution of a single molecule.

4. Possible mechanisms explaining the pattern found for acid DNase are discussed.

5. An outline and discussion of molecular taxonomy are presented.

INTRODUCTION

In a previous paper (Russell *et al.*, 1964) it was shown that certain salts which activate the acid deoxyribonuclease (DNase) from a mollusk, an arthropod and an annelid are inhibitory to calf thymus acid DNase and the acid DNase of an echinoderm.

Since these findings appear significant in the evolution of invertebrate and vertebrate forms, these observations have been extended. The research reported in this paper is a result of a survey of the acid DNase of 38 invertebrates from the Indian Ocean.

Special methods were chosen for this survey which would permit rapid analysis with portable equipment of the enzyme from many animals. Three problems were considered: extraction of the enzyme from tissue of various invertebrates; method of measurement of enzyme activity; and the method by which similarities and differences between enzymes could be demonstrated.

As purification of acid DNase was not possible, the enzyme was extracted from the tissue suspended in deionized water by homogenization in a hand-operated homogenizer built by the author. The homogenate was acidified to pH 2·5 to

* This work was performed at Nossi Bé, Madagascar, and was supported by the National Science Foundation as a part of the United States Program in Biology of the International Indian Ocean Expedition.

† Present address: Research Service, Veterans Administration Hospital, 200 Springs Road, Bedford, Massachusetts 01730.

precipitate contaminants. This pH is used during the purification of vertebrate acid DNase (Bernardi, 1961) and, in the author's experience, does not precipitate acid DNase in a solution of low ionic strength. Heavy precipitates were removed from the solution by centrifugation in a hand-operated centrifuge, and the supernatant used as a source of enzyme. The author has observed by purifying various acid DNases that the presence of impurities in an acid DNase solution depresses the effect of activators and inhibitors of the enzyme, but does not qualitatively change their effect. This has been substantiated by deliberately adding contaminants to purified acid DNase (Cordonnier, 1964).

Acid DNase activity was measured by standard techniques in a capillary viscometer (McCarty, 1946; Tampion, 1965), which was chosen due to its simplicity. The concentration of the substrate deoxyribonucleic acid (DNA) was sufficiently high to avoid the effect of shear on the DNA during the course of the experiment (Robins, 1964).

The similarities and differences between acid DNases from various animals were demonstrated by measuring the effect of three different salts (a divalent cation, a divalent anion and a chelating compound) on the activity of the enzyme against DNA. A concentration for each salt was chosen that has been found to clearly inhibit calf thymus acid DNase and activate previously studied invertebrate acid DNases (Russell *et al.*, 1964).

The addition of salts causes a change in the specific viscosity of DNA solution (Schruggs & Ross, 1964), which in the experiments reported in this paper was found to amount to approximately a 2 per cent increase for the divalent anion and chelating compound, and a 2 per cent decrease for the divalent cation which possibly reflects the interaction of the salts with the phosphate charges on the DNA (Schildkraut, 1965). However, as the substrate salt concentrations are constant for each enzyme studied, differences in activation and inhibition between enzymes is attributable to the salts.

MATERIAL AND METHODS

Marine animals were collected from the coastal areas of Nossi Bé, Madagascar, and were kept alive until used. For preparation of the enzyme solution, dissected tissue was diluted with 1 vol of deionized water and homogenized. The homogenate was acidified to pH 2·5, and centrifuged in a hand-operated centrifuge. The supernatant, containing the enzyme, was used without further treatment.

The enzymatic hydrolysis of DNA was measured in an Ostwald–Fenske viscometer with a flow time for water of 26·8 sec at 30°C. All measurements were performed at 30°C. To measure the rate of hydrolysis, 5 ml of a 0·16 M pH 5·0 acetate buffer solution containing 0·4 mg/ml of salmon sperm DNA (Calif. Corp. Biochem. Res. Lot No. 590493) was placed in the viscometer, and 0·1–0·2 ml of the enzyme solution mixed with the substrate. Rate of flow of the solution through the viscometer was measured at approximately 1 min intervals. The velocity of hydrolysis of DNA by the enzyme was measured by similar techniques in the presence of three separate salts: 0·04 M $MgCl_2$, 0·04 M Na_2SO_4 and 0·04 M

sodium citrate. The data were plotted as previously reported (Russell *et al.*, 1964) and the slope *m* of the resulting lines measured. The slope resulting from the measurement without added salts was made equal to 100, and the slope resulting from the reaction in the presence of the salts was set proportional to this. Consequently, inhibition of the enzyme activity results in a number of less than 100, and activation, in a number greater than 100.

The above data were also plotted as a profile on a graph. The slope *m* for each salt was plotted as a point on the ordinate, while three equidistant points on the abscissa represent the presence of 0·04 M $MgCl_2$, 0·04 M Na_2SO_4 or 0·04 M sodium citrate in the reaction medium. The three points are connected by a line. With this profile it is possible to compare the enzyme reaction from various animals by inspection.

RESULTS

TABLE 1—COMPARATIVE EFFECT OF SALTS ON THE ACTIVITY OF INVERTEBRATE ACID DNASE

Animal	Normalized slope of enzyme reaction in the presence of 0·04 M salt		
	$MgCl_2$	Na_2SO_4	NaCitrate
Starfish			
Protoeaster lincki (Blainville)	175	238	152
Culcita schimideliana (Retzius)	260	149	193
Sea cucumber			
Argiodia nobilis (Selenka)	162	55	15
Thelenota ananas (Jaeger)	151	131	160
Crinoid			
Unidentified crinoid	52	112	71
Brittle Star			
Unidentified ophiuroid	41	84	45
Mollusks			
Asaphis rugosa Lamarck	11	54	30
Malleus malleus (Linné)	77	46	33
Tridacna squamosa Lamarck	162	161	158
Pycnodonta sp.	57	134	109
Chama sp.	28	92	31
Lambis (*Millepes*) *scorpius scorpius* (Linné)	28	46	21
Achatina sp.	190	216	208
Amphineuran	2	27	2
Annelid			
Unidentified polychaete	42	150	100
Coelenterates			
Cassiopea sp.	137	98	130
Unidentified alcyonarian	82	144	109
Radianthus ritteri (Kwietniewski)	0	82	30
Unidentified pennatulid	37	193	110
Sponge			
Siphonochalina fascigera Hentschel	33	95	50

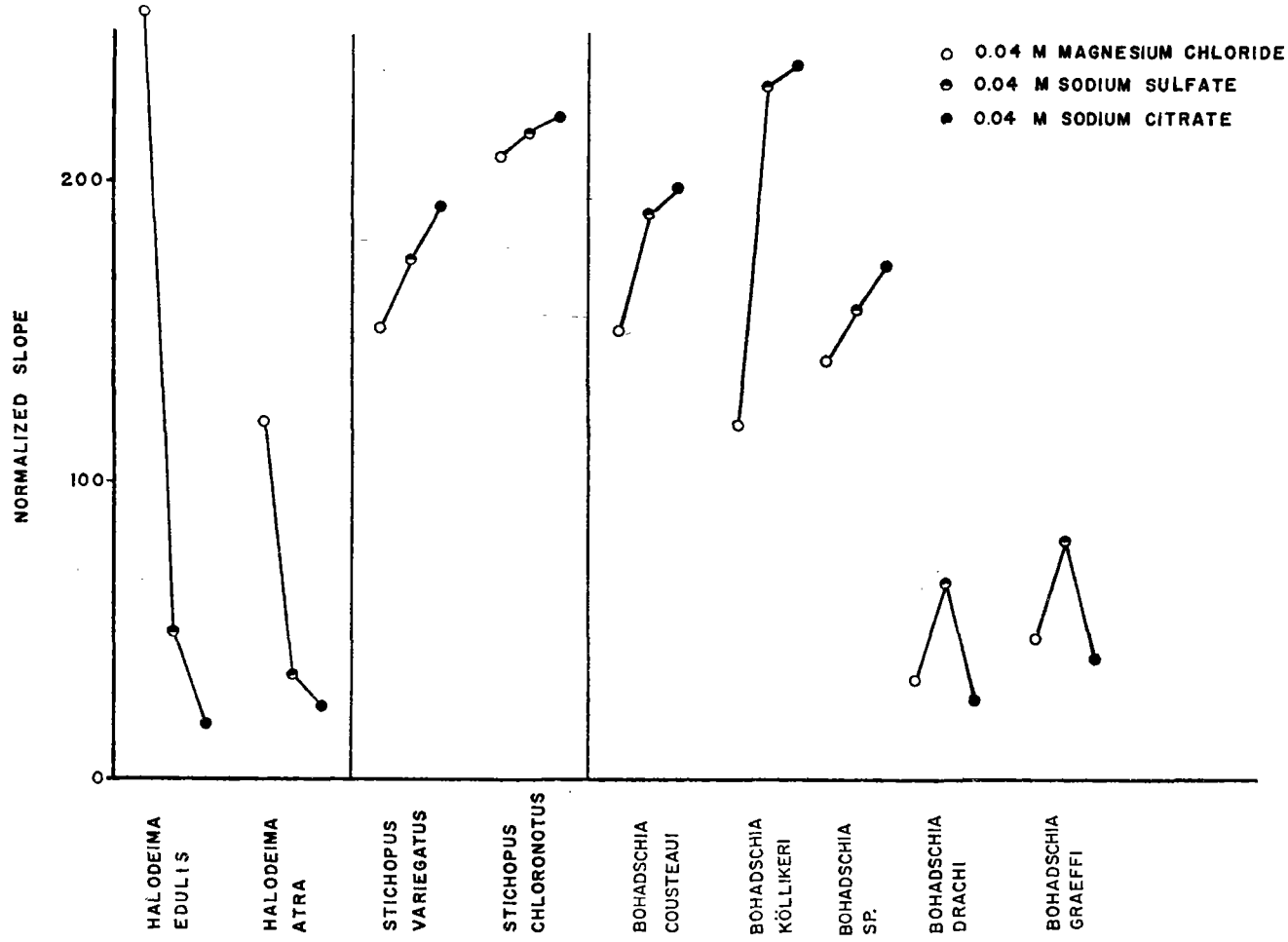


FIG. 1. Profile of the effect of salts on the acid DNase activity of three genera of sea cucumbers.

Acid DNase activity was found in all animals tested. All the enzymes appeared to be endonucleotidases since hydrolysis of DNA proceeded without a time lag. The figures present the profiles of measurements of enzyme activity of animals in taxonomically related groups. It may be seen from the profiles that enzymes which appear to have similar characteristics do not have numerically identical values,

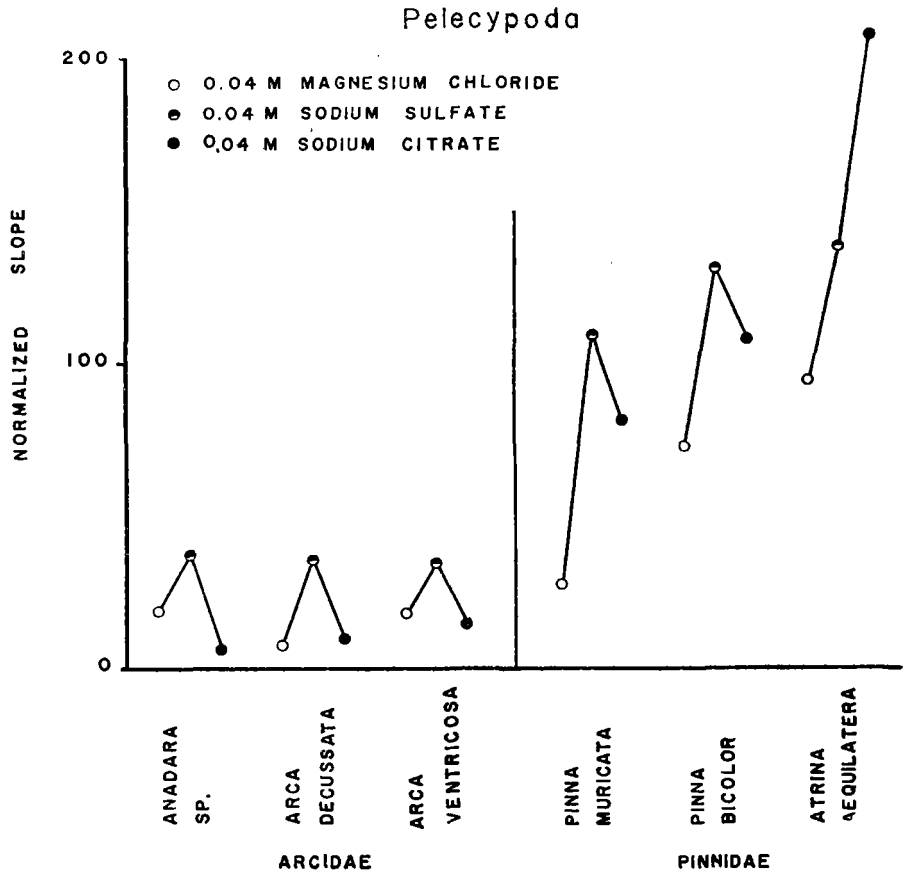


FIG. 2. Profile of the effect of salts on the acid DNase activity of two families of clams.

which in part reflect impurities in the preparations. However, the profiles have the same geometric shape which is striking when compared to the pattern from unrelated enzymes. Table 1 lists the measurements of enzyme activity of animals not included in the profiles. Similarities and differences between the enzymes may be seen, but the animals are too distantly related to include in the profiles.

The Figures show that the effect of the salts on enzyme activity results in a similar profile for all species of any genus except for *Bohadschia* (Fig. 1), a genus which needs redescription (E. Deichmann, personal communication). Fig. 2 shows

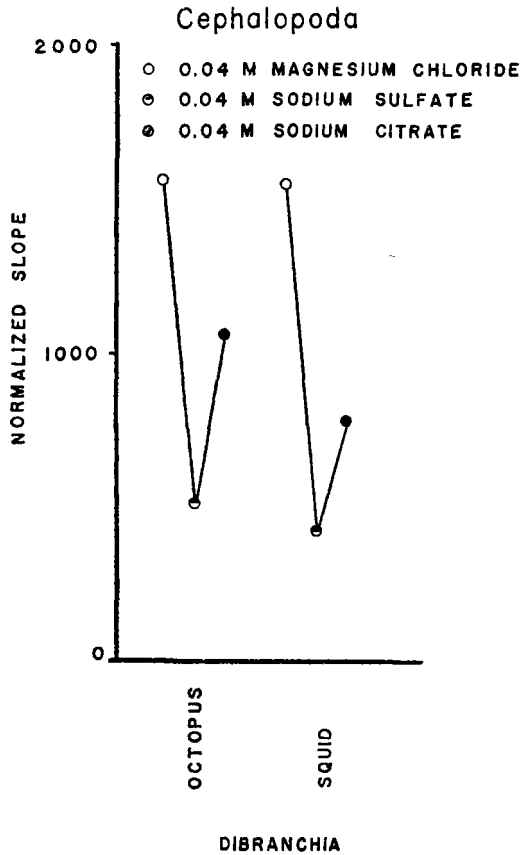


FIG. 3. Profile of the effect of salts on the acid DNase activity of the octopus and the squid which belong to separate orders.

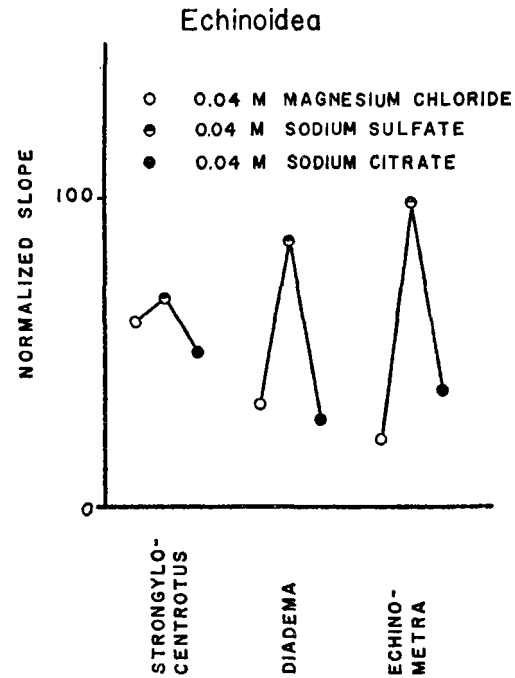


FIG. 4. Profile of the effect of salts on the acid DNase activity of three sea urchins.

the profiles representing two families of mollusks. Two genera of the family Arcidae have enzymes which result in similar profiles, suggesting the enzyme may be similar within the family. However, in the Pinnidae, the profile for the genus *Atrina* differs from that for the genus *Pinna*. The enzymes of the squid and the octopus (Fig. 3), which belong to different orders, have a strikingly similar profile as the activation of their enzymes is ten times greater than the enzymes of other animals. Finally, three genera of the class Echiuroidea (Fig. 4) have a basically similar response to salts. The data on the echiuroid *Strongylocentrotus dröbachiensis* is taken from the previous paper (Russell *et al.*, 1964). The enzyme had been subject to a partial purification.

DISCUSSION

The results suggest that acid DNase may undergo evolutionary changes within one taxon, while in another taxon it appears unchanged. Acid DNases with similar properties occur in taxa of different rank. This finding reflects the evolutionary pattern of a single molecule, which, taken with other molecules, reflect evolution of the species.

The pattern may be interpreted as meaning that the gene coded for acid DNase is undergoing mutations in one taxon, while in another it is not. Since the enzyme was extracted from living animals, the mutations under discussion are presumed to be non-lethal. Moreover, the occurrence of acid DNases of different characteristics appears to represent divergent evolution of one gene. This hypothesis is based on the observation that acid DNase occurs throughout the Animalia, including the Protozoa (Eichel & Roth, 1953) and would therefore appear to be an enzyme basic to cell function. Allfrey & Mirsky (1952) related mammalian acid DNase to the function of the tissue and the ability of cells to divide and regenerate, Zahn (1960) showed it to be a growth substance, and Vorbrodt (1961) showed enzyme to be associated with the chromosomes of liver parenchymal cells. From these observations acid DNase appears intimately associated with cell function, with the consequence that the code for this enzyme would be expected to be a part of the genome of all animal cells. Differences in the enzyme from different animals would therefore represent divergent evolution.

There are three possibilities which could account for changes in acid DNase in one taxon and stability of acid DNase in another related taxon. The stability or instability of the code for the enzyme may be related only to the base sequence of the DNA; those genes being highest in thymine being the most susceptible to mutation, as thymine is the base most sensitive to radiation damage (Weiss, 1964). The second possiblity involves the relationship of acid DNase to cell physiology. In the organisms which show no change in the ionic requirements of acid DNase from one taxon to another, biochemical pathways associated with acid DNase activity might be so delicately balanced that any change in ionic requirements of the enzyme would be lethal. The third possibility involves the evolutionary trend of the organism (Simpson, 1950). If the trend reflects a change in a specific section

of the genome, then variations in acid DNase would suggest that the gene for acid DNase is included in that section of the genome involved in the evolution of the taxon, while the opposite is true in animals belonging to taxa which show no change in acid DNase.

If it is hypothesized that the distribution observed for acid DNase is true of all molecules, it follows that between any two taxa certain of the molecules will be identical and certain ones will differ. It would therefore be possible to make a biochemical definition of a taxon in relationship to other taxa, which would include molecules which are stable between the taxa and those which vary. The biochemical definition of the taxon might have a predictive value. If all the species of a genus have a molecular system which is unchanged throughout the genus, and a non-lethal mutation of this system occurs in one of the species, this species might represent the start of a new genus. It is conceivable that this effect would operate to form higher taxa, as a non-lethal mutation in a previously stable molecule leading to the evolution of a new family, order, etc. It is presupposed that any such mutation would not be disadvantageous to the organism.

The concept of a biochemical definition of the taxon is related to molecular systematics. Basic to the taxonomy are molecules which function in a specific reaction and which are common to all organisms. Nucleic acids would certainly be among these molecules and possibly certain enzymes. Further, there are molecules which reflect the relationship of all species within a kingdom. Acid DNase presumably falls into this category. Divergence to phyla and lower taxa may also be represented by molecules which are characteristic of each of the taxonomic groupings. The extent of homologous sequences in the DNA of vertebrates have been studied by Hoyer *et al.* (1964) who find that approximately 8 per cent of the genome of humans and salmon are exactly homologous. Thus one would expect that at least 8 per cent of the molecules of these vertebrates are similar.

Function is directly correlated with the taxomony of the molecules, from those basic to all life to those which vary from individual to individual. The most basic would be associated with cellular physiology and reproduction. The next would be those associated with cellular differentiation and metazoan physiology. Molecules associated with lower taxa would be expected to be correlated with the especial morphological and physiological characteristics of the taxon and would not be subject to variable expression where interbreeding does not occur. Finally, there are those molecules which are involved in the expression of individual differences, the genetics and chemistry of which have been widely studied. Consequently, the taxonomic rank of a molecule indicates its function.

Further work in molecular taxonomy should not only give information in molecular mechanisms operating in evolution, but should help clarify the function of molecules in the development, morphology and physiology of organisms.

Acknowledgements—I am greatly indebted to Dr. Arthur G. Humes for both helping to collect the animals used in this study and identifying them. I would also like to thank Dr. Donald I. Patt for his interest in this work and discussion of the results.

REFERENCES

ALLFREY V. & MIRSKY A. E. (1952) Some aspects of the deoxyribonuclease activities of animal tissues. *J. gen. Physiol.* **36**, 227–241.

BERNARDI G. (1961) Chromatographic purification of acid ribonuclease from calf thymus. *Biochim. biophys. Acta* **53**, 216–217.

CORDONNIER C. (1964) Etude comparée des désoxyribonucléases acides extraites de tissus différents, p. 37. Thèse présentée à la Faculté des Sciences de l'Université de Strasbourg, France.

EICHEL H. J. & ROTH J. S. (1953) The effect of X-irradiation on nuclease activity and respiration of *Tetrahymena Galeii* W. *Biol. Bull., Woods Hole* **104**, 351–358.

HOYER B. H., MCCARTHY B. J. & BOLTON E. T. (1964) A molecular approach in the systematics of higher organisms. *Science, N.Y.* **144**, 959–967.

MCCARTY M. (1946) Purification and properties of deoxyribonuclease isolated from beef pancreas. *J. gen. Physiol.* **29**, 123–139.

ROBINS A. B. (1964) Non-Newtonian behaviour of dilute DNA solutions. *Trans. Faraday Soc.* **60**, 1344–1351.

RUSSELL A. P., PATT D. I. & TERNER C. (1964) Invertebrate acid deoxyribonucleases. *J. cell. comp. Physiol.* **63**, 71–76.

SCHILDKRAUT C. (1965) Dependence of the melting temperature of DNA on salt concentration. *Biopolymers* **3**, 195–208.

SCHRUGGS R. L. & ROSS P. D. (1964) Viscosity study of DNA. *Biopolymers* **2**, 593–609.

SIMPSON G. G. (1950) *The Meaning of Evolution*, p. 31. Mentor Book, New American Library, New York.

TAMPION J. (1965) New method for the determination of the activity of viscosity-reducing enzymes. *Nature, Lond.* **206**, 510–511.

VORBRODT A. (1961) Histochemical studies on the intracellular localization of acid deoxyribonuclease. *J. Histochem. Cytochem.* **9**, 647–655.

WEISS J. J. (1964) Effects of radiation on nucleic acids. In *Progress in Nucleic Acid Research and Molecular Biology* (Edited by DAVIDSON J. N. & COHN W. E.), Vol. 3, p. 133. Academic Press, New York.

ZAHN R. K. (1960) Deoxyribonucleases as growth substances. *Biochem. J.* **76**, 66 P.

Reprinted from *Comp. Biochem. Physiol.*, vol. 17, 1966, p. 641-660

SALT AND WATER BALANCE IN SELECTED CRABS OF MADAGASCAR

WARREN J. GROSS, ROBERT C. LASIEWSKI, MICHAEL DENNIS and PAUL RUDY, JR.

Department of Life Sciences, University of California, Riverside; Department of Zoology, University of California, Los Angeles; Department of Biological Sciences, Stanford University, and Department of Zoology, University of California, Davis

(*Received* 26 *July* 1965)

Abstract—1. Salt and water regulation were studied in *Cardisoma carnifex*, *Sesarma meinerti*, *Varuna litterata* and *Coenobita cavipes*.

2. The brachyurans, *Cardisoma*, *Sesarma* and *Varuna* show strong osmoregulation in tap water or 150 per cent sea water, the antennary glands being ineffective in the process but able to concentrate magnesium in the urine independently of the magnesium influx from the medium.

3. The anomuran *Coenobita* was not studied in immersion experiments but was shown to control its water balance on land by behavioral means.

4. When desiccated, *Cardisoma* can regain water against an osmotic gradient from sea water dampened sand.

INTRODUCTION

DESPITE numerous studies of osmotic and ionic regulation in the decapod Crustacea, only a small sample of the great variety of species has been examined, partly because so many are found in remote parts of the world. This is especially so in the tropical zones which furnish critical material for comparative studies, since numerous amphibious, terrestrial and fresh-water crabs occur there. The extreme and fluctuating stresses, commonly imposed on such animals, may be expected to have encouraged the selection of a variety of mechanisms concerned with water and salt balance. Yet this wealth of potential, experimental material is relatively inaccessible and, with few exceptions, remains neglected.

The general subject of osmotic and ionic regulation has been reviewed recently by Potts & Parry (1964); Lockwood (1962) has reviewed osmotic regulation among the Crustacea. Several recent studies have been concerned with the physiological and behavioral capacities of crabs inhabiting terrestrial or semi-terrestrial situations. Gross (1964a) examined three species of anomuran land crabs in the field at Eniwetok and found that their success on land is due, for a large part, to their ability to regulate the concentration of their blood by behavioral means. Gross (1963) reported that the terrestrial brachyuran *Gecarcinus lateralis* of Bermuda could live indefinitely on sand dampened with fresh water as its sole source of water, but would dehydrate rapidly and die when placed in a situation where the only source of water was sand dampened with sea water. Gross (1964b) examined an array of crabs showing different degrees of terrestrialness and expanded the

early observation of Jones (1941) that crabs showing some degree of terrestrialness are commonly hypoosmotic regulators as well as strong hyperosmotic regulators.

The primary function of the crab antennary gland seems to be that of ionic rather than osmotic regulation, for the blood and urine are essentially isoosmotic regardless of the salinity of the external medium (Potts & Parry, 1964). This is also true in the few species of fresh-water crabs studied, such as *Eriocheir sinensis* (Scholles, 1933), *Potamon edulis* (Schlieper & Hermann, 1930) and *P. niloticus* (Shaw, 1959), although too few species have been examined to permit the generalization that the antennary glands of all fresh-water crabs have no osmoregulatory function. Green *et al.* (1959) reported that the urine of *Uca pugilator* and *U. pugnax* is hyperosmotic to the blood when the crabs are immersed in 175 per cent sea water. Gross (1964b), on the other hand, found no osmotic difference between blood and urine of *U. crenulata* either under hyper- or hypoosmotic stress. Prosser *et al.* (1955) demonstrated in the shore crab *Pachygrapsus crassipes* that as the medium becomes more concentrated, the urine Mg increases in concentration, but the urine Na decreases in concentration. A similar phenomenon has also been shown in *U. pugilator* and *U. pugnax* (Green *et al.* 1959); in *Cancer antennarius*, *Hemigrapsus oregonensis* and *U. crenulata* (Gross, 1964b). A notable exception to this phenomenon was the highly terrestrial crab *G. lateralis* which was incapable of concentrating Mg in its urine and which showed an increase in urine Na as the medium increased in concentration (Gross, 1964b). Such a dramatic physiological difference suggested a fundamentally different renal mechanism in this family of crabs (Gecarcinidae). However, De Leersnyder & Hoestlandt (1963) studied another gecarcinid, *Cardisoma armatum* and reported high urine Mg concentrations when it was immersed in sea water.

It is apparent that considerable physiological diversity can exist within a single family of crabs, and even within one genus, such as *Uca*. Since knowledge of a few representatives of a taxonomic group in which there is a considerable radiation of species does not permit generalities, more information about the physiology of ionic and osmotic regulation in further species of crabs is needed. The authors had the opportunity to acquire such information during July and August of 1964 while participating in the International Indian Ocean Expedition aboard the Research Vessel *Te Vega*. Four species of Madagascar crabs which had not been studied previously with respect to their osmotic relations were examined. Three of the species were brachyuran crabs, inhabiting fresh water, amphibious and terrestrial situations respectively. The fourth was an anomuran terrestrial hermit crab. This investigation provides information on some of the physiological adaptations for terrestrial life among crabs, and produces further evidence concerning the role of the antennary gland in diverse decapod crustaceans.

MATERIALS AND METHODS

The brachyuran crabs studied were *Sesarma meinerti* de Man, *Varuna litterata* (Fabricius) and *Cardisoma carnifex* (Herbst). The anomuran was the terrestrial hermit crab *Coenobita cavipes* Stimpson. All four species were collected in the vicinity of the Centre d'Oceanographie et des Pêches de Nosy Bé, Madagascar. The terrestrial *Cardisoma* and amphibious

Sesarma were collected in mangrove areas which are periodically inundated with normal sea water, but also occasionally exposed to runoff of rain water. *Varuna* was netted in fresh water about 400 m landward from the mouth of a stream. The total Ca plus Mg of this water was determined to be less than 4 m-equiv/l compared to 125 m-equiv/l for sea water. The collecting sites for this crab were separated from brackish water by a riffle which dropped about 5 m elevation to the highest tidal level of the sea. *Coenobita* was collected in and around sugar-cane fields close to the sea. All crabs were mature and between molts. *Cardisoma* ranged in size from 100 to 485 g; *Sesarma* was larger than 25 g; *Varuna* ranged between 15 and 25 g; and the *Coenobita* were estimated to be larger than 25 g without their adopted shells. Several *Cardisoma* were collected on the island of Anjouan in the Comores, but most of these were used in the exploratory parts of the investigation. Details of the natural history and taxonomy of the four subject species are given by Barnard (1950).

Urine was removed from the nephropores by means of a fine glass cannula. Blood was extracted from all species by puncturing the arthrodial membranes at the bases of the appendages by means of a glass pipette. The blood usually was introduced into a 2 ml graduated plastic beaker where it was allowed to coagulate. The clot was removed and the serum analyzed.

Osmotic concentrations of fluids were determined by means of a Mechrolab vapor pressure osmometer. Each test solution was compared with a standard of normal sea water (salinity: 34‰). Osmotic concentrations could be determined to within ± 1 per cent accuracy for the range of concentrations observed in this study. No obvious difference has been observed between serum and whole blood osmotic concentrations in crabs (Prosser *et al.*, 1955; Gross, 1964a).

Salinity of water was estimated in the field by means of an American Optical Company TS meter (Goldberg refractometer). The range of error for this method is less than 3 per cent for concentrations near normal sea water.

Ca and Mg were determined by titration with ethylene diamine tetra acetic acid (EDTA), a method described by Schwarzenbach *et al.* (1946) and Wallach & Steck (1963). Urine and water were titrated directly. However, blood samples were dialyzed against deionized water and the dialysate was titrated for Ca plus Mg (Gross, 1959). Serum was titrated directly for Ca. Mg was estimated by difference. Exploratory tests showed no obvious difference between whole blood and serum with respect to Ca concentrations. Ca and Mg could be determined with less than a ± 5 per cent error for the minimum concentrations measured. However, volumetric measurements for the rapidly coagulating blood of *Cardisoma* could not be made precisely with the available methods and the error for Mg values in blood was as high as ± 10 per cent. Probability values were determined by means of Student's *t* test.

PROCEDURE AND RESULTS

Ionic and osmotic concentrations of blood (serum) and urine were determined on the four species of crabs under different environmental conditions. *Cardisoma* was investigated in a variety of aquatic and terrestrial situations, *Sesarma* and *Varuna* only in aquatic situations of different salinities and *Coenobita* only in a variety of terrestrial conditions. Immersion experiments involved exposure to the respective media for at least 24 hr and not more than 48 hr. Periods of immersion were in part dictated by the schedule of shipboard activity and, therefore, could not be as uniform as would have been desired. *Cardisoma* was transferred to the experimental medium directly after capture in the field, or was transferred from a box where the crabs were maintained in a terrestrial situation with fresh water, sea water and food accessible to them. *Sesarma* was also transferred to the experimental medium directly after capture in the field. *Varuna* was transferred from fresh water to 100 per cent sea water, but was exposed to 142 per cent sea water only after an intermediate step in 100 per cent sea water for 24 hr. With the exception of *Sesarma*, the

animals were in sufficiently large volumes of medium to cover them completely at all times. Since a limited number of *Sesarma* was available for study, they were permitted to rise partly out of the water and aerate the gill chamber in order to minimize the possibility of drowning. However, the *Sesarma* usually remained completely immersed throughout the experiments, and it is believed that the results would have been little different from those observed had the crabs been in large volumes of medium. The water temperatures for all immersion experiments ranged between 25 and 28°C.

Results of these experiments are presented in Tables 1–4. First, it should be pointed out that neither the amphibious *Sesarma* nor the terrestrial *Cardisoma* showed signs of drowning when immersed. The case of *Cardisoma* is particularly interesting in this respect, because another gecarcinid, *Gecarcinus lateralis*, gives indications of drowning in less than 24 hr when completely immersed (Gross, 1964b). In the present investigation, *C. carnifex* was observed to remain active

TABLE 1 (a)—EFFECTS OF OSMOTIC STRESS ON SERUM AND URINE CONCENTRATIONS IN *Cardisoma*

Medium		Osmotic (per cent S.W.)			Ca m-equiv/l			Mg m-equiv/l		
		Mean	S.D.	No.	Mean	S.D.	No.	Mean	S.D.	No.
	Urine	67·1	3·87	11	9·06	2·39	10	50·0	29·1	11
Tap water	Serum	67·9	4·09	11	22·6	2·91	11	28·2	6·51	5
	U/S	0·99	0·015	11	0·42	0·19	10	1·93	1·61	5
100 per cent	Urine	79·5	3·22	11	14·3	6·01	11	120	54·0	7
sea water	Serum	81·1	3·67	13	30·6	2·78	13	25·8	12·4	8
	U/S	0·99	0·019	11	0·47	0·20	10	4·40	1·88	6
150 per cent	Urine	94·1	8·05	14	11·3	5·64	12	256	85·1	12
sea water	Serum	96·1	8·34	15	27·2	4·39	15	20·8	9·17	10
	U/S	0·99	0·010	14	0·42	0·22	12	15·7	16·6	8

for at least 3 days when completely immersed in 150 per cent sea water or for at least 4 days in tap water. *Varuna* obviously is adapted for a purely aquatic mode of life. Immersion experiments were not performed on *Coenobita*.

Cardisoma, *Sesarma* and *Varuna* are all strong hyperosmotic as well as hypoosmotic regulators (Fig. 1, Tables 1–3). Crabs of all three species remained active in tap water for more than 24 hr, sustaining large osmotic gradients. Individuals of all three species regulated their serum concentrations well below the concentrations of normal sea water (34 ‰) and hypersaline water. Fifty per cent of the *Varuna* placed in 142 per cent sea water died after 24 hr immersion, and the survivors were sub-normal in activity although regulating osmotically (see below). There were about 20 per cent mortalities when *Varuna* was transferred directly from fresh water to 100 per cent sea water. At first, animals so treated were relatively inactive but after a few hours regained normal activity; those which survived the first 24 hr remained viable for indefinite periods immersed in normal sea water. Ten such crabs, for example, were vigorous after a 20 day immersion in 100 per cent sea water.

TABLE 1(b)—SERUM AND URINE CONCENTRATIONS OF *Cardisoma* IN DIFFERENT TERRESTRIAL SITUATIONS

		Osmotic (% S.W.)			Ca m-equiv/l			Mg m-equiv/l			Duration of exposure
		Mean	S.D.	No.	Mean	S.D.	No.	Mean	S.D.	No.	
(a) Natural (field samples)	Urine	77·1	8·60	7	10·9	6·51	6	76·4	24·6	6	—
	Serum	78·0	7·88	7	22·5	3·36	7	—	—	—	—
	U/S	0·99	0·018	7	0·51	0·37	6	—	—	—	—
(b) Sea water (only), food and damp sand	Urine	86·5	4·11	5	—	—	—	—	—	—	At least 7 days
	Serum	82·7	3·43	5	—	—	—	—	—	—	
	U/S	0·97	0·011	5	—	—	—	—	—	—	
(c) Fresh water, sea water, food	Urine	83·4	3·57	5	—	—	—	—	—	—	At least 7 days
	Serum	84·6	4·27	5	—	—	—	—	—	—	
	U/S	0·99	0·009	5	—	—	—	—	—	—	
(d) Fresh water (only), food and damp sand	Urine	69·4	5·58	5	—	—	—	—	—	—	At least 7 days
	Serum	71·2	5·46	5	—	—	—	—	—	—	
	U/S	0·98	0·017	5	—	—	—	—	—	—	

S.W. = Sea water.

TABLE 2—EFFECTS OF OSMOTIC STRESS ON SERUM AND URINE CONCENTRATIONS IN *Sesarma*

Medium		Osmotic (% S.W.)			Ca (m-equiv/l)			Mg (m-equiv/l)		
		Mean	Range	No.	Mean	Range	No.	Mean	Range	No.
Fresh water	Urine	53·2	49·0 –56·3	3	12·3	4·0 –19·2	3	37·2	12·2 –56·0	3
	Serum	54·5	50·8 –57·3	4	26·8	25·6 –30·2	4	—	—	—
	U/S	0·97	0·96– 0·98	3	0·47	0·14– 0·80	3	—	—	—
100 per cent sea water	Urine	73·2	70·0 –76·6	3	6·9	3·7 –10·1	3	132	72·0 –178	3
	Serum	73·9	70·7 –77·5	3	27·9	24·8 –30·6	3	—	—	—
	U/S	0·99	0	3	0·24	0·15– 0·35	3	—	—	—
150 per cent sea water	Urine	91·7	88·6 –97·4	3	8·2	4·0 –14·7	3	383	291–475	3
	Serum	93·2	89·4 –97·9	4	31·4	30·6 –32·9	4	—	—	—
	U/S	0·99	0·98– 1·00	3	0·26	0·13– 0·48	3	—	—	—

S.W. = Sea water.

The osmotic behavior of *C. carnifex* in fresh water and sea water, shown in Table 1 and Fig. 1, is similar to that shown in *C. armatum* by De Leersnyder & Hoestlandt (1963). Thus it maintains its serum hypoosmotic to normal sea water and can regulate strongly in fresh water. Following the trend for other crabs of terrestrial habits (Gross, 1964b), this species as well as *Sesarma* also can regulate strongly in hypersaline water (Tables 1, 2, and Fig. 1).

It is also apparent from Tables 1–3 that the urine is essentially isoosmotic with the blood in *Cardiosoma*, *Sesarma* and *Varuna* for all treatments. Therefore, the antennary glands could have no significant value as osmoregulators. Thus, Fig. 1,

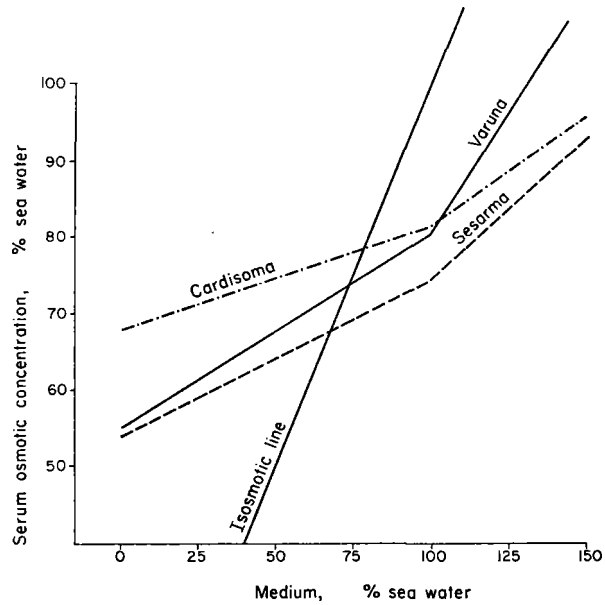


FIG. 1. Osmotic regulation in the crabs, *Cardisoma*, *Sesarma* and *Varuna*. Curves are estimated from mean values given in Tables 1–3.

which represents serum concentrations for crabs immersed in different media, could just as well represent urine concentrations.

It should be emphasized that values for immersion experiments indicated in Tables 1–3 and Fig. 1 cannot be compared precisely for the three subject species of the present investigation, or for species of other investigations. All immersion experiments were conducted under laboratory conditions which could influence the physiological response of each species in a different manner. As pointed out above, conditions aboard ship did not permit uniform or prolonged periods of immersion. There is evidence in the case of *Cardisoma*, the largest species of this study, that osmotic equilibrium is attained soon after 24 hr immersion. In tap water, for example, the serum osmotic concentration of five specimens averaged

69·2 per cent sea water after 24 hr immersion (range: 63·0–72·1); after 48 hr immersion the serum osmotic concentration of three smaller specimens averaged 64·7 per cent sea water (range: 58·6–69·5). Furthermore, five specimens of *Cardisoma*, whose serum osmotic concentrations averaged 90·6 per cent sea water after 24 hr immersion in 150 per cent sea water, increased the average to 95·6 per cent sea water after 48 hr immersion.

TABLE 3—EFFECTS OF OSMOTIC STRESS ON SERUM AND URINE CONCENTRATIONS IN *Varuna*

Medium		Osmotic (% S.W.)			Ca (m-equiv/l)			Mg (m-equiv/l)		
		Mean	S.D.	No.	Mean	S.D.	No.	Mean	S.D.	No.
Rain water	Urine	54·3	4·89	13	18·8	5·58	12	40·7	22·1	12
	Serum	55·0	4·32	13	25·3	3·33	13	—	—	—
	U/S	0·99	0·036	13	0·75	0·22	12	—	—	—
100 per cent sea water	Urine	80·7	4·75	9	33·0	12·1	9	164	147	8
	Serum	80·6	4·44	9	38·1	10·8	9	—	—	—
	U/S	1·00	0·024	9	0·89	0·29	9	—	—	—
142 per cent sea water	Urine	108	4·69	4	30·4	12·0	4	422	62·4	3
	Serum	109	2·94	4	36·6	8·72	4	—	—	—
	U/S	0·99	0·058	4	0·82	0·20	4	—	—	—

S.W. = Sea water.

TABLE 4.—EFFECTS OF AVAILABLE WATER ON SERUM CONCENTRATION IN *Coenobita*

Available water	Period of exposure (Days)	Serum osmotic concentration (% S.W.)		
		Mean	Range	No.
(a) Field samples	—	90·8	87·0– 98·1	5
(b) Sea water	4	105	103 – 108	3
(c) Fresh water	4	77·0	71·5– 87·0	3
(d) None	4	116	108 –131	3

S.W. = Sea water.

Despite the acknowledged, unavoidable shortcomings of the experimental procedure, it is obvious that all three species can sustain tremendous osmotic gradients between the blood and the external medium when exposed to the extreme stresses of tap and hypersaline water.

The osmotic concentration of fluid from the stomach and hind-gut of *Cardisoma* was determined, in an attempt to demonstrate the role of the gut (drinking) in

hyporegulation. After *Cardisoma* had been immersed in 145 per cent sea water for 38 hr, the highest osmotic concentration of hind-gut fluid found in four specimens was equivalent to 128 per cent sea water. This value is well below the concentration of the medium, and indicates that the gut of *Cardisoma* is not solely responsible for the hyporegulating process. In all five cases examined, the stomach fluid was almost isosmotic with the serum, and was never as concentrated as normal sea water. The mean value for the ratio, osmotic concentration of stomach fluid : osmotic concentration of serum, was 1·02 (range of 0·99–1·08). If significant volumes of the medium were drunk, the salts were rapidly absorbed and excreted by an extra-renal pathway. However, there is no evidence that the medium was drunk. In four measured cases the mean osmotic ratio of stomach fluid : hind-gut fluid was 0·90 (range: 0·77–0·97). This might be interpreted to mean that water was absorbed from the gut and/or that salts were added for excretion. If water in the ingested medium were selectively absorbed by the gut and the salts exclusively eliminated by the gut, the hind-gut fluid would have to be hyperosmotic to the medium. On the basis of these data, the role of the gut in hyporegulation cannot be resolved.

The serum concentration of Ca remained relatively constant for all salinities tested in the cases of *Cardisoma* and *Sesarma*. However, while *Varuna* maintained relatively constant serum Ca levels in 100 and 142 per cent sea water (means: 38·1 and 36·6 m-equiv/l respectively), the concentration dropped considerably to an average of 25·3 m-equiv/l when the crab was immersed in fresh water—the medium from which it was collected.

In all species studied, the Ca U/S values were much less than unity, indicating that the antennary glands conserve this ion under the described conditions. Such a phenomenon was also shown for *C. armatum* (De Leersnyder & Hoestlandt, 1963).

Mg concentrations in the blood were measured only in *Cardisoma*. The average value for crabs immersed in sea water was 25·8 m-equiv/l, which compares favorably with that reported by De Leersynder & Hoestlandt (1963) for *C. armatum*. On the other hand, the average blood Mg for *C. carnifex* immersed in tap water (28·2 m-equiv/l) is three times higher than values reported by De Leersynder & Hoestlandt (1963) for *C. armatum*. Such a difference could not be explained by the impreciseness of measurement for blood Mg in the present investigation. The urine Mg concentration for *C. carnifex* was about three times higher than that reported for *C. armatum* in fresh water, and there is no reason to doubt the validity of values for Mg in the urine.

In *Cardisoma*, *Sesarma* and *Varuna* the urine Mg concentration elevated dramatically as the salinity of the external medium increased (Fig. 2). In contrast, *Gecarcinus* showed no such response; the urine Mg remained constant in concentration (Gross, 1964b). It was suggested that since *Gecarcinus* has a marine larva, its ability to concentrate Mg in the urine is secondarily lost when the crab becomes landborne (Gross, 1964b). Inasmuch as *C. carnifex*, as well as *C. armatum* (De Leersynder & Hoestlandt, 1963) can concentrate Mg in the urine, it is obvious

that the inability of *G. lateralis* to do so is not a characteristic of the family Gecarcinidae.

It is interesting to note that the urine Mg of *Cardisoma*, *Sesarma* and *Varuna* was maximal in the hypersaline concentrations of sea water (Fig. 2), even though the high concentrations were achieved by adding NaCl to normal sea water. Therefore, the 150 per cent sea water contained no more Mg than 100 per cent

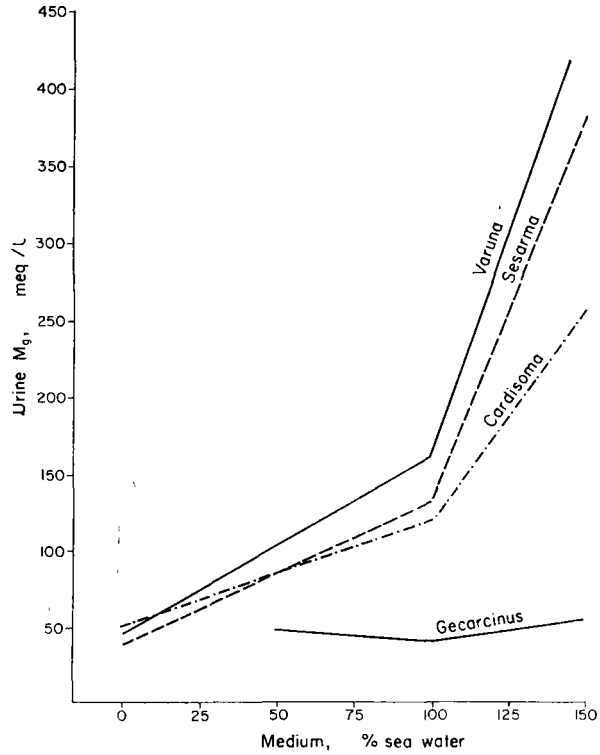


FIG. 2. Concentrations of urine magnesium for crabs immersed in media of different salinities. Curves for *Cardisoma*, *Sesarma* and *Varuna* are estimated from mean values in Tables 1–3. Curve for *Gecarcinus* is taken from Gross (1964b).

sea water. The Mg concentration in the urine of these three species is therefore dictated in some way by the osmotic concentration of the external medium as shown for *Pachygrapsus* (Gross & Marshall, 1960) and not by the Mg influx.

The concentration of body fluids in *Cardisoma* was also determined after exposure to terrestrial environments in which the access to sea water and/or fresh water was varied. The conditions are indicated in Table 1(b) and are as follows: (a) crabs collected from terrestrial situations in nature were returned in dry bags to the laboratory—and in less than 12 hr the blood and urine were sampled without further treatment to the animals; (b) crabs placed in a large box containing sand dampened with sea water were given access to normal sea water in a flat dish and

fed fresh fish and meat scraps; (c) crabs placed in a box where both fresh water and sea water were available in flat dishes were fed fresh scrap meat, fish and vegetable material; (d) crabs placed in a box containing sand dampened with fresh water were given access to fresh water in a flat dish and fed fresh meat scraps. The boxes used in the above experiments were sufficiently large to permit free movement of the crabs.

The serum of *Cardisoma* freshly collected in nature (a) is hypoosmotic to the sea [Table 1(b)]. This also is true for the experimental situations where the availability of fresh and sea water varied. When only sea water was available (*b*), the serum averaged only 82·7 per cent sea water which is not significantly different from the mean (78·0) for field animals (*a*). It is notable that when both fresh water and sea water are available (*c*), the mean serum osmotic concentration (84·6) was not significantly different from the mean (82·7) for crabs which were deprived of fresh water (b). When only fresh water was available (*d*), the mean blood osmotic concentration (71·2) was significantly lower ($P < 0{\cdot}01$) than for both experimental groups offered sea water (*b* and *c*) but not significantly different from the serum concentrations of the field animals (78·0).

The urine of *Cardisoma* in terrestrial situations remained essentially isoosmotic to the serum. Therefore, there is no obvious adaptation in the antennary glands for terrestrial life. The regulation of Ca by *Cardisoma* in a terrestrial situation was about the same as in an aqueous environment. The serum Ca level averaged the same as it did for crabs in tap water and the low U/S ratio indicated Ca conservation. Urine Mg concentrations of field animals were sufficiently high (mean =76·4 m-equiv/l) to suggest that the crabs had recently been exposed to sea water in which Mg was high, and, as indicated above, sea water was indeed available in the regions where this species was captured; in fact, sea water of normal salinity was found in *Cardisoma* burrows.

It might be argued that the food made available to the experimental crabs in terrestrial situations furnished sufficient water of low salinity to neutralize the effects of the different treatments, and to lower the serum osmotic concentrations to hypoosmotic levels. However, as seen above, *Cardisoma* immersed completely in sea water shows strong hyporegulation; further evidence will be produced below that on land this crab can maintain its serum hypoosmotic to normal sea water in the absence of water of low salinity in any form.

Attempts were made to determine the preference of *Cardisoma* for fresh or sea water, but no pattern of behavior could be resolved in this regard by direct observation. Both extremes of salinity were freely entered, and *Cardisoma* was observed to drink water ranging in salinity from 25 to 118 per cent sea water. This was done from shallow puddles by transporting drops by the chelipeds to the mouth. Although it was not observed directly, fresh water probably is drunk in the same manner. This behavior, of course, would be of particular adaptive value for the terrestrial habit.

The terrestrial hermit crab, *Coenobita cavipes*, was examined with respect to its serum osmotic concentration when in different terrestrial situations, as

indicated in Table 4: (a) crabs freshly collected from dry, terrestrial situations were returned to the laboratory and maintained in a dry situation overnight, after which blood was sampled for osmometer determinations; (*b*) freshly collected crabs were placed where they could reach only sea water; (*c*) freshly collected crabs were placed where they could reach only fresh water; (*d*) freshly collected crabs were maintained in a dry container and deprived of water for 4 days. As seen in Table 4 the serum of all crabs sampled soon after collection, without further treatment, was hypoosmotic to the available sea water (mean: 90·8 per cent sea water). The serum of crabs given access to only fresh water for 4 days was even more dilute than that of the field animals (mean: 77 per cent sea water), suggesting that in nature *C. cavipes* has some source of salt other than that in fresh water. When only sea water was available to *Coenobita* for 4 days, the serum of all specimens examined was hyperosmotic to the available water (mean = 105 per cent sea water). These data, coupled with values for freshly collected crabs, suggest that this species in nature does not use the sea as its sole source of water, and that it cannot maintain its blood hypoosmotic to sea water by physiological mechanisms, as is also the case for *C. brevimanus* and *Birgus latro* (Gross, 1964a). Finally, when this crab was deprived of water for 4 days, its blood became hyperosmotic to normal sea water (mean = 116 per cent sea water), suggesting that in nature *C. cavipes* frequents water of lower salinity more often than every 4 days, or that it utilizes microhabitats that decrease the impact of the environment.

Although data in Table 4 suggest that *C. cavipes* does not use the sea exclusively as its source of water, a few specimens were observed in nature to enter quiet ponds of normal sea water. *C. perlatus* is known to enter the sea and to fill its shell with sea water, but this species normally is hyperosmotic to the sea (Gross, 1964a).

In order to determine the availability of water to *Cardisoma* from a damp substrate, the crab first was desiccated by placing it in a wire cage which was suspended on the main deck of the ship where it was protected from the sun, but exposed to air currents. Conditions for desiccation could not be controlled precisely because of varying air currents and occasional exposure to the sun due to the swinging of the ship. Thus, the period of exposure, varying with the climatic conditions, ranged from 21 to 48 hr. Air temperatures were observed to range between 25 and 33°C. Weight loss by evaporation was determined by weighing the animal before and after desiccation. Also, the blood and/or urine were sampled immediately following the weighing process for the determination of osmotic concentration. Then the crab was placed on either: (a) sand dampened with fresh water, or (*b*) sand dampened with normal sea water. In the latter treatment particular attention was paid to the salinity of the sea water used on the sand. First, the salinity of the water used was measured and found to be 100 per cent of normal. Then the sand which was contained within a wooden crate was flushed with a volume of normal sea water which was equal to at least ten times the volume of the sand. This was allowed to drain, was flushed again and was allowed to drain again in a protected location where there was no chance of dilution by rain.

TABLE 5—CHANGES IN BODY WATER AND BODY FLUID CONCENTRATIONS OF *Cardisoma* ON DAMP SAND AFTER DESICCATION

Spec. No.	Weight loss by desiccation (% body wt.)	Weight gain (% body wt.)	Urine (% S.W.)		Serum (% S.W.)		Period on damp sand (hr)
			Before	After	Before	After	
			Fresh Water				
1	9·6	5·0	102	89	104	92	72
2	5·8	7·8	88	79	—	—	72
3	6·7	8·7	84·5	79	—	—	24
4	7·7	8·7	87	82	—	—	72
5	6·1	0	92	99	—	—	24*
			Sea Water				
6	9·4	9·4	92	88	—	—	36
7	10·0	9·8	100	89·5	—	—	36
8	6·3	5·5	105	93	—	—	36
9	4·8	4·0	93	87	—	—	36
10	13·4	8·9	101	87	102	90	48
11	9·6	9·0	109	88	108	95	48
12	7·8	3·0	96	87	97	92	48

* Dead in 48 hr. S.W. = Sea water.

The sand was allowed to dry partially so that the water content was approximately 25 per cent by weight. This also was the approximate amount of water in the sand dampened with fresh water. The desiccated crabs were placed on the damp sand in the container which was covered with cheese cloth. In about 24 hr the crabs were removed, wiped dry, cleaned of sand and reweighed. Blood and/or urine were sampled again for osmotic concentration determinations. By repeating this process, the history of weight gains and body fluid concentration changes could be determined as a function of time for individual specimens. Inasmuch as findings from immersed specimens and freshly collected animals from the field demonstrated in all cases that the urine and serum were isoosmotic, it was felt that determining the osmotic concentration of the urine would also give the osmotic

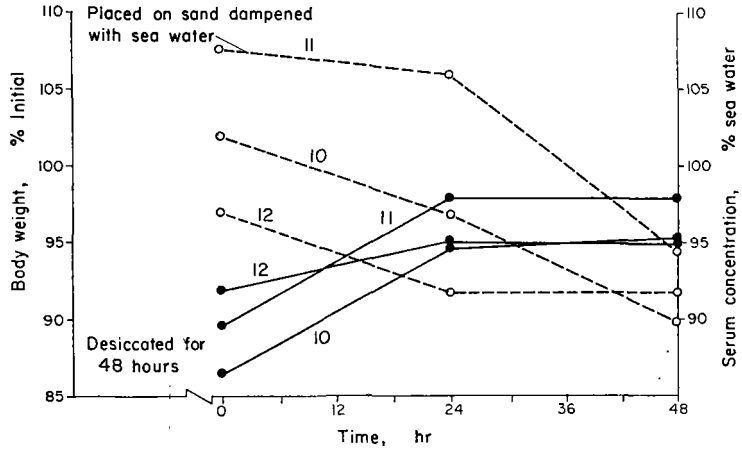


FIG. 3. Weight gains and serum osmotic concentration changes in dehydrated specimens of *Cardisoma* placed on sand dampened with sea water. Each curve represents history of individual specimen indicated by numbers over respective curves. Open circles and broken lines represent serum concentration: solid circles and lines represent weight. Specimens presented here are also represented by respective numbers in Tables 5 and 6.

concentration for the serum, and since urine can be extracted with a minimum disturbance to the animal, it was judged that serial samplings of urine would be more desirable experimentally than sampling the blood. Therefore, no blood was taken from the majority of the animals in this phase of the investigation. However, during the process of rehydration urine and serum were not necessarily isoosmotic (Table 5).

Table 5 shows the weight gains and serum concentration changes for all crabs surviving on damp sand for at least 24 hr after having been desiccated. Here, it can be seen that four out of five crabs placed on sand dampened with fresh water gained weight and reduced the osmotic concentration of their body fluids. The fifth case showed no weight change, and its serum concentration increased. This

specimen died before it had been on damp sand for 48 hr and obviously was irreversibly harmed by the desiccation process.

It can be seen in Table 5 that all seven crabs tested for rehydration on sand dampened with sea water showed large weight gains and significant reductions in the osmotic concentration of urine and/or serum. It will be noted that in every case the final body fluid concentration was less than that of the sea water which was used to dampen the sand. This means, in net effect, that water was taken up against a gradient. It should be emphasized that the crabs were large specimens ranging in weight from 100 to 485 g and that the smallest gain on sand dampened with sea water was 10 g, a quantity that could be measured easily to within ± 1 per cent accuracy. As mentioned above, particular precautions were taken to assure that the sand was flooded sufficiently with normal sea water. Then, too, all osmotic concentration readings were checked against a standard in a vapor pressure osmometer which is accurate to at least ± 1 per cent for this particular range of values.

Figure 3 presents the histories of all three specimens whose serum concentrations were measured during the rehydration process on sand dampened with sea water. It is possible that ingested damp sand was the source of weight gain and that the water and salts in the sand were absorbed from the gut; the excretion of the salts thus effecting a reduction in the body fluid concentrations. The gut contents were not examined for sand, but indirect evidence was obtained that the gut could not serve a major role in water uptake for these conditions, by calculating the solute space from the equation:

$$V = \frac{E}{(C_1/C_2) - 1}$$

where: V = volume of solute space in per cent of initial hydrated body weight (water equivalent);

E = water gained (per cent initial hydrated body weight) on damp sand assuming ingested damp sand is source of pure water and contains 25 per cent water by weight;

C_1 = body fluid concentration after rehydration on damp sand (per cent sea water);

C_2 = body fluid concentration after desiccation (per cent sea water).

Thus, in Table 6 it can be seen that in only one case (specimen no. 6) is the calculated solute space of reasonable value. The mean for seven specimens, 24·8 per cent body weight, is considerably less than most reported values for blood volume. For example, blood volume for *Carcinus* and *Eriocheir* have been reported as about 35 per cent body weight (Webb, 1940; Krogh, 1938). Solute space would be expected to be larger than blood space inasmuch as it includes both intra- and extracellular compartments. Gross (1957) calculated solute space for *Pachygrapsus* to be 54 per cent body weight. The calculated values presented here are based on the assumption that only pure water was absorbed from the gut, but if salts were also assumed to enter, then the calculated values for solute space

would be even smaller than presented in Table 6. From these data it must be concluded that water was absorbed by means other than ingestion of damp sand.

In one experiment a desiccated crab was placed on a cloth dampened with sea water. Although this animal regained most of its lost weight from the damp cloth, it did not show the recovery toward normal body fluid concentrations shown in Table 5. However, the cloth was hardly damp at the end of the experiment, and

TABLE 6.—CALCULATED SOLUTE SPACE IN REHYDRATING *Cardisoma*

Spec. No.	Body fluid measured	Calculated solute space (percentage hydrated body wt.)	Weight gained on damp sand (g)
6	Urine	60·4	10
7	Urine	25·7	14
8	Urine	13·3	23
9	Urine	17·2	18
10	Serum	20·8	20
11	Serum	20·7	31
12	Serum	16·0	14
Mean		24·8	

the available water at that time must have been of high salinity. This does suggest that water can be taken up without drinking or eating wet sand and without altering the body fluid concentration significantly.

DISCUSSION

All three brachyuran crabs studied are strong hypo- as well as hyperosmotic regulators as shown in Fig. 1. Since *Cardisoma* and *Sesarma* have terrestrial habits, this phenomenon adds further evidence to the correlation between terrestrialness in crabs and the ability to hyporegulate. In the case of *Varuna* which was living in fresh water powerful hyporegulation is surprising, although *Eriocheir* and others which invade fresh water also show such tendencies (Krogh, 1939). The presence of hyporegulation in another purely aquatic crab, which probably is not exposed to hypersalinities, strengthens the assertion of Verwey (1957) that hyporegulation is correlated with environments of varying salinity. Certainly, the amphibious *Sesarma* and the terrestrial *Cardisoma* in the Nosy Bé area are exposed to varying salinities caused by tidal periodicities in the mangrove regions and also by the frequent rains that occur even during the dry season. While *Varuna* was found only in fresh water by the authors, it is primarily marine (Chace, personal communication) which was reflected by its ability to concentrate Mg in its urine and to adapt physiologically to normal sea water. Salinity does not seem to be the critical factor limiting the distribution of this species. As pointed out above,

the fresh water in which *Varuna* was collected was separated by a riffle from brackish water, the salinity of which was influenced by the tides. While *Varuna* could easily tolerate such salinities, it was conspicuously absent in water below the riffle, which was populated by predaceous crabs and fish, none of which were found above the riffle. It is suggested that *Varuna* was limited to fresh water of the stream in this area at this season by the presence of predators in brackish water which were physiologically incapable of following it into fresh water.

The antennary glands of the crabs studied do not have an osmoregulatory function. Only when *Cardisoma* was immersed in 150 per cent sea water was the mean U/S value (0·99) different from unity ($P < 0{\cdot}01$), but this could not be adaptive. It is interesting to note that when dehydrated crabs were placed on damp sand, the urine was hypoosmotic to the serum during the rehydration process in all cases where both fluids were analyzed. This was particularly true for specimen Nos. 11 and 12 (Table 5). Again, such hypoosmotic urine would not be adaptive for a terrestrial life.

Cardisoma, *Sesarma* and *Varuna* all show increases in urine Mg concentrations as the osmotic concentration of the external medium increases, and all three do so, at least in part, independently of the Mg influx. As Mg increases in the urine, the blood and urine remain isoosmotic to each other which suggests that Mg is concentrated at the expense of Na, a phenomenon shown in every brachyuran crab investigated except *Gecarcinus lateralis* (Gross, 1964b).

Comparing the results of the present investigation with those of Gross (1963, 1964b), major physiological differences between *Cardisoma* and its close relative *G. lateralis* were observed: (a) *Cardisoma* will not drown as will *Gecarcinus*; (b) *Cardisoma* responds to high ambient salinities by concentrating Mg in the urine which *Gecarcinus* cannot do; (c) *Cardisoma* can absorb water from a substrate dampened with sea water or fresh water; while *Gecarcinus* can live indefinitely on sand dampened with fresh water, it has been shown to dehydrate and die on sand dampened with normal sea water; (d) when given access to only sea water in a terrestrial situation, *Cardisoma* maintains its blood hypoosmotic to sea water and demonstrates high tolerance. *Gecarcinus*, according to Gross (1963), can neither hyporegulate its blood concentration nor even survive when given access to only 100 per cent sea water in a terrestrial situation. Recently, however, Bliss (personal communication) has found that *G. lateralis* can be maintained indefinitely when given access to 88 per cent sea water either in the free state or as damp sand, but the incidence of molting becomes relatively low. Either the threshold of tolerance for this crab lies between 88 per cent and 100 per cent sea water or the experimental treatment by Bliss was different from that of Gross (1963).

Gecarcinus is farther removed from a marine life than is *Cardisoma*, and indeed the exclusive distribution of adult stages of *Gecarcinus* above the intertidal levels (Bliss, 1963; Flemister, 1958) fits well with this crab's relative intolerance to saline water or even sand dampened with sea water. *Cardisoma* is found in nature within the intertidal zones as well as above them. Also, this species will enter sea water and, as shown above, tolerate high salinities. *Cardisoma* is more aquatic than

Gecarcinus, but direct evidence is still lacking to indicate that *C. carnifex* is less adapted to terrestrial life than is *Gecarcinus*. Bliss (1963), however, reports that *Gecarcinus* is better adapted to life on land than is *C. guanhumi*.

Coenobita cavipes performs similarly to *C. brevimanus* and *Birgus* (Gross, 1964a) with respect to water balance; i.e. this terrestrial hermit crab is hypoosmotic to sea water in nature and acquires the low blood concentrations apparently through behavioral means. It differs from *C. perlatus* in which the blood is usually hyperosmotic to the sea (Gross, 1964a). Thus, *C. cavipes*, *C. brevimanus* and *Birgus* seem to be farther removed from the marine habit than *C. perlatus*, because the low blood concentrations of the three former species require that they seek sources other than the sea for water.

The brachyuran *Cardisoma* differs from the anomuran land crabs in its ability to maintain its blood hypoosmotic to sea water by physiological rather than behavioral means. While preference for salinity by *Cardisoma* was not resolved in the present investigation, such a behavioral device may exist but varies from season to season or during the reproductive cycle when the females enter the sea to release the mature eggs. De Leersnyder & Hoestlandt (1963) report that *C. armatum* prefers fresh water to sea water. *C. guanhumi* is known to enter both sea water and fresh water freely (Feliciano, 1962; Herreid & Gifford, 1963).

SUMMARY

1. Salt and water balance was studied in the following Madagascar crabs: the terrestrial *Cardisoma carnifex*, the amphibious *Sesarma meinerti*, the euryhaline *Varuna litterata*, which was captured in fresh water, and finally the anomuran, land crab *Coenobita cavipes*.

2. All three brachyuran crabs, *Cardisoma*, *Sesarma* and *Varuna* demonstrated powerful ability to regulate osmotically for at least 24 hr when immersed in a range of salinities from fresh water to 150 per cent sea water. *Coenobita* was not studied in immersion experiments.

3. Strong hypoosmotic regulation in *Sesarma* and *Cardisoma* conforms with the physiological response to high salinity common to other terrestrial and amphibious crabs.

4. The antennary glands of all three brachyurans are ineffective organs of osmoregulation for all conditions studied, but are capable of concentrating Mg in the urine as the ambient salinity increases. This is done independently of the Mg flux. *Cardisoma* thus differs from another gecarcinid, *Gecarcinus*, which cannot concentrate urine Mg. The antennary glands of the three species also conserve Ca.

5. When *Cardisoma* is immersed in 150 per cent sea water, neither its stomach fluid nor hind-gut fluid differs significantly in osmotic concentration from that of the serum. There is no evidence that the gut in *Cardisoma* has an osmoregulatory function (drinking).

6. Both land crabs, *Cardisoma* and *Coenobita cavipes*, maintain their serum concentrations hypoosmotic to sea water in nature. *C. cavipes* in this regard is

similar to *C. brevimanus* and *Birgus latro*, but different from *C. perlatus*. Evidence suggests that this is accomplished primarily by behavioral means in *Coenobita*, but by physiological and possibly behavioral means in *Cardisoma*.

7. None of the brachyuran crabs studied drowned when completely immersed for prolonged periods. *Cardisoma* therefore differs from its close relative *Gecarcinus* which will drown within 24 hr when completely immersed. *Cardisoma*, in this respect, is not only more aquatic than the most terrestrial brachyuran, *Gecarcinus lateralis*, but also the most terrestrial anomuran, *Birgus latro*, which also will drown.

8. *Cardisoma* can absorb water from sand dampened with fresh or sea water, or from a cloth dampened with sea water. It can regain water lost by evaporation from sand dampened with sea water and lower its blood osmotic concentration toward normal, even though the osmotic gradient favors further loss of water. The evidence suggests that the gut does not participate in this water gain.

9. *Cardisoma* will drink water of different salinities from small, shallow puddles, a behavioral pattern which could prevent dehydration in a terrestrial environment.

10. The population of *Varuna* studied was found only in the fresh water of a stream at sites sharply delimited from tidal influence by a riffle descending about 5 m elevation into brackish water where there were numerous predaceous fish and crabs.

11. Because *Varuna* is a powerful osmoregulator it is suggested that it was prevented from entering brackish water by the presence of predators that were intolerant to fresh water.

Acknowledgements—These studies were conducted while participating in a marine physiological expedition to Madagascar and Iles Comores aboard the Research Vessel *Te Vega* during July and August of 1964. The expedition was supported by the U.S. National Science Foundation in the form of a grant from the U.S. Program in Biology of the International Indian Ocean Expedition and from a general operations grant for the *Te Vega* Expeditions to Stanford University. These studies also were supported by NSF Grant, GB1827 (to R. C. Lasiewski) and GB1092 (to W. J. Gross). We wish to extend our gratitude to the following: Dr. Malcolm S. Gordon for his able leadership in organizing the expedition; Director M. Angot, Associate Director M. Frontier and the staff of the Centre d'Oceanographie et des Pêches de Nosy Bé for their kind cooperation; Dr. A. G. Humes, resident 110E representative at Nosy Bé, for his generous and efficient assistance, particularly in the collecting of experimental animals; Dr. Fenner A. Chace, Jr. for his kind identification of the crabs *Sesarma meinerti* and *Varuna litterata* and Dr. Dorothy Bliss for furnishing us with pertinent information from her unpublished findings.

REFERENCES

BARNARD K. H. (1950) Descriptive catalogue of South African decapod Crustacea. *Ann. S. African Museum*, **38**, 837.

BLISS D. E. (1963) The pericardial sacs of terrestrial Brachyura. In *Phylogeny and Evolution of Crustacea*.. Museum of Comparative Zoology, Special Publication, 1963. Harvard University, Cambridge, Mass.

DE LEERSNYDER M. & HOESTLANDT H. (1963) Premières donnés sur la regulation osmotique et la régulation ionique du crabe terreste, *Cardisoma armatum* Herklots. *Cahiers de Biologie Marine* **4**, 211–218.

FELICIANO C. (1962) *Notes on the biology and economic importance of the land crab* Cardisoma guanhumi, *Latreille, of Puerto Rico.* Special contribution, Institution of Marine Biology, University of Puerto Rico.

FLEMISTER L. (1958) Salt and water anatomy constancy and regulation in related crabs from marine and terrestrial habitats. *Biol. Bull., Woods Hole* **115**, 189–200.

GREEN J. W., HARSCH M., BARR L. & PROSSER C. L. (1959) The regulation of water and salt by the fiddler crabs, *Uca pugnax* and *Uca pugilator. Biol. Bull., Woods Hole* **116**, 76–87.

GROSS W. J. (1957) An analysis of response to osmotic stress in selected decapod Crustacea. *Biol. Bull., Woods Hole* **112**, 43–62.

GROSS W. J. (1959) The effect of osmotic stress on the ionic exchange of a shore crab. *Biol. Bull., Woods Hole* **116**, 248–257.

GROSS W. J. (1963) Cation and water balance in crabs showing the terrestrial habit. *Physiol. Zool.* **36**, 312–324.

GROSS W. J. (1964a) Water balance in anomuran land crabs on a dry atoll. *Biol. Bull., Woods Hole* **126**, 54–68.

GROSS W. J. (1964b) Trends in water and salt regulation among aquatic and amphibious crabs. *Biol. Bull., Woods Hole* **127**, 447–466.

GROSS W. J. & MARSHALL L. A. (1960) The influence of salinity on the magnesium and water fluxes of a crab. *Biol. Bull., Woods Hole* **119**, 440–453.

HERREID C. F. & GIFFORD C. A. (1963) The burrow habitat of the land crab, *Cardisoma guanhumi* (Latreille). *Ecology* **44**, 273–275.

JONES L. L. (1941) Osmotic regulation in several crabs of the Pacific Coast of North America. *J. cell. comp. Physiol.*, **18**, 79–91.

KROGH A. (1938) Extracellular and intracellular fluid. *Acta Med. Scand. Suppl.* **90**, 9–18.

KROGH A. (1939) *Osmotic regulation in aquatic animals.* Cambridge Univ. Press.

LOCKWOOD A. P. M. (1962) The osmoregulation of Crustacea. *Biol. Rev.* **37**, 257–305.

POTTS W. T. W. & PARRY G. (1964) *Osmotic and Ionic Regulation in Animals.* Macmillan, New York.

PROSSER C. L., GREEN J. W., & CHOW T. (1955) Ionic and osmotic concentrations in blood and urine of *Pachygrapsus crassipes* acclimated to different salinities. *Biol. Bull., Woods Hole* **109**, 99–107.

SCHLIEPER C. & HERMANN F. (1930) Beziehungen zwischen Bau und Funktion bei den Exkretionsorganen dekapoder Crastuceen. *Zool. Jb.* **52**, 624–630.

SCHOLLES W. (1933) Ueber die Mineralregulation wasserlebender Evertebraten. *Z. vergl. Physiol.* **19**, 522–554.

SCHWARZENBACH G., BIEDERMANN W. & BANGERTER F. (1946) Komplexone VI. Neue einfache Titriermethoden zur Bestimmung der Wasserharte. *Helv. Chim. Acta* **29**, 811–818.

SHAW J. (1959) Salt and water balance in the East African fresh-water crab, *Potamon niloticus* (M. Edw.). *J. exp. Biol.* **36**, 157–176.

VERWEY J. (1957) A plea for the study of temperature influence on osmotic regulation. *Ann. Biol.* **33**, 129–149.

WALLACH D. F. & STECK T. L. (1963) Flourescence technique in microdetermination of metals in biological materials—II. An improved method for direct complexometric titration of calcium in small serum samples. *Analyt. Biochem.* **6**, 176–180.

WEBB D. A. (1940) Ionic regulation in *Carcinus maenas. Proc. R. Soc.* B. **129**, 107–136.

Reprinted from *Proc. Indo-Pacific Fish. Coun.*, vol. 11, no. II, 1966, p. 156-171

RESULTS OF BOTTOM TRAWLING IN INDIAN SEAS BY R/V ANTON BRUUN IN 1963

by

T.S. Hida and W.T. Pereyra
US Dept. Interior, Fish and Wildlife Service
Bureau of Commercial Fisheries
Honolulu-12, Hawaii

ABSTRACT

One hundred and four successful hauls were made by the Anton Bruun in the Bay of Bengal and in the Arabian Sea, utilizing a 13-m. Gulf of Mexico shrimp trawl.

The highest catch rates in the Bay of Bengal were obtained in depths of 15 - 37 m. in the Burma and East Pakistan regions. Stingrays, guitarfish and croakers were the most important organisms in the catches.

The highest catch rates obtained in Arabian Sea were in depths of 38 - 73 m. off the southeastern Arabian coast. The stingrays were the most important group in the catches. Other prominent groups in the catches were the swimming crabs, sciaenids, croakers, lizardfish, cardinal fish and threadfins.

A large part of the catches consisted of small fish weighing less than 250 g. each which was considered of very low market value.

The highest catch rates generally were obtained on Cruise 4B in areas of well mixed water.

INTRODUCTION

Exploratory bottom trawling surveys were carried out by the U.S. Bureau of Commercial Fisheries in the Bay of Bengal and in the Arabian Sea in 1963 as part of the field work of the U.S. Program in Biology. The program represents a major contribution of the United States to the International Indian Ocean Expediton (IIOE). This expedition, sponsored by UNESCO, is a multi-

nation effort to delineate the topographic features, circulation and distribution of living organisms in the Indian Ocean and adjacent seas.

Bottom trawling was conducted from the R/V Anton Bruun, the former presidential yacht Williamsburg, which has been converted for oceanographic and biological research for the National Science Foundation. This twin screw vessel, which has 1100 SHP direct diesel drive on each shaft plus a 150 SHP active rudder, is 74 m long and weighs 1,421 metric tons (Fig. 1).

The major objectives of these surveys were: (1) to gain information on the distribution and relative abundance of fish and shellfish inhabiting the continental shelf and slope regions, and (2) to obtain specimens for systematic and other biological studies. These objectives were pursued in the hope that information gained would aid those countries bordering the Bay of Bengal and Arabian Sea to utilize the marine resources of these waters to a greater extent. The survey of the Bay of Bengal was carried out from March 12 to April 11, 1963, (Cruise 1) while that of the Arabian Sea took place from November 12 to December 10, 1963, (Cruise 4B).

HISTORICAL BACKGROUND

Surveys of the Bay of Bengal up to 1959 were mostly of the expeditionary type with little emphasis placed on commercial trawling aspects. In 1959, the Government of India started trawling surveys off the coast of Waltair as part of its third 5-year plan. These surveys were directed by a fisheries expert from FAO (Naumov, 1961, p. 60 and Borisov, 1962, p. 29), and the area covered was a narrow band along the northwestern part of the Bay of Bengal. The principal gear used was otter trawls. Explorations were conducted in waters ranging in depth from 12 to 160 m, with most of the trawling being done between 35 and 55 m. The largest catches generally were made in depths from about 40 to 60 m. Fishes frequently taken included sea catfishes (Arridae), lizardfishes (Synodontidae), croakers (Sciaenidae), goatfishes (Mullidae) and threadfin breams (Nemipteridae).

A Burma-Japan cooperative bottom trawling survey was conducted off Burma in the Gulf of Martaban in 1953-1955 (Ba Kyaw, 1956, p. 4). The largest catches were made where the water depth was about 54 m. The most common fishes in the catches were croakers, grunts (Pomadasyidae), snappers (Lutjanidae), leiognathids and lizardifishes. It was reported that from one-fourth to one-third of the catch was comprised of small fishes of no commercial importance.

In the Arabian Sea large scale trawling experiments were started in 1946 after the establishment of a pilot deep-sea fishing station in Bombay. During the period 1949-1955, intensive fishing

with otter and bull trawls was conducted from shallow water to a depth of about 73 m (Jayaraman et al, 1959, p. 87). Largest catches were made in a depth of about 37 m and included perch, threadfins (Polynemidae), sea catfishes, eels and elasmobranchs.

Recently, two Soviet tropical class stern trawlers were reported to have carried out successful bottom trawling operations along the southeastern Arabian coast (Hinds, 1964, p. 3).

Most of the surveys off India and West Pakistan were conducted in depths less than 70 m. This was in line with the idea of providing immediate assistance to the existing fishery which is concentrated along a narrow coastal belt on the inner continental shelf. The Gulf of Kutch region was considered to be one of the richest grounds in the Arabian Sea (Seshappa, 1958, p. 14). The catches usually consisted of many species of fish, and only rarely were they dominated by one or two species. The best catches of shrimp were made in depths less than 22 m.

GEAR AND METHODS

The primary sampling gear was a nylon Gulf of Mexico shrimp trawl (Schaefers and Johnson, 1957, p. 17) measuring 13 m along the foot rope with a mesh size of 3.8 cm (stretched measurement, opening including 1 knot). A 46-m long bridle connected the trawl to a single towing warp. A rectangular otterboard measuring 0.8 x 1.5 m and weighing 73 kg was attached to each wing of the net when trawling to depths to 366 m. Below 366 m heavier boards (179 kg each) were used.

Echo soundings of the ocean bottom were taken whenever the Anton Bruun was under way. A general criterion was followed which required that approximately 5 km of relatively flat bottom was present before a trawl haul was attempted. Echo soundings were supplemented by samples of bottom sediments obtained with a small dredge of a spring-loaded bottom grab prior to trawling.

The trawl was towed from the starboard side off an A-frame and was set out at a vessel speed of about 6 to 8 knots with the cable being payed out at a rate of 40 to 60 m per min. The cable out-to-depth (scope) ratios were consistent with those found to be satisfactory in exploratory trawling with identical gear in the northeastern Pacific Ocean (Pereyra, 1963, p. 4). Ratios ranged from 6:1 in shallow water to about 3:1 in deep water. Except when snags or other hazards were encountered, the trawl fished for 30 to 45 min, (time trawl was on bottom) on Cruise 1 while on Cruise 4B the trawl fished for 45 min. in depths less than 183 m and for an hour at greater depths. Trawling speed ranged between 2 and 3 knots. Several features of the vessel which may have adversely affected the results were: (1) her relatively deep draft made it necessary to trawl only in depths greater than 15 m; (2) her propellers stirred up mud and sand in depths of about 22 m

and shallower which may have frightened fish away from the path of the trawl, and (3) difficulty in maintaining proper trawling speed necessitated intermittent use of an active rudder in conjunction with the port engine which often resulted in a variable speed during the course of a trawl drag.

Following each haul, the cod end was lifted aboard the vessel by a small hydraulic crane and the catch was emptied onto a sorting table (Fig. 2) where it was separated by family (genera or species when possible). The total weight and number of individuals in each family of fish and each group of shellfish were recorded and representative samples of the catches were preserved. The preserved samples were shipped to the Smithsonion Institution in Washington, D.C. Other information obtained for most groups included length ranges and average weights. Length frequencies were taken from representative samples of some groups of fishes. For the larger shrimp catches, estimates of the number of whole shrimp per pound were recorded. Some of the specimens in good condition were photographed on a lightbox (Ronholt, 1963, p. 4) before being preserved.

TREATMENT OF DATA

In order to evaluate the catches in such a large survey area, it was decided to segregate the stations into several regions which generally were made to coincide with the geographic boundaries of the countries involved. The stations on Cruise 1 were divided into the Andaman Islands, Thailand, Burma and East Pakistan (Fig. 3); while regions used for Cruise 4B were India, West Pakistan, Gulf of Oman and Arabia (Fig. 4). Stations in each region then were grouped according to depth ranges of 15-37, 38-73, 74-110, 111-183, 184-366 and 367-549 m. The depth of each haul was determined as the average of the starting and ending depths.

Relative abundance of the fish and shellfish encountered was examined by comparing their catch rates in kilograms caught per hour of trawling. Average catches in kilograms per hour of trawling were computed by dividing the sum of the catches by the total effort for individual depth intervals within regions. Catch rates were computed for elasmobranchs, flatfish, eels, roundfish, squid and crustaceans but were not calculated for snakes, corals, echinoderm, crinoids, gastropods, coelenterates, tunicates and sponges since the latter were not believed to be quantitatively sampled by the trawl.

RESULTS

Bay of Bengal

Between March 12 to April 11, 1963 trawling on Cruise 1 was conducted east of the Nicobar Islands to the west coast of Thailand, off the southern and western coasts of Burma, along the eastern coast of the Andaman Islands and along the coast of East Pakistan. Although sampling was conducted within

the general depth range of 15 to 516 m, most of the trawling occurred on the continental shelf (to depths of 183 m). The continental shelf was usually trawlable but there were occasional outcroppings of coral and rocky bottom which prevented trawling. The continental slope at depths from 183 to about 900 m was usually too precipitous for effective trawling. The bottom at depths greater than about 990 m was usually flat and muddy and suitable for trawling.

Bottom sediments varied considerably between regions. Off Burma they consisted of grey mud with some sand and combinations of mud, sand, shell, shale and coral. Sediments off East Pakistan were mostly greenish-grey mud with some sand. Greenish mud with combinations of sand, shell, hard clay and rock predominated along the eastern coast of the Anadaman Islands. Off Thailand, sediments were mostly greenish clay, shell, mud and coral.

Thirty-one trawl hauls were made in the Bay of Bengal, of which 27 were successful and 4 resulted in extensive damage or loss of the nets. The highest incidence of gear damage occurred off Thailand where there were numerous outcroppings of coral. Largest catches were obtained off Burma and East Pakistan (Fig. 5). Catch rates of fishes and invertebrates for the different regions are shown in Table I through IV.

Andaman Islands

A haul taken in the 38-73 m depth range and two hauls made in the 74-110 m depth range resulted in relatively small catches ranging from 0.5 to 23 kg per hour of trawling. The catches were comprised of 2 families of elasmobranchs, 2 families of flatfish, 16 families of roundfish, and a few squid. Aside from a 23 kg stingray (Dasyatidae), which was caught in the 74-110 m depth range, the catches were negligible. No shrimp or eels were caught in this region.

Thailand

Single hauls taken in the 38-73, 74-110 and 367-549 m depth ranges resulted in relatively poor catches ranging from 1 to 19 kg per hour of trawling. Represented in the catches were 3 families of flatfish, 1 family of elasmobranchs, 2 families of eels, 29 families of roundfish, shrimp, crabs, octopods and cuttlefish. The highest catch rate occurred in the 38-73 m depth range where lizardfishes were the most important group taken.

East Pakistan

Six hauls made in the 15-37 m depth range resulted in catch rates ranging from 11-148 kg per hour of trawling. Five families of elasmobranchs, 2 families of flatfish, 33 families of roundfish, shrimp, crabs, scyllarids, sepiolids and loliginids were present in the catches. The fact that the guitarfishes

(Rhinobatidae) yielded the highest catch rate (27 kg per hour of trawling) was due entirely to the capture of one large individual. Other important fishes in this depth interval were croakers, sea catfishes and threadfins. The average catch of shrimp amounted only to 2 kg per hour of trawling.

Burma

Catches off Burma consisted of 3 families of elasmobranchs, 5 families of flatfish, 57 families of roundfish, eels and 9 groups of invertebrates. Highest catch rates were obtained in the 15-37 m depth range followed by those in the 184-366, 367-549, 38-73 and 74-110 m depth ranges, respectively. Stingrays and croakers were the most prevalent fishes caught in the 15-37 and 38-73 m ranges. Snappers were the most important group in the 74-116 m depth range. The catch in the 367-549 m depth range consisted mainly of an unidentified berycoid fish and shrimp. Only small quantities of shrimp were caught in the shallower depths and the fair quantities of those found in the deeper waters were not the usual commercial species.

Other factors besides the generally small fish catches suggested the ocean floor in the regions surveyed in the Bay of Bengal was rather barren of life. Very few sea stars were encountered anywhere. Many shells of mollusks and other invertebrates were brought up in the trawl, but almost all of them were empty.

Arabian Sea

The survey on Cruise 4B was made from November 12 - December 10, 1963, starting from Angria Bank, off Bombay, then proceeding along the continental shelf into the Gulf of Oman and terminating off the eastern coast of Arabia (South of Al Masirah). The depths trawled ranged from 16-366 m. No trawlable grounds were found in the vicinity of Angria Bank where the bottom was mostly of coral. The area between Bombay and Karachi offered the largest trawling grounds with its wide shelf characterized by extensive flat muddy bottom. The continental shelf from Karachi to the Gulf of Oman was relatively narrow compared to that east of Karachi. The Gulf of Oman contained fairly extensive grounds but there were occasions where coral and great quantities of dead shells hampered trawling. Hard and irregular bottom prevailed off the Arabian coast.

Of the 86 trawl hauls made, 77 were accepted as satisfactory for use in the catch analysis. The total trawling time of 60 hours was broken down as follows: 21.3 hours off India; 22.0 hours off West Pakistan; 15.4 hours in the Gulf of Oman; and 1.3 hours off Arabia. Average catches in kilograms per hour of trawling for each organism caught in the Arabian Sea are shown by depth ranges and regions in tables V through VIII. Highest catch rates were obtained off the Arabian coast, followed by those off Indian and West Pakistan (Fig. 6).

India

Twenty-eight hauls in this region resulted in catches ranging from about 1 to 439 kg per hour of trawling. Represented in the catches were 4 families of

elasmobranchs, 4 families of flatfish, 4 families of eels, 48 families of roundfish, and 8 groups of invertebrates. The most productive depth range surveyed was from 15-37 m, followed by those from 111-183, 74-110, 38-73, 184-366 m, respectively. Threadfin breams provided the highest catch rates in this region, dominating catches in the 111-183 and 74-110 m depth ranges. Stingrays were the next most important group and dominated catches from the 15-37 and 38-73 m depth ranges. Other important fishes caught were croakers, threadfins, and lizardfishes. The small shrimp catches were mostly from the shallower depths.

West Pakistan

Twenty-seven hauls made in this region resulted in catch rates ranging from 0.5 to 349 kg per hour of trawling. Eight families of elasmobranchs, 5 families of flatfish, 3 families of eels, 44 families of roundfish and 8 groups of invertebrates were present in the catches. Highest catch rates were obtained in the 15-37 m depth range followed by those in the 111-183, 74-110, 38-73 and 184-366 m depth ranges, respectively. Stingrays provided the highest catch rates and dominated catches from the 15-37 and 111-183 m depth ranges. Threadfin breams, which followed the stingrays in importance, were mainly taken in the 74-110 m depth range. Other important constituents of the fish catches were guitarfishes, croakers, and grunts. Relatively few invertebrates were caught in this region. Most of the shrimp were taken in the 184-366 m depth range.

Gulf of Oman

Of 27 hauls made in this region, 7 were not used in the catch analysis because the trawl was either badly torn or failed to perform satisfactorily. Catch rates from successful hauls ranged from 1 to 154 kg per hour of trawling. Represented in the catches were 5 families of elasmobranchs, 4 families of flatfish, 5 families of eels, 43 families of roundfish, and 7 groups of invertebrates. Highest catch rates in this region were obtained in the 74-110 m depth range, followed by those in the 38-73, 111-183, 15-37 and 184-366 m depth ranges, respectively. Threadfin breams yielded the highest catch rates and most were caught in the 74-110 and 111-183 m depth ranges. Only stingrays and croakers were of any importance in the remainder of the catches. Shrimp and other invertebrates were caught only in small quantities.

Arabia

Two of the 4 hauls made off Arabia resulted in extensive damage to nets from coral. The 2 successful hauls in the 38-73 m depth range yielded the highest catch rates for both Cruise 1 and Cruise 4 B. A 45-minute haul made at Station 270A (Fig. 7) yielded 834 kg of swimming crabs (Portunidae) and 771 kg of fish -- primarily grunts, stingrays, and cardinal fishes (Apogonidae). At Station 272A, a 30-minute haul yielded the largest catch of the entire survey -- 2,404 kg of stingrays and 45 kg of other fishes. Stingrays were the most important

fish group taken with an average catch of 1,769 kg per hour of trawling. They were followed by swimming crabs with an average catch rate of 556 kg per hour of trawling. No shrimp were caught in this region.

Size of Organisms

Several families of roundfish were caught in substantial numbers, but the individuals were generally too small to be of commercial importance. The small mesh size of the trawl net used in these surveys contributed to the catch of small fish, some of which were only 4 cm in length. Undoubtedly, some of the families would not have been retained had the mesh size been larger.

Since the sizes of fish caught on Cruises 1 and 4B were similar, only the length frequencies and average weights of some that were frequently caught on Cruise 4B are shown in figures 8 and 9. Within the elasmobranchs group, guitarfishes ranged in weight from a few kilograms to 181 kg, sharks usually weighed but a few kilograms, and stingrays ranged from 0.5 to 205 kg. The stingrays taken in large numbers off the Arabian coast averaged about 18 kg each. Most of the eels were small except those that belong to the family Muraenesocidae which weighed from about 0.5 kg to about 9 kg each and reached lengths up to about 1.5 m. Most of the roundfish weighed less than 250 g with a small percentage of sea catfishes, croakers, grunts, sparids, and a few others that weighed up to a few kilograms each.

Shrimp ranged in size from more than 440 individuals per kilogram (heads on) to about 35 individuals per kilogram in the Arabian Sea, and on one occasion, 5 individuals to a kilogram in the Bay of Bengal. Squat lobster (Scyllaridae) which were caught frequently but only in small numbers usually weighed about 250 to 500 g per individual. The swimming crabs which were caught in large numbers off Arabia averaged about 22 individuals to a kilogram with carapace lengths ranging from 3.8 to 10.2 cm.

ENVIRONMENTAL FACTORS

Bathythermograph lowerings, surface and bottom temperatures, and bottom and surface water samples for salinity, phosphate and oxygen determinations were taken at nearly all of the trawl stations on Cruise 4B. Comparison of the catch data with some of the environmental data showed that the bottom oxygen concentrations were correlated with the catches ($r = 0.261$, $P < 0.05$) and that the bottom phosphate concentrations were inversely correlated with the catches ($r = -0.259$, $P < 0.05$). There were no significant correlations between the catches and the bottom salinities or the bottom temperatures.

Bottom temperatures decreased with increasing depth, the decrease being the greatestoff India. Surface temperatures increased slightly progressing away from the coast. The surface salinities were highest in the Gulf of Oman and lowest off India. This was probably due to the fresh water run-off into the Gulf of Cambay

and Kutch. Bottom oxygen levels were lowest off India and increased to the westward with the highest being observed off Arabia where the largest fish catches were taken. Tongues of mixed waters, as indicated by low phosphate concentrations (Fig. 10), intruded over the continental shelf just north and east of Karachi, in the northern part of the Gulf of Oman, along the eastern coast of Arabia, and off the India-West Pakistan border. In general, the larger trawl catches were made in areas of well mixed water. This is shown in figure 11 which illustrates the distribution of catches greater than 45.4 kg per hour of trawling that were obtained on Cruise 4B.

ACKNOWLEDGEMENTS

The authors are indebted to Captain Osterwald and crew of Anton Bruun for their cooperation while carrying out the surveys and to the visiting scientists from the United States, India, Pakistan and Thailand for their assistance in the trawling operation and expecially for their aid in identifying organisms caught during the surveys. They also would like to thank A.T. Pruter of the Exploratory Fishing and Gear Research Base in Seattle, Washington, for his suggestions and review of this manuscript.

REFERENCES

Ba Kyaw, U. (1956). Trawling results of Taiyo Maru No. 11 in Burnese waters. IPFC Procs., 6(2): 261-264.

Borisov, N.I. (1962). Report to the Government of India on experimental and exploration fishing in the Bay of Bengal. FAO/EPTA Rept., 1466: 29.

Hinds, V.T. (1964). International Interest in Gulf of Aden Fisheries. Fish. News. Int., 3(1): 20-22.

Jayaraman, R., G. Seshappa, K.H. Mohamed and S.V. Bapat (1959). Observations on the trawl-fisheries of the Bombay and Saurashtra waters, 1949-50 to 1954-55. Indian J. Fish., 6(1): 58-144.

Naumov, V.M. (1961). Report to the Government of India on a survey of the fishery resources of the Bay of Bengal. FAO/EPTA Rept., 1393: 60.

Pereyra, W.T. (1963). Scope ratio-depth relationships for beam trawl, shrimp trawl, and otter trawl. Comm. Fish. Rev., 25(12): 7-10. [Also separate No. 696].

Ronholt, L.L. (1963). Equipment note No. 14 - A lightbox for photographing fish and invertebrates at sea. Comm. Fish. Rev., 25(9): 8-11. [Also see separate No. 687].

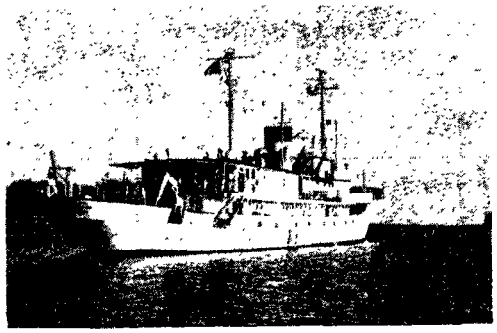
Schaefers, E.A. and H.C. Johnson (1957). Shrimp explorations off the Washington coast, fall 1955 and spring 1956. Comm. Fish. Rev., 19(1): 9-25. [Also separate No. 465].

Seshappa, G. (1958). Offshore Fisheries. In : Fisheries of the west coast of India edited by S. Jones, p. 60-73. Bangalore Press, Bangalore, India. Published by Central Marine Fisheries Research Station; Mandapam Camp.

TABLE I

Average catches in kilograms per hour of trawling, by depth range, obtained in the Andaman Islands region on Cruise 1 of the Anton Bruun. Dashes designate catches of less than 0.2 kg. (half a pound)

No. hauls	(1)	(2)
Depth in meters	38-73	74-110
Elasmobranch		
Carcharhinidae	3.6	
Dasyatidae		22.7
Flatfish		
Bothidae		-
Pleuronectidae		-
Roundfish		
Apogonidae		-
Carangidae	-	
Chaetodontidae		-
Emmelichthyidae		-
Fistulariidae	-	
Gerridae	.9	
Labridae	-	
Leiognathidae	-	
Mullidae	-	-
Nemipteridae	-	.5
Ogcocephalidae		-
Pomacentridae		-
Priacanthidae		-
Scombridae		-
Serranidae		-
Synodontidae	-	-
Invertebrate		
Loliginidae		-



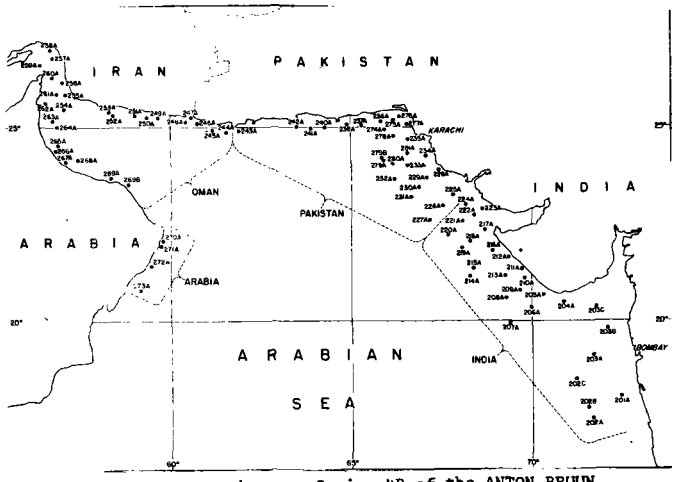


Fig. 4 Trawl stations on Cruise 4B of the ANTON BRUUN in the Arabian Sea, November 12 - December 10, 1963. Dashed lines separate the regions.



Fig. 2 Cod end being lifted over the sorting table.

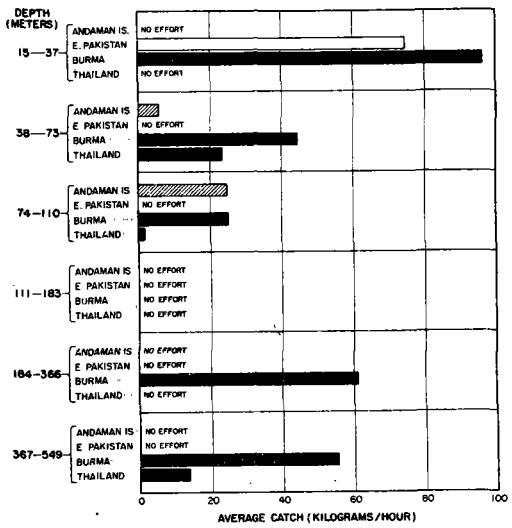


Fig. 5 Average catches in kilograms of fish and invertebrates per hour of trawling by depth ranges and by regions in the Bay of Bengal obtained on Cruise 1.

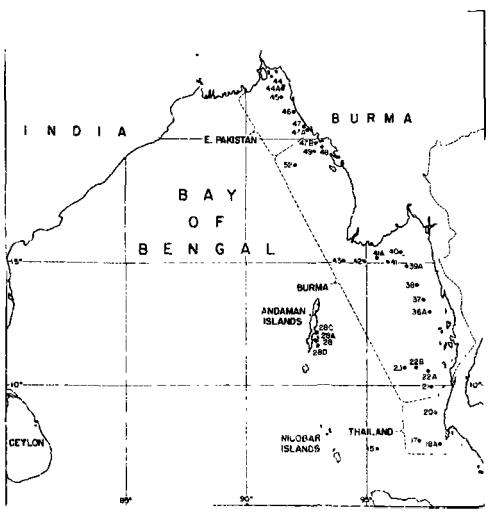


Fig. 3 Trawl stations on Cruise 1 of the ANTON BRUUN in the Bay of Bengal, March 12 to April 11, 1963. Dashed lines separate the regions.

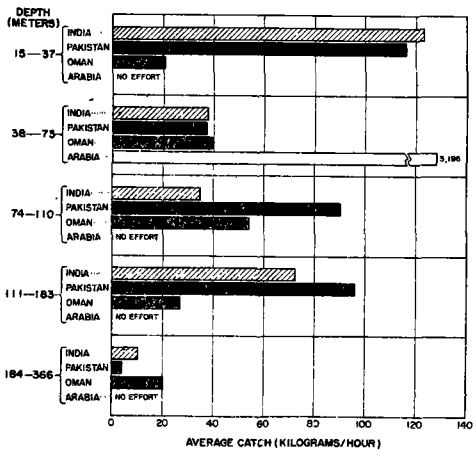


Fig. 6 Average catches of fishes and invertebrates in kilograms per hour of trawling by depth ranges and regions in the Arabian Sea obtained on Cruise 4B.



Fig. 7 Top photo shows the catch obtained at Station 270A on Cruise 4B of the BRUUN. Bottom photo shows the crabs which were caught in abundance.

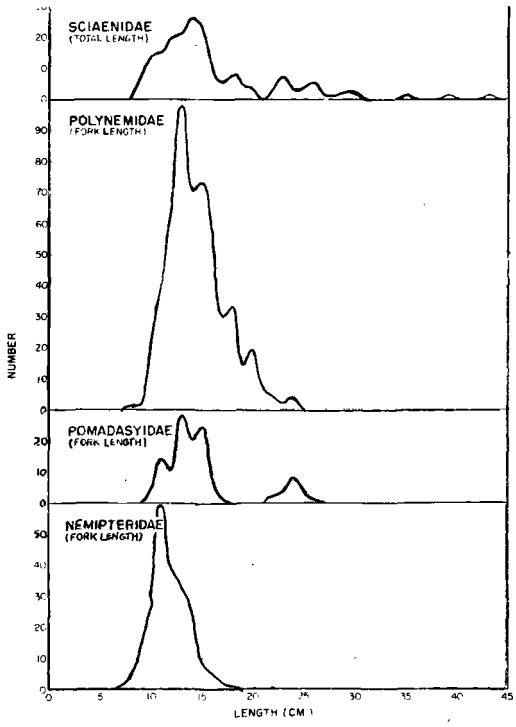


Fig. 8 Length-frequencies of some fishes frequently caught on Cruise 4B.

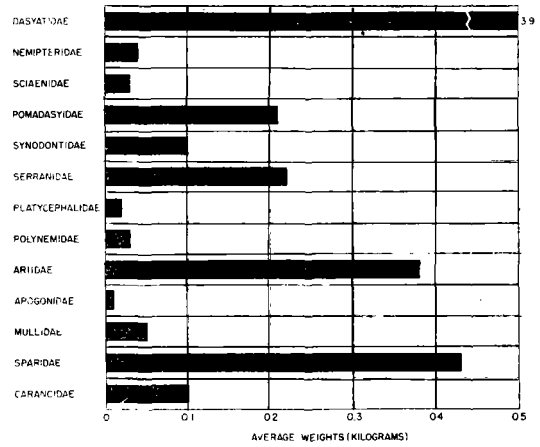


Fig. 9 Average weights of some fishes frequently caught on Cruise 4B.

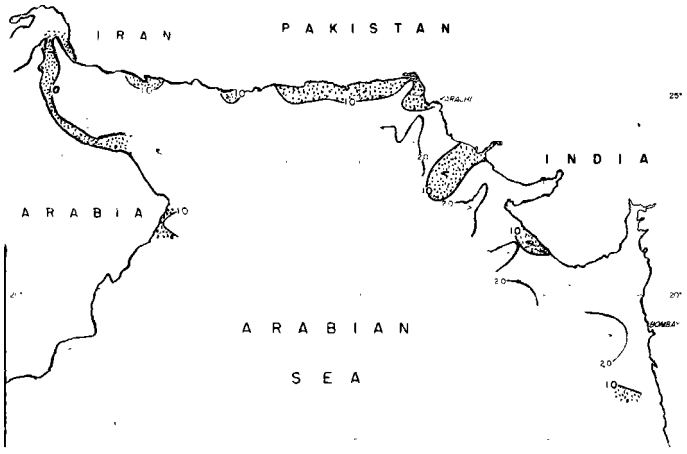


Fig. 10 Schematic illustration of bottom phosphate concentrations observed on Cruise 4B.

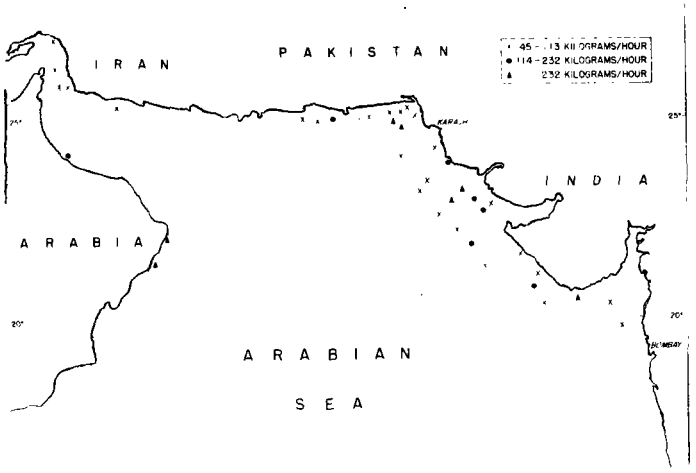


Fig. 11 Distribution of catches larger than 45.4 kg. per hour of trawling on Cruise 4B.

Table II

Average catches in kilograms per hour of trawling, by depth range, obtained in the Thailand region on Cruise 1 of the Anton Bruun. Dashes designate catches of less than 0.2 kg. (half a pound)

No. hauls	(1)	(1)	(1)
Depth in meters	38-73	74-110	367-549
Elasmobranch			
Rajidae			-
Flatfish			
Bothidae	.9		
Psettodidae	1.8		
Soleidae	-		
Eel			
Nemichthyidae			-
Unidentified	-		
Roundfish			
Apogonidae	-		
Brotulidae			-
Callionymidae	-		
Carangidae	.9		
Dactylopteridae	3.6		
Diodontidae		.5	
Drepanidae	-		
Emmelichthyidae	-	-	
Fistulariidae	-		
Grammicolepidae		-	
Labridae	-		
Macruridae			3.6
Mullidae	-		
Myctophidae			-
Nemipteridae	2.7		
Ogcocephalidae	-		
Ostraciontidae	-		
Peristediidae			-
Platycephalidae	.9		
Pomadasyidae	-		
Priacanthidae	-	.5	
Scolopsidae		-	
Scorpaenidae	.9		
Serranidae	-	-	
Stomiatidae			.9
Synodontidae	6.3	-	
Triacanthidae	-		
Zeidae			-
Unidentified			3.6
Invertebrate			
Crab	-		-
Polypodidae	.9		
Sepiolidae	-		
Shrimp	-		3.6

Table III

Average catches in kilograms per hour of trawling, by depth range, obtained in the East Pakistan region on Cruise 1 of the Anton Bruun. Dashes designate catches of less than 0.2 kg. (half a pound)

No. hauls	(6)
Depth in meters	15-37
Elasmobranch	
Carcharhinidae	.9
Dasyatidae	.5
Rhinobatidae	26.8
Sphyrnidae	.5
Torpedinidae	-
Flatfish	
Bothidae	.5
Soleidae	.5
Roundfish	
Apogonidae	-
Ariidae	5.0
Carangidae	.5
Clupeidae	2.3
Dactylopteridae	.5
Engraulidae	.5
Ephippidae	.9
Fistulariidae	-
Gerridae	-
Gobiidae	-
Harpodontidae	2.7
Lagocephalidae	-
Leiognathidae	.9
Lutjanidae	-
Monacanthidae	-
Mullidae	.9
Nemipteridae	.5
Pegasidae	-
Platycephalidae	.5
Polynemidae	5.0
Pomadasyidae	-
Sciaenidae	21.3
Scombridae	-
Scorpaenidae	-
Sillaginidae	-
Sparidae	-
Sphyraenidae	-
Syngnathidae	-
Synodontidae	.5
Tetraodontidae	-
Theraponidae	.5
Triacanthidae	-
Trichiuridae	-
Invertebrate	
Crab	.5
Loliginidae	.5
Scyllaridae	.5
Sepiolidae	-
Shrimp	2.3

Table IV

Average catches in kilograms per hour of trawling, by depth range, obtained in the Burma region on Cruise 1 of the Anton Bruun. Dashes designate catches of less than 0.2 kg. (half a pound)

No. hauls	(3)	(7)	(3)	(1)	(1)
Depth in meters	15-37	38-73	74-110	184-366	367-549
Elasmobranch					
Carcharhinidae	-			.9	3.6
Dasyatidae	41.3	5.9	.9		
Torpedinidae		-	-		
Flatfish					
Bothidae	-	-	.9	-	
Cynoglossidae	.9	2.7		-	
Pleuronectidae		-			
Psettodidae	-	1.4	-		
Soleidae		-	-		
Eel					
Unidentified	-	4.1		-	
Roundfish					
Apogonidae	-	.9	.9		
Ariidae	8.2	.5			
Balistidae		-	1.4		
Bembropsidae				.9	
Blenniidae		-			
Callionymidae			.5		
Carangidae	-	-	.5		
Carapidae			-		
Centriscidae		-			
Chaunacidae				-	
Chlorophthalmidae				18.1	.9
Clupeidae	-	-			
Dactylopteridae	-	.5	-		-
Eleotridae		-			
Ephippidae	.5		-		
Fistulariidae	-	.5	-		
Gerridae	-	-	-		
Gonostomidae					-
Harpodontidae	1.8				
Holocentridae			.5		
Leiognathidae	-	-			
Lophiidae		-	-		-
Lutianidae		1.8	7.7		
Macruridae				.9	3.6
Monacanthidae		-	-		
Monodactylidae	-				
Mullidae	.9	.5	.9		
Myctophidae					-
Nempteridae	3.6	2.3	3.2		
Ogcocephalidae		-	-	-	
Ostraciontidae		-			
Parapercidae			-		
Pegasidae			-		
Platycephalidae	-	-	.5	-	
Polynemidae	6.8	-			
Pomacentridae			-		
Pomadasyidae	.5	1.8			
Priacanthidae		-	-	.9	
Rachycentridae	-				
Sciaenidae	16.3	9.1			
Scombridae			-		
Scorpaenidae	-	-	-	3.6	-
Serranidae		.5	1.4		
Sillaginidae	-				
Sparidae		.5			
Sphyraenidae		-			
Sternoptychidae					-
Stromateidae	-	-		1.8	
Synodontidae	.5	4.5	1.4		
Tetraodontidae	.9	-			
Theraponidae	-				
Triacanthidae	-	-		.9	
Trichiuridae	-	-		-	.9
Triglidae			.5		
Uranoscopidae	-	-	-		
Unident. Berycoid				.9	27.2
Unidentified	-	-		-	.9
Invertebrate					
Argonautidae			-		
Crab	-	-	.5		-
Loliginidae	-	-	.5		
Palinuridae		-		4.5	
Scallop	5.0	-			
Scyllaridae	-	-	.5		
Sepiolidae	.9	-	.5		
Shrimp	5.4	2.7	-	25.4	15.4
Stomatopoda	-	-			

Table V

Average catches in kilograms per hour of trawling, by depth range, obtained in the India region on Cruise 4B of the Anton Bruun. Dashes designate catches of less than 0.2 kg. (half a pound)

No. hauls	(10)	(7)	(5)	(4)	(2)
Depth in meters	15-37	38-73	74-110	111-183	184-366
Rays and sharks					
Dasyatidae	34.5	14.5			
Galeorhinidae			.5		
Rhinobatidae	3.6	-			
Torpedinidae	-				
Flatfish					
Bothidae	-	-	-	.5	
Cynoglossidae	-	-	-		
Pleuronectidae			-		
Soleidae	-	-	-	-	
Eel					
Congridae		-			-
Leptocephalus			-		
Muraenesocidae	4.1	-			
Nemichthyidae		-			
Roundfish					
Aluteridae	-	-			
Anthiidae			-		
Apogonidae	5.9	-	.5	-	2.3
Ariidae	1.8	.5	-		
Brotulidae		-			
Callionymidae		-	-		
Carangidae	.5	-	1.4	.5	
Chaetodontidae				-	
Champsodontidae		-	-	-	4.5
Chirocentridae	-				
Clupeidae	-				
Diodontidae				-	
Drepanidae	.5				
Engraulidae	1.4				
Fistulariidae	-	-	-	-	
Gadidae	-	-			
Gempylidae					.5
Gobiidae	-				
Harpodontidae	6.3				-
Lactariidae	-	-			
Lagocephalidae	-				
Leiognathidae	1.4	-	-	-	
Lutjanidae	.5		-		
Mullidae	.9	2.7	4.1		
Myctophidae					-
Nemipteridae	-	7.3	11.8	55.8	1.8
Ogcocephalidae			-	-	
Parapercidae			-	.5	
Platycephalidae	.5	1.4	5.9	-	
Plotosidae		-			
Polynemidae	18.1	.5	.5		
Pomadasyidae	1.4	-			
Priacanthidae			-		
Rachycentridae		.5			
Sciaenidae	27.7	-	.5		1.4
Scolopsidae		-	-	-	-
Scorpaenidae	-	-	-		
Serranidae	-	1.8	3.2	3.6	
Sparidae	1.8	1.4	.5		
Sphyraenidae		-	.5	-	
Stomiatidae					-
Stromateidae	-	-	-		-
Synanceiidae	-	-	-	-	
Synodontidae	.5	3.2	2.3	9.1	
Therapontidae	-				
Trichiuridae	-	-	-		
Triglidae		.5	-	.9	
Uranoscopidae		-	-		
Invertebrate					
Caridea	1.8	-	-		
Crabs	-	-	.5		-
Loliginidae	.9	.5	.5	.9	
Penaeidae	6.3	.5	.9		-
Polypodidae		-	-	-	
Scyllaridae	.5	.9			
Sepiolidae	-	.9	1.8	-	
Stomatopoda	-	-			

Table VI

Average catches in kilograms per hour of trawling, by depth range, obtained in the West Pakistan region on Cruise 4B of the Anton Bruun. Dashes designate catches of less than 0.2 kg. (half a pound)

No. hauls	(12)	(1)	(8)	(4)	(2)
Depth in meters	15-37	38-73	74-110	111-183	184-366
Rays and sharks					
Carcharhinidae	.9	4.1			
Dasyatidae	43.1	1.4	.5	45.4	
Myliobatidae	-				
Rajidae	-		-		
Rhinobatidae	1.8		31.3	5.4	
Scyliorhinidae	.5		-	-	
Torpedinidae	-				
Unident. shark				-	
Flatfish					
Bothidae	-		-	-	
Cynoglossidae	.5			-	-
Psettodidae	-				
Soleidae	-		-	-	
Unident. flatfish					-
Eel					
Congridae	-		-	-	
Echelidae				-	
Muraenesocidae	1.8		1.8	.5	
Roundfish					
Apogonidae	-		-	-	.5
Ariidae	7.3	3.6	.5	-	
Callionymidae	-			-	-
Carangidae	1.4	3.6	8.2	-	
Cephalacanthidae	-				
Cepolidae			-		
Champsodontidae			-		.5
Chirocentridae	-				
Clupeidae	.9				
Drepanidae	2.7	-	-	-	
Echeneidae			-		
Engraulidae	.9		-	.9	
Fistulariidae	-		-		
Gadidae			-		-
Gerridae	-				
Harpodontidae				-	-
Lactariidae	8.6		.5		
Lagocephalidae	-	1.4	-		
Leiognathidae	2.3	-	.5		
Lutjanidae	-				
Mullidae	.5	.5	-		
Myctophidae					-
Nemipteridae	1.4	3.2	31.3	7.3	
Platycephalidae	.5	-	.5	-	
Polynemidae	4.1		2.7	4.1	
Pomadasyidae	9.5	12.2	.9	3.6	
Priacanthidae			-		
Rachycentridae	.9		.5		
Sciaenidae	19.0		6.8	10.0	.5
Scolopsidae			-	16.3	
Scombridae	-				
Scorpaenidae	-			-	
Serranidae	-		1.4	.5	
Sparidae	3.6	3.2	-		
Sphyraenidae	.9		-		
Stromateidae	.5		-	.5	
Synancidae	-				
Synodontidae	1.8	3.6	.9	-	
Tetraodontidae	.9		-		
Theroponidae	1.4				
Thunnidae			-		
Trichiuridae	.5		-	-	
Triglidae	-		-	.5	
Uranoscopidae	-		-		
Invertebrate					
Argonautidae			-		
Crabs			-	-	
Loliginidae	.9		.5	-	
Palinuridae	-			-	
Penaeidae	.5		-	.5	2.7
Scyllaridae	-				
Sepiolidae	-		.9	-	
Stomatopoda	-				

Table VII

Average catches in kilograms per hour of trawling, by depth range, obtained in the Gulf of Oman region on Cruise 4B of the Anton Bruun. Dashes designate catches of less than 0.2 kg. (half a pound)

No. hauls	(3)	(5)	(6)	(2)	(4)
Depth in meters	15-37	38-73	74-110	111-183	184-366
Rays and sharks					
Carcharhinidae			4.5		
Dasyatidae		26.8		.9	
Rhinobatidae	.5		-		
Scyliorhinidae			.5		1.8
Torpedinidae					-
Flatfish					
Bothidae		.5	-	.5	
Cynoglossidae				1.8	-
Pleuronectidae			-		
Psettodidae	.5	-	-		
Eel					
Congridae		-		-	.9
Leptocephalus				-	
Muraenesocidae		1.8	.5		.9
Nemichthyidae					-
Nettastomidae					-
Roundfish					
Apogonidae	-		-	-	2.7
Ariidae	1.8	.9	3.2		
Brotulidae					-
Callionymidae				-	-
Carangidae	.5	.5	7.3		
Champsodontidae		-	-	-	-
Clupeidae	-		-		
Drepanidae	.5	.5			
Echeneidae	.5				
Engraulidae	-	-			-
Fistulariidae	-	-	-		
Gadidae	-	-	-	-	
Gempylidae					-
Gerridae	-				
Gobiidae				-	
Harpodontidae					.5
Holocentridae					.9
Lactariidae	-				
Lagocephalidae	-		.5		
Leiognathidae	-	.5	.5		
Lutjanidae			5.0		
Menidae	-				
Mullidae	2.7	-	.5		
Myctophidae				-	
Nemipteridae	2.3	.9	13.6	10.9	.9
Ostraciontidae			-		
Platycephalidae	.5	.5	.9		
Polynemidae		-		.5	
Pomadasyidae	2.7	.9	2.7		-
Priacanthidae			.9		
Rachycentridae		1.8			
Sciaenidae	-	-	-	3.6	10.0
Scolopsidae			-	3.2	.5
Scorpaenidae					-
Serranidae	-	.5	3.6	.5	.5
Sparidae		.5	1.8		
Sphyraenidae			.5		
Stromateidae				-	-
Synancidae		-			
Synodontidae	4.1	2.3	2.3		
Trichiuridae				-	.5
Triglidae	-	-	-	.5	
Uranoscopidae		-	-		
Invertebrate					
Crabs	-		3.6	-	-
Loliginidae	.5	-	.9		.5
Penaeidae	.9		-	.9	3.6
Polypodidae			-	-	
Scyllaridae	-	.5			
Sepiolidae	-	-	.9	.9	.5
Stomatopoda			-		-

Table VIII.

Average catches in kilograms per hour of trawling, by depth range, obtained in the Arabin region on Cruise 4B of the Anton Bruun. Dashes designate catches of less than 0.2 kg. (half a pound)

No. hauls	(2)
Depth in meters	38-73
Rays and sharks	
Dasyatidae	2040.8
Flatfish	
Bothidae	-
Cynoglossidae	-
Roundfish	
Apogonidae	76.2
Ariidae	3.6
Carangidae	9.5
Cephalacanthidae	1.8
Gerridae	1.8
Lagocephalidae	1.8
Leiognathidae	1.8
Nemipteridae	28.6
Platycephalidae	3.6
Pomadasyidae	346.9
Sparidae	4.1
Synancidae	1.8
Synodontidae	12.7
Theraponidae	3.6
Triglidae	12.7
Uranoscopidae	-
Invertebrate	
Crabs	641.7
Loliginidae	-

Reprinted from *Aust. J. mar. freshw. Res.*, vol. 17, 1966, p. 135-145

OCEANOGRAPHY
545
COLLECTED REPRINT

THE CONCENTRATION OF CHLOROPHYLLS *a* AND *c* IN THE SOUTH-EAST INDIAN OCEAN

By G. F. HUMPHREY*

[*Manuscript received May* 23, 1966]

Summary

Samples were collected in 1959–62, usually at 0, 25, 50, 75, 100, and 150 m, in the region between 90 and 140°E., and 10°N. and 50°S. At 0 m (and 150 m) the regional average for chlorophyll *a* was 0·08 (and 0·09) μg/l in summer and 0·12 (and 0·09) μg/l in winter; for chlorophyll *c* the values were 0·17 (and 0·21) μg/l in summer and 0·21 (and 0·21) μg/l in winter. Most samples had chlorophyll *c*/*a* ratios between 1 and 2. The average amount of chlorophyll *a* in the water column to 150 m was 15 mg/m² in summer and 23 in winter; for chlorophyll *c* the values were 29 mg/m² in both summer and winter. At most stations the maximum amounts of chlorophyll were at 75 m, often near density and temperature discontinuities. At 75 m the regional average for chlorophyll *a* was 0·14 μg/l in summer and 0·19 in winter; for chlorophyll *c* the values were 0·35 and 0·24. The results of the present and similar work show that the amounts of the chlorophylls in the water column under 1 m² are similar for all oceans.

I. INTRODUCTION

As part of a general study of the oceanography of the Indian Ocean near Australia, determinations were made of the concentration of plankton pigments. The results obtained have allowed specific problems to be formulated, some of which are being investigated separately. The present paper gives the results obtained during the general study, i.e. in 1959–62.

II. METHODS

Sampling and analytical methods, and the data, are in CSIRO AUST. (1962*a*, 1962*b*, 1963*a*, 1963*b*, 1963*c*, 1964*a*, 1964*b*, 1964*c*, 1966*a*, 1966*b*). The values given in these Oceanographical Cruise Reports were calculated using the equations of Richards with Thompson (1952) which gave chlorophyll *c* in arbitrary units. The extinction coefficient of chlorophyll *c* is now known (Jeffrey 1963) and the concentrations in arbitrary units given in the Reports have been divided by 2 to give μg/l before being used in the present paper.

III. RESULTS

(*a*) *Sampling*

Between October 1959 and October 1962, 335 stations were sampled, almost always at 0, 25, 50, 75, 100, and 150 m. In a few cases, sampling was continued to 500 m. The distribution of stations according to month and 5° square, is shown in Figure 1. No samples were taken west of 90°E., or south of 50°S., nor in January, April or December. During October–March 136 stations were sampled and in

* Division of Fisheries and Oceanography, CSIRO, Cronulla, N.S.W.

April–September, 199. The first period will be referred to as summer and the second as winter although it is realized that these seasonal terms do not apply to the 11 stations which were in the Northern Hemisphere.

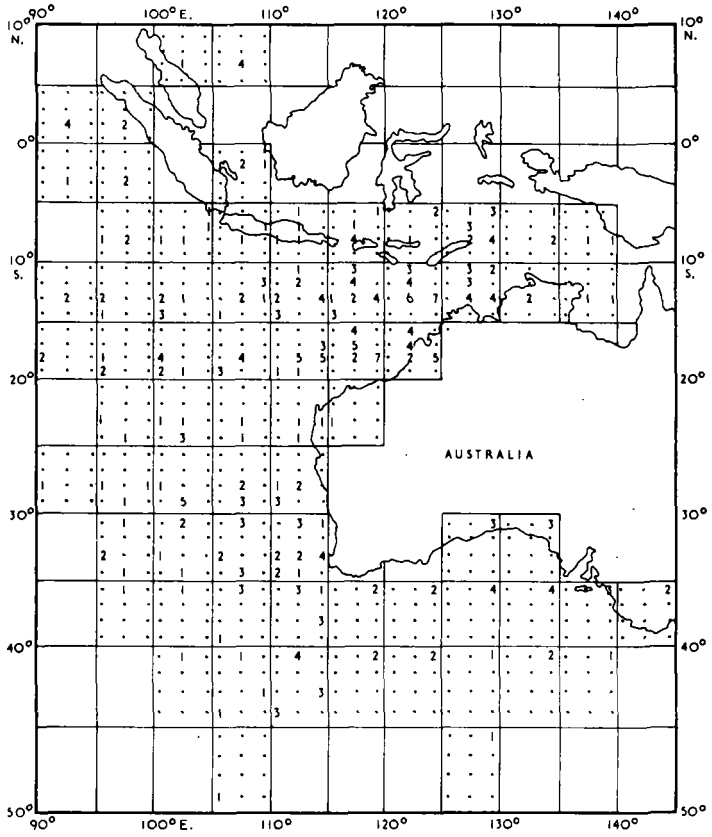


Fig. 1.—Distribution of stations. In each square the 12 months are indicated by (·) or by a numeral; (·) means no sample, the numeral shows the number of samples. The months are arranged in groups of three: J F M, A M J, J A S, O N D.

(*b*) *Surface Chlorophyll*

The mean monthly chlorophyll *a* concentration at 0 m, calculated for each 5° square, ranged from 0·01 to 0·50 μg/l; the corresponding range for chlorophyll *c* was 0·01 to 0·66 μg/l. In nearly all the squares, the maximum monthly value occurred in winter; the exceptions were one square for chlorophyll *a* and seven squares for chlorophyll *c*. The seasonal contours for chlorophyll *a* (Fig. 2) show that its concentration was higher in winter over most of the region; south of 40° there were more samples in summer than in winter, and they had higher concentrations than the rest of the region. For chlorophyll *c*, similar conclusions can be drawn, but not so clearly.

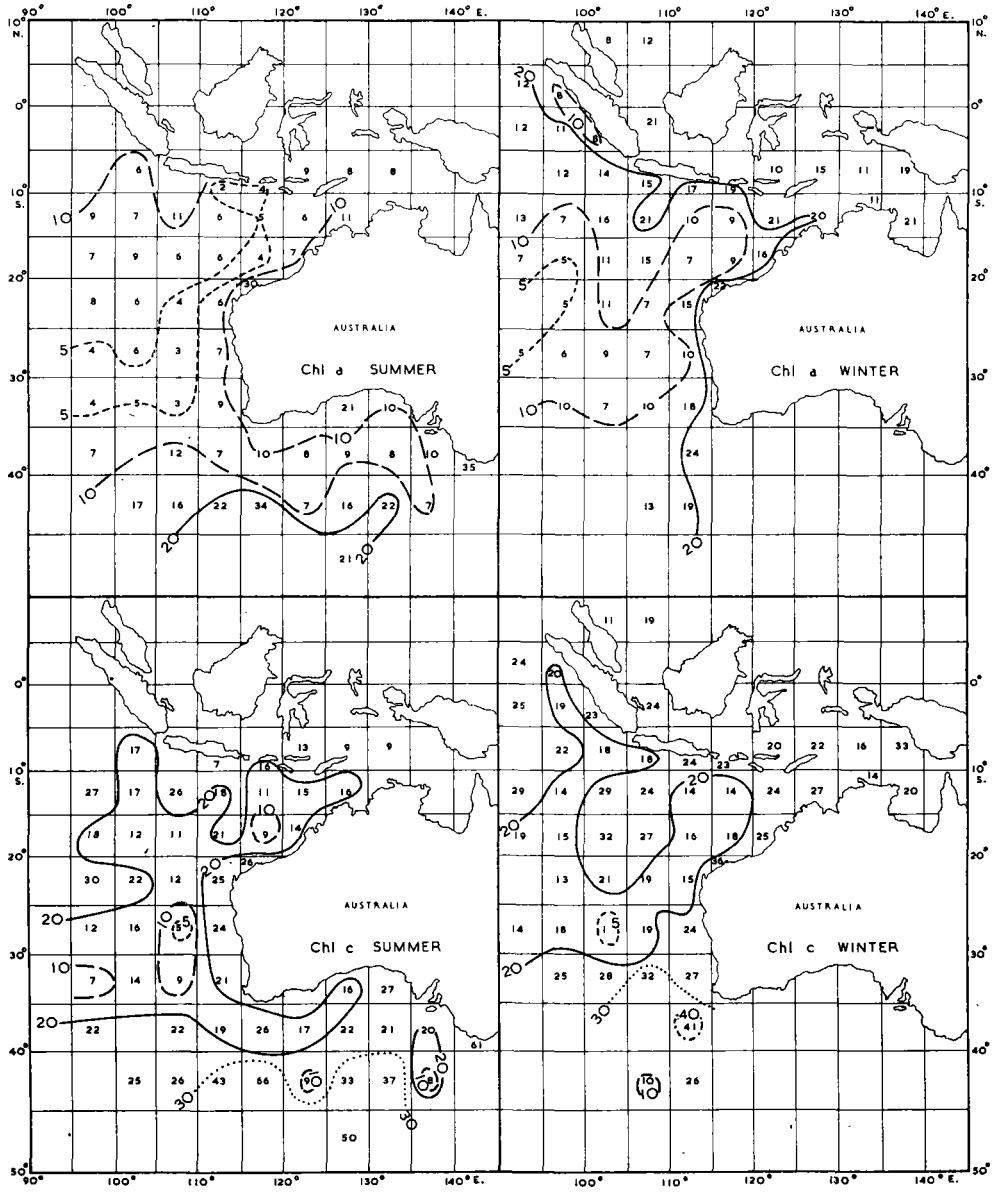


Fig. 2.—Seasonal contours of surface chlorophylls. The value in each square is 100 times the mean of the concentrations (μg/l) found for the season.

For the squares which were sampled in both seasons, the averages of the 5° square means were 0·08 μg/l chlorophyll *a* in summer and 0·12 in winter, and 0·17 μg/l chlorophyll *c* in summer and 0·21 in winter.

(c) *Deep Chlorophyll*

The mean monthly chlorophyll *a* concentration at 150 m, calculated for each 5° square, ranged from 0·02 to 0·36 μg/l; the corresponding range for chlorophyll *c* was

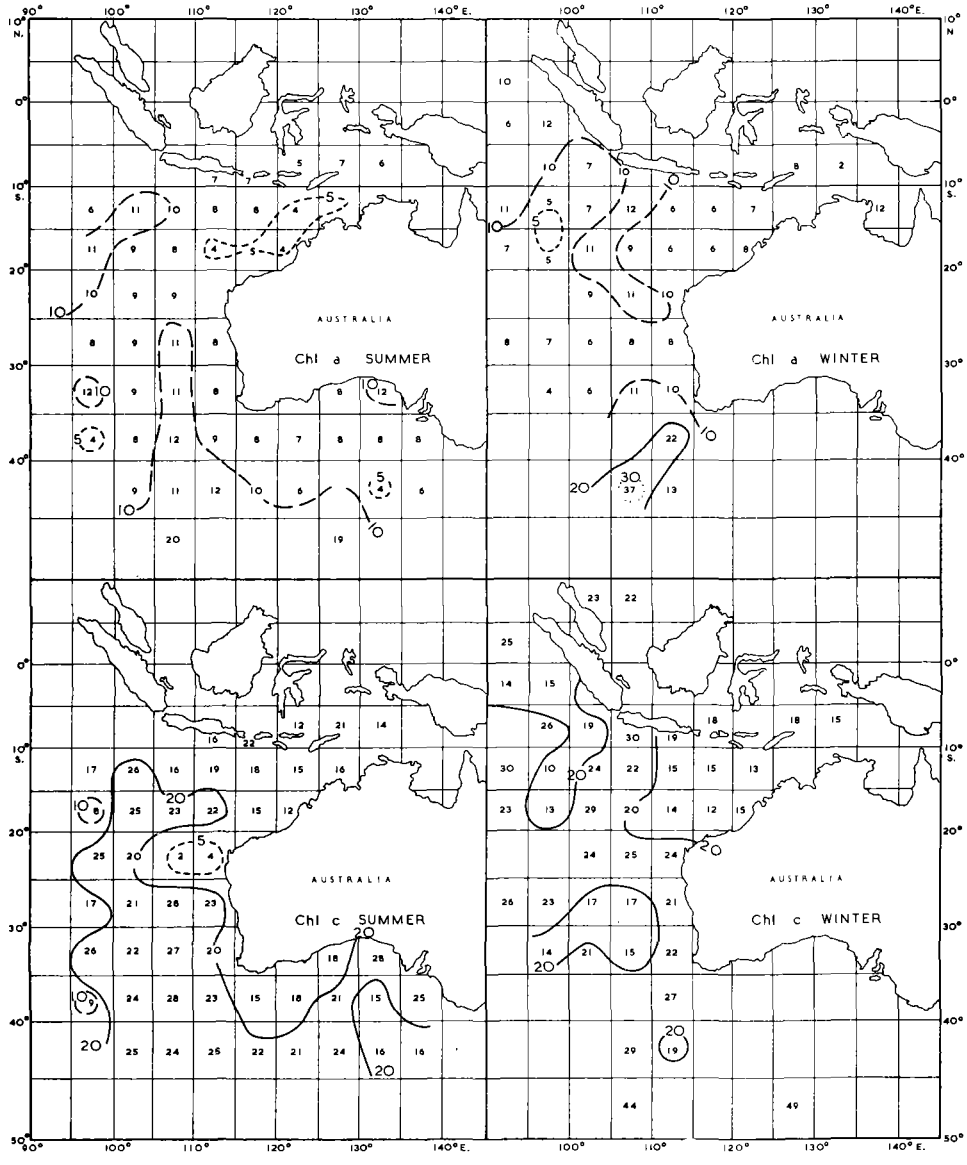


Fig. 3.—Seasonal contours of 150-m chlorophylls. For explanation see Figure 2.

0·04–0·44 μg/l. In most squares, the maximum monthly value occurred in winter; there were 11 exceptions for chlorophyll *a* and 12 for *c*. Although the seasonal contours for chlorophyll *a* (Fig. 3) changed between summer and winter, there was

little variation in concentration throughout the region, except for the south-west of Australia where 0·20 and 0·30 μg/l contours appeared in winter. The mean monthly chlorophyll *c* concentration showed a greater variation throughout the region in

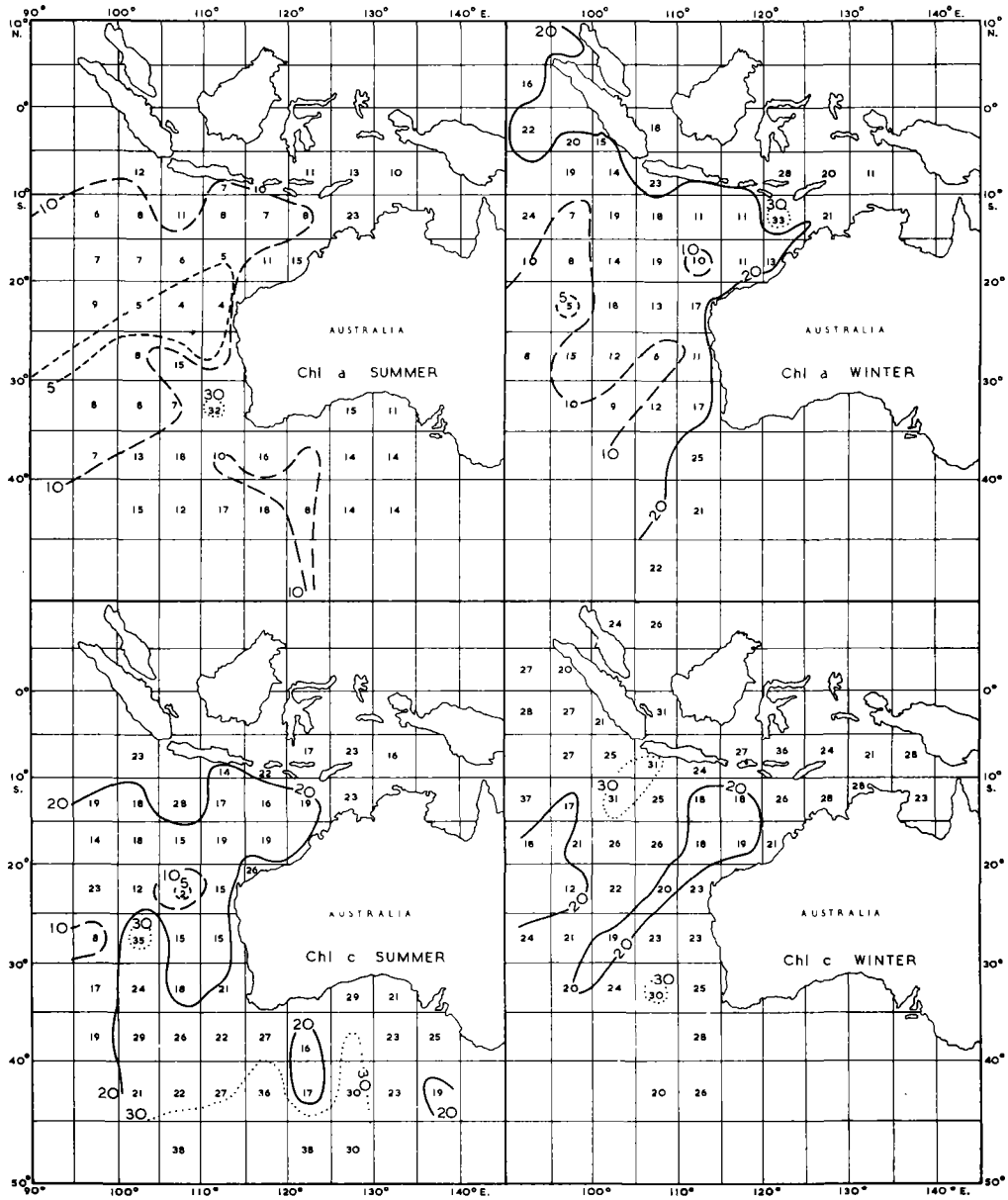


Fig. 4.—Seasonal contours of column chlorophylls. For explanation see Figure 2.

summer than in winter. The highest concentrations were in winter to the south-west of Australia. For the squares which were sampled in both seasons, the averages of the 5° square means were 0·09 μg/l chlorophyll *a* and 0·21 μg/l chlorophyll *c* in both summer and winter.

In July to October, 87 samples were collected below 150 m, usually to 500 m. The mean chlorophyll *a* was 0·08 μg/l; only 16 of the values were greater than 0·10, the highest being 0·25 μg/l. The water column above 150 m had more chlorophyll *a* than that below. The mean chlorophyll *c* was 0·19 μg/l; 28 of the values were greater than 0·20, the highest being 0·56 μg/l. In most cases, the water column above 150 m had more chlorophyll *c* than that below.

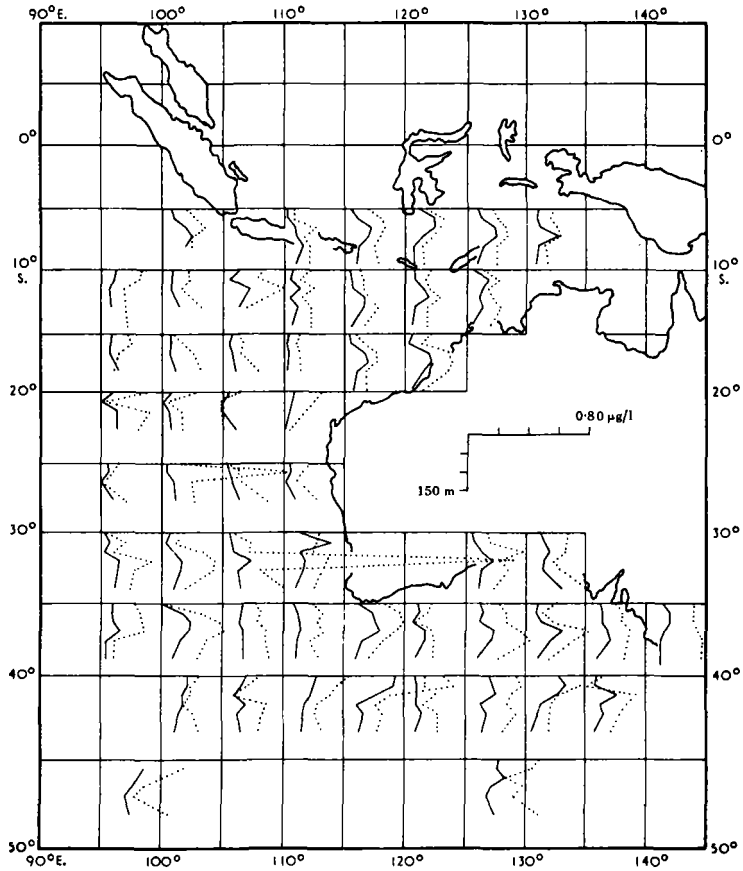


Fig. 5.—Summer depth profiles of chlorophylls *a* (——) and *c* (· · · ·) in micrograms per litre. The mean value at each depth for a given square is plotted.

(*d*) *Column Chlorophyll*

The average concentration of chlorophyll in the water column (down to 150 m) at each station was calculated according to Humphrey (1960). The monthly means of the column concentrations in each 5° square ranged from 0·02 to 0·78 μg/l chlorophyll *a* (equivalent to 3–117 mg/m^2 for the 0–150 m zone) and from 0·01 to 0·44 μg/l chlorophyll *c* (1·5–66 mg/m^2). In nearly all the squares, the maximum value was in winter; there were four exceptions for chlorophyll *a* and seven for chlorophyll *c*. The seasonal contours for the column concentration of chlorophyll *a* (Fig. 4) show higher values in winter over most of the region; south of 40° in summer, the values

were higher than for the rest of the region. For chlorophyll *c*, the seasonal difference was the same, but not so clearly marked; the increased southern concentration began at 35°S.

For the squares which were sampled in both seasons, the averages of the 5° square means were 0·10 μg/l (15 mg/m²) chlorophyll *a* in summer and 0·15 (23 mg/m²) in winter, and 0·19 μg/l (29 mg/m²) chlorophyll *c* in both summer and winter.

(*e*) *Ratio of Chlorophyll* c *to* a

Figures 2–4 show that in most cases the concentration of chlorophyll *c* was higher than that of chlorophyll *a*. Usually the ratio of the concentration of chlorophyll *c* to that of *a* in a single water sample was between 1 and 2. The concentration of chlorophyll *a* was very low in most of the samples, 46% of them having a concentration less than 0·1 μg/l. In the following tabulation the ratios of chlorophyll *a* to chlorophyll *c* have been calculated individually from the chlorophyll concentrations in all the samples collected. The tabulation shows that ratios greater than 1 were found more often with the lower ranges of concentration of chlorophyll *a*.

Range of chlorophyll *a* (μg/l)	Samples where *c*/*a* exceeded 1 (%)
0–0·09	90
0·1–0·19	87
0·2–0·29	72
0·3–0·39	67
0·4–0·49	20
0·5+	20

(*f*) *Chlorophyll Variation with Depth*

Figures 5 and 6 show, for summer and winter, respectively, the mean depth profiles for chlorophylls *a* and *c* in each 5° square. In both periods, the chlorophyll *c* curve was similar to that for chlorophyll *a* but showed higher values. Nearly all the profiles had clearly defined maxima; occasionally, there were two maxima to a profile. For each chlorophyll and for each season, the depth at which there was most frequently a principal maximum was 75 m. In summer, 100 m was the next in frequency, and in winter, 50 m. No evidence was obtained that the depth of the maximum was related to the time of day at which the sample was taken.

For the squares which were sampled at 75 m in both seasons, the averages of the 5° square means were 0·14 μg/l chlorophyll *a* in summer and 0·19 in winter, and 0·35 μg/l chlorophyll *c* in summer and 0·24 in winter. In the 30–35°S., 105–110°E. square, the chlorophyll *c* concentration was exceptionally high; omitting this square the chlorophyll *c* averages were 0·23 μg/l in both summer and winter.

IV. Discussion

(*a*) *Surface Chlorophyll*

Previous work on pigments in the Indian Ocean has dealt only with chlorophyll *a*. In April 1957, Kutyurin and Lisitzin (1962) found surface concentrations of

about 0·2 μg/l in the area 88–97°E., 53–0°S.; a station at 97°E., 29°S. had 0·7 μg/l. In December 1960–January 1961, and March–April 1961, Ichimura and Fukushima (1963) found 0·02–0·2 μg/l on a line from Sumatra to South Africa, and 0·15–0·6 μg/l from South Africa towards the Antarctic (50°E.). In December 1961, Saijo and Kawashima (1964) found 0·02–0·6 μg/l in the region from 37°S. to the Antarctic; only 4 of the 15 values exceeded 0·2 μg/l. In December 1962–January 1963, Saijo (1963) found 0·01–0·02 μg/l along a 78°E. section from Colombo to 20°S. The sampling period of these observations complements that of the present work.

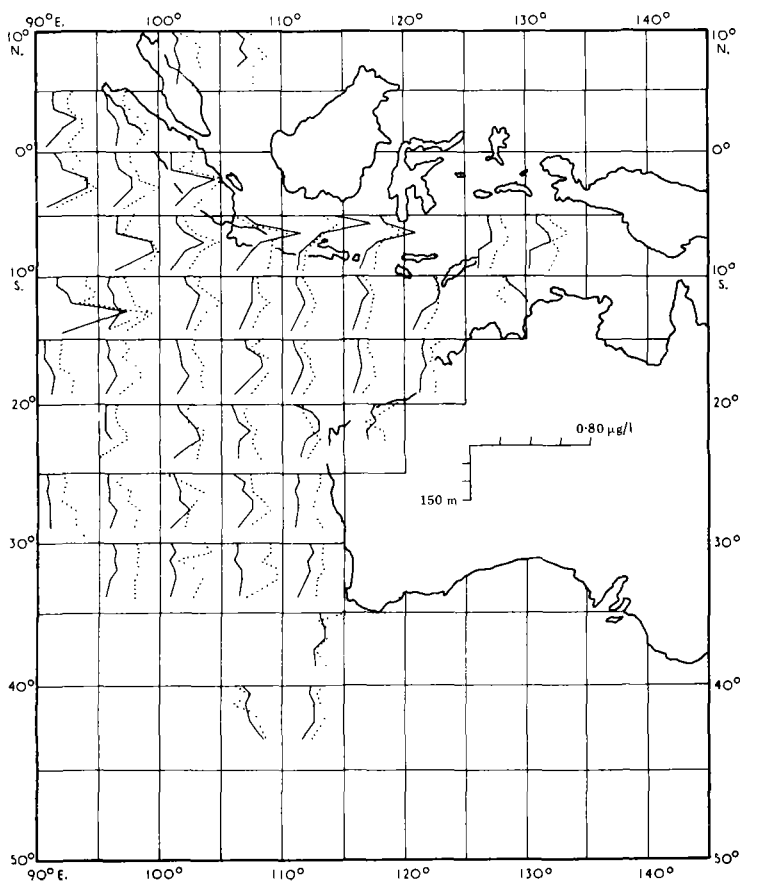


Fig. 6.—Winter depth profiles of chlorophylls. For explanation see Figure 5.

Therefore, for the whole of the year, the surface of the south-eastern and southern parts of the Indian Ocean is characterized by a low level of chlorophyll *a*, i.e. usually no more than 0·2 μg/l. Exceptions to this are coastal regions (Fig. 2), a few stations towards the Antarctic, and the 10–15°S., 105–110°E. square (Fig. 2) near the upwelling area (Rochford 1962; Wyrtki 1962) south of Java. Figure 2 shows that although concentrations were only just over 0·2 μg/l in this square in winter, in both summer and winter the area was richer than surrounding ones. This area also had a relatively higher seston concentration than surrounding ones (Hagmeier 1964).

Information on chlorophyll *c* is available only from the present investigation. It shows that the surface concentration is low (usually 0·1–0·2 μg/l) with the exceptions given above for chlorophyll *a* and some other small areas.

(*b*) *Subsurface Chlorophyll*

In addition to his surface determinations along 78°E., Saijo (1963) measured chlorophyll *a* at 10, 25, 50, 75, 100, 125, 150, and 200 m. Maxima in depth profiles were usually at 75 m; at 12°S. the maximum was at 50 m and at 16°S. it was at 100 m. The largest concentration in any sample was 0·12 μg/l (16°S. at 100 m).

The subsurface concentrations of chlorophyll *a* found in the present investigation are higher than those found by Saijo but the positions of the maxima in profiles are the same. Often the maximum was at the same depth as a density or temperature discontinuity, but sometimes there was no such relation.

(*c*) *Ratio of Chlorophyll* c *to* a

Probably most of the ratios greater than unity found in the present investigation are artefacts arising from the insensitivity of the chlorophyll method. This criticism does not apply to samples where chlorophyll *a* was more than 0·5 μg/l and yet 20% of such samples gave *c*/*a* ratios greater than 1. Many other authors (reviewed by Humphrey 1962) report large *c*/*a* ratios and although most of the values can be discarded as above, there remain some where *c*/*a* exceeds 1. Spectrophotometric and chromatographic analyses of cultures (Humphrey 1963; Madgwick 1966) have not shown ratios greater than 0·9 (after correcting where necessary for differing extinction coefficients). The high ratios found in field studies cannot yet be explained but it might be important that the culture ratio of 0·9 was obtained with a dinoflagellate, and dinoflagellates have been found to predominate in that part of the south-east Indian Ocean examined for species occurrence (Durairatnam 1964).

(*d*) *Comparison with Atlantic and Pacific Oceans*

Menzel and Ryther (1960) determined chlorophyll *a* in 48 samples from 0 to 100 m during 1957–59 at a deep station (32°N., 65°W.) off Bermuda. At all depths, concentrations varied seasonally up to 1 μg/l. In the tropical Atlantic (15–40°W., 14°N.–16°S.) in August–November, Sushchenia and Finenko (1964) determined surface chlorophyll at 24 stations. The range for chlorophyll *a* was 0·02–1·09 μg/l (six stations greater than 0·20) and for chlorophyll *c* (after dividing by 2 to allow for the incorrect extinction coefficient) 0–1·1 μg/l (four stations greater than 0·20). Chlorophyll *a* in 23 subsurface samples (mainly at 25 and 100 m) was from 0·03 to 0·36 μg/l and chlorophyll *c*, 0–0·51 μg/l; the biggest values were at 100 m. The amount of chlorophyll *a* in a 100-m column was 4·9–13·2 mg.

Humphrey (1962) reviewed the distribution of chlorophylls in the Pacific Ocean, noting that most of the values were for 0 and 25 m and usually ranged from 0 to 1·5 μg/l for both chlorophylls *a* and *c* (after dividing the latter by 2). More recently, Aruga and Monsi (1963) give 25–45 mg/m^2 for the amount of chlorophyll *a* in the Kuroshio area and 50–70 mg/m^2 for the Oyashio. Further, Jitts (1965) has examined

the results of several hundred chlorophyll *a* analyses, made by the method used in the present paper, of samples taken in the summer months of 1960–65 in the Coral and Tasman seas. In the five regions studied, mean surface chlorophyll *a* varied from 0·05 to 0·15 μg/l and the amount in a 150-m column of water, from 14 to 26 mg.

The studies of each ocean were not equally comprehensive but it seems that the amounts in a water column under 1 m^2 are of the same order of magnitude for all oceans, although in the Indian Ocean the concentration of chlorophylls per litre of water do not reach the highest values found in the Atlantic and Pacific Oceans. It is not yet possible to correlate any of the recorded chlorophyll distribution patterns with environmental factors or with the physiological properties of the phytoplankton. Such correlations must await more information both on the environment and on the physiology of the algae involved.

V. References

ARUGA, Y., and MONSI, M. (1963).—Chlorophyll amount as an indicator of matter productivity in bio-communities. *Pl. Cell Physiol., Tokyo* **4**, 29–39.

CSIRO AUST. (1962*a*).—Oceanographical observations in the Indian Ocean in 1959. H.M.A.S. *Diamantina*, Cruises Dm 1/59 and Dm 2/59. *CSIRO Aust. Oceanogr. Cruise Rep.* **1**.

CSIRO AUST. (1962*b*).—Oceanographical observations in the Indian Ocean in 1960. H.M.A.S. *Diamantina*, Cruise Dm 1/60. *CSIRO Aust. Oceanogr. Cruise Rep.* **2**.

CSIRO AUST. (1963*a*).—Oceanographical observations in the Indian Ocean in 1960. H.M.A.S. *Diamantina*, Cruise Dm 2/60. *CSIRO Aust. Oceanogr. Cruise Rep.* **3**.

CSIRO AUST. (1963*b*).—Oceanographical observations in the Indian Ocean in 1961. H.M.A.S. *Diamantina*, Cruise Dm 1/61. *CSIRO Aust. Oceanogr. Cruise Rep.* **7**.

CSIRO AUST. (1963*c*).—Oceanographical observations in the Indian Ocean in 1961. H.M.A.S. *Diamantina*, Cruise Dm 2/61. *CSIRO Aust. Oceanogr. Cruise Rep.* **9**.

CSIRO AUST. (1964*a*).—Oceanographical observations in the Indian Ocean in 1961. H.M.A.S. *Diamantina*, Cruise Dm 3/61. *CSIRO Aust. Oceanogr. Cruise Rep.* **11**.

CSIRO AUST. (1964*b*).—Oceanographical observations in the Indian Ocean in 1962. H.M.A.S. *Diamantina*, Cruise Dm 1/62. *CSIRO Aust. Oceanogr. Cruise Rep.* **14**.

CSIRO AUST. (1964*c*).—Oceanographical observations in the Indian Ocean in 1962. H.M.A.S. *Diamantina*, Cruise Dm 2/62. *CSIRO Aust. Oceanogr. Cruise Rep.* **15**.

CSIRO AUST. (1966*a*).—Oceanographical observations in the Indian and Pacific Oceans in 1961. H.M.A.S. *Gascoyne*, Cruise G 2/61. *CSIRO Aust. Oceanogr. Cruise Rep.* **10**.

CSIRO AUST. (1966*b*).—Oceanographical observations in the Indian Ocean in 1962. H.M.A.S. *Diamantina*, Cruise Dm 3/62. *CSIRO Aust. Oceanogr. Cruise Rep.* **18**.

DURAIRATNAM, M. (1964).—Vertical distribution of phytoplankton in an area near Cocos–Keeling Islands, Indian Ocean. *Inf. Bull. Planktol. Japan* **11**, 1–6.

HAGMEIER, E. (1964).—Zum Gehalt an Seston und Plankton im Indischen Ozean Zwischen Australien und Indonesien. *Kieler Meeresforsch.* **20**, 12–17.

HUMPHREY, G. F. (1960).—The concentration of plankton pigments in Australian waters. CSIRO Aust. Div. Fish. Oceanogr. Tech. Pap. No. 9.

HUMPHREY, G. F. (1962).—Phytoplankton pigments in the Pacific Ocean. Proceedings of the Conference on Primary Productivity Measurements, Marine and Freshwater, University of Hawaii, August 21–September 6, 1961. (Ed. M. S. Doty.) (U.S. Atomic Energy Commission Monograph.)

HUMPHREY, G. F. (1963).—Chlorophyll *a* and *c* in cultures of marine algae. *Aust. J. mar. Freshwat. Res.* **14**, 148–54.

ICHIMURA, S., and FUKUSHIMA, H. (1963).—On the chlorophyll content in the surface water of the Indian and the Antarctic Oceans. *Bot. Mag., Tokyo* **76**, 395–9.

JEFFREY, S. W. (1963).—Purification and properties of chlorophyll *c* from *Sargassum flavicans*. *Biochem. J.* **86**, 313–8.

JITTS, H. (1965).—The summer characteristics of primary production in the Tasman and Coral Seas. *Aust. J. mar. Freshwat. Res.* **16**, 151–62.

KUTYURIN, V. M., and LISITZIN, A. P. (1962).—Plant pigments in the suspended matter and bottom sediments of the Indian Ocean. Communication 2. Quantitative distribution and qualitative composition of the pigments in the suspended matter. *Oceanol. Res. (Results of the IGY, Section X)* **5**, 112–29.

MADGWICK, J. C. (1966).—Chromatographic determination of chlorophylls in algal cultures and phytoplankton. *Deep Sea Res.* **13**, 459–66.

MENZEL, D. W., and RYTHER, J. H. (1960).—The annual cycle of primary production in the Sargasso Sea off Bermuda. *Deep Sea Res.* **6**, 351–67.

RICHARDS, F. A. (with THOMPSON, T. G.) (1952).—The estimation and characterization of plankton populations by pigment analyses. II. A spectrophotometric method for the estimation of plankton pigments. *J. mar. Res.* **11**, 156–72.

ROCHFORD, D. J. (1962).—Hydrology of the Indian Ocean. II. The surface waters of the south-east Indian Ocean and Arafura Sea in the spring and summer. *Aust. J. mar. Freshwat. Res.* **13**, 226–51.

SAIJO, Y. (1963).—Technique of primary production measurement used on the Indian Ocean cruise of the *Umitaka Maru* December 1962–January 1963, and suggestions on their improvement on the next cruise. *Inf. Bull. Planktol. Japan* **10**, 17–22.

SAIJO, Y., and KAWASHIMA, T. (1964).—Primary production in the Antarctic Ocean. *J. oceanogr. Soc. Japan* **19**, 190–6.

SUSHCHENIA, L. M., and FINENKO, Z. Z. (1964).—On the study of plankton productivity of the tropical part of the Atlantic Ocean. *Oceanology* **4**, 866–72.

WYRTKI, K. (1962).—The upwelling in the region between Java and Australia during the south-east monsoon. *Aust. J. mar Freshwat. Res.* **13**, 217–25.

Reprinted from *Proc. Biol. Soc. Wash.*, vol. 79, 1966, p. 91-94

A NEW SPECIES OF *DENTIGRYPS* WILSON (COPEPODA, CALIGOIDA) FROM MADAGASCAR

By Roger Cressey
Smithsonian Institution, Washington, D.C.

A new species of *Dentigryps* parasitic on the body surface of the jack, *Caranx hippos* (Linn.) was collected by the author at Nosy Bé, Madagascar during the International Indian Ocean Expedition.

I would like to acknowledge the National Science Foundation-U.S. Program in Biology for supporting the field portion of this work.

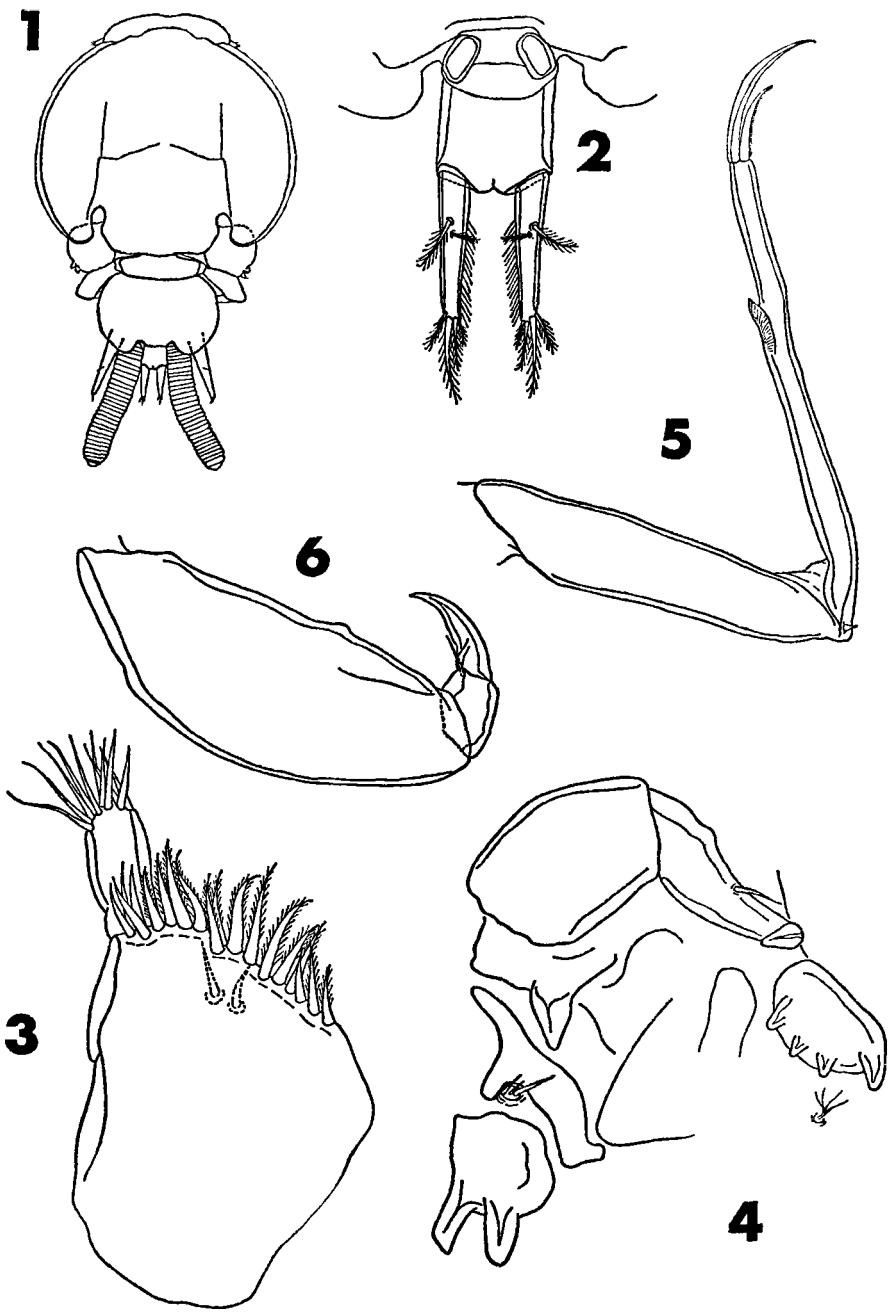
Dentigryps longicauda, new species

Specimens studied: 6 females collected from the body surface of a single specimen of *Caranx hippos* caught off Nosy Bé, Madagascar (Pointe Lokobe), 8 March 1964. Holotype ♀ (USNM 113048) and 4 paratype ♀♀ (USNM 113049) in alcohol deposited in the United States National Museum. One specimen dissected for study and retained in author's personal collection.

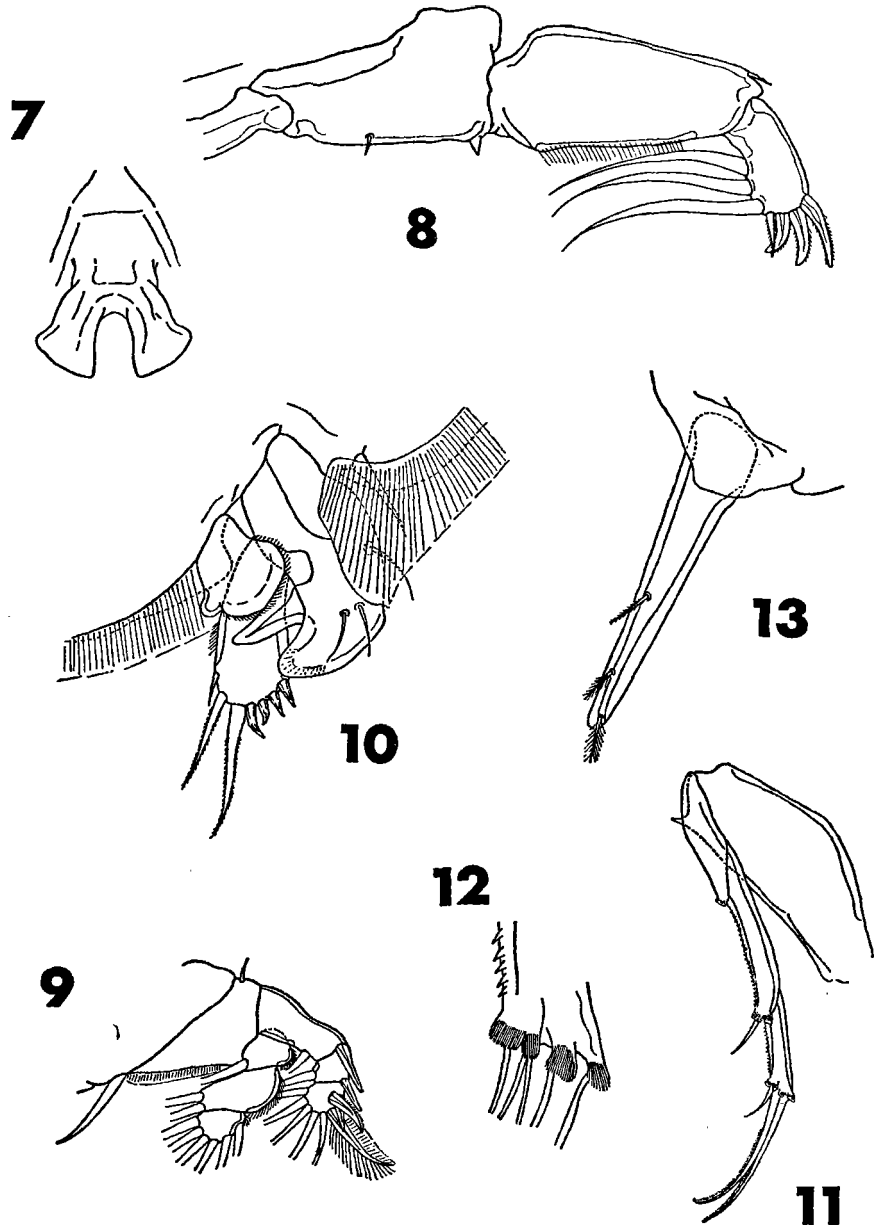
Etymology: *longicauda*—alluding to the length of the caudal rami.

Female holotype: Body form as in Fig. 1. Total length 5.6 mm (not including setae on caudal rami). Greatest width (measured at widest part of cephalon) 3.5 mm. Edge of cephalon with membrane as in Fig. 1. Cephalon nearly round. Thoracic segment 4 free. Genital segment wider than long (1.7 × 1.2 mm), greatest width in anterior third. Posterior corners broadly rounded and projecting. Area for spermatophore attachment near junction of genital segment and abdomen (see Fig. 2). Abdomen 1-segmented, slightly longer than wide (420 μ × 360 μ). Caudal rami (see Fig. 2) about 4 times as long as wide (456 μ long). Each ramus with 4 terminal plumose setae, 2 plumose ventral setae located near middle. Oral area of the typical caligid type.

First antenna (Fig. 3) 2-segmented. First segment bearing several plumose setae on distal border. Last segment with group of 11 naked setae at tip. Second antenna (Fig. 4) 3-segmented. Penultimate segment in form of sclerotized claw. Sclerotized cuticular process directed posteriorly near base of second antenna. Post-antennal process with prominent lateral process and 3 smaller sclerotized processes along



FIGS. 1–6. *Dentigryps longicauda* n. sp., female: 1, female, dorsal; 2, abdomen and caudal rami; 3, first antenna; 4, area of second antenna and first maxilla; 5, second maxilla; 6, maxilliped.



FIGS. 7–13. *Dentigryps longicauda* n. sp., female: 7, sternal furca; 8, leg 1; 9, leg 2; 10, leg 3; 11, leg 4; 12, distal end of last segment of leg 4; 13, leg 5.

posterior border (see Fig. 4). Mandible and mouth tube as in other species of genus. Mandible with 12 teeth at tip. First maxilla reduced to group of 3 setae anterior to postoral process (see Fig. 4). Postoral process with 2 broad sclerotized processes directed posteriorly as shown in

Fig. 4. Second maxilla (Fig. 5) 2-segmented, bearing 2 bladelike setae at tip. Longest seta with double base fusing to form single tip. Maxilliped (Fig. 6) 2-segmented, terminating in claw. Sternal furca (Fig. 7) spatulate.

Leg 1 (Fig. 8) biramose. Exopod 2-segmented, first segment with small spine on outer distal corner and inner margin with row of hairs. Terminal segment with 3 terminal spines, 1 terminal short seta, and 3 long plumose setae along inner margin. Endopod reduced to small process near base of exopod. Leg 2 (Fig. 9) biramose. Each ramus 3-segmented, armed as in figure. Leg 3 (Fig. 10) biramose. Exopod 2-segmented, first segment modified to form clawlike process bearing stout inwardly directed, spine. Last segment with 4 terminal spines and 3 terminal setae. Endopod 1-segmented, unarmed. Leg 4 (Fig. 11) uniramose. Exopod 3-segmented, each segment bearing distal spatulate processes (see Fig. 12). Last segment with 3 setae at tip, 2 longer setae fringed along outer border. Outer border of last 2 segments bearing row of spinules. Leg 5 (Fig. 13) 1.1 mm long (measured along outer border) consisting of a long, heavily sclerotized process bearing 3 short setae as shown in figure. Leg 6 absent.

Egg strings uniseriate and of usual caligoid type, about 2 mm long.

Male: Unknown.

Remarks: Lewis (1964) recognized four species in the genus *Dentigryps*. This new species differs from those four by the nature of the caudal rami, leg 3, and postantennal process. The diagnosis of the genus as given by Lewis states that the caudal rami are flattened, not filiform but his concept should be modified to include *D. longicauda*. The endopods of leg 3 in the four previously described species are 2-segmented and armed with a number of setae, whereas the endopod of leg 3 in *D. longicauda* is reduced to one unarmed segment.

Literature Cited

Lewis, A. 1964. The Caligid Copepod genus *Dentigryps* (Crustacea: Caligoida). Proc. U.S. Nat. Mus. 115(no. 3487): 347–380.

Reprinted from *Bull. mar. Sci.*, vol. 16, no. 2, 1966, p. 324-329

BARIAKA ALOPIAE N. GEN., N. SP. (COPEPODA: CALIGOIDA), A PARASITE ON THE GILLS OF A THRESHER SHARK

ROGER F. CRESSEY
Smithsonian Institution, Washington, D.C.

ABSTRACT

Bariaka alopiae, a new genus and species of caligid copepod is described from the gills of *Alopias superciliosus,* a thresher shark. This copepod has been placed in the family Eudactylinidae and it differs from all other members of the family in having 18 segments in the first antenna.

INTRODUCTION

During a 4-month period of participation in the International Indian Ocean Expedition, I collected many parasitic copepods from the fishes of the area. One of these, from the gills of the big-eye thresher shark, *Alopias superciliosus* (Lowe), represents a new genus of eudactylinids and is described below.

The field portion of this work was supported by the National Science Foundation-U. S. Program in Biology.

EUDACTYLINIDAE Yamaguti, 1963

Bariaka n. gen.

Diagnosis.—Female: body vermiform, considerably longer than wide, not flattened dorsoventrally. Cephalon only about one-sixth of total length Head fused with thoracic segment bearing first pair of thoracic legs. Abdomen of 4 segments. Caudal rami small. First antenna of 18 segments. Second antenna uncinate. Legs 1-4 biramose, all rami 3-segmented. Leg 5 present. Leg 6 reduced to knobs.

Male: body form as in the female. Abdomen 4-segmented. Caudal rami conspicuous. Appendages with same generic characters as female except leg 6 which is represented by 3 setae on the genital segment.

Etymology.—Bariaka, gender feminine, derived from the name of the research vessel AMBARIAKA of the Station d'Océanographie et des Peches, Nosy Bé, Madagascar.

Type species.—B. alopiae, n. sp.

Bariaka alopiae, n. sp.

Material Studied.—Thirteen specimens (11 ♀♀, 2 ♂♂) collected from the gills of *Alopias superciliosus* (Lowe) caught off Nosy Iranja, Madagascar,

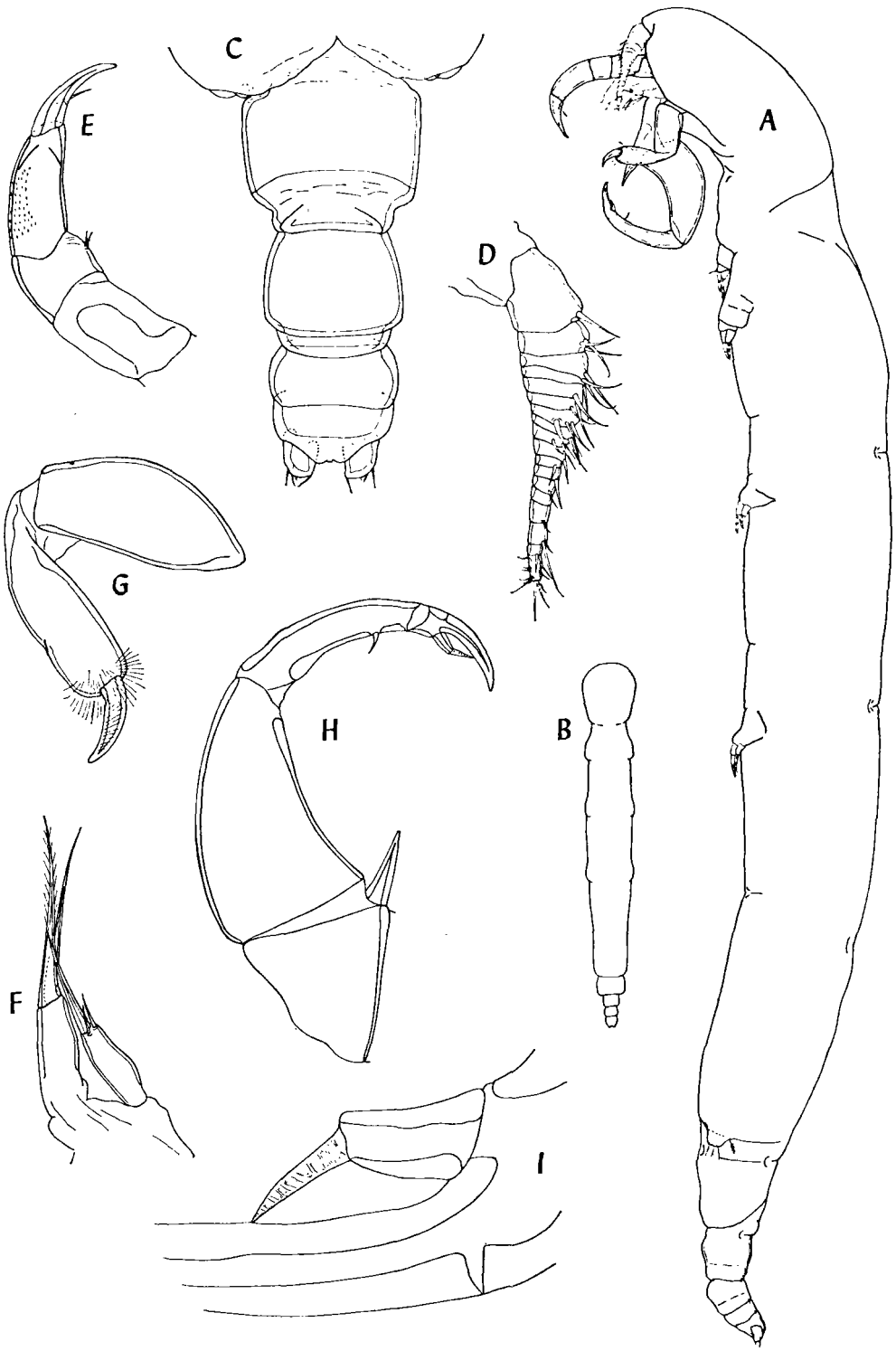


FIGURE 1. *Bariaka alopiae,* n. sp., female: a, lateral view; b, dorsal view; c, abdomen, ventral view; d, first antenna; e, second antenna; f, first maxilla; g, second maxilla; h, maxilliped; i, detail of spine on maxilliped.

UNESCO ARCHIVES

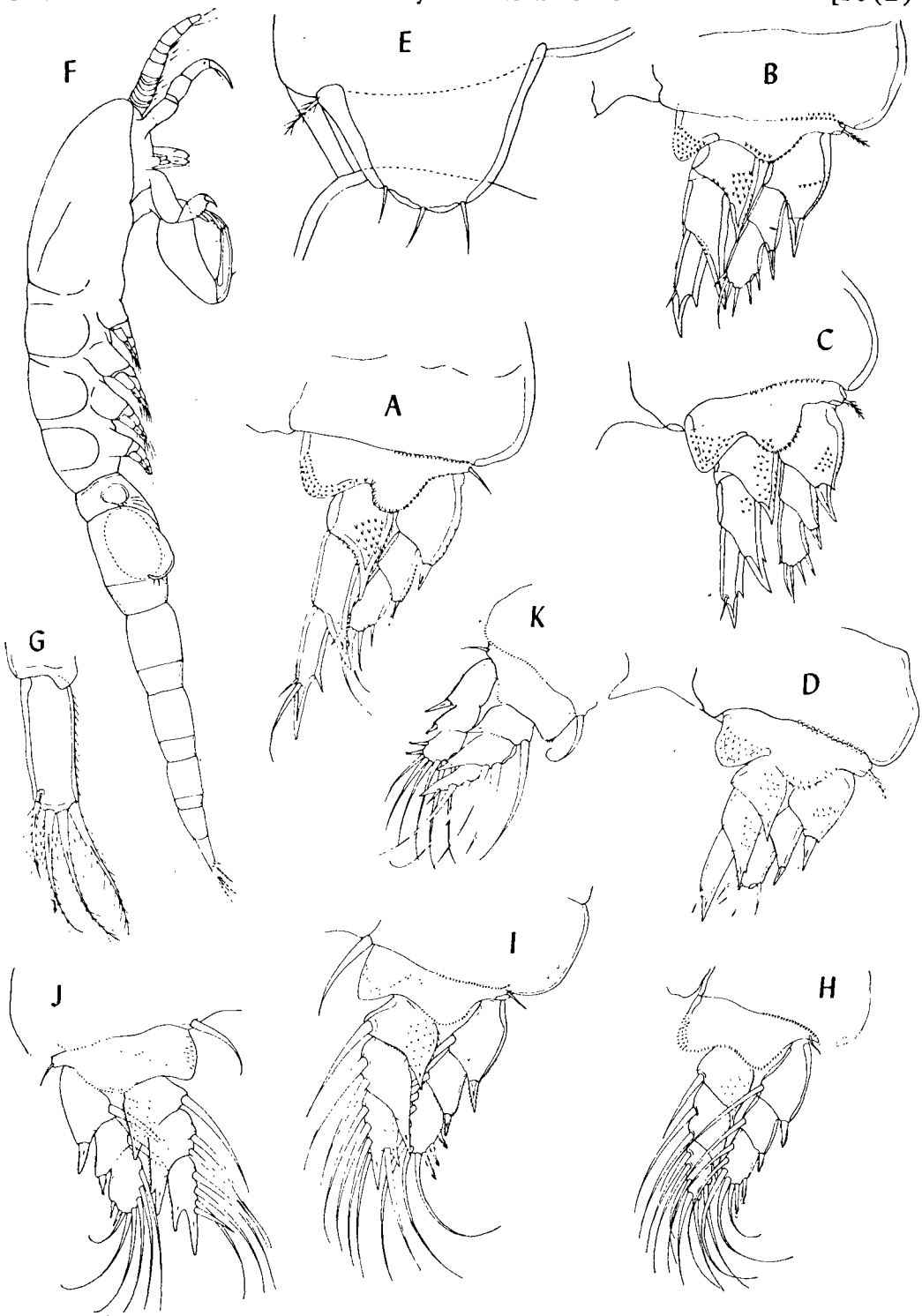


FIGURE 2. *Bariaka alopiae,* female: a, leg 1; b, leg 2; c, leg 3; d, leg 4; e, leg 5; male: f, lateral view; g, caudal ramus; h, leg 1; i, leg 2; j, leg 3; k, leg 4.

April 9, 1964. Two females from the gills of the same host collected by S. Kato, California Fish and Wildlife Service from the Pacific Ocean (0°38'N, 124°23'W).

Types.—The holotype female (USNM 113035), allotype male (USNM 113036), four paratype females (USNM 113037) deposited in the U. S. National Museum, and three paratype females deposited in the Muséum National d'Histoire Naturelle at Paris.

Description.—Female: body form as shown in Figure 1, a and b. Total length 9.4 mm; greatest width 1.0 mm. Cephalon about one-sixth total body length; widest anteriorly, tapering slightly to posterior border; posterior corners merging with thoracic segments and not projecting. No dorsal plates present. Genital segment fused with last thoracic segment and bilobed on its ventral posterior border. Abdomen (Fig. 1c) 4-segmented. Caudal rami small, attached along the lateral edges of the abdomen and bearing 4 short naked setae on the posterior borders. Oral area strongly modified for prehension. First antenna (Fig. 1d) of 18 segments each bearing naked setae as illustrated. Second antenna (Fig. 1e) 4-segmented; inner border of second segment with 2 setae; third segment with median patch of spinules; terminal segment modified as a claw, bearing seta near the middle of inner border. Mandible a styliform process lying within the mouth tube and of the usual caligoid type. First maxilla (Fig. 1f) biramose; exopod with 3 setae at tip, 1 prominent, other 2 small; endopod with 2 prominent setae at tip, shorter one armed with short hairs. Second maxilla (Fig. 1g) 3-segmented; penultimate segment with distal patch of hairs, terminal segment in the form of a stout claw. Maxilliped (Fig. 1h) 3-segmented; inner border of basal segment bearing spine-like process; terminal claw with 2 stout setae, distal seta as in Figure 1i.

Legs 1-4 biramose, with spine and setal formula as follows (Roman numerals refer to spines, Arabic numerals to setae):

	Leg 1		Leg 2		Leg 3		Leg 4	
	exo	end	exo	end	exo	end	exo	end
Seg. 1	I:0	0:0	I:0	0:0	I:0	0:0	I:0	0:0
Seg. 2	I:0	0:0	I:0	0:0	I:0	0:0	I:0	0:0
Seg. 3	6	2	6	1	5	1	4	1

Leg 1 (Fig. 2a) with both rami 3-segmented, armed with patches of spinules on basipod and first segment of endopod; outer distal corners of endopod segments produced to form prominent spiniform processes. Leg 2 (Fig. 2b) in general like leg 1 but with additional spinules on first exopod segment and second endopod segment; terminal endopod segment with tip produced to form prominent non-articulated spine. Leg 3 (Fig. 2c) similar to leg 2 but with 1 less seta on last exopod segment. Leg 4

(Fig. 2d) like leg 3 but with fewer setae. Leg 5 (Fig. 2e) attached somewhat laterally (see Fig. 1b), consisting of lobe bearing 3 naked setae with a plumose seta near base. Leg 6 reduced to a lobe or series of lobes at area of egg string attachment on posterior corners of genital segment. All setae on rami of legs 1-5 naked. Egg strings long, uniseriate, and of the usual caligoid type.

Male: body form as shown in Figure 2f. Total length (including caudal rami but not setae) 5.8 mm; greatest width 1.0 mm at cephalon. Cephalon about one-fourth body length; modified for prehension as in female. Thoracic segments incompletely articulated, with saddle-like sclerotizations on dorsal surface of segments 2, 3, and 4. Abdomen 4-segmented. Caudal rami (Fig. 2g) conspicuous and bearing 6 setae; the 4 terminal setae plumose, the 2 subterminal setae naked. Inner margins of rami plumose.

Oral area as in female.

Legs 1-4 biramose with spine and setal formula as follows:

	Leg 1		Leg 2		Leg 3		Leg 4	
	exo	end	exo	end	exo	end	exo	end
Seg. 1	I:1	0:1	I:1	0:1	I:1	0:1	I:0	0:1
Seg. 2	I:1	0:2	I:1	0:2	I:1	0:2	I:0	0:2
Seg. 3	II:5	6	III:6	5	II:6	4	II:6	3

Leg 1 (Fig. 2h) with patches of spinules on basipod and first endopod segment; exopod spines with lateral clear hyaline membranes; setae long and plumose. Leg 2 (Fig. 2i) with patches of fine spinules on basipod and first endopod segment; exopod spines fringed or with clear hyaline membranes; endopod segments with outer distal corners produced to form spine-like processes; setae long and plumose. Leg 3 (Fig. 2j) with patches of fine spinules on basipod and first 2 endopod segments. Outer distal corners of endopod produced as in leg 2. Leg 4 (Fig. 2k) with 2 rows of spinules as in the figure; exopod spines with hyaline membranes; endopod segments with outer distal corners produced as in preceding legs. Leg 5 as in female. Leg 6 a lobe bearing 3 setae and located on the distal corner of the genital segment.

Etymology.—The name *alopias* is derived from the generic name of the host.

Remarks.—This new genus differs from all other members of the family by the number of segments in the first antenna (18 in *Bariaka,* 13 or less in all others), and by the number of segments in the abdomen (4 in *Bariaka,* 3 or less in all others). It can be further separated from *Kroyeria, Kroyerina,* and *Lamproglena* by the nature of the second antenna; in *Bariaka* it is uncinate, in *Kroyeria* and *Kroyerina* it is chelate, and in *Lamproglena* the claw is lacking.

Collections of this copepod from *Alopias superciliosus* at two widely separated stations (Madagascar and eastern Pacific) suggests a possible affinity of the copepod for this host. It is interesting to note that another new genus was recently described (Cressey, 1964) from this same host. So far, both of these new genera are known only from this species of shark.

SUMARIO

Bariaka alopiae N. GEN., N. SP. (COPEPODA: CALIGOIDA), UN PARÁSITO DE LAS AGALLAS DE UN TIBURÓN ZORRA

Procedente de una especie de tiburón zorra *Alopias superciliosus,* se describe *Bariaka alopiae* n. gen., n. sp. Este nuevo género ha sido colocado en la familia Eudactylinidae Yamaguti, 1963 y difiere de todos los otros géneros de la familia por tener 18 segmentos en la primera antena. El parásito fué recolectado en Madagascar y el Océano Pacífico Oriental y se encuentra en las agallas del huésped.

REFERENCES

CRESSEY, R. F.
1964. A new genus of copepods (Caligoida, Pandaridae) from a thresher shark in Madagascar. Cahiers Orstom-Oceanographie n°6- 1963 (Serie Nosy Bé II): 385-397.

WILSON, C. B.
1922. North American parasitic copepods belonging to the family Dichelesthiidae. Proc. U. S. nat. Mus., *60* (2400): 1-100.

YAMAGUTI, S.
1963. Parasitic copepods and Branchiura of fishes. John Wiley and Sons, N. Y., 1-1104 pp.

Reprinted from *Science*, vol. 152, no. 3,730, 1966, p. 1753-1755

Lipids of the Living Coelacanth, Latimeria chalumnae

Abstract. *The muscle of* Latimeria chalumnae *contains 30 to 71 percent (dry weight) of lipid deposited extracellularly. Wax esters constituted 90 percent or more of the lipids from muscle and fat storage tissues. These esters, by gas-chromatographic analysis, consisted of C_{30} to C_{40} homologs with one or two double bonds.*

The living coelacanth fish, *Latimeria chalumnae*, has excited the interest of biologists concerned with vertebrate phylogeny ever since its discovery off eastern South Africa in 1938 (*1*). In the intervening years over 30 specimens have been captured, all but the first in the vicinity of the islands of Anjouan and Great Comoro in the Comoro Archipelago between Madagascar and Mozambique. Several preserved specimens have been carefully dissected, and aspects of their gross and microscopic anatomy and gross chemical composition have been described (*2*). The rarity of the species has combined with the difficulty of access of the Comoros to prevent all but the sketchiest studies of behavior and ecology (*3*). Nothing is known of the physiology and very little of the biochemistry (*4*) of this form.

We recently obtained a newly caught male coelacanth, perfectly preserved by formalin and deep-freezing (*5*). The freshness and excellent condition of this specimen have permitted us to make a detailed study of the pattern of lipid composition of the various tissues. This pattern, while exotic, resembles that found in several species of bathypelagic fishes. We have examined trunk muscle, liver, spleen, the fat-filled presumptive swim bladder, and fat storage tissues in several locations.

The techniques employed (*6*) were: (i) extraction of the lipid from the tissue with chloroform-methanol as solvent; (ii) separation of the various lipid classes by adsorption column chromatography on silicic acid, monitored by thin-layer chromatography (TLC); (iii) saponification of the chromatographically pure wax esters—the principal lipid type present in the muscle and adipose tissues—and separation of the constituent long-chain alcohols and fatty acids on florisil columns; and (iv) gas-liquid partition chromatography (GLC) of the intact wax esters and of the alcohol and acid moieties (as the trifluoroacetate and methyl ester derivatives, respectively) (Tables 1, 2, and 3).

The liver lipid fraction consisted of triglycerides, 78.4 percent; wax esters plus sterol esters, 8.2 percent; and polar lipids (including phospholipids), 9.1 percent. The composition of the triglyceride fatty acids is given in Table 3. The pattern of the spleen lipids was unusual: hydrocarbons, 3.6 percent; wax esters plus sterol esters, 14.7 percent; triglycerides, 6.2 percent; free fatty acids, 16.1 percent; cholesterol, 12.8 percent; and polar lipids, 46.7 percent. The hydrocarbons were identified by GLC as the C_{20} to C_{32} normal alkanes plus squalene (about one-third of the total). No unesterified long-chain alcohols were detected, and the only phospholipid in the polar lipids was lecithin (by TLC; *6*). Lecithin could not have been the principal constituent of this fraction, since 57.8

Table 1. *Composition of the lipids of Latimeria chalumnae* tissues.

Total lipid (%)			
Wet weight	Dry weight		Wax ester content
	This work	Millot (*8*)	
	Ventral muscle		
34.1	71.4		94.3
	Dorsal muscle		
7.7	29.7	23.9	92.7
	"Swim bladder"		
61.9	98.9	95	97.2
	Pericardial		
81.0	98.7		92.7
	Pericerebral		
76.2	95.5	92.3	92.9
	Postocular		
60.8	92.7		90.0
	Liver		
24.1	67.7	32.3	8.2*
	Spleen		
3.5	18.6		14.7*

* Includes sterol esters.

Table 2. Wax esters of *Latimeria chalumnae*. The composition was determined by gas-liquid chromatography on a glass column (1.8 m by 4 mm inside diameter) packed with stabilized diethylene glycol succinate polyester, originally 12 percent by weight, on Anakrom ABS (70 to 80 mesh) (*11*). The column was operated at 240°C and an inlet gas pressure of 0.84 kg/cm².

Component*	Muscle tissues		Adipose tissues			
	Ventral	Dorsal	"Swim bladder"	Pericardial	Pericerebral	Postocular
30:0	1.7	1.6	2.7	1.5	2.2	1.9
30:1	0.5	0.4	0.6	0.5	0.6	0.6
32:0	1.8	2.0	2.9	2.4	2.9	2.6
32:1†	9.4	8.7	12.8	9.9	10.8	11.3
32:2	1.9	1.6	2.2	1.9	2.0	2.1
34:0	1.0	trace		trace	0.8	trace
34:1	28.1	27.6	20.6	28.7	26.8	29.6
34:2	11.5	11.5	12.5	12.5	12.0	12.2
36:1	9.9	8.8	11.0	9.7	9.3	9.0
36:2	26.6	30.4	28.8	26.7	25.5	24.8
38:1	1.9	1.2	0.8	1.9	2.0	1.7
38:2	5.3	4.9	4.0	4.0	4.5	3.6
40:2	0.3	1.2	0.9	0.3	0.4	0.5

* *The component is designated by the number of carbon atoms in the total compound and the total number of double bonds: hence, 30 : 0 indicates 30 carbon atoms in the ester, and no double bonds.* † The retention time for 32 : 1 was 12.8 to 13.9 minutes.

Table 3. Component fatty acids and alcohols of *Latimeria chalumnae* lipids (results are percentages by weight).

Component*	Fatty acids				Alcohols from wax esters	
	Spleen free fatty acids	Liver triglycerides	Wax esters		Dorsal muscle	"Swim bladder"
			Dorsal muscle	"Swim bladder"		
14:0	1.5	2.4	3.2	3.8	0.05	0.09
15:0	0.45	0.23	0.25	0.24	0.25	0.27
16:0	31.6	20.9	3.1	2.6	45.0	40.1
16:1	6.0	7.3	13.9	18.8	0.04	trace
17:1	0.75	0.74	1.2	1.7	.08	0.50
17:1†	1.1	0.56	1.1	1.5		
18:0	12.8	1.4	0.68	0.35	11.2	8.8
18:1	31.9	60.2	70.6	64.2	40.4	46.7
18:2	0.64	0.10	0.54	0.92		
19:1	0.42	.25	0.27	0.25	0.1	0.39
20:1	2.9	3.5	4.1	3.5	2.7	2.9
20:4	4.6	0.22				
22:1		.59	0.64	0.68		
22:3	3.0	.10				

* The notation 14:0, for example, indicates an acid or alcohol with a total of 14 carbon atoms and no double bond. † Branched chain.

mg of material on methanolysis gave only 6.0 mg of chromatographically pure methyl esters. In Table 3, therefore, the analysis of the largest homogeneous fraction of spleen lipids is given, namely the free fatty acids. The total fatty acids of the polar lipid fraction were similar, but had lower values for palmitic and palmitoleic acids and correspondingly higher values for stearic acid.

We have not yet compared the fatty acid patterns of wax esters, cholesteryl esters, and triglycerides from a single tissue of the coelacanth since the wax esters so predominate in the lipid from muscle and adipose tissues that isolation of either cholesteryl esters or triglycerides is difficult; indeed, the presence of glycerides in these tissues has not been established. With the organ lipids the problem is the separation of the cholesteryl esters from the wax esters quantitatively.

The low percentages of C_{20} and C_{22} polyunsaturated acids in the organ lipids were unexpected. There was no evidence that hydrolysis or autoxidation occurred during the shipping, storage, and extraction of the tissues. The formalin probably would have destroyed any phosphatidyl ethanolamine present (*7*), but it would not be expected to react with the polyunsaturated fatty acids. However, in view of the year which intervened between capture of the fish and completion of the GLC analyses of the methyl esters in the organs, the values in Table 3 for the polyunsaturated acids of the liver triglycerides, in particular, are best considered minimum figures. Additional work with fresh tissue and other lipid fractions will be required to establish whether or not the coelacanth is an exception to the generalization that the lipids of marine fishes contain large amounts of polyunsaturated C_{20} and C_{22} acids. This uncertainty does not apply to our data on wax esters, since all the naturally occurring examples contain only traces of polyunsaturated acids. The methyl esters from the saponified wax esters of four tissues of the coelacanth were analyzed (the earliest analysis being within 90 days of its capture), and none contained more than 0.3 percent of any individual (0.7 percent total) polyunsaturated C_{20} or C_{22} fatty acid.

Three features are seen in the data: the high content of total lipid in the muscle, the large percentage of wax esters in the lipids of the muscle and adipose tissues, and the great uniformity in the composition of the wax esters from the six tissues examined.

Our data for the lipid content confirms those of Millot (*8*), which are listed in Table 1 for comparison. Observations with the light and electron microscopes indicate that the lipid in the muscle is extracellular, whereas that in liver is enclosed in large intracellular vacuoles. The structures observed for adipose tissues are similar to those in corresponding tissues of other vertebrates (*9*). The high percentage of lipid in the muscle is not exceptional for fishes, but the content of wax esters is slightly higher than that reported in the muscle of the oil fish (*Ruvettus pretiosus*) (*6*) and considerably more than that in the muscle lipid of several lantern fishes (family *Myctophidae*) (unpublished work).

The lipid of the fat storage tissues (postocular, pericranial, pericardial, and the "swim bladder") consists almost entirely of wax esters. This fact is support for the idea that *Latimeria* deposits pure wax esters as reserve lipid.

The precision of the GLC analyses of the wax esters is estimated to be better than 9 percent of the observed values for major constitutents (>12 percent of total mixture) and better than 20 percent for minor constituents. Therefore the differences in the compositions given in Table 2 for the wax esters from six different tissues are negligible, with the possible exception of the values for monoenoic C_{34} compound in the "swim bladder." This suggests a common site for the synthesis of wax esters in *Latimeria*, but there is no evidence of where this site might be.

Our study of *Latimeria* lipids, together with the data on *Ruvettus pretiosus* (*6*), unpublished work with other gempylid and with myctophid species, and data reported by others, is consistent with the hypothesis that many fishes deposit massive amounts of wax esters in order to approach neutral buoyancy. The other species are all bathypelagic; *Latimeria* may also have this characteristic.

It is not known why wax esters are deposited rather than the more usual triglycerides. Nor is it obvious which chemical or physical properties of the two lipid types may be relevant to the problem. If bouyancy is the objective, then the densities would be important; the meager data available indicate that the wax esters have slightly lower densities (perhaps by 5 percent) than do the triglycerides of a comparable degree of unsaturation (*10*). Study of the site and pathway of biosynthesis of the wax esters, and the rate of turnover of this lipid type in vivo may provide an answer.

JUDD C. NEVENZEL
WALDTRAUT RODEGKER
JAMES F. MEAD
Department of Biophysics and Nuclear Medicine, University of California, Los Angeles
MALCOLM S. GORDON
Department of Zoology, University of California, Los Angeles

References and Notes

1. J. L. B. Smith, *Nature* **143**, 455, 748 (1939).
2. J. Millot and J. Anthony, *Proc. Intern. Congr. Zool. 15th* (1959), p. 36.
3. J. Millot, *Nature* **175**, 362 (1955); M. Menache, *Mem. Inst. Sci. Madagascar* **9A**, 151 (1954).
4. D. L. Fox and G. F. Crozier, *Science* **150**, 771 (1965); S. de Prailaune, *Compt. Rend. Soc. Biol.* **149**, 655 (1955); M. Vialli, *Rend. Ist. Lombardo Sci. Pt. I* **91**, 680 (1957).
5. Captured on hook and line on octopus bait by local fisherman Ahmed Hussein from about 150 m depth at midnight, 11 Dec. 1964, about 1 km offshore from Mutsamudu, Island of Anjouan, Comores. Fish 1.37 m long, 35.5 kg fresh weight. Successfully preserved and shipped to Los Angeles through the efforts of Dr. P. Liaume, Mutsamudu. Administrative arrangements made with the assistance of President Said M. Cheikh, Governing Council, Territory of the Comores; Ambassador C. Vaughan Ferguson, Jr., American Embassy, Tananarive, Madagascar; and Dr. John H. Ryther, Woods Hole Oceanographic Institution, Woods Hole, Mass. Support for the operation from NSF via U.S. Program in Biology, International Indian Ocean Expedition.
6. J. C. Nevenzel, W. Rodegker, J. F. Mead, *Biochemistry* **4**, 1589 (1965).
7. G. Rouser, C. Galli, G. Kritchevsky, *J. Am. Oil Chem. Soc.* **42**, 408 (1965).
8. J. Millot, "Le troisième coelacanthe," *Naturaliste Malgache*, Suppl. 1 (Inst. de Recherches Scientifique, République Malgache, 1954).
9. Histological studies of tissue lipid localization done by sectioning formalin-fixed material at 15 μ on freezing microtome and staining with oil red O and hematoxylin [G. L. Humaston, *Animal Tissue Techniques* (Freeman, San Francisco, 1962), p. 254]. Histology of all tissues for light microscopy was performed by L. Meiers, of muscle for the electron microscope, by J. Adomian.
10. The density of oleyl oleate is 0.8600 at 30°C; that of triolein is 0.8988 at 40°C [F. Richter, Ed., *Beilsteins Handbuch der Organischen Chemie*, 3rd suppl. (Springer Verlag, Berlin, ed. 4, 1961), vol. II-2, pp. 1415, 1423].
11. Both from Analytical Engineering Labs, Hamden, Connecticut.
12. Supported by contract AT(04-1GEN-12 between the U.S. Atomic Energy Commission and the University of California; in part by PHS research career award GM-K6-19, 177 to J.F.M. and by NSF grant GB 3584 to M.S.G.

18 April 1966

Reprinted from *Limnol. and Oceanogr.*, vol. II, no. 3, 1966, p. 371-380

PRIMARY ORGANIC PRODUCTION IN RELATION TO THE CHEMISTRY AND HYDROGRAPHY OF THE WESTERN INDIAN OCEAN[1]

John H. Ryther, John R. Hall, Allan K. Pease, Andrew Bakun, and Mark M. Jones[2]
Woods Hole Oceanographic Institution, Woods Hole, Massachusetts 02543

ABSTRACT

Primary organic production was measured at 231 stations in the western Indian Ocean. Low levels were measured in the eastern part of the region, both north and south of the Equator. Intermediate levels were encountered in the equatorial area, in the Mozambique Channel, and in the southern part of the region. High productivity was observed in the northern and western portions, particularly in the western Arabian Sea.

The high productivity of the Arabian Sea is attributed to the presence of unusually high concentrations of plant nutrients that extend nearly to the sea surface, from which there is ready transport into the euphotic zone by local advective processes. The distributional pattern of the nutrients, in turn, is believed to result from a major system of upwelling, whereby water from intermediate depths is transported north across the Equator and towards the surface, compensating for the southerly flow of surface water and its loss from the Arabian Sea. The fertility of the region is further enhanced by the mechanism of a nutrient trap which is inherent in all countercurrent upwelling systems.

Annual organic production for the 23×10^6 km^2 area studied was 3×10^{12} kg, averaging about twice that of the oceans as a whole.

INTRODUCTION

As a part of the U.S. Program in Biology of the International Indian Ocean Expedition, primary organic production was measured at 231 stations in the western Indian Ocean on seven oceanographic cruises (*see* Fig. 1) of *RV Anton Bruun* during 1963 and 1964. This report summarizes the productivity data and attempts to relate them to certain chemical and hydrographic features of the region studied.

METHODS

Primary production was measured using the ^{14}C technique as described by Steemann Nielsen (1952) but with the minor modifications described below. Water samples were collected in an all-plastic sampler from the depths to which 100, 50, 25, 10, and 1% of incident light penetrated, as measured with a submarine photometer. Samples were dispensed into paired 125-ml Pyrex bottles to which 10 microcuries of $^{14}CO_3^{2-}$ were added. One bottle from each depth was placed in a darkened container. The other was placed in a clear plastic cylinder covered with perforated metal screening which reduced sunlight reaching the bottle to the same intensity as that to which the water was originally exposed. The screened cylinders were then placed in full sunlight in an unobstructed position on the ship. For cooling purposes, surface seawater was run continuously around all of the bottles.

The samples were incubated for 24 hr beginning at whatever time of day or night the station was occupied and the samples obtained. As each cylinder could hold four bottles, samples from four complete stations could be incubated at any one time.

Following incubation, the samples were filtered through HA Millipore® filters (0.45-μ pore size), rinsed with 10 ml of 0.01 N HCl in 3% NaCl solution, desiccated, and counted with a thin (μmil)-window Geiger counter. Carbon assimilation, or primary

[1] Contribution No. 1709 of the Woods Hole Oceanographic Institution. This study was a part of the U.S. Program in Biology, International Indian Ocean Expedition, and was supported by the National Science Foundation.

[2] Present addresses: AKP, Institute of Oceanography, Univ. Br. Columbia, Vancouver; AB, Dept. of Oceanography, Univ. Wash., Seattle; and MMJ, Dept. of Oceanography, Oregon State Univ., Corvallis.

TABLE 1. *Station positions, dates, and values for daily primary organic production expressed as grams of carbon fixed beneath a square meter of sea surface*

Station	Latitude	Longitude	Date	gC m^{-2} day^{-1}
		Anton Bruun *Cruise 2, 1963*		
106	17°37′ N	70°27′ E	23 May	0.09
107*	15°40′ N	70°07′ E	24 May	0.09
108	13°50′ N	70°07′ E	25 May	0.03
109	11°59′ N	69°55′ E	26 May	0.06
110	09°46′ N	70°06′ E	27 May	0.07
111*	08°09′ N	70°02′ E	28 May	0.12
112	05°48′ N	70°03′ E	29 May	0.04
113	03°33′ N	69°54′ E	30 May	0.09
114	01°30′ N	70°01′ E	31 May	0.04
115	01°07′ S	71°00′ E	1 June	0.06
116*	02°23′ S	70°24′ E	2 June	0.10
117	04°22′ S	69°24′ E	3 June	0.02
118	06°48′ S	70°07′ E	4 June	0.08
119	08°35′ S	69°55′ E	6 June	0.09
120	11°10′ S	70°02′ E	7 June	0.28
121	13°15′ S	69°51′ E	8 June	0.10
122	15°25′ S	69°58′ E	9 June	0.27
123	17°18′ S	70°05′ E	10 June	0.06
124	19°30′ S	69°51′ E	11 June	0.04
125	21°40′ S	67°06′ E	25 June	0.04
126	23°47′ S	69°05′ E	26 June	0.04
127	26°34′ S	70°12′ E	27 June	0.02
129	30°34′ S	69°55′ E	29 June	0.06
130	32°52′ S	69°52′ E	30 June	0.06
131	35°09′ S	69°59′ E	1 July	0.14
132†	37°12′ S	70°10′ E	2 July	0.09
133*	30°11′ S	79°42′ E	5 July	0.31
134	27°31′ S	80°08′ E	6 July	0.03
135	20°02′ S	79°50′ E	8 July	0.06
136*†	14°15′ S	79°52′ E	9 July	0.29
137	14°44′ S	79°44′ E	10 July	0.15
138	11°28′ S	80°00′ E	11 July	0.28
139†	08°37′ S	79°34′ E	12 July	0.12
140	05°53′ S	79°57′ E	13 July	0.10
141	03°13′ S	80°02′ E	14 July	0.11
142*	00°33′ S	80°08′ E	15 July	0.12
143	01°54′ N	79°52′ E	16 July	0.09
144*	04°18′ N	80°08′ E	17 July	0.27
		Cruise 3, 1963		
145†	11°56′ N	60°53′ E	13 Aug	0.52
146	10°12′ N	60°04′ E	14 Aug	0.49
147	07°13′ N	59°57′ E	16 Aug	0.52
148	04°05′ N	59°58′ E	17 Aug	0.88
149*	01°16′ N	60°08′ E	19 Aug	0.16
150†	02°00′ S	59°59′ E	20 Aug	0.31
151*	05°04′ S	60°03′ E	22 Aug	0.28
152*	07°21′ S	59°44′ E	24 Aug	0.15
153†	11°39′ S	58°02′ E	26 Aug	0.46
154	22°58′ S	59°45′ E	4 Sept	0.05
155	25°55′ S	60°01′ E	5 Sept	0.09
156*	29°24′ S	60°05′ E	7 Sept	0.27
157	31°58′ S	59°51′ E	8 Sept	0.41
158	34°57′ S	60°05′ E	9 Sept	0.43
159	38°22′ S	59°51′ E	11 Sept	0.25
160	40°54′ S	60°01′ E	12 Sept	0.09
		Cruise 4 A, 1963		
161	19°14′ S	56°33′ E	25 Sept	0.04
162	17°38′ S	54°58′ E	26 Sept	0.13
163	14°53′ S	55°02′ E	27 Sept	0.85
164†	11°34′ S	54°56′ E	29 Sept	0.49
165†	08°14′ S	55°00′ E	30 Sept	0.69
166	00°24′ S	54°33′ E	5 Oct	1.17
167	02°45′ N	53°51′ E	6 Oct	0.69
168	05°52′ N	52°56′ E	7 Oct	0.55
169†	08°57′ N	52°17′ E	8 Oct	0.28
170	12°04′ N	51°31′ E	9 Oct	1.98
171	13°11′ N	51°28′ E	15 Oct	0.81
172†	14°44′ N	51°02′ E	15 Oct	0.77
173	15°27′ N	52°50′ E	16 Oct	1.64
174†	16°27′ N	54°39′ E	17 Oct	1.03
175	17°26′ N	56°29′ E	17 Oct	2.38
176	16°29′ N	57°09′ E	18 Oct	1.23
177†	15°18′ N	57°43′ E	18 Oct	2.14
178	14°21′ N	58°18′ E	19 Oct	0.95
179†	13°12′ N	58°58′ E	19 Oct	1.40
180	12°15′ N	59°42′ E	20 Oct	0.45
181†	14°09′ N	61°07′ E	21 Oct	0.68
182	15°58′ N	62°33′ E	22 Oct	0.59
183†	23°43′ N	66°21′ E	28 Oct	2.20
184	22°33′ N	65°56′ E	29 Oct	0.84
185†	20°39′ N	64°41′ E	30 Oct	1.00
186	21°31′ N	64°06′ E	30 Oct	2.01
187†	22°23′ N	63°32′ E	31 Oct	1.37
188	23°19′ N	62°50′ E	31 Oct	3.30
189†	24°00′ N	62°04′ E	1 Nov	1.99
190	24°48′ N	61°37′ E	1 Nov	1.61
191†	23°57′ N	60°58′ E	1 Nov	2.17
192	23°08′ N	60°32′ E	2 Nov	1.62
193†	22°48′ N	59°34′ E	2 Nov	1.76
194†	22°22′ N	60°05′ E	3 Nov	6.58
195	21°31′ N	60°41′ E	3 Nov	5.79
196†	20°44′ N	61°15′ E	4 Nov	2.09
197	20°02′ N	62°00′ E	4 Nov	1.80
198†	19°17′ N	62°29′ E	4 Nov	1.74
199	18°31′ N	63°08′ E	5 Nov	1.10
200†	18°32′ N	64°39′ E	6 Nov	1.21
		Cruise 5, 1964		
282	16°13′ N	63°29′ E	29 Jan	0.54
283	15°42′ N	60°52′ E	30 Jan	0.75
284	15°22′ N	58°12′ E	31 Jan	1.09
285	14°22′ N	54°18′ E	1 Feb	0.72
286	13°50′ N	52°59′ E	2 Feb	0.72
287	13°11′ N	50°22′ E	3 Feb	0.84
288	09°28′ N	54°52′ E	5 Feb	0.31
289	07°10′ N	55°05′ E	6 Feb	0.30
290	05°02′ N	55°01′ E	7 Feb	0.33

* Stations not included in the contours shown in Fig. 1.
† Stations at which light extinction coefficient was estimated.

TABLE 1. (*Continued*)

Station	Latitude	Longitude	Date	gC m^{-2} day^{-1}
291	02°31′ N	55°04′ E	8 Feb	0.44
293	00°31′ S	54°56′ E	10 Feb	0.14
294	02°51′ S	54°58′ E	11 Feb	0.47
295*	06°28′ S	55°12′ E	16 Feb	0.13
296*†	08°42′ S	55°07′ E	17 Feb	0.15
297*	10°47′ S	55°15′ E	18 Feb	0.21
298	12°33′ S	54°33′ E	19 Feb	0.10
299†	14°57′ S	54°43′ E	20 Feb	0.07
300	17°14′ S	54°38′ E	21 Feb	0.09
301	19°57′ S	54°58′ E	3 Mar	0.06
302	23°07′ S	54°50′ E	4 Mar	0.11
303	26°00′ S	54°52′ E	5 Mar	0.11
304	28°22′ S	55°02′ E	6 Mar	0.07
305	30°50′ S	55°02′ E	7 Mar	0.11
306	33°13′ S	55°10′ E	8 Mar	0.19
307	35°42′ S	55°15′ E	9 Mar	0.28
308	40°04′ S	75°00′ E	4 Apr	0.11
309	42°23′ S	74°54′ E	5 Apr	0.24
310	37°01′ S	75°19′ E	9 Apr	0.20
311	34°31′ S	74°47′ E	10 Apr	0.09
312	31°26′ S	74°57′ E	11 Apr	0.04
313	29°00′ S	74°51′ E	12 Apr	0.02
314	26°27′ S	75°02′ E	13 Apr	0.04
315*†	24°20′ S	74°52′ E	14 Apr	0.17
316	21°58′ S	74°55′ E	15 Apr	0.05
317	19°44′ S	75°20′ E	16 Apr	0.03
318*	16°43′ S	74°53′ E	17 Apr	0.15
319	14°10′ S	74°55′ E	18 Apr	0.06
320	11°47′ S	74°42′ E	19 Apr	0.09
321	09°21′ S	75°08′ E	20 Apr	0.08
322†	06°50′ S	75°02′ E	21 Apr	0.18
323	04°11′ S	75°00′ E	22 Apr	0.14
324	02°14′ S	75°14′ E	23 Apr	0.06
325	01°04′ N	75°07′ E	28 Apr	0.08
326	03°52′ N	74°57′ E	29 Apr	0.14
327	06°51′ N	72°02′ E	30 Apr	0.14
		Cruise 6, 1964		
328	18°02′ N	65°08′ E	17 May	0.17
329	15°36′ N	64°59′ E	19 May	0.17
330	13°36′ N	65°03′ E	20 May	0.08
331†	11°28′ N	65°04′ E	21 May	0.09
332	10°04′ N	64°59′ E	22 May	0.14
333	07°55′ N	64°56′ E	23 May	0.09
334	06°01′ N	64°59′ E	24 May	0.15
335†	03°59′ N	65°02′ E	25 May	0.22
336†	02°01′ N	65°03′ E	26 May	0.10
337	00°30′ S	65°07′ E	28 May	0.30
338	02°38′ S	65°01′ E	29 May	0.27
339	04°40′ S	65°02′ E	30 May	0.24
340	06°00′ S	65°10′ E	31 May	0.36
341	08°00′ S	64°59′ E	1 June	0.41
342†	09°58′ S	64°55′ E	2 June	0.28
343	12°12′ S	65°29′ E	4 June	0.14
344	14°11′ S	65°17′ E	5 June	0.18
345	16°10′ S	64°50′ E	6 June	0.05
346*†	19°23′ S	65°30′ E	8 June	0.12
347	22°06′ S	64°55′ E	23 June	0.07
348	24°01′ S	65°00′ E	24 June	0.07
349†	26°06′ S	64°58′ E	25 June	0.05
350	28°28′ S	65°03′ E	27 June	0.08
351†	30°06′ S	64°58′ E	28 June	0.03
352*†	34°34′ S	64°55′ E	30 June	0
353†	37°58′ S	64°59′ E	2 July	0.14
354†	40°57′ S	64°27′ E	4 July	0.09
355	29°38′ S	49°23′ E	11 July	0.14
		Cruise 7, 1964		
356†	29°11′ S	31°37′ E	29 July	0.40
358	29°12′ S	32°06′ E	30 July	0.38
359†	28°35′ S	32°40′ E	31 July	0.37
360†	27°38′ S	33°24′ E	31 July	0.41
361†	26°35′ S	35°57′ E	1 Aug	0.11
362	24°53′ S	39°18′ E	3 Aug	0.21
363†	23°46′ S	43°07′ E	4 Aug	0.47
364	23°20′ S	43°36′ E	12 Aug	1.44
365	23°19.6′ S	43°33.3′ E	12 Aug	0.37
366†	23°13′ S	43°13′ E	12 Aug	0.73
367†	22°34′ S	41°16′ E	13 Aug	0.20
368†	23°04′ S	38°35′ E	16 Aug	0.43
369	23°48′ S	36°48′ E	17 Aug	1.00
370	24°19′ S	35°46′ E	17 Aug	1.21
371	24°42′ S	35°23′ E	18 Aug	0.69
372†	24°48′ S	34°59′ E	19 Aug	1.44
373	26°01′ S	33°04′ E	22 Aug	3.05
374	26°57′ S	33°53′ E	23 Aug	0.39
375*	27°58′ S	35°16′ E	24 Aug	0
376†	29°22′ S	37°31′ E	26 Aug	0.24
377	30°09′ S	38°39′ E	27 Aug	0.22
378†	30°51′ S	40°11′ E	28 Aug	0.36
379†	32°22′ S	42°55′ E	29 Aug	0.43
380†	32:58′ S	43°37′ E	30 Aug	0.45
381*	33°13′ S	42°53′ E	30 Aug	0.22
382	34°08′ S	41°15′ E	31 Aug	0.51
383†	34°57′ S	38°49′ E	1 Sept	0.40
384†	35°44′ S	36°47′ E	2 Sept	0.87
385†	34°15′ S	36°04′ E	3 Sept	0.31
386†	32°55′ S	35°21′ E	4 Sept	0.71
387†	31°57′ S	34°18′ E	5 Sept	0.35
388†	30°45′ S	32°58′ E	6 Sept	0.99
389	30°10′ S	32°09′ E	6 Sept	0.57
390†	29°45′ S	31°42′ E	8 Sept	1.64
391	29°29′ S	31°44′ E	9 Sept	1.37
392†	29°18′ S	31°33′ E	9 Sept	3.14
		Cruise 8, 1964		
393	29°32′ S	31°18′ E	25 Sept	1.85
394†	29°26′ S	31°33′ E	25 Sept	0.01
395	29°29′ S	32°04′ E	26 Sept	0.27
396	25°34′ S	33°19′ E	28 Sept	0.66
397†	25°10′ S	33°15′ E	28 Sept	2.17
398†	25°17′ S	34°04′ E	29 Sept	1.57
399	22°30′ S	36°07′ E	1 Oct	0.28
400*†	21°11′ S	36°23′ E	2 Oct	0.42
401†	20°42′ S	35°50′ E	3 Oct	3.18
402†	20°14′ S	35°16′ E	4 Oct	0.89
403†	19°10′ S	36°19′ E	9 Oct	0.50

TABLE 1. (*Continued*)

Station	Latitude	Longitude	Date	gC m^{-2} day^{-1}	Station	Latitude	Longitude	Date	gC m^{-2} day^{-1}
404	18°52′ S	37°41′ E	9 Oct	0.43	413	12°56′ S	46°43′ E	29 Oct	1.25
405*†	18°33′ S	39°48′ E	10 Oct	0.23	414†	12°36′ S	45°55′ E	29 Oct	0.77
406	18°04′ S	41°52′ E	12 Oct	0.62	415	10°34′ S	44°23′ E	31 Oct	0.65
407†	17°41′ S	42°31′ E	13 Oct	0.43	416	08°45′ S	43°39′ E	1 Nov	0.67
408	16°46′ S	43°45′ E	15 Oct	0.89	417	07°03′ S	42°34′ E	2 Nov	0.79
409	16°13′ S	43°41′ E	17 Oct	1.38	418	05°10′ S	41°40′ E	3 Nov	0.40
410	15°25′ S	44°22′ E	20 Oct	0.34	419	04°17′ S	41°10′ E	5 Nov	0.55
411	14°24′ S	46°08′ E	21 Oct	0.27	420†	03°07′ S	40°39′ E	5 Nov	2.38
412†	13°22′ S	47°54′ E	22 Oct	0.32	421*†	02°56′ S	40°23′ E	6 Nov	0.95

production, was calculated from the difference between counts of the paired light and dark bottles in the usual way (Steemann Nielsen 1952). Data have not been corrected for isotopic discrimination. Values obtained at the five individual depths were then integrated by computer over the entire euphotic zone to give a single value for daily primary production beneath a square meter of sea surface.

The temperature, salinity, density, phosphate, and dissolved oxygen data included in this report were obtained from standard oceanographic stations occupied in conjunction with the productivity stations. Temperature and depth determinations were made by means of paired protected and unprotected deep-sea reversing thermometers. Salinity was measured with an inductance-type salinometer. Dissolved oxygen was determined by the Winkler method using biniodate standard, and phosphate was determined by the method of Murphy and Riley (1962). The water samples for chemical analyses were collected in Teflon-coated Nansen bottles.

A flat-plate (cosine collector) submarine photometer was used for measuring light extinction (thereby selecting the sampling depths). The photocell was covered by opal diffusing glass, but no colored filters were used. The submarine light cell was balanced against a deck cell to directly give the percentage of incident radiation at each depth. When this unit was non-operational, as was frequently the case, a more simple photometer of the same general design, but without a deck reference cell, was used.

One of the most serious limitations to this study was the inability to obtain accurate and adequate light penetration data. Such measurements could not be made at any of the night stations and reliable readings also could not be obtained in moderate to heavy sea states or when the ship was drifting appreciably. As a result, no light penetration data were taken at 72 of the stations (*see* Table 1)—approximately one-third of the total. At such stations there was no alternative to using the extinction coefficient from the last station where such measurements were made.

This problem was most serious in the regions of high productivity, as in the Arabian Sea, where the distribution of phytoplankton was patchy. It was, however, probably less serious than indicated from the distribution of primary production and chlorophyll alone, because much of the light extinction in this region was due to nonliving, detrital carbon, which was much more abundant and less variable than the living organisms (Ryther and Menzel 1965).

Nevertheless, the errors introduced by inadequate light penetration data may have been large. For example, a recalculation of carbon assimilation at the highly productive Station 194 was made by the method of Ryther and Yentsch (1957) using chlorophyll and radiation data from that station and an assimilation number (carbon uptake/chlorophyll) taken from the surface ^{14}C-uptake and chlorophyll values. Assuming that the extinction coefficient was 0.14, or double the value obtained by extrapolation from the last station, the value for primary production would be decreased by

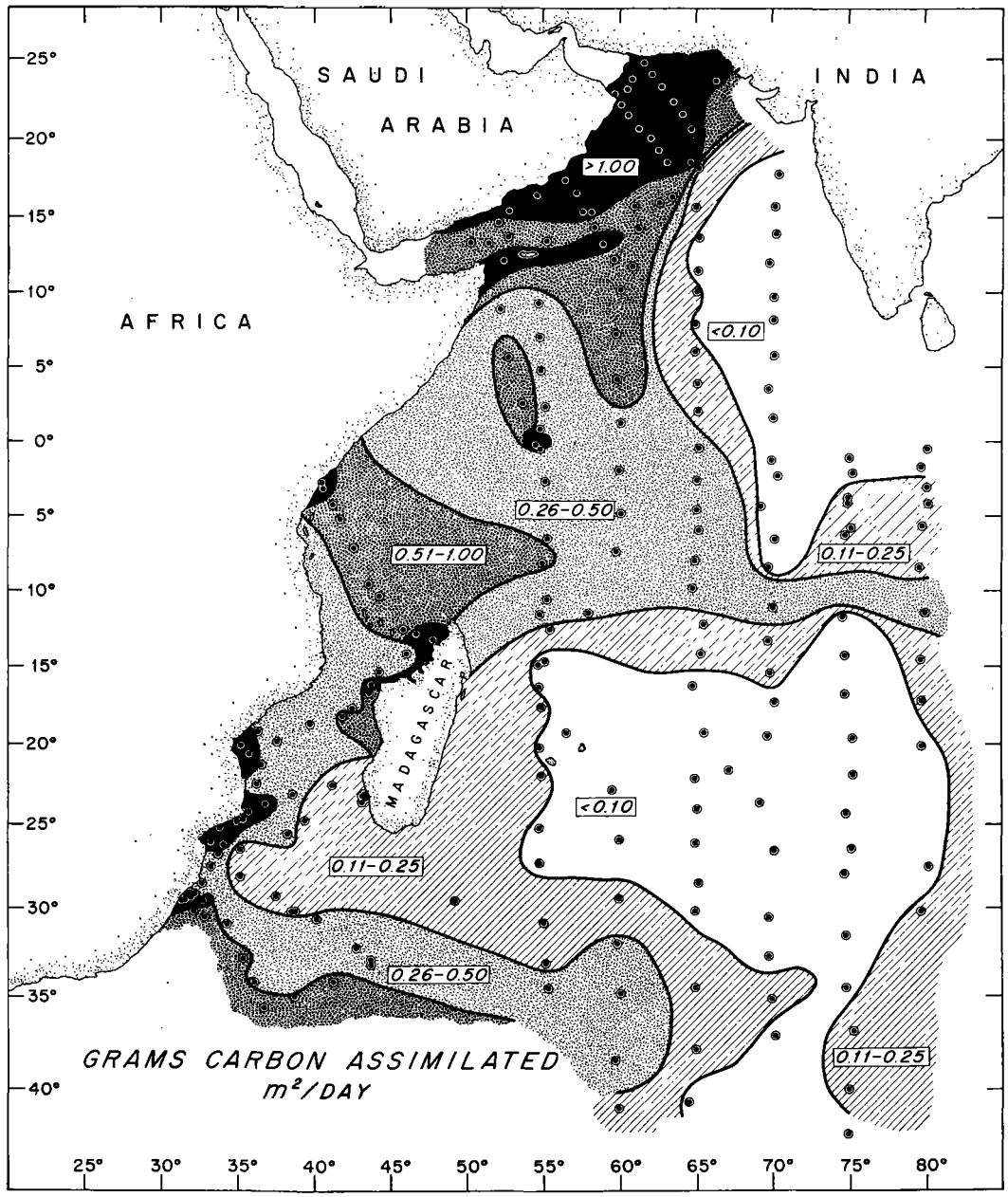


FIG. 1. Chart of the western Indian Ocean showing the positions of oceanographic stations occupied during *Anton Bruun* Cruises 2, 3, 4A, 5, 6, 7, and 8 and the general level of primary organic production.

approximately one-third—from 6.58 to 4.36 g carbon m^{-2} day^{-1}.

All samples were analyzed and all data were calculated at sea by the co-authors (Hall, Pease, Bakun, and Jones). Temperature and depth calculations were subsequently checked by K. G. and E. C. La Fond.

RESULTS

The level of primary production in the western Indian Ocean is shown in Fig. 1. Because the measurements are sparse in some areas and subject to diurnal, microdistributional, and experimental sources of variability, no attempt has been made to describe the data in fine detail or to show minor differences. Rather, the levels of production are reported as falling within one of five rather wide ranges, viz.: < 0.10, 0.11–0.25, 0.26–0.50, 0.51–1.00, and > 1.00 g carbon assimilated m^{-2} day^{-1}. Within these ranges the data are geographically consistent over relatively large areas and their boundaries correspond, in most cases, with recognizable hydrographic features.

But despite the broad grouping, 23 of the values, or 10% of the total number of observations, do not fit within the contours drawn in Fig. 1. In every case these values belonged to the next higher or lower range of values. This license was taken to avoid breaking-up the figure with numerous isolated "islands" of questionable significance. The actual values of primary production and the position and date of each station are given in Table 1.

Two large areas of low productivity (< 0.26 gC m^{-2} day^{-1}) can be seen in Fig. 1. That to the north extends from 80° to nearly 60° E long and from the Indian continent to about 5° S lat. Measurements were not made close to the Indian coast where earlier studies (Jayaraman and Gogate 1957; Banse 1959; Carruthers et al. 1959) have demonstrated local upwelling associated with both the Southwest and Northeast Monsoons.

Another large area of low productivity extends from 10° to about 40° S lat and from 80° E long nearly to the African coast south of Madagascar. The two areas of impoverished water are separated in the eastern portion of the region by a narrow band of moderately productive water (0.26–0.50 gC m^{-2} day^{-1}) between 5° and 10° S lat that presumably represents the divergence between the South Equatorial Current and the Counter Current to its north (*see* Steemann Nielsen and Jensen 1957).

As the South Equatorial Current approaches the coast of Africa, north and east of Madagascar and in the general vicinity of the Seychelle Islands, it divides into two branches, the Somali and Agulhas Currents. The divergence between these produces intensive upwelling (Ivanenkov and Gubin 1960) which accounts for the wedge-shaped region of high productivity north of Madagascar.

Unfortunately, measurements were not made along the Somali coast. Although the region has been assigned a moderately high level of production (0.26–0.50 gC m^{-2} day^{-1}), it is possible that much higher levels occur along the coast and perhaps for some distance offshore, at least during the Southwest Monsoon, where strong coastal upwelling has long been recognized (Schott 1935).

The productive waters formed at the divergence flow in a southerly direction as the Agulhas Current along the western side of the Mozambique Channel, close to the African coast. A portion of the current turns eastward into the central Indian Ocean at 30–35° S lat. (Sverdrup, Johnson, and Fleming 1942). This current pattern is clearly reflected in the level of productivity (Fig. 1). As the Agulhas Current reaches the south African coast, it intensifies and narrows to a position closely approaching the coast. Pockets of very high productivity (> 1.00 gC m^{-2} day^{-1}) along the southeast coast off Durban, Laurenco Marques, and Beira may have resulted partially from geostrophic uptilting of water along the western edge of the Current (Sverdrup et al. 1942; Steemann Nielsen and Jensen 1957). However, the hydrographic conditions at the time the *Bruun* stations were occupied (July–October) show no evidence of this, and it appears more likely that these localized situations resulted from terrigenous contributions. In general, the levels of productivity found by the *Bruun* immediately off the south east African coast were considerably higher than those reported by Steemann Nielsen and Jensen. But on the seaward side of the Agulhas Current (100 miles or less from shore at the latitude of Durban) relatively low levels of productivity (0.11–0.25 gC m^{-2} day^{-1}) were encountered which

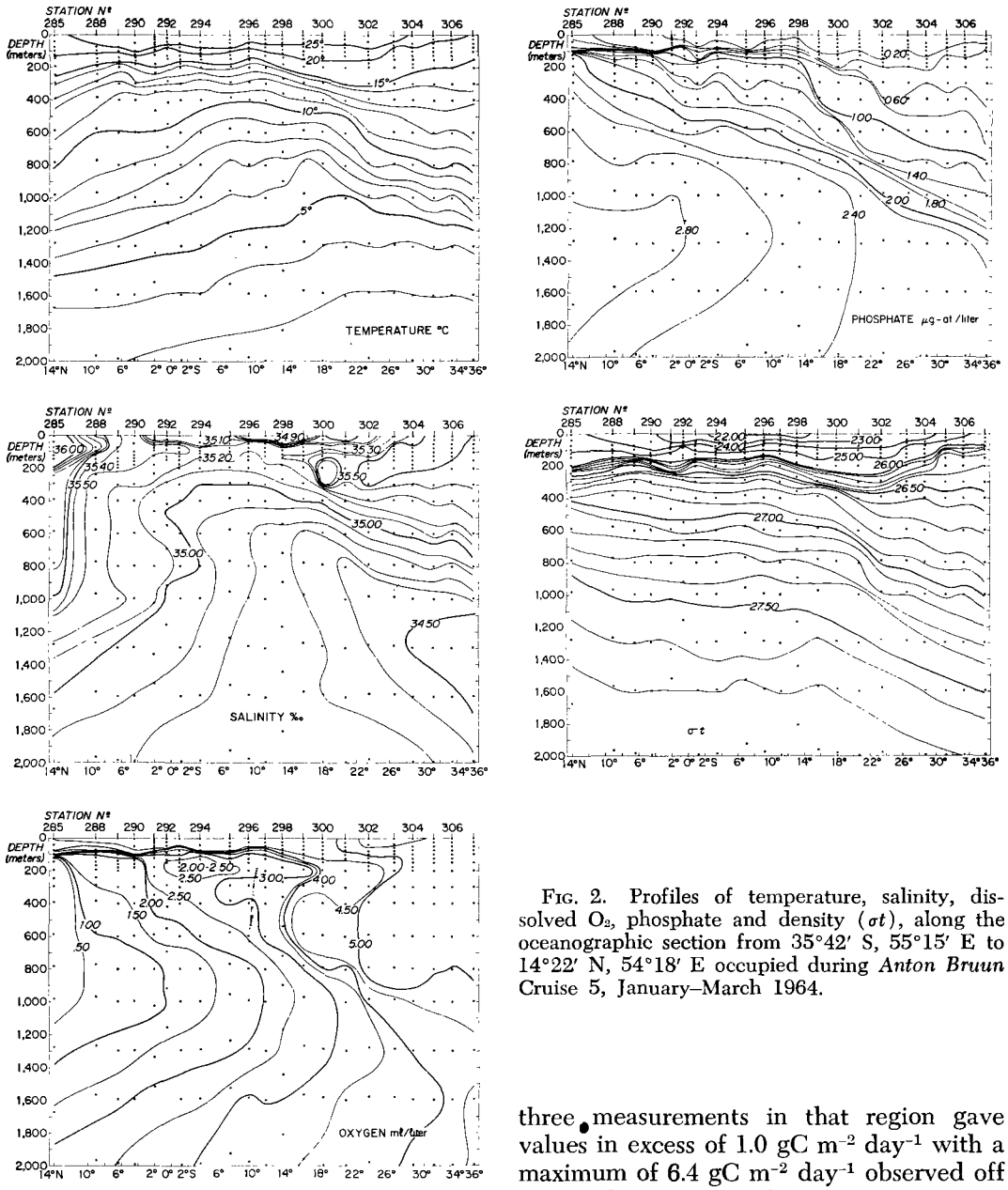


FIG. 2. Profiles of temperature, salinity, dissolved O_2, phosphate and density (σt), along the oceanographic section from 35°42′ S, 55°15′ E to 14°22′ N, 54°18′ E occupied during *Anton Bruun* Cruise 5, January–March 1964.

appear to reflect the intrusion of an eddy of central Indian Ocean water into the Mozambique Channel south of Madagascar.

North of the Equator and into the Arabian Sea the level of organic production increases to the north and west, reaching exceptionally high values off the coasts of Saudi Arabia and West Pakistan. Twenty-three measurements in that region gave values in excess of 1.0 gC m^{-2} day^{-1} with a maximum of 6.4 gC m^{-2} day^{-1} observed off the southeastern tip of Arabia.

The physical and chemical conditions leading to the high productivity of the western Arabian Sea have been described elsewhere (Ryther and Menzel 1965) and need only to be summarized here. Briefly, the explanation lies in the presence of unusually high levels of inorganic nutrients (nitrate, phosphate, silicate) at shallow depths often

within or in close proximity to the euphotic layers. Physical phenomena of both large and small scale capable of inducing even a moderate degree of vertical mixing are sufficient to bring appreciable quantities of these nutrients into the surface layers, thereby sustaining the observed high levels of plant growth. Coastal upwellings along the Somali and Arabian shores and off the west coast of India undoubtedly play a major role in the fertilization of the surface waters of the Arabian Sea at certain times of the year in relation to the monsoons. However, as the high levels of production recorded in this region by the *Anton Bruun* were observed in October–November, during the period of calm seas and winds, it is clear that other forces contribute to the process of vertical advection and the maintenance of high levels of organic production in the Arabian Sea throughout the year. The possible nature of these advective processes is discussed briefly in Ryther and Menzel (1965).

Of basic significance is the origin of the high nutrient and low oxygen levels in the Arabian Sea and their close proximity to the sea surface. These characteristics in the so-called "North Indian Deep Water" of Ivanenkov and Gubin (1960) were attributed by those authors to the Red Sea (the presumed origin of that water mass). However, the phosphate levels of the Red Sea water (Neumann andMcGill 1962) do not even remotely approximate those of the deep Arabian Sea. Moreover, high concentrations of phosphate (> 2.0 μg-at./liter) occur throughout the western Arabian Sea at depths of 100–500 m, well above water with *T–S* characteristics of the Red Sea. It seems unlikely, therefore, that the chemical characteristics of the Arabian Sea owe their origin to the Red Sea, though the deep water itself may be so derived.

Some insight into these problems may be obtained by examination of the oceanographic section along 55° E long occupied during Cruise 5 of *Anton Bruun* in January–March 1964 (Fig. 2). At the northern end of the section, off Cape Guardafui, the intrusion of Red Sea water to the south can be seen at depths of 500–1,500 m. The core of this water (for example, at 1,000 m at Station 288) has a salinity of 35.29‰ and a temperature of 8.66 C, consistent with Ivanenkov and Gubin's North Indian Deep Water.

Above this water mass, the density field and isopleths for phosphate and oxygen tilt sharply from approximately 1,000 m at the southern end to 100–200 m at the northern end of the section. *Anton Bruun* sections along 60, 65, 70, 75, and 80° E long (not shown in this report) show this same feature, modified only by seasonal and geographical factors in the upper 100–200 meters at the northern end of the sections. This water mass is also depicted by Ivanenkov and Gubin (1960) for the Davis Sea–Cape Guardafui section of OB. These authors, referring to this as the "Subtropical Subsurface Water Mass" describe it as an intensive, northerly-flowing, subsurface countercurrent which compensates for the southerly loss of water by surface currents. Their diagram shows the water mass as forming at or near the subtropical convergence, sinking to 1,000–1,500 m at 45–25° S lat, and then rising towards and eventually reaching the surface as it moves northward and crosses the Equator.

While some details are different, the above interpretation is generally consistent with the observations made on the *Anton Bruun* cruises and provides an explanation for the high fertility of the Arabian Sea. What evidently exists here is a major system of oceanographic upwelling. The natural enclosure of the Arabian Sea and its monsoon-driven surface circulation results inevitably in the loss of surface water to the south via the equatorial circulation. It is presumably this loss of surface water that is replaced by the northward-moving "Subtropical Subsurface" water, as described above.

While the deep water is, in itself, rich enough to support a high level of organic production, the two-layered circulation that is common to all upwelling situations constitutes a "nutrient trap" which further reinforces the fertility of the region. This

mechanism was first recognized by Redfield (1955) in his studies of the Gulf of Venezuela, which is also characterized by a two-layered, countercurrent type of circulation. In these situations, rich water is brought up from intermediate depths to the surface, supporting a heavy growth of plankton organisms which then spread seaward with the surface currents in a direction opposite to that of the subsurface flow. The inorganic nutrients that were contained in the upwelled deep water are now incorporated in organic matter. The sinking or migration of these microorganisms, or of the animals that eat them, transports the organic matter down into the subsurface layers that are moving landward and will ultimately contribute to the upwelling process. As the contained organic matter dies and decomposes, the waters become further enriched with inorganic nutrients and depleted in oxygen. The levels of nutrients and oxygen, which are inversely related, depend to a large extent upon the speed of the circulation. When the latter is particularly sluggish, the subsurface waters may approach or reach complete anoxia. The subsequent transport of such water to the surface may well provide an explanation for the periodic mass mortalities of fish and other life in the Arabian Sea as well as in other classical regions of upwelling off Peru and west Africa.

A portion of the rain of organic matter from the rich surface layers penetrates through the subsurface circulation into the North Indian Deep Water. The subsequent decomposition of this material provides the deep water with its characteristic high phosphate and low oxygen concentrations. Thus, while this water appears, from its *T–S* relationships, to originate in the Red Sea, as discussed above, its chemical characteristics are acquired *in situ*. The fact that the deep water contains higher phosphate and lower oxygen than the overlying subsurface water (*see* Fig. 2) merely reflects the relative speed of flow of the two water masses. The outflow from the Red Sea is small relative to the volume of the Deep Indian Water mass, and it is apparently intermittent (Thompson 1939). Consequently, the southward flow of the deep water is undoubtedly extremely sluggish and even low rates of organic decomposition can effect major changes in its chemical composition.

One of the major deficiencies in the *Anton Bruun* survey of the western Indian Ocean is the lack of seasonal coverage in the various regions of interest. By an unhappy coincidence, most of the observations in the eastern portion of the region studied were made during the first half of the year (January–June) while those in the western portion were made during the latter half of the year. The levels of organic production that have been described must therefore be considered in terms of the physical and chemical oceanographic conditions prevailing at the time the measurements were made. How much these conditions vary seasonally and what the resulting effect may be upon the productivity of the region is not known.

With these reservations in mind, the productivity of the entire region studied will be considered. The *Anton Bruun* survey covered an area of 23×10^6 km^2—about one-third of the Indian Ocean as conventionally described and 6.5% of the world's oceans (Sverdrup et al. 1942). From the data appearing in this report, the total annual productivity of this area can be calculated as 3×10^{12} kg, which is 10–12% of Steemann Nielsen and Jensen's (1957) estimate of the range of production for the oceans as a whole. Put in other units, the mean daily rate of production for the western Indian Ocean is 0.35 gC/m^2 or about twice Steemann Nielsen and Jensen's average for the oceans. However, the use of means is misleading in a region where production was found to vary within a range of more than a hundredfold. Over half of the above total organic production occurred in approximately 20% of the region studied; more than one-fifth of the total was in the western Arabian Sea alone, where the mean production is approximately ten times that of the world's oceans. Thus, while the western Indian Ocean as a whole may be considered as somewhat more productive than

most other large oceanic areas, it is a region of great contrast containing both some of the richest and some of the most infertile waters that have been described.

REFERENCES

BANSE, K. 1959. On upwelling and bottom trawling off the Southwest coast of India. J. Marine Biol. Assoc. India, **1**: 33–49.

CARRUTHERS, J. N., S. S. GOGATE, J. R. NAIDU, AND T. LAEVASTU. 1939. Shorewards upslope of the layer of minimum oxygen off Bombay: Its influence on marine biology, especially fisheries. Nature, **183**: 1084–1087.

IVANENKOV, V. N., AND F. A. GUBIN. 1960. Water masses and hydrochemistry of the Western and Southern parts of the Indian Ocean. Trans. Marine Hydrophys. Inst. Acad. Sci. USSR. [Transl. from Russian.] **22**: 27–99.

JAYARAMAN, R., AND S. S. GOGATE. 1957. Salinity and temperature variations in the surface waters of the Arabian Sea off the Bombay and Saurashtra coasts. Proc. Indian Acad. Sci., Sect. B, **45**: 151–164.

MURPHY, J., AND J. P. RILEY. 1962. A modified single solution method for the determination of phosphate in natural waters. Anal. Chim. Acta, **27**: 31–36.

NEUMANN, A. C., AND D. A. MCGILL. 1962. Circulation of the Red Sea in early summer. Deep-Sea Res., **8**: 223–235.

REDFIELD, A. C. 1955. The hydrography of the Gulf of Venezuela. Papers Marine Biol. Oceanog. Deep-Sea Res., **3**: (Suppl.) 115–133.

RYTHER, J. H., AND D. W. MENZEL. 1965. On the production, composition, and distribution of organic matter in the Western Arabian Sea. Deep-Sea Res., **12**: 199–209.

———, AND C. S. YENTSCH. 1957. The estimation of phytoplankton production in the ocean from chlorophyll and light data. Limnol. Oceanog., **2**: 281–286.

SCHOTT, G. 1935. Geographie des Indischen und Stillen Ozeans. Boysen, Hamburg. 413 p.

STEEMANN NIELSEN, E. 1952. The use of radioactive carbon (C^{14}) for measuring organic production in the sea. J. Conseil, Conseil Perm. Intern. Exploration Mer, **18**: 117–140.

———, AND E. A. JENSEN. 1957. Primary oceanic production, the autotrophic production of organic matter in the oceans. Galathea Repts., Copenhagen, **1**: 49–136.

SVERDRUP, H. U., M. W. JOHNSON, AND R. H. FLEMING. 1942. The oceans. Prentice-Hall Inc., Englewood Cliffs, N. J. 1087 p.

THOMPSON, E. F. 1939. Chemical and physical investigations. The exchange of water between the Red Sea and the Gulf of Aden over the "sill." Sci. Rept. John Murray Expedition 1933–34, **2**: 105–119.

Reprinted from *Boll. Mus. Ist. Biol. Univ. Genova*, vol. XXXIV, no. 207, 1966, p. 107-113

N. DELLA CROCE - S. FRONTIER (*)

Istituto di Zoologia della Università di Genova
* Centre O.R.S.T.O.M., Nosy Bé, Madagascar

Thecosomatous Pteropods from the Mozambique Channel

On cruise no. 8 of the R./V. « Anton Bruun », during the International Indian Ocean Expedition, series of tows were made to collect planktonic and bathypelagic organisms for physiological and biochemical studies. The research was carried out by Dr. J.M. Teal of the Woods Hole Oceanographic Institution (WHOI, 1965; Della Croce, 1964-65).

Most of the tows were carried out at night, in surface waters, at depths where heavy traces of scattering were recorded by the PGR, or at day-time and at different depths.

The net, exceeding 4 meters in length, had hexagonal meshes approximately 5 mm long and 2 mm wide, and a square opening of 2,25 m^2. In order to avoid damage to the organisms as much as possible, the collector was a very large one (about 30 cm in diameter).

As the experiments were carried out mostly on Euphausiids and planktonic shrimps, the other specimens (with the exception of Coelenterata which were particularly difficult to handle) were preserved for general observations on taxonomy and geographical distribution, and for classifying them as possible source of scattering. Euphausiids and Siphonophores are already known to be definite components of the scattering layers (Moore, 1950; Barham, 1963).

Because of the mesh size of the net, the collection of animals of the different groups were generally not very abundant. The collections

were made between Durban (South Africa) and Nosy Bé island (Madagascar), at the following geographical positions:

Station	Starting position	Data	Starting time	Tow	Sonic depth
398 D	25° 46′ S - 34° 29′ E	30- 9-'64	0415	Surface	400
398 A	22° 46′ S - 35° 50′ E	1-10-'64	0415	Surface	—
399 D	21° 18′ S - 36° 19′ E	2-10-'64	0415	Surface	1500
400 B	21° 41′ S - 35° 39′ E	3-10-'64	0415	Surface	—
401 A	19° 58′ S - 36° 33′ E	4-10-'64	0415	Surface	—
404 A	19° 34′ S - 40° 19′ E	10-10-'64	0415	Surface	—
405 A	18° 26′ S - 40° 19′ E	11-10-'64	0415	Surface	2520
406 C	18° 27′ S - 41° 20′ E	12-10-'64	1455	(*)	2150
407 B	17° 34′ S - 42° 43′ E	13-10-'64	1530	500 mwo	1950
407 H	17° 22′ S - 43° 10′ E	14-10-'64	1330	600 mwo	710
408 E	16° 11′ S - 43° 29′ E	16-10-'64	0415	Surface	1600
409 D	16° 12′ S - 43° 41′ E	18-10-'63	0415	Surface	600
409 N	15° 29′ S - 44° 42′ E	20-10-'64	0415	Surface	1600
410 B	14° 33′ S - 45° 47′ E	21-10-'64	0410	Surface	2000

(*) Six tows respectively with 10, 50, 100, 150, 200 and 300 meters of wire out (= mwo). Sonic depth in meters.

According to Chen and Bé (1964), since 1888, about thirty five papers dealing with the distribution of Pteropods in the world oceans have been published. The studies devoted to these holoplanktonic organisms are relatively scarce, and most of them are based upon collections of oceanographic expeditions.

The local surveys in the Indian Ocean concerned only the waters off Nosy Bé, North western Madagascar (Frontier, 1963; 1966), to which we refer also in consideration of the fact that sampling in the Nosy Bé area was partially carried out approximately at the same season and day-time of ours.

The following species occured in our samples.

Euthecosomatous Pteropods

Euclio cuspidata (Bosc)

1 specimen. Length: 22 mm? (extremities broken). Station: 410 B. Shell covered by a colony of hydroids.

Eurythermic species previously recorded in the Indian Ocean as far as 40° Lat. S (Tesch, 1948), but not yet off Nosy Bé.

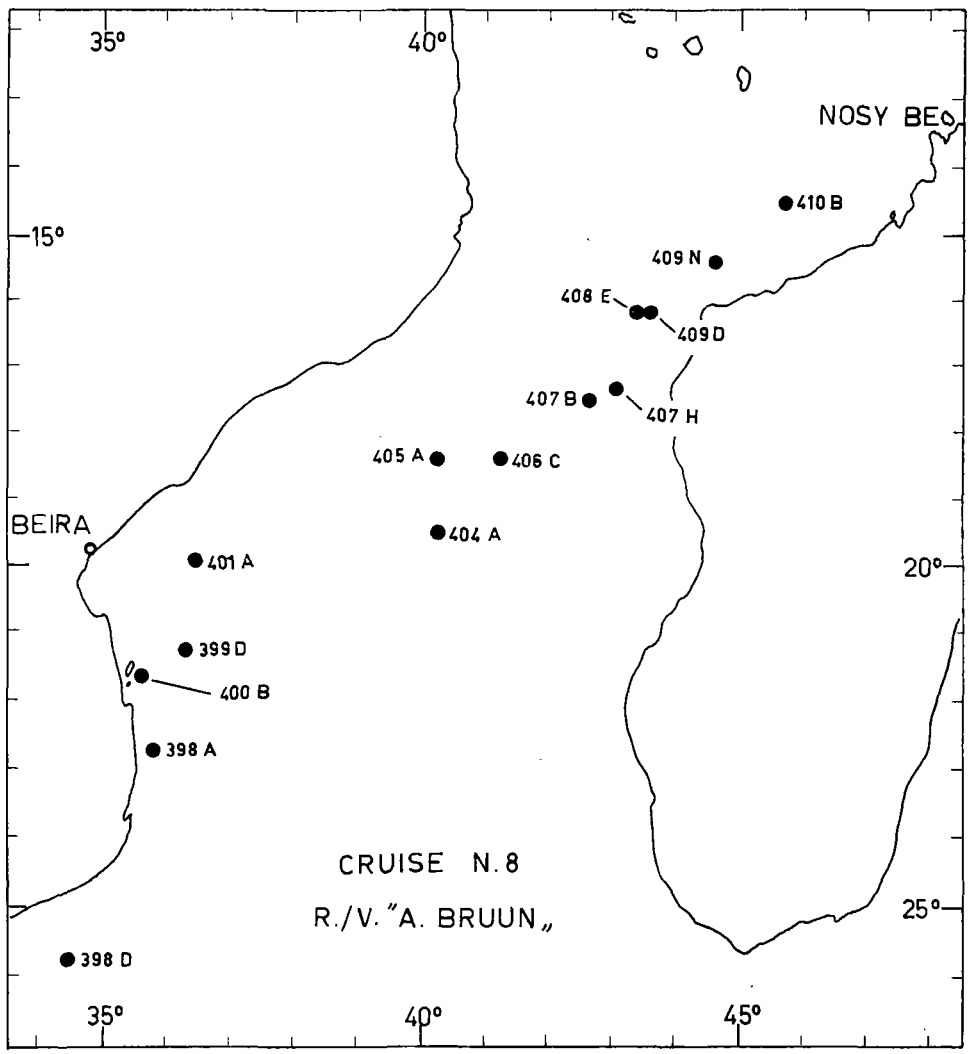
Euclio pyramidata (Linné)

Euclio pyramidata pyramidata L. (= *angusta* Boas)

3 specimens. Length: 8,2-8,5 mm. Stations: 404 A, 405 A, 409 D.

Euclio pyramidata lanceolata (Lesueur) (= *lata* Boas)

7 specimens. Length: 9,5-13,5 mm. Stations: 399 D, 400 B, 401 A, 406 C.



Geographical positions of the sampling stations.

The species is very eurythermic and almost ubiquitous (absent in polar waters only), the subspecies *pyramidata* being characteristic mainly of colder waters, and the subspecies *lanceolata* of the warmer

ones. In our collection, subspecies *lanceolata* was more frequent and found near the african coast and in the center of the channel. *E. p. pyramidata* was caught in the center of the channel only; it occured more frequently than *lanceolata* in surface waters off Nosy Bé.

Diacria trispinosa (Lesueur)

10 specimens. Length (including the young part of the shell): 9,9-10,2 mm. Stations: 404 A, 405 A, 406 C, 409 D, 410 B.

Recorded across the Mozambique Channel. This species occured very rarely off Nosy Bé: only 3 specimens, among which 2 *juveniles*, were found in a three years survey 30 miles around the island. There *Diacria quadridentata* substituted *D. trispinosa* which seems a characteristic species of true pelagic waters. *D. trispinosa* is a very eurythermic and almost ubiquitous species, which is only absent in polar and subpolar waters.

Cavolinia globulosa (Rang)

14 specimens. Length: 5,0-5,8 mm. Stations: 399 D, 400 B, 401 A, 406 C, 410 B.

Scattered across the Mozambique Channel. The species occured in the Nosy Bé area, but scarcely and only at stations 30 miles offshore. *C. globulosa* is characteristic of the tropical waters of the Indo-Pacific.

Cavolinia gibbosa (Rang)

5 specimens. Length: 9,0-9,5 mm. Stations: 405 A, 409 D, 409 N.

The species is almost limited to the Indo-Pacific where it occurs as far as 40° Lat. S. *C. gibbosa* appears to be characteristic of the pelagic waters; it was never collected off Nosy Bé.

Cavolinia inflexa (Rang)
Cavolinia inflexa lata Boas

2 specimens. Length: 7,2 mm. Distance between the lateral edges: 4,4 mm; that is 77% of the length (in agreement with Tesh for the Indian Ocean specimens). Stations: 399 D, 410 B.

Of the two subspecies *longa* and *lata*, the latter is the commonest in the Indian Ocean and western Pacific. In the Nosy Bé area the species occured at stations as far away from the shore as over the edge of the continental shelf.

Cavolinia longirostris (Lesueur)

Cavolinia longirostris longirostris (Lesueur)

2 specimens. Length: 7,2-7,6 mm. Station: 401 A.

This species is very abundant in the warm waters of the world oceans. In the Nosy Bé waters *C. l. longirostris* is the inshore form which is replaced offshore by *C. l. angulata*, the commonest form of the pelagic waters of the Indopacific region (Tesch, 1948). The two forms were frequently represented in the surface samples. The two specimens were collected near the african coast.

Cuvierina columnella (Rang)

Cuvierina columnella columnella (Rang)

1 specimen. Length: 11,2 mm. Station: 406 C.

It is a common tropical species. In the Indo-Pacific the subspecies *urceolaris* Mörch is most common, whilst the subspecies *columnella* is rare. In the Nosy Bé area *C. c. urceolaris* was rather frequent at the stations offshore. In the three years survey only one specimen of *C. c. columnella* has been found.

PSEUDOTHECOSOMATOUS PTEROPODS

Cymbulia sp.

2 specimens without pseudoconcha. Stations: 406 C, 409 N. Cosmopolitan genus.

HETEROPODS

Atlanta gaudichaudi Souleyet

3 specimens. Diameter: 5,1-7,2 mm. Stations: 400 B, 406 C.

Cosmopolitan species, predominant everywhere in the Indo-Pacific. The collected specimens were of great size.

Pterosoma planum Lesson

2 specimens. Length: 10,0-14,5 mm. Station: 400 B.

This species is characteristic of the Indo-Pacific. It has been found only twice in the offshore samples of the Nosy Bé area, and likely limited to the pelagic waters.

Cardiopoda richardi Vayssière

1 specimen. Length: 18,5 mm. Station: 407 H.

Scattered in all tropical waters. In the Nosy Bé area only the nearly related species *C. placenta* has been found.

Pterotrachaea hippocampus Philippi

3 specimens. Length: 16,0-35,0 mm. Stations: 404 A, 406 C. Cosmopolitan species.

Pterotrachaea coronata Forskål

4 specimens. Length: 25,0-50,0 mm. Stations: 401 A, 406 C, 409 D.

Cosmopolitan species not previously found in the Nosy Bé area.

Firoloida demaresti Lesueur

1 male specimen. Length: 16,0 mm. Station: 409 N. Cosmopolitan and very common species.

We may note that several species occuring in our samples were not found in the three years survey which was limited to an area not farther away than 30 miles from shore, and that only at stations farther off very few specimens of some of these species were collected: *Euclio cuspidata, Diacria trispinosa, Cavolinia gibbosa, Pterosoma planum, Cardiopoda richardi, Pterotrachaea coronata.*

On the other hand all these species are well represented in the survey concerning the pelagic area of the South western part of the Indian Ocean (Tesch, 1948; 1949). We may likely conclude that these species belong to the pelagic environment, and that they do not tolerate any mixing with the neritic waters. The pelagic character of our collection would be also confirmed by the scarcity of the *Atlantidae* which, in warm waters, are numerous only inshore and isolated offshore.

Our specimens were of large size, while medium size specimens and small Pteropods as *Limacina* spp. and *Diacria quadridentata* were lacking. It is interesting to note, however, that small specimens of Stomatopods and Amphipods have frequently been found in the samples.

Pteropods of pelagic areas have a mesoplankton habitat, and most of them being collected at dawn in surface waters show that they rise normally from deeper layers at night.

LITERATURE

BARHAM E.G., 1963 - Siphonophores and the deep scattering layer. *Science*, 140 (3568), 826-828.

CHEN C. & BÉ A.W.H., 1964 - Seasonal distributions of Euthecosomatous Pteropods in the surface waters of five stations in the western North Atlantic. *Bull. Mar. Sci. Gulf & Carib.*, 14 (2), 185-220.

DELLA CROCE N., 1964-65 - Crociera No. 8 del R./V. «A. Bruun» nell'Oceano Indiano. *Boll. Mus. Ist. Biol. Univ. Genova*, 33, 5-21.

FRONTIER S., 1963 - Hétéropodes et Ptéropodes récoltés dans le plancton de Nosy Be. *Cah. O.R.S.T.O.M. Océanographie*, n. 6, 213-227.

— — 1966 - Liste complémentaire de Ptéropodes du plancton de Nosy Be (Madagascar). *Cah. O.R.S.T.O.M. Océanographie*, (in press).

MOORE H.B., 1950 - The relation between the scattering layer and the Euphausiacea. *Biol. Bull.*, 99 (2), 181-212.

TESCH J.J., 1913 - Pteropoda. 36. Lieferung in *Das Tierreich*, 1-154.

— — 1948 - The Thecosomatous Pteropods. II. The Indopacific. *Dana Report*, 28, 1-45.

— — 1949 - Heteropoda. *Dana Report*, 34, 1-55.

WHOI, 1965 - U.S. Program in Biology - International Indian Ocean Expedition. Narrative Report: Anton Bruun Cruise 8. *News Bulletin*, n. 10.

— — 1965 - U.S. Program in Biology - International Indian Ocean Expedition. Final Cruise Report: Anton Brunn Cruises, 7, 8, 9. Vol. 1-2.

RIASSUNTO

Gli AA. riportano alcune osservazioni sulla distribuzione dei Pteropodi Tecosomi e degli Eteropodi raccolti prevalentemente di notte, ed in acque superficiali caratterizzate da « scattering » registrato dal PGR. Le raccolte furono effettuate nel corso della crociera n. 8 del R./V. « A. Bruun » in occasione della Spedizione Internazionale nell'Oceano Indiano.

SUMMARY

The AA. report some observations on the distribution of the Thecosomatous Pteropods and Heteropods collected mainly at night in surface waters, where scattering was recorded by the PGR. The samples were collected on cruise n. 8 of the R./V. « A. Bruun » during the International Indian Ocean Expedition.

Reprinted from *Boll. Mus. Ist. Biol. Univ. Genova*, vol. XXXIV, no. 211, 1966, p. 149-164

N. DELLA CROCE - P.H.J. CASTLE *

Istituto di Zoologia della Università di Genova

* Department of Zoology, Victoria University, Wellington

Leptocephali from the Mozambique Channel

Many problems of eel distribution arise from characteristic ability of eel-larvae to traverse considerable oceanic distances by way of wide-ranging currents. There is increasing evidence that certain eel species tend to have a much wider geographical distribution than previously acknowledged, but also that within each species there may be local forms or subspecies recognized by slight differences in the range of vertebral and fin-ray counts, teeth patterns and other characters. Such local forms may be in effective, though limited, contact by movements of larvae. Too few species have been so far investigated to establish this as true for all eel species.

Collections of leptocephali from various areas of the world have vastly increased in recent years incidental to the increased interest in plankton. Studies on eel-larvae rather than on adults therefore offer - perhaps - a more tangible lead to the solution of distribution problems in eels. This is particularly so now that progress is slowly being made in the recognition of the various taxa amongst leptocephali.

Furthermore, eel-larvae make up an important part of oceanic micronekton (nearly 5% in the eastern Indian Ocean), and contribute to some extent to the food of such pelagic fishes as yellowfin tuna (*Neothunnus macropterus*) and lancet fish (*Alepisaurus ferox*) in the South western Pacific (Castle, in press).

Although large collections of eel-larvae have been reported from other parts of the Indo-Pacific and from the Atlantic, knowledge of South African leptocephali is based mainly on the relatively minor account of Barnard (1925, pp. 217-223) which lists eight species. A

few other eel-larvae have been variously reported from the western Indian Ocean.

The present collection of eel-larvae was made on cruise no. 8 of the U.S. National Science Foundation research vessel « Anton Bruun », during the International Indian Ocean Expedition (WHOI, 1965; Della Croce, 1964-65).

Most of the tows were carried out at night, in surface waters, at depths where heavy traces of scattering were recorded by the PGR; or at day-time at different depths. Details on the sampling net and on sampling stations have been reported elsewhere (Della Croce - Frontier, 1966).

Identifications of the various larvae here described are based mainly upon previous systematic studies (Castle, 1963 *et sequ.*) to which we refer for detailed discussion and for illustrations of the various generic types. Except for a new species, which is described in full, brief diagnoses of each species are given, including where possible the important systematic details (e.g. myomere and fin-ray counts). In the case of tentative identifications it is hoped that such information will be of value in permitting future definitive recognition of these larvae, as soon as the relevant information becomes available from adults. The following species occured in our samples.

Family *Congridae*

L. Ariosoma mauritianum (Pappenheim, 1914)

1914. *L. mauritianus* Pappenheim, *Dtsch. Sudpol. Exped.*, 7 (2): 189, pl. 10, fig. 8.

1964 a. *L. Ariosoma mauritianum* (Papp.). Castle, *Zool. Publ. Vict. Univ. N.Z.*, 37: 10.

Material examined: 1 specimen; *A. Bruun* Station 400 B: 21° 41' S - 35° 39' E; 3-10-1964; surface tow at 0415.

Description & Remarks. Total length 93,6 mm; myomeres 125 + 11 = 136; first major vertical blood vessel to the intestine placed at myomere 10, last at myomere 71; anterior margin of gall bladder at myomere 23; teeth $\frac{1 + 1 + IV + 4}{1 + III + 7}$; dorsal rays ca 34; anal rays ca 30; caudal rays not developed.

The specimen conforms closely to the now well known larval type identified with the genus *Ariosoma*, that is, with the type having pigmentation as a series of minute chromatophores on each myoseptum below the midlateral line, along the ventral body-wall and above the intestine, as well as having the dorsal and anal fins restricted until late in growth to the posterior extremity of the body. Previous studies on such larvae discuss the complex of species present in the Indo-Pacific and in the Atlantic (Castle, 1964 a; 1966). Comparative studies on adults have yet to be made to support the systematic and geographical distinctions of the various species as suggested from studies on the leptocephali. There are two species within this complex which are similar as larvae: *A. balearicum* (De Laroche, 1809) with 123–137 myomeres from the Atlantic, and *A. mauritianum* (Pappenheim, 1914) with 134–152 myomeres from the Indo-Pacific. The type locality of the latter is Mauritius, but the species is also known from the Red Sea, off western Australia, and in the South western Pacific. Spawning of the adults is definitely known to occur off western Australia (Castle, 1964 a; p. 12) and the larval life is at least a year long. Castle has previously suggested that spawning may also occur off the eastern coast of Africa, giving rise to a population of adults there, although the species has yet to be recognized from adults in the area. The relatively long larval life of the species suggests that it is at least possible that larvae produced from spawning off western Australia could be transported by East - West trending currents to the western Indian Ocean. An examination of a series of adults or larvae of the species from the two areas for differences in the range of myomere counts or other morphological distinctions (as it occurs in one area to another in the atlantic *A. balearicum*) would determine whether the populations on both sides of the Indian Ocean are continuous or effectively isolated.

L. Gnathophis habenatus (Richardson, 1848)

1848. *Congrus habenatus* Richardson, *Voy. Ereb. Terr., Fish.*, p. 109, pl. 50, figs. 1-5.

1963. *L. Gnathophis habenatus* (Rich.). Castle, *Zool. Publ. Vict. Univ. N.Z.*, 34: 25, text figs. 2 A-F & 5 A-C.

Material examined: 1 specimen; *A. Bruun* Station 399 D: 21° 18′ S - 36° 19′ E; 2-10-1964; surface tow at 0415; sonic depth 1500 m.

Description & Remarks. - Total length 71,0 mm; myomeres 100 + 23 = 123; first major vertical blood vessel to intestine at myomere 11,

last at myomere 39; anterior margin of gall bladder at myomere 35; teeth $\frac{1 + 1 + V + 12}{1 + IV}$; dorsal rays before level of vent 116, dorsal rays 173; anal rays 128; caudal rays 5 + 4; difference between dorsal and anal origins (a — d) equal to + 23 myomeres.

Amongst congrid leptocephali, those of the genus *Gnathophis* (= *Congermuraena* Kaup, in part) are the simplest in pigmentation, having a paired, longitudinal series of rather large, conspicuous chromatophores on the body-wall along the level of the intestine and chromatophores also along the bases of the dorsal, anal and caudal fins. Gnathophid larvae are thus closely similar to those of the majority of species of *Conger* which have, however, at full growth a short, rounded snout and chromatophores continuing from the ventral series along the body-wall above the base of the anal fin. The two species of *Gnathophis* which are present in Australasian waters, *Gnathophis habenatus* (Richardson, 1848) and *G. incognitus* Castle, 1963, were discussed elsewhere (Castle, 1963). At the present time there is sufficient knowledge of only one atlantic species, *Muraena mystax* De Laroche, 1809, for it to be attributed with confidence to *Gnathophis*, although *Congermuraena australis* Barnard, 1923 and *C. bertini* Poll, 1958 from the Atlantic coast of central Africa possibly fall within the limits of the genus. The present specimen conforms most closely with *G. habenatus*, known so far only as far westwards as St. Paul, South Indian Ocean (Kner, 1867, p. 374, pl. 13, fig. 2). Leptocephali of this species are not uncommon in the area to the West of Perth, where spawning of the adults also takes place. Like *A. mauritianum*, it is possible that movement of these larvae may occur westwards across the central Indian Ocean, although it remains to be determined whether such movements have resulted in the establishment of an adult population of *G. habenatus* in african waters.

L. Gnathophis incognitus Castle, 1963.

1963. *Gnathophis incognitus* Castle, *Zool. Publ. Vict. Univ. N.Z.*, 34: 37.
1963. *L. Gnathophis incognitus* Castle, *Zool. Publ. Vict. Univ. N.Z.*, 34: 41.

Material examined: 1 specimen; *A. Bruun* Station 400 B: 21° 41′ S - 35° 39′ E; 3-10-1964; surface tow at 0415.

Description & Remarks. - Total length 62,2 mm (damaged specimen); myomeres 111 to level of vent; last vertical blood vessel to intestine at myomere 57.

This specimen has obviously been damaged at some earlier stage in growth as the posterior end of the body shows no sign of the caudal fin but is rounded and has healed over. A complete myomere count is therefore not possible and the true postanal pigmentation cannot be determined. The larva nevertheless possesses the relatively simple pigmentation typical of *Gnathophis* larvae, although since the postanal region is absent it is impossible to say whether pigment above the anal base (a character which distinguishes larvae of *Conger* from those of *Gnathophis*) would be present. However, as the snout is relatively pointed, not short and rounded (as in full-grown *Conger* larvae), this particular specimen has been identified with *Gnathophis*. There is a relatively high number of preanal myomeres, more than occur at any stage of development of *G. habenatus*, and on this basis the specimen would be referable to *G. incognitus* or *G. mystax*. Although the latter is unknown from the Indo-Pacific, Barnard (1925, pp. 219-220) records (under the names *Leptocephalus Congermuraena australis* or *L. capensis* Kaup) what are clearly *Gnathophis* larvae (including metamorphic specimens) from South Africa having 130-137 segments which could be referred also to either of these two species. Playfair and Gunther (1866, p. 129) record Kaup's *L. capensis* from eastern Africa, but this is an atlantic species probably not found in the Indo-Pacific. The generic position of *Congermuraena australis* and *C. bertini* is as yet unclear, although the former is known to have about 136 vertebrae.

L. Conger wilsoni (Bl. & Schn., 1801)

1801. *Gymnothorax wilsoni* Bloch & Schneider, *Syst. Ich.*, p. 529.
1964 a. *L. Conger wilsoni* (Bl. & Schn.). Castle, *Zool. Publ. Vict. Univ. N.Z.*, 37: 21, text fig. 9 A-C.

Material examined: 1 specimen; *A. Bruun* Station 408 E: 16° 11′ S - 43° 29′ E; 16-10-1964; surface tow at 0415; sonic depth 1600 m.

Description & Remarks. - Total length 85,8 mm; myomeres 116 + 30 = 146; first major vertical blood vessel to intestine at myomere 18, last at myomere 56; anterior margin of gall bladder at myomere 18; teeth $\frac{O + VIII + 12}{O + XV}$; dorsal rays before level of vent 246, dorsal rays 308; anal rays 265; caudal rays 4 + 4; a – d = + 44.

The larvae of *Conger* are similar to those of *Gnathophis* except that they have a more rounded snout (particularly when nearing metamorphosis) and have, as well as chromatophores in a paired longitudinal

series along the intestine, a series of usually inconspicuous chromatophores above the base of the anal fin from the vent to the caudal base. Larvae of *Conger cinereus* (Rüppel, 1828) are known to have, in addition, a longitudinal series of midlateral chromatophores. The present specimen lies well within the range of variation shown for larvae of *Conger wilsoni* (Bl. & Schn.) as previously described (Castle, 1964 a, p. 21, text fig. 9 A-C) but the specimen could also be referred to *Conger jordani* Kanazawa, 1958, known from Japan and possibly South Africa. Relevant to the ease of placing the present larval specimen within the limits of either of these species, great difficulty has been found in separating the two species from published descriptions. The only significant difference between the description of *C. wilsoni* by Kanazawa (1958, pp. 256-257) and Castle (1964 a, pp. 19-20) is that Kanazawa states « two rows of teeth in jaws ». In none of the 25 specimens of *C. wilsoni* examined by Castle from New Zealand waters was this found to be the case, the usual condition in mature specimens being that teeth in both jaws are essentially uniserial with a few teeth in a secondary row, medial to the lateral rows. In this and all other respects, the specimens of *C. wilsoni* from New Zealand are indistinguishable from japanese specimens of *C. jordani*. The two specimens of the latter species which Kanazawa describes from South Africa differ from japanese material in having a more anterior origin of the dorsal fin and fewer dorsal and anal rays. Whatever the true identity of the latter two specimens may eventually prove to be it is clear that the distinction of *C. jordani* from *C. wilsoni* should be reinvestigated to place it on a more workable basis. There appears to be no reason why *C. wilsoni*, a temperate to subtropical species of australasian waters, could not be similar to *C. cinereus cinereus* in having a wide distribution in the Indo-Pacific brought about mainly by the ability of its larvae to traverse some distance across oceanic waters.

L. Uroconger ?braueri Weber & De Beaufort, 1916

1916. *Uroconger braueri* Weber & De Beaufort, *Fish. indo-aust. archip.*, 3: 266.
1964 a. *L. mediopunctatus* Castle, *Zool. Publ. Vict. Univ. N.Z.*, 37: 34, text fig. 11 A-C.

Material examined: 5 specimens; *A. Bruun* Station 400 B: 21° 41′ S - 35° 39′ E; 3-10-1964; surface tow at 0415. *A. Bruun* Station 401 A: 19° 58′ S - 36° 33′ E; 4-10-1964; surface tow at 0415. *A. Bruun* Station 406 C: 18° 27′ S - 41° 20′ E; 12-10-1964; tows at 1455; sonic depth 2150 m. *A. Bruun* Station 408 E: 16° 11′ S - 43° 29′ E; 16-10-1964; surface tow at 0415; sonic depth 1600 m. *A. Bruun* Station 409 D: 16° 12′ S - 43° 41′ E; 18-10-1964; surface tow at 0415; sonic depth 600 m.

Description & Remarks. - Total lengths 80,6–161,8 mm; myomeres 112 - 178 + 47 — 118 = 227 — 236; first major vertical blood vessel to intestine at myomere 14 — 15, last at myomere 64 — 65; anterior margin of gall bladder at myomere 53 — 58; teeth (in a specimen of 134,9 mm total length) $\frac{1 + VI + 13}{1 + VIII + 5}$; dorsal rays before level of vent (two specimens) 248 — 255; dorsal rays (three specimens) 311 — 350; anal rays (four specimens) 276–310; caudal rays 3 + 3, a — d = + 68 (metamorphic specimen) to + 128. The conspicuous midlateral row of chromatophores, spaced at about one per segment, and high myomere count together characterize this larval type amongst congrid leptocephali. Nair (1946; 1948, p. 89; 1960, p. 234) and Nair and Mohamed (1960, p. 182, figs 1-4, tab. 1, pl. 8) have shown that such eel-larvae are the young of *Uroconger* Kaup, 1856 and identified their leptocephali specifically with *U. lepturus* (Richardson, 1844). However, there is some confusion as to the limits of the known species of this genus. Two species have been described from the Atlantic: *U. vicinus* Vaillant, 1888 and *U. syringinus* Ginsburg, 1948. *U. lepturus* and *U. braueri* Weber and De Beaufort, 1916 are Indo-Pacific species, although the distinction of the latter from *U. lepturus* has been questioned. Asano (1962, p. 114) has recently redescribed *U. lepturus* from japanese material and indicates that the species has 203–206 vertebrae, although three specimens examined had 214. Nair and Mohamed (1960) give 204–223 myomeres for their larval material of *Uroconger*, while D'Ancona (1923, p. 46) gives 205–219 for specimens of his larval species *Leptocephalus magnaghii*, which is clearly a larval *Uroconger*. In the type of *L. acuticaudatus* Kaup, 1856 (also a larval *Uroconger*) from Coromandel, India, as re-examined by Bertin (1935, p. 100), there are 200 + myomeres. Dr. J. Blache, of the Institut Français d'Afrique Noire (Dakar), gives counts of 181–184 vertebrae for *U. vicinus* and 191–198 for *U. lepturus* (personal communication). The vertebral count of *U. syringinus* is unknown. A previous account of *Leptocephalus mediopunctatus* Castle, 1964 from the waters of New Caledonia, now recognized as a larva of *Uroconger*, records a myomere count of 239 for this species. Castle recently examined 11 specimens of this species from the eastern Indian Ocean and counted 225–242 myomeres. The present

specimens from the Mozambique Channel conform well with this previous material.

In view of the comparative vertebral counts listed above it seems clear that there is considerable variation in the number of vertebrae in *U.* « *lepturus* » from Japan to the Atlantic, if indeed this species does occur throughout this geographical range. But is is also clear that at least in the southern part of the Indo-Pacific there exists a form of *Uroconger* distinct from other species in having more than 220 myomeres. *U. braueri*, the second known species in the Indian Ocean, has not been examined for vertebral counts but the species has been recorded from the eastern Indian Ocean, including from off Durban. In consideration of the latter record the present larval specimens have been tentatively identified with *U. braueri.*

Leptocephalus maculatus n. sp., Text - fig. 1 A-C

Material examined: type specimen; *A. Bruun* Station 404 A: 19° 34′ S - 40° 19′ E; 10-10-1964; surface tow at 0415. Deposited at the Institute of Zoology, University of Genoa.

Description. - Measurements in mm: total 47,9; head 3,8; snout 1,7; eye 0,8; cleft of mouth 1,8; postorbital 1,7; pectoral 1,2 ;snout-vent 35,7; predorsal ca 23,0; depth just before eye 1,8, at pectoral 2,2, at vent 5,3; maximum depth 6,3. Myomeres 105 + 66 = 171; first major vertical blood vessel to intestine at myomere 22, last at myomere 70; anterior margin of gall bladder at myomere 22; teeth $\frac{1 + VI + 4}{1 + V + 4}$; fin rays not developed, a − d = ca + 45.

Body moderately elongate, much compressed except along head region, relatively shallow, its maximum depth a little posterior to the midpoint of the body and contained 7,6 times in the total length, tapering only gradually in front of, and behind, this point. Head shallower than trunk and thus differentiated from it, relatively short, about 13 times in total; snout moderate, contained a little more than twice in head length, acute, with the dorsal profile concave; nasal organ poorly differentiated; eye oval, its horizontal diameter 4,7 in head length; cleft of mouth oblique, reaching to below anterior margin of pupil; teeth moderately large, acute, three series in each jaw on each side, arranged as follows:

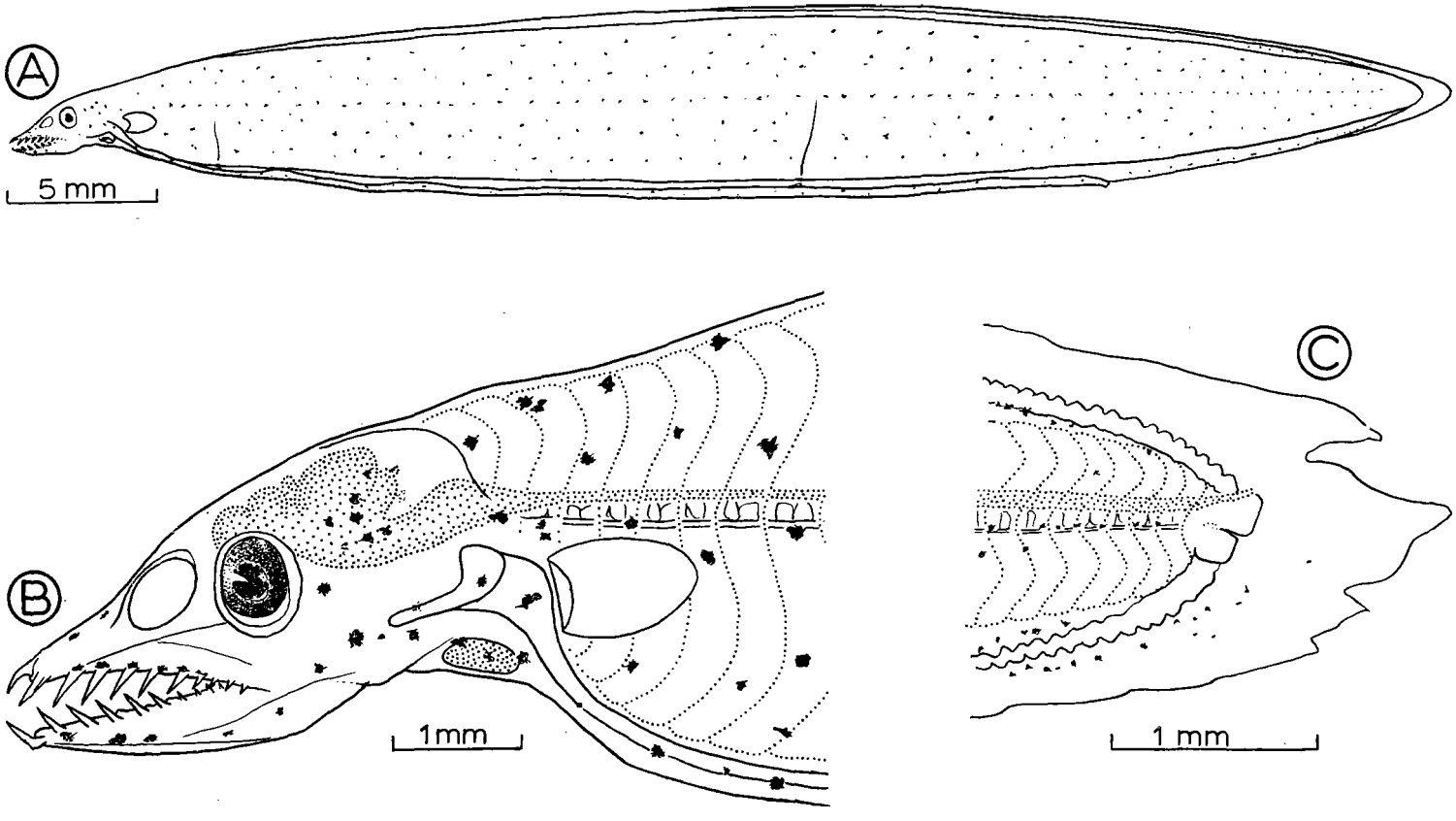


Fig. 1 - *Leptocephalus maculatus* n. sp.; type specimen; 47,9 mm total length. *A. Bruun* Station 404A. Fig. A - lateral view to show pigmentation. Fig. B - lateral view of head. Fig. C - lateral view of caudal région.

an anterior grasping tooth on the tip of the snout, projecting almost immediately forwards, followed by a series of six large teeth and then four much smaller teeth, those on the lower jaw similar in size and distribution. Branchiostegal rays not yet developed. Branchial aperture inconspicuous. Pectoral fin relatively well developed, elongate-oval, its length contained about three times in head; dorsal and anal fins poorly developed, caudal present and supported by two broad hypurals.

Pigmentation conspicuous and characteristic, as follows: dorsal surface of snout with two small, rather diffuse melanophores; a line of six elongate pigment spots along the edge of the upper jaw; six melanophores along the ventral edge of the lower jaw, this series continuing posteriorly to join up with a series scattered over the postorbital region, deep on the surface of the cerebellum, and along the side of the throat; an inconspicuous series of small melanophores along the length of the intestine, spaced at about one pigment spot for every two segments; the whole of the lateral surface of the body covered by rather diffuse, stellate chromatophores, except that these scattered pigment spots extend on to the lateral body-wall above and below the myomeres only at the posterior tip of the body; the bases of the posterior dorsal and anal rays bear minute melanophores.

Remarks. - The unique leptocephalus described above conforms in general features more to the *Congridae* than to any other eel family. It lacks the swollen or looped intestine of moringuid and ophichthid larvae, it possesses a well developed pectoral and a relatively pointed caudal fin and therefore cannot be identified with the *Muraenidae*, and is unlike the larvae of nemichthyids and other similar deepwater families. The pigment scattered across the lateral surface is somewhat reminiscent of that seen in the xenocongrid *Leptocephalus hyoproroides* Strömman, 1896 (although in this species the melanophores are regularly placed so as to follow the edge of each myomere and also extend out on to the dorsal and ventral body-walls) but the present species lacks the characteristic xenocongrid intestinal pigment. A tentative identification with the *Congridae* is given here although there is no pigment patch on the ventral border of the iris, and there is no regular pigment below the lateral line on each myoseptum, the features of the two major divisions of congrid larvae.

Family *Nemichthyidae*

L. Nemichthys scolopaceus Richardson, 1848

1848. *Nemichthys scolopaceus* Richardson, *Voy.* « *Samarang* », 1843-1846, p. 25.
1964 b. *L. Nemichthys scolopaceus* Rich. Castle, *Trans. roy. Soc. N.Z., Zool.*, 5 (7): 79.
1965 a. *L. Nemichthys scolopaceus* Rich. Castle, *Trans. roy. Soc. N.Z., Zool.*, 5 (11): 132, text fig. 1.

Material examined: 1 specimen (total length 155,5 mm); *A. Bruun* Station 405 A: 18° 26′ S - 40° 19′ E; 11-10-1964; surface tow at 0415; sonic depth 2520 m.

Family *Nettastomidae*

L. Nettastoma ?parviceps Günther, 1877

1877. *Nettastoma parviceps* Günther, *Ann. Mag. nat. Hist.*, 20: 446.
1964 b. (non) *L. Nettastoma melanurum* Rafinesque, 1810. Castle, *Trans. roy. Soc. N.Z., Zool.*, 5 (7): 80, text fig. 1 F-G.
1965 a. (non) *L. Nettastoma melanurum* Rafinesque, 1810. Castle, *Trans. roy. Soc. N.Z., Zool.*, 5 (11): 144.

Material examined: 1 specimen; *A. Bruun* Station 399 D: 21° 18′ S - 36° 19′ E; 2-10-1964; surface tow at 0415; sonic depth 1500 m.

Description & Remarks. - Total length 33,9 mm; myomeres 83 + 154 = 237; first major vertical blood vessel to intestine at myomere 25, last at myomere 77; anterior margin of gall bladder at myomere 34; teeth $\frac{1 + \text{VIII}}{1 + \text{IV}}$; fin-rays not developed; postanal midlateral clump of pigment placed at myomeres 96–103.

The broad, leaflike body tapering to a narrow caudal region and the distinctive pigmentation in the form of two conspicuous aggregations of pigment on the intestine with a midlateral, postanal clump of chromatophores, are unmistakable features of this larva, identifying it with the genus *Nettastoma* Rafinesque, 1810. In having 237 myomeres the specimen can be referred to similar material previously described (Castle, 1964 b, p. 80; 1965 a, p. 144) under the name of *L. Nettastoma melanurum* Rafinesque, 1810, from the southwest Pacific. The number of myomeres in this material, greater than that found in larvae of *Nettastoma melanurum* taken in the Atlantic, was considered to be due to the larvae adding myomeres as growth proceeds. The present small specimen throws doubt on this suggestion. It has now become much

more clear that Indo-Pacific leptocephali of *Nettastoma* are distinct from those taken in the Atlantic (Dr. J. Blache, in a personal communication, has informed Castle that the adult of the atlantic *N. melanurum* has 200–206 vertebrae pointing to a distinct species of *Nettastoma* in the Indo-Pacific). The occurrence of the genus *Nettastoma* in the Indo-Pacific has been recorded in the form of *N. parviceps* Günther, 1887 from Japan and from off southeast Africa (Barnard, 1925, p. 194). In view of the distinction shown by the present larva from *N. melanurum* and in consideration of its locality of capture the specimen has been tentatively identified with *N. parviceps*. Thus, similar material from the southeast Pacific recorded as *L. Nettastoma melanurum* must also be referred to this species. The larva described by Barnard (1925, p. 221) from South African waters as *Leptocephalus Nettastomatis* may also be referable to *N. parviceps*.

Family *Muraenidae*

L. Gymnothorax sp.

Material examined: 1 specimen; *A. Bruun* Station 406 C: 18° 27′ S - 41° 20′ E; 12-10-1964; tows at 1455; sonic depth 2150 m.

Description & Remarks. - Total length 45,1 mm; myomeres 55 + 50 = 105; first major vertical blood vessel to intestine at myomere 13, last at myomere 56; anterior margin of gall bladder at myomere 14; teeth $\frac{1 + III + 7}{1 + III + 6}$; dorsal rays before level of vent 105; dorsal rays 285; anal rays 181; caudal rays 2 + 2, a − d = +13.

L. Gymnothorax sp.

Material examined: 1 specimen; *A. Bruun* Station 406 C: 18° 27′ S - 41° 20′ E; 12-10-1964; tows at 1455; sonic depth 2150 m.

Description & Remarks. - Total length 40,2 mm; myomeres 61 + 52 = 113; first major vertical blood vessel to intestine at myomere 15, last at myomere 60; anterior margin of gall bladder at myomere 19; teeth $\frac{1 + III + 6}{0 + IV + 5}$; dorsal rays before level of vent 54; dorsal rays 317; anal rays 226; caudal rays 3 + 2, a − d = +6.

L. Anarchias sp.

Material examined: 1 specimen; *A. Bruun* Station 406 C: 18° 27′ S - 41° 20′ E; 12-10-1964; tows at 1455; sonic depth 2150 m.

Description & Remarks. - Total length 60,7 mm; myomeres 76 + 45 = 121; first major vertical blood vessel to intestine at myomere 12, last at myomere 30; anterior margin of gall bladder at myomere 30; teeth absent; dorsal rays 50; anal rays 41; caudal rays 2 + 2.

Although the characteristic features of the larvae of several genera of muraenids are known, identification to the species level is seldom possible since little is known about comparative vertebral counts in adults of the numerous species in the family, particularly in those from the Indo-Pacific. Reference may be made to a previous paper (Castle, 1965 b) for details of the major larval characteristics of the family *Muraenidae* and particularly of the two genera represented in the present collection, *Gymnothorax* Bloch, 1795 and *Anarchias* Jordan and Starks, 1906. The essential generic features of *Gymnothorax* larvae are the chromatophores in longitudinal series in advance of the dorsal origin, on the body-wall along the ventral aspect of the body, and as a splanchnic series along the upper margin of the intestine from the gall bladder to the vent; the dorsal origin is usually well in advance of the vent. *Anarchias* larvae (like those of *Uropterygius* Rüppell, 1835) and adults both have the dorsal and anal fins reduced to rudiments at the tip of the body, and pigment is entirely absent. Smith (1962, pp. 428-432) lists more than 20 species of *Gymnothorax* and three species of *Anarchias* from the waters of the western Indian Ocean and the Red Sea. The three larval muraenid species described here may therefore be referable to adult species included in this list.

Family *Ophichthidae*

L. ?Leiuranus sp.

Material examined: 1 specimen; *A. Bruun* Station 400 B: 21° 41′ S - 35° 39′ E; 3-10-1964; surface tow at 0415.

Description & Remarks. - Total length 43,2 mm; myomeres 68 + 76 = 144; first major vertical blood vessel to intestine at myomere 10, last at myomere 61; teeth $\frac{1 + V + 4}{1 + V + 3}$; fin-rays not developed; a – d = ca +23.

L. Myrophis sp.

Material examined: 6 specimens; *A. Bruun* Station 405 A (2 specimens): 18° 26′ S - 40° 19′ E; 11-10-1964; surface tow at 0415; sonic depth 2520 m. *A. Bruun* Station 408 E (1 specimen): 16° 11′ S - 43° 29′ E; 16-10-1964; surface tow at 0415; sonic depth 1600 m. *A. Bruun* Station 409 D (2 specimen): 16° 12′ S - 43° 41′ E; 18-10-1964; surface tow at 0415; sonic depth 600 m. *A. Bruun* Station 409 N (1 specimen): 15° 29′ S - 44° 42′ E; 20-10-1964; surface tow at 0415; sonic depth 1600 m.

Description & Remarks. - Total lengths 70,4 mm — 85,4 mm; myomeres 47 — 50 + 89 — 95 = 136 — 144; first major vertical blood vessel to intestine at myomeres 16 — 17, last at myomeres 48 — 52; anterior margin of gall bladder at myomeres 16 — 17; teeth (in a 70,4 mm specimen) $\frac{1 + V + 11}{0 + 10}$; dorsal rays before vent (two specimens) 32 — 58; dorsal rays 303 — 332; anal rays 250 — 287; caudal rays 3 — 4 + 2 — 3; a — d = +10 to +21.

Ophichthid larvae are similar to muraenids in offering considerable difficulty in their identification, not only because of the diversity of genera and species occurring in most areas of the tropical Indo-Pacific but also because of the lack of knowledge of intermediate growth forms which are valuable in the characterisation of larval genera. In a previous account (Castle, 1965 c) of ophichthid larvae occurring in Australasian waters some of the common generic forms, including the two listed above, have been illustrated.

DISCUSSION

The most striking feature of the collection reported above is its diversity: for only 22 specimens at least 5 eel families are represented, including the larvae of five essentially tropical species (the muraenids and ophichthids), three subtropical species (*Ariosoma mauritianum*, *Gnathophis incognitus* and *Conger wilsoni*), one temperate species (*Gnathophis habenatus*), and three species more typical of the deeper oceanic waters (*Nemichthys scolopaceus*, *Uroconger braueri* and *Nettastoma parviceps*). Of these twelve species, at least seven are shared with the eastern Indian Ocean and the southwest Pacific (larvae of these seven species, but not all the adults, have been recognized in collections studies from these areas). Such a sharing can be readily understood for the deep water species and for *Ariosoma mauritianum* which is widely distributed

in Australasian waters and whose type locality is the western Indian Ocean, i.e. Mauritius. On the other hand the present record of the characteristic Australasian species *Gnathophis habenatus*, *G. incognitus* and *Conger wilsoni* is a novelty, pointing to a much closer relationship of Australasian and African congrid faunas than previously acknowledged. In view of (1) the wide distribution of at least some congrid species from Australasia to Africa, (2) the relatively long larval life of congrids, (3) the existence of the necessary East-West trending oceanic currents in the Indian Ocean from an eastern area where all of these species have been recognized (to be reported in a later paper), and (4) the relatively moderate distances involved for the transport of larvae compared with other oceanic areas across which eel-larvae are known to move, there seems to be no barrier to Australasian species becoming established in the western Indian Ocean. However, it remains to be seen whether records of species such as *G. habenatus*, *G. incognitus* and *Conger wilsoni* as suggested by larvae, can be confirmed by the collection and recognition of adults on the eastern coast of Africa.

LITERATURE

ASANO H., 1962 - Studies on the congrid eels of Japan. *Bull. Misaki mar. biol. St. Kyoto Univ.*, 1, 1-143.

BARNARD K.H., 1925 - A monograph of the marine fishes of South Africa. *Ann. S. Afri. Mus.*, 21 (1), 1-418.

BERTIN L., 1935 - Les types du Kaup dans la collection des leptocéphales du Museum. *Bull. Mus. Hist. nat., Paris*, 7, 99-106.

CASTLE P.H.J., 1963 - The systematics, development and distribution of two eels of the genus *Gnathophis* (Congridae) in Australasian waters. *Zool. Publ. Vict. Univ. N.Z.*, 34, 15-47.

— — 1964 a - Congrid leptocephali in Australasian waters with descriptions of *Conger wilsoni* (Bl. & Schn.) and *C. verreauxi* Kaup. *Zool. Publ. Vict. Univ. N.Z.*, 37, 1-45.

— — 1964 b - Eels and eel-larvae of the *Tui* Oceanographic Cruise 1962, to the South Fiji Basin. *Trans. roy. Soc. N.Z., Zool.*, 5 (7), 71-84.

— — 1965 a - Leptocephali of the Nemichthyidae, Serrivomeridae, Synaphobranchidae and Nettastomidae in Australasian waters. *Trans. roy. Soc. N.Z., Zool.*, 5 (11), 131-146.

— — 1965 b - Muraenid leptocephali in Australasian waters. *Trans. roy. Soc. N.Z., Zool.*, 7 (3), 57-84.

— — 1965 c - Ophichthid leptocephali in Australasian waters. *Trans. roy. Soc. N.Z., Zool.*, 7 (6), 97-123.

— — 1966 - The eel larvae (leptocephali). In - Die ichthyologische Ausbeute der ersten Westafrika-Fahrt des fischereitechnischen Forschungsschiffes « Walther Herwig ». *Archiv. für Fischereiwiss.* (in press).

— — 1966 - Les léptocephales dans le Pacifique sud-ouest. *Cahiers O.R.S.T.O.M.* (in press).

D'ANCONA U., 1928 - Murenoidi (Apodes) del Mar Rosso e del Golfo di Aden. Materiali raccolti dal Prof. L. Sanzo nella campagna della R.N. « Ammiraglio Magnaghi » 1923-24. *Mem. R. Com. talassogr. ital.*, 146, 1-146.

DELLA CROCE N., 1964-65 - Crociera No. 8 del R./V. « A. Bruun » nell'Oceano Indiano. *Boll. Mus. Ist. Biol. Univ. Genova*, 33, 5-21.

DELLA CROCE N. & FRONTIER S., 1966 - Thecosomatous Pteropods from the Mozambique Channel. *Boll. Mus. Ist. Biol. Univ. Genova*, 34, 107-113.

KANAZAWA R.H., 1958 - A revision of the eels of the genus *Conger* with descriptions of four new species. *Proc. U.S. nat. Mus.*, 108, 219-267.

KNER R., 1867 - *Reise der österreichischen Fregatte Novara um die Erde in dem Jahren* 1857, 1858, 1859, *unter den Belfchlen des Commodore B. von Wüllerstorf - Urbair. Zoologischer. Theil. Fische.*, Wien, 3, 273-433.

NAIR R.V., 1946 - On the leptocephalus of *Uroconger lepturus* (Richardson) from the Madras plankton. *Curr. Sci.*, 15 (11), 318-319.

— — 1948 - Leptocephali of the Gulf of Mannar. *Proc. Indian Acad. Sci.*, 27 B (4), 87-91.

NAIR R.V. & MOHAMED K.H., 1960 - Studies on the leptocephali of Bombay waters. III. The metamorphosing stages of *Uroconger lepturus* (Richardson). *Proc. Indian Acad. Sci.*, 52 B, 182-190.

PLAYFAIR R.L. & GUNTHER A., 1866 - *The fishes of Zanzibar*, London, v + 153 pp.

SMITH J.L.B., 1962 - The moray eels of the Western Indian Ocean and the Red Sea. *Ichthyol. Bull. Rhodes Univ.*, 23, 421-444.

RIASSUNTO

Esemplari di Leptocefali vennero raccolti nel Canale di Mozambico nel corso della crociera no. 8 del R./V. « A. Bruun » in occasione della Spedizione Internazionale nell'Oceano Indiano. Tale raccolta, che avvenne prevalentemente di notte e in acque superficiali caratterizzate da « scattering » registrato al PGR, comprendeva ventidue larve appartenenti a undici generi e a tredici specie. Una di queste larve, di un tipo non osservato in precedenza, è caratterizzata dall'avere il pigmento sparso irregolarmente sulla superficie laterale del corpo e viene descritta come una nuova specie di *Leptocephalus*. Le altre larve vengono riferite a *Ariosoma mauritianum*, *Gnathophis habenatus*, *G. incognitus*, *Conger wilsoni*, *Uroconger* ? *braueri*, *Nemichthys scolopaceus*, *Nettastoma* ? *parviceps*, a due specie di *Gymnothorax*, ad *Anarchias* sp., ? *Leiuranus* sp. e a *Myrophis* sp.

SUMMARY

Eel-larvae have been collected in the Mozambique Channel on cruise no. 8 of the R./V. « A. Bruun », during the International Indian Ocean Expedition. The collection, which took place mainly at night in surface waters where scattering was recorded by the PGR, included twenty-two larvae belonging to eleven genera and thirteen species. One of these larvae is of a previously unrecorded type, characterized by pigment scattered irregularly over the lateral body surface, and is described as a new species of *Leptocephalus*. The remaining larvae are referred to *Ariosoma mauritianum*, *Gnathophis habenatus*, *G. incognitus*, *Conger wilsoni*, *Uroconger* ? *braueri*, *Nemichthys scolopaceus*, *Nettastoma* ? *parviceps*, two species of *Gymnothorax*, *Anarchias* sp., ? *Leiuranus* sp. and *Myrophis* sp.

Reprinted from *Deep-sea Res.*, vol. 13, 1966, p. 229-234

The Indian Ocean Biological Centre : The centre for sorting plankton samples of the International Indian Ocean Expedition

VAGN KR. HANSEN*

(*Received* 11 *November* 1965)

INTRODUCTION

AT AN early stage in the planning of the International Indian Ocean Expedition (IIOE) it was realized that a large number of zooplankton samples would be collected during the expedition and it was suggested that a sorting centre be organized.

Of all marine biological samples the zooplankton samples require the most time for analysis. A net haul frequently captures a plankton sample with thousands of specimens ranging in size from a few hundred μ to several decimeters. The species represented may run into hundreds—at least in the tropics. The individual biologist is consequently faced with the problem of sorting the species or groups which he wants to study. His own sorting capacity is limited and his institute usually does not have an adequate staff of professional sorters. It is for this reason that an enormous number of plankton samples collected in the past, have never been reported upon, a situation which also prevails at present.

If the zooplankton samples collected during the International Indian Ocean Expedition (IIOE) were not to suffer the same fate, it was obvious that some 'machinery' had to be set up so that the large number of samples could be sorted on a massive scale and be made available for detailed studies by specialists. In order to do this, and also to have comparable samples taken aboard the individual vessels taking part in the IIOE, it was necessary to standardize the methods used both at sea and in the laboratory—in a sorting centre.

The most successfully co-ordinated part of the biological program in the IIOE were the zooplankton investigations. It has been the only biological program to which the participating nations contributed samples taken by the standard methods recommended and for which a single collection with relevant data was maintained. This collection, the International Collection, is located at the Indian Ocean Biological Centre (IOBC) in Ernakulam (near Cochin), Kerala, S. W. India and is by far the largest and most important zooplankton collection from the Indian Ocean in the world today. It can be compared both in quality of material and accuracy of sorting with, for example, the *Dana* Collections, in Denmark.

Development and aims of the Indian Ocean Biological Centre. In the zooplankton program of IIOE the main objective was to study the quantitative and qualitative distribution of planktonic animals. Standardization of the methods to be used at sea were first outlined in New York in 1959 at a meeting of the Special Committee on Oceanic Research (SCOR), held simultaneously with the First Oceanographic Congress. Definite proposals that the analysis of the zooplankton samples collected be made at a centre in India were introduced by the Indian Ocean Working Group in Copenhagen (1960) and again at the meeting of SCOR in Helsinki [INTERGOVERNMENTAL OCEANOGRAPHIC COMMISSION (IOC) 1962; INDIAN COUNCIL ON SCIENTIFIC AND INDUSTRIAL RESEARCH (ICSIR) 1962].

To consider the methods to be used on shipboard and the organization of the sorting centre, UNESCO and SCOR set up a zooplankton working group which met in 1961 in Cochin, S. India, and in New Delhi with representatives of the nations taking part in the IIOE (IOC, 1962; ICSIR, 1962). All participating nations had plans for distributional surveys of the zooplankton. To ensure uniformity in sampling, recommendations were made concerning the adoption of a standard sampling device, as well as uniform procedures in its operation and in the further treatment of the samples (CURRIE, 1963).

*First International Curator, Indian Ocean Biological Centre, Ernakulam, India.

A special net, the Indian Ocean Standard Net was designed, having a mouth area of one square metre and a total length of 5 m. Its filtering area is made of nylon gauze with a mesh aperture of 0·330 mm. It was recommended that each research vessel, every night between 2200 and 0200 hours local time, take one vertical haul from 200 m to the surface, hauling in the net at a speed of 1 m/sec. The samples then were to be preserved in 10% formalin neutralized with hexamethylenetetramine. The displacement volume of the catch should, if possible, be measured at the earliest opportunity by an accepted method. The samples would then be sent to the Sorting Centre for further processing. Many vessels took duplicate hauls, one for the Centre and one for the use of individual scientists in their respective countries.

At the meeting of the International Co-ordination Group for the International Indian Ocean Expedition in January 1964 it was recommended that, in regions with a well-established thermocline between the surface and 200 m depth, an additional haul be taken from the top of the thermocline to the surface.

The functions of the Sorting Centre as discussed in 1960 in Copenhagen are : (1) To sort zooplankton samples taken by the standard method. (2) To examine the samples thus sorted or send them to specialists throughout the world. (3) To maintain a named reference collection of Indian Ocean zooplankton. (4) To prepare named reference collections of Indian Ocean zooplankton for other laboratories throughout the world. (5) To sort other zooplankton samples upon request at the expense of the requesting laboratory. (6) To sort other biological samples by special arrangement with individual laboratories. (7) To organize a training program.

It was recommended that the Centre be located in India, because the country has a rich tradition in taxonomy, a considerable interest in marine studies and a large number of young Indian biologists available for such a Centre. When fully developed the institute may well function as a regional centre for plankton studies in Southeast Asia. During the actual period of the expedition, the location of the Centre in India would be an advantage as many research vessels would call at Indian ports. This would facilitate transfer of biological material to the Centre. The Indian National Committee on Oceanic Research welcomed the establishment of such a Centre in India and recommended that it be located at Ernakulam, a town close to the port of Cochin, one of the three good harbours on the west coast of India. The SCOR–UNESCO working group which met in India in 1961 endorsed this recommendation. UNESCO, represented by the Director of the Office of Oceanography, was prepared to support the Centre which was named the Indian Ocean Biological Centre (IOBC).

As a result, the Indian Council of Scientific and Industrial Research was to provide buildings, staff and running expenses, with a total budget of one million rupees (about U.S. $200,000) for a period of five years. A staff of 29 scientists of whom 20 were to be sorters, and an administrative and technical staff of 24 was proposed. UNESCO was to supply equipment not available in India, up to a value of roughly U.S. $20,000, and on the advice of SCOR, appointed a Consultative Committee for the IOBC as well as a Curator of the International Collection, the expenses incurred for this part of the program were to be paid by UNESCO.

The report from the meetings in India was circulated by SCOR in November 1961. UNESCO reported its action in August 1962 and encouraged those participating in the International Indian Ocean Expedition to send samples to the IOBC (IOC, 1962). This suggestion was promptly acted upon by the Union of South Africa and U.S.A.

Dr. N. K. Panikkar, Director, Indian Program, Indian Ocean Expedition, started organizing the IOBC, and a small staff had been appointed by the end of 1962. Rooms and facilities were placed at their disposal for a period of a few years by the Oceanographic Laboratory of Kerala University. In February 1963, the first meeting of the Consultative Committee was held at the Centre and proposals were made concerning its further development. UNESCO appointed a Curator, Vagn Kr. Hansen from April 1, 1963. The organization of the sorting was started immediately with a staff of 3 scientists. The staff increased gradually as the number of samples increased and in February 1965, when the first curator left the Centre, there were 3 scientific officers, 14 younger scientists (sorters), and a technical and administrative personnel of 17. All the present sorters have academic degrees (11 a M.Sc., 3 a B.Sc.).

The administration of the Collection is delegated to the Deputy Director of the Central Marine Fisheries Research Institute, Dr. R. R. Prasad part-time Chief Scientist-in-Charge of the IOBC and to Mr. L. R. Kasturirangan, Acting Assistant Curator, while Dr. S. Z. Qasim, Assistant Director of the International Biological Programme is Head of Office at the Centre. UNESCO has appointed

Dr. E. Brinton, Scripps Institution of Oceanography, La Jolla, California, as the Second International Curator. He assumed his duties in October 1965 and will be responsible for the International Collection, as well as the loan samples.

The international advisory body to the Indian Ocean Biological Centre is the Consultative Committee. It consists of up to six plankton experts nominated by UNESCO on the advice of SCOR. They will normally serve for three years, but not more than six years. The chairman serves for a term of two years. The Consultative Committee has the following " Terms of Reference " :

To assume responsibility through the Curator for the treatment, loan and further examination of the samples constituting the International Collection.

To work out a general procedure for the maintenance of the International Collection.

To advise on the presentation of data resulting from the examination of samples received by the Centre.

To have its members give lectures and seminars to the scientific and technical staff of Indian marine science institutions.

The present members are Mr. R. S. Glover, Scotland (Chairman); Prof. Dr. J. Krey, W. Germany; Prof. Dr. S. Krishnaswamy, India; Dr. J. A. McGowan, U.S.A.; Prof. S. Motoda, Japan and Dr. M. E. Vinogradov, U.S.S.R. The Committee has thus far had three annual meetings at Cochin, the reports were published by UNESCO (IOC, 1964).

The later meetings have been attended by members of a committee, which determines the policy of the IOBC. This committee is organized under the Indian National Committee on Oceanic Research. Members are representatives of Indian participating agencies, UNESCO and SCOR.

The International Collection. The International Collection is defined as all those plankton samples sent to IOBC by any country during the period of the IIOE and from the area of the IIOE. The International Collection does not, however, include samples sent for contract sorting. The constitution for the International Collection will be published by the Intergovernmental Oceanographic Commission under the title " Provisions for Loan and Examination of the International Collection."

When the sorting started in April 1963, 400 samples were then on hand. It was estimated that there would perhaps be a total of 2300–2500 samples for the whole International Indian Ocean Expedition and as of March 1, 1965, there were actually 1645 samples in the International Collection, of which 88% were taken with the Indian Ocean Standard Net. The other nets used were of a very similar type. Nine nations, Australia, India, Japan, Pakistan, Union of South Africa, U.K., U.S.A., U.S.S.R., and West Germany, have contributed to it.

The areal distribution of samples is fairly good. The Bay of Bengal and the Arabian Sea have received the best coverage, but very few samples were taken in the Madagascar region and in the southeastern Indian Ocean (Fig. 1). Nevertheless, there is no doubt that the International Collection is the most complete and valuable collection of zooplankton from the Indian Ocean—and the most detailed sorted collection. The large number of samples contributed demonstrates the great international interest in supporting the standard zooplankton program of the IIOE, the main object of which is the study of the areal and temporal distribution of the zooplankton in the Indian Ocean. It should also be a source of great encouragement when planning any future international expeditions, as it has now been demonstrated that it is possible to standardize methods used in international surveys.

The sorting technique largely depended on the character of the samples received, taking the following factors into consideration : (1) The time. One of the objects of the Sorting Centre was to have samples processed so that they may be studied by experts as soon as possible after the close of the IIOE in December 1965, the target for completion being 1966. (2) The type of sample sorted. The number of taxa into which the samples were sorted was adjusted to make each subsample of greatest value to the biologist who might request the material for study. (3) The technique. Ideally a plankton sample should be sorted to small taxonomic units (species, genus, etc.). This is essentially impossible and the methods used are thus a compromise. The taxonomic level of the groups selected for identification and/or sorting were such that they can be correctly identified. Thus the subsamples may in some instances be sorted to orders, in others to genus. (4) The size of specimens. Tiny specimens (less than 1–2 mm) of the groups selected for analysis are identified only, but left in the residue, after the larger organisms have been removed.

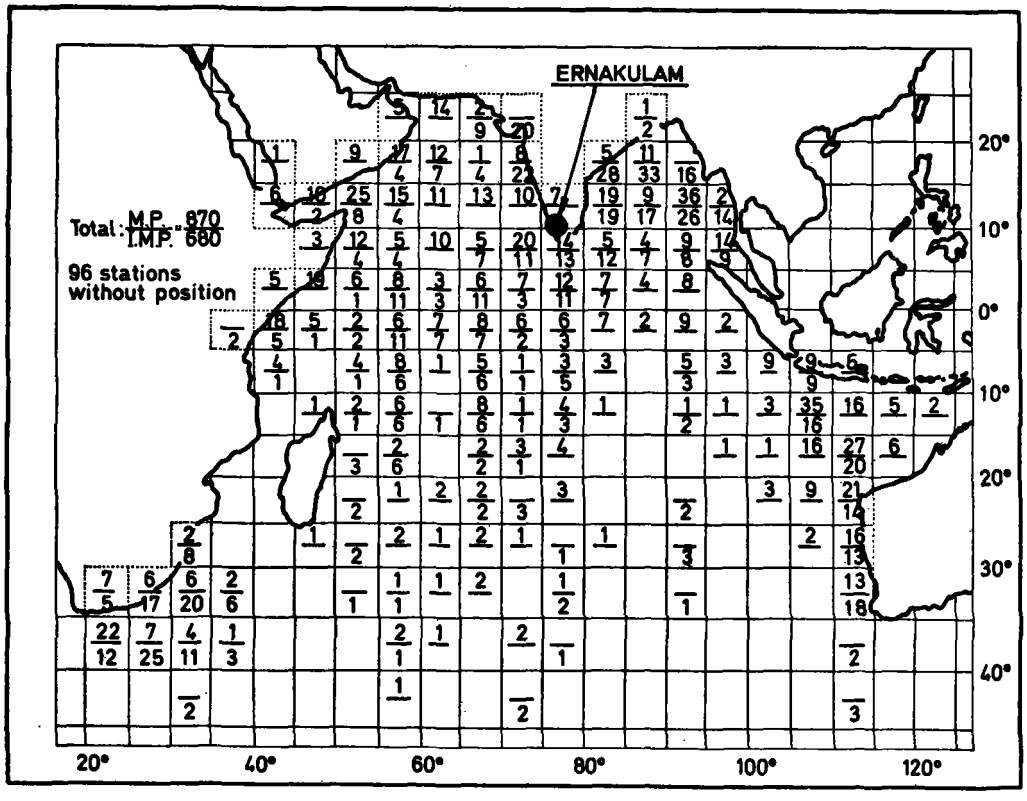


Fig. 1. Location in five degree squares of 1550 samples on file in the International Collection in March 1965. No positions were available for another 96 samples. Numbers above line (M.P.) indicate samples taken in the monsoon periods, numbers below line (I.M.P.) indicate samples from the intermonsoon periods.

The information recorded on the station data sheet is organized for greatest usefulness in ecological studies.

The Curator with the advice of the Consultative Committee defined 77 systematic groups to be used in subdividing the samples. After measuring the total displacement volume and removing all larger organisms including fish eggs, fishes and cephalopods, the remaining organisms are homogeneous in size. A subsample of 3–5 ml is then taken for sorting. The unsorted fraction is stored in the " archives." If the total sample is smaller than 3–5 ml, a standard fraction of 10% is then kept for the " archives." In the processed fraction 63 plankton groups are sorted, counted and preserved separately, and 14 are identified and counted, but left in the residue. The subsamples are stored by coded groups.

The sorting is carried out manually with marten hair brushes under hand lenses; tiny specimens are transferred in pipettes. After sorting, each fraction is checked under a binocular by the individual sorter, and rechecked by the Curator or the senior staff. All samples are stored in the dark and are preserved in 10% formalin neutralized with hexamethylenetetramine. The stored samples are checked for pH at intervals of 3–6 months.

During recent months the average rate of processing has been one sample per week per sorter. By March 1965, 650 samples had been processed, and assuming an increase in the staff of sorters to 20, all the samples from the IIOE will be completed by the end of 1966.

The International Collection and all the sorting activity of the IOBC is still temporarily located in the premises of the Oceanographic laboratory, Kerala University, with floor space available 340 m² (Fig. 2 and 3). This modern building is situated a few meters from the shore of the backwaters,



Fig. 2. General view of the University Oceanographic Laboratory from Foreshore Road.



Fig. 3. View from the main laboratory, where all sorting takes place.

opposite the pier for the University research cutter *Conch*. There is thus ample opportunity for field work both in the vast and very interesting backwaters north and south of Ernakulam and in the open ocean some miles off Cochin harbour, where larger research vessels may be berthed.

The sorters work in a main laboratory (6 m × 19 m) which can accomodate 20 sorters. The Collection is stored in a small room next to the main laboratory. The senior scientific staff and the library occupy three other rooms, two of which are air-conditioned.

Already several foreign scientists have studied the International Collection at the Centre, where an air-conditioned room with laboratory facilities is available. Just behind the University Oceanographic Laboratory a hostel has recently been completed for the University students and staff, which also has rooms for scientists visiting the IOBC.

Reports on the development of the Centre and its activities have been published by UNESCO and various authors (IOC, 1963, 1964; MOTODA, 1964; VINOGRADOV, 1964).

The future of the International Collection. The Centre has been functioning as a sorting agency since 1963. The main task during this initial period has been to organize the sorting of the International Collection. This has been succesfully accomplished because of the foresight of the responsible Indian agencies in appointing a highly qualified staff of sorters. Other activities have also been included, such as sorting of samples on contract for other laboratories (Australia) and, from the beginning, research has been a part of the daily activity at the Centre through the affiliation of Indian research fellows with the permanent scientific staff. This research is a part of the Indian National program of the International Indian Ocean Expedition and includes not only work in zoology but also in chemical oceanography and in primary productivity.

In the future, after sorting has been completed, the main object of research should however be concerned with the International Collection. One of the functions of the Centre is to serve as an agency for sorted samples. These fractions can be sent to approved experts round in the world. Though some specialists interested in the Indian Ocean may want to study the entire collection in their field of interest many may have adequate national collections for basic work but will wish to consult the International Collection for comparative data. This may explain the limited response to the questionnaire circulated to all participating countries requesting the names of experts interested in receiving material for study for they may not have as yet completed the study of their own collections.

It is of great importance that the IOBC come into contract with as many potential collaborators as possible. Scientists interested in receiving samples for study are encouraged to contact the Curator, Indian Ocean Biological Centre, Ernakulam – 6, S. India. It has been proposed that qualified staff members of the IOBC in collaboration with a team of experts should study the data already available for a general description of the qualitative and quantitative distribution of the zooplankton of the Indian Ocean. This team should work at the IOBC and thus encourage foreign and Indian scientists to study the Collection on the spot. The advantage of doing this work at the IOBC is obvious because all data and samples are available there as well as adequate equipment. In addition it will make the institute an extremely valuable training centre in modern ocean ecology. As a result the marine biologists from the Indian Ocean region will continue to receive the advice of the Consultative Committee both on taxonomic studies as well as large scale ecological research based upon the International Collection. It is fortunate that almost all the young scientists at the IOBC have stayed on in the tedious job as sorters. This valuable group of experienced young men working in close collaboration with established research workers may function as a nucleus for future research on the International Collection.

Remarkable progress has been and continues to be made at the Indian Ocean Biological Centre which is now only in its third year. It is most important that support should not only be continued but increased both scientifically and financially.

REFERENCES

CURRIE R. I. (1963) The Indian Ocean Standard net. *Deep-Sea Res.*, **10**, (1), 27–32.

INDIA, COUNCIL ON SCIENTIFIC AND INDUSTRIAL RESEARCH (1962). Indian Scientific Programmes, 1962–1965, 38–40.

INTERGOVERNMENTAL OCEANOGRAPHIC COMMISSION (1962) *International Indian Ocean Expedition, Information Paper*, (1), 5.

INTERGOVERNMENTAL OCEANOGRAPHIC COMMISSION (1963) *International Indian Ocean Expedition, Information Paper*, (4), 15.

INTERGOVERNMENTAL OCEANOGRAPHIC COMMISSION (1964) *International Indian Ocean Expedition, Information Paper*, (7), 1–6, and Appx. I, II and III.

MOTODA S. (1964) Latest information on Indian Ocean Biological Centre. *Inform. Bull. Planktol., Japan*, **11**, 99–102.

PRASAD R. R. and L. R. KASTURIRANGAN (in press) Indian Ocean Biological Centre : an account of its inception, organization and working.

VINOGRADOV M. E. (1964) Second meeting of the Consultative Committee for the Biological Centre (Cochin, India). (In Russian). *Okeanologiia, Akad. Nauk, SSSR*, **4** (4), 735–736.

Reprinted from *Curr. Sci.*, vol. 35, no. 18, 1966, p. 451-455

FISHERY RESOURCES OF THE INDIAN OCEAN*

N. K. PANIKKAR

National Institute of Oceanography, CSIR, New Delhi

I. Introduction

INTEREST in Indian Ocean Fisheries has been a comparatively recent development in the history of world fisheries and has principally stemmed from efforts of countries like India to step up their supply of protein to their large populations. These efforts of the Asian countries have been assisted by United Nations Agencies, notably the Food and Agriculture Organization. A third contributory factor has been the efforts of countries with distant water fishing fleets to operate in the Indian Ocean. Pioneer work of this type has been the fishing effort of Japan in the Indian Ocean, particularly for tuna, and the more recent efforts of the Soviet Union at exploratory fishing. Australia, South Africa and India have been engaged in exploratory surveys in the regions of the Indian Ocean near their own coasts.

When the programmes of the International Indian Ocean Expedition were formulated, fisheries potential was used as an impressive argument to stimulate interest in the project in the Asian and African countries. A quarter of the world's population lives in countries bordering the Indian Ocean, largely in low nutritional standards in terms of calories and acute deficiency in terms of animal protein. Pressure on land use was acute in most countries and added food resources from the sea were clearly indicated as a much needed economic and nutritional corrective. Basic fisheries programmes and attendant biological surveys were included in the earlier draft proposals; physical oceanography was closely dovetailed to chemical biology and plankton studies. In spite of all these, the actual fisheries work accomplished during the expedition itself has been disappointingly small, a fact which is not unconnected with the lack of facilities for exploratory fishing in most ships which took part in the Expedition, with heavily weighted programmes in physical, chemical and geological work. The results of these studies need not be considered negative by those interested in fishery science because the expedition results are clearly bringing out many features of physical and chemical oceanography of the Indian Ocean which have close bearing on the location of fisheries resources, particularly the mapping of areas of upwelling and the movements of the low oxygen waters.

II. Previous Reviews

In a brief account as this, it will not be possible to evaluate critically all the available data but the broad features are given as have emerged from the various studies which are going on in different centres of marine research. Further exploratory and commercial fishing requires more critical evaluation of physical and chemical data collected on a synoptic basis to make fishing operations in specified regions economical. Following the International Indian Ocean Expedition, it is hoped that such critical work will be taken up by the Indian Ocean countries themselves within the forthcoming years.

III. Physical and Chemical Features of the Indian Ocean

Seasonal mixing of surface and deep waters as occurs in the colder latitudes does not occur in most parts of the Indian Ocean and one has to look for the areas of divergence and upwelling to find the turnover of bottom waters to the surface. Two areas of the Indian Ocean, the Red Sea and the Persian Gulf are regions of high salinity and temperature and of these, the higher salinity influences the Northern Arabian Sea. Apart from this, the intense evaporation in the northern part of the Arabian Sea is also responsible for the high salinity of the waters of this region. The Bay of Bengal on the other hand represents waters warmer than the Arabian Sea but with pronounced estuarine influence with several large rivers opening into it. The average salinities are lower here than in the Arabian Sea.

The southern half of the Indian Ocean has characteristics not unlike the southern basins of Pacific and Atlantic bordering on the Antarctic. From the fishery point of view it is noteworthy that for most parts of the entire Indian Ocean, the continental shelf is narrow.

One of the features of the Indian Ocean is the fact that it is largely influenced by the monsoons. The formation of the monsoons and related atmospheric phenomena have been discussed by other speakers at this Congress. The

* Summary of lecture delivered at the Second International Oceanographic Congress, Moscow, 7th June 1966.

monsoon systems are specially pronounced in the Arabian Sea and the Bay of Bengal both the areas being entirely under the regimes of the south-west and north-east monsoons. The southern hemisphere is free from these large-scale wind systems except to a small extent towards west of Australia and to the east of South Africa.

The strong south-west winds during May to early September often deflect large masses of water from the surface and the replenishment of these by the deeper waters result in upwelling. One important area where upwelling following strong offshore winds occurs is the Somali coast, where, in addition, a powerful current going northwards of East Africa in a clockwise direction grazes Arabia, Pakistan and even up to Indian West Coast. This summer pattern is reversed in the north-east monsoon time when offshore winds off the Kathiawar Peninsula result in upwelling particularly in the Gulf of Cambay (Jayaraman and Gogate, 1957).[7] Similarly large-scale upwelling occurs during the south-west monsoons in the south-west coast of India, there is the complex phenomenon of several physical factors acting together the net result of which is the large-scale movement of high nutrient laden, low temperature and low oxygen waters to the surface (Panikkar and Jayaraman, 1956).[2]

One physical feature of the Indian Ocean which has been noted in former years but has come to special comment and observations during the International Indian Ocean Expedition is the regime relating to waters and bottom areas having little or no oxygen. Certain areas in the Arabian Sea have been known as azoic areas from the time of the John Murray Expedition (Sewell, 1955)[5] and several such areas have been noted by Soviet Ships where the azoic conditions prevail in several parts of the western shelf in Gulf of Cambay and off Arabia.

It has been observed by most of the ships participating in the Indian Ocean Expedition that the waters of the Arabian Sea are deficient in oxygen reaching the minimum by about 200–500 meters. It has further been observed by Indian workers and by other ships that the actual oxygen minimum layer comes fairly close to the surface towards the west coast of India during the south-west monsoon regime (Panikkar and Jayaraman, 1966). More critical work is needed to correlate wind force and upwelling. The movements of the oxygen minimum layer may have the beneficial effect of concentrating populations of fish towards the coast in certain seasons but it is equally possible that in the open ocean the surface areas of high productivity do not reach their culmination into profitable fisheries owing to the calamitous effects of low oxygen water. These may well be the cause of large-scale fluctuations in certain fisheries as of the oil sardine of the Indian West Coast and of large-scale mortalities.

IV. Biological Aspects of the Indian Ocean

The major part of the Indian Ocean from the fisheries point of view is composed of a tropical Northern two-thirds of the ocean which is continuous in faunal characters with the larger marine Indo-Pacific area which is a distinct marine zoogeographical division. This area covers the Arabian Sea, Bay of Bengal, Eastern Central Indian Ocean and the smaller seas associated with the eastern archipelago and the equatorial region. The other regions which have specific biological characteristics are the temperate South African region which has characteristic temperate fisheries, the West Australian region which has comparable but different fisheries and an East African tropical region which has tropical fisheries, different from the Indo-Pacific. The Gulf of Aden has certain specific fishery characters but in the main, the commercial species are dominant elements of the Indo-Pacific fauna. Finally, there is the oceanic fishery consisting mainly of stocks of tuna, sail-fish, etc., which assume considerable importance in the Eastern Central Indian Ocean.

The tropical Indian Ocean waters are likewise regions where extensive coral reefs are found with several hundreds of coral islands. While the reefs have contributed much to the remarkable diversity of animal and plant life in the Indian Ocean harbouring several thousands of species forming a reef fauna and flora, it has not contributed to large-scale fishing banks. Even good stocks on reefs are difficult to exploit owing to hazardous fishing on reefs.

The principal features relating to fisheries on the Indian Ocean are that the pelagic and mid-pelagic species dominate the commercial catches with a corresponding reduction in numbers of the ground fish suitable for large-scale trawling. The gadoids which form extensive fisheries in North Atlantic and North Pacific are conspicuous by their absence; this group is represented only by one genus (*Bregmaceros*) whose yield is negligible. Similarly the flat fishes also occupy a low place in the total production and many of them are of small size and confined to the inshore areas.

The southern part of the Indian Ocean to the east of Southern Africa and to the west of Australia, however, present characteristics which are common with the temperate zones with an increased predominance of ground species including the larger gadoids and lobsters.

Most commercial species are characterised by having comparatively longer breeding seasons and one of the peculiarities of fish stocks is the predominance of the younger age groups in the commercial catches. According to a rough calculation, nearly 3/4ths of the entire catches in the Indian Ocean are taken up by fish not more than three years old and even among this, the zero year class is a major contribution to the fisheries in the warmer regions where the rate of growth is rapid. It is in this context that the close relationship between areas of upwelling, high productivity and dense plankton assume special significance in the location of commercial fisheries.

A feature of the Indian Ocean fish fauna in relation to the coastal fisheries whose importance is not often appreciated is that throughout the Indo-Pacific there are important species which are primarily found in the sea and breed in the sea and coastal waters, but ascend estuaries and coastal lagoons when they are young. Annual migrations of young fish of this type take place throughout the coastline and the yield from their harvest in the areas immediately adjoining the coastline is very considerable. To this category belongs the well-known Milk-fish, *Chanos chanos*, species of mullet and of penæid prawns. Species like *Hilsa* which are migratory estuarine fish are important on the coasts of Pakistan and India.

In the Indian Ocean are the areas like Persian Gulf which are shallow platforms forming continental shelves like the North Sea but unfortunately the productivity of these areas is very low. The indications are, therefore, that speaking for the whole area the prospects for trawl fishing are limited except in certain regions where specialised conditions seem to favour such efforts. Areas to the west of Port Okha and west of Ceylon, some regions of the Gulf of Oman and the western coast of Australia and eastern and southern coasts of South Africa are probably areas where efforts in trawling would be commercially successful.

V. Fisheries Yields from the Indian Ocean

Production of fish in the Indian Ocean during the past 15 years or so has, according to FAO fisheries statistics, increased from 1·3 million tons to about 1·8 million tons in 1964 although a still higher figure of 1·9 million tons was touched in 1960. These figures are not likely to be complete. Rass (1965)[4] has estimated the yield at about 2·0 million tons but my own estimate of current production is of the order of 2·5 million tons, but in the following discussions FAO figures have been taken as the basis. The trend of the landings also shows that the increase has taken place both in western and eastern Indian Ocean; but since the output from the western Indian Ocean is greater than the eastern, the present total production is roughly of the order of 1 to 1·1 million tons in the western Indian Ocean, as against 0·8 million tons on the eastern Indian Ocean. In relation to total world marine catch, however, the increase in the Indian Ocean is far from impressive and in fact the percentage contributed by Indian Ocean to the world catch has decreased from about 7% in 1949 to 5% during the past few years. The production from the western and eastern areas in relation to the world total catch is of the order of 3% for the western Indian Ocean and 2% for the eastern Indian Ocean. Considering 1957–59 as the base year at the Index Number 100, the marine fisheries of the Indian Ocean in 1964 has registered an increase to 112, as against the world marine catch increase to the Index Number of 157. These figures show that increase in yield from Indian Ocean has not kept pace with the increase in world catch and indicates the scope of further output. Even assuming that the rate of increase as has taken place in other parts of the world is all that is possible, we should expect the 2·5 million tons to improve to 3·6 million tons with better technology and effort. The rate of increase at least for quite some years could be substantial with more effort because many fisheries have hardly been touched at all, many offshore stocks are not exploited and many inshore stocks are underfished.

At present the major fish-producing country of the region is India with an yield of about 900,000 tons.

The production from the East African countries is at present of the order of 65,000 tons which is shared by 12 countries. The largest yield is from Tanzania, the total production from Zanzibar and Tanganyika accounts for nearly 20,000 tons. Next in importance is the Malagasay Republic 15,000 tons (average for 1961–63) and Ethiopia, mostly on the Red Sea side at 11,000 tons. It is interesting to note

that nearly 45% of the contribution from East African countries are demersal fisheries with the sardines ranking next (18·5%). A very promising area of the African coast is the Mozambique coast as judged by productivity, where the present yield is only 4,000 tons. The Somali region, Gulf of Aden and the areas of Gulf of Oman are promising areas for further effort. This is borne out by nutrient distribution and primary production studies. One of the clear tasks will be to differentiate between pelagic, mid-pelagic and demersal stocks and to assess their intensity, and to establish the niche at which the high productivity results in good commercial fisheries.

VI. Future Prospects of Indian Ocean Fisheries

What then are the prospects for expanding the existing fisheries ? It may be argued with reasonable certainty that productive regions like the Andaman Sea, West coast of Burma, Coasts of Ceylon, West Coast of India, Coast of West Pakistan, Gulf of Aden and Oman, Somali Coast, South African and West Australian coasts are all areas where substantial increase in production is possible from stocks already known and partially exploited. Gulf of Aden, Somali region and South-West Coast of India deserve special mention if phosphates, chlorophyll and phytoplankton are taken into consideration. Some authors have calculated a scope of increase nearly as much as 10 times the present landings and this increase in the yield of the neritic pelagic complex of fishes appears feasible, whereas a much larger increase based on new stocks is quite possible in the newly found productive areas like the Gulf of Aden, Gulf of Oman and Somali coasts.

As regards increased capacity for trawler yields the scope really lies in fishing beyond the marginal seas on the shelf and on the slope of the shelf. Here, experience obtained on the west coast of India in the Kathiawar area might well be indicative of what might be found in the other Arabian Sea areas where the shelf is productive. From trawler fishing the increase may not be much in terms of total yield but substantial in terms of value.

Another bright future is with reference to oceanic fisheries—tunas and other larger Scombroids. Here we may expect a substantial increase from the present 150 thousand tons per annum. The Gulf of Aden is a most promising area for long lining and purse seining for tuna showing some of the highest catch rates recorded and the average Indian Ocean yield of tuna obtained by Japanese vessels are higher than in the Pacific and Atlantic.

The increase in Crustacean fisheries would take place by bringing many areas to fishing but with increased attempts to find out the deep water prawns in the farther waters of the shelf and even on the slope. Prawns which are capable of utilising the coastal inlets for quick growth and development already feature largely in the crustacean production of some Indian Ocean countries and it is to be expected that these practices will become widely spread, based on the breeding oceanic stocks and the young zero year class growing rapidly in coastal belts.

A fishery which is now of low magnitude but which offers great scope in the future relates to the Mollusca which are capable of giving very high yields from the shallow coastal areas of the tropical seas. The yield per acre is exceptionally high and may figure very considerably in future years.

The general picture emerging out of the present information on the fisheries resources of the Indian Ocean and the oceanographic data which are accumulating as a result of the International Indian Ocean Expedition is that there is much scope for increased production from the Indian Ocean than the present rough yield of about 2·5 million tons. Increase in pelagic fisheries is possible in areas which have been diagnosed as areas of divergence and upwelling, higher dissolved nutrients, and higher plankton biomass.

Apart from the well-known pelagic fisheries and the shoaling species of sardines and the scombroids the indications are that the actual fish stocks with reference to an individual species are not of a large magnitude. Instead, there exist a large number of smaller fisheries composed of species with wide range of distribution but forming commercial fisheries in areas widely distant from one another. In many areas of the Indian Ocean the large increase is to come from exploitation of the waters adjoining the coast directed to utilize these miscellaneous fisheries. The technological needs for substantial increase from these fisheries are :—

1. Modern techniques of fish finding and scouting of large concentrations of scombroids and clupeoids in the highly productive areas.
2. Methods to concentrate the somewhat sparse populations of miscellaneous groups of fishes by entirely new techniques

involving the use of light, sound or electricity to make the yield economical.

3. Intensive studies on selected parameters like temperature and oxygen distribution to locate the fish stocks and their area-wise distribution in different seasons.

It was mentioned in an earlier section that the present yield from the Indian Ocean may roughly be put as 2·0 million tons, and taking into account subsistence and unaccounted sources, as about 2·5 million tons. Fisheries expansion is not entirely determined by the availability of resources but influenced by the needs, capabilities and technological improvements taking place in any country. Experience has shown that this change is not rapid. There are the extremes of very slow development at one end where changes are imperceptible and at the other of rapid introduction of modern fishing craft and gear and all attendant facilities. Both these have acted in the Indian experience of marine fish production, where the general trend is that the output is roughly doubled during a 10-year period. It may not be far off the mark if this rate of development is taken as average for most other Asian and African countries, where there is the need for such expansion, economic support and technical feasibility. In this case the output from the Indian Ocean could roughly be indicated as about 20 million tons per annum towards the close of this century. This is apart from large-scale individual fisheries for oceanic stock like tuna, sardines or mackerel mainly in the upwelling areas where newer and imported technology and factory ships might make substantial catches possible. The outlook for the future of Indian Ocean Fisheries is, therefore, one of moderate optimism. The hope that Indian Ocean can provide a substantial contribution to the food supplies of the bordering countries is fully backed by the newer knowledge of oceanography.

1. Jayaraman, R. and Gogate, S. S., *Proc. Ind. Acad. Sci.*, 1957, **45 B**, 151.
2. Panikkar, N. K. and Jayaraman, R., *Proc. 8th Pacific Science Congress*, Philippines (1953)/ 1956, p. 1111.
3. — and —, *Proc. Ind. Acad. Sci.*, B, 1966 (In press),
4. Rass, T. S., *Trudy Institut. Okeanologie*, 1965, **80**, 1.
5. Sewell, R. B. S., *Proc. Linn. Soc. London*, Session 165, 1955, p. 188.

Reprinted from *Proc. Ind. Acad. Sci.*, vol. LXIV, no. 5, sect. B, 1966, p. 231-240

BIOLOGICAL AND OCEANOGRAPHIC DIFFERENCES BETWEEN THE ARABIAN SEA AND THE BAY OF BENGAL AS OBSERVED FROM THE INDIAN REGION

BY N. K. PANIKKAR, F.A.SC. AND R. JAYARAMAN

(National Institute of Oceanography, C.S.I.R., New Delhi)

Received June 3, 1966

ABSTRACT

The paper presents some of the important differences in the oceanographical and biological conditions in the waters of the Arabian Sea and the Bay of Bengal along the Indian coasts. In discussing the biological variability of the two environments from the point of view of fishery productivity, attention is particularly drawn to the extremely complex nature of the oil sardine and mackerel fisheries, especially along the west coast of India, which accounts for the bulk of the fish landings. An attempt is being made to provide a suitable explanation for this on the basis of the nutrient distribution pattern associated with the occurrence of seasonal 'upwelling'. It is also pointed out that the 'upwelling' processes along the west coast of India are also of a complex nature and the forces leading to this are yet to be properly understood. Some comparison is drawn between the conditions on the south-west coast of India and some of the classical upwelling regions of the world, particularly with reference to two important features, namely, formation and disappearance of temporary banks of mud and the occurrence of special planktonic blooms often leading to mass mortality of fish.

INTRODUCTION

FOR several years past the differences in the availability of fish on the west coast (or Arabian Sea Coast) and on the east coast (or the Bay of Bengal Coast) of India, has been quite a puzzling feature in India's sea-fish production. The fact that the coast between Bombay and Cochin accounted for heavy fish landings has been known for several centuries, but only during the past 15 years or so, during which the fisheries statistical system has been slowly evolved, has it been possible to establish that nearly 75% of Indian sea-fish production out of a total annual production of 700-900 thousand tons (Table I) come from the west coast of India and even within this coastline

the strip between Quilon in South, and Ratnagiri in the North accounted for the bulk of the catch, the main components of this neritic-pelagic fishery being the Indian Mackerel, *Rastrelliger kanagurta*, the Malabar Sardine, *Sardinella longiceps* and related *Clupeoids*, the sole, *Cynoglossus semifasciatus* and the penaeid prawns of several species.

TABLE I

Showing the landings of oil sardine, mackerel and sole on the west coast of India during a 16*-year period*, 1950–1965*

[Landings in Metric Tons (Tonnes)].

Year	Oil sardine	Mackerel	Malabar sole
1950	34,420	86,736	..
1951	17,240	1,03,574	..
1952	13,895	77,295	..
1953	51,831	69,597	..
1954	33,952	27,892	1,657*
1955	30,447	21,848	5,507*
1956	7,412	15,023	9,122
1957	1,91,469	86,741	3,687
1958	1,23,282	1,23,282	12,856
1959	69,234	62,198	10,360
1960	1,89,016	1,33,655	14,103
1961	1,67,884	34,485	7,730
1962	1,10,299	29,103	17,644
1963	63,645	72,694	8,062
1964	2,74,307	19,097	4,691
1965	2,61,918	40,836	11,699

* Long tons.

Trend of Fisheries

To the student of geographical distribution who looks for individual species of fish, these present no features of interest, because they are all widely distributed Indo-Pacific species found along the coasts of India and adjoining countries. Both *Rastrelliger* and *Sardinella* occur on both sides of the Indian coast; but while small-scale or negligible landings of these are observed on the Bay of Bengal side, their yields run to a few hundred thousand tons on the south-west coast of India (Table I). The oil sardine which primarily feeds on phytoplankton forms a fishery which is subject to great fluctuations, an extreme instance being provided by its landing of 7,412 tons in 1956 m. and 274,307 m. tons in 1964. The mackerel landings were likewise variable during the past 14 years — on an average, about 60,000 m. tons with higher limits of 1,34,000 m. tons. From the Bay of Bengal side, on the other hand, the total yields in the case of both the fisheries have hardly exceeded 5,000 m. tons and in most of the years they form a very small component of the fish catches of the east coast of India, which themselves are very low by comparison with the west coast catches. A year-to-year comparison of the catch per unit of effort in the two regions is given in Table II.

Table II

Comparative figures of catch of fish per unit of effort for the east and west coasts of India in different years†

Catch/Unit Effort (in kg.)

Year	East coast	West coast
1954	0·61	3·18
1955	0·67	2·85
1956	0·92	2·95
1957	0·95	3·59
1958	0·85	3·19
1959	0·95	3·36
1960	1·30	6·75
1961	1·55	4·88
1962	1·27	5·06
1963	1·66	4·94

Unit Effort = Man-hour

† *Source*: Central Marine Fisheries Research Institute, Mandapam.

The causes of the fluctuations in these fisheries have been engaging the attention of the fishery workers in this country for quite some time and despite years of research in this direction, it has not yet been possible to arrive at a satisfactory solution of this problem. A review of the situation up to 1953 appears in a paper by Panikkar and Jayaraman (1956), who have examined this problem with reference to the differences in the hydrological conditions of the waters along the two coasts. The data presented mainly relate to inshore regions where the physico-chemical features are subject to local conditions and the interactions of the various factors in these environments are, in general, of an extremely complex nature. Since the publication of the paper, more offshore cruises have been undertaken on research vessels like *Kalava*, *Varuna* and *INS Kistna*, and data collected over a wider area have yielded more information on the oceanographic conditions in these regions, and provide the basis for a better comparison of the two environments.

OCEANOGRAPHIC FEATURES

In regard to the oceanography of the Arabian Sea and the Bay of Bengal, a number of papers have appeared in recent years giving us a more or less broad picture of the distribution of the main oceanic parameters, the pattern of circulation, current systems, etc. (Rama Sastry and Myrland, 1959; Ramamritham and Jayaraman, 1960; LaFond, 1957). It is a well-known fact that the circulation of waters in the northern Indian Ocean including its two arms, the Arabian Sea and the Bay of Bengal is very much influenced by the pattern of winds associated with the summer and winter monsoons. While the general circulation in the more oceanic areas conform to the wind pattern, the water movements nearer the Indian coasts are governed more by the physical features such as bottom topography, coastal configuration, etc. In general, along the west coast of India, there is prevalent a south to south-easterly surface current from February to September and north-westerly current from November to January. A similar surface drift is seen along the east coast of India also, but this drift has a north-easterly direction with an occasional easterly component between February and July, changing to south-westerly in the northern part of the coast and and to southerly in the southern part during August-September, and continuing in the same direction up to the end of December. In January a weak westerly drift is observed. While all these drifts are known from pilot charts (1953, 1961; also data sheets of Netherlands Meteorological Institute, 1952) we have very little detailed information on these currents. What is interesting from our point of view is that there are considerable differences in the hydrological

properties of the waters along both the coasts—both seasonal and regional—associated with these water movements. It is not clear how far these differences could be directly attributed to these drifts. It is, however, considered necessary to present here some of the salient features in the various hydrological parameters in the waters along both the coasts, to provide the necessary background for discussions on the variability of the conditions in the two areas.

1. *Salinity*

In regard to the surface salinity in both the areas, it is seen that the Bay of Bengal waters are less saline than the waters of the Arabian Sea. The average values are 30–33‰ for the Bay of Bengal and 34–37‰ for the Arabian Sea. These differences are generally explained by the fact that there is considerable influx of freshwater in the Bay of Bengal owing to number of large river systems both on the east coast of India and the Burmese coast leading to the lowering of salinity of the waters of the Bay; while the absence of any such large river system on the west coast of India combined with the intrusion of waters of very high salinity from the northern Arabian Sea, the Persian Gulf and the Red Sea contribute to the high salinity of the Arabian Sea-waters. These are, no doubt, well established details; it would, however, be necessary to indicate that there are also less understood differences in the vertical circulation patterns in the two areas.

2. *Temperature*

(i) *Surface Temperature.*—In the Bay of Bengal, the surface temperatures normally range between 27° C and 29° C., except in shallow areas nearer the coast. The fluctuations are much wider along the Arabian Sea coast of India, the usual range being 23°–29° C.; the lowest temperatures are reached during the latter part of summer monsoon along the southern west coast and during November-January period along the northern west coast. North of Bombay, along 20° N., the surface temperature sometimes reaches a value of 21° C. during late November and early December (Jayaraman and Gogate, 1957).

(ii) *Vertical Distribution Pattern.*—Although a considerable volume of data have accumulated in recent years on the temperature distribution in the Bay of Bengal resulting from the IIOE cruises, details in regard to the vertical distribution of temperature have not yet been completely worked out for this region. The earlier information pertaining to this region is

mainly based on the work of LaFond and co-workers at the Andhra University, Waltair (LaFond, *loc. cit.*). Some broad features in the recent data are indicated by Jayaraman (1965). On the other hand, for the waters along the west coast of India, between Cape Comorin and Bombay, the patterns have been worked out fairly well and even data on seasonal variations in certain selected areas are also available. The two important aspects that should receive our attention, from the point of view of their application to the problem of variations in biological productivity, are: (i) the variations in the thickness of the isothermal or near isothermal upper mixed layer and (ii) the level of the ' thermocline ' or the discontinuity layer. A comparison of these two regions shows that in the Bay of Bengal off the Indian coast, the thermocline level is usually below 50–55 metres, occasionally going down to 100–125 metre level, and except for a small part off the east central coast, the shelf waters are for most of the time isothermal or near isothermal; whereas off the west coast of India, the thermocline fluctuates a great deal, often showing a definite seasonal trend.

It has been found that during winter, off the south-west coast of India, the thermocline is usually found at 100–125 metres and during the stable period between the winter and summer monsoons, the thermocline level is usually 75–90 metres. With the progress of the summer monsoon there is a gradual " upward migration " of the thermocline reaching to 20–30 metres and even surfacing in some areas towards the later half of the summer monsoon and early post-monsoon. This is seen to be a regular feature every year. It is also seen that in the same period, the shelf is occupied with water, which is cold, dense and poorly oxygenated and also very rich in nutrients (Ramamritham and Jayaraman, *loc. cit.*). Based on these findings, it has been postulated that the season of late monsoon and early post-monsoon is the upwelling season along the west coast of India and all the interesting findings in regard to the rich biological and fishery productivity* have been attributed to this seasonal ' upwelling ' along this coast.

UPWELLING AND NUTRIENTS

This upwelling along the south-west coast of India and its possible connection with the fisheries of the area is slowly emerging as a very complex series of events. With a view to understanding the mechanism of this apparently complex phenomenon along this coast and to work out the role of the various

* A detailed study of zooplankton volumes by Prasad (1966 unpublished) has brought clear evidence of the much higher rate of plankton production in the Arabian Sea coastal waters than in most other regions of the Indian Ocean.

contributing factors, investigations have been carried out on the distribution of temperature, salinity, dissolved oxygen and the nutrient salts, particularly phosphates in the different regions along the west coast and along different sections normal to the coast covering both the inshore and offshore regions. The present indications are that " upwelling " is prevalent along the coast between 7° N. and 16° N. latitudes and the period is usually from August to early October. During this period it is observed that dissolved oxygen occurs in concentrations as low as 0·5 ml./l. below 20 metres. The phosphate occurs in very high concentrations in the entire water column over the shelf. In the nearshore areas off Calicut (depth 10 metres), the surface phosphate concentrations reach a figure of 1·94 mg.—at P/m^3 while at the bottom the values are as high as 2·74 mg.—at P/m^3 (Subrahmanyan, 1959). Recently Reddy and Sankaranarayanan (under publication) have found, in course of their studies on the vertical distribution of nutrients (phosphate, silicate and nitrates) along the west coast of India between Quilon and Ratnagiri, there is considerable enrichment of nearshore waters during the period of summer monsoon and early post-monsoon, while after mid-October up to the end of December the values become quite low.

One of the most noteworthy features in the distribution of phosphate in the coastal and nearshore waters off the south-west coast of India is the direct correlation between high concentration of phosphate and a rich crop of phytoplankton during the monsoon months. This observation has been discussed in detail by Jayaraman and Seshappa (1957) who have advanced the view that the peculiar hydrographical conditions associated with the prevailing south-west monsoon is responsible for the rate of replenishment of nutrients far exceeding the rate of utilization. This again is stated to have been brought about in two ways, namely (i) by local regenerative processes and (ii) the influx of nutrient-rich water into this region. In regard to the local regeneration, the principal mechanism is bacterial action on the dead and decaying matter present in the bottom muds possibly associated with heavy mortality of the bottom animals (Seshappa, 1953). The mortality of the bottom animals may be due to the combination of two factors, intrusion of oxygen-low water at the bottom and prevalence of turbulent conditions. Since it is well known that conversion of organically-bound phosphorus into inorganic phosphate is an anaerobic process (Cviic, 1956) the main contributing factor for the prevalence of anaerobic conditions is the intrusion of oxygen-poor water into this region apparently due to upwelling. It may thus be seen that there are a number of factors contributing to the nutrient enrichment in this region, the main

factor being upwelling. It should be pointed here that, although LaFond and others in the course of their studies along the east coast of India have reported upwelling as a regular seasonal phenomenon in the central part of that coast, the waters there, in general, do not contain nutrients in such high concentrations as those along the west coast.

It is, however, to be mentioned that, in spite of so much supporting evidence for the upwelling along the west coast of India, particularly southern part of west coast (the main region of the sardine-mackerel fishery complex), the processes leading to upwelling in this region have not yet been clearly understood. A study of the wind pattern at this time of the year shows that winds prevalent are most unfavourable for upwelling to take place. The dominant winds are onshore and these winds would promote 'piling' of the surface waters on to the coast rather than upwelling. In other words, this is not the typical wind-induced upwelling usually observed in the classical upwelling regions of the world. It is possible that this upwelling is associated with the southerly coastal current prevalent along the west coast of India during this period of the year. A reference in this connection to the observations by Ryther and Menzel (1965) seems pertinent. According to these authors the factors causing upwelling along the Somali-Arabian coasts are due to the prevalent Somali Current as well as the offshore winds. The main reason for this observation is that in this region upwelling is prevalent not only during the south-west monsoon months but also October-November when there is practically no wind at all, the current however being still strong. On the same analogy it is possible to state that along the south-west coast of India although the winds are not favourable, the upwelling might be due to the dynamical factors associated with the southerly current. A detailed study of this water movement, which has not so far been carried out, would provide the necessary answer.

MUD BANK FORMATION

There are, however, one or two factors which indicate a certain amount of similiarity between the west coast of India and other classical upwelling regions of the world. For example, the regular occurrence of mud banks off the south-west coast of India during the closing phase of the south-west monsoon and their disappearance within a period of 4 to 6 weeks are features which are similar to the occurrence of temporary islands of fine mud in the Benguela upwelling region off the west coast of Africa as reported by Hart and Currie (1960). These authors have, however, stated that these islands

almost completely disappeared within 24 hours whereas the mud banks off the Indian coast remain for a longer duration. According to Ramasastry and Myrland (1959) the formation of the mud banks off the Kerala coast is associated with the upwelling of these waters. It should, however, be mentioned that the mud banks formation and disappearance is the result of a series of events and it would be difficult to isolate a single factor and show it as the main causative factor. More detailed studies on these mud banks are being planned and it is hoped that we shall be able to find the answer soon.

Plankton Blooms

The occurrence of sudden blooms of certain planktonic organisms off the west coast of India is another case of similarity with some of the classical upwelling areas. These occur as discoloured patches over vast areas along the coast and often heavy mortalities of fish are associated with the occurrence of these blooms (Bhimachar and George, 1950). The organisms responsible for these blooms are mostly the flagellates, *Noctiluca*, and *Hornellia* (Subrahmanyan, 1954) and also the blue-green alga, *Trichodesmium* sp. Recently Prakash and Sarma (1964) have reported several discoloured patches in the sea off Cochin as being caused by blooms of *Gonyaulax*.

Conclusion

It may thus be seen that the part of the Indian coast known to support a very rich fishery for the mackerel and the oil sardine is a region of great biological and oceanographical complexity, one might almost say, of biological instability. A thorough understanding of the various factors is the *sine qua non* for finding a satisfactory solution to the major problem of the differences in the fishery productivity of the west and east coasts of India.

References

Admiralty .. *Bay of Bengal Pilot*, 1953.

———— .. *West Coast of India Pilot*, 1961.

Banerji, S. K. and Satyanarayana, A. V. V. "A note on the general trend of marine fish catches in India," *Ind. J. Fish.*, 1958, **5**, 195–200.

Bhimachar, B. S. and George, P. C. "Abrupt set-backs in the fisheries of the Malabar and South Canara coasts and 'Red water' phenomenon as the probable cause," *Proc. Ind. Acad. Sci.*, 1950, **31 B**, 339–50.

Cviic, V. .. "Activity of bacteria in the liberation of phosphate from the sea sediments in bottom water," *Acta Adriatica*, 1956, **8**, (4), 1–32.

Hart, T. J. and Currie, R. I. .. "The Benguela Current" *Discovery Reps.*, 1960, **13**, 123–24.

Jayaraman, R. .. "Upwelling along the east coast of India," *Curr. Sci.*, 1965, **34**, 121–22.

——— and Gogate, S. S. .. "Salinity and temperature variations in the surface waters of the Arabian Sea off the Bombay and Saurashtra Coasts," *Proc. Ind. Acad. Sci.*, 1957, **45 B**, 151–64.

——— and Seshappa, G. .. "Phosphorus cycle in the sea with special reference to tropical inshore waters," *Ibid.*, 1957, **46 B**, 110–25.

LaFond, E. C. .. "Oceanographic studies in the Bay of Bengal," *Ibid.*, 1957, **46 B**, 1–46.

Nederlands (K) Meteorologisch Instituut *Indische Ocean Oceanografische en Meteorologische Gegevens*, 2nd Edition. Publication 135, 1952.

Panikkar, N. K. and Jayaraman, R. "Some aspects of productivity in relation to fisheries of Indian neritic waters," *Proc. Eighth Pac. Sci. Congr., Philippines*, 1953 and published in 1956, **3 A**, 1111–22.

Prakash, A. and Viswanatha Sarma, A. H. "'Red water' phenomenon in the west coast of India," *Curr. Sci.*, 1964, **33**, 168.

Ramamritham, C. P. and Jayaraman, R. "Hydrographical features of the continental shelf waters off Cochin during the years 1958 and 1959," *J. Mar. Biol. Ass. India*, 1960, **2** (2), 199–207.

Ramasastry, A. A. and Myrland, P. "Distribution of temperature, salinity and density in the Arabian Sea along the South Malabar Coast (South India) during the post-monsoon season," *Ind. J. Fish.*, 1959, **6**, 223–55.

Ryther, J. H. and Menzel, D. W. "On the production, composition and distribution of organic matter in the western Arabian Sea," *Deep Sea Res.*, 1965, **12** (2), 199–209.

Seshappa, G. .. "Phosphate content of mud banks along the Malabar Coast," *Nature, London*, 1953, **171**, 526–27.

——— .. "Observations on the physical and biological features of the inshore sea bottom along the Malabar Coast," *Proc. Nat. Inst. Sci. India*, 1953, **19**, 257–79.

Subrahmanyan, R. .. "On the life-history and ecology of *Hornellia marina* gen. et sp. nov. (Chloromonadineae) causing green discoloration of the sea and mortality among marine organisms off the Malabar Coast," *Ind. J. Fish.* 1954, **1**, 182–20.

——— .. "Studies on the Phytoplankton of the West Coast of India, Parts I & II," *Proc. Ind. Acad. Sci.*, 1959, **50 B**, 113–252.

Reprinted from *Veröff. Inst. Meeresforsch. Bremerh.*, Sonderband 11, 1966, p. 131-147

Aus dem Institut für Hydrobiologie und Fischereiwissenschaft
der Universität Hamburg

Quantitative Untersuchungen über die Meiofauna des Tiefseebodens

(Vorläufiges Ergebnis der „Meteor"-Expedition in den Indischen Ozean)[1])

Von Hjalmar Thiel

Über die Meiofauna der Tiefsee liegen bisher nur sehr wenige Angaben vor. Diese sind für die verschiedenen Tiergruppen und für bestimmte Arten von Wieser (1960) zusammengestellt worden. Quantitative Untersuchungen über die Meiofauna der Tiefsee hat es bis 1960 indessen noch gar nicht gegeben, wenn wir die obere Begrenzung der Tiefsee auf die mittlere Tiefe der Schelfkante legen. Die tiefste Probe sublitoraler Untersuchungen stammte bis dahin von Moore (1931) aus 166 m Tiefe aus dem Gebiet der Clyde Sea. In der Zwischenzeit sind zwei Proben vom Kontinentalabhang quantitativ ausgewertet worden. Wigley und McIntyre (1964) bearbeiteten südlich von Massachusetts einen Schnitt mit zehn Stationen, von denen die beiden tiefsten mit 366 bzw. 567 m Tiefe aus dem Bereich der Tiefsee kommen.

Durch die Teilnahme an der Expedition des Forschungsschiffes „Meteor" in den Indischen Ozean war die Möglichkeit gegeben, im Roten Meer, im Golf von Aden, vor der Ostküste Afrikas und vor der Westküste Indiens 56 Proben aus dem Bereich zwischen 1000 m und 5000 m Wassertiefe zu entnehmen. Davon konnten 52 Teilproben für die quantitative Untersuchung der Meiofauna konserviert und 75 weitere Teilproben für die chemische Bestimmung der gesamten organischen Substanz tiefgefroren werden[2]). In der vorliegenden Arbeit werden die Methoden beschrieben und die Ergebnisse von zwölf bisher ausgewerteten Teilproben dargelegt. Die endgültige Bearbeitung wird in den „Meteor-Forschungsergebnissen" (Verlag Bornträger, Berlin) erscheinen. Die Untersuchung wurde mit Unterstützung der Deutschen Forschungsgemeinschaft durchgeführt.

---

[1]) Die Anregung zur Bearbeitung des Benthos der Tiefsee verdanke ich Herrn Prof. Dr. A. Bückmann, dem ich meine erste Arbeit zu diesem Thema zum 65. Geburtstag widme.

[2]) Herrn H. Mayer danke ich für seine Hilfe bei der Entnahme der Proben an Bord von „Meteor" und beim Aussuchen der Proben.

Methoden

1. Die Probennahme

Ein ideales Gerät für die Entnahme von ungestörten Bodenproben, das es auch zuläßt, die Meiofauna quantitativ zu bearbeiten, war bis zu Beginn der Expedition noch nicht bekannt[3]). Die einzige Möglichkeit, relativ ungestörte Proben von der Sedimentoberfläche zu erhalten, schienen mir modifizierte Van-Veen-Greifer zu sein. Auf der Oberseite dieser Greifer sind Klappen angebracht, durch die Teilproben entnommen werden können. Ventile in den Klappen verhindern einen zu großen Stau beim Herablassen und beim Schließen des Greifers. Während das Gerät unter Wasser ist, treten voraussichtlich keine Veränderungen an der Probe auf. Wird es jedoch über die Wasseroberfläche gehievt, so kann das über der Probe stehende Wasser in dem Greifer hin und her schwingen und auslaufen. Dabei wird ein Teil der Meiofauna aufgeschwemmt und kann verlorengehen. Die auf „Meteor" benutzten Greifer schlossen jedoch sehr gut, so daß der Wasserverlust gering war. Das über dem Sediment stehende Wasser wurde mit einem Schlauch abgesogen, filtriert und ebenfalls auf seinen Gehalt an Meiofauna untersucht. Da dieser immer nur sehr gering war, kann auch das ausgelaufene Wasser nur wenige Meiofaunaindividuen enthalten haben. Die ungestörte Sedimentoberfläche war durch aufrechtstehende Wurmröhren und durch ihre Struktur zu erkennen.

Die Verwendung großer Greifer brachte Vorteile für die ganze Expedition. Die Geräte konnten mit 1,5 m/sec gefiert und gehievt werden, einer Geschwindigkeit, die bei leichteren Geräten nicht zu erreichen ist und die bei den großen Tiefen eine beachtliche Zeitersparnis bewirkt. Außerdem konnten von den großen Proben die verschiedenen Arbeitsgruppen an Bord mit Material versorgt werden.

Während der Expedition konnten wir mit einer Erfolgsrate von über 95 % der ausgesetzten Greifer arbeiten. Diese hohe Rate erklärt sich zum Teil aus dem einheitlichen Sediment der Tiefsee, in dem Steine und Korallen fehlen, die den Greifer am vollständigen Schließen hätten hindern können. Eine besonders wertvolle Hilfe für die Entnahme der Proben aber war der Einsatz eines Pingersystems. Das durch die Signale des Pingers aufgezeichnete Echogramm (Abb. 1) gestattet es, den Greifer langsam an den Meeresboden heran- und in das Sediment hineinzufahren.

2. Die Entnahme der Teilproben

Die Entnahme von Teilproben aus Bodengreifern geschieht meist mit einem Rohr, das in das Sediment hineingedrückt und mit der Hand verschlossen herausgehoben wird. Diese einfache Methode eignete sich aber in diesem Falle nicht. Vielmehr wurden folgende Forderungen an ein Gerät für diesen Zweck gestellt:

---

[3]) Von Muus (1964) und Willimoes (1964) sind inzwischen zwei Geräte beschrieben worden, die sich jedoch nicht für Tiefseeuntersuchungen eignen.

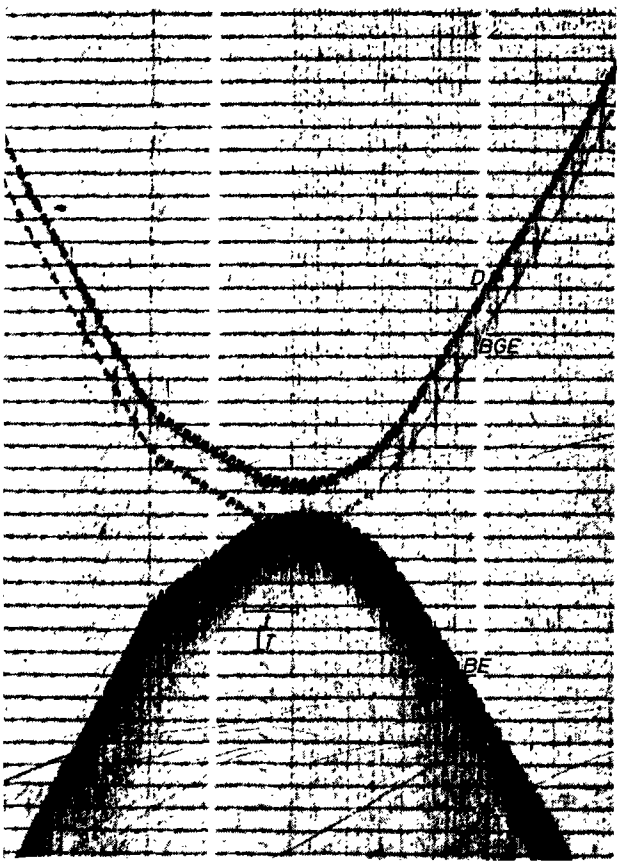


Abb. 1: Echogramm vom Pinger. Zwischen der Aufzeichnung des direkten Schalles (D) und dem Bodenecho (BE) ist das feine Echo vom Bodengreifer (BGE) erkennbar, das in das Bodenecho hineinläuft und sich dann wieder aus ihm löst (t = 60 sec; T = 9.1 m).

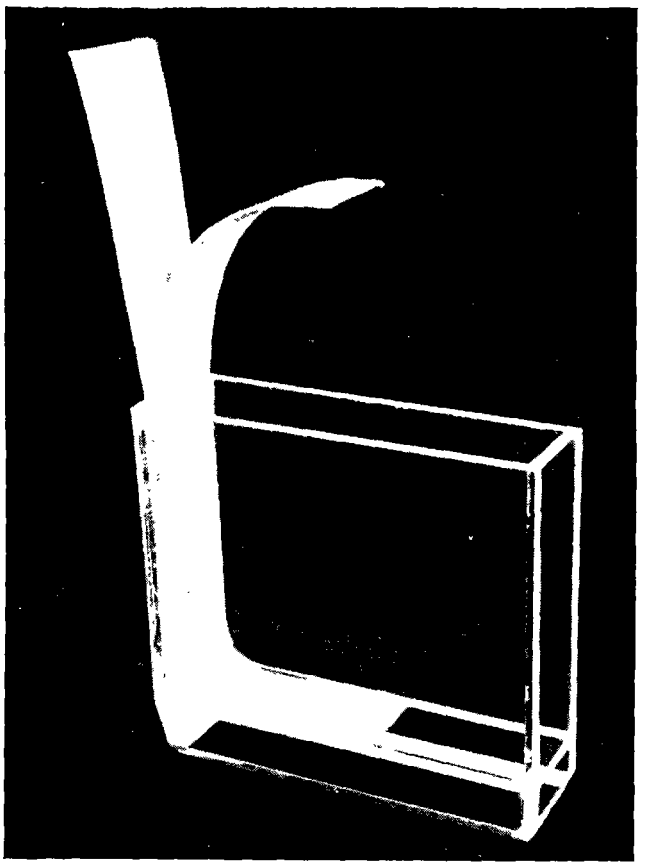


Abb. 2: „Meiostecher" für die Entnahme von Teilproben aus größeren Sedimentproben zur quantitativen Untersuchung der Meiofauna.

1. Die Gesamtprobe sollte nicht gestört werden, um weitere Teilproben entnehmen zu können.

2. Die Teilprobe sollte unten möglichst waagerecht abschließen, um auch geringe Sedimentschichten mit dem Gerät aufteilen und um tiefer gelegene Schichten der Gesamtprobe noch auswerten zu können.

3. Die Form des Gerätes sollte für eine weitere Unterteilung der Teilprobe in senkrechte und waagerechte Schichten nicht rund, sondern eckig sein.

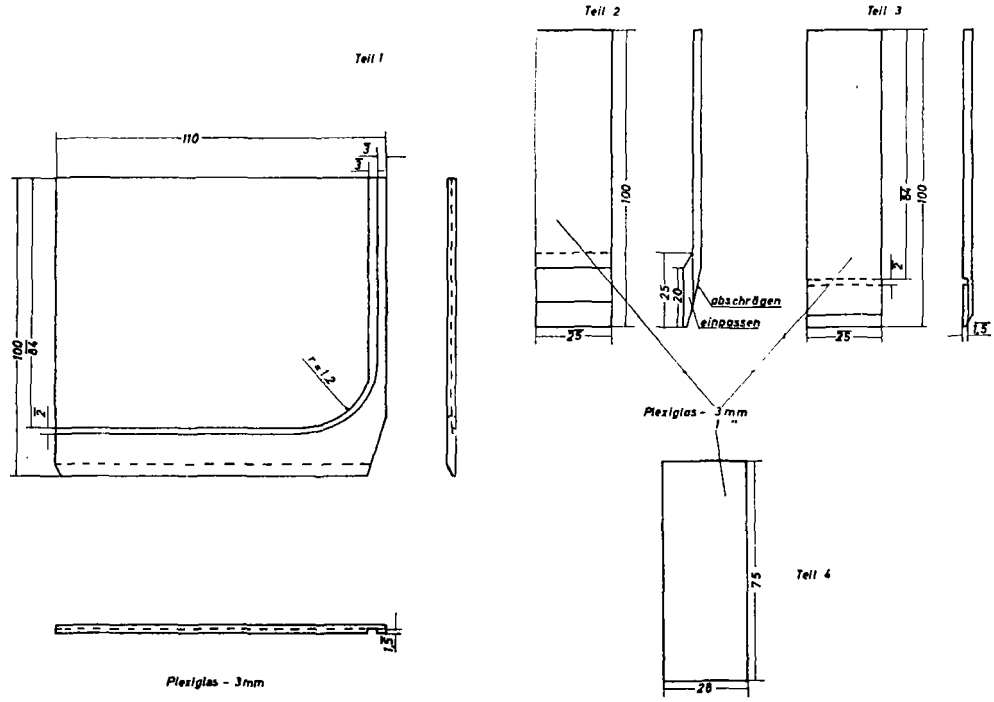


Abb. 3: Konstruktionsskizze des Meiostechers.
Teil 1 entspricht der Vorder- und der Rückseite in Abbildung 2; Teil 2 der linken und Teil 3 der rechten Seite.

Diese Forderungen erfüllt das in den Abbildungen 2 und 3 dargestellte Gerät, das aus Plexiglas gefertigt ist und innen 25×100 mm mißt. Die in Abbildung 2 linke Schmalseite des Gerätes besteht aus einer Doppelwand mit einem schmalen Zwischenraum, der sich seinerseits in eine waagerecht verlaufende Nut in den Seitenwänden fortsetzt. In diesen Zwischenraum wird eine Zunge aus einem $^1/_{10}$ mm starken Phosphorbronze-Federblech eingeschoben. Nachdem der Stecher in das Sediment gedrückt ist, schiebt man das Federblech nach, das in der Nut geführt das Sediment von den tieferen Schichten abschneidet. Da die Schubbelastung für das $^1/_{10}$ mm starke Blech besonders bei grobem Sediment zu hoch wird und es sich beim Einschieben leicht verbiegt, mußte für gleichbleibende Elastizität eine

größere Schubfestigkeit erzielt werden. Das gelang durch die Verwendung von Doppelzungen, die in ihrer Schnittkante scharf gefaltet sind[4]).

Die Größe einer quantitativ auszuwertenden Probe ist abhängig von der Besiedlungsdichte und von der mehr oder weniger gleichmäßigen Verteilung der Tiere über die Fläche. Aber auch die Zeit muß berücksichtigt werden, die die Aufarbeitung einer Probe bedarf. McIntyre (1961 und 1964) und Wigley und McIntyre (1964) verwendeten bei ihren Untersuchungen auf dem Schelf 10 cm^2 als Probenfläche. Die Vergrößerung auf 25 cm^2 bei meinen Untersuchungen ist zwar nicht der vermuteten Abnahme der Individuenzahl pro Flächeneinheit (z. B. Wieser, 1960a) proportional, doch der Zeitaufwand für die Auswertung noch größerer Proben erschien wenigstens zunächst nicht gerechtfertigt.

3. Die Bearbeitung der Proben an Bord

Die Meiofauna wird im allgemeinen lebend aus dem Sediment herausgesucht und dabei auf Grund ihrer Bewegung gegenüber dem Sediment erkannt. Das ist an Bord meist schwierig, obwohl man gerade auf der „Meteor" gut mit dem Binokular arbeiten kann. Es zeigte sich jedoch, daß die Meiofauna aus über 1000 m Wassertiefe bereits tot (Harpacticoida) oder inaktiv (Nematoda) an Bord kam. Das Aussuchen der Tiere aus den Proben war deswegen in der für Flachwasserbiotope üblichen Weise nicht möglich, und es bestand kein Unterschied zu konservierten Proben. Die Proben wurden daher in drei- bis vierprozentigem Formalin konserviert. Durch diese Methode konnten mehr Proben konserviert werden, als an Bord hätten ausgesucht werden können. Zweifellos geht durch die Konservierung ein Teil der feineren und vielleicht systematisch bemerkenswerten Tierarten verloren; sie dürften aber für quantitative Betrachtungen nur eine geringe Rolle spielen.

Zum Aussuchen ist es nicht ratsam, die ganze Probe gleichzeitig zu bearbeiten, und um die Eindringtiefe der Tiere in das Sediment zu bestimmen, muß sie der Tiefe nach in Zentimeterschichten zerlegt werden. Das Aussuchen der sieben oder acht Schichten aller Teilproben ist allerdings nicht möglich, da der Zeitaufwand dafür viel zu groß wäre. Ich habe daher in den meisten Fällen nur den obersten Zentimeter der Teilproben und selten auch die tieferen Zentimeterschichten konserviert. Vermutlich kann man aus dem Verhältnis der Besiedlung in der obersten Schicht zu den Individuendichten in den tieferen Schichten von einigen Proben auf ein entsprechendes Verhältnis in anderen Proben schließen.

Das Aussuchen der Meiofauna aus dem Sediment wird durch die Aufteilung in drei Fraktionen und durch selektives Anfärben der Meiofauna sehr erleichtert.

---

[4]) Der Meiostecher kann durch die Firma Hydrobios-Apparatebau GmbH, Kiel-Holtenau, Jägersberg 7, bezogen werden.

4. Das selektive Anfärben der Meiofauna

Das quantitative Aussuchen der Meiofauna aus Sedimentproben ist wegen der geringen Größe der Tiere und ihrer dem Sediment so sehr ähnlichen Färbung äußerst schwierig. Es war daher naheliegend, durch selektive Anfärbung die Organismen gegenüber dem Sediment hervorzuheben. Entsprechende Methoden sind für die Unterscheidung von lebenden und toten Foraminiferen benutzt worden. WALTON (1952) diskutiert drei ältere Methoden und führt nach Versuchen mit verschiedenen Farbstoffen für die Foraminiferen das Anfärben mit Bengalrosa (Rose Bengal) bei Konservierung in Alkohol neu ein.

McINTYRE (1961 und 1964) und WIGLEY und McINTYRE (1964) haben diese Methode bereits für ihre Untersuchungen der Meiofauna aufgegriffen, doch eigene Vorversuche mit Bengalrosa ergaben, daß diese Methode nicht gleichmäßig alle Tiere erfaßte. Die Färbung war also nicht quantitativ. Trotzdem erbrachte das Aussuchen mit der Färbung mehr Tiere aus der Probe, weil die Meiofauna ungefärbt so schlecht erkennbar ist. Es galt jedoch, vor der weiteren Verwendung von Bengalrosa diese Methode zu überprüfen, sie zu verbessern oder gegebenenfalls eine neue zu finden.

Von einer selektiven Färbemethode war folgendes zu verlangen:

1. Die Meiofauna sollte quantitativ angefärbt werden.
2. Die Färbung des Sedimentes sollte nur oberflächlich und leicht auswaschbar sein.
3. Gute Differenzierung sollte möglich sein, um die Tiere für spätere systematische Untersuchungen wieder durchsichtig zu erhalten.
4. Das Verfahren sollte möglichst einfach sein.

Für die Versuche wurden 3000 Harpacticoida und über 3000 Nematoden verwendet, weil diese die häufigsten Tiere des Meiobenthos sind und sich die Nematoden im Verhältnis zu anderen Tiergruppen bei früheren Experimenten besonders schlecht färben ließen. Diese Untersuchungen führte ich zum Teil an der Biologischen Anstalt Helgoland auf Helgoland aus, weil mir dort die gewünschten Tiere aus dem Bewuchs der Spundwände zur Verfügung standen.

Als Farbstoffe wurden verwendet:

1. Bengalrosa 1 %	nach WALTON (1952).
2. Methylgrün-Eosin	nach RHUMBLER (1935 und früher), das für Foraminiferen verwendet wurde (siehe auch WALTON, 1952).
3. Eosin 1 %	das für zoologische Objekte regelmäßig benutzt wird.
4. Kongorot	mit dem in der Zoologie ebenfalls häufig gefärbt wird.

Als Zusatzmittel wurde verwendet:

5 % Karbolwasser[5])	das CONN (1928) zusammen mit 0.001—0.1 % Calciumchlorid und mit Bengalrosa als Bakterienfarbstoff speziell für Bodenbakterien benutzte.

Methylgrün-Eosin und Kongorot erwiesen sich als ungeeignet, und Calciumchlorid beeinflußte die Färbung nicht. Diese Stoffe werden daher weiter nicht berücksichtigt. Für Bengalrosa und für Eosin wurden die Versuche

[5]) Engl.: aqueous solution of phenol; franz.: eau pheniquée.

zunächst ohne den Zusatz von Karbolwasser ausgeführt. Da die Färbung vom pH-Wert abhängig ist, wurde in einer Serie von Pufferlösungen gefärbt, wie sie von ROMEIS (1948) und von ADAM und CZIHAK (1964) für die Bestimmung des isoelektrischen Punktes angegeben wird. Das Ergebnis ist in Tabelle 1, Spalte 2 und 4, zusammengefaßt.

Tabelle 1. Färbung von Nematoden mit Bengalrosa und Eosin, jeweils mit und ohne Zusatz von Karbolwasser.

Spalte 1	Spalte 2	Spalte 3	Spalte 4	Spalte 5
pH-Bereich	Färbung mit Bengalrosa ohne Zusatz	Färbung mit Bengalrosa, Zusatz von Karbolwasser	Färbung mit Eosin ohne Zusatz	Färbung mit Eosin, Zusatz von Karbolwasser
2— 3	—	gut	gut	gut
3— 4	gut	gut	*gut*	gut
4— 5	*gut*	gut	gut	gut
5— 6	gut	gut	schwach	gut
6— 7	schwach	gut	—	gut
7— 8	sehr schwach	gut	—	gut
8— 9	sehr schwach	gut	—	gut
9—10	—	gut	—	gut

Die Beurteilung der Färbung in der Tabelle richtete sich nach der Erkennbarkeit der Tiere im Sediment. Die stärkste Färbung mit Bengalrosa wurde im pH-Bereich 4—5 erzielt, diejenige von Eosin bei pH 3—4. Bengalrosa färbt etwas dunkler als Eosin. Bei Zusatz von Karbolwasser, das schwach sauer ist und den pH-Wert der Lösungen nicht verschiebt, findet sich eine gleichmäßig gute Färbung aller Tiere in allen pH-Bereichen (Tabelle 1, Spalten 3 und 5).

Als Ergebnis dieser Versuche ist festzustellen, daß man gute und quantitative Färbungen erhält, wenn entweder ein bestimmter, optimaler pH-Bereich eingehalten oder bei Zugabe von Karbolwasser gefärbt wird. Das Sediment wird in keinem Fall mit angefärbt, während Detrituspartikel wenigstens teilweise wie die Tiere reagieren. Wählt man den ersten Weg, so muß zunächst das Fixierungsmittel ausgewaschen werden, das die für die Färbung freien Valenzen blockiert. Anschließend wird in einer auf den optimalen pH-Bereich eingestellten Pufferlösung gefärbt. Bei der Zugabe von Karbolwasser kann indessen unabhängig vom pH-Bereich gearbeitet werden. Die Tiere können vom Konservierungsmittel, Alkohol oder Formalin, in die Farblösung gebracht werden.

Die für den einzelnen Fall beste Methode ist aber auch von der Möglichkeit der Differenzierung abhängig. Grundsätzlich können die mit den vier

Methoden gefärbten Tiere auch wieder entfärbt werden. Bei der Färbung ohne Karbolwasser kann das in entsprechenden Pufferlösungen bei den pH-Werten 7—10 geschehen, es genügt aber auch die Überführung in Wasser oder Formalin. Das gleiche gilt für die Färbungen mit Karbolwasser, nur dauert der Vorgang wesentlich länger. In beiden Fällen differenziert Eosin schneller als Bengalrosa.

Welche Methode im Einzelfall zu verwenden ist, ist von der geforderten Geschwindigkeit des Arbeitsganges abhängig. Hier seien nur die Vorschriften für die Färbungen mit Bengalrosa gegeben, die für Eosin nur durch die Änderung der Pufferlösungen abzuwandeln sind.

1. Färbung mit Bengalrosa, schnelle Differenzierung:

Herstellen der Stammlösungen:	Stammlösung A: 19.43 g Natriumacetat $\times$ 3 H_2O in 1 l aqua. dest. lösen. Stammlösung B: 29.43 g Barbituralnatrium (Merck) = Veronalnatrium in 1 l aqua. dest. lösen.
Herstellen der Farblösung:	10 cm³ Stammlösung A + 10 cm³ Stammlösung B + 20 cm³ 0.1 n Salzsäure + 10 cm³ aqua. dest. Diese Lösung hat den pH-Wert 4.66. Sie ist mit ½ cm³ konzentrierter Lösung von Bengalrosa zu versetzen.
Färben:	a) Probe in ein Sieb spülen. b) Probe mehrfach in Wasser auswaschen, um alles Formalin herauszubringen. c) Probe gut abtropfen lassen und im Sieb in Farblösung bringen d) Probe 10 Minuten färben (oder länger). e) Probe in stehendem Wasser spülen, bis reines Wasser sich nicht mehr sofort färbt.
Aussuchen:	Probe unter dem Binokular aussuchen.
Differenzieren:	Tiere in die Differenzierungsflüssigkeit bringen, die herzustellen ist aus: 10 cm³ Stammlösung A + 10 cm³ Stammlösung B + 3 cm³ 0.1 n Salzsäure + 27 cm³ aqua. dest. Diese Lösung hat einen pH-Wert von 8.68.
Konservieren:	Nach Entfärbung überführen in Formalin.

2. Färbung mit Bengalrosa, langsame Differenzierung:

Herstellen der Farblösung:	50 cm³ Wasser + ½ cm³ konzentrierte Lösung von Bengalrosa + 2½ cm³ konzentriertes Karbolwasser.
Färben:	a) Probe in ein Sieb spülen. b) Kurzes Ausspülen der Probe in Wasser (nicht unbedingt erforderlich). c) Sieb mit Probe für 10 Minuten in Farblösung bringen. d) Probe in stehendem Wasser spülen, bis reines Wasser sich nicht mehr sofort färbt.

Aussuchen, Differenzieren und Konservieren:

Probe unter dem Binokular aussuchen und Tiere direkt in Formalin bringen.

Bei der Anwendung der vier erwähnten Methoden ist darauf zu achten, daß das Anfärben kurz vor dem Aussuchen geschieht, da das Differenzieren in Wasser und Formalin sofort beginnt. Licht hat nur einen sehr geringen Einfluß auf die Differenzierung.

Bei meinen Untersuchungen verwende ich die Färbung mit Bengalrosa + Karbolwasser, wie sie hier unter 2) angegeben ist. Die Methode ist einfach und schnell; sie läßt sich ohne Umstände neben anderen Arbeiten ausführen. Das Differenzieren verläuft indessen nicht zu schnell, sondern es geht später langsam im Formalin vor sich. Kann die zweite Durchsicht einer Probe nicht gleich nach dem ersten Aussuchen stattfinden, so färbe ich die Probe noch einmal.

5. Das Aussuchen der Proben

Jede Probe wird vor dem Aussuchen mit Hilfe eines Siebsatzes in drei Fraktionen zerlegt: 65—100 μ, 100—150 μ und >150 μ[6]). Die Aufteilung in diese Größenstufen läßt sich nicht besonders begründen. Sie hat sich bei der Bearbeitung der Proben als praktisch erwiesen. Weiter kann über diesen Arbeitsgang nichts gesagt werden, denn jeder muß sich seine eigene Methode erarbeiten. Ich bevorzuge es, einen ganz kleinen Teil der Probe in der Mitte einer relativ großen Schale in einer dünnen Schicht auszulegen und diesen dann langsam mit Hilfe einer Lanzettnadel systematisch durchzusuchen. Um eine Genauigkeit von mehr als 95 % zu erreichen, wird jede Probe zweimal ausgesucht.

6. Quantitative Berechnungen

Mit dem Aussuchen der Meiofauna aus dem Sediment erhält man gleichzeitig die Anzahl der Individuen pro Flächeneinheit für die einzelnen Tiergruppen. Diese Werte lassen jedoch nur einen sehr unbefriedigenden quantitativen Vergleich zu, da die Tiere unterschiedlich groß sind und die Tiergruppen nicht den gleichen Teil an Protoplasma, an Eiweiß oder an Kohlenstoff enthalten. Für das Meiobenthos sind entsprechende Untersuchungen von Wieser (1960 b) vorgenommen worden, der von der Größe der Nematoden ausgeht und ein spezifisches Gewicht von 1,13 annimmt. Diese Methode übernehmen auch Wigley und McIntyre (1964) und erzielen eine Annäherung für andere Gruppen durch das Wiegen großer Individuenzahlen. Bessere Vergleichswerte erhält man jedoch nach den Erfahrungen aus der Planktonforschung, wenn man durch Umrechnung Eiweiß- oder Kohlenstoffäquivalente bestimmt (Hagmeier, 1961). Entsprechende Analysen sollen später an größerem Material ausgeführt werden.

---

[6]) Sollen alle Nematoden zurückgehalten werden, so müssen nach neueren Beobachtungen Siebe mit 30 oder 40 μ benutzt werden.

Tabelle 2: Ergebnisse der bisher ausgewerteten 12 Proben

Stationsnummer von METEOR	112	114	115	115	116	116	121	126	126	129	129	130
Probennummer	24	25	26	27	28	29	33	34	34	35	35	36
Nummer der Teilprobe	1	2	2	4	2	2	4	3	4	3	4	2
Tiefe (nicht korrigiert)	5030	3840	3110	3095	1050	1045	2600	2650	2650	4690	4690	4700
1. Nematoda (o. Desmoscolecida)	57	153	181	199	37	41	160	305	259	42	96	161
2. Desmoscolecida	1	3	9	10		7	23	15	26	1	11	19
3. Kinorhyncha		1	1	2			2	5	4	1		
4. Tardigrada			3	1			9	1	1	1		
5. Polychaeta (+ Teilstücke)		4	10	12		1	10	18	10	3	3	17
6. Harpacticoida	1	12	14	29	1	4	41	63	83	8	8	18
7. Nauplien		3	5	13		2	33	13	15	1	5	10
8. Ostracoda	2	1	1	3			4	4	10			1
9. Amphipoda							1	1				
10. Tanaidacea							5					
11. Solenogastres							1					
12. Bivalvia			1	2			1	1				1
13. Pogonophora									3			
Individuen / 25 cm²	61	177	225	271	38	55	290	426	411	57	123	227
Nematoda in % der ges. Individ.-Zahl	96	88	84	77	97	87	63	76	69	76	87	79
unbestimmte Tiergruppen		1	2			5	9	23	12	2	16	4
„Eier und Cysten"	1	5		13	4		23	15	31	6	9	1

Die Ergebnisse der bisher ausgewerteten Proben

Von den 56 Proben für die quantitative Untersuchung der Meiofauna, die während der „Meteor"-Expedition im Indischen Ozean genommen werden konnten, sind 12 bis jetzt ausgewertet worden. Die Ergebnisse lassen keine allgemeinen Schlüsse zu, doch entsprechen sie nicht unseren Erwartungen.

Auf sieben Schnitten, die senkrecht zur afrikanischen Küste verlaufen, wurden auf den in Abbildung 4 dargestellten Stationen Proben entnommen. Besonders hervorgehoben sind die acht Stationen ⊕ auf zwei Schnitten, von denen die 12 ausgewerteten Proben stammen.

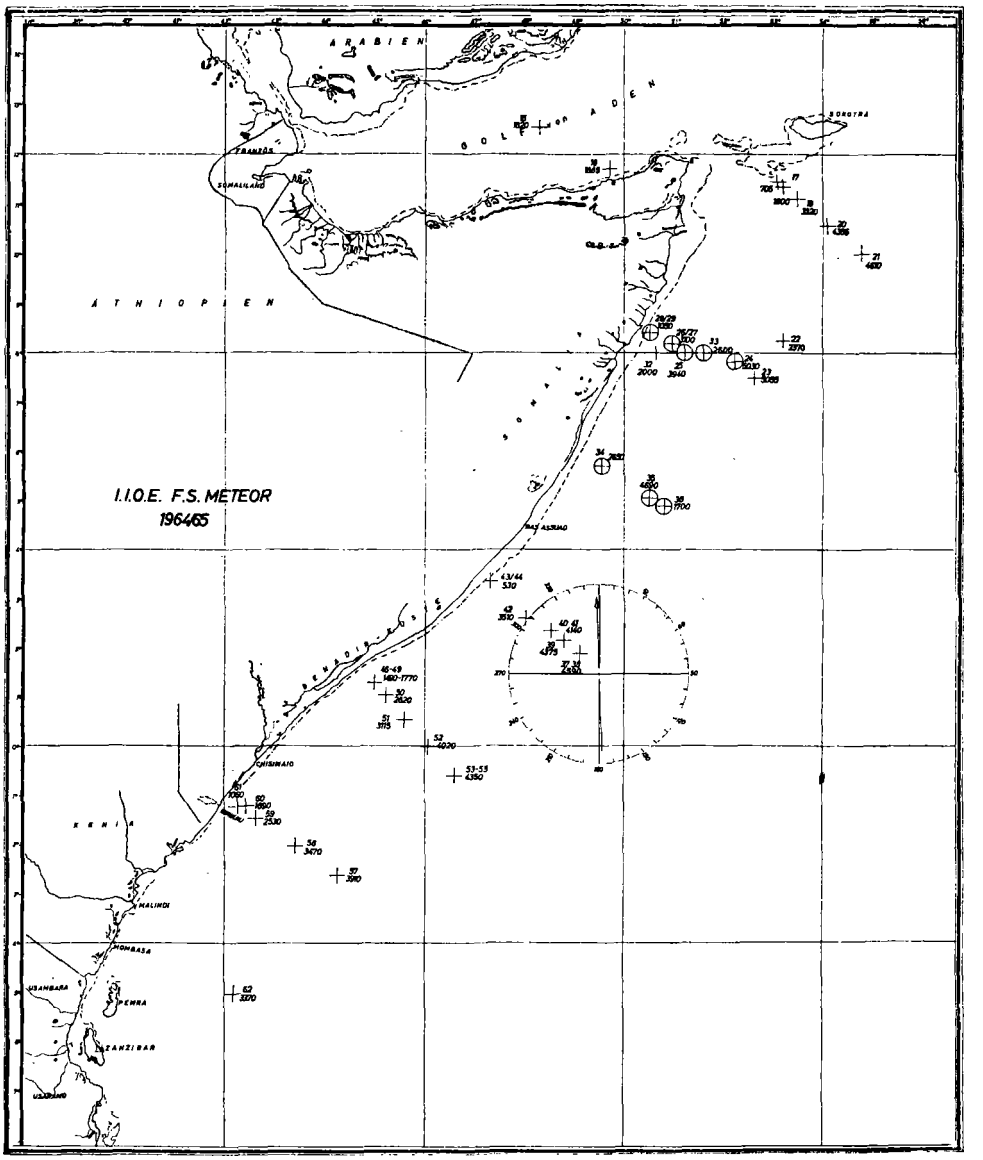


Abb. 4: Karte der „Meteor"-Stationen im Indischen Ozean, auf denen Proben für die Untersuchung der Meiofauna entnommen worden sind. Die bisher ausgewerteten Stationen sind durch ⊕ gekennzeichnet.

In der Tabelle 2 sind die Ergebnisse in der Reihenfolge der Stationen dargestellt, weil eine Ordnung nach natürlichen Gesichtspunkten vorerst noch nicht zu erkennen ist. Die Individuenzahlen auf 25 cm² Probenfläche schwanken zwischen 38 und 426, ohne dabei die Individuen aus den Zeilen „unbestimmte Tiergruppen" und „Eier und Cysten" berücksichtigt zu haben. Der geringste Wert findet sich nicht etwa in der größten Tiefe von 5030 m, sondern bei 1050 m bzw. bei 1045 m[7]). Die höchste Individuendichte, bezogen auf die Größe der Teilproben, kam bei 2650 m vor. Diese unerwartete Verteilung der Meiofauna hängt sicher von verschiedenen Faktoren ab. So fanden die Herren Dr. REINECK und Dr. GUTMANN auf der Station 116 in 1045 m einen pH-Wert von nur 7,0 gegenüber 7,7—8,0 in den anderen Proben, und Herr Dr. GRASSHOFF stellte einen sehr geringen Sauerstoffgehalt des Wassers fest. Beim Aussuchen ergab sich weiterhin, daß das Sediment fast ausschließlich Bestandteile enthielt, die kleiner als 100 μm waren. Wieweit diese Faktoren wirklich von Bedeutung sind, wird erst die Auswertung weiterer Proben zeigen. Die Probe aus 5030 m stammt aus dem roten Tiefseeton und dürfte deswegen so gering besiedelt sein.

Auf der Station 115 konnten zwei Greifer nacheinander gefahren werden: Nr. 26 und 27. Durch die Drift des Schiffes ist die Entnahmestelle nicht ganz die gleiche; die Tiefen unterscheiden sich um 15 m. Die Individuenzahlen zeigen jedoch gleiche Größenordnungen. Bei der Station 126 wurden aus dem Greifer 34 zwei Proben entnommen, die in ihren Individuenzahlen einigermaßen gleiche Werte aufweisen, sich in der Zusammensetzung der Gruppen jedoch bemerkenswert unterscheiden. Ebenso sind aus dem Greifer 35 auf der Station 129 zwei Proben konserviert worden. In diesem Falle aber weichen deren Individuenzahlen stark voneinander ab. Diese hohe Differenz erklärt sich zum Teil wohl durch die erwähnte Schwierigkeit, von der Oberfläche genaue, einen Zentimeter starke Schichten zu isolieren, doch muß auch mit einer hohen Schwankungsbreite der tatsächlichen Werte gerechnet werden.

Bei einer Station wurden auch die tieferen Zentimeterschichten untersucht. Es wurde hierzu die Probe aus 5030 m Tiefe gewählt. Tabelle 3 zeigt die in den verschiedenen Schichten bei doppeltem Durchsuchen aufgefundene Anzahl Tiere.

Wie im sublitoralen Bereich dringen also auch in der Tiefsee Meiofaunaindividuen wenigstens bis zu 7 cm Tiefe in das Substrat ein. Gleichzeitig wird aber deutlich, daß die Individuenzahlen in der Tabelle 2, die sich nur auf den obersten Zentimeter beziehen, nicht die Gesamtzahlen unter 25 cm² darstellen.

Kinorhynchen waren bisher nur aus 385 m Tiefe (cit. nach WIESER, 1960a) und Tardigraden ebenfalls nur aus 385 m Tiefe (MARCUS, 1934) bekannt geworden. Beide Gruppen fand ich noch bei 4690 m.

---

[7]) Bei allen Tiefenangaben handelt es sich um unkorrigierte Anzeigen des Echographen, die bei Bodenberührung des Greifers abgelesen wurden.

Tabelle 3:

Anzahl der Individuen für 1 cm starke Schichten (etwa 25 cm^3) aus einer Probe aus 5030 m Tiefe

Schicht	Nematoda	Harpacticoida	Ostracoda	Nauplien
0—1 cm	58	1	2	
1—2 cm	31	2		1
2—3 cm	7			
3—4 cm	5			
4—5 cm				
5—6 cm	2			
6—7 cm	2			

Wie zu vermuten war, bilden auch in der Tiefsee die Nematoden die individuenreichste Gruppe mit 63—96 % (Tab. 2). Da vor allem Nematoden in den tieferen Sedimentschichten leben (Tab. 3), wird sich ihr Anteil an der Gesamtindividuenzahl bei Berücksichtigung dieser Schichten noch erhöhen.

Bedeutender sind jedoch die Ergebnisse für unsere Vorstellungen über die Besiedlungsdichte der Tiefseeböden. Untersuchungen haben hierzu bisher noch nicht vorgelegen, doch hat WIESER (1960a) theoretische Berechnungen angestellt. Er ging dabei von zwei Annahmen aus: 1. Mit der Tiefe nimmt die Besiedlungsdichte pro Flächeneinheit ab, und 2. die Besiedlungsdichte der Meiofauna beträgt wahrscheinlich das Hundertfache von der der Makrofauna. Demnach sollten in 300—400 m Tiefe 3000 und in 9000 bis 10 000 m Tiefe 500 Individuen pro Quadratmeter vorkommen. Aus dem Tiefenbereich meiner Untersuchungen liegen Angaben über die Makrofauna aus dem Atlantik von SPÄRCK (1951) mit 85 Individuen in 1200 m und mit 30 Individuen pro Quadratmeter in 3782 m vor (hohe Werte aus den Angaben SPÄRCKS). Sowohl die theoretischen Werte von WIESER als auch die aus den Daten von SPÄRCK für die Makrofauna zu berechnenden Werte für die Meiofauna liegen weit unter den von mir gefundenen Individuenzahlen.

Aus sublitoralen Gebieten liegen indessen quantitative Angaben vor, die unabhängig vom Substrat und von der untersuchten Schichtdicke in ihrer Größenordnung meinen Ergebnissen von einer 1-cm-Schicht gegenübergestellt sein sollen (Tab. 4). In der Tabelle sind die Werte für die Individuendichten für 10 cm^2 angegeben, da ihre vermutliche Schwankungsbreite eine Umrechnung auf einen Quadratmeter nicht gestattet. Die Ordnung in Tabelle 4 ist durch die Häufigkeit der Individuen pro Flächeneinheit gegeben, und gleiche Größenordnungen aus dem Sublitoral und aus der Tiefsee sind nebeneinandergestellt. Die Individuenzahlen der Tiefseeproben entsprechen also den geringeren Werten aus dem Sublitoral, und für die Tiefsee wären noch höhere Werte einzusetzen, wenn auch die tieferen Sediment-

Tabelle 4:

Anzahl der Meiofaunaindividuen pro 10 cm² aus Proben vom Sublitoral und vom Kontinentalabhang[1]) nach verschiedenen Autoren (links), im Vergleich mit 12 Proben von acht Stationen aus der Tiefsee des Indischen Ozeans (rechts)

	Verschiedene Gebiete		Indischer Ozean	
Autor	Tiefe in m	Individuen pro 10 cm²	Tiefe in m	Individuen pro 10 cm²
PURASJOKI, 1947	40	4		
PURASJOKI, 1947	35	5—20	1050	16
			1045	22
			4690	23
			5030	24
PURASJOKI, 1947	24	31—40		
KROGH und SPÄRCK, 1936	26	55	4690	50
KROGH und SPÄRCK, 1936	17	56		
KROGH und SPÄRCK, 1936	54	73	3840	70
KROGH und SPÄRCK, 1936	17	84	3110	90
MARE, 1942	45	87	4700	90
PURASJOKI, 1947	55	103		
KROGH und SPÄRCK, 1936	17	108	3095	108
WIGLEY und MCINTYRE, 64	567[1])	117	2600	116
WIGLEY und MCINTYRE, 64	51	127		
WIGLEY und MCINTYRE, 64	366[1])	127		
			2650	164
MOORE, 1931	166	177	2650	170
MOORE, 1931	73	198		
MARE, 1942	45	198		
MOORE, 1931	24	337		
WIESER, 1960b	15—25	169—823		
WIGLEY und MCINTYRE, 64	40—179	235—988		
BOUGIS, 1946 und 1950	30	615—1210		
MCINTYRE, 1964	101	536—2211		
MCINTYRE, 1964	146	878—3117		

schichten ausgewertet worden wären (vergl. Tab. 3). Die offensichtlich hohe Populationsdichte der Meiofauna in der Tiefsee wirft auch neues Licht auf unsere Vorstellung von den Nahrungsketten in diesem Lebensraum. Die Nahrungsbedingungen für die Makrofauna scheinen demnach doch günstiger zu sein, als wir es bisher vermutet haben.

Die Auswertung dieser 12 Proben gibt noch keine Antwort auf entscheidende ökologische Fragen. Ich hoffe, daß nach Aufarbeitung der weiteren Proben allgemeinere Aussagen für dieses Gebiet gemacht werden können. Das wird aber nur dann möglich sein, wenn die Ergebnisse der Expedition von den anderen Fachgebieten vorliegen. Die Unterschiede in der Besiedlungsdichte können von der Art des Sediments abhängig sein und das Sediment seinerseits von der Bodengestalt und den Strömungen. Das monsunabhängige Strömungssystem der Meeresoberfläche des Untersuchungsgebietes, die durch Auftriebwasser zu bestimmten Jahreszeiten bedingte starke Entwicklung von Plankton in den Oberflächenschichten des Wassers und die damit möglicherweise gegebene Eutrophierung des Meeresbodens werden bei der Deutung der Ergebnisse zu berücksichtigen sein.

Zusammenfassung

Methoden und erste Ergebnisse von quantitativen Untersuchungen über die Meiofauna des Tiefseebodens des Indischen Ozeans werden beschrieben. Besonders hervorzuheben ist die hohe Individuenzahl der Meiofauna (Tab. 3), die derjenigen mancher sublitoraler Gebiete entspricht.

Literaturverzeichnis

Adam, H., und Czihak, G. (1964): Arbeitsmethoden der makroskopischen und mikroskopischen Anatomie. G. Fischer, Stuttgart, 583 pp.

Bougis, P. (1946): Analyse quantitative de la microfaune d'une vase marine a Banyuls. C. R. Acad. Sci. **222**, 1122—1124.

Bougis, P. (1950): Méthode pour l'étude quantitative de la microfaune des fonds marins (Meiobenthos). Vie et Milieu **1**, 23—38.

Conn, H. J. (1928): On the microscopic method of studying Bacteria in soil. Soil Sci. **26**, 257—259.

Hagmeier, E. (1961): Plankton-Äquivalente (Auswertung von chemischen und mikroskopischen Analysen). Kieler Meeresf. **17**, 32—47.

Harms, H. (1958): Handbuch der Farbstoffe für die Mikroskopie **2** (3), 225—338; Staufen-Verlag, Kamp-Linfort.

Krogh, A., und Spärck, R. (1936): On a new bottom-sampler for investigation of the microfauna of the sea bottom. Kgl. Danske Vidensk. Selsk. Biol. Medd. **13** (4), 1—12.

Marcus, A. (1934): Tardigrada in: Die Tierwelt Deutschlands **10** (2), 1—150.

Mare, M. F. (1942): A study of the marine benthic community with special reference to the microorganisms. J. Mar. Biol. Ass. U. K. **25**, 517—554.

McIntyre, A. D. (1961): Quantitative differences in the fauna of boreal mud associations. J. Mar. Biol. Ass. U. K. **41**, 599—616.

McIntyre, A. D. (1964): Meiobenthos of sublittoral muds. J. Mar. Biol. Ass. U. K. **44**, 665—674.

Moore, H. B. (1931): The muds of the Clyde Sea area. J. Mar. Biol. Ass. U. K. **17**, 325—358.

Muus, B. J. (1964): A new quantitative sampler for meiobenthos. Ophelia **1** (2), 209 bis 216.

Purasjoki, K. J. (1947): Quantitative Untersuchungen über die Mikrofauna des Meeresbodens in der Umgebung der Zoologischen Station Tvärminne an der Südküste Finnlands. Soc. Scient. Fenn. Comm. Biol. **9** (14), 1—24.

Rhumbler, L. (1935): Rhizopoden der Kieler Bucht, gesammelt durch A. Remane, I. Teil. Schrift. Nat.-wiss. Ver. Schlesw.-Holst. **21** (2), 143—195.

Romeis, B. (1948): Mikroskopische Technik. München, 15. Aufl., 695 pp.

Spärck, R. (1951): Density of bottom animals on the ocean floor. Nature (London) **168**, 4264, 112—113.

Walton, W. R. (1952): Techniques for recognition of living foraminifera. Cushman Found. Foram. Res. Contr. **3** (2), 56—60.

Wieser, W. (1960a): Populationsdichte und Vertikalverteilung der Meiofauna mariner Böden. Int. Revue ges. Hydrobiol. **45** (4), 487—492.

Wieser, W. (1960b): Benthic studies in Buzzard Bay II. The meiofauna. Limnol. Oceanogr. **5** (2), 121—137.

Wigley, R. L., and McIntyre, A. D. (1964): Some quantitative comparisons of offshore meiobenthos and macrobenthos south of Martha's Vineyard. Limnol. Oceanogr. **9** (4), 485—493.

Willemoes, M. (1964): A ball-stopped quantitative sampler for microbenthos. Ophelia **1** (2), 235—240.

Anschrift des Verfassers:
Dr. Hjalmar Thiel, Institut für Hydrobiologie und Fischereiwissenschaft, Hamburg 50, Olbersweg 24

Diskussion

Sterrer: Worauf führen Sie die Tatsache zurück, daß die Meiofauna aus größeren Tiefen gewöhnlich tot oder inaktiv heraufkam?

Thiel: Temperatur und Druck können in gleichem Maße ausschlaggebend sein. Es dauert etwa $1^1/_2$ Stunden, bis eine Bodenprobe aus 5000 m Tiefe an Deck kommt, und sie befindet sich beim Hieven etwa 10 Minuten lang in den oberen erwärmten Wasserschichten. Die Temperaturänderung ist in diesem Zeitraum nur gering. Das gilt ebenfalls für die Zeit der Bearbeitung der Probe, da zum Aussieben des Feinmaterials gekühltes Wasser benutzt wurde. Da wir bisher keine temperatur- und druckgeschützten Geräte für die Probenentnahme haben, kann diese Frage nicht beantwortet werden.

Reprinted from *Veröff. Inst. Meeresforsch. Bremerh.*, Sonderband II, 1966, p. 255-263

Bakteriologische Untersuchungen im Indischen Ozean

(Vorläufiges Ergebnis der „Meteor-Expedition in den Indischen Ozean") [1])

Von Wilfried Gunkel

Bacteriological Investigations in the Indian Ocean

(Preliminary result of the "Meteor"-Expedition in the Indian Ocean)

Abstract

This publication gives some preliminary results of the bacteriological research conducted during the "Meteor"-Expedition in the Indian Ocean 1964/65. Data of the bacterial distribution of four sections, each about 200 miles long and perpendicular to the west coast of India are presented. There is the tendency for bacterial numbers to increase from west to east and from south to north. Bacterial counts from a station in the Gulf of Aden are compared with values of organic bound carbon (Particulate and total). The data of the distribution of bacteria in a deep sea core are presented. Some possible reasons for the distribution are discussed.

Aus der Biologischen Anstalt Helgoland, Meeresstation Helgoland

Unsere Kenntnis über die quantitative Rolle der Bakterien im Stoffkreislauf des Meeres ist sehr gering. Ein wesentlicher Weg zur Erforschung der ökologischen Bedeutung von Meeresbakterien ist die Untersuchung ihrer Verbreitung und Korrelation mit hydrographischen, hydrochemischen und biologischen Faktoren. Im letzten Jahrzehnt sind ausgedehnte Untersuchungen zur Bakterienverbreitung von anderer Seite durchgeführt worden (z. B. KRISS 1961, CVIIC, 1955).

Durch die Teilnahme des FS „Meteor" an der Internationalen Indischen-Ozean-Expedition ergab sich für mich die Möglichkeit, ausgedehnte bakteriologische Untersuchungen auch in diesem Meeresgebiet anzustellen. Dieses Vorhaben erschien besonders lohnend, da von anderen Disziplinen eine Fülle hydrographisch-chemischer Parameter bestimmt wurde.

Die Expedition wurde zur Zeit des Nordostmonsuns durchgeführt. Es mußte erwartet werden, daß hier im indischen Küstengebiet Auftriebswasser vorlag.

Da die endgültige Veröffentlichung erst zu einem späteren Termin erfolgen kann, wenn ein genaues Bild der hydrographischen Situation gezeichnet ist und insbesondere auch die Werte der Planktonuntersuchungen vorliegen, soll an dieser Stelle über einige vorläufige Ergebnisse der bisher ausgewerteten bakteriologischen Untersuchungen berichtet werden.

Methodik

Die Probenentnahme erfolgte unter Berücksichtigung steriler Kautelen mit dem Schöpfer nach ZOBELL (ZOBELL 1941). Die Keimzahl wurde mit dem bewährten Gußplattenverfahren unter Verwendung des Seewassernähragars 2216 E bestimmt. Angelegt wurden mindestens je zwei Parallelplatten mit

---

[1]) Vorausbericht aus den „Meteor-Forschungsberichten". Expedition 1964/65 in den Indischen Ozean.

Die Expedition wurde durch die Deutsche Forschungsgemeinschaft finanziert.

Dem Leiter der Expedition, Herrn Prof. Dr. DIETRICH, Herrn Kapitän LEMBKE und der Besatzung der „Meteor" bin ich für ihre Unterstützung zu besonderem Dank verpflichtet.

Herrn H. H. TREKEL danke ich für die Anfertigung der Abbildungen.

0,5 und 5 ml Seewasser. Die Bebrütung erfolgte bei ca. 18° C. Die Bebrütungszeit betrug 14 Tage. Für die Auswertung wurden alle erhaltenen Werte gemittelt, es sei denn, daß eine zu hohe Koloniendichte auf den 5-ml-Platten die Auszählung unsicher machte. Die verwandten Methoden sind im einzelnen an anderer Stelle (GUNKEL 1963, 1964a) aufgeführt.

Untersuchungen zur systematischen Zugehörigkeit der Bakterien sowie Direktzählmethoden wurden wegen des damit verbundenen Aufwandes, der Schwierigkeiten bzw. Fragwürdigkeiten nicht durchgeführt (GUNKEL 1964c).

Ergebnisse

Die Abb. 1 zeigt Daten einer Station im Golf von Aden („Meteor"-Stat. Nr. 93). Es handelt sich um die Mittelstation eines Schnittes, der von Norden nach Süden quer durch den Golf verlief. Die Wassertiefe betrug hier 3231 m. Da die Tiefenwerte der Bakterien gleichförmig verliefen, sind hier nur die

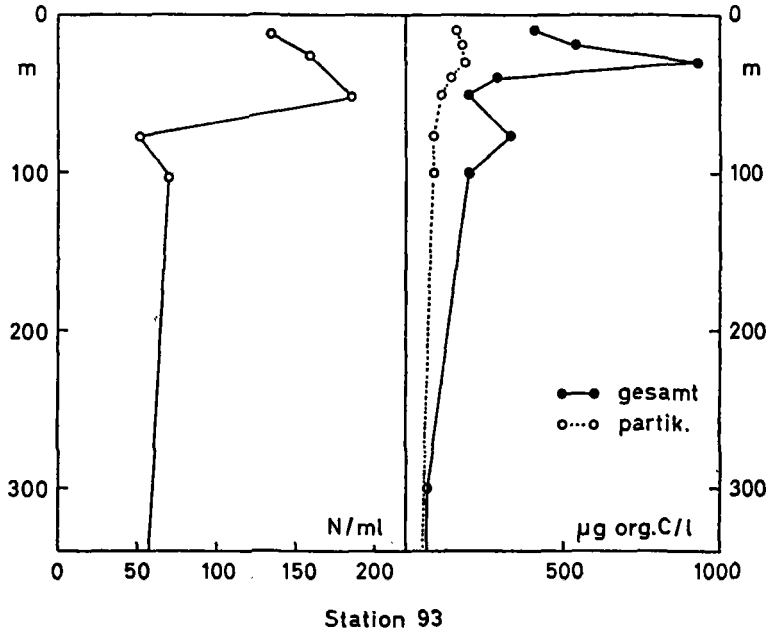


Abb. 1: „Meteor"-Station 93. Bakterienverteilung sowie Gehalt an Gesamt- bzw. partikulär organisch gebundenem Kohlenstoff.

obersten 300 m angeführt. Aufgetragen sind die Anzahlen Bakterien pro ml sowie die Werte für partikulären und Gesamtkohlenstoff, der in organischer Bindung vorlag[1]). Die verschiedenen Kurven haben auf den ersten Blick eine starke Ähnlichkeit. Die höchste Zahl der Bakterien wird in der Probe aus 53 m erreicht, danach fällt sie rasch ab. Das Bakterienmaximum stimmt nicht mit denjenigen des organisch gebundenen Kohlenstoffs überein. Deren

[1]) Herrn Dr. GILLBRICHT sowie Herrn Prof. KREY und Herrn SZEKIELDA danke ich für die freundliche Überlassung der Werte.

Maxima liegen in geringerer Tiefe. Dies erscheint logisch. Das Maximum der Bakterien wird dort erreicht werden, wo schon ein beträchtlicher Teil der als Nahrung dienenden organischen Substanz verbraucht worden ist. Die Werte der Bakterien sind relativ hoch.

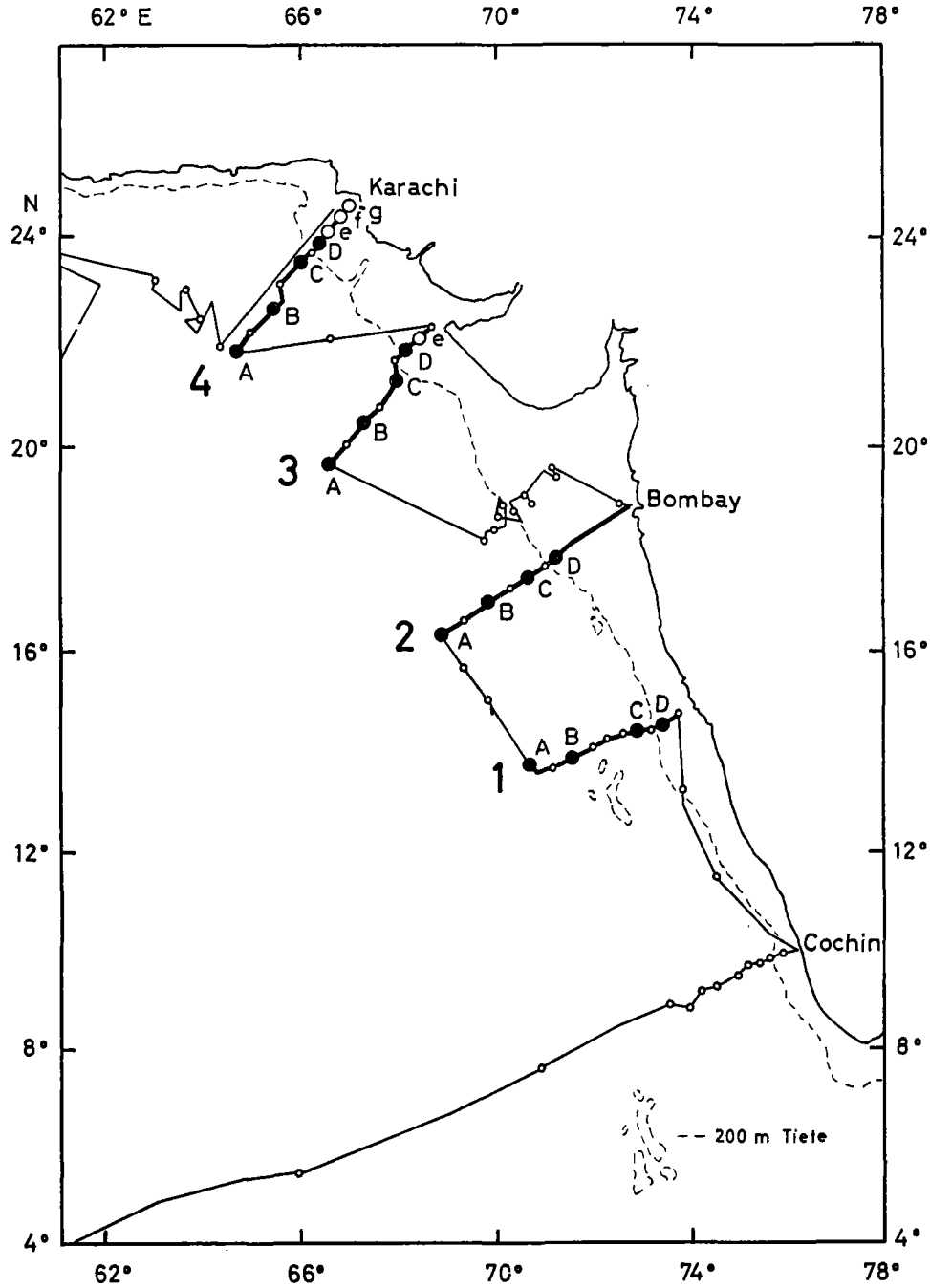


Abb. 2: Expeditionsroute vor der indischen Küste. Die Buchstaben bezeichnen Stationen, auf denen Proben für bakteriologische Untersuchungen entnommen worden sind.

Auf den Stationen in der Arabischen See finden wir bei gleichen Landentfernungen meist beträchtlich niedrigere Werte, insbesondere auch in der Tiefe. Inwieweit hierfür der Einfluß ausströmenden Wassers des Roten Meeres verantwortlich ist, wird ausgesagt werden können, wenn die hydrographischen Daten vorliegen.

Die Abb. 2 zeigt den vor der indischen Küste zurückgelegten Expeditionsweg. Die Schnitte und Positionen, auf denen Proben für bakteriologische Untersuchungen entnommen wurden, sind mit Zahlen und Buchstaben bezeichnet. Die mit großen Buchstaben versehenen Stationen wurden für eine Reihe von Zusammenfassungen verwandt. Die Länge der Schnitte betrug jeweils ca. 200 Seemeilen.

Die Abb. 3, 4, 5, 6 zeigen die Bakterienverbreitung auf den vier Schnitten. Es sind jeweils nur die obersten 100 m dargestellt, obwohl Proben — sofern die Wassertiefe es zuließ — bis mindestens 500 m Wassertiefe, gelegentlich auch noch tiefer, entnommen worden sind. Die Werte unterhalb 100 m sind

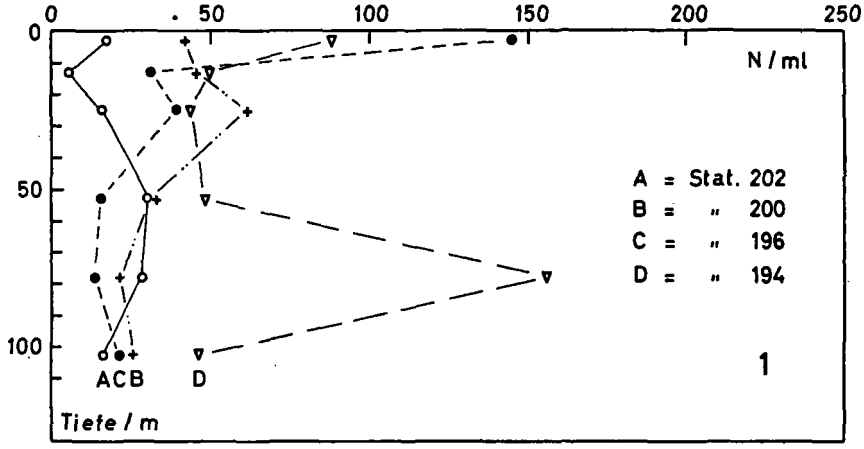


Abb. 3: Bakterienverbreitung auf Schnitt 1.
Die Buchstaben bezeichnen die verschiedenen Stationen (s. Abb. 2).

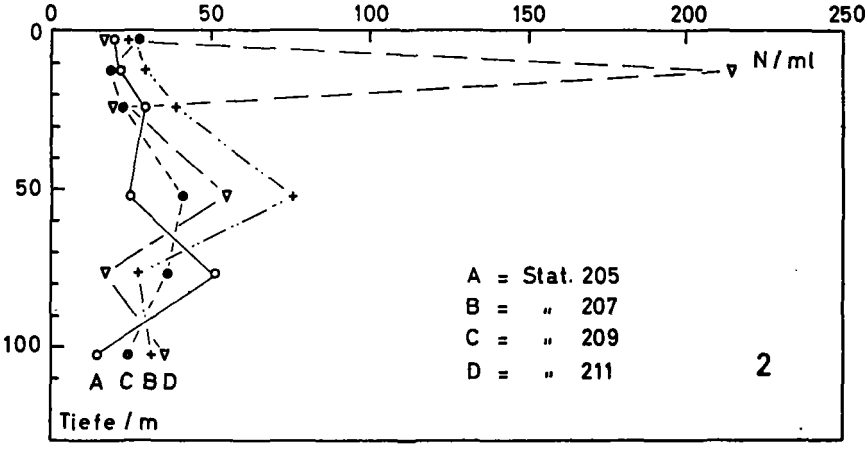


Abb. 4: Bakterienverbreitung auf Schnitt 2.
Die Buchstaben bezeichnen die verschiedenen Stationen (s. Abb. 2).

äußerst niedrig, liegen fast stets unter 10 pro ml und unterscheiden sich bei den einzelnen Stationen kaum. Lediglich die Werte kurz über dem Grund zeigen häufig wieder einen Anstieg. Auf der Abzisse sind jeweils die Entnahmetiefen, auf der Ordinate die Anzahl Bakterien pro ml eingetragen. Das Bild ist zunächst etwas verwirrend, wie auch nicht anders erwartet werden kann, da verschiedene Stationen mit ihren Bakteriengehalten, die ja den verschiedensten Einflüssen unterliegen, hier zusammen dargestellt sind.

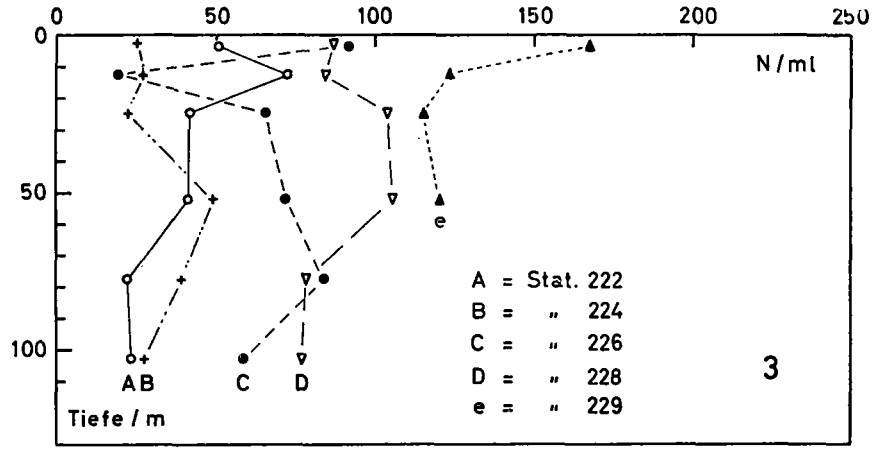


Abb. 5: Bakterienverbreitung auf Schnitt 3.
Die Buchstaben bezeichnen die verschiedenen Stationen (s. Abb. 2).

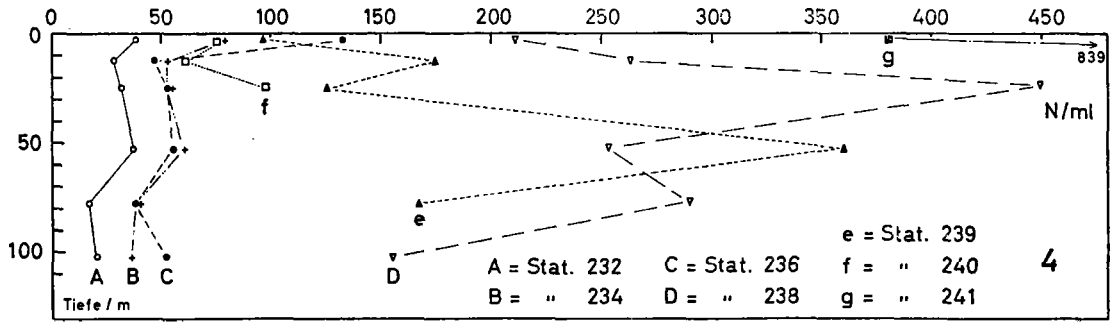


Abb. 6: Bakterienverbreitung auf Schnitt 4.
Die Buchstaben bezeichnen die verschiedenen Stationen (s. Abb. 2).

Die Maxima der Bakterien liegen in verschiedenen Tiefen. Häufig wird auch ein höherer Wert an der Oberfläche, d. h. in ca. 3 m Tiefe, erhalten. Inwieweit dies auf Schiffseinfluß oder auf durch den Wind transportiertes Material beruht, wird noch zu untersuchen sein. Die Maxima liegen niemals tiefer als bei 78 m. Gelegentlich treten stärkere Abweichungen von den Kurven auf, so z. B. der 13-m-Wert bei Schnitt zwei. Bei Schnitt drei (Abb. 5) ist deutlich eine zunehmende Tendenz der Bakterien bei abnehmender Landentfernung festzustellen, obwohl auch hier gelegentlich Überschneidungen vorkommen. Der vierte Schnitt mußte in einem anderen Maßstab gezeichnet werden, da sonst bereits die Station D nicht mehr hätte miterfaßt werden können. Deutlich unterschiedlich verhalten sich hier die Werte der Sta-

tionen A, B und C zu den übrigen Stationen. Um die Tendenz der Bakterienzahlen zum Lande hin noch deutlicher zu machen, wurden noch drei weitere Stationen bearbeitet. Interessanterweise fallen nach Station D die Zahlen wieder ab, insbesondere Station f, während auf der Station g Zahlen bis zu 839 pro ml erhalten werden.

Interessant war hierbei, daß bei der auf dem vierten Schnitt als D bezeichneten Station eine sehr große Anzahl agarverdauender Bakterien auf den Platten auftraten. Sie wuchsen in den Petrischalen, die mit 5 ml Seewasser angelegt waren, so stark, daß eine glatte Oberfläche des Agars nicht mehr vorhanden war, sondern völlig unregelmäßige, aneinanderstoßende Krater.

Um die vorliegenden Tendenzen der Bakterienverbreitung auf den verschiedenen Schnitten deutlich zu erkennen, wurde eine Reihe von Zusammenfassungen vorgenommen.

Die Abb. 7 zeigt die 53-m-Tiefenwerte auf den einzelnen Stationen der vier Schnitte. Die Bakterienzahlen nehmen von Landferne zur Landnähe und

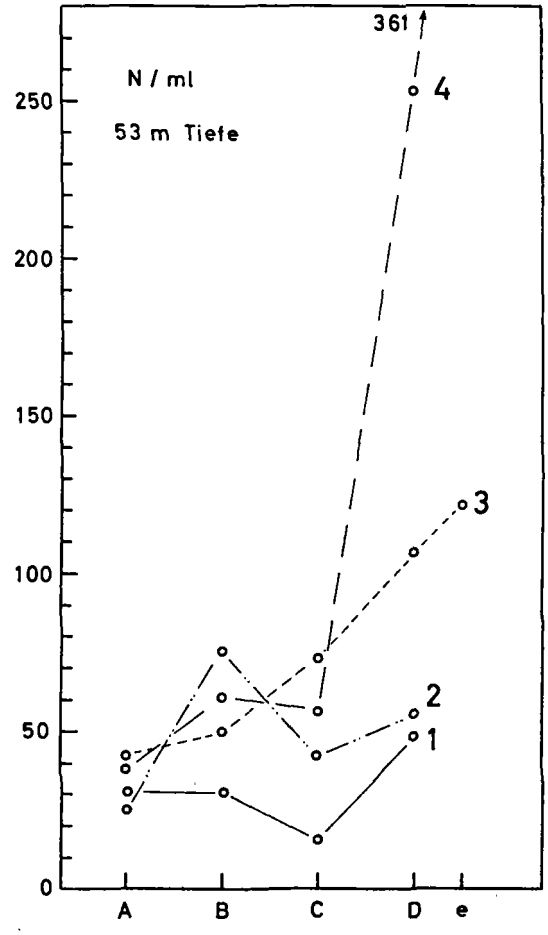


Abb. 7: Bakterienverbreitung in 53 m Tiefe auf den vier bearbeiteten Schnitten.

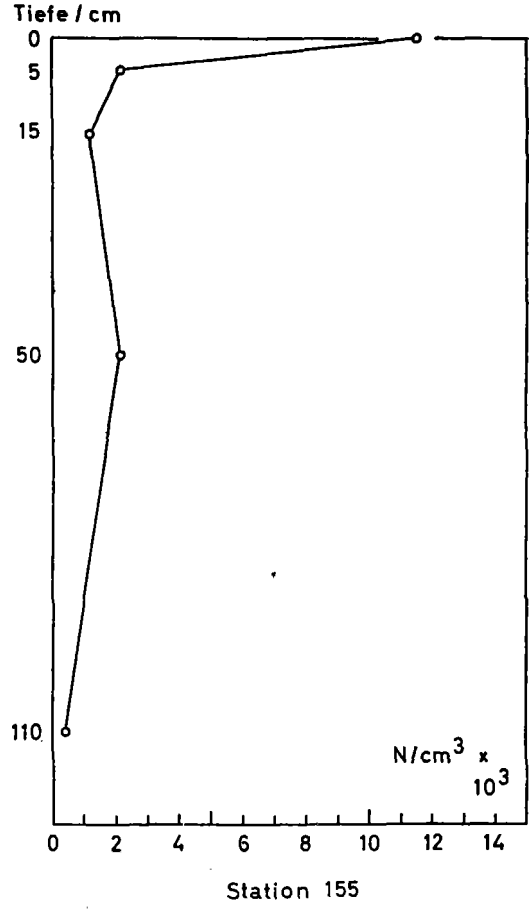


Abb. 8: Verteilung aerober, heterotropher Bakterien in einem Stoßrohrkern (Sediment). „Meteor"-Station 155, Wassertiefe 2530 m.

von Süden nach Norden hin deutlich zu. Um zu untersuchen, ob diese Tendenz nur für die 53-m-Werte gilt oder für die Stationen ganz allgemein zutrifft, wurden die Bakterienzahlen der obersten 103 m addiert. Die erhaltenen Werte sind in Abb. 9 dargestellt. In jeder Säulengruppe ist die jeweilige Summe der Bakterienzahlen von Stationen der verschiedenen Schnitte, die etwa die gleiche Landentfernung hatten, zusammengefaßt. Die Säulen-

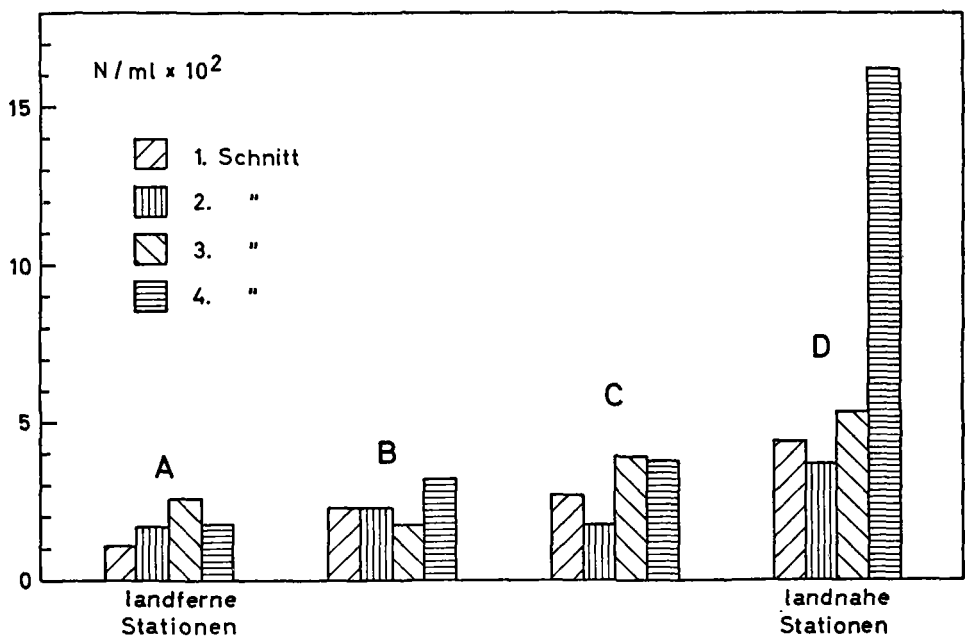


Abb. 9: Zusammenfassende Darstellung der Bakterienverbreitung auf den vier Schnitten. Die Werte der einzelnen Stationen sind addiert worden. 1—4 = Bezeichnung der Schnitte, A—D = Bezeichnung der Stationen auf den Schnitten.

gruppen A bis D entsprechen den jeweiligen Landabständen (s. Abb. 2), und in jeder Gruppe ist die erste Säule die südlichste, die vierte Säule die nördlichste Station. Es ist deutlich zu erkennen, daß sowohl innerhalb der Säulengruppen als auch bei einem Vergleich der Säulen, die zu einem Schnitt gehören, eine Zunahme erfolgt, d. h. es liegt allgemein die Tendenz einer Zunahme der Bakterienwerte in Richtung auf die Küste und nach Norden hin vor.

Abb. 8 zeigt die Anzahl aerober, heterotropher Bakterien in einem Stoßrohrkern, d. h. also einer Sedimentprobe. Aufgetragen ist die Tiefe in cm und die Anzahl Bakterien in Tausend pro cm^3. Der Kern wurde aus einer Wassertiefe von 2530 m vor der afrikanischen Küste entnommen („Meteor"-Station Nr. 155). Es handelte sich um grünen Tiefseeton. Die Bakterienzahlen wurden mit Hilfe der sogenannten Most-Probable-Number-Methode (Verdünnungsmethode) bestimmt. Der weitaus höchste Wert wird im obersten Zentimeter, also dem jüngsten Teil des Sediments, erhalten.

Diskussion

Eine diffizile Diskussion der Ergebnisse, Betrachtung der Ursachen der Maxima und der Zunahmen der Bakterien nach Norden und zum Lande zu kann erst erfolgen, wenn die Daten der anderen Bearbeiter vorliegen und wenn insbesondere ein Bild der hydrographischen Verhältnisse gezeichnet worden ist.

Bisher können wir feststellen, daß sich bei den bakteriologischen Daten Tendenzen abzeichnen, die sinnvoll erscheinen, auch wenn wir zunächst noch nicht erkennen, welches im einzelnen die Ursachen dafür sind.

Wir können bei der Zunahme nach Norden und zum Lande zu an drei Möglichkeiten denken:

1. Landeinfluß durch organische Nahrungsstoffe direkt oder indirekt über eine Zuführung anorganischer Nährsalze und damit der Möglichkeit einer erhöhten Planktonproduktion, die ihrerseits als Nahrung für Bakterien dienen könnte. Hierzu muß jedoch gesagt werden, daß die Untersuchungen zur Zeit des Nordostmonsuns durchgeführt wurden, bei dem keine nennenswerten Niederschläge auf dem indischen Subkontinent stattfanden. So war z. B. die Wasserführung der Flüsse extrem niedrig. Außerdem fallen die Zahlen bis zur jeweils äußersten Station hin ab. Diese Station lag jeweils über 200 Seemeilen vom Land entfernt, so daß, obwohl ablandige Winde vorhanden waren, ein Landeinfluß relativ unwahrscheinlich ist. Sicher wird aber z. B. bei den landnächsten Stationen des vierten Schnittes in irgendeiner Weise ein Landeinfluß vorhanden sein. Darauf deuten z. B. die hohen Zahlen an agarverdauenden Bakterien hin.

2. Eine gewisse Rolle könnte ein Konzentrationseffekt spielen, der durch die geringeren Wassertiefen bei den landnäheren Stationen verursacht wird. D. h. es ist ein günstiges Verhältnis zwischen dem zur Verfügung stehenden Produktionsraum zur unproduktiven Tiefe vorhanden.

3. Mit großer Wahrscheinlichkeit muß damit gerechnet werden, daß zur Zeit des Nordostmonsuns Auftriebswasser an der indischen Küste vorliegt. In den tropischen Meeren ist allgemein das Tiefenwasser im Vergleich zum Wasser der Deckschicht bedeutend reicher an Salzen, die den begrenzenden Faktor für die Produktion darstellen (Stickstoff- und Phosphorsalze). Bei einem Auftrieb findet eine gewaltige Zunahme an Plankton und in dessen Gefolge an Bakterien statt. Der Auftrieb müßte aller Wahrscheinlichkeit nach sich auch gerade am stärksten in den nördlichen Schnitten auswirken. In Richtung dieser Hypothese hindeutende Werte wurden von anderer Seite erhalten (W. Düing, P. H. Koske und G. Krause, persönliche Mitteilung).

Literaturverzeichnis

Cviic, V. (1955): Distribution of bacteria in the waters of the mid Adriatic Sea. Izvesca-Reports **4**, No. 1,44 pp.

Gunkel, W. (1963): Daten zur Bakterienverteilung in der Nordsee. Veröff. Inst. f. Meeresf. Bremerhaven. Sonderband 1, 3. Meeresbiol. Symp., 80—89.

GUNKEL, W. (1964a): Einwirkungen des kalten Winters 1962/63 auf die Bakterienpopulationen vor Helgoland. Helg. Wiss. Meeresunters. **10**, 246—256.
GUNKEL, W. (1964c): Bericht über das Helgoländer Arbeitstreffen der deutschen Gewässermikrobiologen, Juni 1964. Helg. Wiss. Meeresunters. **11**, 327—340.
KRISS, A. E. (1961): Meeresmikrobiologie. 570 pp. Jena.
ZOBELL, C. E. (1941): Apparatus for collecting water samples from different depths for bacteriological analysis. J. Mar. Res. **4**, 173—188.

Anschrift des Verfassers:
Dr. Wilfried Gunkel, Biologische Anstalt, Helgoland

Diskussion

MEYER: Ist eine Spezifikation der Arten vorgenommen worden? Mich interessieren *E. coli, Ps. fluorescens* und Sporenbildner.

GUNKEL: Untersuchungen zur systematischen Zugehörigkeit der Bakterien wurden nicht vorgenommen und waren auch nicht vorgesehen, da sie meine Arbeitskapazität — ich hatte keinen Techniker zur Verfügung — überschritten.

JARKE: Sind Bakterienbestimmungen im Golf von Oman vorgenommen worden? Dort finden sich in der Tiefe — soweit mir bekannt — die einzigen Faulschlammablagerungen im offenen Ozean der Gegenwart.

GUNKEL: Untersuchungen zur Bakterienverbreitung im Golf von Oman wurden durchgeführt, jedoch müssen die Daten noch ausgewertet werden.

Reprinted from *Hvalråd. Skr.*, no. 48, p. 85-93

Salinity adaptation in the mudskipper fish Periophthalmus sobrinus

By

MALCOLM S. GORDON, JAN BOËTIUS, INGE BOËTIUS, DAVID H. EVANS, ROSEMARY MCCARTHY AND LARRY C. OGLESBY

Department of Zoology, University of California, Los Angeles, California; Physiological Laboratory, Danmarks Akvarium, Charlottenlund, Denmark; and "Te Vega" Expeditions, Hopkins Marine Station, Monterey, California

Introduction

Mudskippers are amphibious, euryhaline gobioid fishes, widely distributed in the intertidal environments of much of the Old World tropics. They are usually found in muddy environments, frequently in and around mangrove areas..

Mudskippers resemble anuran amphibians in many aspects of their behavior and ecology (Stebbins and Kalk 1961). In southeast Asia a number of species of mudskippers coexist in the same habitat as the euryhaline crab-eating frog (*Rana cancrivora;* Gordon *et al.* 1961; Smith 1945, pp. 555–559, 564–566). Since mudskippers are teleost fishes which have evolved their adaptations to the littoral environment completely independently of the amphibians, it is interesting to inquire if the physiological responses they give to environmental stresses are similar to those given by the crab-eating frog.

A direct comparison of the various forms *in situ* on the mangrove flats of Thailand would probably have been best. Other considerations, however, led to our making an expedition to Madagascar, where, from June through August, 1964, we studied a population of a widely distributed species of mudskipper, *Periophthalmus sobrinus* Eggert. The present paper describes the results of our studies of salinity adaptation in this fish. Additional information on the natural history and physiology of the amphibious habit in *P. sobrinus* is given by Gordon *et al.* (1966).

This paper is dedicated to Professor Per F. Scholander on his sixtieth birthday. It is a small token of esteem and appreciation for his stimulating role in furthering expeditionary experimental biology.

Materials and methods

Mudskippers ranging in size from recently metamorphosed postlarvae to large adults weighing up to 15 gm were abundant in the intertidal mangrove areas and on stretches of rocky coast along the shores of the island of Nosy Bé, off the northwest coast of Madagascar. They were easily captured in small dipnets during low tide periods at night. Fish ranging in weight from 3–15 gm were used for experimental purposes. No attempt was made to separate the sexes, or to feed them.

Fish were maintained in the laboratory in plastic aquaria with wire covers, with up to twenty fish per aquarium. The aquaria were tipped slightly, so that the 2 liters of water present covered only about half of the bottom surface. The fish thus had their choice of being in or out of water.

Laboratory air temperatures varied with ambient temperature. Ambient temperatures varied diurnally between 23° and 30° C. There was virtually no rain during our working periods at Nosy Bé. Seawater salinities were thus very constant at 34‰ (100% SW; osmotic concentration = 1000 mOsm/1). Salinity measurements were made with an Industrial Instruments Company Model RS-5 inductive salinometer. Precision: ± 0.5‰. In the laboratory dilutions of sea water were prepared volumetrically, by addition of rain water.

Unless noted otherwise, fishes were transferred directly from 100% SW to different sea water dilutions. Adaptation periods of at least two days, usually five days or more, were allowed to pass before any metabolic or chemical measurements were made.

The following measurements were carried out on intact fish:

Body weight change: Fishes were placed in tared, covered plastic cups having perforated bottoms to permit free circulation and drainage of water. Weighings of carefully drained and dried cups were made at intervals following transfers to aquaria containing about 2 cm depth of desired sea water dilutions. Precision: ± 0.1 gm.

Metabolic rate: Small fish (1–5 gm weight) were placed in about 10 ml of water of the appropriate salinity in the chambers of Scholander volumetric microrespirometers (Scholander and Iversen 1958). Six to twelve hours were allowed for temperature equilibration and adjustment of the animals to the apparatus. Oxygen consumption was then measured for about one hour. All measurements were made at temperatures between 23.0 and 24.5°C. Precision: ± 2 mm^3/gm/hr.

Ammonia and urea excretion: Fish were placed in covered plastic boxes containing 100 ml of water of the appropriate salinity. Water samples of 0.25 ml were taken at intervals and analyzed for excreted ammonia and urea using the microdiffusion method of Conway (Natelson 1961, p. 440). Observation periods were approximately 24 hr. Precision: ±0.05 mM ammonia or urea/kg/hr.

To obtain blood and tissue samples fish were killed by a blow on the head. Blood samples were taken from the exposed heart in lightly heparinized glass capillary tubes. Plasma was obtained by centrifugation. Muscle samples were dissected from the lateral musculature. The following analyses were carried out:

Plasma osmotic concentration: Three successive samples, amounting to a total volume of about 15 µl, were placed on the "active" thermistor of a Mechrolab vapor pressure osmometer. Precision: ± 3 mOsm/l.

Plasma chloride: Duplicate 5 µl samples were titrated with mercuric nitrate, using S-diphenylcarbazone as indicator (Schales and Schales, 1957). Precision: ± 5 mEq/l.

Plasma sodium: Duplicate 10 µl samples were diluted 100 × with saturated barium hydroxide solution. Following temperature equilibration in a water bath at 38° C, sodium activity was measured with a micro sodium ion-specific glass electrode connected to a high precision pH meter. Precision: ± 5 mEq/l.

Whole animal inulin space: 100 µl of 10 % inulin solution containing 10 µc/ml activity of inulin-carboxyl-C-14 was injected intraperitoneally into suitably adapted fish. Fish were then kept 4–6 hr in plastic cups, as for weight change experiments, to permit complete internal mixing. Blood samples were taken and 10–25 µl samples of plasma plated on concentrically ringed copper planchets. C-14 activity was measured with a thin end-window geiger tube connected to a Nuclear-Chicago Model 2800 A portable scaler. Whole animal inulin space was calculated from the dilution of activity of the injected solution. Samples were counted for approximately 5000 counts. Overall precision of inulin space calculation: ± 10 ml/kg body weight.

Muscle water content: Duplicate 200–350 mg samples of lateral musculature were weighed wet, then dried overnight at 105°C. Precision: ± 2 ml water/kg wet weight.

Results

Periophthalmus sobrinus is a surprisingly euryhaline fish, tolerating direct transfers from 100% SW to 80%, 60%, 40% and 20% SW. No mortality occurred following these transfers, and the fish survived in good condition for as long as observations continued (over two weeks in several instances). Direct transfer to FW, whether rain water or tap water derived from wells, caused death within 1–3 days. Indefinite survival in FW did occur, however, in a group of six fish which had previously been adapted to 20% SW for six days.

Changes in body weight which occurred following these various transfers are summarized in Fig. 1. For clarity, data from transfers from 100% SW to 80%, 60% and 40% SW are omitted. These three sets of data, just as the 20% SW data plotted, are insignificantly different from the 100% SW controls. All five groups, from 100% SW to 20% SW, increased body

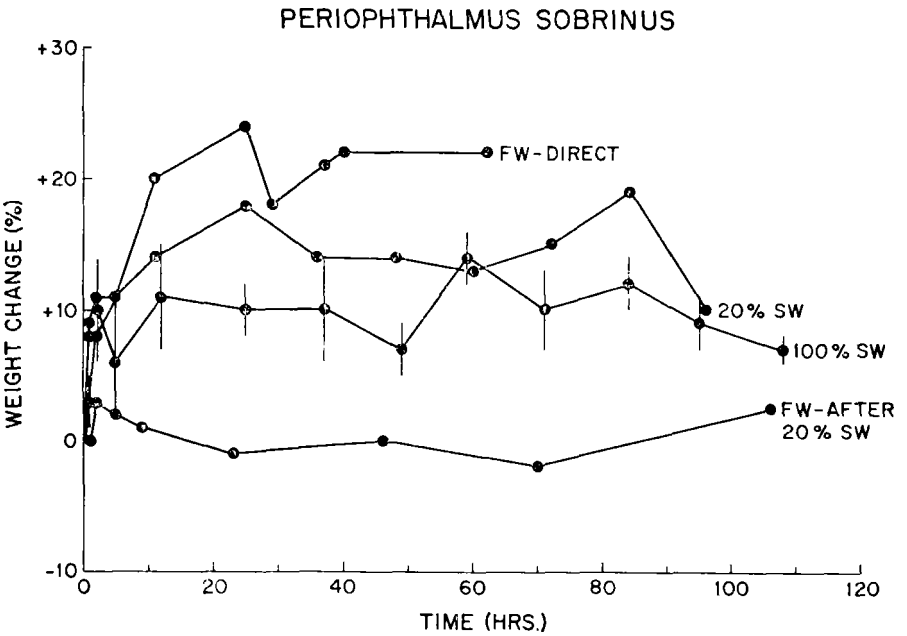


Figure 1: *Percent change in body weight of mudskippers transferred directly from 100% SW to salinities indicated. Solid lines join means for observations on groups of six fish. Vertical lines through points on 100% SW curve, ± 2. S.E.'s Comparable S.E's omitted from other curves for clarity.*

weight 10–15% following transfer. This was probably due to a change in body hydration resulting from the fishes being forced to remain continuously in water during these measurements.

The rapidly fatal direct transfers to FW were associated with a 20% increase in body weight. No further changes in weight followed transfer to FW of fish previously adapted to 20% SW for six days.

Regulation of plasma osmotic and NaCl concentrations was virtually

Table 1. *Plasma concentrations in mudskippers adapted to different salinities*

State of acclimatization	Concentrations [$\bar{X}$ ± S.E. (N)]		
	Δ (mOsm/l)	Cl (mEq/l)	Na (mEq/l)
FW, 2 days	190 ± 23(4)	74 ± 8(5)	136 ± 6 (7)
FW, 7 days	354(1)	–	–
20% SW, 2 days	312 ± 11(8)	130 ± 3(8)	175 ± 4(9)
40% SW, 4 days	359 ± 7(7)	140 ± 2(7)	192 ± 14(6)
60% SW, 6 days	315, 315	147 ± 7(5)	233 ± 8(7)
80% SW, 5 days	325 ± 14(7)	148 ± 9(5)	160 ± 5(3)
100% SW	324 ± 9(5)	143 ± 4(9)	212 ± 8(5)

Table 2. *Whole animal inulin space and muscle water content in mudskippers adapted to different salinities*

State of acclimatization	Whole animal inulin space (ml/kg body wt.) [$\bar{X} \pm$ S.E. (N)]	Muscle water content (ml/kg wet wt.) [$\bar{X} \pm$ S.E. (N)]
FW, 2 days	220 ± 5(3)	816 ± 1(3)
60% SW, 1–3 days	250 ± 16(4)	786 ± 2(5)
100% SW	190 ± 5(4)	775 ± 6(5)

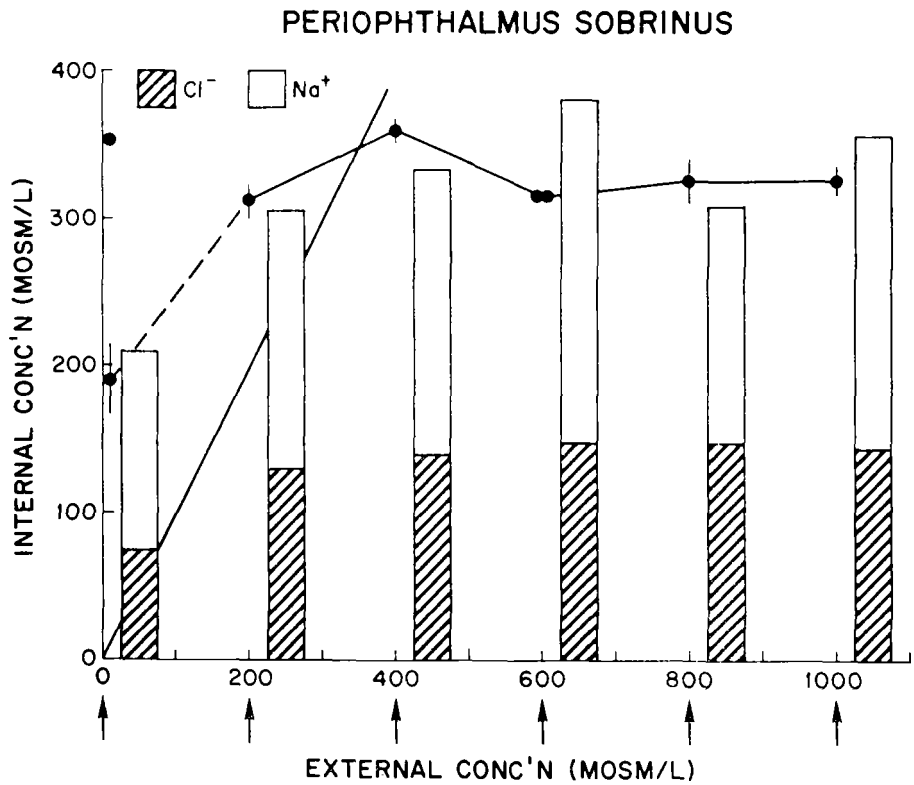


Figure 2: *Pattern of osmotic regulation in mudskippers. Upper line joins means for plasma osmotic concentrations in groups of fish (cf. Table I for numbers) adapted to salinities ranging from* 100% *SW to FW. Experimental salinities indicated by arrows along abscissa. Vertical lines through points* ± 2 *S.E.'s. Diagonal line, line of equality between internal and external concentrations. Vertical bars, mean plasma NaCl concentrations in same salinities.*

perfect over the range from 100% SW to 20% SW (Fig. 2 and Table 1). Relative insensitivity of the analytical procedure used was the probable cause of the variability in plasma Na results. Only nearly moribund fish in FW, following direct transfer from 100% SW, showed significant dilution of the plasma from an average level near 330 mOsm/l. One fish sampled after 7 days in FW, following previous adaptation to 20% SW, had plasma osmolality in the normal range. *P. sobrinus,* therefore, is probably a perfect osmoregulator over the entire range of salinities it is likely to encounter in nature. As is usual with teleosts, over 90% of plasma osmolality in all external concentrations was due to NaCl.

The data on muscle water content (Table 2) also support the picture of great osmoregulatory stability. Only nearly moribund fish in FW showed statistically significant increases in this quantity as compared with 100% controls (at 1% level by "t" test). Whole animal inulin space, however, increased significantly above control level in both 60% SW and FW. The latter two groups did not differ significantly from one another.

Oxygen consumption rates for fish adapted to 60% SW were 40% lower than metabolic rates for 100% SW controls (Table 3; difference statistically significant at 5% level by "t" test). Fish in FW for two days, following direct transfer from 100% SW, showed intermediate rates, not significantly

Table 3. *Oxygen consumption of mudskippers adapted to different salinities*

Environment	Oxygen consumption (mm^3/gm/hr) [$\bar{X} \pm$ S.E. (N)]	Body weight (gm) [$\bar{X}$ (range)]
FW	65 ± 9(4)	2.6 (1.9–3.1)
60% SW	54 ± 4(6)	3.5 (2.6–4.1)
100% SW	84 ± 9(8)	1.8 (1.1–2.5)

Table 4. *Ammonia and urea excretion from mudskippers adapted to different salinities. 24 hr. rates of excretion* [$\bar{X} \pm$ S.E. (N)]

Environment	Ammonia (mM/kg/hr)	Urea (mM/kg/hr)
40% SW	0.77 ± 0.16(5)	0.06 ± 0.04(3)
100% SW	0.49 ± 0.05(5)	0.36 ± 0.05(5)

different from either of the other groups. These differences correlate with the differences in body weights of the fish in the three groups. Salinity *per se* appears to have no significant effect on oxygen consumption.

As a result of technical difficulties associated with work on a ship, data on ammonia and urea excretion rates are less complete than we had wished. The data in Table 4 do permit the following statements: Mudskippers in 100% SW were, for teleosts, highly ureotelic. The difference between ammonia and urea excretion rates in this medium is not statistically significant. Urea/ammonia partitioning was thus about 1:1. Comparing fish adapted to 40% SW with 100% SW controls, ammonia excretion did not change significantly, while urea excretion declined markedly (significant at 1% level by "t" test). Urea/ammonia partitioning in 40% SW was about 1:10 (difference significant at 2% level by "t" test).

Discussion

Mudskippers spend the greater part of their lives out of water, moving about over the surfaces of hot tropical shores some distance from the tide line. Their physical mobility is great enough so that it is unlikely that they are ever trapped in environments such as evaporating tide pools in which they would be exposed to salinities higher than that of the nearby sea. The only serious salinity stress they are likely to encounter is that of low salinity – either as dilution of the inshore waters by torrential rainy season downpours, or as actual fresh water for the numerous populations which live along the shores of rivers to near the limits of tidal action.

The present results demonstrate that, at least from the physiological standpoint, such low salinity stresses are not a serious selective hazard. Indeed, the osmoregulatory capacities of *P. sobrinus* are superior to those of most temperate zone euryhaline fishes, despite the fact that the latter have the advantage of lower environmental temperatures (Gordon 1959; Parry 1961). It seems probable that the gradual onset of the summer rainy seasons would permit additional adaptive increases in these capacities above the levels we found during the winter dry season. In any case, at least in the vicinity of Nosy Bé, the normal 3–4 meters tidal range would ensure that very low salinities would not persist for more than a few hours in coastal localities.

The typically teleostean pattern of osmoregulation shown by *P. sobrinus* differs from the responses to equivalent salinity stresses shown by adult crab-eating frogs (Gordon *et al.* 1961). The frog changes body weight in osmometric fashion, and is an osmoconformer at medium concentrations above 20% SW. As part of its osmoconformity, the frog accumulates large amounts of urea in its body fluids. The tadpoles of *Rana cancrivora,* however, are good osmoregulators and physiologically resemble mudskippers (Gordon and Tucker 1965).

The data on urea and ammonia excretion indicate a shift toward ammoniotelism in lower salinities. These observations agree with much of the work

of Solomon (1962) on the same species. The relatively high rate of urea excretion in 100% SW might be interpreted as a concomitant of the amphibious nature of *P. sobrinus*. However, Wood (1958) indicates that some completely aquatic marine teleosts may show as large a degree of ureotelism.

Summary

Survivorship, changes in body weight, pattern of regulation of plasma osmotic and NaCl concentrations, whole animal inulin space, muscle water content, metabolic rate, and ammonia and urea excretion rates were studied in mudskippers (*Periophthalmus sobrinus*) adapted to different salinities ranging downward from 100% sea water (34‰ salinity) to fresh water.

P. sobrinus tolerated direct transfers from 100% SW to salinities as low as 20% SW. Survival in FW was also possible, following short periods of adaptation to 20% SW. Control of plasma osmotic and NaCl concentrations, and muscle water content was virtually perfect in tolerable salinities. Plasma osmotic concentration averaged about 330 m Osm/l; NaCl contributed over 90% of this amount.

Oxygen consumption was unaffected by salinity. Variations in weight-specific metabolic rates correlated with variations in body weights of experimental fish.

Mudskippers in 100% SW excreted approximately equal amounts of ammonia and urea. Fish in 40% SW excreted less urea, resulting in an ammonia/urea ratio of 10:1.

The ecological significance of these results is discussed, and *P. sobrinus* is compared physiologically with the euryhaline crab-eating frog (*Rana cancrivora*) and other euryhaline fishes.

Acknowledgement

The organization and carrying out of the expedition during which this work was done involved the aid and cooperation of many people and government agencies. We express our sincerest thanks to all. The following were particularly directly concerned: Minister of Foreign Affairs A. Sylla and Consul in Washington H. Jux Ratsimbazafy, Government of the Malagasy Republic; Associate Secretary-General M. Gleizes, Office de la Recherche Scientifique et Technique d'Outre-Mer, Paris; Director M. Angot, Associate Director M. Frontier, and the staff of the Centre d'Oceanographie et des Pêches de Nosy Bé, Prof. R. Bolin, Chief Scientist, "Te Vega" Expeditions, Hopkins Marine Station, Pacific Grove; Drs. J. Ryther and E. Chin, Woods Hole Oceanographic Institution, Woods Hole; Dr. A. G. Humes, Department of Zoology, Boston University, Boston; Captain J. Thomsen and the crew of the R/S "Te Vega."

Support for the expedition derived from the National Science Foundation

via the U. S. Program in Biology of the International Indian Ocean Expedition, the general operations grant to Stanford University for the "Te Vega" Expeditions, and research grant G-23855 (to M. S. Gordon).

Literature cited

Gordon, M. S., 1959: Ionic regulation in the brown trout (*Salmo trutta* L). *J. Exp. Biol., 36*: 227–252.

— Boëtius, J., Boëtius, I., Evans, D. H., McCarthy, R., and Oglesby, L. C., 1966: Natural history and physiology of the amphibious habit in a mudskipper fish (*Periophthalmus sobrinus*). *J. Exp. Biol. 43* (in press).

— K. Schmidt-Nielsen, and Kelly H. M., 1961: Osmotic regulation in the crab-eating frog (*Rana cancrivora*). *J. Exp. Biol., 38*: 659–678.

— and Tucker, V. A., 1965: Osmotic regulation in the tadpoles of the crab-eating frog (*Rana cancrivora*). *J. Exp. Biol., 42*: (in press).

Natelson, S., 1961: Microtechniques of clinical chemistry for the routine laboratory. 2nd ed. Springfield.

Parry, G., 1961: Osmotic and ionic changes in blood and muscle of migrating salmonids. *J. Exp. Biol., 38*: 411–427.

Schales, O., and Schales, S. S., 1953: Chloride. *Std. Methods Clin. Chem., 1*: 37–42.

Scholander, P. F., and Iversen, O., 1958: New design of volumetric respirometer. *Scand. J. Clin. Lab. Invest., 10*: 429–431.

Smith, H. M., 1945: The fresh water fishes of Siam or Thailand. *Bull. U.S. Nat. Mus.*, 188: 1–622.

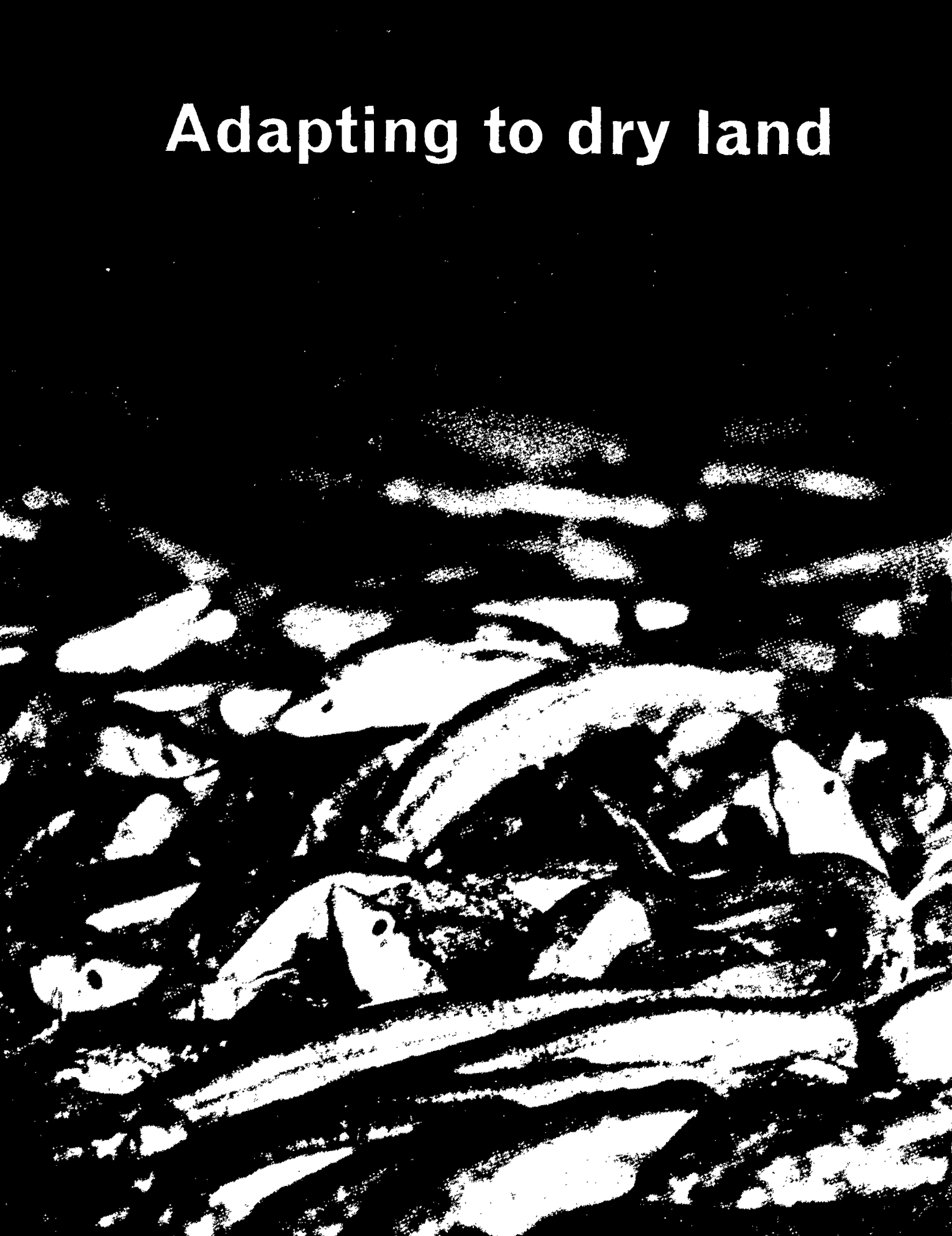
Solomon, L., 1962: An investigation of the excretion of ammonia and urea by *Periophthalmus sobrinus* Eggert in water of different salinities. Unpubl. B. Sc. Honors thesis, Dept. Zoology, University Witwatersrand, South Africa.

Stebbins, R. C., and Kalk, M. 1961: Observations on the natural history of the mudskipper, *Periophthalmus sobrinus*. Copeia, (1): 18–27.

Wood, J. D., 1958: Nitrogen excretion in some marine teleosts. *Can. J. Biochem. Physiol., 36*: 1237–1242.

UNESCO ARCHIVES

Adapting to dry land



Reprinted from *Discovery*, vol. XXVII; nò. 4, 1966, p. 26-30

One of the biggest single evolutionary advances in the history of life came when our fish ancestors struggled from the restricting world of the sea and emerged onto the dry land. Just what physiological and biochemical changes did this giant leap involve?

Malcolm S. Gordon is Associate Professor of Zoology at the University of California, Los Angeles. His interest in the adaptions of animals to natural environments has led him on expeditions to the Canadian Arctic, South-east Asia, Madagascar and the Pacific. At present he is working on the physiological adaptions of deep sea fishes

The very nature of fossils makes them unsuitable subjects for physiological or biochemical study, and hence prevents direct investigations of most of the functional changes which have occurred in the evolutionary histories of living things. For example, the invasion of dry land by the vertebrates, a process which began some 350 million years ago and which may still be going on today, is impossible to study. All we can do is look at the physiology and behaviour of present-day organisms and from them speculate as to some of the possibilities that might have been exploited in the past.

According to paleontologists, our ancestral emergence from the aquatic environment probably occurred in tropical fresh water swamps, where a highly evolved group of fishes (the rhipidistian crossopterygians) apparently gave rise to the earliest true amphibians. This evolutionary development probably occurred a number of times over a considerable span of years, in several or many different places. Thus, the basic functional problems created by the change to a terrestrial environment were probably solved in a variety of ways.

So far only a few species of living amphibians and amphibious fishes have been investigated, but the results already seem to support this concept of alternative solutions. Most present-day fishes taken out of the water react as if they were making a dive into a hostile, asphyxic environment. Did the earliest proto-amphibians react similarly? How did these earliest four-legged creatures adjust to the sudden restriction of liquid water available to them? Did the mode of operation of their kidneys alter? Was the pattern of waste nitrogen excretion changed?

Fig 1 GRUNION spawning on a southern Californian beach. These small fish, related to the whitebait, move onto the wave-washed zone of certain beaches at certain times during the spring. The females deposit their eggs in the sand while the males release their milt in the area around them. Each fish is out of the water for only a few minutes. The grunion show a typical diving syndrome—as soon as they emerge from the water their heart beat slows dramatically and the oxygen supply to all but their essential tissues is cut off

The diving syndrome

Many aquatic birds and mammals dive beneath the water surface. The physiological adjustments during such dives have been intensively studied over the past twenty-five years or so, particularly by Dr P. F. Scholander, his colleagues and students. A clearly defined "diving syndrome" (which may be far more widely distributed than in diving animals) has been outlined; this syndrome has several fundamental features *(see Fig. 1)*.

Since aerobic metabolism, in which oxygen is reduced to water, is the most efficient way of producing energy, the limited supplies of oxygen carried in the animal's body must be conserved if the dive is to be prolonged. Accordingly, most diving animals greatly reduce their metabolic rates, often by as much as 50%, and their heart rate drops dramatically as soon as they dive *(see Fig. 2)*. However, certain areas, such as the nervous system and the heart, cannot function at all without oxygen so that this cutback in aerobic metabolism cannot take place in these critical tissues. Instead, the peripheral circulation taking blood to the muscles—which *can* function anaerobically — is stopped entirely, and virtually all the blood is circulated to those organ systems most in need of oxygen.

The muscles function normally for the first part of the dive, until they use up the oxygen which is dissolved in their own fluids and bound to myoglobin (muscle haemoglobin). For the rest of the time the muscles operate anaerobically, producing large amounts of lactic acid in the process. Since there is no circulation, this lactic acid accumulates until the dive is over and the animal can begin to breathe air again. When breathing begins the blood flow returns to the muscles and there is a rapid, large rise in blood lactic acid concentration as the accumulated stores in the tissues diffuse out. The aerobic machinery of the tissues quickly begins to function again and this lactic acid is rapidly removed and metabolized *(see Fig. 3)*.

Most fishes exhibit the diving syndrome when they are taken out of the water—including types like flying fish which often make brief excursions into the air. Air is deadly for most fishes,

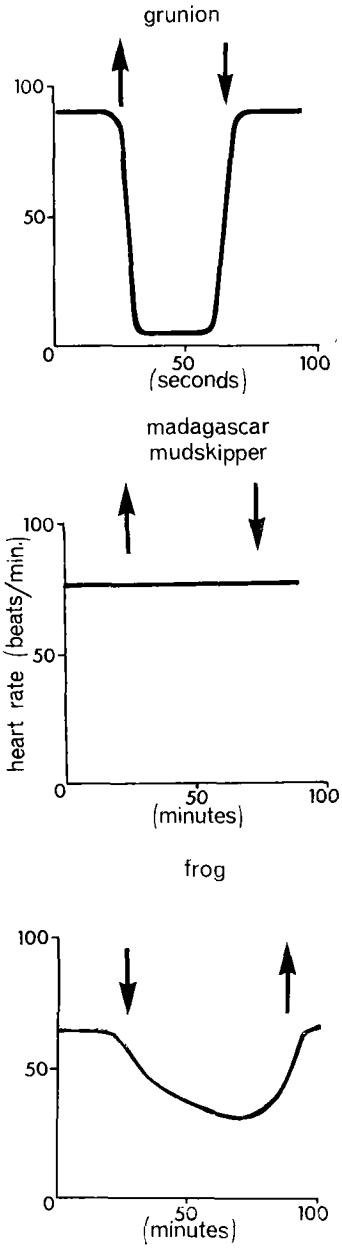


Fig 2 DIVING SYNDROME in a typical fish, amphibious fish and true amphibian, as illustrated by changes in the heart rate. An upward pointing arrow indicates leaving the water, a downward arrow submerging. The grunion exhibits a marked diving syndrome and cannot survive for more than a few minutes on dry land. The mudskipper is well adapted for long periods on dry land, showing no trace of the syndrome. The frog shows a moderate, slower decrease in heart rate while submerged, and can survive for long periods

largely because their gills collapse on themselves and reduce the area of the surface available for respiratory exchange far below the amount required. In such asphyxic environments the diving syndrome is a very useful adaptation for short-term survival, but fish reacting in such a limited way would oviously not be likely candidates for a terrestrial existence. However, a variety of other fishes enter the air and remain there for considerable periods with no apparent harm. What underlying mechanism accounts for their success?

Amphibious fishes

Species of amphibious fish range from the many types of intertidal blennies and gobies, briefly exposed to the air while hopping from one tide pool to another, through their near relatives which may stay out of water for many hours during low tide periods in the protective shelter of wet seaweed, to forms like the common eel which may make extended overland trips on damp nights. Probably the most extreme forms are the highly terrestrial tree climbing "perch" *(Anabas)* of southeast Asia and the goby-like mud-skippers *(Periophthalmus, Boleophthalmus* and related genera) of many tropical seashores *(see Fig. 4)*.

Unfortunately, we know very little about the vast majority of these creatures. Some seem to survive by using another respiratory organ in addition to their gills—a common type is an accessory lung formed from an outgrowth of the gill cavity itself. Another, probably very widespread procedure is to use the skin for respiration—as do most amphibians.

A group of friends and I studied the small mudskipper *Periophthalmus sobrinus* on the island of Nosy Bé, off northwestern Madagascar, as part of the International Indian Ocean Expedition. Although we were specifically looking for the diving syndrome we were unable to detect even a trace of it. This mudskipper, and probably most related species, can survive perfectly well completely submerged in water, deprived of all access to the surface. Normally, however, it spends more than 90% of its time crawling and hopping about on intertidal mudflats, mangrove trees and rocky shores. It shows no change in metabolic rate when entering or leaving fully aerated sea water: there are no changes in heart rate nor in blood lactic acid concentration. The fish appears equally well adapted to either environment, at least with respect to this particular group of physiological characteristics. It probably achieves this independence by means of a highly developed ability to breathe through its skin.

However, it appears that *all* mudskippers may not react in the same way. Several years ago, Mr W. F. Garey, a colleague of Professor Scholander's, investigated changes in heart rate in an Australian species of mudskipper *(Periophthalmodon australis)*. Garey found marked alterations in heart beat frequency between the fish in air and when in water: in fact, his fish reacted to water like terrestrial animals — their hearts slowed down when they were submerged! Evolution may have progressed so far in the Australian fish that it is hardly an aquatic beast at all.

The mudskippers and their relatives—indeed all living varieties of amphibious fishes—are just that: fishes. They are the products of hundreds of millions of years of evolution as fishes. We may assume therefore that they represent the range of physiological variability of which the fishes—the ancestral group from which the proto-amphibians were derived—are capable.

True amphibians

Living amphibians, on the other hand, represent the range of physiological variability of the most closely related of the descendants of the original proto-amphibians. There are completely aquatic species which never leave the water, there are aquatic forms which survive dry periods in their ponds and streams by burrowing into the mud and estivating ("hibernating" during the summer), and there are desert species which spend over 95% of their existence underground, emerging only long enough to mate and lay eggs in temporary pools formed by rare and sporadic heavy rains. The majority of species, like the common frogs, lie between these extremes.

Only a few of even the ordinary species of frogs and toads generally used in laboratories have been studied with respect to the diving reflex, and these few forms are basically terrestrial in their natural behaviour in any case. The hearts of these animals appear to slow down during dives, but since all amphibians can respire across their skins, the onset of this reduced heart rate is slow: for a frog a dive does not mean a complete cut-off of respiratory exchanges. In addition, there appear to be less dramatic reductions in metabolic rate than occur in diving species in other groups. G. Shelton and D. Jones indicated recently

that circulatory adjustments during dives in two species of frogs are similar in pattern to those for birds and mammals. An important difference from these other groups is that the circulation to the skin probably continues—or is enhanced.

Changes in kidney function and nitrogen excretion

Apart from the method employed for respiration, other important functional changes an animal must undergo in emerging from water onto dry land are in its patterns of kidney function and nitrogen excretion. Several species of frogs and toads have been investigated while subjected to a severely restricted water supply, or even under conditions of complete dehydration. J. Balinsky, M. Cragg and E. Baldwin studied patterns of nitrogen excretion *Xenopus lævis*, the completely aquatic South African clawed frog; R. Forster and B. Schmidt-Nielsen studied kidney function and nitrogen excretion in several of the common American species of semi-terrestrial frogs, while K. Schmidt-Nielsen, P. Lee, V. Tucker and I have done similar work with the sole salt water frog known—the crab-eating frog *(Rana cancrivora)* of Thailand.

Unlike the diving syndrome, here the comparison of very different species has led to an impression of widespread uniformity of response—at least in the major features. This is probably because amphibians have only a narrow range of functional pathways available for responding to restrictions in water supply; the ultimate aim is, of course, to limit water loss as much as possible.

The kidneys of frogs have basically the same structure as those found in most vertebrates. Urine is produced by a pressure filtration of blood plasma (leaving all the cells and at least most of the proteins behind) across the walls of tufts of coiled capillary vessels, called glomeruli. The filtrate passes into a double-walled cup called Bowman's capsule, then passes down a long sinuous tubule where the plasma filtrate is greatly reduced in volume and is converted to the appropriate chemical composition for the urine of the animal in its existing physiological state. This process involves water reabsorption and reabsorption of important dissolved substances such as glucose from the urine back into the kidney, and the diffusion of waste materials, such as ammonia and urea, across the walls from the kidney into the urine. Such a mechanism exists in virtually all vertebrates; frogs and toads, and possibly other amphibians, can in addition further modify urine volume and composition through the action of the cells in the walls of the urinary bladder.

Adjusting to water restriction

Anuran amphibians, of which the frogs and toads are the most common members, can use their excretory system to adjust urinary water and nitrogen losses to their needs. They are able to control the amount of plasma initially filtered, the amount of water reabsorbed in the tubules and bladder, and the amounts of dissolved substances permitted to pass out of the body. When the water supply is severely limited the rate of urine production declines markedly; in extreme cases to only 1—2% of the rate in normal animals with access to free water *(see Fig. 6)*. About one-third of this decrease is due to a decline in the volume of blood plasma filtered; the rest is due to increased re-absorption of water in the tubules and the bladder. The decrease in volume is accompanied by an increase in the concentration of the urine, up to the point, in severely stressed animals, where the concentration of dissolved substances in the urine is equal to that in the blood. This increased concentration is largely due to increased amounts of urea. As the amount of urea excreted rises, the proportion of nitrogen wastes excreted as ammonia declines.

Desert anurans, which spend most of their lives underground, apparently excrete virtually no urine at all while beneath the surface. Just how their kidneys function is unknown, but they probably make extensive use of their urinary bladders as water storage organs, absorbing and recycling through their systems water and useful solutes. Anurans are thus able to resist their urinary water losses to a large extent, partially offsetting water losses across their skins which they cannot readily control. The shift in nitrogen excretion from ammonia to urea also permits them to survive periods of water shortage more easily—ammonia appears to be highly toxic to all vertebrates, while much higher concentrations of urea can be tolerated in the blood and body fluids of many species.

Some speculation

Although our knowledge is obviously still very limited, the evidence gathered on these two important functional aspects permits some general speculation about the first vertebrates to emerge onto dry

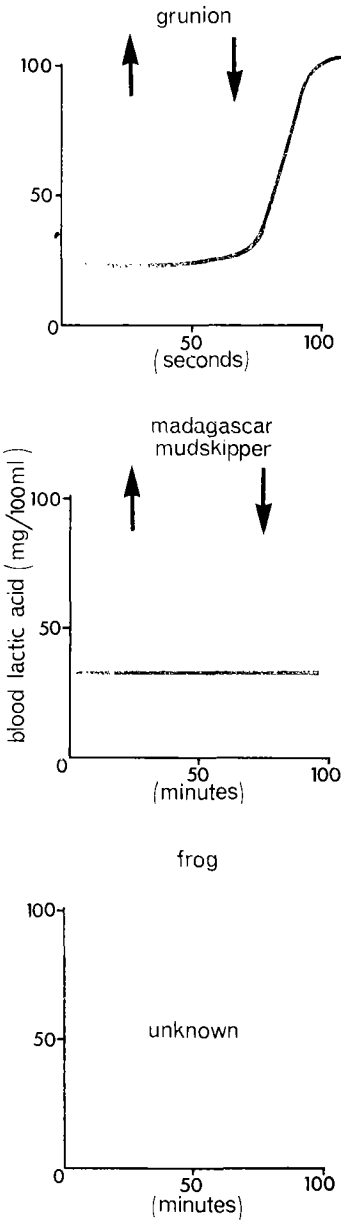
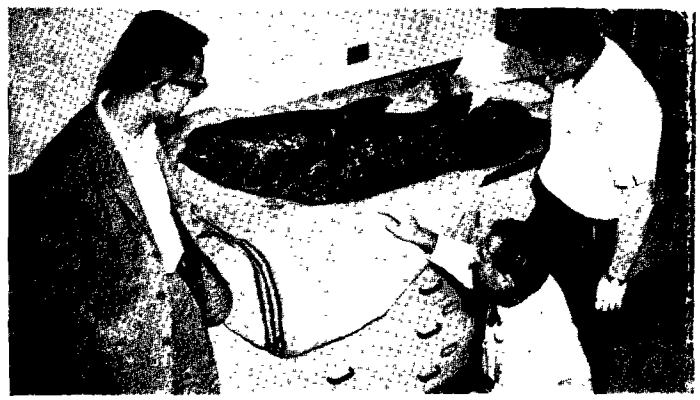
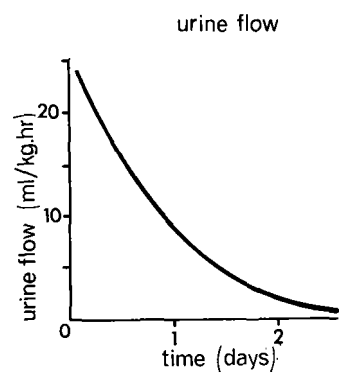
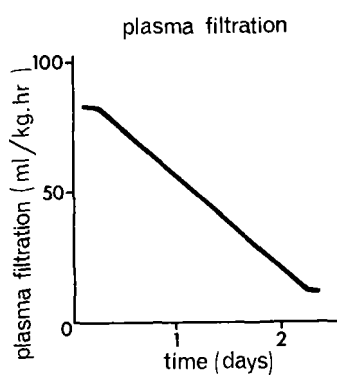


Fig 3 MUSCLES in a creature with a marked diving syndrome, such as the grunion, must continue to function without oxygen when the air supply is cut off, producing large quantities of lactic acid in the process. Since there is no circulation, this lactic acid accumulates until the dive is over and the animal can begin to breathe normally again. There is then a rapid, large rise in the blood lactic acid concentration as the accumulated stores in the tissues diffuse out. The mudskipper does not show this effect









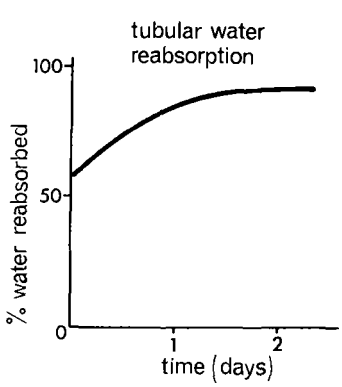


Fig 4 MUDSKIPPER on an intertidal mudflat along the shores of the Gulf of Thailand near Bangkok (left). Although it can survive perfectly well completely submerged in water, with no access to the surface, it normally spends more than 90% of its time crawling and hopping about on the land. It shows no evidence of the diving syndrome and appears equally well adapted to either environment

Fig 5 LIVING COELACANTH fish Latimeria chalumnae (right), caught in December 1964 near the Comores Islands, and now preserved at the University of California, Los Angeles. Closely related to the ancestors of the higher vertebrates, it is the only available source of relatively direct information about the physiology and biochemistry of ancestral groups

land. First, the earliest proto-amphibians probably either showed no diving syndrome or at least were well on their way to eliminating this type of response. The diving syndrome seems to be a set of adjustments permitting short term survival in a hostile, asphytic environment —the selective advantages associated with entering the terrestrial environment were almost certainly associated with *long* term residence there. Probably therefore, adaptions permitting elimination of the diving syndrome were selected in the proto-amphibians; the absence of the syndrome from the Madagascar mudskipper and its appearance only on *submergence* in frogs supports this position.

Secondly, the chances seem good that they were able to adjust their kidney function and pattern of nitrogen secretion in much the same way as in living frogs and toads. These adjustments seem to be virtually universal among living amphibia. Since the various groups of these animals may well be derived from separate paths of evolutionary development after the first emergence onto dry land, the wide distribution of the process argues that it was an early and fundamental step.

Fig 6 CHANGES IN KIDNEY FUNCTION in a common frog, kept out of water but not dehydrated seriously, for 2½ days. The prime aim is, of course, to limit water loss as much as possible. To this end it can control the amount of blood plasma initially filtered, the amount of water reabsorbed into the body from the tubules and bladder, and the amounts of dissolved substances, such as salts and urea, permitted to pass out of the body in urine

I would feel more confident about making even these limited statements if more data were available from a wider variety of life-forms—both fishes and amphibians. We particularly need information from species with 'unusual' life histories; these are often the ones which have solved the difficult problems most clearly and completely. Physiologists must free themselves from their laboratories and be prepared to work in the field, where they can obtain these 'unusual' beasts in adequate numbers, in good condition, and under circumstances where they can become familiar with the ecology and behaviour of their subjects, as well as their physiology.

Finally, we need as much functional information as possible from the single most critical species of all. The living coelacanth fish, *Latimeria chalumnae*, known virtually only from the waters around two of the islands of the Comoro archipelago in the western Indian Ocean, is the nearest thing we are likely to find to the fish which were directly ancestral to the proto-amphibians. Details of the nature of its diving syndrome, its kidney function, mode of osmotic regulation, and pattern of nitrogen excretion, would all be invaluable. *Latimeria*, however, is a rare animal that defies predictions concerning possible times and places of capture. My friends and I made an extended effort at catching a live specimen during the Indian Ocean expedition. We failed, but eventually obtained, at second hand, a well preserved dead one *(see Fig. 5)*. Additional efforts in this direction, profiting by our experience, are called for.

BEAUFORTIA

SERIES OF MISCELLANEOUS PUBLICATIONS

ZOOLOGICAL MUSEUM OF THE UNIVERSITY OF AMSTERDAM

No. 165 Volume 14 November 21, 1966

New species of *Macrochiron* (Copepoda, Cyclopoida) associated with hydroids in Madagascar

ARTHUR G. HUMES

ABSTRACT

From the region of Nosy Bé, Madagascar, three new species of copepods belonging to the lichomolgid genus *Macrochiron*, associated with plumulariid hydrozoans, are described: *M. lytocarpi* and *M. valgum* from *Lytocarpus philippinus* and *M. rostratum* from *L. philippinus* and *L. spectabilis*. Certain features of the external anatomy of *Macrochiron* are briefly discussed.

INTRODUCTION

The genus *Macrochiron* Brady, 1872, has been generally regarded as free-living. However, at Ifaluk Atoll in the Caroline Islands, Vervoort (1964) has recorded *M. cheliferum* (Thompson & A. Scott, 1903) apparently living on hydroids. As a result of recent collecting in the vicinity of Nosy Bé, in north-western Madagascar, three new species of the lichomolgid genus *Macrochiron*, described below, have been found associated with the hydrozoan genus *Lytocarpus* Allman, 1883 (family Plumulariidae).

The hydroids were collected by hand while swimming with a face mask and snorkel tube. In order to avoid the violent stinging sensation received when these featherlike hydroids were disturbed, and to insure that copepods living on them were not dislodged during handling, each colony was cut free at its basal attachment and then floated quickly into a plastic bag which was closed immediately and tied. The copepods were later recovered from the sediment obtained after washing the hydroids in weakly alcoholized sea water.

The material covered in this paper comprises:

Macrochiron lytocarpi n. sp., *Macrochiron valgum* n. sp., and *Macrochiron rostratum* n. sp., all from *Lytocarpus philippinus* (Kirchenpauer, 1872). and

Macrochiron rostratum n. sp., from *Lytocarpus spectabilis* Allman, 1883.

ACKNOWLEDGEMENTS

The copepods were collected by the author in 1960 while a member of an expedition sent to Madagascar by the Academy of Natural Sciences of Phila-

Received: July 1, 1966.

delphia and in 1963-64 while participating in the activities of the U.S. Program in Biology of the International Indian Ocean Expedition.

The study of the specimens has been aided by a grant (GB-1809) from the National Science Foundation of the United States.

I wish to thank Dr. Anita Brinckmann-Voss of the University of Manitoba for the identifications of the hydroids, and to acknowledge the assistance to the field work given by the staff of the Centre d'Océanographie et des Pêches at Nosy Bé.

Macrochiron lytocarpi n. sp. Figs. 1—32.

Type material. — 155 ♀♀, 87 ♂♂, and 6 copepodids washed from a hydroid, *Lytocarpus philippinus* (Kirchenpauer), in a depth of 2 m, at Ambariobe, a small island nearly between Nosy Bé and Nosy Komba, Madagascar. September 19, 1964. Holotype female, allotype, and 90 paratypes (60 ♀♀, 30 ♂♂) deposited in the Zoölogisch Museum, Amsterdam (Z.M.A. Co. 101.017), the same number of paratypes in the United States National Museum, Washington, and the remaining paratypes in the collection of the author.

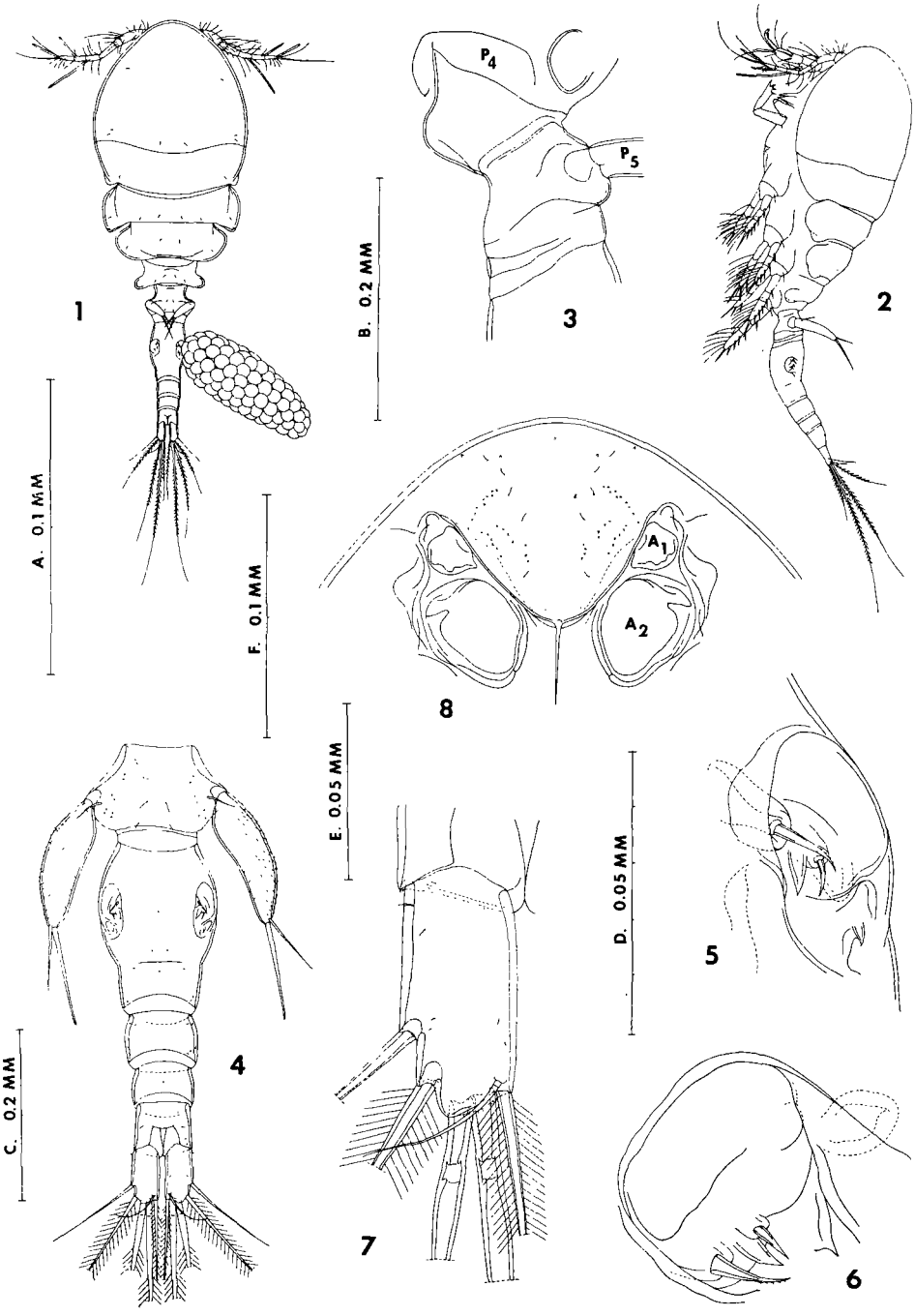
Other specimens. — 15 ♀♀, 28 ♂♂, and 30 copepodids from *Lytocarpus philippinus* in 1 m, Tany Kely, a small island to the south of Nosy Bé, June 23, 1963.

Female. — Body (figs. 1 and 2) rather slender. Length (excluding setae on caudal rami) 1.28 mm (1.18—1.38 mm) and greatest width 0.51 mm (0.46—0.54 mm), based on 10 specimens. Ratio of length to width of prosome 1.7 : 1. Segment bearing leg 1 separated from head dorsally and laterally by a furrow. Epimeral areas of metasomal segments differing in size and form as shown in figures. Posteroventral region of segment of leg 4 produced (fig. 3).

Segment of leg 5 (fig. 4) 91 × 161 μ. Between this segment and genital segment a very short ventral intersegmental sclerite (shown in fig. 3). Genital segment (fig. 4) elongated, 200 μ in length, in dorsal view its anterior two-thirds gently rounded (greatest width 135 μ), its posterior third slightly constricted with nearly parallel margins (width here about 94 μ). Ventral surface of genital segment with very fine transverse striae. Areas of attachment of egg sacs dorsolateral, each area (figs. 5 and 6) bearing 2 setae (7 and 13 μ in length) with a spinous process (8 μ) between them and a small spinous process posteriorly. Three postgenital segments 68 × 78, 47 × 70, and 55 × 66 μ from anterior to posterior. Anal segment with row of minute spinules along posteroventral border.

Caudal ramus (fig. 7) moderately elongated, 66 × 31 μ in greatest dimensions. Ratio of length to width 2.1 : 1. Outer lateral seta 130 μ long and naked. Pedicellate dorsal seta 39 μ and naked. Outermost terminal seta 213 μ with lateral spinules along its proximal two-thirds; innermost terminal seta 239 μ with similar spinules. Two long median terminal setae 370 μ (outer) and 484 μ (inner) with lateral spinules in their midregions; these 2 setae inserted between dorsal (smooth) and ventral (with row of minute spinules) flaps. Ramus with a minute lateral setule 2 μ long on outer basal margin and with a few small hairs on dorsal and ventral surfaces.

Dorsal surface of prosome and urosome with few minute hairs (sensilla) and refractile points; ventral surface of urosome with very little such ornamentation. Ratio of length of prosome to that of urosome 1.65 : 1.



FIGURES 1—8. *Macrochiron lytocarpi* n. sp., female: 1, body, dorsal (A); 2, body, lateral (A); 3, junction of segments of legs 4 and 5, lateral (B); 4, urosome, dorsal (C); 5, area of attachment of egg sac, dorsal (D); 6, area of attachment of egg sac, lateral (D); 7, caudal ramus, dorsal (E); 8, rostrum, ventral (F).

Egg sac (see fig. 1) elongated, in one female 495 × 187 μ, with numerous eggs each about 50 μ in diameter.

Rostrum (fig. 8) well-developed, its posteriorly directed margin rounded and terminating in a slender, needlelike process (57 μ long) lying between bases of second antennae.

First antenna (fig. 9) 7-segmented, lengths of segments (measured along their posterior non-setiferous margins) 44 (55 μ along anterior margin), 78, 26, 59, 45, 33, and 47 μ respectively. Formula for armature: 4, 13 (5 + 8), 6, 3, 4 + 1 aesthete, 2 + 1 aesthete, and 7 + 1 aesthete. Terminal seta 200 μ long. All setae naked. Ventral sclerite on third segment suggesting an intercalary segment.

Second antenna (fig. 10) 3-segmented, last segment 137 μ long. First segment with a short naked seta. Second with a strong spinelike naked seta and minute inner surficial bosses. Third segment proximally with 3 setae (one naked, one unilaterally with spinules, and the third with a spinulose fringe) and an oblique row of bosses; distally with 6 setae (4 of them naked and 2 with fine unilateral barbules, one of these 2 being jointed and slightly unguiform) and a prominent claw 114 μ along its axis. Claw bisegmented with proximal part showing a line of partial further division; teeth along concave surface in a single row.

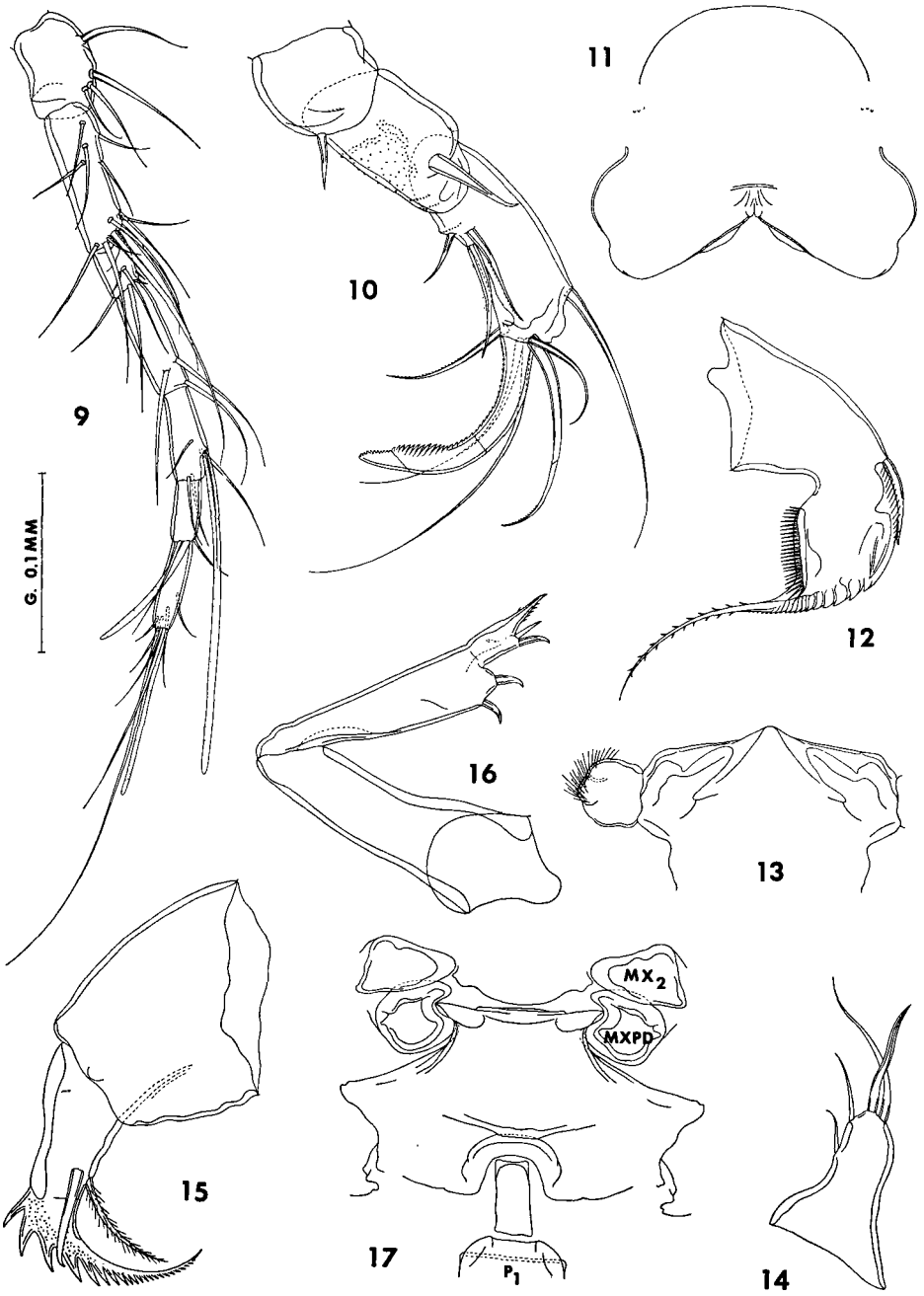
Labrum (fig. 11) with 2 ventral lobes widely divergent.

Mandible (fig. 12) with blade having near its concave edge a row of slender spinules, on its posterior surface a spinous sclerotization, and on its convex edge a pectinate scalelike sclerotization followed by a row of graduated teeth. Lash with spinules along each side. Paragnath (fig. 13) a small lobe with hairs. First maxilla (fig. 14) with 4 setae. Second maxilla (fig. 15) 2-segmented, first segment unornamented; second produced to form a serrated lash and bearing proximally a minute spinule and distally 2 setae, one setose, the other spiniform, hyaline, with a rather blunt tip. Maxilliped (fig. 16) 3-segmented, though separation of last 2 segments not very distinct. Second segment elongated and straight, with 2 recurved spines. Third segment small with 4 elements — a small subterminal setule, a recurved spine, a hyaline seta, and a pectinate spine (without definite articulation).

Area between maxillipeds and first pair of legs (fig. 17) only slightly protuberant (see fig. 2); sclerotized line connecting bases of maxillipeds.

Legs 1—4 (figs. 18, 19, 20, and 21) with trimerous rami except for endopod of leg 4 which consists of a single segment. Armature as follows (Roman numerals indicating spines, Arabic numerals setae):

P_1	protopod 0—1; 1—0	exp I—0; I—1; III,I,4
		end 0—1; 0—1; I,5
P_2	protopod 0—1; 1—0	exp I—0; I—1; III,I,5
		end 0—1; 0—2; I,II,3
P_3	protopod 0—1; 1—0	exp I—0; I—1; III,I,5
		end 0—1; 0—2; I,II,2
P_4	protopod 0—1; 1—0	exp I—0; I—1; III,I,5
		end 2



FIGURES 9—17. *Macrochiron lytocarpi* n. sp., female (continued): 9, first antenna, ventral (G); 10, second antenna, inner (G); 11, labrum, ventral (F); 12, mandible, posterior (E); 13, paragnath and median area, ventral (E); 14, first maxilla, posterior (E); 15, second maxilla, posterior (E); 16, maxilliped, postero-inner (F); 17, area between maxillipeds and first pair of legs, ventral (B).

Inner seta on coxa of legs 1—3 long and plumose, but in leg 4 somewhat shorter (42 μ) and naked. In legs 1—3 inner margin of basis with row of hairs, but this margin smooth in leg 4. In leg 1 margin of basis median to endopod not projected, but in legs 2—4 forming a process. Endopods of legs 1—3 with outer and terminal processes obtuse, but inner processes acute. Three spines on last segment of endopod of leg 2 measuring 37, 34, and 59 μ in length from outer to inner; those on leg 3, 47, 44, and 73 μ. Leg 4 with exopod slightly twisted; endopod 74 μ in length (about as long as first exopod segment), 17.5 μ wide proximal to outer marginal notch, 15.5 μ wide distal to notch, with 2 terminal setae 33 μ (outer) and 91 μ (inner), both with extremely minute barbules, and with a few delicate hairs along outer margin distal to notch. Endopod with very indistinct line of division.

Leg 5 (fig. 22) held erect in specimens in alcohol (see fig. 2). Free segment elongated, 159 $\times$ 44 μ in greatest dimensions, tapered distally, with numerous minute spinules on outer half of dorsal surface, outer terminal seta 72 μ long and naked, inner terminal seta 107 μ with few spinules near its blunt tip (fig. 23). Seta on body near free segment 30 μ and naked.

Leg 6 probably represented by 2 setae near attachment of each egg sac (see figs. 5 and 6).

Color in life in transmitted light varying from slightly opaque to translucid, almost glassy, eye red, egg sacs gray.

M a l e. — Body (figs. 24 and 25) resembling in general that of female. Length (without setae on caudal rami) 1.08 mm (1.00—1.14 mm) and greatest width 0.37 mm (0.34—0.40 mm), based on 10 specimens. Ratio of length to width of prosome 1.65 : 1.

Segment of leg 5 (fig. 26) 60 $\times$ 99 μ. Between this segment and genital segment no ventral intersegmental sclerite. Genital segment longer than wide, 229 $\times$ 180 μ, its lateral margins in dorsal view slightly convex. Four post-genital segments 52 $\times$ 68, 49 $\times$ 62, 31 $\times$ 57, and 43 $\times$ 56 μ from anterior to posterior.

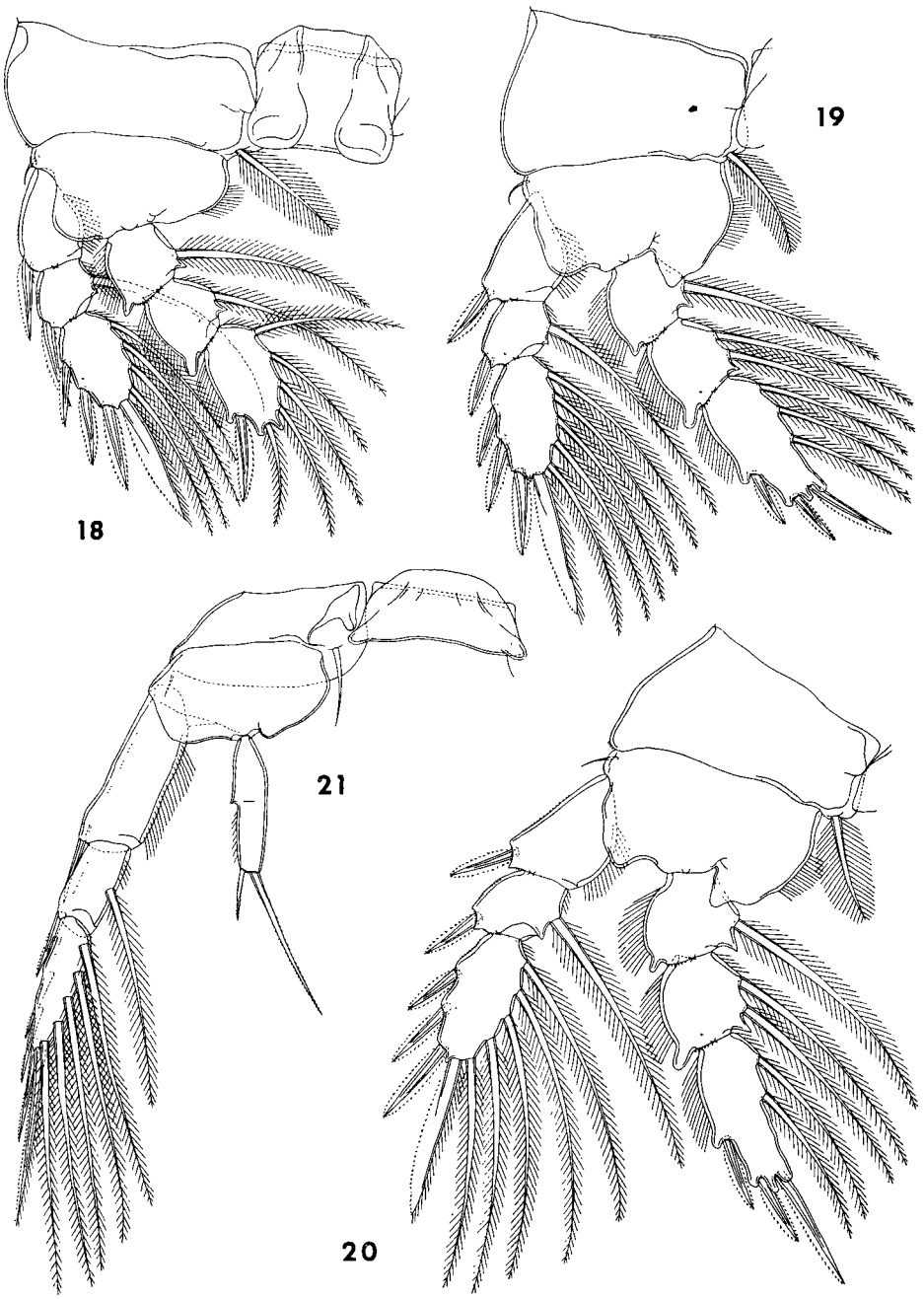
Caudal ramus like that of female but smaller, 53 $\times$ 26 μ.

Surfaces of prosome and urosome with fine hairs and minute refractile points as shown in figs. 24 and 26. Ratio of length of prosome to that of urosome 1.25 : 1.

Rostrum like that of female.

First antenna (fig. 27) resembling that of female but with 3 aesthetes added. Lengths of segments (measured along their posterior non-setiferous margins) 35 (45 μ along anterior margin), 51, 22, 50, 44, 32, and 47 μ respectively. Formula for armature: 4, 13 + 2 aesthetes, 6, 3 + 1 aesthete, 4 + 1 aesthete, 2 + 1 aesthete, and 7 + 1 aesthete. All setae naked.

Second antenna, labrum, mandible, paragnath, first maxilla, and second maxilla like those in female. Maxilliped (fig. 28) slender and elongated (cf. fig. 25), 4-segmented, assuming that proximal half of claw represents a fourth segment. Second segment with 2 naked setae and a row of spinules on inner surface. Claw 153 μ along its axis (including large terminal lamella), partially



FIGURES 18—21. *Macrochiron lytocarpi* n. sp., female (continued): 18, leg 1, anterior (G); 19, leg 2, anterior (G); 20, leg 3, anterior (G); 21, leg 4, anterior (G).

divided about midway, and bearing 2 unequal setae proximally, larger one with small spinules along one edge.

Legs 1—4 segmented as in female and having similar armature and ornamentation, except for leg 1 where last segment of endopod (fig. 29) shows sexual dimorphism, its formula being I,I,4 (outer spinulose spine 37 μ, inner spine 42 μ and naked except for scalelike knobs along edges). Slight sexual dimorphism seen also in spines on last segment of endopod of leg 2 (29, 26, and 37 μ in length from outer to inner) and of leg 3 (42, 29, and 49 μ).

Leg 5 (fig. 30) much smaller than in female, its free segment slender, 44 $\times$ 13 μ, with its 2 terminal naked setae 35 μ (outer) and 46 μ (inner) and with its surface unornamented except for a few minute refractile points.

Leg 6 (fig. 31) a posteroventral flap on genital segment, bearing 2 naked setae 23 and 40 μ in length.

Spermatophore (fig. 32), extruded under slight pressure from body of male, about 208 $\times$ 83 μ, not including neck.

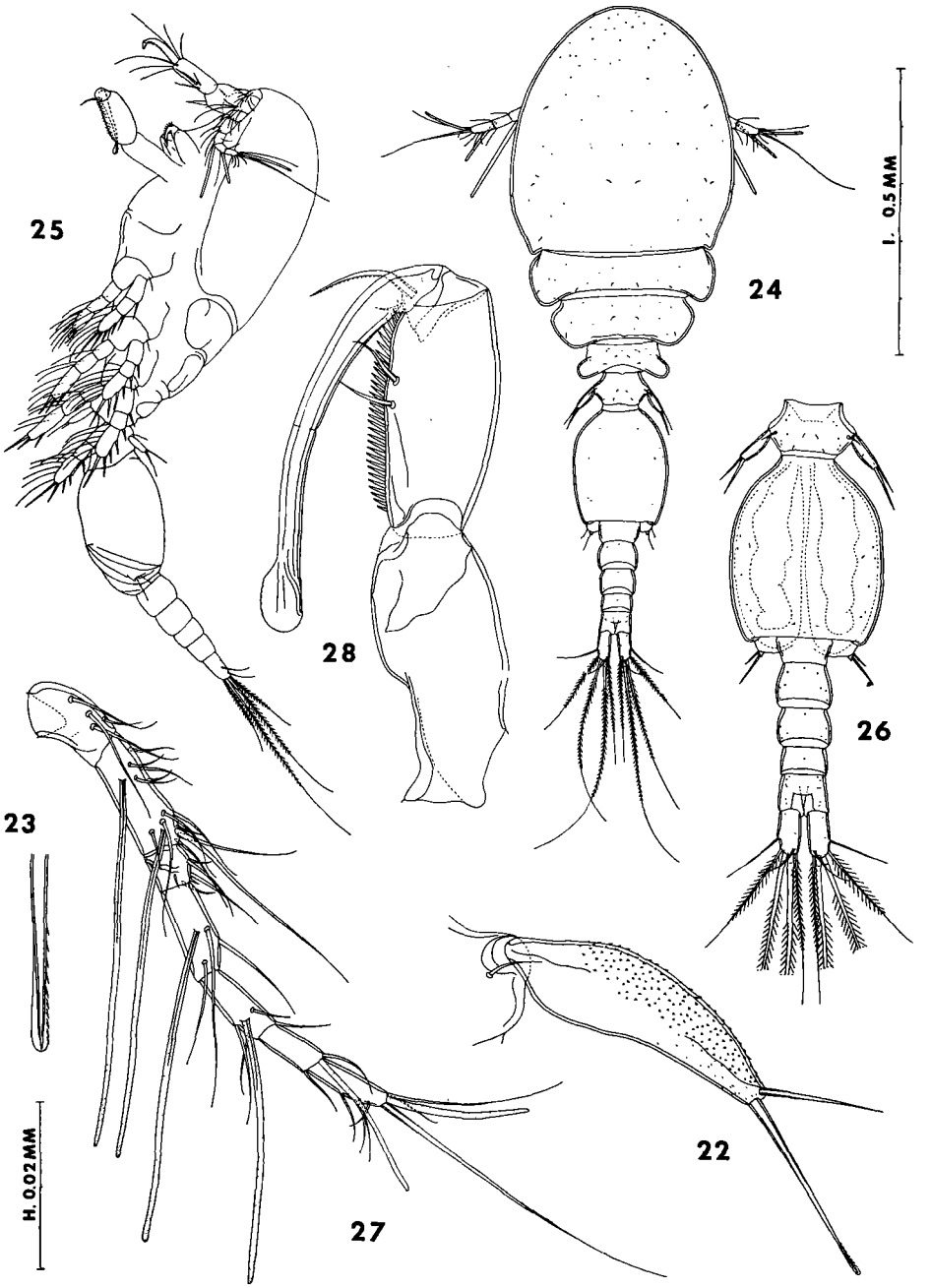
Color in life in transmitted light resembling that of female.

(The specific name *lytocarpi* is based on the generic name of the host.)

Relationship to other species in the genus. Following Stock's (1957) restricted generic definition of *Macrochiron* Brady, 1872, the genus may be recognized by its lichomolgid appearance; the 3-segmented second antenna with a strong, often bisegmented terminal claw; the second maxilla bearing near the base of the apical lash an ornamented seta and a smooth, often hyaline, rather blunt seta; the maxilliped in the female 3-segmented, its last segment small and sometimes indistinctly separated from the preceding segment; legs 1—3 with 3-segmented rami; leg 4 with a 3-segmented exopod and a small 1- or 2-segmented endopod (the line of division often not well-developed) with 2 terminal setae; leg 5 with a long free segment bearing 2 terminal setae.

Many species formerly attributed to *Macrochiron* actually belong to other genera, as Stock (1957) has pointed out. In addition to those listed by Stock, *Macrochiron (Paramacrochiron) ornatum* Krishnaswamy, 1952, does not belong to *Macrochiron,* since it has a 4-segmented second antenna. Instead it probably represents, along with *Macrochiron malayense* Sewell, 1949, and *Pseudanthessius parvus* A. Scott, 1909, a new genus near *Paramacrochiron* Sewell, 1949. (The advisability of erecting a new genus for *M. malayense* and *P. parvus* has already been indicated by Stock, 1957). *Macrochiron (Macrochiron) rigidum* Ummerkutty, 1962, is to be referred to *Lichomolgus* Thorell, 1860, since it has a 4-segmented second antenna and its 2-segmented endopod of leg 4 has the formula 0—1; II.

In *Macrochiron* three species were included by Stock (1957) : *M. fucicolum* Brady, 1872, *M. cheliferum* (Thompson & A. Scott, 1903), and *M. mutatum* Stock, 1957 (= *fucicolum* G. O. Sars, 1917, non Brady). *Macrochiron sargassi* G. O. Sars, 1916 (redescribed by Yeatman, 1962) also belongs almost certainly to the genus, in spite of the fact that Sars showed a small terminal fourth segment on the second antenna (see Yeatman, 1962: 256).



FIGURES 22—23. *Macrochiron lytocarpi* n. sp., female (continued): 22, leg 5, dorsal (G); 23, tip of inner seta on free segment of leg 5, dorsal (H).

FIGURES 24—28. *Macrochiron lytocarpi* n. sp., male : 24, body, dorsal (I); 25, body, lateral (I); 26, urosome, dorsal (C); 27, first antenna, ventral (G); 28, maxilliped, antero-outer (F).

M. lytocarpi differs from both *M. fucicolum* and *M. cheliferum* in the formula for the last segment of the exopod of leg 4 (III,I,5 in *M. lytocarpi*, II,I,5 in *M. fucicolum* and *M. cheliferum).* It may be distinguished from *M. sargassi* by the nature of the terminal armature of the second antenna (a single large claw in *M. lytocarpi*, two unequal claws in *M. sargassi*). It differs from *M. mutatum* in having the large teeth on the claw of the second antenna more distally located than in that species, the outer and terminal processes on the endopod segments of legs 1—3 blunt rather than acute, the second segment of the maxilliped in the female elongated and slender with the two spines far distal rather than relatively short and stout with the two spines in a central position, and the free segment of leg 5 in the female elongated but somewhat widened and spinulose rather than elongated, narrow, and smooth.

Macrochiron valgum n. sp. Figs. 33—60.

Type material. — 31 ♀♀, 48 ♂♂, and 42 copepodids washed from *Lytocarpus philippinus* (Kirchenpauer), in a depth of 1 m, Pte. Lokobe, Nosy Bé, Madagascar. November 3, 1960. Holotype female, allotype, and 28 paratypes (10 ♀♀, 18 ♂♂) deposited in the Zoölogisch Museum, Amsterdam (Z.M.A. Co. 101.018); 27 paratypes (10 ♀♀, 17 ♂♂) in the United States National Museum, Washington; and the remaining paratypes in the collection of the author.

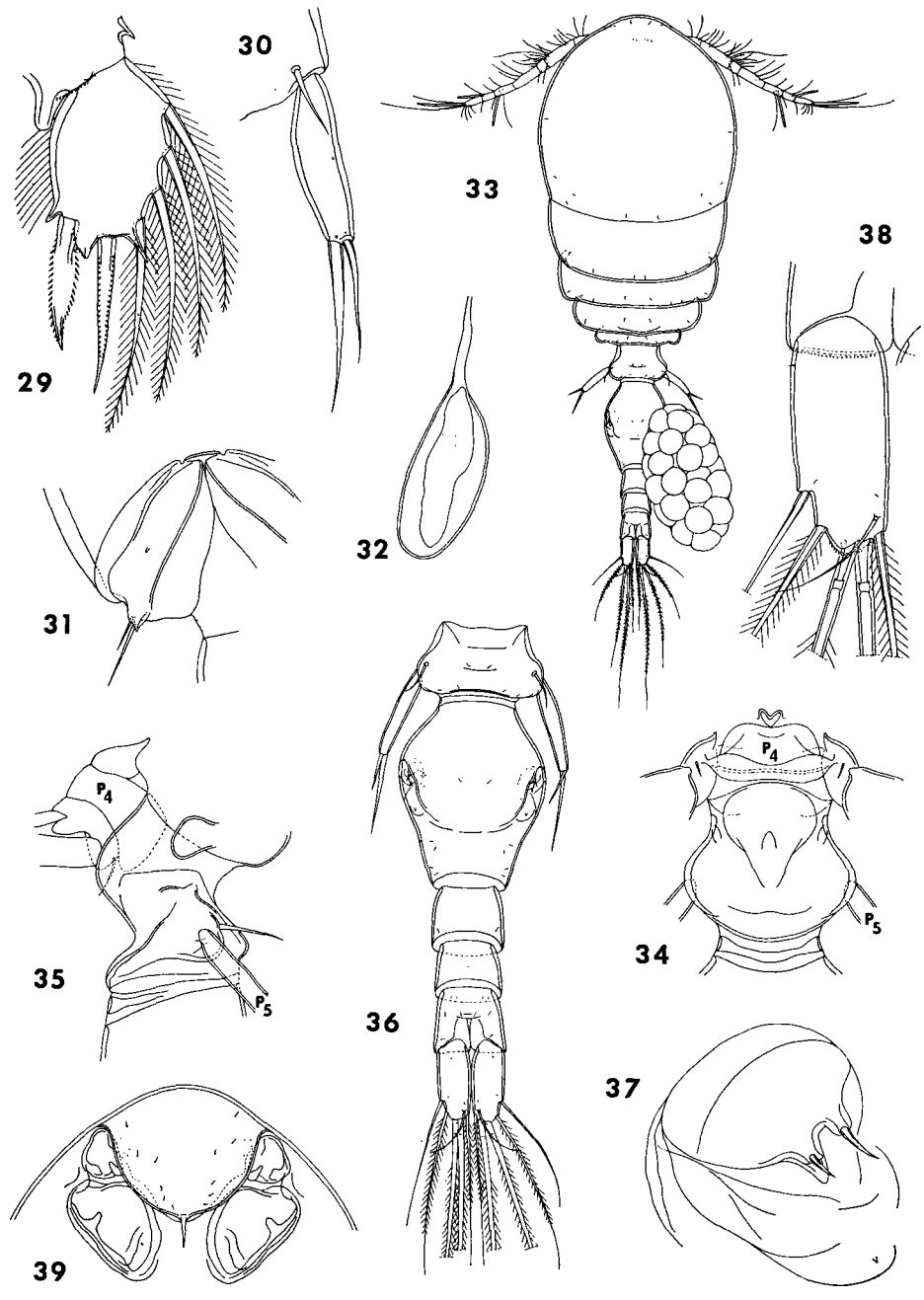
Female. — Body (fig. 33) moderately slender. Length (not including setae on caudal rami) 0.94 mm (0.89—1.01 mm) and greatest width 0.34 mm (0.32—0.36 mm), based on 10 specimens. Ratio of length to width of prosome 1.68 : 1. Segment of leg 1 separated from head by a furrow. Metasomal segments relatively broader than in *M. lytocarpi* and their epimeral areas less prominent. Posteroventral region of segment of leg 4 produced (figs. 34 and 35).

Segment of leg 5 (fig. 36) 57 × 96 μ. Between this segment and genital segment a very short ventral intersegmental sclerite. Genital segment longer than wide, 151 × 117 μ, moderately expanded in its anterior two-thirds and tapered posteriorly. Areas of attachment of egg sacs dorsolateral, each area (fig. 37) bearing 2 naked setae 5 and 7 μ in length, an adjacent spinous process, and more posteriorly a minute spinous process. Three postgenital segments 49 × 56, 39 × 52, and 48 × 54 μ from anterior to posterior. Last segment with row of minute spinules along posteroventral margin.

Caudal ramus (fig. 38) 65 × 26 μ in greatest dimensions, with ratio of length to width 2.5 : 1. Outer lateral seta 83 μ, dorsal seta 33 μ, outermost terminal seta 120 μ, innermost terminal seta 130 μ, and 2 long median terminal setae 200 μ (outer) and 275 μ (inner), the ornamentation of these setae as in preceding species. Minute setule on outer basal margin of ramus only 1 μ long.

Surfaces of prosome and urosome ornamented with hairs and refractile points as in figs. 33 and 36. Ratio of length of prosome to that of urosome 1.49 : 1.

Egg sac (see fig. 33) moderately elongated, in one female 275 × 140 μ, with fewer eggs than in *M. lytocarpi*, each egg about 47 μ in diameter.



FIGURES 29—32. *Macrochiron lytocarpi* n. sp., male (continued): 29, last segment of endopod of leg 1, anterior (E); 30, leg 5, dorsal (E); 31, leg 6, ventral (G); 32, spermatophore, extruded from body of male, dorsal (C).

FIGURES 33—39. *Macrochiron valgum* n. sp., female: 33, body, dorsal (I); 34, segments of legs 4 and 5, ventral (G); 35, junction of segments of legs 4 and 5, lateral (G); 36, urosome, dorsal (B); 37, area of attachment of egg sac, lateral (D); 38, caudal ramus, dorsal (E); 39, rostrum, ventral (B).

Rostrum (fig. 39) broadly rounded, its posterior margin terminating in a needlelike process 24 μ long (relatively shorter than in preceding species).

First antenna (fig. 40) with segmentation and armature as in *M. lytocarpi*. Lengths of segments (measured along their posterior non-setiferous margins) 39 (48 μ along anterior margin), 68, 21, 61, 44, 21, and 29 μ respectively. Terminal seta 110 μ long.

Second antenna (fig. 41) more slender than in preceding species but with generally similar armature and ornamentation. Third segment 122 μ long. Claw bisegmented, 130 μ along its axis, with row of teeth graduating proximally into sharp serrations.

Labrum (fig. 42) with lobes less divergent than in preceding species.

Mandible (fig. 43) similar to that in *M. lytocarpi* but with lateral spinules on lash less prominent. Paragnath and first maxilla as in *M. lytocarpi*. Second maxilla (fig. 44) similar to that in preceding species but teeth on lash more evenly spinelike. Maxilliped (fig. 45) with elongated second segment distinctly bowed; armature as in *M. lytocarpi* though all elements except hyaline seta more spinulose. Separation of last 2 segments not well-developed.

Area between maxillipeds and first pair of legs (fig. 46) only slightly protuberant and resembling that in *M. lytocarpi*.

Legs 1—4 (figs. 47, 48, 49, and 50) with armature as in preceding species, except for last segment of exopod of leg 4 which is II,I,5. Inner seta on coxa of leg 4 small, 7 μ long, and naked. Three spines on last segment of endopod of leg 2 measuring 20, 24, and 37 μ in length from outer to inner; those on leg 3, 36, 30, and 43 μ. Endopod of leg 4 slender, without a line of division, 48 × 8 μ, with a small notch and indistinct hairs on its outer border and with 2 terminal setae, outer 23 μ long and finely barbed, inner 59 μ and fringed.

Leg 5 (fig. 51) with elongated, slender, unornamented free segment, 73 × 12 μ, bearing terminally 2 setae, outer 39 μ and naked, inner 65 μ and fringed along outer edge. Seta on body near attachment of free segment 33 μ and slightly haired.

Leg 6 probably represented by 2 setae near attachment of each egg sac (see fig. 37).

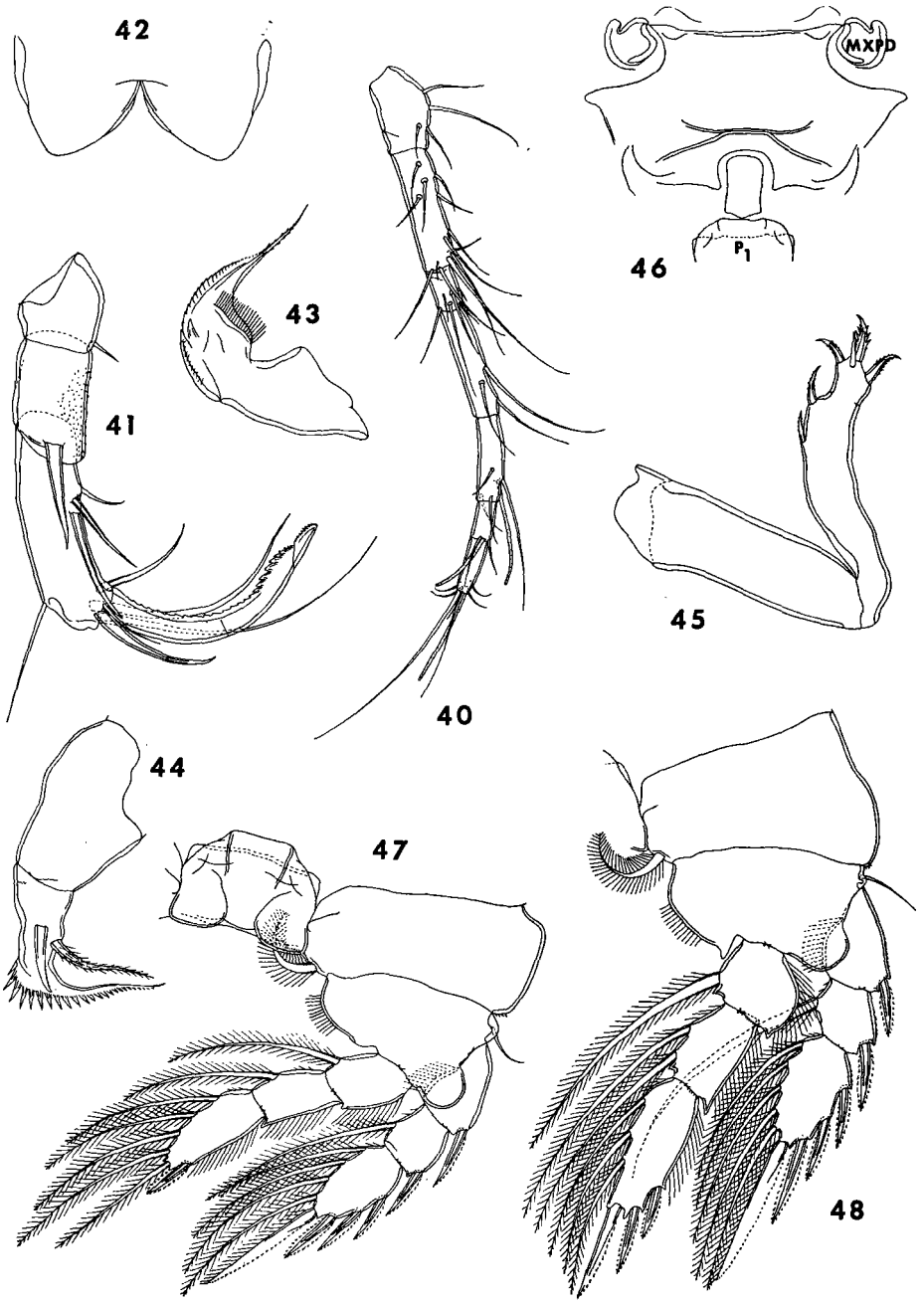
Color in life in transmitted light translucid, eye red, intestine brown, egg sac almost transparent.

M a l e. — Body (fig. 52) resembling in general form that of female. Length (excluding setae on caudal rami) 0.88 mm (0.84—0.95 mm) and greatest width 0.28 mm (0.27—0.29 mm), based on 10 specimens. Ratio of length to width of prosome 1.88 : 1.

Segment of leg 5 (fig. 53) 34 × 75 μ. Between this segment and genital segment no ventral intersegmental sclerite. Genital segment shaped as in previous species, 159 × 133 μ. Four postgenital segments 35 × 53, 34 × 50, 29 × 46, and 36 × 46 μ from anterior to posterior.

Caudal ramus similar to that of female but relatively smaller, 54 × 23 μ.

Surfaces of prosome and urosome with hairs and refractile points as in figs. 52 and 53. Ratio of length of prosome to that of urosome 1.49 : 1.



FIGURES 40—48. *Macrochiron valgum* n. sp., female (continued) : 40, first antenna, ventral (G); 41, second antenna, inner (G); 42, labrum, ventral (E); 43, mandible, posterior (E); 44, second maxilla, posterior (E); 45, maxilliped, antero-outer (E); 46, area between maxillipeds and first pair of legs, ventral (G); 47, leg 1, anterior (F); 48, leg 2, anterior (F).

Rostrum like that of female.

First antenna (fig. 54) segmented and armed as in male of previous species, but aesthetes much shorter. Lengths of segments (measured along their posterior non-setiferous margins) 32 (48 μ along anterior margin), 61, 22, 63, 48, 28, and 35 μ respectively.

Second antenna, labrum, mandible, paragnath, first maxilla, and second maxilla as in female. Maxilliped (fig. 55) more slender than in preceding species, with similar armature. Claw 100 μ along its axis (including large terminal lamella) with only a weak indication of division midway and without a visible fringe along concave margin.

Legs 1—4 segmented as in female, with similar armature and ornamentation, except for leg 1 where last segment of endopod (fig. 56) shows sexual dimorphism, its formula being I,I,4 as in *M. lytocarpi*; outer spine (27 μ) swollen at middle on inner side and bearing a fringe on outer side, inner spine (30 μ) slender and naked. Some sexual dimorphism seen also in spines on last segment of endopod of leg 2 (17, 18, and 33 μ in length from outer to inner) and of leg 3 (23, 22, and 34 μ). Endopod of leg 4 (fig. 57) resembling that of female, 37.5 $\times$ 7.5 μ, but without distinct notch or hairs on outer margin.

Leg 5 (fig. 58) with free segment much shorter than in female, 31 $\times$ 9 μ, with its 2 terminal setae 28 μ (outer) and 36 μ (inner).

Leg 6 (fig. 59) resembling that in previous species, the 2 naked setae 22 and 26 μ in length.

Spermatophore (fig. 60) elongated, 139 $\times$ 62 μ (without neck), distally with a small inner knob on its wall and with a few delicate striations.

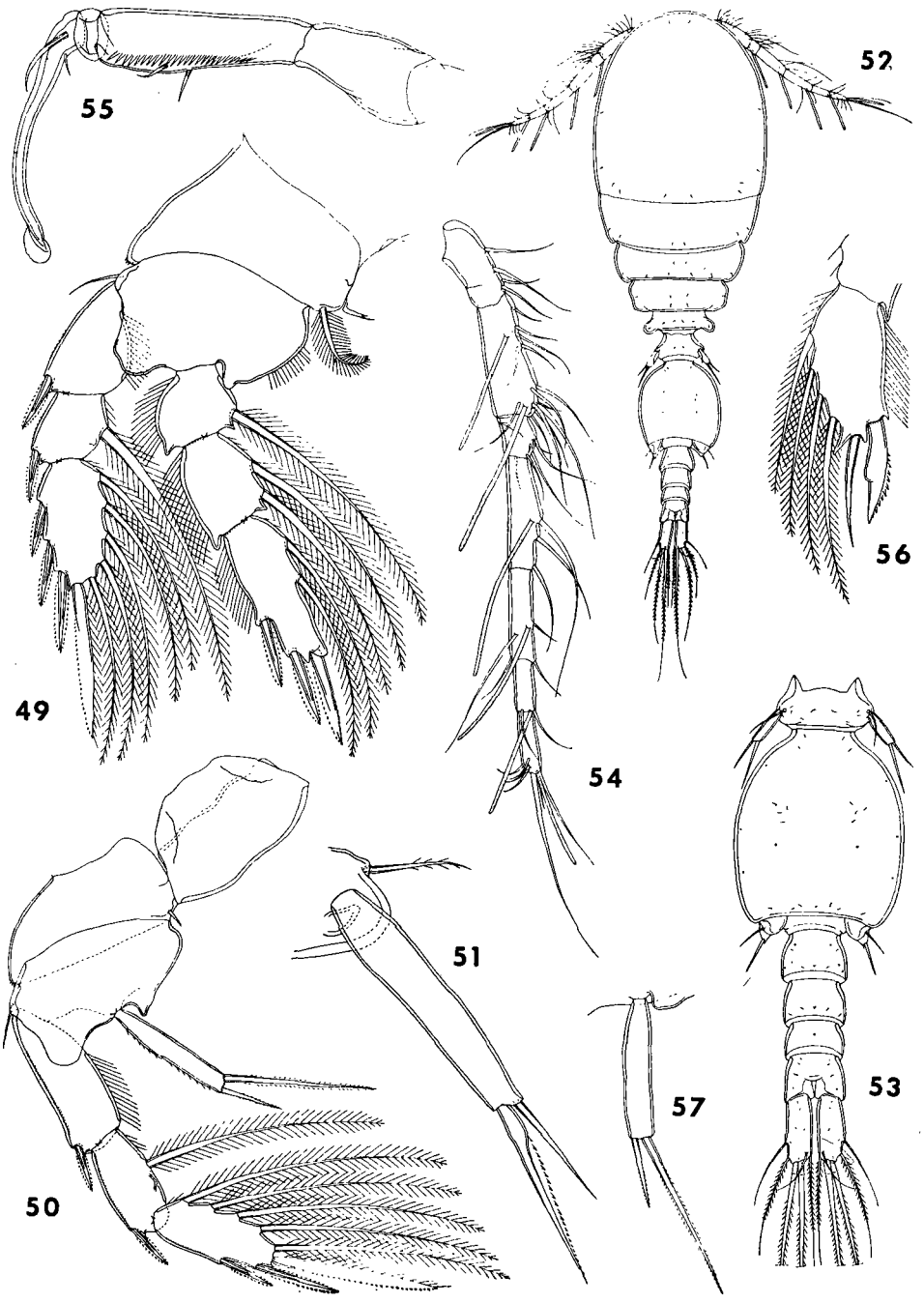
Color in life in transmitted light resembling that of female.

(The specific name *valgum*, from Latin = bowed outwards or bow-legged, alludes to the bowed form of the distal part of the maxilliped in the female.)

Comparison with other species. — *M. valgum* differs from *M. sargassi*, *M. mutatum*, and *M. lytocarpi*, all three of which have the formula III,I,5 on the last segment of the exopod of leg 4. It may be differentiated from *M. fucicolum* by the dentation of the claw of the second antenna (in *M. valgum* the large teeth being distally located near the division of the claw, while in *M. fucicolum* they are in the midregion, as in Brady's pl. III, fig. 12); furthermore, the endopod of leg 4 in *M. valgum* is 1-segmented, with no line of division, while according to Brady this endopod in *M. fucicolum* is 2-segmented (see Stock, 1957: 380). *M. valgum* differs also from *M. cheliferum* which has in the female a more elliptical dorsal outline of the prosome, a more elongated genital segment which is broadest far anteriorly, and a relatively shorter fifth leg.

Macrochiron rostratum n. sp. Figs. 61—88.

Type material. — 21 ♀♀ and 3 ♂♂ washed from *Lytocarpus philippinus* (Kirchenpauer), in a depth of 2 m, Ambariobe, a small island nearly between Nosy Bé and Nosy Komba, Madagascar. September 19, 1964. Holotype female, allotype, and 11 paratypes



FIGURES 49—51. *Macrochiron valgum* n. sp., female (continued): 49, leg 3, anterior (F); 50, leg 4, anterior (F); 51, leg 5, lateral (E).

FIGUPES 52—57. *Macrochiron valgum* n. sp., male: 52, body, dorsal (I); 53, urosome, dorsal (B); 54, first antenna, ventral (G); 55, maxilliped, postero-inner (F); 56, last segment of endopod of leg 1, anterior (E); 57, endopod of leg 4, anterior (E).

(10 ♀♀, 1 ♂) deposited in the Zoölogisch Museum, Amsterdam (Z.M.A. Co. 101.019), 9 paratypic females in the United States National Museum, Washington, and the remaining two paratypes (dissected) in the collection of the author.

Other specimens. — 3 ♀♀ and 2 ♂♂ from *Lytocarpus philippinus* in 1 m, Pte. Lokobe, Nosy Bé, November 3, 1960; 7 ♀♀ and 2 ♂♂ from *Lytocarpus spectabilis* Allman in 1 m, Ambariobe, February 14, 1964.

Female. — Body (fig. 61) resembling in general outline that of *M. lytocarpi*. Length (not including setae on caudal rami) 0.88 mm (0.88— 0.90 mm) and greatest width 0.36 mm (0.35—0.36 mm), based on 5 specimens. Ratio of length to width of prosome 1.7 : 1. Segment of leg 1 separated from head by a furrow. Posteroventral region of segment of leg 4 produced (fig. 62).

Segment of leg 5 (fig. 63) 51 × 94 μ. Between this segment and genital segment a short ventral intersegmental sclerite. Genital segment slightly longer than wide, rather abruptly constricted in its posterior third; 110 μ long, 97 μ in greatest width, and 60 μ wide in the middle of its posterior third; with a row of minute hyaline spinuliform processes along posteroventral border of segment. Areas of attachment of egg sacs dorsolateral, each area (fig. 64) bearing 2 short naked setae (6 and 8 μ long) and 2 sclerotized spinous processes. Three postgenital segments 35 × 47, 26 × 43, and 33 × 45 μ from anterior to posterior. First 2 segments bearing row of minute hyaline spinuliform processes on posteroventral border, anal segment with row of minute spinules along posteroventral margin.

Caudal ramus (fig. 65) moderately elongated, 52 × 21 μ in greatest dimensions, with ratio of length to width 2.48 : 1. Outer lateral seta 83 μ, dorsal seta 36 μ, outermost terminal seta 133 μ, innermost terminal seta 169 μ, and 2 long median terminal setae 248 μ (outer) and 341 μ (inner), the ornamentation of these setae as in 2 previous species. Minute setule on outer basal margin of ramus only 1 μ long.

Surfaces of prosome and urosome ornamented with hairs and refractile points as in figs. 61 and 63. Ratio of length of prosome to that of urosome 1.82 : 1.

Egg sac (see fig. 61) moderately elongated, in one female 352 × 150 μ, with numerous eggs, each about 52 μ in diameter.

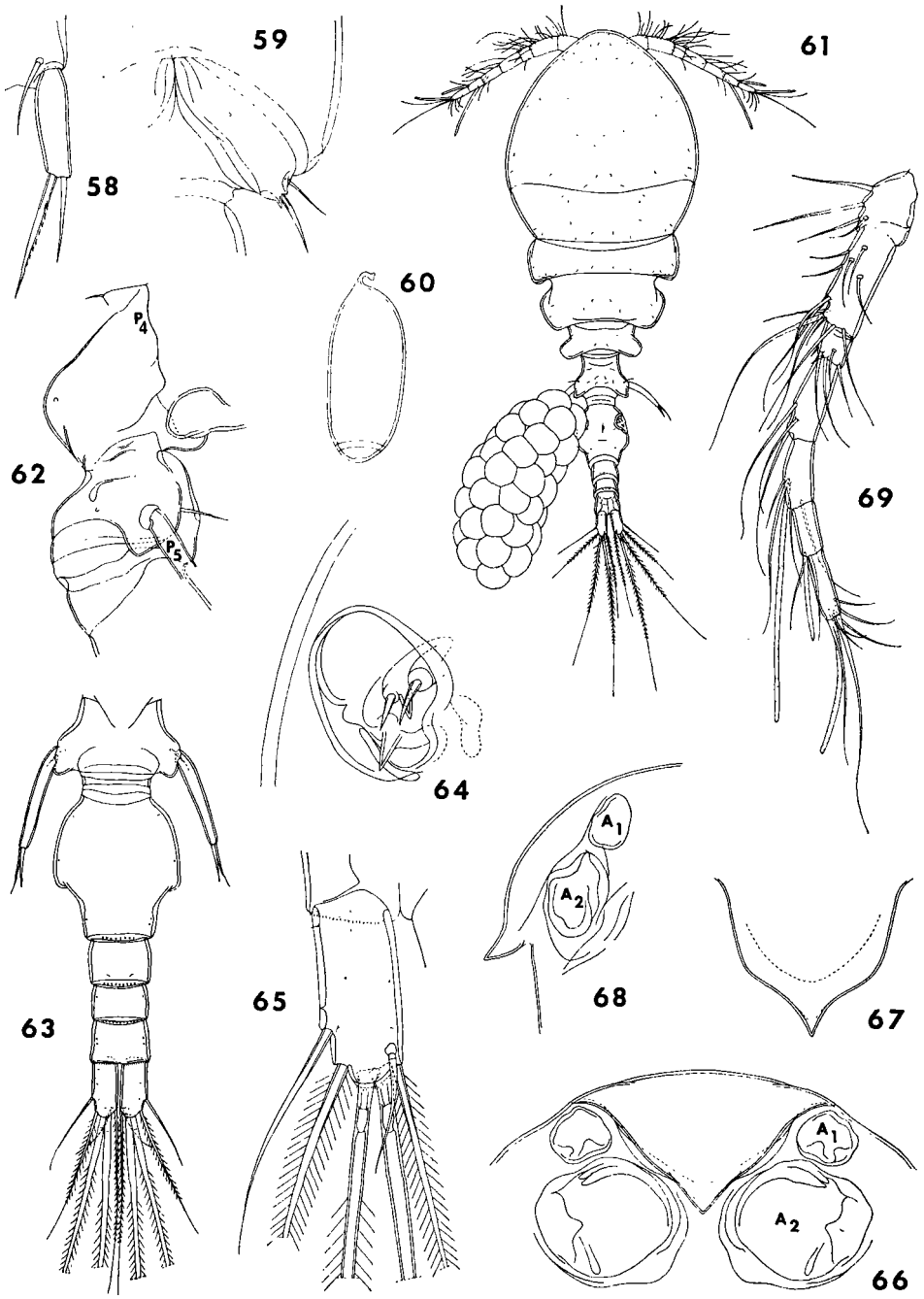
Rostrum (figs. 66, 67, and 68) terminating in a subconical beak turned a little ventrally.

First antenna (fig. 69) with segmentation and armature as in 2 preceding species. Lengths of segments (measured along their posterior non-setiferous margins) 26 (43 μ along anterior margin), 56, 22, 42, 33, 25, and 36 μ respectively. Terminal seta 112 μ long.

Second antenna (fig. 70) resembling in general features that of *M. lytocarpi*, with same segmentation and armature. Third segment 101 μ long. Claw bisegmented, 112 μ along its axis; proximal to few large teeth having 2 rows of denticles which unite in a single row basally.

Labrum (fig. 71) with broad lobes not divergent.

Mandible (fig. 72) similar to that in 2 preceding species, with distinct spinules on lash. Paragnath (see fig. 71) and first maxilla like those in *M. lytocarpi* and *M. valgum*. Second maxilla (fig. 73) resembling that of *M.*



FIGURES 58—60. *Macrochiron valgum* n. sp., male (continued): 58, leg 5, dorsal (E); 59, leg 6, ventral (F); 60, spermatophore, attached to female, lateral (B).

FIGURES 61—69. *Macrochiron rostratum* n. sp., female: 61, body, dorsal (I); 62, junction of segments of legs 4 and 5, lateral (G); 63, urosome, ventral (B); 64, area of attachment of egg sac, nearly dorsal (D); 65, caudal ramus, dorsal (E); 66, rostrum, ventral (F); 67, outline of rostrum as seen in a dissection, ventral (G); 68, rostrum, lateral (G); 69, first antenna, ventral (G).

valgum. Maxilliped (fig. 74) with segments a little stouter than in 2 preceding species, last segment not clearly separated from second. Armature also similar, though ornamentation of elements differing as shown in figure.

Area between maxillipeds and first pair of legs as in *M. valgum*.

Legs 1—4 (figs. 75, 76, 77, and 78) with armature as in *M. valgum*, last segment of exopod of leg 4 being II,I,5. Inner seta on coxa of leg 4 small, 11 μ, and naked. Three spines on last segment of endopod of leg 2 measuring 31, 30, and 40 μ in length from outer to inner; those on leg 3, 30, 44, and 50 μ. Endopod of leg 4 with indistinct line of division as in *M. lytocarpi*. Length 52 μ, width proximal to notch 14 μ, distal to notch 13 μ. Two terminal setae spiniform and fringed, outer 32 μ, inner 55 μ.

Leg 5 (fig. 79) with very slender and elongated free segment, 96 $\times$ 9 μ (taking width at middle). Outer terminal seta 35 μ, swollen basally and fringed, inner terminal seta slender, 41 μ, and naked.

Leg 6 probably represented by 2 setae near attachment of each egg sac (see fig. 64).

Color in life in transmitted light similar to that of *M. valgum*.

Male. — Body (fig. 80) rather like that of female, but anterior part of prosome more rounded. Length 0.71 mm (0.67—0.76 mm) and greatest width 0.23 mm (0.22—0.23 mm), based on 4 specimens (allotype, one paratype, and 2 specimens from Pte. Lokobe, November 3, 1960). Ratio of length to width of prosome 1.89 : 1.

Segment of leg 5 (fig. 81) 39 $\times$ 55 μ. Between this segment and genital segment no ventral intersegmental sclerite. Genital segment 123 $\times$ 100 μ, of a slightly different form than in either *M. lytocarpi* or *M. valgum*, having its lateral margins in posterior half nearly parallel. Four postgenital segments 28 $\times$ 42, 23 $\times$ 39, 20 $\times$ 36, and 25 $\times$ 36 μ from anterior to posterior.

Caudal ramus similar to that of female but smaller, 36 $\times$ 17μ.

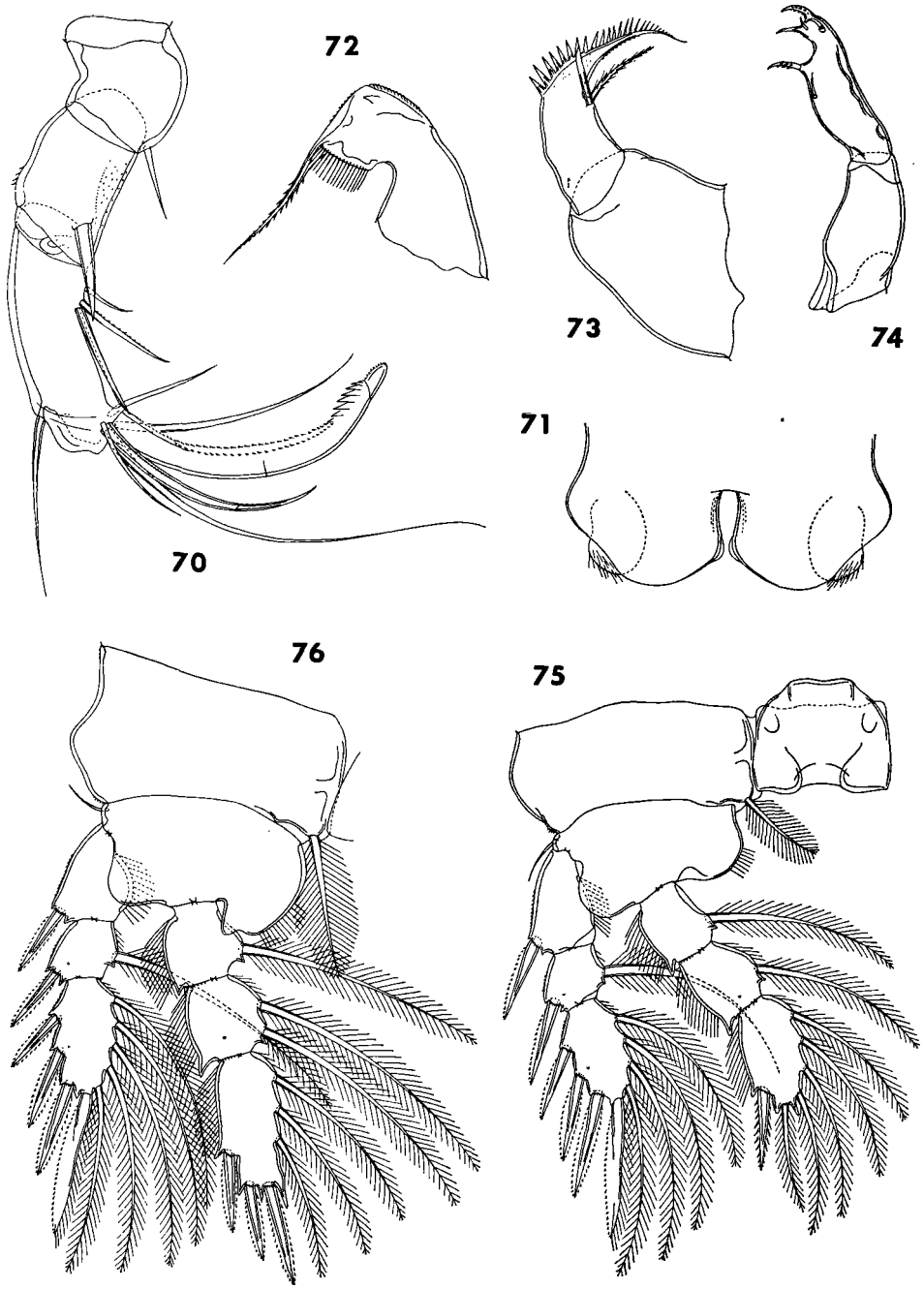
Surfaces of prosome and urosome with hairs and refractile points as in figs. 80 and 81. Ratio of length of prosome to that of urosome 1.57 : 1.

Rostrum like that of female.

First antenna (fig. 82) segmented and armed as in males of 2 preceding species, with very long aesthetes. Lengths of segments (measured along their posterior non-setiferous margins) 22 (36 μ along anterior margin), 41, 14, 33, 27, and 33 μ respectively.

Second antenna, labrum, mandible, paragnath, first maxilla, and second maxilla as in female. Maxilliped (fig. 83) slender, with armature similar to that in 2 preceding species. First segment with a distal sclerotized process. Claw 114 μ along its axis, somewhat swollen in its proximal one-fourth and weakly divided midway.

Legs 1—4 segmented as in female, with similar armature and ornamentation, except for leg 1 where last segment of endopod (fig. 84) shows sexual dimorphism, its formula being I,I,4 as in 2 previous species; both spines fringed, outer 20 μ, inner 29 μ. Slight sexual dimorphism also seen in spines on last segment of endopod of leg 2 (fig. 85), where they are 23, 16, and 26 μ in length from outer to inner, and of leg 3 where they are 21, 29, and 35 μ.



FIGURES 70—76. *Macrochiron rostratum* n. sp., female (continued): 70, second antenna, inner (F); 71, labrum and paragnaths, ventral (E); 72, mandible, posterior (E); 73, second maxilla, posterior (E); 74, maxilliped, antero-outer (F); 75, leg 1, anterior (F); 76, leg 2, anterior (F).

In leg 4 process on basis medial to endopod more pointed than in female; endopod (fig. 86) 34 × 11 μ, with no line of division, 2 terminal setae 22 μ (outer) and 36 μ (inner).

Leg 5 (fig. 87) with free segment shorter than in female, 34 × 8 μ, with 2 terminal elements 21 μ and 25 μ in length.

Leg 6 (see fig. 81) resembling that in 2 preceding species, with its 2 naked setae 13 and 22 μ.

Spermatophore (fig. 88) elongated, 114 × 44 μ (without neck), with a few delicate striations distally.

Color in life in transmitted light as in female.

(The specific name *rostratum*, from Latin = having a beak, refers to the form of the rostrum.)

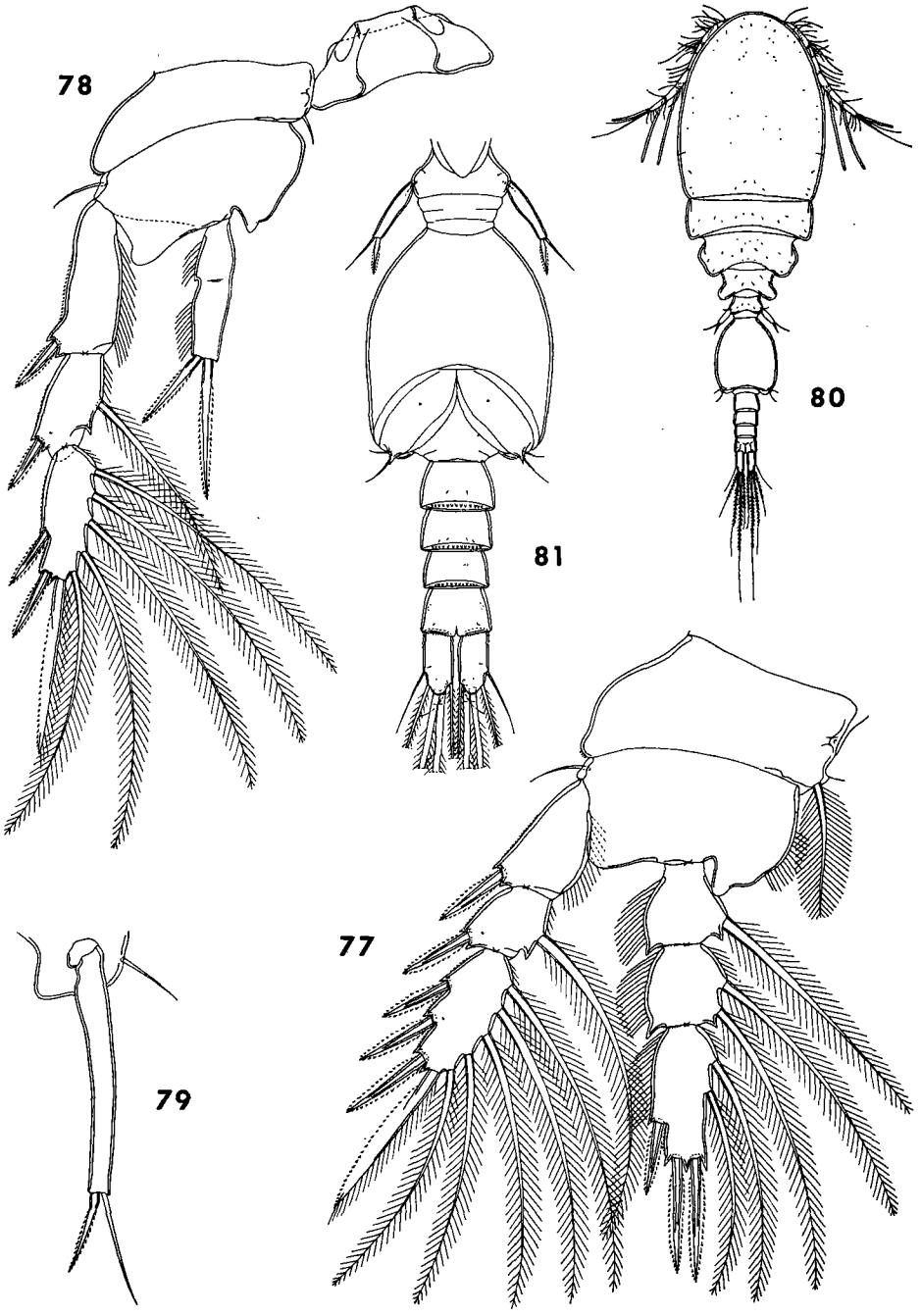
Comparison with other species. — *M. rostratum* may be readily separated from the other six species in the genus by the form of the genital segment in the female (where it is rather abruptly constricted in its posterior third, thus forming conspicuous lateral indentations). It differs further from *M. sargassi*, *M. mutatum*, and *M. lytocarpi* (in which the formula for the last segment of the exopod of leg 4 is III,I,5). It is unlike *M. valgum* in having a subconical beak on the rostrum instead of a needlelike process, and in having the last two segments of the maxilliped in the female much less bowed. *M. rostratum* has a longer fifth leg than in *M. cheliferum* and the last two segments of the maxilliped of the female are less bowed than in that species. It differs from *M. fucicolum* in the dentation of the claw on the second antenna.

REMARKS ON THE GENUS *MACROCHIRON*

The seven species of *Macrochiron* now known constitute a fairly well-defined group. It is of interest to note that the number of outer spines on the last segment of the exopod of leg 4 may vary interspecifically (either II or III), a condition seen also in the genus *Lichomolgus*.

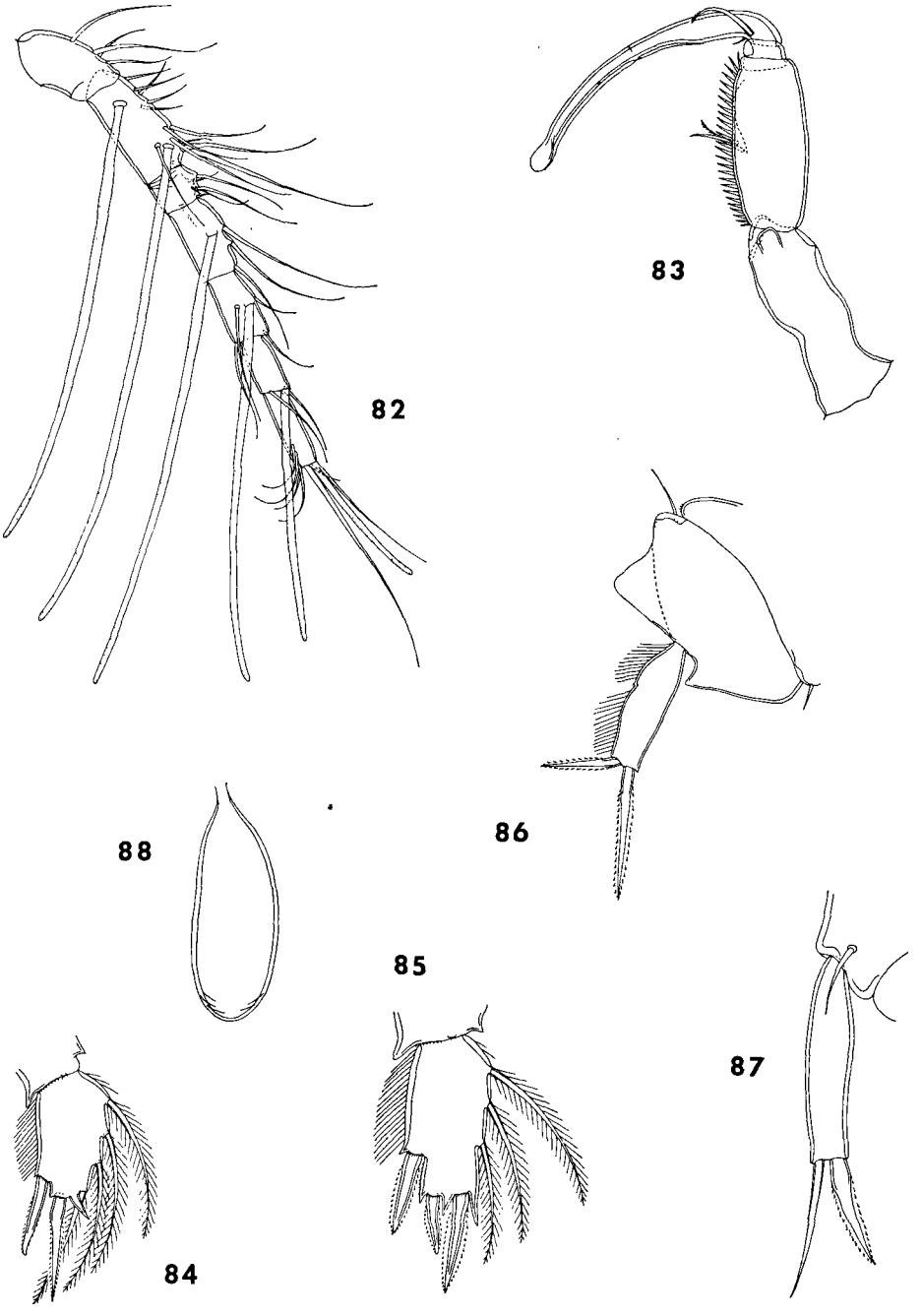
The most conspicuous element in the armature of the last segment of the second antenna is a large denticulated claw. However, in the three species from Madagascar there is also a jointed recurved seta which is slightly unguiform, and may represent either an incipient claw or one which has undergone reduction. Sars (1917: 164) stated that in his *M. fucicolum* (= *M. mutatum*) one seta is „somewhat stronger than the others and may represent the inner claw". The condition of two unequal terminal claws in *M. sargassi* may be regarded as a case where the unguiform seta is more strongly developed and has become distinctly recognizable as a claw. Other features of *M. sargassi* indicate that it is a *Macrochiron*.

The endopod of leg 4 may be a single element, with no line of division, as in *M. valgum*, may show slight indication of segmentation as in *M. lytocarpi* and *M. rostratum*, or may be 2-segmented as reported for *M. fucicolum* (but, as Stock, 1957, has observed, the segmentation line here is sometimes indistinct).



FIGURES 77—79. *Macrochiron rostratum* n. sp., female (continued): 77, leg 3, anterior (F); 78, leg 4, anterior (F); 79, leg 5, lateral (F).

FIGURES 80—81. *Macrochiron rostratum* n. sp., male: 80, body, dorsal (I); 81, urosome, ventral (G).



FIGURES 82—88. *Macrochiron rostratum* n. sp., male (continued): 82, first antenna, ventral (F); 83, maxilliped, postero-inner (F); 84, last segment of endopod of leg 1, anterior (E); 85, last segment of endopod of leg 2, anterior (E); 86, basis and endopod of leg 4, anterior (E); 87, leg 5. dorsal (D); 88, spermatophore, attached to female, lateral (G).

The form of the rostrum is not known for all the species. In *M. lytocarpi* and *M. valgum* there is a posteriorly directed needlelike process. A similar process has been described by Vervoort (1964, fig. 12f) in *M. cheliferum* from Ifaluk Atoll in the Caroline Islands. In *M. rostratum* the rostrum terminates in a subconical beak. For *M. fucicolum* Brady said that it is „short, but distinctly angulated". In *M. sargassi* its form is unknown. For *M. mutatum* (= *M. fucicolum* Sars non Brady) Sars stated that it has a „rostral prominence well defined and pointed at the end". The information available on the nature of the rostrum suggests that it may serve as a useful character for the differentiation of species in the genus.

Explanation of the figures

All figures were drawn with the aid of a camera lucida. The letter after the explanation of each figure refers to the scale at which it was drawn.

Abbreviations used: A_1 = first antenna, A_2 = second antenna, MX_2 = second maxilla, MXPD = maxilliped, P_1 = leg 1, P_4 = leg 4, P_5 = leg 5.

References

Brady, G. S.

1872 Contributions to the study of Entomostraca. — Ann. Mag. nat. Hist., (4) **10**: 1—17.

Kossmann, R.

1877 Entomostraca (1. Theil: Lichomolgidae). — In: Zool. Ergeb. Reise Küstengeb. Rothen Meeres, **1** (4): 1—24.

Krishnaswamy, S.

1952 Some new species of copepods from Madras coast. — Rec. Ind. Mus., 1951, **49** (3/4): 321—336.

Sars, G. O.

1916 Liste systématique des Cyclopoidés, Harpacticoidés et Monstrilloidés recueillis pendant les campagnes de S.A.S. le Prince Albert de Monaco, avec descriptions et figures des espèces nouvelles. — Bull. Inst. océanogr., **323**: 1—15.

1917 An account of the Crustacea of Norway with short descriptions and figures of all the species, **6**. Copepoda Cyclopoida, XI/XII, Clausidiidae, Lichomolgidae (part): 141—172. (Bergen Museum, Bergen).

Scott, A.

1909 The Copepoda of the Siboga Expedition, 1. Free-swimming, littoral and semi-parasitic Copepoda. — Siboga Exped., **29a**: 1—323.

Sewell, R. B. S.

1949 The littoral and semi-parasitic Cyclopoida, the Monstrilloida and Notodelphyoida. — John Murray Exped. 1933—34, sci. Repts., **9** (2): 17—199.

Stock, J. H.

1957 Some notes on the genus Macrochiron Brady, 1872 (Copepoda, Cyclopoida). — Ann. Mag. nat. Hist., (12) **10**: 378—382.

Thompson, I. C. & A. Scott

1903 Report on the Copepoda collected by Professor Herdman, at Ceylon, in 1902. — Rept. Govt. Ceylon Pearl Oyster Fish. Gulf Manaar, **1**, suppl. Rept. 7: 227—307.

Thorell, T.

1860 Bidrag till Kännedomen om Krustaceer, som lefva i Arter af Slägtet Ascidia L. — K. Sv. Vetensk. Akad. Handl., N.F., **3** (2): 1—84.

UMMERKUTTY, A. N. P.
1962 Studies on Indian copepods 5. On eleven new species of marine cyclopoid copepods from the south-east coast of India. — J. mar. biol. Ass. India, **3** (1/2) : 19—69.

VERVOORT, W.
1964 Free-living Copepoda from Ifaluk Atoll in the Caroline Islands. — Bull. U.S. nation. Mus., **236** : 1—431.

YEATMAN, H. C.
1962 The problem of dispersal of marine littoral copepods in the Atlantic Ocean, including some redescriptions of species. — Crustaceana, **4** (4) : 253—272.

DR. A. G. HUMES
Professor of Biology, Boston University, Boston, Massachusetts, U.S.A.

Reprinted from *Océanographie*, vol. IV, no. 2, 1966, p. 147-151

UNE VARIÉTÉ DE *FRITILLARIA PELLUCIDA* (BUSCH), 1851, RÉCOLTÉE DANS LA MER D'OMAN

par R. FENAUX*

Les Appendiculaires récoltés durant la troisième campagne du « Commandant Robert Giraud » en mer d'Arabie, ont fait l'objet d'une publication précédente (FENAUX, 1964). La note présente est destinée à la description d'une variété de l'espèce *Fritillaria pellucida* (Busch), 1851, récoltée dans quelques stations planctoniques de cette campagne.

Le type de cette espèce a été décrit par BUSCH sous le nom d'*Eurycercus pellucidus* (1851, p. 118). Une seconde description en a été donnée par VOGT, en 1854 (p. 76-81), qui l'appelle *Appendicularia furcata*. Par la suite et jusqu'en 1895, le nom de *Fritillaria furcata* prévaut : FOL, 1872, p. 476-477 ; LANGERHANS, 1880, p. 145 ; CARUS, 1889-1893, p. 496 ; LOHMANN, 1892, p. 147. La désignation actuelle date des résultats de la « Plankton Expedition » rédigés en 1896 par LOHMANN (p. 32-34). Depuis les principaux auteurs ayant redécrits ou apportés des précisions sur la morphologie de cette espèce sont les suivants : SALENSKY, 1904, p. 99-134 ; AÏDA, 1907, p. 5-6 ; IHLE, 1908, p. 92-93 ; LOHMANN et BÜCKMANN, 1926, p. 171-172 ; ESSENBERG, 1926, p. 460-463 ; LOHMANN, 1931, p. 145 ; VERNIÈRES, 1933, p. 44 ; LOHMANN, 1933, p. 190 ; HARANT et VERNIÈRES, 1938, p. 28 ; BJÖRNBERG et FORNERIS, 1955, p. 38-41 ; TOKIOKA et CAABRO, 1956, p. 68-69 ; FENAUX, 1967, sous presse.

Les descriptions données par les différents auteurs sont semblables et, pas plus que les illustrations fournies, elles n'ont laissé le moindre doute sur le fait qu'il s'agissait bien, dans tous les cas, d'une seule et même espèce, bien définie et sans variété discernable.

La description suivante en est donnée récemment par FENAUX dans « les Appendiculaires » de la Faune de l'Europe et du bassin méditerranéen :

Le tronc de cette espèce (fig. 1) est à peu près rectangulaire et comprimé dorso-ventralement. Il présente une brusque courbure vers le bas au niveau de la partie pharyngienne. Cette « cassure » marque la position de la couche oïkoplastique qui forme une cavité recouverte par un capuchon. Le tronc est bien caractérisé par la présence constante, à son extrémité postérieure, de deux

* Chargé de Recherches au C.N.R.S., Station zoologique de Villefranche-sur-Mer — 06.

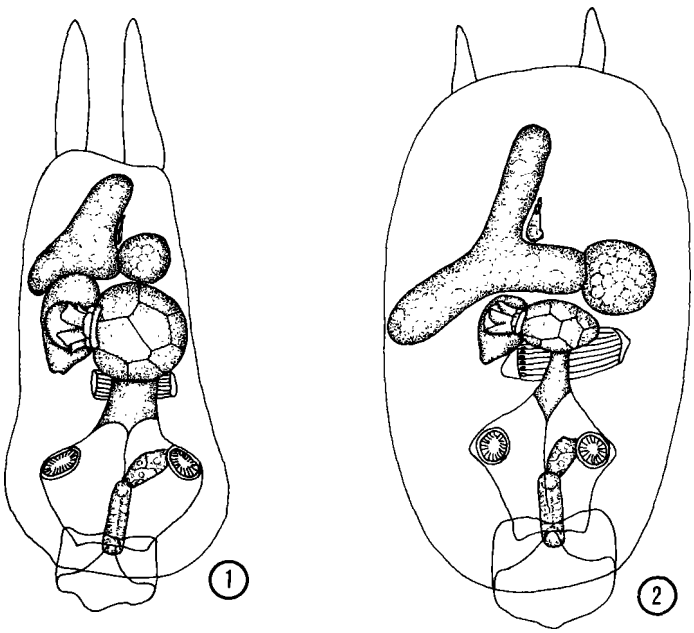
prolongements cuticulaires coniques dont l'aspect varie assez peu avec l'âge de l'individu. Il y a de nombreuses petites cellules glandulaires réparties, pour la plupart, symétriquement en différents emplacements dans le tronc.

La bouche est allongée en une sorte de museau, la lèvre inférieure, bilobée, porte une rangée de cellules tactiles ciliées bien visibles. La lèvre supérieure est de grande taille. La cavité pharyngienne est relativement courte, mais large. Derrière l'endostyle, dont les extrémités sont peu relevées il existe un groupe de quatre cellules glandulaires orientées vers le spiracle gauche. Les spirales sont arrondis. L'œsophage, assez court et large, débouche dans un estomac globuleux placé légèrement à gauche de l'axe longitudinal du tronc. L'intestin, très court, est situé à la partie supérieure droite de l'estomac ; sa partie inférieure donne accès, par le milieu, à un rectum volumineux. Le cœur, de grandes dimensions, est bien visible transversalement sous la partie postérieure de l'œsophage.

Dans le segment génital, l'ovaire apparaît sous forme d'une masse sphérique située à l'arrière et à gauche de l'estomac. Le testicule, cylindrique et transversal chez les jeunes individus, prend rapidement la forme d'un Y dont une branche, très courte, est contiguë à l'ovaire. Chez les exemplaires immatures, ou peu matures, on distingue, à la partie médio-ventrale, une glande assez volumineuse dont le canal évacuateur s'ouvre à la face ventrale. Cette glande s'aplatit ensuite contre le testicule et devient difficilement visible.

La queue, large, à musculature puissante, se rétrécit doucement en allant vers la partie distale qui est échancrée en V. Elle présente, de chaque côté de la bande musculaire, dans son tiers distal, une paire de cellules glandulaires possédant des canalicules d'évacuation très nets. Un certain nombre d'autres très petites cellules « glandulaires » sont visibles sur la queue, surtout chez les jeunes individus.

Parmi les exemplaires de cette espèce, récoltés aux Stations 189, 191, 195, 204 et 205 de la 3e Campagne du Robert Giraud (carte), à proximité des côtes Pakistanaises et Indiennes du Nord-Ouest, figurent des individus présentant certains aspects inhabituels. Il s'agit bien, sans qu'il puisse y avoir un doute, de l'espèce *pellucida* dont toutes les caractéristiques sont présentes. Cependant, l'allure générale ainsi que de nombreux détails sont constamment différents.



Fritillaria pellucida. 1 : Individu typique ; 2 : variété *Omani.*

Le tronc est nettement ovale (fig. 2), sa largeur est donc beaucoup plus importante que dans le type habituel. Les expansions cuticulaires situées à la partie postérieure ont une très faible longueur. Ce dernier caractère a peu de valeur lorsqu'il est seul, puisqu'il est variable avec l'âge des individus (FENAUX, 1965). Pourtant ici, la différence est constante quelle que soit la taille des exemplaires et de plus ce caractère est toujours lié à d'autres variations, ce qui en fait un facteur beaucoup moins aléatoire.

La bouche et la cavité pharyngienne ont l'aspect habituel, mais l'œsophage est sensiblement moins large même si on le compare aux dimensions plus réduites de l'estomac. Tout le tractus digestif est d'ailleurs d'un volume moindre, comparé au volume total du corps. Enfin, dans les gonades, le testicule pris à un stade de maturité comparable, a un aspect plus délié. Il représente un Y d'une façon plus proche que chez les individus décrits habituellement; en particulier, la branche contiguë à l'ovaire est toujours plus distincte.

Quinze Fritillaires (Type II) nous ont ainsi paru différentes des autres. Nous avons effectué une série de mensurations sur ces exemplaires, ainsi que sur quinze autres individus typiques (Type I), choisis au hasard parmi ceux qui ont été récoltés aux mêmes stations.

Le tableau suivant résume les résultats obtenus (valeurs en μ) :

	Type I				Type II			
	Q	L	l	A	Q	L	l	A
Maximum.....	2100	1220	520	360	2380	1760	1020	250
Minimum.....	1320	850	340	240	1720	1200	690	150
Moyenne.....	1713	979	405	289	2118	1551	915	220

TABLEAU n° 1. — Mensurations effectuées sur 15 individus du type normal (I) et 15 individus de la variété (II).

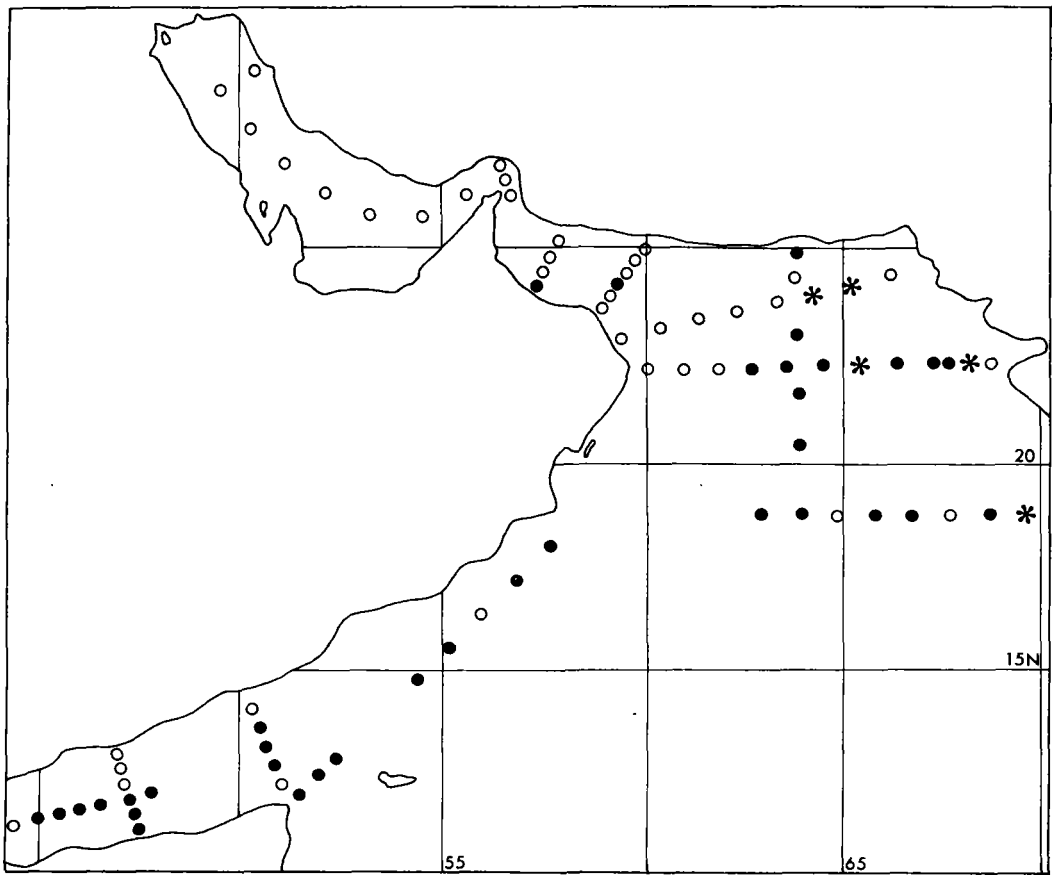
Q : longueur de la queue; L : longueur du tronc; l : largeur du tronc pris au niveau de l'estomac ; A : longueur des appendices cuticulaires.

Il nous est apparu que les différences étaient surtout sensibles dans les rapports existant entre différentes dimensions, aussi est-ce sur eux que nous avons effectué les calculs de variance et d'intervalle de confiance de la moyenne. Les chiffres obtenus sont résumés dans le tableau n° 2.

	Type I			Type II		
	L / l	Q / L	L / A	L / l	Q / L	L / A
Maximum.....	2,78	1,92	3,95	1,87	1,48	8,70
Minimum.....	2,22	1,55	2,94	1,50	1,15	6,66
Moyenne.....	2,41	1,74	3,34	1,69	1,36	7,63
Variance.....	0,4382	0,0301	0,0686	0,0285	0,0254	0,1634
Intervalle de confiance de 99 %	2,753 2,079	1,836 1,658	3,551 3,139	1,780 1,614	1,394 1,337	8,118 7,146

TABLEAU n° 2. — Rapports de diverses mensurations effectuées sur 15 individus normaux (Type I) et 15 individus de la variété (Type II).

L / l : rapport entre la longueur du tronc et sa largeur mesurée au niveau de l'estomac. Q / L : rapport entre la longueur de la queue et celle du tronc. L / A : rapport entre la longueur du tronc et celle des expansions cuticulaires.



3e Campagne du Commandant Robert Giraud en mer d'Arabie.

○ : emplacement des stations planctoniques ;

● : lieu de récolte de *F. pellucida* ;

✱ : lieu de récolte de *F. pellucida* var. *Omani*.

Nous voyons ainsi que les moyennes de tous les rapports calculés diffèrent très significativement. Il est donc fort probable que nous nous trouvons ici en présence de deux variétés bien définies de *F. pellucida*. Comme le type II a été rencontré dans la mer d'Oman, nous proposons de la dénommer *Fritillaria pellucida* var. *omani*.

Nous pensons que l'important matériel récolté dans cette région, durant l'Expédition Internationale de l'Océan Indien, permettra de retrouver de nombreux exemplaires de cette variété et de préciser l'aire de sa distribution géographique.

C.N.R.S. et Station Zoologique de
Villefranche-sur-Mer. — 06.

BIBLIOGRAPHIE

AIDA (T.) 1907. — Appendicularia of Japenese waters. *J. Coll. Sci. Tokyo*, 23, 5, pp. 1-25.

BJÖRNBERG (T.K.S.) et FORNERIS (L.), 1955. — Resultados cientificos do cruzeiro do « Baependi » e do « Vega » a ilha de Trinidade. Copelata. I. — *Univ. de Sao Paulo, Contrib. Avuls do Inst. oceanogr., oceanogr. biol.*, 1, 68 p., 17 pl. h.-t.

BUSCH (W.), 1851. — *Beobachtungen über Anatomie und Entwickelung einiger wirbelloser Seethiere* (pp. 118-120, pl. 16). — Berlin, A. Hirschwald. VIII, 143 p.

CARUS (J.V.), 1889-1893. — *Prodomus faunae Mediterraneae*, 2 (Ordo Copelata, 495-497). Stuttgart, E. Schweizerbart'sche, X, 854 p.

ESSENBERG (C.E.), 1926. — Copelata from the San Diego region and observations on gradual disintegration and death of Copelata. *Univ. Calif. Publ. Zool.*, 28, 22, pp. 399-521 ; 23, pp. 523-525.

FENAUX (R.), 1964. — Les Appendiculaires de la troisième campagne du *Commandant Robert Giraud* en mer d'Arabie. *Bull. Inst. océanogr. Monaco*, 62, n° 1302, 14 p.

FENAUX (R.), 1965. — A propos des expansions cuticulaires du tronc de quelques Fritillaires. *Rapp. Comm. int. Mer Médit.*, 18, 2, pp. 455-456.

FENAUX (R.) (sous presse). — Les Appendiculaires *in* Faune de l'Europe et du Bassin méditerranéen. Masson.

FOL (H.), 1872. — Études sur les Appendiculaires du détroit de Messine. *Mem. Soc. Phys. Genève*, 21, 1, pp. 445-499.

HARANT (H.) et VERNIÈRES (P.), 1938. — Appendiculaires et Thalliacés. *Faune de France*, 33 (2), 59 p.

IHLE (J.E.W.), 1908. — Die Appendicularien der Siboga-Expedition. *Siboga Exped.*, 56 c, 123 p.

LANGERHANS (P.), 1880. — Über Madeiras Appendicularien. *Z. wiss. Zool.*, 34, 1, pp. 144-146.

LOHMANN (H.), 1892. — Vorbericht über die Appendikularien der Plankton-Expedition. *Ergebn. Atlant. Planktonexped.*, 1, pp. 139-149.

LOHMANN (H.), 1896. — Die Appendicularien der Plankton-Expedition. *Ergebn. Atlant. Plankton-Exped.*, 2, EC, 148 p.

LOHMANN (H.), 1931. — Die Appendicularien der Deutschen Tiefsee-Expedition. *Wiss. Ergebn. « Valdivia »*, 21, 1, 158 p.

LOHMANN (H.), 1933-1934. — Tunicata. Appendicularia, *in* : KUKENTHAL (W.) & KRUMBACH (T.). — *Handbuch der Zoologie*, 5, 2, pp. 1-202. — Berlin, de Gruyter.

LOHMANN (H.) & BÜCKMANN (A.), 1926. — Die Appendicularien der Deutschen Sudpolar-Expedition, 1901-1903. *Dtsch. Südpol. Exped.*, 18, pp. 63-231.

SALENSKY (W.), 1903-1904. — Études anatomiques sur les Appendiculaires. I. *Oikopleura vanhoffeni* Lohmann. — II. *Oikopleura rufescens* Fol. — III. *Fritillaria pellucida* Busch. — IV. *Fritillaria borealis* Lohmann. *Mem. Acad. sc. St. Pétersbourg*, 15 (8), 150 p., 17 pl.

TOKIOKA (T.) et SUAREZ CAABRO (J.A.), 1956. — Appendicularias de los mares cubanos. *Mem. Soc. cubana Hist. nat.*, 23, 1, pp. 37-95.

VERNIÈRES (P.), 1933. — Essai sur l'histoire naturelle des Appendiculaires de Banyuls et de Sète. *Bull. Inst. océanogr. Monaco*, 30, n° 617, 60 p.

VOGT (C.), 1854. — Recherches sur les animaux inférieurs de la Méditerranée. *Mem. Inst. nat. Genève*, 2, 102 p.

Reprinted from *Bull. Mus. Nat. d'Hist. Natur.* (Paris), 2nd series, vol. 38, no. 6, 1966 (1967), p. 784-785

LES APPENDICULAIRES DE LA MER ROUGE (Note faunistique).

Par R. FENAUX

La distribution des Appendiculaires en mer Rouge est fort peu connue. Les seuls renseignements que nous possédons sont ceux relatifs au Golfe d'Eylath (FENAUX, 1960) et à la partie centrale (LOHMANN, 1931). Curieusement, seules des Oikopleurides ont été signalées. LOHMANN, cependant, déclare page 75, que les prises contenaient des Fritillaires, qu'elles étaient en petit nombre et qu'elles n'ont pas été triées. « Fritillarien werden sicher auch vorgekommen sein, sind aber nicht ausgelesen. Vielleicht sind sie auch nur spärlich gewesen. »

Lors d'un rapide passage à la Sea Fisheries Research Station de Haifa, nous avons, grâce à l'amabilité du Docteur KIMOR et du Docteur OREN, examiné une partie du plancton récolté durant l'expédition Entedebir. Celle-ci s'est déroulée en 1962 dans la partie sud de la mer Rouge par 39°54'25" E et 15° 43' N (OREN, 1964). Malgré sa brièveté, l'examen de ces prises nous a permis de reconnaître neuf espèces d'Appendiculaires. Parmi celles-ci six Oikopleurides : *O. albicans, O. fusiformis, O. longicauda, O. rufescens, O. parva, Steg. magnum* et trois Fritillaires : *F. tenella, F. formica f. digitata, F. borealis f. sargassi.*

Dans cette liste, six espèces sont nouvelles pour la Mer Rouge, les trois Fritillaires ainsi que *O. albicans, O. parva* et *Steg. magnum.*

A ce jour le nombre des espèces d'Appendiculaires signalés dans cette région s'élève ainsi à quatorze, répartis en quatre genres.

Il s'agit de :

Oikopleura albicans (Leuckart, 1854).
Oikopleura cophocerca (Gegenbaur, 1855).
Oikopleura dioica Fol, 1872.
Oikopleura fusiformis Fol, 1872.
Oikopleura intermedia Lohmann, 1896.
Oikopleura longicauda (Vogt, 1854).
Oikopleura parva Lohmann, 1896.
Oikopleura rufescens Fol, 1872.
Stegosoma magnum (Langerhans, 1880).
Megalocercus abyssorum Chun, 1888.
Megalocercus huxleyi (Ritter, 1905).
Fritillaria borealis f. sargassi (Lohmann), 1905.
Fritillaria formica f. digitata Lohmann et Bückmann, 1926.
Fritillaria tenella Lohmann, 1896.

Centre National de la Recherche scientifique, Station Zoologique de Villefranche-sur-Mer.

BIBLIOGRAPHIE

FENAUX, R., 1960. — Sur quelques Appendiculaires d'Israël. *Bull. Sea Fish. Res. Stat., Haifa*, **29**, 17, pp. 3-7.

LOHMANN, H., 1931. — Die Appendicularien der Deutschen Tiefsee Expedition. *Wiss. Ergebn.* « Valdivia », **21**, 1, 158 p.

OREN, O. H., 1964. — Hydrography of Dahlak Archipelago (Red Sea). *Bull. Sea Fish. Res. Stat., Haifa*, **35**, 1, pp. 3-22.

Reprinted from *C. R. Acad. Sc. Paris*, series D, vol. 263, 1966, p. 1980-1983

PLANCTOLOGIE. – *Sur la variabilité infraspécifique du genre* Ceratium *(Péridinien planctonique) en milieu marin.* Note (*) de M. ALAIN SOURNIA, présentée par M. Théodore Monod.

Les variations morphologiques continues, fréquentes chez *Ceratium*, sont en relation étroite avec la température, mais de nature génétique inconnue. Une terminologie est ici proposée pour les stades transitionnels, et appliquée à 14 espèces courantes.

Il est bien connu des planctologistes que diverses espèces du genre *Ceratium* présentent des séries continues de variations, ou que, du moins, nombre de spécimens sont indéterminables parce que morphologiquement intermédiaires entre deux taxons spécifiques ou infraspécifiques. Synonymes ou autonomes, les noms d'espèces, de sous-espèces, de variétés et de formes abondent dans la bibliographie, mais celle-ci ne compte qu'une monographie mondiale déjà ancienne, celle de Jörgensen (1), complétée postérieurement par le même auteur (2), et légèrement augmentée par Schiller (3).

Dans l'état actuel des connaissances relatives à la physiologie (4) et à la génétique (5) de ces Péridiniens, la nature profonde de telles variations demeure inconnue : génotypes ou phénotypes ? taxons distincts ou morphoses écologiques ? Cependant, leur relation avec la température est évidente, mais le rôle de ce facteur n'a pu encore être prouvé expérimentalement, et son mécanisme reste incertain (adaptation à la flottabilité, ou variation du taux de croissance ?). Il est en effet de règle que les *Ceratium* des hautes latitudes (ou hivernaux) sont « robustes » ou de grande taille, et possèdent des cornes courtes souvent recouvertes de crêtes lamellaires, tandis que les représentants tropicaux (ou estivaux) sont « délicats » ou de petite taille, et pourvus de cornes longues et fines.

A propos du *C. furca*, Pavillard (7) écrivait : « Son extension cosmopolite, son irrégularité quantitative, sa variabilité morphologique sont autant d'obstacles à une discrimination systématique et à une délimitation géographique rigoureuses ». Ce problème, commun à de nombreuses espèces, se pose toutefois différemment, dès lors qu'on admet qu'il n'existe pas en fait de discrimination systématique rigoureuse, pas plus qu'une semblable délimitation géographique. L'écueil réside alors dans la nomenclature.

Celle-ci est partagée entre deux tendances : 1° Multiplication des taxons infraspécifiques, à l'instar de Jörgensen (2); les précisions ainsi apportées se révèlent le plus souvent insuffisantes et conduisent à leur tour à la création de nouveaux noms; 2° Suppression des désignations infraspécifiques, comme il apparaît fréquemment chez Graham et Bronikovsky (8) : c'est là enterrer le problème. Mentionnons enfin les récents travaux de Lopez (9) qui, si intéressants qu'ils soient par ailleurs, ne conduisent pas à une solution taxinomique efficace. Cet auteur propose, pour diverses espèces

TABLEAU I.

Espèces.	Variétés (a).	Stades de transition.
C. candelabrum (Ehr.) Stein	P var. *candelabrum* T var. *depressum* (Pouchet) Jörg.	*C. candelabrum* (Ehr.) Stein, « *candelabrum* — *depressum* »
C. furca (Ehr.) Clap. et Lachm	P var. *furca* T var. *eugrammum* (Ehr.) Schiller	*C. furca* (Ehr.) Clap. et Lachm., « *furca* — *eugrammum* »
C. pentagonum Gourret	P var. *robustum* (Cleve) Jörg. T var. *tenerum* Jörg.	*C. pentagonum* Gourret, « *robustum* — *tenerum* »
C. fusus (Ehr.) Dujardin	P var. *fusus* T var. *seta* (Ehr.) *nov. comb.* = *subsp. seta* (Ehr.) Jörg. [(1), p. 29, *fig.* 55]	*C. fusus* (Ehr.) Dujardin, « *fusus* — *seta* »
C. tripos (Müller) Nitzsch	P (?) var. *atlanticum* Ostf. ou ? var. *tripos* T var. *pulchellum* (Schröder) Lopez	*C. tripos* (Müller) Nitzsch « *atlanticum* — *pulchellum* »
C. breve (Ostf. et Schm.) Schröder	* var. *parallelum* (Schmidt) Jörg. * var. *Schmidtii* (Jörg.) *nov. comb.* = *C. Schmidtii* Jörg. [(1), p. 50, *fig.* 110-111]	*C. breve* (Ostf. et Schm.) Schröder, « *parallelum* — *Schmidtii* »
C. contortum (Gourret) Cleve	* var. *robustum* (Karsten) *nov. comb.* = *C. tripos arcuatum* var. *robustum* Karsten (13) * var. *Karstenii* (Pavillard) *nov. comb.* = *C. Karstenii* Pavillard (6) * var. *longinum* (Karsten) *nov. comb.* = *C. tripos longinum* Karsten (12) * var. *contortum*	Quatre cas connus seulement, parmi les six cas possibles : *C. contortum* (Gourret) Cleve « *contortum* — *Karstenii* » « *contortum* — *robustum* » « *contortum* — *longinum* » « *longinum* — *Karstenii* »
C. gibberum Gourret	* var. *dispar* (Pouchet) *nov. comb.* = *C. tripos* var. *dispar* Pouchet (14) * var. *subæquale* Jörg.	Stades de transition incertains

(a) P, psychrophile; T, thermophile; *, signification thermique incertaine.

TABLEAU I (*suite*).

Espèces.	Variétés (*).	Stades de transition.
C. arietinum Cleve	P var. *bucephalum* (Cleve) *nov. comb.* = *C. tripos* var. *bucephalum* Cleve (11) * var. *arietinum* T var. *gracilentum* (Jörg.) *nov. comb.* = *f. gracilentum* Jörg. [(2), p. 64, *fig.* 62]	Stades de transition incertains : la var. *arietinum* ne représente peut-être qu'une transition entre les deux autres variétés
C. platycorne Daday	P var. *compressum* (Gran) Jörg. T var. *platycorne*	*C. platycorne* Daday « *platycorne — compressum* »
C. macroceros (Ehr.) Vanhöffen	P var. *macroceros* T var. *gallicum* (Kofoid) *nov. comb.* = *C. gallicum* Kofoid (15)	*C. macroceros* (Ehr.) Vanhöffen « *macroceros — gallicum* »
C. massiliense (Gourret) Jörg	P (?) var. *protuberans* (Karsten) Jörg. ou ? var. *armatum* (Karsten) Jörg. T var. *massiliense*	Stades de transition incertains
C. carriense Gourret	P (?) var. *carriense* T (?) var. *volans* (Cleve) Jörg.	*C. carriense* Gourret « *carriense — volans* »
C. horridum (Cleve) Gran	P var. *horridum* T var. *buceros* (Zacharias) *nov. comb.* = *C. buceros* Zacharias (16)	*C. horridum* (Cleve) Gran « *horridum — buceros* »

présentant des variations allométriques continues, une nomenclature infraspécifique basée sur la biométrie : les discriminations sont évidentes au niveau des populations, mais demeurent illusoires chez les individus.

L'étude d'un abondant matériel provenant du canal de Mozambique (récoltes entre 0 et 30° lat. Sud, échelonnées sur 20 mois) m'a fourni l'objet d'une mise à jour systématique portant sur la majorité des espèces mondiales (10), et dont j'expose ici les conclusions essentielles :

Dans le cas de variations apparemment liées à la température, on ne peut actuellement chercher à reconnaître que :

— les « types extrêmes » : généralement au nombre de deux par espèce; l'un est « robuste » et psychrophile, l'autre « délicat » et thermophile;

certaines espèces comportent un ou deux autres types bien individualisés; il est pratique de considérer ces taxons comme des variétés, mais l'avenir dira si ce rang est génétiquement justifié;

— les « stades de transition », pour lesquels je propose une désignation para-taxinomique composée des épithètes des deux variétés réunies par un tiret (dans de tels binomes infraspécifiques, le choix du premier nom à écrire relèvera par simple convention des règles de priorité). Les deux épithètes seront réunies par le signe >, remplaçant le tiret, dans le cas d'un spécimen manifestement plus proche de l'une ou l'autre variété. Au total, trois expressions sont donc possibles pour une série de variations donnée; ainsi, chez *C. fusus* : « *fusus — seta* », ou « *fusus* > *seta* » ou « *seta* > *fusus* ». Dans les trois cas le binome sera écrit entre guillemets, car cette nouvelle terminologie est — malheureusement — en marge de la nomenclature linénenne et, par ailleurs, ne désigne pas des hybrides comme l'emploi du tiret pourrait le suggérer.

Sous cette nouvelle optique j'ai reconsidéré le cas de 14 espèces de variabilité notoire et pour la plupart communes. Ce faisant, j'ai été amené à quelques fusions spécifiques, à quelques nouvelles combinaisons, enfin, à plusieurs reprises, au rétablissement du type de l'espèce sous le nom de variété-type. Ces 14 cas sont reportés dans le tableau I (pour ce qui est des stades de transition je n'ai fait figurer pour plus de clarté que le premier des trois cas envisagés plus haut).

(*) Séance du 7 décembre 1966.

(1) E. JÖRGENSEN, *Int. Revue ges. Hydrobiol. Hydrogr.*, Biol. Suppl., 4, 1911, p. 1-124, *pl.* 1-10.

(2) E. JÖRGENSEN, *Rep. dan. oceanogr. Exped. Mediterr.*, Biol. 2, 1920, p. 1-110.

(3) J. SCHILLER, *Rabenhorst Kryptog. Flora*, 10, (3), 1937, p. 349-432.

(4) *Cf.* E. NORDLI, *Oikos*, 8, (2), 1957, p. 200-265.

(5) *Cf.* H. A. STOSCH, *Helgölander Wiss. Meeresunters*, 10, 1964, p. 140-152.

(6) J. PAVILLARD, *Bull. Soc. bot. Fr.*, 54, 1907, p. 152.

(7) J. PAVILLARD, *Résult. Camp. scient. Prince Albert Ier*, 82, 1931, p. 70.

(8) H W. GRAHAM et N. BRONIKOVSKY, *Scient. Results Cruise VII Carnegie*, Biol. 3, 1944, p. 1-129.

(9) J. LOPEZ, *Investigation Pesq.*, 2, 1955, p. 131-159; 30, 1966, p. 325-427.

(10) A. SOURNIA, *Le genre* Ceratium *(Péridinien planctonique) dans le canal de Mozambique. Contribution à une révision mondiale* (*Vie Milieu*, sous presse).

(11) P. T. CLEVE, A. Rep. Fish Scotl., 15, (3), 1897, p. 302, *fig.* 5.

(12) G. KARSTEN, *Wiss. Ergebn. dt Tiefsee-Exped. « Valdivia »*, 2, (2), 1905, p. 143, *pl.* 21, *fig.* 18.

(13) G. KARSTEN, *Ibid.*, 2, (3), 1907, *pl.* 48, *fig.* 6.

(14) G. POUCHET, *J. Anat. Physiol. Paris*, 19, 1883, p. 423, *vix fig.* D.

(15) C. A. KOFOID, *Univ. Calif. Publs Zool.*, 3, (13), 1907, p. 302, *pl.* 24, *fig.* 10-12.

(16) O. ZACHARIAS, *Arch. Hydrobiol. Planktonk.*, 1, 1906, p. 551, *vix fig.* 15.

(Laboratoire des Pêches Outre-Mer,
Muséum national d'Histoire naturelle,
57, rue Cuvier, Paris, 5e.)

Reprinted from *Proc. U.S. Nat. Mus.*, vol. 121, no. 3,573, 1967, p. 1-24

Proceedings of the United States National Museum

SMITHSONIAN INSTITUTION • WASHINGTON, D.C.

Volume 121 1967 Number 3573

NEW CYCLOPOID COPEPODS ASSOCIATED WITH THE ALCYONARIAN CORAL TUBIPORA MUSICA (LINNAEUS) IN MADAGASCAR

By ARTHUR G. HUMES AND JU-SHEY HO [1]

At Nosy Bé, in the northwestern part of Madagascar, several species of copepods (Humes and Frost, 1964) are known to be associated with members of the alcyonarian order Alcyonacea, but until now none have been reported living with members of the order Stolonifera.

While participating in the work of the U.S. Program in Biology of the International Indian Ocean Expedition at Nosy Bé in 1963–64, the first author collected 4 species of cyclopoid copepods from washings of *Tubipora musica* (Linnaeus), the common organ-pipe coral. These species are described below.

All figures have been drawn with the aid of a camera lucida.

The study of the material has been aided by a grant (GB–1809) from the National Science Foundation. We wish to thank Dr. Michel Pichon for verification of the identity of the coral and to acknowledge the many courtesies received from the staff of the Centre d'Océanographie et des Pêches at Nosy Bé.

[1] Both authors: Department of Biology, Boston University, Boston, Mass.

Family Lichomolgidae Kossmann, 1877

Genus *Lichomolgus* Thorell, 1860

Lichomolgus organicus, new species

FIGURES 1–30

TYPE MATERIAL.—207 ♀♀, 98 ♂♂, and 15 copepodids from a colony of *Tubipora musica* (Linnaeus), in 1 m, Pte. Ambarionaomby, Nosy Komba, near Nosy Bé, Madagascar, collected June 8, 1964: holotype ♀ (USNM 113387), allotype (USNM 113388), and 144 paratypes (USNM 113389) (100 ♀♀ and 44 ♂♂) deposited in the United States National Museum, 80 paratypes (50 ♀♀ and 30 ♂♂) in the Museum of Comparative Zoology, Harvard University, and the remaining paratypes in the collection of A. G. Humes.

OTHER SPECIMENS.—All from *Tubipora musica* collected in 1964: 8 ♀♀ and 8 ♂♂, in 1 m, Pte. à la Fièvre, Nosy Bé, Jan. 5; 1 ♀, in 15 cm, Tany Kely, a small island south of Nosy Bé, Mar. 29; 4 ♀♀ and 8 ♂♂, in 1 m, Pte. Ambarionaomby, Mar. 31; 15 ♀♀ and 1 ♂, in 1 m, Pte. à la Fièvre, Apr. 15; and 14 ♀♀, in 2 m, Pte. Ambarionaomby, Sept. 27.

FEMALE.—Body (fig. 1) with moderately broad prosome. Body length (not including setae on caudal rami) 0.99 mm (0.92–1.05 mm) and greatest width (in middle of cephalosome) 0.49 mm (0.44–0.53 mm), based on 10 specimens. Ratio of length to width of prosome 1.5:1. Segment of first leg separated dorsally and laterally from head by a transverse furrow; lateral areas of this segment not expanded. Lateral areas of segments bearing legs 2 and 3 expanded and rounded posteriorly; those of segment of leg 4 smaller and somewhat truncated.

Segment of leg 5 (fig. 2) wider than long, 61μ x 133μ, with fifth legs borne laterally. Ventrally between this segment and the genital segment no apparent intersegmental sclerite. Genital segment (fig. 2) about as long as wide, 140μ x 142μ, in dorsal view expanded laterally in its midregion, posterior to which the segment is constricted so that its width at the posterior end is only 80μ. Areas of attachment of egg sacs located dorsolaterally on posterior part of expansions. Each area (fig. 3) with 2 naked setae, 12 and 13μ in length; posterior to the setae a small rounded sclerotized protuberance. Three postgenital segments, each without ornamentation except for a few surficial hairs (sensilla), 37μ x 67μ, 26μ x 55μ, and 28μ x 51μ, respectively, from anterior to posterior.

Caudal ramus (fig. 4) only a little elongated, 36μ x 24μ in greatest dimensions, or 1.5 times longer than wide. Length along inner edge

to innermost distal seta 23μ, along outer edge to base of lateral seta 23μ, and to base of outermost distal seta 33μ. Of the usual 6 setae, outer lateral seta naked and 66μ long; remaining 5 feathered: pedicellate dorsal seta 47μ, innermost distal seta 115μ, outermost distal seta 91μ, and the 2 long median terminal setae, both "pegged," 169μ (outer) and 200μ (inner), and inserted between dorsal (unornamented) and ventral (with marginal row of spinules) flaps. In addition, a minute hyaline setule dorsally near insertion of outermost distal seta. Two hairs on dorsal surface of ramus.

Dorsal surface of prosome and dorsal and ventral surfaces of urosome with a few minute hairs. Ratio of length of prosome to that of urosome about 2.1:1.

All ovigerous females observed with broken egg sacs (one shown in fig. 5).

Rostral area (fig. 6) moderately well formed. At level of bases of second antennae a small longitudinal sclerotized ridge between rostrum and anterior part of labrum.

First antenna (fig. 7) 7-segmented, with third segment showing ventrally a proximal sclerotized area suggesting an intercalary segment. Lengths of the segments, measured along their posterior nonsetiferous margins: 28μ (56μ along anterior margin), 95μ, 25μ, 50μ, 50μ, 37μ, and 22μ, respectively. Formula for armature: 4, 13, 6, 3, 4+1 aesthete, 2+1 aesthete, and 7+1 aesthete. All setae naked.

Second antenna (fig. 8) 4-segmented, with last segment moderately elongated, 65μ along its outer edge, 39μ along its inner edge, and 27μ wide. Each of first 2 segments with a small inner seta, third segment with 3 setae (1 of them jointed), and last segment with 7 elements: 5 setae and 2 unequal recurved claws 45μ and 34μ long (measured along greatest axis). All setae naked.

Labrum (fig. 9) with 2 relatively short posteroventral lobes, free border of each lobe showing 2 small hyaline lamellae.

Mandible (fig. 10) with its basal region bearing on its posterior surface a small sclerotized area and separated by a constriction from its distal region, whose inner margin bears a prominent sclerotized pointed toothlike process followed by a striated fringe, whose outer margin has a row of slender spinules and which terminates in a long flagellum with lateral spinules. Paragnath (see fig. 9) a small lobe bearing inner hairs. First maxilla (fig. 11) a single segment bearing 2 terminal setae. Second maxilla (fig. 12) 2-segmented, first segment unarmed, second segment produced distally and bearing row of 4–5 teeth (compare figs. 12 and 13) and slender naked terminal process. (If 4 such teeth, distalmost often slightly bifurcated; if 5, teeth all entire.) On postero-inner surface of second segment 2 setae, one finely pectinate along one margin, other bearing long bluntly tipped

setules along one side. A minute setule on proximal outer edge of this segment. Maxilliped (fig. 14) 3-segmented. Two naked setae on second segment. Third segment (fig. 15) bearing a naked seta, a setiform element with bifurcated tip, and a terminal process about 22μ long and clawlike, with a small hyaline lobe on each side of distal point.

Postoral area (fig. 16) only slightly produced ventrally; an incomplete line of sclerotization between bases of maxillipeds.

Legs 1–4 (figs. 17–20) with trimerous rami except for 2-segmented endopod of leg 4. Armature of legs as follows (Roman numerals= spines, Arabic numerals=setae):

P 1	protopod	0:1	1:0	exp	I:0	I:1	III,I,4
				end	0:1	0:1	I,5
P 2	protopod	0:1	1:0	exp	I:0	I:1	III,I,5
				end	0:1	0:2	I,II,3
P 3	protopod	0:1	1:0	exp	I:0	I:1	III,I,5
				end	0:1	0:2	I,II,2
P 4	protopod	0:1	1:0	exp	I:0	I:1	II,I,5
				end	0:1	II	

Inner seta on coxa of legs 1–3 long and plumose, but in leg 4 short (17μ) and naked. In first 3 pairs of legs inner margin of basis with short row of hairs, but such hairs absent in leg 4. In all 4 legs setae on inner side of last segment of exopod with lateral hairs shorter proximally than distally. Spine on last segment of endopod of leg 1 24μ in length. Endopod of leg 4 shorter than exopod. First segment 33μ x 25μ with inner distal plumose seta 41μ long. Second segment 61μ long (including 2 terminal spinous processes) and 23μ wide in basal half and 19μ wide in distal half, the 2 halves demarcated by very slight indentation. Along outer margin of both segments rows of minute spinules. Terminally second segment with a row of minute spinules near insertion of 2 unequal spines, both with spinulose fringes, outer spine 21μ, inner 39μ long, ratio about 1:1.86.

Leg 5 (fig. 21) with free segment elongated and slightly arcuate in outline, 66μ x 23μ, with short stout spines along outer edge and extending around to distal ventral surface; bearing terminally 2 naked setae 35μ and 37μ in length. Seta on body near free segment slightly feathered with group of spines near its insertion.

Leg 6 probably represented by 2 setae near areas of attachment of each egg sac (see fig. 3).

Color in life in transmitted light rather translucid, eye red.

MALE.—Body (fig. 22) resembling in general form that of female. Length (excluding ramal setae) 0.89 mm (0.85–0.92 mm) and greatest width 0.32 mm (0.30–0.34 mm), based on 10 specimens. Ratio of length of prosome to that of urosome 1.6:1.

Segment of leg 5 (fig. 23) 29μ x 67μ. Genital segment longer than wide, 164μ x 122μ in greatest dimensions, and in dorsal view rather bottle shaped, its lateral borders gently rounded. No intersegmental sclerite ventrally between these 2 segments. Four postgenital segments 18μ x 45μ, 19μ x 43μ, 15μ x 40μ, and 17μ x 43μ, respectively, from anterior to posterior.

Caudal ramus (fig. 24) resembling that of female, but slightly less elongated, its greatest dimensions 31μ x 21μ, or 1.48 times longer than wide.

Surfaces of prosome and urosome with minute hairs as in female. Ratio of length of prosome to that of urosome 1.56:1.

Rostral area like that in female.

First antenna resembling that of female, but an aesthete added on segments 2 and 4 (at exact points indicated by arrows in fig. 7), so that formula is 4, 13+1 aesthete, 6, 3+1 aesthete, 4+1 aesthete, 2+1 aesthete, and 7+1 aesthete. Second antenna (fig. 25) more slender than in female, and last segment elongated, 68μ along outer edge, 52μ along inner edge, and 15μ wide. First segment with inner crescentic row of small spinules. Second segment with numerous small spinules along inner surface, arranged in 2 groups proximal and distal to seta. Last segment with row of very small spinules along inner surface. Armature like that of female, but 2 claws more nearly equal in length (34μ and 35μ), though posterior claw more slender than other.

Labrum, mandible, paragnath, first maxilla, and second maxilla like those in female. Maxilliped (fig. 26) 4-segmented (assuming that proximal part of claw represents fourth segment). First segment unornamented. Second segment bearing on medial surface 2 setae and 2 rows of long spinules. Small third segment unarmed. Slender slightly recurved terminal claw 178μ in length (measured along axis), with narrow terminal lamella, smooth lamellar fringe along its concave surface, and 2 setae near its base, one on posterior surface 44μ long and finely barbed, other on anterior surface 17μ long, naked, and hyaline. Suggestion of division about midway along claw.

Postoral area resembling that of female.

Legs 1–4 resembling those in female and with same spine and setal formula, except for endopod of leg 1 (fig. 27), which has arrangement of 0:1; 0:1; I,I,4. On last segment of this endopod 2 spines, outermost of setae in female being here replaced by a spine; outer spine 29μ long, inner spine 43μ long and recurved distally, and both spines with strong lateral spinules. In alcoholized specimens last segment of endopod flexed outwardly. Terminal spines on endopod of leg 4 in one male 19μ (outer) and 51μ (inner), in another 16μ and 37μ, with an average of 17.5μ and 44μ, ratio of 1:2.5.

Leg 5 (fig. 28) with free segment elongated and slender, 36μ x 9μ, with nearly parallel sides in dorsal view, and with 2 terminal setae unequal, outer 31μ and inner 19μ long. Few minute spinules on outer distal surface of segment. No spinules near insertion of seta on body near free segment.

Leg 6 (fig. 29) a posterolateral flap on ventral surface of genital segment bearing 2 naked setae 23μ and 25μ long.

Spermatophore (fig. 30) inside body of male about 148μ x 68μ plus neck of 14μ.

Color in life resembling that of female.

ETYMOLOGY.—The specific name *organicus*, from Latin, relating to musical instruments, refers to the association of this species with the organ-pipe coral *Tubipora musica*.

COMPARISON WITH RELATED SPECIES.—Among those species in the large genus *Lichomolgus*, wherein the mandible has been described, there are 3 that, like *L. organicus*, show a prominent toothlike process on the proximal inner margin of this appendage. From these, *L. organicus* may be readily distinguished. In *L. actinophorus* Humes and Frost (1964) there is a single claw on the last segment of the second antenna, the free segment of leg 5 in the female is somewhat irregular and has a ratio of 2.1:1, the caudal ramus of the female has a ratio of 3.5:1, and there is a setiferous sphere on the second segment of the second maxilla. In *L. decorus* Humes and Frost (1964) there is one claw and one clawlike spine on the last segment of the second antenna, the last segment of the exopod of leg 4 has the formula III,I,5, and the free segment of leg 5 in the female is 2.2:1 with a basal expansion. In *L. protulae* Stock (1959) the shape of the body is transformed, there are 3 strong claws and 2 setiform claws on the last segment of the second antenna, the caudal ramus of the female has a ratio of about 8.3:1, the free segment of leg 5 in the female is about 2.1:1, and the toothlike process on the mandible is directed distally rather than proximally as in *L. organicus*. In addition, the females of *L. actinophorus* and *L. protulae* are distinctly larger.

There are 8 species of *Lichomolgus* in which the form of the mandible is unknown. These may be separated from *L. organicus*, however, on the basis of other characters (in each case using the female, except in the last mentioned species where the female is unknown). In *L. dentipes* Thompson and A. Scott (1903) the formula for the last segment of the exopod of leg 4 is III,I,5 and the free segment of leg 5 has a prominent toothlike inner process. In *L. elegans* Thompson and A. Scott (1903) there is 1 claw on the second antenna and the body is larger (1.5 mm) and more slender. In *L. gigas* Thompson and A. Scott (1903) there is one claw on the second antenna and the body is larger (2 mm). In *L. longipes* (Sewell, 1949) leg 5 is very long (about

8:1) and the body is larger (1.63 mm) and more slender. In *L. rigidus* Ummerkutty (1962) the formula for the last segment of the exopod of leg 4 is III,I,5 and the body is larger (1.25 mm). In *L. rotundus* Sewell (1949) the free segment of leg 5 is short, swollen, and somewhat produced on the outer margin, with a ratio of about 2:1. In *L. tenuicornis* Brady (1910) the caudal ramus is about 7:1, the free segment of leg 5 has a small basal expansion, and the body is larger (1.7 mm). In *L. vagans* Gurney (1927) (based on the male), the body is larger (1.07 mm) and the last segment of the second antenna (Gurney, 1927, p. 466, fig. C) has a ratio of length of the outer margin to width of about 5.6:1, thus being slightly more slender than in *L. organicus*, where the ratio is about 4.5:1.

Since we still do not know the taxonomic importance of the variation in many characters observed in *Lichomolgus* (such as the terminal armature of the second antenna, the armature of the exopod of leg 4, the exact form of the mandible and leg 5, etc.), we find it impossible in *Lichomolgus* to say with which species *L. organicus* is most closely related. Such a conjecture would seem to be premature in view of the apparent very incomplete knowledge of the species in this genus.

Lichomolgus conjunctus, new species

FIGURES 31–36

TYPE MATERIAL.—163 ♀♀ and 25 ♂♂ from a colony of *Tubipora musica* (Linnaeus), in 1 m, Pte. Ambarionaomby, Nosy Komba, near Nosy Bé, Madagascar, collected June 8, 1964: holotype ♀ (USNM 113391), allotype (USNM 113392), and 89 paratypes (USNM 113393) (79 ♀♀ and 10 ♂♂) deposited in the United States National Museum, 45 paratypes (40 ♀♀ and 5 ♂♂) in the Museum of Comparative Zoology, Harvard University, and the remaining paratypes in the collection of A. G. Humes.

OTHER SPECIMENS.—All from *Tubipora musica* collected in 1964: 121 ♀♀ and 53 ♂♂, in 1 m, Pte. à la Fièvre, Nosy Bé, Jan. 5; 9 ♀♀, in 15 cm, Tany Kely, a small island south of Nosy Bé, Mar. 29; 8 ♀♀, in 1 m, Pte. Ambarionaomby, Nosy Komba, Mar. 31; 14 ♀♀ and 3 ♂♂, in 1 m, Pte. à la Fièvre, Apr. 15; and 43 ♀♀, in 2 m, Pte. Ambarionaomby, Sept. 27.

In the description that follows, morphological features not specifically mentioned may be assumed to be essentially like those in *L. organicus*.

FEMALE.—Body (fig. 31) with prosome more pointed anteriorly than in *L. organicus*. Length of body (without ramal setae) 0.80 mm (0.72–0.87 mm) and greatest width 0.38 mm (0.34–0.40 mm), based on 10 specimens. Ratio of length to width of prosome 1.53:1.

Segment of leg 5 (fig. 32) 46μ x 107μ. Genital segment slightly wider than long, 110μ x 115μ, in dorsal view expanded laterally just behind its midregion, posterior to which segment is constricted, with width at posterior end of segment 60μ. Each area of attachment of egg sacs, located dorsolaterally on expanded part of segment, bearing 2 naked setae and rounded protuberance (more prominent than in previous species). Three postgenital segments 25μ x 53μ, 21μ x 48μ, and 23μ x 46μ, respectively, from anterior to posterior.

Caudal ramus (fig. 33) only slightly longer than wide, 28 $\times$ 23μ in greatest dimensions, ratio of length to width 1.22 : 1. Length along inner edge to innermost distal seta 19μ, along outer edge to base of lateral seta 19μ and to base of outermost distal seta 25μ. Pedicellate dorsal seta apparently naked. Relative lengths of 6 setae approximately those of *L. organicus*.

Ratio of length of prosome to that of urosome 2.6 : 1.

Egg sacs on all ovigerous females broken.

Rostral area (fig. 34) slightly more elongated posteriorly than in *L. organicus*. Segments of first antenna 23μ (44μ), 97μ, 21μ, 46μ, 45μ, 31μ, and 20μ in length (measured as before) and arrangement of naked setae and aesthetes as in previous species. Second antenna resembling that of *L. organicus*, but last segment slightly more slender (63μ along its outer edge, 39μ along its inner edge, and 21μ wide). Larger claw 37μ long, and more slender claw 32μ in length.

Labrum, mandible, paragnath, and first maxilla like those in *L. organicus*. Second maxilla closely resembling that species also, but pectinate seta on second segment slightly longer, reaching nearly to end of first tooth; in females studied 4–5 entire teeth, or 4 teeth with distalmost slightly bifurcated. Maxilliped resembling that of *L. organicus*, but subterminal setiform element apparently not as distinctly bifurcated at its tip.

Postoral area similar to that in previous species.

Legs 1–4 with same segmentation and spine and setal formula as in *L. organicus*. Spine on last segment of endopod of leg 1 27μ long. Endopod of leg 4 (fig. 35) with the following dimensions: first segment 33μ x 25μ with inner seta 40μ long, second segment 60μ x 21μ (greatest width) and 18μ (least width) with 2 terminal spines 25μ (outer) and 54μ (inner) in length, the ratio about 2.16:1.

Leg 5 similar to that of *L. organicus*, dimensions of free segment about 63μ x 24μ.

Leg 6 (represented by 2 setae near attachment of egg sacs) like that in previous species.

Color in life resembling that of *L. organicus*.

MALE.—Body (fig. 36) with prosome more pointed than in previous species. Body length (excluding setae on caudal rami) 0.71 mm (0.65–0.76 mm) and greatest width 0.27 mm (0.23–0.30 mm), based on 10 specimens. Ratio of length of prosome to its width 1.5:1.

Segment of leg 5 25μ x 66μ. Genital segment 151μ x 117μ. Four postgenital segments 14μ x 45μ, 16μ x 42μ, 13μ x 40μ, and 17μ x 42μ, respectively, from anterior to posterior. Caudal ramus 25μ x 21μ, or 1.19:1.

Ratio of length of prosome to that of urosome 1.57:1.

TABLE 1.—*Comparison of certain features of* Lichomolgus organicus *and* L. conjunctus

Characters	*L. organicus*	*L. conjunctus*
Female		
body size	0.99 x 0.49 mm	0.80 x 0.38 mm
anterior border of prosome	rounded	more pointed
ratio of prosome to urosome	2.1:1	2.6:1
caudal ramus	36μ x 24μ (1.5:1)	28μ x 23μ (1.22:1)
genital segment	lateral indentations near middle (fig. 2)	lateral indentations further back (fig. 32)
second antenna	last segment 27μ wide, claws 45μ and 34μ	last segment 21μ wide, claws 37μ and 32μ
spine on last segment of endopod of leg 1	24μ	27μ
spines on last segment of endopod of leg 4	21μ and 39μ (1:1.85)	25μ and 54μ (1:2.16)
Male		
body size	0.89 x 0.32 mm	0.71 x 0.27 mm
anterior border of prosome	rounded	more pointed
caudal ramus	31μ x 21μ (1.48:1)	25μ x 21μ (1.19:1)
spines on last segment of endopod of leg 4	17.5μ and 44μ (1:2.5)	18μ and 50μ (1:2.8)
free segment of leg 5	36μ x 9μ (4:1)	28μ x 8μ (3.5:1)

Rostral area like that of female. First antenna resembling that of *L. organicus*, with same formula for setae and aesthetes. Second antenna also resembling that species; last segment 73μ along outer edge, 54μ along inner edge, and 14μ wide. Two claws (34μ and 35μ) similar to those in *L. organicus*.

Labrum, mandible, paragnath, first maxilla, and second maxilla like those in female; in males observed 4 teeth on distal end of second

221-537—67——2

maxilla, last tooth slightly bifurcated or entire. Maxilliped and postoral area much like those in *L. organicus*.

Legs 1–4 resembling those of female with same spine and setal formula, except for sexual dimorphism in leg 1 (as in *L. organicus*). Two spines on last segment of endopod of leg 1 like those in previous species, outer 27μ and inner 40μ long. Two terminal spines on endopod of leg 4 18μ (outer) and 50μ (inner), ratio of 1:2.8.

Leg 5 resembling that of *L. organicus*, but free segment relatively slightly shorter, 28μ x 8μ.

Leg 6 similar to that in previous species, but 2 naked setae slightly longer (28μ).

Spermatophores, seen only inside body of male, resembling those of *L. organicus*.

Color in life like that of female.

ETYMOLOGY.—The specific name *conjunctus*, from Latin, meaning "closely related or bordering on," refers to the close similarity between this and the preceding species.

COMPARISON WITH RELATED SPECIES.—*L. conjunctus* closely resembles *L. organicus* in general appearance, but a careful study shows certain constant and characteristic differences. These are summarized in table 1.

ASSOCIATION OF THE TWO LICHOMOLGIDS WITH THE ALCYONARIAN.—Both *L. organicus* and *L. conjunctus* were recovered after washing unbroken colonies of *Tubipora musica* in sea water to which about 5 per cent ethyl alcohol had been added. The exact habitat of the copepods is unknown, but there seems to be little doubt of their association with the alcyonarian in view of the large numbers of individuals recovered.

Family Clausidiidae Embleton, 1901

Genus *Hippomolgus* Sars, 1917

Hippomolgus latipes, new species

FIGURES 37–58

TYPE MATERIAL.—8 ♀♀ from a colony of *Tubipora musica* (Linnaeus), in 1 m, Pte. Ambarionaomby, Nosy Komba, near Nosy Bé, Madagascar, collected Mar. 31, 1964: holotypic ♀ (USNM 113395) and 4 paratypic ♀♀, (USNM 113396) deposited in the United States National Museum; remaining 3 ♀♀ (dissected) in the collection of A. G. Humes.

OTHER MATERIAL.—Also from *Tubipora musica*: 1 ♀, in 1 m, Pte. Ambarionaomby, Nosy Komba, June 8, 1964.

FEMALE.—Body (fig. 37) with a rather harpacticoid appearance. Length (excluding setae on caudal rami) 1.13 mm (0.97–1.19 mm)

and greatest width 0.32 mm (0.27–0.37 mm), based on 8 specimens. Ratio of length to width of prosome 1.65:1. Segment bearing leg 1 completely fused with head. Lateral areas of segments of legs 1–3 not produced; those of segment of leg 4 slightly angular posteriorly.

Segment of leg 5 (fig. 38) broad, 94μ x 242μ, with fifth legs borne posterolaterally. Between this segment and genital segment on ventral side a weak intersegmental sclerite. Genital segment (fig. 38) wider than long, 130μ x 198μ. In ventral view its lateral border (fig. 39) with a small notch near middle of segment and a more pronounced indentation posteriorly. Areas of attachment of egg sacs situated dorsolaterally in midregion of segment. Each area (fig. 40) bearing outwardly a rather hyaline flange and inwardly a slender seta 11μ long, a spiniform seta 8μ long, and 2 small spinous processes. On ventral surface of posterior half of genital segment a transverse row of prominent spinules. Three postgenital segments 78μ x 135μ, 60μ x 118μ, and 91μ x 91μ, respectively, from anterior to posterior. Anal segment (fig. 41) bearing anteriorly 4 transverse rows of spinules, 2 rows ventrolateral and 2 ventral; along its posterior border near insertion of each caudal ramus a row of small spinules, this row continued on dorsal side.

Caudal ramus (fig. 42) 104μ x 34μ, or 3 times longer than wide. Minute basal outer spinule 3μ long. Outer lateral seta 22μ long and naked. Outermost terminal seta 41μ long, naked, and composed of 2 parts: a sclerotized proximal half and a more slender distal portion. Innermost terminal seta 57μ long and haired along inner side. Two long terminal setae 209μ (outer) and 462μ (inner), both basally "pegged" and bearing lateral spinules. Pedicellate dorsal seta 39μ long and naked. Dorsal surface of ramus with small hairs and refractile points as indicated in figure.

Dorsal surface of prosome and dorsal and ventral surfaces of urosome with scattered refractile points and hairs. Prosome slightly longer than urosome, ratio 1.1:1.

In single ovigerous female collected egg sac (fig. 43) 319μ x 107μ, extending a little beyond ends of caudal rami, with each egg about 40μ in diameter.

Rostral area (fig. 44) small and well sclerotized. Posterior to it, between bases of second antennae, a small circular sclerotization.

First antenna (fig. 45) 6-segmented and relatively short and robust, its length about 143μ. Lengths of segments measured along their posterior nonsetiferous margins: 15μ (39μ along anterior margin), 19μ, 28μ, 18μ, 13μ, and 24μ, respectively. First segment with 5 setae, proximal one lightly haired, distal one spiniform, with a row of scalelike spinules along one edge. On second segment 2 similar spiniform setae. All remaining setae naked. Each of last 3 seg-

ments with long prominent aesthete. Formula for armature: 5, 14, 9, 4+1 aesthete, 2+1 aesthete, and 7+1 aesthete. Only ornamentation on first antenna consisting of crescentic row of spinules on first segment.

Second antenna (fig. 46) 4-segmented, last segment 32μ x 19μ in greatest dimensions. Each of first 2 segments with a seta, third segment with a spine and 2 slender setae on its inner distal expansion, and last segment bearing 7 elements (a spine and 6 setae). Ornamentation indicated in figure, inner margins of third and fourth segments having rows of scalelike spinules.

Labrum (figs. 47, 48) ornamented with spinules as indicated in figures.

Mandible (fig. 49) bearing 3 terminal elements: a clawlike ventral (outer) spine with 1–2 spinous processes on its concave edge, a spine with lateral spinous projections on its basal half, and a slender barbed seta. No paragnath. First maxilla (fig. 50) bilobed, with 8 setae disposed in groups of 3, 4, and 1. Second maxilla (fig. 51) 2-segmented; first segment unarmed, second with outer haired seta and 2 inner barbed spinulose setae and terminating in a short clawlike process with at either side a setiform barbed process (these 2 processes perhaps setae but their articulation not evident). Maxilliped (fig. 52) 4-segmented, first segment with inner barbed seta, second with 2 naked setae, third unarmed, and fourth (fig. 53) subterminally with small naked seta and terminally with minute spiniform process and fringe of spiniform ornamentations resembling a small fan.

Area behind mouth and between mouthparts (fig. 47) showing anteriorly a transversely elongated median lobe (lingua) with a few very minute lateral spinules, followed immediately by a transverse row of hairs in 2 groups. Posterior to this a row of prominent spinules, with at either end a cluster of hairs. Bases of maxillipeds joined by sclerotized lines. Postoral area between maxillipeds and leg 1 broadly protuberant, especially noticeable in lateral view.

Legs 1–4 (figs. 54–57) with 3-segmented rami. Armature of legs as follows (Roman numerals=spines, Arabic numerals=setae):

P 1	protopod	0:1	1:I	exp	I:0	I:1	III,I,4
				end	0:1	0:1	I,3
P 2	protopod	0:1	1:0	exp	I:0	I:1	III,I,5
				end	0:1	0:2	II,I,3
P 3	protopod	0:1	1:0	exp	I:0	I:1	III,I,5
				end	0:1	0:2	II,II,2
P 4	protopod	0:1	1:0	exp	I:0	I:1	II,I,5
				end	0:1	0:2	II,II,1

Free edges of all 4 intercoxal plates with rows of long slender setules. Inner margin of basis of leg 1 (fig. 54) bearing spinulose

spine 25μ long, with near its insertion an outer row of spinules and an inner spiniform process with slightly bifurcated tip. In legs 2–4 this margin more or less rounded and carrying only a row of hairlike setules. Terminal segment of endopod of leg 1 with 1 spine and 3 setae. Spinous processes at each side of insertion of spine either entire or bifurcated at tip. Ornamentation of legs indicated in figures.

Leg 5 (fig. 58) having an expanded free segment 83μ x 53μ in greatest dimensions. Four elements borne on this segment consisting (from dorsal to ventral) of a finely barbed spine 39μ long, a naked seta 66μ long, a strong spinulose spine 44μ long, and a short weakly barbed spine 23μ in length. Along dorsal edge of segment a row of spinules. Seta borne on body dorsal to insertion of segment 40μ long and naked. (In dorsal or ventral view of undissected animal, segment of leg 5 appearing much less expanded than actually.)

Leg 6 probably represented by seta and spine near attachment of each egg sac (see fig. 40).

Color in life unknown.

MALE.—Unknown.

ETYMOLOGY.—The specific name *latipes*, from Latin, meaning "having broad feet," refers to the wide free segment of leg 5 in this species.

COMPARISON WITH RELATED SPECIES.—Only a single species of the genus *Hippomolgus*, *H. furcifer* Sars (1917), has been known until now. This species was described on the basis of 3 females found free in 60 fathoms, muddy bottom, on the coast of Norway. Males of *Hippomolgus* are unknown, although Nicholls (1944, p. 46) has expressed the view that the male of *Hersiliodes dubia* Thompson and A. Scott (1903) is in reality a *Hippomolgus*. This opinion was followed by Krishnaswamy (1953), who reported males of *Hippomolgus dubia* from the plankton of Madras. It seems improbable to us, however, that *Hersiliodes dubia* is a *Hippomolgus*. The mandible, described by Thompson and Scott as having "2 horizontal plumose projections and 2 plumose setae," is very different. Bocquet and Stock (1957) think it probable that a new genus should be created for *Hersiliodes dubia*.

Like *Hippomolgus furcifer*, *H. latipes* has a body form that is less cyclopoid and more harpacticoid, has a relatively short 6-segmented first antenna with a prominent aesthete on each of the last 3 segments, lacks paragnaths, and has a generally similar structure of the second antennae, mouthparts, and legs 1–5.

There are, however, important differences between these 2 species (based of necessity on the female only). In *H. latipes* the first segment of the first antenna does not bear a spine such as described in *H. furcifer*. The mandible bears 3 terminal elements (2 spines and

1 seta) instead of 4, as in Sars' figure (pl. 82, m). The maxilliped is 4-segmented, the last segment ornamented with a small fanlike fringe, instead of being 3-segmented as in Sars' figure (pl. 82, mp^2). The armature of the last segment of the endopod of leg 1 is I,3 instead of I,II,3 as in Sars' species. The free segment of leg 5 is expanded instead of being narrow as in *H. furcifer*. The caudal ramus is only 3 times longer than wide instead of about 13:1 as in the Norwegian species. The length of the female is 1.13 mm, instead of 1.40 mm as in *H. furcifer*.

Hippomolgus cognatus, new species

FIGURES 59–69

TYPE MATERIAL.—Holotype ♀ (USNM 113397) from a colony of *Tubipora musica* (Linnaeus), in 1 m, Pte. Ambarionaomby, Nosy Komba, near Nosy Bé, Madagascar, collected Mar. 31, 1964, deposited in the United States National Museum.

OTHER MATERIAL.—2 ♀♀ from *Tubipora musica*, in 1 m, Pte. à la Fièvre, Nosy Bé, Jan. 5, 1964, 1 ♀ (USNM 113398) in the United States National Museum, the other (dissected) in the private collection of A. G. Humes.

FEMALE.—Body (fig. 59) resembling that of *H. latipes*. Length (not including setae on caudal rami) 0.90 mm (0.82–0.95 mm) and greatest width 0.29 mm (0.28–0.31 mm), based on 3 specimens. Ratio of length to width of prosome 1.56:1.

Segment of leg 5 broad, 78μ x 188μ. Genital segment (fig. 60) only slightly wider than long, 120μ in length, 132μ wide in its anterior half, and 110μ wide in its posterior half, where sides in dorsal view are nearly parallel. Areas of attachment of egg sacs located dorsolaterally on midregion of segment. Each area (fig. 61) with a slender naked seta 22μ long, a spine 8μ long, and 2 spinous processes. Three postgenital segments 66μ x 101μ, 60μ x 91μ, and 80μ x 82μ, respectively, from anterior to posterior.

Caudal ramus (fig. 62) 64μ x 31μ in greatest dimensions, or 3 times longer than wide. Outer lateral seta 25μ, outermost terminal seta 39μ, innermost terminal seta 88μ, 2 long terminal setae 220μ (outer) and 450μ (inner), dorsal seta 33μ long.

Ratio of prosome to urosome 1.17:1.

In single ovigerous female collected egg sac (fig. 63) 352μ x 138μ, reaching nearly to ends of caudal rami, with each egg about 47μ in diameter.

Rostral area (fig. 64) bearing 2 rows of minute denticles.

First and second antennae like those in *H. latipes*. Labrum (figs. 65, 66) ornamented as indicated in figures. Mandible (fig. 67) bearing 3 terminal elements as in *H. latipes*, but these with different orna-

mentation, i.e., with spinous processes on both sides of 2 spines and with seta naked. Paragnath absent. First and second maxillae and maxilliped like those in *H. latipes*.

Area behind mouth and between mouthparts with median lobe (lingua) weakly developed. Postoral area between maxillipeds and leg 1 (fig. 65) less protuberant than in *H. latipes*.

Legs 1–4 with same spine and setal formula as in *H. latipes*, except for endopod of leg 1 being 0:1; 0:1; I,4. Leg 1 (fig. 68) with inner spine on basis 22μ long and adjacent spiniform process asymmetrically bifurcated; terminal segment of endopod with 4 setae and with 3 small and rather obtuse processes between spine and first seta. Legs 2–4 resembling those of *H. latipes*.

Leg 5 (fig. 69) with relatively slender free segment, 61μ along inner and ventral margin, 51μ along outer and dorsal margin, and 22μ wide. Armature from dorsal to ventral consisting of spine 21μ, seta 50μ, spine 25μ, and spine 40μ in length, all ornamented as in figure.

Leg 6 probably represented by spine and seta near attachment of each egg sac (see fig. 61).

In other respects similar to *H. latipes*.

Color in life unknown.

MALE.—Unknown.

ETYMOLOGY.—The specific name *cognatus*, from Latin, meaning "related or closely allied," refers to apparent close relationship between this species and *H. latipes*.

COMPARISON WITH RELATED SPECIES.—*H. cognatus* differs from *H. furcifer* Sars (1917) in lacking a spine such as described on the first segment of the first antenna in the Norwegian species, in having 3 terminal elements instead of 4 on the mandible, in having a 4-segmented maxilliped with a terminal fanlike fringe, in having the last segment of the endopod of leg 1 armed as I,4 instead of I,II,3 as in Sars' species, and in having a relatively much shorter caudal ramus, 3:1 instead of 13:1 as in *H. furcifer*. The length of the female is 0.90 mm instead of 1.40 mm as in the species described by Sars.

H. cognatus apparently is closely related to *H. latipes* but differs from it chiefly in the form of the genital segment, the presence of denticles on the rostral area, the form and ornamentation of the labrum, the ornamentation of the 3 elements on the mandible, the armature of the last segment of the endopod of leg 1, and the form of the free segment of leg 5.

ASSOCIATION OF THE TWO CLAUSIDIIDS WITH THE ALCYONARIAN.—Whether *Hippomolgus latipes* and *H. cognatus* live in a close association with *Tubipora musica* or occur only sporadically in the coral colony

is difficult to determine on the basis of the relatively few specimens collected. (No *Hippomolgus* were found in 4 other colonies of *Tubipora musica*.)

Literature Cited

BOCQUET, C., and STOCK, J. H.
1957. Copépodes parasites d'invertébrés des côtes de France, 1: Sur deux genres de la famille des Clausidiidae, commensaux de mollusques: *Hersiliodes* Canu et *Conchyliurus* nov. gen. Proc. Koninkl. Nederlandsche Akad. Wetensch. Amsterdam, ser. C, vol. 60, no. 2, pp. 212–222.

BRADY, G. S.
1910. Die marinen Copepoden der Deutschen Südpolar-Expedition 1901–1903, 1: Über die Copepoden der Stämme Harpacticoida, Cyclopoida, Notodelphyoida und Caligoida. No. 5 *of* vol. 11 (Zool. vol. 3) *in* Deutsche Südpolar-Expedition 1901–1903, pp. 497–593.

GURNEY, R.
1927. Zoological results of the Cambridge expedition to the Suez Canal, 1924, XXXIII: Report on the Crustacea: Copepoda (Littoral and semiparasitic). Trans. Zool. Soc. London, vol. 22, no. 4, pp. 451–577.

HUMES, A. G., and FROST, B. W.
1964. New lichomolgid copepods (Cyclopoida) associated with alcyonarians and madreporarians in Madagascar. Cah. O.R.S.T.O.M. Océanogr., Sér. Nosy-Bé, vol. 2, no. 6, pp. 131–212.

KRISHNASWAMY, S.
1953. Pelagic Copepoda of the Madras coast. Journ. Madras Univ., vol. 23 B, no. 1, pp. 61–75.

NICHOLLS, A. G.
1944. Littoral Copepoda from South Australia, II: Calanoida, Cyclopoida, Notodelphyoida, Monstrilloida and Caligoida. Rec. South Australian Mus., vol. 8, no. 1, pp. 1–62.

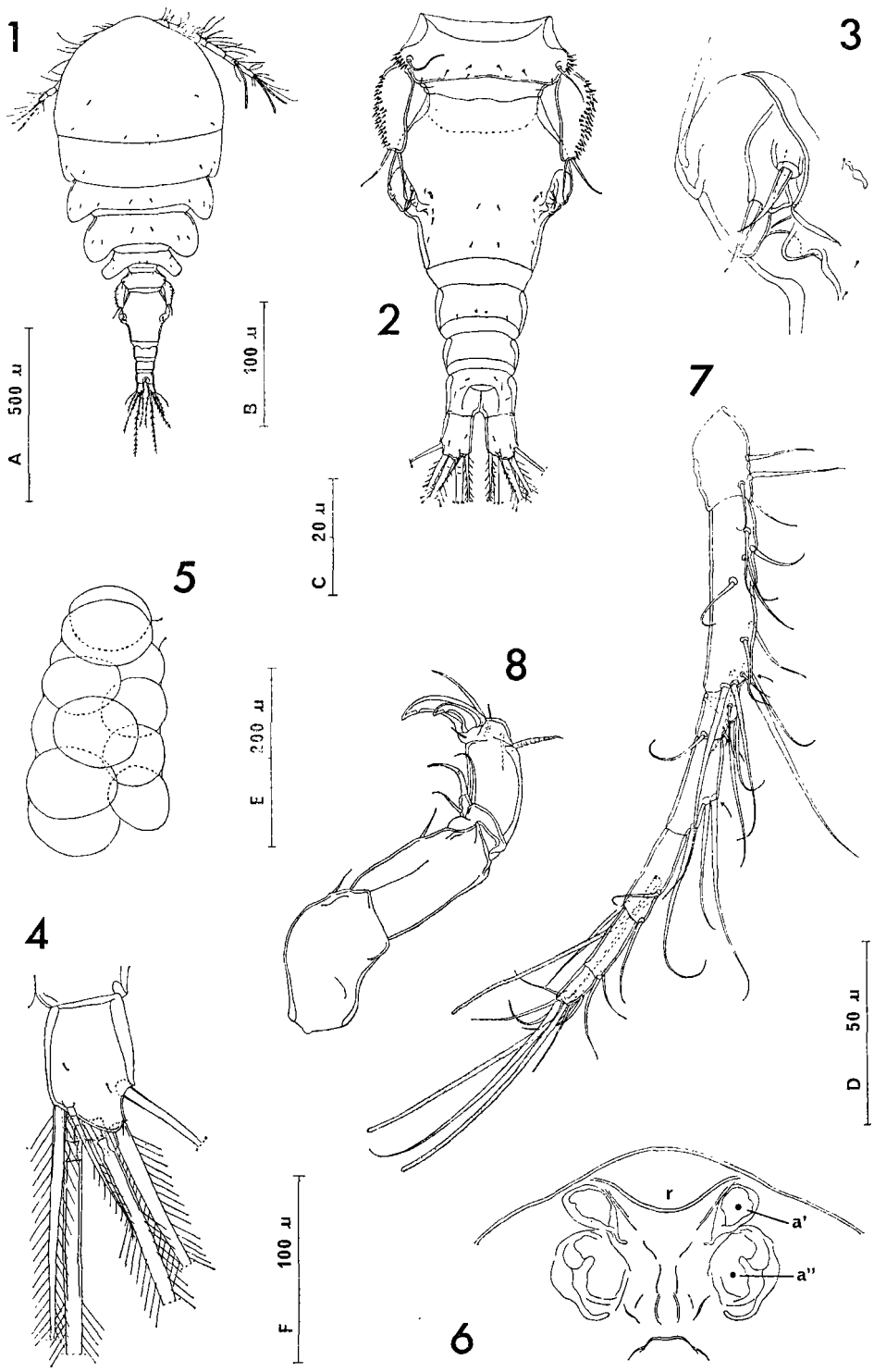
SARS, G. O.
1917. Clausidiidae, Lichomolgidae (part). Pts. 11 and 12 *of* vol. 6 (Copepoda, Cyclopoida) *in* An account of the Crustacea of Norway with short descriptions and figures of all the species, pp. 141–172.

SEWELL, R. B. S.
1949. The littoral and semi-parasitic Cyclopoida, the Monstrilloida and Notodelphyoida. No. 2 *of* vol. 9 *in* John Murray Expedition 1933–34 Scientific Reports, pp. 17–199.

STOCK, J. H.
1959. Copepoda associated with Neapolitan invertebrates. Pubbl. Staz. Zool. Napoli, vol. 31, no. 1, pp. 59–75.

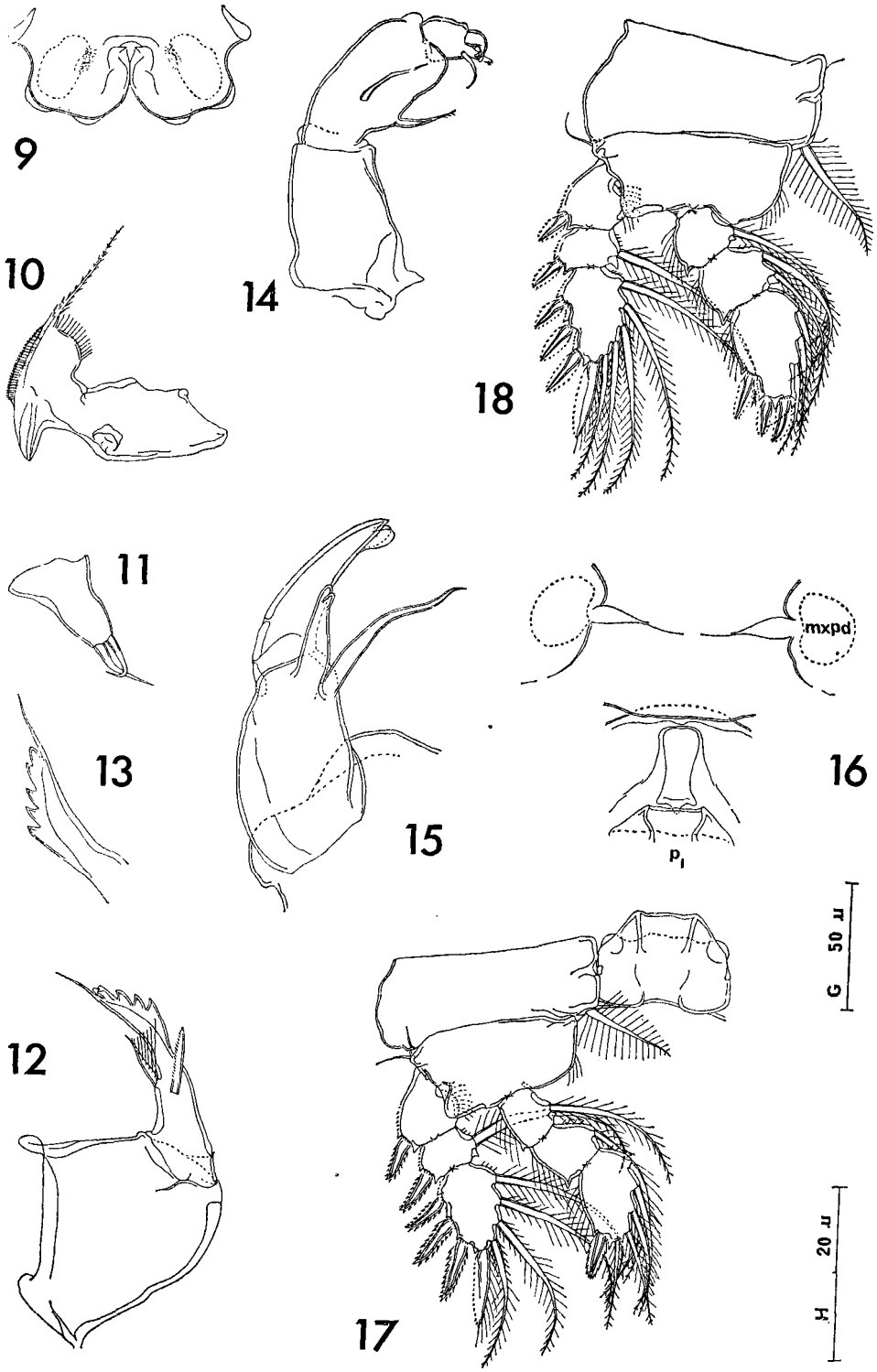
THOMPSON, I. C., and SCOTT, A.
1903. Report on the Copepoda collected by Professor Herdman, at Ceylon, in 1902. Rep. Gov. Ceylon Pearl Oyster Fish. Gulf of Manaar, suppl. rep., no. 7, pp. 227–307.

UMMERKUTTY, A. N. P.
1962. Studies on Indian copepods, 5: On eleven new species of marine cyclopoid copepods from the south-east coast of India. Journ. Mar. Biol. Assoc. India, 1961, vol. 3, nos. 1 and 2, pp. 19–69.



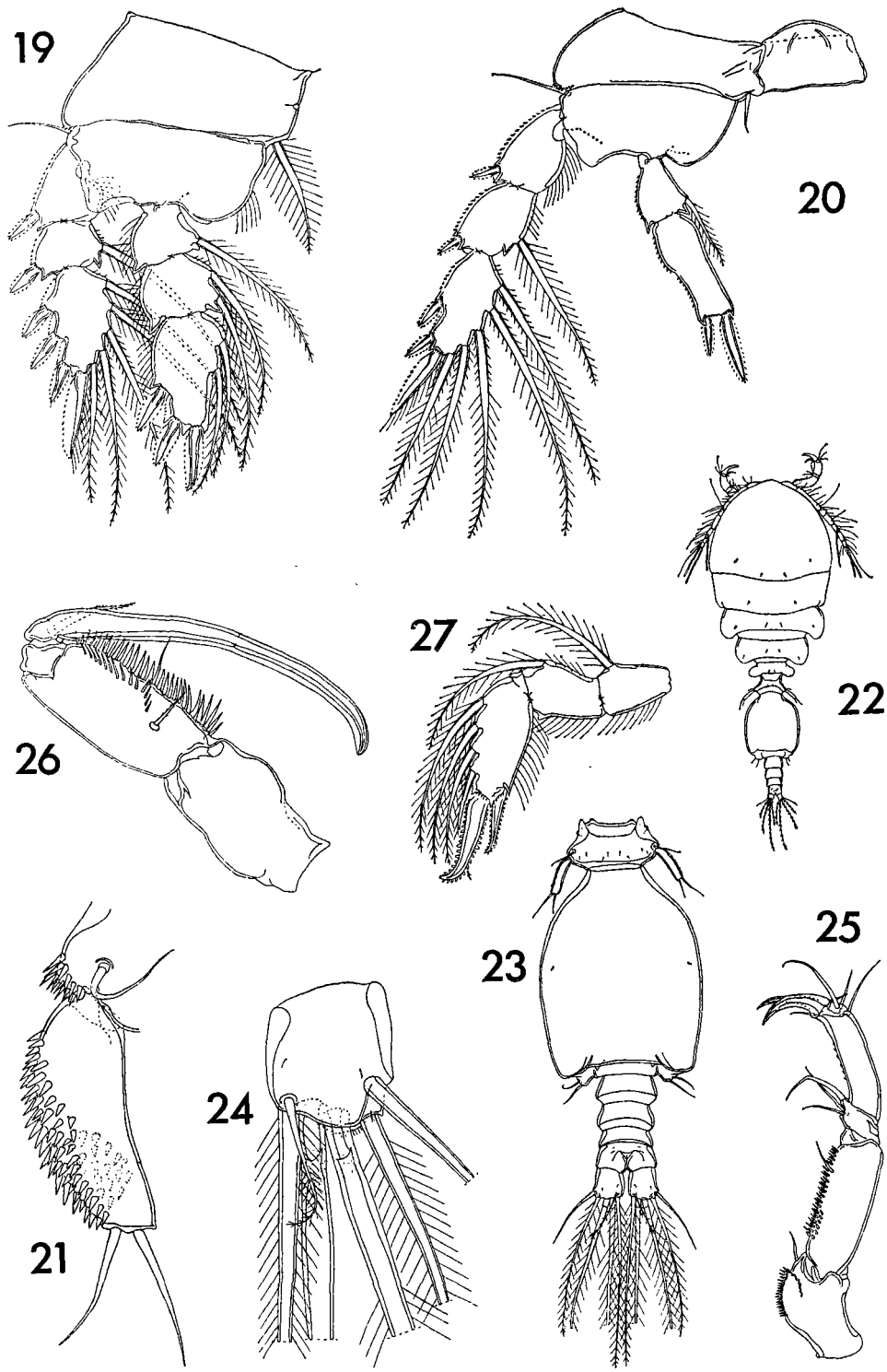
FIGURES 1–8.—*Lichomolgus organicus*, new species, female: 1, dorsal (A); 2, urosome, dorsal (B); 3, area of attachment of egg sac, dorsal (C); 4, caudal ramus, dorsal (D); 5, egg sac, dorsal (E); 6, rostral area, ventral (B); 7, first antenna, with two arrows indicating positions of aesthetes added in male, dorsal (F); 8, second antenna, posterior (F). (Capital letters=scale at which drawn; a'=first antenna, a''=second antenna, r=rostral area.)

17



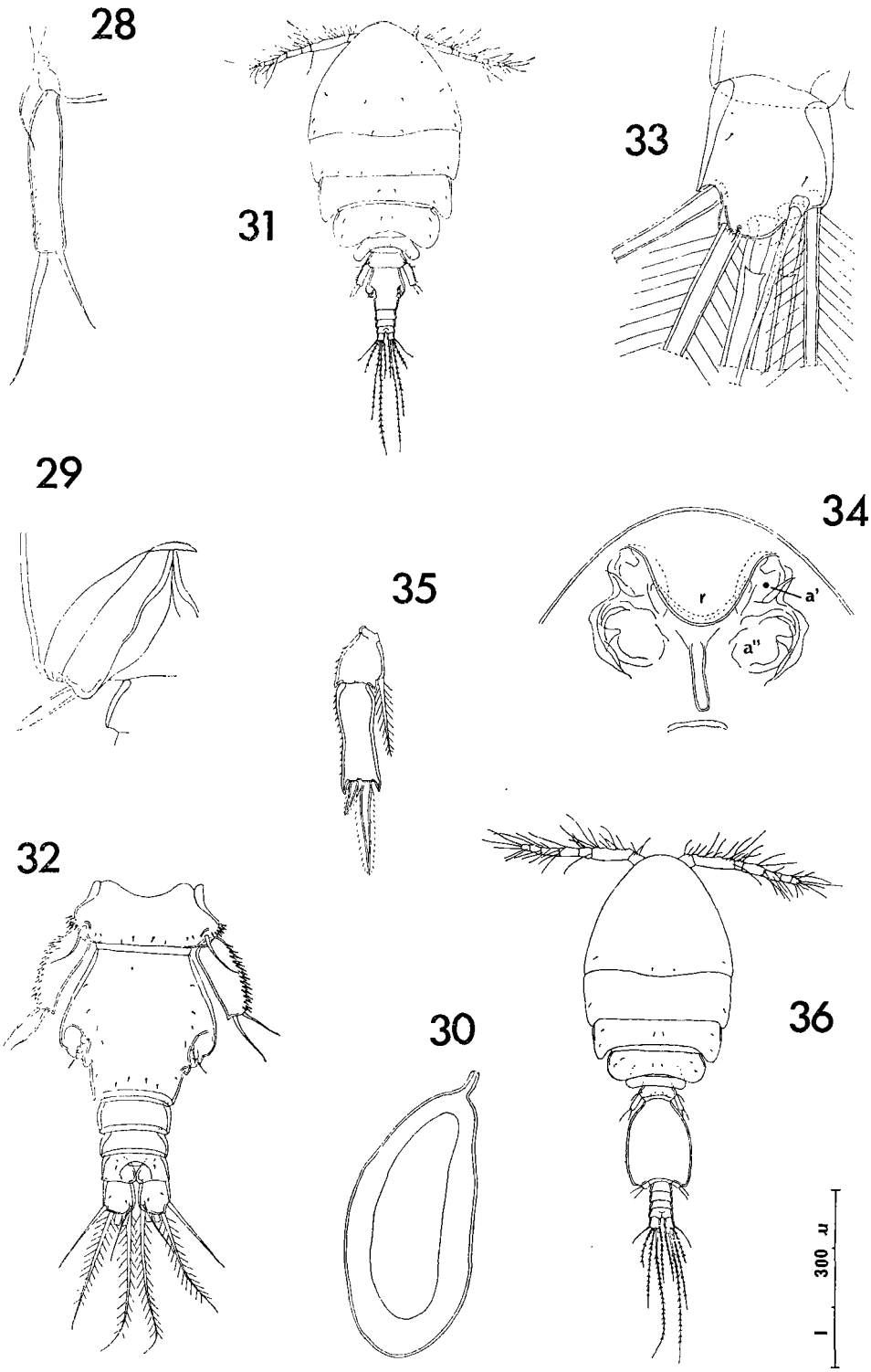
FIGURES 9–18.—*Lichomolgus organicus*, new species, female: 9, posterior part of labrum, with paragnaths indicated by dashed lines, ventral (G); 10, mandible, posterior (G); 11, first maxilla, posterior (G); 12, second maxilla, postero-inner (G); 13, tip of second maxilla, postero-inner (D); 14, maxilliped, posterior (G); 15, terminal segment of maxilliped, antero-inner (H); 16, postoral area between maxillipeds and leg 1, ventral (F); 17, leg 1 and intercoxal plate, anterior (F); 18, leg 2, anterior (F). (Capital letters=scale at which drawn; mxpd=maxilliped, P_1=leg 1.)

18



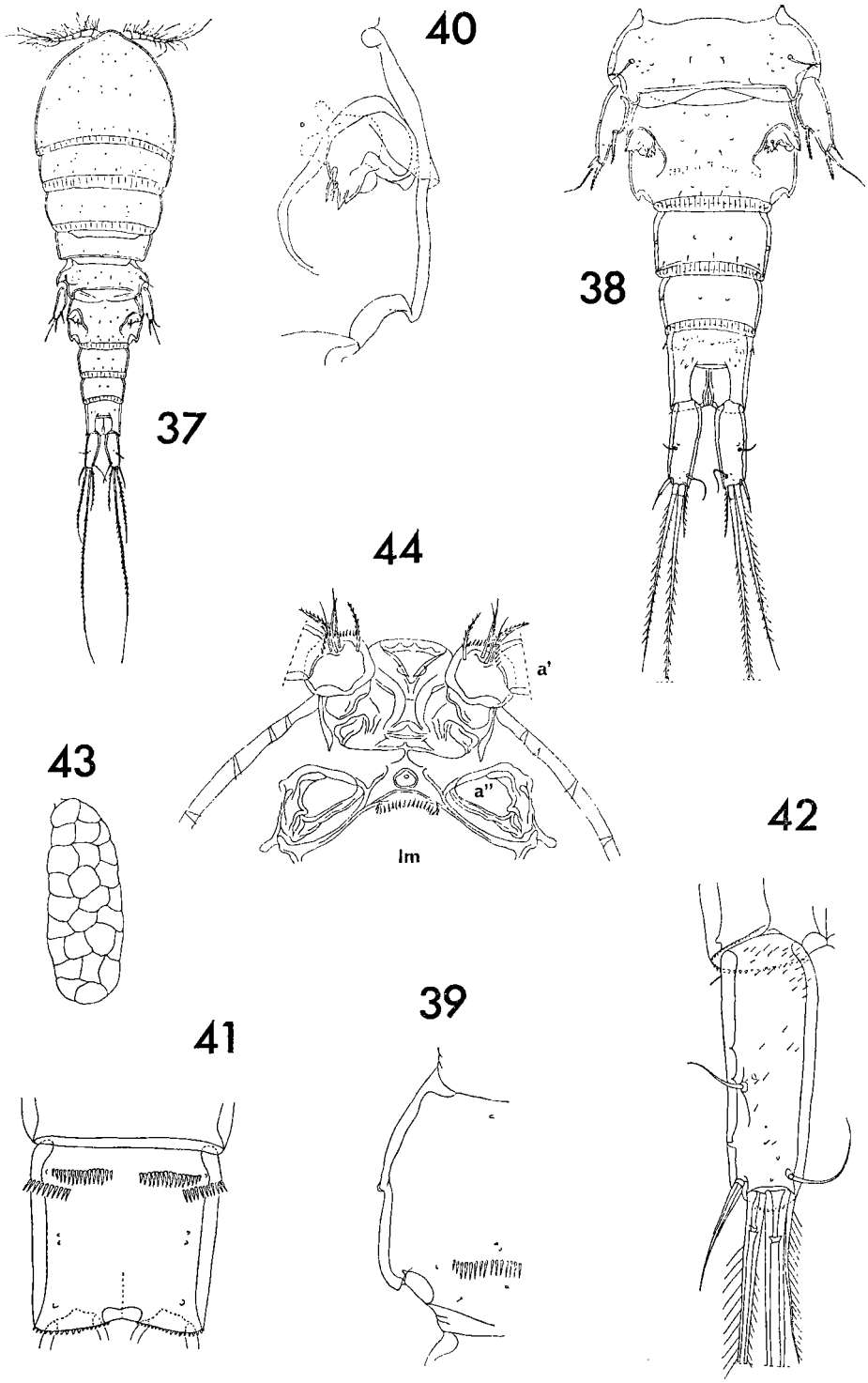
FIGURES 19–27.—*Lichomolgus organicus*, new species, female: 19, leg 3, anterior (F); 20, leg 4 and intercoxal plate, anterior (F); 21, leg 5, dorsal (D). Male: 22, dorsal (A); 23, urosome, dorsal (B); 24, caudal ramus, dorsal (C); 25, second antenna, anterior (F); 26, maxilliped, anterior (F); 27, endopod of leg 1, anterior (G). (Capital letters=scale at which drawn.)

19



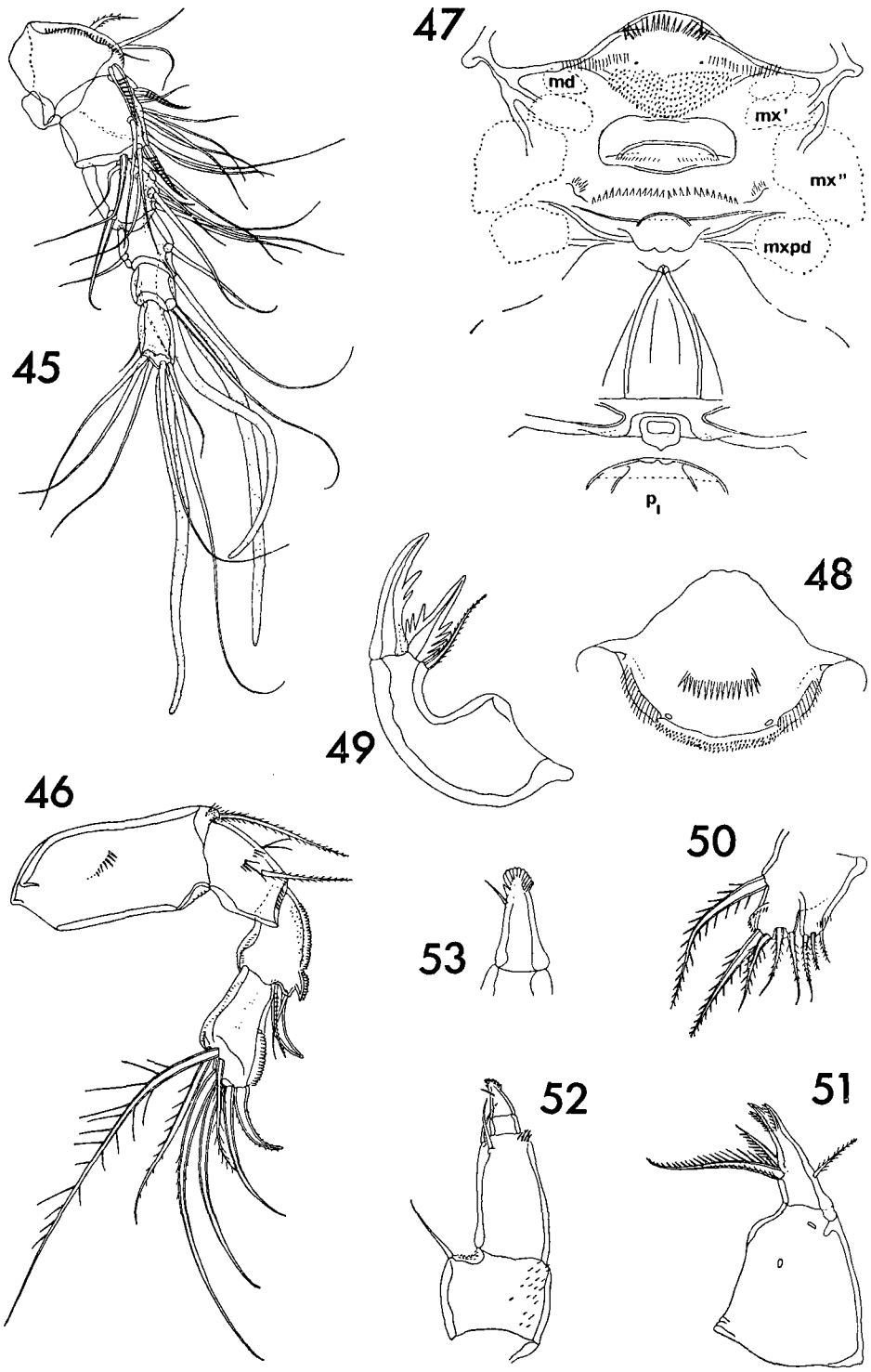
FIGURES 28–36.—*Lichomolgus organicus*, new species, male: 28, leg 5, dorsal (D); 29, leg 6, ventral (G); 30, spermatophore, inside male, ventral (F). *Lichomolgus conjunctus*, new species, female: 31, dorsal (A); 32, urosome, dorsal (B); 33, caudal ramus, dorsal (C); 34, rostral area, ventral (B); 35, endopod of leg 4, anterior (F). Male: 36, dorsal (I). (Capital letters=scale at which drawn; a'=first antenna, a''=second antenna, r=rostral area.)

20



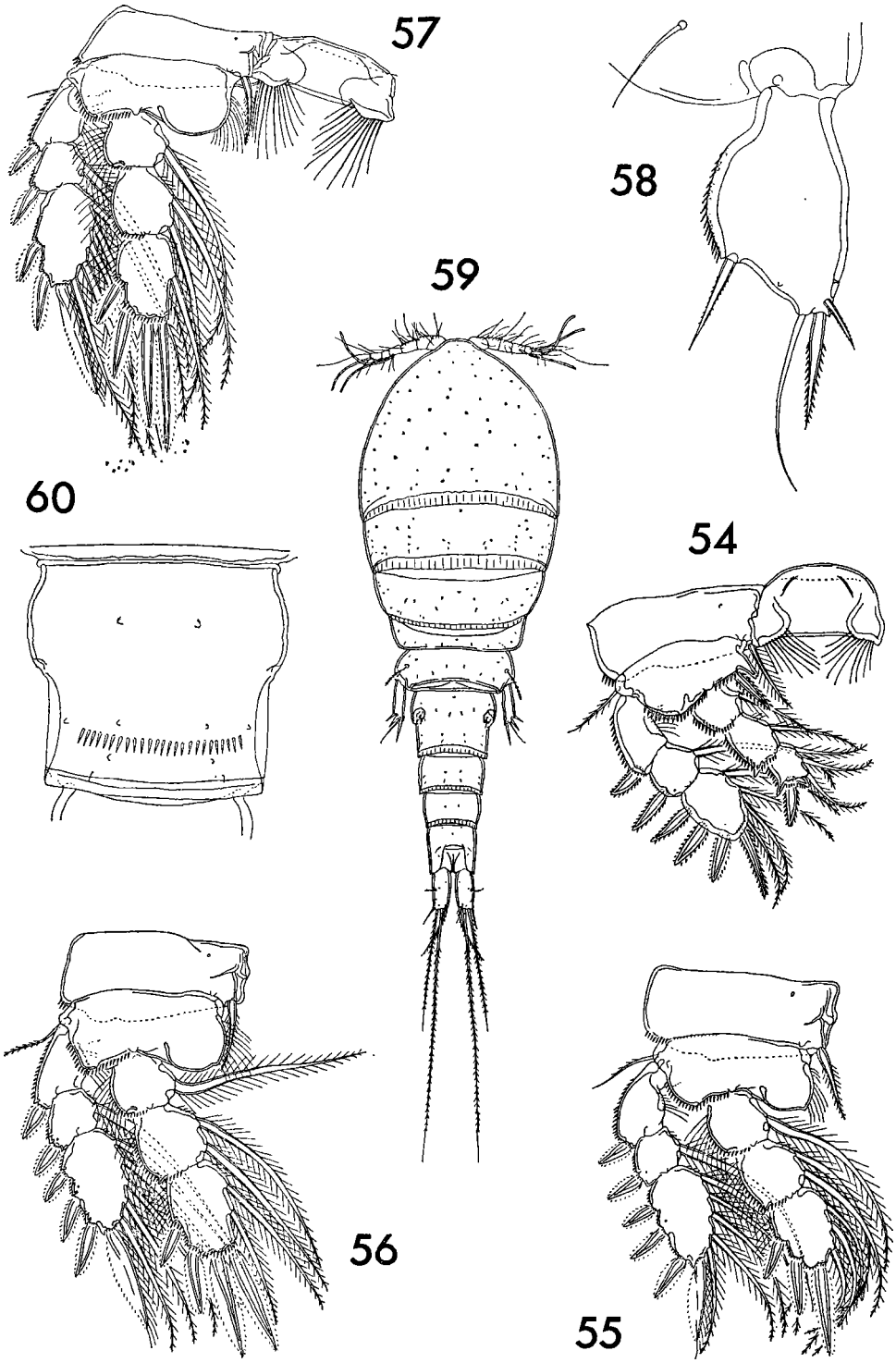
FIGURES 37–44.—*Hippomolgus latipes*, new species, female: 37, dorsal (A); 38, urosome, dorsal (E); 39, right side of genital segment, ventral (F); 40, area of attachment of egg sac, dorsal (G); 41, anal segment, ventral (F); 42, caudal ramus, dorsal (G); 43, egg sac, lateral (I); 44, rostral area, ventral (F). (Capital letters=scale at which drawn; a'=first antenna, a''=second antenna, lm=labrum.)

21



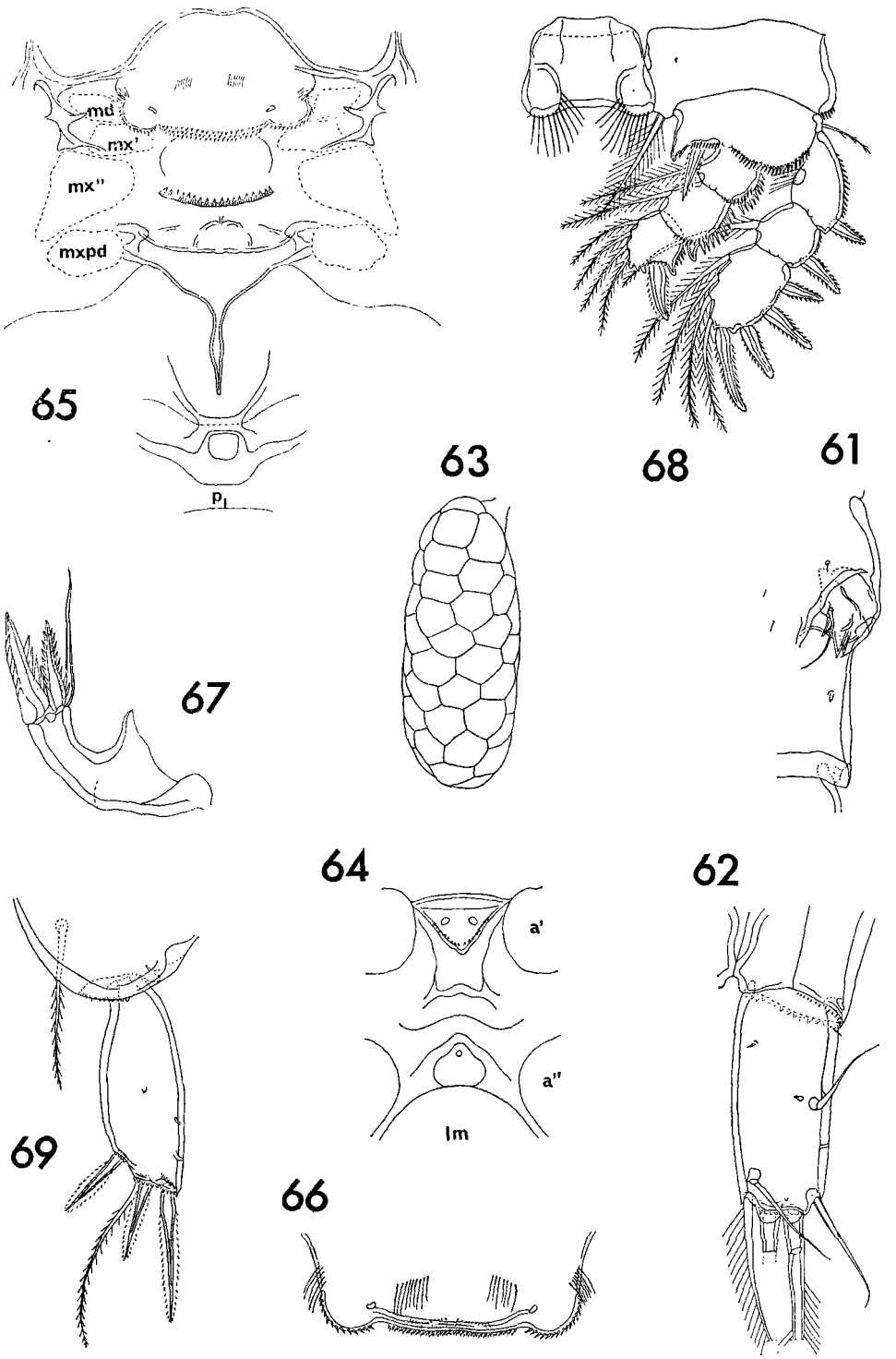
FIGURES 45–53.—*Hippomolgus latipes*, new species, female: 45, first antenna, dorsal (G); 46, second antenna, posterior (D); 47, oral and postoral areas, with labrum erected, ventral (G); 48, labrum, ventral (G); 49, mandible, posterior (C); 50, first maxilla, anterior (D); 51, second maxilla, anterior (D); 52, maxilliped, anterior (D); 53, last segment of maxilliped, ventral (H). (Capital letters=scale at which drawn; md=mandible, mx'=first maxilla, mx"=second maxilla, mxpd=maxilliped, p_1=leg 1.)

22



FIGURES 54–60.—*Hippomolgus latipes*, new species, female: 54, leg 1 and intercoxal plate, anterior (F); 55, leg 2, anterior (F); 56, leg 3, anterior (F); 57, leg 4 and intercoxal plate, anterior (F); 58, leg 5, lateral and outer (G). *H. cognatus*, new species, female: 59, dorsal (I); 60, genital segment, ventral (F). (Capital letters=scale at which drawn.)

23



FIGURES 61–69.—*Hippomolgus cognatus*, new species, female: 61, area of attachment of egg sac, dorsal (G); 62, caudal ramus, dorsal (D); 63, egg sac, lateral (E); 64, rostral area, ventral (G); 65, oral and postoral areas, ventral (G); 66, free edge of labrum, ventral (D); 67, mandible, posterior (C); 68, leg 1, anterior (G); 69, leg 5, ventrolateral (D). (Capital letters=scale at which drawn; md=mandible, mx'=first maxilla, mx''=second maxilla, mxpd=maxilliped; P_1=leg 1, a'=first antenna, a''=second antenna, lm=labrum.)

U.S. GOVERNMENT PRINTING OFFICE: 1967

Reprinted from *Proc. U.S. Nat. Mus.*, vol. 122, no. 3,583, 1967, p. 1-67

Proceedings of the United States National Museum

SMITHSONIAN INSTITUTION • WASHINGTON, D.C.

Volume 122 1967 Number 3583

BATHYPELAGIC CALANOID COPEPODS OF THE WESTERN INDIAN OCEAN[1]

By GEORGE D. GRICE AND KUNI HULSEMANN[2]

The plankton and midwater trawl samples on which this paper is based were obtained during two cruises of R. V. *Anton Bruun* in 1963 and 1964, which, at that time, was participating in the Biological Program of the International Indian Ocean Expedition. The area in which the samples were collected extends from the northern Arabian Sea to approximately the latitude of the subtropical convergence in the southern Indian Ocean. The operation of the *Anton Bruun* in the Indian Ocean provided us with an opportunity to extend our studies on the systematics and the zoogeography of the bathypelagic calanoid copepods from the Atlantic to the Indian Ocean.

We would like to thank Misses Ann Mulcahy and Mary Ann Beecher for their help in sorting and counting the copepods of the plankton samples and Miss Cecilia Simons for inking the original figures. Mr. Bruce Rogers assisted in collecting the samples at sea.

[1] Contribution No. 1807 from Woods Hole Oceanographic Institution. Study supported by National Science Foundation grant (GB 3479) and United States Program in Biology of the International Indian Ocean Expedition.

[2] Both authors: Woods Hole Oceanographic Institution, Woods Hole, Massachusetts.

Methods and Materials

The area in the western Indian Ocean from where the 51 samples considered in this paper were obtained is bounded by latitude 18°N and 40°S and longitude 50°W and 80°W (fig. 1, table 1). Three types of collecting gear were used to sample the deep-living copepods:

Bé multiple plankton sampler: Six of the collections analyzed

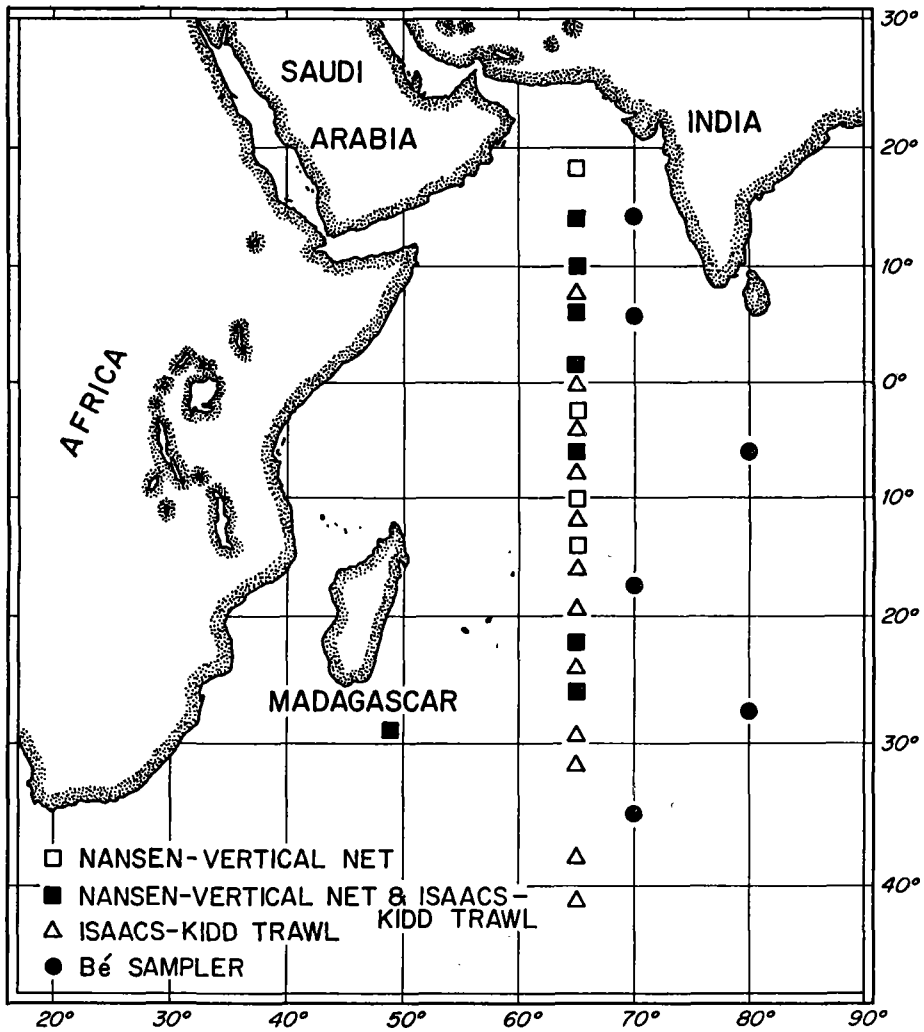


FIGURE 1.—Location of collection stations.

were collected by this sampler (described by Bé, 1962), hereafter designated the Bé net or sampler. The sampler was equipped with a number 3 net (.333 mm aperture), and the samples obtained between the 1000 and 2000 m depth interval on *Anton Bruun* Cruise 2 were studied. A total of 876 adult copepods (139 species) were identified in these samples. No volume measurements were made.

TABLE 1.—*Collection data* (blank space = volume not recorded, a = position at start of trawl, b = maximum depth from time-depth recorder (T) or wire angle (W))

Collection No.	Station No.	Date	Latitude	Longitude	Collection Depth (m)	Volume Plankton (cc)	No. Species Copepods
			Bé Sampler Collections (Cruise 2)				
1	108	25-V-63	13°50′N	70°07′E	2000–1000		40
2	112	29-V-63	05°48′N	70°03′E	2000–1000		50
3	123	10-VI-63	17°18′S	70°05′E	2000–1000		40
4	131	1-VII-63	35°09′S	69°59′E	2000–1000		41
5	134	6-VII-63	27°31′S	80°08′E	2000–1000		52
6	140	13-VII-63	05°53′S	79°57′E	2000–1000		53
			Isaacs-Kidd Midwater Trawl Collections (Cruise 6)				
7	330B	20-V-64	13°58′N [a]	65°02′E [a]	0–2750(T) [b]		3
8	332A	22-V-64	09°56′N	64°59′E	0–3250(W)		8
9	333A	23-V-64	07°55′N	64°55′E	350–2850(W)		21
10	333B	23-V-64	07°33′N	64°41′E	350– 940(W)		14
11	334B	24-V-64	05°48′N	64°57′E	275–2868(W)		17
12	336A	26-V-64	02°03′N	65°04′E	275– 817(W)		10
13	337B	28-V-64	00°14′S	65°03′E	275–2250(W)		26
14	339B	30-V-64	04°14′S	65°02′E	275–2080(W)		12
15	340A	31-V-64	05°55′S	65°10′E	275–2600(T)		21
16	341A	1-VI-64	08°00′S	65°00′E	0–3820(W)		8
17	343B	4-VI-64	12°11′S	64°11′E	225–1930(W)		17
18	345A	6-VI-64	15°57′S	64°46′E	0–2407(W)		7
19	346A	8-VI-64	19°24′S	65°30′E	225–2600(W)		18
20	347A	23-VI-64	22°11′S	64°53′E	350–2500(W)		21
21	348A	24-VI-64	24°03′S	65°00′E	350–3500(W)		17
22	349B	26-VI-64	26°24′S	65°02′E	350–1470(W)		26
23	351B	28-VI-64	29°45′S	64°58′E	350–1710(W)		25
24	351D	29-VI-64	31°45′S	65°08′E	350–1786(W)		16
25	353A	2-VII-64	37°59′S	64°56′E	350–2394(W)		22
26	354A	4-VII-64	40°48′S	65°03′E	0–1650(W)		18
27	355O	12-VII-64	29°29′S	48°43′E	0–3140(W)		22
			Nansen Vertical Net Collections (Cruise 6)				
28	328	17-V-64	18°02′N	65°08′E	2000– 750	1.5	37
29	328	17-V-64	18°02′N	65°08′E	3000–2000	1.0	18
30	330	20-V-64	13°36′N	65°03′E	1980–1050	1.0	40
31	332	22-V-64	10°04′N	64°59′E	2000–1002	0.7	40
32	332	22-V-64	10°04′N	64°59′E	3000–2000	0.5	19
33	332	22-V-64	10°04′N	64°59′E	4000–3000	0.5	8
34	334	24-V-64	06°01′N	64°59′E	2000–1078	0.7	9
35	334	24-V-64	06°01′N	64°59′E	3000–1894	0.5	16
36	336	27-V-64	01°30′N	65°09′E	2000–1000	1.0	41
37	336	27-V-64	01°30′N	65°09′E	3000–1940	0.7	21
38	338	29-V-64	02°38′S	65°01′E	2000–1000	1.0	41
39	338	29-V-64	02°38′S	65°01′E	3000–2000	0.3	26
40	340	31-V-64	06°00′S	65°10′E	1950–1015	1.0	41
41	340	31-V-64	06°00′S	65°10′E	2950–1990	0.5	28
42	342	2-VI-64	10°07′S	64°27′E	1970–1020	1.0	44
43	342	2-VI-64	10°07′S	64°27′E	3000–1980	0.7	32
44	344	5-VI-64	14°11′S	65°17′E	1980–1010	1.0	39
45	347	23-VI-64	22°06′S	64°55′E	2000–1000	0.3	33
46	349	25-VI-64	26°03′S	64°58′E	2000–1000	0.7	23
47	349	25-VI-64	26°03′S	64°58′E	3000–2000	0.5	8
48	349	25-VI-64	26°03′S	64°58′E	4000–3000	0.3	8
49	355	12-VII-64	29°38′S	49°23′E	2000–1000	0.5	11
50	355	12-VII-64	29°38′S	49°23′E	3000–2000	0.7	3
51	355	12-VII-64	29°38′S	49°23′E	4000–3000	0.7	8

Isaacs-Kidd midwater trawl: Twenty-one Isaacs-Kidd midwater samples (IK) collected on *Anton Bruun* Cruise 6 were examined and 10 to 70 copepods removed from each sample. The larger and deeper living species not usually collected in small vertical nets were selected from the trawl sample. The cod end of the trawl was made of number 2 mesh net (.366 mm). The maximum depth of trawling was determined from a time-depth recorder or calculated from measurements of length of wire-out vs. wire angle. Although a catch divider (Foxton, 1963) was attached to the end of the trawl, it apparently did not operate properly. Consequently, no attempt is made to discuss the vertical distribution of the species collected by the midwater trawl. A total of 797 adult copepods (113 species) were identified in these trawl samples.

Nansen vertical net: Twenty-four collections were also obtained on *Anton Bruun* Cruise 6 by a modified Nansen vertical net (NV). This net is similar to the one described by Currie and Foxton (1957) except that a flow-meter was mounted within the mouth of the net and a time-depth recorder (Benthos Mfg. Co., North Falmouth, Mass.) was attached to the weight below the cod end of the net. The net was made of number 6 mesh (.239 mm aperture). The samples from the following depth intervals are considered here: 2000–1000 m, 3000–2000 m, and 4000–3000 m. The time-depth recorder was equipped with a magnetic switch. Upon closure of the net, this switch activated a stylus that marked the recording chart. The maximum depth reached by the net and the depth of net closure was thus indicated on the chart. Since the speed of ascent of the net (60 m/min) and speed of descent of the messenger (200 m/min) that triggered the release and closure of the net was known, it was also possible to compute the depth of closing. In actual practice the depth of closing was clearly indicated in most cases by a severe jerk of the hydrographic wire when the throttling line pursed the net. When this occurred, the amount of wire out was recorded. Good agreement was found between the computed and actual depths of closure. The corrected depths are given in table 1. The method of measuring the volume of the NV samples and treating the copepods are the same as discussed in an earlier paper (Grice and Hulsemann, 1965). A total of 1740 adult copepods (194 species) were identified in these samples.

Contaminants: Twenty-six species of copepods collected by the NV net, which we feel may possibly have entered the net at shallower depths than those indicated, were found in many collections. These species, listed below, are in addition to those previously considered as contaminants in NV samples collected in the northeastern Atlantic Ocean (see Table II, Grice and Hulsemann,

1965). Species considered contaminants in samples collected with Nansen vertical net below 1000 m (in addition to those species listed by Grice and Hulsemann, 1965) are as follows:

Calanus tenuicornis	*Paracalanus denudatus?*	*Scolecithrix nicobarica*
Canthocalanus pauper	*Paracalanus nanus*	*Temora discaudata*
Nannocalanus minor	*Clausocalanus farrani*	*Undinella simplex*
Neocalanus gracilis	*Euaetideus acutus*	*Lucicutia gaussae*
Undinula darwini	*Scolecithricella maritima*,	*Candacia catula*
Acrocalanus longicornis	new species	*Paracandacia bispinosa*
Acrocalanus monachus	*Scolecithricella* species	*Paracandacia truncata*
Calocalanus pavo	*Scolecithrix bradyi*	*Labidocera detruncata*
Calocalanus plumulosus	*Scolecithrix danae*	*Acartia danae*

In addition to the contaminant species recognized in the NV collections from the Indian Ocean, shallow-living species were also observed among the copepods in the six Bé net samples. To illustrate, 14 female *Metridia effusa* (a new species described below), a relatively large species (1.58–1.79 mm), were found in three Bé net samples that presumably sampled the 2000–1000 m depth interval; yet this species (18 females) also occured in five NV samples, all of which were collected in depth intervals between 1000 and 200 m. In none of the 12 NV collections obtained between 2000–1000 m was *M. effusa* observed. It was likewise absent from the 12 other NV collections obtained below 2000 m. These occurrence records for this species suggest that the depth data for species collected in the 2000–1000 m depth interval by the Bé net may not be reliable. For this reason we have included in the following discussion of vertical distribution only those species collected by the NV net as we are more familiar with the operation of this particular type of closing net.

Zooplankton and Copepod Abundance

The discussion in the following two sections is based on the analyses of the NV samples as only these collections were obtained quantitatively from several depth intervals in the water column and in the same manner as those collections previously analyzed by us from the northeastern Atlantic (Grice and Hulsemann, 1965).

DISPLACEMENT VOLUMES.—The displacement volumes of the samples collected by the NV net are shown in figure 2(A). The decrease in zooplankton concentration with increasing depth is clearly evident at all stations but one (station 355). In the depth intervals shown there appeared to be no region along the north-south transect of stations where there were significantly larger or smaller concentrations of zooplankton. On the contrary, omitting one station (station 347), there was no greater than a four-fold difference between the maximum and minimum concentration within the three depth intervals sampled. This is in contrast to our data (unpublished) on

the zooplankton in the upper 1000 m, where differences in volumes within the same depth intervals frequently are much larger.

The mean volumes for each of the three depth intervals can be compared to those we obtained in the northeastern Atlantic between 30° and 40°N (Grice and Hulsemann, 1965). For the depth intervals 2000–1000, 3000–2000, and 4000–3000 m the mean zooplankton volume for the Indian Ocean were .004, .002, and .002 cc/m^3, respectively and for the Atlantic Ocean, .005, .002, and .001 cc/m^3, respectively. These data are certainly similar and indicate how small

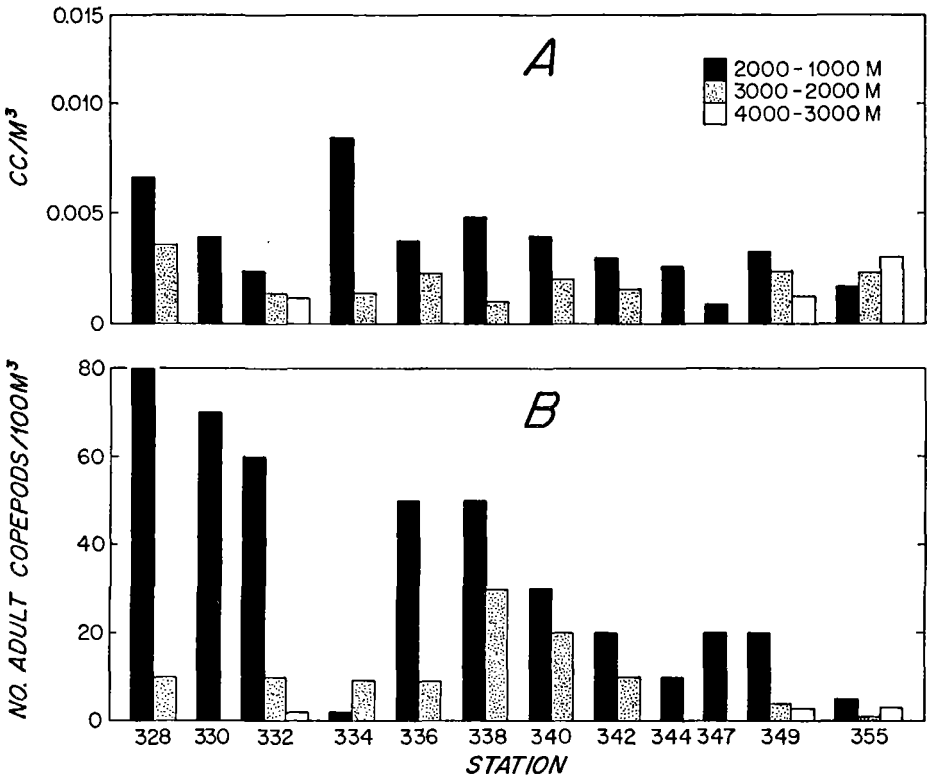


FIGURE 2.—Displacement volumes of the total zooplankton (A) and number of adult copepods excluding contaminant specimens (B).

the zooplankton population is at great depths in the northeastern Atlantic and western Indian Oceans.

COPEPOD ABUNDANCE.—The number of adult copepods per 100 cubic meter computed from the collections taken with the NV net are presented in figure 2(B). In general, the trends in copepod abundance are similar to those found for the total zooplankton. With but one exception the numbers of copepods within the 2000–1000 m interval were much larger than in the intervals below 2000 meters. In no case, however, did the numerical abundance exceed one copepod per

cubic meter and generally the densities were considerably smaller, especially below a depth of 2000 m. The single exception referred to above, where small numbers of copepods were found in the 2000–1000 m interval, was at station 334. Interestingly, the volume of zooplankton at this station exceeded that of all other stations. A large number of contaminant specimens (i.e., copepods that inhabit shallower depths) were noted in this sample. It thus appears that a considerable quantity of zooplankton from the upper 1000 m might have entered the net and was then retained during its descent to 2000 m; or, possibly, material from the 1000–500 m interval, collected just prior to the collection of the 2000–1000 m sample, may have remained attached to the meshes of the net due to incomplete washing of the net. These animals may have been washed into the plankton during the washing of the net after the 2000–1000 m collection. The volume of zooplankton and number of copepods obtained in the 3000–2000 m collection at station 334 does not appear to be unusual.

The number of adult copepods found in the depth intervals below 1000 m in the Indian Ocean are comparable to that previously found by us between 30° and 40°N in the northeastern Atlantic Ocean (Grice and Hulsemann, 1965).

Vertical Occurrence of Copepods

POPULATION MEAN SIZE.—We have measured the total length of 1277 adult copepods from the NV samples amd computed the mean size of the animals, excluding the "contaminant" species, collected within each depth interval. The 4000–3000 m interval will not be considered as only 19 adults were found in the three samples obtained from this interval.

The mean size of the adult copepods between 2000 and 1000 m was 2.36 mm and between 3000 and 2000 m, 2.19 mm. The range of mean sizes in these same intervals at four stations between 30° and 40°N in the northeastern Atlantic (Grice and Hulsemann, 1965) was 2.26–3.04 mm (2000–1000 m) and 1.71–2.38 mm (3000–2000 m). The size of the Indian Ocean copepods living between 1000 and 3000 m are quite comparable to those of the Atlantic.

SPECIES VERTICAL DISTRIBUTION.—Since the present study is based on the analyses of only those NV samples collected in depths below 1000 m, the shallow living species and families are poorly represented. There were present 153 species, excluding contaminants, in 13 families.

The predominantly shallow living families Eucalanidae and Pseudocalanidae were together represented by only seven species. No species, excepting those considered contaminants, of Calanidae, Paracalanidae, Centropagidae, Pontellidae, or Acartiidae, also epi-

pelagic families, were found in the NV samples collected below 1000 m.

The vertical range of many of the species in the 2000–1000 m interval extends into depths of less than 1000 m. Notably among these are species in the large families Aetideidae, Scolecithricidae, Lucicutiidae, and Augaptilidae. Each of these families is represented in our collections by 15 or more species.

Nine families of copepods had one-half or more of their species represented in depths below 2000 m. Only one family (Bathypontiidae) had more than one-half of its species (6 of 11) restricted to depths greater than 2000 m. The range of 9 of the 16 species in the family Spinocalanidae extended below 2000 m, but only 1 species was found exclusively below this depth. Species in these last two families are typical of collections made below 2000 m.

Concerning the 153 species, the largest number was found in the 2000–1000 m depth interval (122), an intermediate number in the 3000–2000 m interval (73), and the least number in the 4000–3000 m interval (13). A similar decrease in species diversity with increasing depth was noted by us (Grice and Hulsemann, 1965) in the northeastern Atlantic, where the decrease in diversity was as follows: 2000–1000 m (71), 3000–2000 m (59), and 4000–3000 m (28). In the Indian Ocean seven species were continually distributed from 1000 to 4000 m: *Mimocalanus cultrifer*, *Spinocalanus abyssalis*, *S. magnus*, *Metridia discreta*, *M. princeps*, *Lucicutia longiserrata*, and *Haloptilus longicornis*. Except for *L. longiserrata*, which we misidentified in our Atlantic samples (see Hulsemann, 1966), these species also occurred below 1000 m in the northeastern Atlantic. The first four we recorded in samples collected in excess of 4000 m.

Zoogeography

GEOGRAPHIC DISTRIBUTION OF SPECIES.—Sewell (1948) has discussed the geographic distribution of copepods in some detail. His account represents an intensive analysis of the literature and attempts to relate the distribution of copepods to ocean currents. The discussion of the copepods in the Indian Ocean is based largely on his own numerous studies made there. A considerable section of his study is devoted to the deep-living copepods of the western Indian Ocean. We are mainly interested here in this discussion and that included in a recent paper by De Decker and Mombeck (1965) as these appear to be the only accounts concerning the zoogeography of the deep-living copepod species of the Indian Ocean.

Sewell (1948) recognized many North Atlantic Ocean species in the northern Indian Ocean. He indicated that these species may be carried southward from the North Atlantic by the North Atlantic

Intermediate water, then eastward into the southwestern Indian Ocean, and finally northward into the northern Indian Ocean by the Antarctic Intermediate water. Citing Sømme's (1933) view that the number of species in a current will decrease in the downstream direction, Sewell examined the occurrence of deep-water copepods at five stations in the Arabian Sea, the Gulf of Aden, and the Gulf of Oman. He indicated that the samples probably came from the Antarctic Intermediate water. He noted a gradual reduction of both deep-sea and North Atlantic copepods in a northward direction; i.e., the number of copepod species decreased from a maximum of 70 (including 56 North Atlantic species) to a minimum of 20 (12 North Atlantic species). The minimum number and the next to the minimum number of species were found in collections obtained in the Gulf of Aden and the Gulf of Oman, respectively. De Decker and Mombeck (1965) cited Sewell's Arabian Sea data and then applied Sewell's technique of examining the contribution of North Atlantic species to an even larger section of the Indian Ocean. These authors compared the number of Atlantic species (134) they found in the bathypelagic fauna of the southwest Indian Ocean with the number of Atlantic species found in the contents of six midwater trawl hauls (described by Sewell, 1929, 1932) made in the area between the Laccadive Sea and west of Andaman Island in the western part of the Bay of Bengal. De Decker and Mombeck pointed out that a gradual decrease of Atlantic species (20 to 0 species) occurred in a northerly and easterly direction.

Our transect of stations extending from approximately 18°N to 40°S along 65°E and 70°E, and one station at 29°S 49°E, in conjunction with the three different methods of collecting deep-water copepods has permitted us to sample a large number of deep-living calanoid species. We have specifically identified 269 species of calanoid copepods excluding the new species and those species found in two Bé net collections made in the eastern Indian Ocean (80°E). As we progressed in our taxonomic analyses of the samples, the similarity of the deep Indian Ocean copepod species to those of the Atlantic became clear. Of interest to us was the appearance of 13 of the 18 species we had recently described from the northeastern Atlantic (Hulsemann and Grice, 1963; Grice and Hulsemann, 1965).

Since our sampling program provided more systematic coverage of bathypelagic species than that of either Sewell (1929, 1932, 1947) or De Decker and Mombeck (1965), it is possible to look more closely into the occurrence of North Atlantic copepod species in the western Indian Ocean. For this analysis we have determined the number of copepod species in our samples in each of 10° latitude intervals

from 20°N to 40°S. A comparison of species found in the western Indian Ocean and the North Atlantic is as follows:

latitude interval western Indian Ocean	*number western Indian Ocean species* [3]	*number species common to North Atlantic* [4]	*percent of species in common*
20°N–10°N	98	90	92
10°N– 0°	117	100	85
0° –10°S	96	95	99
10°S–20°S	120	105	88
20°S–30°S	103	92	89
30°S–40°S	70	55	79

It is quite clear from examination of this tabulation that very large numbers of so-called North Atlantic species are present at all latitudes and that no significant decrease is evident in either the number of species within each interval (north of 30°S) or in the number within each interval that are also present in the North Atlantic Ocean. Thus, Sewell's view of the "falling off" of deep sea copepods and especially the reduction of North Atlantic species northwards in the Antarctic Intermediate water in the northern Arabian Sea is not supported by our data. Since the two stations where Sewell found the least number of copepods are in the Gulf of Oman and Gulf of Aden, the reduction of diversity at these stations may be related to conditions present in these relatively constricted areas.

Other studies on the hydrography of the western Indian Ocean may not entirely support Sewell's interpretation of water mass distribution. Sewell's report of Antarctic Intermediate water in the Arabian Sea is based on an investigation of Mohamed (1940) of pH distribution. Sewell also cited the work of Möller (1929), which indicated that northward flowing subpolar water (500–2000 m) is traceable only to about 5°N (Möller referred only to the eastern Indian Ocean). Sverdrup et al. (1942) indicated that Antarctic Intermediate water and Bottom water flows north and mixes with the deep water in the region north of the Equator. These water masses then flow to the south. According to Ivanenkov and Gubin (1960), in the area between 10° and 16°S the upper part of the southward flowing North Indian Deep water mixes with northward flowing sub-Antarctic Intermediate water and the lower part of the North Indian Deep water mixes with Antarctic Bottom water. This mixing results in the formation of two water masses: the South Indian Deep water (1500–3500 m), which flows southward and North Indian Bottom water (a layer of 200–700 m), which flows northward. Most of the NV and Bé net samples considered in this paper, which were

[3] Present in our samples.

[4] From Grice and Hulsemann (1965) and other literature records from North of 0°.

collected south of approximately 10°S, were probably obtained from within the South Indian Deep water. The midwater trawl (IK) also sampled this water during the greater part of each collection, The North Indian Deep water, formed in the northern Arabian Sea, is centered between 400 and 1500 m north of the Equator and between 800 and 2000 m south of the Equator. Most of our NV, Bé, and IK samples collected north of about 10°S were probably collected in this water mass.

It thus appears from Ivanenkov and Gubin's (1960) work that no sub-Antarctic water is present as such in the Arabian Sea. The continuity that apparently exists between the many species of copepods in the western Indian Ocean and the North Atlantic is apparently due to the transfer or movement of individuals from one water mass to another. Obviously this must be an extremely slow process, but as mentioned below, so might be the rate of speciation in these bathypelagic crustaceans.

Since De Decker and Mombeck's comments relate mostly to the occurrence of North Atlantic copepods (reported by Sewell, 1929, 1932, from six midwater trawl samples) mainly in the eastern Indian Ocean, where we have no samples, we are unable to compare their conclusions with our data. It may, however, be premature to conclude as De Decker and Mombeck did, that Atlantic Ocean copepods decrease in a northerly and easterly direction in the Indian Ocean. The midwater nets used by Sewell were made of "mosquito netting" and the number of copepod species collected in the six hauls was quoted by De Decker and Mombeck to be between only 1 and 54.

Rather than emphasize the decrease of Atlantic Ocean copepods, which our data fail to corroborate anyway, we wish to emphasize the extremely widespread distribution of bathypelagic copepods. The large number of our Indian Ocean species that are also common to the Atlantic (241 in all) is clear evidence for the effective dispersal of copepods by deep currents, slow and sluggish as these may be. Ninety-two percent of the deep-living species in the Arabian Sea, which is included in the northernmost interval (p. 10), are also found in the North Atlantic, some 8000 nautical miles distance. This high degree of similarity in copepod species may indicate a slow rate of speciation in these bathypelagic crustaceans, a suggestion that Day (1963) has already made for planktonic organisms.

ANTARCTIC SPECIES.—As indicated above, most of our collections contained species that are widely distributed in the deep waters. Certain of our collections obtained at the southern end of our sampling area, however, contained species we did not find elsewhere. Although few in number, these species have been included in a list of Antarctic and sub-Antarctic copepod species compiled by Vervoort (1965).

Three of the four collections in which we recognized Antarctic species were obtained from stations located between 35°S and 40°S, which is in the area of the subtropical convergence. The other collection where one Antarctic species occurred was obtained from 29°S.

The species in our collections that are especially indicative of Antarctic or sub-Antarctic waters and which have not been reported from elsewhere are *Calanus australis* Brodsky, *Euchaeta biloba* (Farran), and *Scolecithricella dentipes* Vervoort. *Rhincalanus gigas* Brady, a species much more important in the Antarctic because of its great abundance there, occurred in three of our collections made south of 35°S and in one collection made at 29°S. These four species were obtained in the Bé net and midwater trawl and were probably collected in the upper few hundred meters (see "Methods and Materials"). The occurrence of *R. gigas* at 29°S is considerably north of the subtropical convergence (approximately 40°S) and probably represents the northernmost distribution record for this species in the Indian Ocean. Thompson's (1900) report of *R. gigas* from 20°S has been questioned by Sewell (1929). *Metridia lucens* Boeck was also present in one sample (Bé net) from 35°S. It occurs in the North Atlantic and North Pacific Oceans and is also present in waters of high latitudes in the Southern Hemisphere. Thus, the above five species comprise the Antarctic element in our Indian Ocean copepod species.

INDIAN OCEAN SPECIES.—There are few species in the Indian Ocean including the epi-planktonic ones that are not found elsewhere. Out of a total of 310 species found by us, 40 are not found in the Atlantic Ocean. Of these 40, however, only 7—*Bradycalanus gigas* Sewell, *Amallothrix indica* Sewell, *Scottocalanus dauglishi* Sewell, *Lucicutia bella* Hulsemann, *L. pallida* Hulsemann, *L. rara* Hulsemann, *Euaugaptilus indicus* (Sewell)—are apparently restricted to the Indian Ocean. The remaining ones are also present in Pacific or Antarctic waters. The above 7 species are in addition to the 17 species indicated by Sewell (1947, p. 540) as being possibly endemic to the Indian Ocean. Actually, due to subsequently published distribution records, 3 of these 17 species have been reported from the Pacific: *Chirundina indica* (Grice, 1962), *Cornucalanus indicus* (Brodsky, 1950; Tanaka, 1960), *Lucicutia aurita* (Tanaka, 1963, as *L. maxima*). Further, *L. aurita* has been found in the Malay Archipelago (Scott, 1909) and near the island of South Georgia (Gunther and Hardy, 1935), both times reported as *L. maxima* (see Hulsemann, 1966).

Our list of 310 species includes 78 that have not hitherto been reported from the Indian Ocean. This is not unexpected since the bathypelagic species have not been studied as extensively as the epipelagic ones. The discovery of 17 new species, which are described

in the present paper, is further indication of the paucity of prior taxonomic studies on the deep-water copepods of the Indian Ocean.

Taxonomy

One new genus, 17 new species, 8 previously unknown males, and 1 previously unknown female of calanoid copepods are described below. Systematic or distributional remarks are presented for 25 other species. Also included are descriptions and figures of 9 specimens which, because they may be referable to described species, are not recognized as new. Seven additional species of *Lucicutia* from these collections, which were not previously known from the Indian Ocean, are reported by Hulsemann (1966). In all, 310 species (300 were specifically identified) were found in the collections.

The forms of *Clausocalanus arcuicornis* (Dana) and *Microcalanus pygmaeus* (Sars) were not distinguished. The species designated *Euchaeta* species is being described elsewhere by Dr. Marion Fontaine.

In the description of the species the first to fifth thoracic segments refer to those to which the first to fifth pairs of feet are attached.

Holotype specimens have been deposited in the U.S. National Museum, Washington, D.C., and representative specimens of other species have been deposited in the Woods Hole Oceanographic Institution collections.

Species and collection numbers where they occurred are listed below. (The 78 species not previously known from the Indian Ocean are indicated by an asterisk. See table 1 for collecting data corresponding to collection number.)

CALANIDAE

*1. *Calanus australis* Brodsky, 1959 ---- 4
2. *C. tenuicornis* Dana, 1849 ---- 5, 43–45
3. *Canthocalanus pauper* (Giesbrecht, 1888) ---- 6, 41
4. *Nannocalanus minor* (Claus, 1863) ---- 6, 31, 34, 43–45
5. *Neocalanus gracilis* (Dana, 1849) ---- 3, 5, 43
6. *Undinula darwini* (Lubbock, 1860) ---- 6, 29, 30, 42, 43

MEGACALANIDAE

7. *Bathycalanus bradyi* (Wolfenden, 1905) ---- 7–11, 14, 15, 19, 20, 22–25
*8. *B. princeps* (Brady, 1883) ---- 24, 25
9. *B. richardi* Sars, 1905 ---- 10, 15
*10. *B. sverdrupi* Johnson, 1958 ---- 14, 19
11. *Bradycalanus gigas* Sewell, 1947 ---- 15, 27
*12. *B. sarsi* (Farran, 1939) ---- 9, 15, 18, 21
*13. *B. typicus* A. Scott, 1909 ---- 7, 8, 11
14. *Megacalanus princeps* Wolfenden, 1904 ---- 8–15, 17, 18, 20, 21

EUCALANIDAE

15. *Eucalanus attenuatus* (Dana, 1849) ---- 2, 16, 38, 45
16. *E. crassus* Giesbrecht, 1888 ---- 38
17. *E. elongatus hyalinus* (Claus, 1866) ---- 4–6, 19–24, 45

18. *Mecynocera clausii* Thompson, 1888 41–44
19. *Rhincalanus cornutus* (Dana, 1849) 2, 3, 6, 36
20. *R. gigas* Brady, 1883 4, 25–27
21. *R. nasutus* Giesbrecht, 1888 3–6, 27, 36, 44, 46
PARACALANIDAE
22. *Acrocalanus longicornis* Giesbrecht, 1888 44
23. *A. monachus* Giesbrecht, 1888 34, 42, 44
24. *Calocalanus contractus* Farran, 1926 48
25. *C. pavo* (Dana, 1849) 42, 43
26. *C. plumulosus* (Claus, 1863) 38
27. *C. styliremis* Giesbrecht, 1888 30–32, 34–43, 51
28. *Paracalanus aculeatus* Giesbrecht, 1888 28–30
29. *P. denudatus*? Sewell, 1929 30, 33, 34, 37, 42, 43
30. *P. nanus* Sars, 1907 37, 46, 51
PSEUDOCALANIDAE
31. *Clausocalanus arcuicornis* (Dana, 1849) 4–6, 30, 39–46, 48, 49
32. *C. farrani* Sewell, 1929 38, 40–44
33. *C. furcatus* (Brady, 1883) 6, 28–31, 34, 38–41, 44, 45
34. *C. paululus* Farran, 1926 46–48, 51
35. *Ctenocalanus vanus* Giesbrecht, 1888 40, 42, 43, 45, 51
36. *Farrania frigida* (Wolfenden, 1911) 3, 39, 41
37. *Microcalanus pygmaeus* (Sars, 1900) 28, 30, 31, 36–40
SPINOCALANIDAE
38. *Mimocalanus cultrifer* Farran, 1908 1, 2, 4–6, 28–32, 35–48
39. *M. inflatus*? Davis, 1949 36, 45
*40. *M. nudus* Farran, 1908 6, 31, 46
41. *Mimocalanus* species 39
42. *Monacilla tenera* Sars, 1907 30, 31, 40, 42, 45, 49
43. *M. typica* Sars, 1905 2-6, 34, 36, 38
*44. *Spinocalanus abruptus* Grice and Hulsemann, 1965 29, 31, 42, 45
45. *S. abyssalis* Giesbrecht, 1888 1-3, 5, 28, 30, 31, 35-39, 42, 43, 45, 46, 49
S. abyssalis var. *pygmaeus* Farran, 1926 1, 2, 4-6, 28-49
*46. *S. angusticeps* Sars, 1920 4, 6, 36, 40, 45
*47. *S. longipes* Tanaka, 1956 1, 28
48. *S. magnus* Wolfenden, 1904 1-6, 29, 33, 35, 37, 39, 43, 44
*49. *S. ovalis* Grice and Hulsemann, 1965 35, 51
50. *S. spinosus* Farran, 1908 1-3, 5, 6, 28, 30, 31, 36, 39, 40, 42-46, 50
*51. *S. validus* Sars, 1905 23, 45
52. *S. ventriosus*, new species 31, 32, 38, 41, 46
53. *Spinocalanus* species 46
*54. *Teneriforma naso*, new combination 28, 37, 38
AETIDEIDAE
55. *Aetideopsis retusa*, new species 43
56. *Aetideus armatus* (Boeck, 1872) 5
*57. *Batheuchaeta lamellata* Brodsky, 1950 51
58. *Bradyetes florens*, new species 38
59. *Bradyidius bradyi* (Sars, 1902) 35
60. *Chiridiella macrodactyla* Sars, 1907 28, 38
61. *Chiridius poppei* Giesbrecht, 1892 2, 5
62. *Chirundina indica* Sewell, 1929 3, 13
63. *C. streetsi* Giesbrecht, 1895 5, 6, 16, 19-23, 27
*64. *Chirundinella cara* Tanaka, 1957 12

65. *Euaetideus acutus* (Farran, 1929)---- 44
66. *Euchirella amoena* Giesbrecht, 1888---- 13, 16
67. *E. bella* Giesbrecht, 1888---- 1, 2, 11, 21, 28, 30
68. *E. bitumida* With, 1915---- 22, 27
69. *E. curticauda* Giesbrecht, 1888---- 40
70. *E. formosa* Vervoort, 1949---- 20, 22, 23
71. *E. galeata* Giesbrecht, 1888---- 12, 13
72. *E. maxima* Wolfenden, 1905---- 1, 13, 16
73. *E. messinensis* (Claus, 1863)---- 19, 22, 27
74. *E. pulchra* (Lubbock, 1856)---- 2, 36, 40, 42, 44
75. *E. venusta* Giesbrecht, 1888---- 38
76. *Gaetanus antarcticus* Wolfenden, 1905---- 9, 13-15, 21-26
77. *G. armiger* Giesbrecht, 1888---- 2
*78. *G. brachyurus* Sars, 1907---- 4, 19, 21
79. *G. curvirostris* Sars, 1905---- 42
*80. *G. ferox* With, 1915---- 5
81. *G. kruppii* Giesbrecht, 1903---- 11, 21, 28
82. *G. latifrons* Sars, 1905---- 23
83. *G. minor* Farran, 1905---- 5
84. *G. pileatus* Farran, 1903---- 4, 32
*85. *Gaidius brevicaudatus* (Sars, 1907)---- 37
86. *G. minutus* Sars, 1907---- 36, 40
*87. *G. robustus* (Sars, 1905)---- 17, 22, 25
88. *G. tenuispinus* (Sars, 1900)---- 36
89. *Pseudeuchaeta brevicauda* Sars, 1905---- 4, 11, 13, 14, 17, 19, 22, 37
*90. *Pseudochirella divaricata* (Sars, 1905)---- 19
*91. *P. dubia* (Sars, 1905)---- 9, 50
*92. *P. gibbera* Vervoort, 1949---- 11, 13, 15, 24
93. *P. hirsuta* (Wolfenden, 1905)---- 24–26
94. *P. magna* (Wolfenden, 1911)---- 26
95. *P. obtusa* (Sars, 1905)---- 1, 13, 26
*96. *P. polyspina* Brodsky, 1950---- 25
*97. *P. pustulifera* (Sars, 1905)---- 22?, 24, 25
*98. *P. semispina* Vervoort, 1949---- 13
99. *P. squalida*, new species---- 23
*100. *P. tuberculata* Tanaka, 1957---- 16
101. *Undeuchaeta intermedia* A. Scott, 1909---- 6, 38
102. *U. major* Giesbrecht, 1888---- 17
103. *U. plumosa* (Lubbock, 1856)---- 2–4, 23, 44, 46
104. *Valdiviella brevicornis* Sars, 1905---- 11, 13, 15, 20, 36, 41
105. *V. insignis* Farran, 1908---- 7–17, 19, 21–27, 37, 38
106. *V. oligarthra* Steuer, 1904---- 15

EUCHAETIDAE

107. *Euchaeta barbata* Brady, 1883---- 22, 24, 25
108. *E. biloba* (Farran, 1929)---- 4
109. *E. bisinuata* Sars, 1907---- 6, 20, 22, 36
*110. *E. calva* (Tanaka, 1958)---- 9, 10, 12, 13, 26
111. *E. dubia* Esterly, 1906---- 24–26
112. *E. exigua* Wolfenden, 1911---- 4
*113. *E. farrani* With, 1915---- 26
114. *E. gracilis* Sars, 1905---- 24, 27
115. *E. hanseni* With, 1915---- 11–13

116. *E. malayensis* (Sewell, 1929)---- 3, 26, 27
117. *E. marina* (Prestandrea, 1833)---- 29, 30, 39
*118. *E. robusta* Wolfenden, 1911---- 2
119. *E. sarsi* Farran, 1908---- 12, 17, 25
120. *E. scotti* Farran, 1908---- 8, 9, 20
121. *E. tonsa* Giesbrecht, 1895---- 22, 26, 40
122. *E. weberi* (A. Scott, 1909)---- 12, 13
123. *E. wolfendeni* A. Scott, 1909---- 44
124. *Euchaeta* species---- 24–26
PHAENNIDAE
125. *Cornucalanus chelifer* (Thompson, 1903)---- 25
126. *C. indicus* Sewell, 1929---- 23
127. *C. simplex* Wolfenden, 1905---- 15
*128. *Heteramalla dubia* (T. Scott, 1894)---- 40
129. *Onchocalanus affinis* With, 1915---- 1
130. *O. magnus* (Wolfenden, 1906)---- 17, 23, 24
131. *O. trigoniceps* Sars, 1905---- 1
132. *Xanthocalanus greeni* Farran, 1905---- 10, 14
133. *X. hispidus*, new species---- 49
*134. *X. obtusus* Farran, 1905---- 47
SCOLECITHRICIDAE
135. *Amallothrix arcuata* (Sars, 1920)---- 3
*136. *A. curticauda* (A. Scott, 1909)---- 5
137. *A. emarginata* (Farran, 1905)---- 2, 22, 23, 28, 43, 45, 46
138. *A. gracilis* (Sars, 1905)---- 1, 3
139. *A. indica* Sewell, 1929---- 1, 4, 28, 30, 31, 38, 40, 41
*140. *A. mollis* (Esterly, 1913)---- 2
*141. *A. obtusifrons* Sars, 1905---- 27, 32
142. *A. paravalida* Brodsky, 1950---- 3–6, 31, 38, 49
*143. *A. robustipes* Grice and Hulsemann, 1965---- 6, 40
144. *A. valida* (Farran, 1908)---- 2, 9, 11, 29, 38
145. *Lophothrix frontalis* Giesbrecht, 1895---- 20, 22, 23, 27, 49
146. *L. humilifrons* Sars, 1905---- 11, 13, 23, 27
*147. *L. insignis* Sars, 1920---- 15
*148. *Racovitzanus levis* Tanaka, 1961---- 5
*149. *R. porrectus* (Giesbrecht, 1888)---- 2, 28, 40
150. *?Racovitzanus* species---- 29
151. *Scaphocalanus affinis* (Sars, 1905)---- 6, 19, 30, 44
*152. *S. bogorovi* Brodsky, 1955---- 43, 45
153. *S. brevicornis* (Sars, 1900)---- 1, 4, 6, 28, 30, 31, 45
*154. *S. curtus* (Farran, 1926)---- 5, 6, 36, 38
*155. *S. echinatus* (Farran, 1905)---- 3
156. *S. elongatus* A. Scott, 1909---- 1–3, 5, 29, 36, 38–40, 42, 44, 45
*157. *S. longifurca* (Giesbrecht, 1888)---- 1, 5, 36, 39, 41, 45
158. *S. magnus* (T. Scott, 1894)---- 3, 29, 36, 37, 39, 40
159. *S. major* (T. Scott, 1894)---- 3, 5, 41
160. *S. subbrevicornis* (Wolfenden, 1911)---- 1–6, 28, 30, 31, 36, 38, 40, 42, 43, 45
*161. *Scolecithricella auropecten* (Giesbrecht, 1892)---- 2, 31
162. *S. dentata* (Giesbrecht, 1892)---- 2, 5, 6
163. *S. dentipes* Vervoort, 1951---- 4
164. *S. grata*, new species---- 4
*165. *S. laminata* (Farran, 1926)---- 36, 40, 42

166. *S. maritima*, new species 31, 40
167. *S. ovata* (Farran, 1905) 36
*168. *S. profunda* (Giesbrecht, 1892) 2
*169. *S. spinata* Tanaka, 1962 ..... 2, 6
*170. *S. timida* Tanaka, 1962 ..... 2, 3, 38, 40
*171. *S. unispinosa* Grice and Hulsemann, 1965 47
172. *Scolecithricella* species 36
173. *Scolecithrix bradyi* Giesbrecht, 1888 ..... 42, 43
174. *S. danae* (Lubbock, 1856) 34, 42, 43
*175. *S. fowleri* Farran, 1926 42
176. *S. nicobarica* Sewell,1929 ..... 28, 30
177. *Scottocalanus dauglishi* Sewell, 1929 9
178. *S. helenae* (Lubbock, 1856) 26
THARYBIDAE
*179. *Undinella brevipes* Farran, 1908) 31, 42
TEMORIDAE
180. *Temora discaudata* Giesbrecht, 1889 41
181. *Temoropia mayumbaensis* T. Scott, 1894 ..... 28, 29, 31, 32, 35–39, 41, 44–47
METRIDIIDAE
182. *Gaussia princeps* (T. Scott, 1894) 8–11, 14, 19, 25
183. *Metridia boecki* Giesbrecht, 1889 ..... 2, 4, 28, 37, 38, 44, 46
184. *M. brevicauda* Giesbrecht, 1889 ..... 1–6, 28, 30, 31, 35, 36, 40, 42, 49
*185. *M. discreta* Farran, 1946 ..... 1, 4, 29–33, 35, 39, 41, 43, 46, 48, 49
186. *M. effusa*, new species 1, 5, 6
187. *M. lucens* Boeck, 1864 4
188. *M. macrura* Sars, 1905 ..... 1, 3, 15, 21, 31, 32, 37, 41
189. *M. princeps* Giesbrecht, 1889 ..... 2, 6, 8, 10, 12, 13, 15, 17–28, 31, 35–37, 40 42, 46, 51
190. *M. venusta* Giesbrecht, 1889 2–6
191. *Pleuromamma abdominalis* (Lubbock, 1856) 2, 3, 5, 38
192. *P. gracilis gracilis* (Claus, 1863) 2, 4–6, 44
193. *P. indica* Wolfenden, 1905 ..... 1, 2, 5, 30, 31, 42
194. *P. piseki* Farran, 1929 31
195. *P. quadrungulata quadrungulata* (Dahl, 1893) 2, 6, 36, 40
196. *P. xiphias* (Giesbrecht, 1889) 2–6, 11, 13, 16, 18, 27, 38, 40
CENTROPAGIDAE
197. *Centropages gracilis* (Dana, 1849) 6
LUCICUTIIDAE
198. *Lucicutia aurita* Cleve, 1904 ..... 9, 13–17, 40, 44
199. *L. bella* Hulsemann, 1966 ..... 20, 21, 27, 46
200. *L. bicornuta* Wolfenden, 1905 ..... 17, 22, 27
201. *L. curta* Farran, 1905 ..... 2, 4–6, 30, 31, 36, 40, 43, 46
202. *L. flavicornis* (Claus, 1863) 3–5, 42, 45, 47
203. *L. formosa* Hulsemann, 1966 ..... 27, 51
204. *L. gaussae* Grice, 1963 ..... 3, 42, 43
205. *L. grandis* (Giesbrecht, 1895) 1, 2, 5, 21, 22, 25–28, 30, 31, 40
206. *L. intermedia* Sars, 1905 ..... 1, 30, 40–42, 44, 45
207. *L. longicornis* (Giesbrecht, 1889) 1, 2, 28, 30, 31
208. *L. longiserrata* (Giesbrecht, 1889) 3–6, 30, 31, 42, 44
209. *L. longispina* Tanaka, 1963 ..... 33, 38, 39
210. *L. lucida* Farran, 1908 6
211. *L. magna* (Wolfenden, 1903) 5

228-966—67——2

*212. *L. major* Wolfenden, 1911 ---- 39
213. *L. maxima* Steuer, 1904 ---- 11, 13, 15, 20, 27
214. *L. ovalis* (Giesbrecht, 1889) ---- 1–6, 30, 31, 36–38, 40–42, 44, 45, 49, 50
215. *L. pallida* Hulsemann, 1966 ---- 3, 18, 23
216. *L. parva* Grice and Hulsemann, 1965 ---- 5, 28–32, 35, 36, 38, 39, 41–47
217. *L. polaris* Brodsky, 1950 ---- 38
218. *L. rara* Hulsemann, 1966 ---- 22, 25, 27
219. *L. sewelli* Tanaka, 1963 ---- 32, 41
220. *L. wolfendeni* Sewell, 1932 ---- 4, 9, 13–15, 22, 25, 26, 42
HETERORHABDIDAE
*221. *Disseta minuta* Grice and Hulsemann, 1965 ---- 28, 30–32, 35, 36, 45, 46
222. *D. palumboi* Giesbrecht, 1889 ---- 1, 2, 5, 6, 9–11, 13–15, 17, 18, 20, 22, 23, 30, 36, 44
223. *Hemirhabdus grimaldii* (Richard, 1893) ---- 8, 9, 23, 24
*224. *H. latus* Sars (1905) ---- 17, 19, 44
225. *Heterorhabdus abyssalis* (Giesbrecht, 1889) ---- 2, 5, 6, 28–30, 32, 35–37, 40–42, 45
226. *H. clausi* (Giesbrecht, 1889) ---- 38, 40
227. *H. compactus* (Sars, 1900) ---- 1, 2, 4, 6, 30, 31, 38, 41, 43, 46, 49
228. *H. norvegicus* (Boeck, 1872) ---- 2–4, 6, 36, 38
229. *H. papilliger* (Claus, 1863) ---- 2, 6, 43, 44
*230. *H. robustus* Farran, 1908 ---- 6
231. *H. spinifrons* (Claus, 1863) ---- 3, 4
232. *Heterostylites longicornis* (Giesbrecht, 1892) ---- 1, 28
233. *H. major* (Dahl, 1894) ---- 31
*234. *Mesorhabdus brevicaudatus* (Wolfenden, 1905) ---- 3
AUGAPTILIDAE
235. *Augaptilus glacialis* Sars, 1900 ---- 2, 5
*236. *Centraugaptilus cucullatus* Sars, 1905 ---- 19
237. *C. horridus* (Farran, 1908) ---- 17, 21–23
*238. *Disco inflatus* Grice and Hulsemann, 1965 ---- 3, 28, 30, 32, 36, 37, 39–42, 44, 45
*239. *D. longus* Grice and Hulsemann, 1965 ---- 33, 36
*240. *D. minutus* Grice and Hulsemann, 1965 ---- 28, 32
241. *Disco* species ---- 41
*242. *Euaugaptilus brodskyi* Hulsemann, 1967 ---- 23, 36
243. *E. bullifer* (Giesbrecht, 1889) ---- 30, 31, 38, 42
244. *E. curtus*, new species ---- 1
245. *E. elongatus* (Sars, 1905) ---- 32, 44
246. *E. facilis* (Farran, 1908) ---- 30
*247. *E. farrani* Sars, 1920 ---- 40
248. *E. filigerus* (Claus, 1863) ---- 1, 9
249. *E. fundatus*, new species ---- 1
*250. *E. gracilis* (Sars, 1905) ---- 32, 39
251. *E. grandicornis* Sars, 1920 ---- 1, 2, 9, 30
*252. *E. humilis* Farran, 1926 ---- 5, 28, 36
253. *E. indicus* Sewell, 1932 ---- 14, 15, 30
254. *E. laticeps* (Sars, 1905) ---- 3, 9, 13, 19–22, 46
255. *E. longimanus* (Sars, 1905) ---- 1, 3, 15, 20, 28, 42
*256. *E. longiseta* Grice and Hulsemann, 1965 ---- 28, 39
257. *E. magnus* (Wolfenden, 1904) ---- 1, 9–13, 15 17, 19, 21–25, 27, 30, 31, 35, 44, 49
258. *E. malacus*, new species ---- 5
*259. *E. maxillaris* Sars, 1920 ---- 5

260. *E. nodifrons* (Sars, 1905)---- 1, 4, 5, 9, 17, 21, 23, 26, 28, 37, 38
261. *E. oblongus* (Sars, 1905)---- 1, 2, 10, 13, 29
262. *E. palumboi* (Giesbrecht, 1889)---- 1, 3, 5, 6
263. *E. penicillatus* Sars, 1920---- 3
264. *E. quaesitus*, new species---- 32
265. *E. rectus*, new species---- 13
*266. *E. rigidus* (Sars, 1907)---- 5, 38
267. *E. tenuispinus* Sars, 1920---- 28
268. *Euaugaptilus* species 1---- 28
269. *Euaugaptilus* species 2---- 6
270. *Euaugaptilus* species 3---- 20
271. *Haloptilus acutifrons* (Giesbrecht, 1892)---- 31, 42
272. *H. chierchiae* (Giesbrecht, 1889)---- 1, 2, 28
273. *H. longicornis* (Claus, 1863)---- 1–6, 30, 31, 36, 38, 40, 42–45, 48
274. *H. tenuis* Farran, 1908---- 40
275. *H. validus* Sars, 1920---- 10
*276. *Pachyptilus abbreviatus* (Sars, 1905)---- 9
277. *P. eurygnathus* Sars, 1920---- 20, 22, 23, 27
278. *P. pacificus* Johnson, 1936---- 15, 25
*279. *Pontoptilus mucronatus* Sars, 1905---- 9, 10, 20
*280. *P. robustus* Sars, 1905---- 10
281. *P. lacertosus*, new species---- 20
*282. *Pseudaugaptilus longiremis* Sars, 1907---- 42

ARIETELLIDAE

283. *Arietellus simplex* Sars, 1905---- 17, 18, 20, 25, 26, 42
284. *Phyllopus aequalis* Sars, 1920---- 1
285. *P. bidentatus* Brady, 1883---- 19, 29
286. *P. helgae* Farran, 1908---- 5, 23
287. *P. impar* Farran, 1908---- 6, 28, 31
288. *P. muticus* Sars, 1907---- 45

CANDACIIDAE

289. *Candacia catula* (Giesbrecht, 1889)---- 43
*290. *C. elongata* (Boeck, 1873)---- 4
291. *C. ethiopica* (Dana, 1849)---- 6
292. *C. longimana* (Claus, 1863)---- 5
293. *Paracandacia bispinosa* (Claus, 1863)---- 43, 44
294. *P. truncata* (Dana, 1849)---- 6, 44

PONTELLIDAE

295. *Labidocera detruncata* (Dana, 1849)---- 44

BATHYPONTIIDAE

*296. *Bathypontia elongata* Sars, 1905---- 2, 6, 17, 28
297. *B. major* (Wolfenden, 1906)---- 20
298. *B. regalis*, new species---- 39
*299. *B. sarsi* Grice and Hulsemann, 1965---- 37
*300. *B. similis* Tanaka, 1965---- 39
301. *B. spinifera* A. Scott, 1909---- 2, 3, 5, 6, 36, 42, 44, 46
*302. *Foxtonia barbatula* Hulsemann and Grice, 1963---- 35, 39, 43
303. *Rhinomaxillaris bathybia*, new genus and new species---- 30
*304. *Temorites brevis* Sars, 1900---- 2, 4, 6, 42
*305. *T. discoveryae* Grice and Hulsemann, 1965---- 32, 33, 35
*306. *Zenkevitchiella atlantica* Grice and Hulsemann, 1965---- 33
307. *Z. crassa*, new species---- 41

ACARTIIDAE
308. *Acartia danae* Giesbrecht, 1889 ..... 38, 42, 45
309. *A. negligens* Dana, 1849 ..... 5, 31, 32, 34, 36, 38–40, 43–45, 48
INCERTAE SEDIS
310. Male 41

Calanus australis Brodsky, 1959

FIGURE 3

Remarks: In dorsal view the slightly produced anterior end of the head and the narrow fifth thoracic segment make the specimen referable to Brodsky's *C. australis* var. *atlanticus*. Brodsky (1959) suggests that this is a species of temperate latitudes in the Southern Hemisphere. The single specimen was found in the Bé net sample at 35°09′ S, 69°59′ E. This is the first record of *C. australis* from the Indian Ocean.

Farrania frigida (Wolfenden, 1911)

FIGURES 4–15

Diagnosis (male): Fifth thoracic segment small and rounded. First antenna reaches to end of furca, segments 20–21 (fused) and 22 of right antenna each with patch of thick hair. Proximal end of first antenna highly setose and provided with aesthetasks. Fifth feet asymmetrical, right foot longer than left one. Right exopod 3-segmented, terminal segment provided with 2 terminal setae and subterminal hair. Endopod represented by small, bulblike protuberance. Left exopod 3-segmented. Two unequal spines on terminal segment and one spine on distal lateral corner of first segment. Endopod consists of small rounded protuberance. Total length 2.34 mm.

Remarks: The male of this species, not heretofore known, is distinguished from the male of *F. orbus* (Tanaka) by the rounded fifth thoracic segment and the structure of the fifth feet.

Mimocalanus inflatus? Davis, 1949

FIGURES 16–18

Remarks: As the swimming feet are broken off in both specimens examined it is not possible to determine whether the second endopodal segments are inflated as they are in Pacific and Atlantic specimens of *M. inflatus*. The Indian Ocean specimens have five setae on the second inner lobe and four setae on the second basal segment of the first maxilla. There are four setae and five setae on the corresponding structures of the second maxilla of the Atlantic Ocean specimen described by Grice and Hulsemann (1965). The total length of the present specimens is 1.76 and 2.01 mm. *Mimocalanus inflatus* has not previously been reported from the Indian Ocean.

Mimocalanus species

FIGURES 19–25

Remarks: We are tentatively assigning the two males to this genus. The fifth feet are uniramous and styliform. The terminal segments of the exopods each have a long spine. The fifth feet of *M. cultrifer* and *M. nudus* are not so elongate and the terminal segments of the exopods have short spines. The total length of both specimens is .78 mm.

Spinocalanus longipes Tanaka, 1956

FIGURES 26–27

Remarks: We are referring three male specimens to this species although, as Johnson (1963) points out, the fifth pair of feet is most unlike any described *Spinocalanus*. The total length of the three specimens ranges from 1.60 to 1.76 mm. *Spinocalanus longipes* has not previously been reported from the Indian Ocean.

Spinocalanus magnus Wolfenden, 1904

Remarks: Small differences were noted in the ornamentation (hair, spines) of the terminal exopodal segments of the fifth feet of the present male and that described by Tanaka (1956). The total length of our two male specimens is 2.00 mm.

Spinocalanus validus Sars, 1905

FIGURES 28–31

Diagnosis (male): Anterior end of head knoblike, lateral margin of third thoracic segment with protuberances. Exopods and endopods of fifth feet very elongate, second and third right exopodal segments pubescent. Total length 5.08 mm.

Remarks: The male of this species, heretofore unknown, is distinguished by its large size and details of the fifth feet. Our findings of *Spinocalanus validus* constitute a new record for the Indian Ocean.

Spinocalanus ventriosus, new species

FIGURES 32–34

Occurrence: Station 332 NV, 2000 to 1002 m, 2 ♀♀; 332 NV, 3000 to 2000 m, 3 ♀♀; 338 NV, 2000 to 1000 m, 2 ♀♀; 340 NV, 2950 to 1990 m, 1 ♀; 349 NV, 2000 to 1000 m, 1 ♀.

Diagnosis (female): Head and first thoracic segment incompletely separated, fifth thoracic segment ends in rounded protrusions. First maxilla with four setae on second inner lobe, three on third inner lobe, four on second basal segment and nine on endopod. Total length 1.32–1.52 mm. Female from station 349 is holotype. Holotype: USNM 113513.

Remarks: The knoblike protrusions of the fifth thoracic segment and the number of setae on the first maxilla will distinguish this species from *S. polaris* Brodsky, a species it resembles.

Spinocalanus species

FIGURE 35

Remarks: A single male specimen with fifth feet similar to *S. longipes* is here tentatively referred to the genus *Spinocalanus*. The left exopod is greatly elongate and the endopod is rudimentary. The right foot is small, 1-segmented, and does not exceed the second basal segment of the left foot. The total length of the specimen is 1.28 mm.

Teneriforma, new name

Teneriforma naso, new combination

FIGURES 36–38

Tanyrhinus naso Farran, 1936, pp. 86–87, text-fig. 4.

Diagnosis (male): Head and first thoracic segment separate, fourth and fifth thoracic segments separate. Furca approximately equal to combined length of fourth and fifth abdominal segments. Rostrum large and curved posteriorly. First antenna with 24 free segments (8 and 9 fused), reaching to end of furca. Fifth feet uniramous and asymmetrical. Left foot elongate and consisting of five segments. Right foot small and consisting of two segments. Total length .92 mm. USNM 113514.

Remarks: The male of this monotypic genus has not previously been described. Since the name *Tanyrhinus* has been used for a genus of insects (Coleoptera) by Mannerheim in 1852 (Bull. Soc. Imp. Nat. Moscou, vol. 25, no. 2, p. 349), the genus is here renamed *Teneriforma*. This is the first record of *Teneriforma naso* from the Indian Ocean.

Aetideopsis retusa, new species

FIGURES 39–45

Occurrence: Station 342 NV, 3000 to 1980 m, 1 ♀.

Diagnosis (female): Head and first thoracic segment incompletely separate. Fourth and fifth thoracic segments separate. Rostrum distinct, rami separated by deep invagination. Frontal organ prominent and visible in dorsal view. Posterior lateral corner of fifth thoracic segment acutely pointed. First antenna exceeds furca by last two segments. Total length 1.96 mm. Holotype: USNM 113515.

Remarks: This species is distinguished from others in the genus by its small size and long first antenna.

Bradyetes florens, new species

FIGURES 46–54

Occurrence: Station 338 NV, 2000 to 1000 m, 1 ♀.

Diagnosis (female): Head and first thoracic segment incompletely separate, fourth and fifth thoracic segments separate. Fifth thoracic segment rounded. Rostrum absent. First antenna reaches to end of furca. Terminal five segments of maxilliped equal in length to second basal segment. First and second exopodal segments of first foot without external spines. Total length 1.10 mm. Holotype USNM 113516.

Remarks: This species differs from *B. inermis* Farran and *B. brevis* Farran, the only described species in this genus, by the relatively short first and second basal segments of the maxilliped, by the absence of a spine on the first exopodal segment of the first foot, and by its small size.

Chirundinella cara Tanaka, 1957

FIGURE 55

Remarks: The only difference between this specimen and the description given by Tanaka (1957) are 11 rather than 10 setae on the endopod of the first maxilla and 3 rather than 4 setae on the fifth lobe of the second maxilla. Our specimen measured 7.80 mm, Tanaka's measured 7.44 mm. This species has not heretofore been found in the Indian Ocean.

Gaetanus brachyurus Sars, 1907

Remarks: The female specimen from station 131 differs from the others and from the description of this species in having the exopod of the first foot consisting of two segments. Each segment has one external spine. The animal is also smaller (5.00 mm). The other two females found measured 6.17 and 6.42 mm. *Gaetanus brachyurus* has not previously been found in the Indian Ocean.

Gaetanus ferox With, 1915

FIGURES 56-59

Remarks: Although the right exopod of the fifth foot of the male is 3-segmented in our specimen (With, 1915, shows two segments), the terminal portion of the exopod is similar to With's figure. Possibly the suture separating the two terminal segments was not observed by him. Our specimen measured 3.55 mm; With's measured 3.4 mm. This species has not previously been reported from the Indian Ocean.

Gaidius robustus (Sars, 1905)

FIGURES 60-64

Gaetanus robustus Sars, 1905a, pp. 11-12.
Gaidius maximus Wolfenden, 1906, p. 35, pl. 11, figs. 1, 2.
Gaidius validus Farran, 1908, pp. 32-33, pl. 2, figs. 11-17.
Mesogaidius maximus (Wolfenden).—Wolfenden, 1911, pp. 224-226, pl. 26, figs. 3-6, text-fig. 13.
Pseudogaetanus robustus (Sars).—Brodsky, 1950, pp. 168-169, fig. 86.
not *Gaidius robustus* Vervoort, 1949, pp. 12-15, figs. 5, 6.

Remarks: Vervoort (1952a, 1952b) redefined the genera *Gaidius* Giesbrecht and *Gaetanus* Giesbrecht. Accordingly, the species Sars described in 1905 as *Gaetanus robustus* is here transferred to the genus *Gaidius*. Brodsky (1950) proposed a new genus, *Pseudogaetanus*, for this species. In our opinion, the characters given are insufficient for the erection of a new genus.

The paratype of *Gaidius robustus* Vervoort was kindly loaned to us for examination. We concur with Dr. Vervoort (in litt.) that the specimen is actually referable to *G. intermedius* Wolfenden, the latter species name having priority.

Gaidius robustus (Sars) has not previously been reported from the Indian Ocean.

Pseudochirella gibbera Vervoort, 1949

Remarks: None of the specimens had a spine on the right dorsal side of the fifth thoracic segment as described by Vervoort (1949) in the original description of the species. Our specimens varied in total length from 5.83 to 6.17 mm. Vervoort's single specimen measured 5.50 mm. The species has not been reported from the Indian Ocean.

Pseudochirella squalida, new species

FIGURES 65–70

Occurrence: Station 351B IK, 350 to 1710 m, 1 ♀.

Diagnosis (female): Rostrum strong and directed ventrally. Fifth thoracic segment rounded. First antenna reaches furca. Second endopodal segment of second antenna with seven setae on outer lobe and nine setae on inner lobe. First basal segment of fourth foot with six coarse spines. Genital segment slightly asymmetrical and hairy. Small rounded protuberances on each side. Total length 5.66 mm. Holotype: USNM 113517.

Remarks: This species resembles *P. obesa* Sars but may be distinguished from it by the protuberances on the genital segment. The genital segment of *P. obesa* has neither protuberances nor hair.

***Euchaeta robusta* (Wolfenden, 1911)**

Remarks: Our female specimen differs from Wolfenden's (1911) original description by the absence of hair on the fifth thoracic segment and by a longer second abdominal segment. The first three abdominal segments have a relative length of 20:10:10. Wolfenden gave a ratio of 20:17:15 for his specimens. Our specimen measured 7.85 mm, Wolfenden's 7.8 mm.

***Xanthocalanus hispidus*, new species**

FIGURES 71–79

Occurrence: Station 355 NV, 2000 to 1000 m, 1 ♀.

Diagnosis (female): Head and first thoracic segment fused, fourth and fifth thoracic segments incompletely separate. Ratio of cephalothorax to abdomen 4:1. Posterior lateral corner of fifth thoracic segment somewhat protruded and rounded. Rostral filaments present. First maxilla with two setae on second inner lobe, two setae on third inner lobe, two setae on second basal segment, eight setae on endopod and five setae on exopod. Second maxilla with sensory appendages, coarse setae broken off. Maxilliped setose. Spines on external margin of exopods of first foot long and seta-like. Exopods and endopods of second through fourth feet broken off. Fifth feet 2-segmented. Distal segment with three spines and one spinelike protrusion. Scattered spines on surface of segment and at junction of first and second segment. Total length 1.00 mm. Holotype: USNM 113518.

Remarks: This species resembles *X. paraincertus* Grice and Hulsemann, but the two may be distinguished by the segmentation and structure of the fifth feet. *X. hispidus* has 2-segmented fifth feet and two short outer spines on the terminal segment. *X. paraincertus* has 3-segmented fifth feet and two long outer spines on the terminal segment.

***Amallothrix indica* Sewell, 1929**

FIGURES 80–82

Diagnosis (male): Left fifth foot nearly twice as long as abdomen. Basal segments of left foot very elongate, exopod 3-segmented, endopod 2-segmented. Right foot only slightly longer than first basal segment. Exopod 2-segmented, endopod 1-segmented. Total length 2.68–3.10 mm.

Remarks: The male of this species resembles *Amallothrix emarginata* (Farran) but the right exopod of the latter species exceeds the length of the left exopod. In *A. indica* the right exopod is quite short. The male of this species has not heretofore been described.

Amallothrix paravalida Brodsky, 1950

FIGURES 83–84

Diagnosis (male): The terminal segment of the left fifth foot has two rows of spines and a rounded lamella. Total length 2.30 mm.

Remarks: We are tentatively referring to this species a single male specimen found in a sample containing two female *A. paravalida*. The structure of the terminal segment of the left fifth foot of the male of *A. paravalida* will distinguish this species from *A. valida* (Farran).

Amallothrix robustipes Grice and Hulsemann, 1965

Remarks: The present specimens have 2 setae on the second inner lobe and 10 setae on the endopod of the first maxilla. The two Atlantic Ocean specimens described by Grice and Hulsemann (1965) have four setae on the second inner lobe and nine setae on the endopod of the first maxilla. There are no rostral filaments on the Indian Ocean specimens whereas there are two on the Atlantic Ocean ones. The total length of the specimens is 1.00 and 1.20 mm. This is the first record of *Amallothrix robustipes* in the Indian Ocean.

?*Racovitzanus* species

FIGURES 85–95

Diagnosis (male): Head and first thoracic segment separate, fourth and fifth thoracic segments separate. Posterior lateral corner of fifth thoracic segment indented. Abdominal segments elongate. Rostrum large, without filaments. First antenna exceeds furca by last segment. Segments 8–10 of right first antenna fused. First and second maxilla of the type present in family Scolecithricidae. Maxilliped greatly reduced and with few setae. Exopods of the fifth feet 3-segmented, endopods 1-segmented and pointed. Total length 1.92 mm.

Remarks: We are tentatively assigning this male to the genus *Racovitzanus* based largely on the shape of the rostrum. Since it may represent the undescribed male of a known species, we are not describing it as new species.

Scaphocalanus bogorovi Brodsky, 1955

FIGURES 96–99

Remarks: The present specimens agree with those collected by us in the North Atlantic (Grice and Hulsemann, 1965). The range of this species is here extended to the Indian Ocean.

Scolecithricella grata, new species

FIGURES 100–103

Occurrence: Station 131 Bé, 2000 to 1000 m, 1 ♀.

Diagnosis (female): Head and first thoracic segment fused, fourth and fifth thoracic segments fused. Rostral filaments present. First maxilla of usual scolecithricid structure. Second maxilla with four lobes each bearing setae and without terminal sensory appendages. Fifth feet consisting of one segment ending in a long spine. Total length 1.31 mm. Holotype: USNM 113521.

Remarks: This species differs from others in the genus by the structure of the fifth feet and the absence of sensory appendages on the second maxilla. In the latter respect it is similar to *Scolecithrix fowleri* Farran.

Scolecithricella maritima, new species

FIGURES 104–114

Occurrence: Station 332 NV, 2000 to 1002 m, 2 ♀♀; 340 NV, 1950 to 1015 m, 1 ♀.

Diagnosis (female): Head and first thoracic segment fused, fourth and fifth thoracic segments incompletely separate. Anterior margin of head broadly rounded. Rostral filaments absent. First antenna with 23 free segments (segments 8 and 9 fused), reaching to fifth thoracic segment. Mouth appendages of *Scolecithricella* type. Expods of first through fourth swimming feet 3-segmented, endopod of first foot 1-segmented, of second foot 2-segmented, of third and fourth feet 3-segmented. Scattered spines on terminal endopodal segments of second through fourth feet. Fifth feet 3-segmented with one terminal and one internal spine on distal segment. Total length .76–.77 mm. One female from station 332 is the holotype. Holotype USNM 113522.

Remarks: This species is similar to *S. ctenopus* (Giesbrecht), but the two may be distinguished by the structure of the fifth feet and by their size. *S. maritima* has no surface spines on the second and third segments of the fifth feet and the total length is less than 1 mm. *S. ctenopus* has numerous small spines in the second and third segments of the fifth feet and the total length is about 1.50 mm.

Scolecithricella timida Tanaka, 1962

FIGURES 115-123

Remarks: This species was originally described from Sagami Bay, Japan (Tanaka, 1962). Some additional figures are given here. The total length of the specimens varies from 1.50 to 1.76 mm. This species has not been reported from the Indian Ocean.

Scolecithricella species

FIGURES 124–125

Diagnosis (male): Head and first thoracic segment fused, fourth and fifth thoracic segments separate. First antenna reaches end of second abdominal segment. Right fifth foot uniramous, 2-segmented. Left foot biramous, exopod 3-segmented, endopod 1-segmented. Total length .72 mm.

Remarks: The single male specimen is probably referable to a described female of this species. We therefore will not offer it as a new species.

Scolecithrix fowleri Farran, 1926

FIGURES 126–129

Diagnosis (male): Head and first thoracic segment fused, fourth and fifth thoracic segments separate. Large, ventrally directed rostrum. Fifth feet biramous. Right foot with 3-segmented exopod, 2-segmented endopod. Left foot with 3-segmented exopod and 1-segmented endopod. Total length 1.62 mm.

Remarks: The male of this species has not been heretofore known. Our findings of *Scolecithrix fowleri* represent a new record for the Indian Ocean.

Metridia boecki? Giesbrecht, 1889

FIGURES 130–133

Diagnosis (male): Head and first thoracic segment fused, fourth and fifth thoracic segments fused. Posterior lateral corner of fifth thoracic segment with small protuberance. First antenna reaches to end of second abdominal segment. First segment of left first foot with pubescent swelling. Total length 1.95–2.01 mm.

Remarks: The five male specimens here tentatively recognized as belonging to *M. boecki* differ slightly from *M. discreta* by the large swelling on the first segment of the left fifth foot.

Metridia brevicauda Giesbrecht, 1889

Remarks: The fifth pair or feet of several female specimens were observed to have four rather than three segments. In other respects they agreed with *M. brevicauda*.

Metridia effusa, new species

FIGURES 134–143

Occurrence: Station 108 Bé, 2000 to 1000 m, 1 ♀; 134 Bé, 2000 to 1000 m, 11 ♀♀, 6 ♂♂; 140 Bé, 2000 to 1000 m, 2 ♀♀.

Diagnosis (female): Head and first thoracic segment incompletely separate, fourth and fifth thoracic segments fused. Anterior end of head pointed, posterior lateral corner of fifth thoracic segment rounded.

Genital segment short, in dorsal view sides parallel. Furca longer than wide. First antenna reaches genital segment. First and second segments with prominent teeth. Fifth feet 3-segmented, with extremely small distal segment bearing a long seta. Penultimate segment with small distolateral spine. Total length 1.58–1.79 mm. Holotype: USNM 113525.

Diagnosis (male): Head and first thoracic segment fused, fourth and fifth thoracic segments fused. Anterior end of head with rounded knob. Posterior lateral corner of fifth thoracic segment rounded. Internal spine on second segment of right foot reaches just beyond middle of distal segment. Third segment of left foot with one seta and one spine on internal side. Total length 1.36–1.44 mm. Allotype: USNM 113526.

Remarks: The female of this species resembles *M. venusta* Giesbrecht and *M. brevicauda* Giesbrecht. From the former it is distinguished by the 3-segmented fifth feet and presence of one terminal seta on the distal segment. *M. venusta* has a 2-segmented fifth foot and four setae on the distal segment. From *M. brevicauda* it is distinguished by the spines on the first and second segments of the antenna; in addition, neither *M. venusta* nor *M. brevicauda* have pointed foreheads. The male is distinguished from these species by the rounded knob on the anterior margin of the head and the details of the fifth feet.

Lucicutia major Wolfenden, 1911

FIGURES 144–147

Remarks: This species has not been reported since it was described by Wolfenden in 1911. The one female found differs from the description in that the first antenna exceeds the end of the furca by about the last four segments. Wolfenden stated that the antenna exceeds the furcae by the last two segments. Also, the left furca is only slightly longer than the right one instead of being considerably longer as mentioned in the original description. In all other points our specimen agrees with the description of Wolfenden. The present specimen measures 8.16 mm; Wolfenden's measured 8.0–8.2 mm. Since no figures of *Lucicutia major* have been published, we are presenting figures of this species here. This is the first record of *L. major* from the Indian Ocean.

Disco inflatus Grice and Hulsemann, 1965

FIGURES 148–161

Diagnosis (male): Head and first thoracic segment separate, fourth and fifth thoracic segments fused. Anal segment longer than

preceding segment, slightly shorter than furca. Rostrum absent. First antenna reaches to fourth segment of abdomen. Left antenna geniculate. Endopod of second antenna about equal in length to exopod. First endopodal segment of mandible with row of spines. Mandible palpus elongate, blade with two subequal teeth. First maxilla reduced, endopod (?) with two setae. Second maxilla and maxilliped with reduced number of setae. Exopods of swimming feet 3-segmented, endopod of first foot 2-segmented, of second to fourth feet 3-segmented. Spine of first exopodal segment of first foot large and elongate. Fifth feet biramous, exopods 3-segmented, endopods 2-segmented. Penultimate segment of left exopod indented on internal side. Total length 1.16 mm.

Remarks: The genus *Disco* was described by us (Grice and Hulsemann, 1965) on the basis of female specimens collected in the North Atlantic Ocean. *D. inflatus* has not been previously reported from the Indian Ocean.

Disco species

FIGURES 162–173

Diagnosis (male): Head and first thoracic segment incompletely separate, fourth and fifth thoracic segments fused. Anal segment longer than preceding segment and furca. Rostrum absent. Left antenna geniculate. Endopod of second antenna ⅔ the length of exopod. Mandible palpus elongate, blade with spinelike hairs and three spiniform teeth. First maxilla well developed, internal lobe bearing one seta, exopod with four setae, and second basal segment with one seta. Second maxilla and maxilliped with reduced number of setae. Exopods and endopods of first and second feet 3-segmented. Third and fourth feet broken off. Fifth feet biramous, exopods 3-segmented. Endopod of right foot 3-segmented, of left foot 2-segmented. Total length .80 mm.

Remarks: It appears that the present specimen is referable to the genus *Disco*, but probably not to either of the two described species (*D. longus, D. minutus*) in which the male is unknown. The present male differs from these two species in the absence of a rostrum and in the segmentation of the endopods of the first and second swimming feet. It seems preferable not to refer the male to either species as it may represent the male of an undescribed species of *Disco*.

Euaugaptilus brodskyi Hulsemann, 1967

FIGURES 174–179

Remarks: We found one female measuring 6.83 mm in length, which we believe is *Euaugaptilus brodskyi*. The mandible, first and

second maxilla are figured here since Brodsky (1950) did not figure all of the appendages. In our specimen the exopod of the mandible palpus is reduced and bears four setae. The endopod is represented by one seta. Brodsky described this species as *E. mixtus*. The name was subsequently changed (Hulsemann, 1967) to *E. brodskyi* because it was preoccupied by a species described by Sars in 1905.

There was one male in the collection which measured 3.33 mm. In the structure of the mandible blade and the first maxilla it is closer to the female of *Euaugaptilus mixtus* Brodsky as described and figured by Tanaka (1964) than to the specimens originally described by Brodsky. In our specimen the mandible palpus is biramous. The number of setae on lobes 1–6 of the second maxilla is 1, 1, 2, 3, 2, 3, respectively, and that on lobes 1–5 of the maxilliped is 1, 3, 3, 2, 2, respectively. This male is identical to the one reported as *Euaugaptilus* species by Grice and Hulsemann (1965) from the northeastern Atlantic Ocean. *Euaugaptilus brodskyi* has not previously been reported from the Indian Ocean.

***Euaugaptilus curtus*, new species**

FIGURES 180–186

Occurrence: Station 108 Bé, 2000 to 1000 m, 1 ♀, 1 ♂.

Diagnosis (female): Body slender, head and first thoracic segment incompletely separate. Fourth and fifth thoracic segments fused, posterior lateral corners rounded. Abdomen 3-segmented, genital segment longer than the two following combined. Rostrum with two slender filaments. First antenna exceeds end of furca by about five segments. Exopod of second antenna consisting of eight segments, reaching to end of first endopodal segment. Mandible palpus uniramous composed of five segments, the last three each bearing one seta. Mandible blade with two strong double teeth and one smaller tooth adjacent to the seta. First inner lobe of first maxilla with six spines, second and third inner lobes rudimentary. Fused second basal segment and endopod with one seta. Exopod carrying one very long and one small terminal seta and one slender subterminal seta. External lobe with two setae. Number of setae on lobes 1–6 of second maxilla: 3, 2, 2, 3, 2, 3, respectively; 7 setae on the endopod. Maxilliped bearing 1, 3, 3, 2, 2 setae on the lobes of the basipod. Exopods and endopods of first to fifth pair of swimming feet 3-segmented. Total length 2.81 mm. Holotype: USNM 113528.

Diagnosis (male): Differs from female in the following: Abdomen consisting of five segments. Left first antenna geniculate. Segmentation of mandible palpus incomplete. First inner lobe of first maxilla with five spines. Fifth feet as in figure 186. Total length 2.49 mm. Allotype: USNM 113529.

Remarks: *Euaugaptilus curtus* resembles *E. longiseta* Grice and Hulsemann. The former species differs from the latter, however, in having two teeth on the mandible blade, a uniramous mandible palpus, and a more reduced first maxilla.

Euaugaptilus fundatus, new species

FIGURES 187–192

Occurrence: Station 108 Bé, 2000 to 1000 m, 1 ♀.

Diagnosis (female): Head and first thoracic segment separate, fourth and fifth thoracic segments fused. Posterior lateral corner of fifth thoracic segment rounded. Abdomen 3-segmented. Genital segment longer than the two following combined. Rostral filaments slender, broken short. First antenna exceeding end of furca by about last three segments. Exopod of second antenna 8-segmented. Mandible palpus biramous, endopod small, ending in one setae. Mandible blade with two strong teeth, each with a small side tooth, and one large seta. First inner lobe of first maxilla with four spines; second and third inner lobes absent; fused second basipodal segment and endopod with one seta; exopod with five setae, the two terminal ones largest; external lobes with five setae, the middle one being the largest. Number of setae on lobes 1–6 in the second maxilla: 3, 2, 2, 2, 2, 1, respectively. Two setae each on lobes 3–5 of the maxilliped. Exopod of first swimming foot consisting of three segments, endopod of two segments. Groups of small hairs near base of external spines of second and third exopodal segments. Exopods and endopods of second to fifth swimming feet 3-segmented. Total length 3.64 mm. Holotype: USNM 113530.

Remarks: *Euaugaptilus fundatus* resembles *E. longiseta* Grice and Hulsemann and *E. curtus*. It is distinguished from these by the structure of the mandible blade and palpus, and the development of the first and second maxilla.

Euaugaptilus humilis Farran, 1926

Remarks: These specimens agree in those details discussed by Grice (1963): presence of rostral filaments, symmetrical furcae, symmetrical genital segment, and the presence of a second inner lobe on the first maxilla. *Euaugaptilus humilis* has not previously been reported from the Indian Ocean.

Euaugaptilus longiseta Grice and Hulsemann, 1965

FIGURES 193–195

Diagnosis (male): Rostrum small with slender filaments. Right furca shorter than left. First antenna exceeds end of furca by last four segments. Exopod of second antenna 7-segmented. Mandible palpus biramous, blade as in female. First maxilla with one seta

on fused second basal segment and endopod, five setae on exopod. Number of setae on lobes 1–6 of second maxilla: 2, 2, 2, 3, 2, 1 respectively. Number of setae on lobes 1–5 of maxilliped: 1, 2, 3, 2, 2. Exopods and endopods of fifth feet 3-segmented, terminal segments with one long seta and one short spine. Total length 1.82 mm.

Remarks: Although the first maxilla of the male has no second inner lobe and fewer setae on the fused second basal segment and endopod (one rather than three setae as in the female), the other head appendages agree well with those of the female. The male has not heretofore been described. Our findings of *Euaugaptilus longiseta* represent a new record for the Indian Ocean.

Euaugaptilus malacus, new species

FIGURES 196–200

Occurrence: Station 134 Bé, 2000 to 1000 m, 1 ♀.

Diagnosis (female): Head and first thoracic segment separate, fourth and fifth thoracic segments fused. Posterior lateral corner of fifth thoracic segment rounded, set off by a slight indentation. Abdomen 3-segmented. Rostral filaments very slender. First antenna exceeds end of furca but broken off at segment 22. Exopod of second antenna 8-segmented, shorter than endopod. Mandible blade obliquely cut bearing two strong double-teeth and two slender, shorter teeth. Endopod of mandible palpus rudimentary. First inner lobe of first maxilla with six rather slender and elongate spines, second inner lobe with one seta, third inner lobe lacking; fused second basal segment and endopod with one seta; exopod with two strong and one weak seta; external lobe with three setae. Number of setae on lobes 1–6 of second maxilla: 0, 1, 2, 2, 2, 1, respectively. Number of setae on first five lobes of maxilliped: 1, 2, 3, 2, 2, respectively. Endopods and exopods of first through fifth pair of swimming feet 3-segmented. Total length 3.29 mm. Holotype: USNM 113532.

Remarks: *Euaugaptilus malacus* resembles *E. facilis* (Farran). The obliquely cut mandible blade, the rudimentary endopod of the mandible palpus, the lack of a blunt process on the outer margin of the second and third exopodal segments of the third and fourth swimming feet, and the small size of *E. malacus* will distinguish it from *E. facilis*.

Euaugaptilus nodifrons (Sars, 1905)

FIGURES 201–203

Remarks: A dorsal view of the body, rostrum, and mandible blade of the male are illustrated for the first time. Other appendages of the male are shown by Sars (1924–25) and Sewell (1929).

228-966—67——3

Euaugaptilus oblongus (Sars, 1905)

Augaptilus oblongus Sars, 1905b, pp. 11–12.
Augaptilus rostratus Esterly, 1906, p. 73, pls. 9 (fig. 19), 11 (fig. 42), 12 (figs. 57, 63), 13 (fig. 75).
Augaptilus subfiligerus Wolfenden, 1911, p. 343.
Euaugaptilus oblongus (Sars).—Sars, 1924–1925, pp. 266–267, pl. 81.
Euaugaptilus rostratus (Esterly).—Brodsky, 1950, pp. 374–375, fig. 264.

Remarks: Close examination of two females of *Euaugaptilus rostratus* (loaned to us by Scripps Institution of Oceanography) on which Esterly (1906) probably based the description of that species indicates that *E. rostratus* (Esterly) is identical to *E. oblongus* (Sars, 1905). A comparison of the description of *Augaptilus subfiligerus* Wolfenden, 1911, with *E. oblongus* (Sars) shows that these two species are also identical.

The synonymy of the three species extends the size range of *Euaugaptilus oblongus* to 4.65–7.4 mm.

Euaugaptilus quaesitus, new species

FIGURES 204–209

Occurrence: Station 332 NV, 3000 to 2000 m, 1 ♀.

Diagnosis (female): Head and first thoracic segment separate, fourth and fifth thoracic segments fused. Posterior lateral corner of fifth thoracic segment rounded. Abdomen 3-segmented. Genital segment longer than the two following combined. Rostrum consisting of two points, rostral filaments absent. First antenna barely reaching furca. Exopod of second antenna 8-segmented, segments seven and eight incompletely separated; exopod and endopod of equal length. Mandible blade with two widely separated strong teeth and one slender tooth near the seta. First inner lobe of first maxilla with four spines; second and third inner lobes absent; fused second basipodal segment and endopod with one seta; exopod with five setae, the two terminal ones largest; external lobe with three setae of equal length. Number of setae on lobes 1–6 of the second maxilla: 2, 2,1, 2, 2, 1, respectively. Number of setae on lobes 1–5 of the maxilliped: 0, 3, 3, 2, 2, respectively. Exopod of first swimming foot consisting of three segments, endopod of two segments. Exopods and endopods of second through fourth pair of swimming feet 3-segmented. Exopod and endopod of fifth pair 2-segmented. Total length 1.40 mm. Holotype: USNM 113533.

Remarks: *Euaugaptilus quaesitus* resembles *E. fundatus* in the structure of the mandible blade, the first maxilla, and the 2-segmented endopod of the first swimming foot. The two species can be separated by the smaller size of *Euaugaptilus quaesitus* and by its lack of rostral filaments, its shorter first antenna, and its 2-segmented exopod and

endopod of the fifth feet. *E. quaesitus* is also close to *Euaugaptilus hecticus* (Giesbrecht), but the shorter first antenna in *E. quaesitus* and the more developed mandible palpus and blade distinguish these two species. Finally, *E. quaesitus* differs from *E. humilis* Farran in its shorter first antenna and the structure of the mandible blade and the first maxilla.

***Euaugaptilus rectus*, new species**

FIGURES 210–214

Occurrence: Station 337B IK, 275 to 2250 m, 1 ♀.

Diagnosis (female): Head and first thoracic segment separate, fourth and fifth thoracic segments fused. Posterior lateral corner of fifth thoracic segment rounded. Rostrum consisting of two short and stout cones. No rostral filaments. Exopod of second antenna 8-segmented. Mandible palpus with well-developed rami. Mandible blade obliquely terminated. First maxilla with one seta on second inner lobe, no seta on third inner lobe, three setae on fused second basal segment and endopod, and four setae on exopod. Second maxilla with following setae number on lobes 1–6: 2, 1, 1, 3, 2, 3. Number of setae on lobes 1–5 of maxilliped: 1, 3, 3, 2, 2. Exopod of first foot with one external spine on first segment, one external spine on second segment and two external spines on third segment. Total length 7.98 mm. Holotype: USNM 113534.

Remarks: This species is similar to *E. angustus* (Sars) but the two may be separated by the structure of the rostrum (2-pointed in *E. rectus*, rounded in *E. angustus*), and first foot (two external spines in *E. rectus*, one spine in *E. angustus*).

***Euaugaptilus* species 1**

FIGURES 215–224

Diagnosis (female): Head and first thoracic segment separate, fourth and fifth thoracic segments fused. Genital segment more than one-half the length of the abdomen. Rostral filaments small and fine. First antenna exceeds furca by last five segments. Exopod of second antenna 8-segmented. Mandible palpus without rami. First maxilla with one seta on second inner lobe, no seta on third inner lobe, one seta on fused second basal segment and endopod, and four setae on exopod. Number of setae on lobes 1–6 of the second maxilla: 2, 2, 2, 3, 2, 3, respectively. Number of setae on lobes 1–5 of maxilliped: 1, 3, 3, 2, 2. Maxilliped with indented knob on posterior side. Exopods and endopods of first through fourth feet 3-segmented. Third exopodal segment of third foot cup shaped with two rudimentary spines on external margin and five setae on internal margin. Fifth feet with 3-segmented exopods and endopods and with a small spine on the inne side of the second exopodal segment. Total length 4.87 mm.

228-966—67——4

UNESCO ARCHIVES

Remarks: There is reasonably good agreement between the present specimen and *E. facilis* (Farran), a species also found in these collections. They differ chiefly in the structure of the mandible (no rami in *Euaugaptilus* species 1, biramous in *E. facilis*), first maxilla (three large and one small setae on the exopod in *Euaugaptilus* species 1, three large setae on exopod of *E. facilis*), and third pair of feet (enlarged terminal exopodal segments in *Euaugaptilus* species 1, usual type of terminal segment in exopods in *E. facilis*). The present specimen could possibly be an abnormally developed *E. facilis* and we have therefore not considered it a new species.

***Euaugaptilus* species 2**

FIGURES 225–230

Diagnosis (male): Head and first thoracic segment separate, fourth and fifth thoracic segments fused. Posterior lateral corner of fifth thoracic segment rounded. Abdomen consisting of five segments, anal segment very long, longer than furca. Large rostrum rounded. Rostral filaments slender. Right first antenna reaching anal segment; left first antenna geniculate. Exopod of second antenna 8-segmented, small, extending to two-thirds of first segment of endopod. Mandible blade with four strong and one slender tooth of about the same length, seta small. Mandible palpus biramous. First maxilla much reduced; first endopodal lobe with one spine, second endopodal lobe with one spine, third lobe absent; fused second basal segment and endopod with one seta; exopod with two rather strong setae; external lobe without setae. Number of setae on lobes 1–6 of second maxilla: 1 and a small process, 1 (?), 2, 2, 2, 1, respectively. Number of setae on first 5 lobes of maxilliped: 1, 1, 2, 2, 2, respectively. Exopods and endopods of first to fifth pair of swimming feet 3-segmented. Seta on second basipodal segment of fifth foot short; inner margin of second exopodal segment of right fifth foot with process near proximal corner; external spines of first and second exopodal segments with small knoblike protrusions apically near their base. Total length 3.7 mm.

Remarks: The structure of the mandible and the first maxilla as well as the relatively long genital segment suggest a close relationship of *Euaugaptilus* species 2 to *E. affinis* Sars. The one male specimen found differs from Sars' description (1924–25) of the female in a reduced number of spines or setae, respectively, on the first inner lobe and the outer lobe of the first maxilla, second maxilla and the maxilliped. Also, this male (total length 3.77 mm) is smaller than the female of *E. affinis* (5.40 mm). The male of *E. affinis* is undescribed.

The characteristics pointed out by Brodsky (1950) to distinguish his *Euaugaptilus pseudaffinis* from *E. affinis*—i.e., differences in the

length of the first and second antenna and the structure of the fifth pair of feet—seem insufficient to distinguish *E. pseudaffinis* Brodsky from *E. affinis* Sars. No difference is obvious between Brodsky's and Sars' figure of the fifth feet of the female.

***Euaugaptilus* species 3**

FIGURES 231–240

Diagnosis (male): Head and first thoracic segment fused, fourth and fifth thoracic segments fused. Anal segment twice the length of the preceding segment. Rostrum knoblike , with two short filaments. First antenna exceeds furca by last two segments, left antenna geniculate. Endopod of second antenna about four times longer than exopod. Mandible palpus small, uniramous. First maxilla much reduced. Distal setae of second maxilla and maxilliped with numerous "buttons." Swimming feet with 3-segmented exopods and endopods. Total length 6.16 mm.

Remarks: We are unable to refer this male to a described species but it may be the undescribed male of a known species. The head appendages resemble those of the female of *E. rigidus* (Sars), but the size of the present male exceeds that of the female.

***Pachyptilus abbreviatus* (Sars, 1905)**

FIGURES 241–247

Remarks: Figures of the female of this species, not previously known from the Indian Ocean, are given here. The total length is 5.52 mm.

***Pachyptilus pacificus* Johnson, 1936**

Pachyptilus eurygnathus Sars.—Sewell, 1947, p. 239, text-fig. 65.

Remarks: The species reported by Sewell (1947) as *P. eurygnathus* is referable to *P. pacificus*. Sewell's specimen has a 2-segmented exopod on the first feet, which is the same number found in *P. pacificus*.

***Pontoptilus robustus* Sars, 1905**

FIGURES 248–258

Diagnosis (female): Head and first thoracic segment separate, fourth and fifth thoracic segments fused, posterior lateral corner of fifth thoracic segment protruded. Rostrum absent. First antenna consisting of 25 free segments, exceeding furca by last 3 segments. Structure and setation of head and thoracic appendages similar to *P. muticus* Sars. Total length 8.51 mm.

Remarks: Although closely resembling *P. muticus*, *P. robustus* is distinguished by its larger size, long antenna, and protruding fifth thoracic segment. The female has not been described heretofore. The male was described by Sars in 1905 and later illustrated by him

(Sars, 1924–25). This is the first record of *Pontoptilus robustus* in the Indian Ocean.

Pontoptilus lacertosus, new species

FIGURES 259–265

Occurrence: Station 347A, IK, 350 to 2500 m, 1 ♀.

Diagnosis (female): Head and first thoracic segment fused, fourth and fifth thoracic segments fused. Fifth thoracic segment rounded. Rostrum robust with a single point. First antenna exceeding furca by about five segments. Mandible palpus with three setae. Blade resembling that of *P. ovalis* Sars. First maxilla with five setae on second inner lobe, four setae and a small spine on the endopod, two setae on the second basal segment, five setae on the endopod, three setae on the exopod and one seta on a lobe located just ventrad of the exopod. Setae on lobes 1–5 of the second maxilla as follows: 8, 3, 3, 3, 3, respectively. First to fourth swimming feet with 3-segmented exopods and endopods. Fifth feet with 3-segmented exopods, 2-segmented endopods. Total length 7.17 mm. Holotype: USNM 113535.

Remarks: *P. lacertosus* differs from *P. ovalis* Sars, a species it resembles, in the presence of a rostrum and additional setae on the second basal segment, endopod and exopod of the first maxilla.

Phyllopus muticus Sars, 1907

FIGURES 266–270

Remarks: A very large female (total length 7.21 mm) was found at one station. Figures of this specimen including illustrations of some appendages not heretofore figured are given here.

Bathypontia elongata Sars, 1905

FIGURES 271–274

Remarks: Several figures of the male are given here. The rostrum of the male is rounded and unlike that found in the female. Total length 4.68 mm. *Bathypontia elongata* has not previously been reported from the Indian Ocean.

Bathypontia regalis, new species

FIGURES 275–280

Occurrence: Station 338 NV, 3000 to 2000 m, 1 ♂.

Diagnosis (male): Head and first thoracic segment separate, fourth and fifth thoracic segments separate. Posterior lateral corner of fifth thoracic segment broadly rounded. Rostrum robust and rounded. Exopods of first through fourth feet 3-segmented, endopods of first foot 2-segmented, of second through fourth feet 3-segmented.

Left fifth foot 5-segmented with hair on internal margin of second and third segments. Right fifth foot 5-segmented. Total length 2.32 mm. Holotype: USNM 113537.

Remarks: This species resembles the male of *B. major* (Wolfenden) but the small size of the present specimen and the inflated and pubescent second segment of the left fifth foot will distinguish it from *B. major*.

Rhinomaxillaris, new genus

Type-species: *Rhinomaxillaris bathybia*, new species.

Rhinomaxillaris bathybia, new species

FIGURES 281–292

Occurrence: Station 330 NV, 2000 to 1000 m, 1 ♀.

Diagnosis (female): Head and first thoracic segment incompletely separate, fourth and fifth thoracic segments incompletely separate. Abdomen 4-segmented. Anal segment longer than preceding segment and furca. Rostrum large and obtuse. First antenna reaching to fifth thoracic segment. Segments 8 and 9, 24 and 25 fused. Exopod of second antenna consisting of seven segments, about twice the length of the endopod. Mandible palpus with two setae. First maxilla with two setae on second inner lobe, five setae on endopod and two setae on exopod. Second maxilla with 5 lobes bearing 1, 1, 3, 3, and 2 setae, respectively. Maxilliped large, with long and coarse setae distally. First foot with 3-segmented exopod and 1-segmented endopod. First and second exopodal segments of first foot without external spines. Exopods of second through fourth feet broken off. Endopods of second foot 2- or 3-segmented, of third and fourth feet 3-segmented. Third endopodal segments of third and fourth feet with six setae. Total length 1.12 mm. Holotype: USNM 113538.

REMARKS.—We found one female specimen of a calanoid copepod for which we establish a new genus and species. It was difficult to assign this species to an existing family. Characteristics of this specimen can be found in the genera of the family Bathypontiidae Brodsky: *Bathypontia* Sars, *Temorites* Sars, *Zenkevitchiella* Brodsky, and *Foxtonia* Hulsemann and Grice . The last two of these genera were tentatively placed in this family.

The large, blunt rostrum of *Rhinomaxillaris* is similar to that found in *Bathypontia*. There are 23 free segments in the first antenna of all four genera mentioned except in the species *Temorites discoveryae* Grice and Hulsemann. Segments 24 and 25 are fused in all species in the family. In general, the second maxilla and the maxilliped resemble those in the other genera in the family with respect to their compact form and the strong, spinelike setae on the endopods. The

first and second exopodal segments of the first foot lack external spines as is the case in *Bathypontia*, *Temorites*, and *Foxtonia*. The absence of fifth feet is common to the female of *Foxtonia*.

The new genus *Rhinomaxillaris* is distinguished from *Bathypontia* and *Temorites* by the long exopod in the second antenna, the shape and arrangement of the teeth on the mandible blade, and the absence of fifth feet. *Rhinomaxillaris* differs from *Zenkevitchiella* and *Foxtonia* in the long exopod of the second antenna, the mandible blade, and the peculiar rostrum. From *Zenkevitchiella*, *Rhinomaxillaris* is further distinguished by the absence of external spines on the first and second exopodal segments of the first foot, and the absence of fifth feet. It differs from *Foxtonia* in the increased number of segments in the endopods of the second and third feet and in the absence of spinelike setae between the bases of the first antenna. *Rhinomaxillaris* also resembles certain genera in the family *Pseudocalanidae*. The large and blunt rostrum, the fused 24th and 25th segments in the first antenna, and the absence of external spines on the first and second exopodal segments of the first foot prevent *Rhinomaxillaris* from being placed in this family.

Until a female with intact swimming feet and a male are found, it is not possible to establish the true familial relationship of *Rhinomaxillaris*. In the meantime we have tentatively placed it in the family Bathypontiidae with the full realization that until this family is critically studied it may represent a composite of unrelated genera.

Until additional species are discovered, the genus *Rhinomaxillaris* cannot be diagnosed.

Zenkevitchiella atlantica Grice and Hulsemann, 1965

Remarks: In the single specimen found segments seven and eight of the first antenna are fused as is shown in figure 22(a) in our description of this species from North Atlantic specimens (Grice and Hulsemann, 1965) and not segments eight and nine as stated in the text. Segments 24 and 25 are fused and not segments 23 and 24 as also stated in the text. The distal end of the first antennae are broken off in the Indian Ocean specimen. It may be added here that in the male of *Zenkevitchiella atlantica* described by us (1965), segments seven and eight of the first antenna are fused. No male of this species has yet been found in the Indian Ocean. The occurrence of a female of *Zenkevitchiella atlantica* represents a new record for the Indian Ocean.

Zenkevitchiella crassa, new species

FIGURES 293–305

Occurrence: Station 340 NV, 2950 to 1990 m, 1 ♂.

Diagnosis (male): Head and first thoracic segment incompletely

separate, fourth and fifth thoracic segments separate. Posterior lateral corner of fifth thoracic segment rounded. Rostrum 2-pointed, each point with a filament. Right first antenna geniculate, fifth segment from end with two rounded knobs. Endopod of second antenna about two-thirds the length of exopod. Mandible with two setae on palpus. First maxilla with one seta on second inner lobe, two setae on third inner lobe, one seta on second basal segment, endopod absent, exopod with five setae. Second maxilla with five well-defined lobes bearing 3, 2, 1, 3, 2 setae, respectively. Long and coarse setae on distal lobe and on end of appendage. Maxilliped with coarse setae distally. Exopods of first through fourth feet 3-segmented. Endopods of first foot 1-segmented, of second through fourth feet 3-segmented. Second basal segment of third foot with distolateral spinelike protrusion. Fifth feet with right exopod 2-segmented, left exopod 1-segmented. Right endopod a small knob, left endopod large and bearing a large spine distally. Total length .84 mm. Holotype: USNM 113539.

Remarks: This species is different from *Z. atlantica* Grice and Hulsemann in the structure of the endopods of the fifth feet. In *Z. atlantica* the endopods are bulbous, and neither bears a spine. The male of *Z. abyssalis* Brodsky is not known. It is unlikely that the present specimen is the male of *Z. abyssalis* as this is a relatively large species (2.37 mm).

Unidentified Male

FIGURES 306–319

Diagnosis (male): Head and first thoracic segment separate, fourth and fifth thoracic segments fused. Abdomen 5-segmented, anal segment longer than preceding, equal in length to furca. Rostrum robust, broadly rounded at tip. Left first antenna geniculate, numerous aesthetasks on proximal segments. Endopod of second antenna about two-thirds the length of exopod. Endopod of mandible about two-thirds the length of exopod. Palpus devoid of setae. Blade with one large and two small teeth, distal end covered with numerous small spines. First maxilla with one seta on second inner lobe, three setae on third inner lobe, two setae on second basal segment, nine setae on endopod, and seven setae on exopod. Second maxilla with five lobes bearing 4, 3, 3, 3, and 1 setae, respectively. Maxillipeds broken off distally. Swimming feet broken off. Fifth feet uniramous, each ramus 5-segmented. Distal segment of left foot with 2 spinelike protrusions terminally. Total length .72 mm.

Remarks: In most respects the present male is similar to the males of the two *Disco* species (family Augaptilidae) described earlier. However, the uniramous fifth feet of the present male apparently preclude

its referral to the genus *Disco* and the family Augaptilidae. Until females are discovered, we will not attempt a family designation or generic description.

Summary

Calanoid copepods were identified in 51 samples collected by Bé multiple sampler, Isaacs-Kidd midwater trawl, and modified Nansen vertical net at stations located in the western Indian Ocean between the northern Arabian Sea and approximately the subtropical convergence. The Bé net collections were obtained between 2000 and 1000 m, the midwater trawl samples between the surface and a maximum depth of 3820 m, and the Nansen vertical net samples between 2000 and 1000, 3000 and 2000, and 4000 and 3000 m.

The displacement volumes of the zooplankton and numerical density and size of the copepods collected by the Nansen net were determined and compared to similar collections made in the northeastern Atlantic. In general, the total zooplankton as well as the copepods were more abundant in the 2000–1000 m depth interval than in intervals below 2000 m. The mean size of the animals was larger in the 2000–1000 m interval than in the 3000–2000 m interval. The values obtained for the displacement volumes, numerical abundance, and mean size were similar to those in comparable depth intervals in the northeastern Atlantic.

The greatest number of species in the Nansen vertical collections were found between 2000 and 1000 m (122), a lesser number between 3000 and 2000 m (73), and the least number between 4000 and 3000 m (13). This decrease in diversity with increasing depth is similar to that found in the northeastern Atlantic.

The distribution of 269 species found in the western Indian Ocean was discussed and compared to previous discussions of the geographic distribution of Indian Ocean bathypelagic copepods and to water mass distribution. The very widespread distribution of the bathypelagic species was indicated by the great similarity in species composition between the North Atlantic and western Indian Oceans. Eighty-six percent of the western Indian Ocean species are also present in the North Atlantic. Five typically Antarctic species were found in four samples collected in the southern Indian Ocean near the subtropical convergence.

Included in the 310 species found are 1 new genus, 17 new species, 8 previously unknown males, and 1 previously unknown female. Seventy-eight of the 310 species excluding the newly described ones have not been previously reported from the Indian Ocean. Seven species are apparently known only from the Indian Ocean.

Literature Cited

BÉ, ALLAN W. H.

1962. Quantitative multiple opening-and-closing plankton samplers. Deep-Sea Res., vol. 9, pp. 144–151, figs. 1–5.

BRODSKY, KONSTANTIN A.

1950. Calanoida of polar and far eastern seas of the U.S.S.R. Opredel. Fauna SSSR, Izd., Zool. Inst. Akad. Nauk SSSR, vol. 35, 442 pp., 306 figs. [In Russian.]

1955. On the copepod (Calanoida) fauna of the Kuril-Kamchatka Trench. Trudy Inst. Okean., Akad. Nauk SSSR, vol. 12, pp. 184–209, figs. 1–14a. [Transl. by W. L. Clarke, Woods Hole Oceanogr. Inst.]

1959. Concerning phylogentic relationships of several species of *Calanus* (Copepoda) of the Northern and Southern Hemispheres. Zool. Zhurn., Akad. Nauk SSSR, vol. 38, no. 10, pp. 1537–1552, figs. 1–5. [Transl. by Olga Jones, Scripps Inst. Oceanogr.]

CURRIE, RONALD I., and FOXTON, PETER

1957. A new quantitative plankton net. Journ. Mar. Biol. Assoc. U.K., vol. 36, pp. 17–32, figs. 1–6.

DAVIS, CHARLES C.

1949. The pelagic Copepoda of the Northeastern Pacific Ocean. Univ. Washington Publ. Biol., n.s., vol. 14, pp. 1–118, pls. 1–15.

DAY, JOHN H.

1963. The complexity of the biotic environment. *In* Harding and Tebble, Speciation in the sea. Syst. Assoc. Publ., London, no. 5, pp. 31–49.

DE DECKER, A., and MOMBECK, F. J.

1965. South African contribution to the International Indian Ocean Expedition, 4: A preliminary report on the planktonic Copepoda. Invest. Rep. Div. Sea Fish. South Africa, vol. 51, pp. 10–67, figs. 1–6, pls. 1–14.

ESTERLY, CALVIN OLIN

1906. Additions to the copepod fauna of the San Diego region. Univ. California Publ. Zool., vol. 3, pp. 53–92, pls. 9–14.

FARRAN, GEORGE PHILLIP

1926. Biscayan plankton collected during a cruise of H.M.S. *Research*, 1900, 14: The Copepoda. Journ. Linn. Soc. (Zool.), vol. 36, pp. 219–310, tex-figs. 1, 2, pls. 5–10.

FOXTON, PETER

1963. An automatic opening-closing device for large plankton nets and mid-water trawls. Journ. Mar. Biol. Assoc. U. K., vol. 43, pp. 295–308, text-figs. 1–4, pl. 1.

GIESBRECHT, WILHELM

1889. Elenco dei Copepodi pelagici raccolti dal tenente di vascello Gaetano Chierchia durante il viaggio della R. Corvetta Vettor Pisani negli anni 1882–1885 e dal tenente di vascello Francesco Orsini nel Mar Rosso, nel 1884. Atti Rend. Acc. Lincei ser. 4, vol. 5, no. 1, pp. 811–815; no. 2, pp. 24–29.

GRICE, GEORGE DANIEL
1962. Calanoid copepods from equatorial waters of the Pacific Ocean. U. S. Fish Wildlife Serv. Fish. Bull. 186, vol. 61, pp. 167–246, fig. 1, pls. 1–34.
1963. Deep water copepods from the western North Atlantic with notes on five species. Bull. Mar. Sci., vol. 13, no. 4, pp. 493–501, fig. 1.

GRICE, GEORGE DANIEL, and HULSEMANN, KUNI
1965. Abundance, vertical distribution and taxonomy of calanoid copepods at selected stations in the northeast Atlantic. Journ. Zool., vol. 146, no. 2, pp. 213–262, figs. 1–26.

GUNTHER, E. R., and HARDY, ALISTER C.
1935. The zooplankton, sec. 1. Pp. 88–193 *in* Hardy and Gunther, pt. III, The plankton of the South Georgia whaling grounds and adjacent waters, 1926–1927, *in* vol. 11 of *Discovery* Reports.

HULSEMANN, KUNI
1966. A revision of the genus *lucicutia* (Copepoda: Calanoida) with a key to its species. Bull. Mar. Sci., vol. 16, no. 4, pp. 702–747, figs. 1–126.
1967. Redescription of *Euaugaptilus mixtus* (Sars) (Copepoda: Calanoida). Crustaceana, in press.

HULSEMANN, KUNI, and GRICE, GEORGE DANIEL
1963. A new genus and species of bathypelagic calanoid copepod from the North Atlantic. Deep-Sea Res., vol. 10, pp. 729–734, figs. 1–15.

IVANENKOV, V. N., and GUBIN, F. A.
1960. Water masses and hydrochemistry of the western and southern parts of the Indian Ocean. Transact. Mar. Hydrophys. Inst., Acad. Sci. USSR, vol. 22, pp. 27–99, figs. 1–28. [Transl. by Scripta Technica for American Geophysical Union.]

JOHNSON, MARTIN W.
1936. *Pachyptilus pacificus* and *Centraugaptilus porcellus*, two new copepods from the North Pacific. Bull. Scripps Inst. Oceanogr., Techn. Ser., vol. 4, no. 2, pp. 65–70, figs. A–C.
1963. Zooplankton collections from the high Polar Basin with special reference to the Copepoda. Limnol. Oceanogr., vol. 8, no. 1, pp. 89–102, figs. 1–4.

MOHAMED, A. F.
1940. Chemical and physical investigations: The distribution of hydrogen-ion concentration in the north-western Indian Ocean and adjacent waters. Sci. Rept. John Murray Exped., vol. 2, no. 5, pp. 121–202, figs. 1–34.

MÖLLER, LOTTE
1929. Die Zirkulation des Indischen Ozeans. Veröffentl. Inst. Meeresk., n.s., ser. A, no. 21, 48 pp., 23 figs.

SARS, GEORGE OSSIAN
1905. Liste préliminaire des Calanoides recueillis pendant les Campagnes de S.A.S. le Prince Albert de Monaco, part 1. Bull. Inst. Océanogr. Monaco, no. 26 (1905a), 22 pp.; part 2, no. 40 (1905b), 24 pp.
1907. Notes supplémentaires sur les Calanoides de la Princesse Alice (corrections et additions). Bull. Inst. Océanogr. Monaco, no. 101, 27 pp.
1924–1925. Copépods, particulièrement bathypélagiques provenant des Campagnes Scientifiques du Prince Albert 1er de Monaco. Résult. Camp. Sci. Monaco, vol. 69, text (1925), 408 pp.; atlas (1924), 127 pls.

SCOTT, ANDREW
1909. The Copepoda of the *Siboga* Expedition, 1: Free-swimming, littoral and semi-parasitic Copepoda. Monogr. 29a (livr. 44) *in* Weber, *Siboga*-Expeditie, 323 pp., 69 pls.

SEWELL, R. B. SEYMOUR
1929. The Copepoda of Indian Seas: Calanoida. Mem. Indian Mus., vol. 10, pp. 1–221, text-figs. 1–81, pls. 1, 2.
1932. The Copepoda of Indian Seas: Calanoida. Mem. Indian Mus., vol. 10, pp. 223–407, text-figs. 82–131, pls. 3–6.
1947. The free-swimming planktonic Copepoda: Systematic account. Sci. Rep. John Murray Exped., 1933–1934, vol. 8, no. 1, pp. 1–303, text-figs. 1–71.
1948. The free-swimming planktonic Copepoda: Geographical distribution. Sci. Rep. John Murray Exped., vol. 8, no. 3, pp. 317–592, text-figs. 72–95.

SØMME, IACOB D.
1933. A possible relation between the production of animal plankton and the current-system of the sea. Amer. Nat., vol. 67, pp. 30–52, figs. 1–9.

SVERDRUP, HARALD ULRIK; JOHNSON, MARTIN W.; and FLEMING, RICHARD H.
1942. The oceans: Their physics, chemistry and general biology. New York: Prentice-Hall, 1087 pp., 265 figs.

TANAKA, OTOHIKO
1956. The pelagic copepods of the Izu Region, Middle Japan: Systematic account II: Families Paracalanidae and Pseudocalanidae. Publ. Seto Mar. Biol. Lab., vol. 5, no. 3, pp. 367–406, figs. 6–22.
1957. The pelagic copepods of the Izu Region, Middle Japan: Systematic account IV: Family Aetideidae (part 2). Publ. Seto Mar. Biol. Lab., vol. 6, no. 2, pp. 169–207, figs. 41–61.
1960. The pelagic copepods of the Izu Region, Middle Japan: Systematic account VI: Families Phaennidae and Tharybidae. Publ. Seto Mar. Biol. Lab., vol. 8, no. 1, pp. 85–135, figs. 81–105.
1962. The pelagic copepods of the Izu Region, Middle Japan: Systematic account VIII: Family Scolecithricidae (part 2). Publ. Seto Mar. Biol. Lab., vol. 10, no. 1, pp. 35–90, figs. 127–151.
1963. The pelagic copepods of the Izu Region, Middle Japan: Systematic account IX: Families Centropagidae, Pseudodiaptomidae, Temoridae, Metridiidae and Lucicutiidae. Publ. Seto Mar. Biol. Lab., vol. 11, no. 1, pp. 7–55, figs. 152–174.
1964. The pelagic copepods of the Izu Region, Middle Japan: Systematic account XI: Family Augaptilidae. Publ. Seto Mar. Biol. Lab., vol. 12, no. 1, pp. 39–91, figs. 192–219.

THOMPSON, ISAAC COOKE
1900. Report on two collections of tropical and more northerly plankton. Proc. Liverpool Biol. Soc., vol. 14, pp. 262–294, pl. 15.

VERVOORT, WILLEM
1949. Some new and rare Copepoda Calanoida from East Indian Seas. Zool. Verh., Leiden, no. 5, 53 pp., 23 figs.
1952. Copepoda: Sub-order Calanoida: Family Aetideidae: Genus *Gaidius*. Zooplankton Sheet, Cons. Explor. Mer, no. 45 (1952a), 4 pp.; Genus *Gaetanus*, no. 46 (1952b), 5 pp.

1965. Notes on the biogeography and ecology of free-living marine Copepoda. Pp. 381–400, figs. 1–6, *in* Monographiae Biologicae, 15: Van Oye and Van Mieghem, Biogeography and ecology in Antarctica. The Hague: W. Junk.

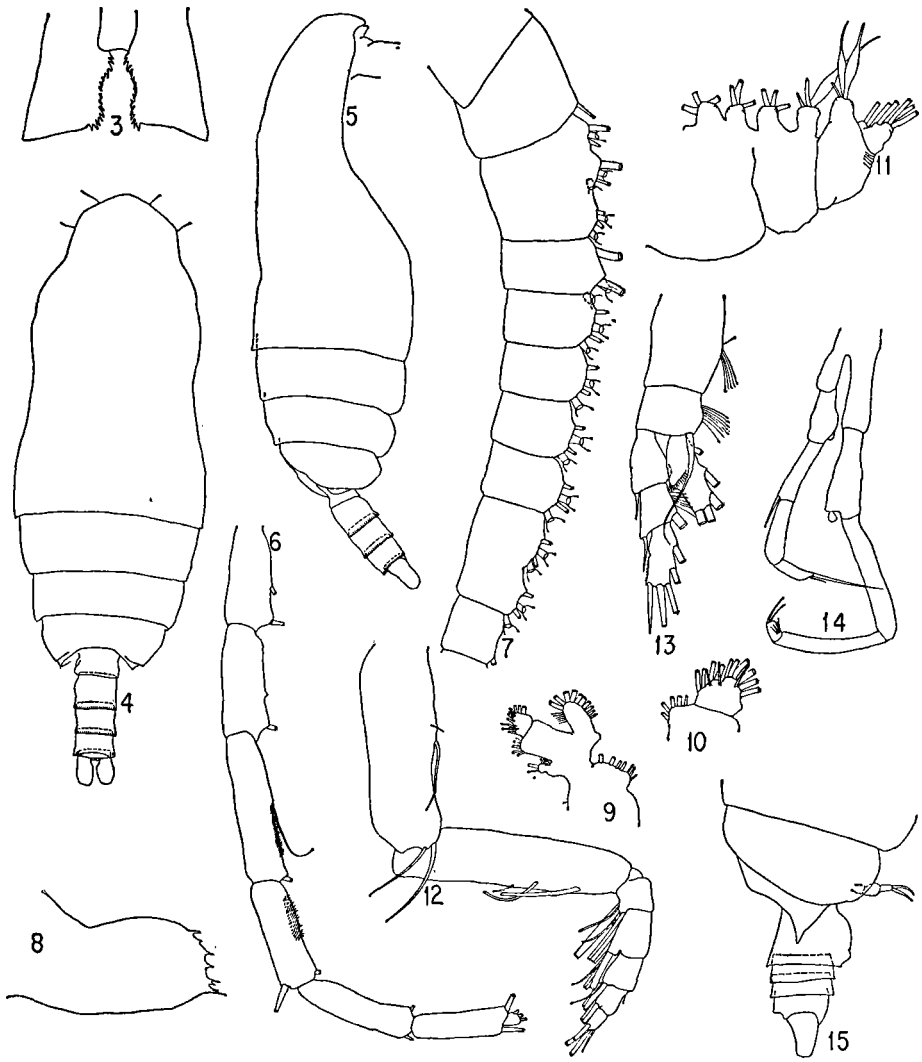
WITH, CARL

1915. Copepoda, I: Calanoida Amphascandria. *In* Danish *Ingolf*-Expedition, vol. 3, no. 4, pp. 1–260, text-figs. 1–79, pls. 1–8.

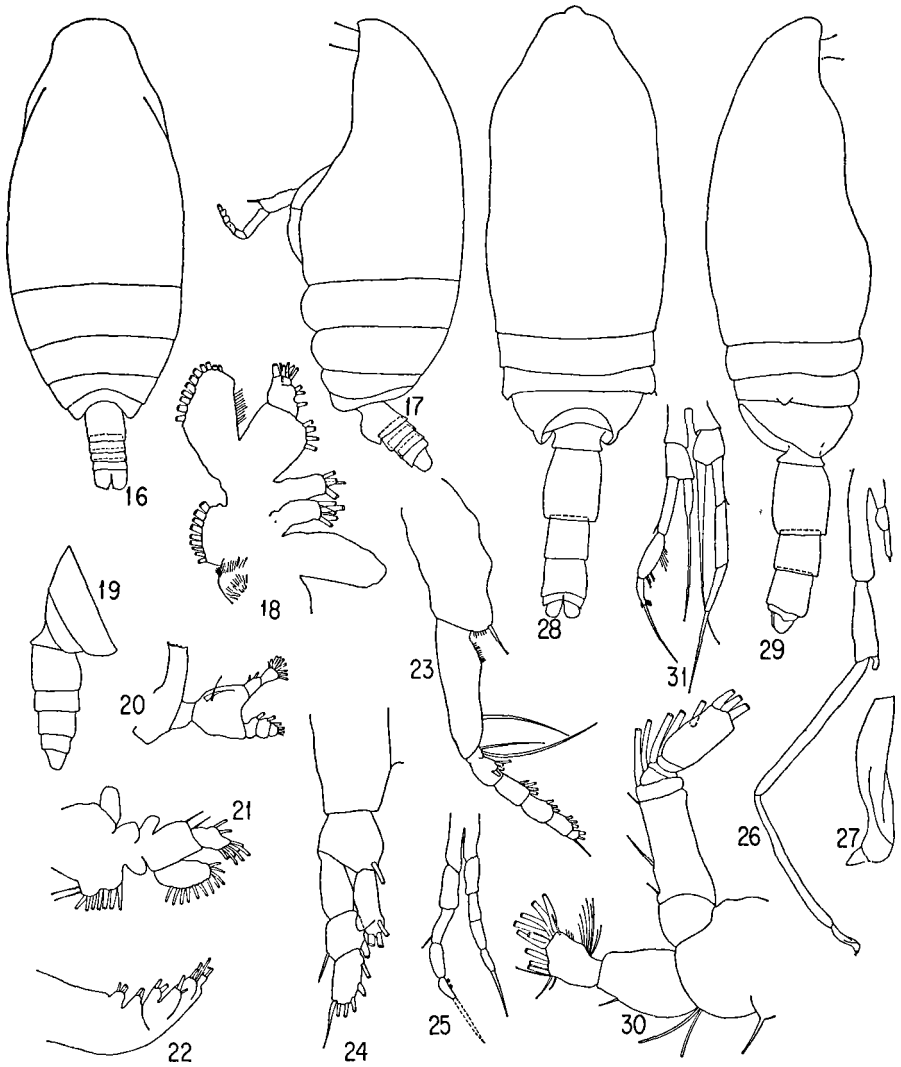
WOLFENDEN, RICHARD NORRIS

1904. Notes on the Copepoda of the North Atlantic Sea and the Faröe Channel. Journ. Mar. Biol. Assoc. U.K., n.s., vol. 7, pp. 110–146, pl. 9.

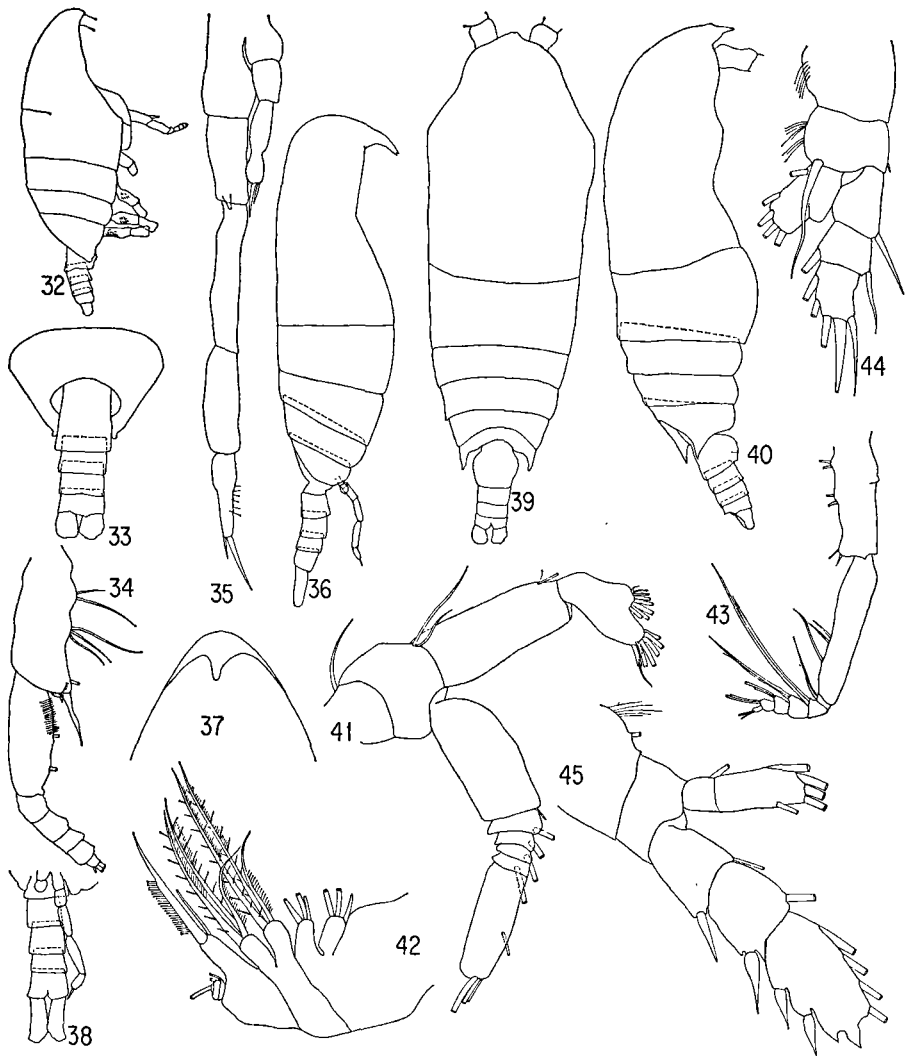
1911. Die marinen Copepoden der Deutschen Südpolar-Expedition 1901–1903, II: Die pelagischen Copepoden der Westwinddrift und des südlichen Eismeers. *In* Deutsche Südpolar-Expedition, vol. 12 (Zool. 4), pp. 181–380, text-figs. 1–82, pls. 22–41.



FIGURES 3–15.—*Calanus australis*, female: 3, first basipodal segments of fifth feet. *Farrania frigida*, male: 4, dorsal view; 5, lateral view; 6, distal end of right first antenna; 7, proximal end of right first antenna; 8, mandible blade; 9, first maxilla (first inner lobe omitted); 10, second basal segment and endopod of first maxilla; 11, second maxilla; 12, maxilliped; 13, first foot; 14, fifth foot; 15, female, posterior end of thorax and abdomen.



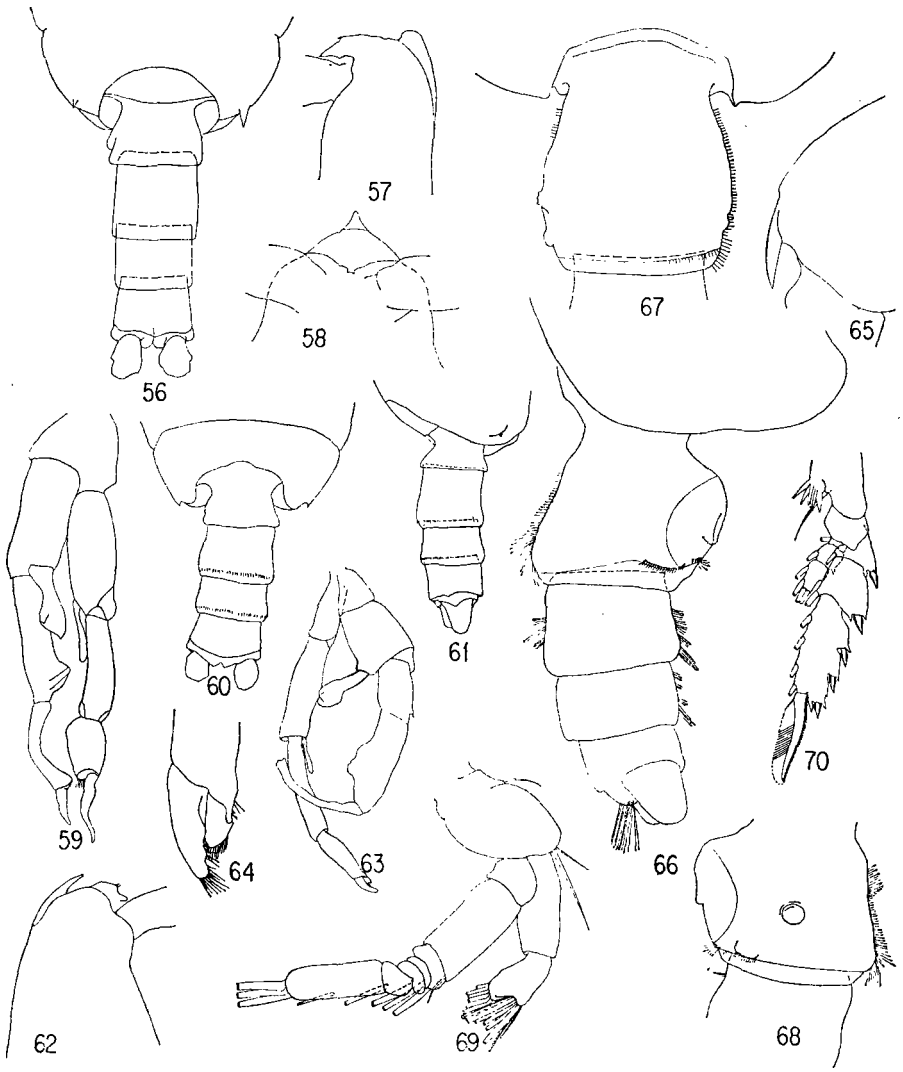
FIGURES 16–31.—*Mimocalanus inflatus?*, female: 16, dorsal view; 17, lateral view; 18, first maxilla (spines on inner lobe omitted). *Mimocalanus* species, male: 19, posterior end of thorax and abdomen, lateral view; 20, mandible; 21, first maxilla; 22, second maxilla; 23, maxilliped; 24, first foot; 25, fifth feet. *Spinocalanus longipes*, male: 26, fifth feet; 27, terminal segment of left fifth foot. *Spinocalanus validus*, male: 28, dorsal view; 29, lateral view; 30, second antenna; 31, fifth feet.



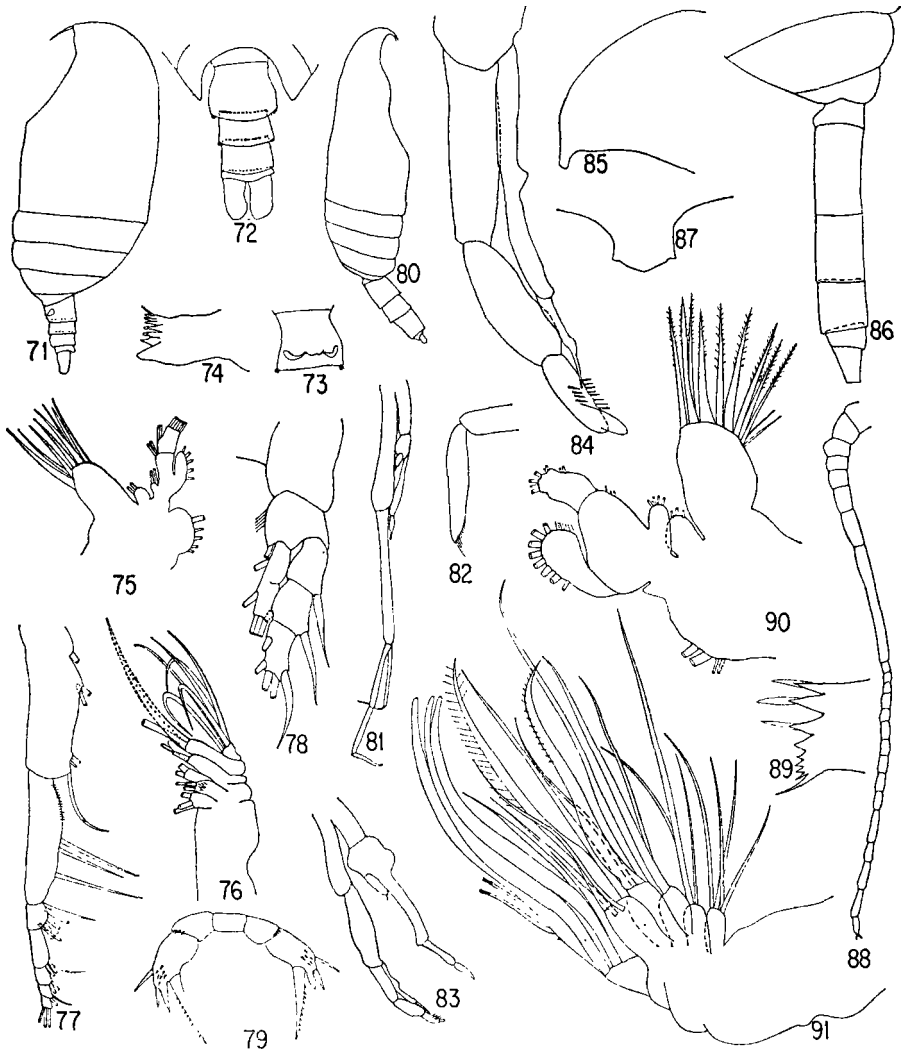
FIGURES 32–45.—*Spinocalanus ventriosus*, new species, female: 32, lateral view; 33, fifth thoracic segment and abdomen, dorsal view; 34, maxilliped (setae on distal segments omitted). *Spinocalanus* species, male: 35, fifth feet. *Teneriforma naso*, male: 36, lateral view; 37, anterior end of head, ventral view; 38, fifth feet and abdomen, ventral view. *Aetideopsis retusa*, new species, female: 39, dorsal view; 40, lateral view; 41, second antenna; 42, second maxilla; 43, maxilliped; 44, first foot; 45, second foot (terminal spine on exopod broken off).



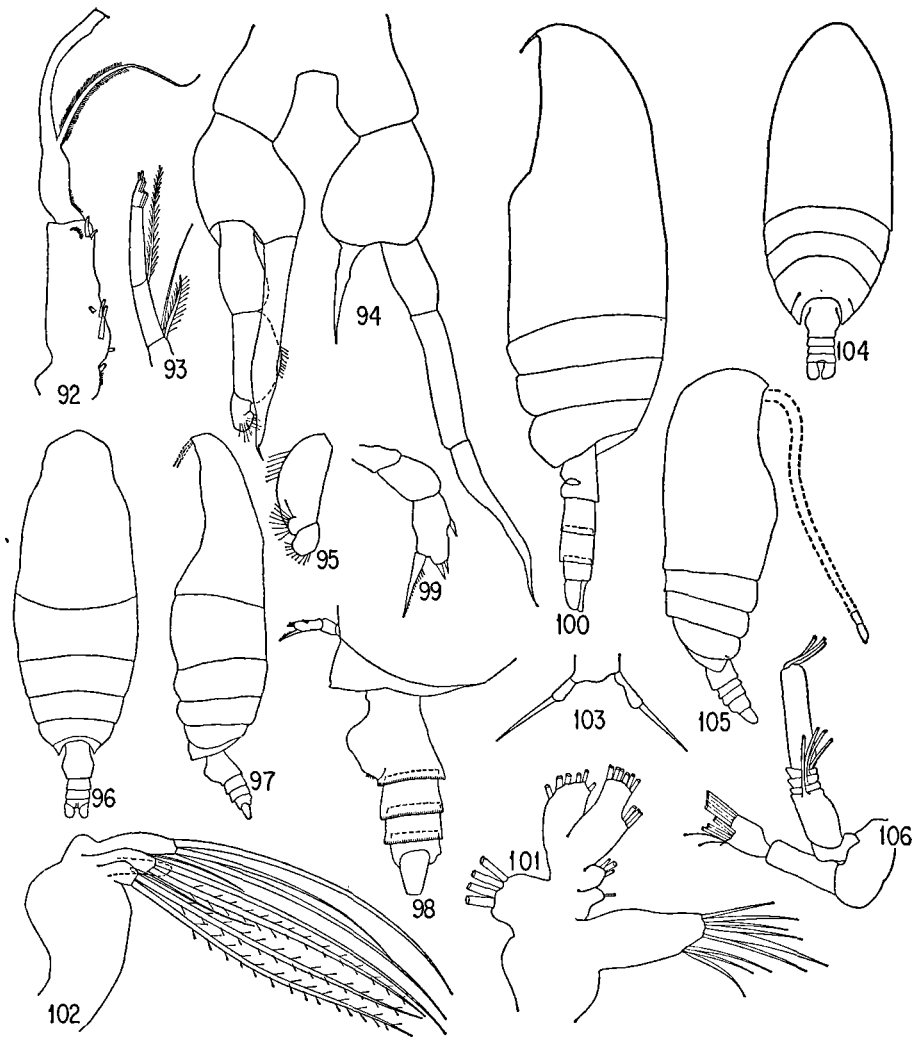
FIGURES 46–55.—*Bradyetes florens*, new species, female: 46, dorsal view; 47, lateral view; 48, second antenna; 49, mandible palpus; 50, mandible blade; 51, first maxilla; 52, second maxilla; 53, maxilliped; 54, first foot. *Chirundinella cara*, female: 55, head, lateral view.



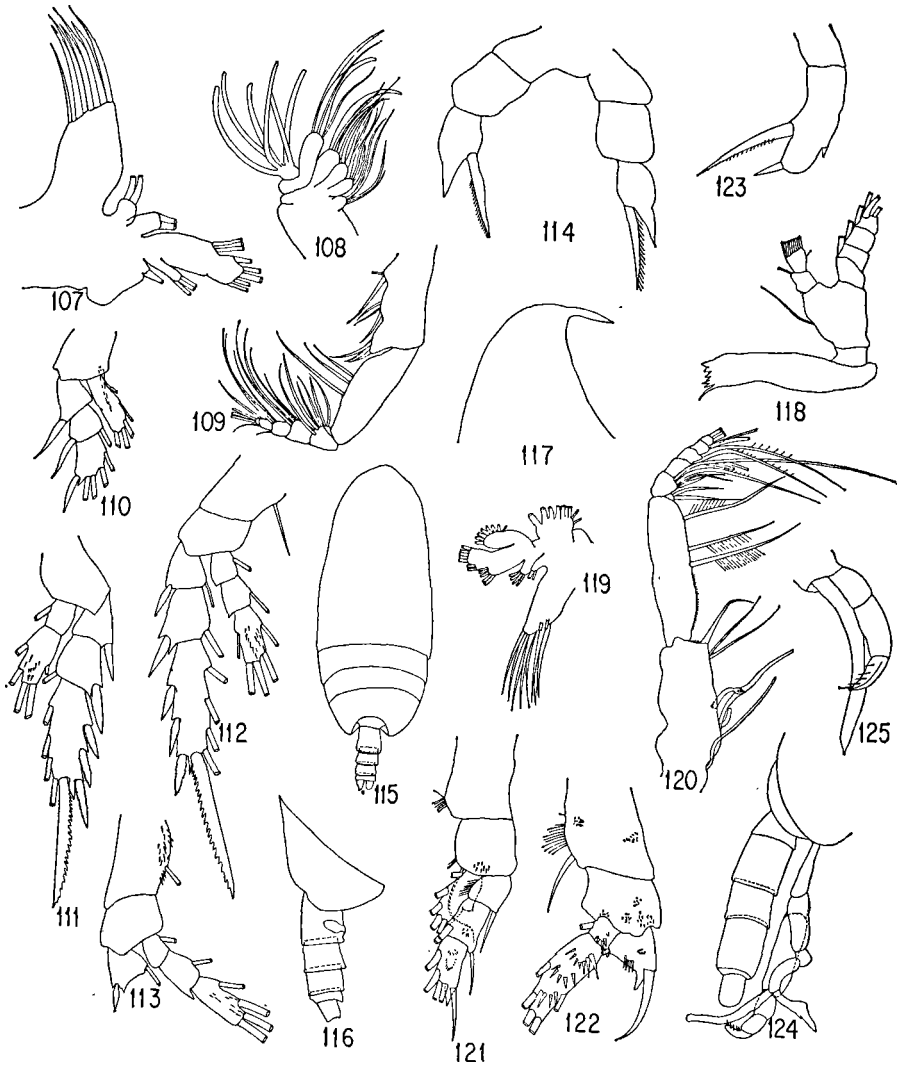
FIGURES 56–70.—*Gaetanus ferox*, male: 56, fifth thoracic segment and abdomen, dorsal view; 57, anterior end of head, lateral view; 58, anterior end of head, ventral view; 59, fifth feet. *Gaidius robustus*, male: 60, fifth thoracic segment and abdomen, dorsal view; 61, fifth thoracic segment and abdomen, lateral view; 62, anterior end of head, lateral view; 63, fifth feet; 64, distal end of left fifth foot. *Pseudochirella squalida*, new species, female: 65, anterior end of head, lateral view; 66, abdomen, lateral view; 67, genital segment, dorsal view; 68, genital segment, left side; 69, second antenna; 70, fourth foot.



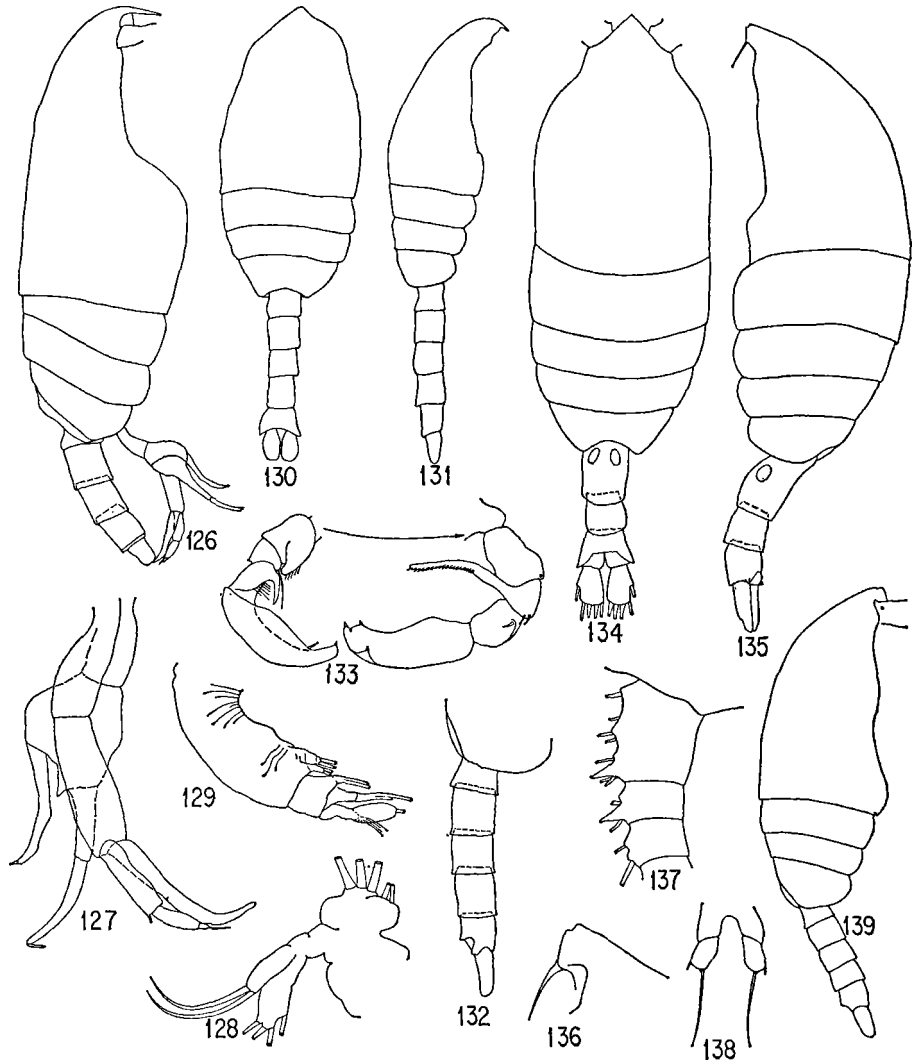
FIGURES 71–91.—*Xanthocalanus hispidus*, new species, female: 71, lateral view; 72, fifth thoracic segment and abdomen, dorsal view; 73, genital segment, ventral view; 74, mandible blade; 75, first maxilla; 76, second maxilla; 77, maxilliped; 78, first foot; 79, fifth feet. *Amallothrix indica*, male: 80, lateral view; 81, fifth feet; 82, distal end of left fifth foot. *Amallothrix paravalida*, male: 83, fifth feet; 84, left fifth foot. *?Racovitzanus* species, male: 85, anterior end of head, lateral view; 86, posterior end of thorax and abdomen, lateral view; 87, rostrum, ventral view; 88, right first antenna; 89, mandible blade; 90, first maxilla; 91, second maxilla.



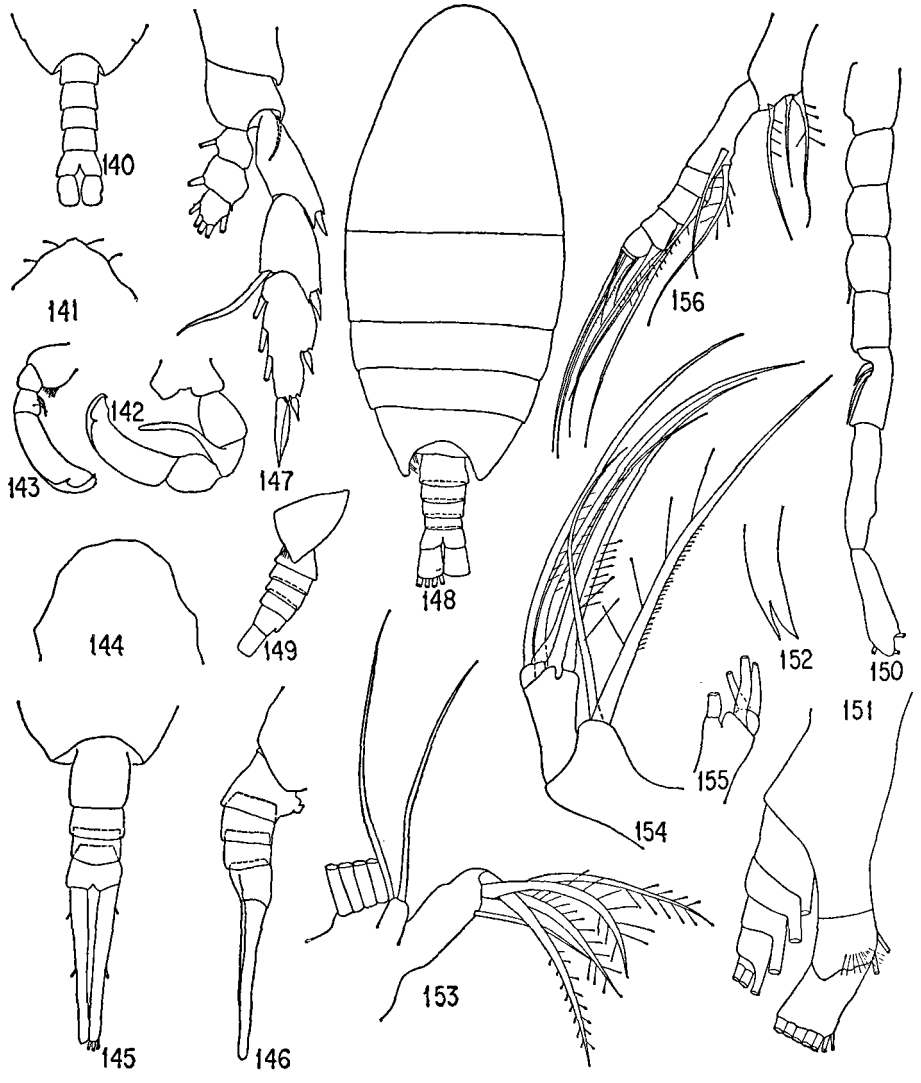
FIGURES 92–106.—?*Racovitzanus* species, male: 92, basipodal segments of maxilliped; 93, distal segments of maxilliped (enlarged); 94, fifth feet; 95, distal segments of left fifth foot. *Scaphocalanus bogorovi*, female: 96, dorsal view; 97, lateral view; 98, fifth thoracic segment and abdomen, lateral view; 99, fifth foot. *Scolecithricella grata*, new species, female: 100, lateral view; 101, first maxilla; 102, second maxilla; 103, fifth feet. *Scolecithricella maritima*, new species, female: 104, dorsal view; 105, lateral view; 106, second antenna.



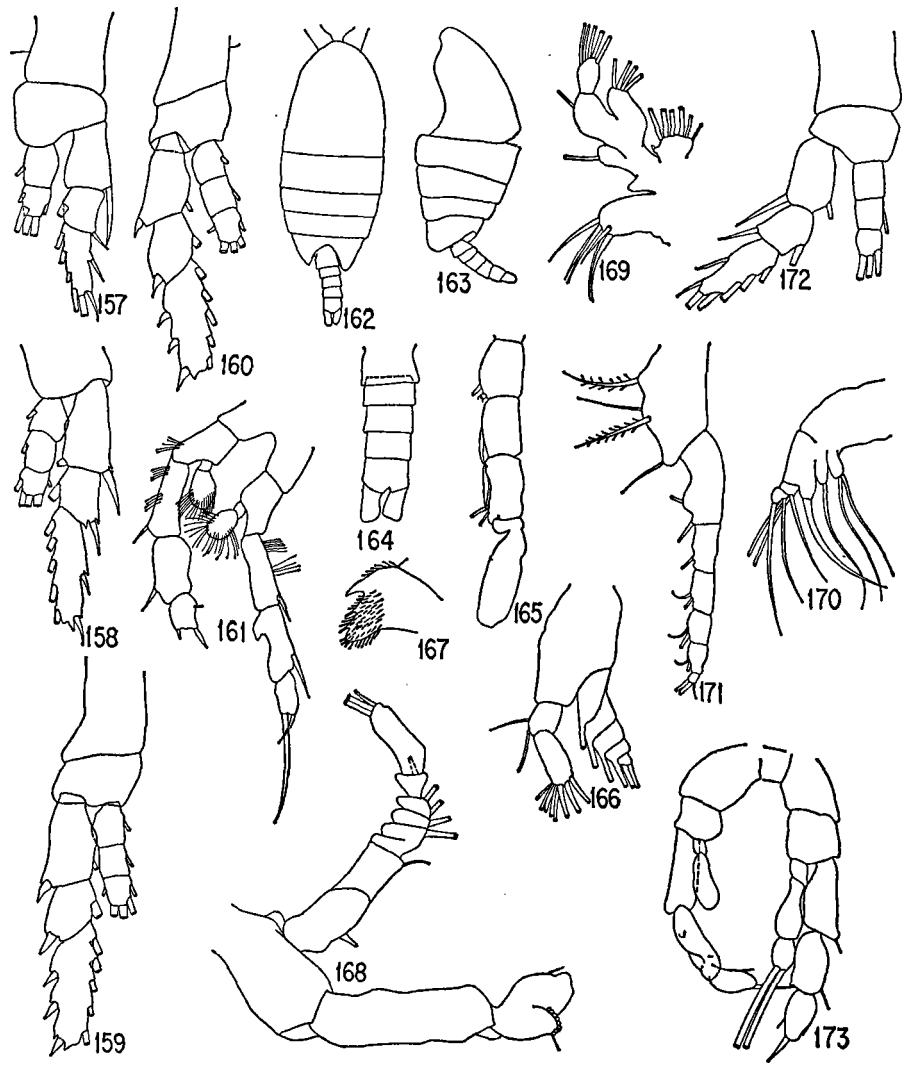
FIGURES 107–125.—*Scolecithricella maritima,* new species, female: 107, first maxilla; 108, second maxilla; 109, maxilliped; 110, first foot; 111, second foot; 112, third foot; 113, fourth feet (second and third exopodal segments broken off); 114, fifth feet. *Scolecithricella timida,* female: 115, dorsal view; 116, fourth and fifth thoracic segments and abdomen, lateral view; 117, anterior end of head, lateral view; 118, mandible; 119, first maxilla; 120, maxilliped; 121, first foot; 122, second foot (second and third exopodal segments broken off); 123, fifth foot. *Scolecithricella,* species, male: 124, abdomen and fifth feet, lateral view; 125, distal end of left fifth foot (enlarged).



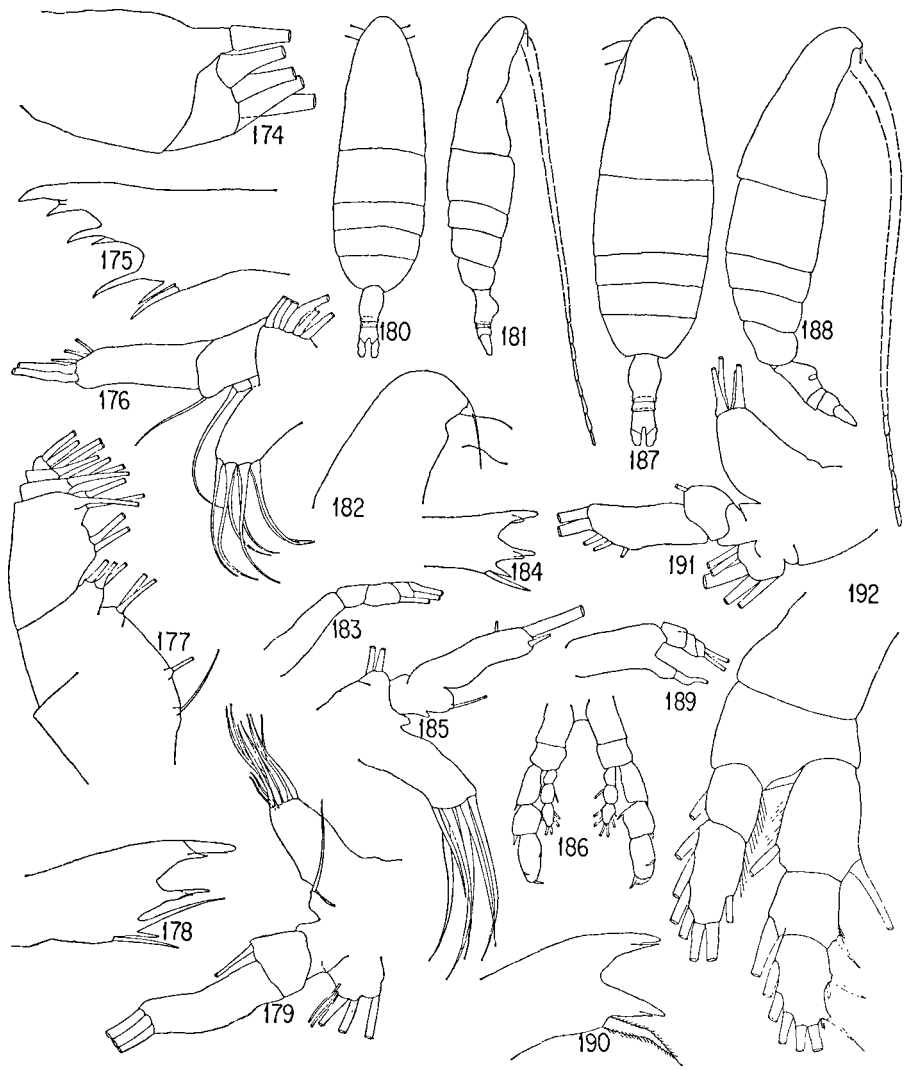
FIGURES 126–139.—*Scolecithrix fowleri*, male: 126, lateral view; 127, fifth feet; 128, first maxilla; 129, second maxilla. *Metridia boecki?*, male: 130, dorsal view; 131, lateral view; 132, fifth thoracic segment and abdomen, lateral view; 133, fifth feet. *Metridia effusa*, new species, female: 134, dorsal view; 135, lateral view; 136, anterior end of head, lateral view; 137, proximal end of first antenna; 138, fifth feet; 139, male, lateral view.



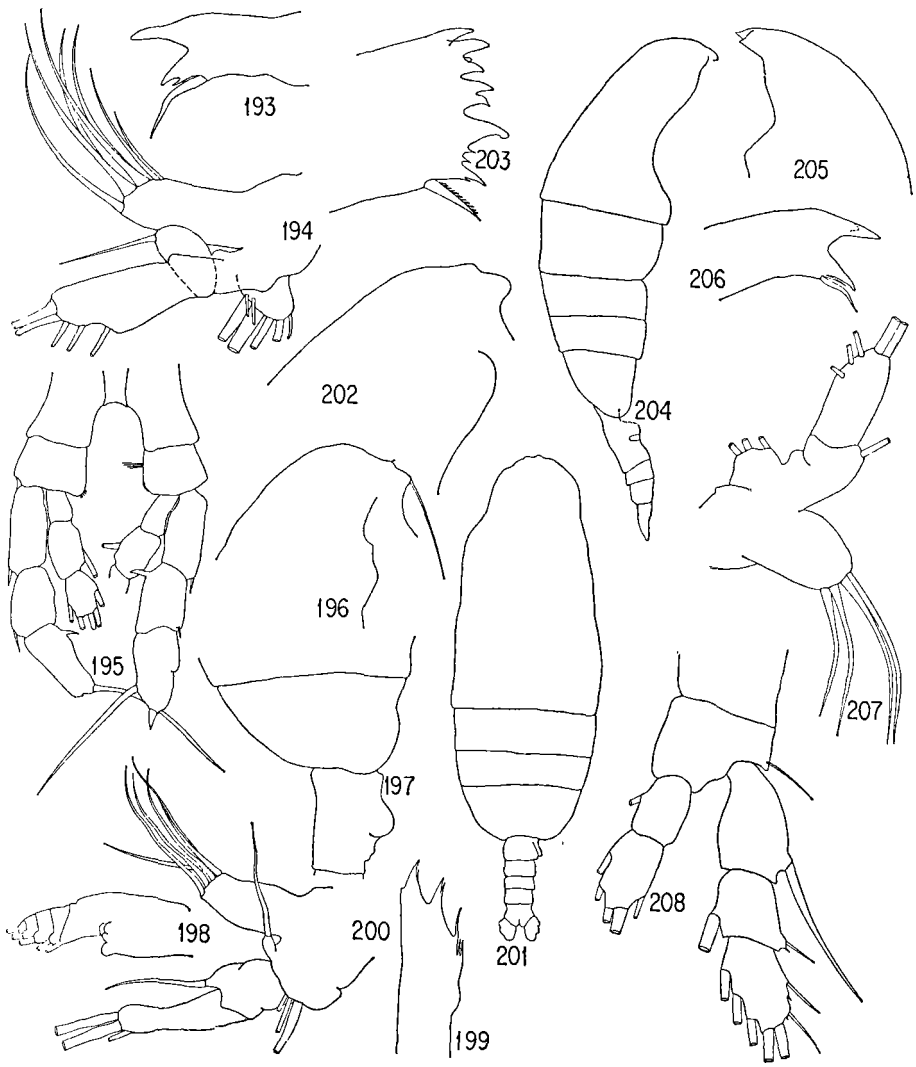
FIGURES 140–156.—*Metridia effusa*, new species, male: 140, fourth and fifth thoracic segments and abdomen, dorsal view; 141, anterior end of head, dorsal view; 142, right fifth foot; 143, left fifth foot. *Lucicutia major*, female: 144, anterior end of head, dorsal view; 145, fifth thoracic segment and abdomen, dorsal view; 146, fifth thoracic segment and abdomen, lateral view; 147, fifth foot. *Disco inflatus*, male: 148, dorsal view; 149, fifth thoracic segment and abdomen, lateral view; 150, distal segments of left first antenna; 151, mandible palpus; 152, mandible blade; 153, first maxilla; 154, second maxilla; 155, distal end of second maxilla, other side; 156, maxilliped.



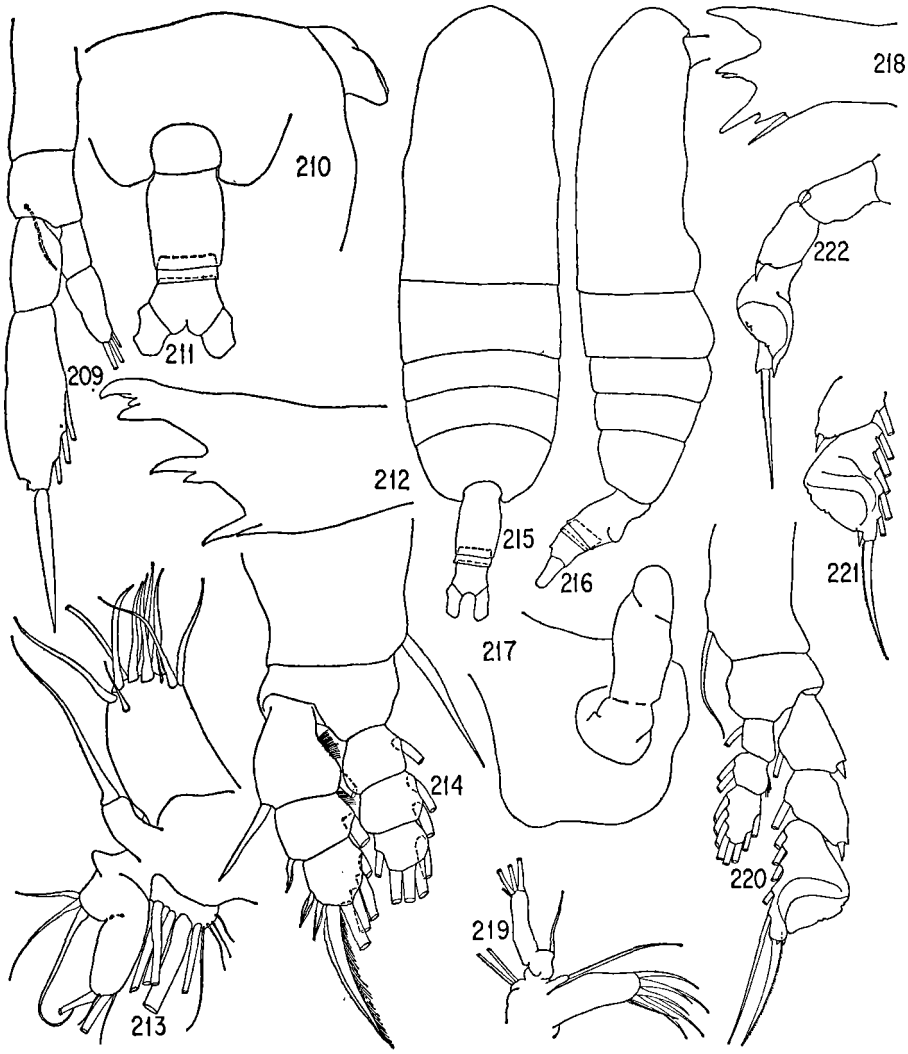
FIGURES 157–173.—*Disco inflatus*, male: 157, first foot; 158, second foot (terminal spine broken off); 159, third foot (terminal spine broken off); 160, fourth foot (terminal spine broken off); 161, fifth feet. *Disco* species, male: 162, dorsal view; 163, lateral view; 164, abdomen dorsal view; 165, segments 15–18 of left first antenna; 166, mandible palpus; 167, mandible blade; 168, second antenna (distal setae of endopod broken off); 169, first maxilla; 170, second maxilla; 171, maxilliped; 172, first foot; 173, fifth feet.



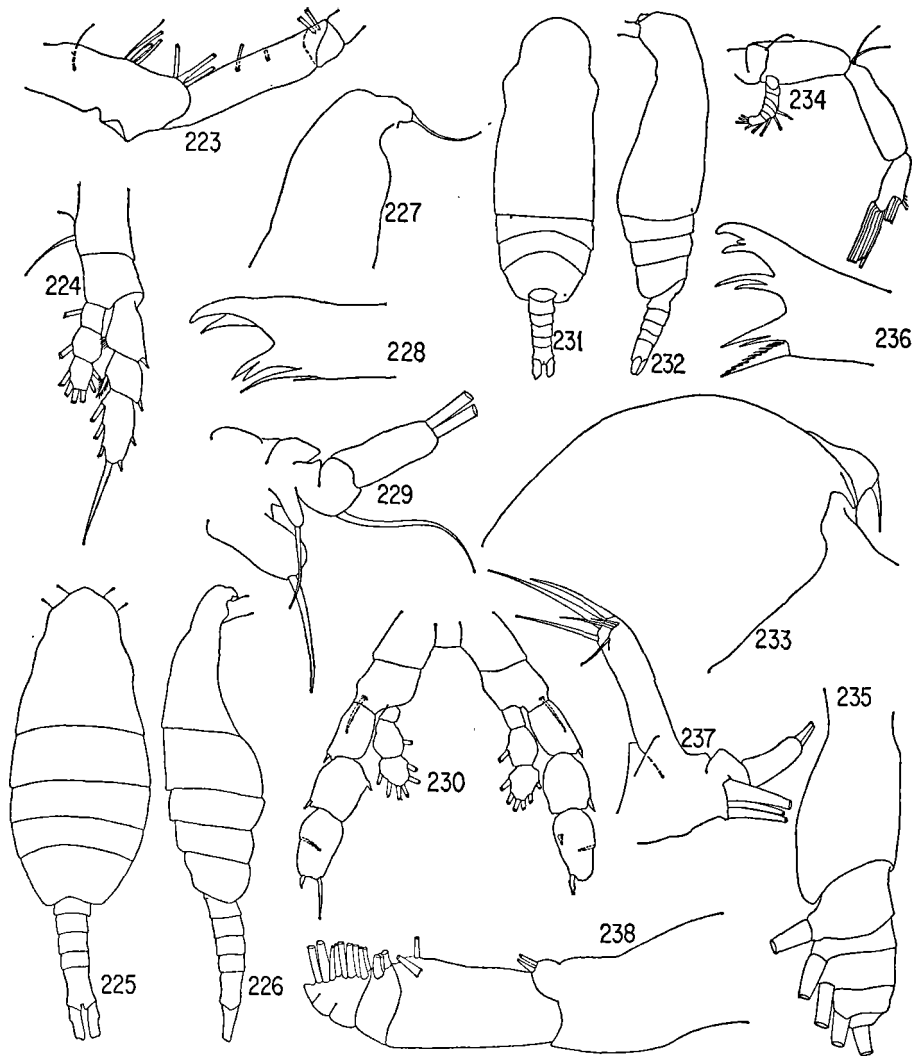
FIGURES 174–192.—*Euaugaptilus brodskyi*, female: 174, mandible palpus; 175, mandible blade; 176, first maxilla; 177, second maxilla; 178, male, mandible blade; 179, first maxilla. *Euaugaptilus curtus*, new species, female: 180, dorsal view; 181, lateral view; 182, anterior portion of head, lateral view; 183, mandible palpus; 184, mandible blade; 185, first maxilla; 186, male, fifth feet. *Euaugaptilus fundatus*, new species, female: 187, dorsal view; 188, lateral view; 189, mandible palpus; 190, mandible blade; 191, first maxilla; 192, first foot.



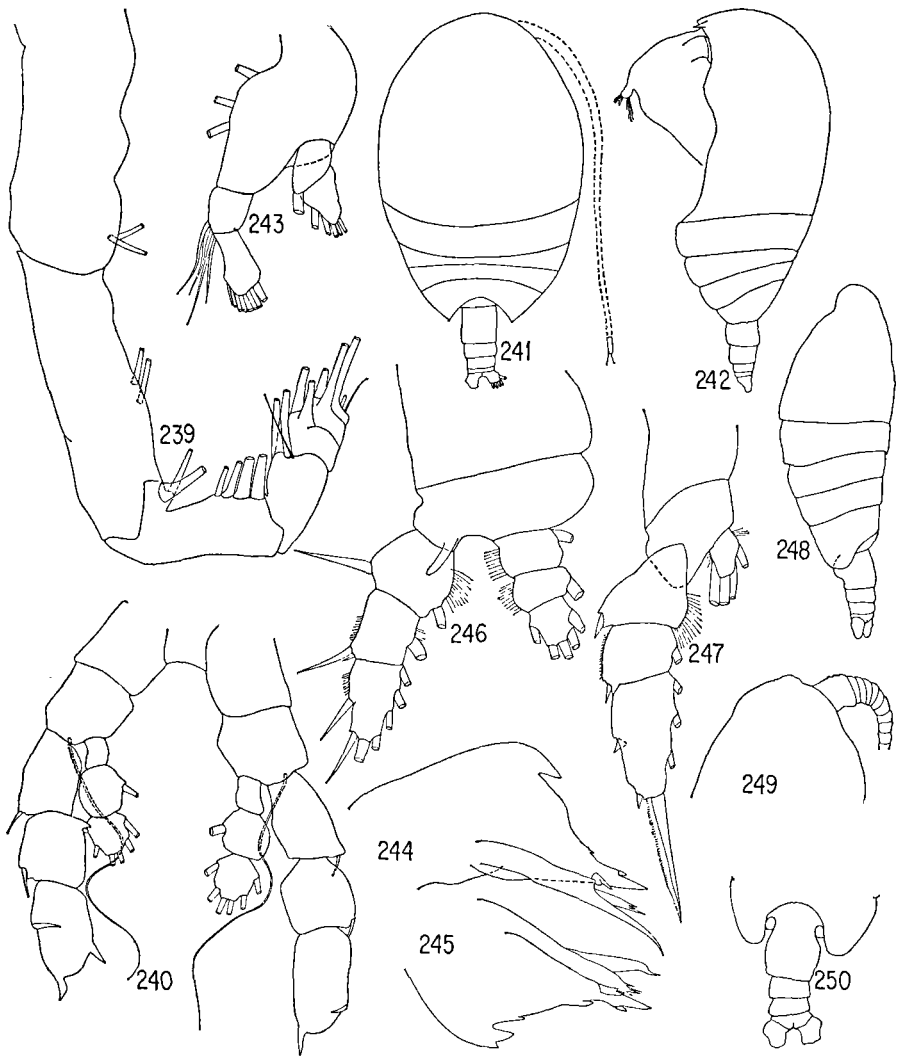
FIGURES 193–208.—*Euaugaptilus longiseta*, male: 193, mandible blade; 194, first maxilla; 195, fifth feet (terminal segment of right endopod incomplete). *Euaugaptilus malacus*, new species, female: 196, anterior portion of head, lateral view; 197, fifth thoracic segment and genital segment; 198, mandible palpus; 199, mandible blade; 200, first maxilla. *Euaugaptilus nodifrons*, male: 201, dorsal view; 202, anterior portion of head, lateral view; 203, mandible blade. *Euaugaptilus quaesitus*, new species, female: 204, lateral view; 205, anterior portion of head, lateral view; 206, mandible blade; 207, first maxilla; 208 first foot.



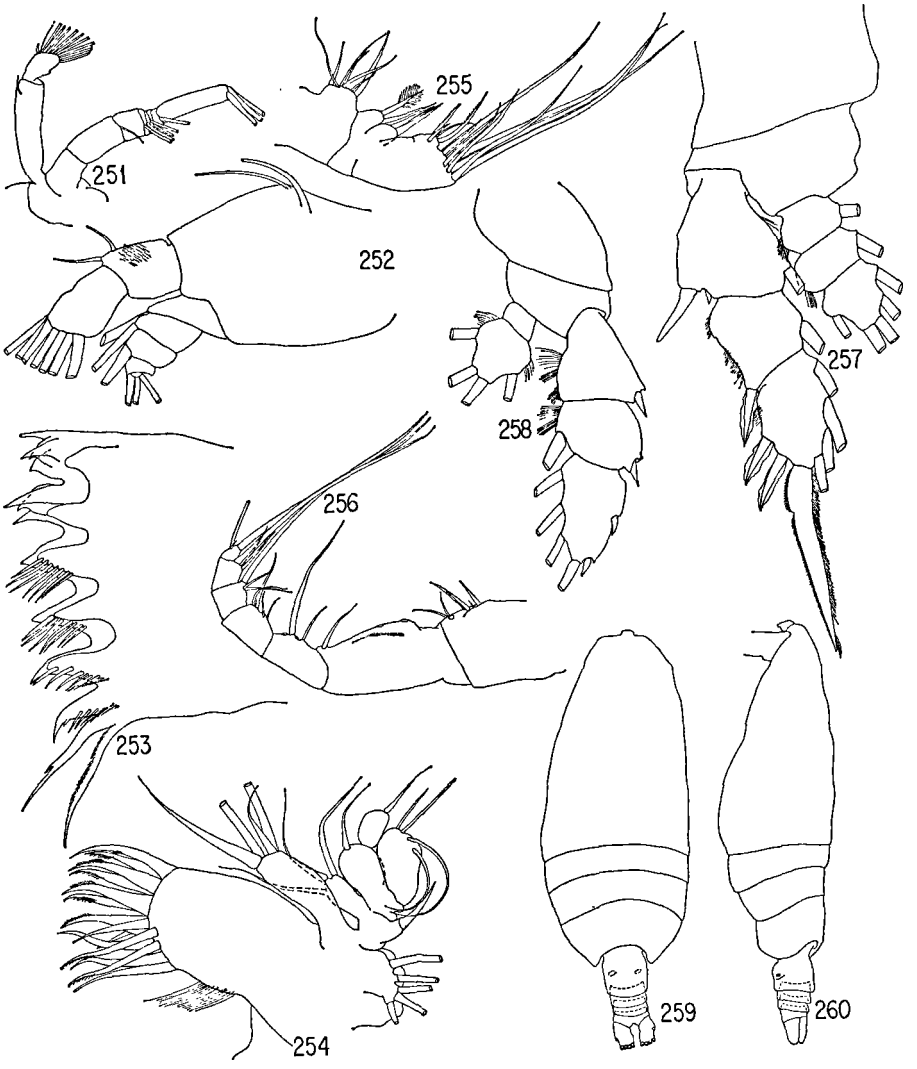
FIGURES 209–222.—*Euaugaptilus quaesitus*, new species, female: 209, fifth foot. *Euaugaptilus rectus*, new species, female: 210, anterior portion of head, lateral view; 211, abdomen, dorsal view; 212, mandible blade; 213, first maxilla; 214, first foot. *Euaugaptilus* species 1, female: 215, dorsal view; 216, lateral view; 217, mandible palpus with basis of mandible blade; 218, mandible blade; 219, first maxilla; 220, third foot, anterior side; 221, second and third exopodal segments of third foot, posterior side; 222, exopod of left third foot, external side.



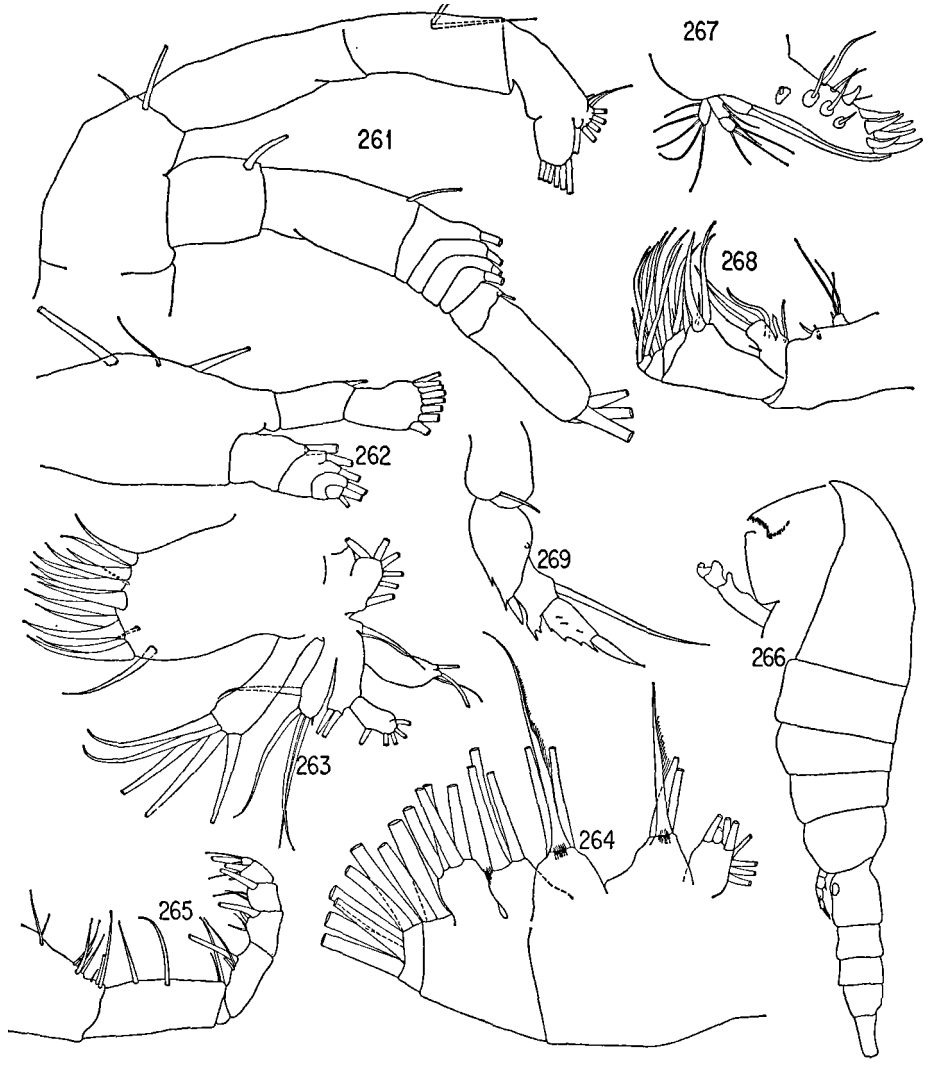
FIGURES 223–238.—*Euaugaptilus* species 1, female: 223, basipodal segments of maxilliped; 224, fifth foot. *Euaugaptilus* species 2, male: 225, dorsal view; 226, lateral view; 227, anterior portion of head, lateral view; 228, mandible blade; 229, first maxilla; 230, fifth feet. *Euaugaptilus* species 3, male: 231, dorsal view; 232, lateral view; 233, anterior portion of head, lateral view; 234, second antenna; 235, mandible palpus; 236, mandible blade; 237, first maxilla; 238, second maxilla.



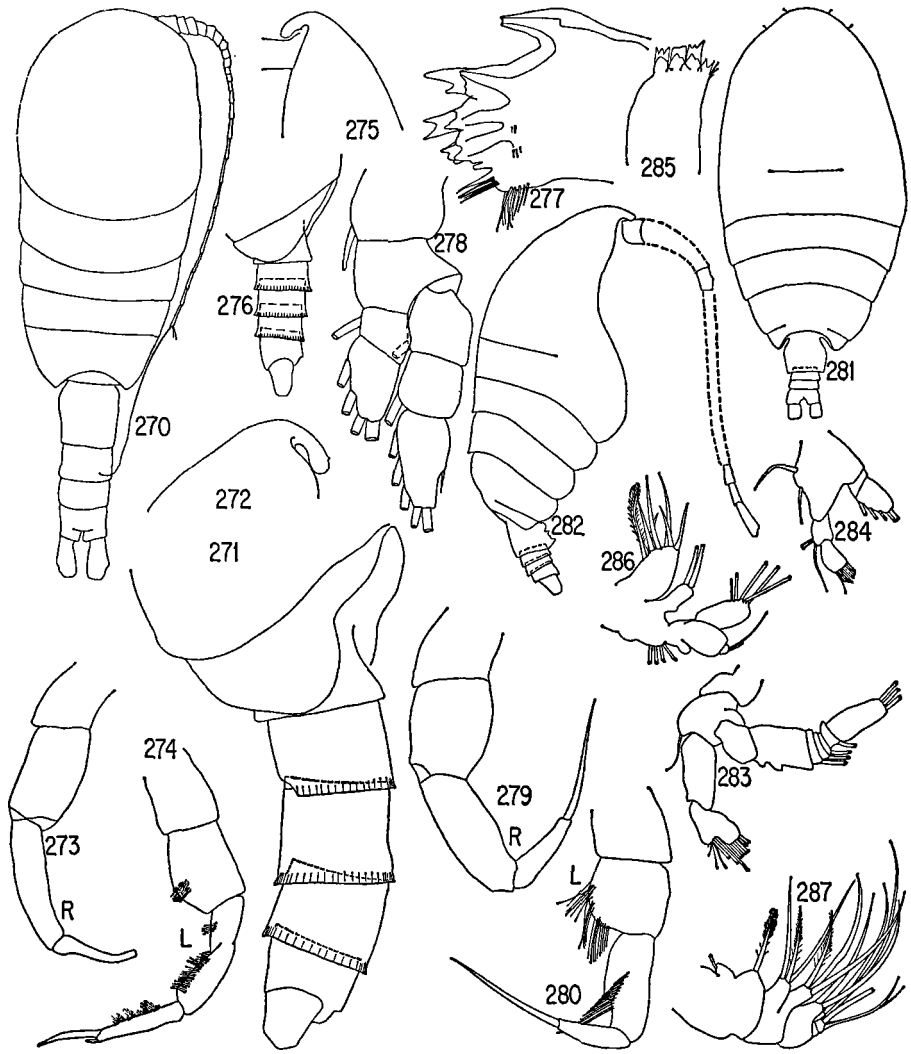
FIGURES 239–250.—*Euaugaptilus* species 3, male: 239, maxilliped; 240, fifth feet. *Pachyptilus abbreviatus*, female: 241 dorsal view; 242, lateral view; 243, mandible palpus; 244, mandible blade; 245, mandible blade, another view; 246, first foot; 247, fifth foot. *Pontoptilus robustus*, female: 248, lateral view; 249, anterior portion of head, dorsal view; 250, fifth thoracic segment and abdomen, dorsal view.



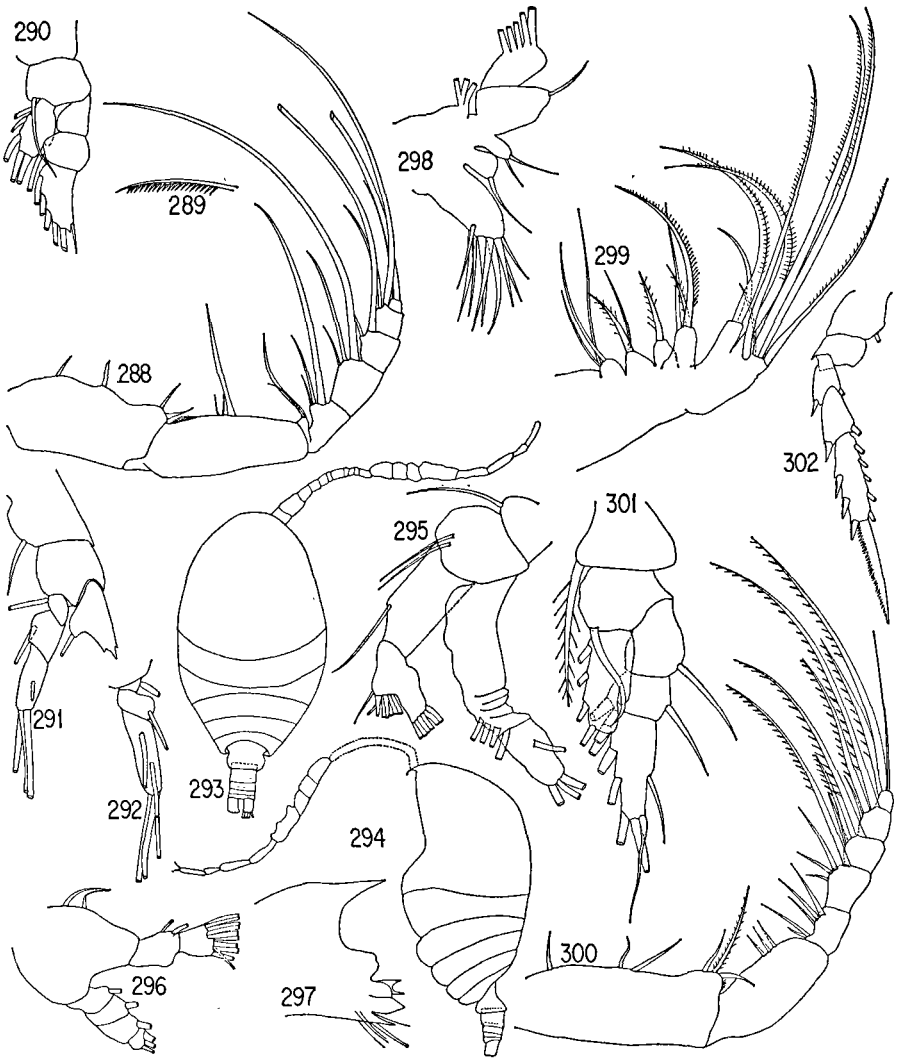
FIGURES 251–260.—*Pontoptilus robustus*, female: 251, second antenna; 252, mandible palpus; 253, mandible blade; 254, first maxilla; 255, second maxilla; 256, maxilliped; 257, first foot; 258, fifth foot. *Pontoptilus lacertosus*, new species, female: 259, dorsal view; 260, lateral view.



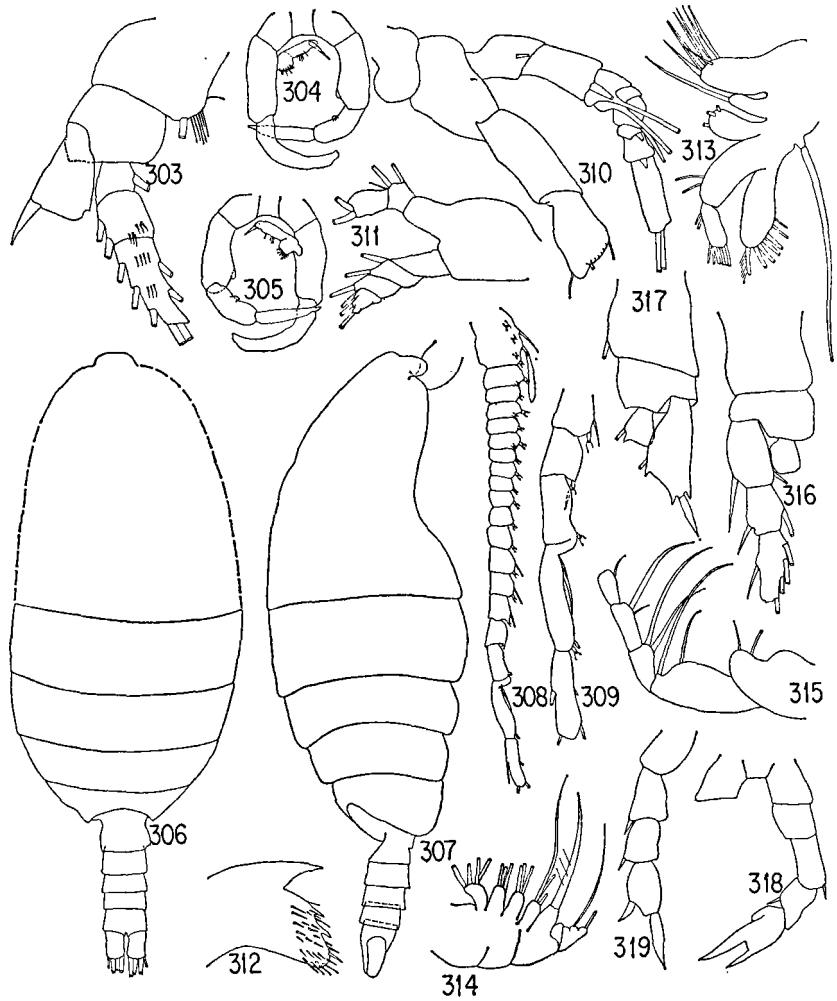
FIGURES 261–269.—*Pontoptilus lacertosus*, new species, female: 261, second antenna; 262, mandible palpus; 263, first maxilla; 264, second maxilla; 265, maxilliped. *Phyllopus muticus*, female: 266, lateral view; 267, first maxilla; 268, second maxilla; 269, fifth foot.



FIGURES 270–287.—*Phyllopus muticus*, female: 270, dorsal view. *Bathypontia elongata*, male: 271, fifth thoracic segment and abdomen, lateral view; 272, anterior portion of head, lateral view; 273, right fifth foot; 274, left fifth foot. *Bathypontia regalis*, new species, male: 275, anterior portion of head, lateral view; 276, fifth thoracic segment and abdomen, lateral view; 277, mandible blade; 278, first foot; 279, right fifth foot; 280, left fifth foot. *Rhinomaxillaris bathybia*, new genus and new species, female: 281, dorsal view; 282, lateral view; 283, second antenna; 284, mandible palpus; 285, mandible blade; 286, first maxilla; 287, second maxilla.



FIGURES 288–302.—*Rhinomaxillaris bathybia*, new genus and new species, female: 288, maxilliped; 289, distal portion of strong spine on maxilliped, enlarged; 290, first foot; 291, fourth foot (exopod incomplete); 292, endopod of fourth foot, another view. *Zenkevitchiella crassa*, new species, male: 293, dorsal view; 294, lateral view; 295, second antenna; 296, mandible palpus; 297, mandible blade; 298, first maxilla; 299, second maxilla; 300, maxilliped; 301, first foot; 302, third foot (endopod omitted).



FIGURES 303–319.—*Zenkevitchiella crassa*, new species, male: 303, second foot (exopod incomplete); 304, fifth feet, posterior side; 305, fifth feet; anterior side. *Unidentified* male: 306, dorsal view; 307, lateral view; 308, left first antenna; 309, distal segments of left first antenna (enlarged); 310, second antenna; 311, mandible palpus; 312, mandible blade; 313, first maxilla; 314, second maxilla; 315, maxilliped; 316, first foot (endopod incomplete); 317, third foot (exopod and endopod incomplete); 318, left fifth foot with first segment of right fifth foot; 319, right fifth foot without first segment.

Reprinted from *Proc. U.S. Nat. Mus.*, vol. 122, no. 3,586, 1967, p. 1-32

Proceedings of the United States National Museum

SMITHSONIAN INSTITUTION • WASHINGTON, D.C.

Volume 122 1967 Number 3586

NEW CYCLOPOID COPEPODS ASSOCIATED WITH THE CORAL PSAMMOCORA CONTIGUA (ESPER) IN MADAGASCAR

By ARTHUR G. HUMES AND JU-SHEY HO [1]

Several species of copepods are known to live in association with madreporarian corals in the region of Nosy Bé, in northwestern Madagascar (Humes, 1962a, 1962b; Humes and Frost, 1964). Only one of these, *Kombia angulata* Humes, 1962, has been recovered from the genus *Psammocora* (family Thamnasteriidae), that is to say, from *Psammocora* species.

An examination of *Psammocora contigua* (Esper) from Ambariobe, a small island situated nearly between Nosy Bé and Nosy Komba, has revealed the four new associated copepods described in this paper.

All collections were made by the senior author while participating in the activities of the U.S. Program in Biology of the International Indian Ocean Expedition at Nosy Bé in 1963–64.

The study of the material has been aided by a grant (GB–1809) from the National Science Foundation.

All figures have been drawn with the aid of a camera lucida. The letter after the explanation of each figure refers to the scale at which it was drawn. Abbreviations used in figures: A_1=first antenna, A_2=second antenna, L=labrum, MD=mandible, P=paragnath,

[1] Both authors: Department of Biology, Boston University, Boston, Massachusetts.

MX_1=first maxilla, MX_2=second maxilla, MXPD=maxilliped, P_1= first leg.

We wish to thank Dr. Michel Pichon for the identification of the coral and to express our appreciation for the many courtesies received from the staff of the Centre d'Océanographie et des Pêches at Nosy Bé.

Family Xarifiidae Humes, 1960

Genus *Xarifia* Humes, 1960

Xarifia diminuta, new species

FIGURES 1–24

TYPE MATERIAL.—148 ♀♀ and 262 ♂♂ washed from a colony of the coral *Psammocora contigua* (Esper) in a depth of 1 m, southeast of Ambariobe, near Nosy Bé, Madagascar. Collected Sept. 6, 1963. Holotype female, allotype, and 155 paratypes (50 ♀♀, 105 ♂♂) deposited in the United States National Museum, Washington; 80 paratypes (30 ♀♀, 50 ♂♂) in the Museum of Comparative Zoology, Cambridge, and in the Zoölogisch Museum, Amsterdam; and the remaining paratypes in the collection of A. G. Humes.

OTHER SPECIMENS (all from *Psammocora contigua* in 1–2 m at Ambariobe, collected during 1963).—10 ♀♀, 2♂♂, Sept. 6; 143 ♀♀, 87 ♂♂, Sept. 8; 173 ♀♀, 116 ♂♂, Sept. 17; and 65 ♀♀, 30 ♂♂, Oct. 6.

FEMALE.—Body (figs. 1, 2) moderately slender, about five times longer than wide. Length (not including setae on caudal rami) 0.98 mm (0.78–1.18 mm), greatest width 0.18 mm (0.14–0.21 mm), based on 10 specimens. Segmentation not defined externally. Region dorsal to fifth legs bearing three long, posteriorly directed processes, median one only slightly shorter than lateral ones. Genital and postgenital segments together (fig. 3) less than one-fifth total body length. Areas of attachment of egg sacs dorsal in position. Behind these areas a pair of minute ventrolateral setules. Caudal ramus (fig. 4) 45μ x 17μ (width taken at middle), about 2.65 times longer than wide; with four short naked setae (one outer and subterminal, others terminal) and a few minute setules. Egg sac (fig. 5), in one female 290μ x 198μ, containing usually five eggs in a flattened cluster (in some females six or seven), eggs about 97μ in average diameter.

Rostral area protuberant in lateral view (fig. 6) between bases of first antennae and bearing relatively long slender setules (fig. 7). First antenna (fig. 7) short (48μ in length without setae) and apparently 3-segmented, though middle segment showing partial division. With numerous naked setae, armature being 3, 20+1 aesthete, and 8+2 aesthetes. Second antenna (fig. 8) 4-segmented, formula being

1, 1, 2, and I,1 (the Roman numeral referring to the claw). Recurved claw on last segment 6μ in length, slender seta 17μ.

Labrum with posteroventral border having two widely separated lateral lobes (fig. 9). Mandible (fig. 10) with an attenuated blade concealed in ventral view under posterior part of labrum (see fig. 9). Paragnath absent. First maxilla (fig. 11) a small rounded lobe bearing two naked setae. Second maxilla (fig. 12) probably 2-segmented, though separation of segments not complete. Second segment bearing two inner elements (a slender setule and a stout hyaline seta) and terminating in a finger-like process with a hyaline lamellate inner margin. Maxilliped (fig. 13) 2-segmented, second segment bearing two small naked setae and terminating in 2 irregular lobate processes.

Legs 1–4 with general form and segmentation like that shown for leg 1 in figure 14; exopods 3-segmented (the articulation obscure), endopods 2-segmented. Spine and setal formula as follows (Roman numerals indicating spines, Arabic numerals setae):

P_1	protopod	0–0	1–0	exp	I–0	I–0	I,3
				end	0–0	2	
P_2	protopod	0–0	1–0	exp	I–0	I–0	I,3
				end	0–0	2	
P_3	protopod	0–0	1–0	exp	I–0	I–0	I,2
				end	0–0	0	
P_4	protopod	0–0	1–0	exp	I–0	I–0	I,2
				end	0–0	2	

In all four legs coxa with a slender setule on posterior outer surface; basis with an outer naked seta and an inner tuft of long hairs. Exopod with stout spines recurved posteriorly (fig. 15); three small slender setae at inner base of terminal spine in legs 1 and 2, two such setae in legs 3 and 4. Long hairs arising from inner margins of first and second segments of exopod. Endopod with long hairs on outer margins of both segments; last segments with two terminal setae in legs 1, 2, and 4, but unarmed in leg 3 (fig. 16).

Leg 5 (fig. 17) elongated and slender, with its free segment not clearly delimited from body. Segment about 120μ in length and somewhat irregular in width, tapered distally, bearing two unequal terminal naked setae 13μ and 26μ long. A slender seta arising from body wall dorsal to base of segment. Leg 6 absent.

Color in life in transmitted light slightly reddish brown, eye red, egg sacs orange red to reddish green.

MALE.—Body (figs. 18, 19) rather slender, slightly longer than female. Length 1.15 mm (0.94–1.35 mm), greatest width 0.16 mm (0.13–0.19 mm), based on 10 specimens. Without external segmentation. Caudal ramus (fig. 20) shorter than in female and not distinctly delimited from anal segment.

Rostral area (fig. 21) as in female. First antenna like that of female but with four aesthetes, one being added on midanterior margin of middle segment. Second antenna, labrum (see fig. 21), mandible, first maxilla, and second maxilla resembling those in female. Paragnath absent. Maxilliped (fig. 22) 4-segmented. First segment short and unarmed. Second large and swollen with two inner setae (one sclerotized proximally, other entirely hyaline) and having its distal outer surface minutely punctate. Third segment very short and unarmed. Fourth segment forming a terminal claw 39μ along its axis, bifurcated at its tip, with an outer hyaline lamella and an inner triangular hyaline process; bearing two setae (one sclerotized proximally, other entirely hyaline).

Legs 1–4 as in female, with same spine and setal forumla. Leg 5 (fig. 23) without a distinct segment and consisting of three small setae, the two more ventral ones forming a pair and probably homologous to the two setae on the end of leg 5 in the female. Leg 6 (figs. 19, 23) represented by a ventrolateral flap bearing two small setae.

Spermatophore (fig. 24) elongated, 255μ x 62μ, not including neck.

Color as in female.

ETYMOLOGY.—The specific name *diminuta*, from Latin=diminished, refers to the relatively small size of this species.

METHOD OF COLLECTION AND RELATION TO HOST.—The number of specimens of *X. diminuta* collected from *Psammocora contigua* depended upon the technique employed. When the corals were washed in weakly alcoholized sea water (with about 5 per cent ethyl alcohol) within one or two hours after being brought to the laboratory, few if any *Xarifia* were obtained. After crushing the corals with a hammer, relatively few *Xarifia* were recovered from the debris and mucus. When, however, the corals were left overnight (12–14 hours) in pails of alcoholized sea water, abundant specimens of the copepods were found in the sediment. This is in accord with the observations of Humes (1962a) on the collection of other species of *Xarifia*. Gerlach, as quoted by Humes (1960), observed that living *Xarifia* in *Pocillopora* in the Maldive Islands crawl about on the surface of the coral but may at times enter the polyps where they seem to tear up the tissue of the coral.

COMPARISON WITH RELATED SPECIES.—There are 10 species presently known in the genus *Xarifia*. *X. diminuta* may be distinguished from eight of these which have the endopods of legs 1–4 composed of a single segment (*X. maldivensis* Humes, 1960; *X. fimbriata* Humes, 1960; *X. gerlachi* Humes, 1962; *X. longipes* Humes, 1962; *X. reducta* Humes, 1962; *X. serrata* Humes, 1962; *X. tenuis* Humes, 1962; and *X. infrequens* Humes, 1962). In the two remaining species, *X. dispar* Humes, 1962, and *X. comata* Humes, 1962, the endopods of legs 1–4 are

2-segmented. The new species differs from *X. dispar*, which is larger (both sexes about 1.4 mm in length), has slender spines on the first two segments of the exopods in legs 1–4, has shorter processes on the region dorsal to the fifth legs, and has a terminal seta on the endopod of leg 3. It seems to be close to *X. comata*, with its fifth legs and three processes dorsal to them being similar to those in that species. *X. diminuta* differs from *X. comata*, however, in the following features: the first segment of the exopods of legs 1–4 has a well-developed outer spine (this spine minute in *X. comata*), the second segment of the exopods of legs 1–4 has an outer spine (lacking in *X. comata*), the endopod of leg 3 lacks terminal elements (two setae in *X. comata*), the endopod of leg 4 has two terminal setae (only one in *X. comata*), the terminal spine and seta of the second antenna are very unequal in length (nearly equal in *X. comata*), the egg sac usually contains five eggs (sometimes six or seven) (in *X. comata* usually two, sometimes one, three, or four), and the maxilliped of the male has a form different from that of *X. comata*.

Family Lichomolgidae Kossmann, 1877

Genus *Lichomolgus* Thorell, 1860

Lichomolgus rhadinus, new species

FIGURES 25–51

TYPE MATERIAL.—199 ♀♀, 227 ♂♂, and 9 copepodids washed from the coral *Psammocora contigua* (Esper) in a depth of 2 m, south of Ambariobe, near Nosy Bé, Madagascar. Collected Sept. 8, 1963. Holotype female, allotype, and 160 paratypes (88 ♀♀, 72 ♂♂) deposited in the United States National Museum, Washington; 85 paratypes (35 ♀♀, 50 ♂♂) in the Museum of Comparative Zoology, Cambridge, and in the Zoölogisch Museum, Amsterdam; and the remaining paratypes in the collection of A. G. Humes.

OTHER SPECIMENS (all from *Psammocora contigua* in 1–2 m at Ambariobe, collected during 1963).—33 ♀♀, 18 ♂♂, Sept. 6; 83 ♀♀, 39 ♂♂, Sept. 8; 9 ♀♀, Sept. 17; and 3 ♀♀, 1 ♂, Oct. 6.

FEMALE.—Body (fig. 25) moderately slender. Length (not including setae on caudal rami) 1.00 mm (0.95–1.04 mm) and greatest width 0.35 mm (0.33–0.36 mm), based on 10 specimens. Ratio of length to width of prosome 1.70:1. Segment of leg 1 separated from head by a dorsal furrow. Epimeral areas of metasomal segments formed as illustrated in figure.

Segment of leg 5 (fig. 26) 47μ x 105μ. Between this segment and genital segment a short ventral intersegmental sclerite. Genital segment about as long as wide, 110μ x 108μ, rather abruptly constricted in its posterior fourth. Areas of attachment of egg sacs situated dorsally (only slightly laterally), each area (fig. 27) bearing two small

setae 5μ and 8μ in length. Three postgenital segments 50μ x 55μ, 39μ x 48μ, and 50μ x 47μ from anterior to posterior. Anal segment with a row of minute spinules along its posteroventral margin on each side.

Caudal ramus (fig. 28) elongated, 73μ x 22μ, about 3.3 times longer than wide. Outer lateral seta 88μ and naked; outermost terminal seta 91μ and naked; innermost terminal seta 112μ with inner hairs proximally. Two long median terminal setae 255μ (inner) and 203μ (outer) with lateral spinules in their midregions; these two setae inserted between dorsal (smooth) and ventral (with a row of minute spinules) flaps. Dorsal pedicellate seta 57μ and naked. Dorsal surface of ramus with scattered hairs.

Dorsal surface of prosome and urosome with few hairs (as in figs. 25, 26); ventral surface of urosome almost devoid of ornamentation. Ratio of length of prosome to that of urosome 1.85:1.

Egg sac (fig. 25) about 278μ x 170μ, containing a relatively small number of large eggs (five–seven), each egg about 92μ in average diameter.

Rostral area (fig. 29) not well developed, without a definite posteroventral margin.

First antenna (fig. 30) slender (280μ in length) and 7-segmented, with sclerite on third segment suggesting an intercalary segment weakly developed. Lengths of segments (measured along their posterior nonsetiferous margins) 28μ (44μ along anterior margin), 99μ, 28μ, 52μ, 28μ, 23μ, and 11μ respectively. Formula for armature, as in other species of *Lichomolgus*, 4, 13 (5+8), 6, 3, 4+1 aesthete, 2+1 aesthete, and 7+1 aesthete. All setae naked.

Second antenna (fig. 31) 4-segmented, slender, and elongated (208μ in length). Outer edge of penultimate segment 52μ in length, and that of last segment 21μ. Armature 1, 1, 3, and I, 1. All setae small and naked; terminal claw 28μ along its axis. Row of slender spinules on inner surface of second segment distal to seta.

Labrum (fig. 32) with two posteroventral lobes.

Mandible (fig. 33) with proximal region constricted, a narrow waist separating basal and distal parts. That part distal to waist having on its inner side a prominent elongated posteriorly directed process followed by a row of minute blunt hyaline spinules; and on its outer side a bilobed margin with setules. Flagellum moderately long with lateral spinules. Paragnath (fig. 37) a prominent well-sclerotized lobe without visible ornamentation but with its distal surface slightly wrinkled. First maxilla (fig. 34) with 3 terminal elements. Second maxilla (fig. 35) 2-segmented. First segment unornamented. Second segment having on its outer (ventral) margin a small proximal setule followed by a seta and on its inner

(dorsal) margin a seta with hyaline lamellae; terminal lash with a row of slender spinules. Maxilliped (fig. 36) 3-segmented. First segment stout and unornamented. Second segment elongated and slender with two inner setae. Third segment with two small setae and a terminal spiniform process with lateral spinules.

Area between maxillipeds and first pair of legs (fig. 37) not protuberant; sclerotized line between bases of maxillipeds.

Legs 1–4 (figs. 38–41) with trimerous rami except for endopod of leg 4 which is 2-segmented. Armature as follows (Roman numerals indicating spines, Arabic numerals setae):

P_1	protopod	0–1	1–0	exp	I–0	I–1	III, I, 4
				end	0–1	0–1	I, 5
P_2	protopod	0–1	1–0	exp	I–0	I–1	III, I, 5
				end	0–1	0–2	I, II, 3
P_3	protopod	0–1	1–0	exp	I–0	I–1	III, I, 5
				end	0–1	0–2	I, II, 2
P_4	protopod	0–0	1–0	exp	I–0	I–1	II, I, 5
				end	0–1	2	

Inner seta on coxa of legs 1 and 2 long and plumose, in leg 3 somewhat reduced in size, and in leg 4 absent. Hairs present on inner margin of basis in legs 1–3 but absent in leg 4. Outer spines on exopod of leg 1 flagellated. Endopod of leg 4 with hairs along outer margins of both segments. First segment 17μ x 13μ with plumose inner seta 26μ long; second segment 29μ long, 9μ wide proximally, 7μ wide distally, and armed with two slightly barbed setae 22μ (outer) and 33μ (inner).

Leg 5 (fig. 42) with an elongated free segment having a proximal inner expansion. This segment 90μ in length, 22μ wide at the expansion, and 17μ wide in its midregion; with a few small spinules on outer dorsal surface of distal half and with two terminal naked setae, outer 44μ, inner 72μ in length. Seta on body near free segment 68μ and slightly haired distally. A few small outer spinules near insertion of free segment.

Leg 6 probably represented by 2 setae near attachment of each egg sac (see fig. 27).

Color in life in transmitted light translucent, eye red, ovary black.

MALE.—Body (fig. 43) slender. Length (without setae on caudal rami) 0.73 mm (0.69–0.76 mm) and greatest width 0.23 (0.22–0.24 mm), based on 10 specimens. Ratio of length to width of prosome 1.72:1.

Segment of leg 5 (fig. 44) 32μ x 73μ. Between this segment and genital segment no ventral intersegmental sclerite. Genital segment longer than wide, 169μ x 135μ. Four postgenital segments 24μ x 43μ, 26μ x 42μ, 21μ x 40μ, and 31μ x 42μ from anterior to posterior.

Caudal ramus (fig. 45) resembling that of female but much shorter, 28μ x 18μ, or 1.55 times longer than wide.

Dorsal surface of body with few hairs (as in figs. 43, 44); ventral surface of urosome almost completely lacking ornamentation. Ratio of length of prosome to that of urosome 1.43:1.

Rostral area like that of female.

First antenna similar to that of female but with 3 aesthetes added, so that formula is 4, 13+2 aesthetes, 6, 3+1 aesthete, 4+1 aesthete, 2+1 aesthete, and 7+1 aesthete. Second antenna resembling that of female but inner margin of second segment with a row of dentiform spinules (fig. 46).

Labrum, mandible, paragnath, first maxilla, and second maxilla similar to those in female. Maxilliped (fig. 47) elongated and slender, 4-segmented, assuming that proximal part of claw represents a fourth segment. First segment unarmed, second with two setae and rows of spinules on inner surface, third short and unarmed. Claw slender and gently recurved, 127μ along its axis (including terminal lamella), with faint indication of division about midway; two unequal setae on proximal part of claw.

Legs 1–4 as in female except for endopod of leg 1 where formula for last segment (fig. 48) is I,I,4, instead of I,5 as in female.

Leg 5 (fig. 49) with elongated free segment, 18μ x 6μ, lacking a basal expansion. Two terminal setae 8μ (inner) and 24μ (outer).

Leg 6 (fig. 50) a posteroventral flap on genital segment bearing two naked setae 18μ and 22μ long.

Spermatophore (fig. 51) moderately elongated, 127μ x 56μ (without neck), often attached to female in pairs.

Color in life in transmitted light similar to that of female.

ETYMOLOGY.—The specific name *rhadinus*, from the Greek word ῥαδινός=slender, refers to the slender form of the body, of the first and second antennae, and of the maxillipeds in this species.

METHOD OF COLLECTION AND RELATION TO HOST.—*Lichomolgus rhadinus* was recovered after washing the coral in alcoholized sea water within a few hours after collection. In contrast to the recovery of *Xarifia diminuta* and *Rhynchomolgus corallophilus*, where the greatest numbers of specimens were found after allowing the coral to remain in alcoholized sea water overnight or after crushing the coral, all *L. rhadinus* were obtained in the first washings and none were found in the second washings after an overnight delay or after crushing. This suggests that *L. rhadinus* lives on the surface of the coral whence it is easily dislodged, rather than in the polyps.

COMPARISON WITH RELATED SPECIES.—The distinctive form of the mandible in *L. rhadinus* sets it apart from almost all of the other 70 or more species already described in the genus. Only five species

have a mandible somewhat resembling that of the new species. *L. actinophorus* Humes and Frost, 1964, has an elongated posteriorly directed process on the inner side of the basal region, but this process is more pointed and dentiform than in *L. rhadinus*. In addition, *L. actinophorus* differs from *L. rhadinus* in lacking a basal expansion on leg 5 in the female. Four species show on the inner basal region of the mandible a dentiform process much shorter than in *L. rhadinus*. These are *L. decorus* Humes and Frost, 1964 (in which the last segment of the exopod of leg 4 is III,I,4), ?*L.* (*Epimolgus*) *protulae* Stock, 1959 (with no basal expansion on leg 5 in the female and with the last segment of the second antenna bearing three strong claws, three setiform claws, and one seta), and *L. organicus* Humes and Ho, 1967, and *L. conjunctus* Humes and Ho, 1967, from the alcyonarian coral *Tubipora musica*. In both of these there is no basal expansion on leg 5 in the female and the last segment of the second antenna bears two claws and five setae. All other species of *Lichomolgus* in which the mandible has been described or figured lack prominent processes of this sort.

Eight species of *Lichomolgus* can not be compared with *L. rhadinus* in respect to the mandible since that appendage in them is unknown. They may be easily separated from the new species, however, on other grounds. *L. dentipes* Thompson and A. Scott, 1903, and *L. rigidus* (Ummerkutty, 1962) have the formula III,I,5 on the last segment of the exopod of leg 4. *L. elegans* Thompson and A. Scott, 1903, has in the female a much shorter caudal ramus and leg 5 without a basal expansion. *L. gigas* Thompson and A. Scott, 1903, is much larger (female 2 mm) and leg 5 lacks a basal expansion. *L. longipes* (Sewell, 1949), *L. rotundus* Sewell, 1949, *L. tenuicornis* Brady, 1910, and *L. vagans* Gurney, 1927, have two claws included in the armature of the last segment of the second antenna.

L. rhadinus appears to be most closely related to *L. actinophorus* Humes and Frost, 1964. It is of interest to note here the strong similarity between the mandible of *L. rhadinus* and that of *Rhynchomolgus corallophilus* (compare figs. 33 and 90). In many other features, however, these two copepods from *Psammocora* are very different.

Genus *Monomolgus* Humes and Frost, 1964

Monomolgus psammocorae, new species

FIGURES 52–79

TYPE MATERIAL.—17 ♀♀, 27 ♂♂, and 2 copepodids washed from the coral *Psammocora contigua* (Esper) in a depth of 2 m, southeast of Ambariobe, near Nosy Bé, Madagascar. Collected Sept. 8, 1963. Holotype female, allotype, and 32 paratypes (12 ♀♀, 20 ♂♂) deposited

228-864—67——2

in the United States National Museum, Washington; 6 paratypes (2 ♀♀, 4 ♂♂) in the Zoölogisch Museum, Amsterdam; and the remaining paratypes in the collection of A. G. Humes.

OTHER SPECIMENS (all from *Psammocora contigua* in 1 m at Ambariobe, collected during 1963).—9 ♀♀, 8 ♂♂, Sept. 6; 2 ♀♀, 2 ♂♂, Sept. 17; and 10 ♀♀, 3 ♂♂, Oct. 6.

FEMALE.—Body (fig. 52) with broadened prosome. Length (excluding setae on caudal rami) 1.25 mm (1.21–1.29 mm) and greatest width 0.65 mm (0.62–0.68 mm), based on 10 specimens. Ratio of length to width of prosome 1.22:1. Segment of leg 1 separated from head by a dorsal furrow. Epimeral areas of segments of legs 1–3 expanded as shown in figure. Segment of leg 4 without such expanded areas.

Segment of leg 5 (fig. 53) 86μ x 213μ. Between this segment and genital segment a short ventral intersegmental sclerite. Genital segment wider than long, 146μ x 172μ, broadest in its anterior half and tapered posteriorly. Areas of attachment of egg sacs situated laterally (only slightly dorsally), each area (fig. 54) bearing two setae 10μ and 6μ in length, with a short spinous process between them. Three postgenital segments 73μ x 99μ, 62μ x 96μ, and 68μ x 97μ from anterior to posterior. Anal segment posteriorly with row of small spinules laterally and ventrally on each side.

Caudal ramus (fig. 55) moderately elongated, 92μ x 35μ in greatest dimensions (77μ along inner edge, 90μ along outer edge). Ratio of length to width 2.63:1. Outer lateral seta 57μ long with minute barbules; outermost terminal seta 58μ and innermost terminal seta 75μ, both with proximal hairs and distal barbules as in figures. Two long median terminal setae 237μ (inner) and 146μ (outer) with proximal spinules and distal barbules; these two setae inserted between dorsal and ventral flaps (both with a row of slender spinules). Dorsal pedicellate seta 37μ and naked. Dorsal surface of ramus with a few hairs and two small hyaline spinules.

Dorsal surface of prosome and urosome with scattered hairs (as in figs. 52, 53); ventral surface of urosome sparsely ornamented. Ratio of length of prosome to that of urosome 1.72:1.

Egg sac (figs. 52, 56) attached in somewhat oblique position, with posterior end lying dorsally over postgenital segments. In lateral view egg sac in one female 400μ x 285μ, containing about 12 large eggs, with their diameters 117μ–130μ.

Rostral area (fig. 57) with broadly rounded posterior margin.

First antenna (fig. 58) 7-segmented, with a small sclerite on third segment suggesting an intercalary segment. Lengths of segments (measured along their posterior nonsetiferous margins) 55μ (71μ along anterior margin), 62μ, 28μ, 28μ, 32μ, 33μ, and 18μ, respectively.

Formula for armature: 4, 13 (5+2+6), 6, 3, 4+1 aesthete, 2+1 aesthete, and 7+1 aesthete. All setae naked. Row of minute spinules on first segment.

Second antenna (fig. 59) 4-segmented, last segment 50μ x 20μ. Armature 1, 1, 3, I, with terminal claw 43μ along its axis. A few minute spinules near bases of setae on third segment; two small setules on opposite surfaces of last segment near insertion of claw.

Labrum (fig. 60) with two posteroventral lobes and bearing numerous hairs.

Mandible (fig. 61) with its inner basal margin smooth, its outer basal margin with a distal row of slender setules and a proximal auricular expansion encircled with setules; lash elongated, its proximal inner margin with blunt hyaline dentations, both margins distal to this with spinules. Paragnath (fig. 62) an elongated lobe with distal hairs. First maxilla (fig. 63) with four elements as in figure. Second maxilla (fig. 64) 2-segmented. First segment somewhat swollen distoventrally, with small spinules. Second segment with a seta (having hyaline lamellae) on its anterior surface, a hyaline element on its inner (dorsal) margin, and a very small setule proximally on its outer (ventral) margin; distal part of segment forming a lash with a marginal row of three large slender proximal teeth gradating rapidly to many slender setules; a crescent of minute spinules at base of lash. Maxilliped (fig. 65) 3-segmented, first segment unarmed, second segment with two naked setae and a short row of minute spinules, and small third segment terminally with a spine, two hyaline setae, and a spinelike process with lateral spinules.

Area between maxillipeds and first pair of legs (fig. 66) not protuberant; sclerotized line connecting bases of maxillipeds.

Legs 1–4 (figs. 67–70) with trimerous rami except for endopod of leg 4 which consists of two segments. Armature as follows (Roman numerals indicating spines, Arabic numerals setae):

P_1	protopod	0–1	1–0	exp	I–0	I–1	III,I,4
				end	0–1	0–1	I,5
P_2	protopod	0–1	1–0	exp	I–0	I–1	III,I,5
				end	0–1	0–2	II,I,3
P_3	protopod	0–1	1–0	exp	I–0	I–1	III,I,5
				end	0–1	0–2	I,I,2
P_4	protopod	0–1	1–0	exp	I–0	I–1	II,I,5
				end	0–0	I	

Inner seta on coxa of legs 1–3 long and plumose, but in leg 4 very small (3μ long) and naked. Lamellae on spines of leg 1 more conspicuously spinulose than in legs 2–4. Spinules in row across distal margin of second segment of endopod of legs 1–3 much larger than those on first segment of these endopods. Endopod of leg 4 with both segments having inner and outer hairs. First segment 23μ x 18.5μ;

second segment 29μ x 13μ, armed with a single terminal spine 50μ in length having minutely spinulose lamellae.

Leg 5 in flat view of anterior surface as shown in figure 71, but in undissected specimens appearing in dorsal view as in figure 72. Free segment elongated and moderately broad, 84μ x 28μ, or three times longer than wide; with a few small spinules on its distal anterior surface and armed with two terminal barbed setae 77μ (outer) and 94μ (inner) in length. Seta on body near free segment 70μ long, haired proximally and barbed distally.

Leg 6 probably represented by two setae near attachment of each egg sac (see fig. 54).

Color in life in transmitted light amber in metasomal region, eye red, ovary gray.

MALE.—Body (fig. 73) with prosome broadened, but a little more spherical in dorsal outline than in female. Length (not including setae on caudal rami) 0.91 mm (0.85–0.97 mm) and greatest width 0.37 mm (0.36–0.38 mm), based on 10 specimens. Ratio of length to width of prosome 1.40 : 1.

Segment of leg 5 (fig. 74) 34μ x 138μ. Between this segment and genital segment no ventral intersegmental sclerite. Genital segment in dorsal view broadly expanded, wider than long, 146μ x 208μ. Four postgenital segments 32μ x 60μ, 33μ x 60μ, 34μ x 58μ, and 33μ x 62μ from anterior to posterior.

Caudal ramus resembling that of female but smaller, 68μ x 26μ.

Dorsal surface of prosome and urosome with scattered hairs (as in figs. 73, 74); ventral surface of urosome almost without ornamentation. Ratio of length of prosome to that of urosome 1.45:1.

Rostral area like that of female.

First antenna (fig. 75) resembling that of female but with three aesthetes added. Lengths of segments (measured as in female) 30μ (50μ along anterior margin), 46μ, 15μ, 14μ, 21μ, 14μ, and 13μ, respectively. Formula for armature: 4, 13+2 aesthetes, 6, 3+1 aesthete, 4+1 aesthete, 2+1 aesthete, and 7+1 aesthete. All setae naked.

Second antenna, labrum, mandible, paragnath, first maxilla, and second maxilla as in female. Maxilliped (fig. 76) elongated and slender, 4-segmented, assuming that proximal part of claw represents a fourth segment. First segment unarmed, second with two naked setae and a row of small blunt spines, third very short and unarmed. Claw strongly recurved, 57μ along its axis (including the lamella), with suggestion of bipartite nature midway along its length; proximal part bearing two unequal setae.

Area between maxillipeds and first pair of legs resembling that of female. Legs 1–4 as in female, without sexual dimorphism in endopod

of leg 1. Endopod of leg 4 with dimensions proportionally much like those in female; first segment 19μ x 17.5μ, second segment 24μ x 11μ, and terminal spine 40.5μ.

Leg 5 in flat anterior view as shown in figure 77, but in undissected specimens appearing in dorsal view as in figure 78. Free segment more rectangular than in female, 34μ x 14μ, or 2.43 times longer than wide; terminal setae 51μ and 69μ in length, respectively.

Leg 6 (fig. 79) a posteroventral flap on genital segment bearing two setae, one 50μ in length and naked, other 45μ with a few lateral hairs.

Spermatophore not observed.

Color in life in transmitted light similar to that of female.

ETYMOLOGY.—The specific name *psammocorae* is based on the generic name of the host.

METHOD OF COLLECTION AND RELATION TO HOST.—Like the preceding species, *M. psammocorae* was recovered in greatest numbers from the first washings of the coral, without allowing the coral to stand overnight in alcoholized sea water and without crushing. Presumably the copepod lives on the surface of the coral rather than in the polyps.

SYSTEMATIC POSITION.—The genus *Monomolgus* is at present founded on a single species, *M. unihastatus* Humes and Frost, 1964, associated with a coral, *Porites* cf. *P. andrewsi* Vaughan (family Poritidae), in Madagascar.

The new species from *Psammocora* may readily be distinguished without dissection from *M. unihastatus* by its shorter and more compact body form, its shorter caudal ramus (in *M. unihastatus* 3.9 times longer than wide in the female, 5.7 times in the male), and its narrower free segment of leg 5 in the female (in *M. unihastatus* 1.7 times longer than wide).

M. psammocorae is similar to *M. unihastatus* in several basic respects, particularly the segmentation and armature of the first antenna, second antenna, leg 1 in the female, leg 2, the exopod of leg 3, the endopod of leg 4, and leg 5. The differences seen in leg 1 of the male (lack of sexual dimorphism in *M. psammocorae*), in the endopod of leg 3 (last segment I,I,2, instead of I,II,2), and in the exopod of leg 4 (last segment II,I,5, instead of III,I,5) are probably only of a specific rather than generic nature.

The mouthparts of *M. psammocorae* exhibit certain detailed differences from those of *M. unihastatus*. The mandible in the species from *Psammocora* has an outer basal auricular expansion and a relatively long terminal lash. The paragnath is elongated. The first maxilla is armed with four elements.

These differences are probably not to be construed as evidence against the congeneric position of the two species; comparable differences in mouthparts exist among the species of the genus *Lichomolgus*. The points of similarity are so great that we think it preferable for the present to regard *M. unihastatus* and *M. psammocorae* as members of the same genus. The form of the endopod of leg 4, regarded as especially diagnostic in lichomolgid copepods, supports this point of view.

The inclusion of *M. psammocorae* in *Monomolgus* will necessitate a revision of the original generic diagnosis, especially in relation to the mandible. We are not attempting such a revision at present, however, in the expectation that further studies will clarify the generic concept of *Monomolgus*.

Rhynchomolgus, new genus

FEMALE.—Cephalosome expanded, urosome narrow. Segment of leg 1 fused with head. Urosome 5-segmented. Rostrum tumid and snoutlike. First antenna 5-segmented. Second antenna 4-segmented with a single terminal claw. Mouthparts lichomolgid. Legs 1 and 2 with 2-segmented rami. Leg 3 reduced to two setae. Leg 4 represented by a single seta. Leg 5 consisting of three setae, without a free segment.

MALE.—Body elongated and rather vermiform. Segment of leg 1 fused with head. Urosome 5-segmented in immature male, 6-segmented in mature male. Caudal ramus reduced and lobate. Rostrum as in female. First antenna 1-segmented. Second antenna indistinctly 3-segmented. Labrum bulbous. Mandibles, paragnaths, and first maxillae absent. Second maxilla a well-developed hook in immature male, a minute spinous process in mature male. Maxilliped 1-segmented with clawlike tip in immature male, absent in mature male. Legs 1 and 2 much reduced, with rami of one segment. Leg 3 represented by a single seta. Legs 4 and 5 absent. Leg 6 present.

Other features as in the species described below.

Living in madreporarian corals.

Type and only known species: *Rhynchomolgus corallophilus*, new species.

Gender masculine.

ETYMOLOGY.—The generic name is a combination of the Greek words ῥύγχος=snout, referring to the prominent rostrum, and μολγός = sack made of leather.

Rhynchomolgus corallophilus, new species

FIGURES 80–115

TYPE MATERIAL.—45 ♀♀, 32 small ♂♂, and 47 large ♂♂ from the coral *Psammocora contigua* (Esper) in a depth of 1 m, southeast of Ambariobe, near Nosy Bé, Madagascar. Collected Sept. 6, 1963. Holotype female, allotype large male, and 58 paratypes (20 ♀♀, 15 small ♂♂, and 23 large ♂♂) deposited in the United States National Museum, Washington; 21 paratypes (7 ♀♀, 7 small ♂♂, and 7 large ♂♂) in the Zoölogisch Museum, Amsterdam; and the remaining paratypes in the collection of A. G. Humes.

OTHER SPECIMENS (all from *Psammocora contigua* in 1–2 m at Ambariobe, collected during 1963).—16 ♀♀, 19 small ♂♂, and 25 large ♂♂, Sept. 8; 5 small ♂♂ and 9 large ♂♂, Sept. 17.

FEMALE.—Body (figs. 80, 81) with cephalosome greatly expanded laterally; segments of metasome and urosome relatively slender and somewhat contractile, the postgenital segments sometimes telescoped. Length (not including setae on caudal rami) 1.07 mm (0.89–1.24 mm) and greatest width 0.56 mm (0.49–0.63 mm), based on 10 specimens in average state of contraction. Two fully extended females 1.49 x 0.54 mm. Ratio of length to width of prosome (not including rostrum) 1.29:1. Segment of leg 1 fused with head, the only indication of separation being an indistinct transverse dorsal fold.

Segment of leg 5 (fig. 82) 91μ x 166μ. Genital segment wider than long, 130μ x 161μ, subrectangular in dorsal outline. Areas of attachment of egg sacs situated dorsolaterally, each area (fig. 83) bearing medially two spiniform setae, both about 19μ in length and directed posteriorly. Three postgenital segments 86μ x 109μ, 65μ x 86μ, and 60μ x 75μ from anterior to posterior. Last segment with a lobate dorsal flap over anal area; at either side of this flap on both dorsal and ventral surfaces a patch of denticles. (Entire urosome in telescoped specimen shown in figure 3 about 325μ in length, but if expanded the length would reach about 475μ.)

Caudal ramus (fig. 84) 44μ x 23μ, with ratio of length to width 1.91:1. Six short naked setae near distal end of ramus, the longest about 36μ. (Of these setae, one more dorsally placed than others, one on outer corner, and two median, shown partly retracted in figure, corresponding respectively to dorsal pedicellate seta, outer lateral seta, and two long median terminal setae seen in less modified lichomolgids such as *Lichomolgus*.) Ramus with a few minute spinules, small setules, and refractile points as shown in figure.

Dorsal surface of prosome with scattered refractile points and setules in metasomal region (as in figs. 80, 81); urosome with dorsal and ventral surfaces similarly ornamented (see fig. 82). Ratio of

length of prosome to that of urosome (in specimen shown in fig. 80) about 2.39:1, but this ratio subject to state of contraction.

Egg sac unknown, since none of females collected was ovigerous.

Rostrum (figs. 80, 81, 85) a conspicuous tumid snoutlike lobe bluntly rounded distally.

First antenna (fig. 86) 5-segmented and relatively short (about 80μ in length). Lengths of segments (measured along their posterior nonsetiferous margins) 21μ (25μ along anterior margin), 15.5μ, 16μ, 11.5μ, and 9μ, respectively. Formula for armature: 3, 10, 4+1 aesthete, 2+1 aesthete, and 7+1 aesthete. Setae with strong lateral spinules, except five naked setae (one on segment 3, one on segment 4, and four on last segment).

Second antenna (fig. 87) 4-segmented and much longer (about 180μ including claw) than first antenna. First and second segments rather large and each with an inner barbed seta. Third and fourth segments smaller, third with three inner barbed setae, fourth (fig. 88) ornamented with five rather hyaline spinules and a short row of minute spinules, and bearing a terminal claw 28μ in length and only slightly recurved. External to base of second antenna and behind base of first antenna a prominent lobe (see figs. 81, 94).

Labrum (fig. 89) with posteroventral margin forming two lobes.

Mandible (fig. 90) with inner margin of basal region having proximally a prominent finger-like extension (directed posteriorly) and distally a row of small dentations; disto-inner margin of basal region with a row of moderately long spinules. Lash relatively short and not finely attenuated, with serrated margins. Paragnath (fig. 89) a small lobe bearing hairs distally. First maxilla (fig. 91) a single small segment with two terminal barbed setae. Second maxilla (fig. 92) 2-segmented, first segment unarmed, second with two barbed elements and extended to form a gladiate blade with short stout teeth along one edge. Maxilliped (fig. 93) 3-segmented, first segment unarmed, second segment with two spinulose elements, and third with one spinulose element and terminating in a spinulose spiniform process.

Area between maxillipeds and first pair of legs (fig. 94) not protuberant.

Legs 1–4 much modified. Legs 1 and 2 (figs. 95, 96) with similar intercoxal plates, protopods, and 2-segmented rami. In leg 1 terminal spine on exopod with a few inner serrations, and anterior surface of basis near insertion of endopod having a row of small spinules; these features absent in leg 2. Spines on both legs obtuse.

Leg 3 (fig. 97) reduced to two unequal setae, inner 7μ, outer 16μ in length. Leg 4 (fig. 98) a single seta 16μ long. These two legs lacking intercoxal plates.

Armature of legs 1–4 as follows (Roman numerals indicating spines, Arabic numerals setae):

P_1	protopod	0–0	1–0	exp	I–0	III,II,2
				end	0–0	I,1
P_2	protopod	0–0	1–0	exp	I–0	III,II,2
				end	0–0	I,II
P_3					2	
P_4					1	

In one female second segment of one endopod of leg 1 with an extra outer spine (I,I,1). In another female second segment of one exopod of leg 2 with an extra inner seta (III,II,3).

Leg 5 (fig. 99) without a free segment, and reduced to three setae, one dorsal 24μ, and two ventral 16μ and 18μ in length.

Color in life, in transmitted light, amber in cephalosome, rest of body translucent, eye red but indistinct.

SMALL IMMATURE MALE.—Body (fig. 100) elongated, rather vermiform, contractile, head region sometimes partly withdrawn into cephalosome and urosome often bent or contracted. Length (excluding setae on caudal rami) 1.17 mm (0.89–1.44 mm) and greatest width 0.26 mm (0.22–0.30 mm), based on 10 specimens not strongly contracted. Ratio of length to width of prosome about 2.61: 1. Segment of leg 1 fused with head.

Urosome (fig. 101) slender. Probably three postgenital segments, but their separation obscure, particularly between last two segments.

Caudal ramus (fig. 102) small, lobate, without distinct articulation with anal segment and bearing three spinules on dorsal surface (ventral surface smooth).

Surfaces of prosome and urosome apparently unornamented, though wrinkled condition of cuticula in preserved specimens makes this difficult to determine. Ratio of length of prosome to that of urosome (in specimen shown in fig. 100) about 1.40 : 1.

Rostrum (fig. 105) a tumid lobe as in female.

First antenna (fig. 103) 1-segmented, very short, about 44μ long, with 13 short terminal spines. Second antenna (fig. 104) probably 3-segmented (segmentation suggested by sclerites, no clear articulations present), about 64μ long. Last segment with eight short spines. External to base of second antenna and behind first antenna a conspicuous lobe (fig. 105), as in female.

Labrum a bulbous area between and behind second antennae, in ventral view (fig. 105) somewhat triangular and attached to a triangular sclerotized framework. Postlabral region forming a fold that slightly overlaps posterior end of labrum. Mouth region apparently located between labrum and postlabral fold. Mandibles, paragnaths, and first maxillae not discernible and apparently absent. Second

228-964—66——3

maxilla (fig. 106) a well-sclerotized recurved hook with a broad base perhaps representing a basal segment. Maxilliped (figs. 107, 108) with a prominent 1-segmented basal area bearing a well-sclerotized short clawlike tip.

Legs 1 and 2 similar in form, each leg far removed from its opposite member, without an intercoxal plate. Leg 1 (fig. 109), located near maxilliped (see fig. 105), with an indefinitely defined protopodal area, a slender setiform unsegmented exopod, and a rather weakly sclerotized unsegmented endopod bearing a single blunt hyaline seta (its articulation indistinct). Leg 3 (fig. 110) consisting of a single seta 22μ in length. Leg 4 absent.

Leg 5 absent.

Leg 6 (figs. 101, 111) consisting of a posteroventral flap on genital segment bearing a well-sclerotized spinous process and two setae 16μ and 22μ in length.

Spermatophores not formed in bodies of these small males.

Color in life, in transmitted light, opaque and grayish, eye not clearly visible.

LARGE MATURE MALE.—In the following description features not mentioned may be regarded as similar to those of the small male already described.

Body (fig. 112) elongated, vermiform, and contractile as in small male. Length (without setae on caudal rami) 2.04 mm (1.86–2.21 mm) and greatest width 0.46 mm (0.41–0.51 mm), based on 10 specimens. (Two other specimens much smaller, 0.69 x 0.18 mm and 0.86 x 0.18 mm). Ratio of length of prosome to that of urosome about 2.60:1.

Four postgenital segments, their separation more distinct than in small male.

Caudal ramus resembling that of small male but a little longer.

Ratio of length of prosome to that of urosome (in specimen shown in fig. 112) about 1.43:1.

Rostrum (figs. 113, 114) similar to that in female and in small male.

First antenna, second antenna, labrum, and postlabral fold as in small male. Mandibles, paragnaths, and first maxillae absent. Second maxillae (figs. 113, 115) represented by small well-sclerotized spinous processes. Maxilliped absent.

Legs 1–3 as in small male. Legs 4 and 5 absent.

Leg 6 (fig. 112) protruding a little more laterally, edge of posteroventral flap less sclerotized, and two setae relatively shorter (15μ and 18μ) than in small male.

Spermatophores fairly well developed inside about two-thirds of large males.

Color in life in transmitted light similar to that of small male.

ETYMOLOGY.—The specific name *corallophilus*, from the Greek words κόραλλον=coral and φίλος=loving, alludes to the association of this species with a coral.

SPECIFIC IDENTITY OF FEMALES, SMALL MALES, AND LARGE MALES.—The differences in external anatomy between males and females of *Rhynchomolgus corallophilus* are so striking that the question arises whether or not they represent opposite sexes of the same species. One can not fail to be impressed by the great difference between the males and females in body form, the nature of the first and second antennae, the labrum, the mouthparts (with mandibles, paragnaths, and first maxillae absent in males), and the form of legs 1–5 (with legs 4 and 5 absent in males). The differences in the second maxillae and maxillipeds in the two kinds of males (with the maxillipeds absent in large males) also contribute to the impression that they represent separate forms.

Since no specimens in our collections were in amplexus, judgment in respect to their specific identity must be made on other grounds than sexual behavior.

We believe that the three groups of specimens represent one species, *R. corallophilus*, for several reasons based on their external anatomy. Both kinds of males and the females have a similar snoutlike rostrum and all possess a prominent lobe external to the base of the second antenna. The small males and large males, differing in their second maxillae (reduced to a spinous process in large males) and maxillipeds (absent in large males), are otherwise similar in their appendages. It is our opinion that the small males are immature, and represent the last pre-adult instar. This interpretation is based on the facts that in small males there seem to be, at most, three postgenital segments and the body does not contain formed spermatophores, while in large males there are four postgenital segments and there are often partly formed spermatophores within. A molt from the small immature male to the large mature male would have to be presumed in order to account for the reduction in the second maxilla and the loss of the maxilliped.

Further justification for considering all three groups as one species may be found in the circumstantial evidence of the numbers of specimens collected. It would seem unlikely, if the males and females represent separate species, that large numbers of females of one species and large numbers of males of the other species would occur together in the same host without there being at least a few of the opposite sex in each case. For this to happen it would be necessary to suppose a very unequal and improbable sex ratio. We therefore

conclude that only one species is involved and that all the specimens represent *R. corallophilus*.

METHOD OF COLLECTION AND RELATION TO HOST.—*Rhynchomolgus corallophilus* apparently lives inside the polyps of the coral. When pieces of the coral were washed intact in alcoholized sea water within one or two hours after being brought into the laboratory, none of these copepods were obtained. After allowing the coral to remain overnight in the alcoholized sea water, considerable numbers were recovered from the sediment. After subsequently crushing the coral, still more *R. corallophilus* were found.

SYSTEMATIC POSITION OF THE NEW GENUS.—Several features of the female of *Rhynchomolgus* suggest that the genus belongs to the family Lichomolgidae. The mandible is lichomolgid in form, resembling rather closely that of *Lichomolgus rhadinus*. The second antenna, labrum, first maxilla, second maxilla, and maxilliped are also basically lichomolgid. The 5-segmented first antenna has fewer segments than in most other lichomolgid genera (where the number of segments is commonly seven). Apparently the reduction in the number of segments in *Rhynchomolgus* has involved the loss of segments 3 and 4, since the arrangement of the setae and aesthetes on the five segments corresponds rather closely (particularly on segments 3–5) to the pattern seen on segments 1, 2, 5, 6, and 7 of the 7-segmented first antenna of *Lichomolgus* and other lichomolgid genera.

There are obvious differences in legs 1–4 between the female of *Rhynchomolgus* and other lichomolgid genera, but these may be attributed to reduction associated with a parasitic way of life. Reduction of legs 1–4, so pronounced in both sexes of *Rhynchomolgus*, is known to occur to a lesser extent in certain other parasitic or associated lichomolgid genera, for example, in *Meomicola* Stock, Humes and Gooding, 1964, and in a new genus from zoanthid coelenterates whose description by Humes and Ho is in press.

Since the male of *Rhynchomolgus* lacks mandibles, paragnaths, and first maxillae, it is more difficult in this sex to demonstrate lichomolgid affinities. The sexual dimorphism seen in the first antenna, second antenna, second maxilla, and maxilliped makes comparison uncertain. However, following our opinion expressed above on the specific identity of the males and females, the males are included with the females as one species in the lichomolgid genus *Rhynchomolgus*. As far as known, no other genus of the Lichomolgidae lacks mandibles, paragnaths; and first maxillae in the male.

Literature Cited

BRADY, G. S.
1910. Die marinen Copepoden der deutschen südpolar-Expedition 1901–1903, I: Uber die Copepoden der Stämme Harpacticoida, Cyclopoida, Notodelphyoida und Caligoida. *In* Deutsche Südpolar-Expedition, 1901–1903, vol. 11, zool. vol. 3, no. 5, pp. 499–593.

GURNEY, R.
1927. Zoological results of the Cambridge expedition to the Suez Canal, 1924, XXXIII: Report on the Crustacea: Copepoda (Littoral and Semi-parasitic). Trans. Zool. Soc. London, vol. 22, pt. 4, pp. 451–577.

HUMES, A. G.
1960. New copepods from madreporarian corals. Kieler Meeresforsch., vol. 16, no. 2, pp. 229–235.
1962a. Eight new species of *Xarifia* (Copepoda, Cyclopoida), parasites of corals in Madagascar. Bull. Mus. Comp. Zool., vol. 128, no. 2, pp. 37–63.
1962b. *Kombia angulata* n. gen., n. sp. (Copepoda, Cyclopoida) parasitic in a coral in Madagascar. Crustaceana, vol. 4, pt. 1, pp. 47–56.

HUMES, A. G., and FROST, B. W.
1964. New lichomolgid copepods (Cyclopoida) associated with alcyonarians and madreporarians in Madagascar. Cahiers ORSTOM Océanogr., 1963, no. 6 (sér. Nosy Bé II), pp. 131–212.

HUMES, A. G., and Ho, J.-S.
1967. New cyclopoid copepods associated with the alcyonarian coral *Tubipora musica* (L.) in Madagascar. Proc. U.S. Nat. Mus., vol. 121, no. 3573, pp.1–24.
In press. New lichomolgid copepods (Cyclopoida) from zoanthid coelenterates in Madagascar.

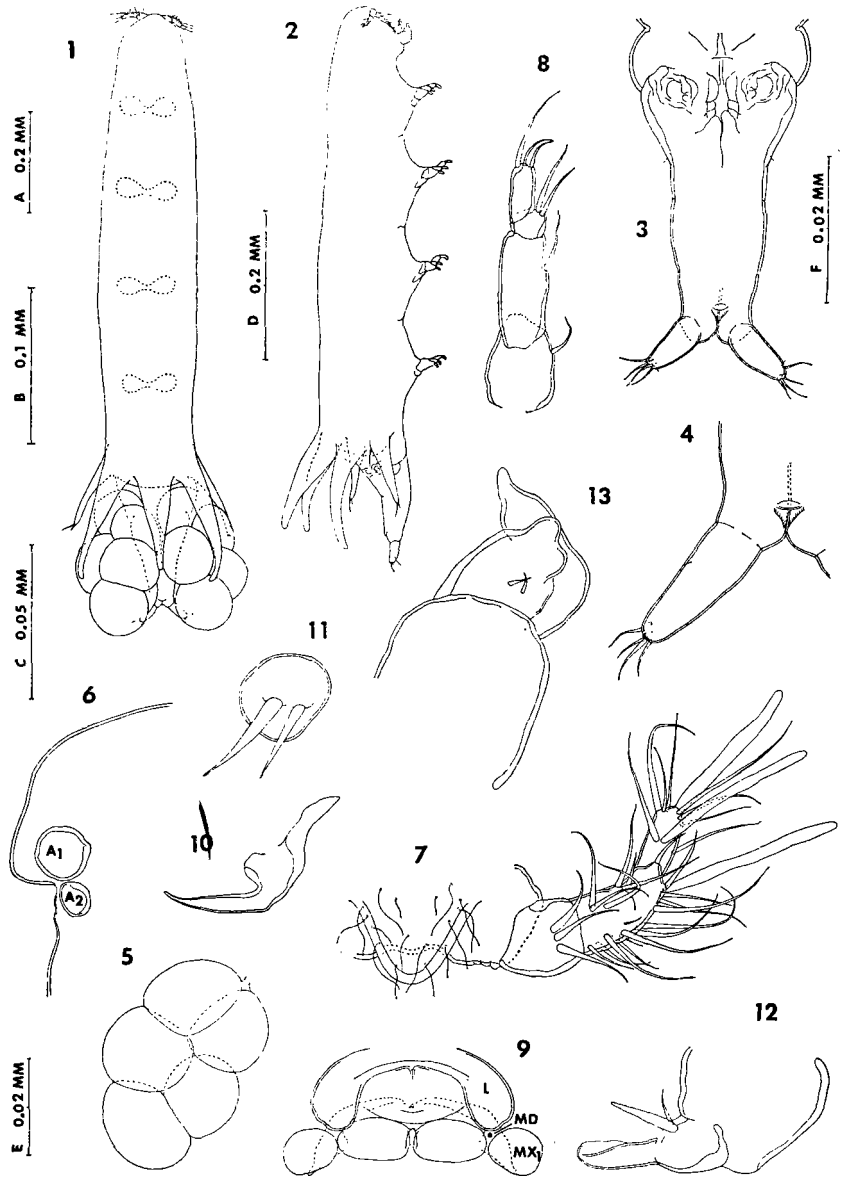
SEWELL, R. B. S.
1949. The littoral and semi-parasitic Cyclopoida, the Monstrilloida and Notodelphyoida. John Murray Exped., 1933–34, Sci. Reps., vol. 9, no. 2, pp. 17–199.

STOCK, J. H.
1959. Copepoda associated with Neapolitan invertebrates. Pubbl. Staz. Zool. Napoli, vol. 31, no. 1, pp. 59–75.

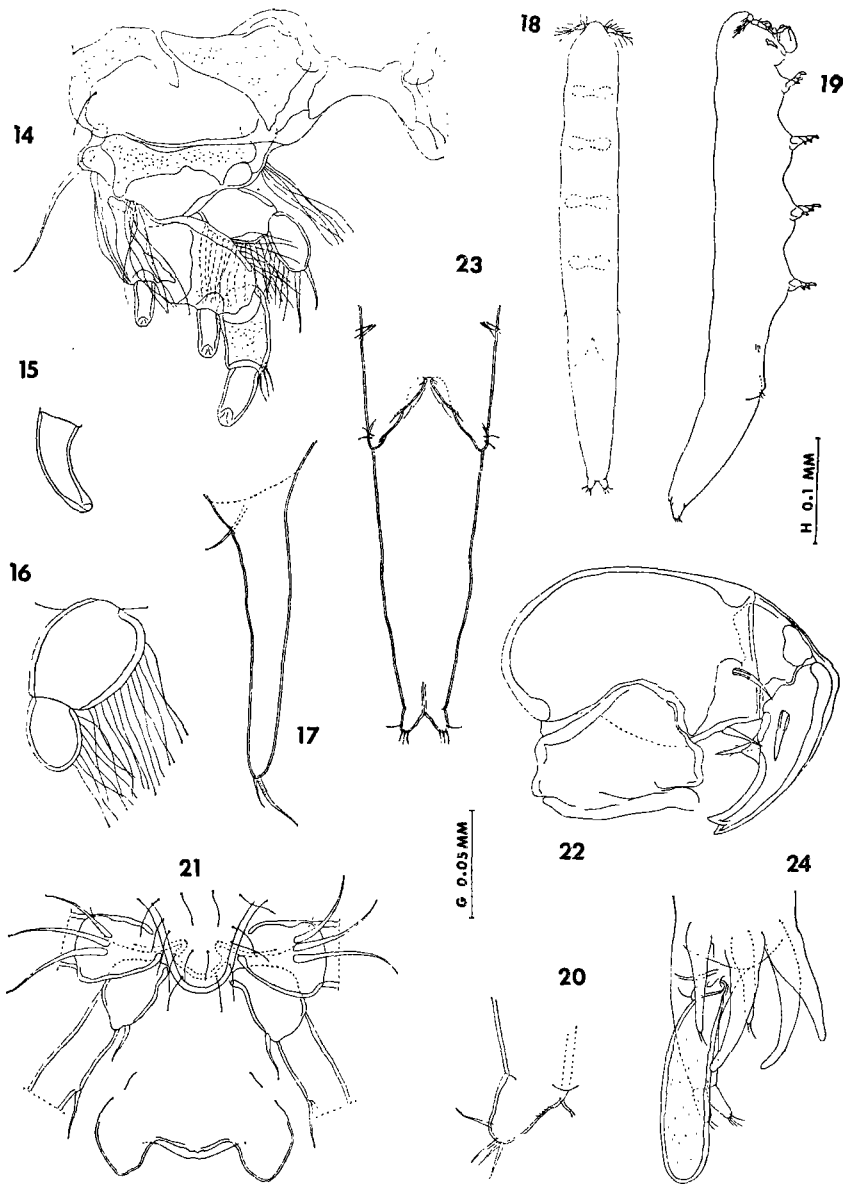
STOCK, J. H.; HUMES, A. G.; and GOODING, R. U.
1964. Copepoda associated with West Indian invertebrates, IV: The genera *Octopicola, Pseudanthessius* and *Meomicola* (Cyclopoida, Lichomolgidae). Stud. Fauna Curaçao and other Caribbean Islands, 1963, vol. 18, no. 77, pp. 1–74.

THOMPSON, I. C., and SCOTT, A.
1903. Report on the Copepoda collected by Professor Herdman, at Ceylon, in 1902. Rep. Gov. Ceylon Pearl Oyster Fish. Gulf of Manaar, suppl. reps., no. 7, pp. 227–307.

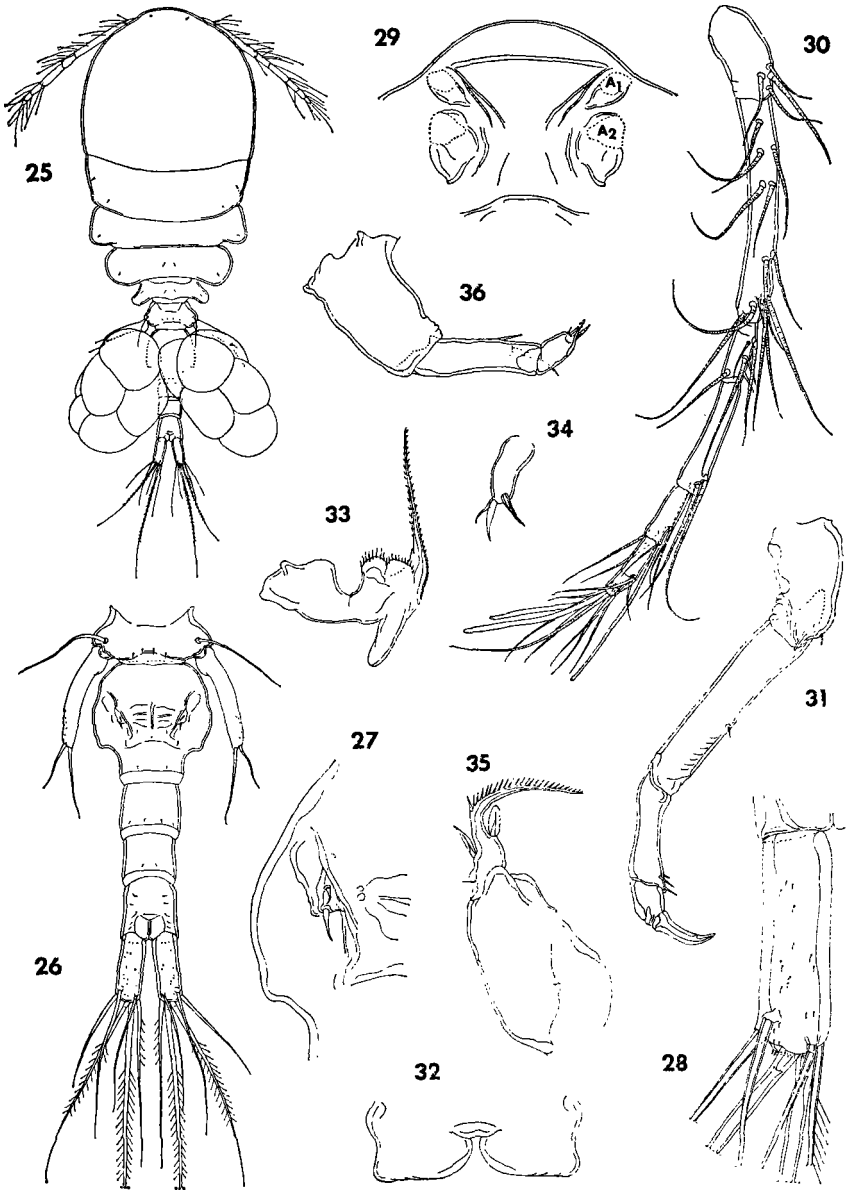
UMMERKUTTY, A. N. P.
1962. Studies on Indian copepods, 5: On eleven new species of marine cyclopoid copepods from the south-east coast of India. Journ. Mar. Biol. Assoc. India, 1961, vol. 3, nos. 1 and 2, pp. 19–69.



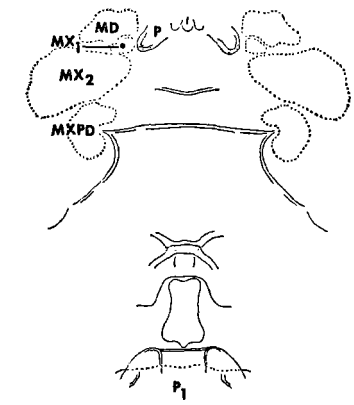
FIGURES 1–13.—*Xarifia diminuta*, new species, female: 1, dorsal (A); 2, lateral (A); 3, genital and postgenital segments, dorsal (B); 4, caudal ramus, dorsal (C); 5, egg sac, lateral (D); 6, outline of rostrum, lateral (C); 7, rostrum and first antenna, anterodorsal (E); 8, second antenna, lateral (E); 9, labrum, posteroventral (E); 10, mandible, anterior (F); 11, first maxilla, ventral (F); 12, second maxilla, anterior (F); 13, maxilliped, anterior (F).



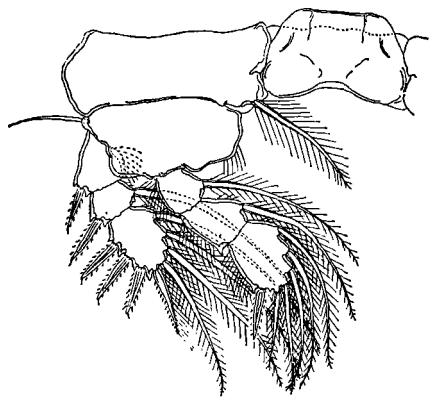
FIGURES 14–24.—*Xarifia diminuta*, new species, female: 14, leg 1 and intercoxal plate, posterior (E); 15, terminal spine on exopod of leg 1, lateral (E); 16, endopod of leg 3 posterior (F); 17, leg 5, medial (G). Male: 18, dorsal (A); 19, lateral (A); 20, caudal ramus, dorsal (C); 21, rostral area and labrum, anterior (E); 22, maxilliped, medial (E); 23, urosome, ventral (H); 24, spermatophore, attached to female, lateral (D).



FIGURES 25–36.—*Lichomolgus rhadinus*, new species, female: 25, dorsal (A); 26, urosome, dorsal (H); 27, area of attachment of egg sac, dorsal (C); 28, caudal ramus, dorsal (C); 29, rostral area, ventral (B); 30, first antenna, dorsal (G); 31, second antenna, inner (G); 32, labrum, ventral (C); 33, mandible, anterior (C); 34, first maxilla, lateral (C); 35, second maxilla, anterior (C); 36, maxilliped, anterolateral (C).



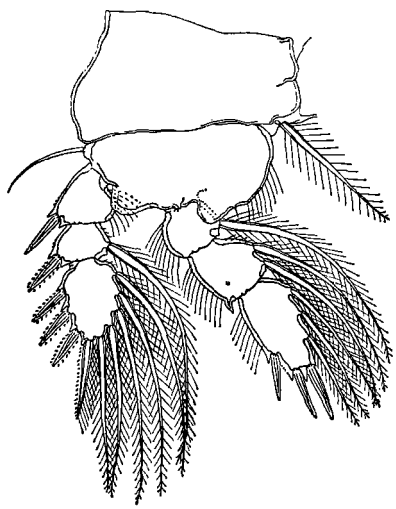
37

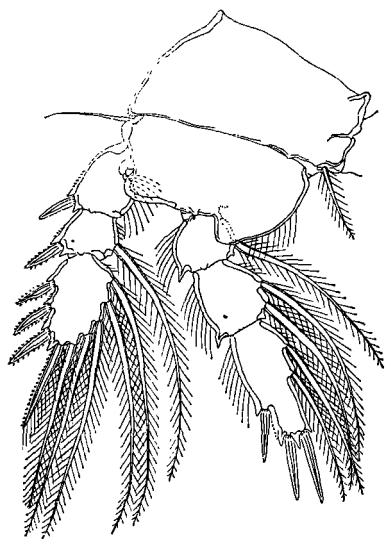


38

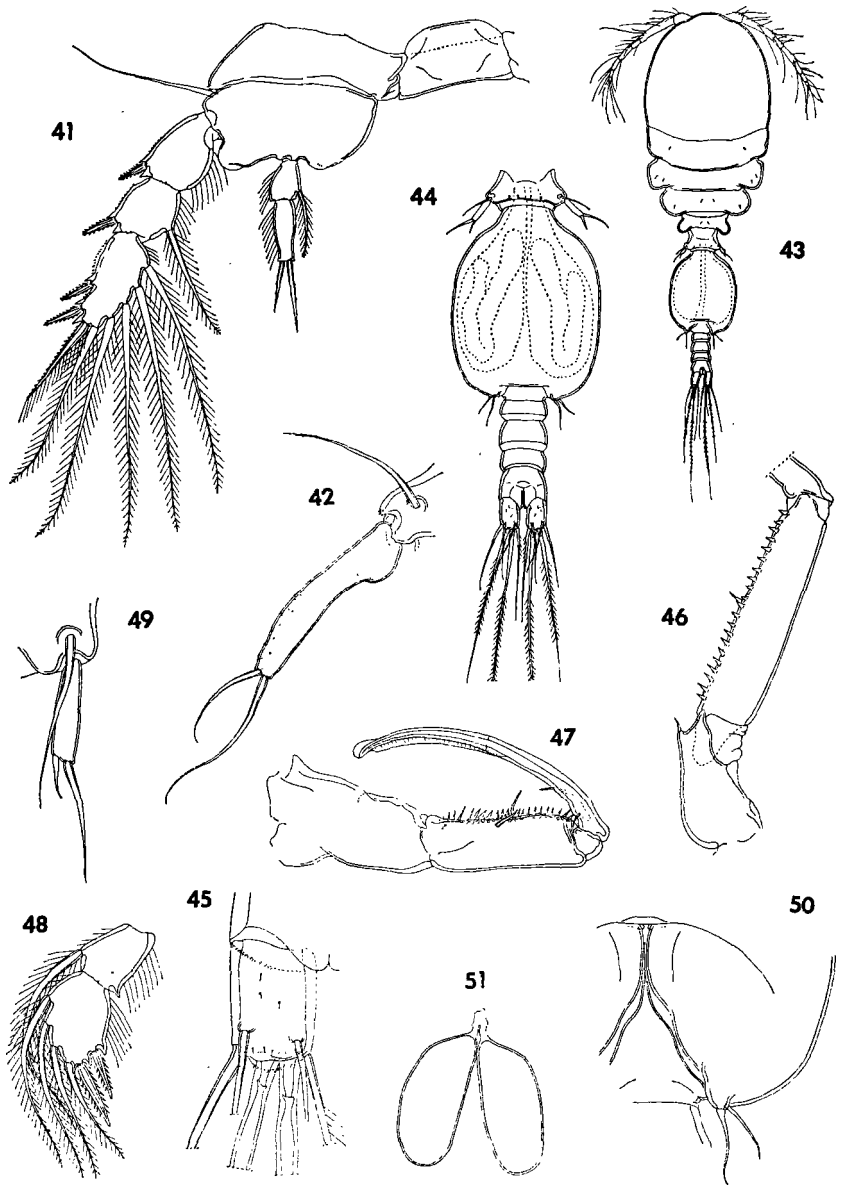
40

39

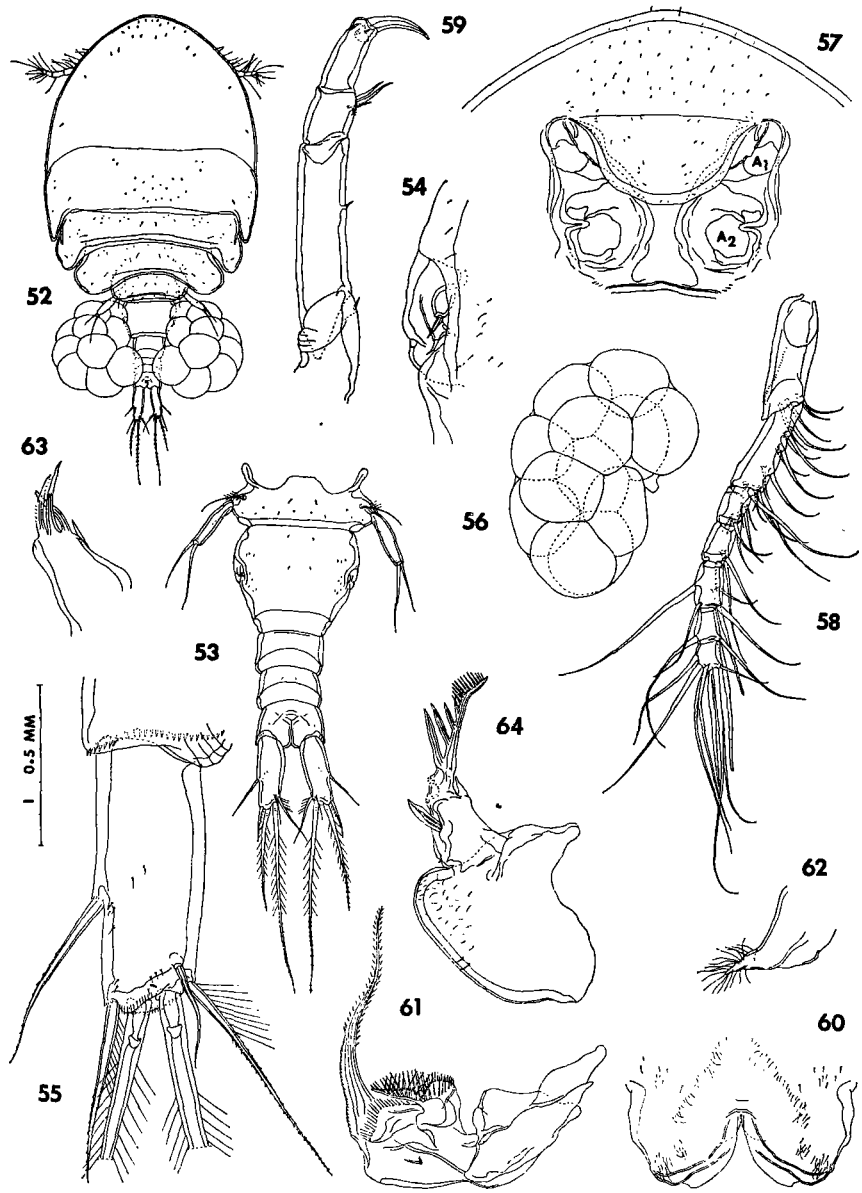




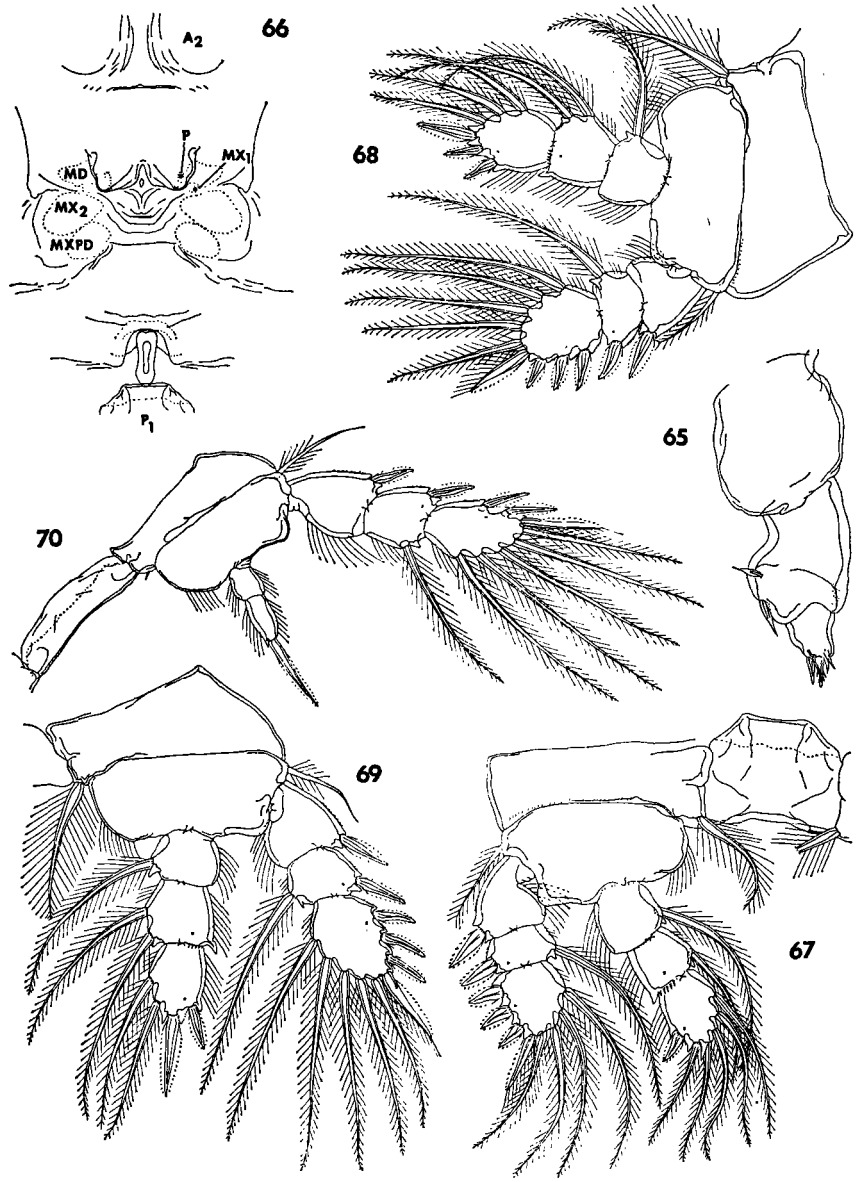
FIGURES 37–40.—*Lichomolgus rhadinus*, new species, female: 37, postoral area, ventral (G); 38, leg 1 and intercoxal plate, anterior (G); 39, leg 2, anterior (G); 40, leg 3, anterior (G).



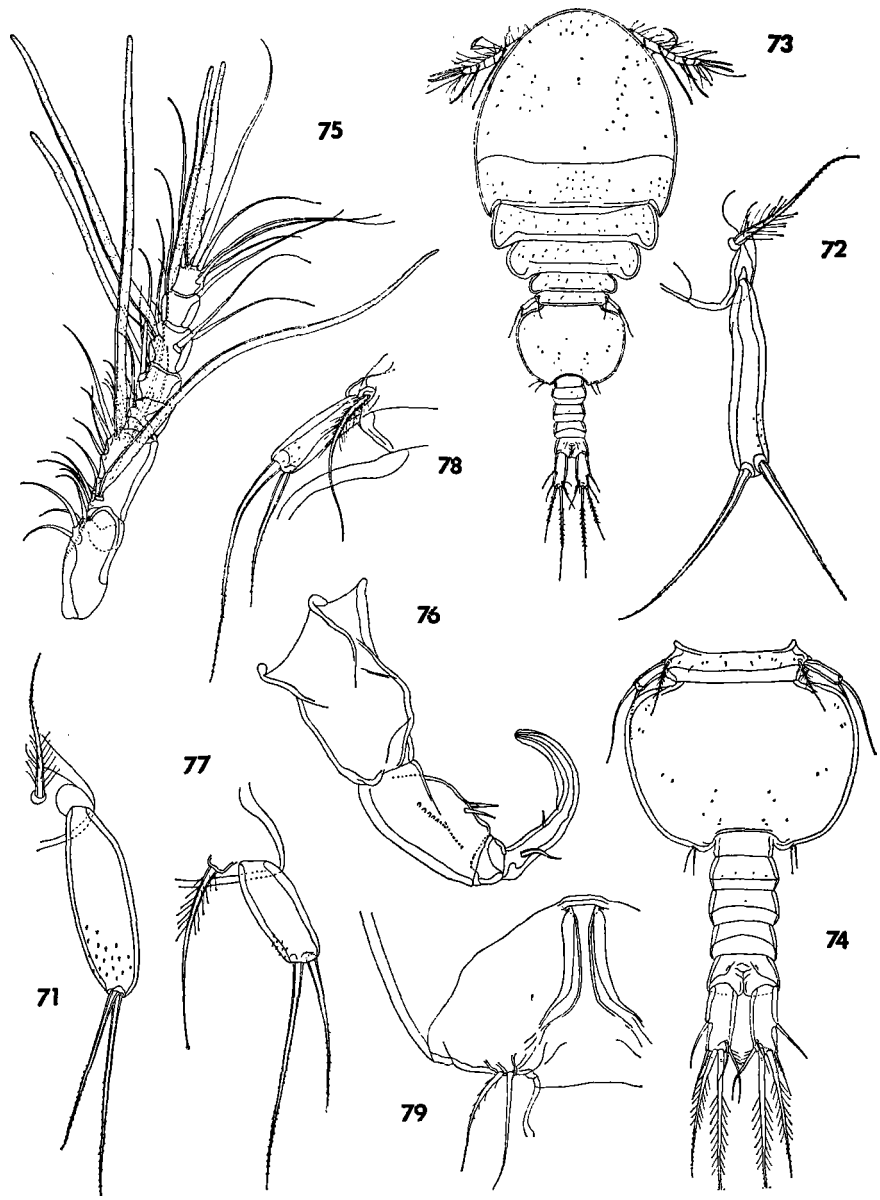
FIGURES 41–51.—*Lichomolgus rhadinus*, new species, female: 41, leg 4 and intercoxal plate, anterior (G); 42, leg 5, dorsal (G). Male: 43, dorsal (A); 44, urosome, dorsal (H); 45, caudal ramus, dorsal (E); 46, first two segments of second antenna, inner (C); 47, maxilliped, outer (G); 48, last two segments of endopod of leg 1, anterior (C); 49, leg 5, dorsal (E); 50, leg 6, ventral (C); 51, spermatophore, attached to female, lateral (H).



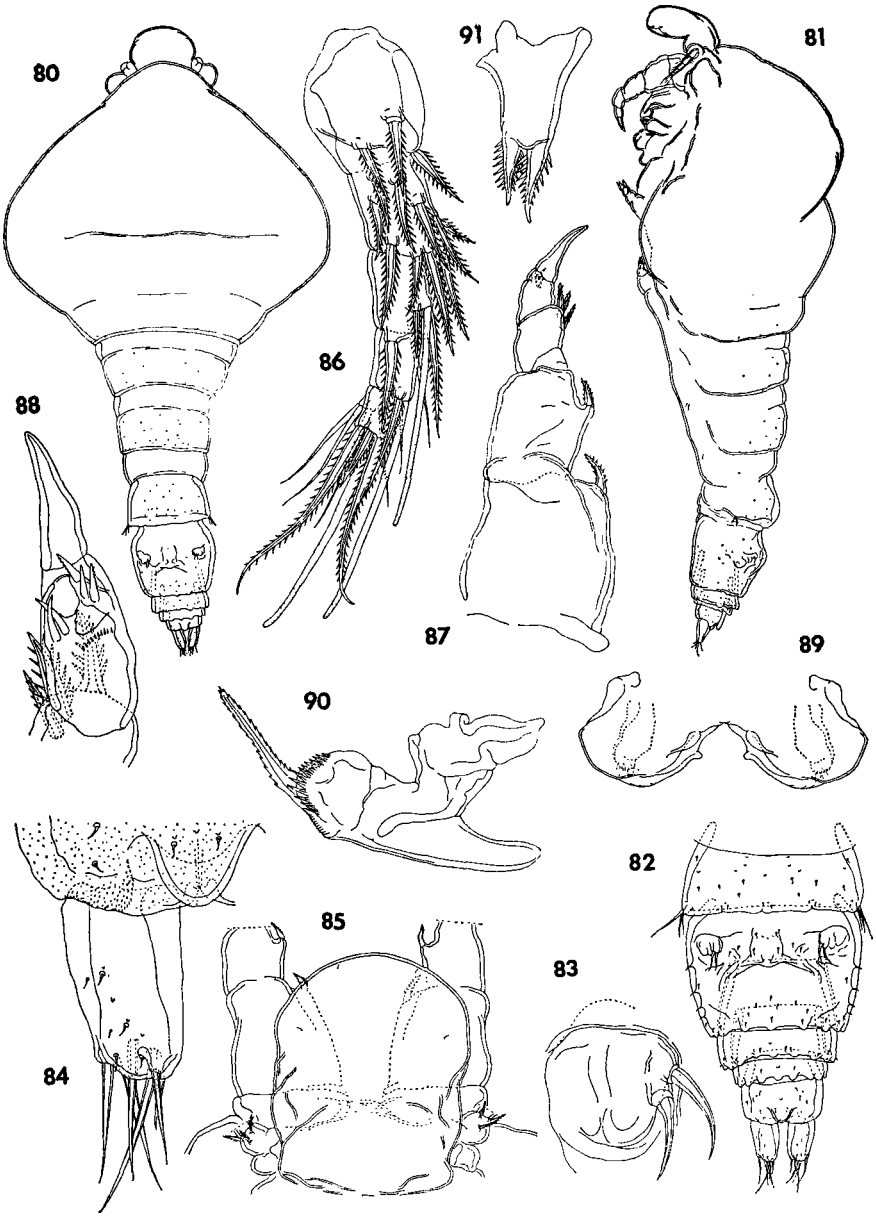
FIGURES 52–64.—*Monomolgus psammocorae*, new species, female: 52, dorsal (I); 53, urosome, dorsal (D); 54, area of attachment of egg sac, dorsal (C); 55, caudal ramus, dorsal (C); 56, egg sac, lateromedial (D); 57, rostral area, ventral (H); 58, first antenna, ventral (B); 59, second antenna, posterolateral (B); 60, labrum, ventral (G); 61, mandible, posterior (C); 62, paragnath, anterior (E); 63, first maxilla, posterior (C); 64, second maxilla, anterior (C).



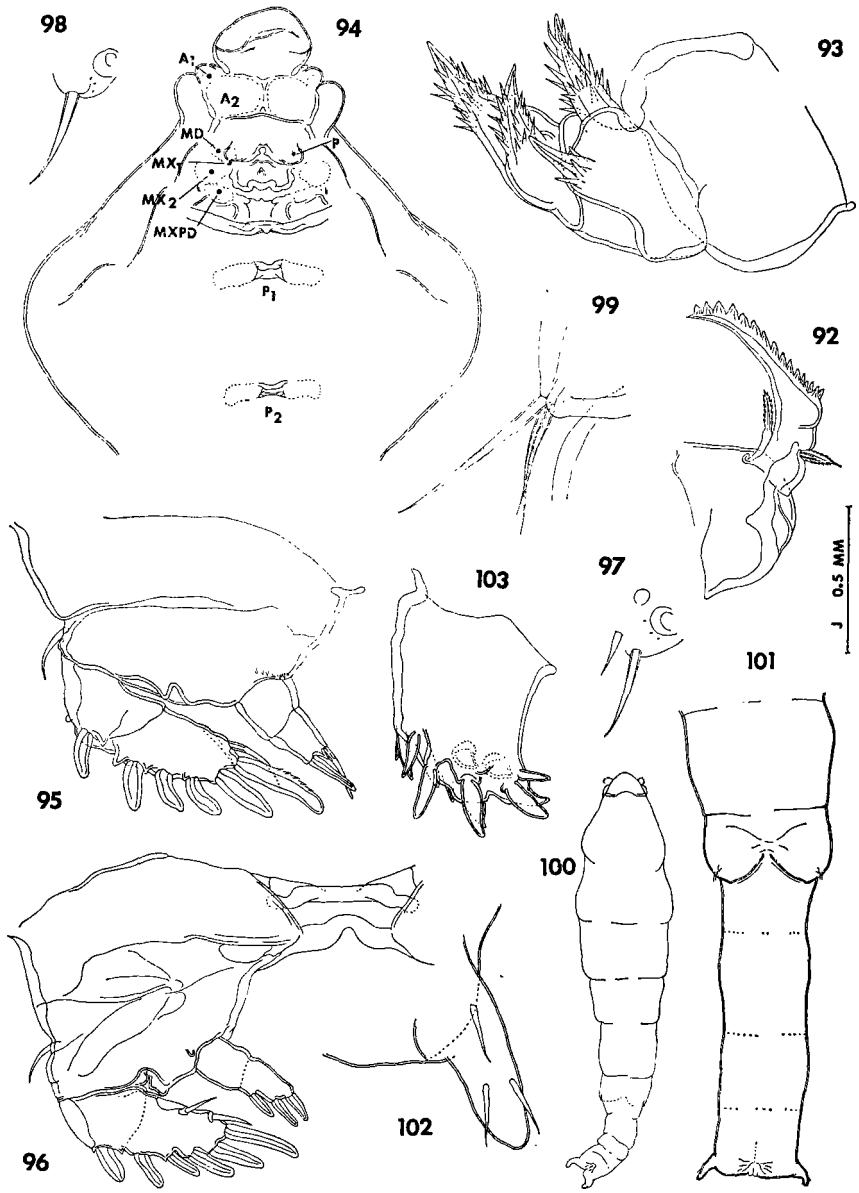
FIGURES 65–70.—*Monomolgus psammocorae*, new species, female: 65, maxilliped, antero-medial (C); 66, oral and postoral area, ventral (H); 67, leg 1 and intercoxal plate, anterior, (B); 68, leg 2, anterior (B); 69, leg 3, anterior (B); 70, leg 4 and intercoxal plate, anterior (B).



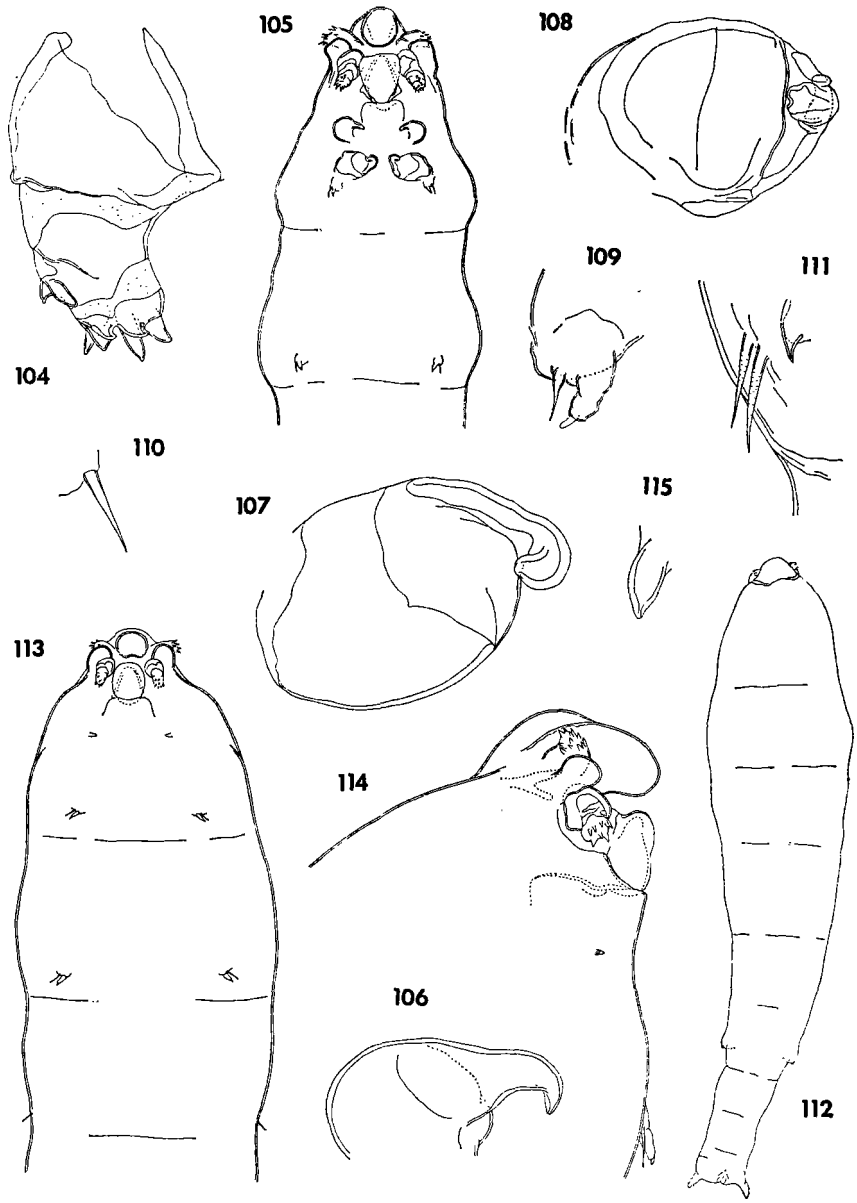
FIGURES 71–79.—*Monomolgus psammocorae*, new species. female: 71, leg 5, anterior (G); 72, leg 5, dorsal (G). Male: 73, dorsal (A); 74, urosome, dorsal (H); 75, first antenna, dorsal (G); 76, maxilliped, inner (C); 77, leg 5, somewhat anterior (C); 78, leg 5, dorsal (C); 79, leg 6, ventral (G).



FIGURES 80–91.—*Rhynchomolgus corallophilus*, new species, female: 80, dorsal (A); 81; lateral (A); 82, urosome, with postgenital segments telescoped, dorsal (H); 83, area of attachment of egg sac, dorsal (E); 84, caudal ramus, dorsal (E); 85, rostrum, dorsal (B); 86, first antenna, anterodorsal (E); 87, second antenna, anterior (G); 88, terminal segment and claw of second antenna, lateral (G); 89, labrum, ventral (G); 90, mandible, anterior (C); 91, first maxilla, anterior (E).



FIGURES 92–103.—*Rhynchomolgus corallophilus*, new species, female: 92, second maxilla, anterior (C); 93, maxilliped, posterior (E); 94, anterior part of body, ventral (D); 95, leg 1, anterior (E); 96, leg 2 and intercoxal plate, posterior (E); 97, leg 3, left side, ventral (E); 98, leg 4, left side, ventral (E); 99, leg 5, dorsal (E). Small immature male: 100, dorsal (J); 101, urosome, ventral (D); 102, caudal ramus, dorsal (E); 103, first antenna, ventral (E).



FIGURES 104–115.—*Rhynchomolgus corallophilus*, new species, small immature male: 104, second antenna, medial (E); 105, anterior part of body, ventral (D); 106, second maxilla, anterior (E); 107, maxilliped, ventral and slightly lateral (E); 108, maxilliped, ventra (E); 109, leg 1, ventral and somewhat anterior (E); 110, leg 3, ventral (E); 111, leg 6, ventral (E). Large mature male: 112, dorsal (J); 113, anterior part of body, ventral (A); 114, cephalosome, lateral (H); 115, second maxilla, ventral (E).

Reprinted from *Bull. Mus. Comp. Zool.* (Harvard), vol. 135, no. 7, 1967, p. 377-413

NEW CYCLOPOID COPEPODS ASSOCIATED WITH POLYCHAETE ANNELIDS IN MADAGASCAR

ARTHUR G. HUMES[1,2] AND JU-SHEY HO[1]

INTRODUCTION

At Nosy Bé, in northwestern Madagascar, copepods are known to be associated with many different marine invertebrates, but as yet none has been described from polychaete annelids. This paper deals with six new cyclopoid copepods collected from polychaetes at Nosy Bé in 1960 and 1963–64.

All collections were made by A. G. Humes, those in 1960 during an expedition of the Academy of Natural Sciences of Philadelphia, and those in 1963–64 as part of the U.S. Program in Biology of the International Indian Ocean Expedition. Type material has been deposited in the large copepod collection of the United States National Museum. Other specimens of the new species (with the exception of *Nasomolgus leptus*) have been placed in the Museum of Comparative Zoology.

The study of the specimens has been aided by a grant (GB-1809) from the National Science Foundation of the United States.

All figures were drawn with the aid of a camera lucida. The letter after the explanation of each figure refers to the scale at which it was drawn.

The abbreviations used are: a_1 = first antenna, a_2 = second antenna, md = mandible, p = paragnath, mx_1 = first maxilla, mx_2 = second maxilla, mxpd = maxilliped, p_1 = leg 1.

We wish to thank Dr. Marian H. Pettibone of the United States National Museum for the identification of the polychaete hosts and to acknowledge with appreciation the assistance to the field work given by the staff of the Centre d'Océanographie et des Pêches at Nosy Bé. We are indebted to Dr. J. P. Harding and Miss P. D. Lofthouse of the British Museum (Natural History) who have examined for us the single type specimen of *Nasomolgus cristatus*.

The copepods described in this paper comprise the following:

1) from *Lepidonotus cristatus* (Grube)
   Cotylomolgus lepidonoti n. gen., n. sp.
2) from *Sabella fusca* (Grube)
   Pseudanthessius ferox n. sp.
3) from *Sabellastarte magnifica* (Shaw)
   Nasomolgus firmus n. sp.
   Nasomolgus leptus n. sp.
   Nasomolgus rudis n. sp.
   Nasomolgus parvulus n. sp.

SYSTEMATIC DESCRIPTION

CLAUSIDIIDAE Embleton, 1901

COTYLOMOLGUS[1] n. gen.

Body cyclopoid, elongated, moderately widened and rather flattened in the pro-

[1] Boston University, Boston, Massachusetts
[2] Associate in Marine Invertebrates, Museum of Comparative Zoology

[1] The generic name is a combination of κοτυλή = a small cup, alluding to the sucker on the second antenna, and μολγός = a sack made of leather.

some. Segment of leg 1 completely fused with the head. Urosome 5-segmented in the female, 6-segmented in the male. Caudal ramus with 6 setae. First antenna 6-segmented. Second antenna 4-segmented, with a large pedunculate sucker on the third segment. Mandible with 4 terminal elements (1 flattened recurved attenuated spine and 3 setae). Paragnath a spinulose lobe. First maxilla a small lobe with 4 elements. Second maxilla probably 2-segmented, with terminally a recurved spine and a long spiniform element. Maxilliped absent in the female, but well formed in the male, where it is 4-segmented (assuming that part of the terminal claw represents the fourth segment).

Legs 1 and 2 with 3-segmented rami. Leg 3 reduced to a single free segment. Leg 4 absent in both sexes. Leg 5 two-segmented in the female, the first segment with a single seta, the second segment armed with 4 setae, 3 of them long and spiniform, the other short and slender. Leg 5 in the male with a single free segment.

Other features as in the species described below.

Living on polychaete annelids.

Type and only known species: *Cotylomolgus lepidonoti* n. sp.

Gender masculine.

Cotylomolgus lepidonoti[1] n. sp.
Figs. 1–29

Type material.—10 females, 8 males, and 3 immature specimens from 5 *Lepidonotus cristatus* (Grube) under intertidal rocks at Antsakoabe, on the northern shore of Nosy Bé, Madagascar. Collected December 1, 1963. Holotype female, allotype, and 11 paratypes (6 females and 5 males) deposited in the United States National Museum, Washington; the remaining paratypes in the collection of A. G. Humes.

Other specimens (all from *Lepidonotus cristatus* collected intertidally at various localities on Nosy Bé).—1 female from 1 host, Ambatoloaka, September 2, 1960; 7 females and 6 males from 2 hosts, Antsakoabe, November 1, 1963; 6 females, 4 males, and 2 immature from 2 hosts, Navetsy, November 3, 1963; 2 females and 3 males from 4 hosts, Antsakoabe, February 16, 1964; 4 females and 4 males from 2 hosts, Antsakoabe, September 7, 1964; and 1 female and 1 male from 1 host, Befifika, October 7, 1964.

Female.—The body (Figs. 1 and 2), with a moderately broadened and somewhat flattened prosome, has a length (excluding the setae on the caudal rami) of 1.41 mm (1.29–1.50 mm) and a greatest width of 0.63 mm (0.59–0.72 mm), based on 8 specimens. The ratio of length to width of the prosome is 1.35 : 1. The segment of leg 1 is completely fused with the head. The epimeral areas of the metasomal segments are rounded posteriorly. These segments are separated by faintly striated intersegmental membranes.

The segment of leg 5 (Figs. 3 and 4) is wider than long, 101 × 257 μ, and bears the fifth legs ventrally on the posterolateral areas. Dorsally the segment bears posteriorly a transverse striated membrane, and ventrally between the insertions of the legs there are 2 patches of spinules arranged in somewhat irregular rows. The genital segment is wider than long, 141 × 177 μ in greatest dimensions, with the broadened anterior two-thirds separated abruptly from the narrowed posterior third (where the width is 130 μ). The posterior margin of the segment bears a striated membrane dorsally and ventrally and has delicate spinules laterally. The areas of attachment of the egg sacs are situated dorsolaterally in the middle of the segment. Each area (Fig. 5) bears 2 small setae about 7 μ in length and a small setiform projection. There are 3 postgenital segments, the first 2 bearing a posterior membrane dorsally and ventrally and lateral spinules as on the genital segment (though the membrane on the second postgenital segment is incomplete midventrally and is indented mid-

[1] The specific name *lepidonoti* is derived from the generic name of the host.

dorsally). The first postgenital segment is 75 × 120 μ, the second 49 × 114 μ, and the third 60 μ (greatest length) × 101 μ. The anal segment, on which the caudal rami are inserted dorsally, bears ventrally near the base of each ramus a patch of very small spinules.

The caudal ramus (Fig. 6) is elongated, 78 μ in length along its outer edge (70 μ along the inner edge) and 33 μ in width, or about 2.4 times longer than wide. The outer lateral seta is 45 μ long and naked. The pedicellate dorsal seta is 36 μ and naked. The outermost terminal seta (86 μ) and the innermost terminal seta (66 μ) are minutely spinulose. There is a single well developed long median terminal seta 314 μ in length and naked. From its outer basal area there arises a finely spinulose slender seta 53 μ in length. This seta has no apparent articulation; presumably it represents the outer of the 2 long terminal setae commonly found in poecilostomes which here has fused with the base of the inner long seta. On the proximal half of the dorsal surface of the ramus there are a few small spinules and on the distal ventral surface there is a patch of very small spinules. A small hair arises on the proximal outer margin of the ramus.

The dorsal surface of the prosome and the dorsal and ventral surfaces of the urosome bear scattered minute setules. The ratio of the length of the prosome to that of the urosome is 2 : 1.

The egg sacs are moderately elongated (Fig. 7), 593 × 246 μ, and contain numerous mostly hexagonal eggs about 55–60 μ in diameter.

The rostral area (Fig. 8) is not well developed and consists of a small lobe lying behind the prominent crescentic ridge between the bases of the first antennae.

The first antenna (Fig. 9) is 6-segmented. The lengths of the segments (measured along their posterior margins) are: 36 (30 μ along the anterior margin), 73, 48, 50, 42, and 32 μ respectively. The first segment bears 5 setae (the posteriormost with lateral hairs); the second bears 11 proximal setae and 3 anterodistal setae; the third 6 medioanterior setae, a single medioposterior seta, and 2 distal setae; the fourth 2 setae and one aesthete proximally and 2 setae distally; the fifth 2 setae and one aesthete distally; and the sixth 7 setae and one aesthete. The formula thus is: 5, 14 (11 + 3), 9 (6 + 1 + 2), 4 + 1 aesthete (2 and 1 aesthete + 2), 2 + 1 aesthete, and 7 + 1 aesthete. All the setae are delicately annulated and naked except for the single haired seta on segment 1.

The second antenna (Figs. 10 and 11) is 4-segmented and distinctly flexed, with the 3 short distal segments directed back toward the relatively elongated proximal segment. The first segment bears anterodistally a cluster of hairs. The second segment bears a row of spinules. The third segment bears a hyaline seta, a spine with its distal third formed like a crooked thumb and spinulose, and a large pedunculate sucker 56 μ in diameter, its cup having well sclerotized supporting rays and with its rim formed by a hyaline lamella ornamented with minute hairlike processes (spinules?). The fourth segment is longer and more slender than the preceding 2 and bears 2 setae on a subterminal expansion and 4 terminal setae, all of them annulated and naked.

The labrum (Fig. 12), held erect in alcoholized specimens, is linguiform in outline, with a small terminal indentation and 2 lateral hyaline lobes.

The mandible (Fig. 13) is a single elongated segment bearing 4 terminal elements: a recurved attenuated flattened spine with a few short lateral spinules, and 3 setae with lateral spinules. The paragnath (Fig. 14) is a rounded lobe bearing slender spinules and showing small circular markings in its cuticle. The first maxilla (Fig. 15) is a small segment armed with 4 elements: 1 seta on the anterior surface, and 3 terminal setae (2 large, the longer 33 μ in length, and 1 shorter and slender). Near the base of the seta on the anterior surface

there is a group of surficial markings. The second maxilla (Figs. 16 and 17) probably consists of 2 segments, though the segmentation is obscure. The proximal portion (first segment?) bears a large ventral patch of small spinules arranged in irregular rows. The distal portion (second segment?) has surficial creases and folds, and bears 2 terminal elements: a greatly recurved spine having on its concave surface 2 relatively long hyaline spinules followed by 2 rows of minute spinules, and a long attenuated spiniform element not clearly articulated with the segment and bearing surficial punctations and a minute subterminal process. The maxilliped is absent.

The postoral area (Fig. 18) shows a number of sclerotized regions, with a transverse lobed area just posterior to the level of the second maxillae having a pair of irregular somewhat spherical sclerotizations. These 2 sclerotized pieces might be considered as remnants of maxillipeds, but since they are so far removed (see Fig. 8) from the usual position of maxillipeds in other poecilostomes they probably do not represent appendages. Posterior to the region shown in Figure 18 there is a balloonlike expansion (see Fig. 2) bearing 2 patches of small spinules arranged in irregular rows (Fig. 19).

As shown in a ventral view of the cephalosome (Fig. 8), the area between the bases of the first antennae is raised to form a crescentic ridge, and bears groups of small spinules. On either side, posterior to the bases of the antennae, the ventral wall of the cephalosome is raised to form a spinulose ridge that extends nearly to the posterolateral corners of the cephalosome. The rostrum and head appendages are thus surrounded by these ridges (except posteriorly). The ridges may aid (together with the 2 suckers on the second antennae) in adhesion to the host.

Legs 1 and 2 (Figs. 20 and 21) have 3-segmented rami. Leg 3 is reduced to a single segment. Leg 4 is absent. The spine and setal formula is as follows (the Arabic numerals indicating setae, there being no spines on the legs):

P 1	protopod	0-0;	1-0 exp	1-0; 1-1; 1,1,4
			end	0-1; 0-1; 4
P 2	protopod	0-0;	1-0 exp	1-0; 1-1; 1,4
			end	0-1; 0-1; 4
P 3	reduced,	1-0;	2	
P 4	absent			

Leg 1 (Fig. 20) shows a row of spinules on the outer distal area of the coxa, but there is no inner spine or seta on this segment. The intercoxal plate is broad and its distal edge is ornamented anteriorly and posteriorly with 2 groups of small spinules arranged in irregular rows. The basis has an outer haired seta and is ornamented on its anterior surface with a row of spinules between the insertions of the rami and with 3 or 4 rows of spinules medial to the insertion of the endopod; on the margin of the inner expansion of the basis there is a row of long hairs. The outer margins of the segments of both rami are well ornamented with spinules. Hairs occur along the inner margin of the first segment of the exopod and along the outer margins of the first and third segments of the endopod. The segments of the exopod bear slender annulated outer setae instead of the spines often seen in other poecilostomes. The inner margin of the third segment of the endopod shows an interruption of the sclerotization.

Leg 2 (Fig. 21) is in general similar to leg 1, but the several rows of spinules on the anterior surface of the basis medial to the insertion of the endopod are absent, the outer seta on the basis is smaller and naked, there is only 1 small annulated seta on the third segment of the exopod, and there is no interruption in the sclerotization of the inner margin of the third segment of the endopod.

Leg 3 (Fig. 22) consists of only a single elongated free segment, 58×22 μ, armed with 2 very unequal terminal setae, the inner 94 μ in length and bearing rows of very short spinules on its distal two-thirds, the outer 35 μ long, slender, and naked.

Near the insertions of the 2 setae there is a ventral patch of minute spinules. Close to the insertion of the free segment there is an outer naked seta 52 μ long arising from the body.

No trace could be found of leg 4.

Leg 5 (Fig. 23) is 2-segmented. The first segment is 88×73 μ, and bears an outer naked seta 52 μ long. On the dorsal surface of the segment there is a diagonal line from the base of the seta to the inner distal angle; on the ventral surface there are transverse rows of minute spinules near the distal margin. The second segment is 117 μ along the inner margin and 68 μ along the outer margin to the base of the first seta; its greatest diagonal length in 135 μ and its greatest width is 70 μ. The segment is armed with 2 outer lateral spiniform setae (99 and 112 μ long respectively) and 2 very unequal terminal setae, 1 slender and 55 μ, the other spiniform and 140 μ in length. All 4 setae bear extremely minute lateral spinules and are delicately annulated. Diagonal rows of minute spinules occur along the distal dorso-inner margin and extend around on the ventral surface to form a patch near the insertion of the innermost long seta. Another patch of minute spinules arranged in diagonal rows may occur (not in all specimens) on the ventral margin just proximal to the first outer seta.

Leg 6 is probably represented by the 2 small setae on the areas of attachment of the egg sacs (see Fig. 5).

The color in life in transmitted light is translucid to slightly opaque, the eye red, the egg sacs opaque gray.

Male.—The form of the body (Fig. 24) resembles that of the female. The length (without the setae on the caudal rami) is 1.06 mm (0.90–1.17 mm) and the greatest width is 0.46 mm (0.39–0.50 mm), based on 10 specimens. The ratio of length to width of the prosome is 1.4 : 1.

The segment of leg 5 (Figs. 25 and 26), measuring 81×172 μ, resembles that of the female. The genital segment is wider than long, 91×143 μ. The 4 postgenital segments are 55×107, 47×97, 33×92, and 40×86 μ from anterior to posterior.

The caudal ramus is like that of the female.

The surfaces of the prosome and urosome bear minute setules as in the opposite sex. The ratio of the length of the prosome to that of the urosome is about 1.8 : 1.

The rostral area, first antenna, second antenna, labrum, mandible, paragnath, first maxilla, and second maxilla resemble those of the female. The maxilliped (Fig. 27) has a rather poorly defined basal segment. The large second segment bears 2 hyaline naked setae on its inner surface and a large patch of small blunt spinules arranged in longitudinal rows on its posterior surface. The third segment is small and unarmed. The fourth segment probably forms part of the short and rather stout terminal claw, which is 54 μ in length (measured along its axis) and bears near its base a slender naked annulated seta and a very small setule. On the concave surface of the claw there is proximally a minute hyaline process and more distally 2 parallel rows of minute denticles.

The postoral area and the cephalosome resemble generally those areas in the female.

Legs 1, 2, and 3 are like those in the female. Leg 4 is absent.

Leg 5 (Fig. 28) has a single free segment and is held against the sides of the genital segment in alcholic specimens (see Fig. 25) rather than diverging as in the female. The free segment is more elongated than in the female, 59×25 μ in greatest dimensions. The 4 setae measure from outer to inner 79, 95, 39, and 127 μ in length. There is a patch of small spinules on the ventral surface near the insertion of the longest seta. The group of spinules seen in the female on the ventral margin proximal to the first outer seta is absent here. The seta arising from the body near the free segment is 55 μ long and naked.

Leg 6 (Fig. 26) consists of a postero-

lateral flap on the ventral surface of the genital segment, ornamented with minute spinules but apparently lacking spines or setae.

The spermatophore (Fig. 29), attached to the female, is elongated, 234 × 68 μ, including the neck.

The color in life in transmitted light resembles that of the female.

Taxonomic position of the genus.—The new genus *Cotylomolgus* appears to be related to *Myzomolgus* Bocquet and Stock, 1957 (Clausidiidae), and to *Catinia* Bocquet and Stock, 1957 (Catiniidae), genera which live on sipunculid worms. As in these two genera, *Cotylomolgus* has the segment of leg 1 fused with the head, the urosome in the female is 5-segmented and in the male 6-segmented, the first antenna is 6-segmented, the second antenna is 4-segmented with a large sucker on the third segment, the first maxilla bears four elements, leg 5 in the female is 2-segmented and in the male has only a single free segment, and the maxilliped in the male is 4-segmented (assuming that the fourth segment forms part of the claw).

Cotylomolgus differs from *Myzomolgus* chiefly in lacking the maxilliped in the female, in the reduction of leg 3 and the absence of leg 4, and in the absence of an inner spine on the basis of leg 1.

The new genus differs from *Catinia* in having a well developed mandible with four terminal elements, in the reduction of leg 3 and the absence of leg 4, and in the absence of an inner spine on the basis of legs 1–3.

Cotylomolgus differs from both *Myzomolgus* and *Catinia* in certain features of legs 1–4, principally, the absence of an inner spine on the basis of legs 1 and 2, the reduction of the outer spines on the exopods of legs 1 and 2 to simple setae, the reduction of leg 3 to a single free segment, and the absence of leg 4.

The nature of the mandible in *Cotylomolgus*, with its four terminal elements, is more like that of *Myzomolgus* than that of *Catinia*. (Gooding, 1963, in an unpublished thesis, after examination of specimens of *Catinia plana* Bocquet and Stock, 1957, has shown that a pair of small, weakly cuticularized mandibles, bent midway almost at a right angle and apparently without major spines or setae, exists in that species.) Since the structure of the mandible in poecilostomes is characteristic within supraspecific groups and thus may be regarded as indicative of phylogenetic relationship, *Cotylomolgus* appears to be closer to *Myzomolgus* than to *Catinia*.

Bocquet and Stock (1957, p. 430) placed their new genus *Myzomolgus* in the Clausidiidae largely on the basis of the structure of the mouthparts, notably the mandible, the antennae, and the well developed thoracic legs. While *Cotylomolgus* shows a reduction of the legs, a feature which is characteristic of many of the genera in the Clausiidae, the form of its mandible is clausidiid rather than clausiid. We are led, therefore, to include provisionally the genus *Cotylomolgus* in the Clausidiidae, recognizing at the same time that there is a close relationship between the Clausidiidae and the Clausiidae and that the two families may actually represent a single category (see Wilson and Illg, 1955, p. 137).

LICHOMOLGIDAE Kossmann, 1877
PSEUDANTHESSIUS Claus, 1889

Pseudanthessius ferox[1] n. sp.
Figs. 30–59

Type material.—14 females, 5 males, and 5 immature specimens from 3 *Sabella fusca* (Grube), in 1 m, at Ambariobe, a small island between Nosy Bé and Nosy Komba, Madagascar. Collected October 4, 1964. Holotype female, allotype, and 14 paratypes (11 females and 3 males) deposited in the United States National Museum, Washington; the remaining paratypes (dissected) in the collection of A. G. Humes.

[1] The specific name *ferox* (from Latin = warlike, savage) alludes to the rather formidable appearance of the labrum.

Other specimens (all from *Sabella fusca*). —1 female and 2 males from 1 host, in 6–8 m, Ambariobe, December 27, 1963; 4 females, 10 males, and 12 immature specimens from 1 host, in 1 m, west of Pte. Mahatsinjo, Nosy Bé, March 27, 1964; and 4 females and 5 males from 1 host, in 2 m, Andraikarebe, Nosy Komba, October 9, 1964 (these specimens placed in the Museum of Comparative Zoology).

Female.—The body (Fig. 30) is rather elongated, with the prosome moderately broadened. The length (not including the setae on the caudal rami) is 1.73 mm (1.63–1.97 mm) and the greatest width is 0.71 mm (0.67–0.75 mm), based on 10 specimens. The ratio of length to width of the prosome is 1.67 : 1. The segment of leg 1 is separated from the head by a dorsal furrow. Near the level of the maxillipeds on each side of the cephalosome there is a slight notch, perhaps indicating the boundary of the maxillipedal segment. The epimeral areas of the metasomal segments are rather pointed posteriorly.

The segment of leg 5 (Fig. 31) is 104 μ long and bears a transverse sclerotized area 153 μ in width. (The exact width of the segment is difficult to determine, since the fifth legs are fused with it.) The genital segment (Figs. 31, 32, and 33) is 224 μ in length. In dorsal view the segment is widened in its anterior two-thirds (180 μ), then narrowed in its posterior third (130 μ). On the ventral surface of the anterior half there are 2 swollen areas, each about 112 × 68 μ. In lateral view these areas protrude conspicuously. These swellings were seen on all females examined. Their size, shape, position, and lack of a neck make it unlikely that they represent spermatophores. The areas of attachment of the egg sacs are located dorsolaterally at the level of the segmental constriction. Each area in dorsal view (Fig. 34) shows a pedicellate naked seta 37 μ long set upon a sclerotized base and 2 spinelike elements, one 22 μ long and naked, the other 14 μ and bearing a subterminal setuliform process. In lateral view (Fig. 35) the armature is more clearly visible. The 3 postgenital segments are 78 × 112, 62 × 95, and 90 × 91 μ from anterior to posterior.

The caudal ramus (Fig. 36) is elongated, 109 × 38 μ, or about 2.9 times longer than wide. The outer lateral seta is 92 μ long, the pedicellate dorsal seta 31 μ, the outermost terminal seta 81 μ, the innermost terminal seta 138 μ, and the 2 median terminal setae 360 μ (outer) and 560 μ (inner). All the setae except the 2 median terminal ones are finely annulated and all are naked except the innermost terminal 1 which bears an inner row of hairs near its base. The dorsal and ventral surfaces of the ramus bear scattered minute setules.

The dorsal surface of the prosome and the dorsal and ventral surfaces of the urosome bear minute setules. The ratio of the length of the prosome to that of the urosome is 1.45 : 1.

The egg sacs are elongated (Fig. 30), in one female measuring 952 × 190 μ, though there is some variation in length in different individuals, and contain numerous eggs, each about 60 μ in diameter.

The rostral area (Fig. 37) is undeveloped and represented by a crescentic line between the bases of the first antennae.

The first antenna (Fig. 38) is 7-segmented, but the third segment has on its ventral surface a small proximal sclerotized area suggesting an intercalary segment. The lengths of the segments (measured along their posterior non-setiferous margins) are: 15 (70 μ along the anterior margin), 75, 33, 51, 47, 33, and 24 μ, respectively. The formula for the armature is 4, 13, 6, 3, 4 + 1 aesthete, 2 + 1 aesthete, and 7 + 1 aesthete. All the setae are naked except 1 on segment 5 and 4 on segment 7 which are haired. One of the terminal setae on the last segment is longer (150 μ) and stronger than any of the others.

The second antenna (Fig. 39) is 4-segmented, with the formula 1, 1, 3, and 5 + II. The last segment, about 55 × 39 μ, bears terminally 2 strong unequal claws 72 and

36 μ long, a slender transversely divided seta, and a small seta near the insertion of the smaller claw; subterminally there are 3 setae, 1 short, the other 2 long. All the setae are naked, and those on the last 2 segments are slightly annulated.

The labrum (Fig. 40) has 2 medial rounded and rather hyaline lobes, external to which there are 2 large well sclerotized spikelike processes about 50 μ in length which extend ventrally to the mouthparts. The labrum lacks fine ornamentation.

The mandible (Fig. 41) has a small naked spinelike element on the convex side at the base of the blade. The blade is attenuated distally and bears a striated flange on the convex side and a row of spinules on the concave side. The paragnath (Fig. 40) is probably represented by a small unoramented rather hyaline lobe about 17 μ long located between the base of the mandible and the outer corner of the labrum. The first maxilla (Fig. 42) consists of a single segment armed with 4 setae, all of which are indistinctly articulated. The second maxilla (Fig. 43) is 2-segmented. The first segment is unarmed. The second segment bears the usual armature consisting of a small hyaline basal outer seta, a larger seta on the posterodorsal surface, and a long subterminal spinulose seta, and terminates in a moderately short lash with prominent dentiform spines proximally becoming slender spinules distally. The maxilliped (Fig. 44) has 3 segments: an elongated unarmed basal segment, a rather swollen second segment partially divided by surficial creases and bearing on the inner surface proximally a patch of spinules and distally 2 naked elements (1 spiniform and 1 setiform), and a small slender terminal segment bearing on its inner surface 2 naked elements (1 spiniform and 1 setiform) and terminating in a spiniform process (not articulated).

The postoral area (see Fig. 37) does not protrude ventrally. A sclerotized line connects the bases of the maxillipeds.

Legs 1–4 (Figs. 45, 47, 48, and 49) have 3-segmented rami, with the exception of the endopod of leg 4 which consists of a single segment. The spine and setal formula is as follows (the Arabic numerals representing setae, the Roman numerals spines):

P 1	protopod	0-1;	1-0 exp	I-0; I-1; III,I,4
			end	0-1; 0-1; I,5
P 2	protopod	0-1;	1-0 exp	I-0; I-1; III,I,5
			end	0-1; 0-2; II,I,3
P 3	protopod	0-1;	1-0 exp	I-0; I-1; III,I,5
			end	0-1; 0-2; II,I,2
P 4	protopod	0-1;	1-0 exp	I-0; I-1; II,I,5
			end	II

The inner seta on the coxa of legs 1–3 is long and feathered, but in leg 4 this seta is minute (12 μ long) and naked. In the first 3 legs the inner margin of the basis bears a row of hairs, but these hairs are absent in leg 4. In leg 1 (Fig. 45) the outer spines of the exopod have short blunt spinules along one side. Between the rami the basis (as in legs 2 and 3 also) forms a sharply pointed process (Fig. 46). In leg 2 (Fig. 47) the outer spines of the exopod have delicate spinulose lamellae. The terminal spine on the last segment of the endopod is 66 μ long, naked, somewhat irregular, and has a minutely pointed tip. Leg 3 (Fig. 48) is similar to leg 2, except for differences in the spine and setal formula. Leg 4 (Fig. 49) has a less prominent and more rounded process on the basis between the rami. The endopod is 1-segmented, though the restriction of the inner lateral hairs to the proximal portion and the interruption in the sclerotization suggest a division of the segment. The segment measures 115×57 μ in greatest dimensions. The outer margin of the endopod is somewhat irregular and on its distal half there are 3 groups of minute denticles borne on 3 marginal lobes. The 2 terminal spines are 44 μ (inner) and 29 μ (outer) in length. There is an anterior row of minute spinules near the insertions of these spines.

Leg 5 (Fig. 50) does not have a free segment and bears terminally a naked spine 37 μ and a naked seta 56 μ in length,

and dorsally a seta 55 μ long with lateral hairs.

Leg 6 is probably represented by the armature on the area of attachment of the egg sacs (see Figs. 34 and 35).

The color in life in transmitted light is slightly opaque, the eye red, the egg sacs gray.

Male.—The form of the body (Fig. 51) resembles that of the female. The length (not including the setae on the caudal rami) is 1.41 mm (1.28–1.52 mm), and the greatest width is 0.46 mm (0.42–0.50 mm), based on 10 specimens (the allotype, 4 paratypes, and 5 specimens from Andraikarebe collected October 9, 1964). The epimeral areas of the segments of legs 2–4 are more rounded posteriorly than in the female. The ratio of length to width of the prosome is 1.66 : 1.

The segment of leg 5 is smaller than in the female, being only 52 × 96 μ, but otherwise similar. The genital segment (Fig. 52) is longer than wide, 161 × 146 μ, with gently arcuate lateral margins in dorsal view. The 4 postgenital segments are 77 × 90, 73 × 77, 50 × 64, and 64 × 64 μ from anterior to posterior.

The caudal ramus is like that of the female.

The surfaces of the prosome and urosome bear minute setules as in the female. The ratio of the length of the prosome to that of the urosome is about 1.15 : 1.

The rostral area and first antenna are like those in the female. The second antenna also resembles that of the female, but the slender transversely divided seta on the last segment next to the 2 claws is longer and more clawlike (Fig. 53). The labrum, mandible, paragnath, and first maxilla resemble those of the female. The second maxilla (Fig. 54) is much like that of the opposite sex, but the first segment appears to be a little more swollen and the terminal lash is relatively shorter. The maxilliped (Fig. 55) is 4-segmented (assuming that the fourth segment forms part of the claw). The first segment bears a prominent weakly sclerotized digitiform process on its distal inner corner. The second segment bears on its inner surface 2 setae (31 and 19 μ long) and a row of small spinules. The short third segment is unarmed. The slender claw (Fig. 56), 130 μ in length (measured along its axis), bears near its base a posterior seta 28 μ and an anterior seta 11 μ in length. The marginal lamella along the concave surface of the claw shows a minute interruption about midway, perhaps representing the distal boundary of the fourth segment. The tip of the claw has a very narrow lamella.

The postoral area resembles that of the female.

Leg 1 (Fig. 57) shows several differences from that of the female, especially in the endopod. The outer spines on the exopod are more slender and acutely pointed. The last 2 segments of the endopod are almost completely fused, the only evidence of the former articulation between them seen on the anterior surface where a line extends halfway across the ramus at the level of the spinous process. The distal part of the endopod is much modified, terminating in a sclerotized clawlike structure. There is a single short (10 μ) naked outer spine and 4 setae (1 naked, 20 μ long, with a narrow lamella, arising from the convex edge; 1 feathered, 32 μ long, arising on the posterior surface; and 2 feathered, 44 and 48 μ long, arising on the inner side). On the anterior surface between the spine and the first seta there is a sclerotized clawlike projection (for which no articulation could be seen). This projection may perhaps be derived from the outermost seta in the female. Two other small projections are located subterminally on the anterior surface. The presence of the clawlike structures and the curvature of the distal part of the endopod suggest a prehensile function. The formula for the endopod is 0-1; 0-1 . . . I,4.

Legs 2-5 resemble those of the female.

Leg 6 (Fig. 58) consists of a posterolateral flap on the ventral side of the genital

segment, bearing 2 naked setae 27 and 44 μ in length and having a surficial spiniform projection 4.5 μ long.

The spermatophore (Fig. 59), as seen within the body of the male, is elongated, 151 × 62 μ, not including the short neck of 10 μ.

The color in life in transmitted light resembles that of the female.

Comparison with other species in the genus.—Pseudanthessius ferox may be readily distinguished from 13 of the 22 species in the genus listed by Stock, Humes, and Gooding (1963) on the basis of three recognition characters: the two spikelike processes on the labrum in both sexes, the process on the first segment of the male maxilliped, and the clawlike modification of the endopod of leg 1 in the male. These 13 species, which lack one or more of the three characters and thereby differ from *P. ferox*, are: *aestheticus* Stock, Humes, and Gooding, 1963; *assimilis* G. O. Sars, 1917; *deficiens* Stock, Humes, and Gooding, 1963; *latus* Illg, 1950; *liber* (Brady, 1880); *luculentus* Humes and Cressey, 1961; *mucronatus* Gurney, 1927; *nemertophilus* Gallien, 1935; *notabilis* Humes and Cressey, 1961; *pectinifer* Stock, Humes, and Gooding, 1963; *sauvagei* Canu, 1892; *thorelli* (Brady, 1880); and *tortuosus* Stock, Humes, and Gooding, 1963. *Pseudanthessius procurrens* Humes, 1966 from a cidarid echinoid in Madagascar lacks all three of the characters just mentioned and thus is easily separated from *P. ferox*.

Unfortunately, in the remaining 9 species no information is available regarding these three recognition characters, and other features must be used to separate them from *P. ferox*. Of these species, *liber, sensu* Sewell, 1949, has two long elements on the first segment of the first antenna; *dubius* G. O. Sars, 1918, has a 4-segmented urosome in the female; and the remaining 7 species (*concinnus* Thompson and A. Scott, 1903, *gracilis* Claus, 1889, *graciloides* Sewell, 1949, *obscurus* A. Scott, 1909, *spinifer* Lindberg, 1945, *tenuis* Nicholls, 1944, and *weberi* A. Scott, 1909) have slender setiform elements instead of strong claws on the last segment of the second antenna.

In addition to these differences, other features, such as the length to width ratio of the caudal rami, may be useful in separating many of the species from *P. ferox*. None of the known species of *Pseudanthessius* seems to be closely related to the new species from Madagascar.

NASOMOLGUS Sewell, 1949

This genus was established by Sewell on the basis of a new species, *Nasomolgus cristatus*, of which he found only a single female in debris at a depth of 38 m off the South Arabian coast. In describing the four new species which follow, we have been unable to compare at firsthand this type specimen (which is in the British Museum). However, Dr. J. P. Harding and Miss P. D. Lofthouse of the Museum staff have examined the permanent slide of *N. cristatus* and have supplied us with information on several critical points.

Nasomolgus firmus[1] n. sp.
Figs. 60–86

Type material.—28 females and 4 males from one sabellid polychaete, *Sabellastarte magnifica* (Shaw), in 2 m, at Ambariotelo, a small island between Nosy Bé and Nosy Komba, Madagascar. Collected May 15, 1964. Holotype female, allotype, and 20 paratypes (females) deposited in the United States National Museum, Washington; the remaining paratypes in the collection of A. G. Humes.

Other specimens (all from *Sabellastarte magnifica*).—14 females and 3 males from 2 hosts, under intertidal dead coral at Antsakoabe, on the northern shore of Nosy Bé, November 1, 1963 (of this collection 7 females and 2 males placed in the Museum of Comparative Zoology); 5 females and 3 males from one host, under intertidal rock at Antsakoabe, September 7, 1964.

[1] The specific name *firmus* (from Latin = firm, strong, robust) refers to the strong sclerotization of the body wall and appendages in this species.

Female.—The body (Fig. 60) is moderately broadened with a flattened prosome. The length (without the setae on the caudal rami) is 0.81 mm (0.78–0.84 mm) and the greatest width is 0.36 mm (0.33–0.38 mm), based on 10 specimens. The ratio of length to width of the prosome is 1.46 : 1. The segment of leg 1 is rather indistinctly set off from the head, and its lateral areas are rounded posteriorly. The epimeral areas of the segment of leg 2 are truncated, those of the segment of leg 3 are broadly rounded, and those of the small segment of leg 4 are rather truncated.

The segment of leg 5 (Fig. 61) is rather narrow, 36 × 68 μ, and bears the small fifth legs slightly ventrally a little posterior to the midlateral areas. There is a narrow weakly sclerotized intersegmental sclerite ventrally between the segment of leg 5 and the genital segment. The genital segment is longer than wide, and (as seen in dorsal view) is expanded in its anterior part to form 2 broadly rounded wings but is narrowed posteriorly where its sides are parallel. The length of the segment is 110 μ, the width at the expanded part 100 μ, and the width in the narrow posterior portion 58 μ. The areas of attachment of the egg sacs are situated dorsolaterally on the posterior halves of the expansions. Each area (Fig. 62) bears 2 small naked setae 20 μ and 10 μ in length. There are 3 postgenital segments, without posterior rows of spinules, the first 46 × 48 μ, the second 41 × 43 μ, and the third 44 × 42 μ.

The caudal ramus (Fig. 63) is moderately elongated, 39 μ along its outer edge, 35 μ along its inner edge, and 43 μ in greatest length (including the subconical terminal expansion). Its width proximal to the lateral seta is 18 μ, and distal to that seta 15.5 μ. Taking the greatest dimensions, the ratio of length to width is 2.9 : 1. The outer lateral seta, situated 21 μ from the base of the ramus, is 33 μ long. The pedicellate dorsal seta is 33 μ, the outermost terminal seta 40 μ, and the innermost terminal seta 39 μ. The 2 long median terminal setae, inserted between unornamented dorsal and ventral flaps, are 180 μ (outer) and 325 μ (inner), and do not show the basal "pegs" often seen in lichomolgids. The surfaces of the ramus are without ornamentation except for a setule and a refractile point dorsally.

The dorsal surface of the prosome is ornamented with minute setules and refractile points, and in addition the posterior half of the cephalosome shows dorsally a broad band of extremely fine transverse striations (visible only under very high magnification and not shown in Fig. 60). In dorsal view there are 2 internal longitudinal sclerotized bars (Fig. 60) extending posteriorly from the rostral area to nearly the middle of the cephalosome. (The dorsal surface of the cephalosome in this region is smooth, there being no crest such as Sewell described in *N. cristatus.*) The dorsal and ventral surfaces of the urosome bear relatively few minute setules and refractile points. The ratio of the length of the prosome to that of the urosome is 1.6 : 1.

The body wall (and, as will be seen below, the appendages) is strongly sclerotized, in contrast to the 3 species whose descriptions follow.

The egg sacs are slender (Fig. 64) and reach well beyond the ends of the caudal rami. Each sac is about 418 × 99 μ, and contains numerous eggs about 47 μ in diameter.

The rostral area (Fig. 65) projects slightly in front of the head. Posterior to it, on the ventral surface of the head between the insertions of the second antennae, there is a slight longitudinal ridge.

The first antenna (Fig. 66) is 7-segmented. The lengths of the segments (measured along their posterior non-setiferous margins) are: 13 (35 μ along the anterior edge), 57, 22, 28, 25, 17, and 13 μ respectively. The entire first antenna (without the terminal setae) is about 185 μ long. The formula is: 4, 13, 6, 3, 4 + 1 aesthete, 2 + 1 aesthete, and 7 + 1 aesthete.

All the setae are naked. The third segment shows ventrally a sclerotization suggesting an intercalary segment.

The second antenna (Fig. 67) is 4-segmented and rather robust. The first and second segments bear a single small inner seta. The short third segment bears 3 setae, one much larger than the other two. The fourth segment bears 7 elements: 3 proximal slender setae, another more distal slender seta, a slender clawlike seta, and 2 stout recurved claws. All the setae are naked. The entire second antenna is about 108 μ in length.

The labrum (Fig. 65) bears anterolaterally a pair of naked setae, each 44 μ in length, directed ventrally and somewhat anteriorly, and rather indistinctly articulated with the surface of the labrum. Near the extreme anterior end of the labrum, between these 2 setae, there is a somewhat triangular raised sclerotized area (rather similar to that described by Sewell in *N. cristatus*). Posteriorly the labrum is bifurcated to form 2 rounded lobes without ornamentation.

The mandible (Fig. 68) has a moderately elongated blade, with a row of small spinules along the concave outer margin and a fringe of large hyaline spiniform elements along the convex inner margin (the proximal spinelike element in this row being slightly more sclerotized and prominent that the succeeding ones). There are 2 sclerotized spiniform elements on the dorsal surface of the blade. The paragnath (Fig. 69) is a small lobe with hairs along its medial side. The first maxilla (Fig. 70) is a small lobe bearing 4 elements: terminally 2 long unilaterally barbed spines and a minute naked setule, subterminally a shorter naked spine. The second maxilla (Fig. 71) is 2-segmented, the first segment bearing a prominent sclerotized conical projection on its outer margin. The second segment bears proximally 2 slender naked inner setae and a minute outer setule; the segment is prolonged to form a short process bearing a row of about 8 outer spines graduated in length and becoming smaller distally. The maxilliped (Fig. 72) is 3-segmented and slender. The first segment is unarmed. The second segment bears 2 small inner naked setae. The clawlike third segment is very long (110 μ) and slender; proximally on the inner side there is a small naked seta and a minute setule. The distal half of the segment is more slender and less sclerotized than proximally and bears a row of short hairs along each side.

The postoral area (Fig. 65) shows a pair of sclerotizations extending medially from the bases of the maxillipeds, but not joining each other. There is a slightly projecting cordiform area just posterior to the mouth region. The area between the maxillipeds and the first pair of legs projects only slightly.

Legs 1–4 (Figs. 73, 74, 75, and 76) have 3-segmented rami except for the endopod of leg 4 which is 2-segmented. The spine and setal formula is as follows (the Roman numerals indicating spines, the Arabic numerals setae):

P 1	protopod 0-1; 1-0	exp	I-0; I-1;	III,I,4
		end	0-1; 0-1;	I,5
P 2	protopod 0-1; 1-0	exp	I-0; I-1;	III,I,5
		end	0-1; 0-2;	I,II,3
P 3	protopod 0-1; 1-0	exp	I-0; I-1;	II,I,5
		end	0-1; 0-2;	II,2
P 4	protopod 0-1; 1-0	exp	I-0; I-1;	II,I,5
		end	0-1; 2	

The inner seta on the coxa of legs 1–3 is long and feathered, but in leg 4 this seta is shorter (20 μ) and naked. A row of hairs occurs on the inner margin of the basis in all 4 legs. The spines on the exopods are recurved posteriorly, with the lateral fringe along their proximal sides more prominent than that on their distal margins. The outer spines on the exopod of leg 1 show small subterminal flagella; the terminal spine on this ramus has a straight tip, while in legs 2–4 the tip is reflexed. The outer spine on the last segment of the endopod of leg 1 is 7 μ in length. The endopod of leg 4 is elongated (Fig. 76). The first segment is 18×11 μ, having a row of hairs on the outer margin and bearing a long feathered

inner distal seta 68 μ in length. The second segment measures 39 × 8 μ, having a row of hairs on both outer and inner margins and bearing 2 unequal terminal naked setae, the outer one 31 μ, the inner one 50 μ in length. In addition, there is an anterior row of minute spinules on the end of the segment near the insertions of the 2 setae.

Leg 5 (Fig. 77) has a very small quadrate free segment, 6 × 6 μ, bearing 2 terminal naked setae, the anterior 1 slender and 28 μ long, the posterior 1 much stouter and 44 μ long. The seta arising from the body wall adjacent to the segment is naked and 26 μ long.

Leg 6 is probably represented by the 2 setae near the attachment of the egg sacs (see Fig. 62).

The color in life in transmitted light is slightly opaque, the eye red, the egg sacs gray.

Male.—The body (Fig. 78) is more slender than in the female. The length (excluding the setae on the caudal rami) is 0.58 mm (0.52–0.63 mm) and the greatest width is 0.16 mm (0.14–0.18 mm), based on 10 specimens (the allotype, 3 paratypes, 3 specimens collected at Antsakoabe on November 1, 1963, and 3 collected at the same locality on September 7, 1964). The ratio of length to width of the prosome is 1.8 : 1. The segment of leg 1 is more distinctly separated from the head than in the female.

The segment of leg 5 (Fig. 79), 37 × 29 μ, resembles that of the female. The ventral intersegmental sclerite between the segment of leg 5 and the genital segment is not evident. The genital segment is longer than wide, 97 × 75 μ, with its lateral borders in dorsal view only slightly rounded. The 4 postgenital segments are 24 × 37, 29 × 34, 23 × 31, and 25 × 30 μ from anterior to posterior.

The caudal ramus (Fig. 80) resembles that of the female, but is relatively shorter, the greatest dimensions being 27 × 13 μ, or 2 times longer than wide. The 2 long terminal setae show basal "pegs."

The surfaces of the prosome and urosome bear scattered hairs and refractile points. The fine transverse striations seen on the dorsal posterior half of the cephalosome in the female are absent here. The ratio of the length of the prosome to that of the urosome is 1.25 : 1.

The rostral area and first antenna resemble those of the female. The second antenna (Fig. 81) is a little more slender than in the female. The first and second segments bear a small seta as in the female, but, in addition, the second segment is ornamented on its inner surface with 2 rows of minute spinules. The third segment bears 4 setae, 3 of them slender, the other larger and placed more distally, very near the base of the fourth segment. The fourth segment bears 7 elements: 3 slender outer setae, 2 setae near the bases of the claws, and 2 recurved claws, 1 slender, the other stout. The labrum, mandible, paragnath, and first maxilla resemble those of the female. The second maxilla (Fig. 82) has on the outer margin of its first segment groups of small spinules and a small process which is perhaps homologous to the prominent conical projection seen in the female. The maxilliped (Fig. 83) is slender and 4-segmented (assuming that the fourth segment forms part of the claw). The first segment shows on its inner edge a small knob and a rather pointed sclerotized process. The second segment has 2 small inner naked setae and 2 inner rows of small spinules. The small third segment is unarmed. The recurved claw, 58 μ in length (measured along its axis), bears proximally a posteromedial, minutely barbed seta 20 μ long and on its inner edge a slender naked setule 6 μ long and a small process. The posteroinner surface of the claw is covered with minute blunt spinules. At the tip of the claw there is a conspicuous lamella.

The postoral area resembles that of the female.

Legs 1–4 in general resemble those of

the female, having the same spine and setal formula. The outer distal corners of the first 2 segments of the endopods in legs 1–3 bear small spinelike processes not present in the female. The outer spine on the last segment of the endopod of leg 1 (Fig. 84) is 11 μ in length, a little longer than in the female.

Leg 5 is like that of the female.

Leg 6 (Fig. 85) consists of a posterolateral flap on the ventral surface of the genital segment, bearing 2 naked setae 17 and 28 μ long.

In 2 females spermatophores (Fig. 86) were attached in pairs. In both cases the 2 elongated spermatophores (86 × 31 μ without the neck) were joined in a common tube which led into the genital segment.

The color in life in transmitted light resembles that of the female.

Comparison with Nasomolgus cristatus.—*Nasomolgus firmus* seems to be close to *N. cristatus*, but shows several differences. In *N. firmus* the caudal ramus is a little longer (with a ratio of length to width of 2.9 : 1 instead of about 2.5 : 1), the lateral seta on the ramus is inserted halfway along the margin instead of at about the junction of the middle and distal thirds as in Sewell's species, the formula for the last segment of the endopod of leg 3 is II,2 instead of I,II,2, the two setae on the end of the last segment of the endopod of leg 4 have a ratio of 1 : 1.6 instead of about 1 : 2.2 as in Sewell's fig. 35E, and the outline of the genital segment in dorsal view is slightly different.

In both *N. cristatus* and *N. firmus* the labrum bears anteriorly a pair of prominent ventrally directed setae, there is a somewhat triangular sclerotized raised area near the front of the labrum at the posterior end of the rostral area, the maxilliped is 3-segmented with the last segment very long and slender, and the arrangement of the spines on the last segment of the exopod of leg 1 is III,I instead of II,I as in Sewell's formula (p. 125). Since it has been impossible to dissect the single type specimen of *N. cristatus*, the mouthparts cannot be compared in detail.

Nasomolgus leptus[1] n. sp.
Figs. 87–109

Type material.—4 females and 4 males from 2 *Sabellastarte magnifica* (Shaw), under intertidal dead coral at Antsakoabe, on the northern shore of Nosy Bé, Madagascar. Collected November 1, 1963. Holotype female, allotype, and 4 paratypes (2 females and 2 males) deposited in the United States National Museum, Washington; the remaining paratypes (both dissected) in the collection of A. G. Humes. (This species was collected in company with *N. firmus*, from the same 2 polychaetes.)

Female.—The body (Fig. 87) is elongated and rather slender, with the prosome not broadened and not as flattened as in the previous species. The length (not including the setae on the caudal rami) is 1.40 mm (1.37–1.44 mm) and the greatest width is 0.35 mm (0.31–0.39 mm), based on 4 specimens. The ratio of length to width of the prosome is 1.8 : 1. The segment of leg 1 is distinctly separated from the head. The epimeral areas of the metasomal segments resemble fairly closely those in the previous species.

The segment of leg 5 (Fig. 88) is 60 × 94 μ, with the small fifth legs borne as in *N. firmus*. A weakly developed intersegmental sclerite occurs ventrally between the segment of leg 5 and the genital segment. The genital segment is longer than wide, in dorsal view being broadly expanded laterally in its anterior half and constricted in its posterior half. The length of the segment is 174 μ, the width at the expansions 140 μ, and the width in the posterior part of the constricted area 73 μ (at this level the segment being slightly wider than more anteriorly). The areas of attachment of the egg sacs are placed

[1] The specific name *leptus* (from λεπτός = thin, slender) refers to the elongated slender form of the body in this species.

dorsolaterally on the posterior halves of the expansions. Each area (Fig. 89) carries 2 naked setae, 11 and 24 μ in length. The 3 postgenital segments, without posterior rows of spinules, are 96×60, 82×52, and 96×55 μ (the last segment being slightly expanded laterally in its posterior half where the width was measured).

The caudal ramus (Fig. 90) is very elongated and slender, 278 μ in length, 25 μ wide in its basal part and 19 μ wide at the level of the outer lateral seta. Taking the latter width, the ratio of length to width is 14.6 : 1. The outer lateral seta, located 177 μ from the base of the ramus, is 36 μ long. The pedicellate dorsal seta is 26 μ, the outermost terminal seta 40 μ, the innermost terminal seta 36 μ, and the 2 long median terminal setae are 143 μ (outer) and 260 μ (inner) and show weak basal "pegs." All the setae are naked. A minute setule 3 μ long occurs on the outer proximal margin of the ramus. The ramus is ornamented with a few minute hairs.

The dorsal surface of the prosome bears very few hairs and no refractile points. The dorsal and ventral surfaces of the urosome are very sparsely ornamented with hairs and refractile points. The urosome is longer than the prosome, the ratio being 1.2 : 1.

The egg sacs (Fig. 87) are elongated and slightly arcuate, reaching beyond the tips of the long caudal rami. Each sac is about 759×198 μ, and contains many eggs approximately 57 μ in diameter.

The rostral area (Fig. 91) does not project forward as in the previous species. Between the rostrum and the labrum there is a low longitudinal ridge (between the bases of the second antennae).

The first antenna (Fig. 92) is 7-segmented, the lengths of the segments (measured along their posterior non-setiferous margins) being: 18 (44 μ along the anterior margin), 94, 35, 45, 31, 18, and 14 μ respectively. The formula for the setae and aesthetes is the same as in *N. firmus*. All the setae are naked.

The second antenna (Fig. 93) is 4-segmented and fairly robust. Each of the first 2 segments bears a short distal inner seta with lamellate margins. The third segment bears 2 such setae plus a longer seta. The fourth segment carries 7 elements (including 2 stout recurved claws) much like those of *N. firmus*.

The labrum (Figs. 91 and 94) bears anterolaterally, as in the previous species, a pair of ventrally directed naked setae, each 55 μ in length. There is no triangular sclerotized area in front of the labrum, such as seen in *N. firmus*. Posteriorly, the edge of the labrum is deeply bilobed, with each lobe elongated, rounded, and unornamented, and with a short median process between the bases of the lobes.

The mandible (Fig. 95), paragnath, and first maxilla (Fig. 96) resemble those of *N. firmus*. The second maxilla (Fig. 97) is 2-segmented. The first segment has a broad sclerotized bulge on its outer margin and an interrupted crescentic row of spinules on its posterodorsal surface. The second segment is similar to that in the previous species, but the spines on the distal prolongation are more numerous and slender. The maxilliped is very similar to that of *N. firmus*, having the same general form and armature and with the slender clawlike segment 122 μ long.

The postoral area (Fig. 98) resembles generally that in the previous species and shows a weak line between the bases of the maxillipeds. The ventral surface between the bases of the maxillipeds and the first pair of legs is slightly protuberant.

Legs 1–4 (Figs. 99, 100, 101, and 102) resemble those of *N. firmus*, with the same spine and setal formula except for the endopod of leg 3 where the formula is 0-1; 0-2; I,II,2, the outer marginal spine on the last segment being retained. The terminal spine on the last segment of the exopods of all 4 legs is not reflexed at the tip. The outer spine on the last segment of the endopod of leg 1 is 14 μ in length. The endopod of leg 4 is elongated (Fig. 102). The first segment is 33×19 μ and bears a short

feathered inner distal seta 22 μ long. The second segment is 74 × 13 μ and bears 2 terminal slightly barbed setae 44 μ (outer) and 77 μ (inner) in length. The ornamentation of the endopod resembles that of *N. firmus*. The inner coxal seta of leg 4 is short (13 μ) and naked.

Leg 5 (Fig. 103) resembles that in the previous species, with the small free segment 7 μ in anterior length, 6 μ in posterior length, and 8 μ in width at the middle.

Leg 6 is probably represented by the 2 setae near the attachment of the egg sacs (see Fig. 89).

The color in life in transmitted light is moderately translucid, the eye red, the egg sacs gray.

Male.—The body (Fig. 104) is more slender than that of the female. The length (excluding the setae on the caudal rami) is 0.94 mm (0.93–0.96 mm) and the greatest width is 0.19 mm (0.18–0.19 mm), based on 4 specimens. The ratio of length to width of the prosome is 2.1 : 1. The segment of leg 1 is less distinctly set off from the head than in the female.

The segment of leg 5, 40 × 58 μ, resembles that of the female. Ventrally between the segment of leg 5 and the genital segment there is no evident intersegmental sclerite. The genital segment (Fig. 105) is elongated, 151 × 50 μ, with its sides in dorsal view slightly rounded. The 4 postgenital segments are 57 × 46, 61 × 40, 47 × 34, and 57 × 33 μ from anterior to posterior.

The caudal ramus (see Fig. 105) is elongated, 135 × 16 μ, about 8.4 times longer than wide. It is a little less tapered distally than in the female, but bears similar armature.

The dorsal surface of the prosome seems to lack ornamentation. The dorsal and ventral surfaces of the urosome are unornamented except for a pair of hairs on the dorsal surface of the anal segment. As in the female, the urosome is longer than the prosome, the ratio being 1.3 : 1.

The rostral area and first antenna resemble those of the female. The second antenna (Fig. 106) is more slender than in the female. The arrangement of the spines and setae is the same as in the male of *N. firmus*, with 4 elements on the third segment instead of 3 as in the female. The 2 terminal claws are distinctly jointed. The slender clawlike seta on the last segment has a more blunt tip than in the female. The fine ornamentation, not present in the female, consists of a small patch of spinules on the inner proximal surface of the first segment and a long patch of small spinules on the inner surface of the second segment.

The labrum, mandible, paragnath, and first maxilla resemble those of the female. The second maxilla is also similar to that in the opposite sex, but the outer bulge on the first segment is much less prominent. The maxilliped (Fig. 107) resembles in general form that of *N. firmus*. The second segment has on its inner surface 2 small naked setae and 2 rows of spinules. The recurved claw, 68 μ in length (measured along its axis), shows a slight indication of division. Proximally the claw bears a posteromedial barbed seta 19 μ long and an adjacent inner naked setule 6 μ long. The concave surface of the claw bears a row of small spinules, instead of being covered with minute blunt spinules as in *N. firmus*.

The postoral area is similar to that in the previous species.

Legs 1–4 are like those of the female, with the same spine and setal formula. The outer distal spine on the last segment of the endopod of leg 1 is 16.5 μ in length, being slightly longer than in the female.

Leg 5 resembles that of the female.

Leg 6 (Fig. 108) consists of a posterolateral flap on the ventral surface of the genital segment, bearing 2 slender naked setae 26 and 31 μ in length.

The spermatophore (Fig. 109), seen only inside the body of a male, is elongated, 113 × 49 μ, not including the neck.

The color in life resembles that of the female.

Comparison with other species.—Nasomolgus leptus may readily be distinguished

from *N. firmus* and *N. cristatus* by its greater length, by its more slender body form, and by the much more elongated caudal rami. It differs further from *N. firmus* in the nature of the protuberance on the first segment of the second maxilla in the female and in the ornamentation of the claw on the maxilliped in the male.

Nasomolgus rudis[1] n. sp.
Figs. 110–135

Type material.—10 females and 5 males from one *Sabellastarte magnifica* (Shaw), in 2 m, at Ambariotelo, a small island between Nosy Bé and Nosy Komba, Madagascar. Collected May 15, 1964. Holotype female, allotype, and 10 paratypes (8 females and 2 males) deposited in the United States National Museum, Washington; the remaining paratypes (dissected) in the collection of A. G. Humes.

Other specimens (all from *Sabellastarte magnifica*, but one host identification uncertain as indicated below).—10 females and 2 males from 2 hosts, under intertidal dead coral, Antsakoabe, on the northern shore of Nosy Bé, November 1, 1963; 11 females from 1 host (only the plume collected, but probably *S. magnifica*), in 14 m, Tany Kely, a small island south of Nosy Bé, December 23, 1963; 9 females and 1 male from 1 host, under intertidal rock, Antsakoabe, September 7, 1964 (these specimens placed in the Museum of Comparative Zoology); and 4 females from 1 host in 1 m, Ambariobe, near Ambariotelo, October 10, 1960.

Female.—The body (Fig. 110) is broadened in the prosomal region. The length (excluding the setae on the caudal rami) is 0.87 mm (0.77–0.97 mm) and the greatest width is 0.41 mm (0.36–0.46 mm), based on 10 specimens. The ratio of the length to the width of the prosome is 1.45 : 1. The segment of leg 1 is clearly set off from the head. The epimeral areas of the pedigerous segments are shaped much as in *N. leptus*.

The segment of leg 5 (Fig. 111) is 55 × 78 μ, with the fifth legs borne as in the 2 previous species. There is a small intersegmental sclerite ventrally between the segment of leg 5 and the genital segment. The genital segment is a little wider than long and in dorsal view is broadly expanded in its anterior two-thirds and constricted in its posterior third. The length of the segment is 99 μ, the width at the expansions 112 μ, and the width in the posterior part of the constricted area 58 μ. The areas of attachment of the egg sacs are situated dorsolaterally on the posterior halves of the expansions. Each area (Fig. 112) bears 2 naked setae 31 and 11 μ in length, a short inner spinous process, and an outer membranous expansion. The 3 postgenital segments, without posterior rows of spinules, are 32 × 52, 24 × 45, and 33 × 43 μ from anterior to posterior.

The caudal ramus (Fig. 113) is short, 25 μ along its inner margin, 27 μ along its outer margin, and 18 μ wide at the level of the outer lateral seta. The ratio of length to width is 1.44 : 1. The outer lateral seta, located 14 μ from the base of the ramus, is 56 μ long. The pedicellate dorsal seta is 33 μ, the outermost terminal seta 54 μ, the innermost terminal seta 72 μ, and the 2 long median terminal setae are 265 μ (outer) and 407 μ (inner) and are basally "pegged." All the setae are naked. Two minute hairs occur on the dorsal surface of the ramus.

The dorsal surface of the prosome is almost devoid of ornamentation, there being only a few hairs on the metasomal segments. The dorsal and ventral surfaces of the urosome have scattered hairs and refractile points. The prosome is much longer than the urosome, the ratio being 2.53 : 1.

The egg sacs are elongated, extending to the ends of the ramal setae. Each sac (Fig.

[1] The specific name *rudis* (from Latin = unaffected, simple) refers to the relatively uncomplicated external anatomy of this species.

114) is about 462 × 132 μ, with numerous eggs 44–47 μ in diameter.

The rostral area (Fig. 115) resembles generally that of *N. leptus*, and there is a low ridge between the bases of the second antennae as in that species.

The first antenna (Fig. 116) is much like that in *N. leptus*, with the same arrangement of setae and aesthetes. The lengths of the segments (measured along their posterior non-setiferous margins) are: 13 (38 μ along the anterior margin), 68, 26, 34, 27, 17, and 15 μ respectively. All the setae are naked.

The second antenna (Fig. 117) also resembles that of *N. leptus*, but the seta on the first segment is hyaline and lacks the lamellate margins.

The labrum (Figs. 115 and 118) resembles in general form that of the 2 previous species. Each of the 2 anterolateral and ventrally directed setae is 36 μ long and naked. The 2 posterior lobes are unornamented. There is no triangular sclerotized area near the front of the labrum, such as seen in *N. firmus*.

The mandible (Fig. 119), paragnath, and first maxilla (Fig. 120) are similar to those in the 2 previous species. The second maxilla (Fig. 121) resembles in general form that of *N. leptus*. There is a lightly sclerotized bulge on the outer margin of the first segment. Of the several spines on the distal end of the second segment the first spine is somewhat larger than the succeeding ones. The maxilliped (Fig. 122) resembles that in the 2 previous species, the slender terminal segment being 113 μ long.

The postoral area (Fig. 123) resembles that of *N. leptus*.

Legs 1–4 (Figs. 124, 125, 126, and 127) have the same spine and setal formula as in *N. leptus*, and closely resemble that species in their fine ornamentation. The outer spine on the last segment of the endopod of leg 1 is 10 μ long. The 3 spines on the last segment of the endopod of leg 2 are 12, 9, and 9 μ in length from distal to proximal; those on leg 3 are 16, 10, and 11 μ respectively. The inner coxal seta of leg 4 is 15 μ long and naked. The endopod of leg 4 is less elongated (Fig. 127) than in either of the 2 previous species. The first segment is 28 × 14 μ and bears a short feathered inner distal seta 29 μ long. The second segment is 47 × 12 μ and bears 2 terminal slightly barbed setae 32 μ (outer) and 66 μ (inner) in length. The fine ornamentation of the endopod is similar to that in the 2 previous species.

Leg 5 (Fig. 128) resembles that of *N. leptus*, with the segment having similar dimensions.

Leg 6 is probably represented by the 2 setae near the attachment of the egg sacs (see Fig. 112).

The color in life in transmitted light resembles that in the 2 previous species.

Male.—The body (Fig. 129) is much more slender than in the female. The length (excluding the setae on the caudal rami) is 0.52 mm (0.50–0.54 mm) and the greatest width is 0.15 mm (0.14–0.16 mm), based on 8 specimens (the allotype, 4 paratypes, 2 specimens collected at Antsakoabe on November 1, 1963, and one specimen collected at the same locality on September 7, 1964). The ratio of the length to the width of the prosome is 2.2 : 1. The separation between the segment of leg 1 and the head is rather weak.

The segment of leg 4, 28 × 44 μ, resembles that of the female. The ventral intersegmental sclerite between the segment of leg 5 and the genital segment is absent. The genital segment (Fig. 130) is elongated, 90 × 73 μ, with its sides in dorsal view nearly parallel. The 4 postgenital segments are 22 × 35, 22 × 33, 16 × 31, and 19 × 30 μ from anterior to posterior.

The caudal ramus (see Fig. 130) is relatively shorter than in the female. The length along the outer edge is 19 μ, along the inner edge 18 μ, and its width is 14 μ, or about 1.3 times longer than wide.

The dorsal surface of the prosome is unornamented. The dorsal and ventral sur-

faces of the urosome bear a few hairs and refractile points. As in the female, the prosome is longer than the urosome, the ratio being 1.54 : 1.

The rostral area resembles that of the female. The ridge seen between the bases of the second antennae in the female appears to be absent.

The first antenna is like that of the female. The second antenna (Fig. 131) has the same arrangement of spines, setae, and claws as in the preceding 2 species, with 4 elements on the third segment instead of 3 as in the female. The seta on the first segment has lamellate margins. The 2 large claws are distinctly jointed. The fine ornamentation is like that in *N. leptus*.

The labrum resembles that of the female, but the 2 large setae are situated more posteriorly. The mandible, paragnath, and first maxilla resemble those in the female. The second maxilla (Fig. 132) lacks the bulge on the outer margin of the first segment, but instead bears groups of small spinules; the spines along the distal end of the second segment are more numerous than in the opposite sex. The maxilliped (Fig. 133) resembles generally that of *N. leptus*, the recurved claw being 50 μ in length (measured along its axis).

The postoral area is like that of the female.

Legs 1–4 have the same spine and setal formula as in the female. The spines on the rami are somewhat longer and often straighter. The outer spine on the last segment of the endopod of leg 1 is 19 μ long. The 3 spines on the last segment of the endopod of leg 2 are 18, 13, and 9 μ long from distal to proximal; those on the last segment of the endopod of leg 3 are 21, 11, and 10 μ respectively. The second segment of the endopod of leg 4 is relatively a little shorter than in the female, being 31×10 μ.

Leg 5 resembles that of the female.

Leg 6 (Fig. 134) consists of a posterolateral flap on the ventral surface of the genital segment, bearing 2 slender naked setae both 22 μ long.

The spermatophore (Fig. 135), attached to the female, is elongated, 74×32 μ, not including the neck. Spermatophores may be attached singly or in pairs with a common stalk as seen in *N. firmus*.

The color in life resembles that of the female.

Comparison with other species.—*Nasomolgus rudis* may be separated from *N. cristatus*, *N. firmus*, and *N. leptus* by the length of the caudal rami. In addition, it may be distinguished from *N. firmus* in that its body wall is less strongly sclerotized, certain setae on the second antenna have lamellate margins, the first segment of the second maxilla in the female has a broad bulge rather than a prominent conical projection, the formula for the last segment of the endopod in leg 3 is I,II,2 rather than II,2, the inner distal seta on the first segment of the endopod in leg 4 is much shorter, and the ornamentation of the claw of the maxilliped of the male is less extensive. From *N. leptus* it may also be distinguished by the shorter second segment in the endopod of leg 4.

Nasomolgus parvulus[1] n. sp.
Figs. 136–142

Type material.—14 females from one *Sabellastarte magnifica* (Shaw), in 2 m, at Ambariotelo, a small island between Nosy Bé and Nosy Komba, Madagascar. Collected May 15, 1964. Holotype and 12 paratypic females deposited in the United States National Museum, Washington; the remaining paratypes (dissected) in the collection of A. G. Humes.

Other specimens (all from *Sabellastarte magnifica*).—2 females from 2 hosts, under intertidal dead coral, Antsakoabe, on the northern shore of Nosy Bé, November 1, 1963 (these specimens placed in the Museum of Comparative Zoology); 2 females from 1 host, under intertidal rock, Ant-

[1] The specific name *parvulus* (from Latin = very small) alludes to the small size of this species.

sakoabe, September 7, 1964; and 1 female from 1 host, in 1 m, Ambariobe, near Ambariotelo, October 10, 1960.

Female.—The body (Fig. 136) has a broad prosome. The length (not counting the setae on the caudal rami) is 0.57 mm (0.49–0.54 mm) and the greatest width is 0.23 mm (0.20–0.26 mm), based on 10 specimens. The ratio of the length to the width of the prosome is 1.35 : 1. The segment of leg 1 is separated from the head by a dorsal furrow. The epimeral areas of the pedigerous segments resemble those of *N. leptus* and *N. rudis*.

The segment of leg 5 is similar to that in *N. rudis*. Between this segment and the genital segment there is a small ventral intersegmental sclerite. The genital segment (Fig. 137) is a little wider than long and in dorsal view is broadly expanded in its anterior three-fourths and constricted in its posterior fourth. The length of the segment is 72 μ, the width in the expanded portion 83 μ, and the width in the constricted part 52 μ. The dorsolateral areas of attachment of the egg sacs are located a little more anteriorly than in *N. rudis*. Each area (Fig. 138) bears 2 naked setae 29 and 10 μ in length. The 3 postgenital segments, without posterior rows of spinules, are 25×41, 19×33, and 24×31 μ from anterior to posterior.

The caudal ramus (Fig. 139) is almost quadrate, 16×14 μ, the ratio of length to width being 1.14 : 1. The outer lateral seta is 35 μ long, the pedicellate dorsal seta 24 μ, the outermost terminal seta 40 μ, the innermost terminal seta 44 μ, and the 2 long median terminal setae are 133 μ (outer) and 237 μ (inner) and are basally "pegged." All the setae are naked. A minute hair is borne on the dorsal surface of the ramus.

The dorsal surface of the prosome and the dorsal and ventral surfaces of the urosome bear a few hairs. The prosome is longer than the urosome, the ratio being 2.0 : 1.

The egg sacs (see Fig. 136) are moderately elongated, 280×128 μ, and contain fewer eggs than in *N. leptus* or *N. rudis*, each egg being 44–50 μ in diameter.

The rostral area, first antenna, second antenna, labrum, mandible, paragnath, and first maxilla resemble those of *N. rudis*. The second maxilla (Fig. 140) lacks the bulge on the first segment seen in *N. rudis*, and the first spine in the row on the distal part of the second segment is less enlarged than in that species. The maxilliped and postoral area resemble those of *N. rudis*.

Legs 1–4 have the same spine and setal formula as in *N. leptus* and *N. rudis*. The outer distal corner of the first segment of the endopod of legs 1 and 2 lacks a spinous process. In leg 3 such a process is absent on both first and second segments of the endopod. The endopod of leg 4 (Fig. 141) resembles in general form that of *N. rudis*. The first segment is 17×9 μ and bears a short feathered inner distal seta 11 μ long. The second segment is 31×7 μ and carries 2 terminal slightly barbed setae 37 μ (outer) and 10 μ (inner) in length. The relationship between the lengths of these 2 terminal setae is about 4 : 1 rather than about 2 : 1 as in *N. rudis*. The fine ornamentation of the endopod is similar to that in the 3 previous species.

Leg 5 resembles that of *N. rudis*.

Leg 6 is represented by the 2 setae near the attachment of the egg sacs.

The spermatophore (Fig. 142), attached to the female in pairs, is 77×31 μ, not including the neck.

The color in life in transmitted light resembles that of the 3 previous species.

Male.—Unknown.

Comparison with other species.—*Nasomolgus parvulus* may be distinguished from all other species in the genus on the basis of its small size, its almost square caudal ramus, and the two very unequal terminal setae on the second segment of the endopod of leg 4. In addition, it differs from *N. firmus* in having a much more weakly sclerotized body wall, in the relative lengths of the prosome and urosome,

in its stouter egg sac, in the absence of a prominent conical projection on the first segment of the second maxilla, and in the armature of the last segment of the endopod of leg 3. From *N. leptus* it is very easily distinguished by its much less elongated body, in having a shorter egg sac with fewer eggs, and in lacking the sclerotized bulge on the first segment of the second maxilla. It differs furthermore from *N. rudis* in the proportional lengths of the prosome and urosome, in its shorter egg sac with fewer eggs, and in the absence of an outer bulge on the first segment of the second maxilla.

REMARKS ON THE GENUS *NASOMOLGUS*

With the finding of these four new species of *Nasomolgus* living on a sabellid polychaete, it seems probable that members of this genus customarily live in association with annelids. One may conjecture that Sewell's specimen of *N. cristatus*, found in dredged debris, may have been dislodged from a polychaete host, but this is impossible to establish.

More than one species of *Nasomolgus* may live on a single polychaete. In two instances (collections at Ambariotelo, May 15, 1964, and at Antsakoabe, September 7, 1964) *N. firmus*, *N. leptus*, and *N. parvulus* occurred on a single *Sabellastarte magnifica*. In one case (collection at Antsakoabe, November 1, 1963) all four species of *Nasomolgus* were recovered from two hosts.

The exact region of the body where the copepods live is not known. It is possible that each species of copepod occupies a region separate from the others, but such a supposition can only be substantiated by careful observation of undisturbed living hosts.

Since the type species, *N. cristatus*, is now known to possess in common with the four new species from Madagascar certain fundamental characters (i.e., the pair of setae on the anterior part of the labrum, the 3-segmented maxilliped with a long slender last segment, and the number of spines [III,I] on the last segment of the exopod of leg 1) which were inadequately mentioned in Sewell's original description, a revision of the diagnosis of the genus *Nasomolgus* would be desirable. However, in view of the fact that we have been unable to make a firsthand study of the single specimen of *N. cristatus*, we are not attempting such a revision at present. There are certain features (especially the structure of the mouthparts) that would be necessary to clarify before undertaking a definitive revision. For the moment, the characteristics given by Sewell, together with the additions and corrections just mentioned, will serve to characterize the genus.

REFERENCES CITED

BOCQUET, C., AND J. H. STOCK. 1957. Copépodes parasites d'invertébrés des côtes de France. IVa. Le double parasitisme de *Sipunculus nudus* L. par *Myzomolgus stupendus* nov. gen., nov. sp., et *Catinia plana* nov. gen., nov. sp., copépodes cyclopoïdes très remarquables. Koninkl. Nederl. Akad. Wetensch. Amsterdam, Proc., Ser. C, **60**(3): 410–431.

BRADY, G. S. 1880. A monograph of the free and semi-parasitic Copepoda of the British Islands. Ray Society, London, **3**: 1–83.

CANU, E. 1892. Les Copépodes du Boulonnais, morphologie, embryologie, taxonomie. Trav. Lab. Zool. Mar. Wimereux-Ambleteuse (Pas-de-Calais), **6**: 1–354.

CLAUS, C. 1889. Über neue oder wenig bekannte halbparasitische Copepoden, insbesondere der Lichomolgiden- und Ascomyzontiden-Gruppe. Arb. Zool. Inst. Univ. Wien, **8**(3): 327–370.

GALLIEN, L. 1935. *Pseudanthessius nemertophilus* nov. sp., copépode commensal de *Lineus longissimus* Sowerby. Bull. Soc. Zool. France, **60**: 451–459.

GOODING, R. U. 1963 (unpublished). External morphology and classification of marine poecilostome copepods belonging to the families Clausidiidae, Clausiidae, Nereicolidae, Eunicicolidae, Synaptiphilidae, Catiniidae, Anomopsyllidae, and Echiurophilidae. Ph.D. Thesis, University of Washington, Seattle.

GURNEY, R. 1927. Zoological results of the Cambridge expedition to the Suez Canal, 1924. XXXIII. Report on the Crustacea:

Copepoda (littoral and semi-parasitic). Trans. Zool. Soc. London, **22**(4): 451–477.

HUMES, A. G. 1966. *Pseudanthessius procurrens* n. sp., a cyclopoid copepod associated with a cidarid echinoid in Madagascar. Breviora, Mus. Comp. Zool., No. 246: 1–14.

HUMES, A. G., AND R. F. CRESSEY. 1961. Deux nouvelles espèces de *Pseudanthessius* (Copepoda, Cyclopoida) parasites des oursins à Madagascar. Mém. Inst. Sci. Madagascar, Sér. F, 1959, **3**: 67–82.

ILLG, P. 1950. A new copepod, *Pseudanthessius latus* (Cyclopoida: Lichomolgidae) commensal with a marine flatworm. Jour. Washington Acad. Sci., **40**(4): 129–133.

LINDBERG, K. 1945. Un nouveau copépode poecilostome de l'Inde de la famille des Lichomolgidae; *Pseudanthessius spinifer*, n. sp. Bull. Soc. Zool. France, **70**: 81–84.

NICHOLLS, A. G. 1944. Littoral Copepoda from South Australia (II). Calanoida, Cyclopoida, Notodelphyoida, Monstrilloida and Caligoida. Rec. So. Austral. Mus., **8**(1): 1–62.

SARS, G. O. 1917. An account of the Crustacea of Norway with short descriptions and figures of all the species. Vol. 6, Copepoda, Cyclopoida, pts. 11 and 12, Clausidiidae, Lichomolgidae (part), pp. 141–172. Bergen Museum, Bergen.

———. 1918. An account of the Crustacea of Norway with short descriptions and figures of all the species. Vol. 6, Copepoda, Cyclopoida, pts. 13 and 14, Lichomolgidae (concluded), Oncaeidae, Corycaeidae, Ergasilidae, Clausiidae. Eunicicolidae, Supplement, pp. 173–225. Bergen Museum, Bergen.

SCOTT, A. 1909. The Copepoda of the Siboga Expedition. Part I. Free-swimming, littoral and semi-parasitic Copepoda. Siboga Exped., **29**a: 1–323.

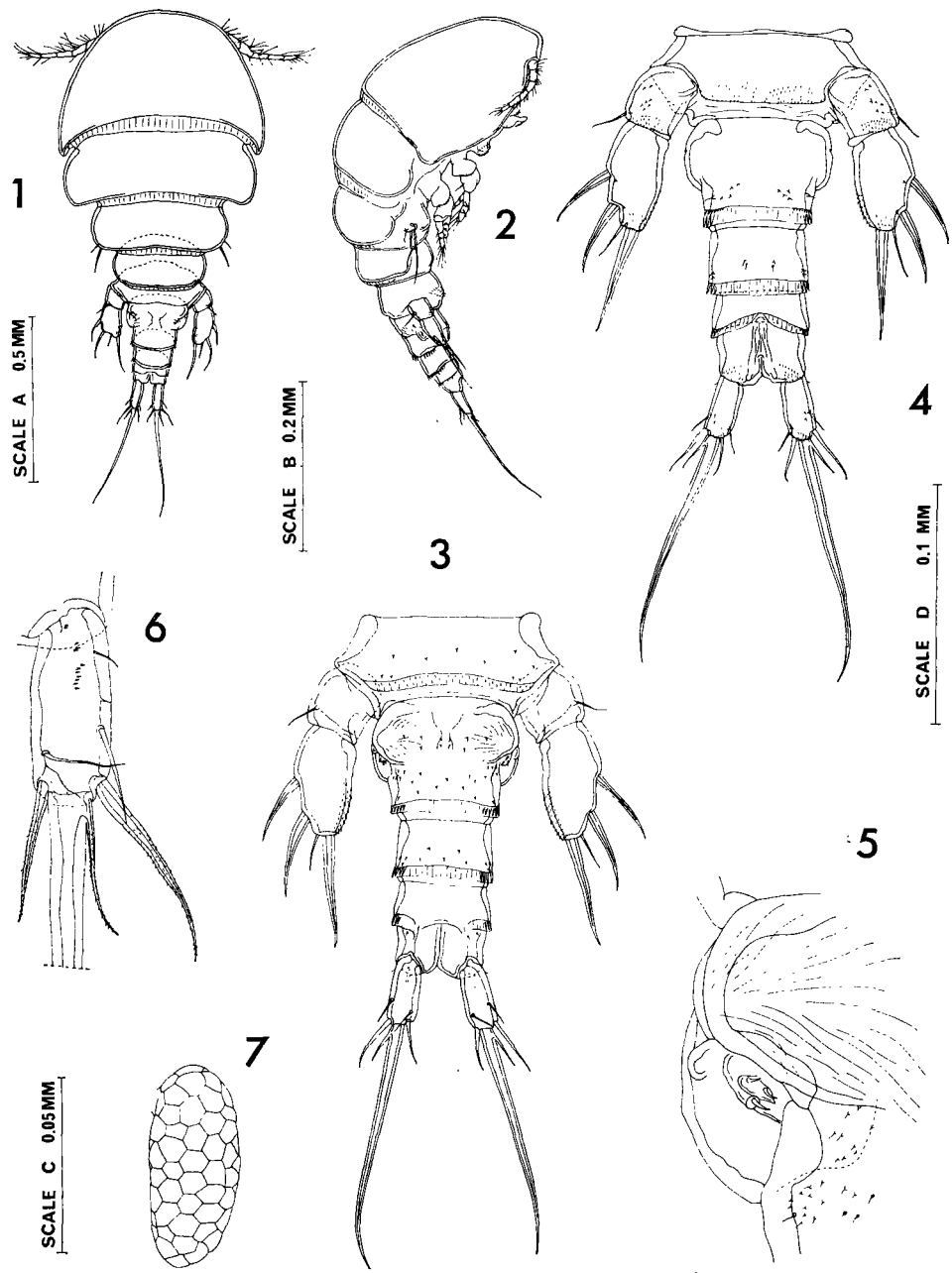
SEWELL, R. B. S. 1949. The littoral and semi-parasitic Cyclopoida, the Monstrilloida and Notodelphyoida. John Murray Exped. 1933–34, Sci. Repts., **9**(2): 17–199.

STOCK, J. H., A. G. HUMES, AND R. U. GOODING. 1963. Copepoda associated with West Indian invertebrates IV. The genera *Octopicola*, *Pseudanthessius* and *Meomicola* (Cyclopoida, Lichomolgidae). Studies Fauna Curaçao and other Caribbean Is., **18**(77): 1–74.

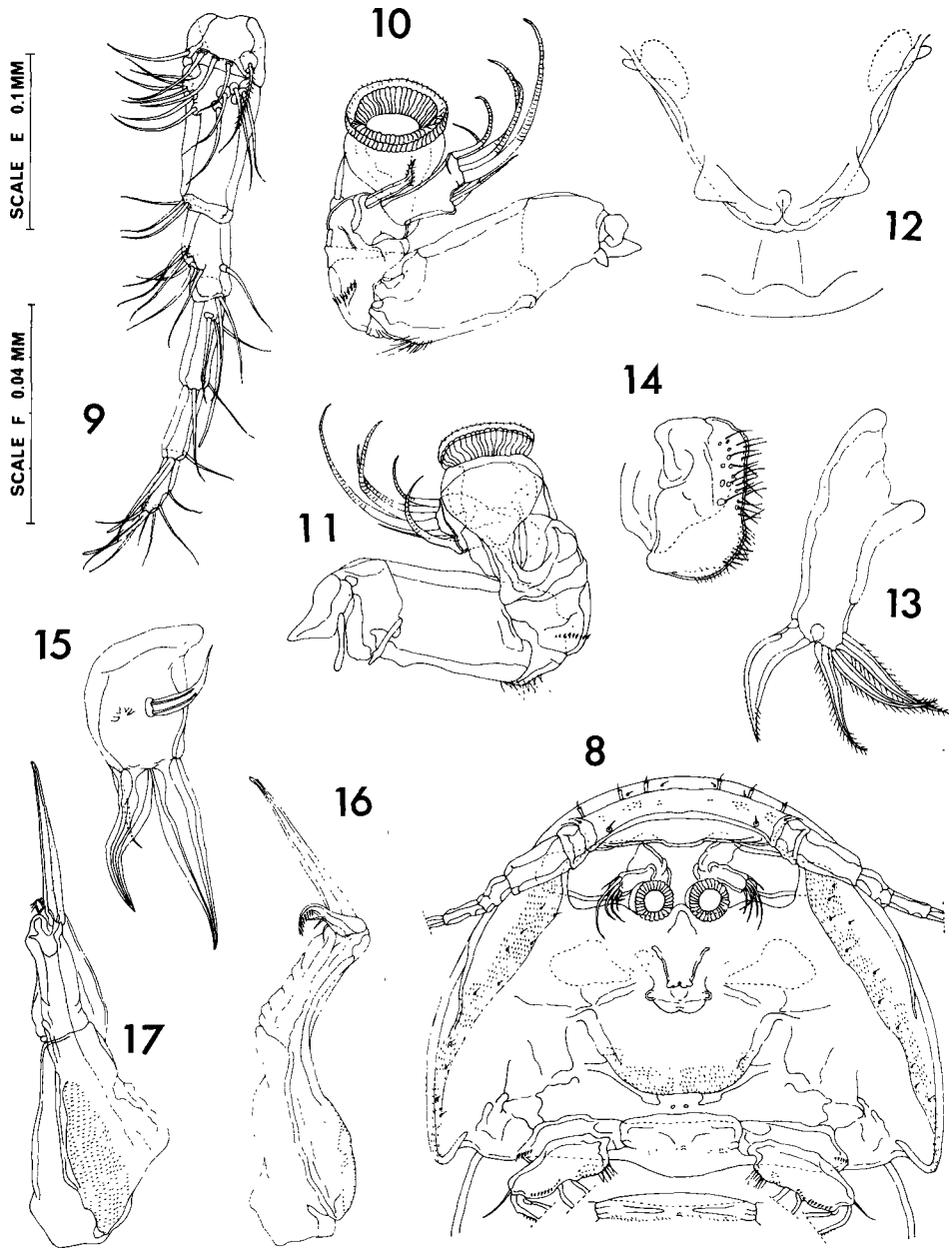
THOMPSON, I. C., AND A. SCOTT. 1903. Report on the Copepoda collected by Professor Herdman, at Ceylon, in 1902. Rept. Govt. Ceylon Pearl Oyster Fish. Gulf of Manaar, pt. I, Suppl. Rept. No. 7: 227–307.

WILSON, M. S., AND P. L. ILLG. 1955. The family Clausiidae (Copepoda, Cyclopoida). Proc. Biol. Soc. Washington, **68**: 129–142.

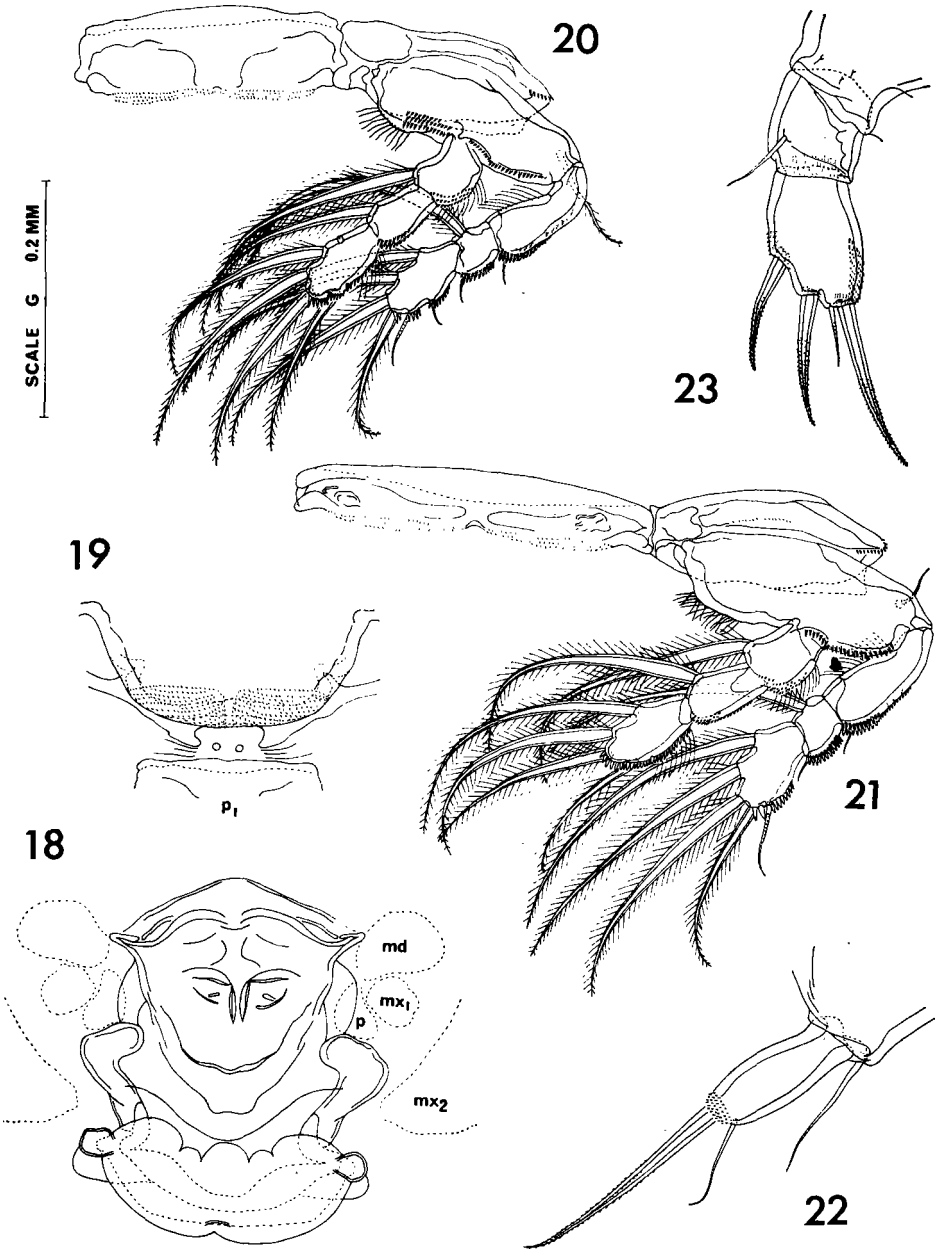
(Received December 10, 1965)



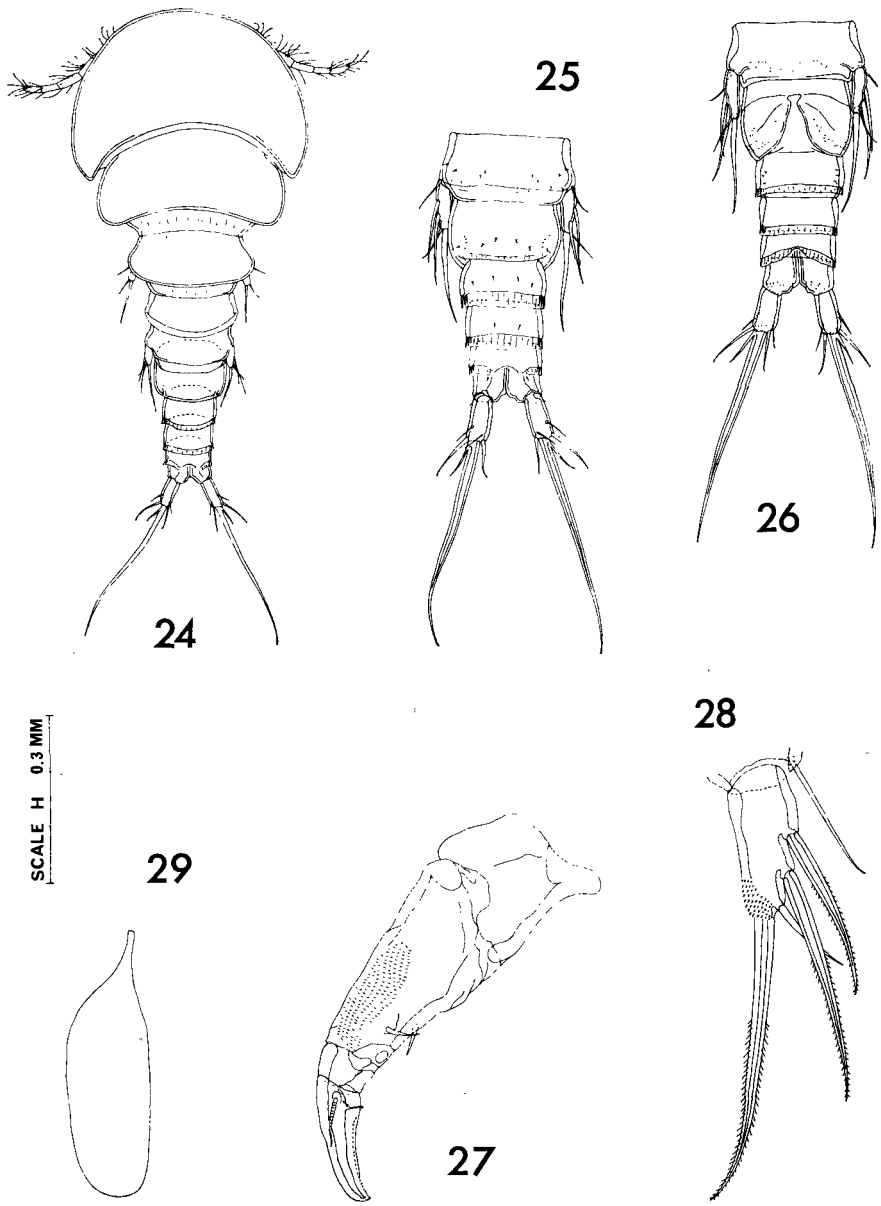
Figures 1–7. Catylomalgus lepidonoti n. gen., n. sp., female. 1, dorsal (A); 2, lateral (A); 3, urosome, dorsal (B); 4, urosome, ventral (B); 5, area of attachment of egg sac, dorsal (C); 6, caudal ramus, dorsal (D); 7, egg sac, dorsal (A).



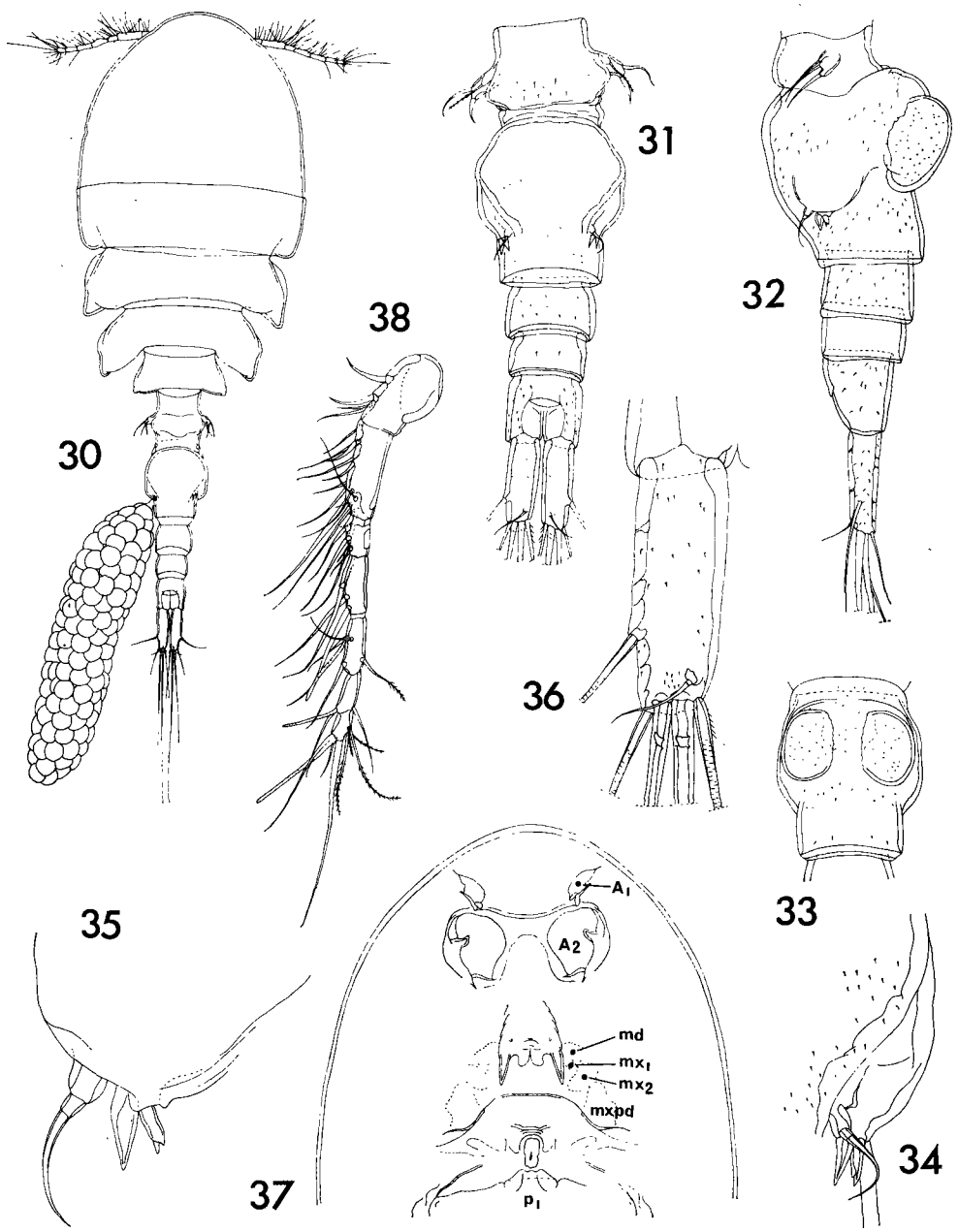
Figures 8–17. *Cotylomolgus lepidonoti* n. gen., n. sp., female (continued). 8, cephalosome, ventral (B); 9, first antenna, ventral (E); 10, second antenna, anterior (E); 11, second antenna, posterior (E); 12, labrum, anterior (C); 13, mandible, lateral (F); 14, paragnath, ventral (F); 15, first maxilla, anterior (F); 16, second maxilla, posterior (E); 17, second maxilla, ventral (E).



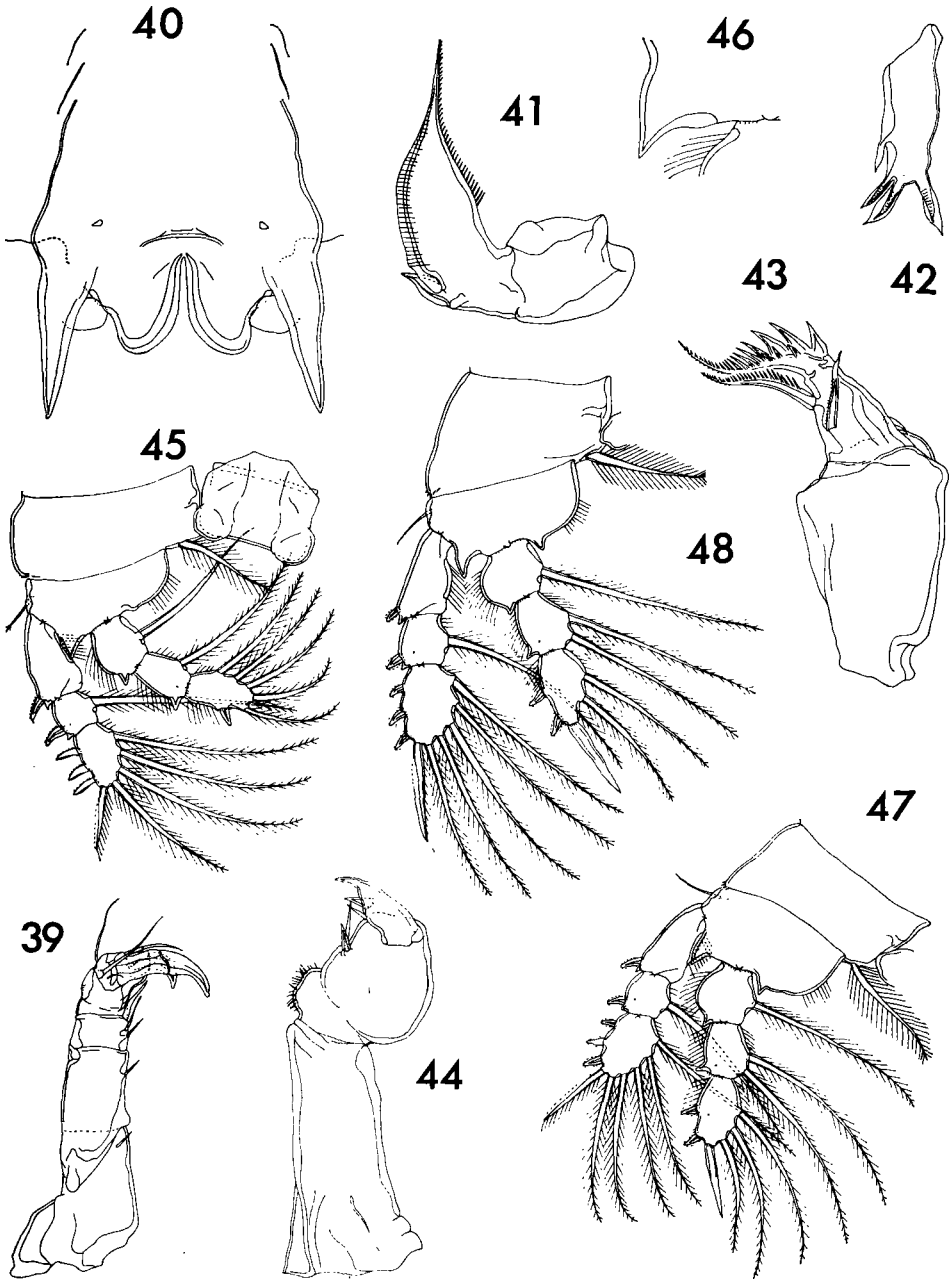
Figures 18–23. *Cotylomolgus lepidonoti* n. gen., n. sp., female (continued). 18, oral area posterior to labrum, ventral (C); 19, postoral protuberance between maxillipeds and leg 1, ventral (G); 20, leg 1 and intercoxal plate, anterior (E); 21, leg 2 and intercoxal plate, anterior (E); 22, leg 3, ventral (D); 23, leg 5, dorsal (G).



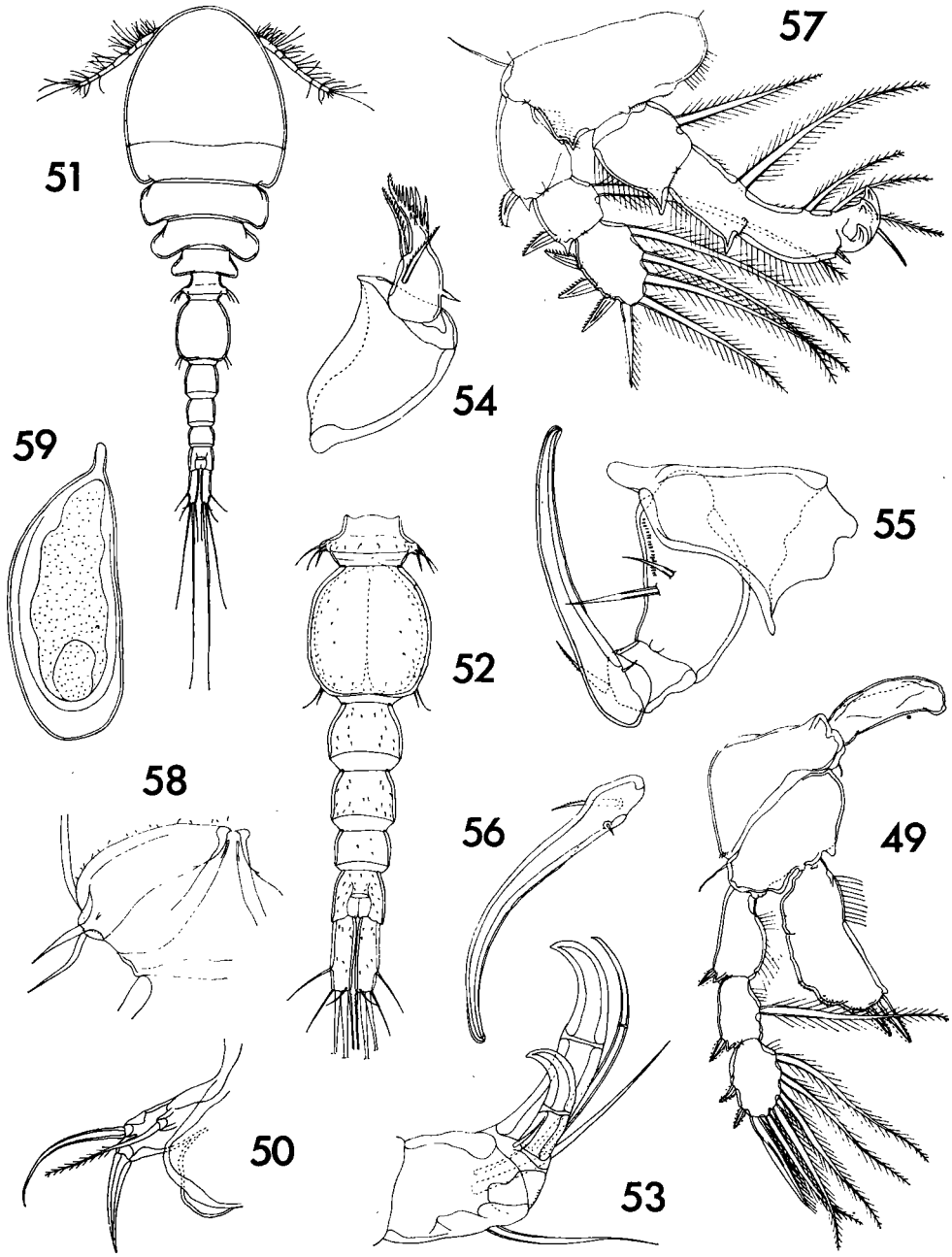
Figures 24–29. *Cotylomolgus lepidonoti* n. gen., n. sp., male. 24, dorsal (H); 25, urosome, dorsal (B); 26, urosome, ventral (B); 27, maxilliped, posterior (D); 28, leg 5, lateral (D); 29, spermatophore, ventral (G).



Figures 30–38. *Pseudanthessius ferox* n. sp., female. 30, dorsal (A); 31, urosome, dorsal (B); 32, urosome, lateral (B); 33, genital segment, ventral (B); 34, area of attachment of egg sac, dorsal (D); 35, enlargement of setae on egg sac attachment area, lateral (C); 36, caudal ramus, dorsal (D); 37, cephalosome, ventral (H); 38, first antenna, ventral (G).

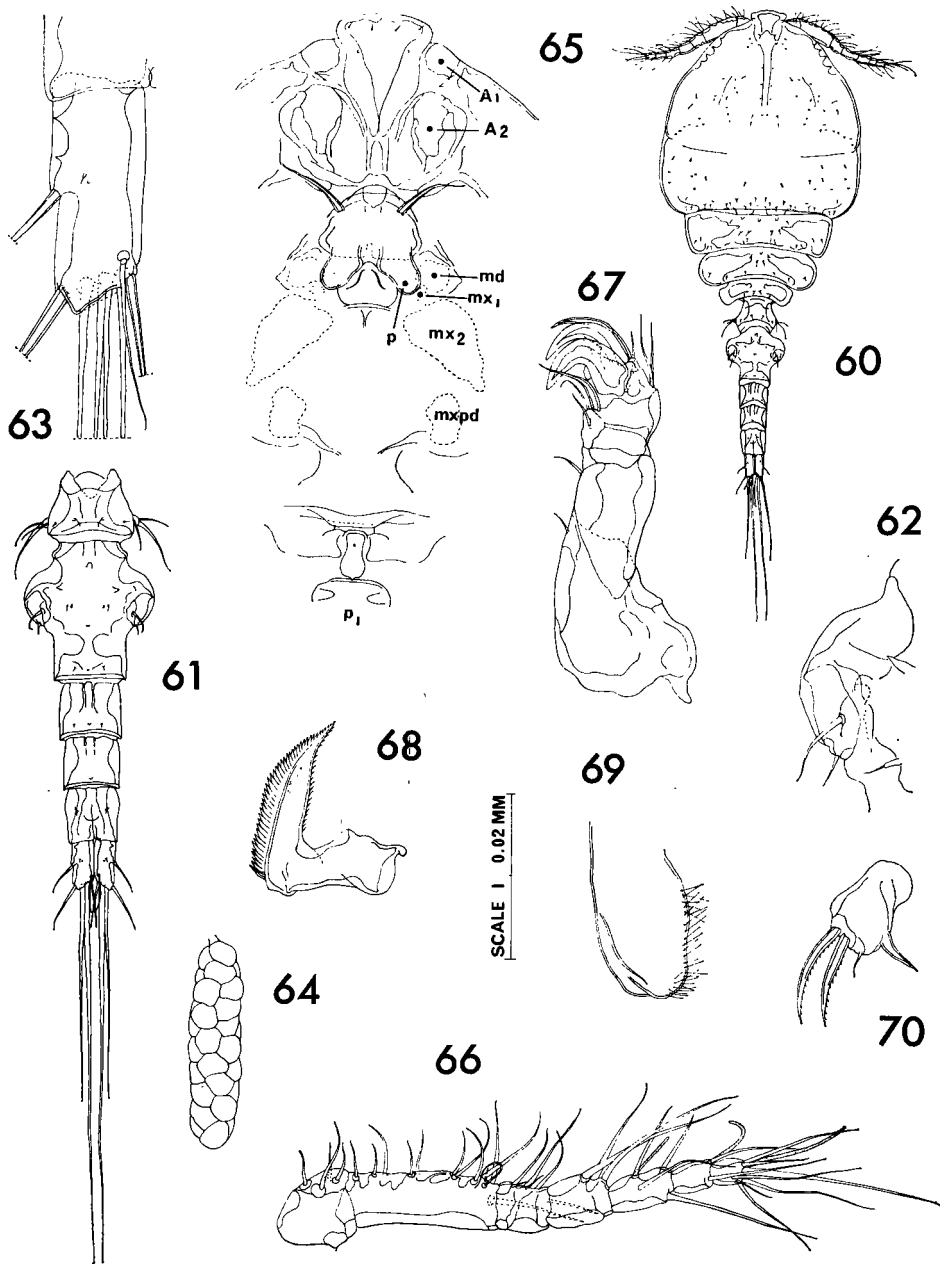


Figures 39–48. *Pseudanthessius ferox* n. sp., female (continued). 39, second antenna, anterior (G); 40, labrum, ventral (D); 41, mandible, anterior (D); 42, first maxilla, anterior (D); 43, second maxilla, posterodorsal (D); 44, maxilliped, anterior (D); 45, leg 1 and intercoxal plate, anterior (G); 46, angular lamella on basis of leg 1, anterior (C); 47, leg 2, anterior (G); 48, leg 3, anterior (G).

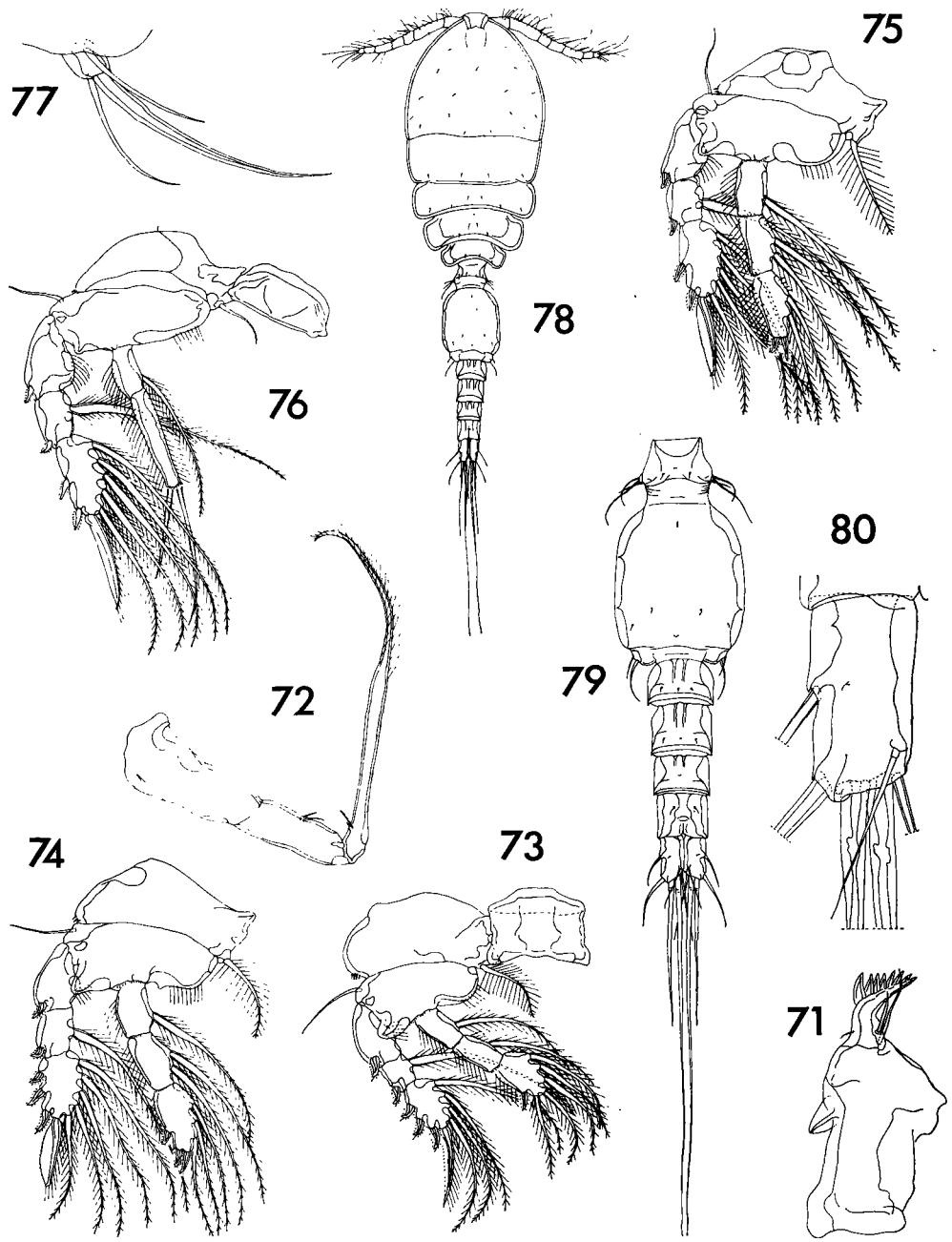


Figures 49–50. *Pseudanthessius ferox* n. sp., female (continued). 49, leg 4 and intercoxal plate, anterior (G); 50, leg 5, dorsal (D).

Figures 51–59. *Pseudanthessius ferox* n. sp., male. 51, dorsal (A); 52, urosome, dorsal (B); 53, last segment of second antenna, posterior (C); 54, second maxilla, posterodorsal (D); 55, maxilliped, anterior or dorsal (D); 56, claw of maxilliped, anterior or dorsal (D); 57, leg 1, anterior (D); 58, leg 6, ventral (D); 59, spermatophore inside male, ventral (E).

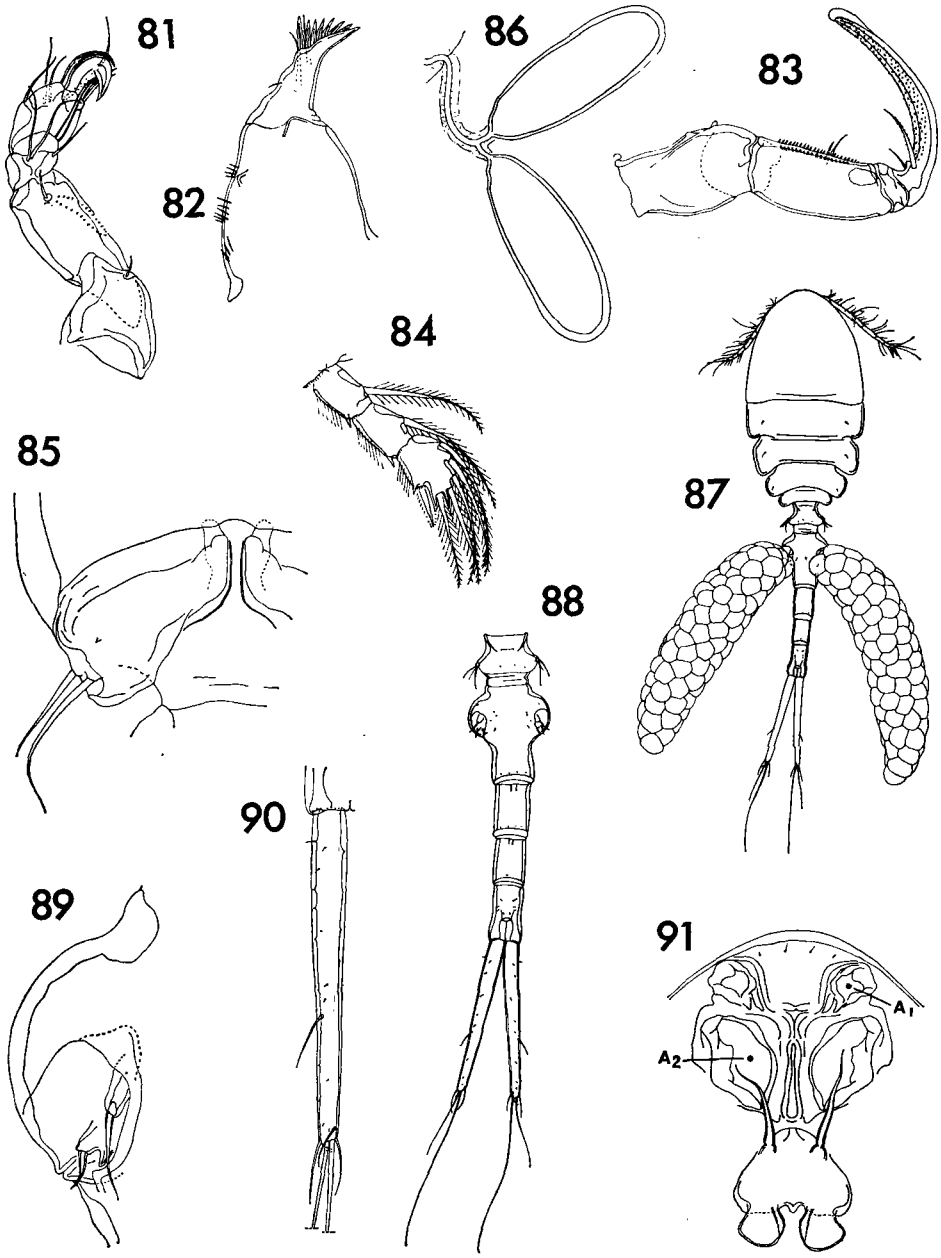


Figures 60–70. *Nasomolgus firmus* n. sp., female. 60, dorsal (H); 61, urosome, dorsal (G); 62, area of attachment of egg sac, dorsal (C); 63, caudal ramus, dorsal (F); 64, egg sac (H); 65, median part of cephalosome, ventral (E); 66, first antenna, ventral (D); 67, second antenna, anterior (C); 68, mandible, ventral (C); 69, paragnath, ventral (I); 70, first maxilla, anteroventral (F).



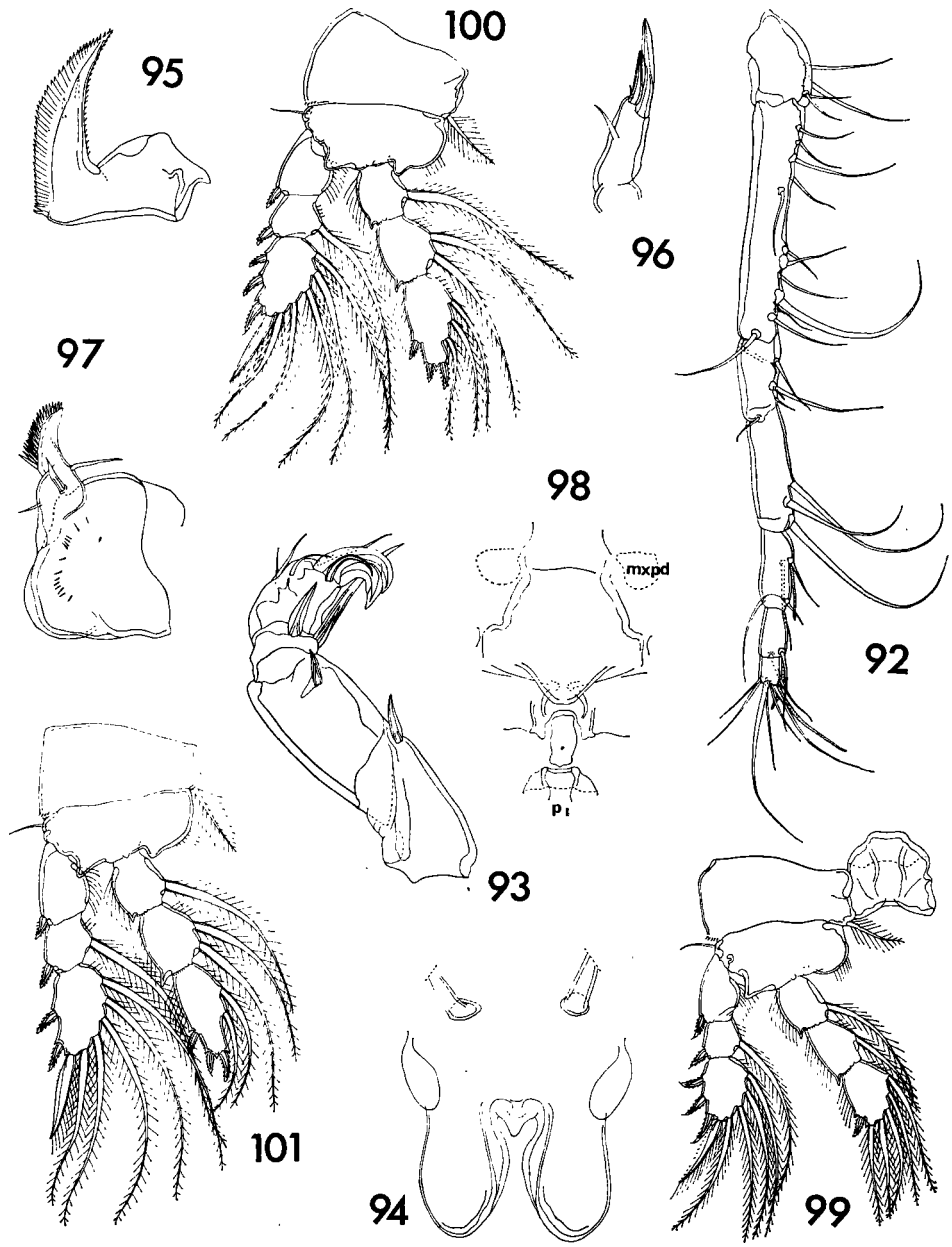
Figures 71–77. *Nasomolgus firmus* n. sp., female (continued). 71, second maxilla, posterodorsal (C); 72, maxilliped, anterior (C); 73, leg 1 and intercoxal plate, anterior (D); 74, leg 2, anterior (D); 75, leg 3, anterior (D); 76, leg 4 and intercoxal plate, anterior (D); 77, leg 5, dorsal (F).

Figures 78–80. *Nasomolgus firmus* n. sp., male. 78, dorsal (B); 79, urosome, dorsal (E); 80, caudal ramus, dorsal (I).

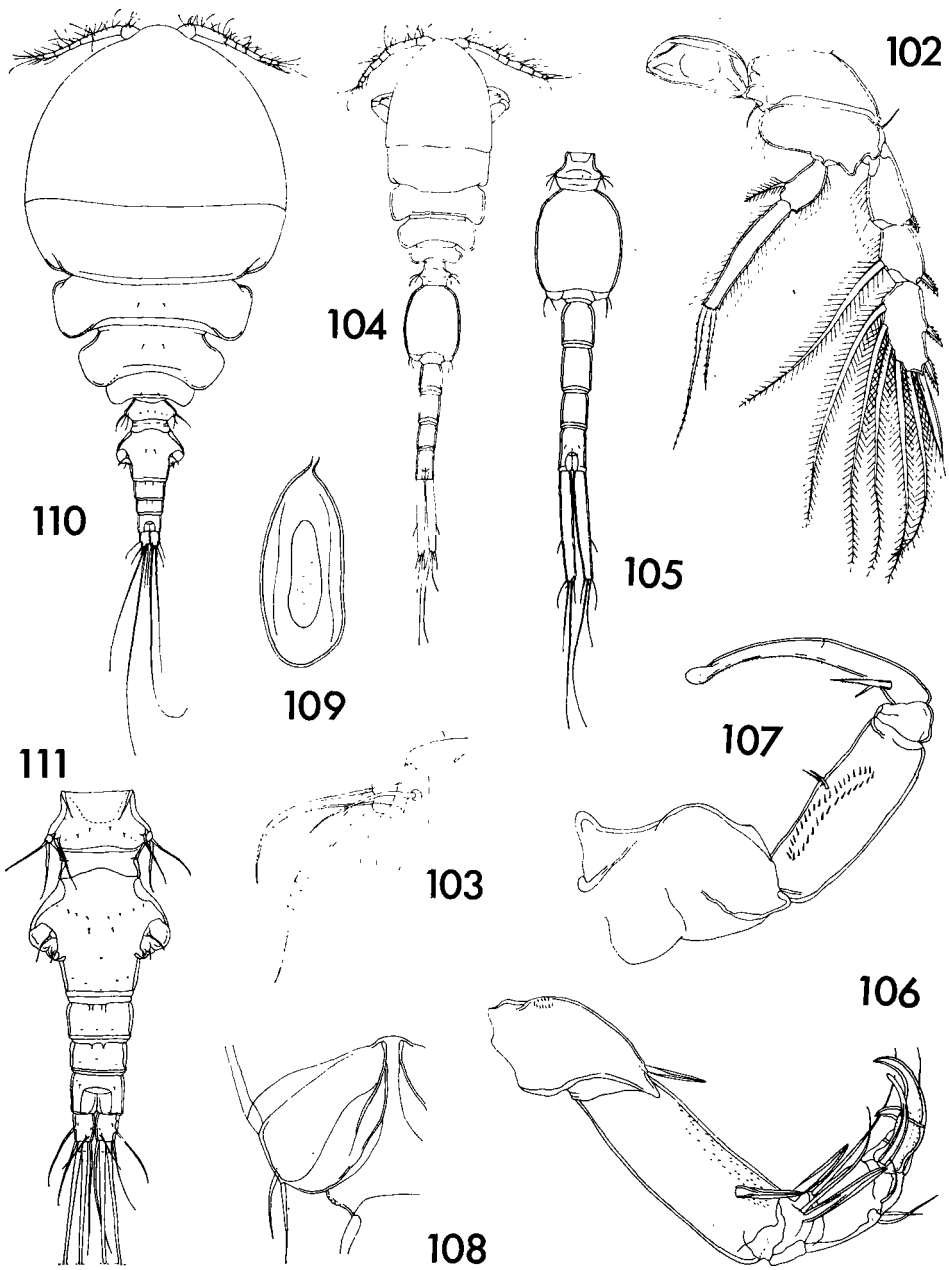


Figures 81–86. *Nasomolgus firmus* n. sp., male (continued). 81, second antenna, inner (C); 82, second maxilla, posterior (F); 83, maxilliped, posteromedial (C); 84, endopod of leg 1, anterior (C); 85, leg 6, ventral (F); 86, spermatophore, attached to female, ventral (D).

Figures 87–91. *Nasomolgus leptus* n. sp., female. 87, dorsal (A); 88, urosome, dorsal (H); 89, area of attachment of egg sac, dorsal (C); 90, caudal ramus, dorsal (G); 91, rostral area and labrum, with labral lobes erected ventrally and thus foreshortened in the drawing, ventral (E).



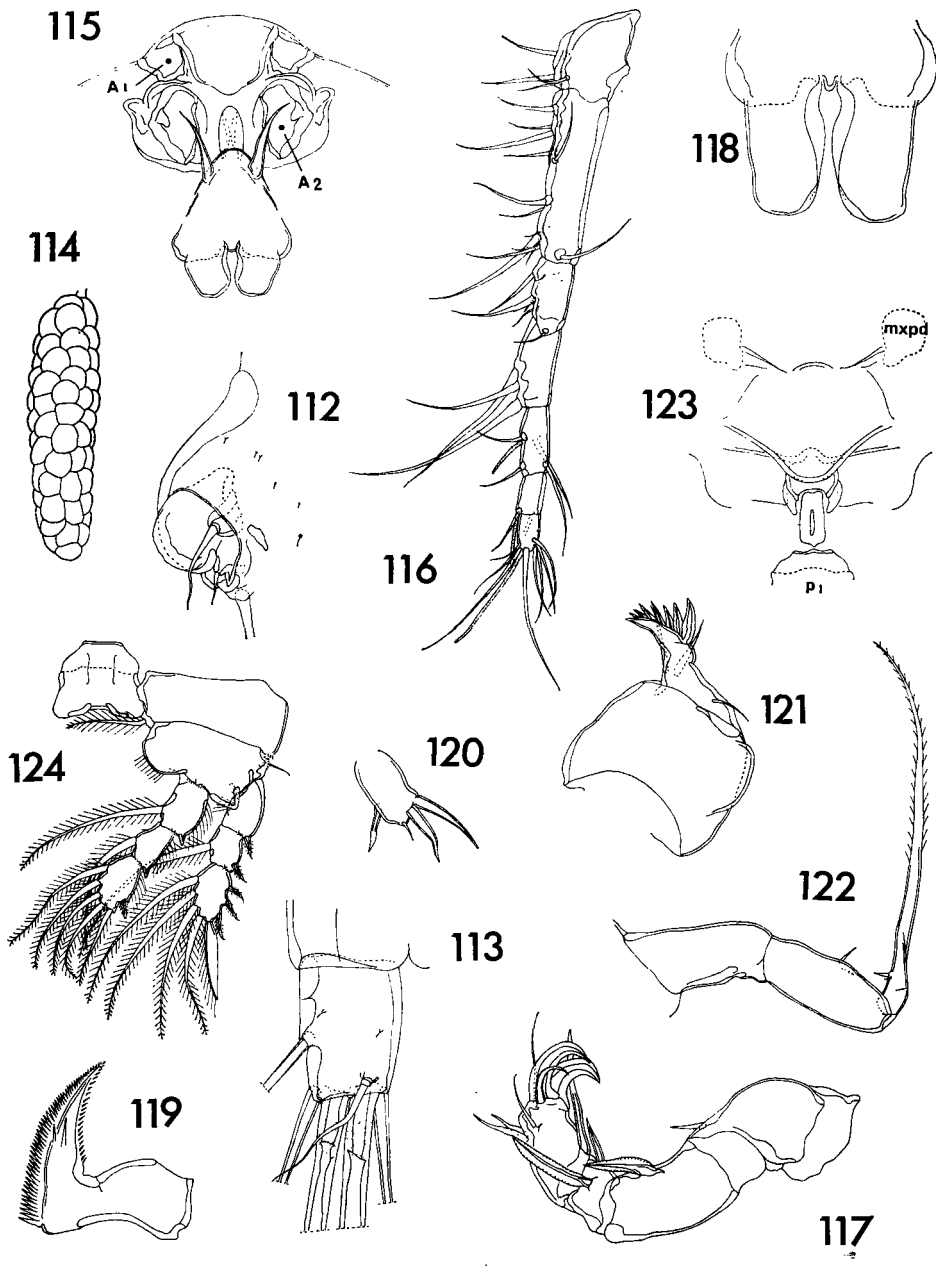
Figures 92–101. *Nasomolgus leptus* n. sp., female (continued). 92, first antenna, dorsal (D); 93, second antenna, posterior (D); 94, posterior part of labrum with bases of two setae, ventral (C); 95, mandible, ventral (C); 96, first maxilla, inner (C); 97, second maxilla, posterodorsal (C); 98, postoral area, ventral (E); 99, leg 1 and intercoxal plate, anterior (E); 100, leg 2, anterior (E); 101, leg 3, anterior (E).



Figures 102–103. *Nasomolgus leptus* n. sp., female (continued). 102, leg 4 and intercoxal plate, anterior (E); 103, leg 5, dorsal (F).

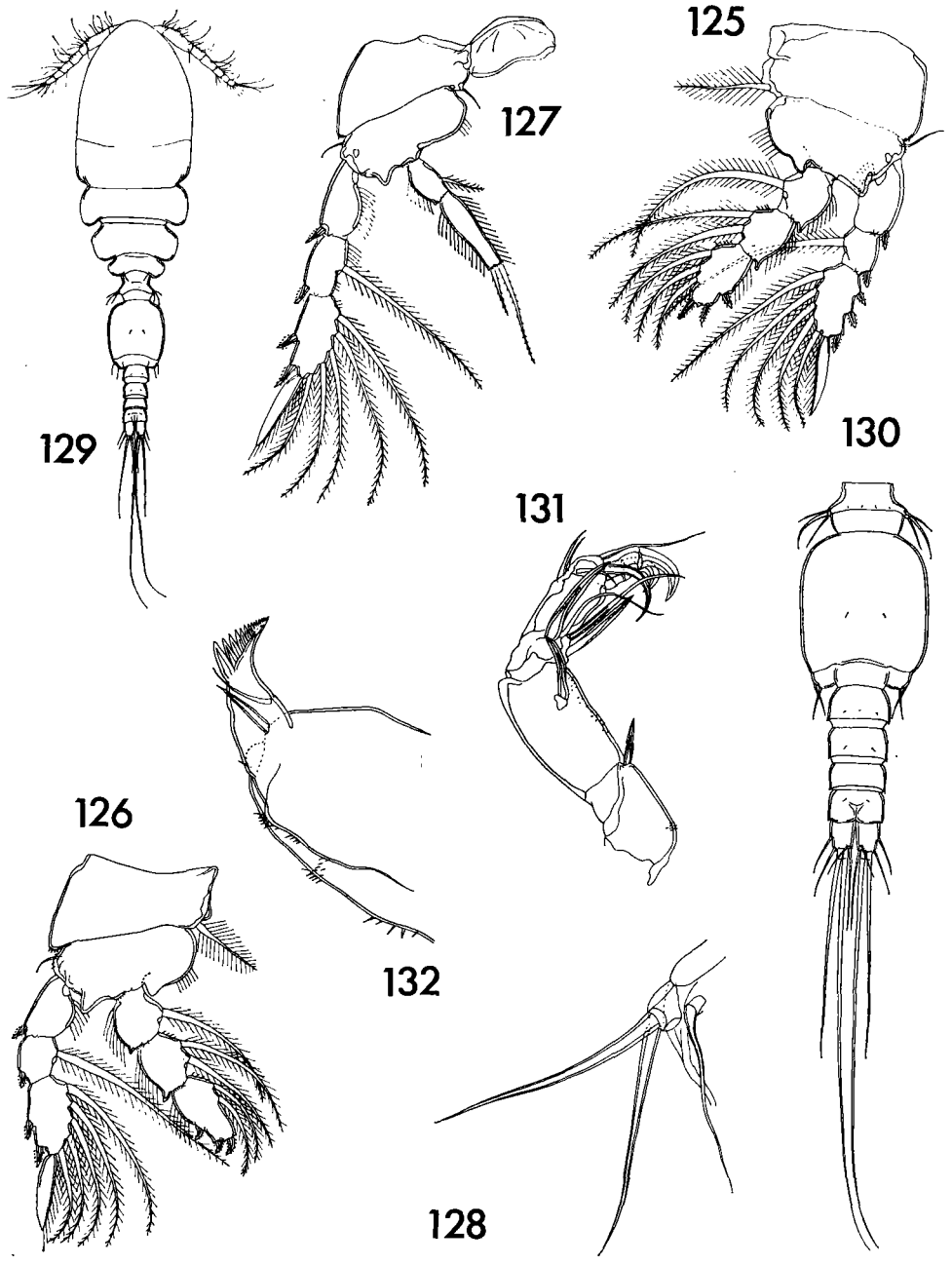
Figures 104–109. *Nasomolgus leptus* n. sp., male. 104, dorsal (H); 105, urosome, dorsal (B); 106, second antenna, posterior (C); 107, maxilliped, posteromedial (C); 108, leg 6, ventral (C); 109, spermatophore, inside male, dorsal (E).

Figures 110–111. *Nasomolgus rudis* n. sp., female. 110, dorsal (H); 111, urosome, dorsal (G).



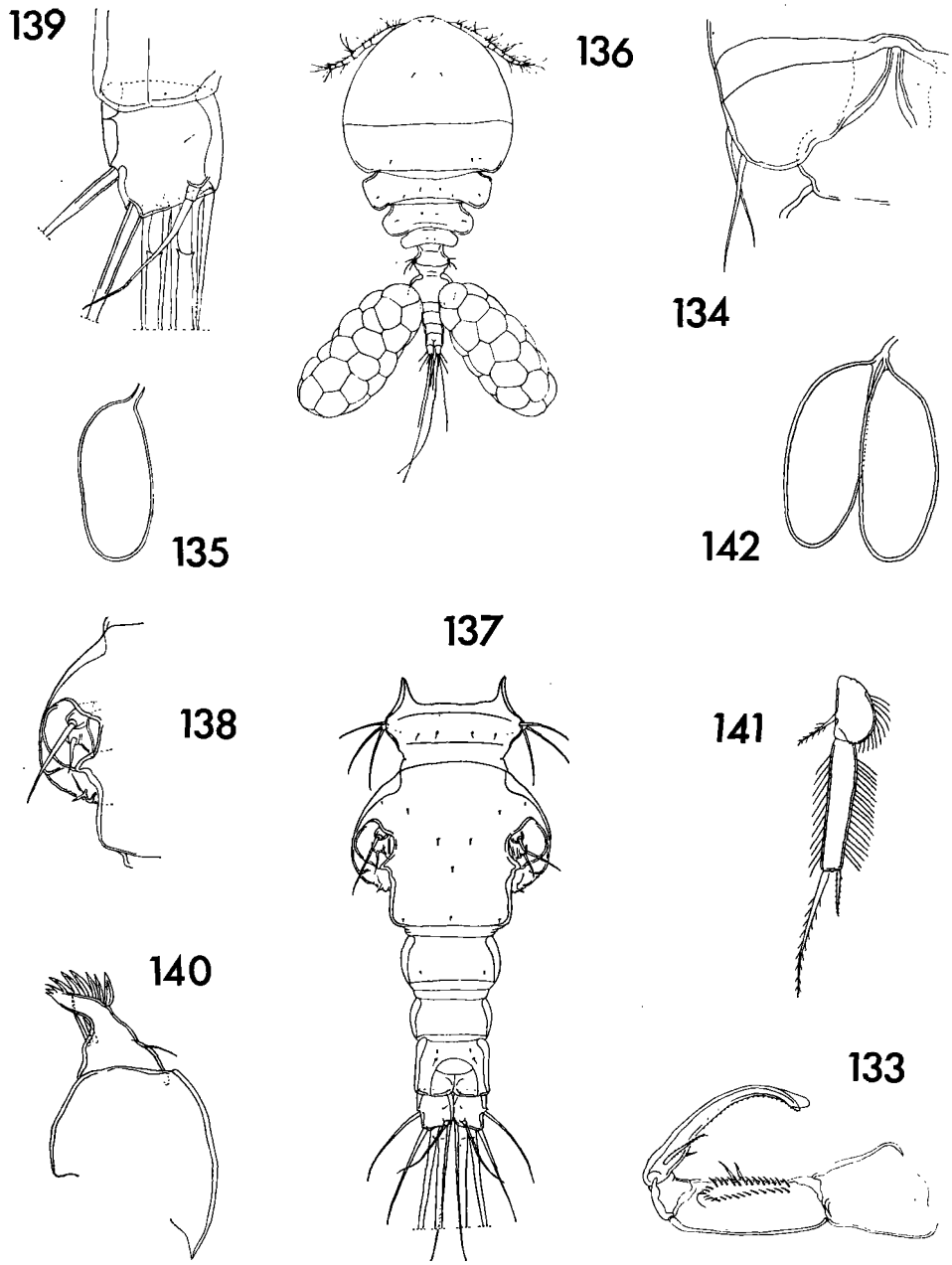
Figures 112–124. *Nasomolgus rudis* n. sp., female (continued). 112, area of attachment of egg sac, dorsal (C); 113, caudal ramus, dorsal (F); 114, egg sac, dorsal (H); 115, rostral area and labrum, with labral lobes erected ventrally and thus foreshortened in the drawing, ventral (E); 116, first antenna, dorsal (D); 117, second antenna, posterior (D); 118, posterior part of labrum, ventral (C); 119, mandible, dorsal (C); 120, first maxilla, ventral (C); 121, second maxilla, posterior (C); 122, maxilliped, posterior (C); 123, postoral area, ventral (E); 124, leg 1 and intercoxal plate, anterior (E).

UNESCO ARCHIVES



Figures 125–128. *Nasomolgus rudis* n. sp., female (continued). 125, leg 2, anterior (E); 126, leg 3, anterior (E); 127, leg 4 and intercoxal plate, anterior (E); 128, leg 5, dorsal (F).

Figures 129–132. *Nasomolgus rudis* n. sp., male. 129, dorsal (B); 130, urosome, dorsal (E); 131, second antenna, posterior (C); 132, second maxilla, anterior (I).



Figures 133–135. *Nasomolgus rudis* n. sp., male (continued). 133, maxilliped, posteromedial (C); 134, leg 6, ventral (F); 135, spermatophore, attached to female, dorsal (D).

Figures 136–142. *Nasomolgus parvulus* n. sp., female. 136, dorsal (H); 137, urosome, dorsal (D); 138, area of attachment of egg sac, dorsal (C); 139, caudal ramus, dorsal (I); 140, second maxilla, posterior (F); 141, endopod of leg 4, anterior (C); 142, spermatophores, attached to female, ventral (D).

Reprinted from *Science*, vol. 156, no. 3,772, 1967, p. 246-248

Heliacus (Gastropoda: Architectonicidae) Symbiotic with Zoanthiniaria (Coelenterata)

Abstract. *Eight species of* Heliacus *are obligate symbionts with* Zoanthus *and* Palythoa, *colonial zoanthid sea anemones. The gastropods live among* Zoanthus *polyps and under the edges of* Palythoa *incrustations, on which they feed and to which they and their egg masses are attached with sturdy but elastic mucous threads.*

Eight species in the marine gastropod genus *Heliacus* are symbiotic with *Zoanthus* and *Palythoa*, colonial zoanthiniarian sea anemones of the family Zoanthidae. *Heliacus* comprises about 30 Recent tropical and warm temperate species in the Architectonicidae (*1*, *2*), a family of mesogastropod prosobranchs with opisthobranch affinities. Hitherto, obligate symbiosis was unknown in the Architectonicidae. Other prosobranch symbionts with coelenterates are the families Epitoniidae, Janthinidae, Ovulidae, and Coralliophilidae, whose post-larval stages all live with and feed on coelenterates (*3*). Little is known as to why these prosobranchs are not deterred by nematocysts.

In the tropics, *Zoanthus* and *Palythoa* are abundant, sessile animals on rock substrata in shallow water. *Palythoa* lives where wave action is strong, such as reefs. At some places, *Palythoa* incrusts as much as 90 to 95 percent of the substratum (*4*). Architectonicids are seldom observed *in situ*, and population densities of *Heliacus* with zoanthids are usually low (Table 1). The abundance of *Heliacus* must be regulated by factors other than the abundance of zoanthids because *Heliacus* can be scarce where zoanthids are luxuriant. Also, the symbiosis with *Zoanthus* and *Palythoa* cannot occur in all species of *Heliacus* because there are several that live in the Mediterranean (*2*), where the Zoanthidae do not occur but where other zoanthiniarian families do (*5*).

Biologically, architectonicids are not well known. They have a very long, invaginable, acrembolic proboscis, with the true mouth at its everted tip; they also have jaws and a radula in a small buccal mass, large salivary glands, and a peculiar excretory organ (*6*). There are no data on the feeding habits of such genera as *Architectonica* and *Philippia*, whose radulae differ greatly from those of *Heliacus*.

In the literature on *Heliacus* there are nine observations on the habitats of six species. Four observations mention associations with zoophytes and corals, vague designations that include zoanthids. Long ago in the West Indies, *H. cylindricus* (Gmelin) was found "inserted in slimy zoophytes on rocks about low-water mark" (*7*). In the Hawaiian Islands, *H. variegatus* (Gmelin) and *H. mighelsi* (Philippi) were "found almost invariably on branched coral, . . . suspend[ing] themselves by strong gelatinous threads" (*8*). At Boynton Beach, southeast Florida, *H. bisulcatus* (Orbigny) was "characteristically . . . closely associated with living coral polyps in shallow water" (*9*). Two observations mention a *Heliacus* with "ascidians." At Carmen Island and near Guaymas, Gulf of California, *H. bicanaliculatus* (Valenciennes) has twice been reported occurring intertidally with a short, olive-green, compound ascidian (*10*). *Zoanthus* resembles some ascidians, and, as expected and already noted in a paper by Robertson and Merrill on abnormal coiling of *Heliacus* (*11*), *H. bicanaliculatus* does live with *Zoanthus*. Two observations do not mention other animals. At Cap Vert, Senegal, *H. perrieri* (Rochebrune) was in spray and foam on boulders (*12*). In the Florida Keys, *H. cylindricus* was mainly upside down in a muddy habitat (*13*).

The new data (Table 1) show that eight species of *Heliacus*, including all those mentioned above except *H. bisulcatus*, occur either with the genus

Table 1. Data on *Heliacus* symbiotic with zoanthids.

Heliacus specimens (No.)	Zoanthid hosts (*14*)	U.S.N.M. catalog No. (hosts)	Localities
	Heliacus bicanaliculatus (Valenciennes)		
7+	*Zoanthus danai* (Le Conte)	52285	South side Bahía San Luis Gonzaga, Gulf of California
	Heliacus cylindricus (Gmelin)		
5	*Palythoa caribaeorum* Duchass. and Mich.	51029	Entrance Point, North Bimini, Bahama Islands
1	*Palythoa caribaeorum* Duchass. and Mich.		North Rabbit Cay, south of southwest end South Bimini, Bahama Islands
4	*Palythoa caribaeorum* Duchass. and Mich.	51681	Bache Shoal, 3 km east of north end Elliott Key, southeast Florida
1	*Palythoa mammillosa* (Ellis and Solander)	52293	Reef east of south end Cay Corker, British Honduras
Many	*Zoanthus pulchellus* (Duchass. and Mich.)	52700	Arasji, northwest Aruba, Netherlands Antilles
	Heliacus discoideus sterkii (Pilsbry and Vanatta)		
5	*Palythoa vestitus* (Verrill)		Reef off Ala Moana Park, Honolulu, Oahu, Hawaiian Islands
	Heliacus implexus (Mighels)		
2*	*Zoanthus confertus* Verrill		4 km south of Koloa, Kauai, Hawaiian Islands
	Heliacus mighelsi (Philippi)		
15	*Zoanthus confertus* Verrill, plus *P. vestitus*		4 km south of Koloa, Kauai, Hawaiian Islands
	Heliacus perrieri (Rochebrune) (*12*)		
2+	*Zoanthus pulchellus* (Duchass. and Mich.)		Arasji, northwest Aruba, Netherlands Antilles
	Heliacus trochoides (Deshayes)		
4	*Palythoa vestitus* (Verrill)		Reef off Kaoio Point, Oahu, Hawaiian Islands
2	*Palythoa tuberculosa* (Esper)	52606	Reef southeast of Imma Island, North Male Atoll, Maldive Islands
3†	*Palythoa tuberculosa* (Esper)	52607	North end Ongu Island, North Malosmadulu Atoll, Maldive Islands
1	*Palythoa tuberculosa* (Esper)	52608	Northwest end Gan Island, Addu Atoll, Maldive Islands
	Heliacus variegatus (Gmelin)		
Many	*Palythoa vestitus* (Verrill)	52387 & 52388	Reef off Ala Moana Park, Honolulu, Oahu, Hawaiian Islands
4	*Palythoa vestitus* (Verrill)		Reef off Kaoio Point, Oahu, Hawaiian Islands
6	*Zoanthus confertus* Verrill		4 km south of Koloa, Kauai, Hawaiian Islands

*Including one empty shell *in situ*. †Including two empty shells *in situ*.

Zoanthus or with *Palythoa* (*14*). There is no indication that postlarval *Heliacus* ever lives far from zoanthiniarians, although in the Hawaiian Islands several *H. trochoides* and *H. variegatus* have been found about a meter from the nearest zoanthid. The observations in Table 1 were made in all months of the year except September through November. The symbiosis occurs intertidally and to a depth of at least 9 m.

Host specificity between *Heliacus* and the various species of *Zoanthus* and *Palythoa* is low. Three or four *Heliacus* species are known to occur with more than one zoanthid species, including *H. cylindricus* with one species of *Zoanthus* and two of *Palythoa*. Some of the shell variability of *H. cylindricus* correlates with the generic identity of the host: large-shelled specimens (up to 14 mm high) that are abraded and brownish have been found only with *Zoanthus*, while those found with *Palythoa* are all smaller (less than 7 mm high), unabraded, and patterned with cream-white and brown. The different growth habits of *Zoanthus* and *Palythoa* account partly for these differences. *Zoanthus* has projecting polyps and a thin basal coenenchyme, while the shorter polyps of *Palythoa* scarcely project above a thicker coenenchyme. With *Zoanthus*, *Heliacus* lives among the projecting polyps where the shells are exposed to abrasive wave action; with *Palythoa*, *Heliacus* is protected under the incrustations in restricted spaces.

The following observations pertain to postlarval *Heliacus cylindricus* and *H. trochoides* with *Palythoa* colonies. *Heliacus* occurs in widely spaced clusters of two or three different-sized animals under the edges of loosely attached (old?) incrustations. Occasionally, *Heliacus* occurs singly, or on top of a colony, or nearby. *Heliacus* animals are fairly sedentary and usually are attached to their hosts and to the substratum with remarkably sturdy but elastic mucous threads. When *Heliacus* does crawl, the conical operculum projects into the umbilicus of the shell. When *in situ* the animals are in various positions, including umbilical side up. In the laboratory, feeding and spawning occurred only at night, and no direct observations were made of either

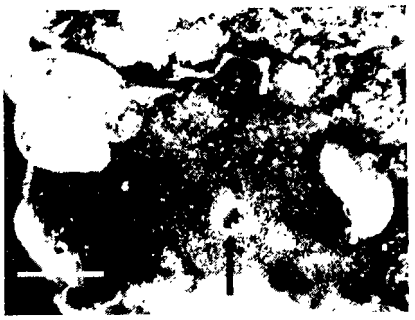


Fig. 1. Pair of live *Heliacus trochoides* on under surface of *Palythoa tuberculosa* colony, with hole where one has fed (arrow). North Male Atoll, Maldive Islands. Scale, 3 mm.

activity. However, *Heliacus* does eat *Palythoa* body tissues; 3- to 4-mm deep holes were made overnight in the surface of the colonies (Fig. 1, arrow). Also, the feces of *Heliacus*, which are uncompacted, are the same pale yellowish brown color as *Palythoa* and contain sand grains derived from the sand-containing *Palythoa* tissues. The spawn of *H. cylindricus* is a U-shaped jelly mass that is attached with mucous threads to the host colony.

This case of symbiosis I consider to be ectoparasitism verging on commensalism. *Heliacus* does not harm its host much (the injured tissues heal speedily), and, relative to a host colony, even a full-grown *Heliacus* is small [rarely larger than a single zoanthid polyp (*15*)].

The larval ecology of *Heliacus* is noteworthy because there is at least occasional transoceanic larval transport by ocean currents. Architectonicid larvae can live in the plankton more than 3 months (possibly 7 months or more), and the West Indian architectonicids (including several species of *Heliacus*) occur in shallow water across the entire tropical Atlantic (*16*). The observations in this paper imply that contact with benthic zoanthiniarians is essential for successful settlement and metamorphosis of these *Heliacus* larvae and for their subsequent growth and attainment of sexual maturity.

ROBERT ROBERTSON
Department of Mollusks,
Academy of Natural Sciences,
Philadelphia, Pennsylvania 19103

References and Notes

1. Architectonicidae and *Heliacus* are also known under the names Solariidae and *Torinia*. Bayer (*2*) lists 54 Recent species of *Torinia*; my estimate is based on his list but excludes synonyms and species in other genera.
2. C. [G. F. H.] Bayer, *Zool. Verhandel. Leiden* **4**, 1 (1948).
3. R. Robertson, *Amer. Malacol. Union Annu. Rep.* **1965**, 6 (1966). Isolated cases are known in three other families: Lamellariidae, Muricidae (*Drupella* spp.), and Columbellidae.
4. R. Sourie, *Mém. Inst. Franç. Afrique Noire* **38**, 342 pp. (1954); L. S. Kornicker and D. W. Boyd, *Bull. Amer. Ass. Petrol. Geol.* **46**, 640 (1962).
5. F. Pax and I. Müller, *Inst. Oceanogr. Ribarstvo Split; Fauna Flora Adriatica* **3**, 110 (1962).
6. F. H. Troschel, *Das Gebiss der Schnecken* (Nicolaische Verlags-Buchhandlung, Berlin, 1875), vol. 2, pp. 155–158; E.-L. Bouvier, *Bull. Soc. Malacol. France* **3**, 77 (1886); J. Thiele, *Wiss. Ergeb. Deut. Tiefsee-Exped. Valdivia* **17**, 113 (1925); ——, *Z. Wiss. Zool.* **132**, 73 (1928); T. Habe, *Jap. J. Malacol.* **13**, 75 (1943); J. Risbec, *J. Conchyliol.* **95**, 45 (1955).
7. H. J. Krebs, *The West-Indian Marine Shells with Some Remarks . . .* (privately printed at Nykjøbing, Falster, Denmark, 1864), p. 63; republished in *Rev. Soc. Malacol. Carlos de la Torre* **5**, 97 (1947). *H. cylindricus* is here referred to as *Solarium Herbertii* Dh.
8. W. H. Pease, *Amer. J. Conchol.* **5**, 80 (1869). *H. variegatus* is referred to as *Torinia areola* Desh.
9. T. L. McGinty, *Nautilus* **54**, 106 (1941).
10. H. N. Lowe, *ibid.* **46**, 110 (1933). *H. bicanaliculatus* is referred to as *H. variegatum* Lam. A. Sorensen, *ibid.* **57**, 5 (1943). *H. bicanaliculatus* is referred to as *H. radiatus*.
11. R. Robertson and A. S. Merrill, *Veliger* **6**, 76 (1963).
12. A. T. de Rochebrune, *Bull. Soc. Philomathique Paris* (7) **5**, 108 (1881). As *Teretropoma perrieri*. Rochebrune mistakenly believed he had discovered a new "subfamily" of land snails. The name *Heliacus perrieri* is used here for the species that is the Atlantic analogue of *H. infundibuliformis* (Gmelin) [the same as *Torinia crenellus* (Linn.) of Bayer (*2*)], an Indo-West-Pacific species.
13. B. R. Bales, *Proc. Phila. Shell Club* **1**(3), 12 (1958). As *Torinia cyclostoma* Menke.
14. The species identifications of the zoanthids are provisional because the taxonomy is in disorder (according to C. E. Cutress, who identified them). The catalog numbers of the host specimens at the United States National Museum (U.S.N.M.), Washington, D.C., are listed to aid eventual revision.
15. *Heliacus bicanaliculatus* is exceptional in attaining the volume of 10 to 15 polyps of *Zoanthus danai*.
16. R. Robertson, *Proc. Acad. Nat. Sci. Phila.* **116**, 1 (1964); R. S. Scheltema, unpublished.
17. My field work was supported by various organizations: in the Bahamas, by the Society of the Sigma Xi and the Lerner Marine Laboratory of the American Museum of Natural History; in Florida, by the Marine Laboratory, University of Miami; in British Honduras, by the Humble Oil and Refining Company in a grant to E. G. Purdy (Rice University); and, in the Maldives, by the National Science Foundation as a part of the U.S. Program in Biology, International Indian Ocean Expedition. For the field observations and specimens from the Hawaiian Islands, I thank Mrs. E. Gage, Mrs. A. M. Harrison, and A. E. Kay; from the Gulf of California, D. R. Shasky; from Aruba, R. T. and S. D. Abbott, and Mrs. J. O. Johnson. For other information, I thank C. E. Cutress, A. M. Keen, T. L. McGinty, A. S. Merrill, and R. S. Scheltema.

24 February 1967

Reprinted from *Bioenergetica i Biologicheskaya Spectrophotometria*. Special issue, 1967, p. 46-52

О БИОЛЮМИНЕСЦЕНЦИИ ПЛАНКТОНА В ИНДИЙСКОМ ОКЕАНЕ ПО МАТЕРИАЛАМ 35-го РЕЙСА ЭКСПЕДИЦИОННОГО СУДНА «ВИТЯЗЬ»

В. В. ЗЕРНОВА

(Институт океанологии АН СССР, Москва)

Материалом для настоящей работы послужили наблюдения, проведенные в северо-восточной части Индийского океана во время 35-го рейса экспедиционного судна «Витязь» с 2 июля по 2 сентября 1962 г. на четырех меридиональных разрезах — по 77, 84, 92 и 104—114° в. д. и от 5—14° с. ш. до 10—32° ю. ш. (рис. 1).

Свечение в море измеряли батифотометром по стандартным горизонтам — 1, 10, 25, 50, 75, 100, 125, 150, 200, 250, 300, 400, 500, 750, 1000, 1250, 1500, 2000, 2500 *м*. Запись сигналов вели в течение 2 мин. на каждом горизонте, затем полученные величины пересчитывали на число вспышек в 1 мин. За время рейса на 48 станциях были сделаны 503 измерения свечения, из них в слое 0—500 *м* измерения проведены 450 раз, в слое 500—1000 *м* — 36 раз, в слое 1000—2500 *м* — 17 раз.

Интенсивность свечения (число вспышек за 1 мин. наблюдения) и величина отдельных вспышек, как это будет показано ниже, существенно менялись в разных районах исследованной акватории и на разной глубине. Полученный материал позволяет наметить пути выяснения причин этих изменений. Наиболее рациональным методом для этого было бы выяснение состава светящихся организмов, а затем изучение их экологии и распространения. Однако при изучении видового состава светящихся форм появился ряд технических трудностей в их поимке и отборе из проб. Обработка полученных в рейсе результатов еще не закончена, и мы пока можем дать лишь предварительный перечень светящихся форм, встреченных в слое 0—500 *м*[1].

[1] Определение Copepoda проводил М. В. Гептнер, Ostracoda — Ю. А. Рудяков (Институт океанологии АН СССР).

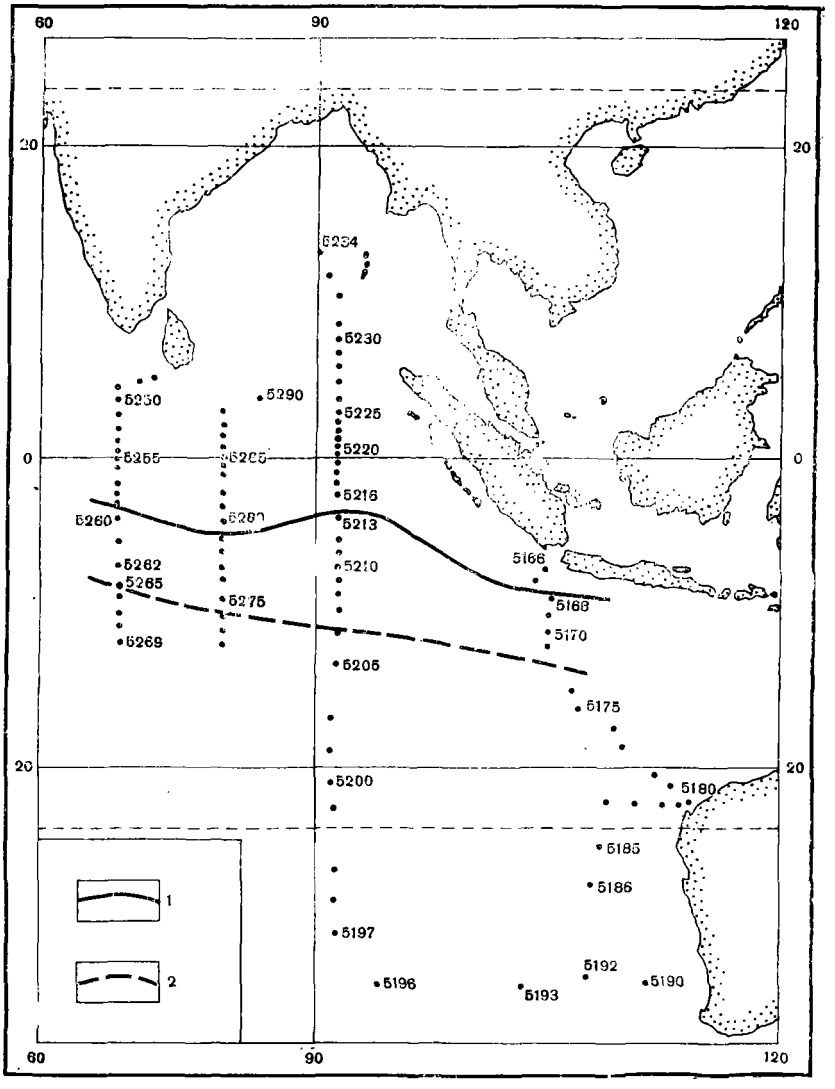


Рис. 1. Карта станций 35-го рейса экспедиционного судна «Витязь»

1 — экваториальная дивергенция; *2* — тропическая конвергенция на глубине 50 *м*

Copepoda: *Lucicutia flavicornis*, *L. ovaliformis*, *Pleuromamma gracilis*, *P. indica*, *P. quadrangulata*, *P. abdominalis* f. *abyssalis*, *Euchaeta marina*, *Heterorhabdus spinifrons*, *Eucalanus* sp., *Scolecithricidae* gen. sp., *Oithona* sp., *Oncaea* sp. *Corycaeus* sp., *Copilia* sp.

Ostracoda: *Cypridina sinuosa*, *C. chierchiae*, *Conchoecia elegans*, *C. daphnoides*, *C. spinirostris*, а также виды Euphaesiidae, Siphonophora и Radiolaria.

В верхнем 100—200-метровом слое, особенно в некоторых районах, подавляющее большинство вспышек дают жгутиковые —

Pyrocystis pseudonoctiluca. Поэтому в дальнейшем мы обратим особое внимание на сравнение ее распространения с распределением общего числа вспышек в поверхностных слоях.

Не имея возможности сравнить интенсивность свечения с распределением непосредственно светящихся организмов, мы попытаемся сопоставить ее с общим распределением планктона [1], так как в первом приближении можно считать, что число светящихся животных пропорционально общему количеству планктона.

В свою очередь распределение планктона чрезвычайно изменчиво и в значительной степени зависит от гидрологических условий и, прежде всего, от системы циркуляции вод.

В районе исследования в период рейса система циркуляции состояла из следующих основных элементов [2]:

1) слабого течения западных ветров, занимающего тропическую область, северной границей которой является тропическая конвергенция (зона опускания вод) (10—14° ю. ш.);

2) пассатного течения (5—10° ю. ш.), ограниченного на севере (5° ю. ш.) экваториальной дивергенцией (зона подъема вод), а на юге — тропической конвергенцией (10—14° ю. ш.);

3) муссонного (северного экваториального) течения, занимающего всю область севернее 5° ю. ш. Муссонное течение было самым мощным потоком с наибольшими скоростями течений на экваторе, так как оно в основном носило поверхностный характер.

Наибольшая интенсивность свечения в слое 0—100 *м* (рис. 2) в восточной части Индийского океана была отмечена в экваториальной области (5—3° с. ш.; 77° в. д.; 5° с. ш.; 3° ю. ш.; 84° в. д.; 1—6° ю. ш.; 92° в. д.) в водах муссонного течения к северу от экваториальной дивергенции, проходящей примерно по 5° ю. ш. В этом районе среднее количество вспышек в 1 мин. превышало 140, достигая максимума — 186 вспышек на станции 5286.

К северу и югу от экваториального района интенсивность свечения уменьшается до 100—140 вспышек. Такая интенсивность свечения была отмечена в юго-восточной части Бенгальского залива, в большей части вод пассатного течения (5—10° ю. ш.) и в тропической области или так называемой области слабого течения восточиых ветров, расположенной южнее 10° ю. ш.

Наименьшая интенсивность свечения (менее 100 вспышек) наблюдалась в узкой зоне, к северу от тропической конвергенции, на 6—7° ю. ш.; 77° в. д.; 6—10° ю. ш.; 84° в. д.; к югу от о. Ява — на 8—16° и на 25° ю. ш., где среднее число вспышек для слоя 0—100 *м* в минуту было 55.

Интенсивность свечения в слое 100—200 *м* (рис. 2, *б*) в общем ниже, чем в слое 0—100 *м*, но амплитуда различий между отдельными районами была больше. Максимальное количество вспышек было отмечено в экваториальном районе по 84° в. д., а минимальное (12 вспышек) — на этом же разрезе на 6° ю. ш. К северу и югу от экватора интенсивность свечения уменьшается

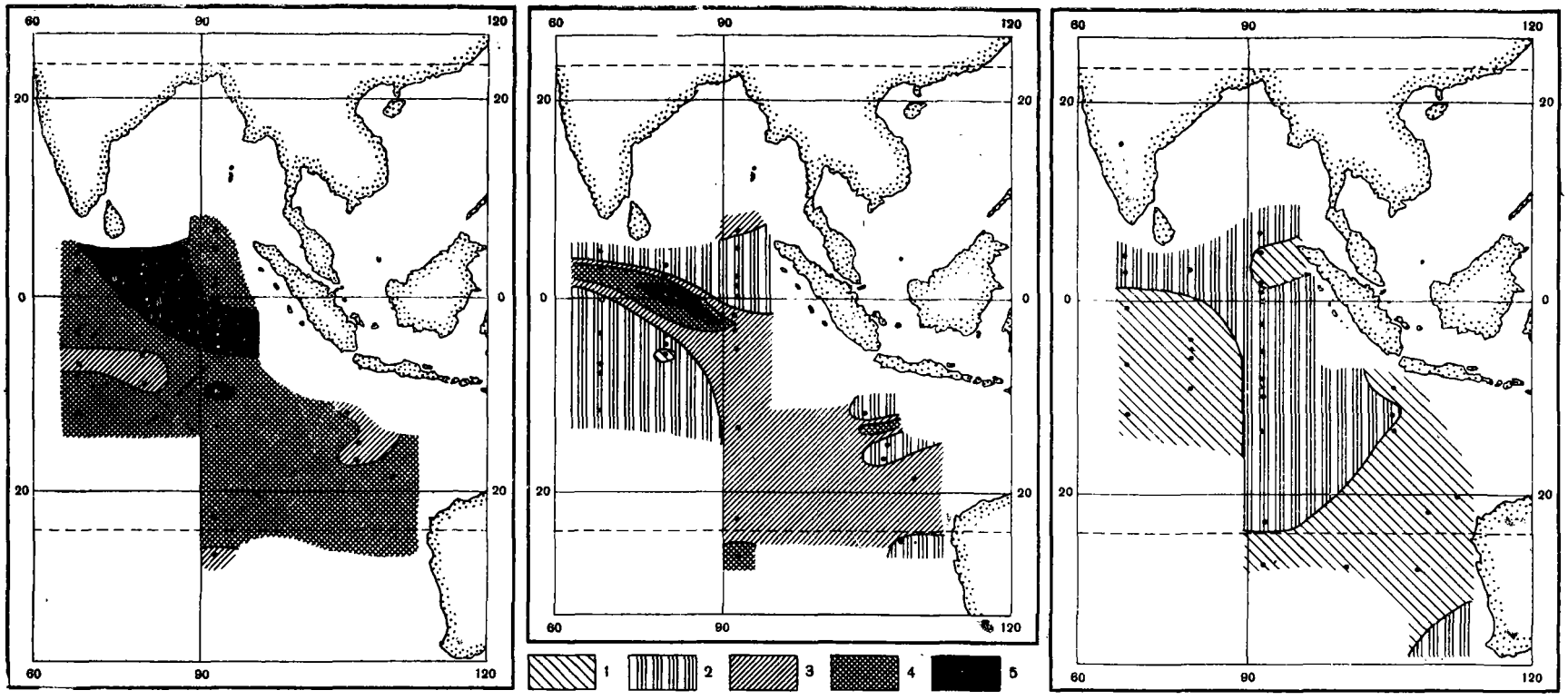


Рис. 2. Распределение интенсивности свечения в слое

а — 0—100 *м*; *б* — 100—200 *м*; *в* — 200—500 *м*; количество вспышек в 1 мин.: *1* — до 20; *2* — 20—50; *3* — 50—100; *4* — 100—150; *5* — свыше 150

и составляет 50—100, а часто и менее 50 вспышек в 1 мин. Особенно низкая интенсивность свечения к югу от Бенгальского залива — на 5° с. ш.— и южнее экватора — на разрезах по 77 и 84° в. д., а также на нескольких станциях между о. Ява и Австралией.

В слое 200—500 *м* интенсивность свечения оказалась значительно меньшей (рис. 2, *в*). Максимальное количество вспышек — 50 (ст. 5196) и минимальное — 2 вспышки (ст. 5186) было отмечено у берегов Австралии. Районы с большей интенсивностью (более 20 вспышек) расположены к северу от экватора — на 77 и 84° в. д., почти на всем разрезе по 92° в. д. и примерно там же, где была отмечена повышенная интенсивность свечения в слое 100—200 *м*. Уменьшение свечения хорошо прослеживается к югу от экватора на разрезах по 77° и 84° в. д. как в слое 200—500 *м*, так и в слое 100—200 *м*. Минимальное свечение было отмечено в слое 200—500 *м* к северо-востоку от Австралии.

Хотя интенсивность свечения на глубине 100—200 *м* ниже, чем в слое 0—100 *м*, а в слое 200—500 *м* — еще ниже, для каждого слоя районы с повышенной или пониженной интенсивностью свечения примерно совпадают.

Максимумы интенсивности свечения для всех слоев приурочены к экваториальной дивергенции (5° ю. ш.) и экватору, на разрезе по 92° в. д.— к тропической конвергенции (10° ю. ш.) и к водам муссонного течения между 5° ю. ш. и экватором. К экваториальному району приурочена максимальная интенсивность свечения и на разрезе по 77° в. д. Таким образом, наибольшая интенсивность свечения на разных глубинах, особенно в верхнем слое (200 *м*), была максимальной в экваториальном районе и уменьшалась в тропических водах.

Полученные данные довольно хорошо согласуются с картиной распределения фито- и зоопланктона [1]. Биомасса фито- и зоопланктона в экваториальном районе втрое больше, чем в центральных водах, в зоне течения западных ветров. Столь же высоко количество планктона в южной части Бенгальского залива, в водах муссонного течения. Для тропических центральных вод характерна очень низкая биомасса планктона (менее 0,05 $см^3/м^3$ в среднем для слоя 0—100 *м*), лишь на отдельных станциях она незначительно повышается.

Распределение *Pyrocistis pseudonoctiluca* носит аналогичный характер. Ее максимальная численность была отмечена к северу и югу от экватора (более 200 клеток в 1 $м^3$ в среднем для слоя 0—100 *м*) — до 5° ю. ш. в западной части исследованного района и до 10° ю. ш.— в восточной.

Сопоставляя распределение интенсивности свечения с распределением количества планктона и количества *P. pseudonoctiluca*, легко видеть, что районы, наиболее богатые планктоном, особенно экваториальный, оказываются зонами наибольшей интенсивности свечения, и наоборот. Конечно, это совпадение касается только

общей тенденции распределения всех упомянутых характеристик, а не его деталей.

Очевидно, после обработки сборов планктона и составления карт распределения всех массовых светящихся организмов картина изменения интенсивности свечения станет яснее.

P. pseudonoctiluca может вызывать многочисленные, но небольшие вспышки. Более яркие вспышки создаются крупными животными. Именно мелкие вспышки (первого и второго порядков) составляют основную массу вспышек в верхнем 100-метровом слое. Более яркие вспышки (третьего и четвертого порядков) наблюдаются гораздо реже. (В среднем 80—100 мелких вспышек в 1 мин. и 0—25 крупных.) В зоне экваториальной дивергенции роль крупных вспышек несколько увеличивается.

При сравнении результатов, полученных в 35-м рейсе экспедиционного судна «Витязь» по биолюминесценции, с картой повторяемости случаев свечения моря, распределенных по десятиградусовым квадратам [3], видно, что в Индийском океане район максимального свечения находится к северу от экватора (0—10° с. ш.). К северу и югу от этого района интенсивность свечения падает.

Можно считать, что воды муссонного течения, в которых было отмечено наибольшее количество планктона, в течение всего года будут иметь постоянно повышенную интенсивность свечения.

ВЕРТИКАЛЬНОЕ РАСПРЕДЕЛЕНИЕ ИНТЕНСИВНОСТИ СВЕЧЕНИЯ

По интенсивности биолюминесценции всю исследованную толщу вод океана можно разделить на три зоны: верхнюю, где число вспышек в течение 1 мин. регистрации батифотометром превышает 50; среднюю, где число вспышек составляет 50—10, и глубинную (менее 10 вспышек).

Уменьшение количества биолюминесцентных организмов соответствует общему уменьшению количества планктона с глубиной.

Максимальное количество вспышек обычно наблюдается в слое 50—100 *м* — более 200 вспышек в минуту (до 283 на глубине 100 *м* станц. 5285). В самом поверхностном слое интенсивность свечения была несколько меньшей и даже в районах с интенсивным свечением не превышала 100—200 вспышек в минуту. Нижняя граница зоны с интенсивной биолюминесценцией (более 50 вспышек в 1 мин.) лежит в среднем на глубине 100—150 *м*, но испытывает заметное колебание. Глубже всего она опускается в районе экватора и в центральных районах океана. Так, например, на экваторе, на разрезе по 84° в. д., даже на глубине 300 *м* было зарегистрировано более 200 вспышек в 1 мин. Примерно то же наблюдалось и на разрезе по 77° в. д. Однако восточнее (разрез по 92° в. д.) ни резкого увеличения светящихся организмов, ни опускания нижней границы зоны интенсивной биолюминесценции

на экваторе отмечено не было. Это, очевидно, связано с некоторым обеднением планктона в районе экватора, в самой восточной части океана.

Зона средней интенсивности биолюминесценции простирается от глубины 100—200 до 200—800 *м*. Выше всего эта граница лежит в бедных планктоном центральных водах (25—30° ю. ш.), а наиболее глубоко опускается в водах с экваториальной структурой. На разрезе по 92° в. д. подъем нижней границы этой зоны имел место и в бедных планктоном водах к северу от экватора.

По мере дальнейшего увеличения глубины интенсивность свечения продолжала уменьшаться и на глубине 1500—2000 *м* обычно отмечалось не более 1—2 вспышек в 1 мин. Однако необходимо подчеркнуть, что не было ни одного случая, чтобы в течение 2 мин. прибор не зарегистрировал ни одной вспышки. С глубиной меняется не только количество вспышек, но и их яркость. В поверхностном слое велико значение сравнительно слабых вспышек, очевидно создаваемых *Pyrocystis pseudonoctiluca* и мелкими копеподами. В более глубоких слоях увеличиваются роль и абсолютное количество ярких вспышек, создаваемых более крупными животными. Обязаны ли эти вспышки своим возникновением крупным копеподам или макропланктонным формам, пока сказать трудно.

ЛИТЕРАТУРА

1. И. Н. Суханова. 1962. Отчет о работах 35-го рейса «Витязя», т. III. Библиотека Ин-та океанол. АН СССР.
2. В. Г. Нейман. 1963. Океанология, 3, вып. 3.
3. Н. И. Тарасов. 1956. Свечение моря. М., Изд-во АН СССР.

Part II

Marine chemistry

Reprinted from *Limnol. and Oceanogr.*, vol. 10, no. 3, 1965, p. 459-462

Size Fractionation of Particulate Organic Carbon in the Surface Waters of the Western Indian Ocean[1]

Although the total standing crop of particulate organic carbon (living organisms and detritus) constitutes the basic food resource for filter-feeding pelagic animals, this crop is not utilized uniformly. The availability of organic carbon as food for any particular species depends partly upon the size of the particles in which it occurs. Wood and Davis (1956), Yentsch and Ryther (1959), and Teixeira (1963) have determined the contributions of net phytoplankton and nannoplankton to the total chlorophyll content, cell numbers, and ^{14}C productivity of seawater, while Holmes and Anderson (1963) and Saijo (1964) performed more complete size fractionations of ^{14}C-labeled primary producers. Since carbon is the basic metabolic substrate and since many zooplankters may feed on detritus or microzooplankton as well as living phytoplankton, the size distribution of particulate organic carbon is perhaps of more importance than is that of chlorophyll in determining the availability of food.

Seawater was taken from a depth of 15 m by a submersible pump along a 55° E long transect or with a large-volume water bottle along a 75° E long transect at 20 stations in the western Indian Ocean from February to April 1964. The pump (loaned by Dr. M. B. Allen) had a 4-cm diameter intake nozzle and delivered about 10 liters/min. After preliminary filtration through No. 00 nylon netting (500 μ apertures) to remove large organisms, the water was drawn by mild suction through a fractional filtration column (Fig. 1), thus dividing the total particulate matter into 7 fractions. Each coarse filter was made from nylon bolting cloth glued to a plastic funnel to obtain an effective filtration area of about 25 cm^2. The funnels were stacked so that the water passed through successively finer filters and finally through glass fiber filters of approximately 2 μ pore size (P. M. Williams, personal communication). Here, the average pore size of these filters is arbitrarily taken as 1 μ to allow for increased retention as the filters clog. The catch from each nylon netting was rinsed onto a glass fiber filter and each filter was rinsed with isotonic Na_2SO_4.

Total particulate carbon was determined from filters A and B (Fig. 1); particles with an effective diameter between 500 and 350 μ were analyzed from filter C, those between 350 and 125 μ from filter D, and so on. Particles between 33 and 10 μ could not be analyzed directly because of the carbon content of the 10 μ filters, but were estimated by difference as $(L + M) = (H + I) - (J + K)$. The sum of the fractional carbon on filters C to G plus J to M should equal the total carbon on filters A and B when all are converted to carbon per liter of water. The null hypothesis that there is no difference between the sum of the fractions and the total is acceptable from the available data ($p > 0.10$ by Wilcoxon signed rank test). This suggests that no significant amount of carbon was lost by the fractionation process or added as contamination during handling.

The carbon on each glass filter was measured within 3 hr of filtration by wet oxidation with dichromic acid. The treatment employed was that of Strickland and Parsons (1960, p. 117) except that the excess dichromate was back-titrated with 0.1

[1] Contribution No. 1592 from the Woods Hole Oceanographic Institution. This investigation was conducted during Cruise 5 of the *RV Anton Bruun* as part of the International Indian Ocean Expedition. Funds were provided by National Science Foundation Grant G-20952 and Postdoctoral Fellowship 43094. Dr. J. D. H. Strickland provided helpful criticism of the manuscript.

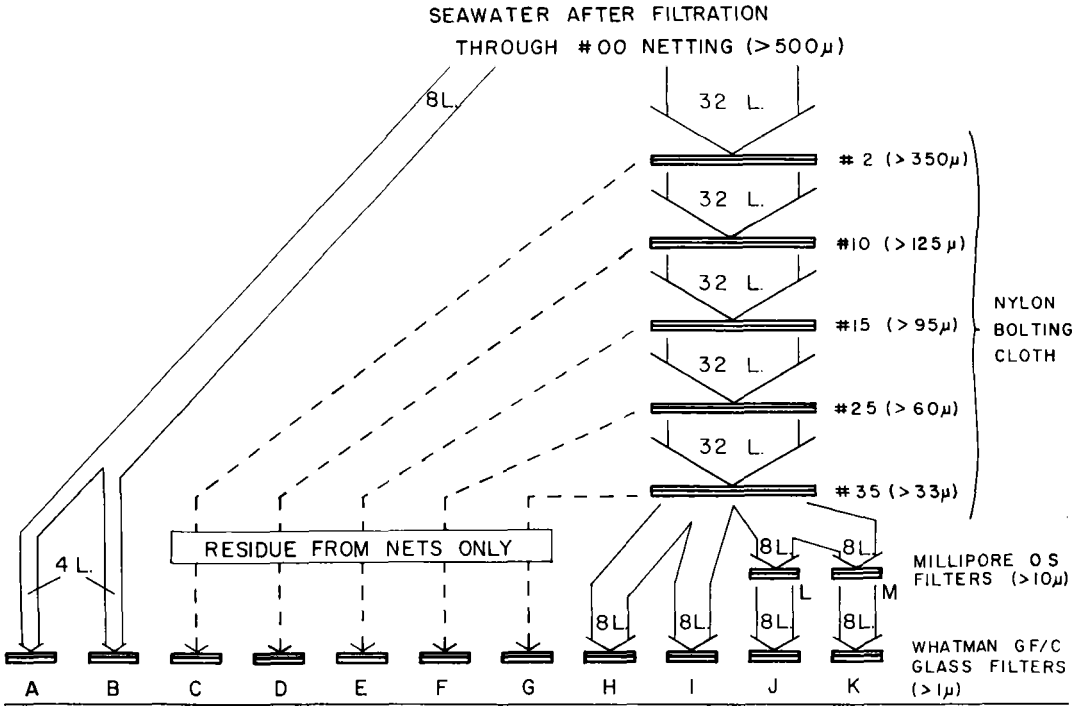


FIG. 1. Fractional filtration of particulate matter prior to organic carbon determinations (modified from Conover and Mullin 1963).

N acidic ferrous ammonium sulfate (*see* Fox, Isaacs, and Corcoran 1952; Maciolek 1962). This method actually measures total oxidizable material. Blanks were determined by repeating the analysis with Na_2SO_4-rinsed fresh filters, and the method was calibrated against a standard glucose solution. As an estimate of the precision of the titration itself, the standard error of the mean was computed for three replicates in each of 20 sets of titrations using reagents alone or reagents plus 300 or 600 μg of carbon as glucose. The mean of the standard errors was equivalent to 6 μg of carbon (range 1 to 18 μg C).

Table 1 indicates that the 10–1-μ fraction (filters J and K in Fig. 1) contributed at least 45% of the total carbon at all but two stations and was the richest single category. At the other two stations, the 33–10-μ fraction contained slightly more carbon than the 10–1-μ fraction. The sum of the carbon in particles larger than 33 μ (filters C through G in Fig. 1) ranged from 14 to 32% of the total. There was no significant correlation between total carbon and the relative contributions of either the 10–1-μ fraction or the fraction larger than 33 μ ($p > 0.10$). The size distribution of carbon-containing particles is therefore not related to the total amount of particulate carbon in the present samples.

The mean total carbon along each transect was identical, but the relative contribution of the 10–1-μ fraction was somewhat lower along 75° E long than along 55° E long. This may be a real effect, but it could occur if the pump used to take samples along the 55° E long transect had a greater tendency to disrupt natural aggregations than the water bottle used along the 75° E long transect.

Table 2 shows the relative distribution of carbon between the different categories, which is similar to that found in the Gulf of Maine during late spring and summer (Mullin 1963), but the amount of carbon within each category is two to three times less.

TABLE 1. *Total particulate organic carbon at 15 m in the western Indian Ocean, and the contribution of particles of 10 to 1 μ size to the total**

Station location lat	long	Total particulate organic C, μg/liter	10–1 μ C / total C
15° N,	58° E	129.5	0.70
10° N,	55° E	87.0	0.56
05° N,	55° E	86.2	0.67
01° N,	55° E	58.6	0.78
03° S,	55° E	57.0	0.78
09° S,	55° E	74.2	0.69
13° S,	55° E	68.5	0.56
17° S,	55° E	110.0	0.51
26° S,	55° E	77.9	0.56
31° S,	55° E	46.5	0.59
36° S,	55° E	69.0	0.66
04° N,	75° E	84.2	0.31
02° S,	75° E	69.5	0.45
09° S,	75° E	64.6	0.56
14° S,	75° E	62.4	0.62
20° S,	75° E	52.5	0.46
26° S,	75° E	70.5	0.75
30° S,	75° E	65.0	0.34
37° S,	75° E	100.0	0.56
40° S,	75° E	138.0	0.46

* Recently, chlorophyll analyses (which permit estimates of organic carbon in living phytoplankton) have become available from these stations and will be published as an addendum in the next issue of this journal.

The method fractionates particles on the basis of effective diameter, that is, the filter aperture necessary to retain the particle. A major source of error in the fractionation technique is the possibility that natural aggregations such as those described by Riley (1963) are broken up during the sampling or filtration. Microscopic examination would be necessary to evaluate the magnitude of this artifact. Colonies or chains of cells may be disrupted and even single cells may be fragmented (Holmes and Anderson 1963). If this occurs, the carbon content of the 33–10-μ and 10–1-μ fractions is artificially increased at the expense of the other fractions. Organic carbon may be somewhat more evenly distributed as to size *in situ* than the results indicate.

Considering the large area samples were taken from, the total particulate carbon is rather constant; the threefold variation is less than might be found in a much smaller area in different seasons. The stations are north of the Subtropical Convergence within the Central and Equatorial water masses and largely outside the influence of land drainage or strong currents and upwelling (Sverdrup, Johnson, and Fleming 1942). Bernard and Lecal (1960) studied this same area from October to February and found that coccolithophorids were the dominant phytoplankters, in terms of biomass, followed by Myxophyceae and dinoflagellates. These authors computed that the standing crop of phytoplankton in the upper 40 m contained at least 50 to 100 μg C/liter from optical measurements of cell volumes and a conversion factor. Most of the values for total particulate organic carbon given in Table 1 fall within this range, suggesting that most of the carbon in the samples was due to phytoplankton rather than to heterotrophs or detritus.

If selective pressures encourage different zooplankton species to feed with maximum efficiency on different sizes of food particles, an increase in the size diversity of available organic particles may permit an increase in the faunal diversity of zooplankton even if the total biomass of particles remains constant. The importance of particle size diversity as measured in the present study is difficult to estimate because of the uncertain role of detritus in the various size categories and in the nutrition of the zooplankton (Krey 1961; Parsons 1963). A portion of the carbon in each size category may not be directly usable by zooplankton, and this portion probably varies from category to category. However, it is apparent that a species feeding on particles larger than 60 μ will have

TABLE 2. *Mean carbon content of various particle size categories at 15 m in the western Indian Ocean*

Particle size category	350 to 500 μ	125 to 350 μ	95 to 125 μ	60 to 95 μ	33 to 60 μ	10 to 33 μ	1 to 10 μ	Total
Mean μg C/liter	2.1	3.9	3.1	5.0	5.0	13.9	45.5	78.5
Mean % of total C	3%	5%	4%	6%	6%	18%	58%	100%

to search considerably more water to find a given amount of food than a species feeding on particles less than 10 μ in size. Since much of the primary production in oceanic areas is carried out by organisms smaller than 10 μ (e.g. McAllister, Parsons, and Strickland 1960), it is obviously advantageous for a herbivore to be able to remove these small particles from suspension efficiently.

MICHAEL M. MULLIN

Institute of Marine Resources,
University of California,
San Diego.

REFERENCES

BERNARD, F., AND J. LECAL. 1960. Plancton unicellulaire récolté dans l'ocean Indien par le *Charcot* (1950) et le *Norsel* (1955–56). Bull. Inst. Oceanog., No. **1166**. 59 p.

CONOVER, R. J., AND M. M. MULLIN. 1963. Preliminary studies of natural plankton communities marked with parachute drogues. Woods Hole Oceanog. Inst., Appendix to Ref. 63–4: 1–14 (unpublished manuscript).

FOX, D. L., J. D. ISAACS, AND E. F. CORCORAN. 1952. Marine leptopel, its recovery, measurement, and distribution. J. Marine Res., **11**: 29–46.

HOLMES, R. W., AND G. C. ANDERSON. 1963. Size fractionation of C^{14}-labeled natural phytoplankton communities, p. 241–250. *In* C. H. Oppenheimer [ed.], Symposium on marine microbiology. Thomas, Springfield, Ill.

KREY, J. 1961. Der Detritus im Meere. J. Conseil, Conseil Perm. Intern. Exploration Mer, **26**: 263–280.

MACIOLEK, J. A. 1962. Limnological organic analysis by quantitative dichromate oxidation. U.S. Fish Wildlife Serv., Res. Rept., **60**: 1–61.

MCALLISTER, C. D., T. R. PARSONS, AND J. D. H. STRICKLAND. 1960. Primary productivity at station "P" in the north-east Pacific Ocean. J. Conseil, Conseil Perm. Intern. Exploration Mer, **25**: 240–259.

MULLIN, M. M. 1963. Comparative ecology of the genus *Calanus* in the Gulf of Maine. Ph.D. Thesis, Harvard Univ. 97 p.

PARSONS, T. R. 1963. Suspended organic matter. *In* M. Sears [ed.], Progress in oceanography, **1**: 203–239. Pergamon Press.

RILEY, G. A. 1963. Organic aggregates in seawater and the dynamics of their formation and utilization. Limnol. Oceanog., **8**: 372–381.

SAIJO, Y. 1964. Size distribution of photosynthesizing phytoplankton in the Indian Ocean. J. Oceanog. Soc. Japan, **19**: 19–21.

STRICKLAND, J. D. H., AND T. R. PARSONS. 1960. A manual of sea water analysis. Bull. Fisheries Res. Board Can., **125**: 185 p.

SVERDRUP, H. U., M. W. JOHNSON, AND R. H. FLEMING. 1942. The oceans. Prentice-Hall, Englewood Cliffs, N. J. 1087 p.

TEIXEIRA, C. 1963. Relative rates of photosynthesis and standing stock of the net phytoplankton and nannoplankton. Bol. Inst. Oceanog., Sao Paulo, **13**: 53–60.

WOOD, E. J. F., AND P. S. DAVIS. 1956. Importance of smaller phytoplankton elements. Nature, **177**: 438.

YENTSCH, C. S., AND J. H. RYTHER. 1959. Relative significance of the net phytoplankton and nannoplankton in the waters of Vineyard Sound. J. Conseil, Conseil Perm. Intern. Exploration Mer, **24**: 231–238.

Reprinted from *Limnol. and Oceanogr.*, vol. 10, no. 4, 1965, p. 610-611

Size Fractionation of Particulate Organic Carbon in the Surface Waters of the Western Indian Ocean: Addendum

Since the previous report on particulate organic carbon (Mullin 1965), information concerning the concentration of chlorophyll *a* at various stations of the survey has been made available. Staff scientists on the *Anton Brunn* used the method of Richards and Thompson (1952) to determine the chlorophyll *a* content of particulate matter retained on glass fiber filters. The organic carbon attributable to living phytoplankton can therefore be estimated, using a factor of 35 to convert chlorophyll *a* to phytoplankton carbon (Ryther and Menzel 1965). This calculation indicates that, although phytoplankton carbon is positively correlated with total particulate organic carbon ($p < .05$ by Kendall rank correlation, tau), less than 10% of the total carbon at any station was in fact in the form of living phytoplankton. Even if a conversion factor of 60 or 70 is used (McAllister, Parsons, and Strickland 1960), phytoplankton carbon still accounted for less than 20% of the total carbon.

Carbon in the form of detritus or heterotrophic microorganisms was therefore considerably more important than suggested in the previous report. The minimal estimates of phytoplankton carbon given by Bernard and Lecal (1960) must be re-interpreted to indicate that phytoplankton crops considerably larger than those observed during the present survey may sometimes be present.

Michael M. Mullin

Institute of Marine Resources,
University of California,
San Diego.

References

Bernard, F., and J. Lecal. 1960. Plancton unicellulaire récolté dans l'ocean Indien par le *Charcot* (1950) et le *Norsel* (1955–56). Bull. Inst. Oceanog. Monaco, No. 1166. 59 p.

McAllister, C. D., T. R. Parsons, and J. D. H. Strickland. 1960. Primary productivity at station "P" in the north-east Pacific Ocean. J. Conseil, Conseil Perm. Intern. Exploration Mer, **25**: 240–259.

Mullin, M. M. 1965. Size fractionation of particulate organic carbon in the surface waters of the western Indian Ocean. Limnol. Oceanog., **10**: 458–462.

Richards, F. A., and T. G. Thompson. 1952. The estimation and characterization of plankton populations by pigment analysis. II. A spectrophotometric method for the estimation of plankton pigments. J. Marine Res., **11**: 156–172.

Ryther, J. H., and D. W. Menzel. 1965. On the production, composition, and distribution of organic matter in the Western Arabian Sea. Deep-Sea Res., **12**: 199–209.

Part III

Physical oceanography and marine meteorology

Reprinted from *Limnol. and Oceanogr.*, vol. 10, supplement, November 1965, p. R25-R37

RADIOCARBON IN THE PACIFIC AND INDIAN OCEANS AND ITS RELATION TO DEEP WATER MOVEMENTS[1]

G. S. Bien, N. W. Rakestraw, and H. E. Suess
University of California, San Diego, La Jolla, California

ABSTRACT

Since 1948, carbon-14 measurements on the bicarbonate of ocean water samples from the Pacific and Indian oceans have been carried out at the Scripps Institution of Oceanography, La Jolla, California. Previous reports of the results of these investigations have been confirmed and amended by many recent measurements. The method of extracting CO_2 from ocean water has been modified and perfected over the past years. The most notable results of the measurements concern the ^{14}C content of deep ocean water which can be interpreted unambiguously by considering the aging of the water during the time of movement from the Weddell Sea eastward and then northward into the North Pacific Ocean.

INTRODUCTION

The principles underlying the method of radiocarbon dating are well known. Natural carbon has an isotopic form, ^{14}C, with a half-life of some 5,730 years. Carbonaceous materials formed subaerially will orginally contain a proportion of ^{14}C practically equal to that in the atmosphere. With time, the radioactive isotope of the fixed carbon will decay and its relative content will indicate the elapsed time since the material was formed from the atmosphere.

Early determinations of the proportion of radiocarbon in the inorganic carbon content of seawater indicated that the results can be accepted only as a relative measure of the "age" of the water, because, in general, surface water cannot be assumed to come into complete equilibrium with the atmosphere before sinking. Therefore, one cannot be certain about the original radiocarbon content in any subsurface sample of seawater. There are also some tenuous assumptions necessary in taking the residence time of the carbon as the residence time of the water itself. Nevertheless, it seems evident that the appropriately defined residence time of the deep water of the oceans is of the order of hundreds of years.

Broecker et al. (1960), in discussing the natural radiocarbon in the Atlantic Ocean, have presented the results of all the prior measurements made in the Atlantic area and have ably discussed the problems involved in their interpretation, including the influence of such factors as the possible introduction of "young" carbon from the oxidation of organic matter and of "old" carbon from the solution of sedimentary carbonate.

The absolute age of the water requires a more or less arbitrary definition; differences in age or residence time, however, are in themselves significant. Differences in radiocarbon content in any large mass of water may be considered from the viewpoint of mixing of the water from different sources or of time spent by the water in going from one place to another. Broecker et al. have been concerned principally with the former alternative in the several water masses of the Atlantic area; we have undertaken to investigate the possibilities of the second alternative in the Pacific and Indian oceans.

As we have already indicated (Bien, Rakestraw, and Suess 1960), the International Geophysical Year afforded us an opportunity to obtain deep samples in a longitudinal section from approximately 40° S lat to 15° N long in the Pacific Ocean. Subsequently, similar samples were obtained in the Indian and the North Pacific oceans, and the results from these have

[1] Contribution from the Scripps Institution of Oceanography, University of California, San Diego.

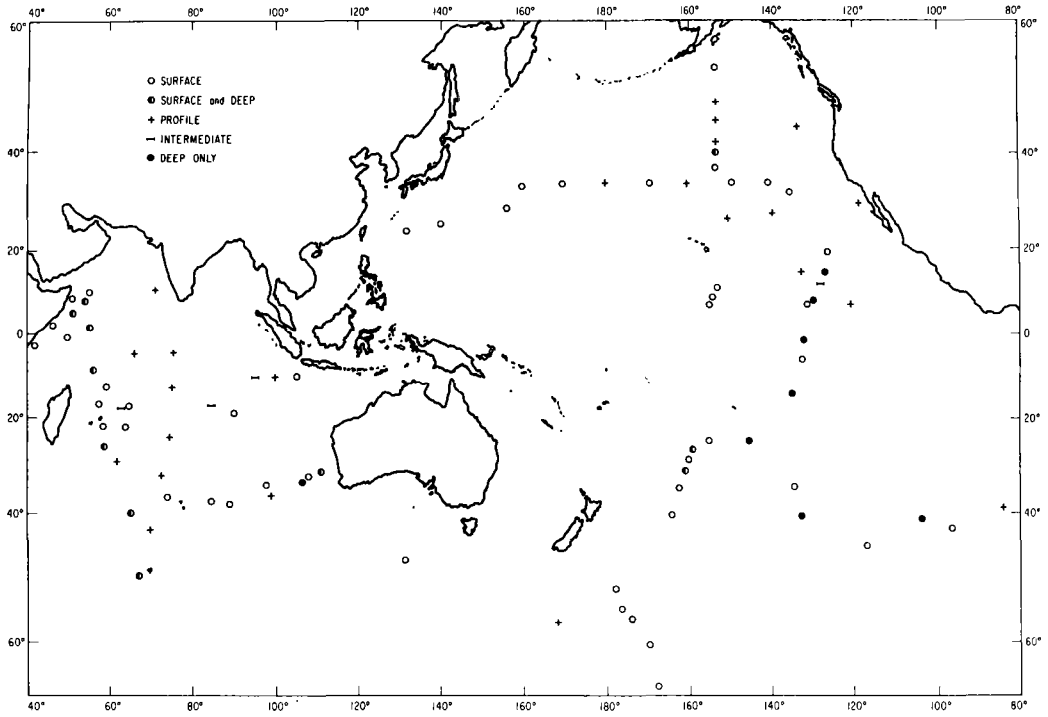


FIG. 1. Location of stations.

been reported elsewhere (Bien et al. 1963*a*, *b*). This paper brings the study up to date with additional results from the Pacific and Indian oceans. Fig. 1 shows the locations from which all samples have been obtained.

METHODS

Water samplers of several designs were constructed, all of an approximate 50-gal (190-liter) capacity. The first of these operated with spring-loaded doors mounted on a central column in the center of the barrel. When cocked, the upper door raised and the bottom lowered, and when tripped off by a falling messenger, both doors snapped shut. These proved reasonably satisfactory, but required frequent attention to adjust the fitting of the doors to prevent leakage when removed from the water.

In a subsequent design, hinged doors opened wide and the barrel went down in the vertical position. When released by a messenger, the barrel turned into the horizontal position and the doors were held firmly shut by a bridle formed by the hoisting cable itself. The weight of the full barrel and the tension of the cable were sufficient to kept the barrel firmly shut even when raised from the water. The loose lines tended to foul, however, and the design was abandoned after the barrel itself was lost in the Indian Ocean.

The final design was a square barrel with spring-loaded doors, the bottom one closing downward inside the barrel. This operated with general satisfaction but was lost in the Indian Ocean before some minor complications were eliminated.

Water samples can be preserved safely for a considerable time in steel drums provided with plastic liners. If closed tightly, exchange of CO_2 with the atmosphere will be insignificant. A few samples were returned in this way, but the usual practice was to treat the samples on shipboard, removing the total CO_2 and precipitating it as insoluble carbonate, in which form it

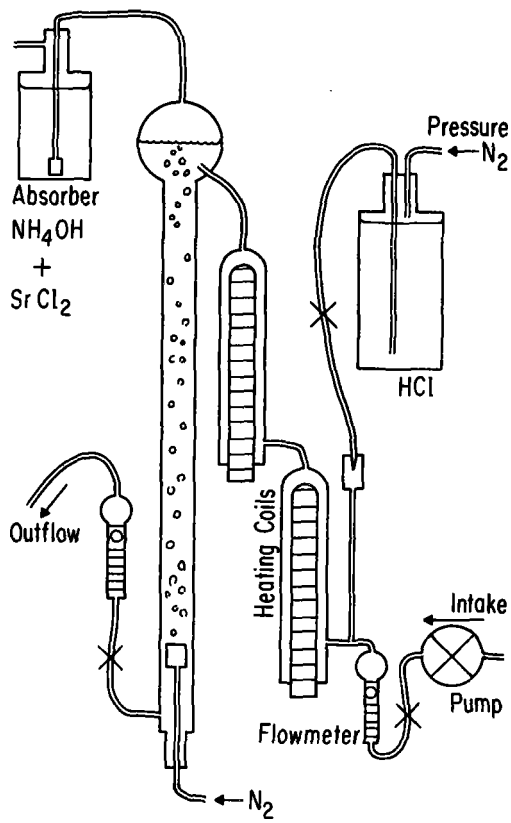


FIG. 2. Processing apparatus. Water enters at the rate of 1.5–2.5 liters/min, is acidified, heated, and the CO_2 stripped by N_2 gas and precipitated as $SrCO_3$.

was returned to the laboratory for further processing and counting.

Originally, the preliminary processing was done in a single batch, the whole sample was acidified in a suitable container, nitrogen gas bubbled through it, and the CO_2 absorbed from the stream in an alkali solution. Complete recovery can require considerable time, however, particularly when cold water must be heated.

In the present method of continuous circulation, the CO_2 can be virtually completely removed from a 50-gal (190-liter) sample in as little as 90 min.

The water is pumped from a plastic drum into the apparatus, and as it enters it is acidified with HCl at a controlled rate. The water passes over electrically heated coils and issues at a temperature of 50 to 70C into the top of a stripping column where it meets a stream of fine bubbles of nitrogen entering the bottom of the column through a sintered-glass diffuser head. The CO_2-free water goes to waste from the bottom of the column while the gas stream passes from the top and enters an absorber bottle through a sintered-glass diffuser. The absorber is a 1-liter Pyrex bottle containing about 800 ml of concentrated NH_4OH made approximately 1 M with $SrCl_2$. Fig. 2 is a diagram of the apparatus. Flowmeters monitor the intake and outflow rates of the water (from 1.5 to 2.5 liter/min), and the rate of addition of HCl is controlled by a needle valve and drop counter.

In our experience, absorption is better in ammonia than in alkali because it can take place in the gas phase as well as in the liquid. The precipitation of $SrCO_3$ is preferable to $BaCO_3$ because barium salts sometimes contain radium, which can cause contamination of the counting gas with radon; strontium salts are usually much less contaminated with radium. The carbonate must be reduced to carbide and hydrolyzed with water to produce C_2H_2, the gas used in our counter.

Our results are expressed as $\Delta^{14}C$; the derivation is as follows:

By definition,

$$\delta^{14}C = \left[\frac{A_{sample}}{A_{std}} - 1\right].$$

Let

$$\delta^{13}C_{sample} = \left[\frac{^{13}C/^{12}C_{sample}}{^{13}C/^{12}C_{std}} - 1\right]$$

from mass spectrograph. $\delta^{13}C_W$ = that of 19th century wood, which has an overall average of ~0.025. To normalize to 19th century wood, $\Delta^{13}C = \delta^{13}C_W - \delta^{13}C_{sample}$,

$$\Delta^{14}C = \frac{1+\delta^{14}C}{1+2\Delta^{13}C} - 1 = \frac{\delta^{14}C - 2\Delta^{13}C}{1+2\Delta^{13}C}$$

$$= \delta^{14}C - 2\Delta^{13}C(1+\delta^{14}C) \quad \text{(neglecting higher terms)}.$$

Inserting numerical values, and expressing in per mill,

$$\Delta^{14}C(‰) = \delta^{14}C(‰) - (2\delta^{13}C + 50) \times \left[1 + \frac{\delta^{14}C(‰)}{1{,}000}\right]$$

TABLE 1. *Pacific Ocean*

Sample number	Lat	Long	Depth (m)	Temp. (°C)	Salinity (‰)	$\delta^{13}C$ (‰)	$\Delta^{14}C$ (‰)	Date collected
LJ-410	64°11′ S	168°58′ W	0	1.70	34.009	*	−120 ± 20	13 Feb 1961
LJ-412	60°12′ S	171°32′ W	0	5.50	34.002	*	−66 ± 20	15 Feb 1961
LJ-321	58°20′ S	168°58′ E	0	6.32	34.038	+0.4	−63 ± 6	7 Feb 1961
LJ-320	"	"	740	3.38	34.224	−0.5	−121 ± 8	"
LJ-319	"	"	1,400	2.43	*	−1.3	−155 ± 12	"
LJ-318	"	"	2,100	*	34.766	−2.0	−165 ± 10	"
LJ-317	"	"	2,944	1.48	34.372	−1.1	−167 ± 10	"
LJ-316	"	"	3,825	*	34.277	−1.4	−180 ± 10	"
LJ-414	57°34′ S	144°15′ W	0	*	*	*	−52 ± 7	16 Feb 1961
LJ-413	55°39′ S	177°51′ W	0	*	*	*	−45 ± 4	17 Feb 1961
LJ-417	52°37′ S	178°57′ W	0	*	*	*	−30 ± 5	19 Feb 1961
LJ-418	49°42′ S	178°52′ W	0	9.3	34.34	*	−35 ± 5	20 Feb 1961
LJ- 90	46°30′ S	116° W	0	9.2	34.67	−0.7	−60 ± 8	8 Dec 1957
LJ- 93	42°43′ S	96°06′ W	0	11.5	*	−0.6	−40 ± 8	15 Dec 1957
LJ- 91	42°37′ S	103°20′ W	3,500	1.85	*	−2.5	−180 ± 8	17 Dec 1957
LJ- 69	40°35′ S	132°10′ W	3,500	1.50	34.67	−1.2	−195 ± 8	30 Nov 1957
LJ-408	40°22′ S	164°24′ W	0	*	*	*	−4 ± 20	3 Mar 1961
LJ- 94	39°33′ S	84°10′ W	3,500	1.46	*	−1.9	−196 ± 8	18 Mar 1957
LJ-409	36°27′ S	163°09′ W	0	*	*	*	−7 ± 5	5 Mar 1961
LJ- 68	34°50′ S	135°53′ W	0	17.7	35.05	−0.4	−38 ± 8	15 Nov 1957
LJ-326	34°04′ S	161°54′ W	0	21.4	35.103	*	−24 ± 10	7 Apr 1961
LJ-327	"	"	3,350	*	*	*	−202 ± 10	7 Mar 1961
LJ-415	30°26′ S	160°32′ W	0	*	34.8	*	−12 ± 4	9 Mar 1961
LJ-325	26°29′ S	160°33′ W	0	27.2	35.56	*	−3 ± 20	11 Mar 1961
LJ-324	"	"	3,500	*	*	*	−197 ± 10	"
LJ- 67	25°00′ S	145°00′ W	3,560	1.54	34.65	*	−204 ± 8	23 Nov 1957
LJ-416	24°41′ S	155°15′ W	0	*	34.88	*	−4 ± 4	12 Mar 1961
LJ-877	16°22′ S	161°49′ W	0	*	*	*	19 ± 10	16 Jan 1964
LJ- 57	14°29′ S	135°30′ W	3,450	1.58	34.69	−1.8	−211 ± 8	7 Nov 1957
LJ-876	11°25′ S	117°30′ W	0	*	*	*	46 ± 8	25 Dec 1963
LJ- 66	7°00′ S	132°00′ W	0	26.7	34.68	−1.0	−31 ± 8	26 Feb 1958
LJ- 63	2°08′ S	131°27′ W	3,473	1.52	34.69	−1.3	−214 ± 8	18 Feb 1958
LJ-878	0°	138°58′ W	0	*	*	*	24 ± 8	19 Feb 1964
LJ- 62	5°00′ N	130°00′ W	0	28.0	34.40	−0.1	−33 ± 8	21 Feb 1958
LJ-879	5°00′ N	134°00′ W	0	*	*	*	61 ± 10	21 Feb 1964
LJ-146	5°32′ N	120°05′ W	10	27.5	33.50	−1.22	−75 ± 8	27 July 1959
LJ-140	"	"	485	7.88	34.67	−2.51	−143 ± 8	"
LJ-147	"	"	1,080	4.12	34.63	−1.81	−213 ± 8	"
LJ-494	7°03′ N	158°38′ W	0	*	*	*	−27 ± 5	26 July 1960
LJ- 61	7°08′ N	129°17′ W	2,987	1.48	34.69	−1.4	−228 ± 8	22 Feb 1958
LJ-495	8°14′ N	156°38′ W	0	*	*	*	−9 ± 3	29 July 1960

* No observation.

In translation of $\Delta^{14}C$ results into age, we have used as a starting point the activity of 19th century wood rather than an assumed activity of water at the surface. This is purely arbitrary and does not yield an absolute age for the water. We believe, however, that it facilitates the comparison of different samples.

Accordingly:

Average age of $^{14}C = 8{,}033$ years (using a half-life of 5,568 years).

$$\text{Age} = 8{,}033 \ln \frac{A_{std}}{A_{sample}}$$

$$= 18{,}500 \log \frac{A_{std}}{A_{sample}}$$

Setting

$A_{std} = 1$,

$A_{sample} = 1 + \Delta^{14}C$, and

$\text{Age} = 18{,}500 \log [1/(1 + \Delta^{14}C)]$.

TABLE 1. Continued

Sample number	Lat	Long	Depth (m)	Temp. (°C)	Salinity (‰)	$\delta^{13}C$ (‰)	$\Delta^{14}C$ (‰)	Date collected
LJ-139	8°29′ N	120°09′ W	2,280	1.97	34.70	−1.66	−253 ± 8	28 July 1959
LJ-137	"	"	3,370	1.58	34.70	−0.74	−211 ± 8	"
LJ-880	*10°00′ N*	*133°00′ W*	*0*	*	*	*	*42 ± 10*	*23 Feb 1964*
LJ-493	10°39′ N	155°56′ W	0	*	*	*	−27 ± 4	30 July 1960
LJ- 60	11°00′ N	128°31′ W	400	10.9	34.65	−1.5	−100 ± 8	23 Feb 1958
LJ-467	14°55′ N	133°30′ W	0	*	34.13	*	42 ± 5	20 Jan 1962
LJ-468	"	to	753	6.8	34.51	*	−100 ± 4	"
LJ-470	"	134°14′ W	1,039	4.3	34.56	*	−188 ± 8	"
LJ-476	"	"	1,240	3.72	34.59	*	−161 ± 7	"
LJ-475	"	"	1,711	2.68	34.61	*	−207 ± 9	"
LJ-473	"	"	2,384	1.89	34.56	*	−207 ± 8	"
LJ-471	"	"	2,757	1.73	34.70	*	−227 ± 9	"
LJ-474	14°55′ N	134°14′ W	3,479	1.53	34.67	*	−207 ± 8	20 Jan 1962
LJ- 59	14°58′ N	127°31′ W	2,987	1.66	34.69	−1.2	−222 ± 8	24 Feb 1958
LJ-881	15°00′ N	130°00′ W	0	*	*	*	67 ± 9	24 Feb 1964
LJ-328	15°42′ N	155°22′ W	0	*	*	+1.8	−12 ± 10	21 July 1960
LJ- 58	19°35′ N	125°00′ W	0	24.4	34.69	−0.5	−33 ± 8	26 Feb 1958
LJ-882	20°00′ N	126°40′ W	0	*	*	*	66 ± 9	26 Feb 1964
LJ-561	24°28′ N	131°25′ E	0	25.0	34.87	*	33 ± 9	7 June 1962
LJ-883	25°00′ N	123°00′ W	0	*	*	*	85.7 ± 10	27 Feb 1964
LJ-560	27°11′ N	140°00′ E	0	25.02	35.00	*	64 ± 9	6 June 1962
LJ-1047	27°21′ N	155°00′ W	0	*	*	*	137 ± 10	12 Sept 1964
LJ-420	27°27′ N	150°35′ W	10	25.04	35.283	*	23 ± 5	20 Aug 1961
LJ-420	"	"	716	4.55	34.194	*	−152 ± 7	"
LJ-425	"	"	1,042	3.84	34.436	*	−190 ± 9	"
LJ-426	"	"	2,300	(1.85)	34.665	*	−225 ± 10	"
LJ-427	"	"	3,165	1.55	34.677	*	−223 ± 10	"
LJ-428	"	"	3,630	1.50	34.684	*	−212 ± 10	"
LJ-285	28°12′ N	139°07′ W	538	*	34.061	*	−153 ± 7	15 June 1960
LJ-282	"	"	1,607	*	34.571	*	−233 ± 10	13 June 1960
LJ-283	"	"	2,468	*	34.649	*	−222 ± 11	13 June 1960
LJ-284	"	"	3,518	*	34.680	*	−217 ± 8	14 June 1960
LJ-149	30°04′ N	118°02′ W	10	19.30	33.48	+1.9	−13 ± 8	14 Oct 1959
LJ-150	"	"	75	15.85	33.44	+1.0	−32 ± 8	"
LJ-151	"	"	120	13.40	33.48	+0.2	−38 ± 8	"
LJ-152	"	"	390	6.60	33.16	−1.9	−100 ± 8	"
LJ-153	"	"	600	5.21	34.35	−6.0	−169 ± 8	"
LJ-154	"	"	2,000	2.00	34.66	−1.6	−239 ± 8	"
LJ-158	"	"	3,300	1.60	34.67	+0.3	−235 ± 8	"
LJ-559	30°16′ N	147°49′ E	0	*	*	*	59 ± 10	4 June 1962
LJ-1048	31°29′ N	155°00′ W	0	*	*	*	131 ± 10	10 Sept 1964
LJ-1026	33°48′ N	135°01′ W	0	*	*	*	187 ± 10	7 Aug 1964
LJ-558	34°47′ N	160°20′ E	0	20.4	34.78	*	23 ± 10	2 June 1962
LJ-557	35°00′ N	170°02′ E	0	*	*	*	59 ± 10	31 May 1962

(Continued on next page)

RESULTS

All the results to date have been collected in Tables 1 and 2, with the collection sources arranged from south to north, in both the Pacific and Indian oceans.

Results from deep water below 3,000 m are plotted in Figs. 3 and 4 to show the gradient of variation with latitude.

In the Pacific Ocean the ^{14}C content decreases constantly from south to north well into the northern hemisphere; thereafter the gradient seems to flatten out. This is consistent with Knauss' circulation pattern, later referred to. Extensive mixing probably also takes place.

In the Indian Ocean, the situation is approximately similar but not so clear. ^{14}C decreases from south to north, though not so regularly, with the exception of two stations in the equatorial region. Indeed, at

TABLE 1. Continued

Sample number	Lat	Long	Depth (m)	Temp. (°C)	Salinity (‰)	$\delta^{13}C$ (‰)	$\Delta^{14}C$ (‰)	Date collected
LJ-540	35°00′ N	150°00′ W	0	17.00	34.35	*	−40 ± 10	22 May 1962
LJ-541	35°01′ N	160°00′ W	0	18.06	34.49	*	53 ± 10	24 May 1962
LJ-542	"	"	50	15.27	34.51	*	44 ± 9	"
LJ-543	"	"	100	14.84	34.48	*	16 ± 9	"
LJ-544	"	"	500	7.38	34.00	*	−150 ± 8	"
LJ-545	"	"	1,000	3.46	34.30	*	−150 ± 8	"
LJ-547	"	"	2,000	1.96	34.59	*	−246 ± 10	"
LJ-548	"	"	3,500	1.54	34.68	*	−226 ± 10	"
LJ-546	"	"	4,500	1.49	34.69	*	−320 ± 20	"
LJ-1027	35°00′ N	155°00′ W	0	24.26	34.716	*	140 ± 12	11 Aug 1964
LJ-538	35°02′ N	140°08′ W	0	16.53	34.30	*	74 ± 10	20 May 1962
LJ-550	35°05′ N	180° W	0	17.79	34.80	*	61 ± 10	28 May 1962
LJ-551	"	"	50	17.40	34.76	*	59 ± 10	"
LJ-552	"	"	100	15.48	34.68	*	−22 ± 10	"
LJ-553	"	"	500	7.99	34.06	*	−46 ± 10	"
LJ-554	"	"	1,050	3.58	34.28	*	−184 ± 10	"
LJ-555	"	"	2,000	1.95	34.59	*	−213 ± 10	"
LJ-556	"	"	3,500	1.52	34.66	*	−312 ± 10	"
LJ-549	35°46′ N	170°13′ W	0	17.50	34.69	*	55 ± 10	26 May 1962
LJ-1046	36°49′ N	155°00′ W	0	*	*	*	131 ± 12	7 Sept 1964
LJ-1030	41°00.9′ N	155°00′ W	0	21.8	34.498	*	62 ± 11	13 Sept 1964
LJ-1045	42°09.2′ N	155°02′ W	0	*	*	*	29 ± 10	4 Sept 1964
LJ-429	44°55′ N	134°55′ W	0	16.70	32.756	*	22 ± 5	21 Sept 1961
LJ-430	"	"	1,200	3.0	34.306	*	−189 ± 9	"
LJ-431	"	"	1,700	2.08	34.567	*	−230 ± 9	"
LJ-432	"	"	2,188	1.80	34.615	*	−227 ± 10	"
LJ-435	"	"	2,600	1.65	34.645	*	−202 ± 10	"
LJ-436	"	"	2,996	1.58	34.625	*	−234 ± 10	"
LJ-439	"	"	3,400	*	34.635	*	−227 ± 10	"
LJ-440	"	"	3,630	1.55	34.679	*	−212 ± 10	"
LJ-1033	45°00′ N	155°00′ W	0	15.85	33.031	*	144 ± 12	15 Aug 1964
LJ-1031	"	"	100	7.68	33.382	*	44 ± 11	"
LJ-1032	"	"	200	7.22	33.905	*	−59 ± 8	"
LJ-1040	"	"	500	3.96	34.00	*	−133 ± 8	"
LJ-1039	"	"	998	3.10	34.354	*	−184 ± 8	"
LJ-1038	"	"	4,064	*	*	*	−226 ± 8	"
LJ-1049	47°38.1′ N	155°00′ W	0	*	*	*	80 ± 10	28 Aug 1964
LJ-1037	49°00′ N	154°58′ W	0	11.59	32.654	*	114 ± 10	16 Aug 1964
LJ-1036	"	"	107	4.48	32.865	*	67 ± 8	"
LJ-1034	"	"	210	3.52	33.687	*	−77 ± 11	"
LJ-1035	"	"	498	3.52	34.106	*	−141 ± 8	"
LJ-1041	"	"	1,021	2.81	34.393	*	−199 ± 10	"
LJ-1044	52°56.5′ N	155°03.3′ W	0	*	*	*	101 ± 10	26 Aug 1964
LJ-1042	54°34′ N	155°00′ W	0	11.5	32.721	*	122 ± 12	18 Aug 1964

these stations, at approximately 5° S lat, there is evidence of upwelling. Radiocarbon is unusually low at both stations (*see* Fig. 9) and unusually high in the deep water. As in the Pacific Ocean, the results here are consistent with the assumption of slowly rising deep water in the northern parts of the ocean.

At the northernmost station, the deepest water has an extraordinarily low ^{14}C content, corresponding to an age of some 2,000 years, which seems to be in regular continuation of the ^{14}C gradient from the far south. The layer above it, with a higher ^{14}C activity, seems to be rising, leaving the older water beneath it.

As we have already reported (Bien et al. 1960), the difference in apparent age of the deep water of the Pacific from 40° S lat to 15° N lat is of the order of 300–400 years,

TABLE 2. *Indian Ocean*

Sample number	Lat	Long	Depth (m)	Temp. (°C)	Salinity (‰)	$\delta^{13}C$ (‰)	$\Delta^{14}C$ (‰)	Date collected
LJ-691	51°07′ S	65°51′ E	0	1.63	33.903	*	−56 ± 9	10 Nov 1962
LJ-693	"	"	3,185	0.74	34.71	*	−147 ± 11	"
LJ-489	49°29′ S	132°17′ E	0	9.3	34.339	*	−45 ± 10	12 Jan 1961
LJ-404	42°03′ S	70°45′ E	0	10.88	34.430	*	−36 ± 4	21 Dec 1960
LJ-403	"	"	100	*	*	*	−52 ± 6	"
LJ-401	"	"	1,000	3.35	34.396	*	−120 ± 6	"
LJ-402	"	"	3,000	1.55	34.742	*	−155 ± 7	"
LJ-374	"	"	3,400	1.25	34.689	*	−150 ± 7	"
LJ-689	39°45′ S	64°00′ E	0	14.57	35.372	*	10 ± 12	7 Nov 1962
LJ-690	"	"	4,800	0.7	34.70	*	−123 ± 11	"
LJ-695	37°56′ S	87°38′ E	0	14.2	35.2	*	−26 ± 11	20 Nov 1962
LJ-488	37°51′ S	84°45′ E	0	*	*	*	−22 ± 8	25 Dec 1960
LJ-359	36°18′ S	98°41′ E	0	15.40	35.151	*	−25 ± 10	29 Dec 1960
LJ-383	"	"	100	*	*	*	−35 ± 10	"
LJ-369	"	"	1,066	4.47	34.377	*	−105 ± 9	"
LJ-355	"	"	3,469	1.17	34.718	*	−152 ± 11	"
LJ-698	34°11′ S	105°49′ E	0	16.64	35.737	*	20 ± 10	25 Nov 1962
LJ-699	"	"	3,430	1.50	34.73	*	−162 ± 11	"
LJ-696	33°48′ S	96°01′ E	0	14.90	35.41	*	−36 ± 11	22 Nov 1962
LJ-697	"	"	4,300	*	*	*	−115 ± 12	"
LJ-342	33°21′ S	72°42′ E	0	18.32	35.50	+0.6	−22 ± 9	18 Dec 1960
LJ-339	"	"	1,000	5.44	34.406	−0.04	−95 ± 4	"
LJ-392	"	"	3,050	1.62	*	0.0	−178 ± 8	"
LJ-340	"	"	3,987	1.15	34.703	−0.6	−190 ± 10	"
LJ-486	33°14′ S	108°45′ E	0	18.32	35.50	*	−15 ± 5	1 Jan 1961
LJ-700	32°49′ S	108°39′ E	5,525	*	*	*	−164 ± 10	26 Nov 1962
LJ-686	30°30′ S	61°53′ E	0	18.66	35.584	*	−6 ± 10	4 Nov 1962
LJ-687	"	"	3,400	1.37	34.720	*	−168 ± 10	"
LJ-688	"	"	4,400	0.58	34.688	*	−171 ± 10	"
LJ-684	26°54′ S	58°11′ E	0	21.84	35.56	*	4 ± 12	2 Nov 1962
LJ-685	"	"	5,450	0.93	34.70	*	−164 ± 11	"
LJ-351	23°56′ S	73°53′ E	0	23.86	35.472	*	−16 ± 15	15 Dec 1960
LJ-350	"	"	1,016	4.69	34.418	*	−110 ± 6	"
LJ-349	"	"	1,956	2.54	34.818	*	−172 ± 10	"
LJ-343	"	"	3,339	1.41	34.803	*	−192 ± 10	"
LJ-683	22°00′ S	57°30′ E	0	*	*	*	37 ± 8	31 Oct 1962
LJ-483	18°49′ S	88°33′ E	0	25.53	34.571	*	−7 ± 6	27 Nov 1960
LJ-496	17°19′ S	84°23′ E	350	14.05	35.410	*	−49 ± 5	29 Nov 1960
LJ-682	17°19′ S	57°42′ E	0	*	*	*	35 ± 8	25 Oct 1962
LJ-487	17°15′ S	63°50′ E	0	*	*	*	7 ± 6	5 Dec 1960
LJ-497	16°56′ S	63°50′ E	350	*	*	*	−49 ± 4	5 Dec 1960
LJ-499	14°05′ S	72°15′ E	350	10.30	34.880	*	−63 ± 4	2 Dec 1960

* No observation.
† Complete date unavailable.

(Continued on next page)

corresponding to an overall average velocity of 0.6–0.7 mm/sec based on the simple assumptions that are made. The corresponding velocities in the southern part of the Indian Ocean are of the order of 0.2–0.3 mm/sec. Our subsequent measurements have not changed these conclusions.

DISCUSSION

It was surprising to find the calculated velocities so low. This is connected with the very long residence times, which were also surprising when they were first reported. It would be even more surprising, however, if long residence time were *not* accompanied by slow motion.

There have been efforts to explain the low ^{14}C activity by contamination or mixture with old carbon from some source. This is difficult, because mixing with another water mass requires that the second mass be still older, and this com-

TABLE 2. Continued

Sample number	Lat	Long	Depth (m)	Temp. (°C)	Salinity (‰)	$\delta^{13}C$ (‰)	$\Delta^{14}C$ (‰)	Date collected
LJ-681	13°41′ S	59°42′ E	0	*	*	*	31 ± 8	25 Oct 1962
LJ-484	10°31′ S	105°34′ E	0	28.4	34.41	*	−16 ± 4	19 Oct 1960
LJ-498	10°31′ S	94°55′ E	350	10.27	34.631	*	−111 ± 6	24 Dec 1960
LJ-396	10°28′ S	99°00′ E	100	*	34.336	*	−104 ± 6	12 Nov 1960
LJ-398	"	"	343	10.44	34.675	*	−182 ± 7	"
LJ-395	"	"	960	4.94	34.624	*	−200 ± 7	"
LJ-392	"	"	2,500	2.68	34.672	*	−222 ± 10	"
LJ-394	"	"	3,424	1.33	34.695	*	−212 ± 10	"
LJ-679	9°54′ S	56°20′ E	0	26.32	35.065	*	22 ± 12	27 Oct 1962
LJ-680	"	"	3,480	*	*	*	−167 ± 8	"
LJ-675	5°54′ S	63°47′ E	0	27.94	34.518	*	−55 ± 14	14 Oct 1962
LJ-676	"	"	1,000	5.85	34.78	*	−180 ± 10	"
LJ-677	"	"	2,943	1.76	34.74	*	−176 ± 10	"
LJ-678	"	"	3,920	1.60	34.72	*	167 ± 10	"
LJ-1063	5°52′ S	55°00′ E	0	25.42	35.226	*	49 ± 7	Oct 1962†
LJ-1066	"	"	100	*	*	*	−16 ± 8	" †
LJ-1067	"	"	200	*	*	*	−54 ± 7	" †
LJ-1065	"	"	300	*	*	*	−68 ± 8	" †
LJ-1064	"	"	500	*	*	*	−122 ± 10	" †
LJ-670	5°21′ S	75°06′ E	0	27.94	34.518	*	−52 ± 14	10 Oct 1962
LJ-672	"	"	1,000	5.78	34.78	*	−143 ± 10	"
LJ-673	"	"	2,970	1.78	34.74	*	−154 ± 10	"
LJ-674	"	"	5,000	1.38	34.72	*	−129 ± 10	"
LJ-1052	1°16′ S	41°30′ E	0	24.62	35.207	*	−1 ± 7	4 Aug 1964
LJ-1053	1°58′ S	49°20′ E	0	25.74	35.246	*	23 ± 6	9 Aug 1964
LJ-1054	2°00′ N	45°38′ E	0	24.30	35.016	*	−5 ± 10	12 Aug 1964
LJ-1061	2°07′ N	55°04′ E	0	27.02	35.321	*	49 ± 7	30 Aug 1964
LJ-1062	"	"	>2,000	*	*	*	−191 ± 7	"
LJ-1055	5°00′ N	50°51′ E	0	25.07	35.462	*	−5 ± 10	15 Aug 1964
LJ-1056	"	"	2,000	*	*	*	−212 ± 8	"
LJ-661	8°16′ N	70°37′ E	0	28.46	36.36	*	−28 ± 14	6 Oct 1962
LJ-662	"	"	100	20.45	35.51	*	−68 ± 11	"
LJ-663	"	"	200	13.37	35.20	*	−13 ± 13	"
LJ-664	"	"	400	10.85	35.17	*	−121 ± 11	"
LJ-665	"	"	600	9.54	35.12	*	−125 ± 12	"
LJ-666	"	"	800	8.38	35.08	*	−128 ± 11	"
LJ-667	"	"	1,000	7.18	35.05	*	−143 ± 12	"
LJ-668	"	"	1,995	2.73	34.80	*	−184 ± 12	"
LJ-669	"	"	3,200	1.71	34.73	*	−192 ± 12	"
LJ-670	"	"	3,800	1.66	34.73	*	−244 ± 14	"
LJ-1058	8°53′ N	53°09′ E	<2,000	*	*	*	−145 ± 7	20 Aug 1964
LJ-1057	9°18′ N	51°03′ E	0	13.32	35.113	*	−93 ± 7	18 Aug 1964
LJ-1059	10°14′ N	53°01′ E	0	25.89	35.837	*	24 ± 10	27 Aug 1964
LJ-1060	"	"	>2,000	*	*	*	−190 ± 7	"

pounds the problem. Solution of sedimentary carbonate has also been suggested as a source of carbon of low activity, but the carbonate in the upper surface of the sedimentary layer, available for solution, contains young carbon supplied continuously from above. It would require unusual erosional processes to bring into solution very much of the old carbon deeper in the sediment. Broecker et al. (1960) have also discussed this source and dismissed it as unimportant.

Mixing of water, contamination with other sources of carbon, oxidation of organic matter, or solution of fresh carbonate—all would result in increasing the ^{14}C content and decreasing the residence time or age.

The calculated velocities are an order of magnitude less than any previously sup-

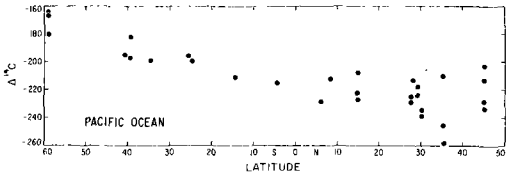


FIG. 3. Carbon-14 in the Pacific Ocean below 3,000 m, vs. latitude.

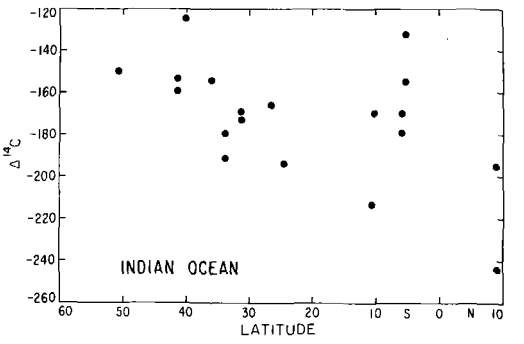


FIG. 4. Carbon-14 in the Indian Ocean below 3,000 m, vs. latitude.

posed for deep water movements. Calculations must always be checked with direct current measurements, and few direct measurements of deep water movements have been attempted. Neutrally-buoyant floats have given useful results in many cases, but in very deep water they have not always been satisfactory. Some unpublished results have been reported to us of such measurements in the Indian Ocean at 2,000 m. A casual inspection of these indicates that while the speed may be 2 cm/sec or more, the resultant velocity vectors at nearby stations may vary in direction by as much as nearly 180°.

We believe that the movement of the deep water is in a large sense random, and that one cannot measure the time it takes for the water to travel long distances in terms of small-scale velocities. For this purpose, we believe that the differences in residence times, which we have measured by radiocarbon dating, are more suitable, even if only approximate.

In the general theory of deep water movement, it is recognized that there are only two sources of deep water—in the very northern Atlantic Ocean (probably including the Norwegian Sea) and in the Weddell Sea in Antarctica. These two water masses not only fill the deep Atlantic basins but also contribute, in unknown proportion, to the eastward drift around the south of Africa into the Indian Ocean and on into the Pacific Ocean. The only source of deep water in the Indian and Pacific oceans, therefore, is in the south.

It is generally supposed that in each

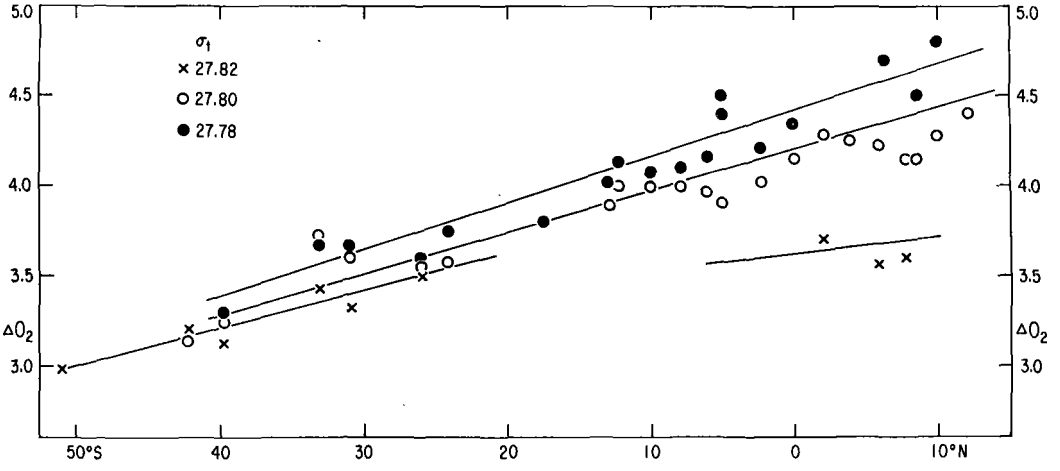


FIG. 5. Oxygen consumption vs. latitude in the deep water of the Indian Ocean. Saturation concentrations of oxygen minus observed values, at different sigma-t surfaces, 27.78, 27.80, and 27.82 (bottom).

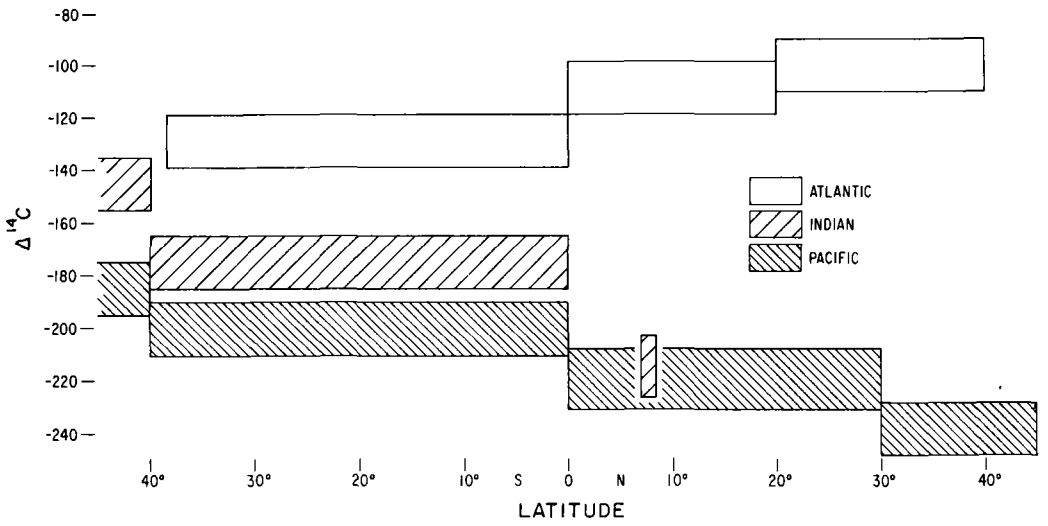


FIG. 6. Average ^{14}C content below 3,000 m in zonal areas in the Pacific, Indian and Atlantic oceans. Width of the bars indicates the average error of determination. Values for the Atlantic quoted from Broecker et al.

ocean, the strongest deep movement is along the western boundary, and Stommel's theory involves return movements along the eastern boundary as well as a slow general diffusion upward through the thermocline.

The circulation in the deep Pacific Ocean has been discussed by Wooster and Volkmann (1960) and by Knauss (1962), who has made use of our earlier results on ^{14}C age. On the basis of the temperature distribution, he suggests a general movement of deep water northward, a little stronger in the western basin, a slow upwelling in the very North Pacific, and a probable widespread return in the upper layers. He is concerned, however, with the difficulty of explaining the transport figures according to the generally accepted model of the circumpolar current. In the latter connection, we would point out that one can calculate a zonal velocity along the edge of the circumpolar current at least, by using the ^{14}C figures at three of our stations: 1), 51°07′ S lat, 65°51′ E long; 2), 58°20′ S lat, 168°58′ E long; and 3), 39°33′ S lat, 84°10′ W long. The last of these is rather too far north, but using the figures for the deep water, one can calculate an overall velocity of 1.4 mm/sec. If this is approximately true, it indicates that the deep circumpolar current moves much more slowly than heretofore supposed.

It should be observed that the ^{14}C measurements confirm the picture of northward movement of deep water in both oceans, without any indication of a return southward in the eastern part of the ocean, as has been suggested. Knauss' theory of slow rise in the north, and Stommel's model of general upward diffusion through the thermocline are both consistent with our results.

The calculation of overall velocities from the differences in radiocarbon age assumes, of course, that the direction of motion is in the direction of decreasing ^{14}C content. This is from south to north, and there is no question of this being the direction in which the deep water moves in the Pacific Ocean. Knauss has clearly shown this from the distribution of temperature. A similar analysis of the Indian Ocean has not yet been made, but there seems to be little doubt of its similarity.

The gradient of oxygen consumption has also been used to indicate the direction of water movement, and Fig. 5 shows the calculated values of oxygen consumption

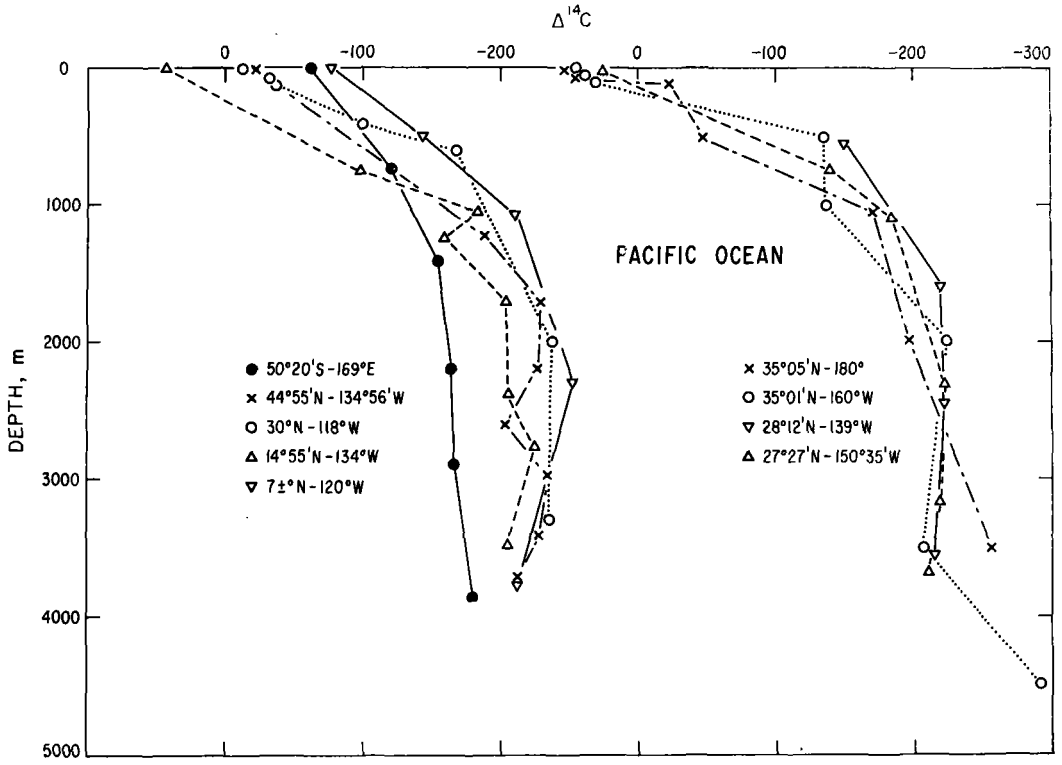


FIG. 7. Vertical profiles of $\Delta^{14}C$ at stations in the Pacific Ocean.

at a number of stations in the Indian Ocean plotted against latitude. Increase of oxygen consumption is a clear indication of northerly movement.

To treat our results in accordance with the general model of deep water circulation, the Pacific and Indian oceans were divided into zonal areas: below 40° S lat; from 40° S lat to the equator; from the equator to 30° N lat; and beyond 30° N lat (in the Pacific Ocean only). All the values for ^{14}C in each of these areas below 3,000 m were averaged and the results are shown in Fig. 6 In similar fashion, the Atlantic Ocean was divided into zonal areas and the deep water values given by Broecker et al. were averaged. ^{14}C activity in the deep water decreases from south to north in both the Pacific and Indian oceans and from north to south in the Atlantic Ocean, approaching a common value where the circulation model postulates continuity between the South Atlantic and the Indian oceans.

VERTICAL DISTRIBUTION

Figs. 7 and 8 extend the data that we reported previously on the vertical distribution of ^{14}C. At any one station, radiocarbon is relatively constant with depth below 2,000 m within a range of ±10%. There are a few notable exceptions, particularly at two stations where activity is abnormally low at the lowest depth. This seems to suggest a source of "dead" carbon from the bottom. We have already dismissed the possibility of solution of sedimentary carbonate, but it is conceivable that local volcanic activity might be responsible. However, we believe that a more likely explanation is the one already given. Both these stations are in the northern parts of the Pacific and Indian oceans, respectively, where slowly rising deep water could leave the deepest and oldest water behind.

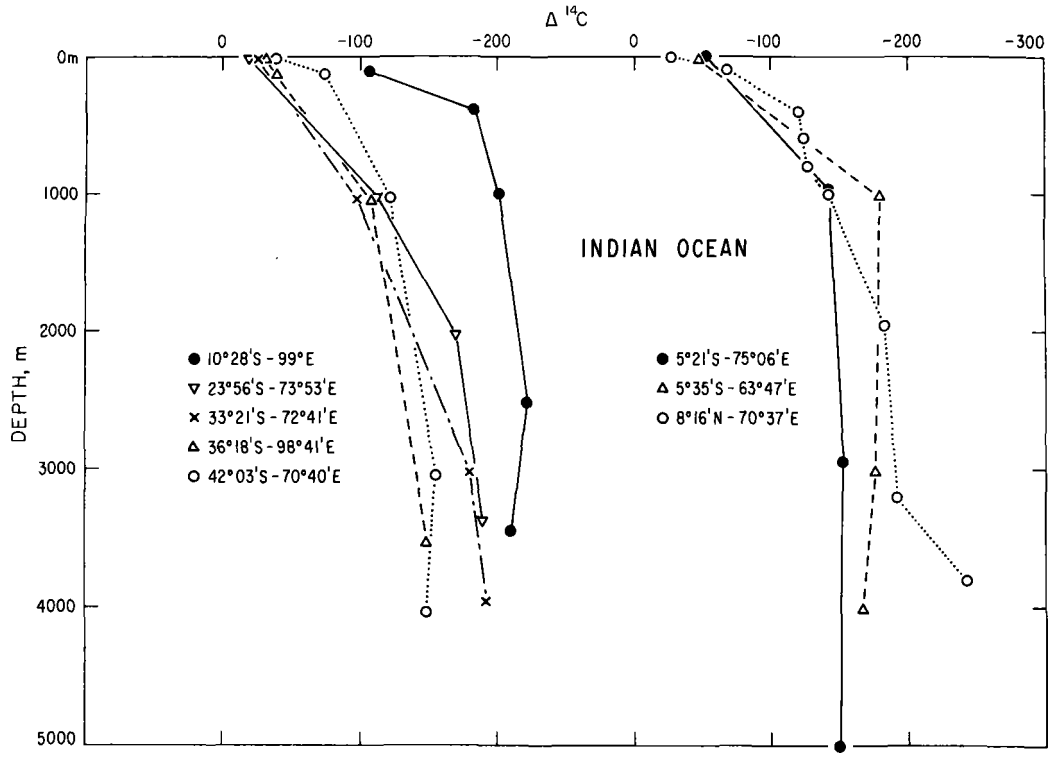


FIG. 8. Vertical profiles of $\Delta^{14}C$ at stations in the Indian Ocean.

The concentration gradients in the upper parts of these profiles may be important in interpreting mixing phenomena and the exchange with the atmosphere.

RADIOCARBON IN THE SURFACE

Fig. 9 shows values for ^{14}C in surface water in the Pacific and Indian oceans, plotted against latitude for different years from 1958 to 1964. Two points are significant: the decrease in ^{14}C from north to south, with extremely low values in the far south; and the general increase of ^{14}C at all latitudes from 1958 to 1964. The overall increase is, of course, the result of artificial nuclear activity, with greater effect in the northern hemisphere. The very low ^{14}C values in the high southern latitudes remain relatively unaffected. As reported before, these doubtless result from upwelling of deep water and its failure to come into equilibrium with the atmosphere. Future observations, extended over several more years, will eventually make it possible to deduce quantitative data for the rates of exchange and mixing that determine the observed ^{14}C concentrations on the surface of the oceans.

ACKNOWLEDGMENT

We gratefully acknowledge help, at various stages of the project, from Warren S. Wooster, John A. Knauss, and Joseph L. Reid, Jr. Ship operations and the collection of samples were completed with the support of Atomic Energy Commission Contract AT (11-1)-34, Project No. 74. Radiocarbon measurements were financed through a National Science Foundation Grant.

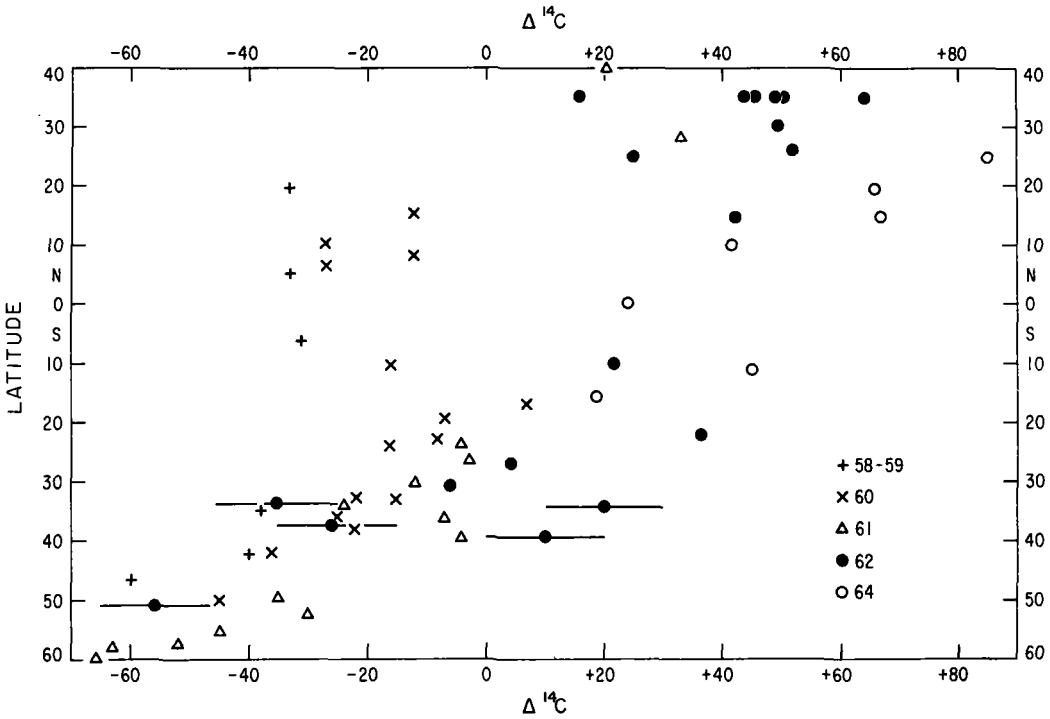


FIG. 9. Carbon-14 in the surface of the Pacific and Indian oceans, vs. latitude and in years from 1958 to 1964.

REFERENCES

BIEN, G. S., N. W. RAKESTRAW, AND H. E. SUESS. 1960. Radiocarbon concentration in Pacific Ocean water. Tellus, **12**: 436–443.

———, ———, AND ———. 1963*a*. Radiocarbon dating of deep water of the Pacific and Indian Oceans. Bull. Inst. Oceanog., **61**: 12–16. *Also in* Radioactive dating, p. 159–173. Intern. Atomic Energy Agency, Vienna.

———, ———, AND ———. 1963*b*. Natural radiocarbon in the Pacific and Indian Oceans. Nuclear Sci. Ser. Rept. No. 38, p. 152–160. Publ. 1075, NAS–NRC, Washington, D.C.

BROECKER, W. S., R. GERARD, M. EWING, AND B. C. HEEZEN. 1960. Natural radiocarbon in the Atlantic Ocean. J. Geophys. Res., **65**: 2903–2931.

KNAUSS, J. A. 1962. On some aspects of the deep circulation of the Pacific. J. Geophys. Res., **67**: 3942–3954.

WOOSTER, W. S., AND G. H. VOLKMANN. 1960. Indications of deep Pacific circulation from the distribution of properties at five kilometers. J. Geophys. Res., **65**: 1239–1249.

Reprinted from *J. atmos. Sci.*, vol. 23, no. 2, 1966, p. 144-150

The Summer Atmospheric Circulation over the Arabian Sea[1]

C. S. RAMAGE
University of Hawaii, Honolulu

(Manuscript received 23 September 1965)

ABSTRACT

The summer heat low system extending from Somalia across southeast Arabia to northwest India is the most extensive and intense on earth. Although it develops in the normal way over desert regions in response to the sun's zenithal march, it is maintained and intensified through the summer by subsidence of air originally lifted and warmed by the release of latent heat in monsoon rain systems to the east and south. The subsidence not only dominates West Pakistan, Arabia, and Somalia, but severely restricts low cloud formation over the central and western Arabian Sea.

The heat low exports cyclonic vorticity in the middle and upper troposphere to the northern Arabian Sea. When a deep layer of moist air is present over the eastern part of this area, subtropical cyclogenesis occurs, producing a burst of west Indian monsoon rains. This in turn, by increasing subsidence above the heat low, intensifies the heat low and its associated low-level monsoon circulation. When the supply of moist air is cut off, the subtropical cyclone fills, the heat low weakens, and a break takes place in the monsoon rains. With renewal of the moisture supply, the sequence is repeated.

1. Introduction

During the International Indian Ocean Expedition oceanographers have concentrated more on studying the western Arabian Sea than any other part of the Indian Ocean. The reason is not hard to find since nowhere else is the difference between summer and winter monsoons so sharp—strong southwesterly winds with vigorous coastal upwelling in summer and moderate to fresh northeasterly winds and near-uniform sea surface temperatures in winter. So far the summer monsoon has been probed more extensively than the winter monsoon and since several of the research vessels made regular radiosonde ascents and U. S. Weather Bureau and Woods Hole Oceanographic Institution research aircraft made drop soundings in the summers of 1963 and 1964, a detailed study of the summer atmospheric circulation over the western Arabian Sea appears to be feasible.

To prepare for this study, I attempt to construct in this paper a climatological framework interrelating gross features of the normal distributions of pressure, temperature, winds, and weather over the Arabian Sea and its littoral.

For surface climatology I have relied on the atlas published by the Royal Netherlands Meteorological Institute (1952) and for upper climatology on Raman and Dixit (1964), Frost and Stephenson (1965), and on observations from research vessels and aircraft.

Traditionally, meteorologists have linked the Arabian Sea summer monsoon circulation with a heat low system over Arabia, West Pakistan, and northern India. The heat low, developing during May, establishes the low-level monsoon wind regime a full month before heavy monsoon rains set in over western India south of the heat low. By mid-July, the low is deepest, the southwest monsoon is strongest, and the west Indian rains are heaviest, while all diminish through August and September. As long ago as 1887, W. L. Dallas questioned how a heat low dependent for its existence on hot sun and clear skies can persist once clouds and rain develop. Surface charts for the Arabian Sea show winds converging into the West Pakistan heat low. Surface relative humidities are high and the air is rising. Why then does the low remain cloud-free and intense while rain falls well to the south? This question and the related question—Why does so little rain fall over the western Arabian Sea?—will be discussed in the remainder of this presentation.

2. Undisturbed heat low circulation

The surface southwesterly winds of the heat low circulation force cold water to upwell along the coast of Somalia and Arabia. The cold water, by modifying the temperature and hence the pressure distribution of the overlying air, produces two pronounced effects; a persistent wind speed maximum offshore from the zone of upwelling (Bunker, 1965) and deflection of inflow to flow parallel to the coast (Fig. 1). Consequently, with moist inflow over West Pakistan and little or none over Somalia and Arabia, we should expect to find a rather weak moist heat low over West Pakistan with plentiful rain, a return current in the middle troposphere, evidence for some compensatory sinking

[1] Contribution No. 128 of the Hawaii Institute of Geophysics. This paper was presented at the Symposium on Meteorological Results of the International Indian Ocean Expedition, 22–26 July 1965, Bombay, India.

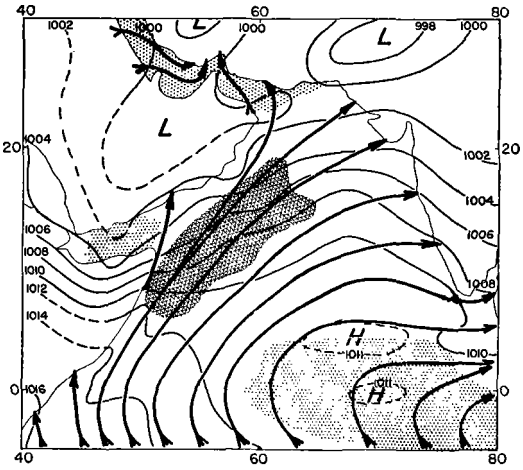


FIG. 1. August mean sea level pressure and mean resultant winds. Speeds less than 10 kt stippled; greater than 25 kt cross-hatched.

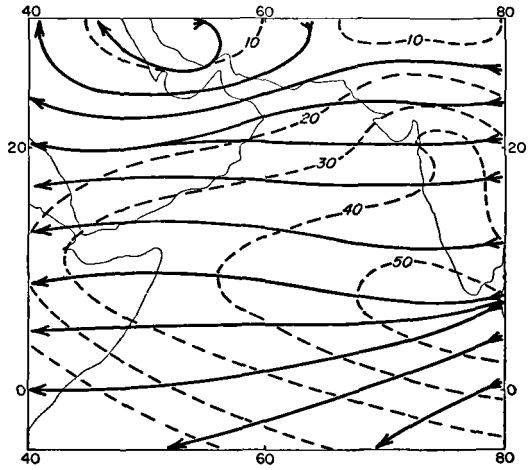


FIG. 3. August 200 mb mean resultant winds. Isotachs are labelled in kt.

over the Arabian Sea (a situation similar to that observed over North Viet Nam and the South China Sea in summer), and a rather vigorous heat low over Arabia and Somalia.

3. Interaction between monsoon rains and heat low

What we do observe is a cloudless heat low which attains its maximum intensity over West Pakistan, and which is so shallow there that cyclonic inflow gives way to anticyclonic outflow below 700 mb. We also observe a subsidence inversion based between 500 and 2000 m over the western Arabian Sea, where precipitation is almost never recorded (Fig. 2).

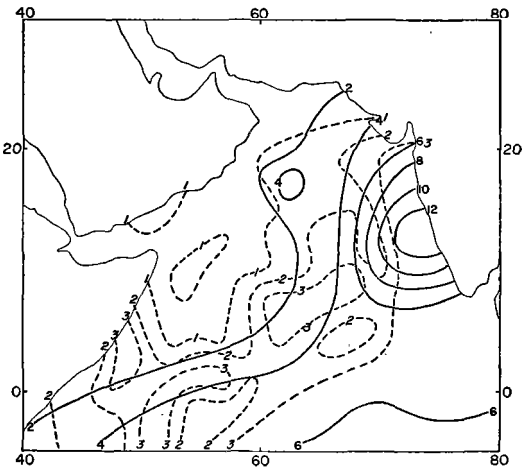


FIG. 2. Percentage duration of precipitation during summer from ship observations (full lines) and level of the inversion base in km from 130 aerological soundings made during the summers of 1963 and 1964 (dashed lines).

To find an explanation, we must take cognizance of conditions over the eastern Arabian Sea and western India. By mid-June monsoon rains have set in over western India. South of Kutch and north of Goa, the precipitation agency is almost always a quasi-stationary mid-tropospheric depression which develops, intensifies, and dissipates over a period of one to three weeks in the vicinity of Bombay. A detailed case study by Miller and Keshavamurthy (1965) shows this "subtropical cyclone" (Simpson, 1952; Ramage, 1962) to be most intense at around 600 mb and to have a cold core

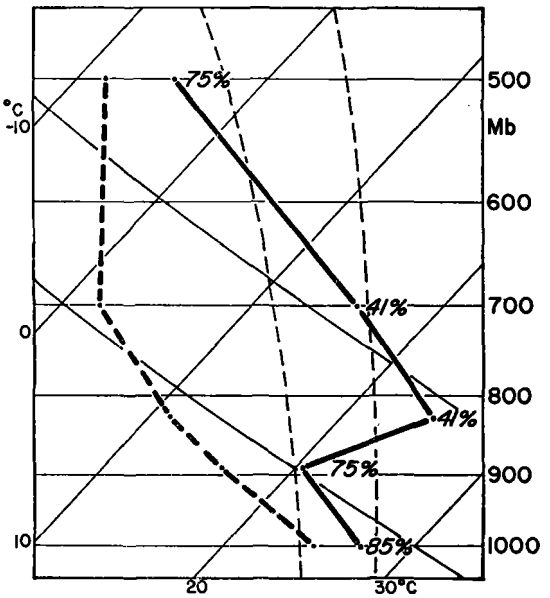


FIG. 4. Median sounding for Karachi (24°55'N; 67°09'E) for August 1963 at 0500 local time.

character below that level and a warm core character above. Convergence is weak at the surface and strongest in the middle troposphere, while above 300 mb the sub-tropical cyclone is overlain by persistent easterlies. Great sheets of cirrostratus or cirrus densus visible day after day over most of the Arabian Sea testify to the role of the easterlies in the energetics of the subtropical cyclone. Subtropical cyclones, and warm-cored systems further east over the Ganges Valley, release massive amounts of latent heat into the upper troposphere. This effect was noted by Raman and Ramanathan (1964) who demonstrated that heavy

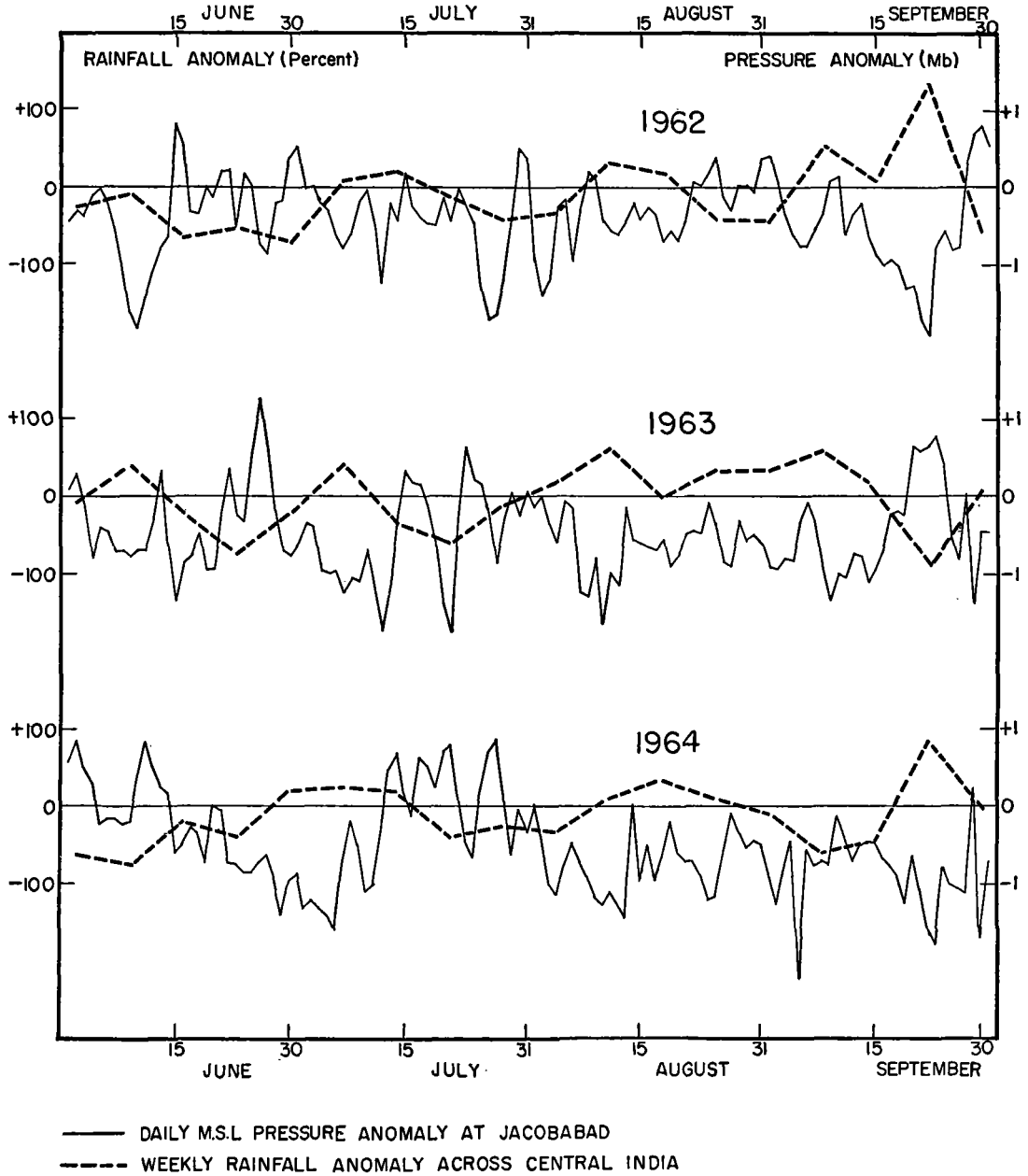


FIG. 5. Daily anomalies in mb of mean sea level pressures measured at 0800 local time at Jacobabad (28°18'N; 68°28'E); 56 m above MSL) (full lines) and weekly percentage anomalies of rainfall for Indian subdivisions lying roughly between 18 and 27N (dashed lines) for the summers of 1962, 1963, and 1964.

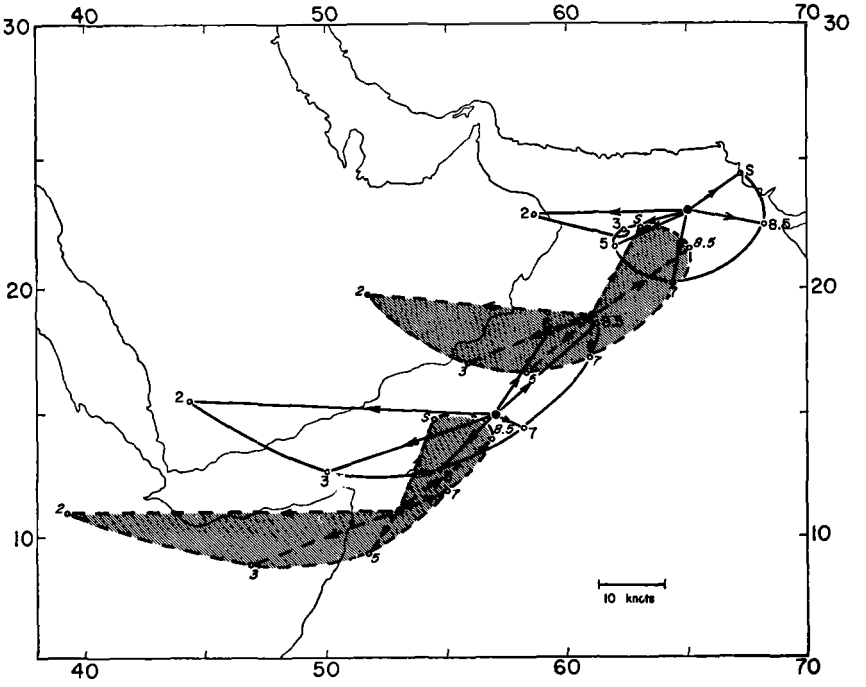


FIG. 6. Hodographs of August mean resultant winds at standard pressure levels (centibars) at four locations in the western Arabian Sea.

monsoon rains over Indo-Pakistan usually precede by several hours, and are found to the north of, a sharply defined jet in the upper tropospheric easterlies, while the easterlies possess a climatological speed maximum roughly coincident with the west coast of India (Fig. 3). Thus, above the heat low and over most of the Arabian Sea, northeast Africa and Arabia, the upper easterlies are convergent and subsidence prevails through the middle troposphere (Flohn, 1964).

Computation of the divergence (Bellamy, 1949) of the mean resultant winds at standard pressure levels over the eastern portion of the heat low (Indo-Pakistan border area) indicates net ascent below 700 mb associated with the heat low circulation and net descent above 700 mb associated with the convergent easterlies.

Observations reveal that the subsidence affects the heat low in two ways:

a) A median August 1963 sounding for Karachi at 0000 GMT (0500 local time) (Fig. 4) shows that the lower layers, originating over the Arabian Sea, are moist. There is a sharp inversion at around 850 mb and relative humidity increases with height above 700 mb. A similar vertical distribution is common inland at Jodhpur, although insolational heating often breaks down the inversion by early afternoon. Subsidence limits the height to which surface air from the Arabian Sea can ascend, restricting cloud development and thus favoring strong insolational heating.

b) Fig. 5 suggests that surface pressure at Jacobabad, near the center of the heat low, is inversely related to the intensity of monsoon rains over a strip of the subcontinent extending eastward to the south and east of the station, while Dixit and Jones (1965), in comparing a monsoon rain with a monsoon lull along the west coast of India, located by far the greatest middle and upper tropospheric temperature differences above the heat low, with the rain situation 2–6C warmer than the lull situation. Hence subsidence over the heat low by raising the temperature of the middle and upper tropospheric air reduces surface pressure below what is observed in heat lows elsewhere.

Both these effects then operate to maintain the heat low circulation and consequently the strength of the low-level monsoon flow. Similar but less marked effects are probably produced over Arabia. However, subsidence into the heat low waxes and wanes in unison with the monsoon rains. When the rains are heavy, the heat low is vigorous, and stronger than normal surface winds prevail over most of the Arabian Sea, hundreds of kilometers distant from the rain systems. When the rains break, the southwest monsoon over the Arabian Sea is weak.

Figs. 6 and 7 illustrate related reasons why the

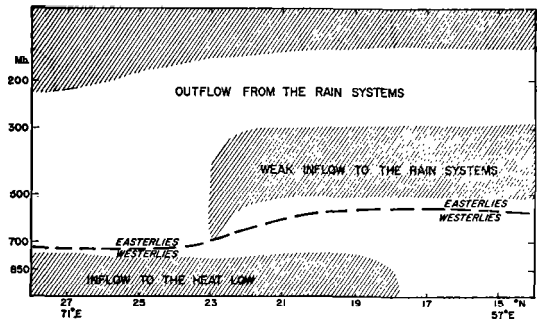


FIG. 7. Schematic section extending southwest from the Indo-Pakistan heat low. Layers with upward motion hatched.

western Arabian Sea, where the subsidence inversion is usually below 1000 m (Fig. 2), probably experiences as little rain as the deserts of Arabia and Somalia.

Fig. 6 shows that the mean resultant vertical wind shear over the western Arabian Sea parallels the Arabian and Somali coasts below 500 mb and is directed from east to west between 500 and 200 mb, reflecting the heating effect of Arabia and Somalia on the lower troposphere and the effect of latent heat release in monsoon rain systems on the upper troposphere. This shift in the shear pattern means that, between 800 and 600 mb, the western Arabian Sea is overlain by desert-dried air from the west.

A schematic cross section of the vertical circulation between the heat low (27N 71E) and 15N 57E (Fig. 7) suggests shallow inflow into the heat low and upward motion downstream from the southwest monsoon speed maximum (Fig. 1). In the middle troposphere south of 23N air is converging into a subtropical cyclone centered just west of Bombay. This results in sinking motion in the lower troposphere accentuated by low-level divergence upstream from the southwest monsoon speed maximum, and rising motion between 500 and 300 mb. In the upper troposphere the section lies west of the easterly jet maximum which in turn is an effect of intense condensation over India. Thus massive subsidence between 200 and 700 mb maintains the intensity of the heat low. The effect of the Arabian and Somali troughs, not explicitly included here, is to elongate the circulation toward the southwest.

4. Subtropical cyclone development

The heat low circulation always develops before the first of the subtropical cyclones which produce western India's monsoon rains. Therefore, an hypothesis that the heat low "causes" subtropical cyclogenesis seems worth exploring.

Because of its nature the heat low is likely to exert a thermodynamic effect rather than a mechanical effect on its environment. Petterssen (1956) discusses large scale thermodynamic influences on the behavior of cyclones and anticyclones. He begins with the vorticity equation for a surface of constant potential temperature and by assuming steady state and neglecting the contribution of vertical advection of the tangential vorticity vector derives the equation

$$\nabla\cdot(Q\mathbf{V})=F-\frac{\partial Q}{\partial\theta}\dot{\theta},$$

in which Q is the component of the absolute vorticity normal to a surface of constant potential temperature, $\mathbf{V}$ is the horizontal wind vector, F is the vorticity of the frictional force, and θ is the potential temperature.

Over Arabia and West Pakistan the heat low slowly intensifies from late May until mid-July then slowly weakens until it disappears after mid-September. Thus one might be justified in assuming steady state condi-

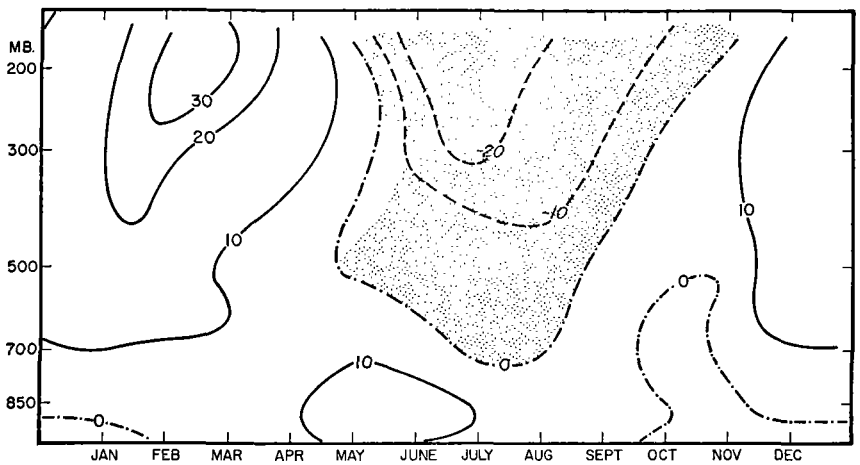


FIG. 8. Relative vorticity of the mean monthly resultant winds over the triangle Peshawar (34°01'N; 71°35'E); Karachi, (24°55'N; 67°09'E); Jodhpur (26°18'N; 73°01'E) in units of 10^{-6} sec^{-1}.

tions and in exploring the implications of Petterssen's equation.

The term on the left measures the intensity of the vorticity source, i.e., the export per unit time of vorticity through the boundaries of a unit area in a surface of constant potential temperature. The export depends on F, the intensity of the heat or cold source, $\dot{\theta}$, and the sign of $\partial Q/\partial\theta$ which differs insignificantly from $\partial Q/\partial Z$.

In only one part of the heat low are mean resultant tropospheric winds available for computing vorticity, the triangle enclosed by the rawinsonde stations of Pehsawar, Jodhpur, and Karachi. Fig. 8 depicts the mean distribution through the year and through the troposphere of the relative vorticity computed by the Bellamy (1949) method for the triangle, whose centroid is located at about 28N 71E, on the axis of the heat low.

If F and $[-\dot{\theta}(\partial Q/\partial\theta)]$ have the same sign, the sign of the vorticity export is known. During summer over the heat low, $\dot{\theta}$ is always positive while in the stippled area of the diagram, $F>0$ and $(\partial Q/\partial\theta)<0$. Fig. 8 shows that beginning in early June cyclonic vorticity is exported from the triangle in the middle and upper troposphere. If vorticity is similarly exported from Arabia then cyclonic vorticity accumulates over the northern Arabian Sea. As long as the air remains dry development is unlikely, but by mid-June moist air reaches the northeast Arabian Sea, usually from the south or east. Then buoyancy forces come into play, a subtropical cyclone develops, and the first burst of monsoon rains drenches the Bombay district. The subtropical cyclone through the agency of subsidence further intensifies the heat low which then exports additional cyclonic vorticity to the middle and upper troposphere over the northern Arabian Sea. It may be no accident that the rains of western India set in (latitude for latitude) later than the rains of eastern India and Burma for the latter probably play a part in initiating the sharp increase in anticyclonic vorticity above the West Pakistan heat low in late May.

As Miller and Keshavamurthy (1965) show, a subtropical cyclone lasts from one to three weeks, modifying its environment so as finally to reduce the supply of moist air to the circulation below the sustaining point. The cyclone fills, and a monsoon "break" ensues. Then when a new supply of moist air becomes available, subtropical cyclogenesis may once more occur in the favored location.

In a more general discussion, Pisharoty (1964) accounts for diminution of monsoon rains in terms of decreasing slope of isentropic surfaces resulting from the release of latent heat in the condensation process.

Fig. 8 shows that the depth of the layer of positive $[F-\dot{\theta}(\partial Q/\partial\theta)]$ over the heat low decreases rapidly through September. At the same time, $\dot{\theta}$ also decreases. By mid-September, in most years, positive vorticity is no longer exported to the northern Arabian Sea and no further subtropical cyclogenesis occurs there. One consequence of the model, indicated by crudely quantitative computations, is that the Arabian Sea subsidence inversion may so limit the supply of moisture as to make appreciably heavy monsoon rains over western India unlikely without significant incursions of deeply moist air from the Bay of Bengal across the peninsula. A burst of west Indian monsoon rains is usually preceded by increased depth of the moist layer to the east.

The worst west Indian summer drought in history occurred in 1899. Over northwest India both surface temperatures *and* pressures were above normal. Over the Arabian Sea surface winds were below normal. Intense insolation favored heat low development but the absence of subsidence above the heat low resulting in turn from the absence of rain systems to the south and east outweighed the effect of insolation. Presumably if "feedback" between rain systems and heat low is interrupted, export of mid-tropospheric cyclonic vorticity to the northern Arabian Sea is reduced, chances of subtropical cyclogenesis are lessened, the heat low remains relatively weak, and drought tightens its grip.

5. Concluding remarks

The foregoing discussion implies a symbiotic relationship between heat lows and subtropical cyclones. Because cold upwelling coastal waters keep Somalia and Arabia dry and hot throughout the summer, because a complex of desiccating influences are at work over West Pakistan, because topography concentrates mid-tropospheric cyclonic vorticity over the northern Arabian Sea, and because deep moist air can reach the region only from south or east, the relationship is strongly developed over West Pakistan and the northeast Arabian Sea.

However, rain-producing systems similar in character to subtropical cyclones have been observed south of the Saharan heat low (Gilchrist, 1960). In early summer, south of the thermal equator over the South China Sea and the Bay of Bengal, subtropical cyclones may also develop (Ramage, 1959, 1964), but as summer advances, warm-cored cyclones dominate these seas and moving inland displace the dry cloud-free air of the heat lows. Thus many meteorologists maintain that the summer lows of North Viet Nam and the Ganges Valley are in reality only the statistical effects of stagnating, dissipating tropical storms (Palmer, 1951).

The summer regime over the Arabian Sea is a strange one whose character seems basically determined by the vast desert arc extending from northeast Africa to northwest India and by coastline orientation. The heat low develops over the deserts but then is maintained and protected by its offspring, upwelling along the west coast and subtropical cyclones in the northeast. The result is the most intense monsoon system on earth, gale force southwesterlies overlain by jet strength easterlies. Despite such vigor, no moving cyclone

system ever enters the region during summer. Tropical hurricanes are unknown (Ramage, 1959), while the subtropical cyclones develop, intensify and fill *in situ* equally as captive to orography as the heat low.

Acknowledgments. This work forms part of an investigation of the general atmospheric circulation of the Indian Ocean region made possible by grant G-22413 from the National Science Foundation.

REFERENCES

Bellamy, J. C., 1949: Objective calculations of divergence, vertical velocity, and vorticity. *Bull. Amer. Meteor. Soc.*, **30**, 45–49.

Bunker, A. F., 1965: Interaction of the summer monsoon air with the Arabian Sea (preliminary analysis). Paper presented at Symposium on Meteorological Results of the International Indian Ocean Expedition, Bombay, 22 July 1965.

Dallas, W. L., 1887: Memoir on the winds and monsoons of the Arabian Sea and north Indian Ocean. Calcutta, Supt. of Govt. Printing, India, 45 pp.

Dixit, C. M., and D. R. Jones, 1965: A kinematic and dynamical study of active and weak monsoon conditions over India during June and July, 1964. International Meteorological Center, Bombay (prepub.) 28 pp. (Available from International Meteorological Center, Colaba Observatory, Bombay-5, India.)

Flohn, H., 1964: Investigations on the tropical easterly jet. *Bonner Meteor. Abhand.*, **4**, 80 pp.

Frost, R., and P. M. Stephenson, 1965: Mean streamlines and isotachs at standard pressure levels over the Indian and west Pacific Oceans and adjacent land areas. *Geophys. Mem.*, **109**, 24 pp.

Gilchrist, A., 1960: Contour charts for July 1960 in the West African area. *Tech. Notes, Brit. W. African Meteor. Services*, **19**, 5 pp.

Miller, F. R., and R. N. Keshavamurthy, 1965: The Arabian Sea summer monsoon. Paper presented at Symposium on Meteorological Results of the International Indian Ocean Expedition, Bombay, 26 July 1965.

Palmer, C. E., 1951: Tropical meteorology. *Compendium of Meteorology*, Boston, Amer. Meteor. Soc., p. 873.

Petterssen, S., 1956: *Weather Analysis and Forecasting, Second Edition.* Vol. I, Motion and motion systems, New York, McGraw-Hill, 428 pp.

Pisharoty, P. R., 1964: Monsoon pulses. Proc. WMO Symposium on Tropical Meteorology, Rotorua, New Zealand, 373–379.

Ramage, C. S., 1959: Hurricane development. *J. Meteor.*, **16**, 227–237.

——, 1962: The subtropical cyclone. *J. Geophys. Res.*, **67**, 1401–1411.

——, 1964: Some preliminary research results from the International Meteorological Center. Proc. WMO Symposium on Tropical Meteorology, Rotorua, New Zealand, 403–408.

Raman, C. R. V., and C. M. Dixit, 1964: Analyses of monthly mean resultant winds for standard pressure levels over the Indian Ocean and adjoining continental areas. Proc. WMO Symposium on Tropical Meteorology, Rotorua, New Zealand, 107–118.

——, and Y. Ramanathan, 1964: Interaction between lower and upper tropical tropospheres. *Nature*, **204**, 31–35.

Royal Netherlands Meteorological Institute, 1952: *Indian Ocean Oceanographic and Meteorological Data, Second Edition*, 31 pp. and 24 charts.

Simpson, R. H., 1952: Evolution of the kona storm, a subtropical cyclone. *J. Meteor.*, **9**, 24–35.

Reprinted from *Curr. Sci.*, vol. 35, no. 15, 1966, p. 378-380

UPWELLING IN THE MINICOY REGION OF THE ARABIAN SEA

L. V. GANGADHARA RAO AND R. JAYARAMAN
Planning and Data Division, National Institute of Oceanography, C.S.I.R., New Delhi

THE coral island, Minicoy (Latitude 8° 7′ N, Longitude 73° 18′ E), which is situated between the Laccadive and the Maldive Archipelagos is a major tuna-fishing centre in the Indian Ocean region.[1] While the importance of this region from the point of tuna fishery has been well recognized, we have very little data on the oceanographic conditions prevalent there. This is particularly noteworthy since in many areas, tuna investigations have always been supported by large-scale oceanographic studies.[2] It may also be mentioned here that one of the most important discoveries in modern oceanography, namely the Cromwell Current, is associated with systematic investigations for tunas in the central and equatorial Pacific by the Pacific Oceanic Fishery Investigations (POFI) group.

In one of the International Indian Ocean Expedition (IIOE) cruises in the Arabian Sea, INS KISTNA worked out a long section of 15 stations along the latitude 8° N from the 27th November to the 2nd December 1962. During the occupation of stations in the vicinity of Minicoy, it was particularly noticed by one of us (R.J.) that the ship was drifting considerably giving rise to large wire angles indicating the possibility of strong water movements in the area. In addition, while examining the distribution of various parameters along this 8° N section, some very interesting features were observed in respect of stations in the Minicoy region. It was, therefore, thought desirable to make a detailed analysis of the data for various parameters in this region in particular (Stns. 84–81). The location of stations and the vertical distribution of various parameters in the upper 200 metres are shown in Fig. 1 (*a-e*).

At Stn. 82, the temperature structure shows a sudden decrease in the thickness of mixed layer and the presence of relatively colder water in it. In association with this feature, a sharp rise of thermocline to 50 m. depth is seen, while in the neighbouring stations it is deeper (75–100 m.). The salinity distribution shows a parcel of relatively low saline water in the surface layers at Stns. 81–82 and the resulting local halocline is seen to be surfacing at Stns. 82–83. The density structure indicates the presence of a parcel of relatively lighter water in the surface at Stns. 81–82 with its westward boundary being situated between Stns. 82–83. The isopycnals exhibit an upward tilt under Stn. 82 at 50–150 m. depth. The dissolved oxygen content is seen to be less at 40–100 m. depth under Stn. 82 compared to its value under the neighbouring stations at the corresponding depths. The distribution of all these parameters clearly indicate that upwelling is present at Stn. 82, which is situated very close to Minicoy. The phenomenon appears to be limited to the upper 150 metres.

Among the various factors examined with a view to finding out the causes of this upwelling, the most obvious seems to be the presence of diverging current systems. As the observations were taken in the last week of November, the typical circulation established for the earlier half of the north-east monsoon season (November to January)[3] can be taken as the representative circulation for the period of observation. During this period, the general set of current in the southern part of the Arabian Sea is westerly. Owing to the coastal conformation, a north-north-westerly current develops off the west coast of India. These two currents diverge in the vicinity of Minicoy leading to upwelling in this region. The relatively low saline lighter water seen in the surface layers at Stns. 81–82 may be the Bay of Bengal water possibly carried westward by the north equatorial current.

It is pertinent to point out here that according to Jones and Kumaran (*loc. cit.*), in the Minicoy area, tuna fishery is operative from September to April, the peak season being from December to March. It is possible that the upwelling, which has been observed during late November, may have considerable impact on the peak tuna catches of this region. The exact sequence of events and the ultimate correlation between these physical processes and the tuna fishery of Minicoy require more detailed investigation.

The authors wish to express their deep sense of gratitude to Dr. N. K. Panikkar, Director, National Institute of Oceanography, C.S.I.R., New Delhi, for advice and encouragement.

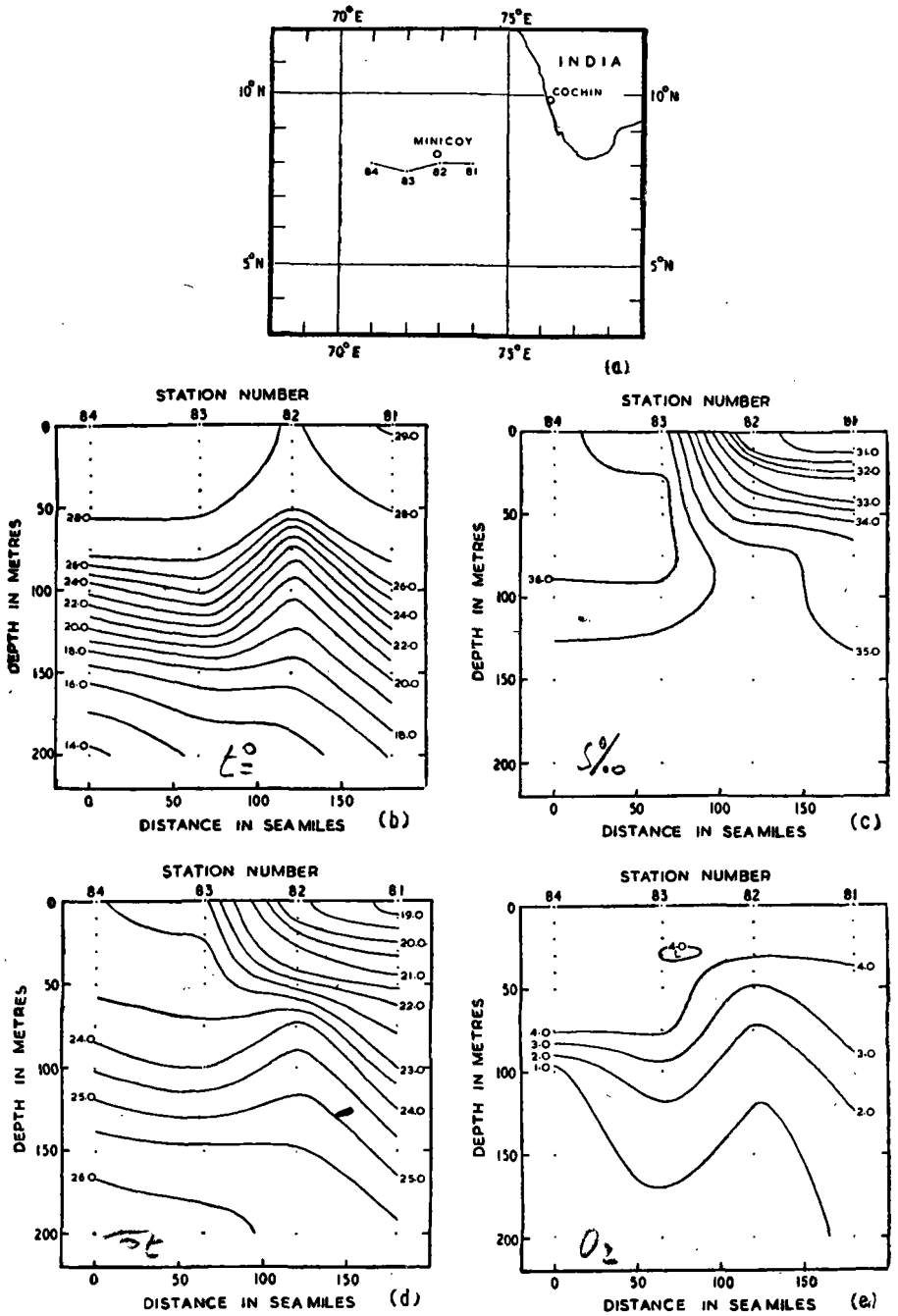


FIG. 1. Vertical distribution of temperature, salinity, density and dissolved oxygen along a section south of Minicoy Island during the last week of November, 1962. (*a*) The location of stations along the section. (*b*) The temperature distribution contour interval 1°C. (*c*) The salinity distribution contour interval 0·5‰. (*d*) The distribution of density in terms of σ_t-contour interval 0·5 gm./litre. (*e*) The distribution of dissolved oxygen contour interval 1 ml./l.

1. Jones, S. and Kumaran, M., *Indian J. Fish.*, 1959, **6** (1), 30.
2. Schaefer, M. B., *Rep. Calif Ocean. Fish Invest.*, (SS/16 b and 22 b, MP/4 b and 7a), 1961, **8**, 41.
3. West Coast of India Pilot, Hydrography Dept., Admiralty, London, 1961.

Reprinted from *Deep-sea Res.*, vol. 13, 1966, p. 861-888

Current measurements off the Somali coast during the southwest monsoon of 1964*

J. C. SWALLOW† and J. G. BRUCE‡

(*Received* 25 *July* 1966)

Abstract—Seven sections out from the East African coast between 1°N and 8½°N showed the Somali Current flowing northeastwards with increasing transport. Differences between directly measured and geostrophic currents could in some cases be related to the local winds. A few deep current measurements, though variable, tended to indicate southward motion at a depth of 1000 m. Near 9°N, the Somali Current turned eastward. In the cold area to the north along the coast, relatively weak currents were found, but farther offshore part of a clockwise loop of warm high-salinity water was observed.

INTRODUCTION

DURING August and early September 1964 the R.R.S. *Discovery* of the British National Institute of Oceanography and the R.V. *Argo* of the University of California co-operated in an oceanographic survey of the Somali Current. A variety of physical and biological observations was made, and accounts of some of the work have already been published. In particular, WARREN *et al.* (1966) have described the water-mass structure of the Somali Basin, as shown by serial observations of temperature, salinity and dissolved oxygen content, and they have inferred flow patterns from the distribution of these properties. The present paper is complementary to that account, in providing further evidence about the circulation from direct measurements of current and from geostrophic calculations.

The main features of the surface currents off the Somali Coast in the southwest monsoon have long been familiar to navigators. FINDLAY (1866, pp. 102–103) wrote " On the eastern coast of Africa the current sets along the coast to the N.N.E. at a velocity of 2 to 4 miles per hour. . . . . To the south of Sokotra, at a distance of about 150 miles, is a great whirl of current. . . . .; it commences about the parallel of Ras Hafun, when the current strikes off to the eastward to the 55th meridian, then to the southward, to the 5th parallel, whence it again curves up to the northeastward, forming a complete whirl. At the northern limit the velocity is very great, being 4 to 5 miles per hour, while at its southern extreme it is only ¾ to 1 mile per hour." This would serve with little alteration as a description of the surface observations made in 1964 (Fig. 2). The current along the coast was indeed strong, with maximum speeds exceeding 6 knots. It turned eastward near 9°N, a little to the south of Ras Hafun, with speeds between 4 and 6 knots, then southeast. The " great whirl " appeared to extend beyond the 55°E meridian, and the weak westward flow was found somewhat to the

* Contribution No. 1831 from the Woods Hole Oceanographic Institution.
† National Institute of Oceanography, Wormley, Godalming, Surrey.
‡ Woods Hole Oceanographic Institution, Woods Hole, Mass.

south of 5°N. A feature not mentioned by FINDLAY, noticed in 1964, was what may have been part of another clockwise " whirl," of warm highly saline water between Socotra and 9°N, in which speeds of 3 to 5 knots were observed.

Below the surface, however, the currents were relatively unknown. This paper is principally concerned with current meter observations in the upper 200 m of the Somali Current, and the volume transports derived from them and from geostrophic calculations. A few deeper current observations are also described, and combined with geostrophic current profiles to give some indications of movement in the intermediate and deep water.

METHODS

Most of the current observations made by *Argo* and *Discovery* were in the form of relative current profiles to a depth of 200 m. At eight of the *Discovery's* stations, these profiles were extended to greater depths using a telemetering current meter lent by the Geophysical Institute at Bergen, but the untimely loss of that instrument brought the deeper current meter observations to an end. On board the *Argo*, the lack of a depth gauge on the current meter meant that its depth had to be estimated from wire out and surface wire angle, and in strong current shear this became too uncertain below 200 m. These relative current profiles have been combined with the best estimate that could be made of the surface current at each station, to give "true" currents down to 200 m. Several different methods, of varying accuracy, were used on board each ship for estimating surface currents, and before presenting the observations themselves it seems appropriate to consider the uncertainties involved.

In the *Discovery*, the relative current measurements were made with a pair of propeller-type direct reading current meters (CARTWRIGHT and WOODS, 1963). One of these was kept at a fixed depth, nominally 10 m, while the other was lowered on an armoured electric cable, together with a depth gauge and temperature–salinity probe. The cable was paid out in increments of 10 m, and readings were taken while the meter was being held steady for a period of 1 or 2 min, at each depth. A complete profile to 200 m depth, with check readings at 40-m intervals on the way up, usually took about an hour.

These readings were corrected according to the calibrations of the individual current meters (which were reproducible to within 5 cm/sec), and components of relative current in north–south and east–west directions were plotted against depth, for each station. Smooth curves were drawn by eye for each component. The standard deviation of single observations from the smooth curves was about 15 cm/sec. Partly this scatter came from fluctuations imposed on the current meters by the irregular motion of the ship, but part of it may be systematic because in strong current shear it was necessary to manoeuvre, during the current meter observations, to maintain an acceptable wire angle on the deep meter. Even though care was taken to wait for steady conditions after any substantial change (> 25 cm/sec) in the shallow meter reading, part of the scatter may still be due to manoeuvring. There may have been systematic over-reading on the shallow current meter due to pumping action induced by ship motion, and it is difficult to estimate how serious this may be. The arrangement used for streaming the shallow meter would tend to reduce this effect, as also would the fact that generally the ship was making appreciable headway.

A different suspension had to be used for the " deep " current meter, which made it more vulnerable to ship motion, at shallow depths. Comparison of the readings of the two meters when they were both at the same depth, at the beginning and end of each profile, suggests that systematic over-reading on the shallow meter due to ship motion may have been of the order of 5 cm/sec.

Coming now to the surface (or 10-m) currents to which the relative profiles have been fitted, these are known with varying accuracy. At about one-third of the stations, positions could be determined by radar relative to the coast or an anchored buoy. Throughout each station, the shallow current meter was read at 5-min intervals, from which the total movement through the water on station could be found. Combining this with the displacement shown by radar fixes gave mean values of current at 10 m depth.

At Sta. 5538, four separate estimates of current, for different intervals during the station, by this method differed from the mean by less than 10 cm/sec; on the other hand, at Sta. 5551, in a very strong current and at 20 miles range on the radar, three measures of the surface current had a standard devia-

tion of 25 cm/sec. It seems reasonable to suppose that at most of the stations where radar fixing was possible the standard deviation of the mean surface current will be of the order of 10–15 cm/sec. Part of this variability may of course be real.

It had been hoped that it would be possible to determine the ship's movement over the ground on station by means of VLF radio nagivation equipment (STANBROUGH and KEILY, 1964), but unfortunately only one component of movement could be obtained at all reliably, and that one ran northwest–southeast, more or less at right angles to the main current.

South of 4°N, surface currents could be obtained by GEK, but farther north (nearer the magnetic equator) the *Discovery's* GEK observations became unreliable and were discontinued. Most of the surface currents, at stations where radar was not available, were in fact determined by combining dead reckoning and star sights. This turned out to be better than might have been expected, despite the fact that *Discovery's* log was out of action. In the stronger parts of the current, stations took about 5 hr each, on average, and time was almost equally divided between stations and steaming.

In choosing a surface current appropriate to a particular station, it was assumed that the current varied linearly between stations, and the mean surface current between a pair of fixes could be portioned out between the stations in that interval. Fixes were frequent enough (or stations slow enough) so that no more than parts of two stations came in any interval between fixes.

Other celestial fixes were used when stars could not be obtained, simultaneous Sun and Venus observations were useful in avoiding uncertainties of running-on Sun position lines. Some systematic error may have been introduced by combining current meter readings on station, at a depth of 10 m, with the set experienced by the ship on passage, with a mean draught of 5 m. From rough estimates of all the likely sources of error, it seems reasonable to suppose that the adopted values of surface current at stations in the main part of the Somali Current may have systematic errors persisting over several stations amounting to 10 cm/sec, as well as random errors of about 15 cm/sec. Farther out along the two longer sections, where the proportion of time on passage was greater and there were fewer fixes per station, estimated surface currents are less certain. However, the real fluctuations in the weaker currents are likely to be less, and the observations relative to anchored buoys at Stas. 5538 and 5544 serve as useful checks on the others: perhaps the errors in these weaker surface currents are not much greater than those in the main current itself. Returning now to the relative current profiles, and combining their uncertainties with those of the near-surface currents, it seems likely that at those stations where radar fixing was possible the subsurface currents may have errors of the order of 15–20 cm/sec, but where the surface current was obtained by celestial navigation the error may be 25 cm/sec, of which some 10 cm/sec may be systematic over several stations.

Differences between successive values in a vertical profile, however, depend only on the current meter readings themselves and might be expected to have random errors of about 15 cm/sec.

In the *Argo* the current meters used were suspended on conducting cable, sensing speed by a Savonius rotor and direction by a vane coupled to an internal compass. The signals representing both speed and direction were recorded continuously on shipboard. Two meters were used, one being lowered to 10 m to obtain movement of the ship relative to that level while the other was lowered in stages to 500–1000 m. During current measurements, the ship was lying-to drifting with the wind.

Unfortunately no depth indicator was available, and current meter depths were determined from the amount of wire out and wire angle. On a later cruise when a depth gauge was added it was found to agree reasonably well for the shallow depths (to 200 m) discussed here. While operating in surface currents from 1–3 knots, errors in depth between 100–200 m would be approximately $\pm$ 5–10 m, whereas in currents of 3–6 knots, errors might be as high as $\pm$ 20 m.

To determine the movement of the ship relative to the bottom during current stations, three methods were used. The most accurate method was by radar, which was limited to approximately 20 miles offshore, and required a distinguishable feature on the coast to serve as a target. GEK surface measurements were continued up to approximately 6°N, north of which the proximity of the magnetic equator made such readings inaccurate. Another method was to observe the ship's heading and speed through the water while a hydrographic cast was down, when the wire angle was kept at nearly zero. This procedure gave good agreement with GEK results in currents above 1 knot, and although not a suitable method for accurate determination of surface current, it seems unlikely that errors would exceed 15–20% in the regions of strong currents.

When the surface current had been determined by one or more of the above three methods, it was

combined with the relative profile obtained from the current-meters and curves of speed and direction versus depth were drawn.

Some deeper current measurements were made by the *Discovery*, by two different methods. The Bergen current meter already mentioned was used at eight stations to extend the relative current profiles to depths between 200 and 1000 m. No depth gauge was available for use with it, but the meter signalled *in situ* temperature as well as revolutions of the Savonius rotor and current direction, and depths could be inferred from the temperature–depth profile at the same station. At four stations off the Somali Coast, and at one station offshore from Mombasa, deep currents were measured with neutrally buoyant floats, the method being much the same as that described by SWALLOW and WORTHINGTON (1960). Care was taken where an anchored buoy was used as a reference point, to check on any movement of the buoy over the ground by repeated echo-sounding surveys.

OBSERVATIONS IN THE UPPER 200 METRES

The positions of the current measuring stations occupied by both ships are shown in Fig. 1. Most of them fall on the numbered sections. Besides the seven sections in the Somali Current between 1°N and 8½°N, there are two in the cold surface water to the north between Somalia and Socotra, and an additional section is shown which had been occupied by the *Discovery* off Mombasa (4°S) just before the start of the Somali Current observations.

The current vectors obtained at depths of 10 m, 100 m, and 200 m off the Somali Coast are shown in Figs. 2, 3, and 4, together with the appropriate dynamic topography relative to 1000 decibars. These three figures show similar features, decreasing in intensity with depth. The current can be seen to be relatively narrow near 1°N, broadening and increasing in speed as it moves northeast along the coast, and turning eastwards at about 9°N. The dynamic height contours run more or less parallel to the current arrows, forming a low area close to the coast near 10°N, and two high areas near 10°N, 55°E and 6°N, 52°E. The current vectors in the neighbourhood of both the high areas suggest clockwise circulations. A sharp boundary was observed, both visually and by bathythermograph, between the northern clockwise loop and the east-going current just to the south of it, near 9°N, and the dynamic height contours crossing the boundary have been drawn with an abrupt change of direction, although the water-sampling data are too sparse to reveal such a discontinuity. The general agreement between the currents observed and those to be expected from the dynamic topography, at all three depths shown, suggests that both non-geostrophic currents and the motion at 1000 decibars are likely to be small compared to the main current. The relative weakness of currents and dynamic topography at 200 decibars (total range 21 dyn . cm compared to 75 at the surface) shows that the strong surface currents are sharply limited in depth.

These charts of current may usefully be compared with the charts of surface temperature and salinity shown by WARREN *et al.* (1966, Figs. 12 and 13). The pattern of flow in the near-surface layer inferred from those charts is substantially the same as that shown by the current measurements. In Figs. 2 and 3, the sinuous nature of the dynamic height contours near the coast at Lat. 4°N. lends some support to the existence of a meander there (WARREN *et al.*, 1966). The observed currents do not suggest such a feature, though this may have been masked at the 100 m level (Fig. 3) by the strong inflow from farther offshore in this latitude. Neither the currents nor the water-sampling observations however, are detailed enough to show clearly whether the meander exists or not.

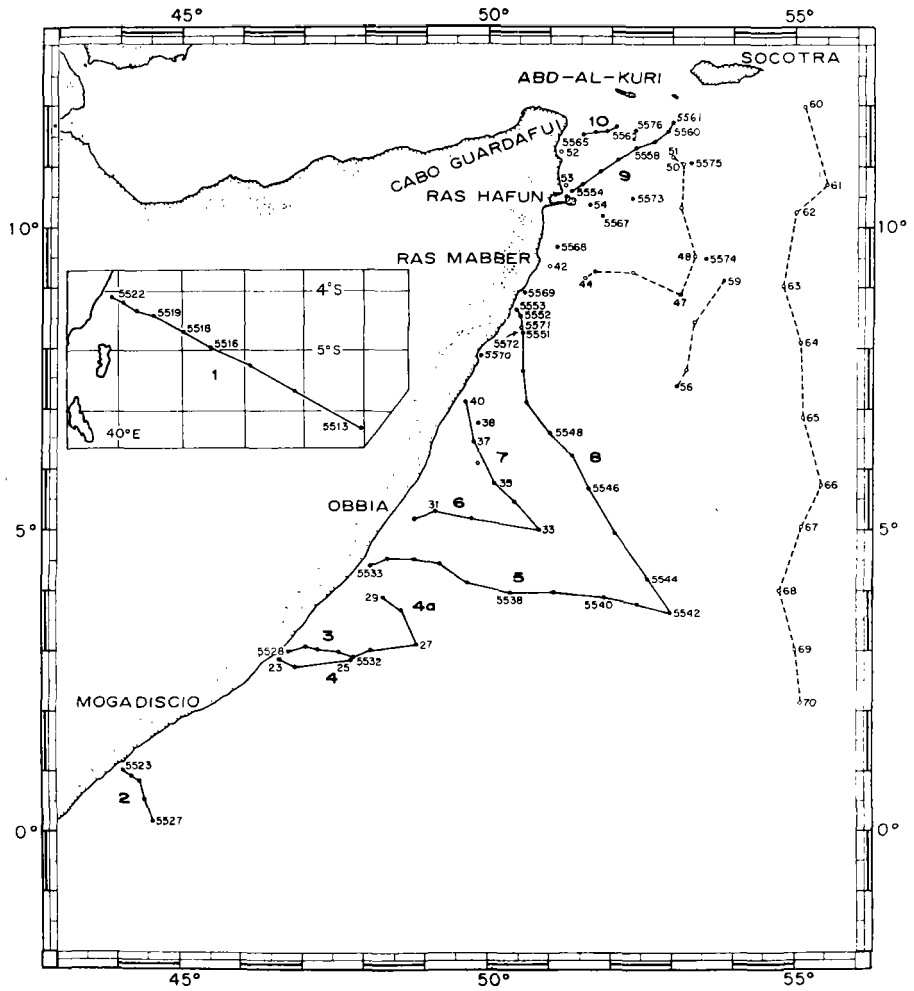


Fig. 1. Station positions and section numbers. Solid dots and lines indicate stations and sections where vertical profiles of current were observed. Dashed lines indicate other sections for which geostrophic currents are presented. Stas. 23–70, *Argo* Dodo VI; Stas. 5513–5576, *Discovery*.

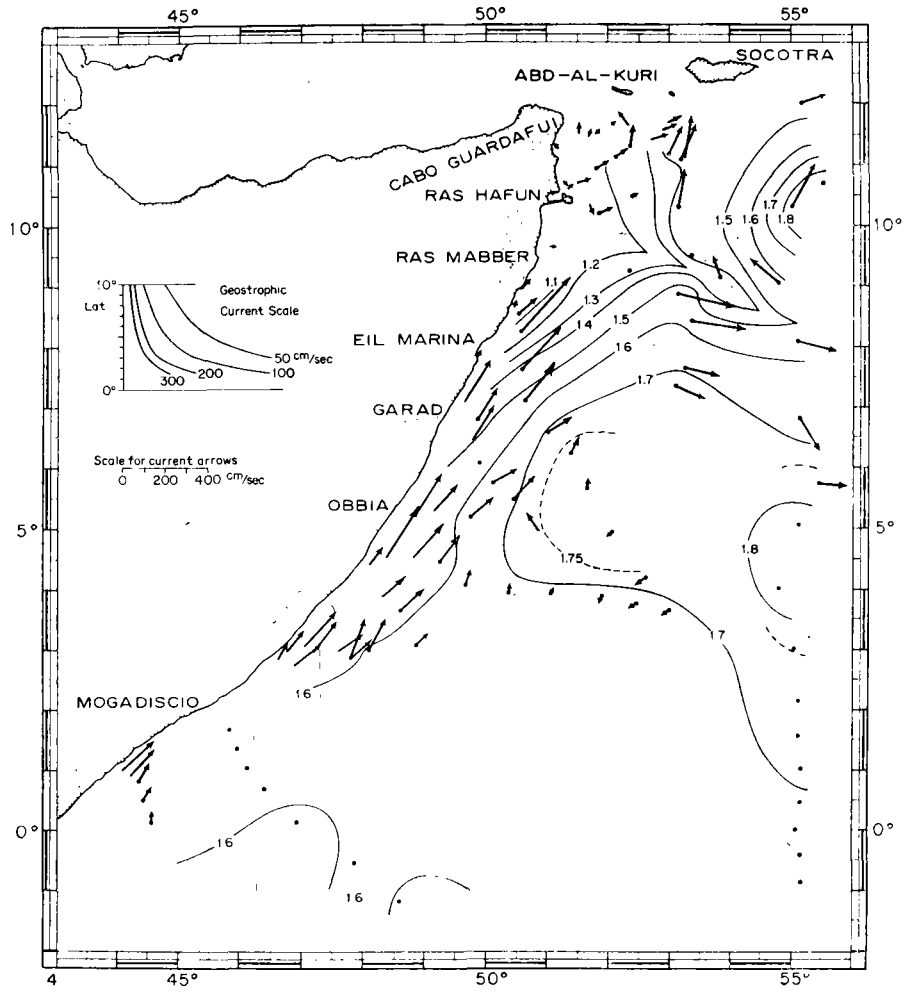


Fig. 2. Currents at 10 m depth, and dynamic height (metres) of the sea surface relative to 1000 decibars. Dots indicate stations on which the dynamic height contours are based. To use the scale of geostrophic currents, pick off the spacing of an adjacent pair of height contours and measure that distance from the left-hand edge of the scale, along the appropriate latitude.

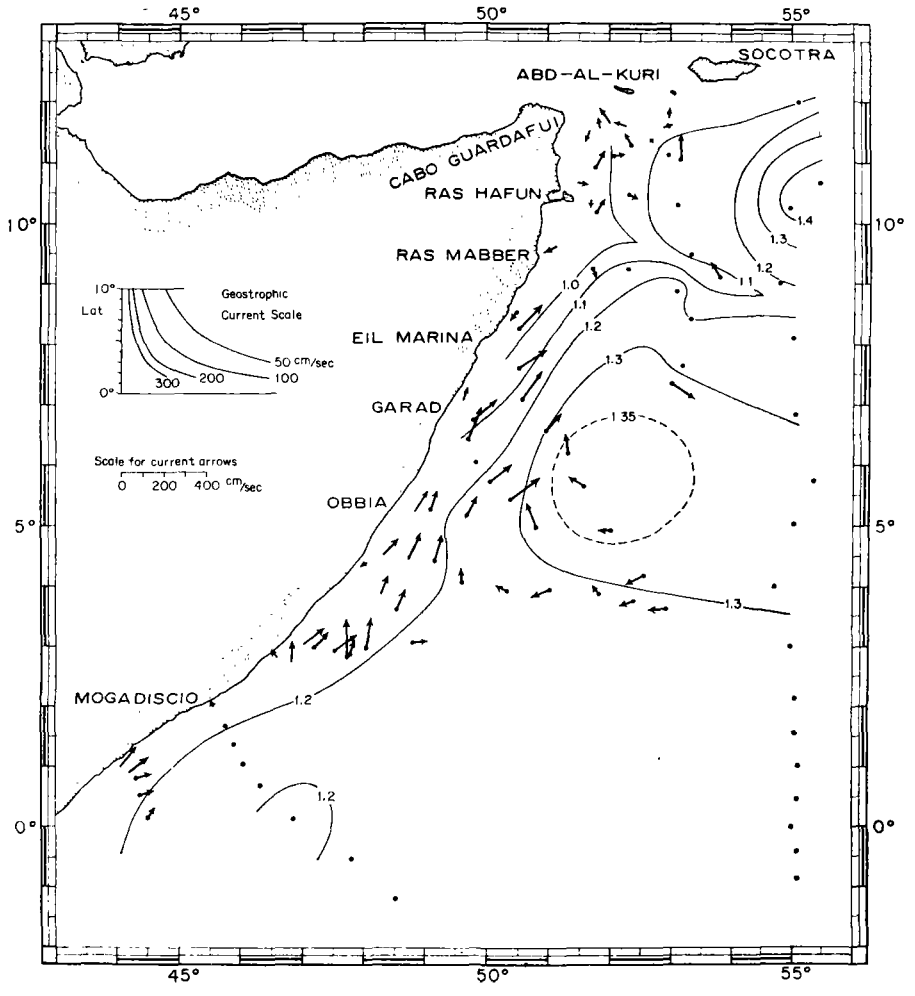


Fig. 3. Currents at 100 m depth, and dynamic height of the 100 decibar surface relative to 1000 decibars. (100 decibars pressure is at 99–100 m).

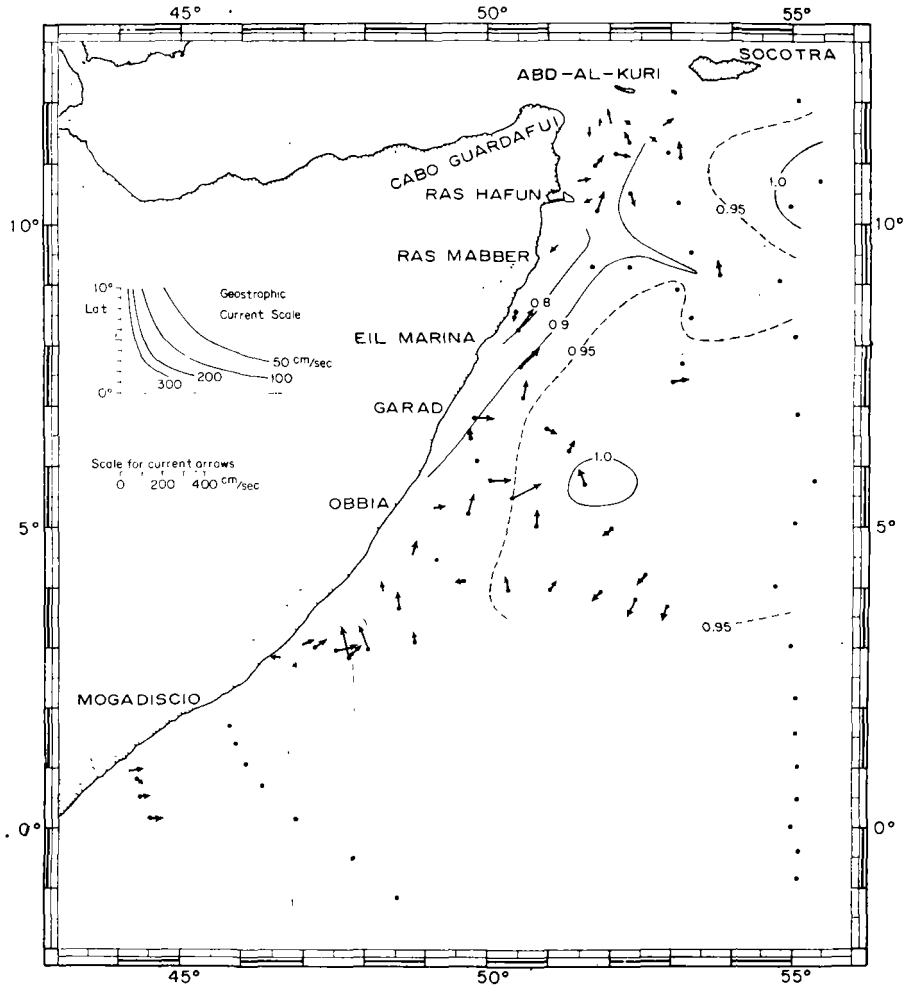


Fig. 4. Currents at 200 m depth, and dynamic height of the 200 decibar surface relative to 1000 decibars. (200 decibars pressure is at 199 m).

It is difficult to estimate quantitatively to what extent these currents are typical of normal conditions, although (as pointed out in the introductory comparison with FINDLAY's description) the main qualitative features seem to be normal. The surface current charts compiled by MICHAELIS (1923) and SCHOTT (1942), though showing the main features clearly, are on too small a scale for detailed quantitative comparison with the present observations. The best compilation of surface currents, for this purpose, is the " Dutch Atlas " (*K. Ned. Met. Inst. Publ.* No. 135, issued in 1952), which

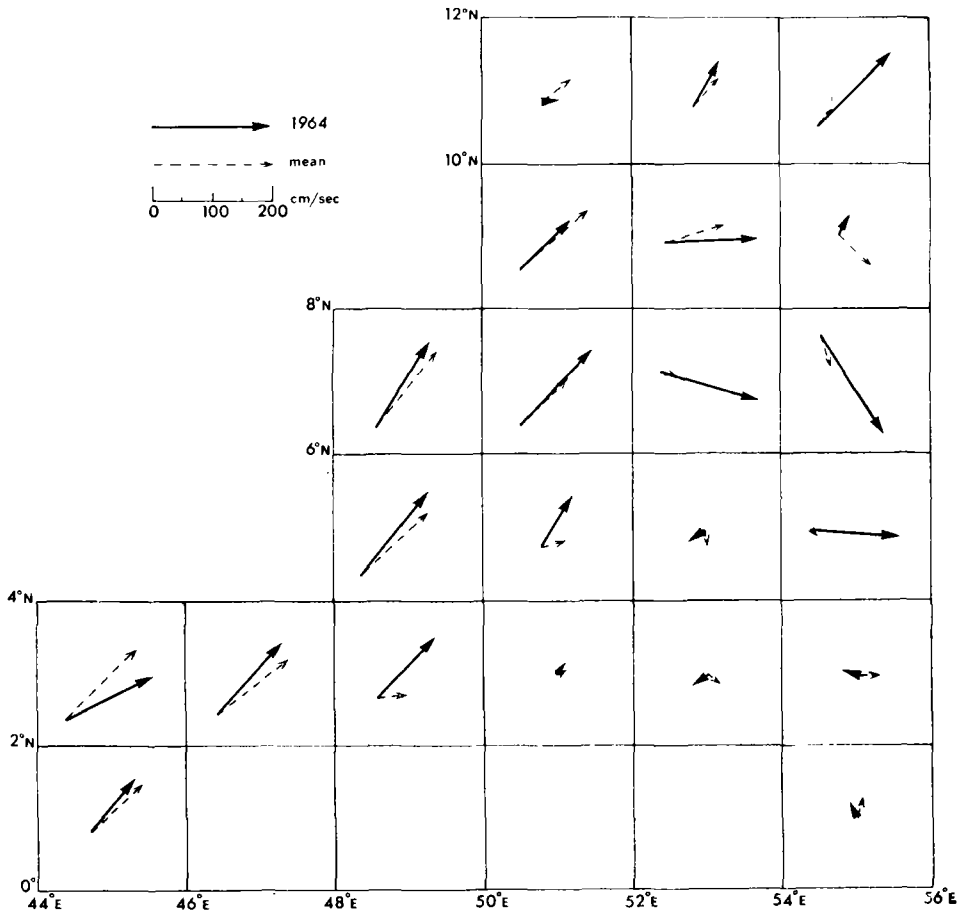


Fig. 5. Comparison of vector mean surface currents in 2° quadrangles in 1964 with mean values for August taken from *K. Ned. Met. Inst. Publ.* No. 135.

gives monthly mean surface current vectors for each 2° quadrangle. The mean vectors for August in the region of the Somali Current are compared with mean values derived from the *Argo* and *Discovery* observations in Fig. 5. In the main current, close to the coast as far as 9°N, there is surprisingly close agreement, but the discrepancies in the quadrangles centred at 3°N, 49°E and 5°N, 51°E suggest that in 1964 the current may have been wider than normal. Differences can also be seen in the quadrangle centred at 7°N, 53°E, and along the 55°E meridian north of 4°N, where in 1964 the eastward

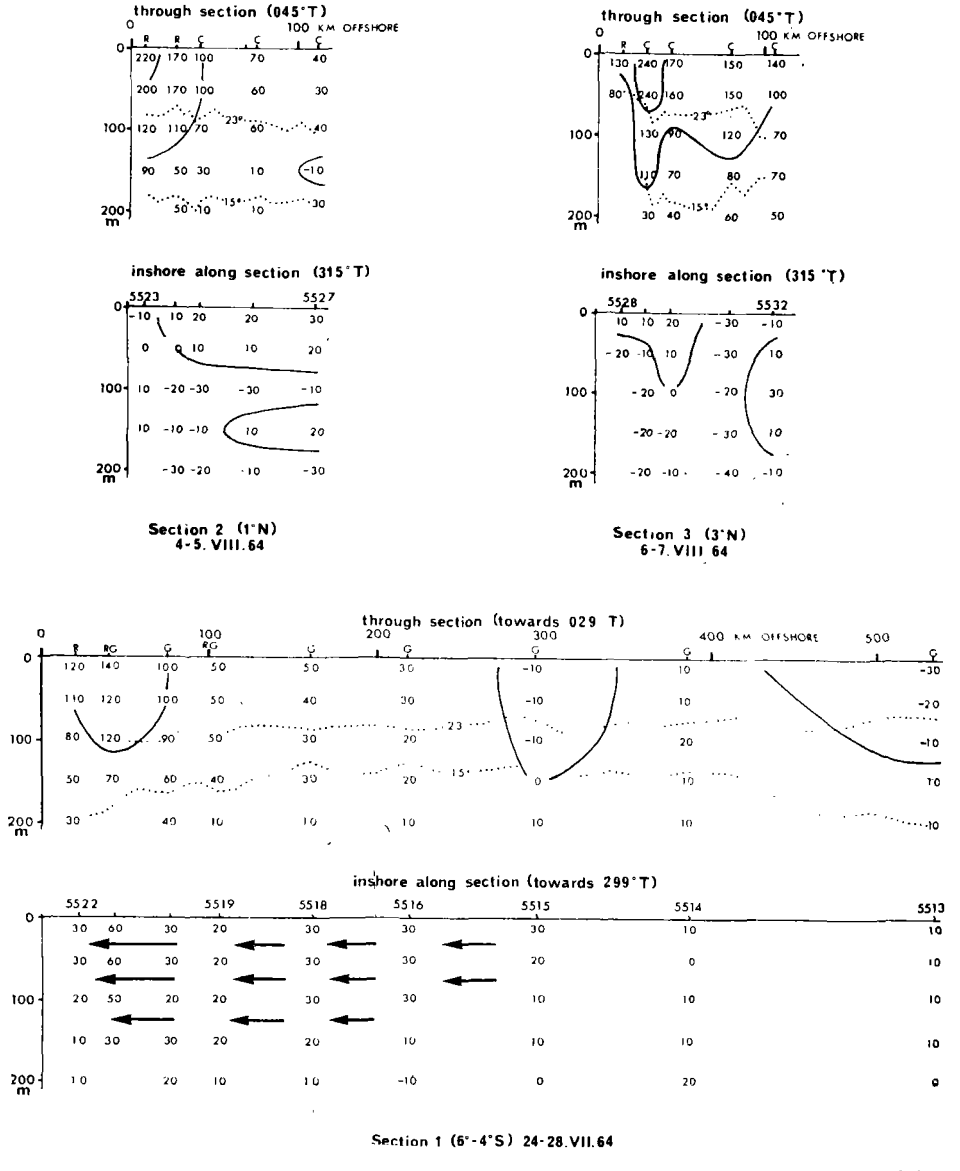


Fig. 6. Sections 1–3. Directly measured current components. Speeds in cm/sec. In this and the following three diagrams, the letters along the top of the sections indicate the source of surface current information at each station: C—celestial navigation, G—GEK, R—radar, S—ship's speed when hove-to on vertical wire.

current seems to have been stronger and spread farther south than usual. Bearing in mind the sparseness of the observations, though, and the non-uniform distribution of ships' tracks on which the mean values must be based, these apparent discrepancies should be regarded with some caution. The high speeds of surface current observed in 1964 (up to 6·9 knots, 350 cm/sec) are not inconsistent with those given in the atlas. The sheet for August (*K. Ned. Met. Inst. Publ.* 135) lists no fewer than 49 observations

of ships' drift exceeding 5 knots (120 miles per day) in the Somali coast area, the fastest one being nearly 7½ knots (179 miles per day).

There are some misfits between the current vectors and the dynamic height contours, particularly in the area near the coast just north of 10°N. Partly that may be due to the surface currents being even more uncertain than usual, but partly also to changes that were occurring in the area at that time. A near-surface current of 240 cm/sec towards 098°T, observed at *Discovery* Sta. 5574, near 9½°N, 53½°E, not plotted in Fig. 2, was directly opposed to the dynamic height contours based on *Argo* stations

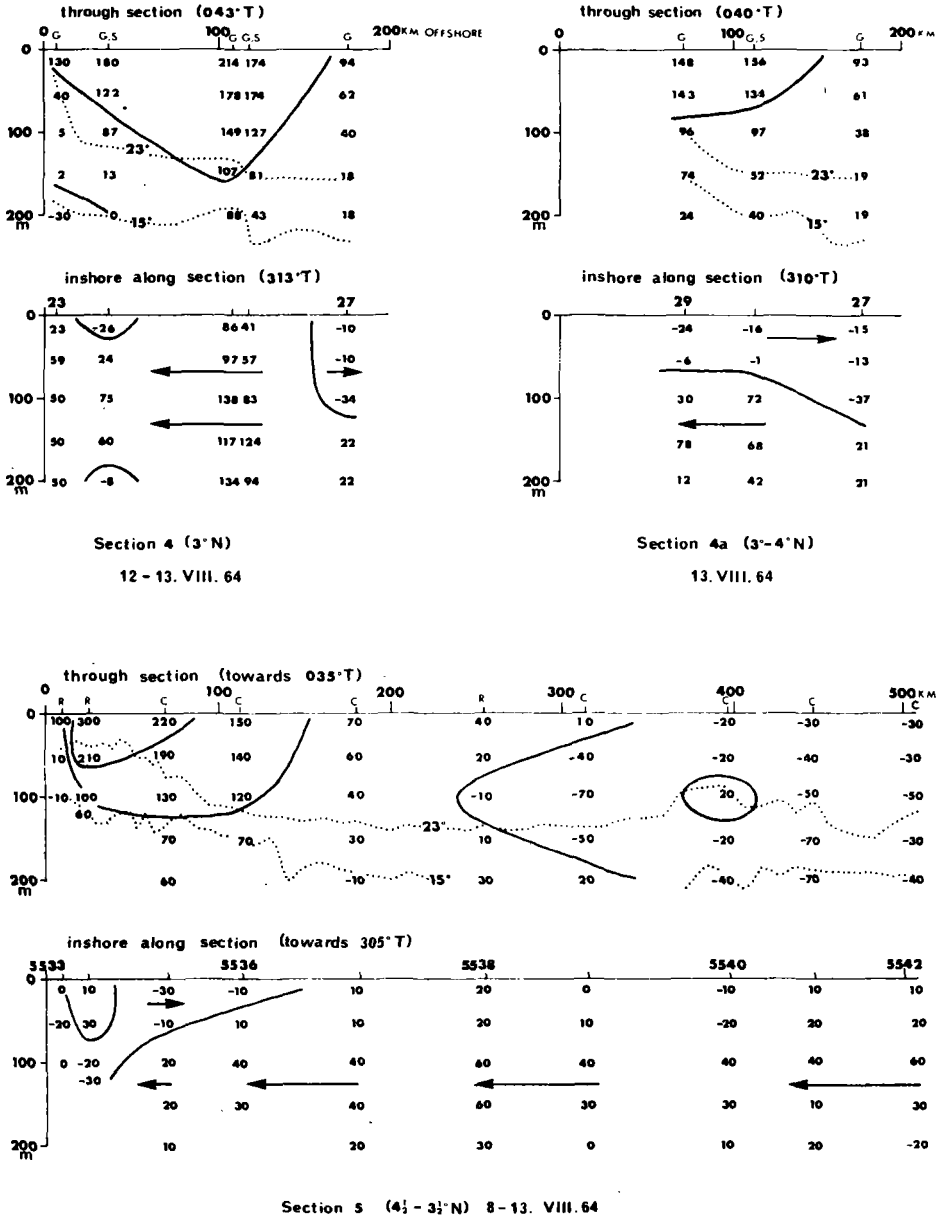
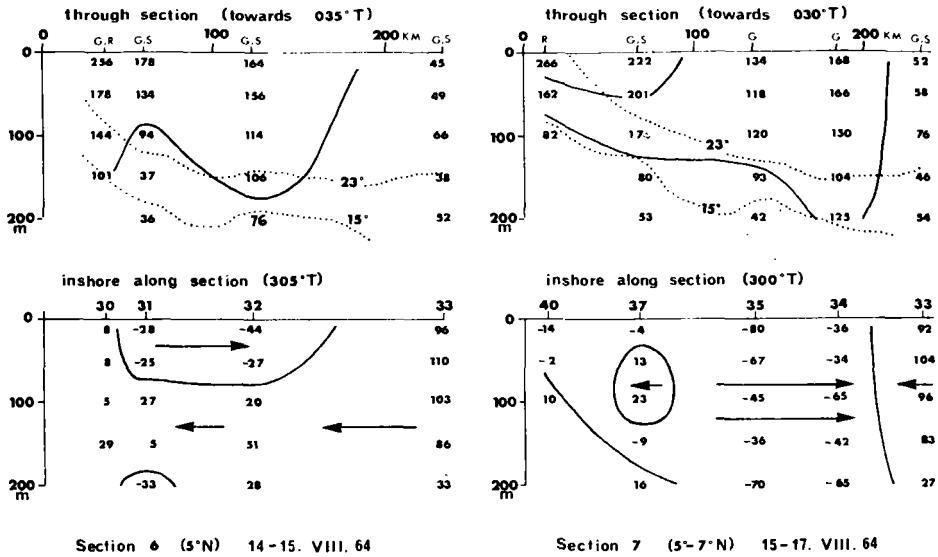


Fig. 7. Sections 4, 4a and 5. Directly measured current components. Speeds in cm/sec.

occupied two weeks previously. The boundary on the north side of the east-going current had moved about 30 miles northward in that interval.

The current meter observations are shown in more detail in the form of vertical sections in Figs. 6–9. For each of the numbered sections in Fig. 1, a line has been chosen at right angles to the general run of the coast and the fathom lines, the stations have been projected on to it, and the current vectors resolved into components parallel to the coast and perpendicular to it. The 23°C and 15°C isotherms have been drawn



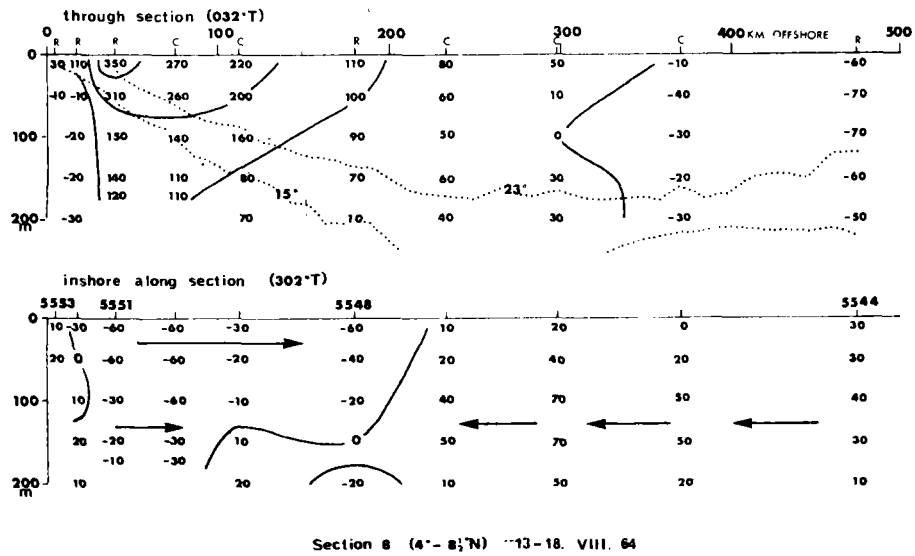


Fig. 8. Sections 6–8. Directly measured current components. Speeds in cm/sec.

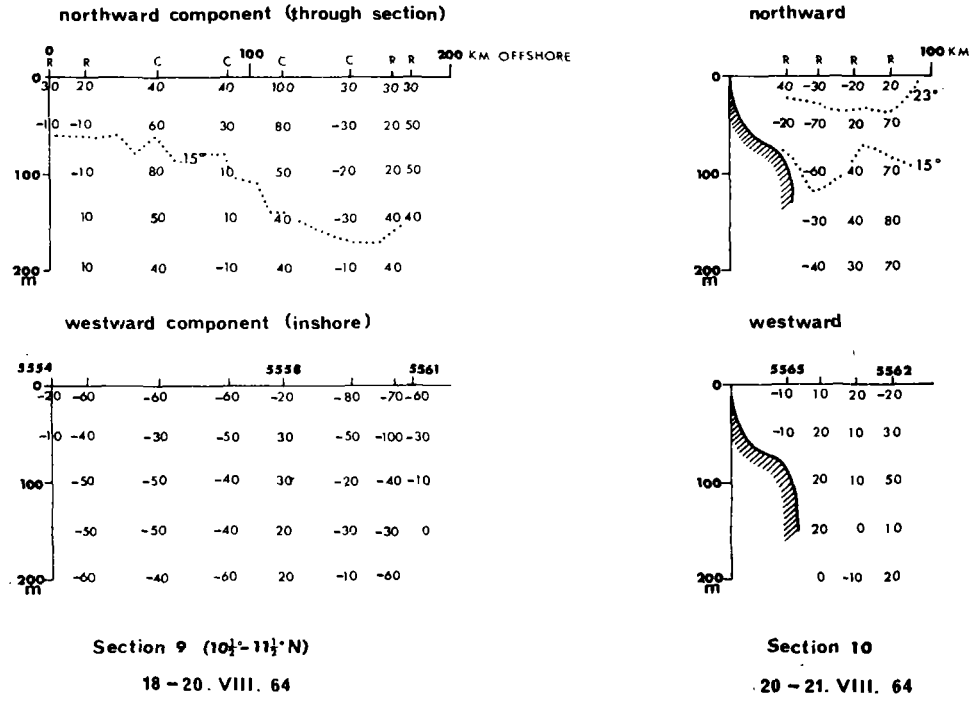


Fig. 9. Sections 9 and 10. Directly measured current components. Speeds in cm/sec.

on these vertical sections; they indicate the upper and lower limits of the steep part of the thermocline, at most stations. Some features, which can be seen more readily in the sections than in the charts of horizontal distribution, are described below.

Section 1, which was outside the area of Figs. 2–4, showed strong northward currents only close to the shore, with a width (to half the maximum speed) of less than 100 km, decreasing more slowly out to 300 km. Except under the strongest part of the current, there was negligible flow at 200 m depth. Some evidence about the steadiness of the current was obtained at Sta. 5519, where a buoy was anchored and the current-meter profile was repeated three times within 24 hr. In the east–west components, differences from the mean of up to 15 cm/sec were observed, but the variations in the north–south components did not exceed $\pm$ 5 cm/sec. Within 300 km of the coast, the current had a marked inshore component in the upper 100 m. If that had persisted steadily as far north as the equator, with no vertical motion, the transport through Sect. 2 would have been doubled. It seems more likely that the observed inshore movement was mainly a local feature due to deflection of the current by Zanzibar and Pemba islands.

In Sect. 2, the current was faster but narrower than at 4°S, but broadened again in Sect. 3. When the latter section was reoccupied by the *Argo* six days later (the first three stations of Sect. 4) the maximum current had moved farther offshore, and strong components in towards the coast were observed, compared to the weak, mainly offshore, movement found earlier. Turning back towards the coast after Sta. 27, the *Argo* found weaker currents at the next two stations, on the short Sect. 4a, than had

been seen at the same distance offshore on the previous section, and the strong inshore flow was confined to depths of 100 m and below.

A very strong surface current, nearly 6 knots, was encountered at the second station of Sect. 5, 24 km from the coast. The current shear was unusually high, $2{\cdot}2 \times 10^{-2}$ sec^{-1} in the upper 100 m, and instead of the usual nearly isothermal layer with a sharp thermocline below it, the temperature profile showed an almost linear decrease with depth. The Richardson number was 0·4, compared to 1·1 across the thermocline at the next station out along the section. There was significant northeastwards flow out to 250 km offshore, with a weak countercurrent beyond 400 km. The inshore components at nearly all stations on this section were strongest at 100–150 m depth, that is, near the top of the thermocline. More will be said of this later, in relation to the geostrophic flow.

Similar features can be seen in Sect. 6, made six days after the inshore part of Sect. 5.

Section 7 and the inshore half of Sect. 8 were occupied simultaneously. On both of them, very strong surface currents were observed; well over 5 knots close inshore on Sect. 7, and nearly 7 knots at 40 km from the coast on Sect. 8. Current shear was again very high, under the strongest surface currents, $2{\cdot}2 \times 10^{-2}$ sec^{-1} at Sta. 40 and $3{\cdot}5 \times 10^{-2}$ sec^{-1} at Sta. 5551, in the upper 50 m. The average Richardson number in the same interval at the latter station was 0·3, and there was a distinct thermocline, though quite shallow, with the 15°C isotherm at 50 m depth. Farther inshore the surface temperature decreased rapidly, to less than 15°C at the coast. The current had already begun to turn towards the east, as shown by the marked offshore components at Stas. 5548–5551. In the outer part of Sect. 8, there was again a maximum of inshore flow at depths of 100–150 m, as in Sect. 5. It is a bit unrealistic plotting the stations of Sect. 8 as if they lay on a line at right angles to the coast; in fact the speed of the current forced the section to run almost due north between Stas. 5549 and 5552, and the apparent convergence along the section, towards Sta. 5548, is really part of a clockwise circulation.

Currents were mainly northward, though variable, in Sects. 9 and 10. They were in the area of cold surface water, near its boundary with the much warmer, more saline surface water of the Gulf of Aden. Violent eddies were seen in the neighbourhood of Cape Guardafui, not far from Sect. 10, and the current measurements there may not have more than a very local significance. Still, the relatively strong northward flow at Sta. 5558 was consistent with that observed at Sta. 5576, two weeks later, and the current profiles at Stas. 5562 and 5563 indicate northward flow of the cold water below a thin layer of warmer surface water.

Volume transports have been calculated from the current components of Sects. 2–8, and are presented in Fig. 10. The rough estimates of uncertainty against some of the values are derived from those estimated previously for the currents. In making these calculations it was assumed that the observed currents were steady, within the errors of observation, during the time of occupation of the section, and that the current varied linearly in the intervals between stations. It is of course very questionable how far these assumptions were justified. Some evidence about steadiness of the current has already been mentioned, at two stations where the observations could be subdivided. The second assumption may not be so drastic as it seems. In the southern part of the area, where the *Argo* made two sets of closely spaced GEK observations across

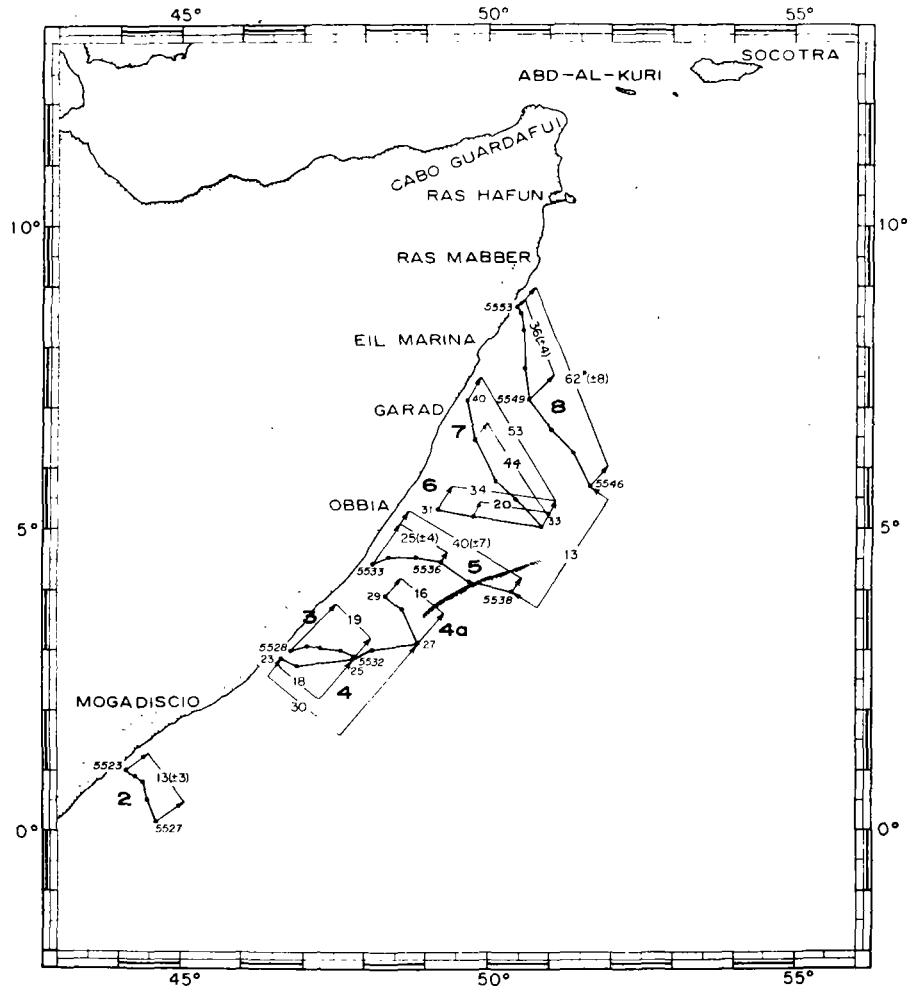


Fig. 10. Volume transport in the upper 200 m, from direct measurements. Transports in units of 10^6 m^3/sec. The transport through Sect. 8 (marked*) may be an overestimate, 54 × 10^6 m^3/sec being a more likely value (see text).

the current, (STOMMEL and WOOSTER, 1965), the fluctuations were not very large. In Sect. 8, where the current was strongest, the smooth slope of the isotherms (which are based on half-hourly bathythermograph observations between stations) makes a smooth variation of current seem probable.

Despite these uncertainties, the large increase in transport between 1°N and 8°N is remarkable. The transport towards the coast between the offshore ends of Sects. 5 and 8 was calculated from the mean of the shorewards components of current at Stas. 5538–5546.

One is tempted to try to stretch the data one stage further, and estimate vertical transport from below the 200 m level by continuity. As they stand, the transport values given in Fig. 10 might be taken to imply that 9 (± about 12) × 10^6 m^3/sec of water were moving upwards from below 200 m, under the main current between Sects. 5 and 8. Dividing the water above 200 m into three categories according to

temperature—the nearly-isothermal water down to the 23°C isotherm, the thermocline region between 23°C and 15°C, and the cold water below 15°C—there was indeed a fortuitously good balance of transports for the two warmer kinds of water, and a deficiency of colder water which could have been supplied from below. However, it seems unlikely that the current was steady throughout the whole period while Sects. 5 and 8 were being made (8th–18th August).

There are several reasons for suspecting unsteadiness of the current, over an interval of a week or two. The boundary between the slowly moving cold water and the strong current where it begins to leave the coast is marked, approximately, by the 20°C surface isotherm. Between longitudes 51°E and 52°E, that isotherm lay south of 9°N on August 18th–19th, but on September 2nd it ran northeastward from 9° 15′N to 9° 40′N between the same longitudes.

The point at which the current turns away from the coast seems to be related to the appearance of the thermocline at the surface at the inshore edge of the current. If the thermocline depth in the slowly moving offshore water remains constant, and if the flow is geostrophic, an increase in transport will bring the thermocline to the surface near the coast at a lower latitude. Presumably this will affect the turning-off point and the northern boundary of the east-going current, and the observed northward shift of the boundary may perhaps be related to a decrease in transport. There was in fact a change in observed current when Sta. 5551 (on 17th August) was reoccupied as Sta. 5572 (1st September), from 350 cm/sec 042°T to 300 cm/sec 036°T, though the horizontal gradient of surface current between stations 5551 and 5552 was so strong that a lateral shift of the current of only 6 km could have produced the observed speed change. Further evidence came from the dead fish seen in the southern part of the cold-water area, described by FOXTON (1965). Of the first ones seen on 18th August, most were only recently dead, but passing through the same area on 31st August more were found in an advanced state of decomposition. It seemed likely that the mortality was due to the extremely cold near-surface water, that it was in an early stage when seen on August 18th, and that the current at that time was stronger than it had been previously, to bring the cold water nearer the surface.

Although the vertical transport could not be estimated reliably from continuity, it seems clear that there was some vertical motion. The 20°C isotherm shoaled gradually by 50 m in going from 1°N to 8½°N under the fastest part of the current, a distance of 600 miles with speed increasing downstream, and a mean speed of 150 cm/sec. It is difficult to imagine this happening without some upward movement, even though the current may not have been steady. If we assume that the 20°C isotherm along the current axis was a streamline, and supposing for the moment that the current had been steady, the vertical velocity corresponding to the observed mean horizontal speed would have been 7×10^{-3} cm/sec, or 6 metres per day. This should be less sensitive to small departures from a steady state, than the estimate of vertical transport from below 200 m derived from continuity would be.

Dynamic heights were shown in Figs. 2–4 relative to an arbitrary reference level of 1000 decibars, and the geostrophic volume transports in the upper 200 metres are shown, relative to that reference level, in Fig. 11. Some stations near the coast, which were too shallow, had to be omitted, and other sections are presented where currents were not measured directly. Where comparisons can be made, the geostrophic transports are similar to the directly measured values, but some of the discrepancies seem

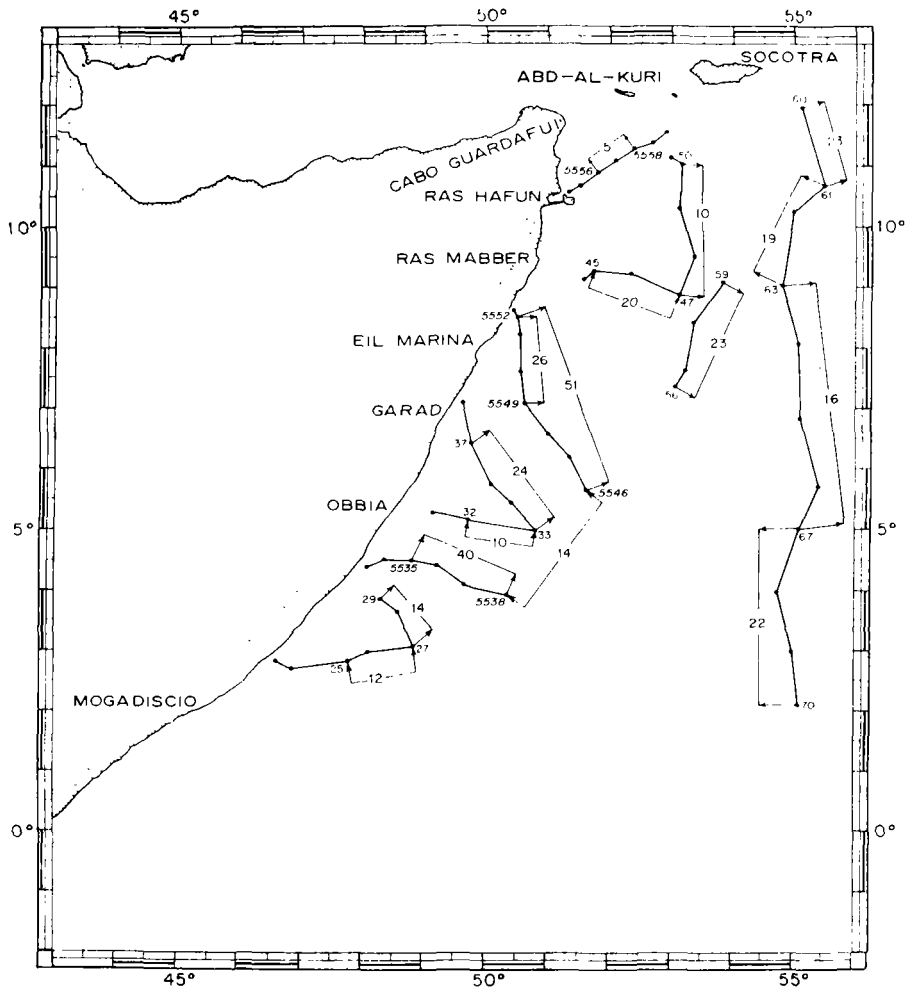


Fig. 11. Geostrophic volume transport, in units of 10^6 m^3/sec, in the interval 0–200 decibars, relative to 1000 decibars. Arrows indicate sense of flow through sections.

to be too large to be entirely due to errors of observation. They can be accounted for partly by non-geostrophic flow due to wind stress on the sea surface, and partly by motion at 1000 decibars, and are discussed in relation to the direct measurements of deep currents below.

DEEP CURRENT OBSERVATIONS AND GEOSTROPHIC CURRENT PROFILES

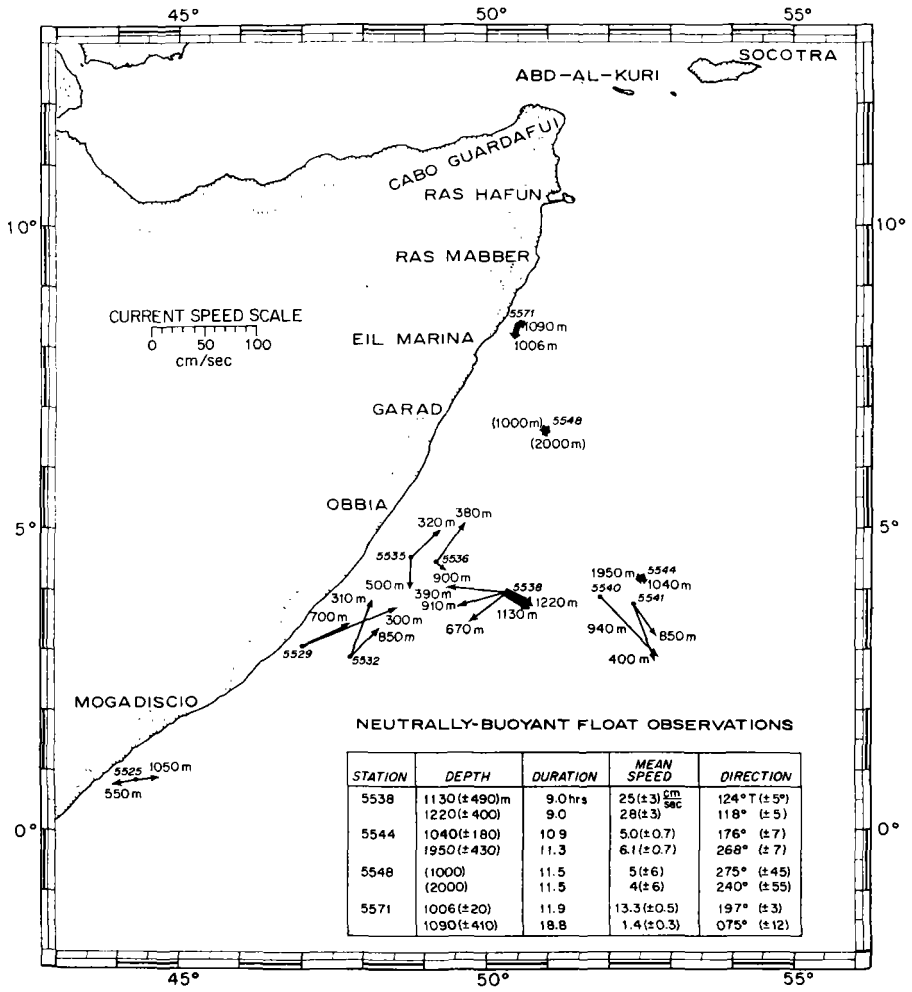
The complexity of the temperature, salinity and oxygen distributions at intermediate depths in the Somali Basin has been commented on by WARREN *et al.* (1966). The field of motion is unlikely to be any simpler, and the few direct measurements of deep currents that were made can hardly be expected to represent the mean flow. The difficulty can be illustrated by considering what evidence there is about deep currents in Sect. 1, made by the *Discovery* on the way in to Mombasa before the start of the Somali Current work.

Volume transport through the section, down to 200 m depth and out to 300 km offshore, amounted to 22 ($\pm$ 8) $\times$ 10^6 m^3/sec from the directly measured currents. Geostrophic transport in the same layer, calculated relative to 1000 decibars or to the bottom where it was too shallow, was 38 $\times$ 10^6 m^3/sec. Most of the discrepancy occurred between Stas. 5515 and 5519; within that interval the geostrophic transport exceeded that from the direct measurements by 16 $\times$ 10^6 m^3/sec, equivalent to an extra 40 cm/sec of current throughout that part of the section. This difference in transport seemed to be too large to be due to errors of measurement, or stretching of thinly spread data, or non-geostrophic flow due to local wind stress. It could only be interpreted as evidence for southward flow, with speeds of the order of 40 cm/sec at 1000 decibars. The salinity maximum at a σ_t of 27·3, characteristic of Gulf of Aden water, was particularly well marked at Stas. 5515–5519, with its core at 800–900 m depth, and that might be regarded as consistent with deep southward flow. One deep current observation was made on that section; at Sta. 5519, a neutrally buoyant float was followed for 13 hr, at an observed depth of 1400 m. It moved at a speed of 17 cm/sec towards 062°T, not at all consistent with the supposed southward movement farther out along the section. It was, of course, deeper than the high-salinity core, though the geostrophic profiles did not suggest any reversal below 1000 m. Possibly the Gulf of Aden water was in the form of a rotating lens moving southwards, and Sta. 5519 was on the western fringe of it, but without more observations the only certain conclusion was that the flow at intermediate depths was irregular, with speeds of the order of a few tens of centimetres per second.

Currents at depths greater than 200 m observed in the Somali Basin are shown in Fig. 12. Those derived from measurements relative to the surface, using the Bergen current meter, naturally depend on the estimated surface current and are consequently uncertain. Currents less than 25 cm/sec obtained in that way are probably not significant. The observations with neutrally buoyant floats are more reliable, being averaged over about 12 hr (instead of the 15–20 min at each depth with the current meter) and being independent of surface current.

In the depth range 300–400 m, there was significant movement northeastwards under the main current close to the coast, as shown by four observations near 3°–5°N. Currents at depths around 1000 m were more variable, but tended to have southward components. The speeds of neutrally buoyant floats at Sta. 5538—25 cm/sec at 1130 m and 28 cm/sec at 1220 m—were unusually high, three times the mean speed from 15 observations at comparable depths elsewhere in the western Indian Ocean. Those at Sta. 5548 were less reliable than the others, because the anchored reference buoy broke adrift during the observation and had to be recovered. The displacement of the floats was determined from star sights and not, as was usual, by reference to the sea floor contours.

In trying to fit these observed deep currents to the relative geostrophic currents, sometimes there was reasonably good agreement, but in other cases it was clear that not enough direct measurements had been made. Profiles from some of the stations in Sect. 5 are shown in Fig. 13. The zero of the geostrophic current profile has been adjusted in each case to fit the mean of the observed components of current at 100–200 m depth. Reasons will be given later for believing that there was appreciable non-geostrophic flow in the upper 100 m. For Stas. 5535 and 5536, the geostrophic current profile fitted fairly well to the mean of the directly observed profiles down to



STATION	DEPTH	DURATION	MEAN SPEED	DIRECTION
5538	1130(±490)m	9.0hrs	25(±3) cm/sec	124°T(±5°)
	1220(±400)	9.0	28(±3)	118° (±5)
5544	1040(±180)	10.9	5.0(±0.7)	176° (±7)
	1950(±430)	11.3	6.1(±0.7)	268° (±7)
5548	(1000)	11.5	5(±6)	275° (±45)
	(2000)	11.5	4(±6)	240° (±55)
5571	1006(±20)	11.9	13.3(±0.5)	197° (±3)
	1090(±410)	18.8	1.4(±0.3)	075° (±12)

Fig. 12. Deep current observations. Lengths of arrows represent current speeds. Current meter observations are shown by thin arrows, neutrally buoyant floats by thick ones. The latter observations are also tabulated since some were too slow to be plotted conveniently as current arrows.

500 m, bearing in mind that within each profile the current meter observations were uncertain relative to each other by about 15 cm/sec. The positions of the directly measured profiles relative to the zero of the current scale were more uncertain, depending on the surface current estimates; even so, the southwestward motion indicated by the geostrophic profile below 500 m seemed strong enough to be significant. It reached a speed of 80 ($\pm$ about 25) cm/sec at 900 m, but that was the mean for the interval between the two stations. There would have to be a much higher southwestward speed (of the order of 160 cm/sec) at 900 m at Sta. 5535, to give a mean value of 80 cm/sec if the near-zero value at 900 m at Sta. 5536 is correct. However, we have no direct evidence of such a strong countercurrent, and the possibility of large errors in the surface currents cannot be excluded.

There was fairly close agreement between the shapes of the geostrophic profile

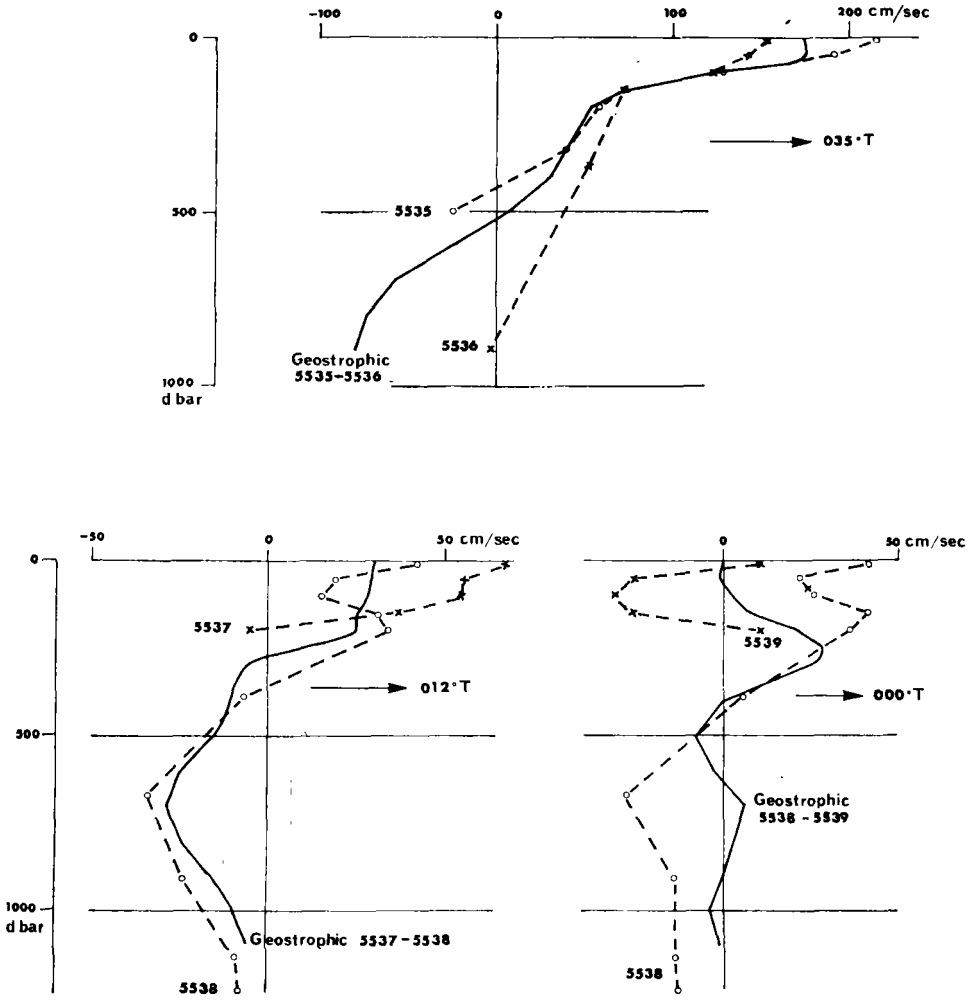


Fig. 13. Section 5. Some profiles of geostrophic current, and directly measured components in the same direction, for the same stations.

for Stas. 5537 and 5538, and the directly measured components of current at the latter station. Vertical gradients of current must have been fairly uniform between the two stations, although no deep current observations were made at Sta. 5537. These comparisons between directly measured and geostrophic current profiles encouraged the belief that the current measurements, even though of short duration, could be related reasonably well to the mean current between stations, and conversely that the main features of the geostrophic profiles represent real currents. Little resemblance could be seen, however, between the directly measured current profile at Sta. 5538 and the geostrophic profile for Stas. 5538–5539. There must have been an appreciable change in the vertical structure of current between the two stations. It seemed probable that, even though these changes were observed in the upper 1000 m, there could also have been changes at the 1000 m level and below. It seemed doubtful whether the accurately known speeds from the neutrally buoyant floats at Sta. 5538 could be assumed to

extend uniformly across to Sta. 5539, to provide a reference for the geostrophic profile in that interval, even though they might possibly apply between Stas. 5537 and 5538. No attempt was made, therefore, to present a complete section of deep geostrophic currents based on a " reference level " derived from the neutrally buoyant floats. It seemed equally unrealistic to construct a section assuming zero velocity at the bottom, in view of the possible countercurrent under Sta. 5535.

On the question of the reality of this countercurrent, it may be mentioned that higher salinities were observed in the Gulf of Aden water (650–900 m depth) at Sta. 5535 than at adjacent stations to the east or south. On the other hand, at Sta. 5538 where there was no doubt of the reality of the deep southward component of current, the salinity maximum was not very pronounced and was 300 m deeper than the southward current maximum.

Although the current measurements were inadequate to determine the transport of Gulf of Aden water through Sect. 5, the available evidence suggests that it was southward, even under the strong surface current.

The subtropical subsurface water showed as a more discrete core in Sect. 5, than did the Gulf of Aden water. It was moving unambiguously northeastwards and it was possible to make a rough estimate of its transport. This water is characterized by its high oxygen content, which exceeded 3 ml/l. at Stas. 5535 and 5536, in the depth range 200–300 m. Using the profiles in Fig. 13 it was found that, between those stations alone, the northeastward transport of that water was $2\frac{1}{2}$ ($\pm$ 1) $\times$ 10^6 m^3/sec. At Sta. 5537, the oxygen content just reached 3 ml/l. in that depth range, and there must have been some such water to the west of Sta. 5535. The total transport of subtropical subsurface water, richer in oxygen than 3 ml/l. through Sect. 5 may well have been close to the " mere guess " of 5 $\times$ 10^6 m^3/sec made by WARREN *et al.* (1966).

Observations were made with neutrally buoyant floats at three stations in Sect. 8, though those at Sta. 5571 were made two weeks after the section was completed. Velocities were much lower than at Sta. 5538, and generally towards southwest. Profiles of geostrophic current for some pairs of stations in Sect. 8 are shown in Fig. 14. Despite the cautionary examples given earlier, and the small-scale variability indicated by the two very different observations at station 5571, zero reference lines have been marked on each profile, based on the nearest deep current observations.

The only justification for this is the uniformity and small size of the observed components of deep current through the section, raising the hope that the unknown fluctuations occurring between observations may be small.

It may be doubted whether the deep currents measured at Sta. 5571 should be used as reference values for the section made two weeks earlier, since there had been changes at the surface during that interval. Nevertheless, there was still a very strong surface current (300 cm/sec) on the second visit, and the geostrophic current profile derived from Stas. 5571 and 5572 had a similar shape to that from Stas. 5551–5552.

In all the profiles in Fig. 14 current shear was strongest in the upper 300 m. At the offshore stations, the shear decreased rapidly below that depth and currents were small and weakly southwestward. Under the stronger surface currents, there was a gradual decrease of current below 200 m, with appreciable northeastward flow to depths of 600–900 m.

In the two deep profiles, the weak southwestward motion is shown continuing down to 2000–3000 m, with a small northeastward current below that. The significance

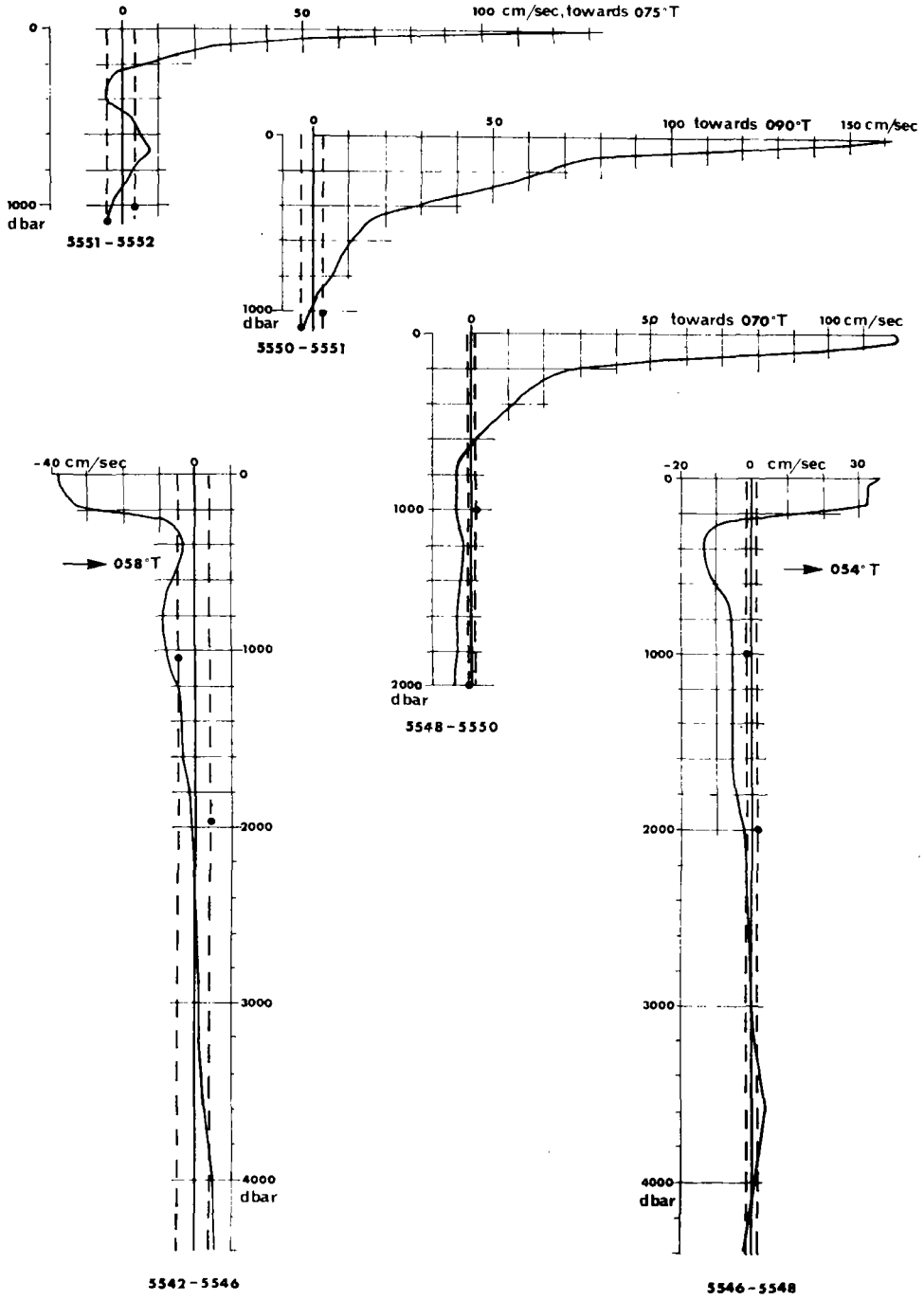


Fig. 14. Section 8. Some adjusted profiles of geostrophic currents. In each case the zero of the current scale is the mean of two estimates (indicated by dashed vertical lines) derived from the nearest neutrally buoyant float observations. Depths of these latter observations are marked by dots.

of such small currents, derived after much horizontal and vertical extrapolation of a few measurements, is however very doubtful.

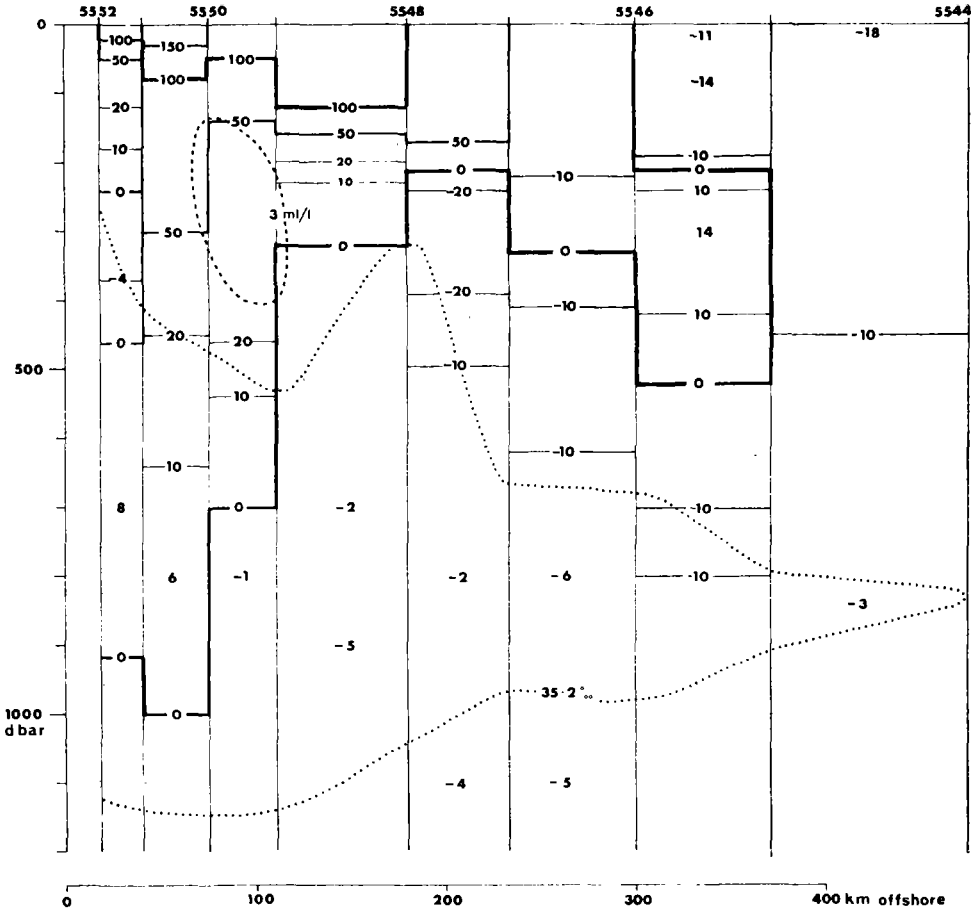


Fig. 15. Part of Sect. 8 showing geostrophic currents fitted to deep current observations. Speeds in cm/sec. Salinity and oxygen contours are explained in text.

Parts of the profiles in Fig. 14 have been combined with others to form a section of geostrophic currents in Fig. 15. It has been drawn as a block diagram, which is simple and unambiguous. Contouring seemed inappropriate, since the section was not straight, and the calculated components of current varied in direction between northeast and east.

The geostrophic transport towards northeast, above the zero line shown in Fig. 15 between Stas. 5546 and 5552, was 64·6 $\times$ 10^6 m^3/sec. The subtropical subsurface water was most conspicuous at Stas. 5549 and 5550, where the dissolved oxygen content exceeded 3 ml/l. in the depth range 140–400 m. The northeastward transport of water within the 3 ml/l. oxygen contour between those stations was 4·5 $\times$ 10^6 m^3/sec.

The 35·2‰ isohaline shown in Fig. 15 was chosen to indicate the Gulf of Aden water in the section, though the water within that contour was far from uniform,

some salinities exceeding 35·3‰ and others, at 700–800 m depth at Stas. 5550 and 5551, being somewhat below 35·2‰.

Water of some other origin may have been included within the 35·2‰ contour at Sta. 5548; there, the σ_t varied from 26·6 to 27·4, though elsewhere it was in the range 27·0–27·4. At stations near the coast, the water within the 35·2‰ isohaline was moving northeast, its total transport in that direction being $4{\cdot}7 \times 10^6$ m³/sec. Offshore, there was a weak broad flow in the opposite direction, the transport southwestwards being $5{\cdot}9 \times 10^6$ m³/sec. However, as may be seen from the profiles in Fig. 14 the reference velocities were uncertain by at least ± 1 cm/sec, and a systematic error of 1 cm/sec would change the net transport within the 35·2‰ contour by $2{\cdot}3 \times 10^6$ m³/sec. It seems, then, that although the separation into a northeastward transport near the coast and a broad southwestward one farther out may be real, their difference was not significantly determined.

NON-GEOSTROPHIC CURRENTS

The geostrophic volume transport through the upper 200 m of Sect. 8, calculated relative to the zero line shown in Fig. 15 between Stas. 5546 and 5552, was 48×10^6 m³/sec. This differs only slightly from the 51×10^6 m³/sec obtained using the 1000-decibar surface as a reference, since the observed components of velocity near 1000 m depth were small. However, it was appreciably smaller than the transport calculated from the directly measured currents, 62×10^6 m³/sec. Comparing the directly measured and geostrophic transports within 50 m depth intervals between each pair of stations, it was found that the discrepancy tended to be greatest near the surface.

The subdivided transports, their differences, and the equivalent mean speed differences are given in Table 1 below.

Table 1. *Transports subdivided in* 50 m *depth intervals, for Sect.* 8 (*offshore from* 8°N) *Stas.* 5546–5552

	Depth interval (m)	*Observed transport* (10^6 m³/sec)	*Geostrophic transport* (10^6 m³/sec)	*Obs. minus geostrophic* (10^6 m³/sec)	*Equivalent mean speed difference* (cm/sec)
	0–50	23·3	16·7	6·6	38
	50–100	17·8	13·8	4·0	23
	100–150	12·5	10·3	2·2	13
	150–200	8·8	6·7	2·1	12
Total	0–200	62·4	47·5	14·9	

Bearing in mind the estimated uncertainties of the direct measurements of current in the upper 200 m, a systematic difference of 12 or 13 cm/sec does not seem significant. The difference of 26 cm/sec between upper and lower layers seems likely to be real, however, since it depends only on the relative observations with the current meters and not on the estimates of surface current. Since the discrepancy was nearly constant in the 100–200 m interval, it seems likely that the components of surface current through the section were on the average 12 cm/sec too high, and that the directly measured transport in the upper 200 m should be reduced to 54×10^6 m³/sec. There remains a

discrepancy of 6·5 $\times$ 10^6 m^3/sec between the directly measured and geostrophic transports, associated with the difference in relative current. This is in the sense to be expected for non-geostrophic transport through the section due to the frictional effect of the local wind on the sea surface. Using the expression given by EKMAN (1905) for the volume transport per unit width of section at right angles to a wind stress, in a uniform deep ocean far from the coast, and assuming a drag coefficient of 0·0024 (WILSON, 1960), the observed r.m.s. wind of 12·5 m/sec from the direction 210°T should cause

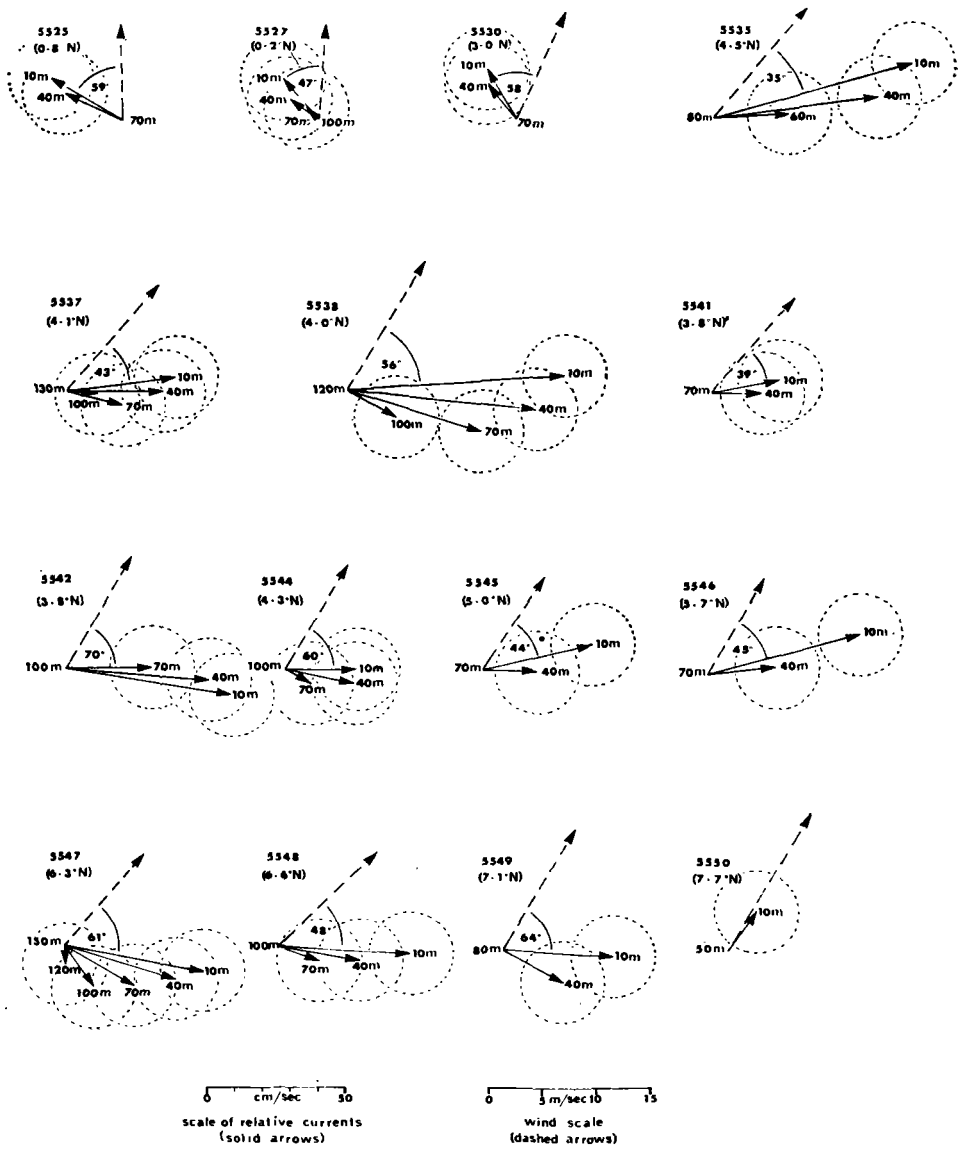


Fig. 16. Relative currents in the nearly isothermal surface layer, at those stations where it was observed, and winds at 10 m height. The depth of the base of the layer is plotted at the origin of the arrows for each station. The dotted circles round each current arrowhead have a radius of 15 cm/sec. (the estimated uncertainty of the relative current vectors).

a transport of $5{\cdot}3 \times 10^6$ m^3/sec between Stas. 5546 and 5552. This may be in error due to neglect of the effects of the coast and of the shallow thermocline, but it agrees fairly well with the observed excess in the directly measured transport.

Taking this excess transport, $6{\cdot}5 \times 10^6$ m^3/sec, as a reasonable estimate of the contribution due to local wind stress, the total northeastwards transport through the section may be obtained by adding this $6{\cdot}5 \times 10^6$ m^3/sec to the geostrophic transport of $64{\cdot}6 \times 10^6$ m^3/sec, calculated for the whole of the section above the reference line shown in Fig. 15. This gives a total of 71×10^6 m^3/sec for the water moving northeastwards through Sect. 8. The accuracy of this figure is difficult to estimate, in view of the assumptions and extrapolations involved. It does not seem sensible to press the data even further and calculate the *net* transport through the section, in view of the uncertain speeds and large cross-sectional area below 1000 m depth.

The effect of the wind could be seen in the current meter profiles at the offshore stations of Sects. 5 and 8, as well as in the transport of the main current itself. As pointed out earlier, there were relatively strong components of current in towards the coast in the depth range 100–150 m, at those stations. Calculations of geostrophic current between pairs of stations such as 5538 and 5546, 5539 and 5545 confirm the inshore flow at 100–150 m but they indicate that the water above that depth range should also have been moving towards the coast at the same speed. The surface water was not observed to be moving so quickly shorewards and was evidently being held off by the wind. In Fig. 16, relative current vectors have been plotted for stations where there was a nearly isothermal upper layer; the current at each chosen level within the layer is plotted relative to that observed at the bottom of the layer. These vectors have been derived from the smoothed relative current profiles, and present a much tidier picture than the individual current observations would have done. However, in so far as one might expect the profiles to be smooth, it seems reasonable to present them in this way. Even allowing an uncertainty of 15 cm/sec on each vector, the general resemblance to parts of Ekman spirals seems fairly convincing, though the magnitude of the uncertainties makes further quantitative investigation seem unwarranted. As a check on the reality of these Ekman spirals, the relative currents in the near-surface mixed layer at stations south of the equator were examined. Although even more scattered, there was a marked tendency for the relative current vectors to lie to the left of the wind.

It may be noticed in Fig. 16 that at the three stations only just north of the equator (5525, 5527 and 5530) the current vectors were to the left of the wind. One might suppose that, since they were in a current that had only recently crossed the equator (within less than 70 hr) they were still showing the effects of wind action south of the equator, and that the time-constant for generating an Ekman spiral in such low latitudes was longer than 70 hr. However, this interpretation seems somewhat uncertain in view of the number of exceptions found earlier elsewhere both north and south of the equator.

SUMMARY AND COMMENTS

The authors are very conscious of the inadequate nature of the current measurements described above. The uncertainties of the surface current estimates, and the brief duration of the current meter observations, are such that their use can only be justified by the great speed of the current and the shortage of other observations in

this area. More uncertainties are brought in by the assumptions and extrapolations needed in calculating transports from the observed currents. In these circumstances, accuracies could not be calculated rigorously, and for the most part the uncertainties quoted are merely the best guess we can make. With so much vague qualification having to be applied to so many of the results, the reader may well be sceptical or confused about their significance, and it seems worthwhile to risk some repetition in summarizing what we think can be concluded from these measurements and what is still uncertain.

The Somali Current was seen to increase in speed and width in the near-surface layers (down to 200 m) as it moved northward from the equator to about 8°N. Speeds exceeded 200 cm/sec near the coast on almost all sections between those latitudes. The highest speeds were found only near the surface, decreasing under the fastest part of the current to one-third the surface value before 200 m depth was reached. These features can be seen clearly in Figs. 6–8.

There was no reason to think that the strong surface currents were abnormal, from the comparison with previous ships' drift observations in Fig. 5.

The turning of the current to the east near 9°N, and the evidence for parts of two clockwise circulations separated by a sharp boundary, are shown in Figs. 2–4. The agreement between the observed currents and the dynamic topography relative to 1000 decibars suggests that the flow was mainly geostrophic and that currents at a depth of 1000 m were generally weak compared to the strong surface currents. The same conclusion can be drawn from comparison of the directly measured and geostrophic transports for the depth range 0–200 m shown in Figs. 10 and 11. The increase in transport along the current was supplied partly from offshore and partly from below 200 m. The current was not steady enough for vertical transport to be determined by continuity.

Although currents were weaker below 200 m they were not negligible. Appreciable northeastwards flow was found only under the strongest parts of the surface current, and even there it appeared to be limited to depths less than 1000 m. There was evidence of southwestward movement at 1000 m under the strong surface current, from one direct observation at Sta. 5571, and indirectly at Sta. 5535, but these are not enough to exclude the possibility of some northeastward flow at that depth. We know that there could be considerable small-scale variability; the two neutrally buoyant floats used at Sta. 5571 were separated only 7 km horizontally and less than 100 m vertically, yet their mean velocities differed by 14 cm/sec. Many more measurements would be needed for an adequate description of the flow at intermediate depths in this area.

Despite their variability, those two float observations were used, together with four others, to define reference velocities for geostrophic profiles in the section across the strongest part of the Somali Current, near 8°N (Figs. 14 and 15). The geostrophic transport towards the northeast, for that part of the section above the fitted reference line, was $64{\cdot}6 \times 10^6$ m^3/sec. The transport of subtropical subsurface water, with dissolved oxygen content exceeding 3 ml/l., was $4{\cdot}5 \times 10^6$ m^3/sec through this section. The fitted velocity profiles were, however, too uncertain for significant estimates to be made of the net flow of the high-salinity water from the Gulf of Aden, or of the deep water below 2000 m.

The difference between the geostrophic and directly measured transport in the upper 200 m of the above section could not all be accounted for by likely systematic

errors in the current measurements. There remained an excess of $6{\cdot}5 \times 10^6$ m^3/sec, of the order of magnitude and in the sense to be expected from the frictional effect of the local wind. Adding this to the geostrophic transport gave 71×10^6 m^3/sec as the total northeastwards transport through the section. Of this, 54×10^6 m^3/sec passed through the upper 200 metres.

The effect of the local wind could also be seen in the relative currents, resembling Ekman spirals, at those stations where there was a nearly isopycnal near-surface layer (Fig. 16).

We have no direct evidence about the movement of deep water below 2000 m. Measurements of long duration, closely spaced under the strong surface current, are needed in the deep and intermediate water; moored current meters with deeply submerged buoyancy could be used. In view of the difficulty of anchoring surface buoys in a current that may exceed 6 knots, near-surface current measurements might best be made using drifting arrays of current meters, but their success would depend on improvements in aids to navigation in that area.

Acknowledgements—The authors are indebted to many colleagues among the scientists, officers and crew of both ships for their helpful cooperation in making observations in this unusually strong current. Provision of equipment to the *Discovery* by the Fisheries Laboratory, Lowestoft, and by the Geophysical Institute, Bergen, is gratefully acknowledged. Much of the reduction of the *Discovery's* current meter and water sampling observations has been done by Miss J. CLEEVE and Mr. C. L. GULLIVER. Work by the *Argo* and the preparation of that data for the paper was sponsored by grants from the National Science Foundation.

REFERENCES

CARTWRIGHT D. E. and A. J. WOODS (1963) Measurements of upper and lower tidal currents at Banc de la Chapelle. *Dt. hydrogr. Z.* **16**, 64–76.

EKMAN V. W. (1905) On the influence of the earth's rotation on ocean-currents. *Ark. Mat. Astr. Fys.* **2**, (11), 1–52, 1 plate. (Reprinted 1963, Royal Swedish Academy of Science, Stockholm).

FINDLAY A. G. (1866), *A directory for the navigation of the Indian Ocean.* London: Richard Holmes Laurie, 1062 pp.

FOXTON P. (1965) A mass fish mortality on the Somali Coast. *Deep-Sea Res.* **12**, 17–19.

KONINKLIJK NEDERLANDS METEOROLOGISCH INSTITUUT (1952) *Indische Oceaan. Oceanografische en Meteorologische gegevens.* 2nd Edition. Publication No. 135, Vol. 1, Text 31 pp. Vol. 2, 24 charts.

MICHAELIS G. (1923) Die Wasserbewegung an der Oberfläche des Indischen Ozeans im Januar und Juli. *Veröff. Inst. Meeresk. Univ. Berl.* n.f., Ser. A, No. 8, 32 pp.

SCHOTT G. (1943) Nachtrag zu dem Aufsatz "Die Grundlagen einer Weltkarte der Meeresströmungen." *Annln Hydrogr. Berl.* **71**, 281–282, Hierzu Tafel 22.

STANBROUGH J. H. and D. P. KEILY (1964) Long-range navigation by means of VLF transmissions. *Deep-Sea Res.* **11**, 249–255.

STOMMEL H. and W. S. WOOSTER (1965) Reconnaissance of the Somali current during the southwest monsoon. *Proc. natn. Acad. Sci. U.S.A.* **54**, 8–13.

SWALLOW J. C. and L. V. WORTHINGTON (1961) An observation of a deep counter-current in the Western North Atlantic. *Deep-Sea Res.* **8**, 1–19.

WARREN B., H. STOMMEL and J. C. SWALLOW (1966) Water masses and patterns of flow in the Somali Basin during the southwest monsoon of 1964. *Deep-Sea Res.* **13**, 825–860 (this issue).

WILSON B. W. (1960) Note on surface wind stress over water at low and high wind speeds. *J. geophys. Res.* **65**, 3377–3382.

Reprinted from *J. atmos. Sci.*, vol. 23, no. 6, 1966, p. 712-719

The Mean Wind Structure over Bahrein and Aden in 1962[1]

A. H. GORDON

University of Hawaii, Honolulu

(Manuscript received 11 July 1966)

ABSTRACT

The mean upper wind structure over Bahrein and Aden in 1962 is studied. Patterns of the zonal and meridional wind speed components are presented. Eddy and advective fluxes of the momentum are calculated and mean annual height profiles drawn for both stations. The transport of momentum by synoptic scale eddies is more important at Bahrein than at Aden. Transport of momentum by the local mean meridional wind is larger in magnitude and fluctuates in an irregular way from month to month at both stations. The vertical integral of the momentum suggests export of relative momentum from the Bahrein-Aden sector in winter and import in summer. These conclusions are supported by 1963 data from the Ahmadabad-Madras sector. In the belt of latitude considered the winter surface winds have an easterly component and gain momentum from the earth while the summer surface winds have a westerly component and lose momentum to the earth. The results of the short period analysis for the sectors studied suggest broad agreement with the synoptic climatology of the region.

1. Introduction

Our knowledge of the structure of the wind in the troposphere and low stratosphere of the Middle East remains incomplete due to the sparseness of upper air reporting stations in the area. This is especially true over the Arabian peninsula. However, the upper air reporting stations at Bahrein (26°16′N, 50°37′E) and Aden (12°50′N, 45°02′E) which are operated by the United Kingdom Meteorological Office fill a big gap in the widely spaced network. The data provide a useful source for the study of the wind field at various pressure levels for each month of the year for two important localities within the tropics. The observations analyzed in this study consisted of the daily components of the wind for the surface, 900, 850, 800, 700, 600, 500, 400, 300, 250, 200, 150, 100, 80 and 60 mb for 0000 and 1200 GMT for each month of the year 1962 for Bahrein and Aden. The daily values of the meridional and zonal wind components and the mean monthly values for each of the two reporting hours had been tabulated by electronic computer and these were available for the calculation of profiles of the meridional and zonal wind and of the eddy and advective fluxes of momentum for each month for both stations.

Ninety per cent of the observations reached at least 200 mb. Above 100 mb the number of observations decreased to 50 per cent or less of the maximum possible. Since Bahrein and Aden are separated by only 5°35′ of longitude it was conveniently approximated that both stations lie along the same meridian for the purpose of representing the variation of wind and momentum with latitude within this sector of Arabia.

[1] Hawaii Institute of Geophysics Contribution No. 155.

2. Mean zonal wind

Bahrein is located at the approximate latitude at which the subtropical jet stream reaches its maximum southward limit in January. It also lies within the influence of the summer upper easterly wind belt. Fig. 1 shows the isotach pattern of the mean westerly wind as a function of height throughout the year for this sta-

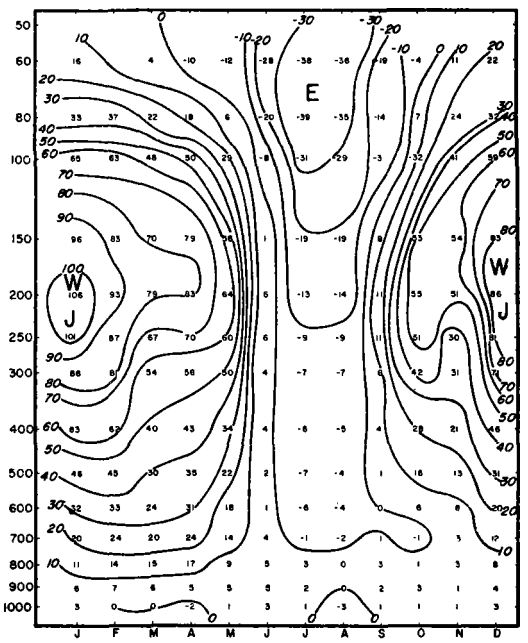


FIG. 1. Mean zonal wind speed at Bahrein in 1962 (kt).

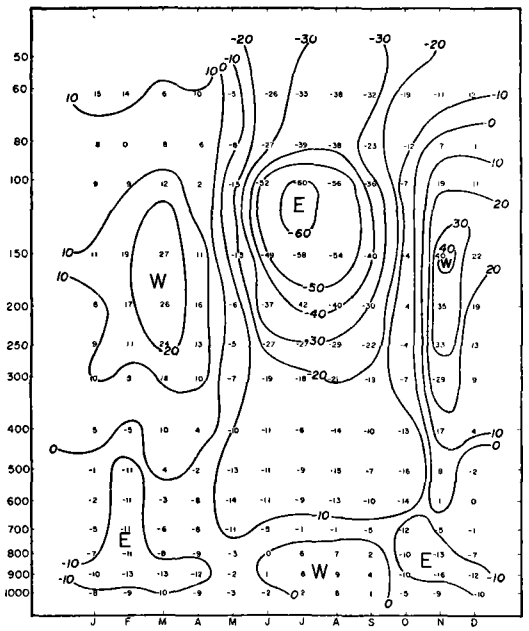


FIG. 2. Mean zonal wind speed at Aden in 1962 (kt).

tion. It is noted that the westerly subtropical jet stream reaches a maximum of over 100 kt at 200 mb in the winter months. During the winter period westerlies extend throughout the whole of the troposphere and lower stratosphere. In summer, easterlies extend upward from 700 mb reaching a maximum in July and August at or above 60 mb. There is a sharp decrease in the mean zonal component of the westerly jet between May and June and a rapid increase between September and October. The abruptness of the transition between premonsoon and summer monsoon conditions over the Indian subcontinent and surrounding oceans has been described by Raman and Dixit (1963) and other authors.

Fig. 2 shows the mean zonal component of the wind for Aden for 1962. The mean zonal wind structure reflects to some extent the general pattern observed at Bahrein but there are important differences. The upper tropospheric westerly is very much weaker than at Bahrein and the maximum isotach is only 20 kt. The summer easterly wind has reached jet stream intensity at this latitude with the core at about 125 mb, somewhat lower than at Bahrein. There is also a change in the lower troposphere where easterly winds exist from the surface to at least 600 mb in winter, whereas there is a transition to a westerly regime below 700 mb in summer.

3. Mean meridional wind

Several workers (Palmén and Vuorela, 1963; Tucker, 1959; and others) have integrated the meridional component of the wind around parallels of latitude throughout the vertical extent of the atmosphere and shown that a Hadley cell circulation exists within the tropics. The Hadley cell is usually described as a mean circulation in the vertical meridional plane extending to about 30 deg latitude on either side of the equator. This mean circulation has been averaged, mainly in the Northern Hemisphere, over time periods ranging from a day to several years. Such cells show upward vertical motion in the vicinity of the equator, a southerly mean meridional flow in the upper troposphere, downward vertical motion within the subtropics and a returning northerly mean meridional flow in the lower troposphere. The quantitative derived circulation is supported by the existence of the equatorial rain belts and subtropical deserts.

The time-averaged meridional component of the wind at single stations does not necessarily imply a Hadley cell type circulation. For example, there might on a given day, or during a period of some days, be an upper-level anticyclone to the east of the station overlying a low-level cyclone. Such a vertical distribution of the pressure field would create a meridional circulation in the Hadley sense, but it would not contribute to the mean meridional circulation when averaged around the globe. However, it is unlikely that such pressure distributions would remain for a period as long as a month. Thus, the mean meridional wind averaged over a month at single stations may well contribute to the Hadley cell circulation. The mean meridional structure at Bahrein and Aden may be regarded in this light.

Fig. 3 shows the mean meridional wind structure over

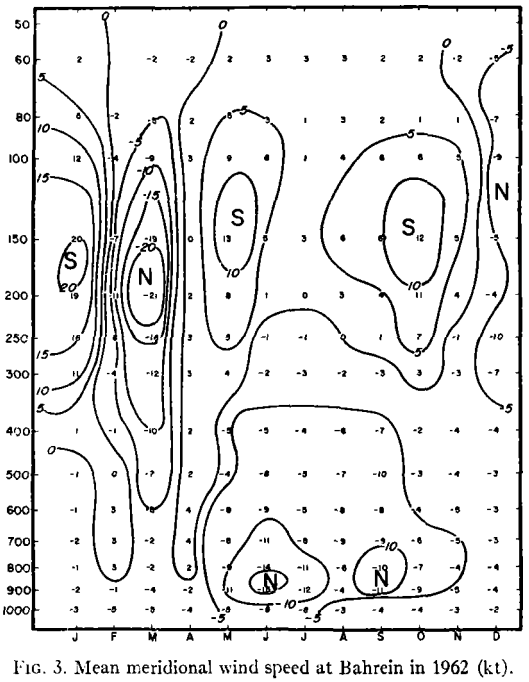


FIG. 3. Mean meridional wind speed at Bahrein in 1962 (kt).

Bahrein in 1962. From May to November a definite meridional circulation exists. During the remaining months considerable variations occur. Thus, in January, there is a light northerly component up to 400 mb which is overlain by a strong southerly component with a maximum at about 175 mb. In February and March the meridional wind in the upper troposphere and lower stratosphere is northerly. In March and December it is northerly throughout the whole column up to 60 mb. The meridional wind structure at Aden shown in Fig. 4 exhibits a toroidal (Hadley cell) regime. At Aden the maximum speeds of the low-level northerly branch are found at 600 mb as compared to Bahrein where the maximum low-level northerlies occur at about 850 mb. Maximum southerlies occur at about the same levels as at Bahrein. Below 900 mb, southerly components blow throughout the year at Aden and these extend to about 850 mb in summer. The upward extension of the surface layer westerlies is accompanied by an upward extension of the levels of the overlying low tropospheric northerlies. In March and December northerly components blow at Aden at all levels and no meridional cell circulation appears for that year.

4. Meridional fluxes at single stations

Priestley (1949) undertook an investigation of the meridional flux of heat, water vapor and momentum for Larkhill on Salisbury Plain in southwest England for the years 1946 and 1947. His purpose was to draw attention to the method and to appeal for a global investigation. Since that time research into the general circulation has advanced to a state where global projects have been undertaken on a large scale. Among those responsible are Mintz (1951), Palmén (1951), Starr (1951), Starr and White (1952a, b), Chiu and Crutcher (1965), and many others. The quantities originally calculated for one or two isolated stations have now been integrated around parallels of latitude and with height on a hemispheric or global scale. Nevertheless, as Priestley (1949) rightly remarked, global projects are too formidable for one or two individuals to undertake. However, useful knowledge can still be extracted from investigations into the quantities which prevail at one or two stations from which accurate upper air observations can be obtained. Consequently, there remains a need to make individual analyses of upper air circulations.

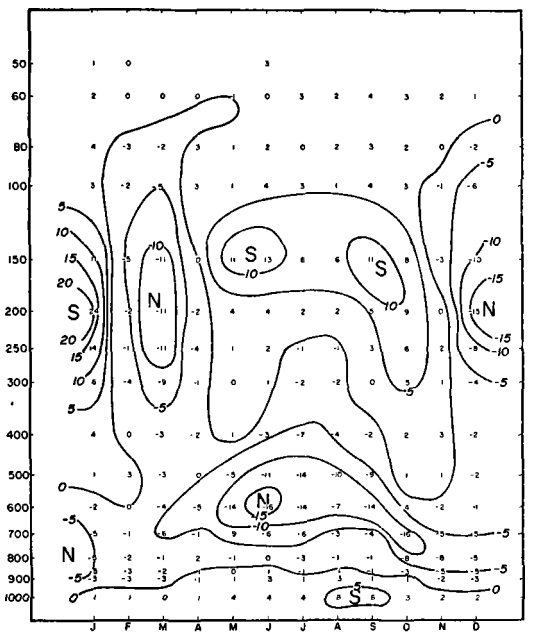


FIG. 4. Mean meridional wind speed at Aden in 1962 (kt).

5. Eddy flux of momentum

The study of the transport of the angular momentum of the atmosphere can be carried out by the use of the perturbation relations. For example, the absolute angular momentum of the air may be written

$$m = a\cos\phi(u + \Omega a\cos\phi), \tag{1}$$

where a is the radius of the earth, ϕ the latitude, Ω the angular velocity of the earth's rotation and u the velocity of the wind along a parallel of latitude measured positively towards the east. The term $au\cos\phi$ is the relative momentum while the transport of relative momentum along a meridian, positive toward the pole, and negative toward the equator, may be expressed by $uva\cos\phi$ in the Northern Hemisphere.

Now the instantaneous velocities u, v along the x and y axes, respectively, may be expressed in the form

$$\left.\begin{aligned} u &= \bar{u} + u' \\ v &= \bar{v} + v' \end{aligned}\right\}, \tag{2}$$

where the overbar represents the time average over a month, and the prime notation signifies the variation of each individual observation from the mean value. Then the sum of the individual values of the transport of the relative momentum is given by the expression

$$\Sigma uva\cos\phi = \Sigma(\bar{u}\bar{v} + u'v')a\cos\phi, \tag{3}$$

and the average total monthly transport by the relation

$$\overline{uv} = \bar{u}\bar{v} + \overline{u'v'}. \tag{4}$$

The term on the left hand side of (4) represents the flux of the relative momentum at some selected level or within a chosen layer of the atmosphere expressed in $cm^2\ sec^{-2}$ or kt^2. The first term on the right hand side represents the northward flux of zonal momentum by the local mean meridional wind while the second term on the right hand side represents the local eddy flux of zonal momentum.

If (4) is integrated throughout the vertical extent of the atmosphere and p_0 is the surface barometric pressure, the term $\int_{p_0}^{p} \overline{uv}dp$ expresses the flux of relative momentum in gm sec^{-2}. The latter units may also be written as dyn cm^{-1} in which units the vertical integral of the Reynolds stress is expressed.

The flux of relative momentum was calculated for Bahrein and Aden for each month of the year 1962 for the levels listed in the introductory paragraph. Then the eddy flux was found from (4). Fig. 5 shows the eddy flux of momentum averaged for the six 2-monthly periods of 1962 for Bahrein. A cell of poleward flux which is associated with eddies of the period of several days in the subtropical jet stream (Fig. 1), is found at about 150 mb in January and February and at about 250 mb in November and December. The flux in the lower troposphere is directed toward the equator at all times of the year. There is also equatorward flux in May-June between 150 and 200 mb, which is associated with the transition from westerlies to easterlies (Fig. 1). Poleward flux occurs at all periods from 500 to 250 mb. The pattern of the eddy flux of momentum at Aden shown in Fig. 6 is very weak. In contrast to Bahrein the flux at low levels is toward the pole. Maximum flux is toward the equator in the low stratosphere in March-April and November-December. This flux is associated with high level northwesterly winds which occurred during the latter months. Starr and White (1952b) reported a tendency for equatorward transport at high levels at 13N. In Fig. 7 the patterns have been averaged to give a mean annual profile with height. The level of zero transport at Bahrein is about 550 mb and the transport is equatorward below this level and poleward above it. Maximum flux in the mean annual profile is 95 kt^2 at 300

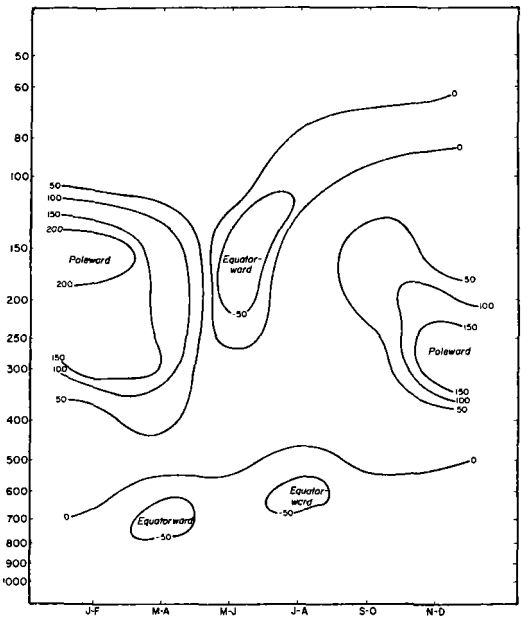


FIG. 5. Eddy flux of momentum at Bahrein in 1962 (kt^2).

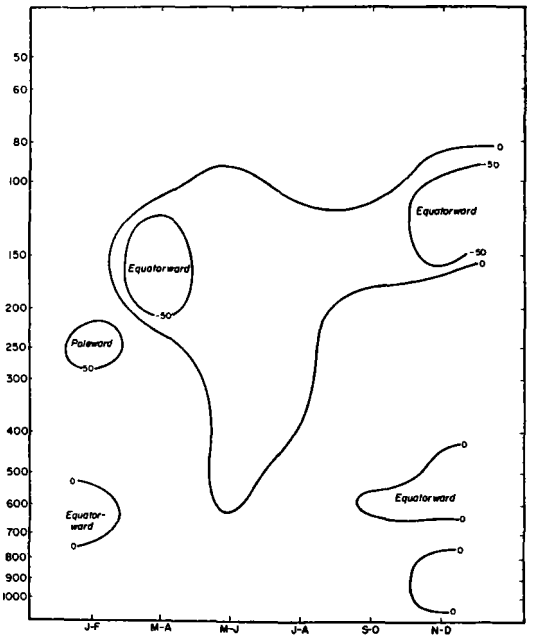


FIG. 6. Eddy flux of momentum at Aden in 1962 (kt^2).

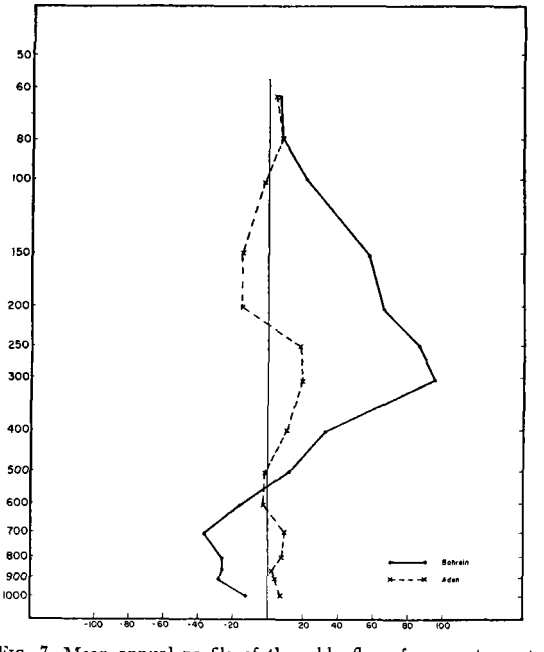


FIG. 7. Mean annual profile of the eddy flux of momentum at Bahrein and Aden in 1962 (kt^2). Positive is poleward.

mb. Conversion to cgs units gives a maximum mean value of 2.5×10^5 cm^2 sec^{-2}. Starr and White (1952a) found a mean winter value of poleward eddy flux of momentum of about 6.2×10^5 cm^2 sec^{-2} at 30N and about 250 mb when averaged around the globe during one year. Tucker (1964) suggests a maximum poleward flux of about 3.8×10^5 cm^2 sec^{-2} at 25N and 300 mb for the winter months averaged over a 2-yr period. The maximum flux at Bahrein, averaged over a month in 1962, was in March at 200 mb with a value of 13.2×10^5 cm^2 sec^{-2}.

The mean annual profile of the eddy flux at Aden is different from that at Bahrein as shown in Fig. 7. The Aden profile shows a poleward flux up to about 225 mb and only a narrow belt of equatorward flux above. The magnitude of the flux is much less than at Bahrein.

6. Advective momentum

The advective momentum flux given by the term $\bar{u}\bar{v}$ was also computed. The month to month patterns are not reproduced here. They are more variable and greater in magnitude when averaged over a month than the eddy momentum flux and closely controlled by the variations in the mean meridional winds (Figs. 3 and 4). Fig. 8 shows the mean annual profiles of advective momentum for Bahrein and Aden for 1962. The profiles below 300 mb show equatorward advection at Bahrein and poleward advection at Aden. The advective flux reaches a maximum toward the equator at Aden at 150 mb. This is brought about by the combination of northwest winds in the spring and winter months and by southeast winds in the summer months of 1962. In contrast to Aden there is relatively little advection at Bahrein.

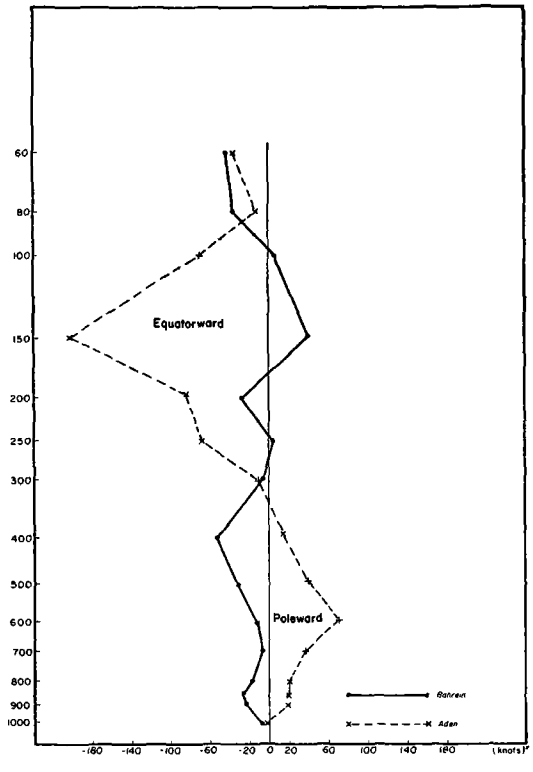


FIG. 8. Mean annual profile of the advective flux of momentum at Bahrein and Aden in 1962 (kt^2).

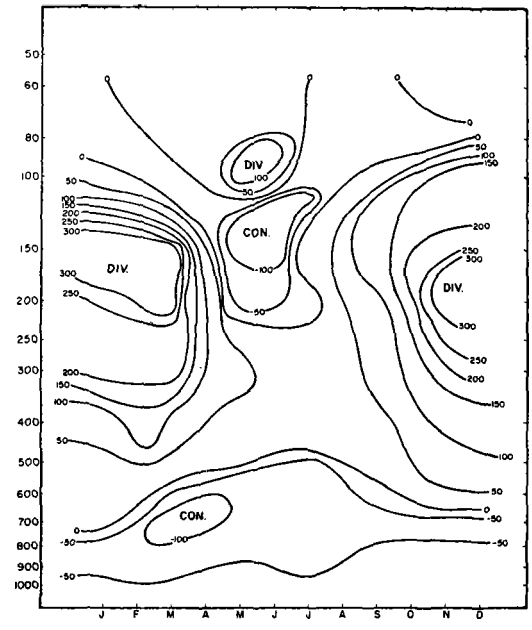


FIG. 9. Divergence of the eddy flux of momentum within the Bahrein-Aden sector in 1962 (10^{-5} cm sec^{-2}).

7. Divergence of momentum

Fig. 9 shows the divergence of the eddy flux of momentum for the Bahrein-Aden sector for 1962. Convergence of flux occurs in the lower troposphere. Centers of maximum divergence occur at about 150 mb in winter. In summer weak divergence overlies the convergence from 500 to 200 mb and a center of convergence is found at about 150 mb. There is some evidence of upward flux in winter whereas in summer the upward flux appears weaker. In 1962 there appears to be some downward flux in May and June in the upper troposphere. The mean annual profile of the divergence of eddy and advective momentum is given in Fig. 10. It is seen that there is low-level convergence and high-level divergence of both fluxes. Such a distribution would give a mean annual upward vertical transport of both fluxes. A study of the mean meridional wind patterns in Figs. 3 and 4 shows that the advection of the Earth's momen-

tum within the sector would also give rise to a mean annual upward transport. However, these conclusions may be limited by the neglect of variations of the wind with longitude due to the fact that the two stations do not lie exactly along the same meridian.

8. The vertical integral of the momentum flux

The patterns of the momentum fluxes illustrated in Figs. 5–10 are based on values computed for selected levels. However, if the vertical integrals of the fluxes throughout the atmospheric column at Aden and Bahrein are subtracted from one another the difference will give the total import or export of momentum within the sector. If this difference is divided by the meridional distance between the two stations the frictional stress needed to balance the divergence of momentum may be obtained. This stress exports westerly momentum from the earth to the atmosphere if the surface wind is easterly and imports momentum from the earth to the atmosphere if the surface wind is westerly.

Table 1 gives the values of $\int_{1010}^{60} \overline{u'v'}dp$ and $\int_{1010}^{60} \bar{u}\bar{v}dp$ for Bahrein and Aden for each month of the year. The units are dyn $cm^{-1} \times 10^8$. On the average, frictional dissipation of excess momentum by surface westerly winds tended to balance the import of momentum from the earth by the deceleration of easterly winds.

9. Comparison with the Ahmadabad-Madras sector

Advective and eddy fluxes of momentum were also computed for a sector within the Indian subcontinent. The two stations used were Ahmadabad (23°04′N, 72°38′E) and Madras (13°00′N, 80°11′E). It was desired, in particular, to compare the divergence of the vertical integrals of momentum between the latter two stations with the divergence between Bahrein and Aden and to evaluate the momentum balance in terms of frictional stress of the surface winds.

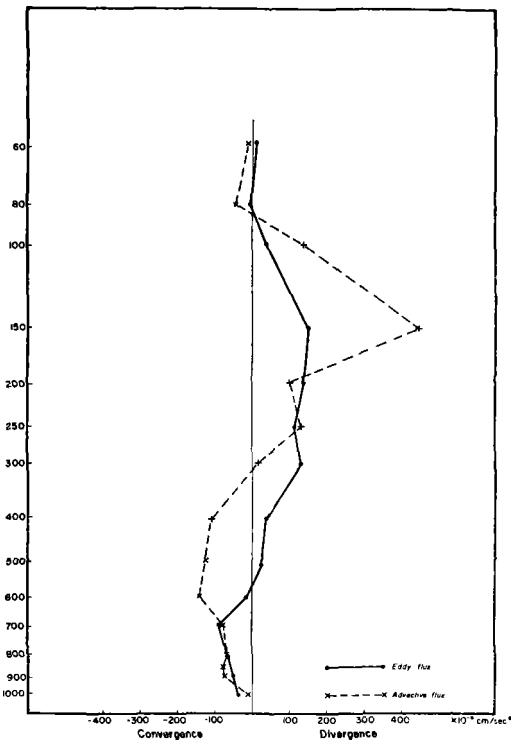


FIG. 10. Mean annual profile of the divergence of the eddy and advective fluxes of momentum within the Bahrein-Aden sector in 1962 (10^{-5} cm sec^{-2}).

The data used for Ahmadabad and Madras were collected during the period of the International Indian Ocean Expedition and were equivalent in quality and

TABLE 1. Vertical integral of the eddy and advective momentum fluxes for Bahrein and Aden, 1962. Units are dyn $cm^{-1} \times 10^8$.

	Bahrein		Aden	
	$\int_{1010}^{60} \overline{u'v'}\,dp$	$\int_{1010}^{60} \bar{u}\bar{v}\,dp$	$\int_{1010}^{60} \overline{u'v'}\,dp$	$\int_{1010}^{60} \bar{u}\bar{v}\,dp$
January	0.0	10.2	0.3	1.1
February	2.3	−3.3	0.3	−0.1
March	2.6	−9.4	0.7	−1.3
April	−1.5	2.1	−0.2	−0.1
May	−0.8	1.4	−0.2	0.6
June	0.2	−0.8	0.1	−1.2
July	−0.6	−0.1	0.1	0.1
August	−0.4	−0.1	0.5	0.4
September	0.1	−0.3	0.3	−0.4
October	−0.3	2.2	−0.1	0.5
November	−0.6	0.1	−0.2	0.5
December	2.1	−7.1	−0.1	−0.8
Mean	0.3	−0.4	0.1	−0.1
Export		0.2×10^8 dyn cm^{-1} eddy momentum		
Import		0.3×10^8 dyn cm^{-1} advective momentum		

TABLE 2. Vertical integral of eddy and advective fluxes of momentum at Ahmadabad and Madras in 1963. Units are dyn $cm^{-1} \times 10^8$. Values in parentheses refer to the station with approximate corresponding latitude in the Arabian sector.

	Ahmadabad		Madras	
	$\int_{1000}^{100} \overline{u'v'}\, dp$	$\int_{1000}^{100} \bar{u}\bar{v}\, dp$	$\int_{1000}^{100} \overline{u'v'}\, dp$	$\int_{1000}^{100} \bar{u}\bar{v}\, dp$
January	2.1 (0.0)	9.0 (10.2)	0.1 (0.3)	1.5 (0.1)
April	1.9 (−1.5)	−1.5 (2.1)	0.6 (−0.2)	0.1 (−0.1)
July	0.1 (−0.6)	−0.2 (−0.1)	−0.1 (0.1)	0.5 (0.1)
October	0.1 (−0.3)	−0.2 (2.2)	−0.1 (−0.1)	0.5 (0.5)
Mean	1.1 (−0.6)	1.8 (3.6)	0.1 (0.0)	0.7 (0.2)

detail to the observations used for Bahrein and Aden, but the periods used were different (January, April, July, October, 1963).

Table 2 shows the values of $\int_{1000}^{100} \overline{u'v'}dp$ and $\int_{1000}^{100} \bar{u}\bar{v}dp$ for the latter four months at Ahmadabad and Madras, where the values in parentheses refer to the stations with corresponding latitudes in the Arabian sector (Bahrein corresponding with Ahmadabad and Aden with Madras, respectively), for 1962. Table 3 compares the total (frictional) stress for both sectors in each of the four months.

The greatest frictional stress occurs in January for both sectors. The mean stress for the year, probably fortuitously, is the same for both sectors when computed for the four months concerned. However, the close agreement suggests that the frictional stress computed for this region is of the right sign when averaged over several comparable months. The maximum net divergence of momentum occurs in winter while in summer there is slight net convergence. This agrees with the synoptic climatology of the region. The northeast winter monsoon gains momentum from the earth while the summer southwest monsoon loses momentum to the earth. The results indicate that there is a net annual gain of earth momentum to the sector and that much of this import is transferred upward to the upper troposphere and lower stratosphere where it is exported.

10. Conclusion

The upper wind structure within the Bahrein-Aden sector in 1962 shows evidence of meridional circulations during much of the year at Bahrein and at Aden. The eddy flux at Bahrein shows a belt of equatorward flux in the lower troposphere for all months in 1962. Strong cores of poleward flux occur at 150–200 mb in the winter while equatorward flux occurs in the high troposphere and low stratosphere in summer. The eddy flux of momentum is much weaker at Aden than at Bahrein. The divergence of the eddy momentum flux suggests upward vertical flux predominating within the sector, particularly in winter.

TABLE 3. Total stress (dyn cm^2) in the Arabian and Indian sectors.

	Arabian sector	Indian sector
January	5.9	8.5
April	0.2	−0.4
July	−0.3	−0.3
October	1.5	−0.8
Mean	1.8	1.8

The advective term is larger and more variable than the eddy term but the mean annual divergence profile of advective momentum also indicates upward vertical transfer. The total momentum balance indicates that momentum is gained from the earth in winter due to the frictional stress of the surface westerlies. These conclusions agree with the synoptic climatology of the region which suggests a mean surface easterly wind in winter and a mean surface westerly wind in summer. The magnitude of the frictional stress may serve, therefore, as a measure of the zonal wind strength at the surface.

The flux of momentum by synoptic scale eddies of the subtropical jet stream appears to be the more systematic and regular process for transporting momentum poleward at Bahrein. Transport in both directions by the meridional wind is irregular and tends to cancel out. At Aden the transport of momentum by eddies is less important. This result agrees with the conclusions of Tucker (1964) and others that the transport of momentum by eddies becomes greater with increasing latitude in the tropics.

The conclusions drawn for the Bahrein-Aden sector are supported by the results of the Ahmadabad-Madras sector which exhibit the same broad features for the four months analyzed.

REFERENCES

Chiu, W. C., and H. L. Crutcher, 1965: The spectra of angular momentum transfer in the atmosphere. *J. Geophys. Res.*, **71**, 1017–1032.

Mintz, Y., 1951: The geostrophic poleward flux of angular momentum in the month of January 1949. *Tellus*, 3, 195–200.

Obasi, G. O. P., 1963: Poleward flux of atmospheric angular momentum in the Southern Hemisphere. *J. Atmos. Sci.*, **20**, 516.

Palmén, E., 1951: A note on the eddy transport of angular momentum. *Quart. J. R. Meteor. Soc.*, **77**, 44–50.

——, and L. A. Vuorela, 1963: On the mean meridional circulations in the Northern Hemisphere during the winter season. *Quart. J. R. Meteor. Soc.*, **89**, 131–138.

Priestley, C. H. B., 1949: Heat transport and zonal stress between latitudes. *Quart. J. R. Meteor. Soc.*, **75**, 28–32.

Raman, C. R. V., and C. M. Dixit, 1963: Analyses of monthly mean resultant winds for standard pressure levels over the Indian Ocean and adjoining continental areas. *Proc. Symposium Trop. Meteor.*, Rotorua, New Zealand, 107–118.

Starr, V. P., 1951: A note on the eddy transport of momentum. *Quart. J. R. Meteor. Soc.*, **77**, 44–50.

——, and R. M. White, 1952a: Seasonal variation of the meridional flux of angular momentum. *Quart. J. R. Meteor. Soc.*, **78**, 62–69.

——, and ——, 1952b: Meridional flux of angular momentum in the tropics. *Tellus*, **4**, 118–125.

Tucker, G. B., 1959: Mean meridional circulations in the atmosphere. *Quart. J. R. Meteor. Soc.*, **85**, 209–224.

——, 1964: Zonal winds over the equator. *Quart. J. R. Meteor. Soc.*, **90**, 405–423.

——, 1965: Equatorial tropospheric wind regime. *Quart. J. R. Meteor. Soc.*, **91**, 140–150.

Part IV

Marine geology and geophysics

Reprinted from *Curr. Sci.*, vol. 33, no. 22, 1964, p. 685

SUBMARINE CANYONS OFF MADRAS COAST

IN the recent 15th Scientific Cruise of INS KISTNA (June 8–20, 1964), as part of the International Indian Ocean Expedition Programme, the writer participated in geological exploration. A series of submarine canyons were identified and interpreted from the echograms taken with an Edo Echosounder. These stretch to a distance of about 45 nautical miles across, off the coast of Madras (between 12° 13′ 30″ N, 80° 20′ E. and 11° 30′ N, 79° 58′.)—between 35 miles northeast of Pondichery and 12 miles east of Porto Novo. It is known that in this region the 100-fathom line bends near to the coast in several places (Shepard, 1963, p. 238).

These submarine canyons, so far noticed, are in two sets and each consists of hill-like projections and V-shaped valleys. The height of the ridges ranges from 300–2,400 feet and the V-shaped valleys range from 30–2,550 feet from a depth of 50–250 fathoms below the sea-level.

The first series, consisting of four hill-like projections and two big and five small V-shaped valleys, covers a distance of about 18 nautical miles. One of the hill-like projections is 1·85 nautical miles wide whereas one of the two big V-shaped valleys is 2,550 feet deep and approximately 2½ nautical miles wide. This is followed by a flat but a deeply inclining shelf, giving rise to the second series which consists of four hill-like projections, and five V-shaped valleys. One of the flat-topped, steep-sided hills is 1·65 nautical miles wide and 2,400 feet high.

Several theories have been put forward regarding the origin of submarine canyons. They are attributed to diastrophism, faulting, erosion during a vast lowering of sea-level, and action of turbidity currents especially during Pleistocene times (Kuenen, 1938; Dietz, 1953). But, in recent years, most of the theories have been discredited, 'leaving only the turbidity current hypothesis and another which combines subærial erosion with drowning and maintenance of the canyons by turbidiy currents, submarine slides, and sand flowes' (Shepard, 1963, p. 337).

However, a detailed investigation of these canyons is necessary before their exact relationship to the continental shelf could be explained.

Particular thanks are due to Dr. N. K. Panikkar, Director, Indian Programme, International Indian Ocean Expedition, for providing the writer an opportunity to participate in the 15th Scientific Cruise of INS KISTNA and to Commander Maitra and ships officers for their assistance.

M. G. ANANTHA PADMANABHA SETTY.*
Indian Ocean Physical
Oceanographic Centre,
Ernakulam (India), *September* 25, 1964.

* Now at Department of Geology, Central College, Bangalore 1.

1. Dietz, R. S., *Bull. Geol. Soc. Amer.*, 1953, **64**, 375.
2. Kuenen, Ph.H., *Geol. Mag.*, 1938, **75**, 241.
3. —, *Marine Geology*, John Wiley & Sons, N.Y., 1950, p. 485.
4. Shepard, F. P., *Submarine Geology*, II Ed., Harper & Row, N.Y., 1963, p. 557.

Okeanologia, vol. V, no. 6, 1965, p. 993-998

Г. Б. УДИНЦЕВ

НОВЫЕ ДАННЫЕ О СТРОЕНИИ ДНА ИНДИЙСКОГО ОКЕАНА

Институт океанологии АН СССР

В результате работ 36-го рейса «Витязя» [1] получен комплекс сведений, характеризующих различные тектонические зоны Индийского океана. Ранее уже делались попытки тектонического районирования этого океана, например, Белоусовым на его известных тектонических картах Мира [1, 2], Хаиным [7], в последние годы Хейзеном и Тарп [8], а также автором этой статьи на «Тектонической карте Евразии» [5] и на карте тектоники Мира в «Физико-географическом Атласе Мира» [6]. Теперь для решения задачи тектонического районирования Индийского океана имеется значительно больше данных — они создают основу для классификации структур океанского дна по комплексной геолого-геофизической характеристике земной коры. Возможно, что последующее изучение собранных материалов поможет дальнейшей разработке проблемы Гондваны.

Предварительное рассмотрение материалов 36-го рейса, собранных большим коллективом исследователей, и анализ материалов, накопленных ранее другими исследователями, советскими и зарубежными, позволяет сейчас сделать некоторые выводы в отношении тектоники дна Индийского океана. Важнейшими структурными зонами океана нам представляются (рис. 1):

а) океанические плиты или монократоны, являющиеся наиболее устойчивыми частями океанических платформ или талассократонов, и испытавшие преимущественно нисходящие вертикальные движения. Монократоны слагают дно котловин Индийского океана (Центральной, Западно-Австралийской и др.) и противостоят разновозрастным платформам материков, областям кайнозойской складчатости и современным геосинклиналям, как области, не испытавшие в последние этапы геологической истории геосинклинального развития. Монократоны Индийского океана разновозрастны, ибо одни из них развились сравнительно недавно на месте древних материковых платформ, другие существуют длительное время. Как известно, гравитационное поле в пределах монократонов характеризуется положительными аномалиями в редукции Буге. Магнитное поле в их пределах имеет неспокойный характер. Тепловой поток из недр Земли примерно соответствует тепловому потоку на материковых платформах. Земная кора состоит из так называемого «базальтового» слоя (скорости сейсмических волн порядка 6,7 *км/сек*) мощностью 4—6 *км*, перекрываемого «вторым» или «надбазальтовым» слоем (скорости сейсмических волн порядка 5 *км/сек*) мощностью 1—3 *км*. Мощность покрова рыхлых осадков подвержена резким колебаниям: от 200 до нескольких десятков метров, а местами рыхлые осадки отсутствуют. Однако вблизи материков мощность рыхлого осадочного покрова возрастает до 1,5—2,5 *км*. Подкоровой слой под моно-

[1] Информационная статья о 36-м рейсе «Витязя» печатается в этом номере журнала.

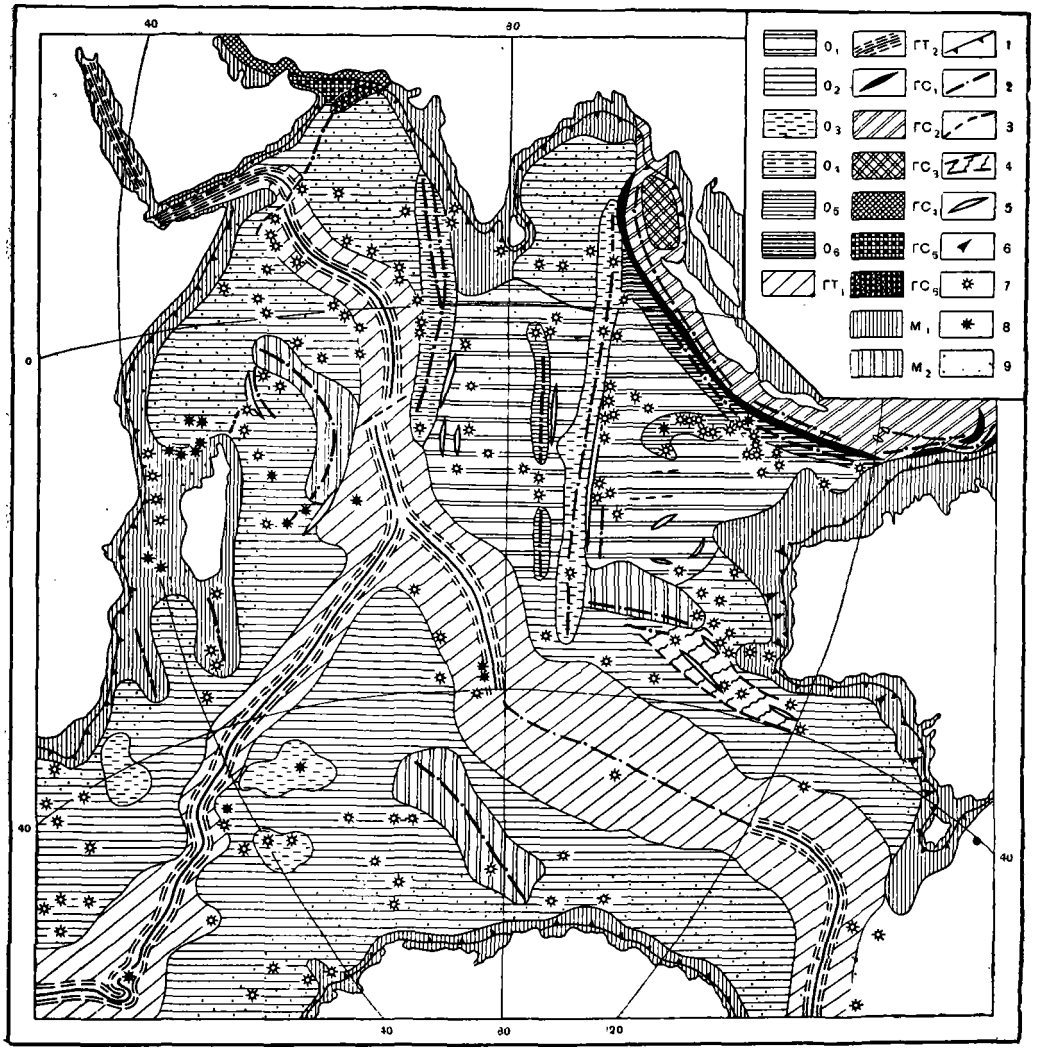


Рис. 1. Тектоническая схема Индийского океана (составили В. Ф. Канаев и Г. Б. Удинцев)

Океанические платформы (талассократоны): O_1 — древние допалеозойские океанические плиты (монократоны); O_2 — океанические плиты (монократоны), возникшие в палеозое и мезозое; O_3 — глыбовые хребты (горсты) с вулканическими надстройками; O_4 — глыбовые хребты (горсты) с коралловыми надстройками; O_5 — сводовые поднятия (валы); O_6 — краевые сводовые поднятия (валы). Геотафрогенальные зоны: $ГТ_1$ — геотафрогенальные хребты (срединноокеанические хребты); $ГТ_2$ — рифтовые зоны (современные геотафрогенали). Кайнозойские и современные геосинклинальные зоны. Океанические геосинклинали (ортогеосинклинали); $ГС_1$ — краевые океанические геосинклинальные желоба (эвгеосинклинали); $ГС_2$ — подводные части складчатых систем (островных дуг); $ГС_3$ — окраинные котловины (миогеосинклинали). Краевые геосинклинали (парагеосинклинали). $ГС_4$ — паралиагеосинклинали (аккумулятивные шельфы); $ГС_5$ — аккумулятивные шлейфы (миогеосинклинали). Материковые платформы (геократоны). $М_1$ — подводные части материковых эпимезозойских платформ различного возраста (макрократоны); $М_2$ — подводные части фрагментарных эпимезозойских платформ различного возраста (микрократоны). Обозначения элементарных структур: *1* — край материковой отмели (шельфа); *2* — оси валов и хребтов; *3* — элементарные разломы; *4* — зоны разломов; *5* — желоба — разломы (авлакогены); *6* — каньоны; *7* — подводные вулканические конусы; *8* — подводные вулканические конусы с надводной вершиной; *9* — осадочной покров повышенной мощности

кратонами характеризуется скоростями сейсмических волн порядка 8,1—8,3 *км/сек.*;

б) океанические хребты глыбовой структуры или асейсмические хребты по терминологии ряда зарубежных исследователей [8]. Это узкие и высокие поднятия, возвышающиеся над монократонами на сотни и даже тысячи метров. Длина их резко превышает ширину. Очертания их очень близки к прямолинейным, а в некоторых случаях, как например, Восточно-Индийский хребет, поразительно прямолинейны. Видимо, это структуры типа горстов. Весьма типичны структуры «асимметричных гребней» — сочетания взброшенного гребня со сброшенным вниз краем плиты. С глыбовыми хребтами часто сочетаются проявления вулканизма, и вследствие этого часто трудно решить, какая часть их сформирована глыбовыми дислокациями, а какая — вулканическими процессами. В строении коры под ними принимают участие сравнительно маломощный (несколько сотен метров) покров рыхлых осадков или коралловых толщ, «второй» слой мощностью 2—4 и «базальтовый» слой мощностью 4—7 *км*. С краевыми разломами этих хребтов связаны аномалии суммарной напряженности магнитного поля. Сведения о существовании корней под этими хребтами разноречивы. Неясен вопрос о их возрасте. Они могут быть либо остатками древних материковых глыб, либо типичными океаническими образованиями;

в) современная Зондская геосинклинальная зона, включающая Зондский краевой океанический геосинклинальный желоб, складчатые пояса Зондской островной дуги и глубокие геосинклинальные котловины краевых морей. Эти структуры типа крупных складок земной коры осложнены по своим крыльям многочисленными разломами и сбросами, а по внутренним крыльям складчатых поясов и вдоль сводов антиклинальных поднятий — вулканическими сооружениями. Особенно крупные разломы протягиваются вдоль внутреннего крыла складчатых зон, отмечаемые аномалиями физических полей Земли. Дно геосинклинальных желобов и котловин является областью интенсивного осадконакопления. Степень компенсации при этом различна и зависит от местных физико-географических условий. Мощность рыхлого осадочного покрова местами достигает 1,5—2,5 *км* и почти компенсирует прогиб северной части Зондского желоба. Различные звенья Зондской островной дуги находятся на разных стадиях геосинклинального развития. Характерно формирование внешнего складчатого хребта, закономерного для зрелой стадии развития многих островных дуг.

В строении земной коры островных дуг, кроме осадочного и «базальтового» слоев, участвует «гранитный» слой со скоростями сейсмических волн порядка 6,0 *км/сек*, а мощность коры достигает 20—30 *км*. Современная геосинклинальная область Зондской дуги высоко сейсмична и изобилует проявлениями вулканизма;

г) зона современного тафрогенеза в области Срединно-океанических хребтов или зона геотафрогеналей. Зона охватывает всю область срединных хребтов, но активной современной частью ее является собственно рифтовая зона, сейсмически и вулканически высоко активная. Рельеф рифтовой зоны очень сложен, в нем сочетаются вытянутые вдоль общего простирания хребта гряды и рифтовые ущелья. В несколько сглаженном виде этот тип рельефа прослеживается и в области склонов срединно-океанических хребтов. Склоны рифтовых ущелий лишены или почти лишены покрова осадков, но дно их заполнено осадочно-вулканогенной толщей, соответствующей «второму» слою земной коры. Толщина этого слоя на дне рифтовых ущелий порядка 2,0—2,5 *км*. Под ним залегают породы, характеризующиеся скоростями 7,0—7,2, а в области склонов хребта — скоростями около 7,5 *км/сек*. Морфология рифтовых ущелий позволяет предполагать возможность обнажения

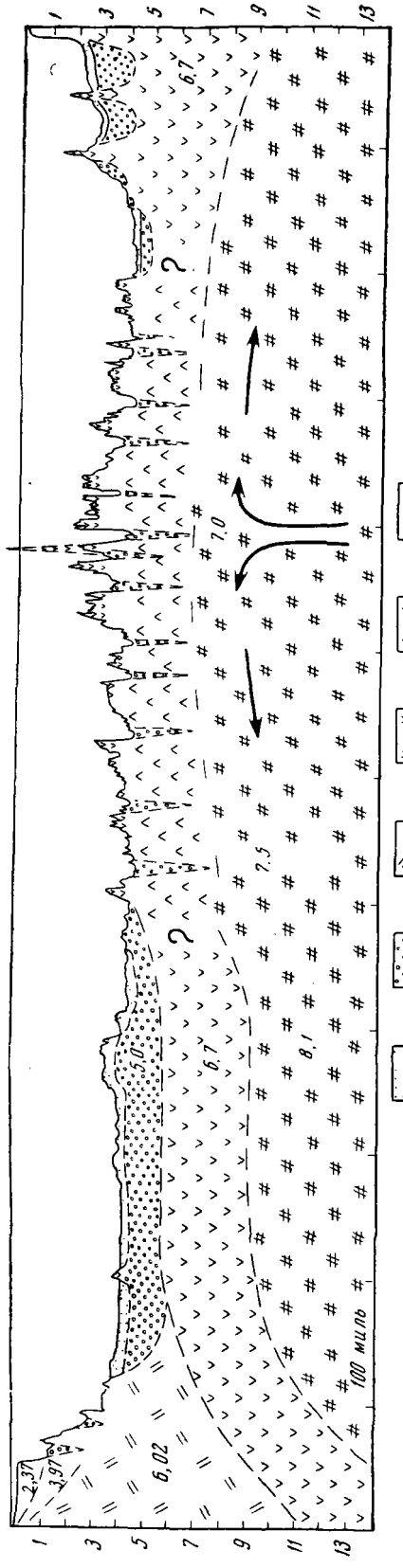


Рис. 2. Схематический разрез земной коры через Срединно-Индоокеанский хребет:

1 — рыхлые осадки; *2* — «второй» сейсмический слой земной коры; *3* — «гранитный» слой земной коры; *4* — «базальтовый» слой земной коры; *5* — поднятые, серпентинизированные и динамометаморфизованные породы верхней мантии; *6* — верхняя мантия Земли. Цифрами показаны скорости распространения сейсмических волн в *км/сек*, стрелки показывают направление предполагаемых конвекционных движений вещества верхней мантии, вертикальная шкала — глубины в *км*, горизонтальная — расстояния в морских милях (100 миль — 185,2 *км*)

этих пород на их склонах. Над ущельями отмечается резкий минимум суммарной напряженности магнитного поля. К ним относятся максимальные значения теплового потока из недр Земли.

Со дна ущелий и с гребней рифтовых гор получены образцы остекловатых базальтовых лав и спекшегося фораминиферового песчаника. Базальты состоят из плагиоклаза, пироксена, содержат включения оливина. Со склонов рифтовых ущелий получены образцы излившихся и глубинных основных и глубинных ультраосновных пород. Основные породы представлены базальтовыми лавами и крупнокристаллическим габбро, состоящим из лабрадора и диаллага. Среди ультраосновных пород преобладающими являются серпентинизированные в различной степени перидотиты (гарцбургиты) и образованные по ним серпентиниты. В меньшем количестве встречены дуниты и хромитит. Для минералогического состава образцов ультраосновных пород характерно наличие магнезиального оливина, сопровождаемого энстатитом и авгитом, при постоянной примеси хромита и пикотита. Во всех образцах наблюдаются псевдоморфозы серпентина по первичным минералам. На поверхности образцов видны плоскости скольжения. Признаки динамометаморфизма заметны также в раздроблении кристаллов оливина, в структуре серпентинитов.

Можно высказать предположение, что обнаруженные в рифтовых ущельях ультраосновные породы являются малоизмененными породами верхней мантии Земли. По своему минералогическому составу они вполне соответствуют современным представлениям о породах верхней мантии, как остаточных породах от выплавления базальта из первичного вещества Земли, аналогичного составу каменных метеоритов, путем зонного плавления [3]. Они должны соответствовать, как нам кажется, не локальным апофизам, типа даек, далеко отходящим от основного массива пород, а кровле сводового поднятия верхней мантии, обусловившего образование Срединно-океанических хребтов Индийского океана: Западно-Индийского, Центрально-Индийского, Аравийско-Индийского и Австрало-Антарктического. Это поднятие отмечается близким к поверхности залеганием границы раздела со скоростями сейсмических волн 7,0—7,2 *км/сек* под дном рифтовых ущелий (рис. 2).

Такие скорости сейсмических волн на столь малой глубине могут соответствовать, судя по результатам лабораторных измерений, скорее всего ультраосновным породам, находящимся в условиях пониженного давления (по сравнению с обычной глубиной залегания пород верхней мантии), относительно высоких температур (учитывая повышенный поток тепла из недр Земли) и подвергшихся серпентинизации [9]. Большой интерес представляет сообщение о том, что динамометаморфизм вызывает анизотропность ультраосновных пород мантии и существенные вариации скоростей сейсмических волн в зависимости от направления разрезов [10]. По этим данным в магнезиальном оливине, в зависимости от ориентировки относительно плоскостей скольжения, скорости сейсмических волн будут 7,73, 8,65 и 9,87 *км/сек*, из которых первое значение уже близко к наблюдавшимся под дном рифтового ущелья. Если же принять во внимание наблюдающуюся серпентинизацию перидотитов, то еще большее снижение скоростей сейсмических волн в ультраосновных породах верхней мантии не будет казаться невероятным. Само же нахождение серпентинизированных ультраосновных пород в рифтовых ущельях больше всего подтверждает такое предположение.

Подъем вещества верхней мантии Земли к поверхности и сопровождающие это динамометаморфизм и серпентинизация происходят наиболее активно в современной рифтовой зоне. Это процесс выжимания пород, а не излияния их, в отличие от излияния базальтовых лав, выплавляемых в процессе зонной плавки. Судя по полученным данным, влияние этого процесса не ограничивается только рифтовой зоной. Можно предполагать, что дивергенция конвекционных течений вещества верхней мантии под рифтовой зоной ведет к растяжению и раздроблению новообразуемой здесь коры и формированию ее во всей области срединно-океанических хребтов. Это подтверждается наблюдениями на склоне Западно-Австралийского хребта. Область срединно-океанического хребта в целом, как это уже отмечали многие исследователи, является особой тектонической зоной Земли. По своим масштабам и по значению протекающего в ней процесса образования особого типа коры она сопоставима с геосинклинальными поясами. Мы предлагаем для ее обозначения термин геотафрогеналь, имеющий в основе предложенный в свое время еще Зюссом для описания процесса образования системы Восточно-Африканских грабенов термин тафрогенез (от греческого слова тафрос — ров). Единство процесса, ведущего к растяжениям и разрывам земной коры и образованию этих грабенов и формированию срединно-океанических хребтов, хотя они и развиваются в различных тектонических условиях, кажется нам весьма вероятным. Рифтовая зона, где наиболее возможны выходы непосредственно на поверхность ультраосновных пород верхней мантии, составляет одну из замечательных особенностей строения Земли — ее срединно-океани-

ческий перидотитовый пояс, противостоящий зеленокаменному поясу островных дуг по периферии Тихого океана.

Обработка материалов, собранных в 36-м рейсе «Витязя», продолжается. Ее ведет большой коллектив ученых Отделения наук о Земле Академии наук СССР. Публикация результатов обработки предполагается в виде специального сборника, посвященного исследованиям земной коры и верхней мантии Индийского океана.

ЛИТЕРАТУРА

1. Белоусов В. В. 1954. Основные вопросы геотектоники. М.
2. Белоусов В. В. 1964. Проект исследований верхней мантии Земли. Геофизический бюллетень, № 15.
3. Виноградов А. П. 1964. Верхняя мантия — земная кора. АН СССР, М.
4. Индийский океан, карта м-ба 1 : 15 000 000, ГУГК ГГК СССР, 1963.
5. Удинцев Г. Б. 1964. Тектоника дна морей и океанов на тектонической карте Евразии. Геология дна океанов и морей, М.
6. Физико-географический атлас Мира. АН СССР, ГУГК ГГК СССР, 1964.
7. Хаин В. Е. 1964. Общая геотектоника, Изд. «Недра», М.
8. Heezen B., Tharp M. 1965. Descriptive sheet to accompany Physiographic Diagram of the Indian Ocean.
9. Hess H. 1962. History of ocean basins. Petrographic studies, a volume to honour A. F. Buddington. Geol. Soc. Amer.
10. Hess H. 1964. Seismic anisotropy of the uppermost mantle under oceans. Nature, **203**, № 4945.

Reprinted from *Okeanologia*, vol. V, no. 6, 1965, p. 1113-1119

ИНФОРМАЦИЯ

УДК 551.46.062(047)

36-й РЕЙС НАУЧНО-ИССЛЕДОВАТЕЛЬСКОГО СУДНА «ВИТЯЗЬ»

36-й рейс «Витязя» проходил в Индийском океане в период с 5.X-1964 г. по 6.III-1965 г. Рейс проводился в соответствии с двумя международными исследовательскими программами: Международной индоокеанской экспедиции и Международного проекта верхней мантии Земли.

36-й рейс «Витязя» являлся завершающим по отношению к предшествующим 31-му, 33-му и 35-му рейсам в Индийский океан, также выполнявшимся по программе Международной индоокеанской экспедиции. Однако то обстоятельство, что рейс проводился также по программе Международного проекта верхней мантии Земли, придало этой экспедиции специализированный геолого-геофизический характер, отличающий ее от предшествующих, носивших характер комплексных океанологических экспедиций. Геологические и геофизические исследования в различных сочетаниях отдельных видов работ выполнялись в экспедициях на «Витязе» и ранее, но полный комплекс геофизических и геологических исследований был осуществлен в 36-м рейсе впервые. Это оказалось возможным после продолжительного периода разработки приборов и методов морских геофизических и геологических исследований, осуществлявшейся как в Институте океанологии, так и в других институтах, принявших участие в 36-м рейсе «Витязя».

Первые три плавания «Витязя» в Индийском океане дали обширные сведения о природе этого океана, ранее изученного совершенно недостаточно. Были получены некоторые фундаментальные данные по геологии дна Индийского океана, позволяющие представить основные черты его геологического строения и правильно организовывать дальнейшие более углубленные исследования. Эти данные были обобщены в ряде статей и в специальных сборниках: в подготовленном к 22-му Международному геологическому конгрессу (Геология дна океанов и морей, 1964 г.) и посвященном результатам исследований в период Международного геофизического года и Года международного геофизического сотрудничества (Океанологические исследования, № 13, 1965). Кроме того, эти результаты получили отражение на новых картах «Физико-географического Атласа Мира» (АН СССР и ГУГК ГГК СССР, 1964) и географической карте «Индийский океан» в масштабе 1 : 15 000 000 (ГУГК ГГК СССР, 1963).

В итоге проведения первых трех рейсов «Витязя» в Индийском океане выявился определенный недостаток данных по тектонике дна, по петрографии коренных пород, по геофизическим характеристикам дна. Такие данные важны как для решения вопросов региональной геологии Индийского океана, так и для разработки ряда фундаментальных вопросов планетарной геологии и геофизики Земли. Это уже само по себе определило геолого-геофизическую направленность настоящего плавания, а дополнительным стимулом в постановке именно геолого-геофизической задачи явилось выдвижение в рамках Международного проекта исследований верхней мантии Земли проблемы рифтовых зон Мирового океана. В Индийском океане существует, как показали предшествующие исследования, развитая система срединно-океанских хребтов с глубокими рифтовыми ущельями в их осевой зоне. Имевшиеся сведения о геологическом строении этих рифтовых зон и о сопутствующих им особенностях физических полей Земли свидетельствовали о тесной связи структуры земной коры в рифтовых зонах с процессами, протекающими в верхней мантии Земли. Таким образом исследования рифтовых зон открывали перспективу проникновения в верхнюю мантию, если не прямого, то косвенного, путем изучения всего комплекса свойственных им геологических явлений.

Основной задачей 36-го рейса «Витязя» были комплексные геофизические и сопутствующие им геологические исследования различных тектонических зон Индийского океана. Известные данные по геологии суши, окружающей Индийский океан, позволяют предполагать в прошлом явления распада древних материков и новообразования коры океанического типа в одних частях океана и явления роста материков за счет причленения к ним складчатых геосинклинальных зон, развивающихся на древних

океанических плитах,— в других. Роль развития рифтовых зон при этом чрезвычайно интересна. Раскрытие ее ведет к пониманию механизма и причин тектонических движений, вулканизма, связей тектоники земной коры с физическими полями Земли и процессами развития верхней мантии. Большой интерес представляет также вопрос о минеральных ресурсах дна Индийского океана.

Подробное изучение всех тектонических зон Индийского океана современными средствами потребовало бы значительного времени, намного превышающего 5 месяцев, предусмотренных для 36-го рейса «Витязя».

Поэтому в качестве основной была принята методика полигонных исследований, предусматривающая детальные комплексные геолого-геофизические исследования лишь некоторых ограниченных, но типичных для каждой из тектонических зон площадей. Перспективность такой методики исследований была установлена еще несколько ранее, в 24-м, 29-м и 30-м рейсах «Витязя», когда по инициативе и под руководством Н. Н. Сысоева впервые были проведены опыты постановки заякоренных буев в открытом океане и привязки к ним различных видов съемки и дрейфовых наблюдений. Точные радиолокационные и визуальные определения места корабля на полигоне относительно заякоренного буя обеспечивают возможность весьма детальных исследований геологического строения дна океана, невыполнимых при обычных навигационных методах определения. Размеры полигонов, как показал опыт 36-го рейса, могут достигать 20×20 миль при одном буе и 20×40 миль при двух заякоренных буях.

Полигонные исследования дополнялись в 36-м рейсе «Витязя» маршрутной геофизической съемкой и дрейфовыми наблюдениями на станциях в некоторых точках маршрута.

Своеобразие задач 36-го рейса наложило отпечаток на состав экспедиции. В связи с использованием ряда новых методов и приборов Институт океанологии, организовывавший экспедицию, привлек к участию в плавании специалистов из других учреждений: Института физики Земли, Геологического института Академии наук СССР, институтов Государственного геологического комитета СССР, Гидрометеослужбы СССР, из Московского университета и др. В экспедиции при выходе судна из Владивостока участвовало 129 человек. Из них 64 человека составляли научный персонал и 65 человек — экипаж судна. Во время стоянки в порту Фримантл (Австралия) к экспедиции присоединился еще один участник, прибывший из СССР самолетом, и численность состава экспедиции достигла 130 человек. Начальником экспедиции был ст. научный сотрудник Института океанологии АН СССР Г. Б. Удинцев, а капитаном «Витязя» — капитан морского флота 1 ранга Е. А. Авраменко.

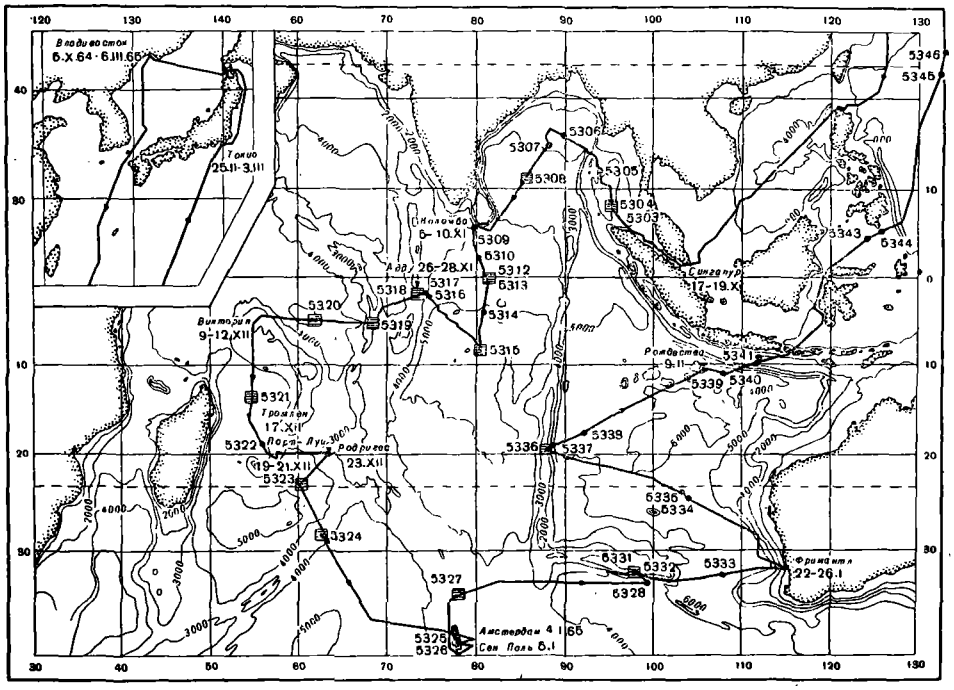
В составе экспедиции было 10 отрядов, обеспечивавших работы по важнейшим направлениям геолого-геофизических исследований и по некоторым разделам океанологических работ, выполнявшихся в экспедиции в качестве вспомогательных и попутных.

Руководителями основных разделов работы были специалисты: В. Ф. Канаев (геоморфология и тектоника дна), Ю. А. Богданов (литология), Е. А. Романкевич (стратиграфия и геохимия донных осадков), Ю. П. Непрочнов (сейсмоакустические исследования), М. Ф. Михно (магнитометрические исследования), В. А. Тулин (гравиметрические исследования), В. И. Маракуев (работы в области развития техники исследований), А. Е. Абаев (гидрографические исследования). Ф. А. Пастернак (гидробиологические исследования), В. И. Кукса (гидрофизические исследования), Л. П. Шкоткин (метеорологические исследования). В составе экспедиции были также научные сотрудники, проводившие отдельные виды исследований: В. А. Сечкин (акустические исследования), Е. А. Любимова (геотермические исследования), В. И. Чернышева (изучение коренных пород дна). Е. Д. Заклинская (спорово-пыльцевой анализ донных отложений), Ю. А. Романов (синоптические исследования).

Примерно половина участников являлась специалистами в области геологии и геофизики. Между всеми отрядами осуществлялось согласованное взаимодействие, обеспечивавшее успешное решение поставленных задач. Тесное взаимодействие существовало также между научным персоналом и экипажем, что было особенно важно, принимая во внимание высокую насыщенность судна в этом рейсе новой техникой, а также применение новых приемов работы.

Маршрут экспедиции был проложен так, чтобы охватить все важнейшие тектонические зоны Индийского океана (рисунок). «Витязь» вышел из Владивостока 5.X 1964 г. и направился через Японское и Восточно-Китайское моря в Филиппинскую котловину Тихого океана. Следуя севернее о. Лусон (Филиппинские о-ва) «Витязь» вошел в Южно-Китайское море и 17.X прибыл в порт Сингапур (Малайзия), где были пополнены запасы воды, топлива и продовольствия, а также осуществлены научные контакты с местными учеными и ботанические сборы. 19.X «Витязь» направился Малаккским проливом в Андаманское море. 22.X на глубине 2500 *м* над плоским аккумулятивным дном геосинклинальной котловины Андаманского моря были начаты работы на первом полигоне (ст. 5304).

Работы на этом и последующих полигонах начинались с постановки заякоренного буя и комплексной геофизической съемки вокруг него, включавшей изучение рельефа дна с помощью эхолота с прецезионным самописцем глубин и магнитную съемку с помощью буксируемого протонного магнитометра. После выполнения съемки вокруг



Маршрут 36-го рейса «Витязя» в Индийском океане

Цифрами указаны номера станций, квадратиками — полигоны. Подписаны названия мест высадок и заходов в порты, с указанием дат. Рельеф дна показан схематическими изобатами через каждые 1000 *м* по карте «Индийский океан» масштаба 1 : 15 000 000 (ГУГК ГГК СССР, 1963)

первого буя корабль отходил в сторону на 5—8 миль и ставил второй заякоренный буй, на удалении от первого в 10—16 миль. Затем выполнялась вторая половина съемки вокруг этого буя. Далее обычно следовало глубинное сейсмическое зондирование, выполнявшееся с помощью двух или трех автономных радиоакустических буев. Один из них часто прикреплялся к заякоренному бую, другие расставлялись по разрезу и находились в свободном дрейфе. Буи принимали и транслировали на корабль сейсмические волны, возбуждаемые взрывами, которые производились с «Витязя», проходившего вдоль разреза; на нем же производилась регистрация.

После работ по глубинному сейсмическому зондированию осуществлялись станционные наблюдения и сборы различных проб: колонок донных осадков с помощью грунтовых трубок (прямоточной и поршневой большого диаметра), поверхностных проб донных осадков и бентической фауны с помощью дночерпателя, коренных пород дна и бентической фауны с помощью драги и трала, гидрологические наблюдения с помощью серий батометров и батитермографа, сбор проб водной взвеси, геотермические измерения с помощью термоградиентографа, телевизионные наблюдения, различные экспериментальные работы (с донным сейсмографом, с измерителем придонных течений и др.), ловы планктона сетями и ловы рыб, гидрооптические измерения и т. д. Обычно продолжительность работ на полигонах колебалась от 2,5 до 6 суток.

Переходы между полигонами и местами высадок на острова и заходами в иностранные порты осуществлялись, в основном, по кратчайшим расстояниям, но с учетом изученности океана и положения основных тектонических структур дна. На переходах велось изучение рельефа дна, магнитная съемка, батитермографические наблюдения, местами — сбор колонок донных осадков грунтовыми трубками и геотермические измерения.

Работы на первом полигоне были закончены 25.X, и «Витязь» направился к выходу из Андаманского моря. Миновав срединное складчатое поднятие Андаманской котловины, корабль пересек неизученную ранее подводную вулканическую гряду, образующую восточный хребет горного сооружения геосинклинальной Андаманской островной дуги. Два вулкана этой гряды выступают над водой — это острова Баррен и Наркомдан — а остальные скрыты водами Андаманского моря. Глубокий межгорный желоб отделяет эту вулканическую гряду от складчатого внешнего хребта Андаманской дуги. Восточный склон хребта, судя по сильной магнитной аномалии, осложнен крупным разломом. Пересекши Андаманскую островную дугу, «Витязь» вышел Кокок-

совым проходом в Бенгальский залив. Здесь было проведено сейсмическое зондирование по методу отраженных волн на широтном разрезе поперек северного окончания Зондского (Яванского) глубоководного геосинклинального желоба. Было обнаружено, что под поверхностью почти плоской аккумулятивной равнины существует прогиб фундамента примерно на 1000 *м*, позволяющий продолжить структуру Яванского желоба в этот район и, возможно, далее к северу, на соединение с Предгималайским предгорным прогибом.

По выходе в центральную часть Бенгальского залива 30 ноября там были начаты работы на втором полигоне (ст. 5308) на глубине около 3500 *м* над аккумулятивной равниной, пересекаемой руслами суспензионных потоков. Работы на этом полигоне закончились 3.XI, после чего «Витязь» направился к о. Цейлон и 5.XI зашел в порт Коломбо. Стоянка в Коломбо с целью пополнения запасов воды и продовольствия была использована также для проведения геологических и ботанических сборов в различных частях острова и для научных контактов с местными учеными.

10.XI «Витязь» вышел из Коломбо и направился к югу, следуя примерно по 80-му меридиану в. д. и останавливаясь несколько раз для сбора колонок донных осадков. 12.XI экспедиция достигла экватора и близ него на глубине 4500 *м* были начаты работы на третьем полигоне (ст. 5312), расположенном уже в Центральной котловине Индийского океана над зоной разлома, ориентированной примерно в широтном направлении. Эта зона разлома ограничивает с юга один из участков аккумулятивной равнины, протягивающейся сюда из Бенгальского залива. 14.XI работы на третьем полигоне были закончены и «Витязь» продолжил свое движение на юг. По достижении 8-й параллели ю. ш. 16 ноября были начаты исследования на четвертом полигоне (ст. 5315), располагавшемся также в Центральной котловине, над холмистым ложем океана, на глубинах порядка 5200 *м*. Эти работы продолжались 5,5 суток и закончились 22.XI.

После этого «Витязь» повернул на северо-запад, в направлении к атоллу Адду, самому южному из Мальдивских о-вов. На пути к этому острову был пересечен желоб — разлом Чагос, с глубиной более 5000 *м*, протягивающийся вдоль восточного подножья Мальдивского подводного горного хребта. На склоне этого глыбового хребта была проведена драгировка, а по выходе на его платообразную вершинную поверхность, лежащую на глубине около 2000 *м*, осуществлены работы на пятом полигоне (ст. 5318). Эти работы были начаты 25 и закончены 26.XI, после чего «Витязь» зашел в лагуну атолла Адду. Стоянка в лагуне этого атолла имела целью выполнение опорных геофизических наблюдений, биологические и геологические сборы. Утром 28.XI «Витязь» покинул атолл Адду и направился на юг до места пятого полигона, чтобы продолжить поперечное пересечение Мальдивского хребта, а затем — на юго-запад через южную оконечность Аравийской котловины к подводному Аравийско-Индийскому хребту.

После двукратного рекогносцировочного пересечения рифтовой зоны Аравийско-Индийского хребта утром 30.XI были начаты работы на шестом полигоне (ст. 5319), расположенном непосредственно в рифтовой зоне хребта, гребень которого находится на глубине около 2000 *м*. Эти работы дали исключительно интересные результаты почти по всем разделам исследований, но особенно интересными оказались данные, полученные путем глубинного сейсмического зондирования вдоль дна рифтового ущелья на глубине 5800 *м* и драгировок на его склонах. Были установлены признаки подъема глубинных границ раздела земных недр и выходы на поверхность склонов рифтового ущелья глубинных ультраосновных пород. Образцы этих пород рассматриваются нами, как образцы пород верхней мантии Земли. Работы на шестом полигоне продолжались почти 6 суток и были закончены 5.XII.

Следуя курсом на запад, «Витязь» направился к Сейшельским о-вам 7.XII в центральной части Сомалийской котловины были начаты работы на седьмом полигоне (ст. 5320). Полигон располагался на глубинах 3300 *м* над краем подводного плато, получившего в работах исследовавших его английских геофизиков название плато Мединги-райз (по названию холма, на котором расположен геофизический факультет Кембриджского университета), и над ложем котловины на глубине около 4000 *м*. 8.XII работы на этом полигоне были закончены, и утром 9.XI. «Витязь» вышел на край Сейшельской банки, представляющей собой вершинную поверхность северной части подводного Маскаренского хребта. Сейшельская банка, как показали исследования английских и американских экспедиций последних лет, имеет типичное материковое строение коры, в составе которой имеется гранитный слой. Это согласуется и с тем, что сами Сейшельские о-ва сложены гранитами, возраст которых 650 млн. лет. Сейшельские острова с Сейшельской банкой представляют редкий пример фрагмента материковой коры среди океана и сходны в этом отношении с Мадагаскаром.

9.XII «Витязь» зашел в порт Виктория, на о. Маэ (Сейшельские о-ва). Здесь были проведены опорные геофизические наблюдения, осуществлены геологические, ботанические и гидробиологические сборы, а также пополнены запасы питьевой воды и продовольствия. Весьма полезными были контакты с местными учеными, а также с американскими учеными судна Национального научного фонда США «Антон Бруун», работавшего также по программе Международной индоокеанской экспедиции и находившегося в порту Виктория в эти же дни.

12.XII «Витязь» покинул порт Виктория и направился к югу. Миновав Амирантскую котловину, экспедиция вышла в Маскаренскую котловину, в центральной части которой на глубине около 4500 *м* были проведены исследования на восьмом полигоне (ст. 5321). Этот полигон располагался над холмистым ложем дна котловины. Работы на нем были начаты 14 и закончены 16.XII. После этого экспедиция посетила о. Тромлен, расположенный в центре Маскаренской котловины. Это поднятый над уровнем моря коралловый атолл, построенный на вершине большого подводного вулкана. В результате поднятия острова из-под воды обнажились базальтовые лавы, лежащие в основании коралловой постройки. Продолжая движение на юг, «Витязь» достиг 19.XII о. Маврикий. Стоянка в порту Луи на этом острове дала возможность пополнить запасы топлива, питьевой воды и продовольствия, а также провести опорные геофизические наблюдения, собрать геологические и ботанические коллекции. О. Маврикий имеет вулканическое происхождение и испытывает небольшое поднятие. Весьма полезными были контакты с местными учеными из музея и краеведческого института, из Сельскохозяйственного департамента и Гидрометеослужбы.

22.XII «Витязь» вышел из порта Луи и 23.XII подошел к о. Родригес, расположенному на Центрально-Индийском подводном хребте. Это вулканический остров, испытывающий значительное поднятие в связи с развитием системы срединно-океанического хребта. Коралловые известняки подняты на этом острове на высоту до 170 *м*. Во время стоянки «Витязя» на рейде сотрудники экспедиции совершили геологические исследования острова, изучали также фауну литорали. От о. Родригес «Витязь» прошел на юго-запад и вышел в Мадагаскарскую котловину океана. 24.XII были начаты исследования на девятом полигоне (ст. 5323).

Этот полигон располагается на глубинах от 3000 до 5000 *м* в нижней части северо-западного склона Западно-Индийского хребта. Интересно, что и здесь были отмечены признаки подъема глубинных границ раздела недр Земли и выходы ультраосновных глубинных пород, отмечавшиеся ранее для рифтовой зоны Аравийско-Индийского хребта. Работы на полигоне были закончены 26.XII, и «Витязь» направился к юго-востоку, пересекая Западно-Индийский хребет. После двукратного рекогносцировочного пересечения рифтовой зоны этого хребта 26.XII были начаты работы на десятом полигоне (ст. 5324). Подобно шестому этот полигон располагался точно в рифтовой зоне хребта. Глубинное сейсмическое зондирование и здесь проводилось вдоль дна рифтового ущелья, находящегося на глубине 5100 *м*, а драгирoвки — на склонах ущелья и гребне рифтовых гор, расположенном на глубине 2700 *м*. Здесь также были получены признаки поднятия глубинных границ раздела и образцы ультраосновных пород, а кроме того отмечен значительный поток тепла из недр Земли.

31.XII работы на десятом полигоне были закончены. «Витязь» продолжил движение на юго-восток и вошел в котловину Крозе. В этой котловине была отмечена резкая смена характера рельефа дна, связанная, видимо, с важными различиями в структуре дна, возможно, с переходом от молодой (послепалеозойской) океанической платформы к более древней (допалеозойской). На дне котловины Крозе отмечены также резко выраженные в рельефе зоны разломов. Штормовая погода не позволила провести в этой котловине полигонные исследования, и «Витязь» подошел 4.I—1965 г. к о. Новый Амстердам, расположенному на западной рифтовой гряде Центрально-Индийского хребта. Остров представляет собой базальтовый купол, рассеченный трещинами, параллельными рифтовому ущелью. Вдоль этих трещин располагается ряд вулканических кратеров. Структура острова в миниатюре напоминает структуру Исландии. Участники экспедиции совершили высадку на остров и провели там геологические сборы. Весьма интересными были контакты с сотрудниками французской геофизической обсерватории, расположенной на этом острове. По окончании высадки «Витязь» провел съемку рифтовой зоны хребта и спустился на юг к о. Сен-Поль, где 5.I также была проведена высадка с целью геологических наблюдений на берегу и комплексных исследований в кратерной бухте острова. Остров представляет собой базальтовый стратовулкан на гребне рифтовых гор, край которого разрушен сбросом и кратер открывается в океан. По окончании высадки «Витязь» продолжил движение на юг примерно до 40° ю. ш. со съемкой рифтовой зоны Австрало-Антарктического подводного хребта. Однако дальнейшее резкое ухудшение погоды, исключавшее возможность геофизических работ, заставило экспедицию повернуть на север.

7.I «Витязь» вышел на 34-ю параллель ю. ш. и в связи со значительным улучшением погоды начал поперечное пересечение Центрально-Индийского хребта и выбор места для полигона в его рифтовой зоне. После двукратного рекогносцировочного пересечения хребта 7.I были начаты работы на одиннадцатом полигоне. Подобно шестому и десятому он располагался в рифтовой зоне хребта. Глубинное сейсмическое зондирование проводили вдоль дна рифтового ущелья, лежащего здесь на сравнительно небольшой глубине — около 3300 *м*, а драгировки на гребне рифтовых гор (глубина 2000 *м*) и на склонах рифтового ущелья. Работы были закончены 10.I, и «Витязь» направился на восток, к берегам Австралии.

Следуя на восток вдоль 33-й параллели ю. ш., «Витязь» вышел в Юго-Западную Австралийскую котловину Индийского океана. Здесь были отмечены неизвестные ранее подводные вулканические горы, мало характерные для западной части Индийского океана и широко распространенные в Тихом океане. Одна из таких гор, открытых «Витязем», была детально исследована. «Витязь» пересек южное окончание Восточно-

Индийского хребта, представляющее собой невысокое плато, ограниченное сбросами. Затем был пересечен глубокий желоб Оби, названный ранее по имени обнаружившего его судна Советской антарктической экспедиции. Проведя ряд работ (сбор колонок донных отложений, непрерывное сейсмическое профилирование и др.) в желобе Оби и на протягивающемся вдоль него краевом валу океанского ложа, «Витязь» вышел на Западно-Австралийский хребет.

15.I на вершинной поверхности этого хребта, на глубинах порядка 1600 *м*, были начаты работы на двенадцатом полигоне (ст. 5331). В ходе этих работ на гребне, располагающемся у южного края плато Западно-Австралийского хребта, был получен с помощью драги образец коренной породы — кварцевого долерита. По мнению проф. Прайдера из Университета Западной Австралии, эта порода во многом напоминает кварцевые долериты Австралии и Антарктиды. 18.I работы на Западно-Австралийском хребте были закончены, и «Витязь» продолжил движение на восток. В районе восточного окончания желоба Оби была исследована подводная гора с глубиной над вершиной 1180 *м*, открытая «Витязем» ранее, в 35-м рейсе.

22.I «Витязь» вошел в порт Фримантл (Австралия). Здесь были пополнены запасы топлива, питьевой воды и продовольствия. Не менее важными были контакты с австралийскими учеными из университета Западной Австралии, Геологической службы и Геофизической обсерватории Западной Австралии, способствовавшие развитию научного сотрудничества с ними. Были проведены при содействии австралийских ученых опорные гравиметрические наблюдения на пункте, где в свое время проводил измерения один из пионеров морской гравиметрии, голландский ученый Венинг-Мейнес, проведены геологические экскурсии и сборы, а также ботанические экскурсии и сборы гербария.

26.I «Витязь» вышел из Фримантла и направился на северо-запад. На своем пути он пересек Западно-Австралийскую котловину, в которой были проведены геотермические измерения, и вышел на Восточно-Индийский хребет. После рекогносцировочного пересечения хребта близ 20° ю. ш. 2 февраля были начаты работы на последнем тринадцатом полигоне (ст. 5336). Этот полигон располагался на платообразной вершинной поверхности хребта, лежащей на глубинах 1800—2000 *м*. Работы на полигоне закончились 4.II и после небольшого перехода проведена драгировка на восточном склоне того же хребта. После этого «Витязь» направился на северо-восток, к выходу из Индийского океана. Работы экспедиции в основном были закончены, но продолжались попутные наблюдения и некоторые экспериментальные работы.

9.II «Витязь» подошел к о. Рождества — поднятому на высоту до 400 *м* древнему коралловому атоллу. Кратковременная высадка на этот остров позволила собрать образцы горных пород и гербарий. Остров сложен в основном коралловыми известняками. В верхней части острова, в лагуне древнего атолла, залегают богатейшие запасы фосфатов, интенсивно разрабатываемые. В результате поднятия острова близ берега из-под коралловой постройки обнажились базальтовые лавы вулкана, служащего основанием острова.

Продолжая движение на северо-восток, «Витязь» пересек Зондский (Яванский) желоб, затем — внешний складчатый хребет Зондской геосинклинальной островной дуги (так называемый Балийский хребет) и межгорный Балийский желоб. Здесь велись работы по непрерывному сейсмическому зондированию. Проливом Ломбок «Витязь» вышел 14.II из Индийского океана и вошел в Индонезийские моря. Следуя Макассарским проливом, он вышел в море Сулавеси, где были проведены работы по непрерывному сейсмическому зондированию и измерению теплового потока из недр Земли.

17.II «Витязь» пересек Филиппинскую островную дугу и вышел в Тихий океан. Двигаясь в северо-восточном направлении, он пересек Филлипинскую котловину. 25.II «Витязь» вошел в порт Токио (Япония) с целью провести научные контакты с японскими учеными, для обмена информацией о результатах исследований по программе Международной индоокеанской экспедиции, а также для обмена опытом в области морских геологических и геофизических исследований. В Токио были проведены опорные гравиметрические измерения. 3.III «Витязь» вышел из Токио и прошел вдоль восточного побережья о. Хоисю к Сангарскому проливу. 5.III был пройден Сангарский пролив, а 6.III «Витязь» вошел в порт Владивосток и 36-й рейс был закончен.

Экспедиция продолжалась 153 суток. За это время был пройден маршрут протяженностью 23 294 мили, что заняло 85 суток. Из этого маршрута 7200 миль приходится на Тихий океан (26 суток) и 16 000 миль на Индийский океан (59 суток). Работы на полигонах и станциях заняли 41,5 суток, причем работы на тринадцати полигонах потребовали 34,5, а на 30 отдельных станциях в различных точках маршрута — 7 суток. Высадки для береговых работ на восьми островах и четыре захода в порты для снабжения заняли 26,5 суток.

Наибольшие затраты времени падают на геолого-геофизические исследования и организацию полигонов, где они проводились. На первом месте по затратам времени оказывается глубинное сейсмическое зондирование на двенадцати разрезах — 232 часа, несколько более 100 часов потребовала организация полигонов, 152 часа — комплексная геофизическая съемка на двенадцати полигонах. Сбор образцов коренных пород со дна океана на 22 точках занял 106 и сборы проб донных осадков на 92 точках —

111 часов. По остальным разделам работ (в т. ч. 14 гидрологических серий, 11 бентосных тралов и драг и др.) затраты времени были значительно меньше — в среднем по 20—40 часов. В течение рейса было сделано 255 астрономических обсерваций, 1740 радиолокационных обсерваций и 654 навигационных определения места корабля. Кроме того, большое количество материалов было получено в рейсе путем попутных наблюдений без специальных затрат времени. Например, эхолотный промер велся на протяжении 22 683 миль пути, магнитная съемка — на протяжении 8 000 миль пути, попутно собрано большое число проб водной и атмосферной взвеси, проведены актинометрические наблюдения, запуски радиозондов и т. д.

Г. Б. Удинцев

Reprinted from *Dokl. Akad. Nauk SSR*, vol. 165, no. 5, 1965, p. 1147-1150

УДК 551.14

ГЕОЛОГИЯ

Г. Б. УДИНЦЕВ, В. И. ЧЕРНЫШЕВА

ОБРАЗЦЫ ПОРОД ВЕРХНЕЙ МАНТИИ ЗЕМЛИ ИЗ РИФТОВОЙ ЗОНЫ ИНДИЙСКОГО ОКЕАНА

(Представлено академиком А. П. Виноградовым 31 VII 1965)

Широко распространено представление, что по своему составу верхняя мантия должна быть близка к ультраосновным породам: перидотитам, дунитам и пироксенитам. Это представление основано на сопоставлении скоростей распространения сейсмических волн, наблюдаемых в мантии Земли и измеренных в образцах ультраосновных пород. Оно основано также и на том, что наблюдаемые в пределах земной коры интрузии и выбросы наиболее глубинных пород являются ультраосновными, притом весьма однородными по своему химическому и минеральному составу. А. П. Виноградовым было экспериментально доказано по продуктам выплавления и дегазации каменных метеоритов при зонном плавлении, что вещество мантии Земли должно отвечать составу каменных метеоритов, а ультраосновные породы верхней мантии следует рассматривать в качестве остаточной породы от выплавления базальта [1].

Известно, что ультраосновные породы встречаются в земной коре лишь на большом удалении от кровли верхней мантии в виде обнаженных эрозионным срезанием глубинных интрузий в геосинклинальных складчатых поясах, в виде даек, поднимающихся по зонам глубинных разломов, а также в алмазных трубках взрывов. Широко распространены ультраосновные ксенолиты, вынесенные из недр Земли базальтовыми лавами [2]. Значительное удаление ультраосновных пород от раздела Мохоровичича допускает сомнения в полном соответствии их по составу породам верхней мантии и затрудняет решение вопроса о ее природе.

Наиболее близкими по своему залеганию к границе Мохоровичича являются образцы ультраосновных пород, полученные в области океанов. Известны находки ультраосновных пород в Атлантическом океане [3, 4]. Они были обнаружены в 33-м рейсе «Витязя» в Индийском океане на Аравийско-Индийском хребте [5]. Однако при этих находках не было возможности ясно представить связь с теми или иными структурами дна океана. Ультраосновные породы известны на о. Скалы св. Петра и Павла в Центральной части Атлантического океана, на Срединно-Атлантическом хребте [6] и на о. Сент-Джон в Красном море. Определения возраста ультраосновных пород о. Скалы св. Петра и Павла дали весьма значительную величину, а именно, 4,5 млрд лет, что древнее самых древних пород земной коры и приближается к предполагаемому возрасту Земли [7].

Связь ультраосновных пород упомянутых островов с рифтовой зоной, которая является структурой планетарного значения [8, 9], вызвала представления о подъеме в этой зоне к поверхности Земли вещества верхней мантии [10–12], что связывается некоторыми исследователями с конвекционными движениями вещества мантии [4, 13].

Изучение рифтовой зоны океанов было включено в программу исследований по Международному проекту верхней мантии [14]. Такие исследования были проведены советской геолого-геофизической экспедицией на «Витязе» в 36-м рейсе с 5 X 1964 г. по 6 III 1965 г. Маршрут экспедиции охватил различные тектонические зоны Индийского океана, в том числе три ветви Срединно-Индоокеанского хребта: Аравийско-Индийский, За-

падно-Индийский и Центрально-Индийский хребты (рис. 1). В каждой из этих зон были проведены детальные геолого-геофизические исследования на полигонах площадью примерно 30 × 50 км, включавшие изучение рельефа дна, донных осадков, суммарной напряженности магнитного поля, теплового потока из недр Земли, глубинное сейсмическое зондирование, а также сбор образцов коренных пород путем драгирования. Всего было исследовано 13 полигонов. Три из них (станции №№ 5319, 5324 и 5327) располагались непосредственно в рифтовой зоне Срединно-Индоокеанского хребта, а один (№ 5323) — на склоне хребта. Драгирование в рифтовой зоне проводилось на гребнях рифтовых гор, на склонах рифтового ущелья и на его дне, глубинное сейсмическое зондирование — вдоль дна рифтовых ущелий.

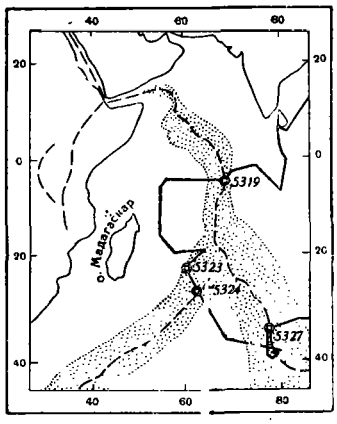


Рис. 1. Маршрут 36-го рейса «Витязя» в Индийском океане и места драгировок коренных пород на Срединно-Индоокеанском хребте. Цифры — номера станций

Можно отметить следующие характерные особенности рифтовой зоны (рис. 2). По данным, полученным В. Ф. Канаевым, она имеет весьма сложный рельеф и разбита глубокими трещинами. Склоны рифтовых ущелий лишены или почти лишены покрова осадков, но дно их заполнено осадочно-вулканогенной толщей (Е. А. Романкевич и Ю. А. Богданов). Толщина слоя, заполняющего дно ущелий и характеризующегося скоростями сейсмических волн порядка 5,0 км/сек, по данным Ю. П. Непрочнова, составляет всего 2,0—2,5 км. Под ним залегают породы, характеризующиеся скоростями 7,0—7,2 км/сек. Морфология ущелья позволяет предположить возможность обнажения на его склонах пород со скоростями 7,0—7,2 км/сек или, во всяком случае, их очень близкое залегание к поверхности. По данным М. Ф. Михно, над ущельем наблюдается резкий минимум напряженности магнитного поля. Максимальное значение величин теплового потока из недр Земли в Индийском океане относится также к рифтовому ущелью (Г. Б. Удинцев, Е. А. Любимова и др.).

Сбор образцов коренных пород производился модифицированной биологической драгой. В рифтовой зоне осуществлено шесть успешных сборов и на склоне хребта — один сбор. Образцы пород были изучены на корабле визуально и в шлифах под микроскопом. Со дна ущелья и гребней рифтовых гор получены плиты фораминиферового песчаника, свежие угловатые глыбы остеклованных базальтовых лав. Это — оливиновые или безоливиновые базальты, состоящие из лейст плагиоклаза (лабрадора), крупных офитовых зерен пироксена (авгита). В некоторых образцах наблюдаются также включения оливина.

Со склонов рифтовых ущелий получены обломки основных и ультраосновных пород. Основные породы представлены серым крупнокристаллическим габбро, состоящим из лабрадора и диаллага. Среди ультраосновных пород преобладают серпентинизированные в различной степени гарцбургиты (перидотиты) и образованные по ним серпентиниты. В меньшем количестве встречены дуниты и хромитит. Наиболее распространенным типом серпентинитов являются хризотил-антигоритовые апогарцбургитовые серпентиниты.

Для минерального состава рассмотренных образцов гипербазитов характерен магнезиальный оливин, сопровождаемый энстатитом, реже авгитом. Хромит и пикотит присутствуют как постоянные примеси. Почти во всех образцах обнаружено проявляющееся в различной степени замещение оливина серпентинитом и во многих случаях полный переход

перидотитовых пород в серпентиниты. Последние имеют мелкопетельчатую структуру, основу которой создают тонкие пересекающиеся прожилки, сложенные параллельно-волокнистым хризотилом. Центральная часть этих петель выполнена почти изотропным, участками колломорфным, мелкочешуйчатым серпофитом. В серпентиновой массе обильно рассеян пылевидный магнетит, образующий скопления в хризотиловых петлях. По концентрации магнетитового агрегата можно определить, что петельчатым серпентиновым минералом замещены зерна бастита. На мелкопетельчатую структуру накладываются более поздние выделения антигорита.

Во всех изученных образцах наблюдаются явные псевдоморфозы серпентина по первичным минералам. Во многих случаях оливин нацело пе-

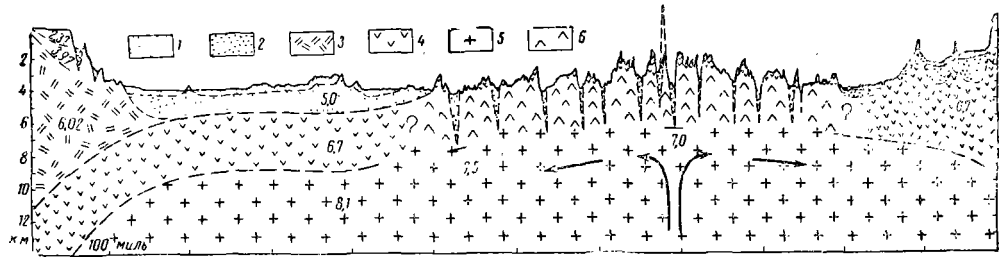


Рис. 2. Схематический разрез земной коры в Индийском океане через Срединно-Индоокеанский хребет по обобщенным данным (в том числе по данным «Витязя» и ([8], [13], [15], [16])). *1* — рыхлые осадки, *2* — 2-й сейсмический слой земной коры, *3* — «гранитный» слой земной коры, *4* — «базальтовый» слой земной коры, *5* — верхняя мантия Земли, *6* — зона подъема пород верхней мантии и их серпентинизации. Цифры — скорости распространения сейсмических волн (км/сек). Стрелки — направление конвекционных движений вещества верхней мантии

реходит в серпентин, и тем не менее определяется первичная форма каждого оливинового кристалла. Пироксен, как правило, не затрагивается серпентинизацией, но в некоторых случаях наблюдаются и его изменения. Благодаря сохранению характерной трещиноватости оливина и спайности, а также диаллаговой отдельности пироксена, можно отличить серпентин, образовавшийся по оливину от образованного по пироксену.

На поверхности отдельных образцов отчетливо видны плоскости скольжения. Признаки динамометаморфизма видны также в раздробленных кристаллах оливина перидотитов и дунитов, в структуре серпентинитов. Судя по предварительному изучению образцов, серпентинизация развивалась снаружи внутрь.

В настоящее время организована обработка всех собранных образцов по широкой программе, возглавляемой акад. А. П. Виноградовым и осуществляемой различными институтами Академии наук СССР.

Анализируя данные, полученные экспедицией «Витязя» и другими исследователями ([4], [5], [8], [13], [15], [16]), мы считаем возможным высказать предположение, что эти породы являются малоизмененными породами верхней мантии Земли. По своему минеральному составу они вполне соответствуют современным представлениям о веществе верхней мантии. Нам кажется также, что выходы ультраосновных пород соответствуют не локальным апофизам пород верхней мантии, а кровле массивного сводового поднятия, обусловившего образование Срединно-Индоокеанского хребта. Признаки этого поднятия можно видеть прежде всего в самом факте встречаемости выходов ультраосновных пород на обширном пространстве, в точках, удаленных друг от друга на тысячи километров. Его признаком может служить также близкое к поверхности дна залегание границы раздела со скоростями сейсмических волн 7,0—7,2 км/сек.

UNESCO ARCHIVES

Такие скорости сейсмических волн на малой глубине залегания границы раздела должны соответствовать скорее всего ультраосновным породам, находящимся в условиях пониженного давления, относительно высоких температур и подвергнувшихся серпентинизации и динамометаморфизму. Известно, что лабораторные измерения показывают возможность снижения скоростей упругих волн в ультраосновных породах верхней мантии до 7,0 км/сек и ниже за счет изменения давления, разогревания, серпентинизации ([4]), а также за счет анизотропности этих пород, вызванной динамометаморфизмом ([17]). По сторонам Срединно-Индоокеанского хребта нижняя граница «базальтового» слоя со скоростями сейсмических волн 6,7 км/сек залегает глубже, чем лежит в рифтовой зоне граница раздела со скоростями 7,0—7,2 км/сек. Трудно предполагать, что данные скорости соответствуют кровле «базальтового» слоя. Повышенные значения потока тепла из недр Земли, превышающие в рифтовой зоне примерно в 3—4 раза обычные для океанических платформ значения, свидетельствуют также о подъеме глубинного вещества. Признаки серпентинизации и динамометаморфизма выражены на собранных образцах очень ярко.

Мы полагаем, что подъем вещества мантии Земли к поверхности и сопровождающие его динамометаморфизм и серпентинизация происходят наиболее активно в рифтовой зоне. Это не излияния, а выжимание ультраосновных глубинных пород. Дивергенция конвекционных течений вещества мантии в рифтовой зоне вызывает растяжение коры Срединно-Индоокеанского хребта. Рифтовая зона, где наиболее вероятен выход на поверхность ультраосновных пород, образует одну из замечательных особенностей строения Земли — ее перидотитовый срединно-океанический пояс. Ведущими процессами формирования коры в этом поясе являются серпентинизация вещества верхней мантии и растяжение и разрывы на поверхности. В тектоническом отношении это самостоятельная зона Земли, по масштабам сопоставимая с геосинклинальными поясами. Мы предлагаем для нее термин геотафрогеналь (тафрос (греч.) — ров).

Авторы считают своим долгом выразить признательность Л. В. Дмитриеву (Институт геохимии и аналитической химии АН СССР), любезно оказавшему помощь в определениях части описываемых образцов пород.

Институт океанологии
Академии наук СССР

Поступило
19 VII 1965

ЦИТИРОВАННАЯ ЛИТЕРАТУРА

[1] А. П. Виноградов. Верхняя мантия — земная кора (геохимический аспект), М., 1964. [2] C. Ross, M. Foster, A. Myers, Am. Mineral., 39, № 9—10 (1954). [3] S. J. Shand, J. Geol., 57, № 1 (1949). [4] H. H. Hess, Petrologic Studies, Geol. Soc. Am., 1962. [5] П. Л. Безруков, Геология дна океанов и морей, «Наука», М., 1964. [6] W. Tressler, S. Bershad et al., Hydrographic Office Technical Report, 1956, p. 31. [7] S. Hart, Carnegie Inst. Wash. Year Book, 1964, p. 63. [8] B. C. Heezen, Sci. Am., 203, № 4 (1960). [9] B. C. Heezen, M. Ewing, Geol. Arctic, Toronto, 1961. [10] J. Ewing, M. Ewing, Bull. Geol. Soc. Am., 70, № 3 (1959). [11] R. Raitt, G. Shor, Prelim. Rep. Exp. Downwind, IGY Gen. Rep. Ser., World Data Center A., Washington, 2, 1958. [12] H. Menard, Science, 132, № 3441 (1960). [13] E. C. Bullard, Quart. J. Geol. Soc. London, 120, № 1 (1964). [14] В. В. Белоусов, Сов. геол., № 1, 1964. [15] R. Fisher, Ed., Preliminary Report on Expeditions Monsoon and Lusiad, 1960—1963, University of California, San Diego, Scripps Institution of Oceanography Cruises to the Indian Ocean, S. I. O. Ref. 64—19, University of California, San Diego, 1964. [16] D. Davies, T. Francis, Deep-Sea Res., 11, № 11 (1964). [17] H. H. Hess, Nature, 203, № 4945 (1964).

Reprinted from *International upper mantle project—The world rift system*, p. 33-61

RED SEA SEISMIC REFLECTION STUDIES[1]

S.T. Knott, E.T. Bunce and R.L. Chase
Woods Hole Oceanographic Institution
Woods Hole, Massachusetts

Abstract

Seven continuous seismic reflection profiles were made across the main trough of the Red Sea north of 17°N latitude. These were accompanied by short-pulse echo-soundings and measurements of the total intensity magnetic field and the free-air gravity anomaly.

The horst-and-graben structure of the Gulf of Suez continues southward beneath the western marginal zone of the main trough at least as far as latitude 20°05'N. Deformation of sediments in the grabens indicates fault activity during and after deposition. Short-pulse echo-soundings reveal several episodes of faulting, probably Pleistocene, in the top 20 metres of sub-bottom sediments in the Gulf of Suez.

The main trough between the shelves of the Red Sea can be divided into mildly deformed marginal zones and a deeper, intensely fractured axial zone. Sedimentary sequences in places over 1.8 km thick are found in the marginal zones. Sediment-filled depressions in the western marginal zone at latitudes 18° and 25°N appear to be basins partially closed at their eastern margins by buried blocks of crystalline basement. A strong reflector 0 to 500 metres below all zones of the main trough is postulated to be an unconformity of late Miocene or early Pliocene age. If this postulate is correct, the following can be stated about ages of deformation in the main trough: (1) Most of the deformation in the axial zone appears to have taken place in two periods, one before the beginning of the Pliocene, and the other in late Plio-Quaternary times. These periods of deformation were separated by a period of tectonic quiescence during the early part of Plio-Quaternary time. (2) In the marginal zones, horsts and sediment-filled grabens similar to those of the Gulf of Suez were formed before the Pliocene, and lie buried beneath little-disturbed sediments of Pliocene and younger age.

Recently deposited layered sediment ponds exist in the north and south ends of the Red Sea.

---

[1]Contribution No. 1747 of the Woods Hole Oceanographic Institution.

INTRODUCTION

This paper is concerned primarily with the structure beneath the floor of the Red Sea, determined by continuous seismic reflection profiling (Hersey, 1963). During March 1964, R/V Chain, en route eastward for the International Indian Ocean Expedition, made ten crossings of the axial part of the Red Sea north of latitude 17°N. Continuous seismic profiles, believed to be the first in the region, were made on seven of the crossings (Fig. 1). Gravity, magnetic, and high-resolution echo-sounding observations were made on all ten crossings. Five of the reflection profiles were run across or closely paralleled positions of refraction profiles made in 1958 aboard R/V Atlantis (Woods Hole Oceanographic Institution) and R/V Vema (Lamont Geological Observatory) in order that the reflection measurements might be correlated with the refraction results reported by Drake and Girdler (1964).

INSTRUMENTATION AND DATA PROCESSING

The sound source used for the continuous seismic profiling was an underwater spark, produced by discharging the stored energy of a 1920 μfd capacitance charged at about 8kv. Reflection measurements were taken every ten seconds. The receiver was a Chesapeake Instruments hydrophone array, consisting of five hydrophones in line, ten feet apart, that was towed about 500 ft. behind the ship. The combined output of the five hydrophones connected in parallel was preamplified and fed via the tow cable to additional amplifiers aboard ship. Signals from the array were then recorded on Precision Graphic Recorder (PGR) and magnetic tape. Variable bandpass filters were used when required before the signals were recorded on the PGR, but no filter was used before the magnetic tape recorder. The tapes were then played back at later times through filter-bandwidths not previously used. Ship speeds during profiling were 7-9 knots.

The free-air gravity anomaly and total-intensity magnetic-field measurements presented here with the interpretations of the seismic reflection data are preliminary results obtained from a LaCoste-Romberg sea gravimeter and a Varian proton-precession magnetometer, respectively. They were computed by a shipboard IBM 1710 computer (Bernstein and Bowin, 1963).

RESULTS

The chart of the Red Sea (Fig. 1) shows the ship's track and the locations of seismic reflection profiles described in this paper, and the location of the refraction profiles described by Drake and Girdler (1964).

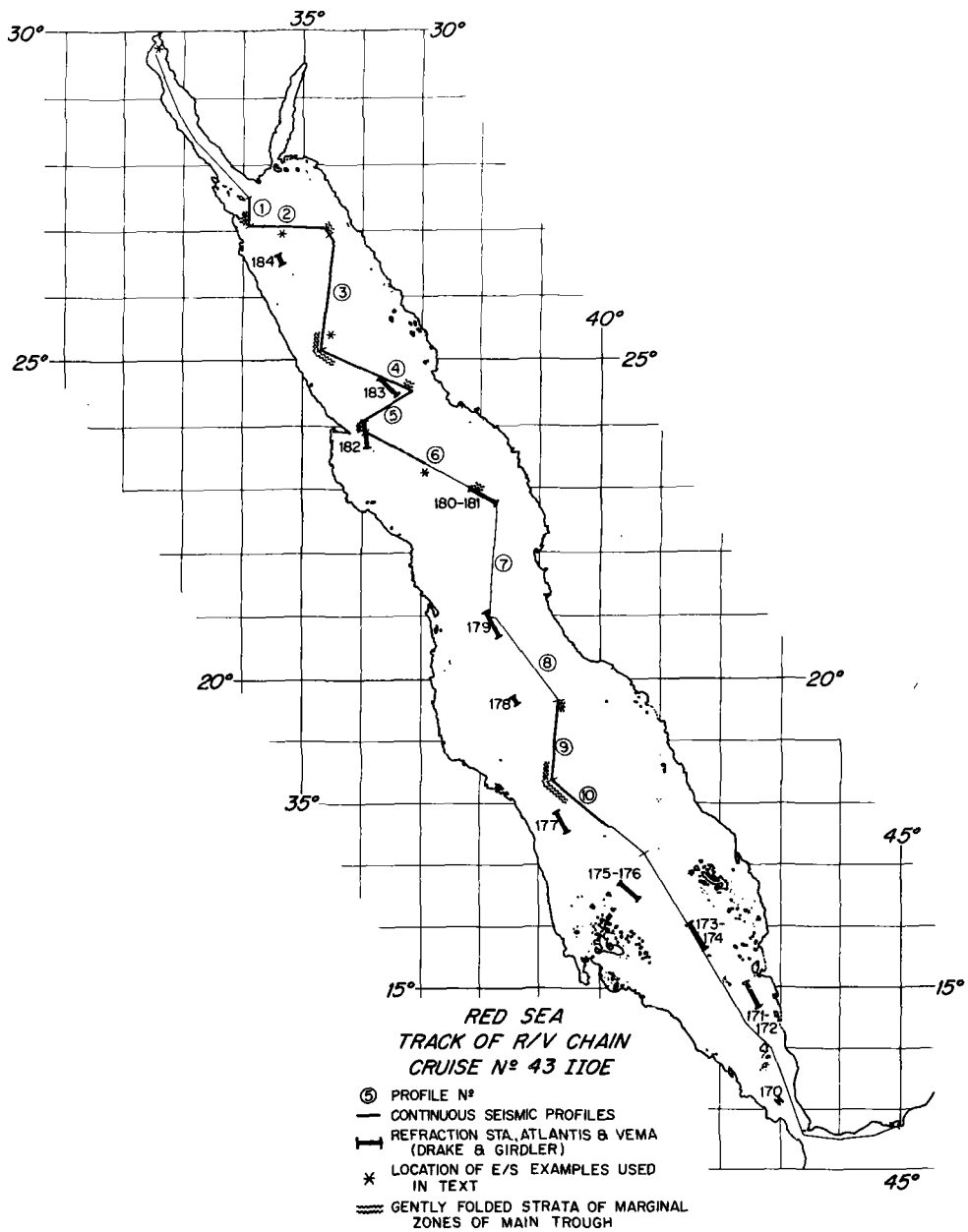


Figure 1. Track of R/V Chain and locations of observations in the Red Sea.

Examples of the seismic profiles recorded by the PGR are given in Figures 2-4. The apparent configuration of reflectors from the reflection profiles is shown by means of line drawings in Figures 2 and 5-16 together with profiles of total intensity magnetic field and free-air gravity anomaly. Bathymetry only is given for those crossings where seismic reflection profiles were not taken. In the line drawings, corrections have been made for varying ship and recorder speeds to bring the tracings to a common horizontal scale. The vertical scale is a time scale whose spatial equivalent varies with the compressional wave velocity of the materials traversed by the sound. Bathymetric scales are based on the assumption that the speed of sound in water is 1500 m/sec. The vertical exaggeration of the bathymetry is about 20:1, and of the configuration of the sub-bottom layers, somewhat less. The exaggeration in the reproductions of original records (Figs. 2-4) is about the same.

In the line drawings, solid lines indicate continuously received and well-correlated echoes (in this case "correlation" refers to how well successive measurements compare with one another in travel time and signal shape); broad lines indicate strong reflections and broken lines indicate interrupted and poorly correlated reflections. Ambiguities may exist where many reflecting horizons are closely spaced in depth. Closely spaced interfaces may be clearly identified at one point in a profile and at another appear to merge and form a single prominent reflecting horizon; in such case the interpretations may show more than one solid line joining a broad line.

ECHO SOUNDINGS

High-resolution echo-sounding records were made on all the tracks by using intense, short (0.2 millisecond) 12-kcps pulses. Sections of records are shown in Figure 17 (for their positions see Fig. 1).

DISCUSSION

The terminology of Drake and Girdler (1964), somewhat amplified, is used for physiographic regions of the Red Sea in the following discussion. New terms which are introduced below are the "axial zone" and the "marginal zones" of the main trough. The former is not to be confused with the axial trough, a previously defined term for a distinct region.

Three physiographic regions of the Red Sea are apparent: the coastal shelves, the main trough, and the axial trough (Fig. 18a; Drake and Girdler, 1964; Heezen and Tharp, 1964; Admiralty Chart C6359, 1965). The shelves slope gently from the shores to depth of 300 to 600 metres. The

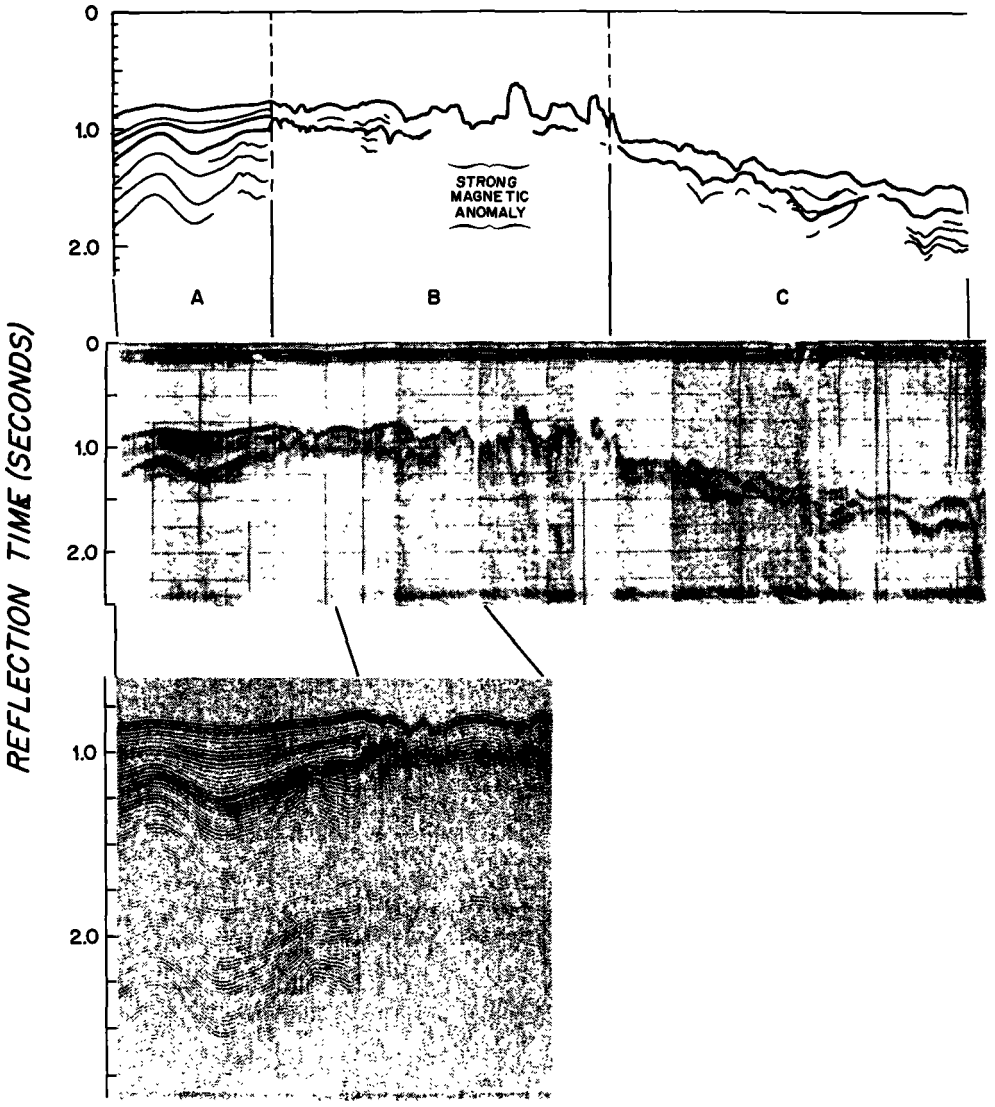


Figure 2. Western half of Profile 4: (top) line-drawing interpretation; (middle) seismic reflection record, recording bandwidth 37.5 to 300 cps; (bottom) section of reflection record, recording bandwidth 37.5 to 75 cps. A. Gently folded strata of western marginal zone. B. Acoustically opaque ridge which trends across the Red Sea. C. Axial zone of the main trough.

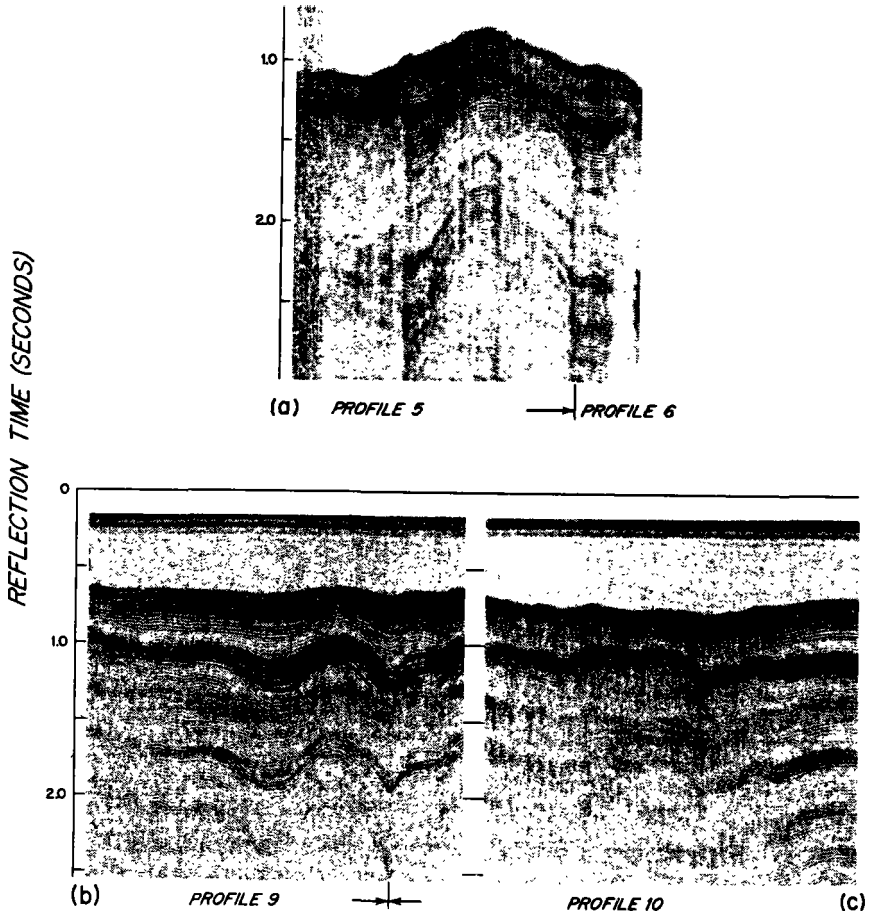


Figure 3. Photographs of continuous seismic reflection records. Recording bandwidth 20 to more than 3000 cps. (a) Western marginal zone of the main trough (lat. 24°N). The anticline is probably the submarine extension of the Ras Banas Peninsula. A sequence of reflectors beneath the anticline, 0.9 to 1.5 seconds below sea-level, is cut off abruptly on the north (left) side, possibly along a steeply dipping fault. Reflectors below the sequence are multiples. The strong reflector 0.25 seconds below the sea floor is postulated to be the Miocene-Pliocene contact. (b) Strata beneath the broad embayment in the western shelf at 18°N. The strong reflector at 0.9 seconds at the south end (left) laps up onto acoustically opaque substrata. (c) The central part of the profile shows an opaque unit, apparently a horst, below the strong reflector at 1.0 secs below sea-level. The strong reflector continues across a sediment-filled graben to the right (south-east) of the horst.

irregular broken floor of the main trough varies from 600 metres to more than 1,000 metres deep. This trough is 100 to 150 kilometres wide north of latitude 20°N, but becomes generally narrower southward. Between 23° and 26°N isolated deeps occur in the main trough. South of 23°N a continuous deep, the axial trough, is developed within the main trough. In places the axial trough is more than 2,000 m deep and greater than 20 km wide. It is incised by deeps that appear to trend parallel with the axis (Swartz and Arden, 1960). South of 19°N, the depth of the axial trough decreases, the shelves widen, and the main trough narrows. At 17°N, the axial and main troughs become indistinguishable.

The Red Sea reflection profiles discussed here cut only the main and axial troughs. The shelves were not investigated. Profile 1 (Fig. 8) runs along the boundary between the shelf and the main trough. Profiles 2-6 (Figs. 8-12) cut the trough, and Profiles 7-10 (Figs. 13-16) cut both the main and axial troughs.

Profile 1 (Fig. 8) is parallel to the margin of the main trough just south of the Gulf of Suez, and Profile 2 cuts across the north end of the main trough. Information from surface geology and exploratory wells just north of Profile 1 shows that this region is one of elongated horsts of crystalline basement and grabens filled by Tertiary sedimentary rock. The controlling faults trend north-northwest (Said, 1962, Figs. 25, 26 and 47). This structural picture is supported by the reflection profiles. Profile 1 extends 35 km south from a point near Shadwan Island. Two grabens filled with layered rock at least one kilometre thick lie between three horsts of crystalline basement or older more consolidated sedimentary rock. The northern horst is probably the southern continuation of a basement high passing beneath Shadwan Island (Said, 1962, Fig. 25). The northern graben may be a continuation of the graben beneath Tawila Island (ibid, Figs. 26 and 68) that, some 40 km north, is known to be filled with about 4 km of post-Eocene strata. The southern graben of Profile 1 appears again as the deep western graben of Profile 2. Deformation within the grabens indicates reactivation of the boundary faults and of other faults in the underlying basement during and after deposition.

Examination of the shape of the sea floor and sub-bottom reflectors of the profiles over the main trough (Figs. 8-12, Profiles 2-6) reveals that this trough is generally divisible into three zones – namely, a deep axial zone of rugged floor and intense sub-bottom deformation, and shallower marginal zones of more gentle topography and milder deformation, which bound the axial zone to east and west. Examples of reflection profiles across places where the boundary between zones is abrupt are shown in Figure 4. The transition from one zone into another is not in all places so sharp and unequivocal, however. Parts of Chain's track underlain by the gently folded strata of the marginal zones are shown in Figure 1, and the

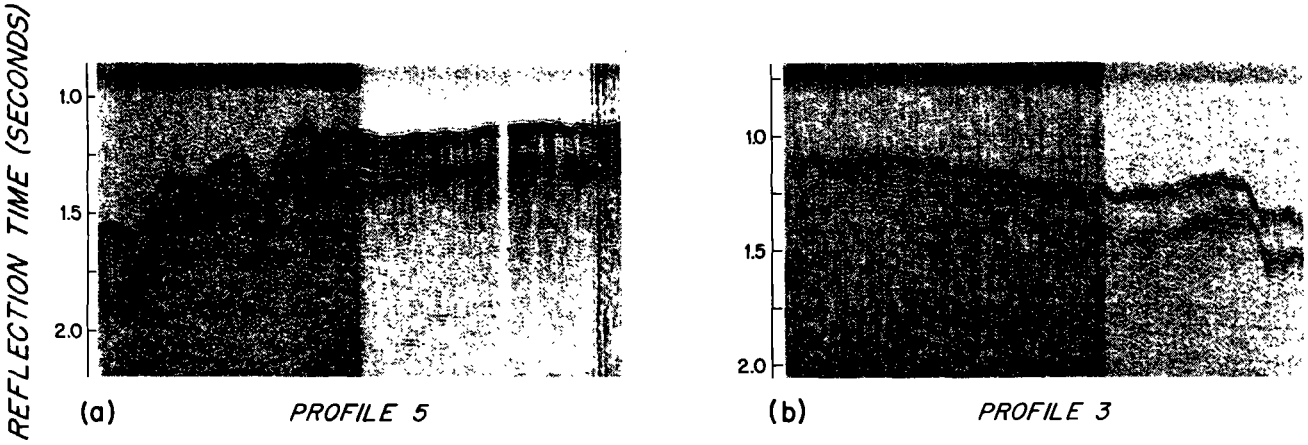


Figure 4. Continuous seismic reflection profiles across the transition between the marginal and axial zones of the main trough. (a) Near lat. 24°N. Strata of the western marginal zone appear to crop out on the fault scarp which marks the boundary. (b) Near lat. 27°N. The strong reflector beneath the eastern marginal zone appears about 450 metres (0.3 secs) deeper in the axial zone (sections viewed from the north).

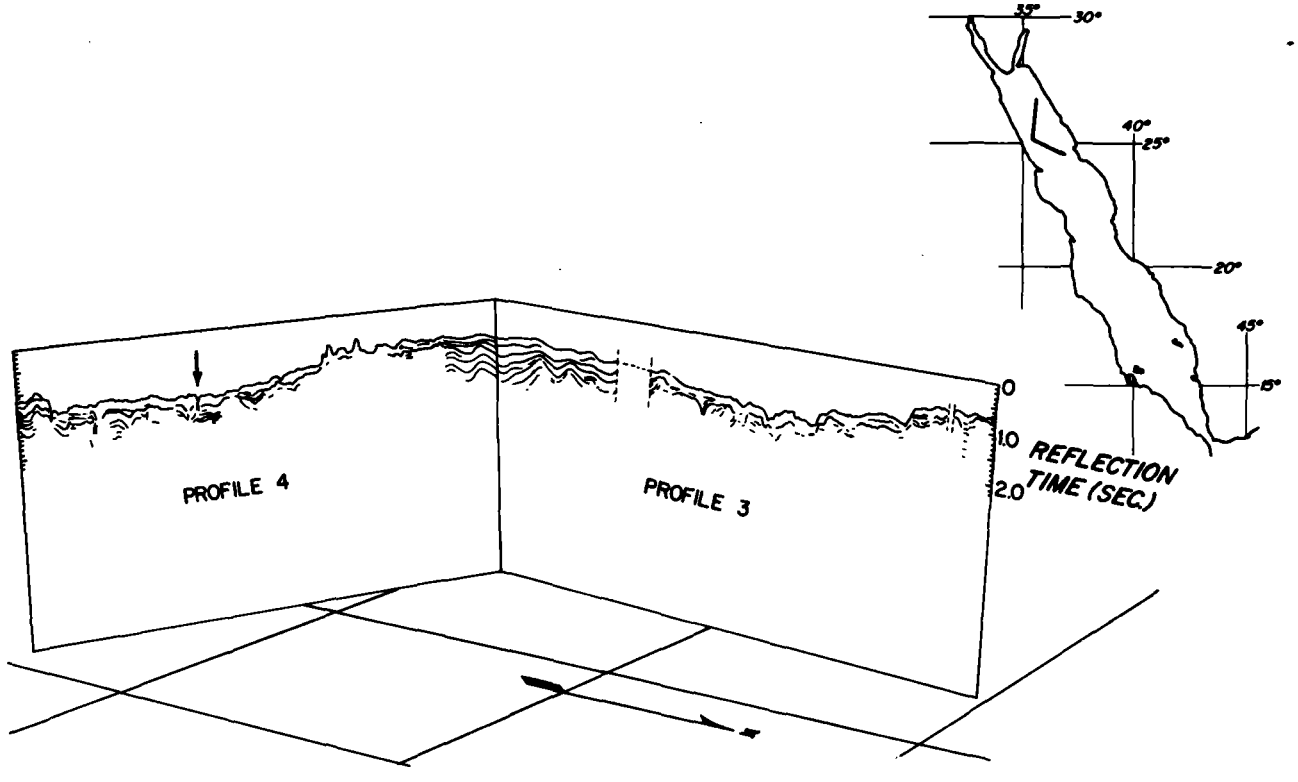


Figure 5. Panel diagram showing seismic reflection Profiles 3 and 4 of northern part of the main trough of the Red Sea, showing a basin beneath the western marginal zone (centre) and two sections through the axial zone. Note narrow axial deep below arrow.

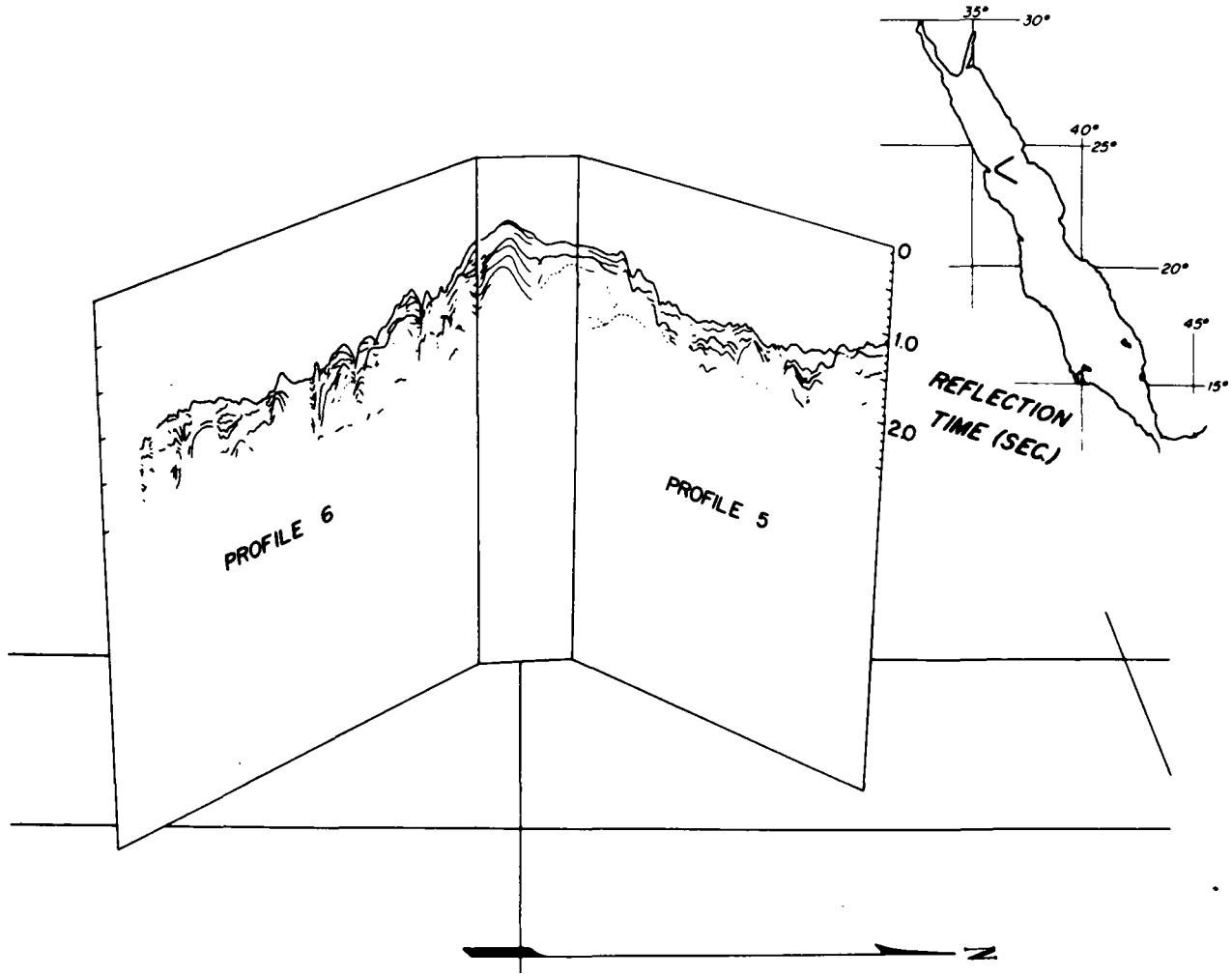


Figure 6. Panel diagram of seismic reflection Profiles 5 and 6 across the seaward extension of the Ras Banas Peninsula (centre) near St. John's Island, and across the axial trough in two places.

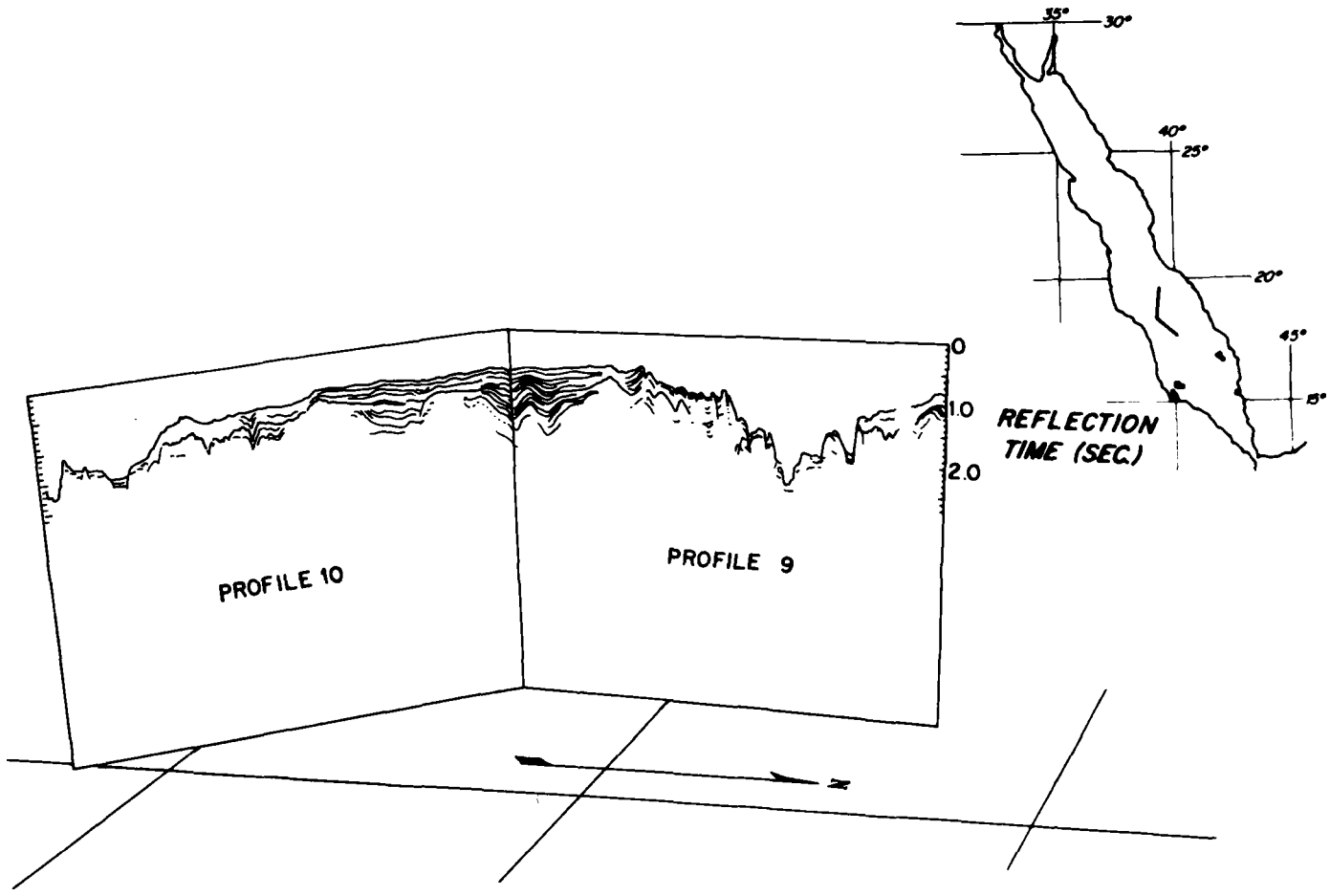


Figure 7. Panel diagram of seismic reflection Profiles 9 and 10 in the southern part of the Red Sea showing gently folded strata of the marginal zone of the main trough under a broad re-entrant into the western shelf (centre of diagram) and two cuts across the axial trough.

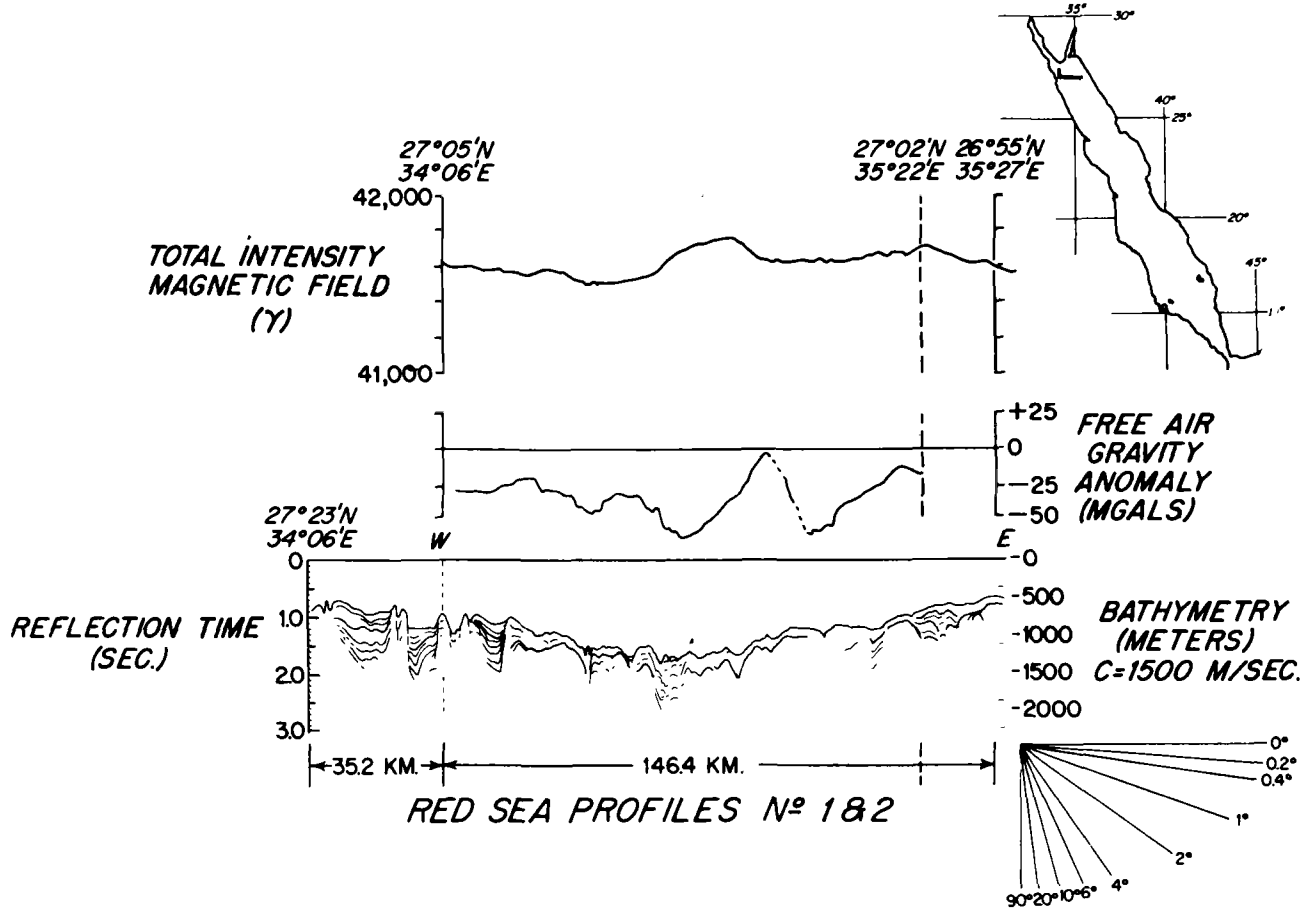


Figure 8. Profiles 1 and 2: seismic reflections, bathymetry, gravity and magnetics (course changes indicated by vertical dashed lines).

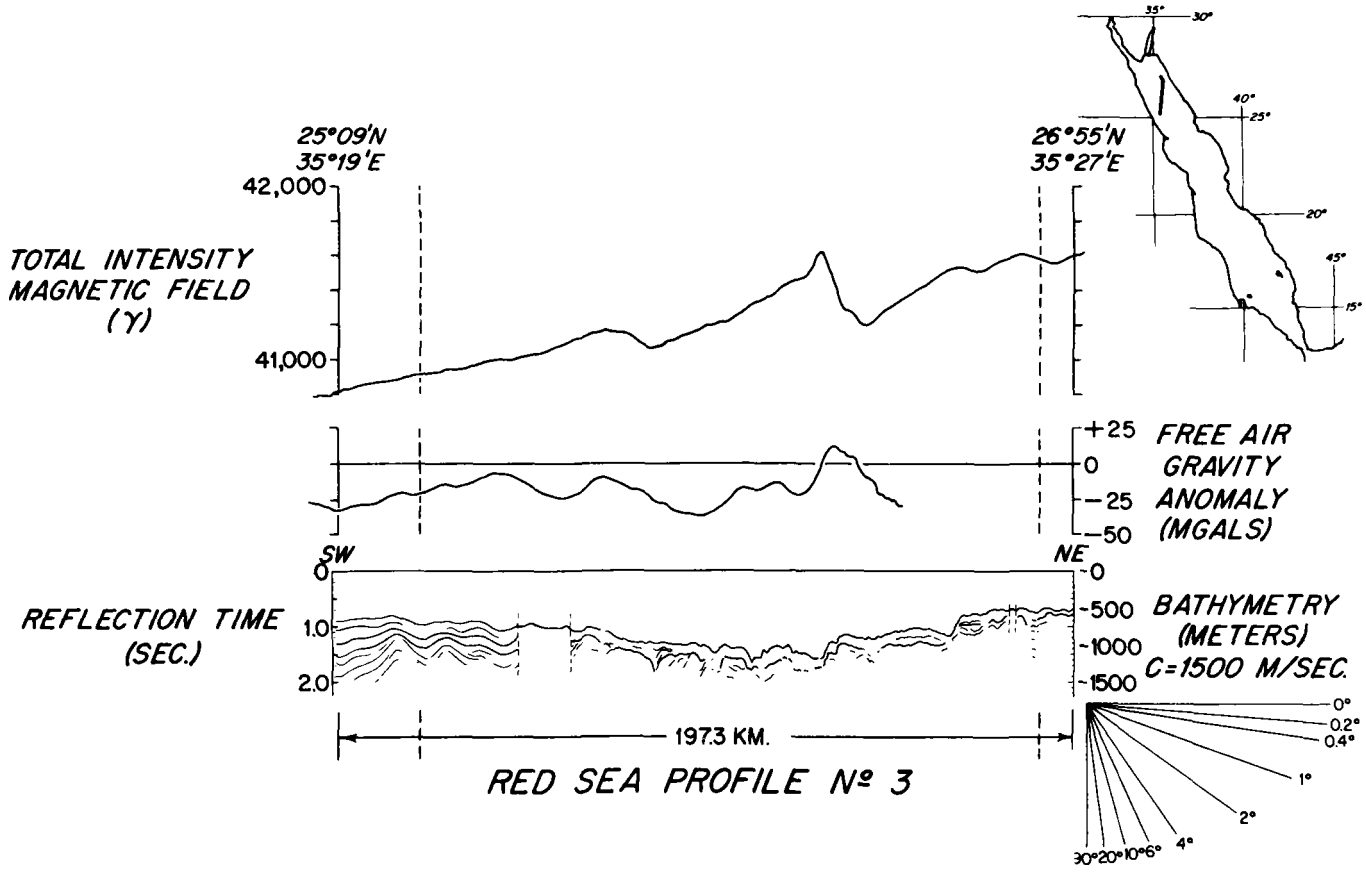


Figure 9. Profile 3: same as in Figure 8.

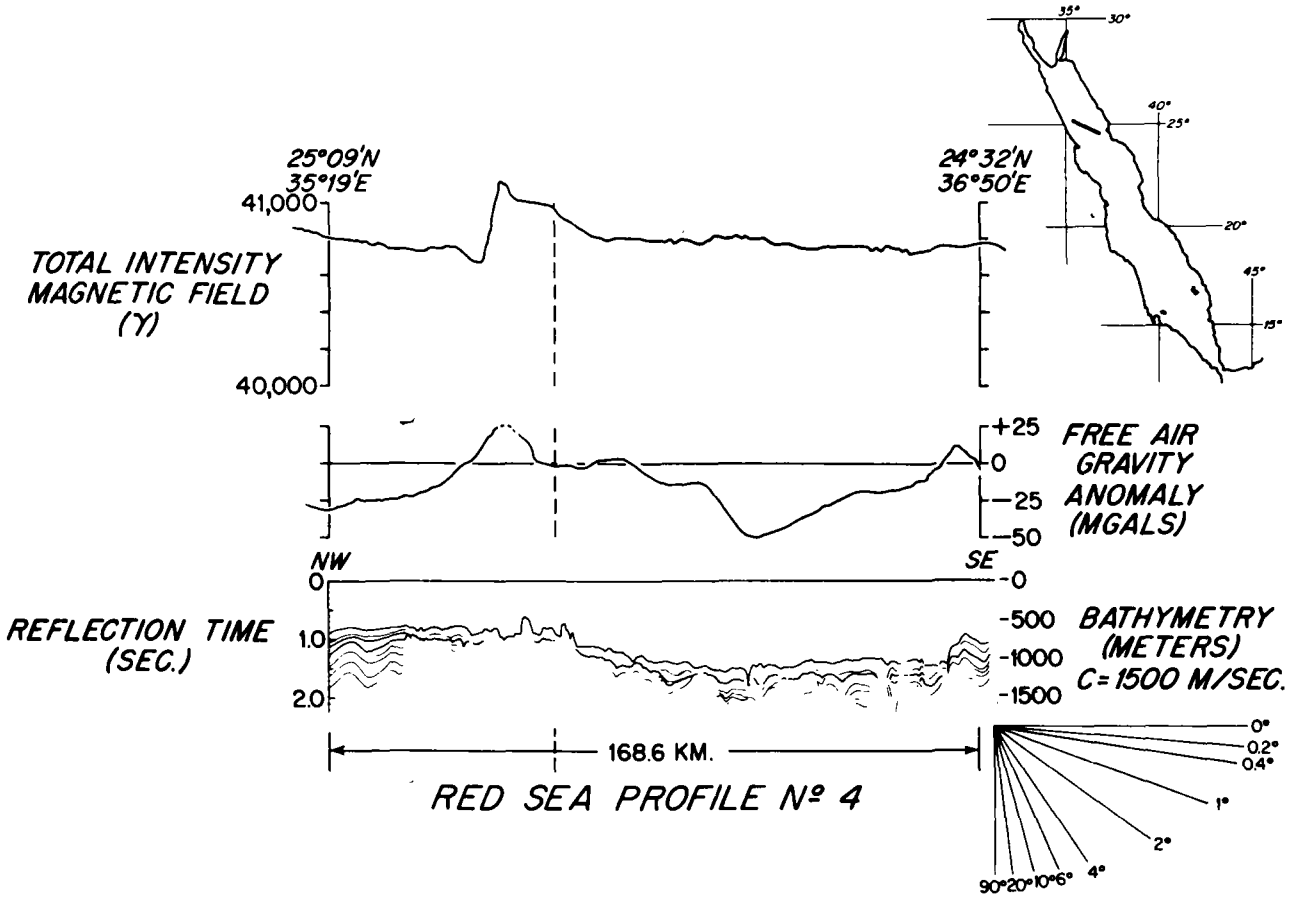


Figure 10. Profile 4: same as in Figure 8.

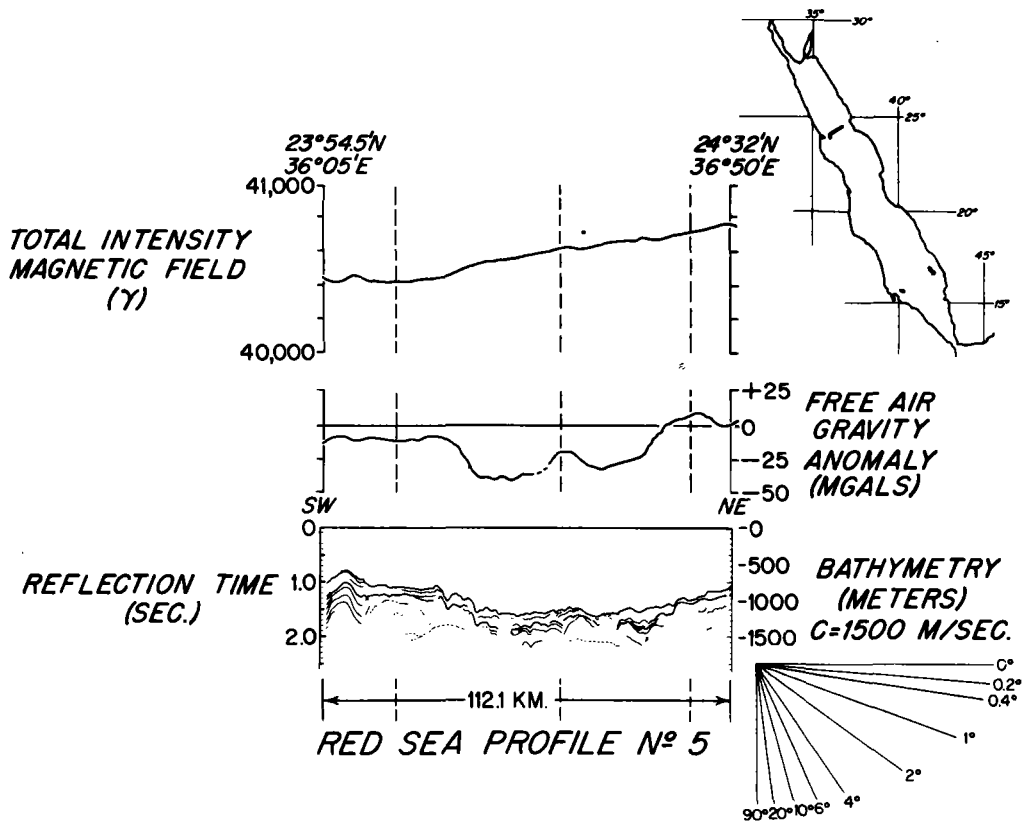


Figure 11. Profile 5: same as in Figure 8.

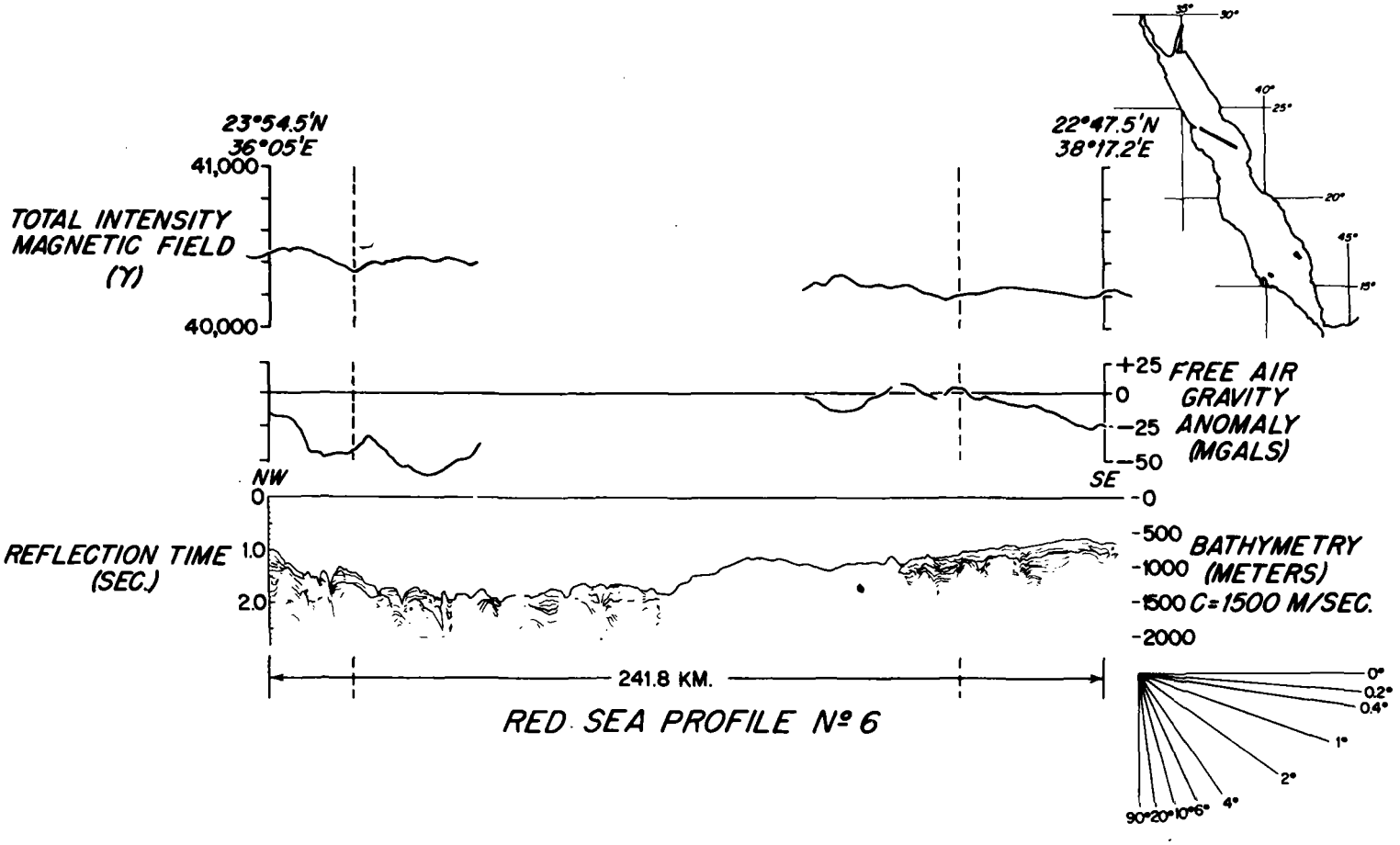


Figure 12. Profile 6: same as in Figure 8.

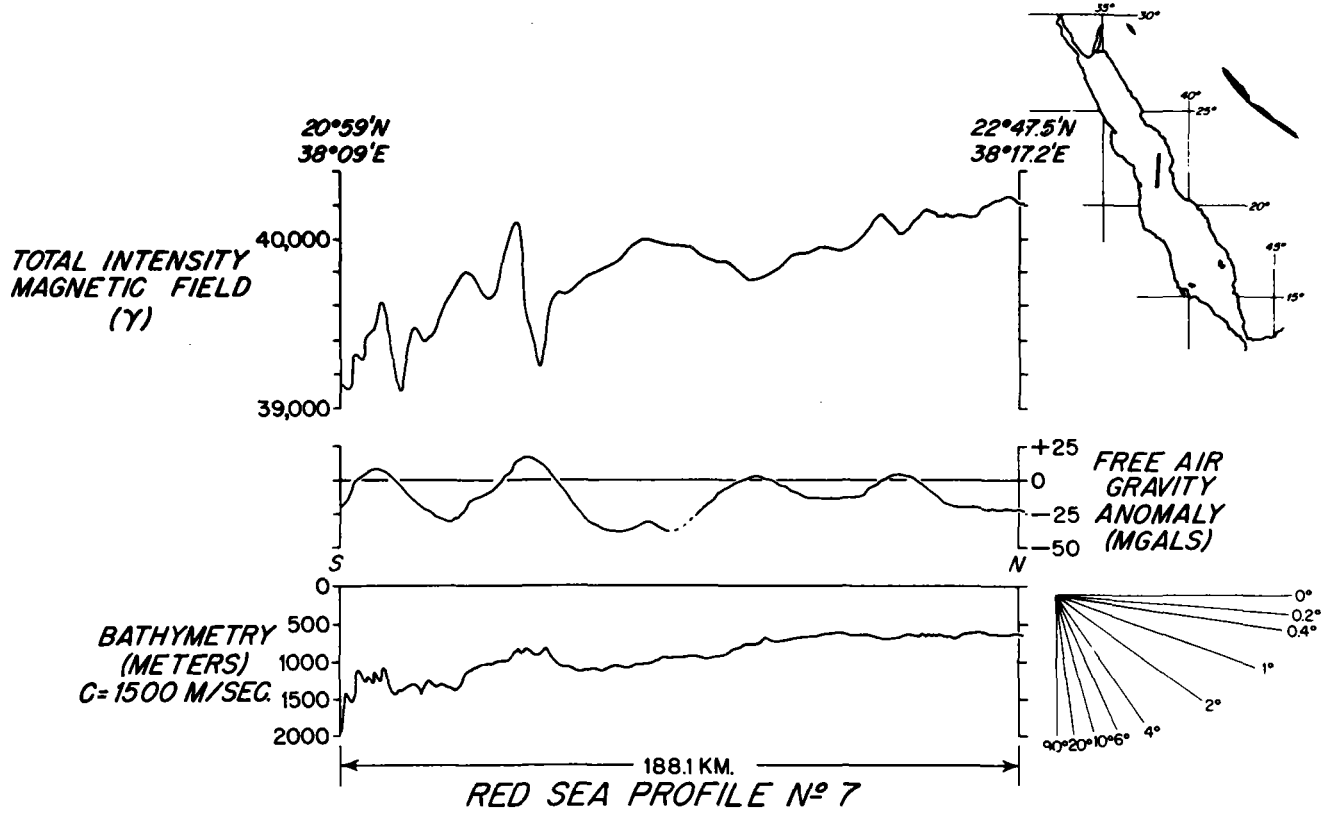


Figure 13. Profile 7: Bathymetry, gravity and magnetics (course changes indicated by vertical dashed lines).

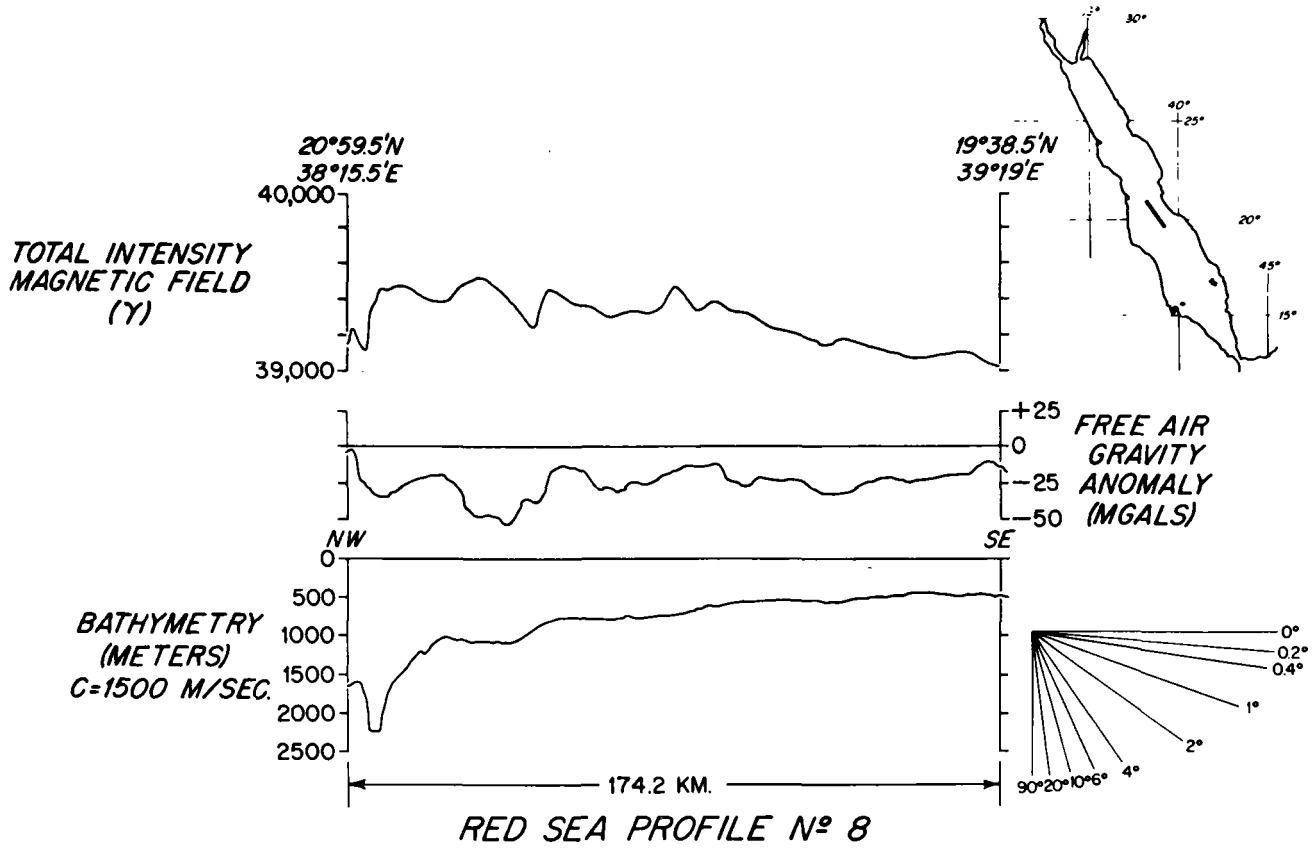


Figure 14. Profile 8: same as Figure 13.

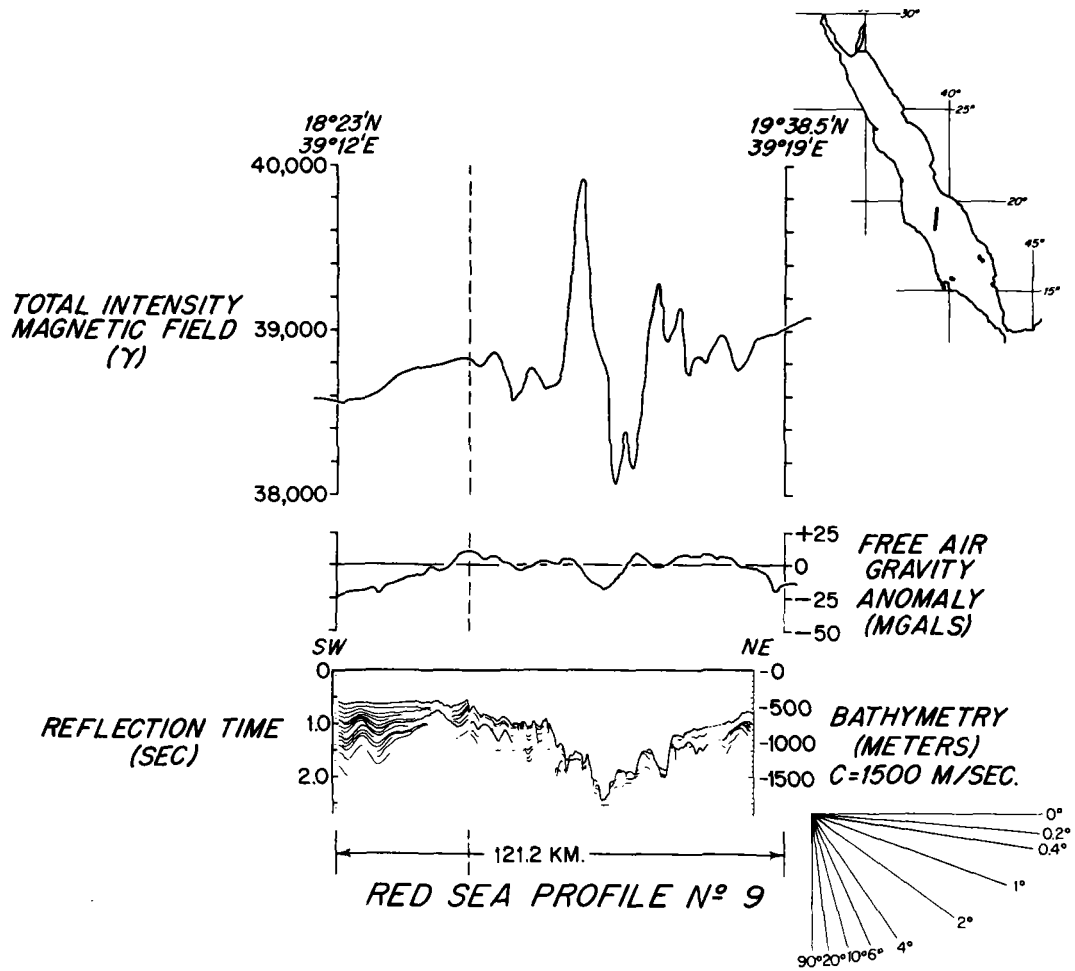


Figure 15. Profile 9: same as in Figure 8.

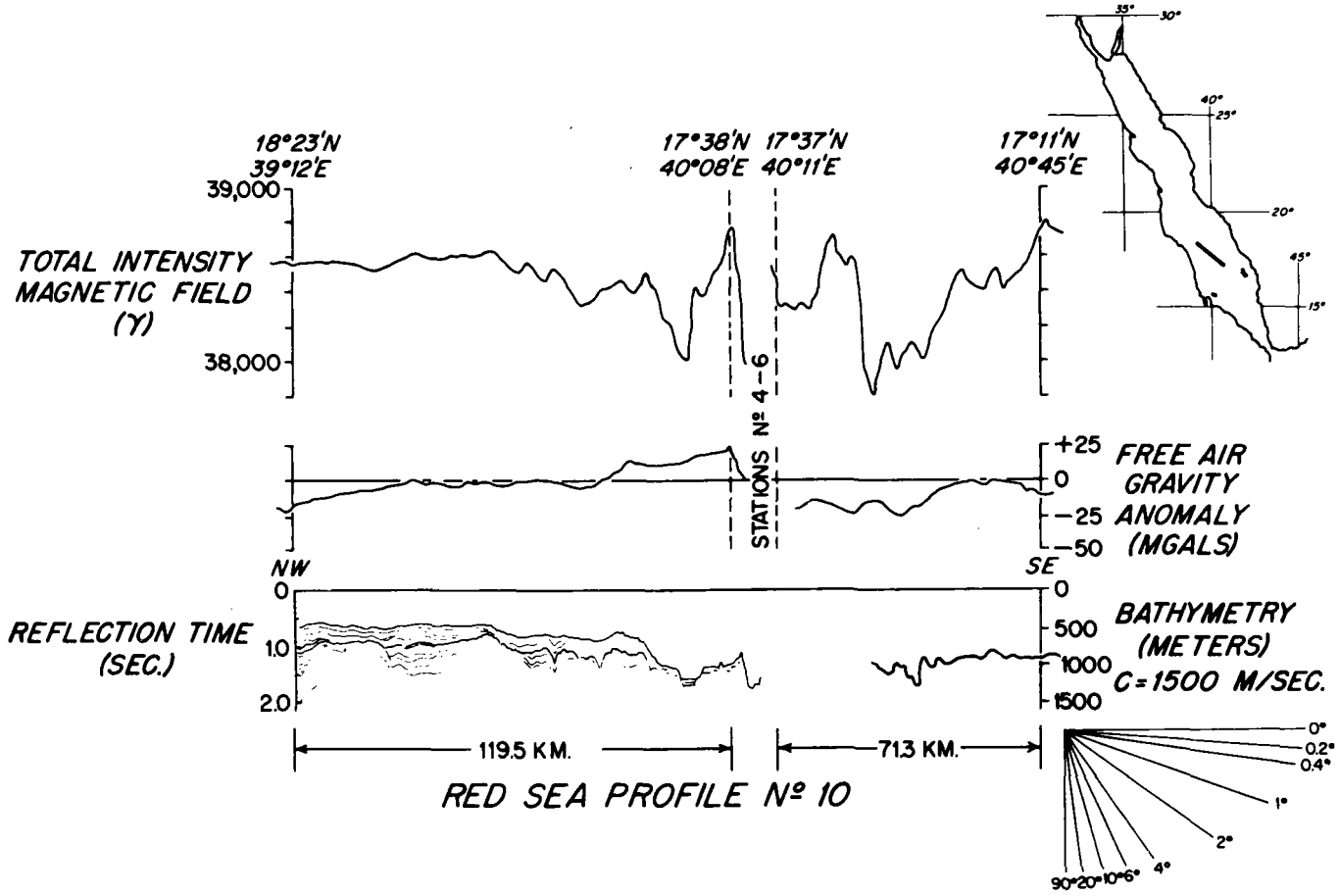


Figure 16. Profile 10: same as in Figure 8.

approximate boundaries of the axial zone in Figure 19. The central part of Profile 2 (Fig. 8), through the axial zone of the main trough, shows distorted, laterally discontinuous sequences of reflectors, this being evidence of many faults. A marked free-air gravity high near the eastern margin of the axial zone may be the result of much greater differential movement of basement blocks and consequent variations in thickness of semi-consolidated superficial material in this locality than is apparent from the reflection profiles. On the other hand, it may instead mark an intrusive igneous body at depth, though the associated magnetic anomaly is small compared with those farther south in the axial trough (cf. Figs. 13-16).

Profile 3 (Figs. 5 and 9) cuts obliquely across the main trough. At its southwest end, penetration was obtained into a sequence of gently folded strata which also appear at the northwest end of Profile 4 (Figs. 5 and 10). In the latter profile, penetration is less beneath an area of relatively rugged bottom to the southeast of the folded strata. This area forms part of an irregular northeast-trending ridge shown on Admiralty Chart C6359. An extension of the ridge forms the northern side of an isolated deep in the axial zone. High free-air gravity anomalies coupled with a magnetic anomaly over this ridge indicate that it is an upfaulted basement block, or an intrusive mass, or perhaps both. It seems to form the southern side of a sediment-filled depression (Fig. 5). There is a suggestion on Profile 3 that sedimentary strata in the depression also shallow to the north before they reach the axial zone. Thus the depression may be a closed basin.

One strong reflector (about 1.5 sec below sea-level at the west end of Profile 3) beneath the western marginal zone appears to be a surface of mild unconformity. A similar though rougher reflector is present beneath the axial zone in both profiles, although there the attitudes of beds above and below it are more divergent. Similar strong reflectors appear in all the other reflection profiles, beneath both marginal and axial zones of the main trough (Figs. 3 and 4), but not beneath the axial trough in Profile 9 (Fig. 15). It is postulated here that all the above-mentioned strong reflectors are one and the same, and that this one strong reflector is a surface of unconformity, dating from the end of the Miocene or the beginning of the Pliocene and representing a period when blocks in the axial zone were differentially elevated, depressed and tilted, and sediments beneath the marginal zones were more gently warped over faults in the underlying crystalline basement. The argument supporting this postulate is as follows. The depth of the reflector beneath the sea bottom varies between zero and 0.5 seconds under both axial and marginal zones of the main trough. If a compressional wave velocity appropriate for unconsolidated sedimentary rock is assumed (that is, about 2 km/sec), the thickness of rock above the reflector is 0 to 500 m. The Red Sea refraction results of Drake and Girdler (1964) (Fig. 18b) indicate that in most places a layer of material of about

this thickness and velocity overlies rock of higher velocity that they assume comprises consolidated sediments and evaporites beneath the shelves and main trough, and lava flows and sediments beneath the axial trough. There is evidence from exposed and subsurface geology of the margins of the Red Sea (Said, 1962; Sestini, 1965, USGS Map I-270A) that tectonic activity at the end of the Miocene or the beginning of the Pliocene terminated the deposition of a Miocene succession of limestone, evaporite and clastic rock. Pliocene and Pleistocene deposits, mainly clastic sediments and reef limestones, overlie the Miocene succession. The thickness of the post-Miocene deposits in the Gulf of Suez varies from 0 to 1.6 km (Said, 1962, p. 279). On the coast south of the Gulf of Suez, near Q'seir, the Pliocene succession is about 100 m thick (Said, 1962, p. 117), and beneath the Sudan coast, it is known to be as thick as 400 m (Sestini, 1965, p. 1465). Thus the thickness of the post-Miocene sediments on the margins of the Red Sea is similar to that of the rocks above the strong reflector, and to that of the unconsolidated material of the refraction profiles. Hence it is postulated that the strong reflector is a discontinuity which resulted from tectonic activity at the end of the Miocene.

Post-Miocene deformation in the western marginal zone is indicated in Profile 5 (Figs. 3a and 11), which approaches St. John's Island from the northeast, and shows simultaneous folding of the postulated Miocene-Pliocene unconformity and of the sequence below it. In Profile 5 there is a rough correspondence, between western marginal and axial zones, of the number and separation of weaker reflectors above the unconformity. To explain this and similar correspondence found in Profiles 2-4 (Figs. 8-10), it is postulated that during the Pliocene a blanket of sediments extended across the main trough without such a marked break as is now apparent between marginal and axial zones (photographs of the original records illustrating the break are shown in Fig. 3), and that the present broken and tilted structure of the axial zone is in part post-Pliocene.

Profile 6 (Fig. 12) shows that considerable deformation, pre-unconformity and thus presumably pre-Pliocene, took place beneath the eastern marginal zone north of Jidda. Post-Pliocene deformation is indicated by the roughness of the unconformity and discontinuity and variable dip and thickness of beds above it.

The southern end of Profile 7 and the northeastern end of Profile 8 (Figs. 13 and 14) for which there are no reflection data, show strong magnetic anomalies over the axial trough and eastward similar to those of Profiles 9 and 10. The latter (Figs. 15 and 16) are crossings of the region in which the axial trough is well developed, where strong linear magnetic anomalies were found by Drake and Girdler (1964) and Allan (1964). The positive free-air gravity anomaly of Profile 9 agrees generally with the measurements of Vening Meinesz (1934) and of Girdler and Harrison (1957).

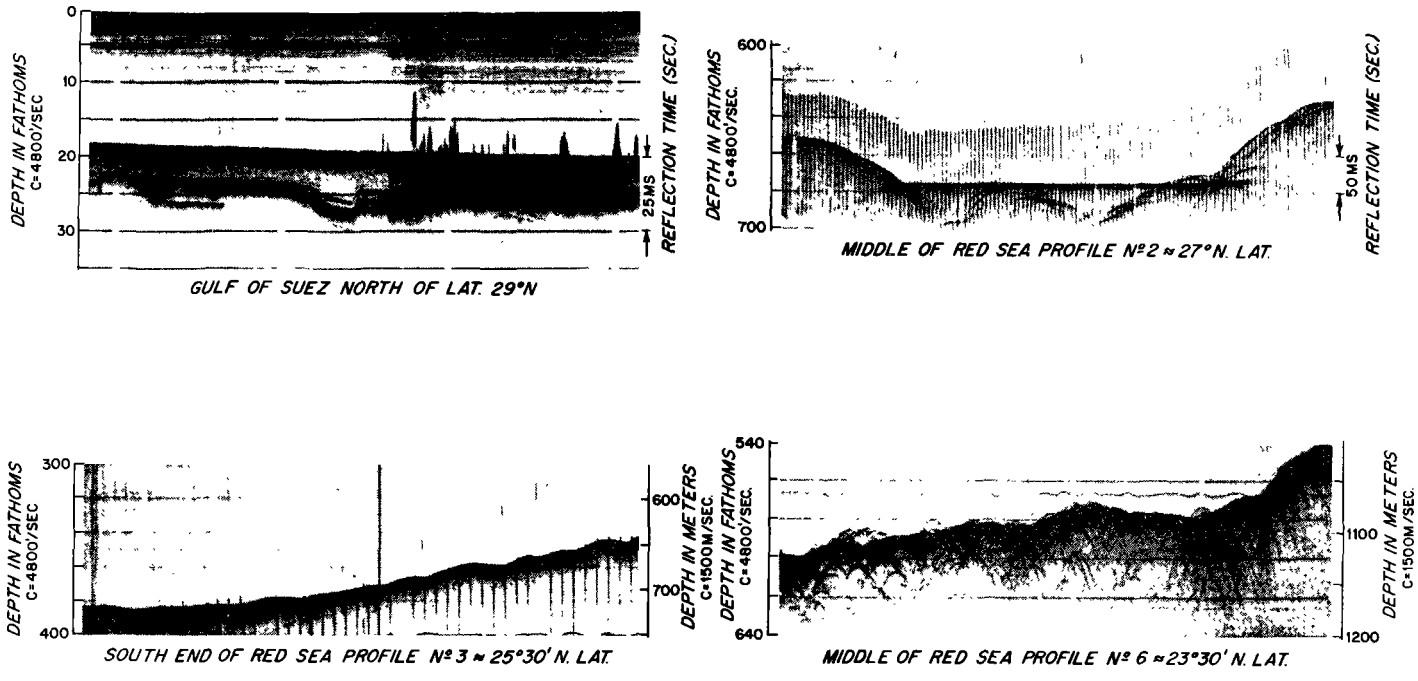


Figure 17. Echo-sounding records showing surficial sediment structures and bottom roughness.

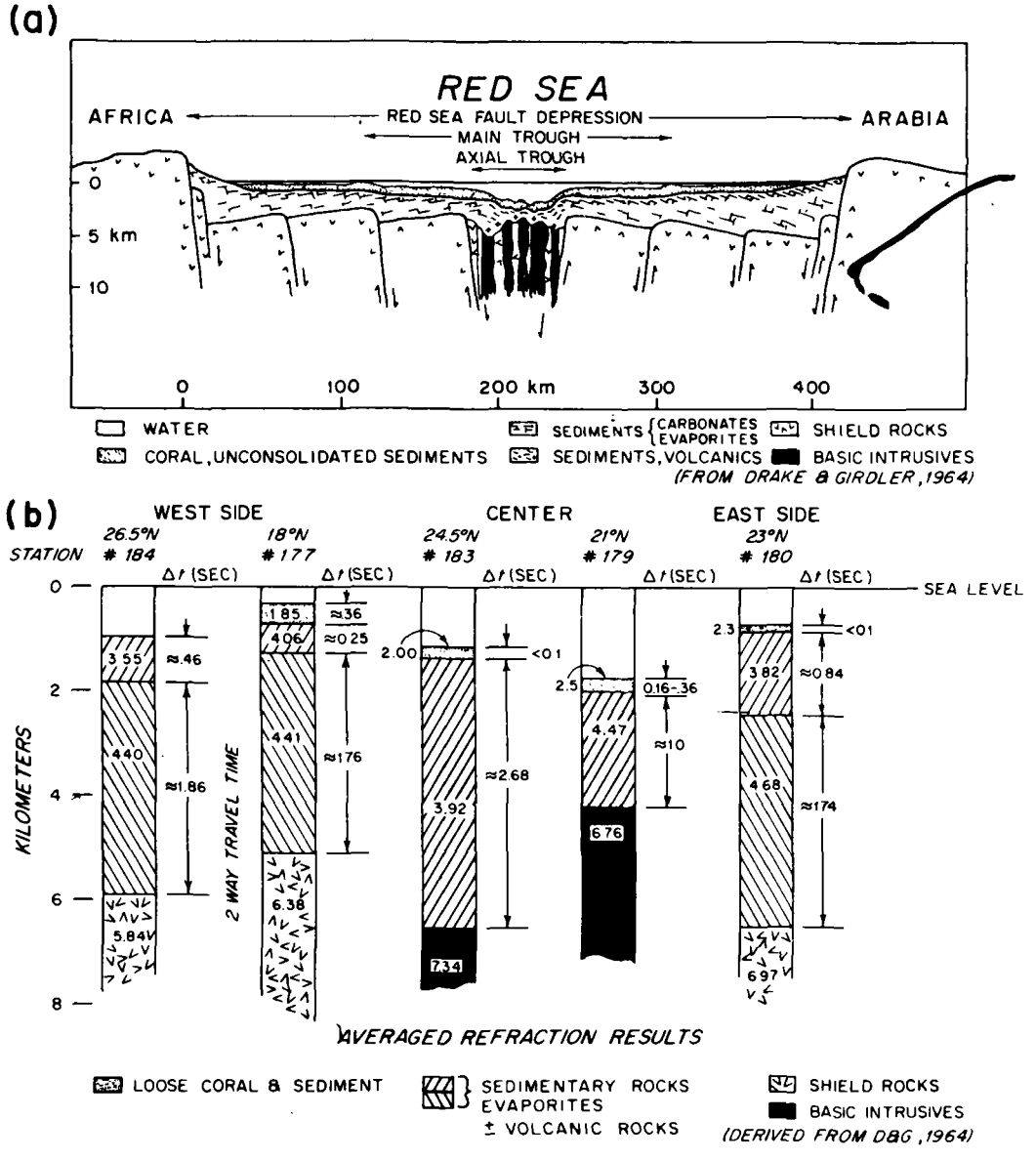


Figure 18. (a) Generalized geological cross section of the Red Sea, from Drake and Girdler (1964).
(b) Averaged seismic sections of the main trough. Depth in kilometres at left; approximate two-way travel times through each layer at right of each column; seismic velocities in kilometres per second within each column.

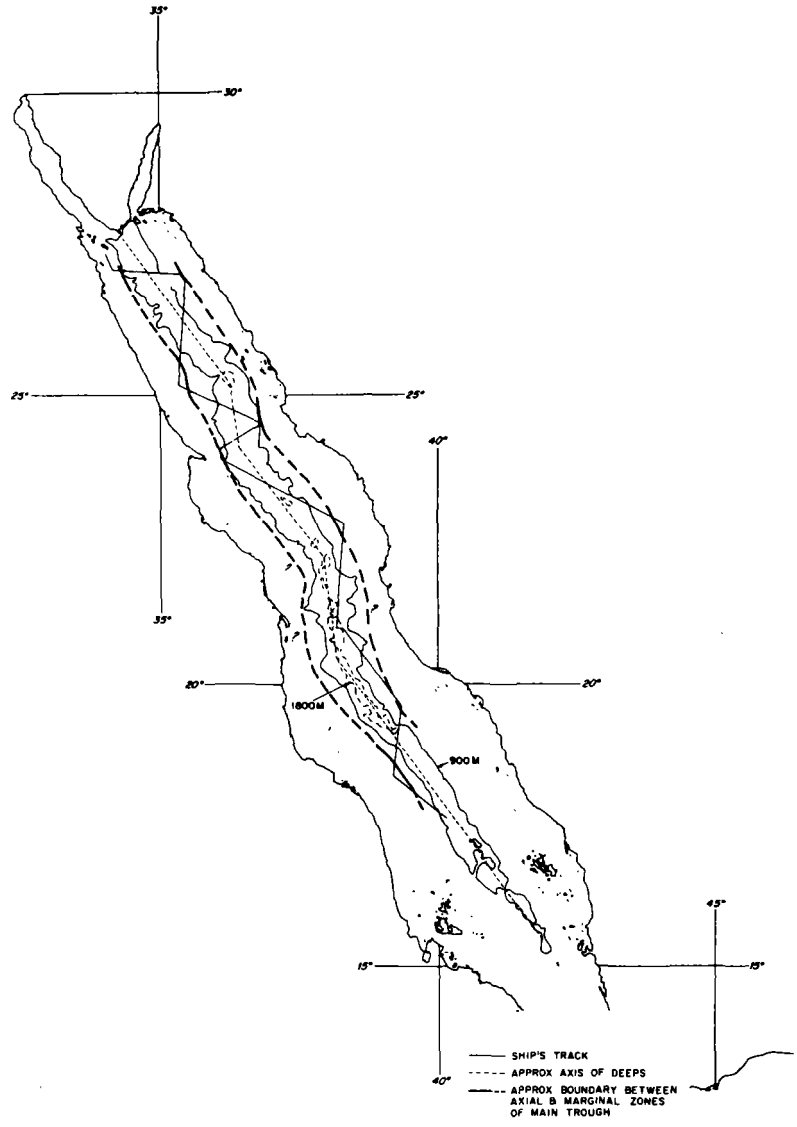


Figure 19. Chart of the Red Sea illustrating the boundaries of the axial zone of the main trough, and the trends of the successive segments of the axis of the sea. (Bathymetric contours taken from British Admiralty Chart C6359 with some modifications based on soundings of R/V Chain.)

The southwest end of Profile 9 (Figs. 7 and 15) shows the structure beneath a broad re-entrant or embayment into the western shelf, that to the north and south is wide and shallow (Admiralty Chart C6359). The free-air anomaly becomes increasingly negative towards the centre of this embayment in Profile 9, and also in Profile 10 which cuts obliquely across the seaward margin of the embayment. The gently folded strata which underlie the embayment appear to thin northeastwards in Profile 9 (Figs. 3b and 15) and lap up onto a buried block of acoustically opaque material that presumably consists of consolidated sedimentary or crystalline rock. The upper surface of the block has an apparent dip of about 1.5° south-southwest. If it is assumed that the azimuth of the true dip is normal to the axis of the trough, the value of the true dip of the block surface is something over 2° southwest. Farther northeast, Profile 9 makes an oblique cut across a narrow southern extension of the main trough and the axial trough. Laterally restricted stratified sequences exist beneath the former (Fig. 15, left centre), as they do in the better developed sections of the main trough to the north. In contrast, beneath the axial trough, equally thick sequences of several parallel reflectors are not seen.

In Profile 10 (Figs. 3, 7 and 16) the unconformity discussed above and postulated to date from the beginning of the Pliocene extends beneath the floor of the embayment across the tops of acoustically opaque volumes of rock and intervening depressions filled with stratified, gently folded material. The near parallelism of this profile with the main structural trends prevents confident interpretation of the sub-bottom structure. Most likely the latter consists of horsts and grabens bounded by faults which, judged by the low relief of the unconformity, have moved little since the latter was formed.

HIGH FREQUENCY ECHO SOUNDINGS

The sea-floor in the echo sounding record from the Gulf of Suez shown in Figure 17, upper left, varies between 18 and 20 fathoms in depth. The "spikes" above the bottom are reflections from schools of fish. Below the floor, penetration of up to 27 milliseconds (about 20 metres) was achieved. A complex sequence of events is indicated, as follows:

1. Deposition of the material now below the lowest reflector on the left hand side of the record.
2. Erosion or faulting to form the buried hill on the same side of the record.
3. Deposition of the material between the lowest and the next layer.

4. Formation of the depression in the centre part of record, probably by faulting, possibly assisted by fluvial erosion.
5. Deposition of a layered sequence up to 10 metres thick in the depression.
6. Renewed faulting of the basement to distort the layered sequence.
7. Deposition of about 10 metres of acoustically transparent material above the layered sequence.

This part of the Gulf of Suez is shallow enough to have been above sea-level during the Pleistocene. Thus, some of the layers seen in the record may be of sub-aerial or fluviatile origin. The faulting mentioned in 2, 4 and 6 above is probably Pleistocene in age.

The two echo-sounding records reproduced on the right hand side of Figure 17 come from the axial zone of the main trough of the Red Sea. The upper record shows a sediment pond near the northern end of the sea in which some 5 metres of layering is apparent. Other sediment ponds in the axial trough were crossed in the south (Figs. 15 and 16), but few, if any, occur in the middle latitudes of the sea. The lower record is made up of numerous parabolas each representing a small reflecting area, an indication of a very rugged floor, unmasked by recent sediment accumulation. This record is to be contrasted with the smoother, acoustically opaque bottom underlain by the gently folded strata of the western marginal zone of the main trough (Fig. 17, lower left).

CONCLUSIONS

1. On the basis of the relative depth and ruggedness of the sea floor, and the degree of deformation of the sub-bottom reflectors, the main trough of the Red Sea can be divided into an intensely deformed axial zone flanked by mildly deformed marginal zones.

2. Sedimentary sequences in the mildly deformed zones are in places over 1.8 km thick.

3. A strong reflector 0 to 500 metres below all zones of the main trough is postulated to be a discontinuity, in some places an unconformity, of late Miocene or early Pliocene age. On the assumption that this postulate is correct, the following can be stated about ages of deformation in the main trough.

(a) The similarities in the reflecting characteristics and the number of Post-Miocene strata beneath the axial and marginal zones in some

regions is taken to indicate that most of the intense deformation of the axial zone of the main trough occurred in two periods, one before the beginning of the Pliocene, and the other in late Plio-Quaternary times. These periods of deformation were apparently separated by a period of tectonic quiescence during the early part of Plio-Quaternary time.

(b) Pre-Pliocene horsts and sediment-filled grabens similar to those of the Gulf of Suez lie buried beneath layers of little-disturbed Pliocene and younger sediments under the eastern marginal zone around latitude 23°N, and under the western marginal zone around latitude 18°N.

4. Sediment-filled depressions in the western marginal zone at latitudes 18° and 26°N appear to be basins partially closed at their eastern margins by buried blocks of crystalline basement.

5. Layered sediment ponds exist in the north and south ends of the Red Sea.

6. The horst-and-graben structure of the Gulf of Suez continues southward beneath the western marginal zone of the main trough of the Red Sea at least as far as latitude 20°05'N. Deformation of the sediments in the grabens indicates fault-activity during and after deposition. Short-pulse echo soundings reveal several episodes of faulting, probably Pleistocene, in the top 20 metres of sub-bottom sediments in the Gulf.

ACKNOWLEDGMENTS

This work was supported at the Woods Hole Oceanographic Institution by the National Science Foundation under Research Grant GP-2370 and the Office of Naval Research under Contract Nonr-4029(00). The authors wish to express their gratitude to the scientific party, the officers, and the crew of the Research Vessel Chain for their assistance during collection of the data, and to Mrs. B. Collins, F.L. Lynch, and A. Zwilling, among others, who helped in the working up and drafting of the results. Criticism and review of the text by Dr. J.B. Hersey is gratefully acknowledged.

REFERENCES

Admiralty Chart C6359. 1965. Compiled by the N.A.T.O. Research Centre, La Spezia. Scale 1:2,300,000.

Allan, T.D. 1964. A preliminary magnetic survey in the Red Sea and Gulf of Aden. Bollettino di Geofisica Teorica ed Applicata, 6(23), 199-214.

Bernstein, R. and Bowin, C.O. 1963. Real-Time digital computer acquisition and computation of gravity at sea. IEEE Trans. on Geoscience Electronics, GE-1, 2-10.

Drake, C.L. and Girdler, R.W. 1964. A geophysical study of the Red Sea. The Geophysical Journal of the Royal Astronomical Society, 8(5), 473-495.

Girdler, R.W. and Harrison, J.C. 1957. Submarine gravity measurements in the Atlantic Ocean, Indian Ocean, Red Sea and Mediterranean Sea. Proceedings of the Royal Society, Section A, 239, 202-213.

Heezen, B.C. and Tharp, M. 1964. Physiographic Diagram of the Indian Ocean. The Geological Society of America.

Hersey, J.B. 1963. Continuous reflection profiling. In M.N. Hill (Ed.) The Sea: Ideas and Observations on Progress in the Study of the Seas, 3, Interscience Publishers (Wiley) New York, pp. 47-72.

Said, R. 1962. The Geology of Egypt. Elsevier, New York.

Sestini, J. 1965. Cenozoic stratigraphy and depositional history, Red Sea coast, Sudan. Bull. Amer. Assoc. Petrol. Geol., 49, 1453-1472.

Swartz, D.H. and Arden, D.D., Jr. 1960. Geologic history of Red Sea area. Bulletin of the Amer. Assoc. Petrol. Geol., 44(10), 1621-1637.

U.S.G.S. Map I-270A. 1963. Geologic Map of the Arabian Peninsula, compiled by the U.S. Geological Survey and the Arabian American Oil Company under the joint sponsorship of the Kingdom of Saudi Arabia, Ministry of Petroleum and Mineral Resources, and the U.S. Department of State.

Vening Meinesz, F.A. 1934. Gravity Expeditions at Sea, 2, 1923 to 1932, Netherlands Geodetic Commission, Delft.

Reprinted from *Trans. N.Y. Acad. Sci.*, series II, vol. 28, no. 1, 1965, p. 81-89

MORPHOLOGY AND SEDIMENTS OF THE SAHUL SHELF, NORTHWESTERN AUSTRALIA*†‡

Tjeerd H. van Andel

Scripps Institution of Oceanography, University of California, La Jolla, Calif.

The Sahul Shelf is a stable continental platform bordered on one side by the ancient, low-lying and deeply weathered Australian craton and, on the other side by the moderately deep geosynclinal basin of the Timor Trough. The purpose of this paper is to define and characterize the recent sedimentary facies of the shelf and their distribution patterns and to compare them with the facies of other continental shelves. Two cruises in 1960 and 1961 provided field observations, soundings and 376 sample stations. Additional soundings were made available by the Royal Australian Navy. Assistance and advice have been provided by many; their help is gratefully acknowledged. A detailed report has been prepared by Van Andel and Veevers (in press).

The Sahul Shelf contains a central basin with a depth of 145 m., the Bonaparte Depression, which is connected to the Timor Trough by a long, narrow, deep channel, the Malita Shelf Valley (FIGURE 1). The Bonaparte Depression is surrounded on three sides by broad, gentle rises with crestal depths of 30 to 50 m. A flat depositional apron connects the depression with the littoral zone. On the seaward side, the shelf terminates with a clear break in slope marked generally with an erosional scarp at 100 to 125 m. Just outside the shelf edge, numerous small, steep-sided banks with flat tops rise from 200 to 400 m. on the continental slope to within 20 m. from the surface. These banks probably originated in shallow water as a broken fringing reef and continued to grow during subsidence of the shelf margin (Fairbridge, 1953).

Superimposed on the regional relief of the shelf is a complex system of flat-top banks, terraces and channels. Many channels entirely traverse the rises. The relief, particularly that of the Van Diemen Rise, is very similar to that of Bathurst and Melville Islands or of the Aru Islands farther north (Fairbridge, 1951; Verstappen, 1959). The tops of banks and terraces can be shown by correlation to be parts of several regional subhorizontal surfaces (Van Andel & Veevers, 1965). The upper surfaces appear to be the seaward extensions of Tertiary erosional plains of the adjacent land, thus indicating uplift and denudation of the shelf during the Tertiary. Subsequently, the shelf was epeirogenetically deformed, and the drainage system became antecedent. In the Pleistocene, the area subsided to its present elevation, and the lower

*This paper, illustrated with slides, was presented at a meeting of the Section on February 1, 1965.

†Contribution of Scripps Institution of Oceanography, New Series.

‡This investigation has been supported by grants from the National Science Foundation and by a contract of the Office of Naval Research with Scripps Institution of Oceanography.

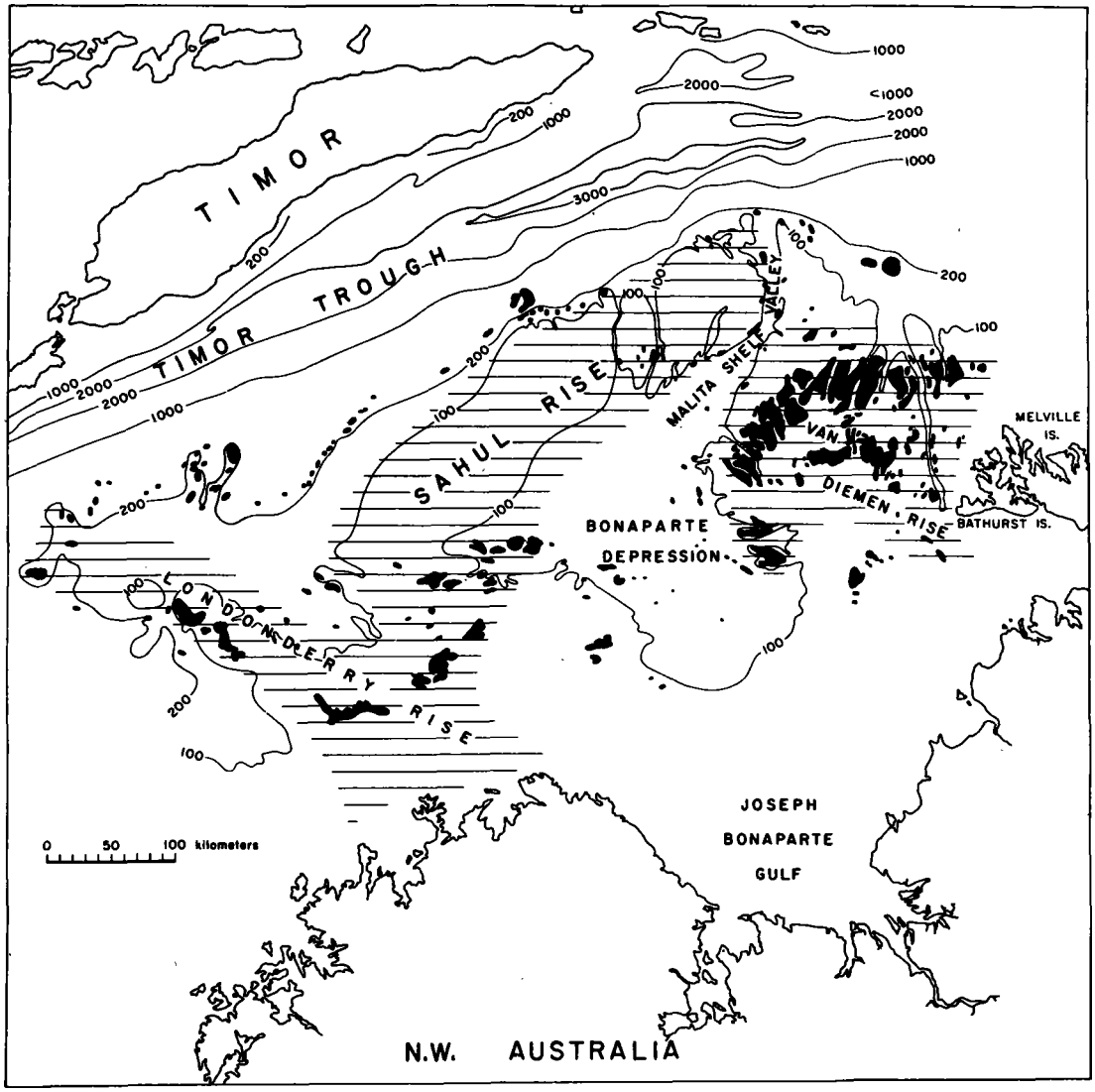


FIGURE 1. Submarine topography of the Sahul Shelf. Black areas indicate banks. Rises shown by shading. Depth contours in meters.

surfaces were formed by erosion and aggradation during glacial low stands of sea level.

During the maximum of the last Pleistocene glaciation, sea level stood at approximately 120 m. below its present position. The entire shelf was exposed, with the exception of the Bonaparte Depression, which formed an almost enclosed lagoon (FIGURE 2). As sea level rose after the glacial period, the rapid transgression covered the shelf with a blanket of shallow water and nearshore deposits. As a result of the concentration of drainage into the Bonaparte lagoon, no coarse terrigenous material reached the outer

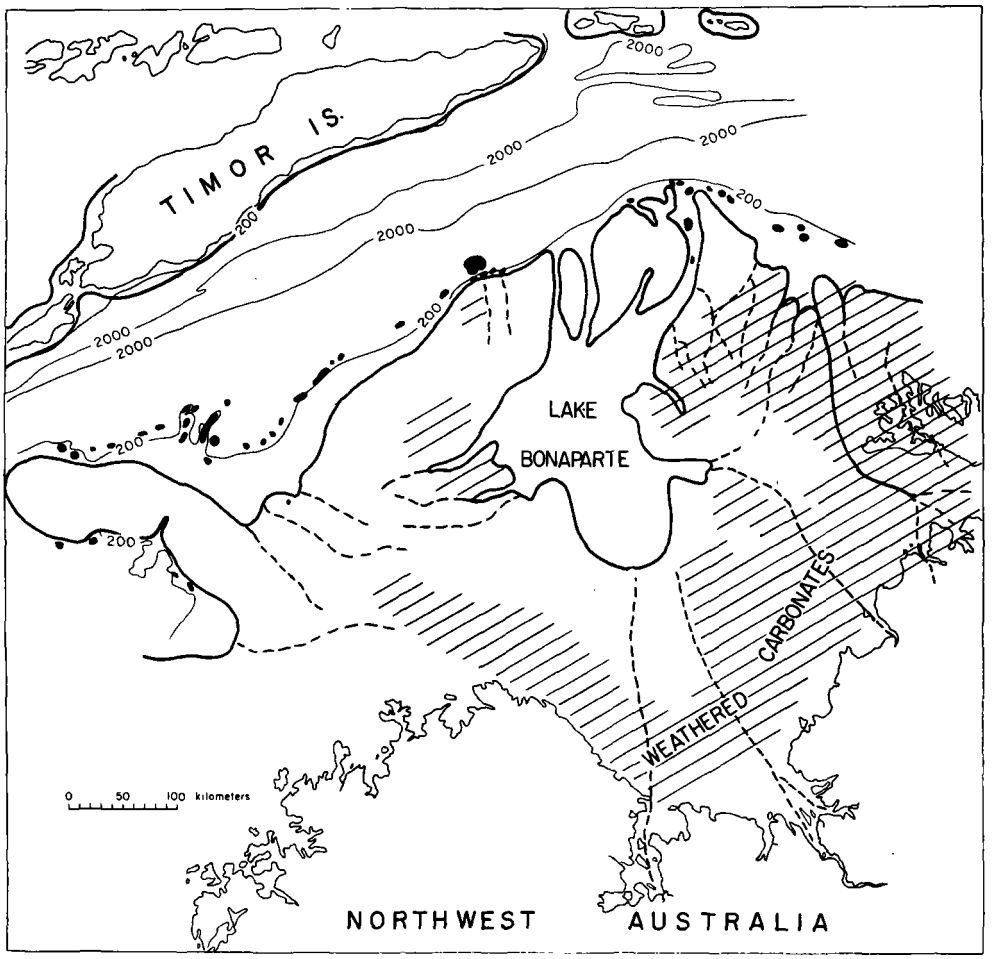


FIGURE 2. Physiography of the Sahul Shelf during the late Wisconsin glaciation. Shaded areas indicate distribution of reworked calcareous soil concretions (kunkar). Depth contours in meters.

and middle shelf at any time. Hence, the outermost and older transgressive deposits are skeletal calcarenites consisting mainly of broken shell and Foraminifera, mixed with coral debris and Bryozoa near the eroded edges of the bank complexes. Only when the transgression passed the 70-m. contour landward of the Bonaparte Depression, did terrigenous sand become incorporated in the nearshore deposits. Consequently, the transgressive blanket can be divided into two parts: an older skeletal calcarenite on the outer and middle shelf, and a younger quartzose calcarenite or calcareous quartz sand on the inner shelf (FIGURE 3). Temporary still stands or brief reversals during the sea level rise from 70 to 0 m. produced littoral zones of high quartz concentration parallel to the old shorelines.

Present sedimentation is restricted to a few areas of the shelf. Near the Australian coast to a depth of approximately 20 m., littoral and coastal deposits are accumulating rapidly. Estuarine, marsh, tidal flat, beach and

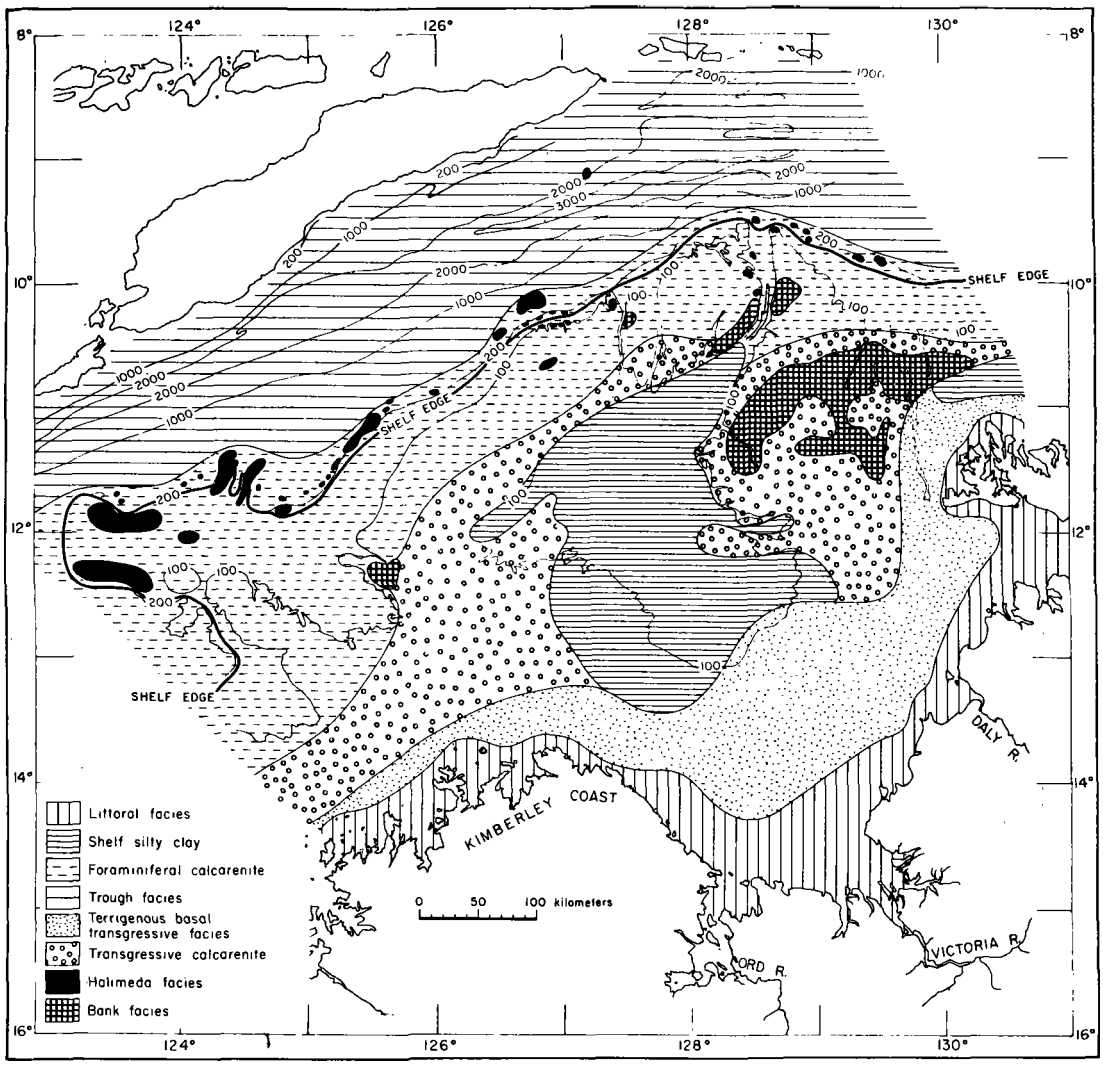


FIGURE 3. Depositional facies of the surface sediments of the Sahul Shelf. Depth contours in meters.

nearshore facies are represented. Coral reefs fringe the shores of Melville and Bathurst Islands and are fairly abundant off the Kimberley coast. Marine currents carry fine suspended clay from the large rivers for hundreds of miles across the shelf. Over most of the shelf, wave turbulence prevents this material from settling, but it accumulates as calcareous mud in deep or sheltered places, mainly in the Bonaparte Depression. This shelf mud facies usually is rich in coarse shell debris, and it appears to accumulate relatively rapidly, especially in the southern part of the Bonaparte Depression.

On the outer shelf and upper continental slope, foraminiferal deposits are accumulating slowly. Toward the shelf edge, these sediments become finer and more planktonic in composition, grading from calcarenites to cal-

cilutites, with a corresponding change in the ratio of planktonic to benthonic Foraminifera from 0.7 at the 100-m. contour to more than 10.0 at the 500-m. contour. This region has been under essentially the same environmental conditions much longer than any other part of the shelf; all early transgressive deposits are buried by the foraminiferal calcarenite, notwithstanding the probable slow rate of deposition.

Calcirudites consisting mainly of calcareous algae and large Foraminifera (*Amphistegina, Heterostegina, Cycloclypeus, Peneroplids* and others) cover the flat tops of the banks (25 to 40 m.) on the rises, while *Halimeda* is the dominant constituent of the shallower (20 m.) shelf-edge bank sediments. The sediments are very coarse as a result of continuous winnowing by waves. Coral is rare; live or fresh coral has been found in only seven samples, and old coral debris is abundant mainly in transgressive sediments near the edges of banks.

On most of the shelf, including nearly all of the middle and inner parts, the coarse relict transgressive sediments exposed at the surface are continuously reworked by waves and burrowing organisms. The skeletal material is generally of very shallow origin and is mixed with a minor proportion of recent material, mainly Foraminifera. Much of the skeletal debris, mainly foraminiferal tests and gastropod shells, is glauconitized, with glauconite molds and replacement of carbonate by glauconite. Reworked brown calcareous soil nodules (kunkar), which were formed apparently during the Pleistocene exposure of the shelf, are abundant in most relict sediments (FIGURE 2).

Facies and facies distribution of the Sahul Shelf are similar, even in details of texture and composition, to those of the western Florida (Gould & Stewart, 1955) and Yucatan shelves (Williams, 1963; Harding, 1964). The Yucatan and Florida shelves have essentially the same sediment distribution (FIGURE 4). The outer shelf and upper continental slope are covered with foraminiferal deposits which are recent in age and grade outward from calcarenites to calcilutites. Between 50 and 90 m, there is a scattering of low banks covered with and surrounded by coarse algal and foraminiferal debris. Between the banks and the shelf-edge foraminiferal calcarenites is a broad belt of oolitic sediments that is attributed to littoral deposition during a late Quaternary low stand of sea level. Relict transgressive deposits consisting mainly of shell debris are found landward of the bank area. These transgressive sediments grade shoreward into modern littoral deposits, which, depending upon the availability of a supply of terrigenous sand, vary from skeletal calcarenites to calcareous quartz sands. Oolites and other nonskeletal carbonates are absent or are of minor consequence in the coastal sediments.

Studies of the Bahamas (for summaries, see Illing, 1954; Purdy, 1963) and similar areas (Gulf of Batabano, Cuba: Daetwyler & Kidwell, 1959; Persian Gulf: Sugden, 1963; Kinsman, 1964) show that the formation of oolites and other nonskeletal carbonates depends on the availibility of a supply of cool, carbon dioxide-rich sea water, which warms up while rising over a very shallow bank, causing precipitation of oolites, grapestone and aragonite muds in the turbulent water. In the Bahamas, this condition is fulfilled by the presence of a steep slope from the bank top at 10 to 15 m. to oceanic depths; elsewhere, a special circulation pattern may provide a favorable situation (Persian Gulf: Sugden, 1963). The late Quaternary oolites of the

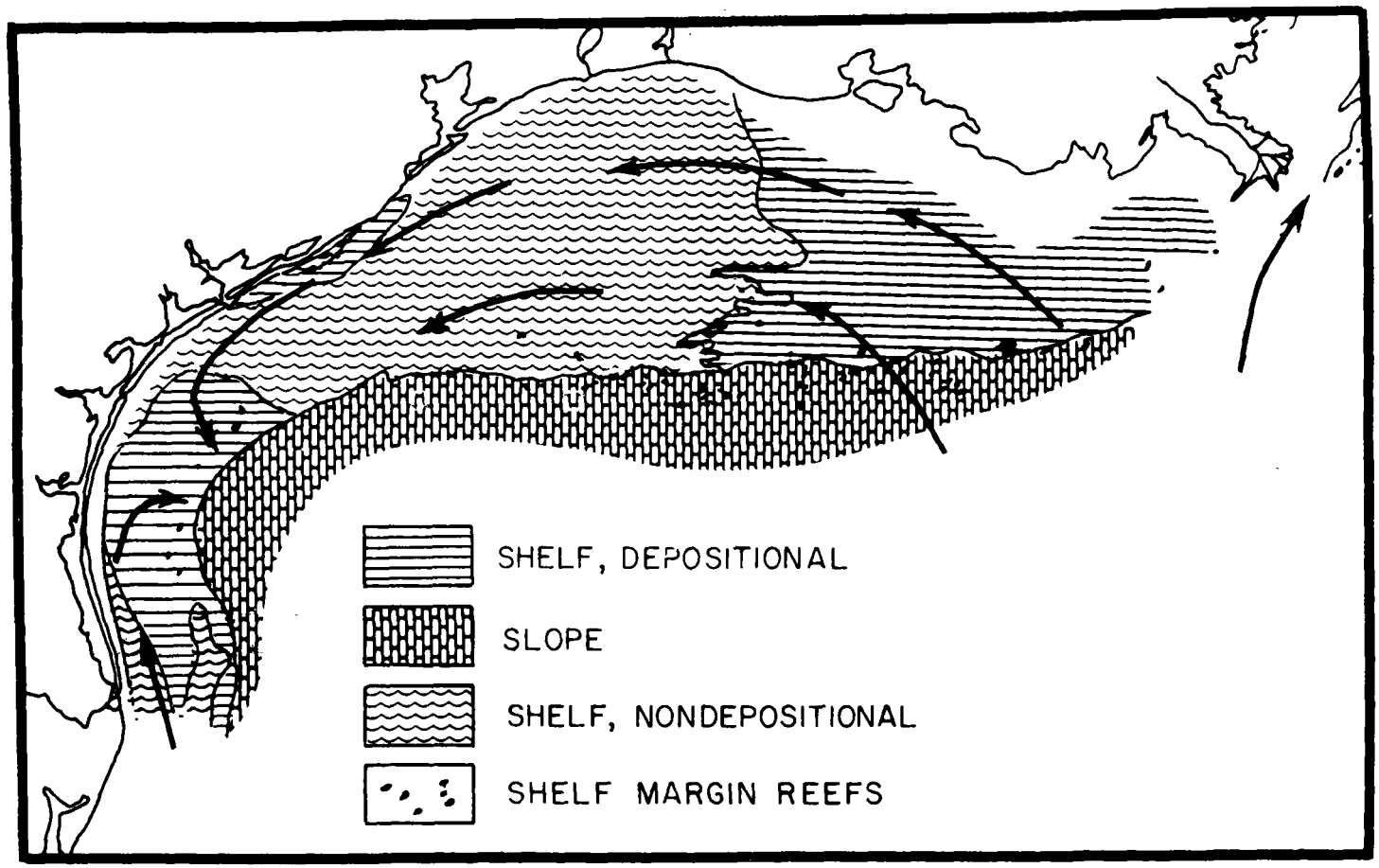


FIGURE 4. Depositional facies of the western Florida shelf (*A*, compiled from Gould & Stewart, 1955) and the Yucatan Shelf (*B*, compiled from Williams, 1963; Harding, 1964).

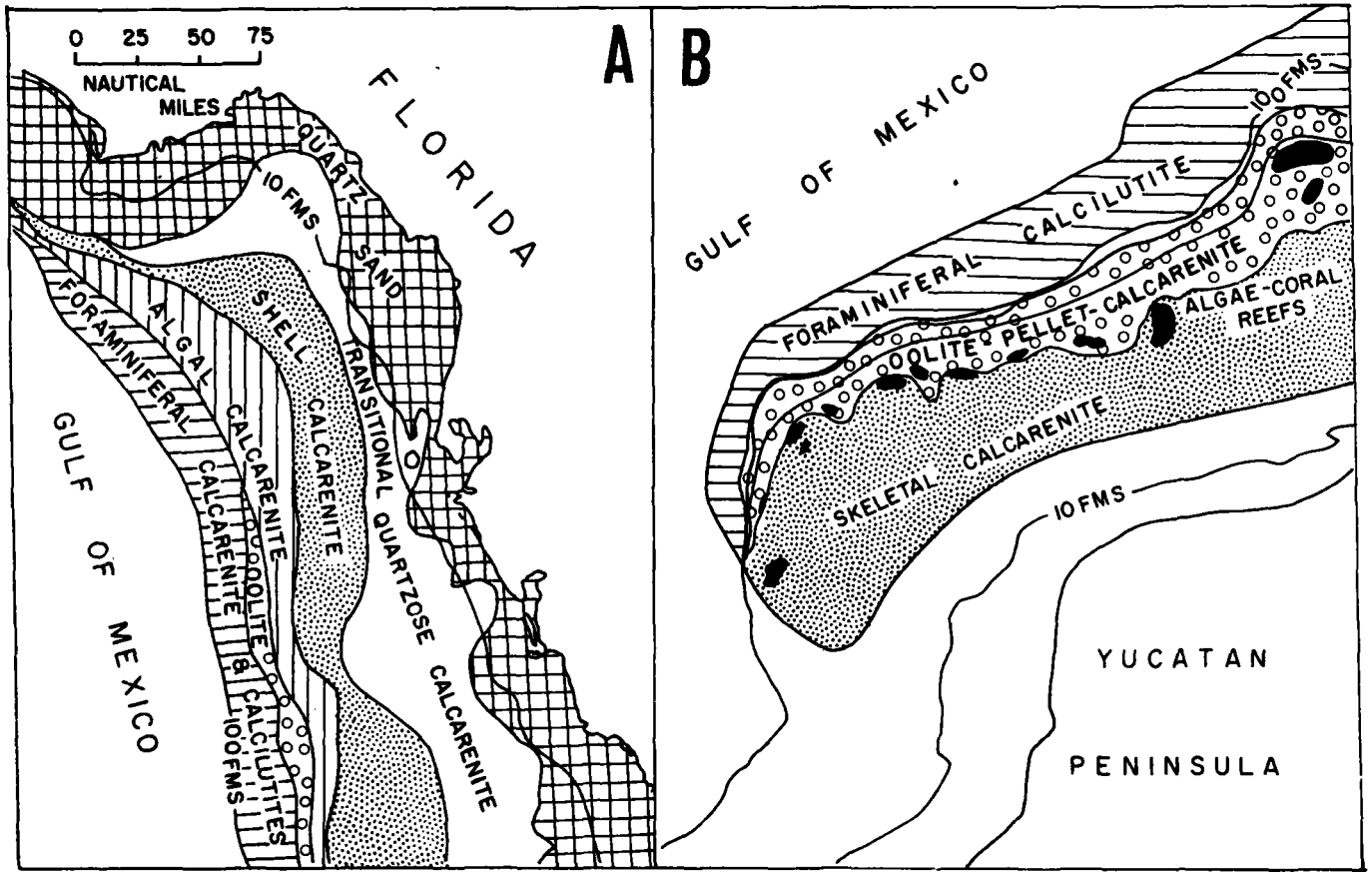


FIGURE 5. Depositional facies of the northwestern Gulf of Mexico shelf. *Shelf depositional facies* consists of current-transported mud; *slope facies* is foraminiferal silty clay; *shelf nondepositional facies* represents relict, transgressive, glauconitic muddy sand and sandy mud.

outer Florida and Yucatan shelves were formed near the edge of the continental platform, whereas the modern littoral water sediments of these areas and of the Sahul Shelf accumulate at a great distance from open ocean water.

Comparison of the three calcareous shelves discussed above shows that the deposition of sediment takes place mainly in three areas: the outer shelf, the littoral zone and the shallow tops of banks. The sediment types produced are distinctive. If a supply of fine suspended clay exists, a fourth type, consisting dominantly of terrigenous mud, may be found in deep or sheltered areas. These modern sediments are superimposed on a thin blanket of littoral transgressive sediments, which overlies an erosional unconformity (Gould & Stewart, 1955; Williams, 1963; Harding, 1964) and is exposed at the surface over large areas of the shelf.

In the examples discussed, the predominance of skeletal calcareous material over noncalcareous terrigenous sediment appears to be mainly because of a lack of terrigenous supply during the postglacial transgression and at the present time. An unusually high production of calcareous material need not be assumed.

In principle, the facies types and sediment distribution patterns of these shelves are similar to those of shelves covered with terrigenous sediment. The relict glauconitic transgressive calcarenites, the algal-foraminiferal bank deposits, the calcareous shelf muds and the outer shelf foraminiferal deposits find their counterparts in lithology, genesis and distribution in the facies of the Gulf of Mexico (FIGURE 5) and of the Guayana Shelf (Van Andel & Curray, 1960). Although the nature of the components is different, the major controlling factors of location and rate of terrigenous sediment supply, of current patterns, wave reworking and the dominance of the effect of the postglacial transgression are similar and have produced similar results.

References

DAETWYLER, C. C. & A. L. KIDWELL. 1959. The Gulf of Batabano, a modern carbonate basin. Proc. 5th World Petrol. Congress, New York 1: 1-21.

FAIRBRIDGE, R. W. 1951. The Aroe Islands and the continental shelf north of Australia. Scope, J. Sci. Union Univ. W. Aust. 1 (6): 24-29.

FAIRBRIDGE, R. W. 1953. The Sahul Shelf, northern Australia; its structure and geological relationships. J. Roy. Soc. W. Aust. 37: 1-33.

GOULD, H. R. & R. H. STEWART. 1955. Continental terrace sediments in the northeastern Gulf of Mexico. *In* Finding Ancient Shorelines. 3: 2-20. Soc. Econ. Pal. Min., Spec. Publ. Tulsa, Okla.

HARDING, J. L. 1964. Petrology and petrography of the Campeche lithic suite, Yucatan Shelf, Mexico. Texas Ag. & Mech. Coll. Dept. Oceanog. Rept. 64-11T: 1-140.

ILLING, L. V. 1954. Bahama calcareous sands. Bull. Amer. Assoc. Petrol. Geol. 38 (1): 1-95.

KINSMAN, D. J. J. 1964. The recent carbonate sediments near Halat el Bahrani, Trucial Coast, Persian Gulf. *In* Developments in Sedimentology. L. M. J. U. van Straaten, Ed. 1: 185-192. Elsevier. Amsterdam, Holland.

PURDY, E. G. 1963. Recent calcium carbonate facies of the Great Bahamas Banks. J. Geol. 71 (3): 334-355; 71 (4): 472-497.

SUGDEN, W. 1963. The hydrology of the Persian Gulf and its significance in respect to evaporite deposition. Amer. J. Sci. 261: 741-755.

VAN ANDEL, TJ. H. & J. R. CURRAY. 1960. Regional aspects of modern sedimentation in northern Gulf of Mexico and similar basins. *In* Recent Sediments, Northwestern Gulf of Mexico. F. P. Shepard, F. B Phelger and Tj. H. van Andel, Eds.: 345-364. Amer. Assoc. Petrol. Geol. Tulsa, Okla.

VAN ANDEL, TJ. H. & J. J. VEEVERS. 1965. Submarine morphology of the Sahul Shelf, northwestern Australia. Bull. Geol. Soc. Amer. 76 (6): 695-700.

VAN ANDEL, TJ. H. & J. J. VEEVERS. Morphology and sediments of the Timor Sea. Bur. Min. Resources, Commonwealth of Australia, Bull. (in press).

VERSTAPPEN, H. TH. 1959. Geomorphology and crustal movements of the Aru Islands in relation to the Pleistocene drainage of the Sahul Shelf. Amer. J. Sci. 257: 491-502.

WILLIAMS, J. D. 1963. The petrology and petrography of sediments from the Sigsbee Blanket, Yucatan Shelf, Mexico. Texas Ag. & Mech. Coll. Dept. Oceanog. Rept. 63-12T: 1-59.

Reprinted form *C. R. Acad. Sc. Paris*, series D, vol. 263, 1966, p. 1052-1054

OCÉANOGRAPHIE. — *Découverte de turbidités hétérogènes dans le bassin australien.* Note (*) de MM. **Wladimir D. Nesteroff**, **Bruce C. Heezen** et **John R. Conolly**, présentée par M. Pierre Pruvost.

On observe dans les turbidités de la plaine abyssale située au Sud de l'Australie une séquence très particulière : sables terrigènes grossiers, sables bioclastiques, boue calcaire, argile. C'est l'équivalent de la séquence type des Flyschs à Helmintoïdes. Les données sédimentaires et climatiques du Sud australien nous suggéraient ainsi les conditions probables de formation du flysch à Helmintoïdes.

Au Sud du continent australien, dans la région de la « Great Australian Bight », la marge continentale est bordée par une longue plaine abyssale : la *Great Bight Abyssal Plain* (1).

Une série de campagnes des bâtiments océanographiques *Vema* et *Conrad*, du Lamont Geological Observatory (Columbia University, New York), a permis d'en préciser la structure et de ramener des carottes « longues » prélevées au carottier à piston. La plaine abyssale, comme c'est la règle, est remplie de couches granoclassées déposées par des courants de turbidité (1).

Toutefois la composition pétrographique de ces turbidités est assez particulière. Dans les carottes décrites jusqu'à présent chaque séquence appartient, selon l'origine de ses matériaux, à l'un des deux grands groupes sédimentaires : terrigène ou bioclastique (2). Dans la Great Bight Abyssal Plain par contre, la séquence est hétérogène, formée d'une succession de couches de matériaux d'origines différentes. Cette *séquence type* peut s'observer par exemple dans la section 603-285 cm de la carotte V 18.220 (37°27'S-133°40'E, 5552 m de profondeur).

Elle débute par une dizaine de centimètres de *sable terrigène* grossier composé de 90 % de grains de quartz de 1 à 2 mm bien arrondis, émoussés luisants et ronds mats. Des débris biologiques grossiers : Bryozoaires, Oursins, Foraminifères, complètent le tableau.

En montant dans la séquence les grains de quartz deviennent plus petits (200 à 500 μ) et vers le niveau 590 cm leur pourcentage tombe à 1 %. Le sédiment passe à un *sable bioclastique* grossier composé surtout de Foraminifères (70 %) et de gros débris (2 à 5 mm) de Bryozoaires, Oursins, Ptéropodes, coquilles de Lamellibranches et de rares Ostracodes. Cette couche de sable bioclastique est épaisse (595-285 cm) et granoclassée. Au fur et à mesure qu'on s'élève les gros débris organogènes disparaissent pour laisser la place aux Foraminifères (vers 450 cm). Le diamètre de ceux-ci, autour de 500 μ à la base, diminue lui aussi (200 μ à 400 cm) tandis que de petits débris biologiques, difficilement identifiables, envahissent graduellement le sédiment. Ils représentent 50 % à 350 cm et plus de 70 % au-dessus de 300 cm.

Une couche de *boue calcaire* blanche (285-259 cm) surmonte ce sable bioclastique.

La séquence se termine par une couche de *vase chocolat* (259-253 cm) faiblement calcaire : 20 % $CaCO_3$. Les passages d'une couche à l'autre sont graduels mais se produisent rapidement, sur une faible épaisseur. De nombreuses perforations soulignent et traversent la limite boue blanche-vase chocolat.

Nous ne disposons que d'un petit nombre de carottes assez espacées les unes des autres dans cette longue plaine abyssale. Cependant toutes, sauf une, contiennent au moins une séquence hétérogène complète (V 16-106, 108, 110; V 18-218, 220, 221). Dans les séquences incomplètes c'est le plus souvent la couche de base de sable terrigène qui manque. Une seule carotte (V 16-107) ne contient que des séquences incomplètes.

Dans le cas le plus général il s'agit d'une séquence à quatre membres : deux couches de sables surmontées de deux couches de vases, la première et la dernière de ces couches étant d'origine terrigène, tandis que les deux couches intermédiaires, sable bioclastique et boue calcaire, sont essentiellement biologiques.

Nous retrouvons ainsi, à la nature des organismes près, l'équivalent exact de la séquence-type des Flyschs à Helmintoïdes des Alpes franco-italiennes et plus spécialement la séquence de la « série à dominante calcaire » décrite par Lanteaume ([3]). Cette correspondance concerne même la position dans la séquence des perforations et pistes de vers concentrées vers la limite des boues calcaires et des vases faiblement calcaires.

Ce type de sédimentation n'avait été décrit, jusqu'à présent ([4]), que dans les séries géologiques et la découverte, dans nos mers modernes, d'un grand bassin sédimentaire recevant simultanément des apports biologiques calcaires et des détritiques terrigènes nous permet enfin de préciser les conditions de formation de tels dépôts.

Comme dans la plupart des plaines abyssales, les couches prélevées par les carottiers, c'est-à-dire la dizaine de mètres superficiels, semble correspondre à la grande période d'érosion et de dépôt des glaciations quaternaires.

Au Sud de l'Australie, le plateau et la pente continentale étaient au Plio-Miocène et sont encore actuellement, le siège d'une sédimentation biologique calcaire : sables coquilliers et boues à Globigérines. Le continent australien par contre est relativement désertique avec des bassins d'alimentation où se forment des détritiques terrigènes. Durant les périodes interglaciaires, des courants de turbidité chargés de matériel terrigène traversent le plateau continental, érodent les sédiments bioclastiques qui s'y trouvent et entraînent vers les grands fonds et la plaine abyssale du matériel hétérogène.

En tenant compte de la différence de dimension entre la Great Bight Abyssal Plain, longue d'environ 1000 km et les petits bassins alpins nous pouvons supposer, comme l'avait prévu Nesteroff ([2]), que c'est dans des conditions similaires que se sont déposés les flyschs à Helmintoïdes, la taille du bassin récepteur, ainsi que les proportions de sédiments de diverses origines qu'il reçoit, déterminant, dans chaque cas, la prépondérance d'un type de séquence particulier.

(*) Séance du 3 octobre 1966.

(1) B. C. HEEZEN et LAUGHTON, *The Sea*, John Wiley, 3, 1963, p. 312-364.

(2) W. D. NESTEROFF, *Bull. Soc. géol. Fr.*, (7), 4, 1962, p. 849-856.

(3) *Thèse Sc.*, Paris, 1962.

(4) Actuellement plusieurs exemples de bassins contenant des turbidités hétérogènes ont été reconnus mais n'ont pas encore fait l'objet de publications.

(*Lamont Geological Observatory,*
Columbia University, Palisades, New-York,
Contribution 930
et *Laboratoire de Géologie dynamique à la Sorbonne, Paris.*)

Reprinted from *J. sedimentary Petrology*, March 1967, p. 102-127

SEDIMENTS OF THE MALACCA STRAIT, SOUTHEAST ASIA[1]

GEORGE H. KELLER[2] AND ADRIAN F. RICHARDS
Department of Geology, University of Illinois, Urbana, Illinois

ABSTRACT

The Malacca Strait is a shallow passage between the Malay Peninsula and Sumatra with oceanographic and bottom-sediment characteristics closely related to strong currents, debouching rivers, climatic variation, and the close proximity of bordering land masses. The strait assumed its present configuration as a result of the postglacial rise of sea level which drowned the Sunda Shelf. An essentially tidal northwest current flow prevailing in the strait throughout the year is largely responsible for the hydrographic and oceanographic conditions in the region. Surface salinities and temperatures are generally found to be lower than in the surrounding seas. A prominent wedge of cool-temperature, high-salinity bottom water is found to extend from the Andaman Sea into the strait.

Bottom sediments primarily consist of muddy sands, with large areas of mud occurring in the vicinity of river mouths and in the Andaman Sea. Calcium carbonate, primarily composed of mollusk shells and foraminiferal tests, and organic carbon are generally found only in minor amounts in the strait. Higher concentrations of calcium carbonate are confined to local shell deposits and larger percentages of organic matter are found in the vicinity of river mouths and in the fine sediments of the Andaman Sea. The non-calcareous detrital fraction is dominated by quartz with minor amounts of orthoclase and plagioclase feldspars. The heavy mineral suite is complex because of the varied geology of the bordering land areas and consists primarily of leucoxene, ilmenite, staurolite, biotite and amphiboles. Kaolinite and mixed-layer minerals constitute the dominant clay minerals; lesser amounts of illite and montmorillonite also are present. A slight decrease in illite and an increase in mixed-layer minerals with depth was observed in some cores. Volcanic ash of an andesitic origin is found throughout much of the area. Many cores penetrate what appears to be a Late Pleistocene surface consisting of stiff, slightly indurated silty clay. The clay contains much peat, some of which has given a radiocarbon date of 10,000 years B. P.; it appears to represent a former tidal flat or estuarine deposit.

INTRODUCTION

The Malacca Strait, a shallow passage between the Malay Peninsula and Sumatra, connects the Indian Ocean with the South China Sea (fig. 1). It is approximately 805 km long and varies in width from 64 km in the south to 257 km in the north. The strait provides a depositional environment of considerable complexity owing to its physiography, oceanographic and climatological conditions, and the varied sediment source areas provided by the adjacent land masses. This study was initiated to investigate the importance of these variables upon the sediments of the strait.

Previous studies were largely made to support fisheries research or as a minor portion of a more extensive study of the Sunda Shelf. The earliest recorded observations were those of the Dana Expedition between 1928 and 1930, from which plankton and oceanographic data were obtained from two stations in the strait. Surface salinity measurements over varying periods of time were reported by Soeriaatmadja (1956) and Selvarajah (1962). Additional oceanographic stations were occupied by the Indonesian research vessel SAMUDERA (Anonymous, 1957) and the French vessel JEANNE D'ARC (Anonymous, 1963). Wyrtki (1961) discussed the climatology and oceanography in the region of the strait as part of his study of the physical oceanography of the southeast Asia waters. Van Baren and Kiel (1950) include 18 samples from the strait in a sedimentary petrology study of the Sunda Shelf. According to the files of World Oceanographic Data Center A, five sediment samples were collected by the Russian Oceanographic vessel VITYAZ (cruise 35), but as yet these data are not available (B. S. Richmond, personal communication).

In the spring of 1961, the U. S. Naval Oceanographic Office began an investigation of the general sediment distribution and hydrographic conditions within the Malacca Strait; a more detailed survey and sampling program was undertaken later in 1961. During March and April 1964, the senior author, while aboard the U. S. Coast and Geodetic Survey Research Vessel PIONEER, obtained additional hydrographic data as well as bottom samples to supplement those collected by the Naval Oceanographic Office. Data collected during these three cruises include observations obtained from 24 oceanographic stations (temperature and salinity), 155 bottom sediment stations, and five 26- to 33-hour anchor

[1] Manuscript received June 29, 1966.
[2] Present address: Institute for Oceanography, ESSA, Silver Spring, Maryland 20910.

stations for the determination of the spatial and temporal variations of currents (fig. 2). It is upon these data that this study is based. The locations of all stations plus the sedimentological and oceanographic data obtained at each site are on file at the National Oceanographic Data Center, Washington, D. C. (NODC geology acquisition number 051866-1 and cruise numbers 00545 and 00639).

PHYSIOGRAPHY AND AREAL GEOLOGY

Bordering Lands and Islands

The regional physiography and geology of the adjacent lands is germane to this investigation because sediments brought to the strait are controlled by the nature of these bordering provinces, as will be demonstrated later.

Sumatra can be divided topographically into three parallel provinces extending along the island from northwest to southeast; the Barisan Mountains, a transition zone, and a wide coastal plain. The volcanic Barisan Mountain chain largely consists of Late Paleozoic crystalline schists with some shallow depressions containing Mesozoic, Tertiary and Quaternary sediments. Tertiary-Quaternary volcanics, including rhyolite and pumice tuffs as well as andesite cones, cover wide portions of the province. Some isolated intrusives of plutonic rock of possible Quaternary age constitute the remaining outcrops (fig. 2). The mountains descend gradually eastward to a transition zone of rolling hills composed of Paleozoic schists and Mesozoic and Tertiary sediments. Minor amounts of Tertiary-Quaternary rhyolithic tuff and plutonic intrusions also occur in the transition zone. The third zone is an extensive flat lowland of Quaternary and Recent sediments that borders the strait; it is 48 to 193 km wide. Most of this coastal zone is swampy and covered by jungle. Although numerous rivers drain both sides of Sumatra, the majority have their headwaters in the Barisan Mountains and drain into the strait. The east coast of Sumatra has generally shifted considerably toward the strait owing to the deposition of the large sediment load of these streams (Van Bemmelen, 1949, p. 702). A recent mariner's report based on actual observations compared with existing charts for the area by H. P. Hansen (personal communication) indicates, however, that the shoreline along northeastern Sumatra in the vicinity of Belawan has receded as much as 2 km. Hansen has also observed drowned tree stumps 300 m off shore in this same area.

The Malay Peninsula consists of a hilly and mountainous interior bordered on both sides by

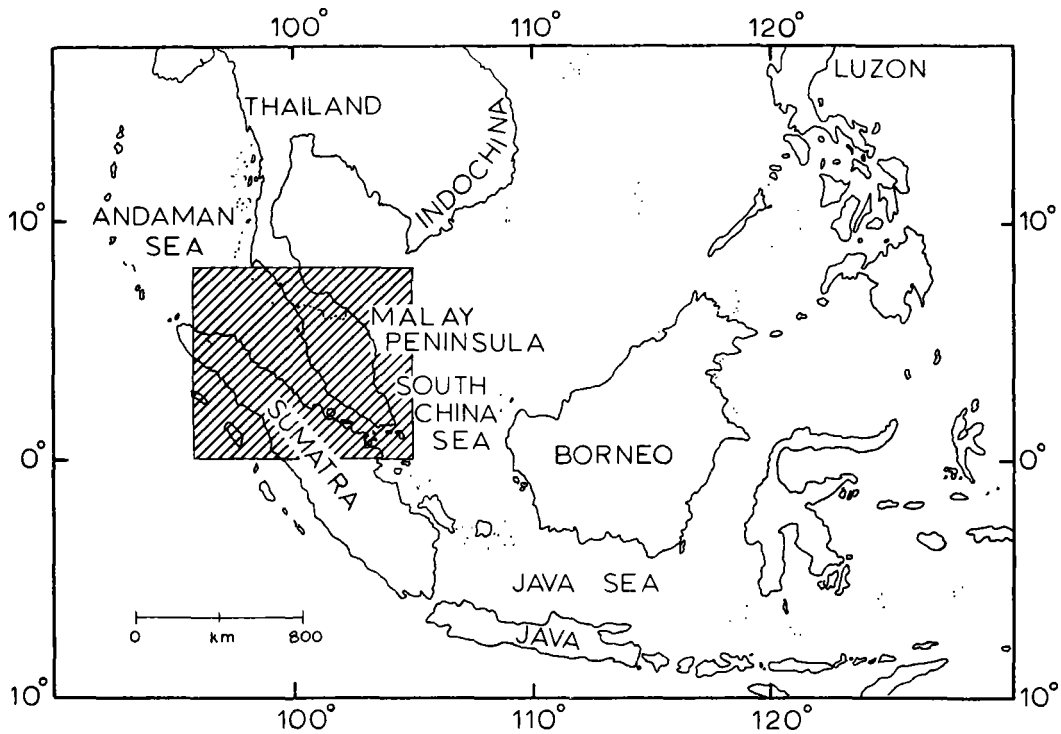


FIG. 1.—Index map, Malacca Strait and adjacent seas.

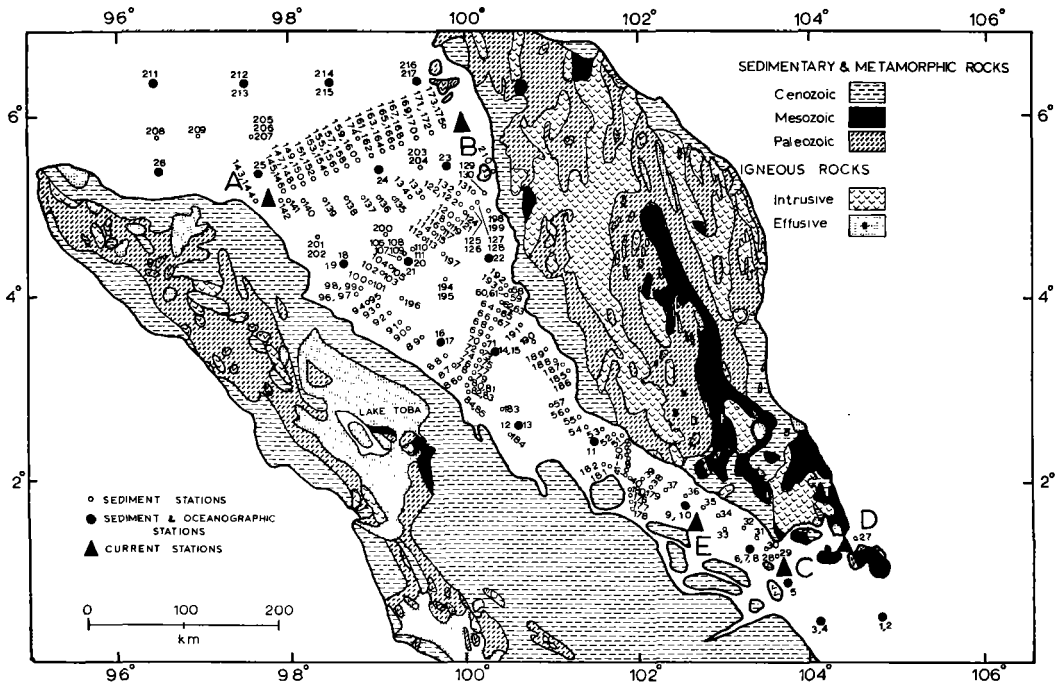


FIG. 2.—General geology of the bordering land areas and station locations in the Malacca Strait.

coastal lowlands. Several north–south trending mountain ranges extend from the Thailand border across approximately two-thirds of the peninsula, becoming discontinuous in the southern third. Granitic intrusives of Jurassic age crop out along the entire length of these ranges as well as in the south, where little of the high relief remains. A hilly topography exists between the ranges, which consists mainly of Permo-Carboniferous limestones and shales and Triassic arenaceous deposits (Van Bemmelen, 1949, p. 360). Effusive rocks of unknown composition are common throughout much of this region. Rolling hills and lowland plains of Paleozoic and Quaternary sediments extend out from the mountains toward the coast where the coastal lowlands bordering the strait have an average width of 64 km. The extensive volcanism that occurred on Sumatra in the Quaternary also resulted in the widely distributed ash deposits on the Malay Peninsula (United Nations Economic Commission for Asia and the Far East, 1961, p. 36).

The islands in the vicinity of Singapore consist mainly of sedimentary rocks and granites of Mesozoic age. To the north, Penang Island is also composed of Mesozoic granites, and Langkawi Island near the border of Thailand consists predominantly of an Ordovician-Silurian calcareous sequence (Alexander, 1959). Islands along the coast of Sumatra in the narrow portion of the strait are formed of Recent sediments.

Determination of the sedimentary provenance in the strait is difficult as a result of the numerous streams and rivers draining the complex and varied geology of the adjacent lands. Sumatra has the greatest influence on the sediments of the Malacca Strait although Malayan drainage contributes large quantities of material. Much of the sediment entering the strait from Sumatra appears to be finer than that from streams draining the Malay Peninsula. This is attributed to the extensive drainage system from western Sumatra eastward across the lowlands and finally through the wide coastal plains covered with thick vegetation. There is a tendency in the coastal region for much of the coarser part of the sediment load, that otherwise reaches the strait, to be intercepted. Islands south of Singapore contribute only minor amounts of material to the southern portion of the strait, as indicated by the concentration of various iron minerals believed to have come from the laterite deposits on these islands. Wind-derived sediment is present in the form of volcanic ash and pumice, but it is of minor importance relative to the quantity of stream-borne material. Much of the ash found in the strait is considered to be detri-

tal rather than wind-borne. Sediment entering from the Andaman Sea consists mainly of planktonic foraminifera carried in by southeast-flowing bottom currents. Organic production in the strait is the only remaining source of sediment, and in some regions it is a significant source.

Strait Floor

The topography of the strait floor prior to 1961 was only generally known because of the lack of adequate bathymetric surveys. Data from the recent cruises of the Naval Oceanographic Office and the Coast and Geodetic Survey have provided much more detail. Contours at 10 fathom (18.3 m) intervals in the strait and 100 fathom (183 m) intervals beyond the continental shelf have been drawn (fig. 3) based on these recent soundings that are corrected for sound velocity and those from the U. S. Hydrographic Office Chart 1595 that are mainly wire-line soundings.

Numerous islands clutter the southern entrance to the strait where water depths seldom exceed 20 fathoms (37 m) and more commonly are about 15 fathoms (27 m). Within the narrow portion of the strait, from Singapore northwestward to approximately Port Swettenham, water depths increase slightly toward the middle portion with shallower sill-like depths at both ends. The shallow areas that occur at either end may be due to relict deposits which are expressions of the topography prior to an eustatic rise of sea level.

The broad shallow areas bordering Sumatra along the southern portion of the strait result from the large quantity of sediment supplied by local rivers. In this region, prominent fine sand and mud ridges trend parallel to the axis of the strait. Some of these ridges rise as much as 21.9 m above the bottom and are up to 48 km long (fig. 4, profiles A & B). Present orientation of these ridges appears to be maintained by bottom currents, which may reach velocities of 77 to 103 cm/sec. Umbgrove (1949, p. 5) reports the presence of similar features to the south in Banka Strait, between Sumatra and Banka Island,

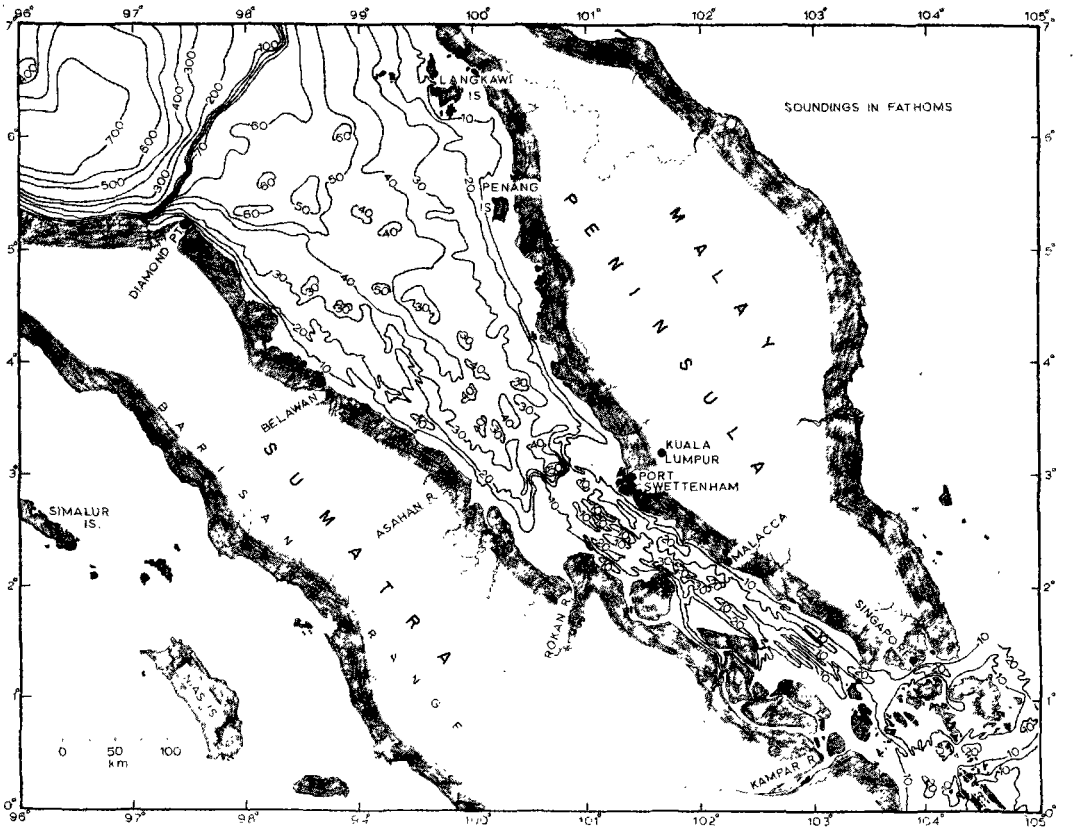


FIG. 3.- Bathymetry of the Malacca Strait with a 10-fathom (18.3 m) contour interval from 10 to 100 fathoms and a 100-fathom (183 m) interval beyond 100 fathoms.

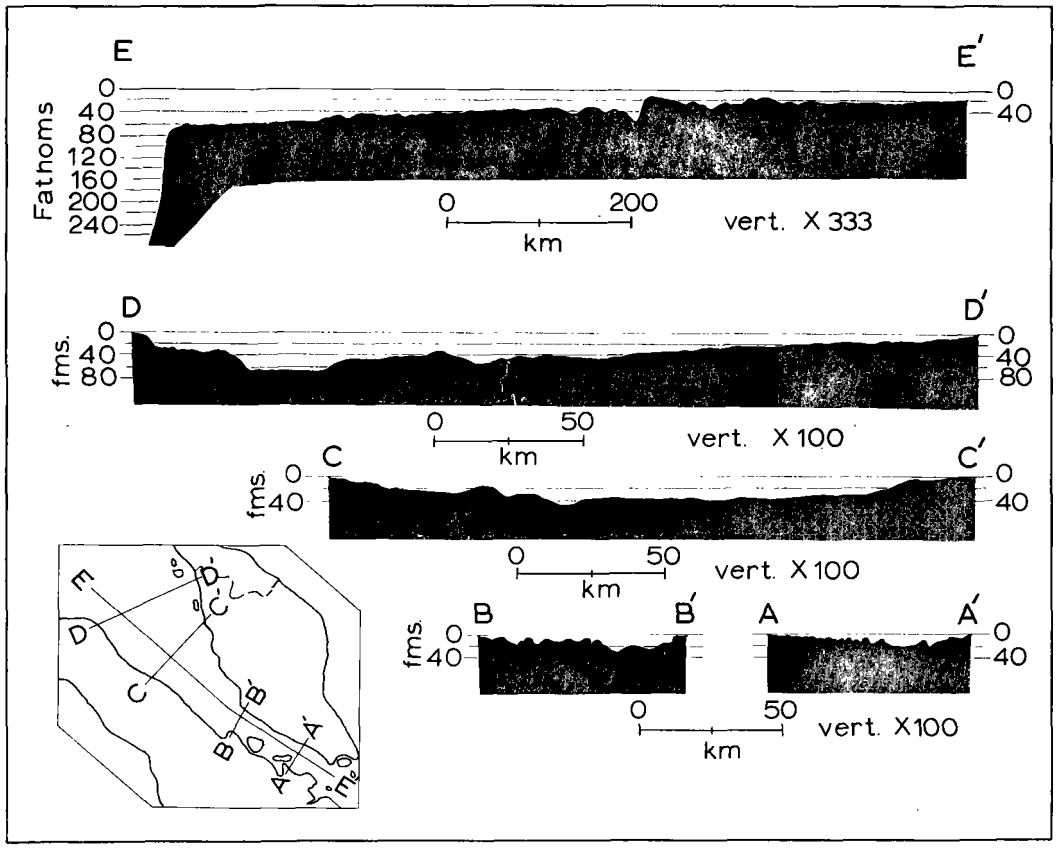


FIG. 4.—Depth profiles.

which he describes as remanent features resulting from currents eroding numerous channels in the floor of the strait and leaving ridges between the channels. The term "channel," as used by Umbgrove is a misnomer in that the bathymetry shows no indication of trenches or channels having been cut in the strait floor. Ridges occur above the sea floor in the Malacca Strait and the depressions one commonly associates with channels are not found. If these ridges are the result of erosion by sea currents, as Umbgrove (1949, p. 6) suggests, one would expect the ridge tops to be at the same depth as the floor of the strait surrounding the area where these features are found. This is not the case. We believe the ridges in both straits are depositional rather than erosional features. Once the sediments from the Kampar River and its tributaries enter the strait they are carried northwestward by the currents. Farther out in the strait some of these sediments are deposited to form linear ridges parallel to the current flow and extending away from the river mouths. Some ridges show a gradual tapering in width away from the rivers. Many of the ridge tops are composed of mud, but sand is generally found in the troughs. Shepard, Emery, and Gould (1949, p. 28) suggested that the presence of sand between the ridges may possibly be attributed to erosion of the ridges. Since the ridges result from the deposition of fine sediments entering the strait from nearby rivers, the possibility that enough sand would be available from erosion of the ridges seems doubtful. It is more likely that the sand is transported into the area (and concentrated in the troughs) by currents moving through the strait. Van Veen (1936, p. 198) believes that these features are similar to the sand ridges he has observed in the Straits of Dover. The only similarity between the ridges in these two areas is that they are depositional features formed parallel to the current flow. The ridges in the Strait of Dover are attributed to strong currents and a small supply of sand, whereas those in the Malacca Strait are the result of strong currents and large quantities of fine sediment.

The general physiography of the strait floor was probably established during a period of

lower sea level in the Late Pleistocene. Present sea currents tend to maintain the bottom configuration except in areas where large quantities of sediment are deposited from nearby rivers such as in the southern portion of the strait.

Sand waves occur in the region consisting entirely of coarse to medium sand in the area of maximum current velocity between Malacca and Port Swettenham. These waves are oriented perpendicular to the axis of the strait and have wave lengths of approximately 241 to 900 m and heights of 4.6 to 15.3 m (fig. 5). The larger waves show a definite asymmetry with steep slopes to the northwest. Smaller waves tend to show a greater degree of symmetry. Small sand waves also occur near One Fathom Bank, west of Port Swettenham (Wyrtki, 1961, p. 9).

In the central portion of the strait (lat. 4° 42′ N., Long. 99° 07′ E), underwater photographs revealed the presence of small ripple marks having heights of 3 to 4 cm that trend in a northwest–southeast direction. This unusual trend, parallel to the general current flow, is attributed to local variation in current direction.

The strait widens to the northwest from a width of 64 km at Port Swettenham to about 257 km where it enters the Andaman Sea. Over this distance the axis of the strait gradually deepens (fig. 4, profile E). The slope off the coast of the Malayan Peninsula decreases to the north, but increases along the Sumatra coast (fig. 4, profiles C and D). The 50 fathom (91.4 m) "hole" west of Port Swettenham may be a relict feature of Pleistocene drainage or possibly structurally controlled. Little can be said about the latter possibility without subbottom information. The presence of Pleistocene submarine terraces, similar to those found in the neighboring South China Sea (Krempf and Chevey, 1934, p. 849), were not observed in any of the echo-sounding records from the strait. If present, they may have been masked by Recent sediments. Bottom contours indicate the presence of a drowned river channel extending northward from the mouth of the Rokan River. Numerous submerged river valleys have been reported and described on the Sunda Shelf by Molengraaff (1921), Umbgrove (1949, p. 2), and Kuenen (1950, p. 482).

DEPOSITIONAL ENVIRONMENT

Climate

Climatological variation directly influences depositional conditions in the strait in two major ways: runoff from bordering land provinces and general circulation in the strait. Since both factors are significant to an understanding of the sediments in the Malacca Strait a brief

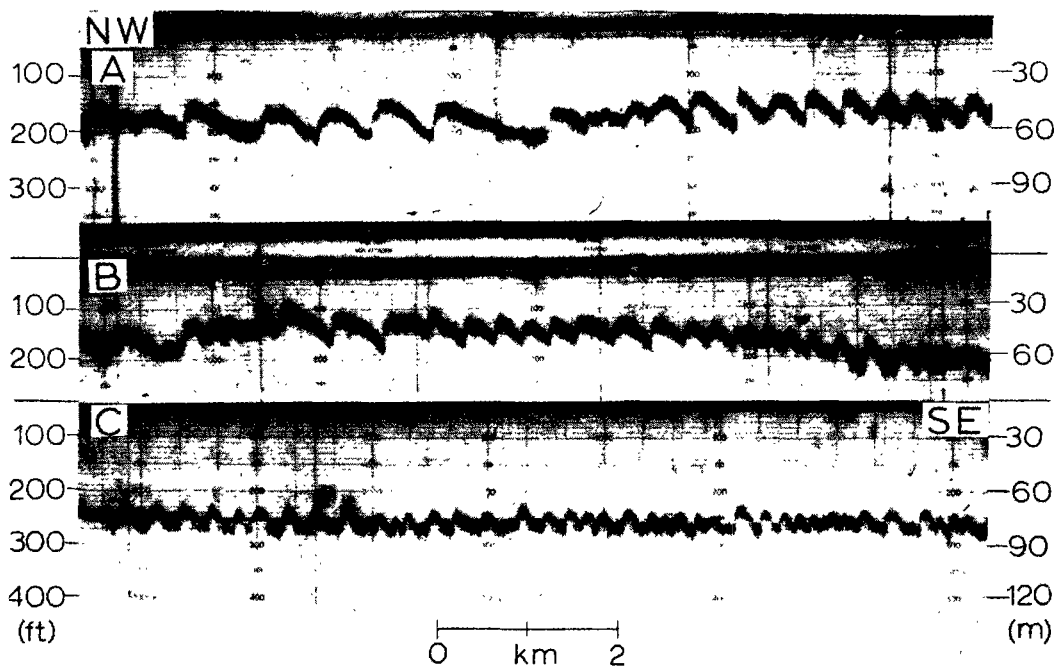


FIG. 5.—Sand waves. Series of nearly continuous echo-sounding records taken from an area extending south-east from Port Swettenham.

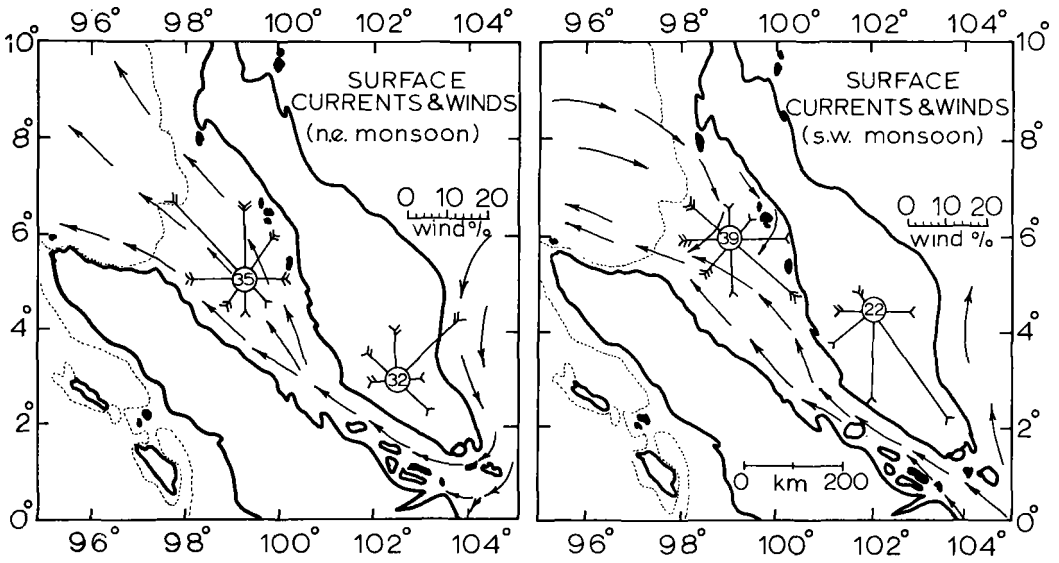


FIG. 6.—Surface currents and winds during the northeast and southwest monsoons. Wind roses fly with the wind, and the number of barbs on the arrow indicate the Beaufort scale of average wind force. The length of the arrow measured from the center of the circle gives the average percent of time the wind blows in a particular direction. The number in the circle indicates the percent time of calms. Modified from the U. S. Navy Hydrographic Office (1944).

discussion of the climatological aspects is pertinent. The climate of the region is typically equatorial—hot and humid. Monsoonal effects are not as severe in the strait as in the more open surrounding seas because of the sheltering effect offered by the Malay Peninsula and the island of Sumatra. Indirectly, however, the monsoon seasons greatly influence the circulation in the strait. As a result of the monsoons, two rainy seasons of unequal magnitude occur without any really dry period. Average annual rainfall over most of the area ranges from 1961 to 2649 mm, with the greater rainfall occurring in the lower latitudes (U. S. Navy Hydrographic Office, 1951, p. 18).

Variation in surface wind direction and force follow the monsoonal seasons. Northeast monsoon conditions prevail from December to March. Near the equator during this time the variable winds have an average Beaufort force of 2 or 3 and originate mainly from the north. The southwest monsoon season extends from May to October and is preceded by squally weather, strong winds and considerable rain. Winds are mainly from the south and southwest and are of about the same force as those occurring during the northeast monsoon (Royal Netherlands Meteorological Institute, 1935). Severe squalls with gale force winds often accompany the southwest monsoon, but have little influence on the circulation in the strait because of their limited fetch (Great Britain Hydrographic Department, 1958, p. 31). Wind roses and the associated surface currents for the two monsoon seasons are shown in figure 6.

Oceanography

An understanding of tides, currents, salinity and water temperature is important in the interpretation of a shallow-water marine sedimentary environment. Currents normally account for the grain-size distribution. Temperature and salinity measurements delineate various water masses, which usually have considerable influence on the type of sediments deposited, particularly those of organic origin that are dependent on the properties of the overlying water.

Oceanographic conditions in the Malacca Strait differ considerably from those of the surrounding seas yet they are greatly influenced by the currents and water masses driven into the strait from these seas by the monsoons. The most significant effect of the monsoons is their regulation of the circulation in the South China and Java Seas as well as the Indian Ocean, which in turn control conditions in the strait. Within the strait only a minor effect is noted directly from the monsoons because of the shielding provided by the bordering land masses. Heavy rainfall in the higher elevations of the bordering lands, however, results in a large runoff into the strait which does influence salinity conditions.

Tides and Currents.—Currents flow through the strait in a general northwest direction throughout the year as a result of monsoonal effects on the neighboring seas. This flow is also strongly influenced by tides. It is a continuation of the south-flowing current during the northeast monsoon which rounds the tip of the Malay Peninsula from the South China Sea and passes into the strait (fig. 6). During the southwest monsoon, part of the northwestward-flowing water moving from the Java Sea into the South China Sea passes directly into the Malacca Strait (U. S. Navy Hydrographic Office, 1945). Currents are weak in June, July and August, and often a southeast flow is recorded as a result of the Indian Ocean current pattern that causes a pile up of water in the Andaman Sea. The difference in sea level during this period from the southern to the northern entrance of the strait is of the order of 10 to 15 cm with the slope toward the Andaman Sea. At the time of maximum flow to the northwest in January to March a difference in sea level of 50 cm has been reported by Wyrtki (1961, p. 126). Measurements during similar periods on both sides of the strait at various points indicate that there is little if any difference in sea level across the strait (Wyrtki, 1961, p. 125).

Tides are of the semidiurnal type throughout the strait except in the southern portion near Singapore where they are of a "mixed type." Flood currents set to the southeast and ebb to the northwest in the strait. The combination of tide and the general northwesterly flow causes the ebb to last longer and run slightly stronger than the flood. Current velocities average between 55 and 103 cm/sec. in the center of the strait, but closer to shore and in restricted channels they may reach 180 cm/sec. during spring tides.

Five current stations were occupied for periods of 26 to 33 hours during November 1961 (fig. 2). All measurements were made with a Roberts current meter. Surface and bottom currents for four of these stations as well as the respective tides are shown in figure 7. Tidal conditions at stations A and B are more uniform and the curves show less inequality than at stations C and D, which would be anticipated in an area of semidiurnal tides. North of Penang Island at station B, bottom currents are of about the same or slightly higher velocity than surface currents during times of flood, but appear to be slower during ebb (fig. 7). Bottom currents tend to be stronger than surface currents during periods of flood along the western margin of the strait at station A. The general surface current pattern during the southwest monsoon indicates that currents turn away from the vicinity of Penang Island and flow westward toward Sumatra (fig. 6). This is believed to account for the slightly higher current velocities observed near Sumatra at station A. Tidal currents are complex in the narrow part of the strait, particularly just north of Singapore. At station C, between the Kampar River mouth and Singapore, surface currents flowing towards the northwest are strongest during ebb flow while bottom currents in the opposite direction are strongest during flood. A surface velocity of 108 cm/sec. at station C was the highest measured in the strait during this series of current observations. Station D, southeast of Singapore, is in an area affected by tides from both the Malacca Strait and the South China Sea. Surface and bottom currents at this station have essentially the same velocity. These currents are variable in direction and little information can be gained from this single station when compared with the local tide data.

Sediments within the strait are predominantly

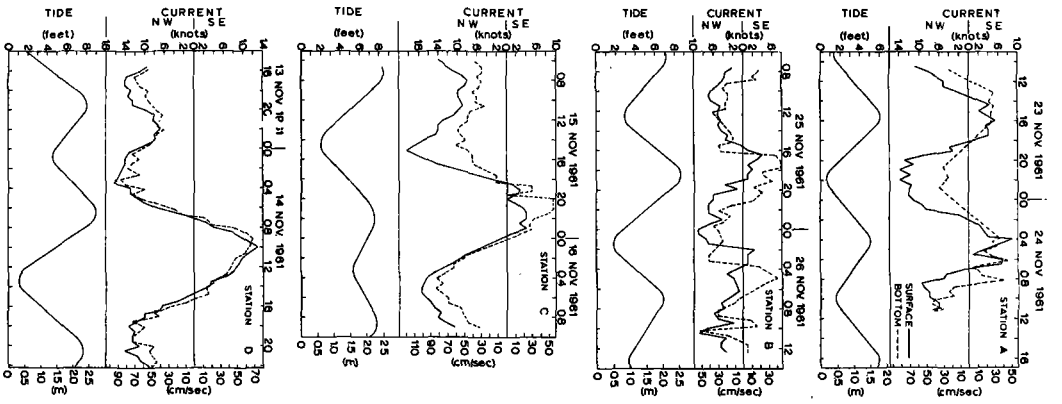


FIG. 7.—Tide and current observations from various portions of the Malacca Strait. The locations of stations A to D are shown in figure 2.

transported to the northwest, because of the general current pattern. This is particularly evident in the narrow portion of the strait between Malacca and Port Swettenham where the steep slopes of the large asymmetrical sand waves are inclined to the northwest. Local variations in currents and bottom topography in the northern and central parts of the strait also account for the movement of sediment in directions other than to the northwest as indicated by the small ripple marks mentioned earlier. The relatively short period of current observations presented here gives only an indication of the general current conditions with depth during the beginning of the northeast monsoon. Longer and more frequent observations are required to interpret more adequately the current-sediment relationship. While the above-mentioned currents are of great importance in transporting sediment throughout much of the strait, streams draining the adjacent land areas are also significant with respect to sediment distribution along the coastal margins. Stream currents in these regions appear to be stronger than the currents in the strait and account for much of the sediment transported into these areas.

Salinity.—A south-flowing current rounds the Malay Peninsula from the South China Sea and causes water of salinity greater than 32.0% to enter the Malacca Strait, displacing the low salinity waters in the southern portion of the strait during the northeast monsoon (Soeriaatmadja, 1956, p. 31). This low salinity water moves northward mixing with the higher salinity water of the central and northern portions of the strait. The result of this movement is a salinity maximum in the southern part of the strait during the northeast monsoon in spite of the heavy rainfall.

A decrease in salinity in the southern portion of the strait is thought to be caused by runoff from the large rivers on the east coast of Sumatra and the low salinity water entering from the Java Sea during the southwest monsoon (Selvarajah, 1962, p. 2). The annual variation of surface salinities in the northern and central parts of the strait shows two maxima and two minima, essentially a mirror image of the amount of rainfall (Soeriaatmadja, 1956, p. 30). Rainfall and salinity are not interdependent factors to the south.

Surface salinity measurements made during late March and early April 1961 do not agree with the general pattern described by Soeriaatmadja (1956, p. 40) for that time of the year. Soeriaatmadja shows an almost uniform surface salinity throughout the eastern half of the strait and lower salinities along much of the Sumatra coast. Data used in the present investigation indicate an increase in salinity from Port Swettenham to the Andaman Sea and a distribution pattern clearly reflecting the general current flow to the northwest. Additional measurements obtained by the Research Vessel JEANNE D'ARC during late March 1963 (Anonymous, 1963) are in concurrence with the pattern shown in figure 8. The salinity distribution pattern shown by Soeriaatmadja (1956) represents an averaging of data over a five year period which may account for the discrepancy mentioned here. The pattern of bottom salinity shows an even more pronounced high salinity wedge extending southeastward into the strait. This wedge is more evenly distributed across the strait at depth than at the surface. The bottom currents flowing to the southeast during periods of flood may help to maintain the position of this wedge. Salinity profiles also show this wedge to be thicker along the western margin of the strait and sloping towards the east (fig. 9). The penetration of higher salinity water from both the Indian Ocean and the South China Sea is readily apparent in the axial profile. The influence of large rivers is also clearly evident from the profiles and areal patterns, particularly in the southern entrance to the strait. Within the narrow, shallow part of the strait very little variation is found both laterally and vertically as a result of mixing.

Temperature.—The average annual variation of sea surface temperature is approximately 1.5° C. and is closely related to changes in the air temperature (Wyrtki, 1957, p. 21). Measurements made during March and April 1961, indicate that surface temperatures increase from off the Sumatra coast northeastward across the strait (fig. 8). This gradient, transverse to the axis of the strait, probably results from less mixing and weaker currents along the eastern margin of the strait.

Bottom temperature measurements during this same period show a cooler wedge of water extending into the Malacca Strait from the Andaman Sea and a general increase in temperature to the southeast. Isothermal conditions exist in the narrow portion of the strait because of vertical mixing.

Temperature profiles across the strait show a distinct tongue of warmer water along the eastern margin of the strait. The southeastward extension of cooler Indian Ocean water along the bottom is clearly shown in the axial profile (fig. 9).

An important influence on the sedimentary environemnt of the north and central portions of the strait is the large wedge of cool, high salinity water that extends into the area from the Anda-

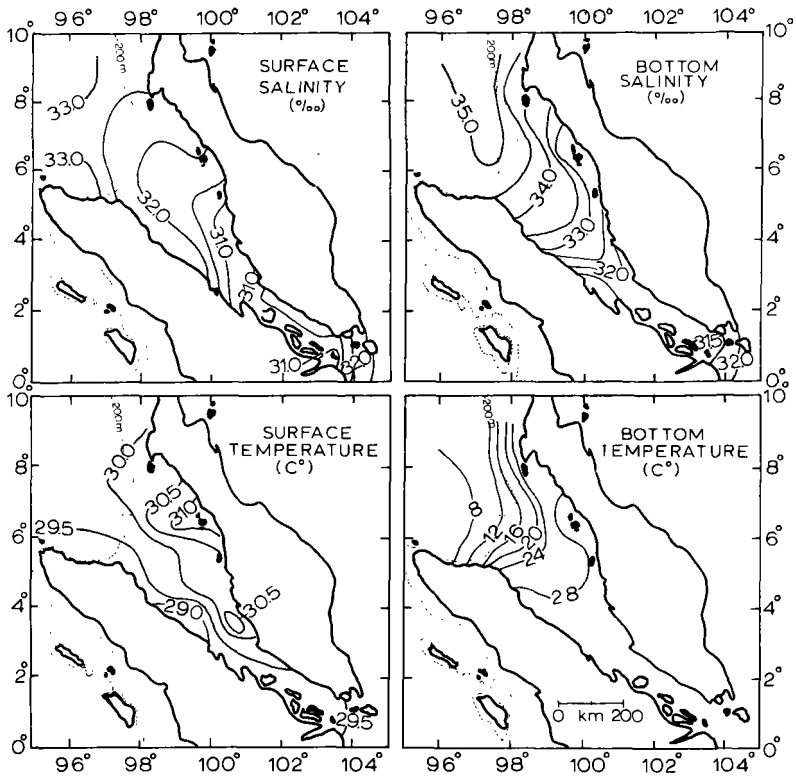


FIG. 8.—Water temperature and salinity distribution for April 1961.

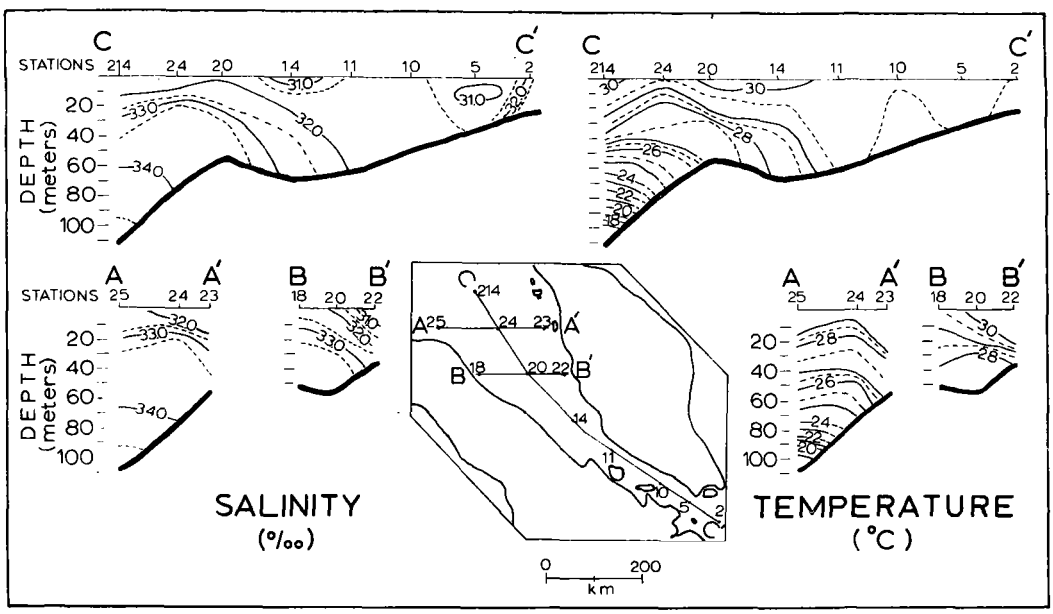


FIG. 9.—Water temperature and salinity sections.

man Sea. We believe this wedge is more or less stationary and is not an actively moving water mass. The fluctuation of bottom currents with changes in the tide is probably largely responsible for the location of this wedge. The significance of this water mass with respect to the sedimentary constituents is discussed in a later section.

Sediments

The complexity of the depositional environment in the Malacca Strait is mainly attributed to the varied sediment source areas provided by the bordering land provinces and to the oceanographic conditions in and around the strait. Tectonic activity in the adjacent land masses has resulted in extensive areas of igneous intrusion and associated zones of metamorphic rock which contribute numerous mineral suites to the rivers entering both sides of the strait. In addition, the remains of both planktonic and benthonic faunas are found in the bottom sediments. Factors other than source material tend to further complicate the environment. The magnitude of river discharge increases considerably during the winter and summer months as the result of monsoonal rains. Sediment entering the strait is subjected to a strong annual northwest current that has superimposed upon it a semidiurnal tidal current having a flow of nearly 55 cm/sec. to the southeast, then later reverses direction to flow northwest at velocities up to 100 cm/sec. Bottom irregularities account for isolated patches of coarse or fine material within areas of nearly uniform sediment type. As a result of these many factors constituting the depositional environment, the various sediment parameters of size, sorting, mineral content and other constituents undergo short term spatial and temporal variations of considerable magnitude.

One hundred-forty-one grab samples and 76 sediment cores were collected at 155 stations (fig. 2). An orange-peel bucket sampler (Sumner, and others, 1914, p. 7) and the Shipek grab sampler (manufactured by Hydro Products, San Diego, California) were used to obtain the surface samples. All cores with the exceptions of those at stations 184, 185, 195, 199, 202, 204 and 209 were collected with a Phleger corer (U. S. Hydrographic Office, 1955, p. 54–57), and the remainder was taken with a modified Hydroplastic corer using a piston (Richards and Keller, 1961). Core lengths vary from 10 to 349cm, averaging about 46 cm. Only relatively short cores were obtained from much of the area because of the coarse surface sediment and an underlying stiff clay.

Cores taken in the vicinity of large rivers indicate that the thickness of silt and lutite extends throughout the sampled interval, while farther away from the rivers sand overlies finer sediments. Sediment grain size and calcium carbonate content vary considerably with depth from station to station. In some areas only minor variations of the sedimentary parameters are noted with depth, while in others a pronounced change is seen where the core penetrates a prominent silty clay layer. The influence of local conditions is clearly evident from the sediment cores.

Textures

Prior to this investigation the only available textural information on the bottom sediments in the Malacca Strait came from chart notations which were based on brief visual examinations of sediment adhering to the tallowed lead used in early hydrographic surveys. The validity of many of the notations is questionable because of the manner in which samples were collected and the crude field descriptions usually logged by mariners. Shepard, Emery, and Gould (1949) compiled these notations into a series of sediment distribution charts for the east Asiatic shelf areas. Their study of the Malacca Strait shows that along the axis the bottom is composed mainly of firm sand and mud and irregular patches of sand and rock. Mud was found to predominate in the north-central and northeastern sections of the strait.

Based on the surface distribution of various textural parameters determined during this investigation, the depositional environment of the Malacca Strait can be divided into four distinct regions (fig. 10), if local irregularities are ignored: north of Penang Island (Northern); Penang Island to Port Swettenham (Central); Port Swettenham to Malacca ("Narrows"); and Malacca to Singapore (Southern).

Sediment samples are assigned to one of four types based on grain-size analysis data: sand (at least 90 percent of the sample consisting of material coarser than 4 phi); muddy sand (50 to 90 percent sand grains); sandy mud (10 to 50 percent sand); and mud (at least 90 percent consists of material finer than 4 phi). While the distribution of these textures shows a vague agreement with the bottom notations mentioned above, the more detailed classification used here affords a better delineation of the sediment types. Mud deposits are less extensive than indicated by Shepard, Emery, and Gould (1949), particularly in the Northern region; they are found mainly in the vicinity of river mouths and in the Andaman Basin. The present study finds that muddy sand is the dominant sediment type in the strait. Sand occurs throughout large

areas, but mainly in association with gravel and large shell fragments along the axis of the strait as well as along the continental shelf break where currents tend to winnow out the finer material (fig. 11). An attempt was made to verify the presence of rock areas reported by Shepard, Emery, and Gould (1949), but none were found.

Vertical variation of the textural properties appears to be minor. Most cores penetrating only the Recent surface sediments show little variation whereas those reaching the underlying stiff clay reveal a distinct change in textural properties. Grain size decreases markedly and sorting generally is poorer below this contact. Within the clay the properties again are remarkably uniform. A 3.84 m core from the southern portion of the Andaman Basin shows little change in the textural parameters with depth.

Color.—Color of the grab samples was determined at the time of their collection by comparison with the Rock-Color Chart devised by Goddard, *et al.*, (1948). Color determination of the wet core samples was made later in the laboratory. Nearly all samples can be approximated by five main colors if minor transitions are ignored: grayish olive (10Y4/2), olive gray (5Y3/2), light olive gray (5Y5/2), dusky yellow green (5GY5/2), and medium gray (N5). Sediment colors often indicate different depositional environments and are commonly related to such parameters as grain size, sorting, or carbonate content (Niino and Emery, 1961, p. 749). This relationship does not appear to hold true for the Malacca Strait. The grayish-olive material found over much of the Central and Northern regions includes sediments varying in texture from mud to sand. This variation of texture is also true for the other colors. It appears that in the Malacca Strait sediment color is not significantly indicative of the conditions in the depositional environment, but rather of the source areas from which the sediments are derived. Although there is a lack of samples from the vicinity of river mouths, there is a strong indication that the observed color patterns are related to the sediments coming from the rivers (fig. 11). Each area delineated by a different color is found to be associated with one or more streams. An indication of this relationship is noted in samples collected off the mouth of one river in the southern portion of the strait, where the freshly collected river sediment has the same color as that found further away from shore.

The large extent of grayish-olive material across the northern portion of the strait is probably related to the current system in the area. Examination of samples from north of the strait and in the Andaman Sea appears to indicate a less complex pattern as one might expect where local drainage is not significant.

Median Diameter.—Grain-size analyses were

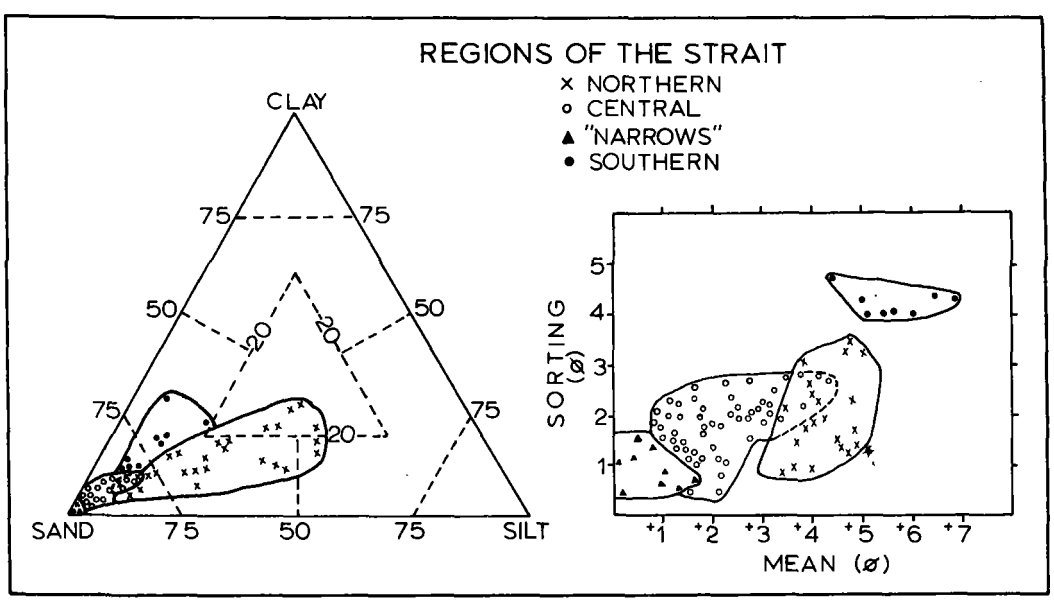


FIG. 10.—Delineation of regions in the Malacca Strait based on textural properties as shown by the sand-silt-clay content and the relationship of sorting to mean grain size.

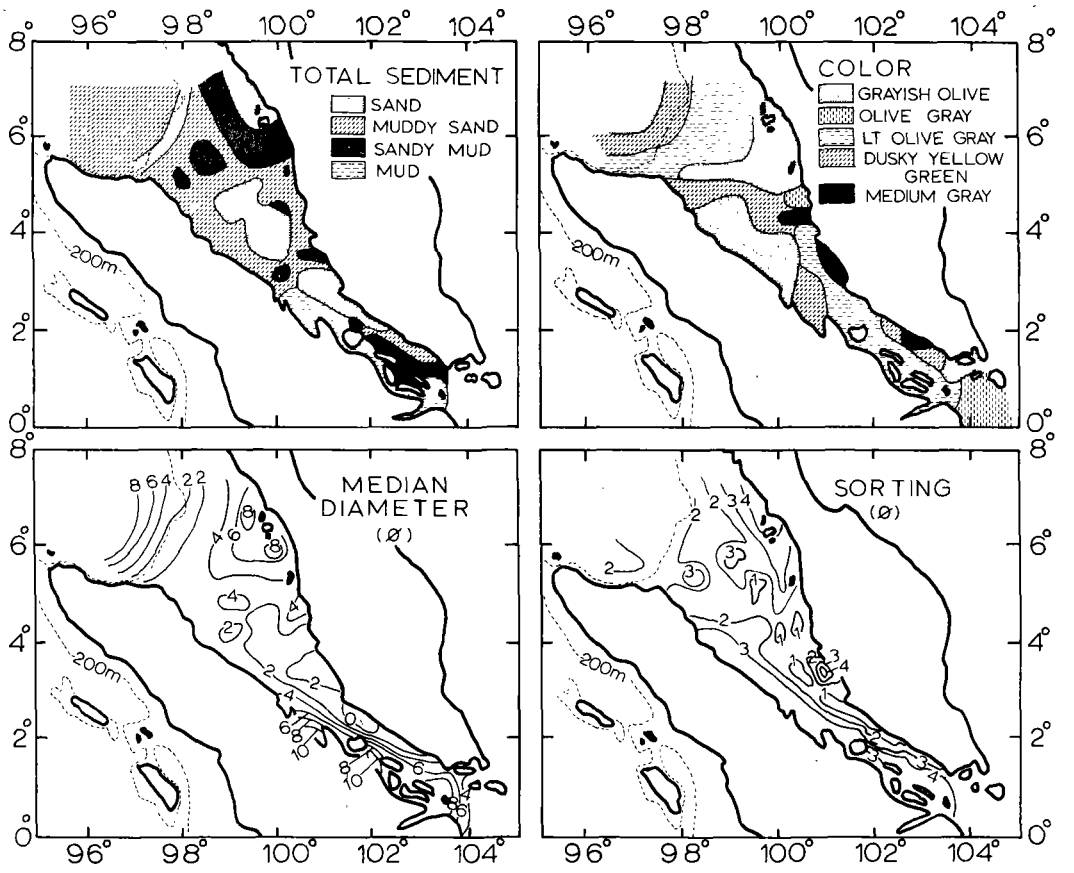


FIG. 11.—General description of total sediment, color, median diameter and sorting of surface sediments from the Malacca Strait and adjacent Andaman Sea. Median diameter and sorting are the descriptive measures of Inman (1952).

made on the whole sample with the coarse and fine fractions separated by wet-sieving through a 0.062 mm screen. The dried coarse fractions were further separated by sieving, and the fine fractions pipetted (Krumbein and Pettijohn, 1938, p. 165). The various measures used in this study to describe size distribution such as central tendency, dispersion and skewness follow the procedure recommended by Inman (1952). Median diameters and quartiles were picked from cumulative curves drawn on arithmetic probability paper.

The effects of currents and debouching rivers on the depositional environment in the strait are clearly shown by the grain-size distribution pattern (fig. 11). Water depth appears to have little influence on the sediment distribution. Although the southern portion of the strait—Singapore to Port Swettenham—is a high-energy environment, it is nearly choked with fine material from the numerous rivers of Sumatra that drain extensive low-lying areas of alluvium. Clean coarse to very coarse sands are only found in the "Narrows," where a constriction occurs in the strait. In this region the currents often reach velocities of 140 cm/sec. which is sufficient for the removal of finer sediment.

The large area of fine-grained sediment northwest of Penang Island, which extends westward beyond the axis of the strait, is a clear reflection of the general current pattern. The northwest current emerging from the narrow part of the strait tends to veer away from the Malayan Peninsula as it approaches the Andaman Sea. The southeast current from the Indian Ocean begins to enter the northern portion of the strait and then turns westward just north of Penang Island during the southwest monsoon. The resulting large eddy forms an area of lower current velocities and transport energy between the two

westward moving currents (fig. 6). Clay-size sediments, with minor amounts of fine sand-size foraminiferal tests, predominate in the deep Andaman Basin.

The percentages of sand-silt-clay clearly show the sediment variation in the major regions of the strait (fig. 10). In the Southern region, the finer size fraction is largely made up of lutite rather than silt-size material, indicating that the rivers in this section of the strait are carrying more clay- than silt-size particles. Silt, rather than clay-size material, comprises the bulk of the fine sediment in the Northern region. The Southern region shows the effect of local drainage, while the Northern is more indicative of an environment farther from land in which the textural properties are related to the energy level rather than the sediment supply. The greater concentration of sand in the "Narrows," relative to all other regions, is indicative of the strong currents found there. The fine detrital sediment from local drainage into the "Narrows" apparently moves northward along the coast and does not reach the axial portion of the strait.

Sorting.—Sorting is poor off the coast of Sumatra particularly in the Southern region as a result of the sediment supply from rivers (fig. 11) Low sorting values characterize the sediments along the axis of the strait where the strong current and less fluvial material result in better sorting. Isolated patches of poorer or better sorted sediments can be related to topographic depressions and elevations, respectively. Poor sorting in the vicinity of Penang Island is probably related to the current pattern discussed above.

Sorting related to mean grain-size shows the distinct characteristics of the four major environments in the strait. Coarse sands are the best sorted whereas the fine silts are the poorest Sorting isopleths reveal a marked similarity to those of the median diameter, especially in the Southern region.

Skewness.—A study of the areal distribution of skewness shows very little relationship to other measured parameters. Coarse and fine (negative and positive) skewness is found in both areas of sand- and clay-size material. The sands of the "Narrows" and the Central region of the strait are largely near-symmetrical to strongly coarse-skewed while in the Northern and Southern regions finely-skewed sediments predominate as the quantity of fine silt- and clay-size material increases. Sediments are fine-skewed, in the vicinity of some rivers although near others they are coarse-skewed even though the median diameters are similar. Skewness plotted against mean grain size indicates a general correlation between these two parameters and does suggest a sinusoidal relationship as has been reported by Folk and Ward (1957, p. 19) and Hubert (1964, p. 777). However, since this correlation is not more diagnostic than median diameter or sorting, it is neither illustrated nor further discussed.

Organic Constituents

Calcium Carbonate.—The fraction of the whole sample that is soluble in dilute hydrochloric acid is primarily organic material in the form of shell fragments and foraminiferal tests. Values are reported here as calcium carbonate, although minor amounts of magnesium carbonate may also be present. Acid-soluble fractions range from 0 to 69 percent. Low concentrations (trace to 17 percent) occur throughout most of the strait. Two exceptions occur in the Central region, where shells tend to concentrate on banks and to the north, where there are more shell fragments and foraminiferal tests (fig. 12).

Areal distribution of calcium carbonate bears little or no relationship to any of the textural parameters because of its biogenic origin. The lowest percentages are found in the narrow portion of the strait where calcium carbonate may be completely absent, possibly because of strong currents that break-up and winnow-out shell fragments. Low calcium carbonate percentages in the vicinity of large rivers results from the high sedimentation rate of fine material that is detrimental to the living habits of shell-contributing organisms. The carbonate concentration increases both to the south of the strait and to the north into the Andaman Basin where the calcium carbonate fraction consists mainly of foraminiferal tests.

Although shells and foraminiferal tests are present in most samples, they constitute only a small percent of the entire sample and are often masked by large quantities of fine detrital material.

Shells.—The areal distribution of both shell fragments and foraminiferal tests (fig. 12) resembles that of total calcium carbonate: each is absent in the "Narrows," most abundant in the Northern and Southern regions, and of intermediate abundance in the Central portion except for two isolated areas with relatively high concentrations. Mollusks contribute the major portion of the shell material; pelecypods are the predominant forms in shallow water and gastropods are more commonly found in deeper water.

Foraminifera.—Foraminiferal tests are particularly abundant in the Andaman Sea and in the Northern region; their numbers decrease to the

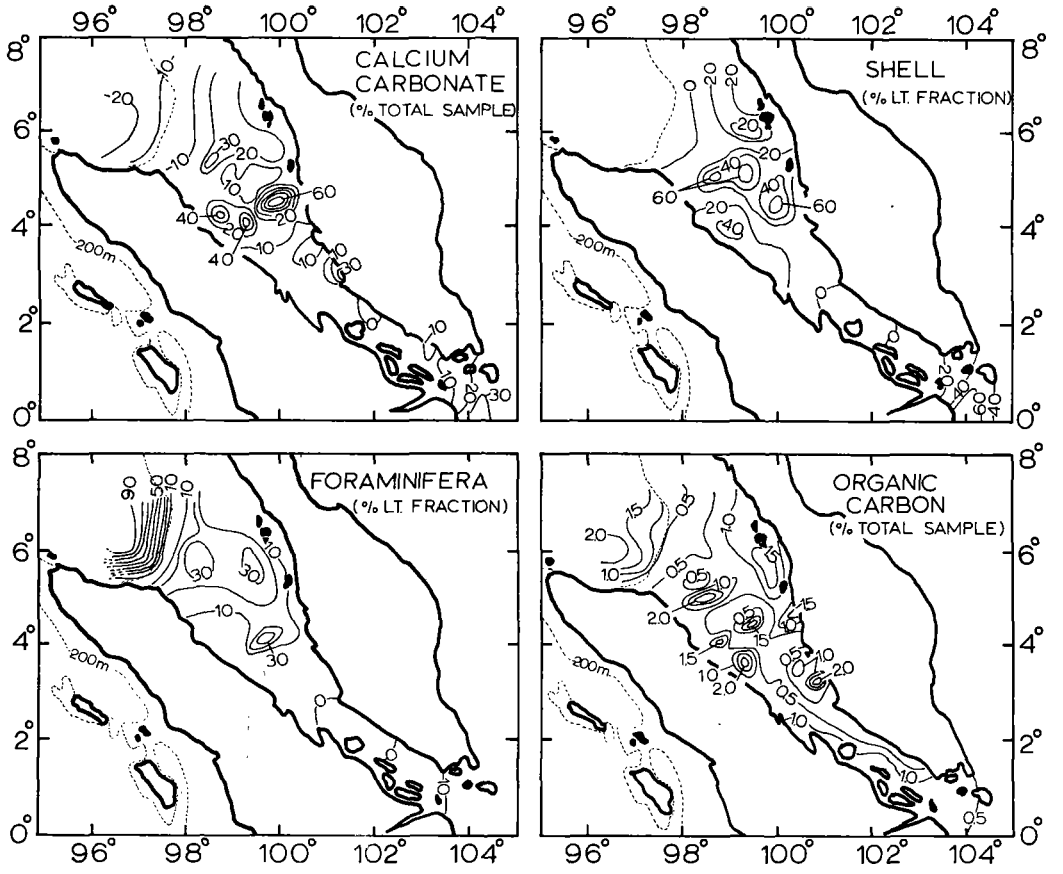


FIG. 12.—Surface distribution of calcium carbonate, shell, foraminifera, and organic carbon, Malacca Strait and adjacent Andaman Sea.

southeast. The shelf break is a distinct divide between the high-test concentrations in the Andaman Sea and the relatively low abundance in the strait. The tongue-like area of foraminiferal tests projecting into the strait from the Andaman Sea is attributed to the environment caused by the wedge of cool, high salinity bottom water that also extends from the Andaman Sea into this region (fig. 8).

Organic Matter.—Duplicate organic carbon determinations were made using the potassium dichromate-ferrous ammonium sulfate titration method of Allison (1935). The values obtained are only approximate because this method is based on the assumption that all organic matter in sediments is at the same state of oxidation. Percentages of organic carbon range from 0.01 to 2.71. The lowest concentrations are found in the area of maximum current velocity between Port Swettenham and Malacca (fig. 12). A fair correlation exists between the areal distribution of grain size and organic carbon; low organic carbon normally is associated with the coarser sediments. High organic carbon content along portions of the coastal margin reflects the influence of river discharge. This is particularly evident in the Southern region and north of Penang Island. Isolated areas of relatively high organic carbon also occur where organic matter has collected in topographic depressions. A pronounced deficiency of organic carbon occurs along the shelf break where the currents tend to winnow away the finer material. Organic carbon percentage increases beyond the continental shelf towards the Andaman Basin.

Nitrogen content was determined for 77 surface samples using a modified micro-Kjeldahl method (Henwood and Garey, 1955). Values ranging from a trace to 0.235 percent, all of which is considered to be organic nitrogen. Areal distribution of nitrogen content throughout

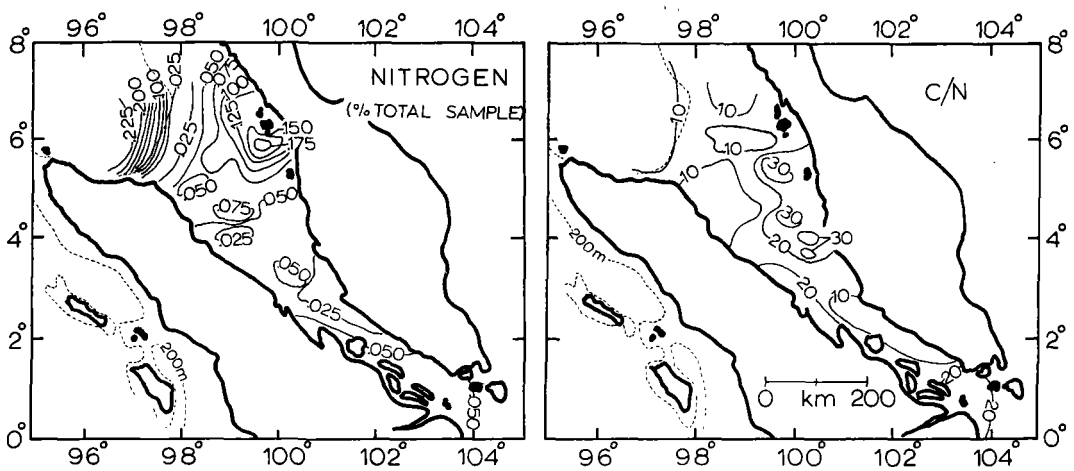


FIG. 13.—Surface distribution of nitrogen and carbon to nitrogen ratio, Malacca Strait and adjacent Andaman Sea.

most of the strait is usually less than 0.050 percent (fig. 13). Lowest values occur in the coarse to medium sands in the "Narrows" and in the sands along the shelf break. A noticeable increase in nitrogen is observed in the Southern region along the Sumatra coast where organic-rich sediments are deposited from nearby rivers. Values to the north increase in areas of finer sediment with the highest percentages occurring in the Andaman Basin.

In the Malacca Strait, C/N ratios vary between 0.4 and 36.9; smaller values occur in the "Narrows" (fig. 13). High ratios are found along the Sumatra coast and in the vicinity of Penang Island indicating abundant drainage from nearby streams of terrestrial humus, such as peat, which is often found disseminated throughout the finer sediments. Carbon-nitrogen ratios of 56 samples give a mean of 15.4, which is slightly higher than the mean of 13 found for the Gulf of Thailand sediments (Emery and Niino, 1963, p. 548) and considerably higher than the 8.4 reported by Trask (1932, p. 21) for all Recent marine sediments. The large mean found in the Malacca Strait is attributed to the high influx of high-carbon organic matter from rivers draining areas of heavy vegetation.

Although organic carbon and nitrogen content is indicative of the amount of total organic matter present in the sediment, there is no consensus as to the proportion of these constituents in organic matter (Bader, 1954; Kaplan and Rittenberg, 1963, p. 593). For this reason, no attempt is made here to determine the total organic content, but only to show its relative concentration by means of the organic carbon and nitrogen content.

Sponge spicules are the dominant siliceous organic remains in these samples. They are most abundant in the Central and Northern regions where, however, they constitute only a very small percentage of the whole sample. Minor amounts of radiolaria are found in most samples; larger numbers occur in samples from the Andaman Sea and the Northern region.

Vertical variation of organic constituents is only significant in core samples that penetrate the stiff, silty clay underlying the coarser Recent sediments. A noticeably lower calcium carbonate content is almost always found in the underlying clay. Organic carbon and nitrogen content is generally higher in the clay than in the overlying sediment in most areas, except in the Southern region where the reverse is true. Variation of the C/N ratio between the sediment above the clay and in the clay may amount to a factor of four.

Variation of the sedimentary parameters with depth is often masked or completely altered by burrowing organisms. Burrow holes or passages are readily apparent in many cores owing to the sharp contacts between the coarse material filling the passages and the finer surrounding sediment. Organisms appear to have dragged the coarser surface sediment downward in some areas. In others, they have apparently concentrated the quartz and volcanic glass shards from the finer sediment through which they are burrowed. Mottling, which is commonly an indication of organism activity is quite noticeable in the finer sediments of the Andaman Basin, but is not observed in cores taken from the strait. The presence or absence of mottling is attributed to the different forms of burrowing organisms and the types of sediment found in the two areas.

TABLE 1.—*Mineralogy of the coarse fraction from various regions of the Malacca Strait and the southern part of the Andaman Basin*

		Percent Light Mineral Fraction							Percent Heavy Mineral Fraction													
Station Area	Station No.	Quartz	Orthoclase	Plagioclase	Rock Frag.	Organic Remains	Other*	Wt. pct. of coarse fraction	Leucoxene	Ilmenite-Magnetite	Amphibole	Tourmaline	Zircon	Garnet	Biotite	Rutile	Staurolite	Kyanite	Siderite	Goethite	Other**	Wt. pct. of coarse fraction
Southern Region	1	44		tr	4	38	14	99.6	60	17	7	3	2			1	3			5	2	0.4
	3	tr		tr	2	98		99.7	74	19	4	1	2									0.3
	6	28	tr	tr	18	36	18	98.2		1									98			1.8
	9	64	tr		17	17	2	97.9												100		2.1
	179	93	6	1	tr			99.8	35	37		4		6		18		tr				0.2
Narrows	11	100	tr					97.8	3	9		1					1			86		2.2
	47	98				tr	2	98.8	5	10		2					tr			83		1.2
Centra Region	12	88	2		1	8	1	99.6	32	31	3	7	6				19				2	0.4
	16	47	2	tr	7	16	28	96.0							100							4.0
	18	1	tr	tr	20	36	43	99.7	17	4	39	7	6		2	1	16	5			5	0.3
	20		3	tr	1	93	2	99.7	20	12	22	3	7		15		12	5			4	0.3
	184	86	8	2	2	2	tr	98.9	44	33	4	6	3		7		1				2	1.1
	188	73	5	13	7	tr	2	99.0	19	42	5	4	2		20		7				1	1.0
	196	43	1	1	15	32	7	99.7	tr		tr		tr		99						tr	0.3
Northern Region	23	77	3	tr		20		99.7	30	11	3	11					39				6	0.3
	24	66	3	tr	tr	21		99.4	31	2	24	9			6		24				4	0.6
	25	92	5	tr	tr	3		99.4	26	16	24	6			6		18				4	0.6
	214	94	3		tr		3	99.7	32	19	6	6	4			1	27				5	0.3
Andaman Basin	211	5			5	90		99.7	31	15	23	4	2				23				2	0.3
	26	5			2	93		98.9	7	24	25	8				1	30				5	1.1
	208	31	3	tr	1	65		97.6	5	8	50	22			9	2	1				4	2.4
	209	5				95		96.6	4	89	3		1				3					3.4

* Glauconite, volcanic glass
** Allanite, Andalusite, Cassiterite, Corundum, Epidote, Monazite, Muscovite, Pyrite, Sillimanite, Titanite, Topaz

Disturbances due to organisms are observed to a depth of 84 cm in cores from the strait, while in the soft sediments of the Andaman Basin, mottling attributed to organisms is found as deep as 2 m below the sea floor.

Detrital Constituents

Separation of the sand-size particles into light and heavy mineral fractions was made by a heavy liquid technique using tetrabromoethane (specific gravity 2.96). The light minerals were identified by the staining technique described by Laniz, Stevens, and Norman (1964), and examination under a binocular microscope. Heavy mineral fractions were weighed and their weight percent in the total sand sample determined. Identification of the mineral constituents was made using a petrographic microscope. The results of this examination are given in table 1.

Light Minerals.—Light minerals dominate the coarse sediment fraction (75 to 100 percent by weight) and are generally concentrated in the sands along the axis of the strait. Quartz comprises over 50 percent of the light fraction in all but a few samples and makes up the entire sample in the high energy zone between Port Swettenham and Malacca. An area of low quartz content (1 to 35 percent) and high glauconite, volcanic glass and shell fragments extends across the strait from Belawan to Penang Island. Isolated areas of low quartz content sediments are observed in the Northern region in topographic depressions where shell material predominates. Quartz content is also low in the southern entrance to the strait (trace to 44 percent).

Orthoclase is generally more abundant than plagioclase; concentrations of a trace to 9 percent are found in the Central and Northern regions, and a trace in the Southern region. Traceable amounts of plagioclase occur throughout the strait with a few samples along the Malaysian coast, north of Port Swettenham, containing as much as 5 to 13 percent. The other few samples in which plagioclase dominates over orthoclase occur in low energy environments either close to shore or in topographic depressions. No distinct distribution pattern can be detected for either of the feldspars as a result of the numerous rivers and the different areas drained by these rivers.

Heavy Minerals.—With a few exceptions, the

heavy mineral assemblages present are composed of stable to moderately stable minerals derived from intermediate to silicic igneous rocks and from associated crystalline metamorphic rocks. These rocks are abundant in both the bordering land provinces and the islands at the southern entrance to the strait. However, in view of the lack of information concerning coastal detritals, only generalizations can be made about provenance.

A few minerals dominate the assemblages in most instances. Opaques consisting of leucoxene, ilmenite and magnetite constitute large percentages of the majority of the samples. It is believed that most of the black opaques are ilmenite rather than magnetite because of the observed partial alteration to leucoxene of many grains of similar appearance. The percent of leucoxene compared to ilmenite is high in two areas: the extreme southern end of the strait and a large area occupying the north-central axial portion of the strait and extending beyond the shelf into the Andaman Sea. This relationship is reversed towards the coastal margins and southward from the Northern region of the strait.

Biotite is concentrated in an elongate area paralleling the northern Sumatra coast and in another area beyond the shelf in the Andaman Sea. Large hexagonal books of biotite are found to make up an entire heavy fraction of a surface sample collected in this area off the Sumatra coast. These concentrations indicate an adjacent source, possibly entering from the nearby Asahan River of Sumatra. The northwesterly current in the strait may account for the northward distribution of the biotite along the coast and into the Andaman Basin.

Amphiboles and staurolite occur in high percentages in most samples from the northern and central portions of the strait. The largest quantity of staurolite is found in the north while amphiboles are concentrated in the west-central strait area; a source for both minerals in the crystalline schists of Sumatra is suggested. Tourmaline is usually found in relatively high concentrations (3 to 13 percent) in association with staurolite. Both minerals are also abundant in the vicinity of the Rokan River, indicating a possible source in the metamorphics of the Barisan Range of Sumatra.

Heavy fractions from the "Narrows" are composed almost entirely of siderite or goethite. A few of these grains contain an olive-brown rounded aggregate of minute crystals, while others have a similar oval shape with colors varying from yellow-brown and brownish-red to brick-red, and display an earthy surface appearance. Chemical tests on selected grains of the olive-brown material show it to be siderite. X-ray analysis of these various grains indicate siderite in some cases and goethite in others although the outward appearance of the grains is similar. Alteration of the siderite appears to be the answer, with oxidation of the ferrous iron and leaching of carbonate. Partial alteration has masked the surface of some grains and gone to completion in the crystallization of goethite in the other samples.

Heavy-mineral weight percentages of the total sand-size fraction are low, generally less than one percent, and correlate with the relative abundance of medium to fine sand. Heavy mineral concentrations greater than 1 percent are confined, with few exceptions, to those samples in which a single mineral comprises all or nearly all of the heavy-mineral fraction.

Van Baren and Kiel (1950) divided the sediments of the Malacca Strait into three distinct groups based on the mineral suites from 18 samples. Their results are not corroborated by the present study (table 1).

In an environment like the Malacca Strait, with its large number of debouching rivers and varied sediment source areas, it is not believed that distinct mineral suites can be delineated for the major portion of the area. Some distinction is possible, however, in the Northern region where the effect of reduced local drainage is shown by the distribution of the amphibole-staurolite-tourmaline suite that does appear to have a definite distribution.

Clay Minerals.—The clay minerals were identified in 54 surface samples as well as in selected intervals from four cores by means of X-ray diffraction.

The less-than-two micron fraction was taken from samples which had been treated with sodium hexametaphosphate and used for the grain-size analyses. Two glass slides of oriented aggregate were prepared from each sample. Each set of slides was X-rayed (Cu Kα radiation) after drying at room temperature and again after solvation in ethylene glycol. Additional X-ray analyses were obtained from selected samples treated in warm 8 N HCl.

The clay minerals observed in this study—montmorillonite, kaolinite, undifferentiated mixed-layer minerals, illite and chlorite—were identified by their characteristic X-ray diffraction peaks.

Clay minerals of the montmorillonite group were identified by a (001) peak reflection which shifts to 17Å after ethylene glycol treatment. However, this could be a true montmorillonite or an illite and/or chlorite which has been stripped of its inter-layer cations and now absorbs two layers of ethylene glycol (Griffin and Goldberg,

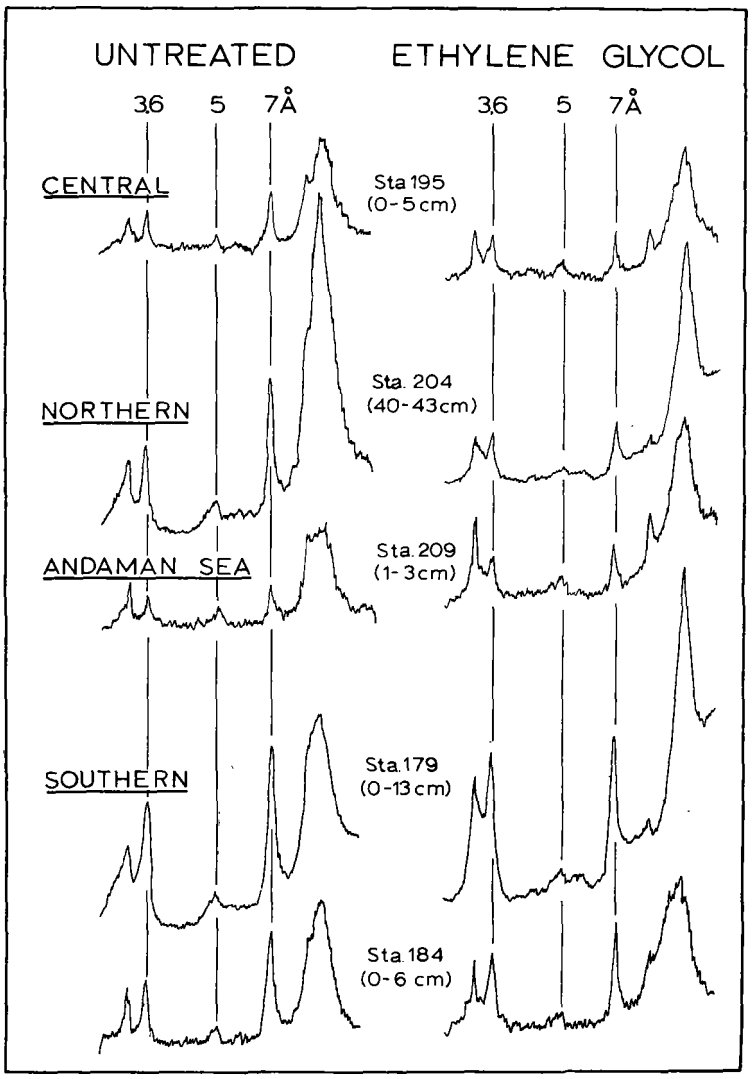


FIG. 14.—Typical X-ray diffraction patterns of clays from various parts of the Malacca Strait and adjacent Andaman Sea.

1963). Diffraction peaks at 7 and 3.5Å are attributed to kaolinite. Using a modification of the procedure described by Brindley (1961, p. 264), a representative number of the samples were placed in warm 8 N HCl for two hours and then X-rayed to distinguish between kaolinite and chlorite. Broad, asymmetrical diffraction peaks varying between 15.5 and 16.8Å after ethylene glycol solvation characterized the undifferentiated mixed-layer minerals. These consist of a complex grouping of three-layered minerals interlayered with montmorillonite. It appears that illite may be the significant mineral mixing with montmorillonite, although chlorite is undoubtedly also present. Diffraction peaks at 10, 5 and 3.3Å which are not affected by ethylene glycol treatment are defined here as belonging to minerals of the illite group. A diffraction peak at 4.7Å as well as a slight reduction of the 3.5Å peak after acid treatment is used as evidence of chlorite. Typical X-ray patterns for samples from different regions of the Malacca Strait and Andaman Sea are shown in figure 14.

A semi-quantitative determination was made utilizing the intensities of the X-ray peaks to study the clay-mineral distribution. The pro-

cedure used is similar to that described by Johns, Grim, and Bradley (1954), with the exception that the area of the 17Å peak was divided by three rather than four. This procedure was used by Ferrell (1965, p. 21–22) and found to be satisfactory. Values are reported in percent rather than in parts in 10 as a matter of convenience. This method, although not truly quantitative, is suitable for comparison of relative abundance.

Kaolinite, mixed-layer minerals, illite, montmorillonite and chlorite comprise the clay-mineral assemblage found in the Malacca Strait in order of decreasing abundance. Kaolinite and mixed-layer minerals constitute from 60 to 85 percent of the clay minerals present in most samples. Illite is present in all samples, but is never found to be the dominant clay mineral. Montmorillonite is the predominant clay mineral at only a few locations and combines with other minerals to form the mixed-layer minerals in all other samples. Chlorite was only observed in trace amounts although it is present in many samples.

The highest concentrations of kaolinite are observed in the shallow areas along the Sumatra coast and in the southern portion of the strait (fig. 15). Kaolinite is common in all samples as might be expected of sediments collected relatively close to land in a tropical climate. The kaolinite content bears a close relationship to the isobaths; a decrease in kaolinite occurs with increasing water depth. Minor concentrations are found in the Andaman Basin. Undifferentiated mixed-layer minerals constitute the dominant clay minerals in the Northern and deeper portions of the strait as well as in the southern part of the Andaman Basin (fig. 15). However, mixed-layer minerals comprise a large portion of the clay minerals in most of the samples analyzed. Montmorillonite is the predominant clay mineral at only six stations, all of which are

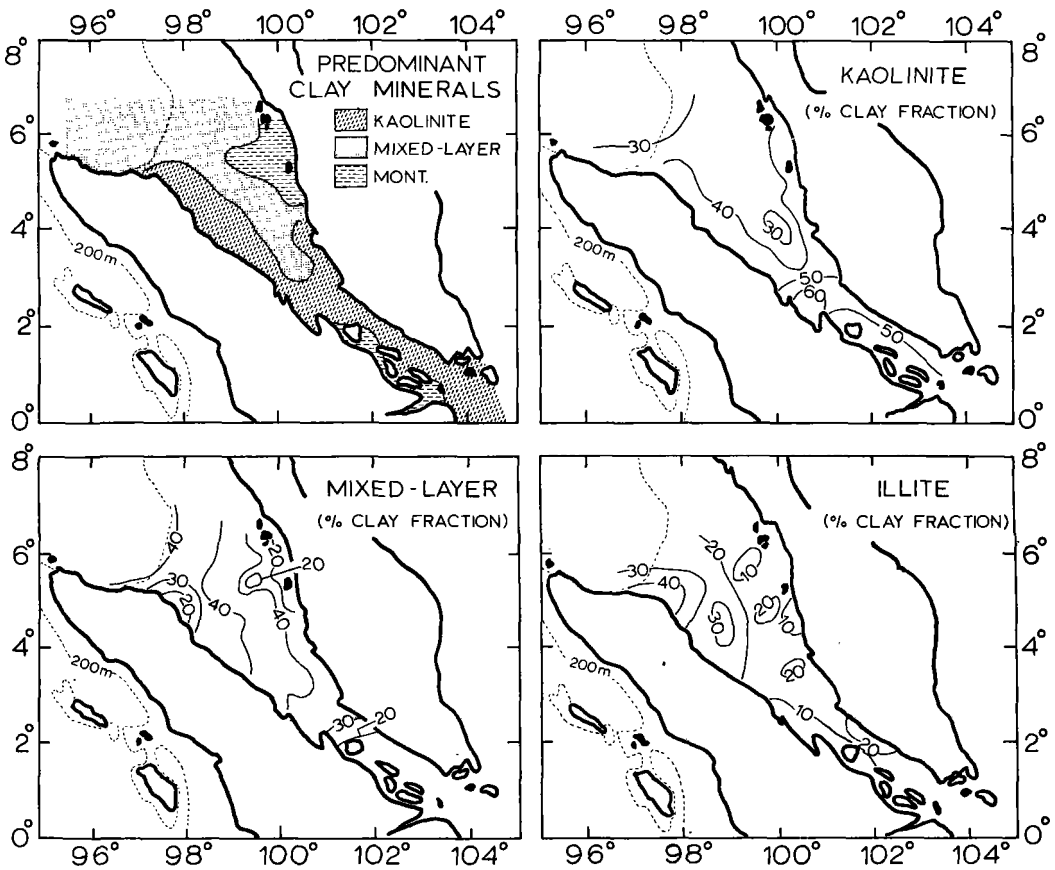


FIG. 15.—Surface distribution of the predominant clay minerals, kaolinite, mixed-layer minerals and illite in the Malacca Strait and adjacent Andaman Sea.

close to shore and generally in the vicinity of river mouths. The concentration of montmorillonite (46 to 53 percent of the clay minerals) in the southern portion of the strait decreases away from the rivers. Drainage through the Tertiary tuffs on Sumatra provides the probable source material for these clays. Streams draining Permian shales on the Malay Peninsula in the vicinity of Penang and Langkawi Islands may be responsible for the montmorillonite in this area. Although illite is present in all the samples it seldom makes up more than 25 percent of the clay minerals and usually is much less. The largest concentrations of illite are found east of northern Sumatra in an area where sediments also contain large amounts of biotite. This association plus the presence of glauconite, which is mentioned later, may indicate a diagenic relationship between these minerals (Burst, 1958, p. 493). The illite and biotite could also have been transported to the strait from a source area in Sumatra.

The montmorillonite peak in samples collected progressively farther from land in the Southern region is observed to lose its character and assume that of a mixed-layer peak. This change may be caused by the occurrence of degraded illite with the montmorillonite. The presence of degraded illite can be explained by the loss of potassium ions during transport in slightly acid river waters. As the rivers empty into the strait these ions are normally regained (Bradley, 1953). Although degraded illite may fix potassium from the sea water in a matter of days as suggested by Weaver (1958), it might be a long time before the illite has completely achieved its characteristic 10Å peak. In such a situation, the presence of a certain amount of degraded and crystalline illite would cause the montmorillonite peak to broaden and assume the characteristics of a mixed-layer mineral. The amount of magnesium ion fixation by chlorite could have a similar effect on the montmorillonite peak (Grim and Johns, 1954, p. 100).

Four cores ranging in length from 0.8 to 3.5 m were examined for their clay mineral content, and, of these, only three showed any discernible variation with depth. The predominant minerals are the same as those found in the surface sediments.

The percentage of mixed-layer minerals increases slightly and illite decreases with depth in the three cores. It is generally reported in the literature that there is little or no variation in clay mineral composition with depth for cores in Recent marine sediments (Emery, 1960, p. 231; Griffin and Goldberg, 1963, p. 739; Heezen, and others, 1965, p. 5821). This unusual occurrence found in the Malacca Strait may possibly be explained by an upward migration of slightly acidic water that strips potassium ions from the illite. This would result in a decrease in 10Å illite and an increase in the mixed-layer minerals. Each of the cores displaying this change with depth contains some finely disseminated peat which would reduce the pH of the interstitial water.

Volcanic Fraction.—Volcanic material found in the sand-size fraction consists mainly of shards of volcanic glass and pieces of pumice. Shards are colorless and triangular, plate-like or irregular in shape and often have inclusions of oval-shaped bubbles. The refractive index is 1.512 ± 0.002. Glass of the same refractive index consists approximately of 67 percent silica and is derived from an andesitic magma according to George (1924).

Glass shards occur in almost all the samples in amounts varying from a trace to 25 percent of the light fraction. The highest concentration is found along the Sumatra margin of the strait between the Asahan River and Belawan, where percentages range from 10 to 25.

Volcanic glass is also quite common in many cores where its presence is clearly noted by the numerous layers of glass shards. These layers are very distinct owing to their light gray color in contrast to the darker surrounding material. Ash layers vary in thickness from 0.1 to 4 cm, but are usually less than 0.25 cm thick (fig. 16).

There appears to be a correlation of an ash layer, occurring at a depth of 30 cm below the sea floor, among three adjacent cores from the Central region of the strait. This may be a coincidence because it is not seen in nearby cores, and other ash layers cannot be traced from one core to another. A 4 cm-thick ash layer found in the bottom of core 103 probably represents a local deposit in a former topographic depression because it is not observed in adjacent cores less than 3.2 km away. Shards are also concentrated in irregular bands or pockets that are probably the result of burrowing organisms.

Light gray layers similar in appearance to the ash are observed in certain parts of the strait. These layers, however, are largely composed of clean quartz and glass shards of a single grain size (4 phi). Such is the case west of Singapore where, upon initial examination, the cores look much the same as those containing layers of shards, but on closer scrutiny clean quartz rather than volcanic glass is found to be the dominant constituent. Similar occurrences of such layers are found in a few cores from the Central region of the strait.

It is believed that the ash layers do not represent wind-borne tephra erupted from nearby volcanoes, but rather detrital deposits of ash

eroded from the neighboring land areas. Large ash concentrations off the Sumatra coast in the vicinity of rivers draining tuff deposits on Sumatra lends support to this conclusion. The numerous ash layers in relatively short intervals of the core section, 25 laminae in a 10 cm interval, may be more indicative of heavy runoff during the monsoons than volcanic eruptions. Reworking by currents may also account for the ash distribution.

Authigenic Constituents

Glauconite is found extensively throughout the strait occurring mainly as pellets of dark-green grains and to a lesser extent occupying the cavities of foraminiferal tests. Percentages of glauconite range from a trace to 80 percent of the light fraction with a mean of about 6 percent. The highest concentrations occur in the Central region along the Sumatra margin. Only traceable amounts are found in the coarser sediments between Malacca and Port Swettenham. No apparent correlation is observed between the occurrence of glauconite and grain size because of the way in which the pellets are deposited. Glauconite pellets become part of the sediment as the foraminiferal tests surrounding the pellets are broken. Most of the broken tests are winnowed away leaving the pellets behind. Excluding the narrow portion of the strait in the vicinity of Port Swettenham, there appears to be a general inverse relationship between the presence of foraminifera and glauconite as a result of the removal of the broken tests.

Pyrite occurs in the form of internal molds of foraminifera and radiolaria and is frequently found in the surface sediments. The possibility that reducing conditions may exist in the microenvironment within cavities of various tests and shells may be significant in explaining the origin of such authigenic minerals as pyrite and glauconite in an environment often oversaturated with oxygen. Emery (1960, p. 267) reported similar occurrences of pyrite off the coast of southern California. No indication of phosphorite or manganese oxide coating of gravel was observed in any of the samples.

PLEISTOCENE-RECENT HISTORY

The Malacca Strait is a part of the Sunda Shelf, which is one of the major continental shelf areas of the world. This shelf, unlike most others, is believed to have been a peneplain formed in the Late Tertiary or Early Pleistocene. The peneplain was further denuded during the Pleistocene, when sea level was lowered between 73 and 91 m (Dickerson, 1941, p. 30). The present Sunda Shelf was drowned and the Malacca Strait, as it is essentially found today, came into existence as a result of the postglacial eustatic rise of sea level. Molengraaff (1921, p. 100) suggests that no crustal movement was involved in the submergence. The rather uniform depth of the shelf, between 55 and 64 m, and the numerous drowned river valleys tend to support this hypothesis. Additional evidence from a study of Pleistocene geology on Sumatra and Java by Smit Sibinga (1952) lends further cre-

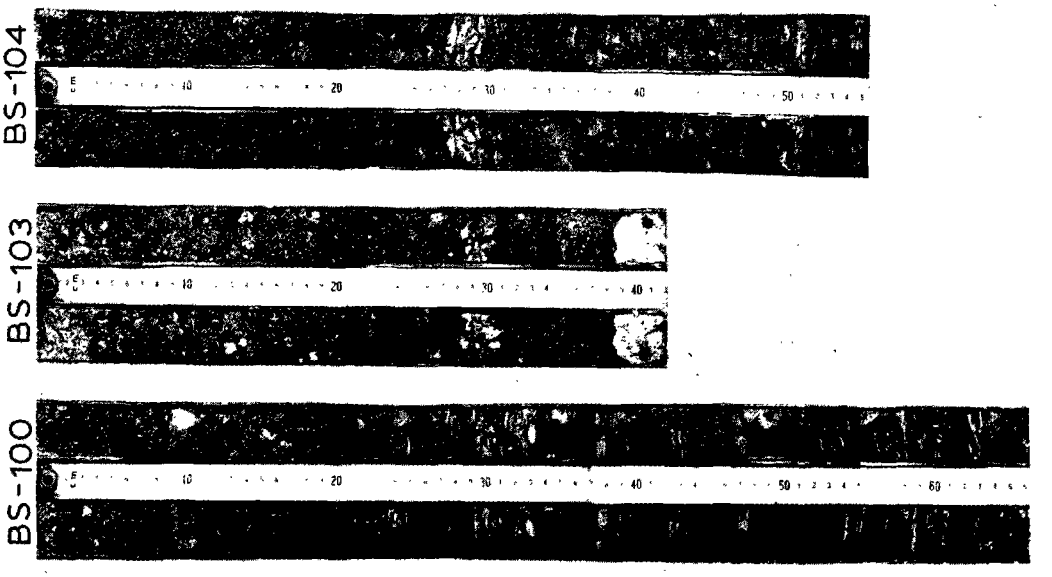


FIG. 16.—Volcanic ash layers in the cores from the Central region of the Malacca Strait.

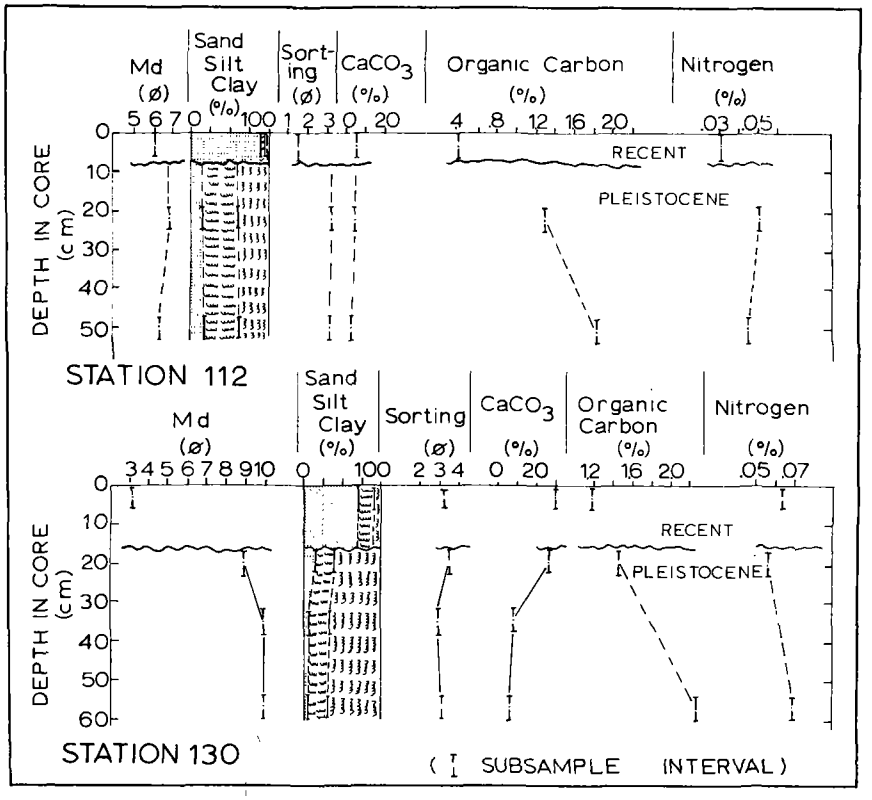


FIG. 17.—Vertical variation of textural and chemical properties in cores penetrating the Pleistocene sediments.

dence to the hypothesis. A carbon-14 date for peat found in a core approximately 24 km north of Port Swettenham at a depth of 26.5 m below sea level gave an age of 10,000 ± 200 years B. P. (U. S. Geological Survey No. W-1675). This date is on the curve established by Curray (1960) and Shepard (1960) for the rise of sea level since the Late Quaternary. It is evident that the Malacca Strait has remained stable during the last 10,000 years.

Evidence of the Pleistocene-Recent history is seen in many core samples as well as in the bathymetry of the strait. Numerous cores exhibit two distinct sediment layers: an upper layer of sand with shell debris and an underlying stratum of stiff, silty clay. The sand is characteristically dirty and composed of medium to fine sand-size particles of quartz, shell debris, glauconite and rock fragments. The underlying gray silty clay is relatively clean and contains only minor or traceable amounts of shell fragments, glauconite and rock fragments. Peat is usually disseminated throughout the silty clay both as fine particles and as large fragments of wood or plant roots. The lower 15 cm of core 185, from just north of Port Swettenham, was entirely composed of peat. In many cores the silty clay section is relatively stiff and appears to have become indurated before the overlying sand was deposited. The pronounced change in sedimentary characteristics across this contact is quite evident from figure 17.

These two types of sediment are indicative of two distinctly different environments of deposition. The silty clay with its abundant peat and few shell fragments is similar to that found in some tidal flat or estuarine areas today (Hantzschel, 1939, p. 197; Guilcher, 1963, p. 624; Van Straaten, 1963, p. 164). The overlying coarse sediments represent the present high energy environment of the strait. We believe that the stiff clay represents a Late Pleistocene tidal flat or estuarine deposit, which is in agreement with the Pleistocene paleogeography proposed by Molengraaff (1921) for this area. The stiffness of the clay indicates that it may have been partially indurated as a result of being subaerially exposed for some period prior to its submergence. This material was probably eroded during the period of exposure and the drainage pattern now ob-

served in the present bottom topography is a result of that erosion. As a result of the radiocarbon date mentioned earlier, from a peat sample taken 23.5 cm below the sand-clay contact, it seems feasible that the stiff, silty clay is of Late Pleistocene age.

The depth at which this Pleistocene surface occurs below the present strait floor differs considerably depending on the local rates of deposition in the strait. The surface is often found at depths of less than 20 cm in the axial portion of the strait, while between Langkawi and Penang Islands it occurs at a depth of 41 cm. Cores that do not display any indication of this surface may not have penetrated deep enough, or the surface may have been obliterated by burrowing organisms.

CONCLUSIONS

The sediments in the Malacca Strait are largely derived from the adjacent land provinces of Sumatra and the Malay Peninsula where the geologic condition varies considerably. Minor amounts of sediment are also transported into the strait from the islands south of Singapore.

Although the Malacca Strait is in a part of the world where monsoons strongly influence climatological and oceanographic conditions, little direct effect is observed because of the protection provided by the bordering land masses. The current circulation is mainly caused by the movement of water into the strait from the South China and Java Seas and to a lesser extent from the Andaman Sea. The depositional environment is primarily influenced by the currents and the numerous streams draining into the strait. Although rivers account for the movement of most sediment into the strait, as well as along its coastal margins in some sections, a northwest current provides the mode of transport for the sediments within the strait. Deposition of biogenic constituents, however, shows a greater dependence on the physical and chemical characteristics of the overlying water mass. This is evident from the similarity of the foraminifera distribution with that of a pronounced wedge of cool-temperature, high-salinity water extending into the strait from the Andaman Sea.

The depositional environment of the Malacca Strait can be divided into four regions based on the textural parameters of the surface sediments: Northern, Central, "Narrows" and Southern. Each region also shows a difference in oceanographic conditions as well as in the influence of streams on the environment. Sediment distribution in the Northern region is almost entirely controlled by currents; in the Southern region both currents and local streams are the controlling factors.

The significance of sediment color in the Malacca Strait is not as an indication of the conditions in the depositional environment, as is often reported in the literature (Emery, 1960, p. 234; Niino and Emery, 1961, p. 749), but rather as a property of the sediments entering the strait. Various streams are depositing sediments of different colors, which is clearly shown by the sediment color distribution in the strait.

Organic matter is generally concentrated in the vicinity of river mouths or in the deep Andaman Sea. High carbon to nitrogen ratios near debouching rivers are an indication of the greater abundance of high-carbon, terrestrial organic matter being deposited in these areas. Peat is believed to be the source of the organics. The lower ratios in the Andaman Sea sediments are attributed to the partly decomposed remains of marine plankton and benthos.

The mineralogy of sediments in the strait is complex because of the numerous streams draining the varied geology on the Malay Peninsula and Sumatra. Delineation of mineral suites is particularly difficult because of the interfingering of the sediments from these streams. Only along the western margin of the Northern and Central regions of the strait can any inference be made as to sediment provenance based on the mineral suites. The concentration of amphiboles, staurolite, tourmaline and biotite in these regions suggests a possible source in the metamorphics of the Barisan Range of Sumatra. Sumatra rather than the Malay Peninsula appears to be the predominant source area for the detrital sediments in the strait.

Kaolinite is the predominant clay mineral found in the strait, as would be expected in marine sediments derived from land masses in a tropical climate. Undifferentiated mixed-layer clay minerals are abundant in the deeper areas as the result of what appears to be the combining of montmorillonite with degraded illite and possibly chlorite. Most of the clay minerals are detrital although some of the illite may be a diagenic product of glauconite.

Slight increases in the percent of mixed-layer minerals and decreases in the illite content with depth are believed to be due to leaching of potassium ions from the illite in an inferred acidic environment. The degraded illite then combines with the montmorillonite to form the mixed-layer minerals.

Although volcanic glass is found throughout most of the strait no ash layers can be traced over any great distance. The layers are normally very thin (0.25 cm) and are repeated frequently in a cored interval. This evidence, together with an increase in ash concentration off some of the rivers, indicates that most of these sediments are

carried into the strait by streams draining tuff deposits rather than being wind-borne material from nearby volcanoes. The numerous layers in a short core interval may possibly reflect seasonal changes in runoff. The lack of eolian ash deposits is attributed to the strong water currents that do not allow the ash to settle into distinct layers as is found in some deep-sea sediments.

Authigenic minerals such as glauconite and pyrite are common constituents of the sediments in the strait. These minerals are all believed to have formed within the tests of foraminifera and radiolaria and do not, by their presence, suggest a reducing environment.

The Sunda Shelf, of which the Malacca Strait is a part, is believed by many investigators to represent a Tertiary-Quaternary peneplain drowned as a result of an eustatic rise of sea level at the close of the last glacial period. Cores examined during this study support this hypothesis and further indicate that the area now occupied by the strait was a tidal flat or estuarine environment prior to submergence.

ACKNOWLEDGEMENTS

We gratefully acknowledge the assistance of Mr. Richard Stewart and others of the Oceanographic Division of the U. S. Naval Oceanographic Office who collected much of the field data and performed many of the textural and chemical analyses. Thanks are also extended to Dr. Kelvin Rodolfo for carrying out the nitrogen analyses and to Dr. Meyer Rubin for the carbon-14 determination. Discussions with Dr. J. B. Alexander of the Malaysian Geological Survey proved most helpful during this investigation.

We acknowledge with appreciation the assistance of Professors A. V. Carozzi, R. E. Olson, M. F. Wahl and H. R. Wanless of the University of Illinois who critically read and made helpful suggestions to this manuscript

The U. S. Naval Oceanographic Office, the U. S. Coast and Geodetic Survey and the Institute for Oceanography of the Environmental Science Services Administration provided both the oceanographic vessels and funds for this study.

REFERENCES

ALEXANDER, J. B., 1959, Geology and palaeontology in Malaya: Nature, v. 183, p. 230–232.
ALLISON, L. E., 1935, Organic carbon by reduction of chromic acid: Soil Sci., v. 40, p. 311–320.
ANONYMOUS, 1957, Oceanographic station list, 1957: Marine Res. Indonesia, no. 4, p. 26–29.
ANONYMOUS, 1963, Observations Océanographique, Croiseur-Ecole d'Application "Jeanne d'Arc," Cahiers Océanographiques, XV Annee no. 9, p. 666–671.
BADER, R. G., 1954, Use of factors for converting carbon or nitrogen to total sedimentary organics: Science, v. 120, p. 709–910.
BAREN, F. A. VAN, AND KIEL, H., 1950, Contribution to the sedimentary petrology of the Sunda Shelf: Jour. Sedimentary Petrology, v. 20, p. 185–213.
BEMMELEN, R. W. VAN, 1949, The geology of Indonesia: Vol. IA, General geology of Indonesia and adjacent archipelagoes. The Hague, Gov't Printing Office, 732 p.
BRADLEY, W. F., 1953, Analysis of mixed-layer clay mineral structures: Analytical Chem., v. 25, no. 5, p. 727–730.
BRINDLEY, G. W., 1961, Chlorite minerals, *in* The X-ray Identification and Crystal Structures of Clay Minerals: Brown, G., ed., Mineralogical Society, London, p. 242–296.
BURST, J. F., 1958, Mineral heterogeneity in "glauconite" pellets: Am. Mineralogist, v. 43, p. 481–497.
CURRAY, J. R., 1960 Sediments and history of Holocene transgression continental shelf, northwest Gulf of Mexico, *in* Recent Sediments, Northwest Gulf of Mexico: Shepard, F. P., Phleger, F. B. and Andel, Tj. H. van, eds., Am. Assoc. Petroleum Geologists, Tulsa, Okla., p. 221–266.
DICKERSON, R. E., 1941, Molengraaff River: A drowned Pleistocene stream and other Asian evidences bearing upon the lowering of sea level during the ice age, *in* Shifting of Sea Floors and Coast Lines. University of Pennsylvania, Bicentennial Conference, University of Pennsylvania Press, Philadelphia, 30 p.
EMERY, K. O., 1960, The sea off Southern California: a modern habitat of petroleum. John Wiley & Sons, New York, 366 p.
EMERY, K. O., AND NIINO, H., 1963, Sediments of the Gulf of Thailand and adjacent continental shelf: Geol. Soc. America Bull., v. 74, p. 541–554.
FERRELL, R. E., 1965, Paleoenvironmental significance of clay minerals in the Shell Creek Shale, Muddy Sandstone, and Thermopolis Shale on the East Flank of the Bighorn Mountains, Wyoming, Unpub. M. S. Thesis, University of Illinois, 66 p.
FOLK R. L., AND WARD, W. C., 1957, Brazos River bar: a study in the significance of Grain size parameters: Jour. Sedimentary Petrology, v. 27, p. 3–26.
GEORGE, W. O., 1924, The relation of the physical properties of natural glasses to their chemical composition: Jour. Geology, v. 32, p. 353–372.
GODDARD, E. N., TRASK, P. D., DE FORD, R. K., ROVE, O. N., SINGEWALD, J. T., JR., AND OVERBECK, R. M., 1948, Rock-color chart: Washington, D. C., Nat. Research Council Comm. on Rock-color chart, 6 p. (distributed by The Geological Society of America).
GREAT BRITAIN HYDROGRAPHIC DEPARTMENT, 1958, Malacca Strait Pilot, 4th Ed. London, 491 p.
GRIFFIN, J. J., AND GOLDBERG, E. D., 1963, Clay mineral distributions in the Pacific Ocean, *in* The Sea: Ideas and Observations on Progress in the Seas. Hill, M. N. ed., v. 3, p. 728–741, Interscience Publishers, New York.

GRIM, R. E., AND JOHNS, W. D., 1954, Clay mineral investigation of sediments in the northern Gulf of Mexico, *in* Clays and Clay Minerals: Swineford, A., and Plummer, N. V. eds., Nat'l Res. Council Pub. 327, p. 81–103.

GUILCHER, A., 1963, Estuaries, deltas, shelf, slope, *in* The Sea: Ideas and Observations on Progress in the Seas: Hill, M. N. ed., v. 3., p. 620–654, Interscience Publishers, New York.

HANTZSCHEL, W., 1939, Tidal flat deposits (Wattenschlick), *in* Recent Marine Sediments: Trask, P. D. ed., Am. Assoc. Petroleum Geologists, Tulsa, Okla, p. 195–206.

HEEZEN, B. C., NESTEROFF, W. D., OBERLIN, A., AND SABATIER, G., 1965, Découverte d'attapulgite dans les sediments profonds du golfe d'Aden et de la mer Rouge: C. R. Acad. Sc. Paris, t. 260, p. 5819–5821.

HENWOOD, A., AND GAREY, R. M., 1955, A modified technique for the Kjeldahl procedure: Hengar Company, Phila., Pa., 4 p.

HUBERT, J. F., 1964, Textural evidence for deposition of many western North Atlantic deep-sea sands by ocean-bottom currents rather than turbidity currents: Jour. Geology, v. 72, p. 757–785.

INMAN, D. L., 1952, Measures for describing the size distribution of sediments: Jour. Sedimentary Petrology, v. 22, p. 125–145.

JOHNS, W. D., GRIM, R. E., AND BRADLEY, W. F., 1954, Quantitative estimations of clay minerals by diffraction methods: Jour. Sedimentary Petrology, v. 24, p. 242–251.

KAPLAN, I. R., AND RITTENBERG, S. C., 1963, Basin sedimentation and diagenesis, *in* The Sea: Ideas and Observations on Progress in the Seas: Hill, M. N. ed., v. 3, p. 583–619. Interscience Publishers, New York.

KREMPF, A., AND CHEVEY, P., 1934, The continental shelf of French Indo-China and the relationship which formerly existed between Indo-China and the East Indies: Proc. Fifth Pac. Scien. Congress, Canada 1933, v. 2, p. 849–852.

KRUMBEIN, W. C., AND PETTIJOHN, F. J., 1938, Manual of sedimentary petrography: Appleton-Century-Crofts, New York, 549 p.

KUENEN, PH. H., 1950, Marine Geology: John Wiley & Sons, New York, 568 p.

LANIZ, R. V., STEVENS, R. E., AND NORMON, M. B., 1964, Staining of plagioclase feldspar and other minerals with F. D. and C. Red. No. 2: U.S. Geol. Survey Prof. Paper 501-B, p. B152–B153.

MOLENGRAAFF, G. A. F., 1921, Modern deep-sea research in the East Indian Archipelago: The Geographical Jour., v. LVII, no. 2, p. 95–121.

NIINO, H., AND EMERY, K. O., 1961, Sediments of shallow portions of East China Sea and South China Sea: Geol. Soc. America Bull., v. 72, p. 731–762.

RICHARDS, A. F., AND KELLER, G. H., 1961, A plastic-barrel sediment corer: Deep-Sea Res., v. 8, p. 306–312.

ROYAL NETHERLANDS METEOROLOGICAL INSTITUTE, 1935, Oceanographic and meteorological observations in the China Seas and in the western part of the North Pacific Ocean: The Hague, Gov't Printing Office folio 115, 80 p.

SELVARAJAH, V., 1962, A study in the North Malacca Strait from salinity determinations: Indo-Pacific Fisheries Council, 9th Session Proceedings, Section II (1961), p. 1–6.

SHEPARD, F. P., 1960, Rise of sea level along northwest Gulf of Mexico, *in* Recent Sediments, Northwest Gulf of Mexico: Shepard, F. P., Phleger, F. B., and Andel, Tj. H. van, eds., Amer. Assoc. of Petroleum Geologists, Tulsa, Okla., p. 338–344.

SHEPARD, F. P., EMERY, K. O., AND GOULD, H. R., 1949, Distribution of sediments on East Asiatic continental shelf: Univ. of Southern Calif., Allan Hancock Found., Occasional paper 9, 64 p.

SMIT SIBINGA, G. L., 1952, Interference of glacial eustasy with crustal movements and rhythmic sedimentation in Java and Sumatra: Geol. en Mijnb., New series, v. 14, p. 220–226.

SOERIAATMADJA, R. E., 1956, Surface salinities in the Strait of Malacca: Marine Res. Indonesia, no. 2, p. 27–48.

STRAATEN, L. M. J. V. VAN, 1963, Aspects of the Holocene sedimentation in the Netherlands: Verhand. Kon. Ned. Geol. Mijnb. Gen., Geol. Ser., v. 21, p. 149–172.

SUMNER, F. B., LOUDERBACK, G. D., SCHMITT, W. L., AND JOHNSON, C. E., 1914, A report upon the physical conditions in San Francisco Bay, based upon the operations of the United States Fisheries Steamer "Albatross" 1912–1913: Univ. of California Publ. Zool., v. 14, p. 1–198.

TRASK, P. D., 1932, Origin and environment of source sediments of petroleum: Gulf Publ. Co., Houston, 323 p.

UMGROVE, J. H. F., 1949, Structural history of the East Indies: University Press, Cambridge, England, 63 p.

UNITED NATIONS ECONOMIC COMMISSION FOR ASIA AND THE FAR EAST, 1961, Geological map of Asia and the Far East: Calcutta, India, 6 sheets.

U. S. NAVY HYDROGRAPHIC OFFICE, 1944, Atlas of surface currents, Indian Ocean: Hydrographic Office Publication No. 566, Washington, 12 charts.

U. S. NAVY HYDROGRAPHIC OFFICE, 1945, Currents in the South China, Java, Celebes, and Sulu Seas: Hydrographic Office Publication No. 236, Washington, 14 p.

U. S. NAVY HYDROGRAPHIC OFFICE, 1951, Sailing directions for the Malacca Strait and Sumatra, 4th ed.: Hydrographic Office Publication No. 70, Washington, 485 p.

U. S. NAVY HYDROGRAPHIC OFFICE, 1955. Instruction manual for oceanographic observations: Hydrographic Office Publication No. 607, Washington, 210 p.

VEEN, J. VAN, 1936, Onderzoekingen in de Hoofden in verband met de gesteldheid der Nederlandsche kust: 'S Gravenhage-Alegemeene Landsdrukkerij, 252 p.

WEAVER, C. E., 1958, The effects and geological significance of potsasium "fixation" by expandable clay minerals derived from muscovite, biotite, chlorite, and volcanic materials: Am. Mineralogist, v. 43, p. 838–861.

WYRTKI, K., 1957, Precipitation, evaporation, and energy exchange on the surface of the southeast Asian waters: Marine Res. Indonesia, no. 3, p. 7–40.

——— 1961, Naga Report v. 2: The University of California, Scripps Institution of Oceanography, La Jolla, 195 p.

Reprinted from *J. geophys. Res.*, vol. 72, no. 10, 1967, p. 2547-2555

Structure of the Western Somali Basin[1]

ELIZABETH T. BUNCE,[2] M. G. LANGSETH,[3] R. L. CHASE,[2] AND M. EWING[3]

The western Somali Basin in the northwestern Indian Ocean is covered by thick deposits of terrigenous sediments. Seismic reflection profiles show, however, the northern and southern parts to be very different. The northern sections is a deep basin filled with thick uniformly stratified sediments. It is enclosed by the continental margin to the west and north, Chain ridge to the east, and shallow basement structure to the south. A change in depth of basement occurs along an approximately east–west line at latitude 3°30'N very near the southern end of Chain ridge. In the southern portion of the basin the basement is shallow, and, immediately south of latitude 3°30'N, it has high relief. Stratified flat-lying sediments fill the basement depressions, and isolated hills formed of basement material rise above the abyssal plain deposits. Farther to the south the abyssal plain becomes very narrow. Gabbro dredged from the southeast slope of Chain ridge has been dated by the potassium-argon method as 89.6 ± 4.5 m.y., which should be considered a minimum age. The evidence suggests that the entire sediment sequence of the northern basin was deposited subsequent to the formation of the ridge. The thin sediment cover of the southern portion of the basin is probably no older than Tertiary.

INTRODUCTION

The Somali Basin, in the northwestern Indian Ocean, is partially enclosed by the coast of Africa to the west and northwest and by the Carlsberg ridge to the east and northeast. Its southern boundary is taken as an east–west line through the Comores Islands and northern tip of Madagascar, the Seychelles bank, and the flanks of the mid-ocean ridge (Figure 1). The basin is divided into eastern and western parts. The western basin, which includes the Somali abyssal plain, is bounded to the east by Chain ridge and several less prominent structures, oriented approximately north northeast–south southwest, extending from the region of the Owen fracture zone [*Matthews*, 1963, 1966] to Madagascar.

During August 1963 the R.V. *Vema* of Lamont Geological Observatory made three crossings of the western Somali basin. In April 1964 the R.V. *Chain* of the Woods Hole Oceanographic Institution, participating in the International Indian Ocean Expedition, traversed the basin from the continental rise south of Socotra to the Seychelles bank. The pertinent tracks are shown in Figure 1. Parts of the traverse by *Chain* were planned to investigate in detail structures found during *Vema*'s crossings and the earlier British geophysical investigations conducted from H.M.S. *Owen* and R.R.S. *Discovery* [*Admiralty Marine Science Publications*, 1963, 1966; *Anonymous*, 1964].

Both *Vema* and *Chain* conducted continuous measurements of the gravity and magnetic field intensity and bathymetry. Continuous seismic reflection profiles were obtained over the entire track of *Vema* and over a major portion of *Chain*'s track. Cores and heat flow measurements were obtained by both vessels, and rock was dredged from the southeast slope of Chain ridge by *Chain*.

Gravity and magnetic measurements aboard *Vema* were obtained by a Graf sea gravimeter and a Lamont Geological Observatory proton precession magnetometer; aboard *Chain* a La-Coste-Romberg sea gravimeter and a Varian proton-precession magnetometer were used and the data computed by a shipboard IBM 1710 computer [*Bowin et al.*, 1965]. The continuous seismic profiler (CSP) [*Hersey*, 1963; *Bunce and Hersey*, 1966] aboard *Chain* was used throughout with the 100,000-joule sparker, operated at a repetition rate of 10 sec, as sound source and a towed Chesapeake hydrophone array as receiver.

[1] Woods Hole Oceanographic Institution Contribution 1855 and Lamont Geological Observatory Contribution 1037.

[2] Woods Hole Oceanographic Institution, Woods Hole, Massachusetts 02543.

[3] Lamont Geological Observatory, Columbia University, Palisades, New York 10964.

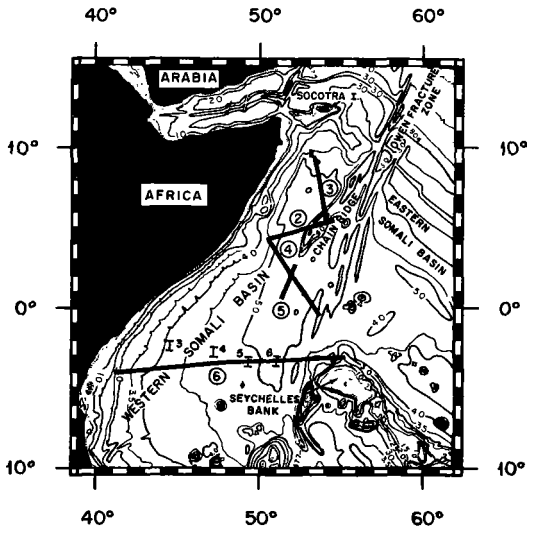


Fig. 1. Bathymetry of the Somali basin showing location of observations. Drafted on a portion of the bathymetric sketch accompanying the physiographic diagram of the Indian Ocean, published by the Geological Society of America. (Copyright 1964 by B. C. Heezen and M. Tharp. Reproduced by permission.) Contours in kilometers. Circled numbers refer to profiles of Figures 2–6, uncircled numbers, to refraction profiles reported by *Francis et al.* [1966].

The *Vema* profiles were obtained by the technique of seismic profiling described by *Ewing and Tirey* [1961]. One-half pound explosive charges detonated at 1-min intervals were used as source and a Lamont Geological Observatory EEL was towed as receiver.

This paper presents the geophysical data and proposes an interpretation of the structure of the western Somali basin based on these data.

Geophysical Results

Geophysical evidence presented here suggests a natural structural division of the western Somali basin into two sections, northern and southern. The northern section extends from the continental rise south of Socotra to near latitude 3°30′N. Two profiles cross this section. The southern section between latitude 3°30′N and the Comores Island chain is traversed by four profiles. The investigations reported here are limited to the basin north of 4°S.

Northern section. The *Vema* profile (Figure 2) crosses the abyssal plain from east to west, from Chain ridge to a small ridge east of the Somali continental slope. The *Chain* profile (Figure 3) starts in the north on the slope of a seamount near the base of the continental rise, angles southeast and east, then turns south to traverse the abyssal plain to Chain ridge.

The echo-sounding records show several continuous reflectors in the upper 20 meters of sea floor material. This shallow stratification is observed on the continental rise. It becomes clearly defined and can be traced continuously in the abyssal plain as well as southwest of Chain ridge. Both the number of layers and their clear definition diminish toward the southeast margin of the plain.

The significant features of the reflection profiles are the total thickness and the lateral uniformity of layering of the sediments covering the floor of the abyssal plain. The sediments are about 2 sec (two-way reflection travel time) thick near the continental rise at the northern margin of the plain and reach a maximum thickness of 2.2 sec near the foot of the small ridge on the western margin (Figure 2). It is possible to identify three zones of different reflective properties on this profile (Figure 2). The uppermost sequence, 0.65 to 0.75 sec thick, is strongly stratified. Although its thickness appears remarkably uniform across the basin, it does increase gradually to the east and north. Below this sequence is acoustically transparent sediment showing little or no stratification; i.e., there are few reflecting interfaces. The equivalent sequence on the profile of Figure 3 shows some stratification in this region. This difference may be more apparent than real, possibly caused by the difference in profiling methods and recording resolutions of the two systems [*Bunce and Hersey*, 1966].

In the profile of Figure 2 the transparent layer thickens toward the continent to the west. The thickening results from the abrupt deepening of the deepest reflector which dips down toward the ridge only partially crossed by the track. The upper portion of the acoustically transparent sequence is continuous with layers that slope upward on the ridge and thin toward its top. The sediment on the slope is less stratified than the upper zone of the basin but is more clearly stratified than the sequence forming the acoustically transparent layer. The material forming the ridge gives strong reverberant returns and shows no stratification.

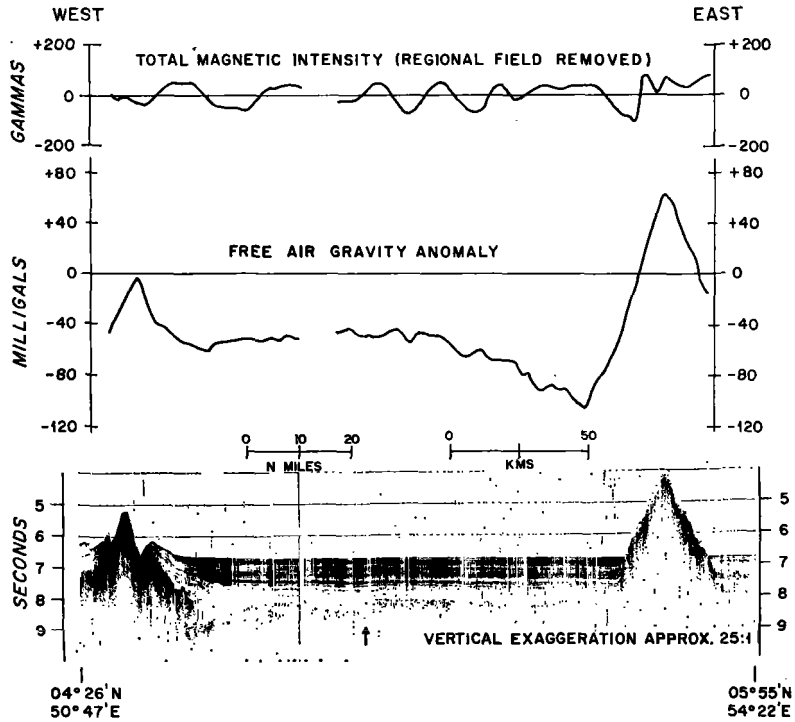


Fig. 2. Northern Somali basin. East–west crossing of *Vema*. Total magnetic intensity (regional variation removed), free-air gravity anomaly, and seismic reflection profile. The vertical scale of the reflection profiles of Figures 2–6 is expressed as seconds of two-way travel time. To convert this to meters knowledge of the compressional wave velocity of the layers is necessary. An approximate value for sea water is 1500 m/sec.

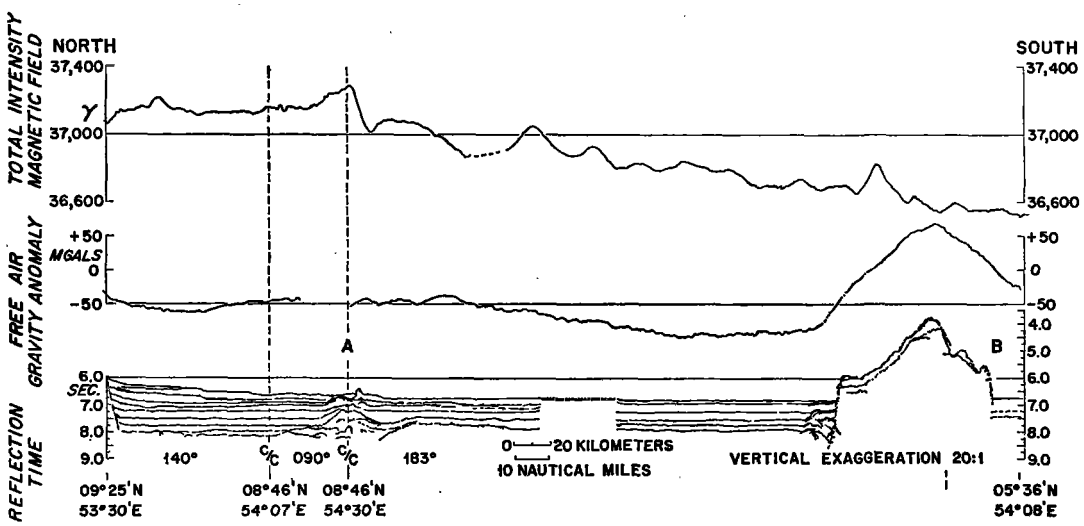


Fig. 3. Northern Somali basin. North–south traverse of *Chain*. Total magnetic intensity, free-air gravity anomaly, and seismic reflection profile. Ship heading and course changes shown, lower left. (Modified from *Bunce et al.* [1966, Figure 2].)

The profile of Figure 3 shows the sediments thickening gradually toward the north. At point A in the profile the flat-lying layers are disturbed near the foot of a partially buried hill.

To the east, the northern portion of the basin is bounded by the Chain ridge. The uppermost highly stratified sediments, 0.5 sec or approximately 500 meters thick, terminate abruptly against the ridge structure, whereas the deeper layers are disturbed and appear to turn up so as to conform with the ridge slope. This is more clearly seen in Figure 2. Because of the large vertical exaggeration of the figures, the steep appearance of this ridge on the reflection profiles is misleading, its average slope being slightly more than 5° on several crossings.

The magnetic profile along the essentially north–south track (Figure 3) shows undulations superposed on the regional trend. The east–west profile (Figure 2), from which the regional trend has been removed, is also undulating in character. These variations may be due to high relief or variation in directions of magnetization of the basement that underlies the thick sediments but is not observed on the seismic profiles. An anomaly of approximately 200 gammas is found on the crossing of Chain ridge, a lower value than might be expected for a volcanic feature at this latitude.

Rocks were dredged from the southeastern slope of the ridge near 5°36′N, 54°02′E, in the profiler depth interval between 4.75 and 6.5 sec, or 3200- and 4700-meter water depth (Figure 3, B). About twenty-five fragments of rock were hauled aboard, the largest of which weighed about 3 kg. The fragments comprised fresh gabbro, gabbro in various stages of alteration to clay minerals, and soft light-brown clay with numerous tubular pores, partially coated with manganiferous material. A potassium-argon radiogenic age of 89.6 ± 4.5 m.y. was determined from a pyroxene concentrate from the fresh gabbro by J. A. Miller and R. Grasty of the Department of Geodesy and Geophysics, Cambridge University (J. Cann, personal communication). A chemical analysis of the gabbro, which will be published at a later date, shows it to have the normative composition of an olivine tholeiite. Incipient alteration of the pyroxene and development of small amounts of nontronite seen in this section suggests that escape of argon may have taken place since initial crystallization. Thus the age of 89.6 ± 4.5 m.y. should be considered a minimum, and the gabbro is at youngest of Cretaceous age.

Southern section. Three reflection profiles traverse this area of the basin. One crosses from the ridge on the western margin southeast toward the Seychelles (Figure 4), the second runs south-southwest from Chain ridge (Figure 5), the third crosses the basin from the Seychelles bank to the coast of Kenya at Mombasa (Figure 6*a* and 6*b*). These profiles show that the structure differs markedly from that of the northern basin. The rough basement surface is buried beneath relatively thin sediment deposits. The vertical relief varies by 0.5 to 1 sec (1–2 km). The depressions in the basement topography have been filled by stratified sediment forming an abyssal plain in the central part of the basin through which some of the basement hills protrude. The sediment of the sea floor is finely stratified, as in the northern section, and is probably continuous with it.

The sediments near the slope of the small ridge on the western margin of the basin (Figure 4, right-hand side) are stratified but are neither flat lying nor always conformable with the basement structure. About 50 km from this ridge the basement is not detected, and the profile suggests that it may drop off rapidly. A negative free-air gravity anomaly of about 80 mgal associated with this small area and a two-dimensional Bouguer calculation [*Talwani et al.*, 1959] show that the basement probably lies no deeper than 2 km.

The eastern margin of the abyssal plain is clearly defined topographically by a small but abrupt upward change in bottom slope. The depth to basement decreases gradually east of this slope break, and the sediments thin to 0.25 sec or less.

Except for the anomaly already described, the gravity field is smooth along the profile, the free-air anomaly decreasing toward the southeast to a value of −20 mgal. The variation in magnetic intensity increases from northwest to southeast along the profile, perhaps corresponding to the rising basement. A 300-gamma anomaly is observed over the marginal structure east of the slope break.

The profile south of Chain ridge (Figure 5) crosses the track of Figure 4 near 1°50′N, 52°10′E. It shows the characteristically rough

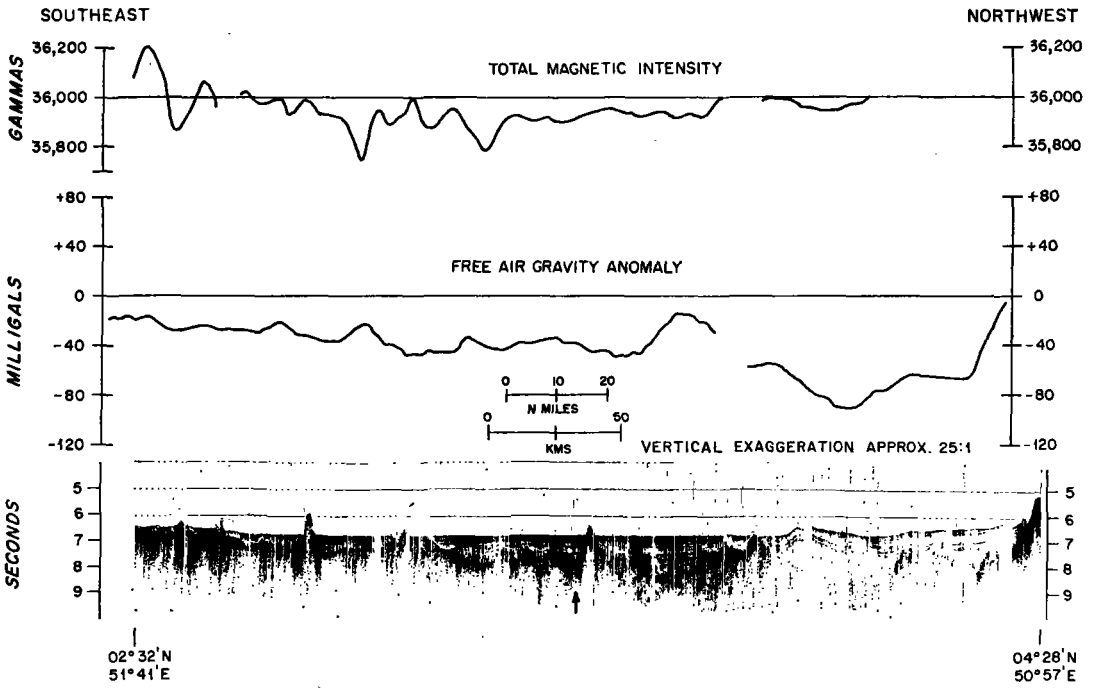


Fig. 4. Somali basin south of Chain ridge. Northeast–southwest crossing of *Vema*. Total magnetic intensity, free-air gravity anomaly, and seismic reflection profile. Arrow indicates intersection of profile 5 (*Chain*).

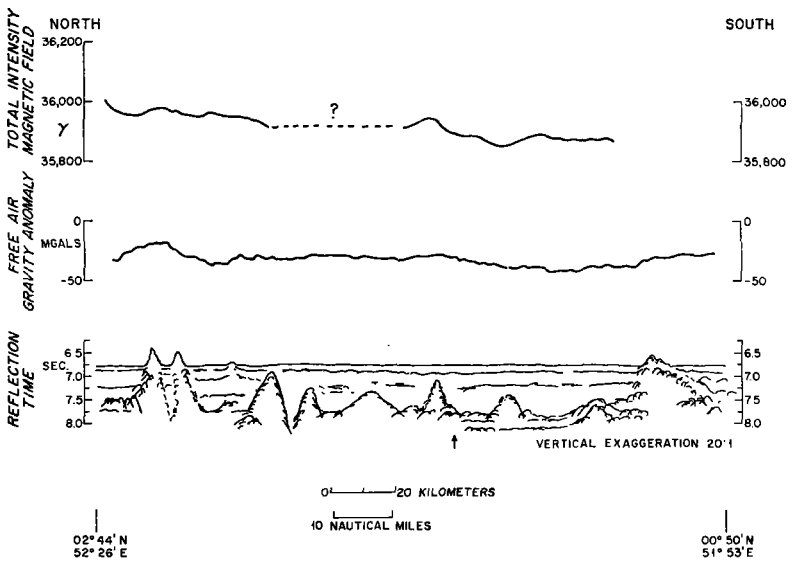


Fig. 5. Somali basin south of Chain ridge. Portion of north–south traverse of *Chain*. Total magnetic intensity, free-air gravity anomaly, and seismic reflection profile. Arrow indicates intersection of profile 4 (*Vema*).

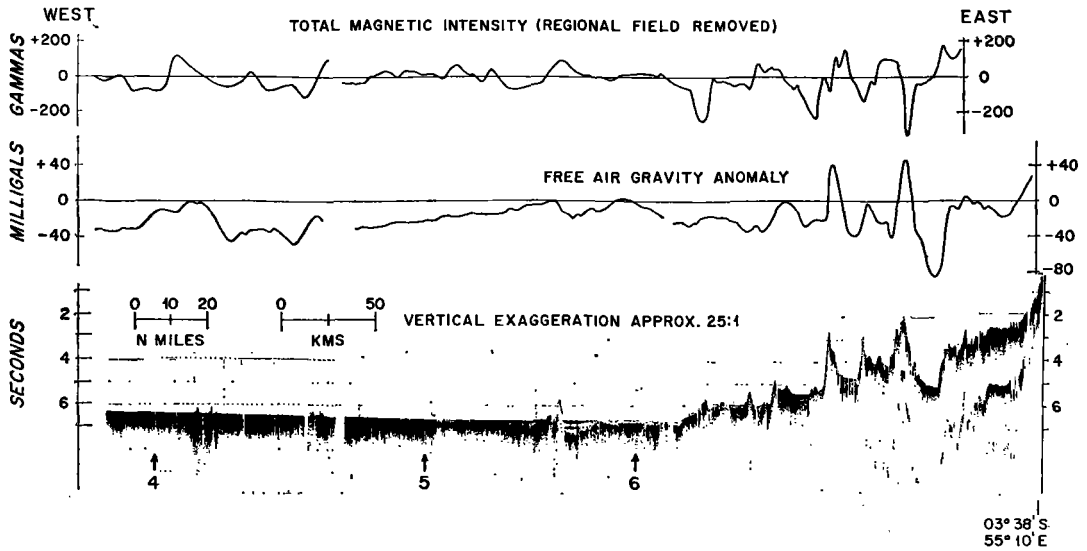


Fig. 6*a*. Somali basin, southern portion. Eastern part of *Vema's* crossing. Total magnetic intensity (regional field removed), free-air gravity anomaly, and seismic reflection profile. Numbers show projected positions of refraction profiles 4, 5, and 6 [*Francis et al.*, 1966].

basement structure of the southern basin, with little or no accompanying variation in the gravity and magnetic profiles.

The southernmost profile runs almost due west across the basin. The Seychelles bank (Figure 6*a*, right-hand side) slopes down steeply to a terrace about 50 km wide having a rough highly reflective surface almost devoid of sediment. The terrace terminates abruptly in a steep slope (12°), dropping into a 3650-meter

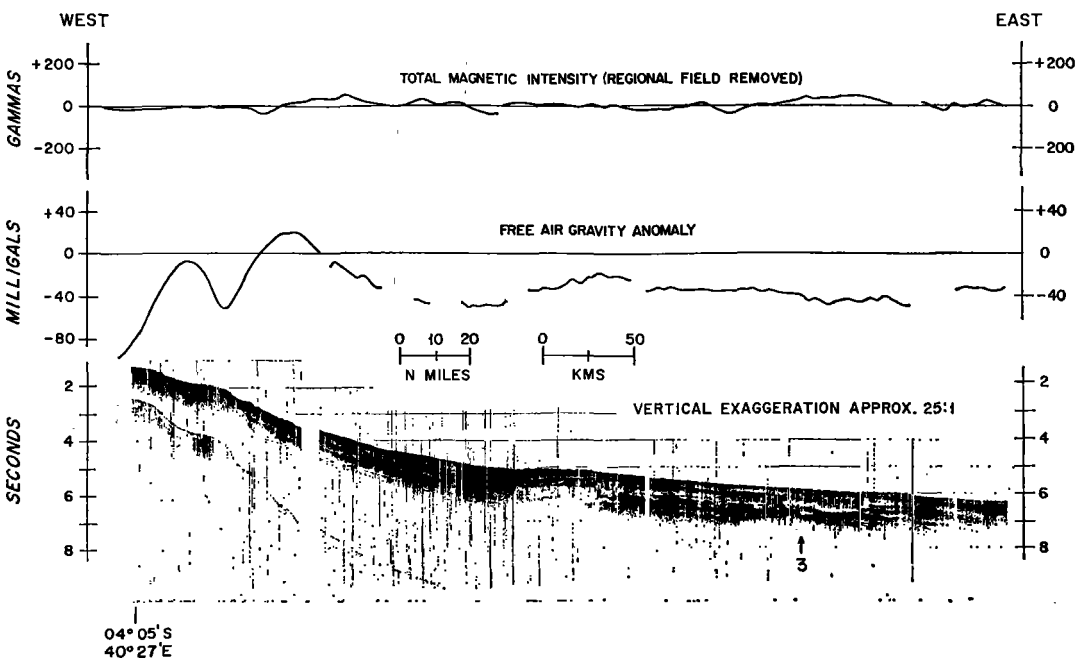


Fig. 6*b*. Somali basin, southern portion. Western part of *Vema's* crossing. Number shows projected position of refraction profile 3 [*Francis et al.*, 1966].

valley. Continuing west, a few small peaks border sediment-filled pockets whose surfaces form terraces that step down gradually to the basin. An abyssal plain about 140 km in extent lies in the floor of the basin. The sediment sequence of the abyssal plain is not well defined, except in a pocket on the eastern side of an isolated steep hill near 6 in Figure 6*a*. From a point near 5 (Figure 6*a*) the bottom rises gradually from the abyssal plain to the continental shelf on the western side of the basin. The sediments on this slope are thick and clearly stratified.

In the deep part of the basin (near 4, Figure 6*a*), the gravity and magnetic anomalies suggest a shallow rough basement structure. The presence of isolated hills piercing the sediment confirms that basement is nowhere very deep.

Seven seismic refraction profiles were made in the southwestern basin and reported by *Francis et al.* [1966]. Three are close enough to the reflection profile to make comparisons of the results for the sedimentary section. The relative accuracies of the positions, shown in Figures 1, 6*a*, and 6*b*, are of course subject to the errors inherent in comparing positions obtained by celestial fixes and dead reckoning. All the refraction profiles were oriented SSW–NNE, oblique to the line of the reflection profile, which crosses within 2 km of profile 6 on the eastern margin, lies about 8 km south of profile 5 and about 40 km south of profile 4.

The comparison has been made by computing vertical reflection times for the wave velocity and layer thickness data of the refraction profiles, and direct reading of the seismic-profiler reflection times.

Table 1 presents the results for refraction profiles, 4, 5, and 6. On profile 4, which lies near the foot of the continental rise, 700 meters of 1.79-km/sec material were measured. The reflection profile, about 40 km to the south, shows clearly stratified sediment in the upper 0.7 sec above a more acoustically transparent layer (not clearly shown on the reproduction of Figure 6*a*). The bottom of the stratified layer possibly corresponds to the top of the 2.5-km/sec layer. A deeper reflector at 1.3 sec is also observed on the original profiler records.

The uppermost sediment section indicated by the data of profile 5 and the reflection profile are comparable. The base of the thin (0.1 sec) transparent layer appears to be the top of a 2.5-km/sec layer. Below the transparent layer there are indistinct reflections, suggestive of stratified sediments, to a depth of 0.5 sec.

TABLE 1

Profile	V_L, km/sec	T_L, km	t_L, sec	t_p, sec
4	1.79 2.49	0.7	0.8	0.7
5	1.91 (2.5)	0.10	0.10	0.10
6	(1.8) 6.2	0.3	0.33	0.15 (average)

V_L, wave velocity in km/sec, refraction measurement [*Francis et al.* 1966, p. 243].

T_L, layer thickness in km, refraction measurement.

t_L, computed reflection time, using the relation $2T_L/V_L$.

t_p, measured reflection time from profiler record.

In the vicinity of refraction profile 6, the reflection record shows a relatively thin veneer of sediment (average thickness about 0.15 sec), in a region of gently rolling bottom topography and moderately rough basement surface. The refraction profile thickness of 300 meters (0.33 sec) is based on an assumed sedimentary velocity of 1.8 km/sec. This difference in sediment thickness is not surprising in view of the basement surface roughness and the averaging nature of the refraction process.

The location of refraction profile 3 (2°31′S, 44°56′E) is 110 km north of the reflection line. However, comparison of the two shows that the depth of the deepest observed reflector of the stratified sequence of the rise is comparable to that of the top of the 2.5-km/sec velocity layer as identified by *Francis et al.* [1966].

Discussion and Summary

The deep floor of the entire western Somali basin is covered by abyssal plain sedimentation. Seismic reflection results show, however, that the northern and southern parts are very different. An abrupt change in depth to basement occurs across a line at about latitude 3°30′N, which is very near the southern end of Chain ridge.

The abyssal plain is most extensive in the northern area. Small abyssal hills intrude the plain deposits in the central region, and the plain is narrow and appears to pinch out to the south.

The northern portion is characterized by a sedimentary sequence 2 km or more thick, ponded between the continental rise of Africa, Chain ridge, and shallow basement to the south.

The clearly defined stratification in the upper part of the sedimentary sequence is probably the result of deposition by a long series of turbidity flows, the reflectors being interfaces of coarse material at the base of each flow. The underlying acoustically transparent layer contains fewer turbidity flows and less clastic material. The sharp change in character from transparent to strongly stratified sediment possibly resulted from uplift of the East African watershed with a consequent increase in the influx of more clastic material. The deepest reflector, because of its relative flatness and occasional stratification, is interpreted as a deep sedimentary layer.

The abrupt deepening of the deepest reflector (Figure 2, arrow) appears to be a fault. If the fault exists it must be older than the overlying sediments, because it does not extend upward into them. The faulting and the formation of the ridge on the western margin of the basin may be contemporaneous. The reflection profile suggests that the ridge was formed during deposition of the stratified and transparent sediment layers. It appears to have formed slowly, lifting on its slopes some of the sedimentary layers originally deposited on a level sea floor.

In contrast, the upper 0.50 sec (500 meters) of sediments terminate abruptly against the western slope of Chain ridge, whereas the deeper layers have a slight upturn. This implies deposition of the upper sequence after the last uplift of the ridge. The gentle upturn of the deeper layers may be the result of a small uplift of the ridge subsequent to their deposition, or alternatively the upturn could have resulted from differential compaction of the sediment. Thus, it is possible that the entire sediment sequence seen on the profile of the basin postdates this ridge, and, if the date of 89.6 ± 4.5 m.y. determined for the dredged gabbro represents the age of Chain ridge, deposition of the sediment seen in the profiles started no earlier than the Cretaceous.

Matthews [1966, p. 176] suggests that Chain ridge is a continuation of the Owen fracture zone system; however, *Heezen and Tharp* [1964] interpret it as an isolated feature. The lack of change in sediment level on the two reflection profiles (Figures 2 and 3) that cross it suggests the ridge is not continuous with the Owen fracture zone. Profiles crossing the Owen fracture zone north of the Carlsberg ridge show that recent sediments are displaced along the fracture zone (J. Ewing, personal communication). In contrast, the profiles of Figures 2 and 3 show Chain ridge to be relatively a stable feature in late Tertiary and Quaternary times. It is obvious that the structural relation between the Chain ridge and Owen fracture zone is not clear and surveys farther north are required.

In the southwestern Somali basin, the continental rise and slope are covered with thick, well stratified sediments. *Francis et al.* [1966, p. 260] have correlated the results of two refraction profiles (2 and 3), on the rise west of longitude 45°E, with the geological column at Lamu on the Kenya coast. They suggest that the material having 2.5-km/sec velocity 'is possibly consolidated sediment of Jurassic and Cretaceous age, laid down perhaps when the water depth in these areas was not so great. The soft sediments (1.8 km/sec) probably started to form during the Tertiary.'

The reflection profiler results show stratified sediments to a depth of 1 km on the continental slope (Figure 6*b*). This section of sediment can be correlated with a layer having a velocity of 1.9 km/sec observed by *Francis et al.* [1966] The reflection profile shows that the sequence continues without significant thinning into the deep basin. In the vicinity of refraction profile 4 it is overlain by a wedge of flat-lying sediment. This means that the top of the 2.5-km/sec velocity layer lies deeper than the interpretation of the refraction profile suggests. The covering wedge of sediments is possibly more recent, Tertiary or later.

Acknowledgments. We wish to acknowledge the helpful cooperation of the officers and crews of R.V. *Vema,* Captain H. C. Kohler, and R.V. *Chain,* Captain C. A. Davis, and the assistance of the scientific members of both institutions who

participated in the cruises. Professors C. L. Drake and J. E. Nafe provided constructive criticism during the preparation of this manuscript.

This work has been supported at the Woods Hole Oceanographic Institution by the Office of Naval Research under contract Nonr-4029(00) and the National Science Foundation under research grants GP-2370 and GA-283; and at Lamont Geological Observatory by the Office of Naval Research under contract Nonr-266(48) and the National Science Foundation under research grants G-22260 and 5538.

References

Admiralty Marine Science Publication 4, Bathymetric, magnetic, and gravity investigations, H.M.S. *Owen,* 1961–1962, London, 1963.

Admiralty Marine Science Publication 9, Bathymetric, magnetic, and gravity investigations, H.M.S. Owen, 1962–1963, London, 1966.

Anonymous, International Indian Ocean Expedition, R.R.S. *Discovery* cruise 2 report, 1963, Dept. of Geophysics, Cambridge University, The Royal Society, London, 60 pp., 1964.

Bowin, C., R. Bernstein, R. Madigan, and E. Ungar, Improved shipboard geophysical data-processing system (abstract), *Geol. Soc. Am. Special Paper, 82,* 17, 1965.

Bunce, E. T., and J. B. Hersey, Continuous seismic profiles of the Outer ridge and Nares basin north of Puerto Rico, *Bull. Geol. Soc. Am., 77*(8), 803–812, 1966.

Bunce, E. T., C. O. Bowin, and R. L. Chase, Preliminary results of the 1964 cruise of R/V *Chain* to the Indian Ocean, *Phil. Trans. Roy. Soc., London, A, 259,* 218–226, 1966.

Ewing, J. I., and G. B. Tirey, Seismic profiler, *J. Geophys. Res., 66*(9), 2917–2927, 1961.

Francis, T. J. G., D. Davies, and M. N. Hill, Crustal structure between Kenya and the Seychelles, *Phil. Trans. Roy. Soc., London, A, 259,* 240–261, 1966.

Heezen, B. C., and M. Tharp, *Physiographic diagram of the Indian Ocean,* Geological Society of America, 1964.

Hersey, J. B., Continuous reflection profiling, *The Sea,* vol. 3, pp. 47–72, John Wiley & Sons (Interscience Publications), New York, 1963.

Matthews, D. H., A major fault scarp under the Arabian Sea displacing the Carlsberg ridge near Socotra, *Nature, 198,* 950–952, 1963.

Matthews, D. H., The Owen fracture zone and the northern end of the Carlsberg ridge, *Phil. Trans. Roy. Soc. London, A, 259,* 172–186, 1966.

Talwani, M., J. L. Worzel, and M. Landisman, Rapid gravity computations for two-dimensional bodies with application to the Mendocino submarine fracture zone, *J. Geophys. Res., 64*(1), 49–59, 1959.

(Received October 6, 1966.)

Reprinted from *Litologia i Poleznye Iskopaemye*, no. 3, 1967, p. 43-56

УДК 550.4 : 551.46.062.4 : 553.32 (97 : 267)

ХИМИЧЕСКИЙ СОСТАВ ЖЕЛЕЗО-МАРГАНЦОВЫХ КОНКРЕЦИЙ ИНДИЙСКОГО ОКЕАНА

А. Б. ИСАЕВА

Открытие железо-марганцовых конкреций в глубоководных осадках во время известного рейса «Челленджера» в 1873—1876 гг. положило начало серии исследований, посвященных химическому составу, генезису и закономерностям распределения этих своеобразных образований. За последние годы интерес к изучению железо-марганцовых конкреций сильно возрос не только в связи с тем, что процессы формирования конкреций помогают изучению диагенетических преобразований, происходящих в морских отложениях, но и потому, что в конкрециях накапливается большое количество рассеянных элементов, промышленную добычу и разработку которых можно считать вопросом не очень далекого будущего.

Работами ряда исследователей (Скорнякова, Андрущенко, Фомина, 1962; Arrhenius, Mero, Korkisch, 1964; Mero, 1960$_{1, 2}$, Willis, Ahrens, 1962, и др.) установлено, что химический состав железо-марганцовых конкреций не только во многом различен для разных водоемов, но также существенно меняется в пределах одного океана. Поэтому особенно важны новые данные, касающиеся химического состава конкреций из неизученных районов. Сейчас в литературе имеется довольно много сведений о составе конкреций Тихого океана, есть данные о конкрециях Атлантического океана и наименее всего изучены конкреции Индийского океана.

I. МАТЕРИАЛ И МЕТОДИКА ИЗУЧЕНИЯ

В настоящей работе приводятся данные о химическом составе железо-марганцовых конкреций и вмещающих их илов, собранных во время 35-го рейса э/с «Витязь» в 1962 г. и любезно предоставленных в распоряжение автора проф. П. Л. Безруковым. Сведения о распределении конкреции на дне Индийского океана приведены в работах П. Л. Безрукова (1962, 1963). Всего было проанализировано 11 проб конкреций с семи станций и четыре пробы вмещающих осадков. В основном анализировали наружный слой конкреций: в двух случаях наряду с наружным слоем химическому анализу подвергались ядра и в двух случаях анализировали среднюю пробу конкреций. Ниже приводится описание проанализированного материала.

Станция 5186 в области распространения красных глин 26°48′ ю. ш., 108°19′ в. д., гл. 5258 *м*. Орудие сбора — трал. Большое количество крупных шаровидных конкреций.

Пробы № 1 и 2. Большая трехслойная конкреция диаметром 85—90 *мм*. Наружный слой темно-коричневый, хрупкий, легко крошится, толщина около 5—8 *мм*. Вес наружного слоя 221 *г*.

Промежуточный слой светло-бурый, мягкий, легко крошится, толщина ~5 *мм*. Ядро того же цвета, что и промежуточный слой, но более плотное, твердое диаметром 55—60 *мм*. Вес ядра 206 *г*.

На анализ были взяты наружный слой (проба № 1) и ядро (проба № 2).

Станция 5193 в области распространения красных глин 32°48′ ю. ш., 103°55′ в. д., глубина 5300 *м*. Орудие сбора — трал. Большое количество «мозговидных» округлых конкреций.

Проба № 3. «Мозговидная» округлая двухслойная конкреция. Наружный слой черный, довольно твердый, толщина 10—17 *мм*. Ядро замещенное, темно-коричневое, твердое. Химическому анализу подвергнут наружный слой.

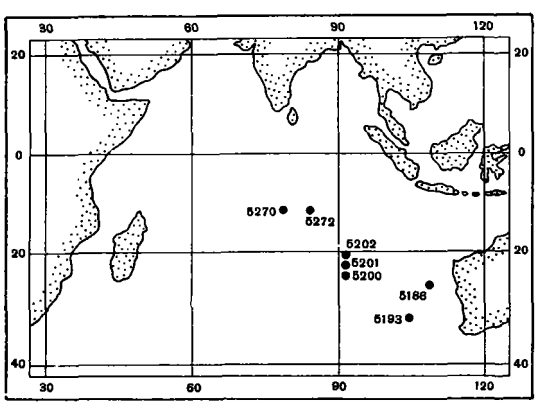
Результаты химического анализа железо-марганцовых конкреций

Лабораторный номер пробы	Станция	Характеристика пробы	SiO_2	B_2O	Fe_2O_3	TiO_2	Al_2O_3	CaO	MgO	MnO	O_2 активн.
1	5186	Конкреция, наружный слой	14,54	0,10	22,90	1,10	3,39	2,72	1,72	21,59	4,88
2	5186	Конкреция, ядро	39,79	0,04	16,82	0,79	5,20	1,92	1,48	12,38	2,73
3	5193	Конкреция, наружный слой	19,17	0,14	17,69	0,86	2,22	2,24	2,09	22,16	5,00
4	5200	Конкреция, средняя проба	16,71	0,18	17,02	1,45	3,10	2,84	1,94	22,58	5,03
12	5200	Конкреция, наружный слой	11,63	0,12	17,74	1,15	3,70	2,72	1,99	25,12	5,66
14	5200	Коричневый известковый ил	25,02	0,16	4,87	0,28	8,12	22,74	1,87	0,98	—
5	5201	Конкреция, наружный слой	13,21	0,14	17,42	1,04	3,14	2,74	2,02	24,88	5,60
6	5201	Плита, наружный слой	12,59	0,14	18,80	1,06	4,15	2,84	1,68	24,64	5,55
7	5202	Конкреция, наружный слой	9,32	0,13	16,91	1,06	3,44	2,78	2,20	28,52	6,33
10	5202	Коричневый карбонатный ил	29,37	0,16	4,86	0,43	8,87	18,48	1,86	1,15	—
13	5270	Конкреция, средняя проба	12,85	0,20	6,44	0,23	3,21	2,10	2,85	37,92	8,26
15	5270	Темно-коричневый глинистый радиоляриевый ил	54,54	0,29	3,50	0,42	7,82	0,59	2,08	0,50	—
8	5272	Конкреция, наружный слой	10,91	0,15	18,58	0,85	3,51	2,69	1,97	36,82	5,96
9	5272	Конкреция, ядро	17,85	0,16	17,20	0,84	4,49	2,78	1,77	22,27	5,00
11	5272	Светло-коричневый радиоляриевый ил	50,98	0,30	3,76	0,32	8,63	2,26	1,89	0,72	—

Станция 5200.23°55′ ю. ш., 91°40′ в. д., гл. 4560 *м*. Дночерпатель принес конкреции размером от 2 до 7,5 *см* в коричневом известковом иле. В связи с тем, что конкреции на этой станции заметно отличались одна от другой по внешнему виду, было проанализировано две конкреции.

Проба № 4. Двухслойная конкреция неправильной формы. Наружный слой темно-коричневый с бурым оттенком, с серыми прослоями, не очень твердый, легко крошится, толщина 15—17 *мм*. Ядро маленькое, диаметром 15—18 *мм*. На анализ взята средняя проба марганцового слоя.

Проба № 12. Округлая «мозговидная» двухслойная конкреция размером 40×45 *мм*, общий вес 61 *г*. Наружный слой черный, твердый, легко отделяется от ядра. Толщина слоя около 10 *мм*, вес 44 *г*. Ядро полностью замещенное, черное, очень плотное, с трудом раскалывается. Диаметр ядра около 20 *мм*, вес 17 *г*. В центре ядра светло-желтое образование диаметром 1—2 *мм*. На границе наружного слоя и ядра желтовато-бурый прослой окислов железа. Проанализирован наружный слой.



Фиг. 1. Карта станций, на которых были получены конкреции

Проба № 14. Коричневый известковый вмещающий ил, принесенный дночерпателем вместе с конкрециями.

Станция 5201 в области распространения красных глин. 22°25′ ю. ш., 91°39′ в. д., гл. 5280 *м*. Орудие сбора — трал. Большое количество округлых конкреций и плит.

Проба № 5. Двухслойная округлая конкреция. Наружный слой буро-черный, мягкий, крошится, легко отслаивается от ядра, толщина 5—10 *мм*. Ядро замещенное, очень твердое, тяжелое, коричневого цвета. Проанализирован наружный слой.

Проба № 6. Двухслойная плита. Наружный слой буро-черный, толщиной 8—10 *мм*, легко отслаивается, крошится. На границе с внутренним слоем плиты оранжевая пленка окислов железа, очень легко отслаивается от внутреннего слоя. Внутренний слой желтовато-коричневый, более мягкий, крошится, толщина 10—15 *мм*. На анализ взят наружный слой.

Станция 5202. 20°54′ ю. ш., 91°25′ в. д., гл. 4565 *м*. Дночерпатель принес небольшие конкреции и обломки пород в коричневом карбонатном иле.

Проба № 7. Двухслойные конкреции. Наружный слой черно-бурый, хрупкий, легко крошится, толщина 3—4 *мм*. Ядро светло-серое, с буроватым оттенком и бурыми про-

Таблица 1

и вмещающих илов Индийского океана, вес. %

NiO	CoO	CuO	V_2O_5	Cr_2O_3	MoO_3	WO_3	ZrO_2	P_2O_5	SO_3	CO_2	$C_{орг}$	П.п.п.
0,39	0,41	0,16	0,070	0,0016	0,043	0,016	0,060	0 67	0,46	0,61	0,07	27,90
0,28	0,13	0,15	0,058	0,0006	0,029	0,009	0,0 6	0,53	0,27	0,28	0,03	17,63
0,65	0,18	0,34	0,073	0,0004	0,048	0,009	0,060	0,58	0,38	0,34	0,06	26,16
0,56	0,28	0,22	0,069	0,0016	0,0 0	0,013	0,055	0,55	0,44	0,44	0,06	26,87
0,73	0,36	0,27	0,077	0,0002	0,048	0,010	0,065	0,65	0,49	0,63	0,04	29,38
0,037	0,016	0,028	0,012	0,0056	0,0004	0,0001	0,013	0,39	0,74	17,79	0,34	30,85
0,65	0,40	0,26	0,078	0,0002	0,068	0,013	0,057	0,57	0,47	0,49	0,06	28,14
0,57	0,35	0,23	0,080	0,0001	0,057	0,015	0,070	0,61	0,43	0,53	0,06	28,72
0,89	0,42	0,36	0,084	<0,0002	0,040	0,015	0,055	0,55	0,51	0,55	0,07	30,46
0,050	0,014	0,033	0,014	0,0055	0,0012	0,0016	0,013	0,37	0,55	14,16	0,24	28,22
1,80	0,060	1,71	0,061	0,0004	0,076	0,0033	0,018	0,27	0,17	0,32	0,06	23,45
0,020	0,008	0,024	0,008	0,0031	0,0004	0,0007	0,013	0,20	1,29	0,18	0,39	17,75
0,75	0,30	0,46	0,068	<0,0002	0,037	0,0079	0,062	0,46	0,39	0,54	0,06	29,58
0,47	0,35	0,31	0,069	0,0004	0,037	0,011	0,060	0,45	0,36	0,47	0,05	26,00
0,034	0,009	0,018	0,014	0,0040	0,0005	0,0012	0,013	0,27	0,94	0,97	0,35	17,08

растаниями, размером 20×25×30 *мм*. Анализировали наружный слой (средняя проба из двух конкреций).

Проба № 10. Коричневый карбонатный вмещающий ил.

Станция 5270. 12°00′ ю. ш., 79°08′ в. д., гл. 5495 *м*. Дночерпатель принес округлые конкреции в радиоляриевом иле.

Проба № 13. Округлая многослойная конкреция с губчатой поверхностью размером 30×35 *мм*, общий вес 22 *г*. Конкреция очень хрупкая, при расколе наблюдается чередование марганцовых и тонких глинистых слоев. Ядро замещенное. Была проанализирована средняя проба (наружный слой и ядро).

Проба № 15. Темно-коричневый глинистый радиоляриевый вмещающий ил.

Станция 5272. 11°55′ ю. ш., 84°10′ в. д., гл. 5253 *м*. Орудие сбора — дночерпатель, много конкреций в радиоляриевом иле.

Пробы № 8, 9. Продолговатая двухслойная конкреция овальной формы размером 80×40×45 *мм*. Наружный слой черно-бурый с металлическим блеском, легко отслаивается, крошится, толщина 4—6 *мм*. Вес 45 *г*. Ядро желто-оранжевое, твердое, по объему значительно больше наружного слоя, вес 60 *г*. На анализ взяты наружный слой (проба № 8) и ядро (проба № 9).

Проба № 11. Светло-коричневый радиоляриевый вмещающий ил.

Карта станций, на которых были получены конкреции, приведена на фиг. 1.

Для изучения состава конкреций и вмещающих илов были применены обычные химические методы, весовые, объемные и колориметрические, с помощью которых в исследуемых пробах определяли содержание кремнекислоты, бария, железа, титана, алюминия, кальция, магния, марганца, активного кислорода, меди, никеля, кобальта, ванадия, хрома, молибдена, вольфрама, серы, фосфора, циркония, карбонатов и органического углерода. Кроме того устанавливали потерю при прокаливании. Анализ проводили по следующей схеме: из так называемой главной навески определяли Si, Ba, Fe, Ti, Al, Ca и Mg. Все остальные определения проводили из отдельных навесок.

II. КОРРЕЛЯЦИОННЫЕ ОТНОШЕНИЯ ЭЛЕМЕНТОВ В КОНКРЕЦИЯХ

Результаты химических анализов конкреций и вмещающих илов сведены в табл. 1. Уже при беглом ознакомлении с таблицей заметно значительное накопление, помимо железа и марганца, еще никеля, кобальта, меди, ванадия, молибдена, вольфрама, циркония. Однако по степени концентрирования элементов конкреции Индийского океана отличаются от конкреций как Тихого, так и Атлантического океана. В табл. 2 приведены сравнительные данные среднего химического состава конкреций из трех океанов, причем данные по составу конкреций Индийского океана базируются на наших определениях и цифрах, опубликованных Дж. Меро (Mero, 1965). Как видно из табл. 2, по накоплению химических элементов конкреции Индийского океана занимают в известной степени промежуточное положение между конкрециями Тихого и Атлан-

тического океанов. Это становится особенно заметным при сравнении марганцовых модулей (отношения Mn : Fe) конкреций из разных океанов. В Атлантическом океане марганцовый модуль меньше единицы (0,93), а для конкреций Индийского и Тихого океанов равен соответственно 1,38 и 1,76, т. е. процесс накопления марганца по сравнению с накоплением железа, достигающий наибольшей интенсивности в осадках Тихого океана (Страхов, 1965), значительно развит и в Индийском

Таблица 2

Средний химический состав железо-марганцевых конкреций из Индийского, Тихого и Атлантического океанов, вес. %

Элемент	Индийский океан *				Тихий океан ** среднее	Атлантический океан *** среднее
	количество проб	максимальное	минимальное	среднее		
Mg	11	1,72	0,89	1,19	1,76	1,7
Al	16	5,60	1,17	2,43	3,27	3,1
Si	17	18,56	4,35	8,93	8,27	11,0
Ca	15	2,03	1,04	1,73	1,98	2,7
Ti	17	0,87	0,14	0,52	0,66	0,8
V	11	0,047	0,032	0,041	0,054	0,07
Mn	16	29,36	9,50	17,50	21,06	16,3
Fe	17	20,90	4,50	12,67	11,97	17,5
Co	17	0,32	0,05	0,22	0,31	0,31
Ni	17	1,41	0,13	0,58	0,67	0,42
Cu	17	1,81	0,11	0,40	0,43	0,20
Zr	11	0,052	0,013	0,041	0,063	0,054
Mo	16	0,054	0,008	0,029	0,04	0,032
Ba	15	0,50	0,04	0,19	0,32	0,17
Mn:Fe	—	—	—	1,38	1,76	0,93

* — по данным автора и J. Mero (1965, табл. 36).
** — *по данным Н. С. Скорняковой и П. Ф. Андрущенко (1964, табл. 1).*
*** — по данным J. Mero (1965, табл. 28).

океане. Такое промежуточное положение Индийского океана проявляется не только в составе конкреций, его можно в еще большей степени проследить и при сравнении илов (табл. 3); в Индийском океане концентрации большинства малых элементов в илах выше, чем в илах Атлантического и ниже, чем в осадках Тихого океана. Марганцовые модули в осадках Индийского и Тихого океанов практически равны (0,13 и 0,12).

Обращает на себя внимание низкая концентрация железа в осадках Индийского океана (см. табл. 3). Для сравнения химического состава осадков Индийского океана с осадками Тихого и Атлантического океанов нами была использована табл. 10 из работы Н. М. Страхова (1965), в которой приведены данные по содержанию железа и марганца в красных глинах Тихого океана, пересчитанные на бескремнево-бескарбонатное вещество (Скорнякова, 1964), исследованные же нами четыре пробы осадков Индийского океана и четыре пробы, взятые из работы S. K. El Wakeel и J. Y. Riley, (1961) среднее значение из которых и дано в табл. 3 настоящей работы, состояли в основном из известковых и радиоляриевых илов. Если содержание железа и марганца в этих восьми пробах пересчитать на бескарбонатный материал, то средние значения будут равны 4,77% Fe и 0,65% Mn, а марганцовый модуль составит 0,136.

В работе Виллиса и Аренса (Willis, Ahrens, 1962) приведена таблица, иллюстрирующая связи между отдельными элементами в конкрециях. Среди 19 исследованных авторами образцов имелись две конкреции с низким содержанием железа (0,38 и 1,8%), и в этих двух образцах концентрации ряда металлов были также очень низкими. Анализируя эту таблицу, авторы выделили три группы элементов в соответствии

с различиями между их средними концентрациями в обычных конкрециях и в конкрециях с низким содержанием железа.

В табл. 4, составленной по методу Виллиса и Аренса, сравниваются средние концентрации элементов во всех 11 пробах с содержаниями элементов в пробе № 13 с низким количеством железа. В исследованных Виллисом и Аренсом конкрециях вместе с понижением содержания железа (в 14 раз) уменьшаются концентрации кобальта (в 39 раз) меди, никеля и титана (в 8—11 раз), а концентрации ванадия и молибдена почти не меняются. В пробе № 13, анализированной нами, наблюдается иная картина. Одновременно с уменьшением количества железа (в 2,6 раза) падают концентрации кобальта, титана, вольфрама и циркония (в 3—4,5 раза), фосфора (в 2 раза), но при этом возрастает содержание никеля, меди (в 2,5—4 раза), марганца, молибдена и бария (в 1,5 раза). Концентрация ванадия меняется мало.

Таблица 3

Среднее содержание железа, марганца и малых элементов в осадках Тихого, Индийского и Атлантического океанов, вес. %

Элемент	Илы Атлантического океана *	Илы Индийского океана **	Илы Тихого океана *
Fe	5,74	3,54	5,65
Mn	0,40	0,45	0,67
Ti	0,51	0,27	0,46
V	0,014	0,016	0,013
Cr	0,0086	0,0036	0,0078
Co	0,0038	0,0100	0,0110
Ni	0,014	0,026	0,030
Cu	0,013	0,036	0,040
Mo	0,0009	0,0016	0,0046
Ba	0,07	0,19	0,40
Zr	0,013	0,012	0,016
Mn:Fe	0,07	0,13	0,12

* — по данным Н. М. Страхова (1965, табл. 10).

** — по данным автора и S. El Wakeel и J. Riley (1961), среднее из 8 проб.

Таким образом, в изученной нами конкреции можно выделить три группы элементов: группа, в которой концентрации элементов убывают вместе с железом — Co, Ti, W, Zr и P; группа, в которой концентрации элементов возрастают, сюда относятся Ni, Cu, Mn, Mo и Ba, и группа, представленная только V, количество которого почти не меняется.

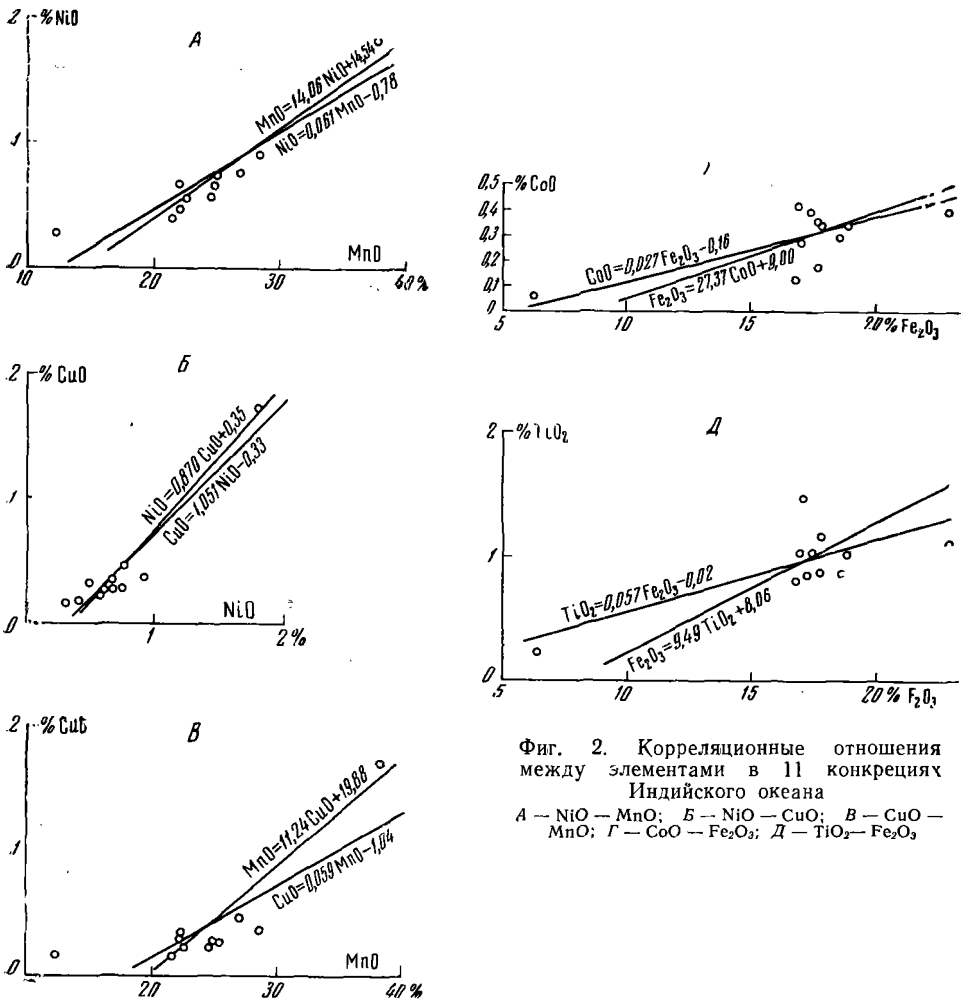
Разумеется, на основании одной пробы нельзя сделать однозначных выводов относительно того, какие из малых элементов сопутствуют при образовании конкреций железу и какие — марганцу. Однако в литературе приводятся такого рода данные. Так, Виллис и Аренс (1962) считают, что кобальт сопутствует железу, а магний и никель марганцу и подчеркивают очень тесную корреляцию, существующую между никелем и медью. Титан, по их мнению, не ассоциирует ни с марганцем, ни с железом. Е. Гольдберг (Goldberg, 1954) нашел, что железу сопутствуют титан, кобальт и цирконий, а марганцу — медь и никель в то время как алюминий и фосфор не зависят ни от Fe ни от Mn. Дж. Райли и П. Синхасени (Riley, Sinhaseni, 1958) обнаружили зависимость между железом и титаном — кобальтом и отрицают связь между железом и цирконием или марганцем и медью.

Таблица 4

Сравнение концентраций элементов в конкреции с низким содержанием железа со средними значениями для всех проб, %

Элемент	Средняя концентрация в 11 конкрециях (A)	Концентрация в 10 конкрециях с обычным содержанием железа		Концентрация в конкреции с низким содержанием железа (B)	A : B
		максимальное	минимальное		
Fe	11,92	—	11,76	4,50	2,6
Co	0,23	—	0,10	0,05	4,6
Ti	0,57	—	0,47	0,14	4,1
W	0,009	—	0,006	0,003	3,0
Zr	0,041	—	0,041	0,013	3,2
P	0,23	—	0,20	0,12	1,9
Mn	18,93	22,08	—	29,36	0,64
Ni	0,55	0,70	—	1,41	0,39
Cu	0,33	0,37	—	1,37	0,24
Mo	0,032	0,045	—	0,051	0,63
Ba	0,12	0,16	—	0,18	0,67
V	0,041		0,032	0,034	1,2

Е. Гольдберг и Г. Аррениус (Goldberg, Arrhenius, 1958) нашли отчетливую связь Mn с Ni, Co и Mo. О связи кобальта и никеля с марганцем говорит также Р. Дитц (Dietz, 1955). Н. С. Скорнякова и П. Ф. Андрущенко (1964) обнаружили, что распределение никеля, меди, молибдена и цинка в конкрециях по площади дна Тихого океана сходно с распределением марганца, а кобальта, свинца и титана — с железом.



Фиг. 2. Корреляционные отношения между элементами в 11 конкрециях Индийского океана

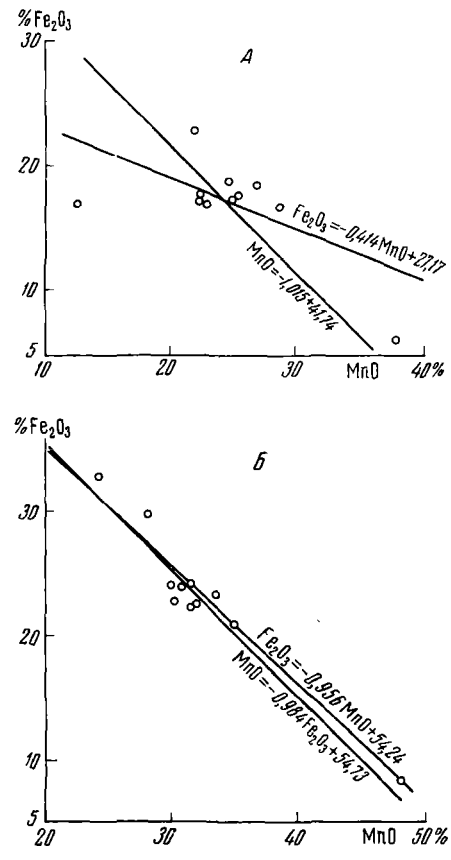
А — NiO — MnO; *Б* — NiO — CuO; *В* — CuO — MnO; *Г* — CoO — Fe_2O_3; *Д* — TiO_2 — Fe_2O_3

Ввиду таких разноречивых сведений было интересно проследить имеющиеся в конкрециях корреляционные связи между элементами на примере изученных нами 11 проб из Индийского океана. Для этого полученные данные были подвергнуты статистической обработке: для них были вычислены коэффициенты корреляции по методу, применяемому для малого числа наблюдений, а также составлены линейные корреляционные уравнения (Леонтьев, 1952), причем расчеты были сделаны как для всей пробы, так и в пересчете на осадок, из которого были исключены карбонаты и основные компоненты глинистых минералов (кремнекислоты, алюминий, карбонаты кальция и магния).

Судя по полученным коэффициентам корреляции (табл. 5), в изученных пробах существует явная связь между марганцем и медью, никелем, магнием (коэффициент корреляции $r=0,8—0,9$) и до известной степени молибденом ($r=0,7$), с одной стороны, и между железом и ко-

бальтом, цирконием, вольфрамом, фосфором ($r=0{,}8$—$0{,}9$) и отчасти титаном ($r=0{,}7$) — с другой. Между никелем и медью также наблюдается высокая степень корреляции ($r=0{,}956$). Между марганцем и кобальтом корреляция полностью отсутствует ($r=-0{,}08$).

Однако при пересчете на бескремнево-бескарбонатный материал коэффициент корреляции между кобальтом и марганцем увеличивается до 0,444 и становится равным коэффициенту корреляции между кобальтом и железом, который при пересчете на бескремнево-бескарбонатный материал снижается почти вдвое: с 0,853 до 0,440. Таким образом, помимо связи кобальта с железом существует некоторая зависимость и между кобальтом и марганцем. Будучи связанным в основном с железом, кобальт тем не менее проявляет и существенные различия в своем геохимическом поведении, в частности способность накапливаться в конкрециях с относительно низким содержанием железа (Мего, 1960[2]). Н. С. Скорнякова и П. Ф. Андрущенко (1964), Дж. Виллис и Л. Аренс (1962) также отмечали такого рода аномалии в поведении кобальта. Можно полагать, что эти отклонения объясняются способностью кобальта соосаждаться как с гидроокислами железа, так и с гидроокислами марганца.



Фиг. 3. Корреляционные отношения между железом и марганцем в 11 конкрециях Индийского океана

А — в расчете на всю пробу; *Б* — в расчете на бескремнево-бескарбонатный материал

На фиг. 2 графически показаны некоторые отношения между элементами в конкрециях. Пересекающиеся прямые построены на основании линейных корреляционных уравнений, приведенных в табл. 5. Угол между ними характеризует величину коэффициента корреляции, а точки дают разброс фактических данных. Графики показывают тесную связь, существующую между никелем и марганцем и никелем и медью (см. фиг. 2, *А* и *Б*). Несколько больший разброс точек наблюдается для отношения $CuO:MnO$ (см. фиг. 2, *В*), а для отношения $CoO:Fe_2O_3$ этот разброс довольно велик (см. фиг. 2, *Г*), хотя малый угол между прямыми свидетельствует о высокой степени корреляции, что подтверждает сказанное выше о специфическом поведении кобальта. То же самое можно отнести к титану (см. фиг. 2, *Д*), особое положение которого отмечали Виллис и Аренс (Willis, Ahrens, 1962). Большой интерес для выявления взаимосвязи между элементами представляют три конкреции: № 13 (ст. 5270, см. табл. 1) — с низким содержанием железа и высоким содержанием марганца; № 1 (ст. 5186) — с повышенной концентрацией железа и № 2 (ст. 5186) — с малым количеством марганца. Именно благодаря наличию таких экстремальных точек наиболее ясно проявляются корреляционные связи между элементами (фиг. 2 и 3), когда речь идет о сравнительно малом числе проб.

Таблица 5

Коэффициенты корреляции и линейные корреляционные уравнения, рассчитанные для 11 проб конкреций Индийского океана

Отношение окислов элементов	Коэффициент корреляции	Достоверность коэффициента корреляции	В пересчете на бескремнево-бескарбонатный материал		Линейные корреляционные уравнения	
					в расчете на весь материал	в пересчете на бескремнево-бескарбонатный материал
	r	S	r	S		
NiO:MnO	0,924	21,0	0,966	48,3	NiO=0,061MnO—0,78 MnO=14,06NiO+14,54	NiO=0,079MnO—2,54 MnO=11,86NiO + 21,30
MgO:MnO	0,895	14,9	—	—	MgO=0,055MnO + 0,62 MnO=14,49MgO—4,10	
CuO:MnO	0,812	7,6	0,920	20,0	CuO=0,059MnO—1,04 MnO=11,24CuO+19,88	CuO=0,085MnO—2,21 MnO=9,97CuO + 26,94
MoO_3:MnO	0,731	5,2	0,651	3,6	MoO_3=0,007MnO + 0,006 MnO=317,94MoO_3 + 9,34	
CoO:MnO	—0,075	—	0,444	—		
ZrO_2:Fe_2O_3	0,893	14,2	0,913	18,3	ZrO_2=0,0030Fe_2O_3 + 0,003 Fe_2O_3=263,79ZrO_2 + 2,28	ZrO_2=0,0031Fe_2O_3—0,64 Fe_2O_3=266,98ZrO_2 + 2,78
WO_3:Fe_2O_3	0,857	10,7	0,769	6,2		
P_2O_5:Fe_2O_3	0,841	9,5	0,929	22,6	P_2O_5=0,025Fe_2O_3 + 0,11 Fe_2O_3=28,46P_2O_5 + 1,83	P_2O_5=0,028Fe_2O_3 + 0,08 Fe_2O_3=31,09P_2O_5 + 0,65
CoO:Fe_2O_3	0,853	10,4	0,440	1,8	CoO=0,027Fe_2O_3—0,16 Fe_2O_3=27,37CoO + 9,00	
TiO_2:Fe_2O_3	0,734	5,3	0,728	5,1	TiO_2=0,057Fe_2O_3—0,02 Fe_2O_3=9,487TiO_2 + 8,06	TiO_2=0,050Fe_2O_3 + 0,11 Fe_2O_3=10,54TiO_2 + 9,66
NiO:CuO	0,956	36,8	0,959	40,0	NiO=0,870CuO + 0,35 CuO=1,051NiO—0,33	NiO=0,862CuO + 0,47 CuO=1,087NiO—0,47
MnO:Fe_2O_3	—0,648	3,7	—0,970	54,5	MnO=—1,015Fe_2O_3 + 41,74 Fe_2O_3=—0,414MnO + 27,17	MnO=—0,984Fe_2O_3 + 54,73 Fe_2O_3=—0,956MnO + 54,24

Известно, что для железо-марганцовых конкреций характерна обратная зависимость между концентрациями главных компонентов — железа и марганца. Для 11 образцов из Индийского океана эта зависимость тоже ярко выражена, особенно в расчете на бескремнево-бескарбонатное вещество (см. фиг. 3, *А* и *Б*). Н. С. Скорнякова и П. Ф. Андрущенко (1964) объясняют противоположную направленность процессов концентрации в конкрециях железа и марганца их различной геохимической подвижностью в процессе седиментации и диагенеза. Действительно, большая геохимическая подвижность марганца может способствовать образованию конкреций с высоким содержанием марганца особенно в центральных областях океана, но не объясняет формирования конкреций с низким марганцовым модулем. Объяснение этого процесса скорее следует искать в том, что, по Н. М. Страхову, в ходе рудогенеза происходит не дифференциация Fe и Mn, а их возрастающая интеграция, смешение при диагенетическом перераспределении рудных компонентов в тех соотношениях, в которых они находятся в осадке (Страхов, 1965, стр. 48).

III. НАКОПЛЕНИЕ ЭЛЕМЕНТОВ В КОНКРЕЦИЯХ ОТНОСИТЕЛЬНО ИХ СОДЕРЖАНИЙ ВО ВМЕЩАЮЩИХ ИЛАХ

Как было упомянуто выше, конкреции Индийского океана занимают второе место после конкреций Тихого океана по степени накопления в них рассеянных элементов. Для более точной оценки было полезно сравнить, какова степень концентрации рассеянных элементов в конкрециях из Индийского и Тихого океанов. В табл. 6 приводятся коэффициенты концентрации (обогащения) некоторых элементов в конкрециях по отношению к их средним содержаниям в земной коре и в красных глинах.

Таблица 6

Коэффициенты концентрации (обогащения) некоторых элементов для конкреций Индийского и Тихого океанов

Элемент	Средний химический состав, %				Коэффициент концентрации				А:Б
					Тихого океана (А) по сравнению		Индийского океана (Б) по сравнению		
	земной коры*	глубоководных глин**	конкреций Тихого океана***	конкреций Индийского океана****	с земной корой	с глубоководными глинами	с земной корой	с глубоководными глинами	
Mn	0,10	0,67	21,06	17,05	210	31,4	175	26,1	1,2
Ce	0,002	0,0074	0,31	0,22	155	41,9	110	29,8	1,4
Cu	0,01	0,025	0,43	0,40	43,0	17,2	40,0	16,0	1,1
Mo	0,001	0,0027	0,04	0,029	40,0	14,8	29,0	10,1	1,4
Ni	0,02	0,022	0,67	0,58	33,5	30,4	29,0	26,4	1,2
Fe	4,20	6,5	11,97	12,67	2,8	1,8	3,0	2,0	0,9
V	0,02	0,012	0,054	0,041	2,7	4,5	2,0	3,4	1,3
Zr	0,025	0,015	0,063	0,041	2,5	4,2	1,6	2,7	1,6
P	0,12	0,15	0,17	0,24	1,4	1,1	2,0	1,6	0,7
Ti	0,61	0,46	0,66	0,52	1,1	1,4	0,8	1,1	1,4

* — по данным F. M.Clarke (1924); ** — по данным K. K. Turekian и K. H. Wedepohl (1961); *** — по данным Н. С. Скорняковой и П. Ф. Андрущенко (1964); **** — из табл. 2, настоящая работа.

Выделяются четыре группы элементов. К первой группе относятся марганец и кобальт, которые накапливаются в конкрециях в 100—200 раз по отношению к кларку в земной коре и в 30—40 раз по отношению к глубоководным глинам. Во вторую группу входят медь, молибден и никель, коэффициенты концентрации которых составляют 30—40 для земной коры и 10—30 для глубоководных глин. Третья группа объ-

единяет железо, ванадий и цирконий, которые концентрируются в 2—4 раза по сравнению с кларком земной коры и с глубоководными глинами. В четвертую группу можно выделить фосфор и титан с очень мало изменяющимися концентрациями. Все эти элементы накапливаются в конкрециях Тихого океана больше в 1,1—1,6 раза по сравнению с конкрециями Индийского океана (среднее 1,3), за исключением железа и фосфора, концентрации которых в конкрециях Индийского океана выше, чем Тихого.

Интенсивность накопления элементов в конкрециях Индийского океана в общих чертах соответствует ряду геохимических подвижностей элементов в процессе формирования конкреций, приведенному в работе Н. С. Скорняковой и П. Ф. Андрущенко (1964):

$$Mn \rightarrow Co \rightarrow Ni \rightarrow Cu \rightarrow Pb \rightarrow Mo \rightarrow Sr \rightarrow V \rightarrow Zn \rightarrow Fe \rightarrow Ti \rightarrow La,$$

особенно при сопоставлении с красными глинами. В данном случае речь идет только о последовательности, в которой располагаются элементы по степени накопления их в конкрециях и о порядке величин коэффициентов концентрации. Дело в том, что в работах различных авторов приводятся иногда довольно значительно отличающиеся друг от друга данные по химическому составу природных объектов. Поэтому трудно сравнивать абсолютные величины коэффициентов концентрации, можно говорить лишь о порядках этих величин и, соответственно, о последовательности их расположения.

Однако все сказанное выше относится к средним содержаниям химических элементов в конкрециях и в осадках. Поскольку в настоящей работе для четырех проб конкреций были анализированы вмещающие осадки, представляло определенный интерес рассмотреть конкретные случаи перераспределения элементов в системе конкреция — осадок. В табл. 7 сопоставляется химический состав конкреций и вмещающих их илов, причем для станций 5200 и 5272, на которых было исследовано по две пробы, приводятся средние значения этих проб. Окислы элементов в таблице расположены в порядке убывания их коэффициентов концентрации.

При рассмотрении табл. 7 прежде всего бросаются в глаза очень высокие коэффициенты концентрации для молибдена. Если в приведенном выше ряду молибден стоит на шестом месте по степени его накопления, то в четырех пробах Индийского океана он занимает первое место, и коэффициенты его концентрации превышают коэффициенты концентрации марганца в 1,5—4,5 раза (максимальное значение 190,0; минимальное — 33,3). Далее порядок расположения элементов в точности соответствует ряду геохимических подвижностей элементом для Тихого океана. Коэффициенты концентрации марганца и кобальта составляют 20—35, никеля — 17, меди и вольфрама 8—11, ванадия, циркония, железа и титана 2,5—6, магния и фосфора 1—1,5; всеми остальными элементами (Ba, S, Al, Si, Ca, Cr) исследованные конкреции обеднены по сравнению с осадками.

Следует особо выделить конкрецию со станции 5270, о которой уже говорилось выше. Это конкреция с низким содержанием железа и большим количеством марганца. Ее марганцовый модуль равен 6,5, в то время как для остальных трех проб он составляет 1,5; 1,9 и 1,5. Помимо того что для нее характерны очень высокие коэффициенты концентрации молибдена, марганца, никеля и меди, абсолютные значения концентраций этих элементов также являются наибольшими из всех изученных проб (см. табл. 1) и этим максимальным содержанием Mo, Mn, Ni и Cu в конкрециях соответствуют минимальные количества их во вмещающих илах. Марганцовый модуль в осадке станции 5270 также ниже, чем в осадках остальных трех станций. Следовательно, при необычно

Таблица 7

Перераспределение элементов между конкрециями и вмещающими их осадками
(содержание, %)

Окислы элементов	Станция 5200			Станция 5202			Станция 5272			Станция 5270		
	конкреция	карбонатный ил	коэффициент концентрации	конкреция	карбонатный ил	коэффициент концентрации	конкреция	радиоляриевый ил	коэффициент концентрации	конкреция	радиоляриевый ил	коэффициент концентрации
MoO_3	0,044	0,0004	110,0	0,040	0,0012	33,3	0,037	0,0005	74,0	0,076	0,0004	190,0
MnO	23,85	0,98	24,3	28,52	1,15	24,8	24,54	0,72	34,1	37,92	0,50	75,8
CoO	0,32	0,016	20,0	0,42	0,014	30,0	0,32	0,009	35,6	0,060	0,008	7,5
NiO	0,64	0,037	17,3	0,89	0,050	17,8	0,61	0,034	17,9	1,80	0,020	90,0
CuO	0,25	0,028	8,9	0,36	0,033	10,9	0,38	0,038	10,0	1,71	0,024	71,2
WO_3	0,012	0,0004	30,0	0,015	0,0016	9,4	0,0095	0,0012	7,9	0,0033	0,0007	4,7
V_2O_5	0,073	0,012	6,1	0,084	0,014	6,0	0,068	0,014	4,8	0,061	0,008	7,6
ZrO_2	0,060	0,013	4,6	0,055	0,013	4,2	0,061	0,013	4,7	0,018	0,013	1,4
Fe_2O_3	17,39	4,87	3,6	16,91	4,86	3,5	17,90	3,76	4,8	6,44	3,50	1,8
TiO_2	1,30	0,28	4,6	1,06	0,43	2,5	0,85	0,32	2,6	0,23	0,42	0,5
P_2O_5	0,60	0,39	1,5	0,55	0,37	1,5	0,46	0,27	1,7	0,27	0,20	1,4
MgO	1,96	1,87	1,0	2,20	1,86	1,2	1,87	1,89	1,0	2,85	2,08	1,4
BaO	0,15	0,16	0,9	0,13	0,16	0,8	0,15	0,30	0,5	0,20	0,29	0,7
SO_3	0,46	0,74	0,6	0,51	0,55	0,9	0,38	0,94	0,4	0,17	1,29	0,1
Al_2O_3	3,40	8,12	0,4	3,44	8,37	0,4	4,00	8,63	0,5	3,21	7,82	0,4
CaO	2,78	22,74	0,1	2,78	18,48	0,2	2,74	2,26	1,2	2,10	0,59	3,6
SiO_2	14,20	25,02	0,6	9,32	29,37	0,3	14,38	50,98	0,3	12,85	54,54	0,2
Cr_2O_3	0,0004	0,0056	0,07	<0,0002	0,0055	0,04	0,0003	0,0040	0,08	0,0004	0,0031	0,1
Mn:Fe	1,5	0,22	—	1,9	0,26	—	1,5	0,21	—	6,5	0,16	—

большом накоплении молибдена, марганца, никеля и меди в конкреции вмещающий осадок заметно обедняется этими элементами.

Такого рода зависимость для марганца уже отмечалась прежде. J. Murray A. F. Renard (1891) считают, что конкреции стягивают почти весь марганец из илов, так как во вмещающих конкреции осадках количество марганца значительно ниже, чем в осадках темно-шоколадного цвета, не содержащих конкреции. Этого же мнения придерживается H. Pettersson (1942). При изучении подвижных форм железа и марганца в осадках Индийского океана (Исаева, 1963) было отмечено, что в поверхностном слое осадка, в котором было найдено большое количество конкреций, концентрация четырехвалентного марганца была меньше, чем в подстилающем этот слой осадке.

В настоящем случае это явление обеднения осадка наблюдается только для марганца и связанных с ним молибдена, никеля и меди. Так например, в конкреции со станции 5200 сильно сконцентрирован вольфрам (коэффициент концентрации 30,0), но его абсолютное содержание на этой станции (0,012% WO_3) не является максимальным для исследованных проб, наоборот, наибольшему его содержанию — 0,015% WO_3 (ст. 5202) соответствует и максимальное количество его во вмещающем осадке. Правда, эта максимальная концентрация W в конкреции не является необычно высокой, как в случае Ni, Mo и Cu, она лишь слегка повышена, в то время как концентрации никеля и меди в конкреции со станции 5270 отличается на порядок от содержания этих элементов в остальных пробах, а концентрация молибдена — в два раза.

Известно, что в формировании железо-марганцовых конкреций принимают участие вмещающие конкреции осадки. В процессе своего роста конкреции находятся в постоянном контакте с осадком, и частицы осадка включаются в физическую структуру конкреций. Иногда можно проследить очень тонкие прослои осадка, заключенные между слоями конкреции. Наличие или отсутствие таких прослоев, а также толщина слоев окислов марганца и железа в конкрециях, по мнению Дж. Меро (Мего, 1965), является показателем изменения скорости образования конкреций и вмещающих осадков. Изменение коэффициентов корреляции некоторых элементов при пересчете на материал, из которого исключены карбонаты и основные компоненты глинистых минералов (см. табл. 5), условно можно считать показателями того, в какой мере накопление данного элемента в конкреции обязано непосредственно включенному в конкрецию осадку.

Решению проблемы количественного участия осадков в образовании конкреций могли бы, возможно, до некоторой степени помочь корреляционные уравнения. Например, S. El. Wakeel и J. Riley (1961) приводят для пелагических осадков следующую линейную зависимость между содержанием титана и общим содержанием железа: $TiO_2 = 0{,}1046\ Fe_2O_3 - 0{,}02$. Из табл. 5 эта же зависимость для конкреций выражается уравнением: $TiO_2 = 0{,}057\ Fe_2O_3 - 0{,}02$. Любое уравнение такого типа можно представить в общем виде, как $y = ax + b$. В данном случае свободные члены обоих уравнений b равны, а коэффициент a для конкреций вдвое больше, чем для илов. Если в оба уравнения подставить, допустим, 10% Fe_2O_3, то значение для титана в осадке будет составлять 1,026%, а в конкрециях 0,55% TiO_2, т. е. на каждую единицу железа при миграции осадок — конкреция будет приходиться почти вдвое меньшее количество титана, точнее, 1,9: иными словами, железо мигрирует вдвое быстрее титана. Эти выкладки можно проверить другим путем. Средние значения для четырех проб конкреций (см. табл. 7) составляют: 14,66% Fe_2O_3 и 0,86% TiO_2. Их отношение, т. е. коэффициент концентрации железа относительно титана, равно 17,0. Для четырех проб вмещающих илов средние значения составляют 3,75% Fe_2O_3 и 0,36 TiO_2 и коэффициент кон-

центрации железа относительно титана равен 10,4. Отношение коэффициента концентрации в конкрециях к коэффициенту концентрации в осадке равно 17,0 : 10,4 = 1,7, т. е. число, довольно близкое к полученному из корреляционных уравнений значению 1,9. Отсутствие полного совпадения, возможно, обусловлено малым количеством проб вмещающих илов. По этой же причине не удалось вычислить коэффициенты корреляции и линейные корреляционные уравнения для осадков.

В заключение следует коротко остановиться на изменении концентраций химических элементов внутри конкреций. Виллис и Аренс (1962) анализировали четыре слоя одной конкреции Индийского океана и нашли, что количество марганца, магния, никеля и меди возрастает по направлению от ядра к наружному слою, содержание железа и кобальта убывает в том же направлении, а концентрации молибдена, ванадия и титана почти не меняются во всей толще конкреции.

Нами были исследованы в двух пробах конкреций (станции 5186 и 5272) ядро и наружный слой (см. табл. 1). Как видно из этой таблицы, в обеих конкрециях в наружном слое по сравнению с ядром возрастают количества марганца, никеля, меди, магния, железа и серы и убывают концентрации алюминия и кремния. Поведение остальных элементов неодинаково в двух конкрециях: содержание Mo, Ti, Co, W, P, Zr, Ca, V, Cr и Ba увеличивается в наружном слое конкреции со станции 5186 и остается неизменным или уменьшается в наружном слое конкреции со станции 5272.

Причину этого явления, по-видимому, следует искать в разнице концентраций марганца и железа в наружном слое и ядре конкреций. В конкреции со станции 5186 эта разница весьма значительна: 9,21% MnO и 6,08 Fe_2O_3. Количества марганца и железа в наружном слое и ядре конкреции со станции 5272 отличаются гораздо меньше, разница составляет 4,55 MnO и 1,38% Fe_2O_3. Поэтому элементы, связанные корреляционными отношениями с марганцем и железом, накапливаются в большей степени в наружном слое конкреции со станции 5186, а в наружном слое конкреции со станции 5272 их накопление несколько отстает от накопления железа и марганца. Исключение представляют никель и медь, которые больше концентрируются в наружном слое конкреции со станции 5272. Возможно, это связано с составом вмещающих осадков, но, к сожалению, пробы конкреций на станции 5186 были получены при помощи трала, т. е. без вмещающих осадков.

Для получения более полных данных дальнейшее изучение конкреций должно включать исследование химического состава вмещающих конкреции осадков.

ЛИТЕРАТУРА

Безруков П. Л. Распределение железо-марганцовых конкреций на дне Индийского океана.— Океанология, т. 2, вып. 6, 1962.

Безруков П. Л. Исследования Индийского океана в 35 рейсе э/с «Витязь».— Океанология, т. 3, вып. 3, 1963.

Исаева А. Б. Геохимические исследования осадков северной части Индийского океана.— Тр. Ин-та океанологии, т. 64, 1963.

Леонтьев Н. Л. Статистическая обработка результатов наблюдений. Гослесбумиздат, 1952.

Скорнякова Н. С. Рассеянные железо и марганец в осадках Тихого океана.— Литология и полезн. ископаемые, № 5, 1964.

Скорнякова Н. С., Андрущенко П. Ф., Фомина Л. С. Химический состав железо-марганцовых конкреций Тихого океана.— Океанология, т. 2, вып. 2, 1962.

Скорнякова Н. С., Андрущенко П. Ф. Железо-марганцовые конкреции Тихого океана.— Литология и полезн. ископаемые, № 5, 1964.

Страхов Н. М. Типы накопления марганца в современных водоемах и их значение для познания марганцоворудного процесса.— Литология и полезн. ископаемые, № 4, 1965.

Arrhenius G., Mero J., Korkisch J. Origin of oceanic manganese minerals. Science, 144, N 3615, 1964.

Clarke F. M. The date of geochemistry, 5 th ed. U. S. Geol. Surv., Bull. N 770, 1924.
Dietz R. S. Manganese deposits on the northeast Pacific Sea floor. Calif. J. Mines Geol. v. 51, N 3, 1955.
El Wakeel S. K., Riley J. P. Chemical and mineralogical studies of deep-sea sediments.— Geochim. et Cosmochim. Acta, v. 25, N 2, 1961.
Coldberg E. D. Marine geochemistry, 1. Chemical scavengers of the sea. J. Geol., v. 62, N 3, 1954.
Goldberg E. D., Arrhenius G. O. S. Chemistry of Pacific pelagic sediments. Geochim. et Cosmochim. Acta, v. 13, N 2/3, 1958.
Mero J. L. Minerals on the ocean floor.— Sci. Amer., 203, N 6, 1960_1.
Mero J. L. Mineral resources on the ocean floor. Mining Congr. J., v. 46, N 10, 1960_2.
Mero J. L. The mineral resources of the sea. Elsevier publishing Compahy. Amsterdam — London — New-York, 1965.
Murray J., Renard A. Report on deep-sea deposits. In: C. Wyville Thompson (Ed). Report on the Scientific results of the voyage of H. M. S. «Challenger». Eyre and Spottiswoode, London, 5, 1891.
Pettersson H. Manganese nodules and the chronology of the ocean floor. Göteborgs Kungl. Vetens-kapsoch vitterhets-samhälles Handlingar.— Sjätte följden. Ser. B., v. 2, N 8, 1942.
Riley J. P., Sinhaseni Prapas. Chemical composition of three manganese nodules from the Pacific ocean. J. Marine Res.,v.17, 466—482, 1958.
Turekian K. K., Wedepohl K. H. Distribution of the elements in some major units of the earth's crust.— Bull. Geol. Soc. America, v. 72, N 2, 1961.
Willis J. P., Ahrens L. H. Some investigations on the composition of manganese nodules, with particular reference to certain trace elements. Geochim. et Cosmochim. Acta, v. 26, 751—764, 1962.

Институт океанологии АН СССР
Москва

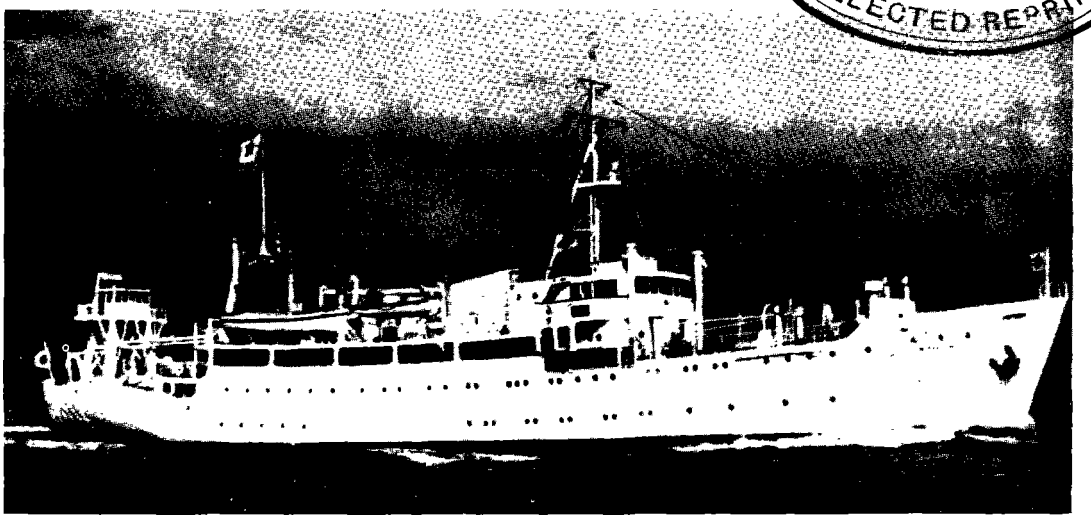
Дата поступления
8.VII.1966

Part V

Cruise and general reports

Reprinted from *Aust. natur. Hist.*, vol. XIV, no. 10, 1964, p. 323-325

C.S.I.R.O. DIV. FISHERIES & OCEANOGRAPHY AUST. 544 COLLECTED REPRINT



The *Umitaka Maru*, one of the many ships built in Japan for research in fisheries and oceanography. Together with the *Koyo Maru*, *Oshoro Maru* and *Kagoshima Maru*, this fine ship has been exploring the eastern Indian Ocean as part of the International Indian Ocean Expedition. [Photo: *Umitaka Maru*.]

THE INTERNATIONAL INDIAN OCEAN EXPEDITION

By D. J. TRANTER
C.S.I.R.O., Division of Fisheries and Oceanography

AT the present moment, the research ships of many nations are exploring the Indian Ocean. This activity has been going on since 1959 and will continue till 1965. Previous to this, research expeditions to the Indian Ocean were few and far between. Less was known about this expanse of water than any other, not excluding the Antarctic. This is no longer the case, and the credit is due to the active encouragement of international bodies, particularly the Scientific Committee for Oceanic Research (SCOR). In fact it was this body of scientists which put forward in 1957 the proposal for an International Indian Ocean Expedition. Since then, UNESCO has become a co-sponsor and the administrative co-ordination is handled by the Intergovernmental Oceanographic Commission.

It is a tribute to the responsibility of science that the stimulus to initiate this work lay not only in the scientific merit of such a programme, but also in its economic and humanitarian implications. Around the shores of the Indian Ocean are distributed some of the most densely populated and under-nourished nations in the world. There is no doubt that these will come to depend more and more on the

protein resources of the open ocean, just as Japan does today. The location of these resources, and the mechanisms by which they are formed, are now becoming apparent as the International Indian Ocean Expedition gathers momentum.

The term "Expedition" is somewhat of a misnomer, since there have already been many expeditions, and more are to follow. Early cruises were carried out by the Soviet Union, France, Australia and U.S.A., and later ones by Japan and Britain. Other cruises were made by South Africa, Pakistan, India and Indonesia.

As well as pursuing a policy of helpful encouragement, SCOR and UNESCO are making other contributions to this programme. Scholars from countries bordering the Indian Ocean are offered studentships at oceanographic laboratories throughout the world, and arrangements are made for them to participate in cruises. These are the people who will form the nucleus of oceanographic effort in this area in the years to come, and who will build upon the store of knowledge amassed during the expedition.

Unique Institution

Oceanography is a science which has developed its own methods and equipment. This is in many respects a healthy characteristic, but it has the disadvantage that where standard gear is not available a multiplicity of equivalents comes into use and it becomes difficult to compare the results obtained by different ships, even though they may be observing the same phenomena. Thus there is a pressing need to intercalibrate the observational methods. With the assistance of SCOR-UNESCO, it has been possible to gather together at Hawaii in 1961 and at Perth in 1962 the scientists and equipment from many participating countries, and to carry out a series of intercalibrations.

Out of the recognition for this need has arisen a unique institution, the Indian Ocean Biological Centre in Cochin, India. The IOBC is located within the precincts of the Oceanographic Laboratory of the University of Kerala, and is staffed and maintained by India's CSIR in co-operation with UNESCO. Its purpose is to act as a receiving centre for zooplankton samples taken with the Indian Ocean Standard net by the ships of the expedition. In charge of the international collections is a curator appointed by UNESCO, the first appointee being Dr. Vagn Hansen, of Denmark.

The Indian Ocean Standard net was agreed upon at a meeting of zooplanktologists in 1962, and was quickly put to use on many ships. It is not without fault as a sampling instrument, but these limitations are far outweighed by the fact that it has become widely used and provides the standard for the comparative zooplankton investigations of the expedition. Standard zooplankton samples are sorted at the IOBC by a team of expert technicians, and studied both at the Centre and abroad by specialists in the various fields of zooplankton systematics. By now the Centre has received a magnificent collection of samples, and will probably develop into the foremost institute for zooplankton research in our area.

Wind Systems

The Indian Ocean is unique in many respects, the chief of which are the relative disposition of land and water and the character of the wind systems in the area. The



The Indian Ocean Standard net, adopted for general use in the expedition. This is a nylon net with a mouth area of one square metre. It is hauled vertically from 200 metres to the surface. [Photo: Commonwealth Film Unit.]



A C.S.I.R.O. scientist at work in the laboratory of one of the Australian oceanographic frigates. The bottles in the rack contain samples of sea-water from various depths. These samples are filtered through fine "millipore" membranes (in the tray) and the concentration of activity of minute phytoplankton organisms measured. [Photo: Commonwealth Film Unit.]

powerful influence of the wind systems upon the productivity of the oceans is not generally realized. In the Indian Ocean it is most marked, for this is the domain of the monsoons, which change their direction from season to season and spread their influence over vast regions of the central and northern Indian Ocean. These winds exert their effect by way of ocean currents and other lateral movements of water, accompanied by upwelling of the deeper nutrient-rich waters so essential for oceanic productivity.

These are the processes which make the Arabian Sea and the Bay of Bengal so fertile, as well as the larger part of the equatorial Indian Ocean. Closer to home, similar influences are at work in the region between the north-west coast of Australia and Indonesia. This is a region which has received particular attention by our own laboratory. Among the 20 or so cruises we have made in the Indian Ocean since 1960, has been a series of six identical cruises between Fremantle and Singapore within a period of 12 months. This is a unique attempt to study the seasonal nature of oceanic productivity and to follow its effect from the point where deeper water is brought up into the lighted zone and triggers off the first phytoplankton bloom, to the stage where abundant food becomes available for populations of large migratory fish such as the tuna.

It seems to us that there may be three systems at work in this region, each with an enriching influence. North of 15° South, there is upwelling associated with the South Equatorial Current, which makes the region south of Indonesia one of the most productive in the entire Indian Ocean. South of this and north of 25° South is an entirely different system, depending for its seasonal enrichment on a deepening of the wind-induced mixed layer. Further south, in the region west of Perth, there is also periodic blooming of the plankton. This seems to be associated with the development of a large anti-clockwise gyral which may be accompanied by vertical uplift of deeper water.

The story is only now beginning to unfold. Our findings will be relevant to the expedition's work in other parts of the Indian Ocean and that work will be relevant to our own. Together, our combined results will provide not only the answers we are seeking, but also answers to problems not yet formulated.

UNESCO ARCHIVES

Reprinted from *Nautilus*, no. 1, 1966, p. 7-8

International co-operation in the Indian Ocean

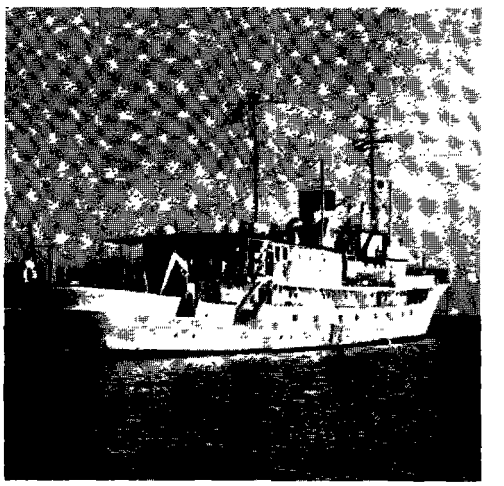
Collective research in the Indian Ocean has been one of the more important recent achievements of oceanography. This work has yielded information about one of the most neglected ocean areas, and the results will be of great economic significance for the many populations living around this broad ocean. More than 20 nations took part in the research programme sponsored by UNESCO.

In December 1964, the U. S. research ship, *Anton Bruun* (Fig. 1), completed its last mission for the International Indian Ocean Expedition (IIOE) and sailed for the United States. In 2 years, the *Bruun* completed nine scientific cruises covering a distance of more than 116,000 kilometres in the Indian Ocean (Fig. 2). Today, 8 months after the end of the field programme, we are still asked such questions as: What is the International Indian Ocean Expedition about? What is the scope of the Expedition? What are some of the results of the Expedition?

With reference to the last question, it is too soon to describe and assess the scientific contributions of the Expedition accurately. The mass of accumulated data will take time to analyze, so the results will continue to be published for years to come. At present, we can only briefly review the background of the Expedition and present a few highlights of the *Anton Bruun* cruises.

The idea of an international oceanographic programme was first proposed at a meeting of the Scientific Committee on Oceanic Research (SCOR) held in Paris in 1957. The plan developed at the meeting was to apply to a single ocean basin the kind of complex international scientific cooperation that produced such fruitful results during the International Geophysical Year (IGY). The Indian Ocean was selected for this extensive study because so little was known about this body of water, which covers one-seventh of the earth's surface. In addition, it was felt that the knowledge gained from the Expedition would lead to increased utilization of the natural resources of the Indian Ocean and adjacent seas by the more than 500 million people living around the border of these waters.

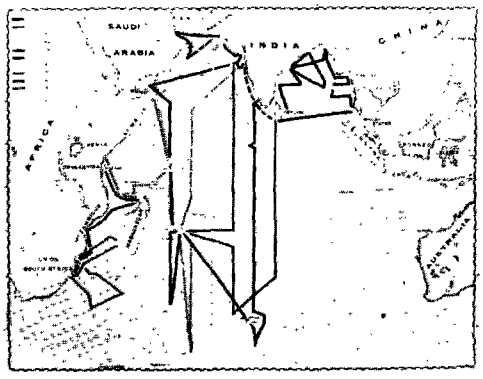
The Expedition began in 1961, reached a peak in 1963, and has since tapered off. No termination



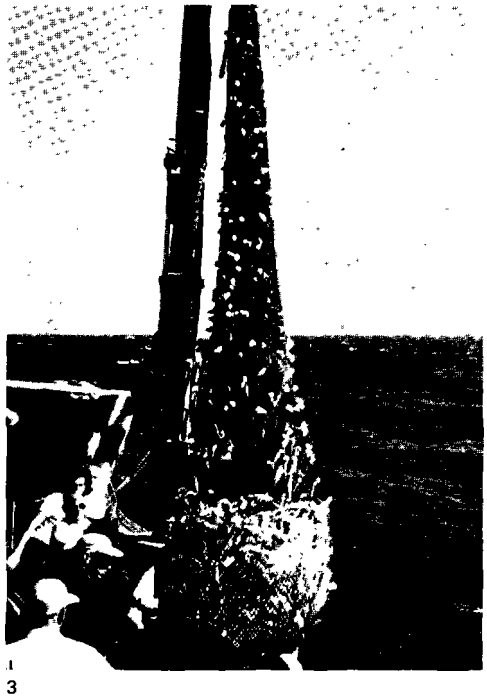
1

date has been set, since it was hoped that countries bordering the Indian Ocean will continue to pursue the types of research undertaken during the early years of the Expedition. To date, 25 countries utilizing more than 40 research ships have participated in the field programme.

As plans of participating countries developed, it became apparent that if the objectives of scientists were to be met, it would not be possible to lay down rigid cruise patterns for all of the ships. Consequently, each country agreed to devote approximately one-half of each cruise to collecting data for systematic surveys and the remainder to individual interests of its scientists. Studies carried out during the Expedition covered the entire range of modern oceanography. Included were studies in meteorology, physical and chemical oceanography, submarine geology, and the various specialized fields in marine biology.



2



1

3

The programme in biology, representing only one part of the total U. S. contribution to the International Indian Ocean Expedition, was supported by the National Science Foundation, with the major effort being based on a series of nine cruises of the *Anton Bruun*.

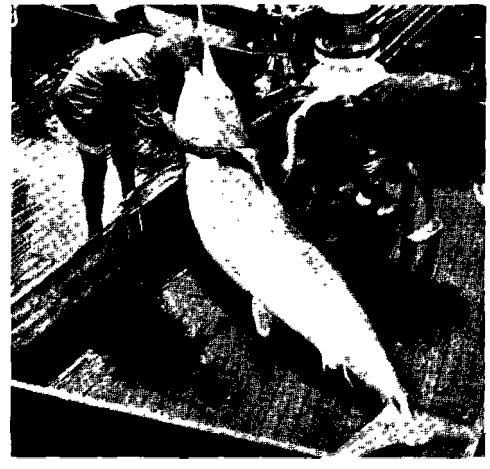
Descriptions of a few highlights of the cruises follow. To a considerable degree, the topics selected reflect the authors' own major interests. They do not necessarily represent the most important accomplishments of the cruises; such judgment must await completion of the vast number of studies now under way in the laboratory.

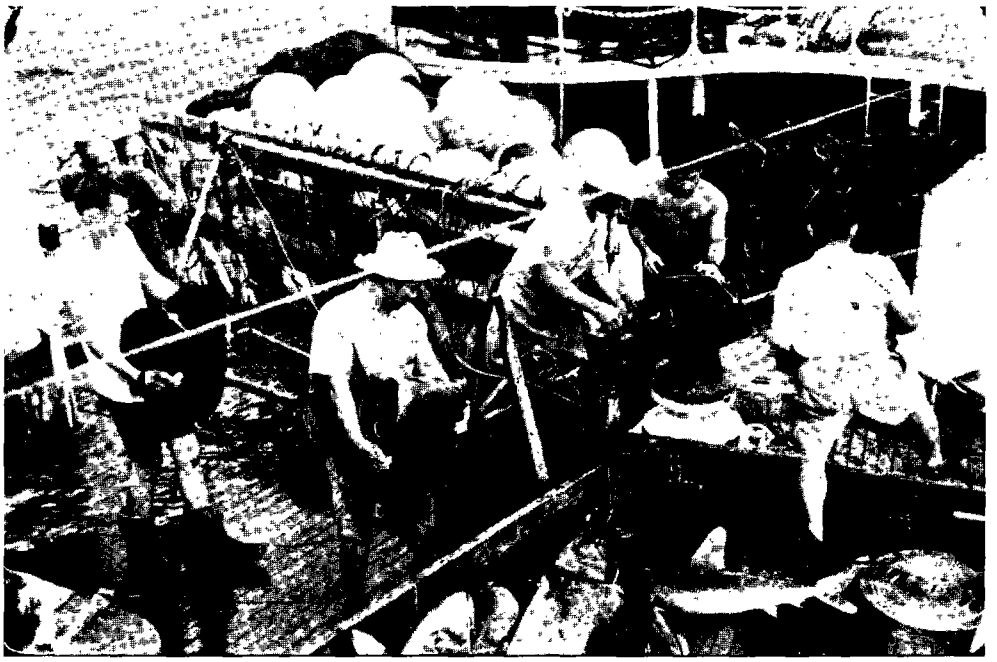
Productivity. – Reports by merchant ships and casual observations of opportunity by research vessels of mass fish mortalities and large plankton blooms in the Western Arabian Sea have long suggested that the production of life in these waters must be high. Accordingly, a cruise was made by the *Anton Bruun* in the Western Arabian Sea in October-November 1963 to investigate this area of indicated high productivity (Fig. 3). Extremely fertile waters were found in an area of diverging currents located some 240–320 kilometres off the Arabian Coast. In terms of carbon assimilation, primary productivity in these waters was an order of magnitude greater than that of the oceans as a whole. At two stations off the Gulf of Oman, rates of productivity were 5.7 and 6.4 g carbon/m^2/day–values considerably higher than ever before reported for the open sea. Dense phytoplankton populations of bluegreen algae, dinoflagellates, and diatoms were commonly observed at the surface between the Arabian Coast and the diverging-current region offshore. The plankton production was characterized by a patchy distribution. While on station, the *Anton Bruun* would commonly drift through areas of extremely dense plankton blooms, which varied in diameter from a hundred metres or less to several kilometres.

Results of this cruise offer an explanation of the probable course of events causing previously reported mass fish mortalities in the Western Arabian Sea. The concentration of dissolved oxygen was observed to decrease rapidly with depth, reaching less than 1.0 ml/litre at 100 metres and less than 0.1 ml/litre at mid-depths of 500 to 1000 metres at some stations. Sinking and decomposition of organic matter could create anaerobic conditions. Subsequent mixing of this anoxic water with surface water might easily lead to the death of fishes.

Mollusks. – Rich hauls of snails (Gastropoda), tooth shells (Scaphopoda), and bivalves (Pelecypoda) were dredged and trawled by the *Anton Bruun* from the ocean floor in the Gulf of Oman.

5





4

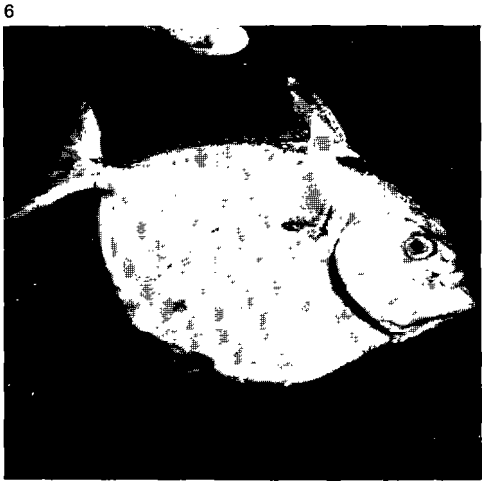
One 5-minute trawl haul made at a depth of 82 metres yielded 90 kilos of shells. The most exciting mollusks caught were 5 adult and 12 juvenile snails, *Strombus listeri*. Prior to the *Bruun*'s find, only 5 specimens of this species had been reported. All the latter were found 70 years ago off Ceylon and Burma.

Bottomfish. – Trawling surveys to assess the latent bottomfish and shellfish resources of the Arabian Sea and Bay of Bengal were made on two cruises of the *Anton Bruun*. Both cruises yielded specimens and data of great scientific interest that will help to describe Indian Ocean fauna and contribute to an understanding of the relation of its benthic fauna to physical and chemical oceanographic features of the region.

Largest trawl catches were obtained in the Western Arabian Sea in the same general area where, on the immediately preceding cruise, very fertile waters (as measured by primary productivity) had been observed. Considering the small size of the trawl nets used, two successful trawl hauls made off the Southeast Arabian Coast yielded exceedingly large catches of fish. One 30-minute haul produced 2 545 kilos; the other, of 45-minutes duration, yielded 773 kilos of fish and 836 kilos of swimming crabs (Fig. 3). Together, these two hauls produced almost as much fish as was caught in the remaining 84 trawl hauls made on the Arabian Sea cruise.

Most of the fish caught in trawls off Arabia were stingray, the largest specimen weighing 204 kilos. The second most abundant fish caught off Arabia was grunt, a desirable food fish.

6



Bathypelagic Fish. – Midwater trawl nets were used on several cruises to catch bathypelagic fishes over a wide range of depths. Two midwater trawl catches were of unique zoological interest. One haul contained a leptocephalus, or larval stage of a deep-sea eel, which was bright orange-red. All other known eel larvae, which number in the tens of thousands, are transparent. The other exciting specimen captured was a metamorphosing eel, over 1 metre long. Identification of this eel is presently in doubt. On the one hand, it seems referable to the "giant lepto-



7

cephalus" caught years ago by the Danish research ship *Dana*. On the other hand, it may be an adult nemichthyoid or snipe eel.

Pelagic Fishes. – Japanese-type longline gear was fished on two cruises of the *Anton Bruun* (Fig. 4). Inasmuch as a Japanese commercial longline fishery has operated in the Indian Ocean since the early 1950's, studies from the *Bruun* were designed to aid in understanding the interrelations between species and to delineate the distribution of these pelagic fishes in relation to their environment. Preliminary analyses of the data indicate an intimate association of certain species with specific types of water. For example, all of the albacore tuna caught on the two cruises were taken in the more southerly latitudes in waters identified as South Indian Ocean Central Water Type. Nearly 400 tunas were caught with the longline gear. Other pelagic fishes that were caught included the various species of billfishes (Fig. 5) wahoo, sharks, lancet fish, and the unusual moonfish (Fig. 6).

One of the most fruitful aspects of the programme was the opportunity for scientists to exercise a high degree of personal judgment in attaining their particular research goals. Of equal importance was the international aspect of shipboard activities (Fig. 7). Excluding the permanent staff assigned to the vessel, approximately one-fourth of the scientists participating on the cruises of the *Anton Bruun* were from countries other than the United States. Researchers from Australia, Austria, Brazil, Denmark, Egypt, Hong Kong, India, Israel, Italy, Madagascar, Pakistan, South Africa, Spain, Sweden, Thailand, and Zanzibar were included in the scientific complement.

The fondest memories of cruise participants are the friendships they formed with scientists of other countries. The general feeling of scientists concerning the programme aboard the *Anton Bruun* was expressed in a letter written by a participant from India, a portion of which is quoted below:

> "I very much appreciated the brotherly attitude of the scientific staff, all working in a team, imbibed with the spirit of exploration and pursuit of knowledge and, at the same time, with individual freedom and choice. I enjoyed this inspiring experience and also the hospitality, for which I am certainly grateful to the United States Programme in Biology of the International Indian Ocean Expedition."

A. T. Pruter and R. Shomura
U. S. Department of the Interior
Fish and Wildlife Service
Bureau of Commercial Fisheries
Seattle, Washington USA

Figure 1
U.S. research vessel *Anton Bruun* at anchor off Phuket, Thailand.

Figure 2
Cruise tracks of the *Anton Bruun* during the International Indian Ocean Expedition, 1963–1964.

Figure 3
Trawl catch of swimming crabs and grunt fish taken off southeast Arabia.

Figure 4
Storing longline fishing gear on the stern of the *Anton Bruun*.

Figure 5
Examining a large white marlin for external parasites.

Figure 6
A large longline-caught moonfish (opah).

Figure 7
Shallow-water fishes collected at Astola Island, West Pakistan, are examined by Dr. H. G. Kewalramani, Indian Department of Fisheries.

Part VI

Papers presented by title only

Department of Ichthyology, Rhodes University, Grahamstown, South Africa

Bibliography of papers by J. L. B. Smith on ichthyology of the Indian Ocean

350. The fishes of the family Sphyraenidae in the western Indian Ocean. *R.U. ich. Bull.*, no. 3, July 1956, p. 34-47.
351. The fishes of the family Scorpaenidae in the western Indian Ocean. Part I: The sub-family Scorpaninae. *R.U. ich. Bull.*, no. 4, July 1957. p. 48-72.
352. The fishes of the family Scorpaenidae in the western Indian Ocean. Part II: The sub-families Pterornae, Apistanae, Setarchinae and Sebastinae. *R.U. ich. Bull.*, no. 5, August 1957, p. 73-88.
353. Sharks of the genus *Isurus* Rafinesque 1810. *R.U. ich. Bull.*, no. 6, September 1957, p. 89-96.
354. List of the fishes of the family Labridae in the western Indian Ocean with new records and five new species. *R.U. ich. Bull.*, no. 7, October 1957, p. 98-114.
355. The Labrid fishes of the subgenus *Julis* Cuvier 1814 (in Coris Lacepede 1802) from South and East Africa. *R.U. ich. Bull.*, no. 8, November 1957, p. 117-120.
356. The gunnellichtbrid fishes with description of two new species from East Africa and of *Gunnellichthys (Clarkichthys) Bilineatus* (Clark) 1936. *R.U. ich. Bull.*, no. 9, January 1958, p. 121-129.
357. Sharks of the genus *Pterolamiops* Springer 1951 with notes on isurid sharks. *R.U. ich. Bull.*, no. 10, June 1958, p. 130-135
358. The fishes of the family Eleotridae in the western Indian Ocean. *R.U. ich. Bull.*, no. 11, July 1958, p. 136-165.
359. Fishes of the families Tetrarogidae, Caracanthidae and Synanciidae from the western Indian Ocean, with further notes on Scorpaenid fishes. *R.U. ich. Bull.*, no. 12, October 1958, p. 166-183.
360. Gobioid fishes of the families Gobiidae, Periophthaluridae, Trypauchenidae, Taenicoididae and Kraemeriidae of the western Indian Ocean. *R.U. ich. Bull.*, no. 13, February 1959, p. 184-226.
361. Fishes of the families Blenniidae and Salariidae of the western Indian Ocean. *R.U. ich. Bull.*, no. 14, May 1959, p. 227-253.
362. Serioline fishes (Yellowtails: amberjacks) from the western Indian Ocean. *R.U. ich. Bull.*, no. 15, August 1959, p. 254-261.
363. The identity of *Scarus gibbus* Ruppell 1828 and of other parrot fishes of the family Callyodontidae from the Red Sea and the western Indian Ocean. *R.U. ich. Bull.*, no. 16, September 1959, p. 262-282.
364. Fishes of the family Lethrinidae from the western Indian Ocean. *R.U. ich Bull.*, no. 17, November 1959. p. 284-297.
365. A new Grammicolepid fish from South Africa. *Ann. Mag. nat. Hist.*, ser. 13, vol. 3, April 1960, p. 231-235.
366. Fishes of the family Gobiidae in S.A. *R.U. ich. Bull.*, no. 18, 1960, p. 299-314.
367. A new clinid fish from South Africa. *Ann. Mag. nat. Hist.*, ser. 13, vol. 3, November 1960, p. 689-691.
368. A rare Lutianid fish from Kenya. *Ann. Mag. nat. Hist.*, ser. 13, vol. 3, December 1960, p. 753-755.
369. Coral fishes of the family Pomacentridae from the western Indian Ocean and the Red Sea. *R.U. ich. Bull.*, no. 19, 1961, p. 317-349, 8 plates.
370. A new stromateid fish from South Africa and another new to that area. *S. Afr. J. Sci.*, vol. 57, no. 6, June 1961, p. 158-159.
371. Fishes of the family Xenopoclinidae. *R.U. ich. Bull.*, no. 20, 1960-1961, p. 351-356, 4 figs.
372. Fishes of the family Anthiidae from the Red Sea and the western Indian Ocean. *R.U. ich. Bull.*, no. 21, 1961, p. 359-369, 2 plates.
373. Fishes of the family Apogonidae. *R.U. ich. Bull.*, no. 22, 1961, p. 373-418, plates 46-52.
374. Nomenclatorial change for a long-known south African fish. *Ann. S. Afr. Mus.*, vol. XLVI, part X, February 1962, p. 257-260.
375. The moray eels of the western Indian Ocean and the Red Sea. *R.U. ich. Bull.*, no. 23, 1962, p. 421-444, plates 53-62.
376. Sand-dwelling eels of the western Indian Ocean and the Red Sea. *R.U. ich. Bull.*, no. 24, 1962, p. 447-466, plates 63-68.
377. Fishes of the family Gaterinidae of the western Indian Ocean and the Red Sea with a resumé of all known Indo-Pacific species. *R.U. ich. Bull.*, no. 25, 1962, p. 469-503, plates 69-72.
378. The rare 'Furred-tongue' *Uraspis uraspis* (Gnthr) from S.A. and other new records from there. *R.U. ich. Bull.*, no. 26, 1962, p. 505-510, plates 73 and 74.
379. New species and new records of fishes from the western Indian Ocean. *Ann. Mag. nat. Hist.*, ser. 13, vol. 6, January 1963, p. 33-37.
380. Fishes of the family Syngnathidae from the Red Sea and the western Indian Ocean. *R.U. ich Bull.*, no. 27, 1963, p. 515-543, plates 75-82.
381. Fishes of the families Draconettidae and Callionymidae from the Red Sea and the western Indian Ocean. *R.U. ich. Bull.*, no. 28, 1963, p. 547-564, plates 83-86.
382. Identity of Hapologenys pictus Tortonese 1935. *Ann. Mag. nat. Hist.*, ser. 13, vol. 5, October 1963, p. 637-638.
383. Fishes of the family Pentacerotidae. *R.U. ich. Bull.*, no. 29, 1964, p. 567-576, plates 87-91.
384. The clingfishes of the western Indian Ocean and the Red Sea. *R.U. ich. Bull.*, no. 30, 1964, p. 581-596, plates 92-97.
385. The rediscovery in South Africa of a rare form of Labrid fish from Mauritius and its sexual dichromatic relation to *Lepidaplois axillaris* (Bennett 1831). *Ann. Mag. nat. Hist.*, ser. 13, vol. 2, March 1964, p. 177-183.
386. A new Gobiid fish of unusual type from Mozambique *(Cottogobius platycephalops)*. *Ann. Mag. nat. Hist.*, ser. 13, vol. 7, March 1964, p. 173-176.
387. A new sponge-dwelling Apogonid fish from the Red Sea. *Ann. Mag. nat. Hist.*, ser. 13, vol. 7, September 1964, p. 529-531.
388. An interesting new fish of the family Chiasmodontidae from South Africa, with redescription of *Odontonoma kerberti* Weber, 1913. *Ann. Mag. nat. Hist.*, ser. 13, vol. 7, September 1964, p. 567-574.
389. The discovery in Mozambique of the little known eel, *Opichthys tenuis* Gunther, 1870. A redescription of the type of *Caecula pterygera* Vahl, 1794, notes on other species and on generic relationships. *Ann. Mag. nat. Hist.*, ser. 13, vol. 7, December 1964, p. 711-723.
390. Fishes of the family Atherinidae. *R.U. ich. Bull.*, no. 31, 1965, p. 98-102.
391. An interesting new Callionymid fish from Madagascar and the first record of a clingfish from there. *Ann. Mag. nat. Hist.*, ser. 13, vol. 8, June 1965, p. 321-324.
392. New records and new species of fishes from South Africa, chiefly from Natal. *R.U. occ. Pap.*, no. 4, 1965, p. 27-34, plates 6-11.
393. *Kaupichthys diodontus*, Schultz. in the western Indian Ocean. A problem in systematics. *R.U. occ. Pap.*, no. 5, 1965, p. 45-54, plate 12.
394. A new clingfish from southern Mozambique. *Ann. Mag. nat. Hist.*, ser. 13, vol. 8, November 1965, p. 641-644.
395. A rare Acanthurid fish from Mauritius in South Africa. *Ann. Mag. nat. Hist.*, ser. 13, vol. 9, January-March 1966, p. 5-8.
396. Certain rare fishes from South Africa with other notes. *R.U. occ. pap.*, no. 7, April 1966.
397. Fishes of the sub-family Nasinae with a synopsis of the Prionurinae. *R.U. ich. Bull.*, no. 32, November 1966, p. 635-682, 13 figs., 2 plates.
398. Interesting fishes from South Africa. *R.U. occ. Pap.*, no. 8, December 1966, p. 82-94.
399. The rare big-eye Pristigenys niphonia (Cand V.) in South Africa. *R.U. occ. Pap.*, no. 9, December 1966, p. 96-102.

Annales de la Faculté des Sciences et des Techniques de Madagascar (Travaux de la station marine de Tuléar)

No. 1, 1962

400. PERES, J.-M.; PICARD, J. Note préliminaire générale sur le benthos littoral de la région de Tuléar (Madagascar), p. 145-151. (cf. IIOE Collected Reprints, vol. II, contribution no. 104).
401. PICHON, M. Note préliminaire sur la topographie et la géomorphologie des récifs coralliens de la région de Tuléar, p. 154-168.
402. VASSEUR, P. Note préliminaire sur l'aspect topographique, morphologique et biologique des surplombs et des grottes sous-marines sciaphiles en avant du récif de Songeritelo, p. 169-179.
403. PLANTE, R. Note préliminaire sur la répartition et les peuplements des substrats solides dans la région de Tuléar, p. 181-200.
404. DERIJARD, R. Note préliminaire sur la localisation et le peuplement de certains atterrissements sablo-vaseux et vaseux intertidaux dans la région de Tuléar, p. 201-219.
405. PICHON, M. Note préliminaire sur la répartition et le peuplement des sables fins et des sables vaseux non fixés dans la zone intertidale dans la région de Tuléar, p. 221-235.
406. CHASSE, C. Remarques sur la morphologie et la bionomie des herbiers de monocotyledones marines tropicales de la province de Tuléar, p. 237-248.

No. 2, 1964

407. VASSEUR, P. Contribution à l'étude bionomique des peuplements sciaphiles infralittoraux de substrat dur dans le récif de Tuléar.
408. PICHON, M. Contribution à l'étude de la répartition des Madrépores sur le récif de Tuléar, p. 81-203.
409. PLANTE, R. Contribution à l'étude des peuplements des hauts niveaux sur substrats solides non récifaux dans la région de Tuléar, p. 207-315.

No. 3, 1965

410. DERIJARD, R. Contribution à l'étude du peuplement des sédiments sablo-vaseux et vaseux intertidaux compactés ou fixés par la végétation de la région de Tuléar, p. 1-85.

No. 4, 1966

411. MINAS, M. La substance organique et le calcaire dans deux types de vasières littorales de la région de Tuléar, p. 57-70.
412. VACELET, J.; VASSEUR, P. Spongiaires des grottes et surplombs des récifs de Tuléar, p. 71-123.
413. TRAVERS, A.; TRAVERS, M. Introduction à l'étude du phytoplancton et des Tintinnides de la région de Tuléar, p. 125-162.

Admiralty marine science publications. Hydrographic Department 1963

414. Bathymetric magnetic and gravity investigations. H.M.S. *Owen*. 1961-1962. International Indian Ocean Expedition. (No. 4.)
415. Surface temperature and salinity observations. H.M.S. *Owen*, 1961-1962. International Indian Ocean Expedition. (No. 5.)
416. Bathymetric and magnetic investigations. H.M.S. *Dalrymple*, 1961-1962 and 1962-1963. (H.D. 566, January 1966.) (No. 8.)
417. Bathymetric, magnetic and gravity investigations, H.M.S. *Owen*, 1962-1963. International Indian Ocean Expedition. Part I: Text. Part 2: Profiles. (H.D. 567, February 1966.) (No. 9.)

National Oceanographic Data Center (Washington)/World Data Center A (Oceanography) publications

418. *Indian Ocean atlas. Interpolated values of depth, salinity and temperature on selected sigma-T surfaces.* Compiled by the Hydrodynamics Branch. (Publication G-12, 1967.)
419. *Special catalogue of data from the International Indian Ocean Expedition.* Washington, D.C., World Data Center A (Oceanography), September 1967.